

Communications

Selectfluor-Mediated Dialkoxylation of Tungsten η^2 -Pyridinium ComplexesGeorge W. Kosturko,[†] Daniel P. Harrison,[†] Michal Sabat,[†] William H. Myers,[‡] and W. Dean Harman^{*†}

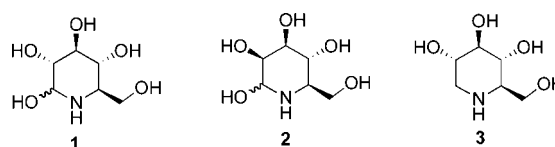
Departments of Chemistry, University of Virginia, Charlottesville, Virginia 22904 and University of Richmond, Richmond, Virginia 27173

Received November 7, 2008

Summary: η^2 -coordinated pyridinium complexes of {Tp-W(NO)(PMe₃)} undergo a stereoselective dialkoxylation reaction when treated with Selectfluor in an alcohol. The alkoxy groups add to the 5- and 6-positions in a *syn* fashion (proven by X-ray diffraction). When the *N*-acetylpyridinium complex is dialkoxylated, the resulting acyldihydropyridinium system readily undergoes nucleophilic addition with cyanide ion to stereoselectively generate a third stereocenter at C2 of the pyridine ring. Treatment with CAN decomplexes the tetrahydropyridine.

A multitude of polyhydroxylated piperidine alkaloids have been isolated from plants and animals, and several show promise as potential therapeutics.¹ For example, nojirimycin (**1**) and mannojojirimycin (**2**) are potential therapeutic agents for diabetes and tumor metastasis,^{2,3} and derivatives of 1-deoxynojirimycin (**3**) have been shown to inhibit the development of HIV *in vitro*.⁴ Most syntheses of these molecules incorporate the nitrogen

moiety through an azide nucleophilic addition⁵ or Garner aldehyde.^{6,7} However, Comins et al. showed the potential of utilizing a pyridine as a synthon to oxygenated piperidines with their elegant synthesis of 1-deoxynojirimycin (**3**) from 4-methoxy-3-(triisopropylsilyl)pyridine.⁸



With the advent of the dearomatization agent {Tp-W(NO)(PMe₃)},⁹ new synthetic opportunities have emerged for arenes and aromatic heterocycles that use this tungsten moiety to activate the aromatic ring through η^2 coordination.¹⁰ We

* To whom correspondence should be addressed. E-mail: wd5z@virginia.edu.

[†] University of Virginia.

[‡] University of Richmond.

(1) Pearson, M. S. M.; Mathé-Allainmat, M.; Fargeas, V.; Lebreton, J. *Eur. J. Org. Chem.* **2005**, 2159–2191.

(2) Heightman, T. D.; Vasella, A. T. *Angew. Chem., Int. Ed.* **1999**, *38*, 750–770.

(3) Haukaas, M. H.; O'Doherty, G. A. *Org. Lett.* **2001**, *3*, 401–404.

(4) Asano, N.; Nash, R. J.; Molyneux, R. J.; Fleet, G. W. J. *Tetrahedron: Asymmetry* **2000**, *11*, 1645–1680.

(5) Hudlicky, T.; Rouden, J.; Luna, H.; Allen, S. *J. Am. Chem. Soc.* **1994**, *116*, 5099–5107.

(6) Takahata, H.; Banba, Y.; Ouchi, H.; Nemoto, H.; Kato, A.; Adachi, I. *J. Org. Chem.* **2003**, *68*, 3603–3607.

(7) Takahata, H.; Banba, Y.; Sasatani, M.; Nemoto, H.; Kato, A.; Adachi, I. *Tetrahedron* **2004**, *60*, 8199–8205.

(8) Comins, D. L.; Fulp, A. B. *Tetrahedron Lett.* **2001**, *42*, 6839–6841.

(9) Graham, P. M.; Meiere, S. M.; Sabat, M.; Harman, W. D. *Organometallics* **2003**, *22*, 4364.

(10) Keane, J. M.; Harman, W. D. *Organometallics* **2005**, *24*, 1786–1798.

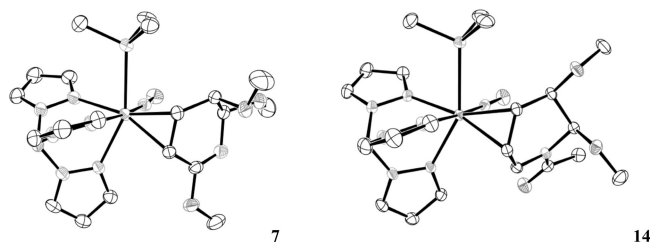


Figure 1. ORTEP diagrams of the complexes **7** and **14**.

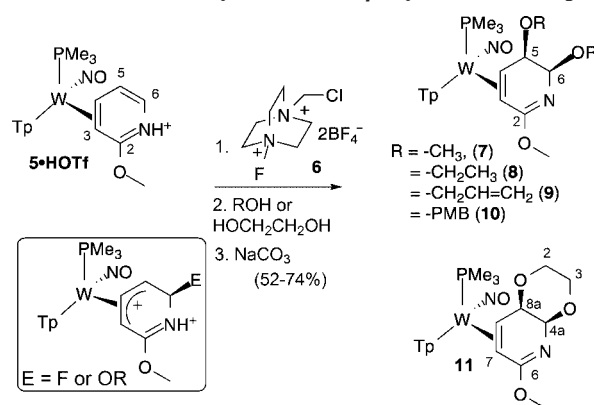
questioned whether common pyridines could be elaborated into oxygenated piperidines through such a strategy.¹¹

The complex $\text{TpW}(\text{NO})(\text{PMe}_3)(\eta^2\text{-benzene})$ (**4**) serves as a convenient precursor to η^2 complexes of many aromatic molecules. In the case of pyridines, nitrogen coordination is suppressed by utilizing a π -donor group at the 2-position of the heterocycle.¹¹ Hence, our studies commenced with the 2-methoxypyridine complex **5**, prepared from **4** in 79% yield.¹¹ While this species is isolated as a 2:1 ratio of coordination diastereomers, they are easily separated by selective precipitation from methanol. An earlier exploration of 2*H*-phenol complexes of tungsten revealed that electrophilic heteroatoms could be added to the uncoordinated π system without oxidation of the metal.¹² Unfortunately, treatment of **5** with *m*CPBA resulted in an intractable mixture of products, presumably a result of oxidative degradation of the complex. Earlier studies have shown that the reduction potential for the W(I/0) couple dramatically increases when **5** is protonated ($E_{\text{p.a}} = +0.74$ V for **5**·HOTf; cf. -0.06 V for **5**), indicating that the conjugate acid **5**·HOTf is substantially more difficult to oxidize. Unfortunately, the reaction of **5**·HOTf with *m*CPBA or with NMO/OsO₄ (Upjohn process) also resulted in decomposition. However, when the oxidant Selectfluor (**6**; Aldrich)¹³ was combined with **5**·HOTf in the presence of methanol,^{14,15} a ligand-based reaction product was isolated (**7**; 74%).

A ³¹P–¹⁸¹W coupling constant of 266 Hz and nitrosyl stretching frequency of 1570 cm⁻¹ suggested a neutral, non-aromatic π complex.¹¹ A positive shift in the anodic peak potential from $E_{\text{p.a}} = -0.06$ V (**5**) to $+0.84$ V (**7**) (NHE) indicated the presence of electron-withdrawing groups on the pyridine framework. ¹H NMR data did not reveal any H–F coupling, but singlets between 3 and 4 ppm signified the incorporation of two methoxy groups. Ultimately, an X-ray diffraction study (Figure 1) confirmed that **7** was a trimethoxy-dihydropyridine complex, the product of a syn-dimethoxylation reaction at C5 and C6 of the pyridine ring (Scheme 1).

Selectfluor has previously been used in the electrophilic addition of a primary alkoxide and fluoride across a CC double bond, sometimes en route to α -keto ethers.^{16,17} However, the

Scheme 1. Dimethoxylation of an η^2 -Pyridinium Complex



dialkoxylation of alkenes using this fluorinating reagent appears to be previously undocumented.

The dialkoxylation of the pyridinium complex **5**·HOTf was successful with other primary alcohols, including ethanol (**8**; 68%), allylic alcohol (**9**; 52%), 4-methoxybenzyl alcohol (PMB) (**10**; 59%), and ethylene glycol (**11**; 66%). Secondary or tertiary alcohols failed to react in this manner. Both ³¹P NMR and cyclic voltammetric data indicated that the dialkoxylation of the pyridine ring occurred within seconds at ambient temperature. These four products (**8**–**11**) show electrochemical and spectroscopic features similar to those of **7**. Further, proton–proton coupling data for H4–H5 (~2 Hz) and H5–H6 (~3 Hz) of **8**–**10** suggest that these products have the same configurations at C5 and C6 as does **7**. A single diastereomer resulted (dr > 10:1) in all cases but for compound **9** (dr = 3:1).¹⁸

The dialkoxylation reaction is potentially a valuable new synthetic tool for pyridines, and its optimization and mechanism are currently under investigation. The tungsten apparently stabilizes the purported allyl cation intermediate (see Scheme 1) resulting from addition of either E⁺ = “MeO⁺” or “F⁺”.¹² Rozen and Kol have described the ability of MeO⁺ (via methyl hypofluorite) to act on alkenes to form fluoroalkoxides.^{19,20} However, those reactions were carried out in acetonitrile; utilizing an alcohol as the solvent either pre-empts fluoride addition, or the F is replaced by the alkoxide in a subsequent substitution reaction. Possibly relevant is a report by Shreeve et al. describing the formation of 6-alkoxylated bipyridyls from primary alcohols and the potent fluorinating agent MeC-31.¹⁷ Finally, it is noteworthy that while Selectfluor often participates in single-electron-transfer (SET) processes,¹⁵ the tungsten is not oxidized in the conversion of **5**·HOTf to **7**. The intact W(0) center of **5**·HOTf not only activates the pyridinium ligand but also protects the bound azadiene products from further oxidation.

With the oxygenated dihydropyridine complexes in hand, we hoped to hydrolyze the imidate functionality in order to prevent the rearomatization of the pyridine ring upon decomplexation. Hence, treatment of **7** with 1 M HCl for 16 h yields the lactam **12** in 67% yield (eq 1). Unfortunately, the other dialkoxyated products (**8**–**11**) failed to yield the corresponding lactam products with 1 M HCl (20–55 °C, 5 days) and attempts to hasten this reaction by heating (>55 °C) resulted in decomposition. Furthermore, attempts to oxidatively decomplex **12** proved to be futile, as treatment of this lactam complex with CAN,

(11) Delafuente, D. A.; Kosturko, G. W.; Graham, P. M.; Harman, W. H.; Myers, W. H.; Surendranath, Y.; Klet, R. C.; Welch, K. D.; Trindle, C. O.; Sabat, M.; Harman, W. D. *J. Am. Chem. Soc.* **2007**, *129*, 406–416.

(12) Todd, M. A.; Sabat, M.; Myers, W. H.; Smith, T. M.; Harman, W. D. *J. Am. Chem. Soc.* **2008**, *130*, 6906–6907.

(13) Syvret, R. G.; Butt, K. M.; Nguyen, T. P.; Bulleck, V. L.; Rieth, R. D. *J. Org. Chem.* **2002**, *67*, 4487–4493.

(14) While Selectfluor is a common source of an electrophilic fluorine atom, it also has the ability to chemically modify heteroatomic nucleophiles to potential electrophiles.

(15) Nyffeler, P. T.; Duron, S. G.; Burkart, M. D.; Vincent, S. P.; Chi-Huey, W. *Angew. Chem., Int. Ed.* **2004**, *44*, 192–212.

(16) Stavber, S.; Sotler, T.; Zupan, M. *Tetrahedron Lett.* **1994**, *35*, 1105–1108.

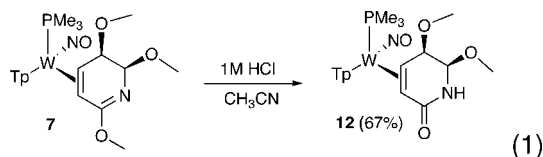
(17) Manandhar, S.; Singh, R. P.; Eggers, G. V.; Shreeve, J. M. *J. Org. Chem.* **2002**, *67*, 6415–6420.

(18) For **9**, a minor impurity was detected that we believe could be the other coordination diastereomer.

(19) Rozen, S.; Mishani, E.; Kol, M. *J. Am. Chem. Soc.* **1992**, *114*, 7643–7645.

(20) Kol, M.; Rozen, S.; Appelman, E. *J. Am. Chem. Soc.* **1991**, *113*, 2648–2651.

*m*CPBA, CuBr₂, Fe(Cp)₂⁺, or NBS under neutral or basic conditions yielded only intractable mixtures.

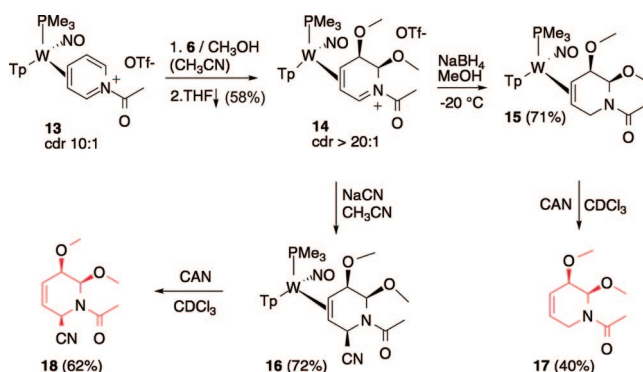


An attractive alternative to the 2-methoxypyridine synthon (**5**) was the recently reported *N*-acylpyridinium complex **13**.²¹ This air-stable complex derived from pyridine–borane was also expected to be resistant to oxidation at the metal and offered an additional position (C2) for eventual elaboration of the pyridine ring. Treatment of **13** (available as a 10:1 mixture of coordination diastereomers)²¹ with 1.05 equiv of Selectfluor and methanol resulted in the dialkoxylation product **14**, in a coordination diastereomer ratio of 8:1. Conveniently, we found that the major isomer could be isolated in pure form (55% yield) by precipitating it from a THF solution (Scheme 2). Significant back-bonding by the tungsten greatly stabilizes the acyliminium group in **14**, and it resists reaction, even in the presence of water. However, C2 is still sufficiently electrophilic to smoothly react with NaBH₄ and NaCN to form the dihydropyridine complexes **15** and **16**, respectively (Scheme 2).

Oxidative demetalation of **15** and **16** is accomplished using CAN in CDCl₃ solution to generate **17** (40%) and **18**, respectively (62%). H NMR spectra indicate that **17** and **18**, as well as their precursors, are present as two-component mixtures; NOESY, HSQC, and COSY data confirm that, in all cases, the two NMR-resolved species are conformational isomers resulting from the hindered rotation of the amide C–N bond.

(21) Harrison, D. P.; Welch, K. D.; Nichols-Nielander, A. C.; Sabat, M.; Myers, W. H.; Harman, W. D. *J. Am. Chem. Soc.* **2008**, *130*, 16844.

Scheme 2. Bis-Alkoxylation of the *N*-Acetylpyridinium Complex and Elaboration



In conclusion, this work demonstrates that a transition-metal complex may be used to stereoselectively elaborate a pyridine into a highly functionalized piperidine. Specifically, a new approach to the preparation of polyoxygenated piperidines has been described that utilizes Selectfluor, a primary alcohol, and a η^2 -pyridinium complex. Dihapto coordination of the heterocycle allows for predictable stereocontrol of all electrophilic and nucleophilic addition reactions, and decomplexation un-masks the remaining alkene carbons.

Acknowledgment. Acknowledgement is made to the donors of the American Chemical Society Petroleum Research Fund (Grant No. 47306-AC1) and to the NSF (Grant No. CHE-0116492 (UR)).

Supporting Information Available: CIF files giving crystallographic data for **7** and **14** and text and figures giving details of the syntheses, characterization data, and ¹H and ¹³C NMR spectra of all new compounds. This material is available free of charge via the Internet at <http://pubs.acs.org>.

OM801068U

A Convenient Method for the Synthesis of Protic 2-(Tertiary phosphino)-1-amines and Their Cp*RuCl Complexes

Masato Ito, Akihide Osaku, Chika Kobayashi, Akira Shiibashi, and Takao Ikariya*

Department of Applied Chemistry, Graduate School of Science and Engineering, Tokyo Institute of Technology, 2-12-1-S1-39 O-okayama, Meguro-ku, Tokyo 152-8552, Japan

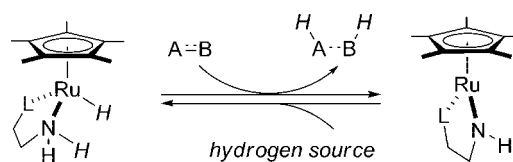
Received October 30, 2008

Summary: A variety of protic 2-(tertiary phosphino)-1-amines ($R_2PCH_2CHR'NHR''$, $P-NH$) have been prepared from 2-oxazolindiones and secondary phosphines using a newly developed acid-promoted decarboxylative C–P bond formation reaction. Treatment of the resulting chiral P–NH compounds with $Cp^*RuCl(isoprene)$ in CH_2Cl_2 smoothly furnished chiral $Cp^*RuCl(P-NH)$ complexes with a typical three-legged piano-stool structure, which prove to be excellent catalyst precursors for asymmetric reactions, including the isomerization of allylic alcohols and hydrogenation of imides.

Recently, optically active nitrogen-containing compounds have been widely used as versatile ligands in transition-metal-catalyzed asymmetric reactions.¹ We have developed conceptually new molecular catalyst systems consisting of Cp^*RuCl complexes bearing chelating protic amine (L–NH) ligands and successfully applied them to a variety of catalytic reactions. The “Ru/NH bifunctionality”^{2,3} is a key structural feature of these catalysts, which facilitates either abstraction or addition of dihydrogen to enable a number of transformations (Scheme 1).

The coordinating elements (L) in the L–NH ligand play a decisive role in controlling the catalytic performance by tuning the electron density of the metal center in the molecule of a catalyst.⁴ Thus, changing the group L from tertiary amine to tertiary phosphine causes a significant broadening of applicable substrates with a polarized C–O bond (polar functionalities) in the hydrogenation.⁵ For example, the catalytic hydrogenation of epoxides,^{5b} imides,^{5c} *N*-acylcarbamates, and *N*-acylsulfon-

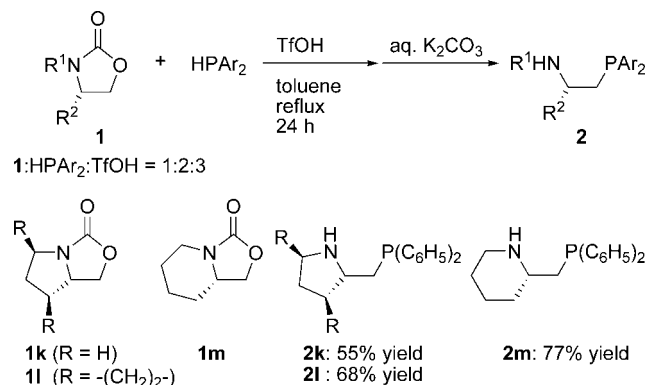
Scheme 1. $Cp^*Ru(L-NH)$ Catalysts with Ru/NH Bifunctionalities



Representative L–NH ligands:



Scheme 2. Preparation of 2-(Diarylphosphino)-1-amines (2) from 2-Oxazolindiones (1)



* To whom correspondence should be addressed. E-mail: tikariya@apc.titech.ac.jp.

(1) For example, see: (a) Noyori, R. *Asymmetric Catalysis in Organic Synthesis*; Wiley: New York, 1994. (b) *Comprehensive Asymmetric Catalysis I–III*; Jacobsen, E. N., Pfaltz, A., Yamamoto, H., Eds.; Springer: Berlin, 1999. (c) *Catalytic Asymmetric Synthesis*, 2nd ed.; Ojima, I., Ed.; Wiley-VCH: New York, 2000. (d) Fache, F.; Schulz, E.; Tommasino, M. L.; Lemaire, M. *Chem. Rev.* **2000**, *100*, 2159–2231.

(2) For reviews: (a) Noyori, R.; Hashiguchi, S. *Acc. Chem. Res.* **1997**, *30*, 97–102. (b) Noyori, R.; Ohkuma, T. *Angew. Chem., Int. Ed.* **2001**, *40*, 40–73. (c) Noyori, R.; Yamakawa, M.; Hashiguchi, S. *J. Org. Chem.* **2001**, *66*, 7931–7944. (d) Ikariya, T.; Murata, K.; Noyori, R. *Org. Biomol. Chem.* **2006**, *4*, 393–406. (e) Ikariya, T.; Blacker, A. J. *Acc. Chem. Res.* **2007**, *40*, 1300–1308.

(3) (a) Alonso, D. A.; Brandt, P.; Nordin, S. J. M.; Andersson, P. G. *J. Am. Chem. Soc.* **1999**, *121*, 9580–9588. (b) Yamakawa, M.; Ito, H.; Noyori, R. *J. Am. Chem. Soc.* **2000**, *122*, 1466–1478. (c) Petra, D. G.; Reek, J. N. H.; Handgraaf, J.-W.; Meijer, E. J.; Dierkes, P.; Kamer, P. C. J.; Brusse, J.; Shoemaker, H. E.; van Leeuwen, P. W. N. M. *Chem. Eur. J.* **2000**, *6*, 2818–2829. (d) Casey, C. P.; Johnson, J. B. *J. Org. Chem.* **2003**, *68*, 1998–2001.

(4) Ito, M.; Ikariya, T. *Chem. Commun.* **2007**, 5134–5142.

(5) (a) Ito, M.; Hirakawa, M.; Murata, K.; Ikariya, T. *Organometallics* **2001**, *20*, 379–381. (b) Ito, M.; Hirakawa, M.; Osaku, A.; Ikariya, T. *Organometallics* **2003**, *22*, 4190–4192. (c) Ito, M.; Sakaguchi, A.; Kobayashi, C.; Ikariya, T. *J. Am. Chem. Soc.* **2007**, *129*, 290–291. (d) Ito, M.; Koo, L.-W.; Himizu, A.; Kobayashi, C.; Sakaguchi, A.; Ikariya, T. *Angew. Chem., Int. Ed.*, in press.

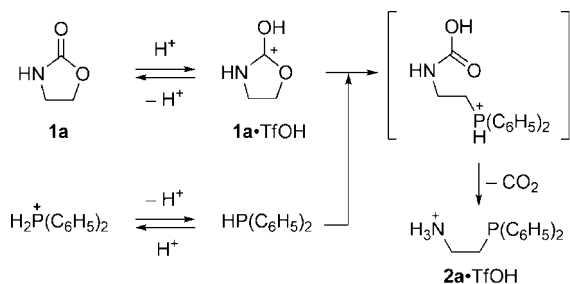
amides^{5d} are effectively promoted by $Cp^*Ru(P-NH)$ complexes but not by $Cp^*Ru(N-NH)$, which serve as chemoselective catalysts for the hydrogenation of ketones.^{5a} The same change in the structure of the catalyst also leads to considerable rate enhancement in the reversible oxidation of primary and secondary alcohols.^{6a} This extremely rapid hydrogen transfer between alcohols and carbonyl compounds was successfully applied to the isomerization of allylic alcohols^{6b} and the selective lactonization of 1,4-diols using acetone.^{6c} These findings prompted us to explore convenient methods for the chiral modification of the essential P–NH framework in the ligand for developing catalytic asymmetric processes.

Conventionally, the chiral P–NH compounds with a carbon-centered chirality on the ethylene backbone have been prepared by reactions of alkali-metal phosphides with partially *N*-

(6) (a) Ito, M.; Osaku, A.; Kitahara, S.; Hirakawa, M.; Ikariya, T. *Tetrahedron Lett.* **2003**, *44*, 7521–7523. (b) Ito, M.; Kitahara, S.; Ikariya, T. *J. Am. Chem. Soc.* **2005**, *127*, 6172–6173. (c) Ito, M.; Osaku, A.; Shiibashi, A.; Ikariya, T. *Org. Lett.* **2007**, *9*, 1821–1824.

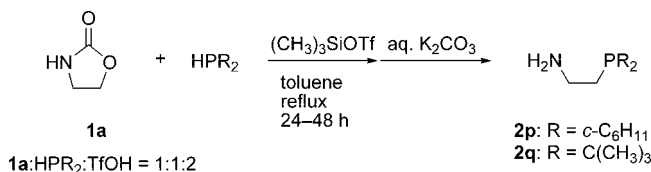
Table 1. Reactions of **1a–m** with Diarylphosphines in the Presence of TfOH

entry	1	R ¹	R ²	HPar ₂	2	yield, %
1	1a	H	H	HP(C ₆ H ₅) ₂	2a	93
2	1b	CH ₃	H	HP(C ₆ H ₅) ₂	2b	95
3	1c	CH ₂ C ₆ H ₅	H	HP(C ₆ H ₅) ₂	2c	80
4	1a	H	H	HP(2-CH ₃ C ₆ H ₄) ₂	2d	49
5	(<i>S</i>)- 1e	H	CH ₃	HP(C ₆ H ₅) ₂	(<i>S</i>)- 2e	80
6	(<i>S</i>)- 1f	H	CH(CH ₃) ₂	HP(C ₆ H ₅) ₂	(<i>S</i>)- 2f	88
7	(<i>S</i>)- 1g	H	CH ₂ CH(CH ₃) ₂	HP(C ₆ H ₅) ₂	(<i>S</i>)- 2g	85
8	(<i>S</i>)- 1h	H	C(CH ₃) ₃	HP(C ₆ H ₅) ₂	(<i>S</i>)- 2h	66
9	(<i>S</i>)- 1i	H	C ₆ H ₅	HP(C ₆ H ₅) ₂	(<i>S</i>)- 2i	70
10	(<i>S</i>)- 1j	H	CH ₂ C ₆ H ₅	HP(C ₆ H ₅) ₂	(<i>S</i>)- 2j	70
11	(<i>S</i>)- 1j	H	CH ₂ C ₆ H ₅	HP(4-CH ₃ C ₆ H ₄) ₂	(<i>S</i>)- 2n	69
12	(<i>S</i>)- 1j	H	CH ₂ C ₆ H ₅	HP{3,5-(CH ₃) ₂ C ₆ H ₃ } ₂	(<i>S</i>)- 2o	66

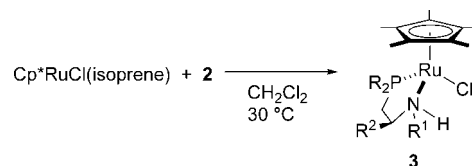
Scheme 3. Possible Reaction Pathway for the Formation of **2a**

protected aminoalkyl halides or pseudohalides as a key step.⁷ However, these methods have certain limitations in synthetic versatility and substrate scope.⁸ One notable side reaction is intramolecular cyclization of partially N-protected aminoalkyl halides induced by the deprotonation of untouched protons on nitrogen with highly basic phosphides to form aziridine derivatives.⁹ In order to preclude this side reaction, we have focused our attention on the acid-promoted degradation of 2-oxazolidinones (**1**),^{10,11} to develop an operationally simple and general synthetic protocol providing a wide variety of chiral P–NH compounds. Herein we describe the details of this novel synthetic method as well as the complexation of the resulting P–NH compounds with the Cp*RuCl fragment.

Our initial screening of acid promoters in the reaction of a 1:1 mixture of 2-oxazolidinone (**1a**) and HP(C₆H₅)₂ in refluxing

Scheme 4. Preparation of 2-(Dialkylphosphino)-1-amines (**2p,q**) from 2-Oxazolidinone (**1a**)

Scheme 5. Preparation of Cp*RuCl(P–NH) Complexes



toluene for 24 h showed that 1.1 equiv of trifluoromethanesulfonic acid (TfOH) promotes the desired decarboxylative C–P bond formation to give a TfOH salt of **2a**, whereas trifluoroacetic acid, montmorillonite K10, AlCl₃, TiCl₄, and BF₃·O(C₂H₅)₂ are not effective promoters under identical conditions. The salt-free **2a** was successfully isolated after treatment with aqueous K₂CO₃ in 28% yield. After optimization of the reaction conditions using TfOH, we found that **2a** is obtainable in reasonably high yield (93%) when the initial molar ratio of **1a**, HP(C₆H₅)₂, and TfOH is set to 1:2:3. It should be noted that the reduction of the amount of HP(C₆H₅)₂ to 1 equiv markedly decreased the product yield (60%). As shown in Scheme 2, the optimized reaction conditions were applicable to the preparation of a variety of P–NH compounds with a diarylphosphino group. The reactions of N-substituted 2-oxazolidinones **1b,c** with HP(C₆H₅)₂ proceeded equally well to furnish the secondary amines **2b,c** in high yields (Table 1, entries 2 and 3). Furthermore, the reaction of **1a** with HP(2-CH₃C₆H₄)₂ afforded the corresponding **2d** in moderate yield (entry 4).

The advantage of the present method was further demonstrated by the preparation of chiral P–NH compounds. A wide variety of chiral 2-oxazolidinones with a stereogenic carbon α to the nitrogen ((*S*)-**1e–m**) afforded the chiral P–NH compounds (*S*)-**2e–m** (entries 5–10), in good to excellent yields.¹² Additionally, the reactions of (*S*)-**1j** with HP(4-CH₃C₆H₄)₂ and HP{3,5-(CH₃)₂C₆H₃}₂ furnished (*S*)-**2n** and (*S*)-**2o** in 69% and 66% yields, respectively (entries 11 and 12). Notably, no measurable loss of optical purity in the products was observed in this process, since (*R*)-**2j** prepared from (*R*)-**1j** showed the specific rotation value of –66 that is opposite in sign to (*S*)-**2j** with +67 (*c* = 1.1, CHCl₃) (see the Supporting Information).

The delicate balance of stoichiometry for the successful C–P bond formation can be explained by the possible mechanism outlined in Scheme 3. Thus, a 3-fold excess of TfOH is required to fully protonate **1a** to generate **1a**·TfOH,¹³ since HP(C₆H₅)₂

(7) (a) Ogata, I.; Mizukami, F.; Ikeda, Y.; Tanaka, M. *Jpn. Kokai Tokkyo Koho* **1976**, 76, 43754; *Chem. Abstr.* **1976**, 85, 124144z. (b) Kashiwabara, K.; Kinoshita, I.; Ito, T.; Fujita, J. *Bull. Chem. Soc. Jpn.* **1981**, 54, 725–732. (c) Hiroi, K.; Abe, J. *Chem. Pharm. Bull.* **1991**, 39, 616–621. (d) Davies, I. W.; Gallagher, T.; Lamont, R. B.; Scopes, D. I. C. *J. Chem. Soc., Chem. Commun.* **1992**, 335–337. (e) Sakuraba, S.; Okada, T.; Morimoto, T.; Achiwa, K. *Chem. Pharm. Bull.* **1995**, 43, 927–934. (f) Kanai, M.; Nakagawa, Y.; Tomioka, K. *Tetrahedron* **1999**, 55, 3843–3854. (g) Saitoh, A.; Uda, T.; Morimoto, T. *Tetrahedron: Asymmetry* **1999**, 10, 4501–4511. (h) Saitoh, A.; Achiwa, K.; Tanaka, K.; Morimoto, T. *J. Org. Chem.* **2000**, 65, 4227–4240.

(8) (a) Christoffers, J. *Helv. Chim. Acta* **1998**, 81, 845–852. (b) Quirnbach, M.; Holz, J.; Tararov, V. I.; Börner, A. *Tetrahedron* **2000**, 56, 775–780. (c) Anderson, J. C.; Cubbon, R. J.; Harling, J. D. *Tetrahedron: Asymmetry* **2001**, 12, 923–935.

(9) For the synthesis of related PN compounds using aziridines, see: (a) Liu, S.-T.; Liu, C.-Y. *J. Org. Chem.* **1992**, 57, 6079–6080. (b) Katagiri, T.; Takahashi, M.; Fujiwara, Y.; Ihara, H.; Uneyama, K. *J. Org. Chem.* **1999**, 64, 7323–7329. (c) Dahlsburg, L.; Götz, R. *J. Organomet. Chem.* **2001**, 619 (2), 88–98. (d) Caiazzo, A.; Dalili, S.; Yudin, A. K. *Org. Lett.* **2002**, 4, 2597–2600. (e) Krauss, I. J.; Leighton, J. L. *Org. Lett.* **2003**, 5, 3201–3203. (f) Kawamura, K.; Fukuzawa, H.; Hayashi, M. *Org. Lett.* **2008**, 10, 3509–3512.

(10) (a) Joutteau, C.; Le Perche, P.; Forestière, A.; Sillion, B. *Tetrahedron Lett.* **1980**, 21, 1719–1722. (b) Poindexter, G. S.; Owens, D. A.; Dolan, P. L.; Woo, E. J. *Org. Chem.* **1992**, 57, 6257–6265.

(11) For the related base-promoted 2-aminoethylation of thiols, see: (a) Ishibashi, H.; Uegaki, M.; Sakai, M. *Synlett* **1997**, 915–916. (b) Ishibashi, H.; Uegaki, M.; Sakai, M.; Takeda, Y. *Tetrahedron* **2001**, 57, 2115–2120.

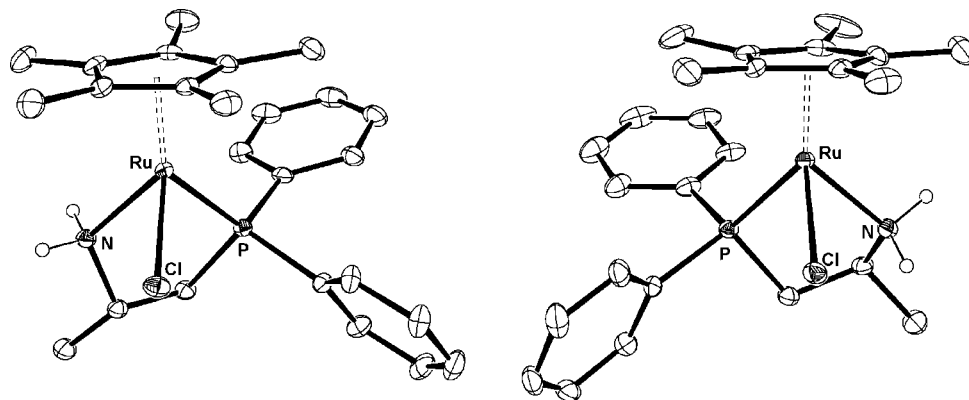


Figure 1. Molecular structures of **3e** composed of S_{Ru},S_C (left) and R_{Ru},S_C (right) configurations. Hydrogens, except those on N, are omitted for clarity.

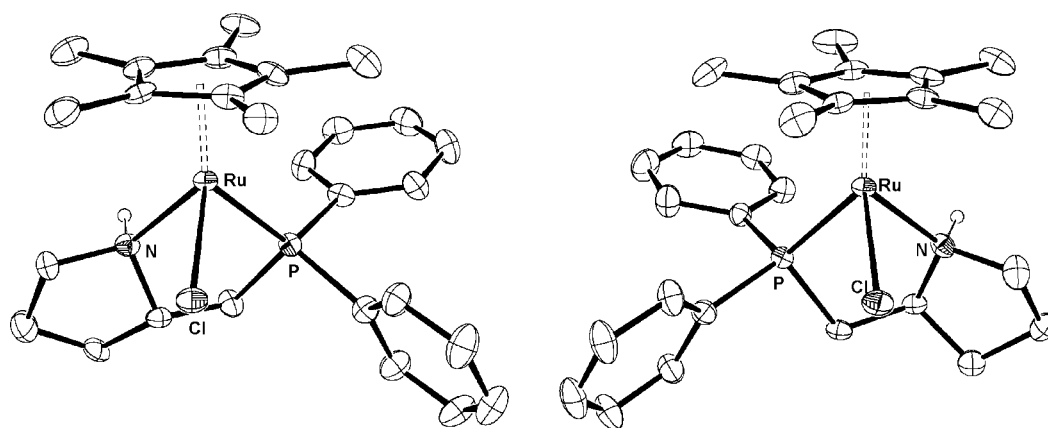


Figure 2. Molecular structures of **3k** composed of S_{Ru},R_N,S_C (left) and R_{Ru},S_N,S_C (right) configurations. Hydrogens, except those on N, are omitted for clarity.

possibly serves as a competing proton acceptor. Also, a 2-fold excess of $HP(C_6H_5)_2$ is necessary to maintain a sufficient concentration of the nonprotonated molecules, which undergo nucleophilic attack at the 5-position of **1a**·TfOH, thereby allowing the subsequent release of CO_2 to produce **2a**·TfOH.

Unfortunately, the optimized stoichiometry was not effective for the reaction of dialkylphosphines, possibly due to their stronger Brønsted basicity compared to that of diarylphosphines.^{14,15} Nevertheless, the similar C–P bond forming process between **1a** and dialkylphosphines was realized when $(CH_3)_3SiOTf$ was used in place of TfOH. As shown in Scheme 4, the reaction of a 1:1 mixture of **1a** and $HP(c-C_6H_{11})_2$ or $HP[C(CH_3)_3]_2$ in refluxing toluene containing 2 equiv of $(CH_3)_3SiOTf$ for 24–48 h furnished **2p,q** in 23 and 13% yields, respectively. These results indicate that the highly oxophilic nature of $(CH_3)_3SiOTf$ allows selective electrophilic activation of **1a** in preference to dialkylphosphines.

As we reported previously,^{5b} a mononuclear Cp^*RuCl (isoprene) complex reacted smoothly with P–NH compounds (**2**) in CH_2Cl_2 , yielding the corresponding pseudotetrahedral Cp^*RuCl (P–NH) (**3**) bearing a primary or secondary NH group (Scheme 5). In principle, the unsymmetrical structure of P–NH compounds inevitably induces a new stereogenic center at the Ru center upon complexation with a Cp^*RuCl fragment.¹⁶ Since complexes **3b,c** with a secondary amine ligand have a stereogenic center at the N atoms and complexes **3e–j** with a primary amine ligand have a stereogenic center at the configurationally fixed carbons, they could be a mixture of two diastereomeric complexes, depending on the absolute configuration at the Ru center. Indeed, an X-ray diffraction study of the single crystals

of **3e** revealed that it exists in the solid state as two crystallographically independent molecules with different absolute configurations¹⁷ of S_{Ru},S_C and R_{Ru},S_C , as shown in Figure 1. However, the CD_2Cl_2 solution of complex **3b** exhibited only a single peak at 62.2 ppm and those of the complexes **3e–j** also showed a single peak around 55–60 ppm in the $^{31}P\{^1H\}$ NMR at 30 °C. These results suggest that the stereogenic Ru center in **3a–j** might retain its configuration, at least in the solid state, but epimerizes¹⁸ readily in solution to converge into the more thermodynamically stable diastereomer.^{19,20}

On the other hand, more confusing stereochemical behavior was observed when the chiral nonracemic ligands (*S*)-**2k,m** with a secondary amino group were used in the complexation. Since **3k** with a pyrrolidine ring and **3m** with a piperidine ring have two stereogenic centers at both the Ru and N atoms in addition to the configurationally fixed carbons, they can be a mixture of four diastereomeric complexes. However, the $^{31}P\{^1H\}$ NMR spectrum of **3k** in CD_2Cl_2 showed only two signals at 59.6 and 61.8 ppm with an intensity of 1:1 that did not change in the temperatures range from –90 to 30 °C. Also, an X-ray diffraction study of the single crystal of **3k** revealed that it is composed of two crystallographically independent molecules with absolute configurations of S_{Ru},R_N,S_C and R_{Ru},S_N,S_C , as shown in Figure 2. Therefore, only two stereoisomers were preferentially formed among four possible diastereomers in the formation of **3k**, possibly due to the configurational lability either of the Ru or N atom, but the stereomutation between these two complexes should require sufficiently high energy even in solution to allow the observation of two independent signals in the $^{31}P\{^1H\}$ spectra.

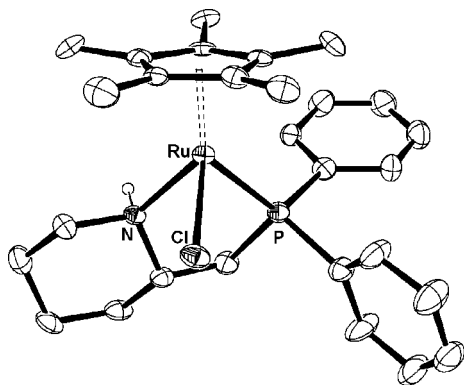


Figure 3. Molecular structure of **3m**. Hydrogens, except those on N, are omitted for clarity.

In contrast, the $^{31}\text{P}\{^1\text{H}\}$ NMR spectrum of **3m** in CD_2Cl_2 showed only one signal at 55.0 ppm, and its solid-state structure determined by X-ray diffraction revealed that it consists of only one stereoisomer with $S_{\text{Ru}}, R_{\text{N}}, S_{\text{C}}$ configuration (Figure 3).

These results led us to conclude that the stereogenic centers at the nitrogen and carbon atoms alone do not inhibit the epimerization at the Ru center in solution and hence the absolute configuration in the solid state should be determined during the course of crystallization by subtle intramolecular interactions, although a synergistic combination of multiple stereogenic elements occasionally retards the epimerization at the Ru center in solution, as in the case of **3k**. The configurational flexibility of the Ru centers in the $\text{Cp}^*\text{RuCl}(\text{P}-\text{NH})$ complexes may be attributed to the ease of ionic dissociation of their Ru-Cl bonds, which is in accord with the very long bond lengths (**3e**, 2.4918(8) Å; **3k**, 2.470(2) and 2.489(2) Å; **3m**, 2.4881(18) Å). Also, it should be noted that the chiral complex **3k** serves as an excellent catalyst upon treatment with $\text{KO}-t\text{-Bu}$ for asymmetric reactions, including the isomerization of allylic alcohols^{6b} as well as hydrogenation of symmetrical glutarimides,^{5c} despite the fact that **3k** is composed of a mixture of diastereomeric molecules both in solution and in the solid state. Therefore, it will be the subject for a further study to elucidate the stereochemistry of catalytically active species^{16c,21} derived from **3k** and other chiral complexes in these asymmetric catalytic processes.²²

In summary, we have developed a convenient method for the preparation of P-NH compounds starting from readily available 2-oxazolidinones. These compounds readily afforded the corresponding $\text{Cp}^*\text{RuCl}(\text{P}-\text{NH})$ complexes, which constitute a new family of chiral half-sandwich type Ru complexes with a stereogenic Ru.¹⁶ Studies on the catalytic performance of these new complexes in our recently developed asymmetric reactions are underway and will be reported in due course.

Acknowledgment. This research was supported by the MEXT (Nos. 16750073 and 18065017 “Chemistry of Con-

certo Catalysis”) and by the Asahi Glass Foundation (M.I.). This work was partly supported by the 21 Century COE Program. We are grateful to Prof. Takayuki Doi and the personnel at the Tokyo Institute of Technology for the mass spectrometric analysis.

Supporting Information Available: Text giving experimental procedures and CIF files giving X-ray crystallographic data for **3e, k, m**. This material is available free of charge via the Internet at <http://pubs.acs.org>.

OM801042B

(15) A toluene- d_8 solution of a 1:1 mixture of $\text{HP}(\text{C}_6\text{H}_5)_2$ and TfOH showed a very broad signal centered at -22 ppm in the $^{31}\text{P}\{^1\text{H}\}$ NMR spectrum at 70 °C, while a similar experiment with $\text{HP}(\text{C}-\text{C}_6\text{H}_{11})_2$ showed a quintet at -3.5 ppm with the coupling constant $^1J_{\text{PD}} = 73$ Hz. Since the formation of TfOD by rapid H-D scrambling between toluene- d_8 and TfOH likely precedes the salt formation, the former may indicate an equilibrium between $\text{DP}(\text{C}_6\text{H}_5)_2$ and $[\text{D}_2\text{P}(\text{C}_6\text{H}_5)_2]\text{OTf}$ but the latter may suggest the irreversible formation of $[\text{D}_2\text{P}(\text{C}-\text{C}_6\text{H}_{11})_2]\text{OTf}$.

(16) (a) Brunner, H. *Acc. Chem. Res.* **1979**, *12*, 250–257. (b) Brunner, H. *Adv. Organomet. Chem.* **1980**, *18*, 151–205. (c) Consiglio, G.; Morandini, F. *Chem. Rev.* **1987**, *87*, 761–778. (d) Brunner, H. *Angew. Chem., Int. Ed.* **1999**, *38*, 1194–1208. (e) Ganter, C. *Chem. Soc. Rev.* **2003**, *32*, 130–138.

(17) (a) Sloan, T. E. *Top. Stereochem.* **1981**, *12*, 1–36. (b) Stanley, K.; Baird, M. C. *J. Am. Chem. Soc.* **1975**, *97*, 6598–6599. (c) Cahm, R. S.; Ingold, C.; Prelog, V. *Angew. Chem., Int. Ed. Engl.* **1966**, *5*, 385–415.

(18) (a) Consiglio, G.; Morandini, F.; Bangerter, F. *Inorg. Chem.* **1982**, *21*, 455–457. (b) Morandini, F.; Consiglio, G.; Straub, B.; Ciani, G.; Sironi, A. *J. Chem. Soc., Dalton Trans.* **1983**, 2293–2298. (c) Ganter, C.; Brassat, L.; Glinzböckel, C.; Ganter, B. *Organometallics* **1997**, *16*, 2862–2867. (d) Nishibayashi, Y.; Takei, I.; Hidai, M. *Organometallics* **1997**, *16*, 3091–3093. (e) Koelle, U.; Rietmann, C.; Raabe, G. *Organometallics* **1997**, *16*, 3273–3281. (f) Brunner, H.; Neuhierl, T.; Nuber, B. *J. Organomet. Chem.* **1998**, *563*, 173–178. (g) van der Zeeijden, A. A. H.; Jimenez, J.; Matthes, C.; Wagner, C.; Merzweiler, K. *Eur. J. Inorg. Chem.* **1999**, 1919–1930. (h) Slugovc, C.; Simanko, W.; Mereiter, K.; Schmid, R.; Kirchner, K.; Xiao, L.; Weissensteiner, W. *Organometallics* **1999**, *18*, 3865–3872. (i) Trost, B. M.; Vidal, B.; Thommen, M. *Chem. Eur. J.* **1999**, *5*, 1055–1069. (j) Onitsuka, K.; Ajioka, Y.; Matsushima, Y.; Takahashi, S. *Organometallics* **2001**, *20*, 3274–3282. (k) Brunner, H.; Muschiol, M.; Tsuno, T.; Takahashi, T.; Zabel, M. *Organometallics* **2008**, *27*, 3514–3525.

(19) (a) Cesarotti, E.; Chiesa, A.; Ciani, G. F.; Sironi, A.; Vefghi, R.; White, C. *J. Chem. Soc., Dalton Trans.* **1984**, 653–661. (b) Consiglio, G.; Morandini, F. *Inorg. Chim. Acta* **1987**, *127*, 79–85. (c) Kataoka, Y.; Saito, Y.; Nagata, K.; Kitamura, K.; Shibahara, A.; Tani, K. *Chem. Lett.* **1995**, 833–834. (d) Koelle, U.; Bücken, K.; Englert, U. *Organometallics* **1996**, *15*, 1376–1383. (e) Rasley, B. T.; Rapta, M.; Kulawiec, R. *J. Organometallics* **1996**, *15*, 2852–2854.

(20) The $^{31}\text{P}\{^1\text{H}\}$ NMR measurements for **3e** at lower temperature (–90 °C) allowed the observation of a minor signal at higher field with respect to the major signal with an intensity of 10%, which gradually diminished to 0% as the temperature was raised to 30 °C. These results support the notion that the two possible diastereomers are readily interconvertible and the Ru-centered chirality of **3e** in CD_2Cl_2 is very labile.

(21) Consiglio, Morandini, and co-workers thoroughly investigated the stereochemistry of some ligand substitution for a series of $\text{CpRu}[(R)-(\text{C}_6\text{H}_5)_2\text{PCH}(\text{CH}_3)\text{CH}_2\text{P}(\text{C}_6\text{H}_5)_2]$ complexes: (a) Consiglio, G.; Morandini, F.; Ciani, G.; Sironi, A. *Angew. Chem., Int. Ed. Engl.* **1983**, *22*, 333–334. (b) Consiglio, G.; Morandini, F.; Ciani, G.; Sironi, A.; Kretschmer, M. *J. Am. Chem. Soc.* **1983**, *105*, 1391–1392. (c) Morandini, F.; Consiglio, G.; Lucchini, V. *Organometallics* **1985**, *4*, 1202–1208. (d) Consiglio, G.; Bangerter, F.; Morandini, F. *J. Organomet. Chem.* **1985**, *293*, C29–C32. (e) Consiglio, G.; Morandini, F.; Sironi, A. *J. Organomet. Chem.* **1986**, *306*, C45–C48. (f) Consiglio, G.; Morandini, F. *J. Organomet. Chem.* **1986**, *310*, C66–C68. (g) Morandini, F.; Consiglio, G.; Sironi, A. *Gazz. Chim. Ital.* **1987**, *117*, 61–63.

(22) By a similar method reported previously,^{5b} the treatment of the chloride complex **3e** (103 mg, 0.20 mmol) with KOH (11.0 mg, 0.30 mmol) in 2-propanol (5.0 mL) afforded a novel Cp^*RuH complex bearing (S)-**2e** (82.0 mg, 85% yield) as a diastereomeric mixture in an approximately 1:1 ratio, which was determined by their hydride signals at –10.6 ppm (d, $^2J_{\text{PH}} = 40.3$ Hz) and –9.9 ppm (d, $^2J_{\text{PH}} = 37.5$ Hz) in ^1H NMR (THF- d_6). This result contrasts remarkably with the stereospecificity observed in the conversion of $\text{CpRuCl}[(R)-(\text{C}_6\text{H}_5)_2\text{PCH}(\text{CH}_3)\text{CH}_2\text{P}(\text{C}_6\text{H}_5)_2]$ to $\text{CpRuH}[(R)-(\text{C}_6\text{H}_5)_2\text{PCH}(\text{CH}_3)\text{CH}_2\text{P}(\text{C}_6\text{H}_5)_2]$ with methanolic CH_3ONa .^{21c}

(12) The substituents at the 5-position in 2-oxazolidinones seem to inhibit the efficient C-P bond-forming process; 5-methyl-, 5-phenyl-, 5,5-dimethyl-, and 5,5-diphenyl-2-oxazolidinones did not afford any product under these conditions.

(13) (a) Olah, G. A.; Heiner, T.; Rasul, G.; Prakash, G. K. S. *J. Org. Chem.* **1998**, *63*, 7993–7998. (b) Olah, G. A.; Calin, M. *J. Am. Chem. Soc.* **1968**, *90*, 401–404. (c) Armstrong, V. C.; Moodie, R. B. *J. Chem. Soc. B* **1968**, 275–277. (d) Remko, M. *Collect. Czech. Chem. Commun.* **1988**, *53*, 1141–1148.

(14) Henderson, W. A., Jr.; Streuli, C. A. *J. Am. Chem. Soc.* **1960**, *82*, 5791–5794.

Nitroso Compounds Serve as Precursors to Late-Metal $\eta^2(N,O)$ -Hydroxylamido Complexes

Ryan L. Holland and Joseph M. O'Connor*

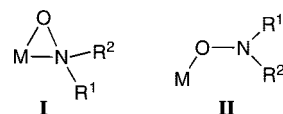
Department of Chemistry and Biochemistry 0358, University of California, San Diego, La Jolla, California 92093-0358

Received November 19, 2008

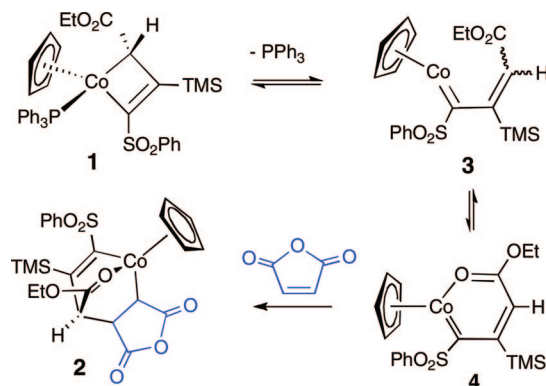
Summary: The metallacyclobutene complex $(\eta^5-C_5H_5)(PPh_3)Co\{\kappa^2(C^1,C^3)-C(SO_2Ph)=C(SiMe_3)CH(CO_2Et)\}$ undergoes a regio- and stereoselective reaction with both nitrosobenzene and 2-methyl-2-nitrosopropane to give ring-expanded metallacycles with an $\eta^2(N,O)$ -hydroxylamido ligand. These transformations represent a new synthetic route toward late-metal $\eta^2(N,O)$ -hydroxylamido complexes.

N,N-Dialkylhydroxylamido complexes, **I** and **II**, are intriguing intermediates that may prove useful for the formation of highly functionalized organic compounds (Chart 1).¹ Both monodentate and bidentate coordination to transition metals have been observed, with early metals more often adopting η^2 bonding (**I**)^{2,3} and late metals typically adopting κ^1 bonding (**II**).^{4–7} Of particular interest for potential synthetic applications are the less oxophilic late-metal hydroxylamido complexes. The most common synthetic routes toward late-metal hydroxylamido complexes employ preformed nitroxyl⁵ or hydroxylamine⁶ reagents. The development of late-metal hydroxylamido chemistry would be facilitated by new methods for the preparation of $\eta^2(N,O)$ -*N,N*-dialkylhydroxylamido complexes which contain two different alkyl groups bound to nitrogen. Here we report the first syntheses of late-metal $\eta^2(N,O)$ -*N,N*-dialkylhydroxylamido com-

Chart 1. $\eta^2(N,O)$ - and $\kappa^1(O)$ -Hydroxylamido Coordination



Scheme 1. Mechanistic Speculation for the Conversion of **1** and Maleic Anhydride to **2**¹⁰



plexes via a formal insertion of nitroso compounds into a metal–carbon bond.^{8,9}

We recently reported the reaction of the cobaltacyclobutene complex $(\eta^5-C_5H_5)(PPh_3)Co\{\kappa^2(C^1,C^3)-C(SO_2Ph)=C(SiMe_3)-CH(CO_2Et)\}$ (**1**) with maleic anhydride to give metallacyclohexene products (**2**, Scheme 1).¹⁰ The observed selectivity for reaction at C(3) in preference to C(1) of the metallacycle contrasts with the reactions of **1** with carbon monoxide, ethyl diazoacetate, and isonitriles, all of which undergo coupling at the Co–C(1) bond to form vinylketene, vinylketenimine, and 1,3-diene products.¹¹ In principle, all four reactions of **1** could proceed via the vinylcarbene intermediate **3** (Scheme 1).¹² Reaction of **3** with CO, isocyanides, and carbenes would involve substrate coordination to cobalt followed by coupling to the carbene ligand. In the case of maleic anhydride, a [4 + 2]

* To whom correspondence should be addressed. E-mail: jmoconnor@ucsd.edu.

(1) Complexes with the connectivity shown for **I** and **II** are also referred to in the literature as “hydroxylaminato”, “hydroxylamino”, “nitroxide”, and “nitroxyl” complexes. The last two terms typically are used for paramagnetic complexes. Nitroxyl also refers to HN=O.

(2) For leading references to early-metal κ^1 -hydroxylamido complexes: (a) Kraft, B. M.; Huang, K.-W.; Cole, A. P.; Waymouth, R. M. *Helv. Chim. Acta* **2006**, *89*, 1589. (b) Rehder, D.; Jaitner, P. *J. Organomet. Chem.* **1987**, *329*, 337.

(3) For leading references to early-metal η^2 -hydroxylamido complexes: (a) Smee, J. J.; Epps, J. A.; Teissedre, G.; Maes, M.; Harding, N.; Yang, L.; Baruah, B.; Miller, S. M.; Anderson, O. P.; Willsky, G. R.; Crans, D. C. *Inorg. Chem.* **2007**, *46*, 9827. (b) Dove, A. P.; Xie, X.; Waymouth, R. M. *Chem. Commun.* **2005**, 2152. (c) Wiegardt, K.; Quilitzsch, U.; Nuber, B.; Weiss, J. *Angew. Chem., Int. Ed.* **1978**, *17*, 351.

(4) Late-metal κ^1 -nitroxyl complexes often display interesting magnetic properties: (a) Sessoli, R. *Angew. Chem., Int. Ed.* **2008**, *47*, 5508, and references therein. (b) Ishii, N.; Okamura, Y.; Chiba, S.; Nogami, T.; Ishida, T. *J. Am. Chem. Soc.* **2008**, *130*, 24.

(5) For leading references to late-metal η^2 -hydroxylamido complexes prepared from nitroxyl radicals: (a) Mindiola, D. J.; Waterman, R.; Jenkins, D. M.; Hillhouse, G. L. *Inorg. Chim. Acta* **2003**, *345*, 299. (b) Laugier, J.; Latour, J. M.; Caneschi, A.; Rey, P. *Inorg. Chem.* **1991**, *30*, 4474.

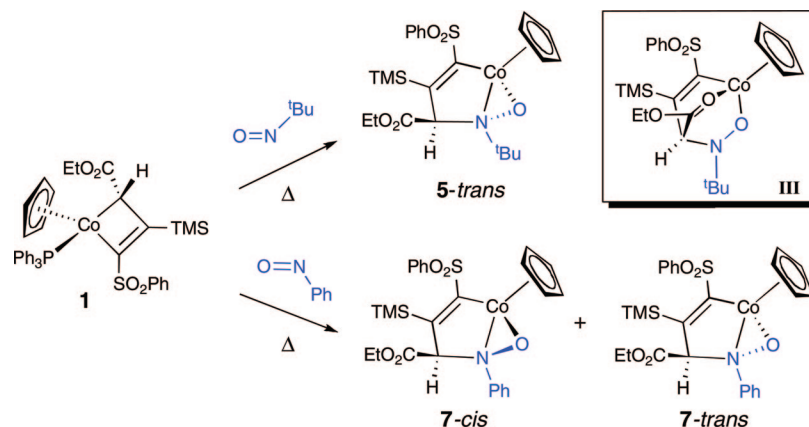
(6) For leading references to late-metal η^2 -hydroxylamidoximes prepared from hydroxylamines: (a) Vogel, S.; Huttner, G.; Zsolnai, L.; Emmerich, C. *Z. Naturforsch.* **1993**, *48b*, 353. (b) Middleton, A. R.; Thornback, J. R.; Wilkinson, G. *J. Chem. Soc., Dalton Trans.* **1980**, 174.

(7) For a late-metal η^2 -hydroxylamido complex prepared from a metal nitrosyl complex: Kura, S.; Kuwata, S.; Ikariya, T. *Angew. Chem., Int. Ed.* **2005**, *44*, 6406.

(8) Nitroso insertions into early-transition-metal–carbon bonds have been observed: (a) Erker, G.; Humphrey, M. G. *J. Organomet. Chem.* **1989**, *378*, 163. (b) Doxsee, K. M.; Juliette, J. J.; Weakley, T. J. R.; Zientara, K. *Inorg. Chim. Acta* **1994**, *222*, 305. (c) Nakamoto, M.; Tilley, T. D. *Organometallics* **2001**, *20*, 5515. (d) Cummings, S. A.; Radford, R.; Erker, G.; Kehr, G.; Fröhlich, R. *Organometallics* **2006**, *25*, 839.

(9) The reactions of nitroso compounds with aromatic iridacycles give addition products without ring expansion: Bleeke, J. R. *Acc. Chem. Res.* **2007**, *40*, 1035. Bleeke, J. R.; Behm, R.; Xie, Y.-F.; Chiang, M. Y.; Robinson, K. D.; Beatty, A. M. *Organometallics* **1997**, *16*, 606. Bleeke, J. R.; Blanchard, J. M. B.; Donnay, E. *Organometallics* **2001**, *20*, 324. Bleeke, J. R.; Hinkle, P. V.; Rath, N. P. *Organometallics* **2001**, *20*, 1939.

(10) Complex **2** was formed as both endo and exo products: Holland, R. L.; Bunker, K. D.; Chen, C. H.; DiPasquale, A. G.; Rheingold, A. L.; Baldrige, K. K.; O'Connor, J. M. *J. Am. Chem. Soc.* **2008**, *130*, 10093.

Scheme 2. Formation of $\eta^2(N,O)$ -*N,N*-Dialkylhydroxylamido Complexes from **1** and Nitroso Reagents

cycloaddition reaction involving **3** or oxametallacycle **4** would lead directly to metallacyclohexene **2**. In this respect, **3** and **4** may be viewed as “metalladiene” participants in a Diels–Alder reaction with activated alkenes. This speculation has now led us to examine the reactions of **1** with the classic heterodienophiles nitrosobenzene and 2-methyl-2-nitrosopropane. In both cases the nitroso compounds undergo regioselective coupling to C(3) of the metallacycle and formation of ring-expanded metallacycles which contain an $\eta^2(N,O)$ -*N,N*-dialkylhydroxylamido ligand.

A toluene solution (25 mL) of metallacycle **1** (245 mg, 0.35 mmol) and excess 2-methyl-2-nitrosopropane dimer (0.66 mmol) was heated under a nitrogen atmosphere at 70 °C for 4 h, followed by chromatography on silica gel (35% ethyl acetate/hexanes), to provide **5-trans** as a dark burgundy powder in 83% yield (Scheme 2). Analytically pure **5-trans** was obtained by recrystallization from chloroform/hexanes. In the ¹H NMR (CDCl₃) spectrum of **5-trans**, singlets were observed at δ 4.93 (C₅H₅) and 4.08 (CHCO₂Et). Both resonances were significantly downfield of the corresponding signals for **1** (δ 4.20 (C₅H₅), 1.43 (d, $J_{\text{PH}} = 7.0$ Hz, CHCO₂Et)) and appeared at chemical shift values very similar to those observed for metallacyclohexene **2** (δ 5.02 (C₅H₅), 4.05 (d, $J_{\text{HH}} = 4.2$ Hz, CHCO₂Et)). In the ¹³C{¹H} NMR spectrum (CDCl₃) of **5-trans**, the carbon bearing the ester substituent was observed at δ 80.6 (CHCO₂Et), which is substantially downfield of the δ 49.6 (CHCO₂Et) resonance observed for the corresponding carbon in **2**. In the

IR spectrum (thin film) of **5-trans**, a strong $\nu(\text{C}=\text{O})$ stretch was observed at 1748 cm⁻¹, which is at much higher frequency than that observed for **2** (1638 cm⁻¹). Thus, the spectroscopic data for **5-trans** suggested that nitroso coupling to C(3) had occurred, but the data were inconsistent with the anticipated structure **III** (Scheme 2).

A single-crystal X-ray diffraction study on **5-trans** confirmed that the ester oxygen was not chelating and revealed a much different type of bicyclic structure, with $\kappa^1(\text{C})-\eta^2(\text{N},\text{O})$ coordination to cobalt (Figure 1, Table S1 (Supporting Information)).¹³ The relative stereochemistry at the cobalt, nitrogen, and carbon stereocenters is *S*^{Co}*S*^N*R*^C, *R*^{Co}*R*^N*S*^C, with O(1) and the ester substituent C(13) located on opposite faces of the five-membered azametallacycle defined by (Co, C(1), C(2), C(3), N). The trans relationship for the ester substituent and O(1) is reflected in a C(13)–C(3)–N(1)–O(1) dihedral angle of 172.95(0.12)°. The fold angle between the Co–N(1)–O(1) and C(1)–Co–N(1) planes is 87.37(5)°, and the largest deviations of ring atoms from the C(1)–Co–N(1) plane are 0.150(2) Å for C(2), 0.410(2) for C(3), and –1.289(1) for O(1). The quaternary carbon of the *tert*-butyl substituent, C(16), is displaced only 0.207(2) Å from the C(1)–Co–N(1) plane.

To our knowledge, **5-trans** is the first cobalt(III)- $\eta^2(N,O)$ -hydroxylamido complex and the only example of an $\eta^2(N,O)$ -hydroxylamido group which is incorporated into a [3.1.0] fused-ring framework. The constraints of this bicyclic structure cause significant perturbations on the geometry at N(1). The

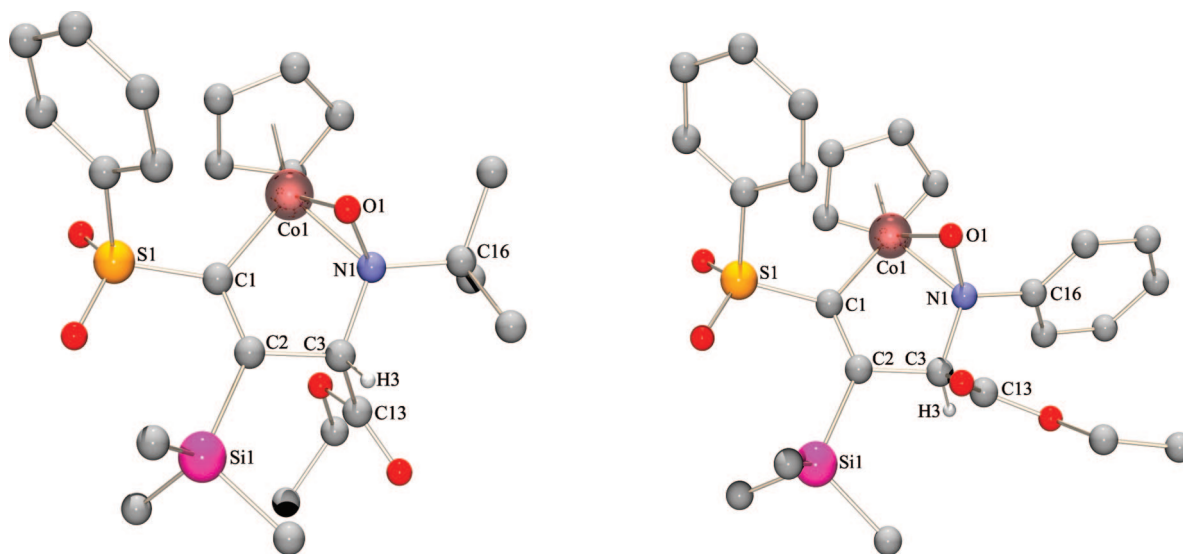
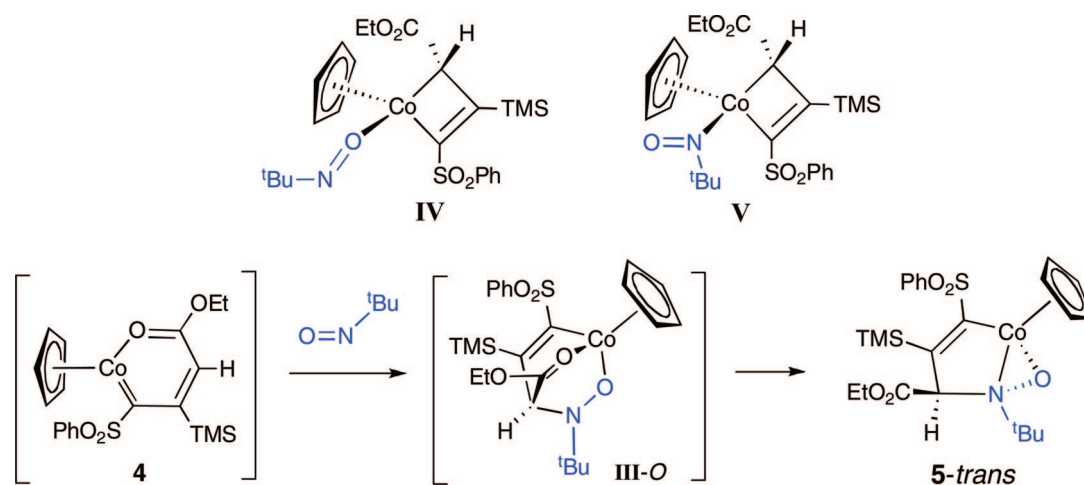


Figure 1. Solid-state structures of **5-trans** (left) and **7-cis** (right). For clarity, H(3) is the only hydrogen atom shown.

Scheme 3. Mechanistic Speculation for the Formation of *5-trans* from **1** and Nitroso Compounds

Co–N(1)–O angle is constrained to 68.4(1)° by the three-membered ring, the Co–N(1)–C(3) angle is constrained to 111.51(10)° by the five-membered ring, and the Co–N(1)–C(16) angle is opened up to 127.6(1)°. The corresponding Co–N–C angles in the cobalt(I) complex (triphos)Co{ $\eta^2(N,O)$ -Me₂NO} (**6**; triphos = 1,1,1-tris(diphenylphosphinomethyl)ethane)^{6a} are 121.5(5) and 122.7(4)°. The Co–N and N–O bond distances in **6** are similar to the 1.917(1) and 1.388(2) Å distances in *5-trans*; however, the 1.908(1) Å Co–O(1) bond distance in *5-trans* is significantly longer than the 1.854(4) Å distance observed in **6**. For comparison the Co–N and N–O bond distances in the $\kappa^1(N)$ -nitroso complex (η^5 -C₅H₅)(PPh₃)Co{ $\kappa^1(N)$ -N(=O)CH₃} are 1.7822(16) and 1.2846(19) Å, respectively.¹⁴

The nature of the nitroso reagent has a dramatic effect on the diastereoselectivity observed for the reactions of **1**. Heating a toluene solution (25 mL) of **1** (0.37 mmol) and excess nitrosobenzene (1.27 mmol) at 70 °C leads to the formation and isolation of an 8:1 mixture of *7-cis* and *7-trans*, in 71% combined yield. The structure of the minor isomer, *7-trans*, was tentatively assigned on the basis of the ¹H NMR spectral data, by comparison to those for *5-trans*. Specifically, in the ¹H NMR spectrum (CDCl₃) of the minor isomer, singlets are observed at δ 4.78 (C₅H₅) and 3.90 (CHCO₂Et), which are chemical shift values similar to those observed for *5-trans* (δ 4.93 (5H) and 4.08 (1H)). In contrast, the major isomer, *7-cis*, exhibits resonances in the ¹H NMR spectrum (CDCl₃) at δ 4.48 (C₅H₅) and 5.23 (CHCO₂Et). Attempts to separate the two isomers by chromatography and recrystallization failed, and extended heating at 70 °C led to eventual decomposition of the compounds without evidence for a change in the 8:1 cis:trans ratio. An analytically pure sample of the mixture was obtained by

recrystallization from chloroform/hexanes, and an X-ray diffraction study was carried out on a crystal of *7-cis* (Figure 1, Table S1). The structural data for *7-cis* revealed a bicyclic structure with $\kappa^1(C)$ - $\eta^2(N,O)$ coordination to cobalt, as was observed for *5-trans*, but with the ester substituent and O(1) on the same face of the five-membered azametallacycle ring. The cis relationship of the ester substituent and O(1) leads to a C(13)–C(3)–N(1)–O(1) dihedral angle of –62.80(0.23)°. The *ipso* carbon of the phenyl substituent, C(16), is displaced only –0.354(2) Å from the C(1)–Co–N(1) plane. The relative stereochemistry at the cobalt, nitrogen, and carbon stereocenters is *S*^{Co}*S*^N*S*^C, *R*^{Co}*R*^N*R*^C. With the exception of a 6.8° smaller Co–N(1)–C(16) angle in *7-cis* and the difference in stereochemistry at C(3), the bond distance and angle data for *7-cis* are very similar to those observed for *5-trans* (Table S1).

In the case of **1**, the available data do not allow us to distinguish between a traditional metallacycle insertion mechanism, involving intermediates such as **IV** and **V**, from a [4 + 2] cycloaddition reaction involving the nitroso compound and intermediate **4** (Scheme 3).¹⁵ Regardless of the mechanism, it is becoming clear that, for the late-metal metallacyclobutene **1**, one-atom addends (CO, carbenes, and isocyanides)¹¹ exhibit selective coupling at the Co–C(sp²) bond, whereas two-atom cycloaddends (alkenes,¹⁰ nitroso compounds, and possibly alkynes^{11c}) exhibit selective coupling at the Co–C(sp³) bond. Efforts are underway to elucidate the factors that control the diastereoselectivity observed for *5-trans* and *7-cis* and to extend this novel reaction chemistry to acyclic late-metal alkyl and vinyl complexes.

Acknowledgment. Financial support by the National Science Foundation (Grant No. CHE-0518707 and instrumentation Grant Nos. CHE-9709183, CHE-0116662, and CHE-0741968) is gratefully acknowledged.

Supporting Information Available: Text, figures, and tables giving synthesis details, characterization data, and crystallographic data. This material is available free of charge via the Internet at <http://pubs.acs.org>.

OM801105X

(11) (a) O'Connor, J. M.; Ji, H.; Iranpour, M.; Rheingold, A. L. *J. Am. Chem. Soc.* **1993**, *115*, 1586. (b) O'Connor, J. M.; Ji, H.-L.; Rheingold, A. L. *J. Am. Chem. Soc.* **1993**, *115*, 9846. (c) O'Connor, J. M.; Fong, B. S.; Ji, H.-L.; Hiibner, K.; Rheingold, A. L. *J. Am. Chem. Soc.* **1995**, *117*, 8029. (d) O'Connor, J. M.; Chen, M.-C.; Frohn, M.; Rheingold, A. L.; Guzei, I. A. *Organometallics* **1997**, *16*, 5589. (e) O'Connor, J. M.; Chen, M.-C.; Rheingold, A. L. *Tetrahedron Lett.* **1997**, *38*, 5241.

(12) A model structure for intermediate **4**, (η^5 -C₅H₅)Co{ $\kappa^2(C,O)$ -C(SO₂Me)C(SiH₃)CH(CO₂Me)}, has been studied using quantum-mechanical methods, and the electrostatic potential map indicates relatively high charge density at the CH ring carbon.¹⁰

(13) The reactions of nitroso compounds with early-transition-metal metallacyclobutenes also leads to insertion into the metal–carbon (sp³) bond, but the ring-expanded product does not engage in metal–nitrogen bonding.^{8b}

(14) O'Connor, J. M.; Bunker, K. D. *Organometallics* **2003**, *22*, 5268.

(15) We are also unable to rule out associative mechanisms. Attempts at kinetic studies were unsuccessful due to the reaction of the nitroso compounds with triphenylphosphine.

Articles

Unprecedented π -Bonded Rhodio- and Iridio-*o*-Benzoquinones as Organometallic Linkers for the Design of Chiral Octahedral Bimetallic Assemblies

Jamal Moussa,[†] Marie Noelle Rager,[‡] Lise Marie Chamoreau,[†] Louis Ricard,[§] and Hani Amouri^{*†}

Laboratoire de Chimie Inorganique et Matériaux Moléculaires, UMR 7071, Université Pierre et Marie Curie-Paris 6, case 42, UPMC 4 Place Jussieu 75252 Paris Cedex 05, France, NMR Facility of Ecole Nationale Supérieure de Chimie de Paris, 11 Rue Pierre et Marie Curie, 75231 Paris Cedex 05, France, and Laboratoire Hétéroéléments et Coordination, Ecole Polytechnique, CNRS UMR 7653, 91128 Palaiseau Cedex, France

Received June 26, 2008

We report the first synthesis of π -bonded rhodio and iridio-*o*-benzoquinones [Cp*M(*o*-benzoquinone)] (M = Rh (**3a**); M = Ir (**3b**)) following a novel synthetic procedure. These compounds were fully characterized by spectroscopic methods; in particular the X-ray molecular structure of **3b** was determined. Compounds **3a,b** were used as chelating *organometallic linkers* for the design of a new family of chiral octahedral bimetallic complexes, **4–9**. The X-ray molecular structure of [(bpy)₂Ru(**3b**)](OTf)₂ (**5**) is presented and shows that the *organometallic linker 3b* is chelating the ruthenium center. In particular, the carbocycle of the *organometallic linker 3b* adopts a η^4 -quinone form, where the Cp*Ir is also bonded to only four carbons. Further our strategy to design new assemblies with organometallic linkers is successfully achieved. These assemblies hold promise for new properties relative to those made from organic bidentate ligands.

Introduction

We recently described the synthesis of *p*-benzoquinone complexes of rhodium and iridium [Cp*M(*p*-benzoquinone)] (M = Rh (**1a**); M = Ir (**1b**)) as well as the related [Cp*Ir(*o*-dithiobenzoquinone)] and [Cp*Ir(*p*-dithiobenzoquinone)] complexes (Figure 1a).¹ The latter were successfully used as organometallic linkers, “OM-linkers”, for the design of an impressive range of new supramolecular assemblies and coordination polymers when treated with cationic inorganic building blocks of different geometry.² Some of these complexes exhibited useful luminescent properties.³ Unlike the *p*-benzoquinone metal complexes, the related *o*-benzoquinone compounds can be used as OM-chelates to generate new chiral

assemblies, which may exhibit different properties when compared to those with *p*-benzoquinone metal complexes. The OM-linkers **1a,b** are obtained simply by treatment of [Cp*M(solvent)₃]²⁺ (M = Rh, Ir), prepared *in situ*, and hydroquinone.⁴ In stark contrast the reaction of the solvated species [Cp*M(solvent)₃]²⁺ with catechol does not lead to a π -bonded compound. Instead a catecholato complex is formed where the Cp*M is chelated to the two oxygen atoms of the catechol as reported by Maitlis and co-workers (Figure 1b).⁵ Although we have previously obtained the 3-methoxy-*o*-benzoquinone complex [Cp*Ir(η^4 -(3-methoxy)-C₆H₃O₂)] through a nucleophilic *ortho*-functionalization reaction,^{1a} no direct method for the synthesis of Cp*M- π -bonded catechol compounds has been reported so far. On the other hand we note that clusters of ruthenium and palladium incorporating one or more catecholato ligands have been studied by Pierpont, Bohle, Churchill, and Keister.⁶ However these examples cannot be considered as a rational synthetic method to prepare simple mononuclear π -bonded *o*-quinone complexes as described in the current work.

In this paper we report the first synthesis of π -bonded rhodio- and iridio-*o*-benzoquinones [Cp*M(*o*-benzoquinone)] (M = Rh

* To whom correspondence should be addressed. E-mail: hani.amouri@upmc.fr.

[†] Université Pierre et Marie Curie-Paris 6.

[‡] NMR Facility of Ecole Nationale Supérieure de Chimie de Paris.

[§] Ecole Polytechnique, CNRS UMR 7653.

(1) (a) Le Bras, J.; Vaissermann, J.; Amouri, H. *Organometallics* **1998**, *17*, 1116–1121. (b) Moussa, J.; Guyard-Duhayon, C.; Herson, P.; Amouri, H.; Rager, M. N.; Jutand, A. *Organometallics* **2004**, *23*, 6231–6238. (c) Moussa, J.; Lev, D. A.; Boubekour, K.; Rager, M. N.; Amouri, H. *Angew. Chem., Int. Ed.* **2006**, *45*, 3854–3858. (d) Moussa, J.; Boubekour, K.; Rager, M. N.; Amouri, H. *Eur. J. Inorg. Chem.* **2007**, 2648–2653.

(2) (a) Moussa, J.; Boubekour, K.; Amouri, H. *Eur. J. Inorg. Chem.* **2005**, 3808–3810. (b) Moussa, J.; Guyard-Duhayon, C.; Boubekour, K.; Amouri, H.; Yip, S.-K.; Yam, V. W. W. *Cryst. Growth Des.* **2007**, *7*, 962–965. (c) Moussa, J.; Amouri, H. *Angew. Chem., Int. Ed.* **2008**, *47*, 1372–1380.

(3) Moussa, J.; Wong, K. M. C.; Chamoreau, L. M.; Amouri, H.; Yam, V. W. W. *Dalton Trans.* **2007**, 3526–3530.

(4) Le Bras, J.; Amouri, H.; Vaissermann, J. *J. Organomet. Chem.* **1998**, *553*, 483–485.

(5) Espinet, P.; Bailey, P. M.; Maitlis, P. M. *J. Chem. Soc., Dalton Trans.* **1979**, 1542–1547.

(6) (a) Fox, G. A.; Pierpont, C. G. *Inorg. Chem.* **1992**, *31*, 3718–3723. (b) Bohle, D. S.; Christensen, A. N.; Goodson, P. A. *Inorg. Chem.* **1993**, *32*, 4173–4174. (c) Churchill, M. V.; Lake, C. H.; Paw, W.; Keister, J. B. *Organometallics* **1994**, *13*, 8–10.

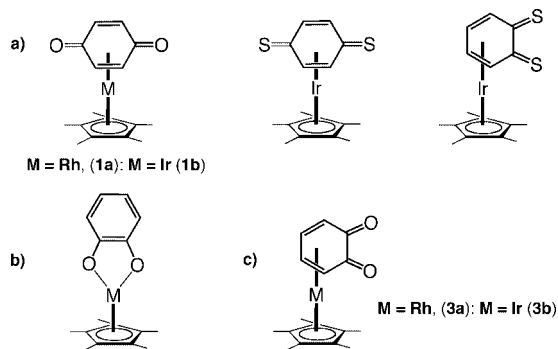


Figure 1. Schematic drawings of some π -bonded and O–O'-bonded benzoquinone and thiobenzoquinone complexes.

(**3a**); M = Ir (**3b**) (Figure 1c) following a new synthetic procedure and their use as chelating OM-linkers for the design of a new family of chiral octahedral bimetallic complexes.

Results and Discussion

Treatment of $[\text{Cp}^*\text{M}(\text{solvent})_3][\text{OTf}]_2$ prepared *in situ* with catechol in acetone, in the presence of excess $\text{BF}_3 \cdot 2\text{H}_2\text{O}$, followed by precipitation with Et_2O ⁷ provided the π -bonded catechol complexes $[\text{Cp}^*\text{M}(\eta^6\text{-C}_6\text{H}_6\text{O}_2)][\text{BF}_4]_2$ (M = Rh, **2a**; M = Ir, **2b**). Subsequent deprotonation with Cs_2CO_3 in acetone afforded the target π -bonded OM-linkers $[\text{Cp}^*\text{M}(o\text{-benzoquinone})]$ (M = Rh (**3a**); M = Ir (**3b**)) in 85–92% yields (Scheme 1).

Unlike those reported by Maitlis, which are blue in color, our compounds are orange and yellow, respectively. Moreover the ¹H and ¹³C NMR studies carried out on **3a** and **3b** confirmed that the *o*-benzoquinone moiety " $\eta\text{-C}_6\text{H}_4\text{O}_2$ " is π -bonded⁸ through the arene ring to the Cp^*M fragment. Thus the ¹H NMR spectrum of **3b** recorded in MeOD at room temperature showed the presence of a singlet assigned to the methyl protons of Cp^*Ir moiety at δ 2.03 ppm and two doublets of doublets centered at δ 5.22 and 5.75 ppm attributed to the protons of the η^4 -bonded arene ring. In a similar fashion the ¹H NMR spectrum of complex **3a** showed a singlet at 1.85 ppm for the Cp^*Rh unit and two doublets of doublets at δ 4.74 and 5.44 ppm, respectively. Furthermore, the ¹³C NMR spectrum of **3a** showed two doublets for the CH groups of the carbocycle at δ 82.4 and 84.7 ppm. These doublets arise from the coupling with a rhodium nucleus with $J_{\text{C-Rh}} = 8.7$ and 7.3 Hz, respectively. Further the carbonyl groups appeared as a singlet at δ 168.2 ppm, proving clearly that the metal is η^4 -bonded to *o*-benzoquinone. These compounds were fully characterized; see Experimental Section. In particular the structure of complex **3b** was confirmed by single-crystal X-ray diffraction study (*vide infra*).

X-ray Molecular Structure of 3b. Suitable crystals of **3b** for X-ray analysis were obtained from a $\text{CH}_2\text{Cl}_2/\text{hexane}$ mixture using a slow evaporation technique. Complex **3b** crystallizes in the monoclinic space group $P2_1/m$. The structure confirms the formation of the desired compound as described by the spectroscopic data (Figure 2a).

The carbocyclic ring is π -bonded to the organometallic Cp^*Ir moiety in the expected η^4 -fashion. We note that the structure displays a crystallographic plane of symmetry that passes through O(1), C(1), C(4), and C(5) and Ir(1) and bisects the molecule into two equivalent disordered halves. Further the structure shows that the quinone moiety is slightly bent upward away from the metal center with angle $\theta = 4.7(8)^\circ$ between the planes "C(3), C(4), C(3'), C(2a')" and "C(3), C(2), C(1), C(2a')".

At this stage a short comment on the resonance form of the π -bonded ring is required. Previously Pierpont and co-workers^{9a} reported the X-ray structure of a disubstituted catecholate complex, $(t\text{-Bu})_2\text{-C}_6\text{H}_2\text{O}_2\text{Mn}(\text{CO})_3$. In this compound the $\text{Mn}(\text{CO})_3$ fragment is σ -bonded to the oxygen atoms rather than π -bonded to the cyclic ring (Figure 3). Further the structure confirms that the carbocyclic ring is aromatic and is better described as a catecholate dianion. More recently Sweigart and co-workers^{11a} reported the molecular structure of an isomeric complex to the precedent example where the $\text{Mn}(\text{CO})_3$ moiety is π -bonded to the carbocyclic ring; further, one of the carbonyl oxygens is coordinated to a sodium cation and the complex was isolated as a dimer (Figure 3). In this example the *o*-benzoquinone complex is not a free molecule as in our case but rather an "*organometallic ligand*" that coordinates to a sodium cation (*vide infra*).

In our example, the solid state structure of **3b** indicates that the major resonance form is that of a π -bonded η^4 -quinone (**3b**) (Figure 4). Moreover in solution, the ¹H and ¹³C NMR of this complex exhibited two multiplets shifted upfield, which is in accord with that of a diene, i.e., resonance form **3b**.^{1a,b,4}

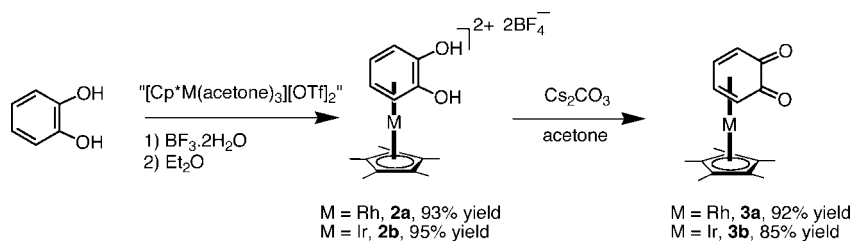
Further examination of the packing in the unit cell suggested that $[\text{Cp}^*\text{Ir}(o\text{-quinone})]$ (**3b**) individual molecules interact through π - π interactions ($d = 3.38 \text{ \AA}$, $\alpha = 18.23^\circ$) between the electron-rich Cp^*Ir moiety and the η^4 -quinone fragment, thus describing a 1D supramolecular chain (see Figure 2b). To our knowledge, this is the first X-ray molecular structure of an η^4 -*o*-quinone π -bonded to the Cp^*M family. In previous work we have isolated the first examples of *o*- and *p*-dithiobenzoquinone complexes $[\text{Cp}^*\text{Ir}(\eta^4\text{-}o\text{-C}_6\text{H}_4\text{S}_2)]$ and $[\text{Cp}^*\text{Ir}(\eta^4\text{-}p\text{-C}_6\text{H}_4\text{S}_2)]$.^{1c,1d,2c} In order to understand the role of " Cp^*Ir " in stabilization of the short-lived *p*-dithiobenzoquinone, we have taken an *ab initio* computational approach employing the hybrid density functional B3LYP method. Computational analyses using density functional theory confirm a net transfer of about 0.8 unit of electron density to the π^* ligand LUMO and 0.2 unit of electron density to each sulfur atom. This additional electron density is largely localized around the thiocarbonyl bonds, resulting in a reduction in C=S bond order as well as the anticipated decrease in C=C bond order. These calculations also prove that the sulfur atoms in the metalated thioquinone $[\text{Cp}^*\text{Ir-}p\text{-}(\eta^4\text{-C}_6\text{H}_4\text{S}_2)]$ (**2e**) are more nucleophilic and hence are good assembling organometallic ligands to construct novel supramolecular structures with transition metal electrophiles. Thus it is not surprising that the Cp^*Ir moiety stabilizes the η^4 -*o*-quinone form through back-donation, as illustrated by the solid state structure of **3b**.

Pierpont and co-workers⁹ investigated the charge distribution in several catecholate complexes where the metal center is chelated to the oxygen atoms. In these compounds the quinone ligands bonded in both semiquinone and catecholate electronic

(7) Moussa, J.; Chamoreau, L. M.; Boubekeur, K.; Amouri, H.; Rager, M. N.; Grotjahn, D. B. *Organometallics* **2008**, *27*, 67–71.

(8) (a) Le Bras, J.; Amouri, H.; Vaissermann, J. *Organometallics* **1996**, *15*, 5706–5712. (b) Le Bras, J.; Rager, M. N.; Besace, Y.; Vaissermann, J.; Amouri, H. *Organometallics* **1997**, *16*, 1765–1771. (c) Amouri, H.; Le Bras, J. *Acc. Chem. Res.* **2002**, *35*, 501–510.

(9) (a) Hartl, F.; Vlcek, A., Jr.; DeLearie, L. A.; Pierpont, C. G. *Inorg. Chem.* **1990**, *29*, 1073–1078. (b) Pierpont, C. G.; Langi, C. W. *Prog. Inorg. Chem.* **1994**, *41*, 331–442. (c) Pierpont, C. G. *Coord. Chem. Rev.* **2001**, *216–217*, 99–125.

Scheme 1. Synthesis of the OM-Linkers **3a,b**

forms. The latter is described as a “valence tautomerism” or “redox isomerization”. The authors demonstrated that facile intramolecular electron transfer between the metal and the organic *o*-quinone unit occurs and is temperature dependent. The novelty in our work involves a Cp*M unit (M = Rh, Ir) instead of a first-row metal ion, and in our case the metal fragment is π -bonded to the *o*-quinone system.

Having elucidated the structures of these novel OM-linkers [Cp*M(*o*-benzoquinone)] (**3a,b**), we decided to explore their coordination chemistry toward cationic inorganic building blocks with adequate geometry, i.e., having two empty sites in a *cis*-position for chelation by the two O–O' oxygen centers of the η^4 -*o*-benzoquinone fragment of **3a,b**.

Indeed, treatment of the luminophore building blocks¹⁰ such as “(bpy)₂Ru(II)²⁺”, “(ppy)₂Rh(III)³⁺”, and “(ppy)₂Ir(III)³⁺ {bpy = 2,2'-bipyridine, ppy = 2-phenylpyridine} with our OM-linkers [Cp*M(*o*-benzoquinone)] (M = Rh (**3a**); M = Ir (**3b**)) provided after reaction workup the novel family of chiral octahedral homo- and heterobimetallic complexes with C₁-symmetry [(bpy)₂Ru(**3a**)] [OTf]₂ (**4**, **RuRh**), [(bpy)₂Ru(**3b**)] [OTf]₂ (**5**, **RuIr**), [(ppy)₂Rh(**3a**)] [OTf] (**6**, **RhRh**), [(ppy)₂Rh(**3b**)] [OTf] (**7**, **RhIr**), [(ppy)₂Ir(**3a**)] [OTf] (**8**, **IrRh**), and [(ppy)₂Ir(**3b**)] [OTf] (**9**, **IrIr**) (Figure 5). These compounds were obtained as racemates.

All these complexes (**4–9**) were fully characterized by spectroscopic techniques (¹H, ¹³C NMR, IR) and elemental analysis (see Experimental Section). The NMR data suggest that in solution the bimetallic assembly is maintained. For each bimetallic compound, the ¹H and ¹³C NMR spectra showed two series of resonances for the bicyclic “bpy” or “ppy” entities. We also note the ¹³C NMR spectra of *o*-benzoquinone moieties permitted to distinguish the six different carbons, indicating clearly a loss of symmetry. For instance, the ¹H NMR spectrum of [(ppy)₂Ir(**3a**)] [OTf]₂ (**8**, **IrRh**) presented 15 multiplets in a range of 6.05 to 8.75 ppm, corresponding to the two nonequivalent ppy ligands, three doublets of doublets at δ 5.51, 5.57, and 5.95 ppm, which are attributed to the coordinated *o*-benzoquinone, and a singlet at δ 1.86 ppm for the η -Cp*Rh. These latter signals are downfield relative to the free OM-linker **3a**.

The ¹³C NMR spectrum of **8** permitted to distinguish 19 peaks for the two ppy patterns in the range 118.7–167.9 ppm. The *o*-benzoquinone moiety showed four doublets at δ 85.3 ppm ($J_{C-Rh} = 6.8$ Hz), 87.2 ppm ($J_{C-Rh} = 6.8$ Hz), 88.0 ppm ($J_{C-Rh} = 7.6$ Hz), and 89.1 ppm ($J_{C-Rh} = 7.6$ Hz) corresponding to the carbons in α - and β -positions relative to the ketonic groups

and two singlets at δ 159.9 and 166.3 ppm attributed to the –C=O functions (Figure 6a). Finally a singlet at δ 9.3 ppm and one doublet at δ 103.0 ppm ($J_{C-Rh} = 7.6$ Hz) were attributed to the η -Cp*Rh moiety. Assignment of individual resonances was achieved using COSY (Figure 6b), HMQC, and HMBC

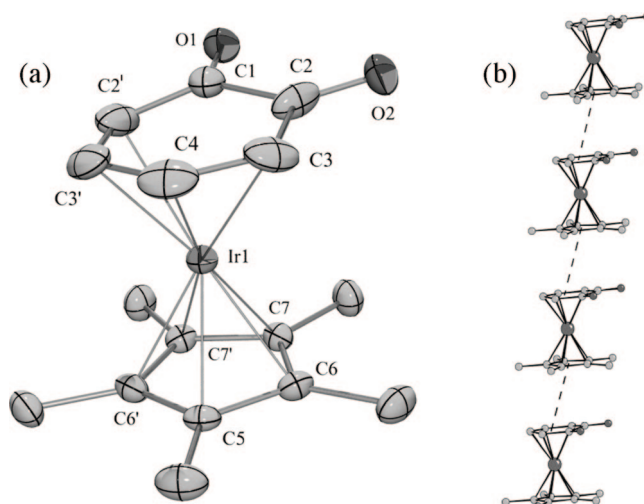


Figure 2. (a) X-ray molecular structure of **3b** with atom-numbering system. (b) 1D supramolecular chain formed through π - π interactions between individual units of [Cp*Ir(*o*-quinone)] (**3b**). Selected bond distances (Å) and angles (deg): Ir(1)–C(1) 2.574(5); Ir(1)–C(2) 2.51(2); Ir(1)–C(3) 2.182(4); Ir(1)–C(4) 2.144(6); Ir(1)–C(2') 2.27(2); C(1)–O(1) 1.250(7); C(2)–O(2) 1.27(1); C(2')–C(1)–C(2) 116.7(7); C(1)–C(2)–C(3) 112.3(9); C(2)–C(3)–C(4) 125.1(6); C(3)–C(4)–C(3') 118.9(5); C(4)–C(3')–C(2') 117.2(8); C(3')–C(2')–C(1) 128.0(1.5).

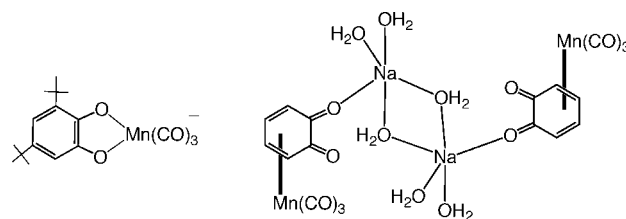


Figure 3. Some organometallic compounds displaying a catecholate ligand as a σ -bonded ligand or a benzoquinone as a π -bonded ligand.

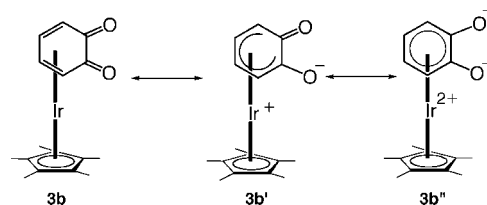


Figure 4. Possible resonance forms displayed by the π -bonded benzoquinone ligand in complex **3b**.

(10) (a) Juris, A.; Balzani, V.; Barigelletti, F.; Campagna, S.; Belsler, P.; von Zelewsky, A. *Coord. Chem. Rev.* **1988**, *84*, 85–277. (b) Lamansky, S.; Djurovich, P.; Murphy, D.; Abdel-Razzaq, F.; Lee, H. E.; Adachi, C.; Burrows, P. E.; Forrest, S. R.; Thompson, M. E. *J. Am. Chem. Soc.* **2001**, *123*, 4304–4312. (c) Lo, K. K.-W.; Chan, J. S.-W.; Lui, L.-H.; Chung, C.-K. *Organometallics* **2004**, *23*, 3108–3116. (d) Lo, K. K.-W.; Hui, W.-K.; Chung, C.-K.; Tsang, K. H.-K.; Lee, T. K.-M.; Li, C.-K.; Lau, J. S.-Y.; Ng, D. C.-M. *Coord. Chem. Rev.* **2006**, *250*, 1724–1736. (e) Flamigni, L.; Barbieri, A.; Sabatini, C.; Ventura, B.; Barigelletti, F. *Top. Curr. Chem.* **2007**, *281*, 143–203.

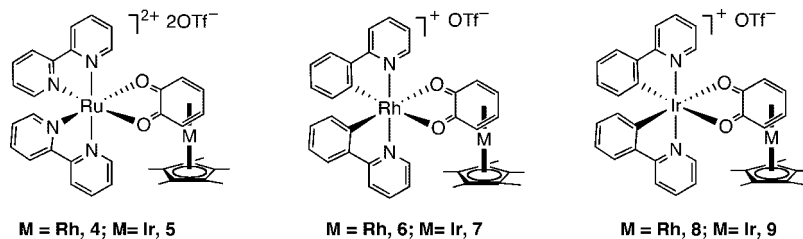
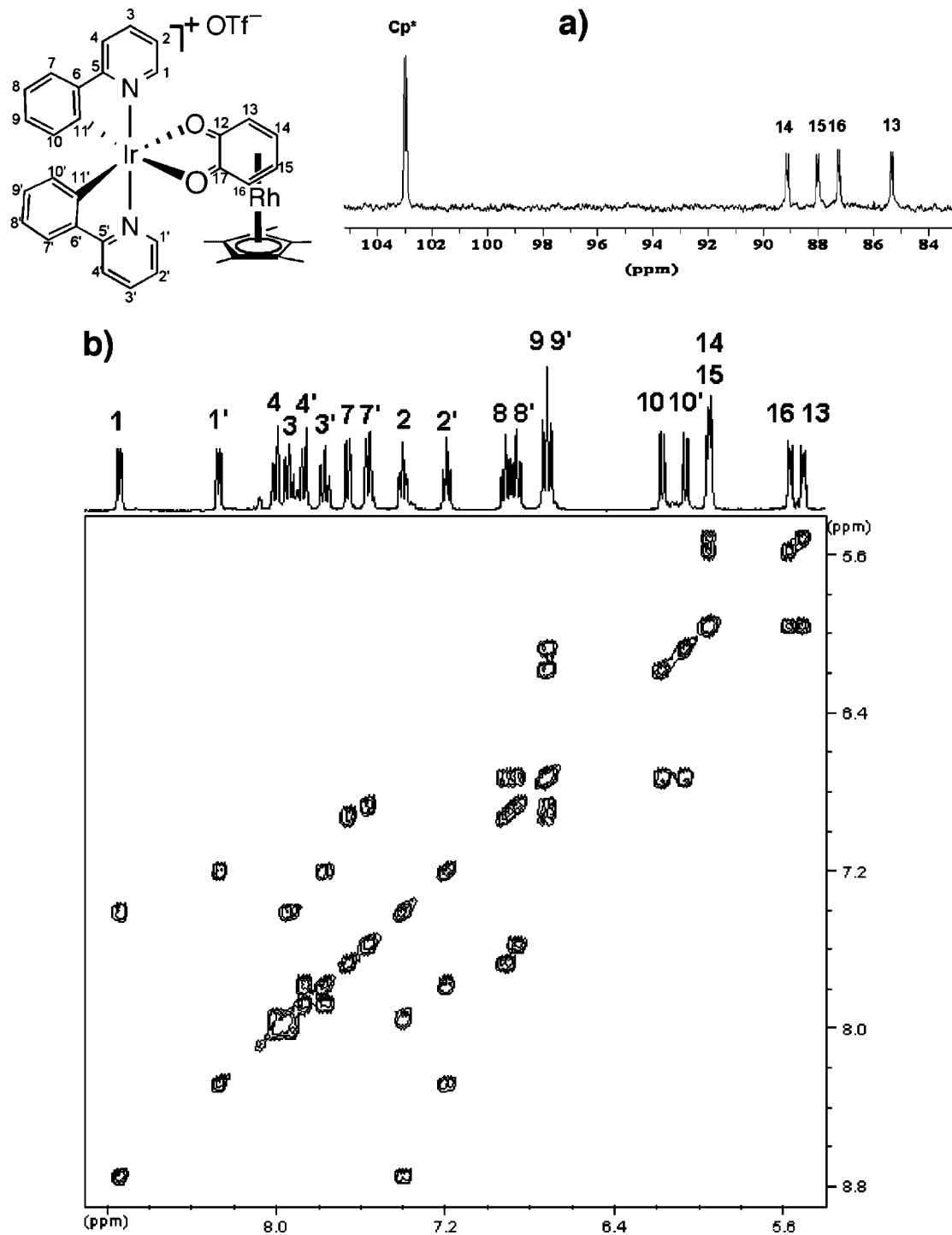


Figure 5. Schematic drawings of 4–9.

Figure 6. (a) Section of the $^{13}\text{C}\{^1\text{H}\}$ NMR spectrum of **8** showing doublets related to $J_{\text{C-Rh}}$ coupling. (b) 2D COSY NMR spectrum of **8** showing full proton assignments.

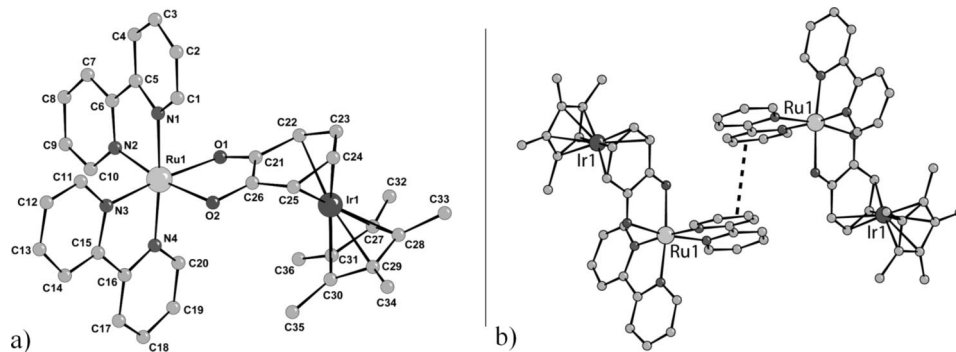


Figure 7. (a) X-ray structure of the cationic part of **5** (**RuIr**); (b) π - π interactions between two bpy units describing a supramolecular dimer. Selected bond distances (Å) and angles (deg): Ru(1)–O(1) 2.143(4); Ru(1)–O(2) 2.125(4); Ru(1)–N(1) 2.057(4); Ru(1)–N(2) 2.040(4); Ru(1)–N(3) 2.026(5); Ru(1)–N(4) 2.066(5); Ir(1)–C(21) 2.548(6); Ir(1)–C(22) 2.241(6); Ir(1)–C(23) 2.191(6); Ir(1)–C(24) 2.187(6); Ir(1)–C(25) 2.259(6); Ir(1)–C(26) 2.597(6); O(1)–Ru(1)–O(2) 79.42(15); N(1)–Ru(1)–N(2) 79.08(18); N(3)–Ru(1)–N(4) 78.85(18).

2D experiments; the latter permitted in particular linking without ambiguity each phenyl group to its pyridine for the two ppy ligands.

A complete NMR study was carried out for all complexes **4–9**. In the case where $[\text{Cp}^*\text{Rh}(o\text{-benzoquinone})]$ was used as a linker, it is noteworthy to mention that ^{13}C NMR spectra showed doublets for each *o*-benzoquinone “CH” carbon, except the carbonyl groups. These doublets arise from the coupling constants $J_{\text{C-Rh}}$. Interestingly the NMR studies highlight the nature of the η^4 -bonded *o*-benzoquinone in the bimetallic complexes. All these NMR data confirm that our assemblies are also stable in solution. Further, the structure of one of these bimetallic assemblies (**5**, **RuIr**) was ascertained without ambiguity by single-crystal X-ray diffraction study (*vide infra*). For instance the ^1H NMR of $[(\text{bpy})_2\text{Ru}(\text{3b})][\text{OTf}]_2$ (**5**, **RuIr**) recorded in CD_2Cl_2 is very informative and showed a singlet for the $\eta\text{-Cp}^*\text{Ir}$ at δ 1.94 ppm. Further, as a result of loss of symmetry in **5**, four multiplets are now visible to the coordinated OM-linker **3b** and appear at δ 5.74, 5.76, 5.92, and 5.99 ppm, which are assigned to the four protons of the chelating η^4 -bonded *o*-benzoquinone. These signals are downfield relative to the free OM-linker **3b**. Moreover, the lack of symmetry is also manifested by the appearance of 15 multiplets in the range 7.14–9.07 ppm and are attributed to the two nonequivalent bpy ligands.

The X-ray structure of **5** (Figure 7) confirms the O,O' σ -chelating mode of the OM-linker **3b** to the Ru(II) core via both oxygen atoms. The Ru(II) center is also coordinated to four nitrogen atoms of two bpy ligands, which describes a distorted octahedral geometry around the metal center. The structure shows also that the *o*-benzoquinone is coordinated to the $\text{Cp}^*\text{Ir(I)}$ moiety via the four diene carbons in η^4 -fashion similar to that of the free complex **3b**. The Ir---C21 and Ir---C26 distances are 2.548 and 2.597 Å, respectively, indicating absence of interaction. Further the C21---O1 and C26---O2 bond distances are 1.294 and 1.293 Å, suggesting a double-bond character. Moreover the two quinone functional groups are bent upward relative to the Cp^*Ir moiety with a hinge angle $\theta = 12.74^\circ$. In summary, in the bimetallic assembly **5**, the carbocycle of the organometallic linker **3b** adopts a η^4 -benzoquinone form. On the other hand, examination of the crystal packing revealed that the bimetallic assembly **5** undergoes π - π interaction ($d = 3.601$ Å, $\alpha = 30.33^\circ$) with one of its neighbors via the bpy unit to form a supramolecular dimer.

All new octahedral assemblies (**4–9**) were stable in air and soluble in most organic solvents, and they can be stored under argon for a long period of time. It is worth mentioning that

some neutral 2D networks were prepared from anionic $[\text{Na}][(\text{CO})_3\text{Mn}(o\text{-benzoquinone})]$ and divalent transition metal ions; however the synthesis and structures of these compounds are completely different from those described here.¹¹ We believe that our OM-linkers may be used as assembling ligands to construct an impressive range of chiral supramolecular assemblies, which may present different properties than those made via classical organic linkers.^{12–15}

In summary, we have reported the first synthesis of π -bonded rhodio- and iridio-*o*-benzoquinones $[\text{Cp}^*\text{M}(o\text{-benzoquinone})]$ ($\text{M} = \text{Rh}$ (**3a**); $\text{M} = \text{Ir}$ (**3b**)) using a new efficient synthetic method. The X-ray molecular structure of complex **3b** was determined and shows that a η^4 -quinone form is stabilized at least in the solid state. Complexes **3a,b** were used as OM-linkers to prepare a new family of octahedral bimetallic assemblies **4–9** via chelation of the appropriate inorganic building blocks such as “ $(\text{bpy})_2\text{Ru}(\text{II})^{2+}$ ”, “ $(\text{ppy})_2\text{Rh}(\text{III})^{3+}$ ”, and “ $(\text{ppy})_2\text{Ir}(\text{III})^{3+}$ ” {bpy = 2,2'-bipyridine, ppy = 2-phenylpyridine}. The X-ray molecular structure of $[(\text{bpy})_2\text{Ru}(\text{3b})][\text{OTf}]_2$ (**5**, **RuIr**) was determined. The X-ray data of the binuclear assembly **5** show that the carbocycle of the organometallic linker **3b** adopts a η^4 -quinone resonance form. Our future studies are devoted to the resolution of these chiral assemblies using optically pure anions.¹⁶ Moreover the luminescent properties of **4–9** are currently under investigation.

(11) (a) Oh, M.; Carpenter, G. B.; Sweigart, D. A. *Organometallics* **2002**, *21*, 1290–1295. (b) Oh, M.; Carpenter, G. B.; Sweigart, D. A. *Organometallics* **2003**, *22*, 1437–1442.

(12) (a) Stang, P. J. *Chem.-Eur. J.* **1998**, *4*, 19–27. (b) Stang, P. J.; Olenyuk, B. *Acc. Chem. Res.* **1997**, *30*, 502–518.

(13) (a) Caulder, D. L.; Raymond, K. N. *Acc. Chem. Res.* **1999**, *32*, 975–982. (b) Seeber, G.; Tiedemann, B. E. F.; Raymond, K. N. *Top. Curr. Chem.* **2006**, *265*, 147–183. (c) Saalfrank, R. W.; Uller, E.; Demleitner, B.; Bernt, I. *Struct. Bonding (Berlin)* **2000**, *96*, 149–175.

(14) (a) Bartik, T.; Weng, W.; Ramsden, J. A.; Szafert, S.; Falloon, S. B.; Arif, A. M.; Gladysz, J. A. *J. Am. Chem. Soc.* **1998**, *120*, 11071–11081. (b) Dembinski, R.; Bartik, T.; Bartik, B.; Jaeger, M.; Gladysz, J. A. *J. Am. Chem. Soc.* **2000**, *122*, 810–822.

(15) (a) Fujita, M.; Umemoto, K.; Yoshizawa, M.; Fujita, N.; Kusukawa, T.; Biradha, K. *Chem. Commun.* **2001**, 509–518. (b) Fujita, M.; Tomimaga, M.; Hori, A.; Therrien, B. *Acc. Chem. Res.* **2005**, *38*, 369–378.

(16) (a) Gruselle, M.; Thouvenot, R.; Caspar, R.; Boubekour, K.; Amouri, H.; Ivanov, M.; Tonsuaadu, K. *Mendeleev Commun.* **2004**, 282–283. (b) Amouri, H.; Caspar, R.; Gruselle, M.; Guyard-Duhayon, C.; Boubekour, K.; Lev, D. A.; Collins, L. S. B.; Grotjahn, D. B. *Organometallics* **2004**, *23*, 4338–4341. (c) Mimassi, L.; Guyard-Duhayon, C.; Rager, M. N.; Amouri, H. *Inorg. Chem.* **2004**, *43*, 6644–6649. (d) Mimassi, L.; Cordier, C.; Guyard-Duhayon, C.; Mann, B. E.; Amouri, H. *Organometallics* **2007**, *26*, 860–864.

Experimental Section

General Procedures. All manipulations were carried out at room temperature under an argon atmosphere using standard Schlenk tube techniques. Solvents were dried and distilled under argon by standard procedures. ^1H and ^{13}C NMR spectra were recorded on Bruker AC 300 or Avance 400 spectrometers. IR spectra were recorded on a Bruker Tensor 27 equipped with a Harrick ATR.

Synthesis of $[\text{Cp}^*\text{Rh}(\eta^6\text{-catechol})][\text{BF}_4]_2$ (2a**).** An acetone solution (10 mL) of AgOTf (415 mg; 1.60 mmol) was added to an orange suspension of $[\text{Cp}^*\text{Rh}(\mu\text{-Cl})\text{Cl}]_2$ (249 mg; 0.40 mmol) in acetone (10 mL). The resulting white AgCl precipitate was filtered off through Celite after stirring for 15 min. The yellow filtrate was then directly added to catechol (340 mg; 3 mmol), the solution turned brown, and the solvent was removed under vacuum. Then $\text{BF}_3 \cdot 2\text{H}_2\text{O}$ (2 mL) was added to the sticky brown solid, and the mixture was stirred for 30 min. Then diethyl ether (50 mL) was added to precipitate the complex $[\text{Cp}^*\text{Rh}(\eta^6\text{-catechol})][\text{BF}_4]_2$ as a light yellow microcrystalline powder, which was filtered through cotton, washed twice with diethyl ether (30 mL each), and dried under vacuum (386 mg; 0.74 mmol). Yield: 93%. Anal. Calcd for $\text{C}_{16}\text{H}_{21}\text{O}_2\text{B}_2\text{F}_8\text{Rh}$: C, 36.82; H, 4.06. Found: C, 37.71; H, 3.85. ^1H NMR (300 MHz in CD_3OD): 2.01 (s, 15H, Cp*); 6.00 (dd, 2H, catechol); 6.22 (dd, 2H, catechol). IR (ATR): 3101; 1555; 1540; 1492; 1425; 1387; 1311; 1019; 876; 819; 764; 736; 637; 588; 540; 520; 463; 387; 339; 228 cm^{-1} .

Synthesis of $[\text{Cp}^*\text{Ir}(\eta^6\text{-catechol})][\text{BF}_4]_2$ (2b**).** This compound was prepared using the procedure described for complex **2a** using the following amounts: AgOTf (520 mg; 2.00 mmol), $[\text{Cp}^*\text{Ir}(\mu\text{-Cl})\text{Cl}]_2$ (400 mg; 0.50 mmol), and catechol (340 mg; 3 mmol). Complex **2b** was obtained as a white microcrystalline powder (580 mg; 0.95 mmol). Yield: 95%. Anal. Calcd for $\text{C}_{16}\text{H}_{21}\text{O}_2\text{B}_2\text{F}_8\text{Ir}$: C, 31.44; H, 3.46. Found: C, 32.38; H, 3.41. ^1H NMR (300 MHz in CD_3OD): 2.14 (s, 15H, Cp*); 6.45 (dd, 2H, catechol); 6.82 (dd, 2H, catechol). IR (ATR): 3560; 3100; 1630; 1555; 1534; 1491; 1425; 1390; 1311; 1027; 889; 838; 819; 764; 735; 639; 578; 540; 520; 467; 388; 342; 309; 210 cm^{-1} .

Synthesis of $[\text{Cp}^*\text{Rh}(o\text{-benzoquinone})]$ (3a**).** An acetone solution (10 mL) of **2a** (386 mg; 0.74 mmol) was added to a white suspension of Cs_2CO_3 (540 mg; 1.67 mmol) in acetone (10 mL). The reaction mixture was stirred for 1 h at room temperature and was then filtered through Celite. The yellow filtrate was allowed to evaporate under vacuum, and the residue was dissolved in methanol (50 mL) and filtered through basic alumina. Evaporation of methanol under vacuum provided complex **3a** as an orange microcrystalline solid, which was dried under vacuum (274 mg; 0.68 mmol). Yield: 92%. Anal. Calcd for $\text{C}_{16}\text{H}_{19}\text{O}_2\text{Rh} \cdot 3\text{H}_2\text{O}$: C, 47.74; H, 6.76. Found: C, 47.01; H, 5.48. ^1H NMR (400 MHz in CD_2Cl_2): 1.85 (15H, s, Cp*); 4.74 (2H, dd, $^3J = 4.7$ Hz, $^4J = 3.2$ Hz, H α); 5.44 (2H, dd, $^3J = 4.7$ Hz, $^4J = 3.2$ Hz, H β). $^{13}\text{C}\{^1\text{H}\}$ NMR (100 MHz in CD_2Cl_2): 8.6 (CH $_3$ -Cp*); 82.4 (d, $J_{\text{C-Rh}} = 8.7$ Hz, C α); 84.7 (d, $J_{\text{C-Rh}} = 7.3$ Hz, C β); 98.8 (d, $J_{\text{C-Rh}} = 7.3$ Hz, Cq-Cp*); 162.8 (s, C=O). IR (ATR): 3351; 2910; 1669; 1533; 1442; 1382; 1367; 1260; 1152; 1030; 869; 734; 679; 637; 585; 517; 456; 433; 353; 304; 218 cm^{-1} .

Synthesis of $[\text{Cp}^*\text{Ir}(o\text{-benzoquinone})]$ (3b**).** This compound was prepared using the procedure described for complex **3a** using **2b** (580 mg; 0.95 mmol) instead of **2a** and Cs_2CO_3 (720 mg; 2.00 mmol). Complex **3b** was obtained as a yellow microcrystalline solid (380 mg; 0.81 mmol). Yield: 85%. Anal. Calcd for $\text{C}_{16}\text{H}_{19}\text{O}_2\text{Ir} \cdot 2\text{H}_2\text{O}$: C, 40.75; H, 4.92. Found: C, 40.86; H, 4.92. ^1H NMR (400 MHz in MeOD): 2.03 (15H, s, Cp*); 5.22 (2H, dd, $^3J = 4.7$ Hz, $^4J = 2.7$ Hz, H α); 5.75 (2H, dd, $^3J = 4.7$ Hz, $^4J = 2.7$ Hz, H β). $^{13}\text{C}\{^1\text{H}\}$ NMR (100 MHz in MeOD): 9.1 (CH $_3$ -Cp*); 77.9 (C α); 80.6 (C β), 95.9 (Cq-Cp*); 161.1 (C=O). IR

(ATR): 3362; 2919; 1670; 1555; 1473; 1425; 1385; 1353; 1046; 891; 732; 596; 521; 428; 250; 226 cm^{-1} .

Synthesis of $[(\text{bpy})_2\text{Ru}(\mathbf{3a})][\text{OTf}]_2$ (4**).** An acetone solution (10 mL) of AgOTf (103 mg; 0.40 mmol) was added to a dark purple acetone solution (10 mL) of $[(\text{bpy})_2\text{RuCl}_2]$ (104 mg; 0.20 mmol). The reaction mixture was stirred for 30 min at room temperature and was then filtered through Celite. The dark red filtrate was added to **3a** (77 mg; 0.20 mmol), and the reaction mixture was stirred for 1 h at room temperature. Then the solvent was removed under vacuum and the residue was dissolved in dichloromethane (50 mL) and filtered through Celite. Evaporation of CH_2Cl_2 under vacuum provided complex **4** as a dark red microcrystalline solid, which was dried under vacuum (196 mg; 0.18 mmol). Yield: 90%. Anal. Calcd for $\text{C}_{38}\text{H}_{35}\text{N}_4\text{O}_8\text{F}_6\text{-RhRuS}_2 \cdot 2\text{H}_2\text{O}$: C, 41.73; H, 3.59; N, 5.12. Found: C, 41.94; H, 3.69; N, 5.56. ^1H NMR (400 MHz in CD_2Cl_2): 1.83 (15H, s, Cp*); 5.62 (1H, dd, $^3J = 6.2$ Hz, $^4J = 1.2$ Hz, H-13); 5.72 (1H, dd, $^3J = 6.2$ Hz, $^4J = 1.2$ Hz, H-16); 5.97 (1H, td, $^3J = 6.2$ Hz, $^4J = 1.2$ Hz, H-14); 6.01 (1H, td, $^3J = 6.2$ Hz, $^4J = 1.2$ Hz, H-15); 7.12–7.17 (2H, m, H-9',9), 7.47 (1H, d, $^3J = 5.9$ Hz, H-10'); 7.65 (1H, d, $^3J = 5.9$ Hz, H-10); 7.66–7.71 (1H, m, H-2'); 7.74 (1H, td, $^3J = 7.8$ Hz, $^4J = 1.5$ Hz, H-8'); 7.82 (1H, td, $^3J = 7.8$ Hz, $^4J = 1.5$ Hz, H-8); 7.94–7.98 (1H, m, H-2); 8.06 (1H, td, $^3J = 8.2$ Hz, $^4J = 1.2$ Hz, H-3'); 8.25 (1H, d, $^3J = 7.8$ Hz, H-7'); 8.29 (1H, td, $^3J = 7.8$ Hz, $^4J = 1.2$ Hz, H-3); 8.38 (1H, d, $^3J = 8.2$ Hz, H-4'); 8.41 (1H, d, $^3J = 7.8$ Hz, H-7); 8.59 (1H, d, $^3J = 7.8$ Hz, H-4); 8.67 (1H, d, $^3J = 5.9$ Hz, H-1'); 9.12 (1H, d, $^3J = 5.9$ Hz, H-1). $^{13}\text{C}\{^1\text{H}\}$ NMR (100 MHz in CD_2Cl_2): 9.4 (CH $_3$ -Cp*); 84.8 (d, $J_{\text{C-Rh}} = 6.7$ Hz, C-13); 86.5 (d, $J_{\text{C-Rh}} = 6.7$ Hz, C-16); 88.1 (d, $J_{\text{C-Rh}} = 7.8$ Hz, C-15); 88.8 (d, $J_{\text{C-Rh}} = 7.8$ Hz, C-14); 103.4 (d, $J_{\text{C-Rh}} = 6.7$ Hz, Cq-Cp*); 122.9 (C-4'); 123.1 (C-7'); 123.3 (C-7); 123.5 (C-4); 125.4 (C-9'); 125.5 (C-9); 126.9 (C-2'); 127.0 (C-2); 134.7 (C-8'); 135.0 (C-8); 136.5 (C-3'); 136.7 (C-3); 150.1 (C-1'); 151.1 (C-1); 152.7 (C-10'); 153.4 (C-10); 157.5 (C-5'); 158.2 (C-5); 159.4 (C-6,6'); 161.0 (C-17); 167.3 (C-12). IR (ATR): 3470; 3076; 2964; 2921; 1719; 1603; 1498; 1462; 1420; 1386; 1341; 1252; 1148; 1026; 878; 800; 760; 727; 659; 633; 591; 572; 538; 515; 422; 343; 254; 208 cm^{-1} .

Synthesis of $[(\text{ppy})_2\text{Ru}(\mathbf{3b})][\text{OTf}]_2$ (5**).** This compound was prepared according to the procedure described for complex **4** and using compound **3b** (95 mg; 0.20 mmol) instead of **3a**. Complex **5** was isolated as a dark red microcrystalline solid (225 mg; 0.19 mmol). Yield: 95%. Anal. Calcd for $\text{C}_{38}\text{H}_{35}\text{N}_4\text{O}_8\text{F}_6\text{IrRuS}_2 \cdot 2\text{H}_2\text{O}$: C, 38.58; H, 3.32; N, 4.74. Found: C, 38.37; H, 3.45; N, 4.74. ^1H NMR (400 MHz in CD_2Cl_2): 1.94 (15H, s, Cp*); 5.76 (1H, dd, $^3J = 6.3$ Hz, $^4J = 1.2$ Hz, H-13); 5.87 (1H, dd, $^3J = 6.3$ Hz, $^4J = 1.2$ Hz, H-16); 5.92 (1H, td, $^3J = 6.3$ Hz, $^4J = 1.2$ Hz, H-14); 5.99 (1H, td, $^3J = 6.3$ Hz, $^4J = 1.2$ Hz, H-15); 7.11–7.16 (2H, m, H-9',9); 7.45 (1H, d, $^3J = 5.9$ Hz, H-10'); 7.65 (1H, d, $^3J = 5.9$ Hz, H-10); 7.70–7.76 (2H, m, H-2', H-8'); 7.80 (1H, td, $^3J = 7.8$ Hz, $^4J = 1.2$ Hz, H-8); 7.91–7.95 (1H, m, H-2); 8.08 (1H, td, $^3J = 7.8$ Hz, $^4J = 1.5$ Hz, H-3'); 8.24–8.29 (2H, m, H-7',3); 8.39 (2H, d, $^3J = 7.8$ Hz, H-4',7); 8.58 (1H, d, $^3J = 8.2$ Hz, H-4); 8.72 (1H, d, $^3J = 5.9$ Hz, H-1'); 9.07 (1H, d, $^3J = 5.4$ Hz, H-1). $^{13}\text{C}\{^1\text{H}\}$ NMR (100 MHz in CD_2Cl_2): 9.2 (CH $_3$ -Cp*); 76.1 (C-13); 78.3 (C-16); 80.2 (C-15); 80.5 (C-14); 97.0 (Cq-Cp*); 122.9 (C-7'); 123.0 (C-4'); 123.3 (C-7); 123.5 (C-4); 125.3 (C-9'); 125.4 (C-9); 126.9 (C-2); 127.0 (C-2'); 134.6 (C-8'); 135.0 (C-8); 136.5 (C-3'); 136.6 (C-3); 150.0 (C-1'); 150.9 (C-1); 152.7 (C-10'); 153.5 (C-10); 157.5 (C-5'); 158.1 (C-5); 159.4 (C-6,6',17); 166.6 (C-12). IR (ATR): 3453; 3072; 2974; 1698; 1603; 1499; 1461; 1419; 1388; 1328; 1251; 1148; 1027; 879; 762; 728; 659; 634; 591; 572; 539; 423; 346; 256 cm^{-1} .

Synthesis of $[(\text{ppy})_2\text{Rh}(\mathbf{3a})][\text{OTf}]_2$ (6**).** This compound was prepared according to the procedure described for complex **4**

using AgOTf (52 mg; 0.2 mmol) and the precursor [(ppy)₂Rh(μ -Cl)]₂ (89 mg; 0.1 mmol) instead of [(bpy)₂RuCl₂]. Complex **6** was isolated as an orange microcrystalline solid (169 mg; 0.18 mmol). Yield: 90%. Anal. Calcd for C₃₉H₃₅N₂O₅F₃Rh₂S·2H₂O: C, 49.69; H, 4.17; N, 2.97. Found: C, 49.64; H, 4.06; N, 2.77. ¹H NMR (400 MHz in CD₂Cl₂): 1.86 (15H, s, Cp*); 5.41–5.43 (1H, m, H-13); 5.49–5.51 (1H, m, H-16); 5.86–5.89 (2H, m, H-14,15); 6.08 (1H, d, ³J = 7.8 Hz, H-10'); 6.19 (1H, d, ³J = 7.8 Hz, H-10); 6.79–6.84 (2H, m, H-9',9); 6.97 (1H, t, ³J = 7.8 Hz, H-8'); 7.01 (1H, t, ³J = 7.8 Hz, H-8), 7.22 (1H, q, J = 5.0 Hz, H-2'); 7.44 (1H, t, ³J = 5.9 Hz, H-2); 7.62 (1H, d, ³J = 7.8 Hz, H-7'); 7.71 (1H, d, ³J = 7.8 Hz, H-7); 7.88 (2H, d, ³J = 4.0 Hz, H-3',4'); 7.98–8.07 (2H, m, H-4,3); 8.25 (1H, d, ³J = 5.0 Hz, H-1'); 8.74 (1H, d, ³J = 5.9 Hz, H-1). ¹³C{¹H} NMR (100 MHz in CD₂Cl₂): 9.4 (CH₃-Cp*); 83.8 (d, J_{C-Rh} = 7.3 Hz, C-13); 85.9 (d, J_{C-Rh} = 7.3 Hz, C-16); 87.4 (d, J_{C-Rh} = 8.1 Hz, C-15); 88.5 (d, J_{C-Rh} = 7.3 Hz, C-14); 102.3 (d, J_{C-Rh} = 8.1 Hz, Cq-Cp*); 119.0 (C-4'); 119.2 (C-4); 122.2 (C-2); 122.5 (C-2',8,8'); 123.8 (C-7'); 124.0 (C-7); 128.9 (C-9'); 129.1 (C-9); 133.1 (C-10'); 133.6 (C-10); 137.7 (C-3'); 137.9 (C-3); 143.7 (C-6); 143.9 (C-6'); 147.8 (C-1'); 149.4 (C-1); 160.0 (C-17); 162.6 (C-11'); 162.8 (C-11); 164.3 (C-5'); 164.8 (C-5); 166.1 (C-12). IR (ATR): 2965; 1604; 1580; 1518; 1501; 1479; 1415; 1384; 1352; 1254; 1222; 1150; 1026; 863; 796; 755; 735; 636; 607; 579; 535; 514; 415; 318; 234; 219 cm⁻¹.

Synthesis of [(ppy)₂Rh(3b)][OTf] (7). This compound was prepared according to the procedure described for complex **4** using AgOTf (52 mg; 0.2 mmol), **3b** (95 mg; 0.20 mmol), and the precursor [(ppy)₂Rh(μ -Cl)]₂ (89 mg; 0.1 mmol) instead of [(bpy)₂RuCl₂]. Complex **6** was isolated as a yellow microcrystalline solid (204 mg; 0.19 mmol). Yield: 98%. Anal. Calcd for C₃₉H₃₅N₂O₅F₃IrRhS·H₂O: C, 46.20; H, 3.68; N, 2.76. Found: C, 46.71; H, 3.86; N, 2.58. ¹H NMR (400 MHz in CD₂Cl₂): 1.96 (15H, s, Cp*); 5.54 (1H, dd, ³J = 5.9 Hz, ⁴J = 1.2 Hz, H-13); 5.63 (1H, dd, ³J = 5.9 Hz, ⁴J = 1.2 Hz, H-16); 5.83 (1H, td, ³J = 5.9 Hz, ⁴J = 1.2 Hz, H-14); 5.88 (1H, td, ³J = 5.9 Hz, ⁴J = 1.2 Hz, H-15); 6.06 (1H, d, ³J = 7.8 Hz, H-10'); 6.18 (1H, d, ³J = 7.8 Hz, H-10); 6.78–6.84 (2H, m, H-9',9); 6.95–7.03 (2H, m, H-8',8); 7.23–7.27 (1H, m, H-2'); 7.43 (1H, t, ³J = 5.9 Hz, H-2); 7.63 (1H, d, ³J = 7.8 Hz, H-7'); 7.70 (1H, d, ³J = 7.8 Hz, H-7); 7.87–7.90 (2H, m, H-3',4'); 7.99 (1H, d, ³J = 7.8 Hz, H-4); 8.04 (1H, t, ³J = 7.8 Hz, H-3); 8.29 (1H, d, ³J = 5.9 Hz, H-1'); 8.66 (1H, d, ³J = 5.5 Hz, H-1). ¹³C{¹H} NMR (100 MHz in CD₂Cl₂): 9.2 (CH₃-Cp*); 74.8 (C-13); 77.3 (C-16); 79.3 (C-15); 80.0 (C-14); 95.9 (Cq-Cp*); 119.0 (C-4'); 119.2 (C-4); 122.2 (C-2); 122.5 (C-8,8'); 122.6 (C-2'); 123.8 (C-7'); 123.9 (C-7); 128.9 (C-9'); 129.1 (C-9); 133.0 (C-10'); 133.5 (C-10); 137.7 (C-3'); 137.8 (C-3); 143.7 (C-6); 143.9 (C-6'); 147.7 (C-1'); 149.2 (C-1); 160.0 (C-17); 162.2 (d, J_{C-Rh} = 37.0 Hz, C-11'); 162.6 (d, J_{C-Rh} = 37.0 Hz, C-11); 164.2 (C-5'); 164.7 (C-5); 166.6 (C-12). IR (ATR): 3520; 3066; 2960; 2911; 1698; 1605; 1525; 1502; 1479; 1418; 1386; 1350; 1335; 1257; 1222; 1149; 1062; 1027; 878; 797; 755; 735; 669; 636; 611; 580; 538; 515; 442; 418; 323; 256; 232; 216 cm⁻¹.

Synthesis of [(ppy)₂Ir(3a)][OTf] (8). This compound was prepared according to the procedure described for complex **4** using AgOTf (52 mg; 0.20 mmol), **3a** (77 mg; 0.20 mmol), and the precursor [(ppy)₂Ir(μ -Cl)]₂ (107 mg; 0.10 mmol) instead of [(bpy)₂RuCl₂]. Complex **8** was isolated as an orange microcrystalline solid (186 mg; 0.18 mmol). Yield: 90%. Anal. Calcd for C₃₉H₃₅N₂O₅F₃IrRhS·2H₂O: C, 45.39; H, 3.81; N, 2.71. Found: C, 45.57; H, 3.67; N, 2.62. ¹H NMR (400 MHz in CD₂Cl₂): 1.86 (15H, s, Cp*); 5.51 (1H, dd, ³J = 4.9 Hz, ⁴J = 2.9 Hz, H-13); 5.57 (1H, dd, ³J = 4.9 Hz, ⁴J = 2.9 Hz, H-16); 5.95 (2H, dd, ³J = 4.9 Hz, ⁴J = 2.9 Hz, H-14,15); 6.06 (1H, dd, ³J = 7.8 Hz, ⁴J = 0.8 Hz, H-10'); 6.17 (1H, dd, ³J = 7.8 Hz, ⁴J = 0.8 Hz, H-10); 6.72 (2H, td, ³J = 7.8 Hz, ⁴J = 1.2 Hz, H-9,9');

6.86 (1H, td, ³J = 7.8 Hz, ⁴J = 1.2 Hz, H-8'); 6.91 (1H, td, ³J = 7.8 Hz, ⁴J = 1.2 Hz, H-8); 7.19 (1H, ddd, ³J = 8.2 Hz, ³J = 5.9 Hz, ⁴J = 1.2 Hz, H-2'); 7.40 (1H, ddd, ³J = 8.2 Hz, ³J = 5.5 Hz, ⁴J = 1.2 Hz, H-2); 7.56 (1H, dd, ³J = 7.8 Hz, ⁴J = 1.2 Hz, H-7'); 7.66 (1H, dd, ³J = 7.8 Hz, ⁴J = 1.2 Hz, H-7); 7.77 (1H, td, ³J = 8.2 Hz, ⁴J = 1.5 Hz, H-3'); 7.86 (1H, d, ³J = 8.2 Hz, H-4'); 7.94 (1H, td, ³J = 8.2 Hz, ⁴J = 1.5 Hz, H-3); 8.00 (1H, d, ³J = 8.2 Hz, H-4); 8.27 (1H, d, ³J = 5.9 Hz, H-1'); 8.74 (1H, d, ³J = 5.5 Hz, H-1). ¹³C{¹H} NMR (100 MHz in CD₂Cl₂): 9.3 (CH₃-Cp*); 85.3 (d, J_{C-Rh} = 6.8 Hz, C-13); 87.2 (d, J_{C-Rh} = 6.8 Hz, C-16); 88.0 (d, J_{C-Rh} = 7.6 Hz, C-15); 89.1 (d, J_{C-Rh} = 7.6 Hz, C-14); 103.0 (d, J_{C-Rh} = 7.6 Hz, Cq-Cp*); 118.6 (C-4'); 118.9 (C-4); 121.2 (C-8'); 121.3 (C-8); 122.0 (C-2); 122.2 (C-2'); 123.9 (C-7'); 124.1 (C-7); 128.9 (C-9'); 129.1 (C-9); 131.8 (C-10'); 132.7 (C-10); 137.5 (C-3'); 137.6 (C-3); 141.1 (C-11,11'); 144.1 (C-6); 144.2 (C-6'); 147.2 (C-1'); 148.8 (C-1); 159.9 (C-17); 166.3 (C-12); 167.5 (C-5'); 168.1 (C-5). IR (ATR): 3470; 3064; 2966; 2927; 1719; 1607; 1582; 1501; 1460; 1418; 1385; 1341; 1256; 1223; 1152; 1062; 1028; 863; 796; 757; 730; 671; 636; 584; 537; 516; 459; 420; 380; 347; 231; 223 cm⁻¹.

Synthesis of [(ppy)₂Ir(3b)][OTf] (9). This compound was prepared according to the procedure described for complex **4** using AgOTf (52 mg; 0.20 mmol), **3b** (95 mg; 0.20 mmol), and the precursor [(ppy)₂Ir(μ -Cl)]₂ (107 mg; 0.10 mmol) instead of [(bpy)₂RuCl₂]. Complex **8** was isolated as an orange microcrystalline solid (189 mg; 0.17 mmol). Yield: 85%. Anal. Calcd for C₃₉H₃₅N₂O₅F₃Ir₂S·H₂O: C, 42.46; H, 3.38; N, 2.54. Found: C, 42.47; H, 3.51; N, 2.35. ¹H NMR (400 MHz in CD₂Cl₂): 1.95 (15H, s, Cp*); 5.63 (1H, dd, ³J = 5.9 Hz, ⁴J = 1.2 Hz, H-13); 5.70 (1H, dd, ³J = 5.9 Hz, ⁴J = 1.2 Hz, H-16); 5.90–5.97 (2H, m, H-14,15); 6.01 (1H, d, ³J = 7.4 Hz, H-10'); 6.13 (1H, d, ³J = 7.4 Hz, H-10); 6.70 (2H, t, ³J = 7.4 Hz, H-9,9'); 6.85 (1H, t, ³J = 7.4 Hz, H-8'); 6.90 (1H, t, ³J = 7.4 Hz, H-8); 7.23 (1H, ddd, ³J = 7.8 Hz, ³J = 5.9 Hz, ⁴J = 1.5 Hz, H-2'); 7.38 (1H, ddd, ³J = 7.8 Hz, ³J = 5.9 Hz, ⁴J = 1.5 Hz, H-2); 7.57 (1H, dd, ³J = 7.8 Hz, ⁴J = 1.2 Hz, H-7'); 7.65 (1H, dd, ³J = 7.8 Hz, ⁴J = 1.2 Hz, H-7); 7.79 (1H, td, ³J = 7.8 Hz, ⁴J = 1.5 Hz, H-3'); 7.88 (1H, d, ³J = 7.8 Hz, H-4'); 7.93 (1H, td, ³J = 7.8 Hz, ⁴J = 1.5 Hz, H-3); 7.99 (1H, d, ³J = 7.8 Hz, H-4); 8.30 (1H, d, ³J = 5.9 Hz, H-1'); 8.66 (1H, d, ³J = 5.9 Hz, H-1). ¹³C{¹H} NMR (100 MHz in CD₂Cl₂): 9.1 (CH₃-Cp*); 76.4 (C-13); 78.9 (C-16); 80.1 (C-15); 80.8 (C-14); 96.5 (Cq-Cp*); 118.7 (C-4'); 118.9 (C-4); 121.2 (C-8'); 121.3 (C-8); 122.1 (C-2); 122.3 (C-2'); 123.9 (C-7'); 124.1 (C-7); 129.0 (C-9'); 129.2 (C-9); 131.5 (C-10'); 132.4 (C-10); 137.5 (C-3'); 137.6 (C-3); 140.6 (C-11,11'); 144.2 (C-6); 144.4 (C-6'); 147.1 (C-1'); 148.6 (C-1); 159.2 (C-17); 166.3 (C-12); 167.4 (C-5'); 167.9 (C-5). IR (ATR): 3500; 3061; 2963; 2917; 1698; 1606; 1583; 1527; 1502; 1476; 1386; 1350; 1338; 1254; 1222; 1148; 1062; 1027; 878; 796; 756; 729; 670; 635; 611; 584; 572; 538; 513; 458; 419; 381; 332; 303; 240; 207 cm⁻¹.

Summary of the Crystallographic Details. Crystal data for 3b. Nonius KappaCCD diffractometer, ϕ and ω scans, Mo K α radiation (λ = 0.71073 Å), graphite monochromator, T = 150 K, structure solution with SIR97, refinement against F^2 using SHELXL97 with anisotropic thermal parameters for all non-hydrogen atoms, calculated hydrogen positions with riding isotropic thermal parameters. Data collection for **3b**: yellow plate, 0.20 × 0.20 × 0.12 mm; monoclinic, $P2_1/m$, a = 7.121(5) Å, b = 13.743(1) Å, c = 8.296(1) Å, β = 105.022(1)°, V = 784.13(12) Å³, Z = 2, ρ_{calc} = 1.997 g cm⁻³, μ = 8.526 cm⁻¹, $F(000)$ = 456, θ_{max} = 30.01°, hkl ranges: -10 8; -19 17; -11 9, 5678 data collected, 2366 unique data (R_{int} = 0.0293), 2232 data with $I > 2\sigma(I)$, 119 parameters refined, GOF(F^2) = 1.073, final R indices ($R1 = \|F_o\| - \|F_c\|/\|F_o\|$, $wR2 = [w(F_o^2 - F_c^2)]/w(F_o^2)^{1/2}$), $R1 = 0.0260$, $wR2 = 0.0607$, max/min residual electron density 1.841(0.161)/-2.7500(0.161) e Å⁻³. Disorder

is induced by a symmetry plane that contains O1, C1, C4, Ir1, and C5. Crystallographic data for the structure reported in this paper have been deposited with the Cambridge Crystallographic Data Center as supplementary publication no. CCDC-702607. Copies of the data can be obtained free of charge on application to CCDC, 12 Union Road, Cambridge CB21EZ, UK (fax (+44)1223-336-033; e-mail: deposit@ccdc.cam.ac.uk).

Crystal Data for [(bpy)₂Ru(3b)](OTf)₂ (5). Red plate-like crystals: C₃₈H₃₅F₆IrN₄O₈RuS₂, monoclinic, *P*2₁/*c*, *a* = 8.6500(12) Å, *b* = 39.336(4) Å, *c* = 12.8186(17) Å, β = 108.822(10), *V* = 4128.4(9) Å³, *Z* = 4, *T* = 250(2) K, μ = 3.770 mm⁻¹, 28 952 reflections measured, 8332 independent (*R*_{int} = 0.0432), 6044 observed [*I* = 2σ(*I*)], 545 parameters, final *R* indices *R*1 [*I* = 2σ(*I*)] = 0.0452 and *wR*2 (all data) = 0.1210, GOF on *F*² = 1065, max./min. residual electron density = 0.88/−1.71 e Å⁻³. A single crystal of compound **5** was selected, mounted onto a glass fiber, and transferred in a cold nitrogen gas stream. Intensity data were collected with a Bruker-Nonius Kappa-CCD with graphite-monochromated Mo Kα radiation. Unit-cell parameter determination, data collection strategy, and integration were

carried out with the Nonius EVAL-14 suite of programs (A. J. M. Duisenberg, L. M. J. Kroon-Batenburg, A. M. M. Schreurs, *J. Appl. Crystallogr.* **2003**, *36*, 220). Multiscan absorption correction was applied (R. H. Blessing, *Acta Crystallogr.*, **1995**, *A51*, 33). The structure was solved by direct methods using the SHELXS-97 program (G. M. Sheldrick, University of Göttingen, 1997) and refined anisotropically by full-matrix least-squares methods using the SHELXL-97 software package (G. M. Sheldrick, University of Göttingen, Germany, 1997).

Acknowledgment. This work was supported by Université Pierre et Marie Curie, Paris-6 and CNRS.

Supporting Information Available: Crystallographic data of **3b** and **5** (CIF). This material is available free of charge via the Internet at <http://pubs.acs.org>.

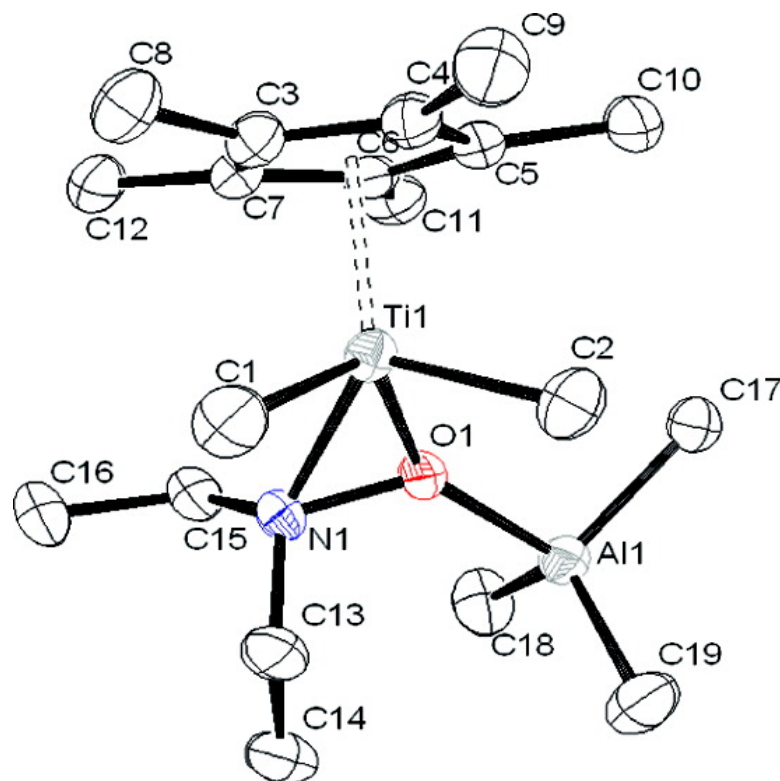
OM800594G

Propylene Polymerization with Cyclopentadienyltitanium(IV) Hydroxylamino Complexes

Andrew P. Dove, Elizabeth T. Kiesewetter, Xavier Ottenwaelder, and Robert M. Waymouth

Organometallics, 2009, 28 (2), 405-412 • DOI: 10.1021/om800571j • Publication Date (Web): 11 December 2008

Downloaded from <http://pubs.acs.org> on April 28, 2009



More About This Article

Additional resources and features associated with this article are available within the HTML version:

- Supporting Information
- Access to high resolution figures
- Links to articles and content related to this article
- Copyright permission to reproduce figures and/or text from this article



ORGANOMETALLICS

Subscriber access provided by SHANGHAI INST OF ORG CHEM

[View the Full Text HTML](#)



ACS Publications
High quality. High impact.

Organometallics is published by the American Chemical Society, 1155 Sixteenth Street N.W., Washington, DC 20036

Propylene Polymerization with Cyclopentadienyltitanium(IV) Hydroxylaminate Complexes

Andrew P. Dove,[†] Elizabeth T. Kiesewetter, Xavier Ottenwaelder,[‡] and Robert M. Waymouth*

Department of Chemistry, Stanford University, Stanford, California 94305

Received June 19, 2008

Complexes of the type Cp*TiX₂(ONR'R'') (Cp* = η⁵-C₅Me₅; X = Me, Cl; R = R' = Et, TEMPO (2,2,6,6-tetramethylpiperidine-*N*-oxyl); X = R' = Me, R'' = ^tBu) were synthesized by several routes. Upon activation with [Ph₃C]⁺[B(C₆F₅)₄]⁻ and AlⁱBu₃, these complexes generate highly active catalysts for propylene polymerization, although significant catalyst deactivation was observed. Activation with B(C₆F₅)₃/AlⁱBu₃ or methylaluminoxane (MAO) resulted in reduced polymerization activity, the latter leading to increased catalyst lifetime. Model studies showed that the interaction of AlMe₃ with Cp*Ti(Me)₂(ONEt₂) led to the formation of Cp*Ti(Me)₂(η²-O(AlMe₃)NEt₂). The X-ray crystal structure confirmed that the hydroxylaminate ligand remained η² bound to the titanium center with the AlMe₃ bound to the complex through the oxygen atom of the hydroxylaminate ligand. Exchange reactions with organic ethers revealed the metalloether to be a comparable donor to PhOMe. Cp*Ti(Me)₂(ON^tBu(Me)) was revealed to be a weaker donor than Cp*Ti(Me)₂(ONEt₂); Cp*Ti(Me)₂(TEMPO) did not bind to AlMe₃. AlⁱBu₃ bound more weakly to Cp*Ti(Me)₂(ONEt₂) than AlMe₃. Reaction of Cp*Ti(Me)₂(ONEt₂) and Cp*Ti(Me)₂(ON^tBu(Me)) with B(C₆F₅)₃ resulted in clean formation of the zwitterionic contact ion pairs [Cp*Ti(Me)(η²-ONEt₂)]⁺[MeB(C₆F₅)₃]⁻ and [Cp*Ti(Me)(η²-ON^tBu(Me))]⁺[MeB(C₆F₅)₃]⁻, respectively, whereas reaction of Cp*Ti(Me)₂(η²-ON^tBu(Me)) with [Ph₃C]⁺[B(C₆F₅)₄]⁻ resulted in the clean formation of the solvent-separated ion pair [Cp*Ti(Me)(η²-ON^tBu(Me))]⁺[B(C₆F₅)₄]⁻. Reaction of Cp*Ti(Me)₂(η¹-TEMPO) with B(C₆F₅)₃ results in the elimination of methane to result in the formation of the contact ion pair [Cp*Ti(η²-TEMPO)]⁺[MeB(C₆F₅)₃]⁻, in which one of the TEMPO methyl groups has undergone C–H activation, resulting in a η²-bound TEMPO ligand, confirmed by ¹H, gROESY, and ¹H–¹⁵N HMBC NMR. Addition of AlⁱBu₃ or AlMe₃ to the cationic [Cp*Ti(Me)(ON^tBu(Me))]⁺[B(C₆F₅)₄]⁻ resulted in decomposition of the cations.

Introduction

New classes of coordination complexes have spawned a renaissance in olefin polymerization catalysis. The application and study of these catalysts has led to both improved catalysts and polymers on an industrial scale and new insights into the mechanisms of enchainment.^{1–10} While considerable studies

have focused on bis-cyclopentadienyl metallocenes,^{1,4,11–14} investigations of coordination compounds lacking cyclopentadienyl ligands^{15–18} or half-metallocenes containing only one

* Corresponding author. E-mail: waymouth@stanford.edu.

[†] Department of Chemistry, University of Warwick, Coventry, U.K. CV4 7A.

[‡] Current address: Department of Chemistry, Concordia University, Montreal, Quebec, Canada.

(1) Brintzinger, H. H.; Fischer, D.; Mülhaupt, R.; Rieger, B.; Waymouth, R. M. *Angew. Chem., Int. Ed. Engl.* **1995**, *34*, 1143–1170.

(2) Coates, G. W. *Chem. Rev.* **2000**, *100*, 1223–1252.

(3) Kaminsky, W. *J. Polym. Sci. Part A* **2004**, *42*, 3911–3921.

(4) Resconi, L.; Cavallo, L.; Fait, A.; Piemontesi, F. *Chem. Rev.* **2000**, *100*, 1253–1345.

(5) Lai, S. Y.; Wilson, J. R.; Knight, G. W.; Stevens, J. C.; Chum, P. S. *U.S. Patent* 5,272,236, 1993.

(6) Scheirs, J.; Kaminsky, W. *Metallocene-based Polyolefins: Preparation, Properties, and Technology*; John Wiley & Sons Ltd.: Chichester, 2000; Vol. 1, p 2.

(7) Stevens, J. C. *Stud. Surf. Sci. Catal.* **1994**, *89*, 277–284.

(8) Landis, C. R.; Rosaaen, K. A.; Sillars, D. R. *J. Am. Chem. Soc.* **2003**, *125*, 1710–1711.

(9) Ferreira, M. J.; Martins, A. M. *Coord. Chem. Rev.* **2006**, *250*, 118–132.

(10) Gladysz, J. A. *E. Chem. Rev.* **2000**, *100*, Special Issue on Frontiers in Metal-Catalyzed Polymerization.

(11) Kaminsky, W. *Macromol. Chem. Phys.* **1996**, *197*, 3907–3945.

(12) Dankova, M.; Waymouth, R. M. *Macromolecules* **2003**, *36*, 3815–3820.

(13) Jensen, T. R.; Yoon, S. C.; Dash, A. K.; Luo, L. B.; Marks, T. J. *J. Am. Chem. Soc.* **2003**, *125*, 14482–14494.

(14) Lofgren, B.; Kokko, E.; Seppala, J. *Adv. Polym. Sci.* **2004**, *169*, 1–12.

(15) Gibson, V. C.; Spitzmesser, S. K. *Chem. Rev.* **2003**, *103*, 283–315.

(16) Zuo, W. W.; Sun, W. H.; Zhang, S.; Hao, P.; Shiga, A. *J. Polym. Sci. Part A* **2007**, *45*, 3415–3430.

(17) Gendler, S.; Groysman, S.; Goldschmidt, Z.; Shuster, M.; Kol, M. *J. Polym. Sci. Part A* **2006**, *44*, 1136–1146.

(18) Capaccione, C.; Proto, A.; Ebeling, H.; Mülhaupt, R.; Okuda, J. *J. Polym. Sci. Part A* **2006**, *44*, 1908–1913.

(19) Nomura, K.; Liu, J. Y.; Padmanabhan, S.; Kitiyanan, B. *J. Mol. Catal. A Chem.* **2007**, *267*, 1–29.

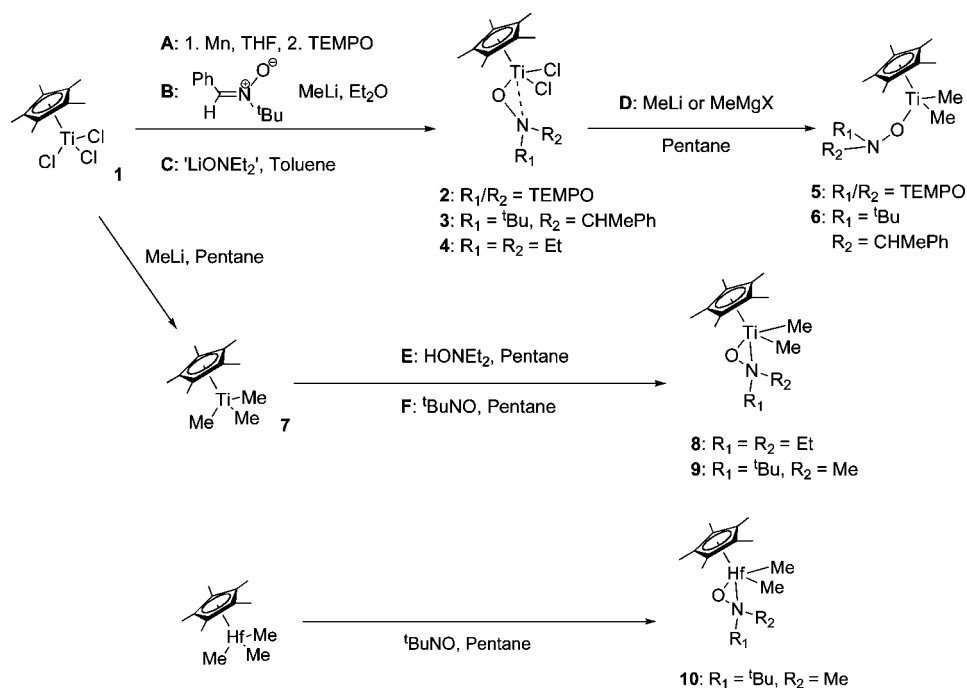
(20) Dove, A. P.; Xie, X.; Waymouth, R. M. *Chem. Commun.* **2005**, 2152–2154.

(21) Mahanthappa, M. K.; Cole, A. P.; Waymouth, R. M. *Organometallics* **2004**, *23*, 836–845.

(22) Stephan, D. W.; Stewart, J. C.; Guerin, F.; Courtenay, S.; Kickham, J.; Hollink, E.; Beddie, C.; Hoskin, A.; Graham, T.; Wei, P. R.; Spence, R. E. V.; Xu, W.; Koch, L.; Gao, X. L.; Harrison, D. G. *Organometallics* **2003**, *22*, 1937–1947.

(23) Stephan, D. W.; Stewart, J. C.; Guerin, F.; Spence, R. E. V. H.; Xu, W.; Harrison, D. G. *Organometallics* **1999**, *18*, 1116–1118.

(24) Guerin, F.; Beddie, C. L.; Stephan, D. W.; Spence, R. E.; Wurzel, R. *Organometallics* **2001**, *20*, 3466–3471.

Scheme 1. Synthetic Routes to Cp**M*(hydroxylaminato) Complexes

cyclopentadienyl ligand^{19–36} have expanded the scope of coordination catalysts for olefin polymerization. The remarkable success of the titanium “constrained geometry” catalysts such as [(Me₂Si)(η⁵-C₅Me₄)(N('tBu))TiCl₂]^{7,37–41} has stimulated renewed interest in the behavior of monocyclopentadienyl complexes with different monoanionic coligands.^{19–36} In conjunction with cocatalysts such as methylaluminoxane (MAO), triphenylcarbenium tetrakis(pentafluorophenyl)borate ([Ph₃C]⁺[B(C₆F₅)₄][−]), or tris(pentafluorophenyl)borane (B(C₆F₅)₃), many of these complexes have been shown to be effective catalysts for the homopolymerization of ethylene and the copolymerization of ethylene with higher olefins such as 1-hexene or

1-octene,^{19,25} but the activities and catalyst lifetimes depend sensitively on the nature of the catalyst precursor as well as the activation strategy. Studies to examine the interaction of these complexes with the cocatalyst system have revealed several deactivation pathways.^{32,42–45}

Hydroxylamines (or nitroxides) are an intriguing class of anionic ligands with tunable M–L bond strengths^{46–49} that can bind as either monodentate (η¹) or bidentate (η²) ligands, depending on the hydroxylamine substituents and the ancillary ligation at the metal.^{21,49–58} We recently reported that monocyclopentadienyl titanium hydroxylaminato complexes exhibit high activities for propylene polymerization.²⁰ In this paper, we describe the synthesis and propylene polymerization behavior of a series of monocyclopentadienyl hydroxylaminato complexes, their propylene polymerization behavior, and the reaction chemistry of these complexes with alkylaluminum reagents and a series of activators (MAO, [Ph₃C]⁺[B(C₆F₅)₄][−], and B(C₆F₅)₃).

Results and Discussion

Synthesis of (Cyclopentadienyl)titanium(hydroxylaminato) Complexes. We have developed several synthetic routes to monocyclopentadienyl titanium hydroxylaminato complexes (Scheme 1).^{20,21,49,53} For hydroxylamines that form stable nitroxyl radicals such as TEMPO (2,2,6,6-tetramethylpiperidine-*N*-oxyl), coupling of the nitroxyl radical with a reduced Ti(III) precursor generates stable TEMPO complexes (Scheme 1A).^{21,51,53} Nitroxides generated by deprotonation of hydroxylamines or by alkylation of nitrones react with titanium halides to generate the hydroxylaminato titanium complexes (Scheme 1B,C).^{21,53}

(25) Mcmeeking, J.; Gao, X.; Von Haken Spence, R. E.; Brown, S. J.; Jeremic, D. *US Patent* 6,114,481, 2000.

(26) Zhang, W.; Sita, L. R. *J. Am. Chem. Soc.* **2008**, *130*, 442.

(27) Zhang, W.; Sita, L. R. *Adv. Synth. Catal.* **2008**, *350*, 439–447.

(28) Harney, M. B.; Zhang, Y. H.; Sita, L. R. *Angew. Chem., Int. Ed.* **2006**, *45*, 2400–2404.

(29) Nomura, K.; Fujii, K. *Macromolecules* **2003**, *36*, 2633–2641.

(30) Nomura, K.; Fujita, K.; Fujiki, M. *J. Mol. Catal., A Chem.* **2004**, *220*, 133–144.

(31) Manz, T. A.; Phomphrai, K.; Medvedev, G.; Krishnamurthy, B. B.; Sharma, S.; Haq, J.; Novstrup, K. A.; Thomson, K. T.; Delgass, W. N.; Caruthers, J. M.; Abu-Omar, M. M. *J. Am. Chem. Soc.* **2007**, *129*, 3776–3777.

(32) Zhang, S.; Piers, W. E.; Gao, X. L.; Parvez, M. *J. Am. Chem. Soc.* **2000**, *122*, 5499–5509.

(33) Dias, A. R.; Duarte, M. T.; Fernandes, A. C.; Fernandes, S.; Marques, M. M.; Martins, A. M.; Da Silva, J. F.; Rodrigues, S. S. *J. Organomet. Chem.* **2004**, *689*, 203–213.

(34) Fenwick, A. E.; Phomphrai, K.; Thorn, M. G.; Vilardo, J. S.; Trefun, C. A.; Hanna, B.; Fanwick, P. E.; Rothwell, I. P. *Organometallics* **2004**, *23*, 2146–2156.

(35) Tamm, M.; Randoll, S.; Herdtweck, E.; Kleigrewe, N.; Kehr, G.; Erker, G.; Rieger, B. *Dalton Trans.* **2006**, 459–467.

(36) Sinnema, P. J.; Spaniol, T. P.; Okuda, J. *J. Organomet. Chem.* **2000**, *598*, 179–181.

(37) Mcknight, A. L.; Waymouth, R. M. *Chem. Rev.* **1998**, *98*, 2587–2598.

(38) Okuda, J. *Chem. Ber.* **1990**, *123*, 1649–1651.

(39) Stevens, J. C. In *Studies in Surface Science and Catalysis*; Hightower, J. W., Delgass, W. N., Iglesia, E., Bell, A. T., Eds.; Elsevier: Amsterdam, 1996; Vol. 101, pp 11–20.

(40) Canich, J. M.; Hlatky, G. G.; Turner, H. W. *WO 92-00333*, 1992.

(41) Chen, Y. X.; Marks, T. J. *Organometallics* **1997**, *16*, 3649–3657.

(42) Nomura, K.; Fudo, A. *Inorg. Chim. Acta* **2003**, *345*, 37–43.

(43) Byun, D. J.; Fudo, A.; Tanaka, A.; Fujiki, M.; Nomura, K. *Macromolecules* **2004**, *37*, 5520–5530.

(44) Zhang, S. B.; Piers, W. E. *Organometallics* **2001**, *20*, 2088–2092.

(45) Kickham, J. E.; Guerin, F.; Stewart, J. C.; Urbanska, E.; Stephan, D. W. *Organometallics* **2001**, *20*, 1175–1182.

(46) Huang, K. W.; Han, J. H.; Cole, A. P.; Musgrave, C. B.; Waymouth, R. M. *J. Am. Chem. Soc.* **2005**, *127*, 3807–3816.

(47) Huang, K. W.; Han, J. H.; Musgrave, C. B.; Waymouth, R. M. *Organometallics* **2006**, *25*, 3317–3323.

Table 1. Propylene Polymerization Using Cp* Titanium Hydroxylaminato Complexes

entry	cat.	activator	scav.	pP (psig)	[Ti] (mM)	yield (g)	prod ^g	Mw ^h (kDa)	PDI ^h	m ⁴ⁱ	r ⁴ⁱ
1	8 ^a	[Ph ₃ C] ⁺	Al ⁱ Bu ₃ ^d	liq	0.25	1.3	153.2	2505	1.90	2.6	17.3
2	9 ^a	[Ph ₃ C] ⁺	Al ⁱ Bu ₃ ^d	liq	1.25	1.6	37.4	2490	1.90	0.9	16.6
3	5 ^a	[Ph ₃ C] ⁺	Al ⁱ Bu ₃ ^d	liq	1.25	0.5	11.4	2500	2.00	0.9	16.3
4	8 ^a	B(C ₆ F ₅) ₃	Al ⁱ Bu ₃ ^d	liq	25	0.2	0.3	1380	2.45	3.6	17.6
5	8 ^a	MAO ^c		liq	25	1.3	1.5	1675	2.03	1.1	21.1
6	8 ^b	[Ph ₃ C] ⁺	Al ⁱ Bu ₃ ^d	60	0.3	1.5	50.0	1340	2.02	1.3	19.8
7	8 ^b	B(C ₆ F ₅) ₃	Al ⁱ Bu ₃ ^d	60	30	trace					
8	8 ^b	MAO ^c		60	0.3	1.1	37.3	1870	2.07	2.1	18.6
9	4 ^b	MAO ^c		60	0.3	0.4	13.3	1610	1.87	2.1	17.3
10	8 ^b	[Ph ₃ C] ⁺	AlMe ₃ ^e	60	30						
11	8 ^b	[Ph ₃ C] ⁺	MAD ^f	60	30						

^a Polymerizations were carried out in 90 mL of liquid propylene, 10 mL of toluene containing 60 mg of AlⁱBu₃ at 20 ± 1 °C for 20 min, [Ph₃C]⁺ = [Ph₃C]⁺[B(C₆F₅)₄]⁻. ^b Polymerizations were carried out in 100 mL of toluene containing 60 mg of AlⁱBu₃ at 20 ± 1 °C for 60 min. ^c Dry MAO. ^d AlⁱBu₃ = triisobutylaluminum. ^e AlMe₃ = trimethylaluminum. ^f MAD = bis(2,6-di-*tert*-butyl-4-methylphenoxy)methylaluminum. ^g Productivity kg poly(propylene) (mmol Ti⁻¹) (h)⁻¹. ^h Determined by gel permeation chromatography. ⁱ Determined by ¹³C NMR.

Conversion of the dichloro complexes to the dimethyl analogues can be achieved by treatment with 2 equiv of methyl lithium or methyl Grignard reagent (Scheme 1D).

Hydroxylaminato titanium alkyl complexes can also be prepared from the alkyl precursors. Addition of HONeEt₂ to Cp*TiMe₃, **7**, in pentane generates Cp*Ti(Me)₂(ONeEt₂), **8** (Scheme 1E). Alternatively nitrosoalkyl compounds can be cleanly and selectively inserted into a single titanium or hafnium methyl bond to generate a hydroxylaminato ligand *in situ*.^{20,59–61} Thus, Cp*Ti(Me)₂(ONⁱBu(Me)), **9**,²⁰ or Cp*Hf(Me)₂(ONⁱBu(Me)), **10**, was generated in high yield by treatment of Cp*TiMe₃ or Cp*HfMe₃ with 1 equiv of ⁱBuNO in pentane (Scheme 1F).

The hapticity of the hydroxylaminato ligands depends sensitively on the nature of the hydroxylamine and the ancillary ligation at the metal.^{20,21,49,51,56,57} X-ray crystallographic analysis of the TEMPO complex **2** reveals a η¹-bound coordination geometry, whereas the hydroxylamine in **8**²⁰ and in Cp*Ti(Cl)₂(ONMe₂)⁵⁶ is bound η² through both oxygen and nitrogen. The sterically demanding TEMPO ligand also adopts an η² coordination geometry in the absence of cyclopentadienyl ligands as in (TEMPO)TiCl₃.^{53,57}

In solution, the ¹⁵N NMR chemical shift provides a useful indicator of the hapticity of the hydroxylamine ligand. The ¹⁵N NMR chemical shifts can be measured by ¹H–¹⁵N heteronuclear multiple-bond correlation spectroscopy (HMBC). These studies revealed that Cp*Ti(Me)₂(TEMPO), **5**, displays two resonances at δ = 217 and 228 ppm, which we attribute to two ring-flip isomers of an η¹-bound TEMPO ligand. The ¹⁵N NMR resonance of **9** occurs farther upfield at δ = 134 ppm, indicative of an η² coordination geometry in solution, consistent with that observed in the solid state. Similar analysis of the diethyl hydroxylaminato complexes **4** and **8** revealed ¹⁵N NMR chemical shifts of δ = 129 and 143 ppm, respectively, indicative of a bidentate coordination of the less sterically hindered hydroxylamine ligands. Analysis of high-field (500 MHz) ¹H NMR spectra of **4** reveals a doublet of doublets for the methylene resonances of the diethyl hydroxylamine, indicative of restricted rotation of the *N*-ethyl groups due to the η² binding of the hydroxylaminato ligand.

Propylene Polymerization Using Cp*TiX₂(hydroxylaminato) Complexes. In liquid propylene, activation of the Cp* titanium dialkyl complexes **5**, **8**, and **9**, bearing an η²-bound hydroxylaminato ligand, with [Ph₃C]⁺[B(C₆F₅)₄]⁻ at room temperature in the presence of AlⁱBu₃ leads to highly active catalysts for propylene polymerization and yields high molecular weight atactic polypropylene.²⁰ Under these conditions, narrow molecular weight distributions are observed, indicative of single-

site behavior. The productivity of Cp*Ti(Me)₂(ONeEt₂), **8**, at room temperature approaches 153 (kg PP) (mmol Ti)⁻¹ (h)⁻¹, comparable to some of the most active constrained geometry type catalysts.⁶² Catalysts derived from the η²-bound hydroxylaminato ligands **8** and **9** are more active than those derived from the η¹-bound TEMPO ligand **5**. In contrast, the hafnium complex **10** shows no activity for the polymerization of propylene upon activation with [Ph₃C]⁺[B(C₆F₅)₄]⁻ at room temperature in the presence of AlⁱBu₃.

In liquid propylene, the highest activities were observed upon activation with [Ph₃C]⁺[B(C₆F₅)₄]⁻; activation of **8** with B(C₆F₅)₃ in the presence of AlⁱBu₃ or with dry MAO resulted in a significantly reduced polymerization activity (Table 1, entries 1, 4 and 5).

Solution Propylene Polymerization. The time course of propylene conversion was monitored in toluene with a gaseous monomer feed at 4 atm to study the catalyst lifetime as a function of activation conditions. Propylene was introduced at constant pressure from a ballast vessel of known volume, temperature, and propylene pressure, and gas uptake was recorded from the pressure drop in the gas ballast.⁶³ Activation of **8** with B(C₆F₅)₃/AlⁱBu₃ in solution at 4 atm of propylene

(48) George, S. D.; Huang, K. W.; Waymouth, R. M.; Solomon, E. I. *Inorg. Chem.* **2006**, *45*, 4468–4477.

(49) Huang, K. W.; Waymouth, R. M. *J. Am. Chem. Soc.* **2002**, *124*, 8200–8201.

(50) Nagy, S.; Etherton, B. P.; Krishnamurti, R.; Tryrell, J. A. *US Patent 6,204,216 B1*, March 20, 2001.

(51) Mahanthappa, M. K.; Cole, A. P.; Waymouth, R. M. *Organometallics* **2004**, *23*, 1405–1410.

(52) Huang, K. W.; Waymouth, R. M. *J. Chem. Soc., Dalton Trans.* **2004**, 354–356.

(53) Mahanthappa, M. K.; Huang, K. W.; Cole, A. P.; Waymouth, R. M. *Chem. Commun.* **2002**, 502–503.

(54) Mitzel, N. W.; Parsons, S.; Blake, A. J.; Rankin, D. W. H. *J. Chem. Soc., Dalton Trans.* **1996**, 2089–2093.

(55) Wieghardt, K.; Tolksdorf, I.; Weiss, J.; Swiridoff, W. Z. *Anorg. Allg. Chem.* **1982**, *490*, 182–190.

(56) Hughes, D. L.; Jimeneztenorio, M.; Leigh, G. J.; Walker, D. G. *J. Chem. Soc., Dalton Trans.* **1989**, 2389–2395.

(57) Golubev, V. A.; Voronina, G. N.; Chernaya, L. I.; Dyachkovskii, F. S.; Matkovskii, P. E. *Zh. Obs. Khim.* **1977**, *47*, 1825–1832.

(58) Brindley, P. B.; Scotton, M. J. *J. Organomet. Chem.* **1981**, *222*, 89–96.

(59) Doxsee, K. M.; Juliette, J. J. J.; Weakley, T. J. R.; Zientara, K. *Inorg. Chim. Acta* **1994**, *222*, 305–315.

(60) Nakamoto, M.; Tilley, T. D. *Organometallics* **2001**, *20*, 5515–5517.

(61) Cummings, S. A.; Radford, R.; Erker, G.; Kehr, G.; Frohlich, R. *Organometallics* **2006**, *25*, 839–842.

(62) Grandini, C.; Camurati, I.; Guidotti, S.; Mascellani, N.; Resconi, L.; Nifant'ev, I. E.; Kashulin, I. A.; Ivehenko, P. V.; Mercandelli, P.; Sironi, A. *Organometallics* **2004**, *23*, 344–360.

(63) Lin, S.; Tagge, C. D.; Waymouth, R. M.; Nele, M.; Collins, S.; Pinto, J. C. *J. Am. Chem. Soc.* **2000**, *122*, 11275–11285.

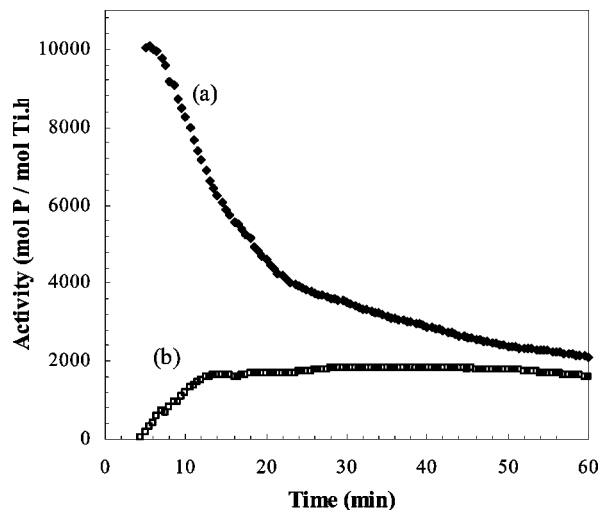


Figure 1. Representative activity versus time profiles for propylene polymerization by $\text{Cp}^*\text{Ti}(\text{Me})_2(\text{ONeEt}_2)$, **8**, activated by (a) $[\text{Ph}_3\text{C}]^+[\text{B}(\text{C}_6\text{F}_5)_4]^-/\text{Al}^i\text{Bu}_3$, \blacklozenge , and (b) MAO, \square (Table 1, entries 6 and 8).

resulted in only a trace amount of polymer. Activation of **8** with $[\text{Ph}_3\text{C}]^+[\text{B}(\text{C}_6\text{F}_5)_4]^-/\text{Al}^i\text{Bu}_3$ yielded an active catalyst, but activation with $[\text{Ph}_3\text{C}]^+[\text{B}(\text{C}_6\text{F}_5)_4]^-$ in the presence of AlMe_3 as a scavenger led to an inactive catalyst for propylene polymerization. Analysis of propylene conversion upon activation of **8** with $[\text{Ph}_3\text{C}]^+[\text{B}(\text{C}_6\text{F}_5)_4]^-/\text{Al}^i\text{Bu}_3$ reveals that the polymerization activity approached a maximum of 10 000 (mol propylene) (mol Ti) $^{-1}$ (h) $^{-1}$ after approximately 6 min, followed by a decrease in monomer uptake; after 15 min, the activity is half of its maximum (Figure 1a). In contrast, activation of **8** with MAO revealed a lower rate of monomer consumption and a gradual increase in activity over 12 min followed by a constant rate of monomer conversion (Figure 1b). One interpretation of these data is that activation of **8** with $[\text{Ph}_3\text{C}]^+[\text{B}(\text{C}_6\text{F}_5)_4]^-/\text{Al}^i\text{Bu}_3$ generates a high concentration of active sites that decay over time, whereas MAO is less efficient in activating the metallocene initially but results in a constant generation of active sites at a rate comparable to catalyst deactivation. Activation of the dichloride precursor **4** with MAO generated a less active catalyst than the dimethyl **8**, but yielded a polymer with similar molecular weight, molecular weight distribution, and tacticity.

Previous studies on the ethylene/hexene copolymerization with the TEMPO derivatives **5** and **2** revealed that activation of the dialkyl derivative **5** with $[(2,6\text{-}i\text{PrC}_6\text{H}_3)\text{NMe}_2\text{H}]^+[\text{B}(\text{C}_6\text{F}_5)_4]^-/\text{Al}^i\text{Bu}_3$ yielded a more active catalyst than that obtained upon activation of the dichloride derivative **2** with MAO. Moreover, bimodal molecular weight distributions were observed for the ethylene/hexene polymers derived from **2**/MAO ($M_w/M_n = 18.3$), whereas those from **5**/ $[(2,6\text{-}i\text{PrC}_6\text{H}_3)\text{NMe}_2\text{H}]^+[\text{B}(\text{C}_6\text{F}_5)_4]^-/\text{Al}^i\text{Bu}_3$ were narrower ($M_w/M_n = 3.1$). For the propylene polymerizations reported here, monomodal molecular weight distributions were observed irrespective of the activator ($[\text{Ph}_3\text{C}]^+[\text{B}(\text{C}_6\text{F}_5)_4]^-/\text{Al}^i\text{Bu}_3$ vs $\text{B}(\text{C}_6\text{F}_5)_3/\text{Al}^i\text{Bu}_3$ vs MAO); nevertheless the bimodal molecular weight distributions observed in EH copolymerizations imply that under some conditions activation by MAO can generate multiple active sites, presumably by transmetalation of the hydroxylamine ligand from Ti to Al.

Model Studies. In an effort to identify the nature of the organometallic species generated upon reaction of the monocyclopentadienyl precursors with either alkylaluminum scavengers or activators, we carried out model studies on the interaction of the catalyst precursors with selected activators

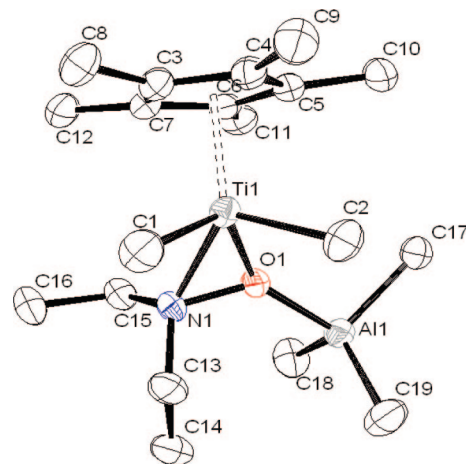


Figure 2. ORTEP diagram of $\text{Cp}^*\text{Ti}(\text{Me})_2(\text{O}(\text{AlMe}_3)\text{NEt}_2)$ (**11**). Representative bond lengths (Å) and angles (deg): Ti–C(1) 2.120(2); Ti–C(2) 2.107(2); Ti–N(1) 2.1696(16); Ti–O(1) 2.0027(12); O(1)–N(1) 1.4496(18); O(1)–Al1 1.9311(13); N(1)–Ti–O(1) 41.41(5); C(1)–Ti–C(2) 91.68(9); Ti–O(1)–Al 147.07(7).

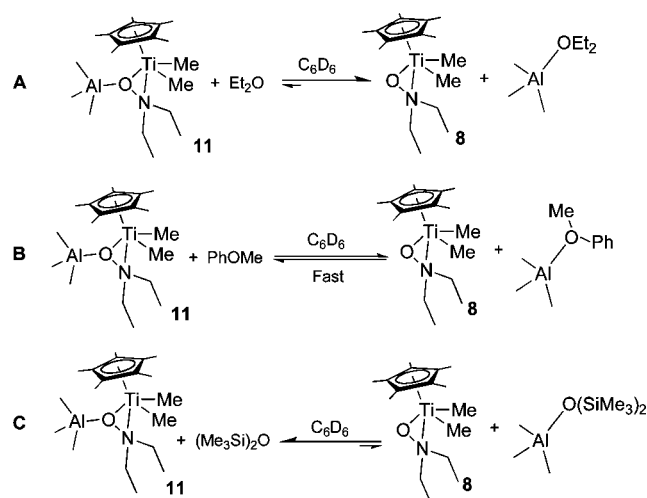
and scavengers. Studies by Stephan,⁴⁵ Piers,^{32,44} and Park⁶⁴ have revealed that monocyclopentadienyl titanium complexes with monoanionic coligands undergo a variety of reactions with alkylaluminum reagents that have helped to identify some of the catalyst decomposition pathways.

To assess the stability of the hydroxylamines in the presence of alkylaluminum scavengers, we first investigated reactions of the neutral hydroxylaminato complexes **5**, **8**, and **9** with alkylaluminum reagents. Addition of AlMe_3 to $\text{Cp}^*\text{Ti}(\text{Me})_2(\text{ONeEt}_2)$, **8**, led to the formation of a stable trimethylaluminum adduct, $\text{Cp}^*\text{Ti}(\text{Me})_2(\text{O}(\text{AlMe}_3)\text{NEt}_2)$, **11**. X-ray quality crystals of **11** were grown from a saturated pentane solution at -30°C ; an ORTEP diagram is shown in Figure 2. The X-ray diffraction structure of **11** reveals AlMe_3 bound to the oxygen of the η^2 -bound diethylhydroxylamine ligand. In contrast to complex **9**²⁰ and the previously reported $\text{CpTi}(\text{Cl})_2(\text{ONMe}_2)$,⁵⁶ the geometry of the ONeEt_2 ligand is twisted with respect to the Ti–Cp centroid vector such that O(1) and N(1) are bound almost parallel to the plane described by Ti, C(1), and C(2) [C(2)–Ti–O(1) = $91.63(7)^\circ$, C(1)–Ti–N(1) = $89.65(7)^\circ$]. The binding of AlMe_3 to the hydroxylamine ligand results in an increase in the Ti–O distances in **11** (O(1)–Ti = 2.0027(12) Å) relative to that of **9** (O–Ti = 1.895(3) Å)²⁰ and $\text{CpTi}(\text{Cl})_2(\text{ONMe}_2)$ (O–Ti = 1.866(1)),⁵⁶ whereas the Ti–N distances are similar (N–Ti = 2.1696(16), 2.178(4), and 2.128 Å, respectively).

The ^1H NMR spectrum of complex **11** at 25°C in solution (Figure S1, Supporting Information) reveals only one set of resonances for the AlMe_3 and N–Et groups, indicating that either the molecule is symmetric in solution or it is fluxional as a result of either the fast rotation of the η^2 -bound hydroxylaminato ligand or rapid dissociation/reassociation of the AlMe_3 . Examination of the ^1H NMR spectrum at -80°C reveals only slight broadening of the resonances, suggesting that even under these conditions the dynamic process is fast. Nevertheless, the multiplet assigned to the NCH_2 protons at $\delta = 3.21$ ppm and triplet at $\delta = 0.85$ ppm for **11** are indicative of an η^2 -bound hydroxylaminato ligand.

To assess the stability of the AlMe_3 adducts, we examined the interaction of **11** with a range of organic ethers (Scheme 2). Addition of 1 equiv of Et_2O to **11** led to the complete

(64) Park, J. T.; Yoon, S. C.; Bae, B. J.; Seo, W. S.; Suh, I. H.; Han, T. K.; Park, J. R. *Organometallics* **2000**, *19*, 1269–1276.

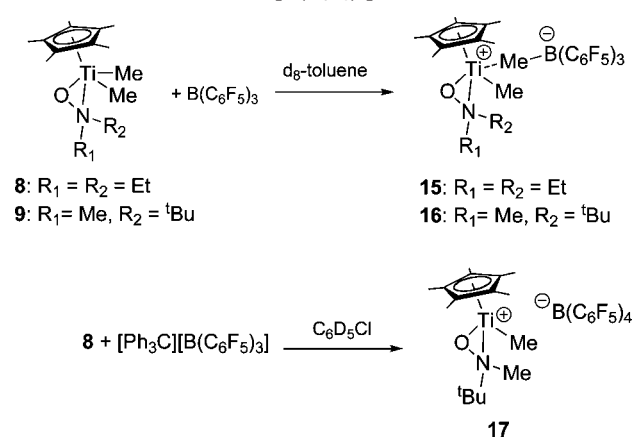
Scheme 2. Reaction of **11** with Ethers

dissociation of the AlMe_3 adduct, whereas the addition of 1 equiv of anisole, PhOMe , led to an equilibrated mixture. At 20 °C the ^1H NMR spectrum of the latter reaction displays only one Cp^* resonance at $\delta = 1.79$ ppm, which is distinct from Cp^* resonance of **8** ($\delta = 1.88$ ppm) and **11** ($\delta = 1.74$ ppm), indicative of a rapid equilibrium. At -80 °C, separate resonances for **8** and **11** could be resolved, enabling a determination of the equilibrium constant for the reaction of **11** with PhOMe of $K_{\text{eq}} = 0.066 \pm 0.003$ (-80 °C). In contrast, the addition of 1 equiv of hexamethyldisiloxane led to no significant change in the resonances attributed to **11** in the ^1H NMR spectrum. This indicates that the bound hydroxylamine of **8** is a significantly stronger donor than $(\text{Me}_3\text{Si})_2\text{O}$. This study demonstrates the order of ether donor strength is $\text{Et}_2\text{O} > \text{PhOMe} \sim \mathbf{8} > (\text{Me}_3\text{Si})_2\text{O}$. In addition, this suggests that the AlMe_3 can readily dissociate from **11** in solution.

Addition of 1 equiv of Al^iBu_3 to **8** led to significant shifts in the ^1H NMR spectrum, indicative of the formation of an adduct analogous to **11**. Addition of 1 equiv of anisole to this mixture regenerated **8** and the anisole adduct of Al^iBu_3 , $\text{Ph}(\text{Me})\text{O} \cdot \text{Al}^i\text{Bu}_3$. These data suggest that AlMe_3 binds more strongly than Al^iBu_3 to **8**.

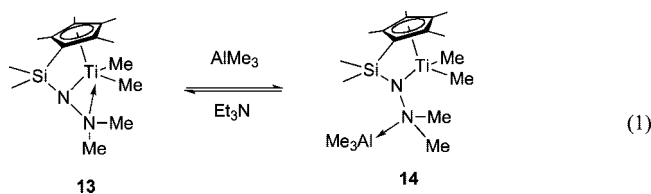
Addition of AlMe_3 to $\text{Cp}^*\text{Ti}(\text{Me})_2(\text{ON}^i\text{Bu}(\text{Me}))$, **9**, affords a related adduct, $\text{Cp}^*\text{Ti}(\text{Me})_2(\text{O}(\text{AlMe}_3)\text{N}^i\text{Bu}(\text{Me}))$, **12**, as evidenced by significant shifts in the ^1H NMR chemical shifts of the Cp^* and AlMe_3 resonances at $\delta = 1.82$ and -0.31 ppm, respectively (**9**: Cp^* $\delta = 1.87$ ppm; free AlMe_3 $\delta = -0.37$ ppm, Figure S1b). Attempts to isolate and crystallize this complex on a preparatory scale were unsuccessful. The equilibrium constant for the reaction of anisole with **12** at -80 °C was measured to be $K_{\text{eq}} = 1.74 \pm 0.23$, a much larger value that observed for the reaction of **11** with anisole. This result indicated that the ONET_2 ligand binds more strongly to AlMe_3 than the $\text{ON}^i\text{Bu}(\text{Me})$ ligand.

Investigations of **11** and **12** in C_6D_6 over a longer period show that some degradation of the titanium species occurs. In the case of **11**, degradation is slow. After 3 days approximately 30% Cp^*TiMe_3 is observed. However, the degradation of **12** is much more rapid. The ^1H NMR spectrum becomes broad after only a few hours and the reaction becomes increasingly green in color due to the probable formation of a $\text{Ti}(\text{III})$. These observations are consistent with the transmetalation of the hydroxylaminato ligand, a possible degradation route for the catalytic species. Addition of AlMe_3 to the η^1 hydroxylaminato complex, $\text{Cp}^*\text{Ti}(\text{Me})_2(\text{TEMPO})$, **5**, does not cause a shift in

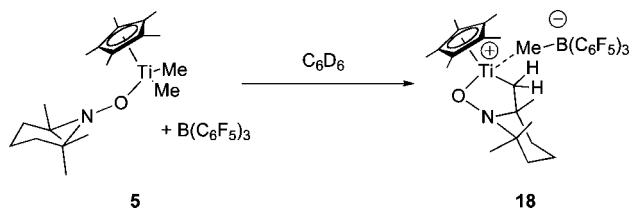
Scheme 3. Activation of **8** and **9** with $\text{B}(\text{C}_6\text{F}_5)_3$ or $[\text{Ph}_3\text{C}][\text{B}(\text{C}_6\text{F}_5)_4]$ 

any ^1H NMR resonances of **5**, suggesting that the more sterically hindered TEMPO ligand does not form an adduct with AlMe_3 .

The reversible formation of AlR_3 adducts of **5**, **8**, and **9** is analogous to the behavior observed by Park for dimethylsilyl-bridged tetramethylcyclopentadienylhydroazidotitanium complexes (eq 1).⁶⁴ The η^2 hydrazido complex **13** reacts with AlMe_3 to form the stable AlMe_3 adduct **14**, and treatment of **14** with Et_3N regenerates **13**. However, though AlMe_3 binds to the oxygen of the η^2 hydroxylaminato complexes **5**, **8**, and **9**, it binds to the terminal Me_2N of the hydrazido ligand, inducing a change in the hapticity of the hydrazido ligand from an η^2 to an η^1 coordination geometry.



Reaction of $\text{Cp}^*\text{Ti}(\text{Me})_2(\text{hydroxylaminato})$ Complexes with $\text{B}(\text{C}_6\text{F}_5)_3$ and $[\text{Ph}_3\text{C}][\text{B}(\text{C}_6\text{F}_5)_4]$. Treatment of $\text{Cp}^*\text{Ti}(\text{Me})_2(\text{ONET}_2)$, **8**, with $\text{B}(\text{C}_6\text{F}_5)_3$ in d_8 -toluene yielded the zwitterionic complex $[\text{Cp}^*\text{Ti}(\text{Me})(\text{ONET}_2)]^+[\text{MeB}(\text{C}_6\text{F}_5)_3]^-$, **15** (Scheme 2). The complex displays two broad resonances attributable to the ethyl CH_2 at $\delta = 2.89$ and 2.56 ppm, a single broad resonance due to the ethyl CH_3 at $\delta = 0.62$ ppm, and Cp^* , TiMe , and $[\text{MeB}(\text{C}_6\text{F}_5)_3]^-$ resonances occurring at $\delta = 1.46$, 0.45, and 0.73 ppm, respectively. The broadening of the ^1H NMR spectra is likely a consequence of a dynamic process involving migration of the $[\text{MeB}(\text{C}_6\text{F}_5)_3]^-$ counterion between binding sites at the titanium.³² In contrast, treatment of $\text{Cp}^*\text{Ti}(\text{Me})_2(\text{ON}^i\text{Bu}(\text{Me}))$, **9**, with $\text{B}(\text{C}_6\text{F}_5)_3$ in d_8 -toluene resulted in sharp ^1H NMR resonances consistent with formation of the contact ion pair $[\text{Cp}^*\text{Ti}(\text{Me})(\text{ON}^i\text{Bu}(\text{Me}))]^+[\text{MeB}(\text{C}_6\text{F}_5)_3]^-$, **16** (Scheme 3). This complex was isolated as a pentane-insoluble orange powder on a 500 mg scale. Investigations by ^1H gROESY NMR and $^1\text{H}-^{15}\text{N}$ HMBC NMR spectroscopy (^{15}N $\delta = 158$ ppm) were consistent with a bidentate η^2 coordination geometry for the hydroxylamine ligand of **16**. NOEs were observed between $\text{N}-\text{CH}_3$ ($\delta = 2.49$ ppm) and $\text{Ti}-\text{CH}_3$ ($\delta = 0.46$ ppm), between $\text{N}-\text{C}(\text{CH}_3)_3$ ($\delta = 0.46$ ppm), and between $\text{Ti}-\text{CH}_3$ and $\text{N}-\text{C}(\text{CH}_3)_3$ and $(\text{C}_6\text{F}_5)_3\text{B}-\text{CH}_3$ ($\delta = 0.89$ ppm). The absence of an NOE between $\text{N}-\text{CH}_3$ and $(\text{C}_6\text{F}_5)_3\text{B}-\text{CH}_3$ suggests that the $[\text{MeB}(\text{C}_6\text{F}_5)_3]^-$ counterion binds strongly and selectively *syn* to the ^iBu group. Similarly, the reaction of **9** with $[\text{Ph}_3\text{C}]^+[\text{B}(\text{C}_6\text{F}_5)_4]^-$ in d_5 -chlorobenzene results in the clean

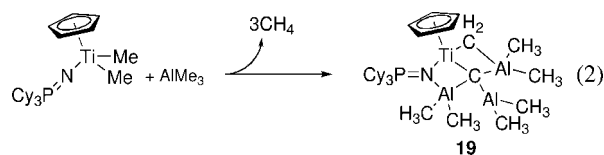
Scheme 4. Activation of **5** with $B(C_6F_5)_3$ 

abstraction of one methyl group from the titanium center with the elimination of Ph_3CMe to yield $[Cp^*Ti(Me)(ON^iBu(Me))]^+[B(C_6F_5)_4]^-$, **17**. 1H NMR resonances attributable to Cp^* , ONMe, ON iBu , and TiMe are observed at $\delta = 1.73, 2.57, 0.55,$ and 0.50 ppm, respectively. 1H gROESY NMR and $^1H-^{15}N$ HMBC NMR spectroscopy confirm that the hydroxylamino ligand remains η^2 bound to the titanium in **17** (^{15}N $\delta = 153$ ppm). Examination of the ^{19}F NMR spectrum of **17** indicates that there is no interaction between the titanium cation and aryl groups of the borate counterion.^{65,66}

Activation of $Cp^*Ti(Me)_2(TEMPO)$, **5**, with $B(C_6F_5)_3$ also results in the clean formation of the bridged zwitterionic titanium- μ -methylborate species **18**, which has undergone C–H activation of one of the methyl groups of the TEMPO ligand (Scheme 4). The 1H NMR spectrum reveals the evolution of methane, and three singlets at $\delta = 0.86, 0.65,$ and 0.50 ppm attributable to three TEMPO methyl signals and a doublet of doublet resonance are observed at $\delta = 0.80$ and -0.59 ppm with $^2J_{H-H}$ splitting constant = 11.4 Hz for the diastereotopic methylene resonances. The 1H NMR shifts of these resonances are comparable to those observed for the recently reported C–H activation of one methyl group on TEMPO upon the reaction of $(TEMPO)Ti(CH_2Ph)_3$ with $B(C_6F_5)_3$.⁵¹ Thus, upon activation of **5**, the zwitterionic product undergoes rapid C–H activation from one TEMPO-methyl group to result in the formation of $[Cp^*Ti(\kappa^2-ON(C(Me)_2(CH_2)_3C(Me)CH_2))]^+[MeB(C_6F_5)_3]^-$, **18** (Scheme 4). 1H gROESY NMR data support this conclusion. Analysis of **18** using $^1H-^{15}N$ HMBC NMR reveals a ^{15}N resonance at $\delta = 163$ ppm. Though this is slightly downfield of other ^{15}N resonances for η^2 -bound hydroxylamino ligands, this is indicative of an η^2 binding of the hydroxylamino ligand in this complex. Our polymerization studies imply that despite the C–H activation mechanism, **18** is still able to initiate the polymerization of propylene.

Reaction of $[Cp^*Ti(Me)(ON^iBu(Me))]^+[B(C_6F_5)_4]^-$ with Alkylaluminum Complexes. Our investigations on the reactivity of the neutral complexes **5**, **8**, and **9** with trialkylaluminum reagents reveal that the hydroxylamino ligands do not readily transmetalate, but rather form stable adducts. However the cations derived from these complexes are much more reactive toward alkylaluminum reagents. The cation $[Cp^*Ti(Me)(ON^iBu(Me))]^+[B(C_6F_5)_4]^-$, **17**, began to degrade immediately upon addition of the Al^iBu_3 to give a mixture of isobutylene and other unidentified products. Resonances due to the hydroxylamine decrease rapidly, suggesting the decomposition pathway may involve loss of the nitroxide ligand via transmetalation. After 2 h, complete decomposition occurs. Addition of $AlMe_3$ to the cation **17** also results in decomposition, but the reaction occurs more slowly and depends on the Al/Ti stoichiometry. With 1 equiv of $AlMe_3$ only two-thirds of the cation was consumed, suggesting that more than 1 equiv of $AlMe_3$ is participating in

this reaction. Of the cation that reacted, no signals attributable to the hydroxylamine could be observed, and for each hydroxylamine consumed, approximately half an equivalent of methane is generated. After 2 h, complete decomposition occurs to unidentified products. Addition of 2 equiv of $AlMe_3$ results in complete disappearance of resonances due to the hydroxylamine ligand along with the liberation of approximately 1 equiv of methane. These results suggest that the hydroxylamine ligands of the cationic species are much more reactive toward trialkylaluminums and likely undergo rapid transfer to the aluminum species along with activation of either the Al–Me or Ti–Me bonds to liberate methane. The rate of decomposition of these complexes appears to be sensitive to both the nature of the activator and the alkylaluminum. We were unable to characterize the organometallic products of these reactions, but the liberation of methane is analogous to the reactivity observed by Piers³² and Stephan,⁴⁵ where $CpTi(Me)_2(NPCy_3)$ reacts with 3 equiv of $AlMe_3$ to generate the carbide complexes $CpTi(\mu^2-Me)(\mu^2-NPCy_3)(\mu^4-C)(AlMe_2)_3$, **19**, along with the liberation of methane (eq 2).



Summary

We have synthesized a variety of Cp^*Ti (hydroxylamino) catalysts via several different synthetic routes. These complexes show a high activity toward the polymerization of propylene in the presence of $[Ph_3C]^+[B(C_6F_5)_4]^-$ and Al^iBu_3 and show a lower activity in both the $B(C_6F_5)_3/Al^iBu$ and MAO catalyst systems. In contrast, these complexes are inactive toward the polymerization of propylene in the presence of $[Ph_3C]^+[B(C_6F_5)_4]^-$ and $AlMe_3$. The interaction of $AlMe_3$ with $Cp^*Ti(Me)_2(ONEt_2)$ led to the formation of $Cp^*Ti(Me)_2(\eta^2-O(AlMe_3)NEt_2)$, while Al^iBu_3 was found to bind more weakly to $Cp^*Ti(Me)_2(ONEt_2)$ than $AlMe_3$. Reaction of $Cp^*Ti(Me)_2(ONEt_2)$ and $Cp^*Ti(Me)_2(ON^iBu(Me))$ with $B(C_6F_5)_3$ resulted in clean formation of the zwitterionic contact ion pairs $[Cp^*Ti(Me)(\eta^2-ONEt_2)]^+[MeB(C_6F_5)_3]^-$ and $[Cp^*Ti(Me)(\eta^2-ON^iBu(Me))]^+[MeB(C_6F_5)_3]^-$, respectively, whereas reaction of $Cp^*Ti(Me)_2(\eta^2-ON^iBu(Me))$ with $[Ph_3C]^+[B(C_6F_5)_4]^-$ resulted in the clean formation of the solvent-separated ion pair $[Cp^*Ti(Me)(\eta^2-ON^iBu(Me))]^+[B(C_6F_5)_4]^-$. However, addition of Al^iBu_3 or $AlMe_3$ to the cationic $[Cp^*Ti(Me)(ON^iBu(Me))]^+[B(C_6F_5)_4]^-$ resulted in decomposition of the cations, likely through rapid transfer of the aluminum species and activation of either the Al–Me or Ti–Me bond to eliminate methane. These results suggest that the hydroxylamine ligands of the cationic species are much more reactive toward trialkylaluminums than those in the neutral complex.

Experimental Section

General Considerations. All reactions were performed under a nitrogen atmosphere, using either standard Schlenk techniques or a dinitrogen-filled glovebox. All solvents and reagents were purchased from Aldrich unless otherwise stated. Pentane and toluene were passed through purification columns packed with activated alumina and copper catalyst, and diethyl ether was passed through a purification column packed with activated alumina. 2-Methyl-2-nitrosopropane was sublimed and then recrystallized from dry diethyl ether prior to use. Diethylhydroxylamine was distilled from

(65) Krossing, I.; Raabe, I. *Angew. Chem., Int. Ed.* **2004**, *43*, 2066–2090.

(66) Jia, L.; Yang, X. M.; Stern, C. L.; Marks, T. J. *Organometallics* **1997**, *16*, 842–857.

potassium hydride. Propylene was purchased from Matheson TriGas (Research Purity) and passed through a purification column packed with activated alumina and copper catalyst. Cp*TiCl₃, **1**, was purchased from Strem, and Cp*TiMe₃, **7**, was prepared by a literature procedure.⁶⁷ Cp*HfCl₃ was purchased from Strem, and Cp*HfMe₃ was prepared by a literature procedure.⁶⁸ Triphenylcarbenium tetrakis(pentafluorophenyl)borate and tris(pentafluorophenyl)borane were kindly donated by Albermarle Corporation. Triphenylcarbenium tetrakis(pentafluorophenyl)borate was reprecipitated from a dichloromethane/pentane mixture, and tris(pentafluorophenyl)borane was recrystallized from a saturated pentane solution at -50 °C. Modified methylaluminoxane (type IV) was purchased from Akzo Nobel as a solution in toluene; before use, the volatile materials were removed *in vacuo* to yield a powdery solid.

Physical Methods. NMR spectra were recorded using a Varian UI-600, UI-500, UI-400, or UI-300 spectrometer and referenced to the residual proton peaks (C₆D₆ = δ 7.15 ppm). ¹³C NMR spectra for polymer analysis were obtained at 75.4 MHz using a 10 mm broadband probe operating at 100 °C. Samples were prepared as solutions of ca. 80 mg polymer in 2.5 mL of 90:10 (v/v) 1,2-dichlorobenzene/benzene-*d*₆ containing ca. 2 mg of chromium(III) acetylacetonate as a spin relaxation agent. An inverse-gated decoupled pulse sequence was used. GPC measurements were taken using a Waters GPC using THF as an eluent. The samples were analyzed through a Waters Styragel HR5E, HR4 and two HR2 columns and analyzed using a Waters 410 differential refractometer. The molecular weight of the samples was determined by comparison to PS standards between 1.25 × 10³ and 2.95 × 10⁶ g/mol using Millenium v3.2. Elemental analyses were performed at Atlantic Microlabs Ltd. Kinetic measurements were made by drawing gas from a ballast vessel of known pressure, volume, and temperature, and results were extrapolated using a previously determined method.⁶³

General Polymerization Procedures. Liquid Propylene Polymerizations. In a 300 mL stainless steel Parr reactor a solution of 60 mg of AlⁱBu₃ (0.30 mmol) in 8 mL of toluene was equilibrated for 30 min at 20 °C with 90 mL of liquid propylene. A solution of catalyst in toluene (1 mL) was injected into the reactor followed by a solution of trityl borate (1 mL) via argon pressure. The polymerization was run for 20 min and quenched by addition of methanol (10 mL). The polymer was precipitated from acidified methanol, filtered, washed with methanol, and dried under vacuum at 60 °C. **Solution Propylene Polymerizations, Kinetic Studies.** In a 300 mL stainless steel Parr reactor a solution of 60 mg of AlⁱBu₃ (0.30 mmol) in 98 mL of toluene was equilibrated for 30 min at 20 °C. A solution of catalyst in toluene (1 mL) was injected into the reactor followed by a solution of trityl borate (1 mL) via a small vent (1–2 psig) and injection with propylene pressure. The polymerization was run for 1 h and quenched by addition of methanol (10 mL). The polymer was precipitated from acidified methanol, filtered, washed with methanol, and dried under vacuum at 60 °C.

Synthesis of Cp*Ti(Cl)₂(ONeT₂) (4). *n*-Butyl lithium (2.5 M in hexanes, 1.36 mL, 3.40 mmol) was added dropwise to a stirred solution of HONeT₂ (0.35 mL, 3.40 mmol) in toluene (50 mL) at 0 °C. The solution was stirred for ca. 30 min before addition to a rapidly stirred suspension of Cp*TiCl₃ (0.99 g, 3.40 mmol) in toluene (70 mL) at -78 °C. The solution was stirred for 4 h at room temperature before being filtered and reduced under vacuum to yield an orange solid (0.94 g, 3.22 mmol, 94.7%). Crystals were grown from a saturated pentane solution at -30 °C.

¹H NMR (C₆D₆, 500 MHz): δ 3.10, 3.06 (ddq, ONCH₂CH₃, ³J_{H-H} = 6.3, 6.5, 7.0, 7.3 Hz, ²J_{H-H} = 13.9, 14.0 Hz, 4H), 1.97 (s, C₅(CH₃)₅, 15H), 0.94 (t, ONCH₂CH₃, ³J_{H-H} = 7.3 Hz, 6H). ¹³C{¹H} NMR (C₆D₆, 500 MHz): δ 129.4 (C₅(CH₃)₅), 51.0 (ON CH₂CH₃), 12.2 (C₅(CH₃)₅), 10.2 (ONCH₂CH₃). ¹⁵N NMR (C₆D₆, 600 MHz): δ 143. Anal. Calcd for C₁₄H₂₅ONTiCl₂ (found): C, 49.13 (49.80); H, 7.37 (7.36); N, 4.09 (4.34).

Synthesis of Cp*Ti(Me)₂(ONeT₂) (8). HONeT₂ (0.35 mL, 3.4 mmol) was added dropwise to a stirred solution of Cp*TiMe₃ (0.78 g, 3.4 mmol) in pentane (70 mL) at 0 °C. The solution was stirred for 4 h before being reduced under vacuum to yield a yellow oil. The oil was washed in 10 mL of pentane at -78 °C and yielded a yellow solid (0.78 g, 2.6 mmol, 76%). Crystals were grown from a saturated pentane solution at -30 °C.

¹H NMR (C₆D₅CD₃, 300 MHz): δ 3.16, 3.00 (ddq, ONCH₂CH₃, ³J_{H-H} = 6.8, 7.3 Hz, ²J_{H-H} = 13.5 Hz, 4H), 1.86 (s, C₅(CH₃)₅, 15H), 1.07 (t, ONCH₂CH₃, ³J_{H-H} = 7.2 Hz, 6H), 0.05 (s, TiCH₃, 6H). ¹³C{¹H} NMR (C₆D₆, 500 MHz): δ 120.2 (C₅(CH₃)₅), 51.4 (ON CH₂CH₃), 46.6 (TiCH₃), 11.3 (C₅(CH₃)₅), 9.8 (ONCH₂CH₃). ¹⁵N NMR (C₆D₆, 600 MHz): δ 129. Anal. Calcd for C₁₆H₃₁ONTi (found): C, 63.78 (63.72); H, 10.37 (10.34); N, 4.65 (4.61).

Synthesis of Cp*Ti(Me)₂(ONⁱBu(Me)) (9). A solution of 2-nitroso-2-methylpropane (0.39 g, 4.5 mmol) in pentane (20 mL) was added slowly to a stirred solution of Cp*TiMe₃ (1.00 g, 4.4 mmol) in pentane (70 mL) at 0 °C. The solution was stirred for 4 h before being reduced under vacuum to yield a pale yellow solid (0.97 g, 3.1 mmol, 70%). X-ray quality crystals were grown from a saturated pentane solution at -30 °C.

¹H NMR (C₆D₆, 500 MHz): δ 2.88 (s, ONCH₃, 3H), 1.87 (s, C₅(CH₃)₅, 15H), 1.06 (s, ONC(CH₃)₃, 9H), 0.47, -0.03 (s, TiCH₃, 3H). ¹³C{¹H} NMR (C₆D₆, 500 MHz): δ 120.5 (C₅(CH₃)₅), 62.9 (ONC(CH₃)₃), 52.4, 44.3 (Ti CH₃), 43.7 (ON CH₃), 26.4 (ONC(CH₃)₃), 11.5 (C₅(CH₃)₅). ¹⁵N NMR (C₆D₆, 600 MHz): δ 134. Anal. Calcd for C₁₇H₃₃ONTi (found): C, 64.75 (64.56); H, 10.55 (10.58); N, 4.44 (4.49).

Synthesis of Cp*Hf(Me)₂(ONⁱBu(Me)) (10). A solution of 2-nitroso-2-methylpropane (0.081 g, 0.93 mmol) in pentane (10 mL) was added slowly to a stirred solution of Cp*HfMe₃ (0.33 g, 0.93 mmol) in pentane (20 mL) at 0 °C. The solution was stirred for 4 h before being reduced under vacuum to yield a white solid (0.27 g, 0.61 mmol, 66%). Crystals were grown from a saturated pentane solution at -30 °C.

¹H NMR (C₆D₆, 500 MHz): δ 2.64 (s, ONCH₃, 3H), 1.97 (s, C₅(CH₃)₅, 15H), 0.98 (s, ONC(CH₃)₃, 9H), -0.035, -0.28 (s, HfCH₃, 3H). ¹³C{¹H} NMR (C₆D₆, 500 MHz): δ 117.1 (C₅(CH₃)₅), 61.9 (ONC(CH₃)₃), 44.4, 42.8 (HfCH₃), 40.9 (ONCH₃), 25.7 (ONC(CH₃)₃), 10.9 (C₅(CH₃)₅). Anal. Calcd for C₁₇H₃₃ONHf (found): C, 45.79 (45.50); H, 7.46 (7.43); N, 3.14 (2.99).

Synthesis of Cp*Ti(Me)₂(O(AlMe₃)NEt₂) (11). A solution of AlMe₃ (0.1 g, 1.43 mmol) in pentane (15 mL) was added dropwise to a stirred solution of **8** (0.43 g, 1.43 mmol) in pentane (30 mL) in a drybox. The solution was removed from the drybox and stirred for 20 min before being reduced under vacuum to yield a yellow solid (0.44 g, 1.18 mmol, 82.5%). Crystals were grown from a saturated pentane solution at -30 °C.

¹H NMR (C₆D₆, 500 MHz): δ 3.51, 2.90 (ddq, ONCH₂CH₃, ³J_{H-H} = 13.9, 14.1 Hz, ²J_{H-H} = 6.8, 7.0 Hz, 4H), 1.74 (s, C₅(CH₃)₅, 15H), 0.85 (t, ONCH₂CH₃, ³J_{H-H} = 7.3 Hz, 6H), 0.48 (s, Ti CH₃, 6H), -0.21 (s, Al(CH₃)₃, 9H). ¹³C{¹H} NMR (C₆D₆, 500 MHz): δ 123.9 (C₅(CH₃)₅), 62.06 (TiCH₃), 53.6 (ONCH₂CH₃), 12.1 (C₅(CH₃)₅), 11.2 (ONCH₂CH₃), -4.0 (Al(CH₃)₃).

NMR Scale Synthesis of Cp*Ti(Me)₂(O(AlⁱBu₃)NEt₂). ¹H NMR (C₆D₆, 500 MHz): δ 3.30, 3.01 (ddq, ONCH₂CH₃, ³J_{H-H} = 7.5 Hz, ²J_{H-H} = 13.5 Hz, 4H), 2.11 (sept, AlCH₂CH(CH₃)₂, ³J_{H-H} = 13.5 Hz, 3H), 1.81 (s, C₅(CH₃)₅, 15H), 1.18 (d, AlCH₂CH(CH₃)₂,

(67) Mena, M.; Royo, P.; Serrano, R.; Pellinghelli, M. A.; Tiripicchio, A. *Organometallics* **1989**, *8*, 476–482.

(68) Schock, L. E.; Marks, T. J. *J. Am. Chem. Soc.* **1988**, *110*, 7701–7715.

$^3J_{\text{H-H}} = 6.6$ Hz, 6H), 0.93 (t, ONCH_2CH_3 , $^3J_{\text{H-H}} = 7.2$ Hz, 6H), 0.31 (s, Ti CH_3 , 6H), 0.30 (d, $\text{AlCH}_2\text{CH}(\text{CH}_3)_2$, $^3J_{\text{H-H}} = 9.6$ Hz, 6H).

Synthesis of $[\text{Cp}^*\text{Ti}(\text{Me})(\text{ON}^i\text{Bu}(\text{Me}))]^+[\text{MeB}(\text{C}_6\text{F}_5)_3]^-$ (16**).** A solution of $\text{B}(\text{C}_6\text{F}_5)_3$ (0.54 g, 1.05 mmol) in pentane (10 mL) was added slowly to a stirred solution of **9** (0.34 g, 1.07 mmol) in pentane (50 mL) at 0 °C. The solution was stirred for 1 h before the colorless solution was filtered from the orange precipitate. The solid was dried *in vacuo* (0.785 g, 0.95 mmol, 90.4%).

^1H NMR ($\text{C}_6\text{D}_5\text{CD}_3$, 500 MHz): δ 2.49 (s, ONCH_3 , 3H), 1.50 (s, $\text{C}_5(\text{CH}_3)_5$, 15H), 0.88 (br s, CH_3BAR_3 , 3H), 0.46 (s, $\text{ONC}(\text{CH}_3)_3$, 9H), 0.46 (s, Ti CH_3 , 3H). $^{13}\text{C}\{^1\text{H}\}$ NMR ($\text{C}_6\text{D}_5\text{CD}_3$, 500 MHz): δ 150.2, 147.0, 140.8, 139.2, 137.7, 135.7 (CAr) 137.3 ($\text{C}_5(\text{CH}_3)_5$), 71.2 ($\text{ONC}(\text{CH}_3)_3$), 63.9 (Ti CH_3), 42.8 (ONCH_3), 24.4 ($\text{ONC}(\text{CH}_3)_3$), 15.1 (br CH_3BAR_3), 11.3 ($\text{C}_5(\text{CH}_3)_5$). ^{15}N NMR ($\text{C}_6\text{D}_5\text{CD}_3$, 600 MHz): δ 153. ^{19}F NMR (C_6D_6 , 400 MHz): δ -132.9, -160.6, -165.3 ($\text{CH}_3\text{B}(\text{C}_6\text{F}_5)_3$). Anal. Calcd for $\text{C}_{35}\text{H}_{33}\text{ONTiF}_{15}\text{B}$ (found): C, 50.78 (48.94); H, 4.02 (3.93); N, 1.69 (1.86).

NMR Scale Activations. The borane and titanium complexes were combined in ca. 0.6 mL of C_6D_6 , $\text{C}_6\text{D}_5\text{CD}_3$, or $\text{C}_6\text{D}_5\text{Cl}$ in a scintillation vial before being transferred to a J-Young NMR tube. Spectra were collected immediately.

$[\text{Cp}^*\text{Ti}(\text{Me})(\text{ONe}t_2)]^+[\text{MeB}(\text{C}_6\text{F}_5)_3]^-$ (15**).** ^1H NMR ($\text{C}_6\text{D}_5\text{CD}_3$, 600 MHz): δ 2.89, 2.56 (br s, ONCH_2CH_3 , 4H), 1.46 (s, $\text{C}_5(\text{CH}_3)_5$, 15H), 0.73 (br s, CH_3BAR_3 , 3H), 0.62 (br s, ONCH_2CH_3 , 6H), 0.45 (s, Ti CH_3 , 3H).

$[\text{Cp}^*\text{Ti}(\text{Me})(\text{ON}^i\text{Bu}(\text{Me}))]^+[\text{B}(\text{C}_6\text{F}_5)_4]^-$ (17**).** ^1H NMR ($\text{C}_6\text{D}_5\text{Cl}$, 600 MHz): δ 6.97–7.15 (m, Ar, 15H), 2.57 (s, ONCH_3 , 3H), 1.73 (s, $\text{C}_5(\text{CH}_3)_5$, 15H), 0.55 (s, $\text{ONC}(\text{CH}_3)_3$, 9H), 0.50 (s, Ti CH_3 , 3H).

$^{13}\text{C}\{^1\text{H}\}$ NMR ($\text{C}_6\text{D}_5\text{Cl}$, 600 MHz): δ 149.3–125.8, (Ar), 125.6 ($\text{C}_5(\text{CH}_3)_5$), 74.2 ($\text{ONC}(\text{CH}_3)_3$), 65.0 (Ti CH_3), 43.3 (ONCH_3), 30.5 ($\text{ONC}(\text{CH}_3)_3$), 11.5 ($\text{C}_5(\text{CH}_3)_5$). ^{15}N NMR ($\text{C}_6\text{D}_5\text{Cl}$, 600 MHz): δ 153. ^{19}F NMR ($\text{C}_6\text{D}_5\text{Cl}$, 400 MHz): δ -132.2, -162.7, -166.6.

$[\text{Cp}^*\text{Ti}(\text{Me})(\text{TEMPO})]^+[\text{MeB}(\text{C}_6\text{F}_5)_3]^-$ (18**).** ^1H NMR (C_6D_6 , 600 MHz): 1.51 (s, $\text{C}_5(\text{CH}_3)_5$, 15H), 1.39–1.10 (m, CH_2 , 6H), 1.09 (br s, CH_3BAR_3 , 3H), 0.86, 0.65, 0.50 (s, TEMPO- CH_3 , 3H), 0.80, -0.59 (dd, TEMPO- CH_2Ti , 2H). ^{15}N NMR (C_6D_6 , 600 MHz): δ 162.

Crystal Data for 17. See Supporting Information for details: $\text{C}_{19}\text{H}_{40}\text{AlNOTi}$, $M = 373.4$, rhombic, $a = 9.143(1)$, $b = 18.171(1)$, $c = 13.708(1)$ Å, $U = 2253.8(2)$ Å³, $T = 166$ K, space group $P21/n$, $Z = 4$, $\mu(0.71073$ Å radiation) 0.42 cm⁻¹, 13 110 reflections measured, 4601 unique ($R_{\text{int}} = 0.0261$), which were used in all calculations, residuals: R_1 ; wR_2 0.0368; 0.1011.

Acknowledgment. We acknowledge the NSF (CHE-0611563) for financial support. Albermarle Inc. is thanked for their donation of borate activators. Dr. Stephen Lynch is gratefully acknowledged for assistance with NMR measurements. We thank Dr. Frederick J. Hollander and Allen G. Oliver of the UC Berkeley Diffraction Facility (CHEXRAY) for collection of X-ray diffraction data.

Supporting Information Available: A CIF file and crystallographic details for **17** are available free of charge via the Internet at <http://pubs.acs.org>.

OM800571J

Star-Shaped Silacyclobutene-Containing π -Systems: Synthesis and Optical Properties

Junhui Liu,[†] Shaoguang Zhang,^{†,‡} Wen-Xiong Zhang,[†] and Zhenfeng Xi^{*,†}

Beijing National Laboratory for Molecular Sciences (BNLMS), Key Laboratory of Bioorganic Chemistry and Molecular Engineering of Ministry of Education, College of Chemistry, Peking University, Beijing 100871, People's Republic of China, and School of Chemical Engineering and Environment, Beijing Institute of Technology, Beijing 100081, People's Republic of China

Received September 1, 2008

Well-defined π -conjugated systems containing two or three silacyclobutene units have been synthesized in high yields via regioselective coupling of bis(phenylethynyl)silanes with dialkynylbenzene or trialkynylbenzene in the presence of $\text{Cp}_2\text{ZrBu}^n_2$ (Negishi reagent). The UV–vis absorption and fluorescence spectra of these new π -conjugated systems have demonstrated that the increase in silacyclobutene units per molecule from two or three brings about an increase of the extinction coefficient.

The continued activity in developing new π -conjugated organic materials has been spurred on by an interest in their applications in organic electronics and optoelectronics. One crucial issue in their molecular designs is how to tune their electronic structures in order to produce desirable photophysical and electronic properties. In this regard, increasing attention has been paid to the π -electron systems containing main-group elements, wherein the orbital interaction between the main-group-element units with the π -conjugated organic framework plays a crucial role in producing varied electronic structures.¹

Theoretical calculations revealed that unsaturated silacycles, such as siloles and silacyclobutenes, could have an unusually high electron affinity.² These silacycles can exhibit strong photoluminescence emission in the solid state as well as a strong aggregation-induced photoluminescence, which is a favored characteristic for various photonic and optoelectronic applications.³ Siloles as the core or side groups have been incorporated

into starburst and dendrimer-type molecules very recently.⁴ However, incorporation of silacyclobutene units into well-defined π -conjugated systems has not yet been developed.^{3a} In view of our interest in unsaturated silacycles,⁵ we tried to develop synthetic methods for well-defined π -conjugated systems containing silacyclobutene units, with the expectation of finding interesting and useful properties for applications in organic electronics and optoelectronics. Herein we report a synthetic method for well-defined benzene-based π -conjugated systems containing two or three silacyclobutene units, by using low-valent zirconocene chemistry. Their optical properties have also been preliminarily studied.

Results and Discussion

The regioselective coupling of alkynes mediated by zirconocene is an important carbon–carbon bond formation reaction. For example, Tilley and co-workers have shown coupling of diynes with zirconocene as an efficient route to new macrocycles,⁶ oligomers,⁷ and polymers.⁸ Takahashi and co-workers have developed the synthesis of alkylidenesilacyclobutenes **3** from bis(alkynyl)silanes **1** (Scheme 1).⁹ Rosenthal and others also have reported such reaction chemistry of

* To whom correspondence should be addressed. E-mail: zfxi@pku.edu.cn. Tel/fax: (+86)10-62759728.

[†] Peking University.

[‡] Beijing Institute of Technology.

(1) (a) Yamaguchi, S.; Tamao, K. *The Chemistry of Organic Silicon Compounds*; Rappoport, Z., Apeloig, Y., Eds.; Wiley: Chichester, U.K., 2001; pp 641–694. (b) Hissler, M.; Dyer, P. W.; Réau, R. *Coord. Chem. Rev.* **2003**, *244*, 1–44. (c) Baumgartner, T.; Réau, R. *Chem. Rev.* **2006**, *106*, 6481–4727. (d) Lo, S.-C.; Burn, P. L. *Chem. Rev.* **2007**, *107*, 1097–1116.

(2) (a) Yamaguchi, S.; Tamao, K. *Bull. Chem. Soc. Jpn.* **1996**, *69*, 2327–2334. (b) Yamaguchi, S.; Tamao, K. *J. Chem. Soc., Dalton Trans.* **1998**, 3693–3702. (c) Yu, G.; Yin, S.; Liu, Y.; Chen, J.; Xu, X.; Sun, X.; Ma, D.; Zhan, X.; Peng, Q.; Shuai, Z.; Tang, B.; Zhu, D.; Fang, W.; Luo, Y. *J. Am. Chem. Soc.* **2005**, *127*, 6335–6346.

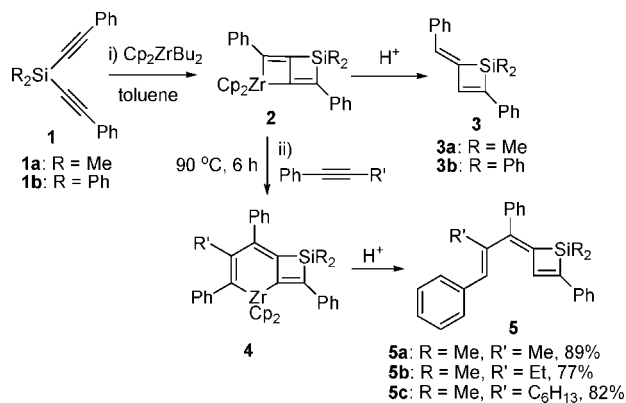
(3) For siloles: (a) Luo, J.; Xie, Z.; Lam, J. W. Y.; Cheng, L.; Chen, H.; Qiu, C.; Kwok, H. S.; Zhan, X.; Liu, Y.; Zhu, D.; Tang, B. Z. *Chem. Commun.* **2001**, 1740–1741. (b) Chen, J.; Law, C. C. W.; Lam, J. W. Y.; Dong, Y.; Lo, S. M. F.; Williams, I. D.; Zhu, D.; Tang, B. Z. *Chem. Mater.* **2003**, *15*, 1535–1546. (c) Chen, J.; Xie, Z.; Lam, J. W. Y.; Law, C. C. W.; Tang, B. Z. *Macromolecules* **2003**, *36*, 1108–1117. (d) Chen, J.; Peng, H.; Law, C. C. W.; Dong, Y.; Lam, J. W. Y.; Williams, I. D.; Tang, B. Z. *Macromolecules* **2003**, *36*, 4319–4327. For silacyclobutenes: (e) Barton, T. J.; Ijadi-Maghsoodi, S.; Pang, Y. *Macromolecules* **1991**, *24*, 1257–1260. (f) Yan, D.; Mohsseni-Ala, J.; Auner, N.; Bolte, M.; Bats, J. W. *Chem. Eur. J.* **2007**, *13*, 7204–7214. (g) Yan, D.; Bolte, M.; Auner, N. J. *Organomet. Chem.* **2008**, *693*, 908–916.

(4) (a) Sanji, T.; Ishiwata, H.; Kaizuka, T.; Tanaka, M.; Sakurai, H.; Nagahata, R.; Takeuchi, K. *Chem. Lett.* **2005**, *34*, 1130–1131. (b) Son, H.-J.; Han, W.-S.; Kim, H.; Kim, C.; Ko, J.; Lee, C.; Kang, S. O. *Organometallics* **2006**, *25*, 766–774.

(5) (a) Yu, T.; Deng, L.; Zhao, C.; Li, Z.; Xi, Z. *Tetrahedron Lett.* **2003**, *44*, 677–679. (b) Sun, X.; Wang, C.; Li, Z.; Zhang, S.; Xi, Z. *J. Am. Chem. Soc.* **2004**, *126*, 7172–7173. (c) Wang, Z.; Fang, H.; Xi, Z. *Tetrahedron Lett.* **2005**, *46*, 499–501. (d) Yu, T.; Sun, X.; Wang, C.; Deng, L.; Xi, Z. *Chem. Eur. J.* **2005**, *11*, 1895–1902. (e) Wang, C.; Luo, Q.; Sun, H.; Guo, X.; Xi, Z. *J. Am. Chem. Soc.* **2007**, *129*, 3094–3095. (f) Liu, J.; Sun, X.; Miyazaki, M.; Liu, L.; Wang, C.; Xi, Z. *J. Org. Chem.* **2007**, *72*, 3137–3140. (g) Liu, J.; Zhang, W.-X.; Guo, X.; Hou, Z.; Xi, Z. *Organometallics* **2007**, *26*, 6812–6820.

(6) (a) Mao, S. S. H.; Liu, F.-Q.; Tilley, T. D. *J. Am. Chem. Soc.* **1998**, *120*, 1193–1206. (b) Nitschke, J. R.; Zürcher, S.; Tilley, T. D. *J. Am. Chem. Soc.* **2000**, *122*, 10345–10352. (c) Nitschke, J. R.; Tilley, T. D. *J. Am. Chem. Soc.* **2001**, *123*, 10183–10190. (d) Nitschke, J. R.; Tilley, T. D. *Angew. Chem., Int. Ed.* **2001**, *40*, 2142–2145. (e) Schafer, L. L.; Tilley, T. D. *J. Am. Chem. Soc.* **2001**, *123*, 2683–2684. (f) Schafer, L. L.; Nitschke, J. R.; Mao, S. S. H.; Liu, F.-Q.; Harder, G.; Haufe, M.; Tilley, T. D. *Chem. Eur. J.* **2002**, *8*, 74–83.

(7) (a) Jiang, B.; Tilley, T. D. *J. Am. Chem. Soc.* **1999**, *121*, 9744–9745. (b) Suh, M. C.; Jiang, B.; Tilley, T. D. *Angew. Chem., Int. Ed.* **2000**, *39*, 2870–2873.

Scheme 1. Zirconocene-Mediated Regioselective Coupling of Bis(phenylethynyl)silanes with Alkynylbenzenes


bis(alkynyl)silanes **1**.¹⁰ We have demonstrated previously that insertion of an alkyne into the zirconacyclobutene–silacyclobutene intermediate **2** occurred to generate the zirconacyclohexadiene–silacyclobutene fused-ring compound **4**; the latter gave a conjugated system containing a silacyclobutene unit (**5**) in high yields upon hydrolysis.^{5d} In order to realize the synthesis of well-defined benzene-based π -conjugated systems containing silacyclobutene units, we first investigated the regiochemistry of such reactions of unsymmetric internal alkynes bearing a phenyl substituent. As shown in Scheme 1, silacyclobutene derivatives **5** with a terminal phenyl ring could all be prepared in high yield by reactions of the respective alkynylbenzene and bis(alkynyl)silanes **1**. The insertion reaction was highly regioselective.

We applied the above method to the synthesis of well-defined benzene-based π -conjugated systems containing two and three silacyclobutene units. The reaction of the 1,4-dialkynylbenzene **6** with a mixture of 2 equiv of a bis(phenylethynyl)silane and Cp₂ZrBu₂ at 90 °C for 6 h proceeded smoothly and highly selectively to afford the 1,4-bis(silacyclobutene)-containing benzene **7** in excellent yield after hydrolysis (Scheme 2). The formation of the 1,4-bis(silacyclobutene)-containing benzene **7b** was confirmed by single-crystal X-ray structure analysis (Figure 1). A similar reaction with the bis(phenylethynyl)silane **1a** and 1,3-dialkynylbenzene **8** led to the 1,3-bis(silacyclobutene)-containing benzene **9** in 90% yield (Scheme 2). Thus, we realized the synthesis of well-defined benzene-based π -conjugated systems containing two silacyclobutene units, in one pot from three components.

Organic π -conjugated systems that have a star shape are an important class of amorphous molecular materials, due to their good processability, transparency, and homogeneous proper-

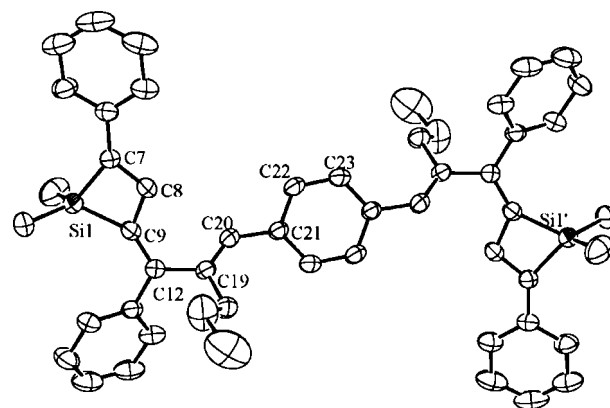


Figure 1. X-ray structure of **7b**.

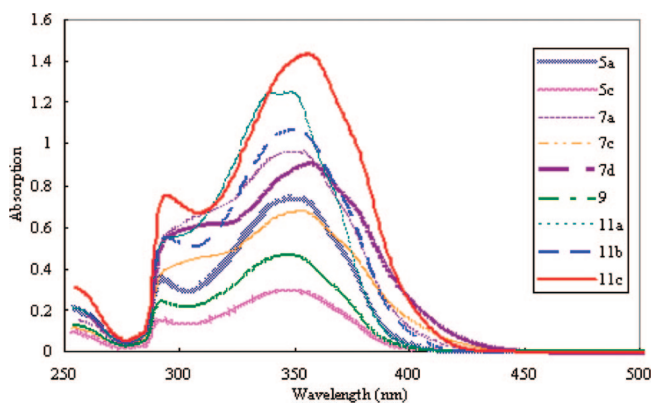


Figure 2. UV-vis absorption spectra of silacyclobutene-containing benzene derivatives.

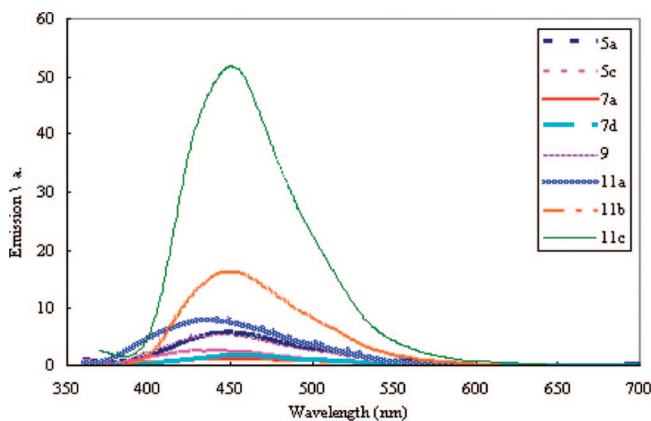


Figure 3. Fluorescence spectra of silacyclobutene-containing benzene derivatives.

(8) (a) Mao, S. S. H.; Tilley, T. D. *Macromolecules* **1997**, *30*, 5566–5569. (b) Lucht, B. L.; Mao, S. S. H.; Tilley, T. D. *J. Am. Chem. Soc.* **1998**, *120*, 4354–4365. (c) Lucht, B. L.; Buretea, M. A.; Tilley, T. D. *Organometallics* **2000**, *19*, 3469–3475. (d) Johnson, S. A.; Liu, F.-Q.; Suh, M. C.; Zürcher, S.; Haufe, M.; Mao, S. S. H.; Tilley, T. D. *J. Am. Chem. Soc.* **2003**, *125*, 4199–4211.

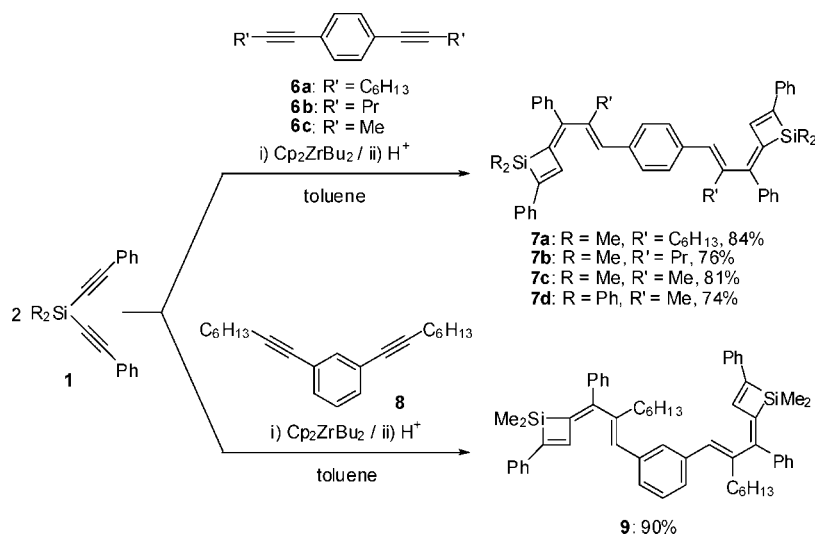
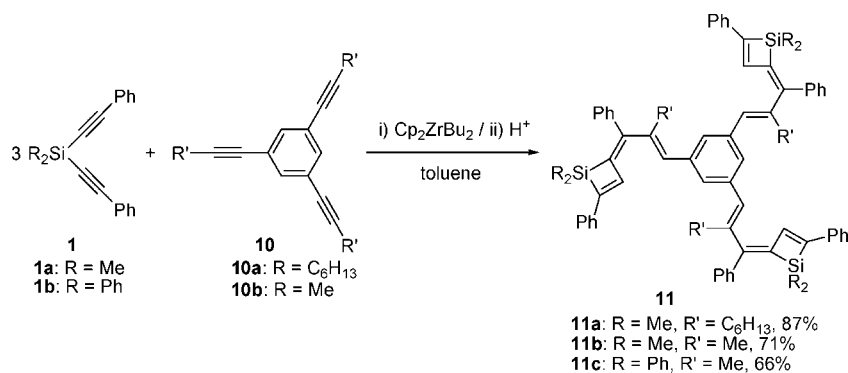
(9) (a) Takahashi, T.; Xi, Z.; Obora, Y.; Suzuki, N. *J. Am. Chem. Soc.* **1995**, *117*, 2665–2666. (b) Xi, Z.; Fischer, R.; Hara, R.; Sun, W.; Obora, Y.; Suzuki, N.; Nakajima, K.; Takahashi, T. *J. Am. Chem. Soc.* **1997**, *119*, 12842–12848.

(10) (a) Pellny, P.-M.; Peulecke, N.; Burlakov, V. V.; Baumann, W.; Spannberg, A.; Rosenthal, U. *Organometallics* **2000**, *19*, 1198–1200. (b) Horáček, M.; Bazyakina, N.; Štepiňka, P.; Gyepes, R.; Čisářová, I.; Bredeau, S.; Meunier, P.; Kubišta, J.; Mach, K. *J. Organomet. Chem.* **2001**, *628*, 30–38. (c) Horáček, M.; Štepiňka, P.; Gyepes, R.; Čisářová, I.; Kubišta, J.; Lukešová, L.; Meunier, P.; Mach, K. *Organometallics* **2005**, *24*, 6094–6103. (d) Jin, C. K.; Yamada, T.; Sano, S.; Shiro, M.; Nagao, Y. *Tetrahedron Lett.* **2007**, *48*, 3671–3675.

ties.¹¹ We then attempted the synthesis of star-shaped 1,3,5-tris(silacyclobutene)benzene derivatives via zirconocene-mediated coupling of bis(phenylethynyl)silanes **1** with 1,3,5-trialkynyl benzenes **10a,b** (Scheme 3). We found that 3 equiv of both bis(phenylethynyl)dimethylsilane **1a** and bis(phenylethynyl)diphenylsilane **1b** could react smoothly with 1 equiv of 1,3,5-trialkynylbenzenes **10a,b** mediated by 3 equiv of Cp₂ZrBu₂, leading to 1,3,5-tris(silacyclobutene)benzenes **11a–c** upon quenching with 3 N HCl (aq) (Scheme 3).

The optical properties of these silacyclobutene-containing π -conjugated systems were the subjects of a preliminary

(11) (a) Shirota, Y. *J. Mater. Chem.* **2000**, *10*, 1–25. (b) Shirota, Y. *J. Mater. Chem.* **2005**, *15*, 75–93.

Scheme 2. One-Pot, Three-Component Coupling Reaction Leading to Benzene-Bridged π -Conjugated Systems Containing Two Silacyclobutene Units**Scheme 3. One-Pot, Four-Component Coupling Reaction Leading to the Synthesis of Star-Shaped π -Conjugated Systems Containing Three Silacyclobutene Units**

investigation. In comparison with silacyclobutenes **3a,b**,^{5f} the absorption spectra of all the silacyclobutene-containing benzene derivatives **5**, **7**, **9**, and **11** are red-shifted only to a small extent. This implies that the delocalization length is not significantly increased from silacyclobutenes **3a,b** to the silacyclobutene-containing benzene derivatives **5**, **7**, **9**, and **11**. However, a clear dependence of the extinction coefficient on the number of silacyclobutene units was observed. For all silacyclobutene-containing benzene derivatives **5**, **7**, **9**, and **11**, the increase in silacyclobutene units brings about an increase of the extinction coefficient (Figure 2).

As illustrated in Figure 3, the fluorescence of silacyclobutene-containing benzene derivatives **11** in cyclohexane solution is slightly shifted to longer wavelengths with much higher intensity. The reason for this phenomenon is probably due to their star-shaped structure.⁴

Conclusions

In summary, a series of π -conjugated organic systems containing two or three silacyclobutene units have been efficiently synthesized via zirconocene-mediated coupling with perfect regioselectivity. In comparison to the simple silacyclobutenes **3a,b**, these bis- or tris(silacyclobutene)-containing benzenes are much better candidates for electronic and optoelectronic applications due to their much larger π system and good physical properties. Further research on functionalized

silacyclobutene-incorporated macromolecules, including their applications, is currently in progress.

Experimental Section

General Methods. The coupling reactions of bis(phenylethynyl)silanes with alkynebenzenes in the presence of Cp_2ZrBu_2 were conducted under a slightly positive pressure of dry and prepurified nitrogen using standard Schlenk techniques. Bis(phenylethynyl)silanes **1a,b** were prepared by reactions of lithium phenylacetylide with dichlorodimethylsilane or dichlorodiphenylsilane. The compounds **5b**,^{5d} **6a**,^{12c,d} **8**,^{12c,d} and **10a**^{12c,d} were prepared according to the literature procedures. Unless otherwise noted, all other chemicals were commercially available and were used without further purification. Toluene was refluxed and distilled from sodium benzophenone ketyl under a nitrogen atmosphere. ¹H and ¹³C NMR spectra were recorded at 300 and 75.4 MHz, respectively, at room temperature, unless otherwise noted. Elemental analysis of all new compounds was performed on an Elementar Vario EL instrument (Germany). UV-vis spectra were recorded on Perkin-Elmer Lambda 35 UV-vis spectra, and PL spectra were conducted on a PerkinElmer LS 55 luminescence spectrometer. MALDI-TOF mass spectra were recorded on a Bruker BIFLEX III time-of-flight (TOF) mass spectrometer (Bruker Daltonics, Billerica, MA).

Typical Procedure for Synthesis of Silacyclobutene-Containing Benzene Derivatives **5a,c from Bis(phenylethynyl)silane **1a** and Alkynebenzenes in the Presence of Cp_2ZrBu_2 .**^{5a,d} To a toluene (8 mL) solution of Cp_2ZrCl_2 (280 mg, 0.96 mmol) at $-78^\circ C$ in a 20 mL Schlenk tube was added dropwise *n*-BuLi (1.92

mmol, 1.6 M, 1.2 mL) with a syringe. After the addition was complete, the reaction mixture was stirred at $-78\text{ }^{\circ}\text{C}$ for 1 h. Then 0.96 mmol of bis(phenylethynyl)silane **1a** was added, and the reaction mixture was warmed gradually to room temperature and stirred at this temperature for 1 h. After 0.96 mmol of alkynylbenzene was added, the reaction mixture was heated at $90\text{ }^{\circ}\text{C}$ for 6 h. The resulting solution was cooled to room temperature and quenched with 3 N HCl. The organic layer was washed successively with water and brine and then dried over MgSO_4 . After evaporation of the solvent, column chromatography (silica gel, hexane/ether = 50:1) afforded **5**.

5a: colorless oil, isolated yield 89% (322 mg). ^1H NMR (CDCl_3 , Me_4Si): δ 0.52 (s, 6H, CH_3), 2.06 (s, 3H, CH_3), 6.57 (s, 1H, CH), 7.20–7.45 (m, 15H, CH), 7.99 (s, 1H, CH). ^{13}C NMR (CDCl_3 , Me_4Si): δ -0.61 (2 CH_3), 18.87 (1 CH_3), 126.43 (1 CH), 126.80 (1 CH), 126.85 (2 CH), 127.06 (2 CH), 127.63 (1 CH), 128.19 (2 CH), 128.22 (2 CH), 128.58 (2 CH), 129.09 (2 CH), 130.88 (1 CH), 137.26 (1 quart C), 137.38 (1 quart C), 138.05 (1 quart C), 141.73 (1 quart C), 142.76 (1 quart C), 143.88 (1 quart C), 147.86 (1 CH), 158.43 (1 quart C). HRMS: m/z calcd for $\text{C}_{27}\text{H}_{26}\text{Si}$ 378.1804, found 378.1801. Anal. Calcd for $\text{C}_{27}\text{H}_{26}\text{Si}$: C, 85.66; H, 6.92. Found: C, 85.82; H, 6.81.

5c: white solid, isolated yield 82% (352 mg). ^1H NMR (CDCl_3 , Me_4Si): δ 0.53 (s, 6H, CH_3), 0.80 (t, $J = 6.9$ Hz, 3H, CH_3), 1.15–1.45 (m, 8H, CH_2), 2.36 (t, $J = 6.9$ Hz, 2H, CH_2), 6.55 (s, 1H, CH), 7.29–7.41 (m, 15H, CH), 7.97 (s, 1H, CH). ^{13}C NMR (CDCl_3 , Me_4Si): δ -0.52 (2 CH_3), 14.04 (1 CH_3), 22.56 (1 CH_2), 28.34 (1 CH_2), 29.27 (1 CH_2), 30.54 (1 CH_2), 31.57 (1 CH_2), 126.46 (1 CH), 126.79 (1 CH), 126.85 (2 CH), 126.99 (2 CH), 127.60 (1 CH), 128.19 (2 CH), 128.25 (2 CH), 128.60 (2 CH), 128.88 (2 CH), 130.61 (1 CH), 137.47 (1 quart C), 138.01 (1 quart C), 141.76 (1 quart C), 142.42 (1 quart C), 142.86 (1 quart C), 144.00 (1 quart C), 148.11 (1 CH), 158.17 (1 quart C). HRMS: m/z calcd for $\text{C}_{32}\text{H}_{36}\text{Si}$ 448.2586, found 448.2584. Anal. Calcd for $\text{C}_{32}\text{H}_{36}\text{Si}$: C, 85.65; H, 8.09. Found: C, 85.54; H, 8.22.

Synthesis of 1,4-Dipentynylbenzene (6b).¹² To a solution of 1,4-diiodobenzene (330 mg, 1.0 mmol) in 10 mL of THF were added CuI (40 mg, 0.2 mmol), Pd(PPh₃)₂Cl₂ (30 mg, 0.04 mmol), 1-pentyne (236 μL , 2.4 mmol), and 10 mL of Et₃N at room temperature, and this mixture was stirred for 4 h. The solution was quenched by a saturated aqueous solution of ammonium chloride. The organic layer was washed successively with water and brine and then dried over MgSO_4 . After evaporation of the solvent, column chromatography (silica gel, hexane) afforded **6b**.

6b: white solid, isolated yield 90% (189 mg). ^1H NMR (CDCl_3 , Me_4Si): δ 1.04 (t, $J = 7.5$ Hz, 6H, CH_3), 1.56–1.68 (m, 4H, CH_2), 2.38 (t, $J = 6.9$ Hz, 4H, CH_2), 7.30 (s, 4H, CH). ^{13}C NMR (CDCl_3 , Me_4Si): δ 13.57 (2 CH_3), 21.46 (2 CH_2), 22.18 (2 CH_2), 80.53 (2 quart C), 91.73 (2 quart C), 123.17 (2 quart C), 131.35 (4 CH). HRMS: m/z calcd for $\text{C}_{16}\text{H}_{18}$ 210.1409, found 210.1402. Anal. Calcd for $\text{C}_{16}\text{H}_{18}$: C, 91.37; H, 8.63. Found: C, 91.27; H, 8.71.

Synthesis of 1,4-Dipropynylbenzene (6c).¹² To a solution of anhydrous zinc bromide (326 mg, 2.4 mmol) in 10 mL of THF was added dropwise 1-propynylmagnesium bromide (0.5 M, THF, 4.8 mL) at $0\text{ }^{\circ}\text{C}$ followed by Pd(PPh₃)₄ (86 mg, 0.08 mmol) and 1,4-diiodobenzene (330 mg, 1.0 mmol). The cooling bath was removed, the reaction mixture was heated at $50\text{ }^{\circ}\text{C}$ for 4 h, and the solution was cooled to room temperature and quenched by a saturated aqueous solution of ammonium chloride. The organic layer was washed successively with water and brine and then dried over MgSO_4 . After evaporation of the solvent, column chromatography (silica gel, hexane) afforded **6c**.

6c: white solid, isolated yield 83% (128 mg). ^1H NMR (CDCl_3 , Me_4Si): δ 2.04 (s, 6H, CH_3), 7.29 (s, 4H, CH). ^{13}C NMR (CDCl_3 , Me_4Si): δ 4.38 (2 CH_3), 79.48 (2 quart C), 87.30 (2 quart C), 123.14 (2 quart C), 131.10 (4 CH). HRMS: m/z calcd for $\text{C}_{12}\text{H}_{10}$ 154.0783, found 154.0787; Anal. Calcd for $\text{C}_{12}\text{H}_{10}$: C, 93.46; H, 6.54. Found: C, 93.37; H, 6.61.

Typical Procedure for Synthesis of Bis(silacyclobutene)-Containing Benzene Derivatives 7 and 9 from Bis(phenylethynyl)silane 1 and Dialkynylbenzenes 6 and 8 in the Presence of $\text{Cp}_2\text{ZrBu}^n_2$. To a toluene (8 mL) solution of Cp_2ZrCl_2 (280 mg, 0.96 mmol) at $-78\text{ }^{\circ}\text{C}$ in a 20 mL Schlenk tube was added dropwise *n*-BuLi (1.92 mmol, 1.6 M, 1.2 mL) with a syringe. After the addition was completed, the reaction mixture was stirred at $-78\text{ }^{\circ}\text{C}$ for 1 h. Then 0.96 mmol of bis(phenylethynyl)silane **1** was added, and the reaction mixture was warmed gradually to room temperature and stirred at this temperature for 1 h. After 0.48 mmol of dialkynylbenzene **6** or **8** was added, the reaction mixture was heated at $90\text{ }^{\circ}\text{C}$ for 6 h. The resulting solution was cooled to room temperature and quenched with 3 N HCl. The organic layer was washed successively with water and brine and then dried over MgSO_4 . After evaporation of the solvent, column chromatography (silica gel, hexane/ether 30/1) afforded **7** or **9**.

7a: yellow solid, mp 122–124 $^{\circ}\text{C}$, isolated yield 84% (660 mg). ^1H NMR (CDCl_3 , Me_4Si): δ 0.54 (s, 12H, CH_3), 0.82 (t, $J = 6.9$ Hz, 6H, CH_3), 1.20–1.49 (m, 16H, CH_2), 2.43 (t, $J = 7.5$ Hz, 4H, CH_2), 6.57 (s, 2H, CH), 7.21–7.46 (m, 24H, CH), 7.99 (s, 2H, CH). ^{13}C NMR (CDCl_3 , Me_4Si): δ -0.51 (4 CH_3), 14.06 (2 CH_3), 22.57 (2 CH_2), 28.36 (2 CH_2), 29.30 (2 CH_2), 30.73 (2 CH_2), 31.61 (2 CH_2), 126.81 (2 CH), 126.86 (4 CH), 127.04 (4 CH), 127.61 (2 CH), 128.21 (4 CH), 128.61 (4 CH), 128.83 (4 CH), 130.41 (2 CH), 136.19 (2 quart C), 137.48 (2 quart C), 141.80 (2 quart C), 142.50 (2 quart C), 143.05 (2 quart C), 144.06 (2 quart C), 148.17 (2 CH), 158.19 (2 quart C); HRMS: m/z calcd for $\text{C}_{58}\text{H}_{66}\text{Si}_2$ 818.4703, found 818.4701. Anal. Calcd for $\text{C}_{58}\text{H}_{66}\text{Si}_2$: C, 85.02; H, 8.12%. Found: C, 84.96; H, 8.30.

7b: yellow solid, isolated yield 76% (557 mg). ^1H NMR (CDCl_3 , Me_4Si): δ 0.54 (s, 12H, CH_3), 0.90 (t, $J = 7.5$ Hz, 6H, CH_3), 1.46–1.57 (m, 4H, CH_2), 2.43 (t, $J = 7.5$ Hz, 4H, CH_2), 6.59 (s, 2H, CH), 7.18–7.47 (m, 24H, CH), 8.00 (s, 2H, CH). ^{13}C NMR (CDCl_3 , Me_4Si): δ -0.51 (4 CH_3), 14.24 (2 CH_3), 21.87 (2 CH_2), 32.90 (2 CH_2), 126.82 (2 quart C), 126.85 (2 quart C), 127.00 (4 CH), 127.61 (4 CH), 128.21 (4 CH), 128.60 (2 CH), 128.86 (4 CH), 130.52 (4 CH), 136.19 (2 quart C), 137.46 (2 quart C), 141.79 (2 quart C), 142.38 (2 quart C), 142.99 (2 quart C), 144.03 (2 quart C), 148.12 (2 CH), 158.26 (2 quart C). HRMS: m/z calcd for $\text{C}_{48}\text{H}_{46}\text{Si}_2$ 734.3764, found 734.3771. Anal. Calcd for $\text{C}_{48}\text{H}_{46}\text{Si}_2$: C, 84.96; H, 7.40. Found: C, 84.74; H, 7.38.

7c: yellow solid, mp 210–212 $^{\circ}\text{C}$, isolated yield 81% (527 mg). ^1H NMR (CDCl_3 , Me_4Si): δ 0.52 (s, 12H, CH_3), 2.11 (s, 6H, CH_3), 6.58 (s, 2H, CH), 7.20–7.49 (m, 24H, CH), 8.00 (s, 2H, CH). ^{13}C NMR (CDCl_3 , Me_4Si): δ -0.59 (4 CH_3), 19.12 (2 CH_3), 126.83 (2 CH), 126.89 (4 CH), 127.17 (4 CH), 127.66 (2 CH), 128.26 (4 CH), 128.62 (4 CH), 129.02 (4 CH), 130.74 (2 CH), 136.29 (2 quart C), 137.35 (2 quart C), 137.43 (2 quart C), 141.82 (2 quart C), 142.94 (2 quart C), 144.06 (2 quart C), 147.95 (2 CH), 158.47 (2 quart C). HRMS: m/z calcd for $\text{C}_{48}\text{H}_{46}\text{Si}_2$ 678.3138, found 678.3130. Anal. Calcd for $\text{C}_{48}\text{H}_{46}\text{Si}_2$: C, 84.90; H, 6.83. Found: C, 84.65; H, 6.86.

7d: white solid, mp 212–214 $^{\circ}\text{C}$, isolated yield 74% (658 mg). ^1H NMR (CDCl_3 , Me_4Si): δ 2.14 (s, 6H, CH_3), 6.71 (s, 2H, CH), 7.15–7.61 (m, 44H, CH), 8.38 (s, 2H, CH). ^{13}C NMR (CDCl_3 , Me_4Si): δ 19.21 (2 CH_3), 127.11 (2 CH), 127.24 (2 CH), 127.79 (4 CH), 127.89 (2 CH), 128.14 (10 CH), 128.64 (4 CH), 129.12 (5 CH), 130.31 (5 CH), 131.02 (2 CH), 133.35 (4 quart C), 135.48 (10 CH), 136.29 (2 quart C), 136.84 (2 quart C), 137.20 (2 quart C), 140.86 (2 quart C), 141.67 (2 quart C), 145.28 (2 quart C), 151.61 (2 CH), 156.64 (2 quart C). HRMS: m/z calcd for $\text{C}_{68}\text{H}_{54}\text{Si}_2$

(12) (a) Brandsma, L. *Preparative Acetylenic Chemistry*, 2nd ed.; Elsevier: Amsterdam, 1988; p 254. (b) Sonoda, M.; Inaba, A.; Itahashi, K.; Tobe, Y. *Org. Lett.* **2001**, *3*, 2419. (c) Lucas, N. T.; Notaras, E. G. A.; Petrie, S.; Stranger, R.; Humphrey, M. G. *Organometallics* **2003**, *22*, 708–721. (d) Alonso, D. A.; Nájera, C.; Pacheco, M. C. *Adv. Synth. Catal.* **2003**, *345*, 1146–1158.

926.3764, found 926.3760. Anal. Calcd for $C_{68}H_{54}Si_2$: C, 88.07; H, 5.87. Found: C, 87.93; H, 5.87.

9: colorless oil, isolated yield 90% (706 mg). 1H NMR ($CDCl_3$, Me_4Si): δ 0.54 (s, 12H, CH_3), 0.77 (t, $J = 6.9$ Hz, 6H, CH_3), 1.15–1.49 (m, 16H, CH_2), 2.44 (t, $J = 7.5$ Hz, 4H, CH_2), 6.62 (s, 2H, CH), 7.27.45 (m, 24H, CH), 8.02 (s, 2H, CH). ^{13}C NMR ($CDCl_3$, Me_4Si): δ -0.53 (4 CH_3), 14.03 (2 CH_3), 22.52 (2 CH_2), 28.36 (2 CH_2), 29.26 (2 CH_2), 30.59 (2 CH_2), 31.57 (2 CH_2), 126.80 (4 CH), 126.84 (4 CH), 127.00 (4 CH), 127.59 (2 CH), 128.19 (4 CH), 128.59 (4 CH), 129.58 (2 CH), 130.66 (2 CH), 137.45 (2 quart C), 137.99 (2 quart C), 141.80 (2 quart C), 142.56 (2 quart C), 142.83 (2 quart C), 144.02 (2 quart C), 148.04 (2 CH), 158.26 (2 quart C). HRMS: m/z calcd for $C_{58}H_{66}Si_2$ 818.4703, found 818.4698. Anal. Calcd for $C_{58}H_{66}Si_2$: C, 85.02; H, 8.12. Found: C, 85.24; H, 8.21.

Synthesis of 1,3,5-Tripropynylbenzene (10b).¹² To a solution of anhydrous zinc bromide (666 mg, 3 mmol) in 10 mL of THF was added dropwise 1-propynylmagnesium bromide (0.5 M, THF, 6 mL) at 0 °C followed by $Pd(PPh_3)_4$ (86 mg, 0.08 mmol) and 1,3,5-tribromobenzene (312 mg, 1.0 mmol). The cooling bath was removed, the reaction mixture was heated at reflux for 8 h, and the solution was cooled to room temperature and quenched by a saturated aqueous solution of ammonium chloride. The organic layer was washed successively with water and brine and then dried over $MgSO_4$. After evaporation of the solvent, column chromatography (silica gel, hexane/ether 50/1) afforded **10b**.

10b: white solid, mp 106–108 °C, isolated yield 78% (150 mg). 1H NMR ($CDCl_3$, Me_4Si): δ 2.02 (s, 9H, CH_3), 7.28 (s, 3H, CH). ^{13}C NMR ($CDCl_3$, Me_4Si): δ 4.31 (3 CH_3), 78.53 (3 quart C), 86.60 (3 quart C), 124.31 (3 quart C), 133.51 (3 CH). HRMS: m/z calcd for $C_{15}H_{12}$ 192.0939, found 192.0941. Anal. Calcd for $C_{15}H_{12}$: C, 93.71; H, 6.29. Found: C, 93.67; H, 6.39.

Typical Procedure for Synthesis of 1,3,5-Tris(silacyclobutene)-Containing Benzene Derivatives 11 from Bis(phenylethynyl)silanes 1 and Trialkynylbenzenes 10 in the Presence of Cp_2ZrBu_2 . To a toluene (8 mL) solution of Cp_2ZrCl_2 (280 mg, 0.96 mmol) at -78 °C in a 20 mL Schlenk tube was added dropwise *n*-BuLi (1.92 mmol, 1.6 M, 1.2 mL) with a syringe. After the addition was completed, the reaction mixture was stirred at -78 °C for 1 h. Then 0.96 mmol of bis(phenylethynyl)silane **1** was added, and the reaction mixture was warmed gradually to room temperature and stirred at this temperature for 1 h. After 0.32 mmol of trialkynylbenzene **10** was added, the reaction mixture was heated at 90 °C for 6 h. The resulting solution was cooled to room temperature and quenched with 3 N HCl. The organic layer was washed successively with water and brine and then dried over $MgSO_4$. After evaporation of the solvent, column chromatography (silica gel, hexane/ether 10/1) afforded **11**.

11a: colorless oil, isolated yield 87% (991 mg). 1H NMR ($CDCl_3$, Me_4Si): δ 0.54 (s, 18H, CH_3), 0.72 (t, $J = 6.9$ Hz, 9H, CH_3), 1.11–1.52 (m, 24H, CH_2), 2.47 (t, $J = 7.5$ Hz, 6H, CH_2), 6.65 (s, 3H, CH), 7.19–7.46 (m, 33H, CH), 8.04 (s, 3H, CH). ^{13}C NMR ($CDCl_3$, Me_4Si): δ -0.52 (6 CH_3), 14.00 (3 CH_3), 22.51 (3 CH_2), 28.41 (3 CH_2), 29.31 (3 CH_2), 30.70 (3 CH_2), 31.61 (3 CH_2), 126.81 (3 CH), 126.87 (6 CH), 127.05 (6 CH), 127.60 (3 CH), 127.66 (3 CH), 128.22 (6 CH), 128.61 (6 CH), 130.76 (3 CH), 137.50 (3 quart C), 137.99 (3 quart C), 141.92 (3 quart C), 142.70 (3 quart C), 142.81 (3 quart C), 144.09 (3 quart C), 148.04 (3 CH), 158.34

(3 quart C). HRMS: m/z calcd for $C_{84}H_{96}Si_3$ 1188.6820, found 1188.6827. Anal. Calcd for $C_{84}H_{96}Si_3$: C, 84.79; H, 8.13. Found: C, 84.22; H, 8.31.

11b: colorless oil, isolated yield 71% (666 mg). 1H NMR ($CDCl_3$, Me_4Si): δ 0.52 (s, 18H, CH_3), 2.16 (s, 9H, CH_3), 6.64 (s, 3H, CH), 7.19–7.43 (m, 33H, CH), 8.04 (s, 3H, CH). ^{13}C NMR ($CDCl_3$, Me_4Si): δ -0.60 (6 CH_3), 19.10 (3 CH_3), 126.84 (3 CH), 126.91 (6 CH), 127.17 (6 CH), 127.66 (3 CH), 128.11 (3 CH), 128.27 (6 CH), 128.63 (6 CH), 130.98 (3 CH), 137.42 (3 quart C), 137.64 (3 quart C), 137.96 (3 quart C), 141.82 (3 quart C), 143.03 (3 quart C), 143.88 (3 quart C), 147.90 (3 CH), 158.59 (3 quart C). HRMS: m/z calcd for $C_{69}H_{66}Si_3$ 978.4472, found 978.4469. Anal. Calcd for $C_{69}H_{66}Si_3$: C, 84.61; H, 6.79. Found: C, 84.42; H, 6.94.

11c: yellow solid, mp 167–170 °C, isolated yield 66% (855 mg). 1H NMR ($CDCl_3$, Me_4Si): δ 2.20 (s, 9H, CH_3), 6.78 (s, 3H, CH), 7.17–7.61 (m, 63H, CH), 8.42 (s, 3H, CH). ^{13}C NMR ($CDCl_3$, Me_4Si): δ 19.21 (3 CH_3), 127.12 (3 CH), 127.28 (6 CH), 127.78 (6 CH), 127.89 (3 CH), 128.15 (18 CH), 128.31 (1 CH), 128.66 (6 CH), 130.32 (6 CH), 131.23 (2 CH), 133.33 (3 quart C), 135.51 (16 CH), 136.84 (3 quart C), 137.55 (3 quart C), 137.95 (3 quart C), 140.95 (3 quart C), 141.63 (3 quart C); 145.09 (3 quart C), 151.60 (2 CH), 156.75 (3 quart C). Anal. Calcd for $C_{99}H_{78}Si_3$: C, 87.95; H, 5.82. Found: C, 87.62; H, 5.98.

X-ray Crystallographic Studies of 7b. Crystals for X-ray analyses of **7b** were obtained as described in the preparations. The crystals were sealed in thin-walled glass capillaries. Data collections were performed at 20 °C on a Rigaku RAXIS RAPID IP, using graphite-monochromated Mo $K\alpha$ radiation ($\lambda = 0.71073$ Å). The determination of crystal class and unit cell parameters was carried out by the Rapid-AUTO (Rigaku 2000) program package. The raw frame data were processed using Crystal Structure (Rigaku/MSC 2000) to yield the reflection data file. The structure was solved by use of the SHELXTL program. Refinement was performed on F^2 anisotropically for all the non-hydrogen atoms by the full-matrix least-squares method. The hydrogen atoms were placed at calculated positions and were included in the structure calculation without further refinement of the parameters. Crystallographic data (excluding structure factors) have been deposited with the Cambridge Crystallographic Data Centre as supplementary publication no. CCDC-699064 (**7b**). Copies of these data can be obtained free of charge from the Cambridge Crystallographic Data Centre via www.ccdc.cam.ac.uk/data_request/cif.

Acknowledgment. This work was supported by the Natural Science Foundation of China (Grant Nos. 20632010, 20521202, and 20702003) and the Major State Basic Research Development Program (Grant No. 2006CB806105). Cheung Kong Scholars Programme, Qiu Shi Science & Technologies Foundation, BASF, Dow Corning Corporation, and Eli Lilly China are gratefully acknowledged.

Supporting Information Available: Figures giving scanned NMR spectra of all new products and tables and CIF files giving X-ray data for **7b** (CCDC 699064). This material is available free of charge via the Internet at <http://pubs.acs.org>.

OM800841S

Chemical, Electrochemical, and Theoretical Investigations of $[(\text{Cp})\text{Ru}(\text{CO})_3]^+$ and $[(\text{Ind})\text{Ru}(\text{CO})_3]^+$

Robert C. Badger,[†] Jason S. D'Acchioli,^{*,†} Benjamin C. Gamoke,[†] Sang Bok Kim,[‡] Tracey A. Oudenhoven,[†] Dwight A. Sweigart,[‡] and Robin S. Tanke[†]

Department of Chemistry, The University of Wisconsin–Stevens Point, 2001 Fourth Avenue, Stevens Point, Wisconsin 54481, and Department of Chemistry, Brown University, Box H, 324 Brook Street, Providence, Rhode Island 02912

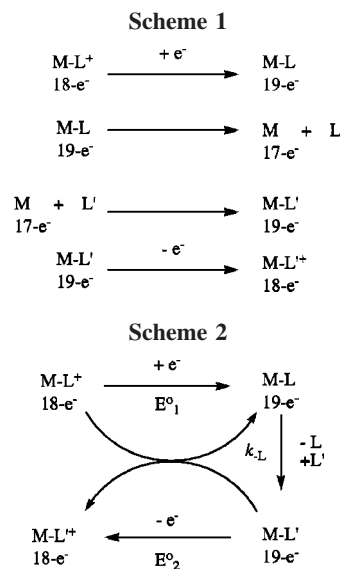
Received August 14, 2008

The complexes $[(\text{Cp})\text{Ru}(\text{CO})_3]^+$ and $[(\text{Ind})\text{Ru}(\text{CO})_3]^+$ were subjected to chemical, electrochemical, and spectroelectrochemical investigations in an attempt to gauge their similarity to $[(\text{Cp})\text{Fe}(\text{CO})_3]^+$ and $[(\text{Ind})\text{Fe}(\text{CO})_3]^+$. While the Fe complexes exhibited reversible electrochemical behavior—the indene analogue exhibiting a so-called “inverse indenyl effect”—the Ru complexes exhibited limited electrochemical reversibility, even at $-30\text{ }^\circ\text{C}$ and higher scan rates. The formation of the hydride complexes $[(\text{Cp})\text{Ru}(\text{CO})_2\text{H}]$ and $[(\text{Ind})\text{Ru}(\text{CO})_2\text{H}]$ was observed via ^1H NMR and IR. The X-ray crystal structure of $[(\text{Ind})\text{Ru}(\text{CO})_3]^+$ is presented here for the first time.

1. Introduction

The reactions of 17- and 19-electron organometallic radicals have been, and continue to be, an area of interest.¹ Of special consideration is the propensity with which such radicals undergo ligand substitution, the mechanism of which is seen in Scheme 1. When an 18-electron organometallic species $\text{M}-\text{L}^+$ undergoes reduction, either chemically or at an electrode surface, the resulting 19-electron species, $\text{M}-\text{L}$, typically dissociates a ligand to form a 17-electron species, M . The 17-electron species can then undergo associative addition with any adventitious ligand present, forming a 19-electron species, $\text{M}-\text{L}'$, which is typically oxidized to a stable 18-electron species, $\text{M}-\text{L}'^+$. Mechanisms in which $\text{M}-\text{L}^+$ is reduced to a 19-electron radical, followed by associative addition of a ligand and the formation of a highly unstable 21-electron species, are typically disfavored.^{2a,b}

A special case occurs if the 19-electron species $\text{M}-\text{L}'$ —formed after L' has ligated to the metal center after dissociation of L —has a less favorable reduction potential than $\text{M}-\text{L}^+$. That is, if $E^\circ_{\text{M}-\text{L}'} > E^\circ_{\text{M}-\text{L}^+}$, then the reaction pathway is termed electron transfer catalyzed (ETC). Ligand substitution is then completely and efficiently effected by the presence of only a trace or catalytic amount of reducing agent, whether chemically



or electrochemically at the electrode surface.² The general process of an ETC mechanism can be found in Scheme 2. Specific examples of ETC mechanisms of ligand substitution have involved the dissociation of CO in the compounds $[(\text{MeCp})\text{Mn}(\text{CO})_2\text{NO}]^+$, $[(\text{Ind})\text{Mn}(\text{CO})_2\text{NO}]^+$, $[(\text{Cp})\text{Fe}(\text{CO})_3]^+$, and $[(\text{Ind})\text{Fe}(\text{CO})_3]^+$ ($\text{MeCp} = \eta^5$ -methylcyclopentadienyl; $\text{Cp} = \eta^5$ -cyclopentadienyl, $\text{Ind} = \eta^5$ -indenyl).^{2a,b}

The cases of $[(\text{Cp})\text{Fe}(\text{CO})_3]^+$ and $[(\text{Ind})\text{Fe}(\text{CO})_3]^+$ (Figure 1) are quite interesting. Electrochemical studies of both compounds afforded information about their rate of CO dissociation, $k_{-\text{CO}}$, in the presence of donor ligands such as AsPh_3 , PPh_3 , $\text{P}(\text{OPh})_3$, $\text{P}(\text{OEt})_3$, $\text{P}(\text{OMe})_3$, $\text{P}(\text{C}_2\text{H}_4\text{CN})_3$, and diphos.³ The truly salient aspect of the study was the unexpected difference in $k_{-\text{CO}}$

* Corresponding author. E-mail: jdacchio@uwsp.edu.

[†] The University of Wisconsin–Stevens Point.

[‡] Brown University.

(1) For an excellent perspective, see: (a) Geiger, W. E. *Organometallics* **2007**, *26*, 5738. (b) Cahoon, J. F.; Kling, M. F.; Schmatz, S.; Harris, C. B. *J. Am. Chem. Soc.* **2005**, *127*, 12555. (c) Chong, D.; Laws, D. R.; Nafady, A.; Costa, P. J.; Rheingold, A. L.; Calhorda, M. J.; Geiger, W. E. *J. Am. Chem. Soc.* **2008**, *130*, 2692. (d) Hapiot, F.; Tilloy, S.; Monflier, E. *Chem. Rev.* **2006**, *106*, 767. (e) Munisamy, T.; Gipson, S. L. *J. Organomet. Chem.* **2007**, *692*, 1087. (f) Ruiz, J.; Oglaro, F.; Saillard, J. Y.; Halet, J. F.; Varret, F.; Astruc, D. *J. Chem. Soc.* **1998**, *120*, 11693. (g) Srinivas, G. N.; Lu, Y.; Schwartz, M. J. *Mol. Struct.* **2005**, *726*, 149. (h) Srinivas, G. N.; Yu, L. W.; Schwartz, M. J. *Organomet. Chem.* **2003**, *677*, 96. (i) Sukcharoenphon, K.; Moran, D.; Schleyer, P. V.; McDonough, J. E.; Abboud, K. A.; Hoff, C. D. *Inorg. Chem.* **2003**, *42*, 8494. (j) Sun, S.; Sweigart, D. A. *Adv. Organomet. Chem.* **1996**, *40*, 171. (k) Torraca, K. E.; McElwee-White, L. *Coord. Chem. Rev.* **2000**, *206*, 469.

(2) (a) Huang, Y.; Neto, C. C.; Pevear, K. A.; Holl, M. M. B.; Sweigart, D. A.; Chung, Y. K. *Inorg. Chim. Acta* **1994**, *226*, 53. (b) Neto, C. C.; Baer, C. D.; Chung, Y. K.; Sweigart, D. A. *J. Chem. Soc., Chem. Commun.* **1993**, 816. (c) Reingold, J. A.; Son, S. U.; Kim, S. B.; Dullaghan, C. A.; Oh, M.; Frake, P. C.; Carpenter, G. B.; Sweigart, D. A. *Dalton* **2006**, 2385.

(3) Pevear, K. A.; Holl, M. M. B.; Carpenter, G. B.; Rieger, A. L.; Rieger, P. H.; Sweigart, D. A. *Organometallics* **1995**, *14*, 512.

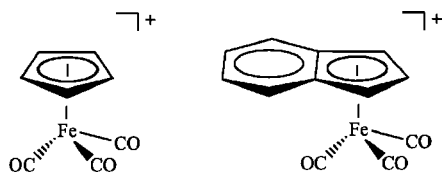


Figure 1. Fe complexes originally studied.

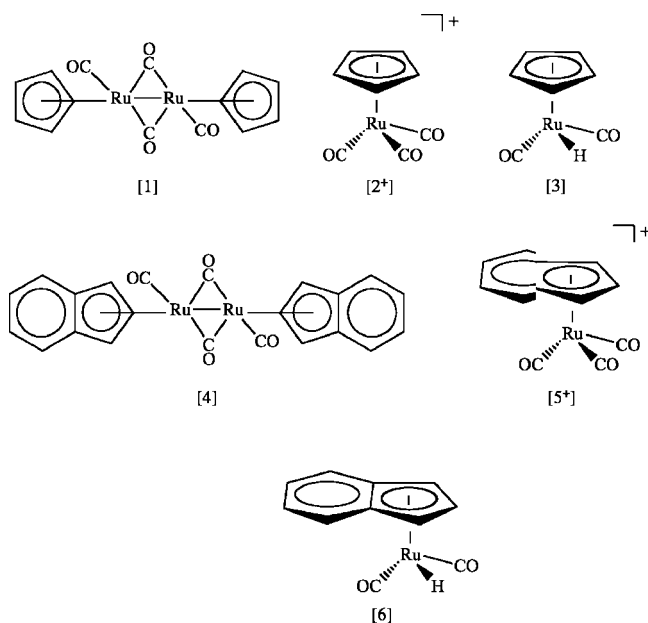


Figure 2. Ruthenium complexes considered in this study.

for $[(Ind)Fe(CO)_3]$ as compared to $[(Cp)Fe(CO)_3]$. That is, k_{-CO} for $[(Ind)Fe(CO)_3]$ is much slower than expected when compared to k_{-CO} for $[(Cp)Fe(CO)_3]$. Metal complexes containing the indenyl ligand are expected to experience an increase in the rate of ligand substitution, the so-called "indenyl effect". This increase is attributed to the ease with which the benzene moiety of indene can accommodate electron density freed as a result of the metal slipping from η^5 to η^3 coordination upon ligand addition. For example, $[(Ind)Rh(CO)_2]$ becomes a 19-electron radical upon reduction, but η^5 to η^3 slippage results in a 17-electron radical capable of undergoing ligand substitution approximately 10^8 times faster than $[(Cp)Rh(CO)_2]^+$.³ In the case of $[(Ind)Fe(CO)_3]$, the slower k_{-CO} is attributed to a stabilization of the 19-electron radical without the necessity of ring slippage. This stabilization results in a decrease in k_{-CO} compared to $[(Cp)Fe(CO)_3]$.

Using the aforementioned rationale, it was believed that electrochemical studies of the ruthenium analogues $[(Cp)Ru(CO)_3]^+$, $[2]^+$, and $[(Ind)Ru(CO)_3]^+$, $[5]^+$ (Figure 2), would offer an interesting comparison to the Fe systems. The outcomes of such a study, however, yielded quite unexpected results. First, both $[2]^+$ and $[5]^+$ showed no electrochemical reversibility, even at lower temperature and higher scan rate. The irreversibility of the systems is evidence that, upon reduction, the 19-electron radicals that are formed subsequently decompose. Even though ligand substitution occurred in the presence of phosphine donor ligands, the rate of the competing decomposition is unknown; there is no way to obtain an absolute k_{-CO} for such systems. Second, under certain conditions of electrochemical reduction (*vide infra*), both $[2]^+$ and $[5]^+$ form the hydride complexes $[3]$ and $[6]$, respectively.

The hydride complex $[3]$ has been known since Wilkinson and co-workers first observed the air-sensitive product;⁴ several syntheses are known.^{4,5} Photochemical experiments involving k_{-CO} from $[3]$ have also been of recent interest in the literature.⁶ The indenyl analogue of $[2]^+$, namely $[5]^+$, has never been reported; its X-ray crystal structure is presented (*vide infra*).

2. Experimental Section

2.1. Synthetic Methods. All reagents used were purchased from commercial sources and used without further purification. CH_2Cl_2 used in synthesis was dried over P_2O_5 and stored over 4 Å molecular sieves; CH_2Cl_2 used in electrochemical measurements was HPLC grade and used without purification. Et_2O was dried using an MBraun solvent purification system and used directly for crystallization. CD_2Cl_2 was stored over 4 Å molecular sieves under nitrogen. $AgBF_4$ was opened and handled in a nitrogen-filled glovebag. Low-temperature IR experiments were performed using a Remspec IR fiber optic immersion probe. Electrochemical experiments were performed with EG&G model 173, 175, and 179 equipment.

2.1.1. Synthesis of $[2]PF_6$. The complex was synthesized according to literature methods.³ For $[2]PF_6$, IR (CH_3CN) ν_{CO} [cm^{-1}] 2134, 2080; 1H NMR (CD_3CN) δ 5.96 (s, 5 H, H^1-H^5).

Preparation of the Hydride $[3]$. Preparation of $[3]$ was effected by the addition of either the reducing agents $CoCp_2$ (1 equiv) or a trace amount of NEt_3 to a solution containing $[2]PF_6$. Samples were prepared on an IR/NMR scale (0.001 g of $[2]PF_6$ dissolved in CH_3CN or CD_3CN) inside a glovebox. The air-sensitive product was never isolated. All chemistry for this compound was performed in CH_3CN . For $[3]$, IR (CH_3CN) ν_{CO} [cm^{-1}] 2024, 1958; 1H NMR (CD_3CN) δ 5.40 (s, 5 H, H^1-H^5), -11.05 (s, 1 H, H^-). The IR and NMR agree with the literature.⁸

2.1.2. Synthesis of $[4]$. The synthesis of $[4]$ was based upon a modified literature procedure.⁷ Glassware was dried with a Bunsen burner under N_2 , with N_2 dried by passage through a Drierite column. Heptane (60 mL) was added to a 250 mL round-bottom flask. Indene (4.5 mL) was added to the flask ($d = 0.996$ g/mol, 38.6 mmol) via syringe, and then 1.020 g of $Ru_3(CO)_{12}$ (1.60 mmol). The solution was left exposed to the air and allowed to stir for 1 h; it was then refluxed for 24 h while exposed to the air. The solution was allowed to cool to room temperature, at which time a red, oily solution was decanted and discarded, leaving behind a black solid.

The black solid was dissolved in CH_2Cl_2 . Impurities were precipitated from CH_2Cl_2 using petroleum ether. The impurities were collected via vacuum filtration and discarded. The filtrate was taken to dryness, and impurities were again precipitated from CH_2Cl_2 /petroleum ether. A rust-colored sample was isolated and dried *in vacuo*. All chemistry for this compound was performed in CH_2Cl_2 .

While spectroscopic data have been reported previously,⁷ the IR data are given below, along with a more refined set of 1H NMR

(4) Davison, A.; McCleverty, J. A.; Wilkinson, G. *J. Chem. Soc.* **1963**, 1133.

(5) (a) Doherty, N. M.; Knox, S. A. R.; Morris, M. J. *Inorg. Synth.* **1990**, 28, 189. (b) Humphries, A. P.; Knox, S. A. R. *J. Chem. Soc.* **1973**, 326.

(6) (a) Bitterwolf, T. E. *Coord. Chem. Rev.* **2000**, 419. (b) Bitterwolf, T. E.; Linehan, J. C.; Shade, J. E. *Organometallics*. **2000**, 19, 4915. (c) Bitterwolf, T. E.; Linehan, J. C.; Shade, J. E. *Organometallics*. **2001**, 20, 775.

(7) Nataro, C.; Thomas, L. M.; Angelici, R. J. *Inorg. Chem.* **1997**, 36, 6000.

(8) Apex2, Version 2 User Manual; Bruker Analytical X-ray Systems, Inc.: Madison, WI, 2006.

Table 1. Crystallographic Data for [5]BF₄

formula	C ₁₂ H ₇ O ₃ RuBF ₄
fw	387.06
cryst sys	orthorhombic
space group	P2 ₁ 2 ₁ 2 ₁
a, Å	8.6715(2)
b, Å	10.7016(2)
c, Å	14.3849(3)
α, deg	90
β, deg	90
γ, deg	90
V, Å ³	1334.90(5)
Z	4
D _{calcd} , g/cm ³	1.926
F(000)	752
cryst size, mm	0.20 mm × 0.26 mm × 0.30 mm
θ range, deg	3–68
no. of rflns collected	8297
no. of data/restraints/params	2345/0/192
goodness of fit on F ²	0.99
final R indices (I > 2σ(I))	
R1	0.0196
wR2	0.0475

data. For [4], yield 13%; IR (CH₂Cl₂) ν_{CO} [cm⁻¹] 1999, 1958, 1782; ¹H NMR (CD₂Cl₂) δ 7.27 (m, 4 H, H⁴⁻⁷), 5.69 (d, ³J_{H^{1,3}-H²} = 2.88 Hz, 2 H, H^{1,3}), 5.58 (t, ³J_{H²-H^{1,3}} = 2.91 Hz, 1 H, H²).

2.1.3. Synthesis of [5]BF₄. All glassware was dried with a Bunsen burner under CO, with the CO dried by passage through a Drierite column. HPLC grade CH₂Cl₂ (25 mL) was added to a 50 mL round-bottom flask. The solvent was bubbled with CO for 10 min in order to saturate it. Complex [4] (54 mg) was added to the flask in a 5 mL aliquot of HPLC grade CH₂Cl₂. The flask was immediately wrapped in aluminum foil to prevent light from striking the solution. Then 0.141 g of AgBF₄ (0.717 mmol) was added to the solution, which was stirred for 10 min under CO. The solution was filtered on a Celite pad on a 30 mL medium frit. The light yellow filtrate was then reduced and recrystallized three times from CH₂Cl₂/Et₂O. The product, a yellow powder, was collected on a 15 mL fine filter frit and dried *in vacuo*. Diffraction-quality single crystals were grown by slow vapor diffusion of diethyl ether into a CH₂Cl₂ solution of the complex. All chemistry for this compound was performed in CH₂Cl₂. For [4], yield 49.2%; IR (CH₂Cl₂) ν_{CO} [cm⁻¹] 2130, 2080; ¹H NMR (CD₂Cl₂) δ 7.82 (dd, ³J_{H⁷-H⁶} = 6.75 Hz, ⁴J_{H⁷-H⁵} = 3.11 Hz, 2 H, H^{6,7}), 7.65 (dd, ³J_{H⁴-H⁵} = 6.64 Hz, ⁴J_{H⁴-H⁶} = 3.01 Hz, 2 H, H^{4,5}), 6.44 (d, ³J_{H^{1,3}-H²} = 2.57 Hz, 2 H, H^{1,3}), 6.41 (t, ³J_{H²-H^{1,3}} = 2.37 Hz, 1 H, H²).

Preparation of the Hydride [6]. Synthesis of [6] was effected by the addition of a trace amount of Et₃N to a solution containing [5]BF₄. Samples were prepared on a IR/NMR scale (0.001 g of [5]BF₄ dissolved in CH₂Cl₂ or CD₂Cl₂) inside the glovebox in order to maintain the integrity of the reducing agents and sample. The air-sensitive product was never isolated. All chemistry for this compound was performed in CH₂Cl₂. For [6], IR (CH₂Cl₂) ν_{CO} [cm⁻¹] 2024, 1961; ¹H NMR (CD₂Cl₂) δ 7.53 (dd, ³J_{H⁷-H⁶} = 6.36 Hz, ⁴J_{H⁷-H⁵} = 3.04 Hz, 2 H, H^{6,7}), 7.17 (dd, ³J_{H⁴-H⁵} = 6.52 Hz, ⁴J_{H⁴-H⁶} = 3.14 Hz, 2 H, H^{4,5}), 5.79 (t, ³J_{H²-H^{1,3}} = 2.92 Hz, 1 H, H²), 5.53 (d, ³J_{H^{1,3}-H²} = 2.86 Hz, 2 H, H^{1,3}), -13.25 (s, 1 H, H⁻).

2.2. Single-Crystal X-ray Structure. Single crystals of η⁵-indenyltricarbonylruthenium tetrafluoroborate were grown by slow diffusion of diethyl ether into methylene chloride. A crystal with dimensions 0.20 mm × 0.26 mm × 0.30 mm was mounted. X-ray diffraction data were collected on a Bruker APEX-II CCD area-detector diffractometer at UCSD with Cu Kα radiation (λ = 1.54178 Å) using φ and ω scanning mode (Table 1). APEX2⁸ was used for data collection computing. The cell refinement and data reduction were performed using Bruker SAINT⁸ software. The structure was solved by direct methods using SHELXS97.⁹ The non-hydrogen atoms refined by full-matrix least squared on F² with CRYSTALS.¹⁰ All H atoms were positioned geometrically and refined using a riding model, with C–H = 0.93 Å, and with U_{iso}(H) = 1.2U_{eq}(C).

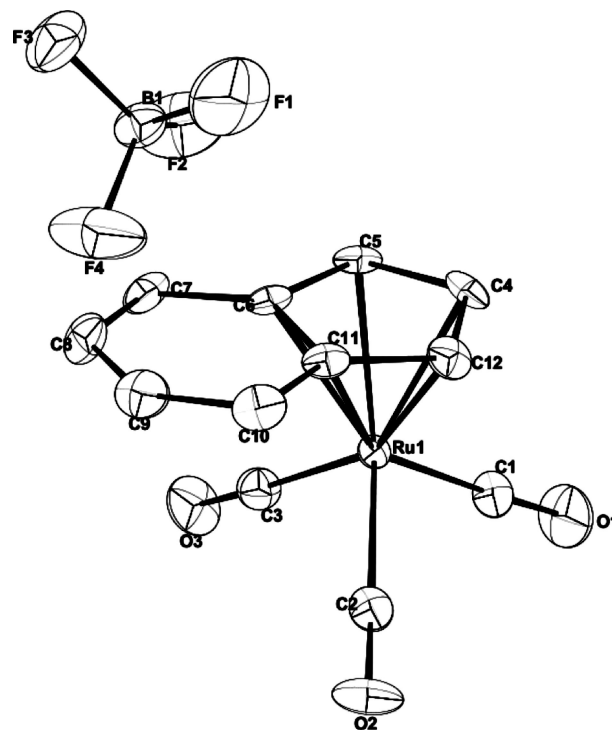


Figure 3. ORTEP plot of [5⁺]BF₄ with displacement ellipsoids drawn at the 50% probability level.

An extinction correction¹¹ was applied. An ORTEP diagram is shown in Figure 3.

2.3. Computational Methods. All calculations were performed using density functional theory as implemented in the Gaussian03 suite of programs.¹² The B3LYP exchange–correlation functional was used for each complex.¹³ The Stuttgart–Dresden (SDD) basis set/effective core potential was used on Fe and Ru atoms,¹⁴ and the Popel-style 6-31G* basis set was used on all nonmetal atoms.¹⁵ Geometry optimizations in C₁ symmetry were performed on [(Cp)Fe(CO)₃]⁺, [(Ind)Fe(CO)₃]⁺, [2⁺], and [5⁺]. All complexes were local minima on their respective potential energy surfaces, as verified by vibrational frequency analyses; Cartesian coordinates

(9) Sheldrick, G. M. *Acta Crystallogr., Sect. A: Found. Crystallogr.* **1997**, *64*, 112.

(10) Betteridge, P. W.; Carruthers, J. R.; Cooper, R. I.; Prout, K. *Appl. Crystallogr.* **2003**, *11796*.

(11) Larson, A. C. In *Crystallographic Computing*; Ahmed, F. R., Ed.; Munksgaard: Copenhagen, 1970; p 291.

(12) Frisch, M. J.; Trucks, G. W.; Schlegel, H. B.; Scuseria, G. E.; Robb, M. A.; Cheeseman, J. R.; Montgomery, J. A., Jr.; Vreven, T.; Kudin, K. N.; Burant, J. C.; Millam, J. M.; Iyengar, S. S.; Tomasi, J.; Barone, V.; Mennucci, B.; Cossi, M.; Scalmani, G.; Rega, N.; Petersson, G. A.; Nakatsuji, H.; Hada, M.; Ehara, M.; Toyota, K.; Fukuda, R.; Hasegawa, J.; Ishida, M.; Nakajima, T.; Honda, Y.; Kitao, O.; Nakai, H.; Klene, M.; Li, X.; Knox, J. E.; Hratchian, H. P.; Cross, J. B.; Adamo, C.; Jaramillo, J.; Gomperts, R.; Stratmann, R. E.; Yazyev, O.; Austin, A. J.; Cammi, R.; Pomelli, C.; Ochterski, J. W.; Ayala, P. Y.; Morokuma, K.; Voth, G. A.; Salvador, P.; Dannenberg, J. J.; Zakrzewski, V. G.; Dapprich, S.; Daniels, A. D.; Strain, M. C.; Farkas, O.; Malick, D. K.; Rabuck, A. D.; Raghavachari, K.; Foresman, J. B.; Ortiz, J. V.; Cui, Q.; Baboul, A. G.; Clifford, S.; Cioslowski, J.; Stefanov, B. B.; Liu, G.; Liashenko, A.; Piskorz, P.; Komaromi, I.; Martin, R. L.; Fox, D. J.; Keith, T.; Al-Laham, M. A.; Peng, C. Y.; Nanayakkara, A.; Challacombe, M.; Gill, P. M. W.; Johnson, B.; Chen, W.; Wong, M. W.; Gonzalez, C.; Pople, J. A. *Gaussian 03, Revision D.02*; Gaussian, Inc.: Pittsburgh, PA, 2003.

(13) (a) Becke, A. D. *Phys. Rev. A: At. Mol. Opt. Phys.* **1988**, *38*, 3098. (b) Becke, A. D. *J. Chem. Phys.* **1993**, *98*, 5648. (c) Lee, C.; Yang, W.; Parr, R. G. *Phys. Rev. B: Condens. Matter* **1988**, *37*, 785.

(14) Andrae, D.; Hauessermann, U.; Dolg, M.; Preuss, H. *Theor. Chim. Acta* **1990**, *77*, 123.

(15) Hehre, W. J.; Radom, L.; Schleyer, P. v. R.; Pople, J. A. *Ab initio Molecular Orbital Theory*; John Wiley & Sons: New York, 1986.

Table 2. Results of Electrochemical and Chemical Reductions.

reactant	product		
	bulk electrolysis (-1.0 V)	chemical reductions	
		CoCp ₂	NEt ₃
$[(Cp)Fe(CO)_3]^+$	D ^a	D	D
$[(Ind)Fe(CO)_3]^+$	D	D	D
$[2^+]$	H ^b	H	H
$[5^+]$	D	D	H

^a The corresponding dimer of the reactant. ^b The corresponding hydride of the reactant.

Table 3. ν_{CO} (cm⁻¹, in CH₂Cl₂) of $[2^+]$, $[3]$, $[4]$, $[5^+]$, $[6]$

$[2^+]$	$[3]$	$[4]$	$[5^+]$	$[6]$
2134, 2080	2024, 1958	1999, 1958, 1782	2130, 2080	2024, 1961

of all optimized structures are provided in the Supporting Information. The SCPA population analyses of Ros and Schuit were performed using the AOMix package.¹⁶ SCPA considers the atomic orbital contribution, χ_a , to the i th molecular orbital to be equal to $(c_{ai}^2)/(\sum_k c_{ki}^2)$, where k runs over all AOs.^{16c} Molecular orbital isosurface plots were made using the VMD software package.¹⁷ The mean absolute error (MAE) for selected bond lengths and angles, respectively, were calculated by taking the absolute values of the difference between the selected crystal structure parameters and the calculated values. These deviations were then averaged.

3. Results and Discussion

3.1. Chemical Reductions of $[2^+]$ and $[5^+]$. Chemical reduction of $[(Cp)Fe(CO)_3]^+$ and $[(Ind)Fe(CO)_3]^+$ with NEt₃ and CoCp₂ resulted in clean conversion to their respective dimers, $[(Cp)Fe(CO)_2]_2$ and $[(Ind)Fe(CO)_2]_2$.⁷ It was similarly believed that chemical reduction of $[2^+]$ and $[5^+]$ would yield their respective dimers, $[1]$ and $[4]$. Surprisingly, the results of chemical reduction were quite different than anticipated (see Table 2). While chemical reduction of $[5^+]$ with CoCp₂ cleanly yielded a dimer as verified by IR (see Table 3 and Supporting Information Figure 1, S1) and ¹H NMR (section 3.2.4), it was found that reduction of $[2^+]$ with either 1 drop of NEt₃ or 1 equiv of CoCp₂ and reduction of $[5^+]$ with 1 drop of NEt₃ gave ν_{CO} values that differed from the known dimer peaks (see Table 3). The peak pattern corresponded to those for typical $[(Cp)M(CO)_2X]$ ($M = Fe, Ru, X = Cl, I, \text{carboalkoxy, and carboxamido groups, and various amines}$) dicarbonyl species.¹⁸ In the case of $[2^+]$ there was a suspicion that the species formed was that of the hydride $[3]$ since the ν_{CO} values agreed with those reported in the literature.^{4,5a} The ¹H NMR of $[2^+]$ after chemical reductions with both NEt₃ and CoCp₂ verified the presence of $[3]$. There was a hydride resonance at $\delta -11.05$, as well as an upfield shift in the resonance of the η^5 -Cp protons compared to $[2^+]$.

While $[5^+]$ is not known in the literature, its chemistry was found to be analogous to that of $[2^+]$. It was verified by IR (Table 2 and S2) that chemical reduction of $[5^+]$ with NEt₃ most likely formed the hydride derivative. The ¹H NMR of the reduction product showed a hydride resonance at $\delta -13.25$, as

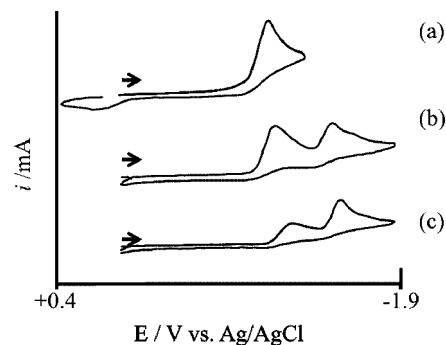


Figure 4. Cyclic voltammograms of 1.0 mM $[2^+]$ in CH₃CN/0.10 M TBAPF₆ under N₂ at the indicated temperatures and in the presence of the indicated nucleophiles: (a) 23 °C, none; (b) 23 °C, 30 equiv PPh₃; (c) -30 °C, 30 equiv PPh₃. The working electrode was a 1 mm diameter glassy carbon disk, and the scan rate was 0.50 V/s. All potentials are relative to the ferrocene/ferrocenium couple ($E_{1/2} = 0.50$ V).

well as an upfield shift of the resonances for the η^5 -Ind protons. Curiously, chemical reduction of $[5^+]$ with CoCp₂ indicated the formation of $[4]$.

3.2. In Situ Bulk Electrolysis of $[2^+]$ and $[5^+]$. *In situ* bulk electrolysis experiments were performed with an IR probe under N₂ at a constant potential of -1.0 V. Both electrolyses were used to ascertain the effects of electrochemical reduction on $[2^+]$ and $[5^+]$, as well as to determine the number of electrons that would effect such changes. IR spectra recorded during the room-temperature bulk electrolysis of 50 mL of a 1 mM sample of $[2^+]$ indicated conversion to $[3]$ —as well as an unidentified minor product—after the passage of 6.0 C (**S3**). This indicates that conversion to the hydride is a one-electron process. This result differs markedly from that recorded during the bulk electrolysis of $[(Cp)Fe(CO)_3]^+$; the one-electron reduction of that complex indicated complete conversion to its corresponding dimer.³

IR spectra recorded during the room-temperature bulk electrolysis of 50 mL of a 1 mM sample of $[5^+]$ indicated complete conversion to $[4]$ after the passage of 5.0 C (**S4**). This result indicates that the one-electron reduction of $[5^+]$ leads to the dimer, again highlighting the contrasts in reactivity with $[2^+]$. It is also interesting to note that the bulk electrolysis of $[5^+]$ was analogous to that of $[(Ind)Fe(CO)_3]^+$, as the one-electron reduction of that complex yielded its corresponding dimer.³ This behavior is in marked contrast to that of $[2^+]$ and $[(Cp)Fe(CO)_3]^+$ under similar conditions (*vide supra*).

3.3. Cyclic Voltammetry of $[2^+]$ and $[5^+]$. An investigation of $[2^+]$ by cyclic voltammetry showed its reduction to be chemically irreversible under indicated experimental conditions, including a faster scan rate of 2 V/s and a lower temperature of -30 °C. The first reduction wave occurred at -1.15 V (Figure 4a). A second chemically irreversible reduction wave, found by increasing the potential range to -2.40 V, was found at -2.31 V. Since bulk electrolysis of $[2^+]$ at -1.0 V yielded $[3]$, it is strongly believed that the reduction wave at -2.31 V corresponds to the hydride.

In the presence of a 30 equiv excess of PPh₃ a second chemically irreversible reduction wave appeared at -1.54 V (Figure 4b). This peak was assigned to the reduction of the ligand-substituted product $[(Cp)Ru(CO)_2(PPh_3)]^+$, formed after loss of CO from the 19-electron radical generated at -1.15 V, addition of PPh₃, and ETC oxidation. IR scale chemical reductions indicated this was the product formed (*vide infra*). The ratio of the peak current for the PPh₃-substituted product

(16) (a) Gorelsky, S. I. *AOMix*: Program for Molecular Orbital Analysis; University of Ottawa, 2007. (b) Gorelsky, S. I.; Lever, A. B. P. *J. Organomet. Chem.* **2001**, 635, 187. (c) Ros, P.; Schuit, G. C. A. *Theor. Chem. Acc.* **1966**, 4, 1.

(17) Humphrey, W.; Dalke, A.; Schulten, K. *J. Mol. Graphics Modell.* **1996**, 14, 33.

(18) (a) Blackmore, T.; Bruce, M. I.; Stone, F. G. A. *J. Chem. Soc. A.* **1971**, 2376. (b) Angelici, R. J.; Blacik, L. J. *Inorg. Chem.* **1972**, 11, 1754. (c) Byrne, S.; Cox, M. G.; Manning, A. R. *J. Organomet. Chem.* **2001**, 629, 182.

to that of the original cation, $i(\text{PPh}_3)/i([\mathbf{2}]^+)$, was equal to 0.746. Lowering of the temperature to $-30\text{ }^\circ\text{C}$ resulted in slight shifts in reduction potentials (from -1.15 and -1.34 V to -1.22 and -1.55 V, respectively), as well as an increase in $i(\text{PPh}_3)/i([\mathbf{2}]^+)$ to a value of 2.10 (Figure 4c). The currents in Figure 4c were diminished compared to those in Figure 4b, owing to the temperature dependence of the diffusion rate. An IR spectrum recorded immediately after the CVs also showed that no reaction had occurred in the bulk solution.

A cursory inspection of the CV in Figure 4b might indicate that the mechanism of CO substitution is not an ETC mechanism, since the reduction wave at -1.15 V was not completely suppressed. An IR spectrum recorded after chemical reduction of $[\mathbf{2}]^+$ with 0.1 equiv of CoCp_2 in the presence of a 5 equiv excess of PPh_3 , however, indicated complete conversion to the PPh_3 -substituted product (**S5**), and thus supports an ETC mechanism. The reason for the similar values of $i(\text{PPh}_3)$ and $i([\mathbf{2}]^+)$, then, may be attributed to competition between CO substitution in $[\mathbf{2}]^+$ and its decomposition to the hydride. At lower temperature there is a significant decrease in $i([\mathbf{2}]^+)$ compared to $i(\text{PPh}_3)$. The resulting increase in $i(\text{PPh}_3)/i([\mathbf{2}]^+)$ indicates that, at lower temperature, the competition between CO substitution and hydride formation favors CO substitution; the pathway to hydride formation is suppressed. There is, then, an increase in the concentration of $[(\text{Cp})\text{Ru}(\text{CO})_2(\text{PPh}_3)]^+$ near the electrode surface. The abundance of the 19-electron PPh_3 -substituted species can effectively reduce any $[\mathbf{2}]^+$ in its vicinity, thus leading to a diminished wave for its reduction.

The behavior of $[\mathbf{2}]^+$ is similar to that of its Fe analogue, $[(\text{Cp})\text{Fe}(\text{CO})_3]^+$, in that both demonstrated irreversible one-electron reductions.³ Beyond that minor point, however, the chemistry of the compounds differs. Photolysis of $[(\text{Cp})\text{Fe}(\text{CO})_2]_2$ provided its rate of dissociation, k_D , to $[(\text{Cp})\text{Fe}(\text{CO})_2]$ to be $3 \times 10^9 \text{ M}^{-1} \text{ s}^{-1}$.³ Since this rate constant was known, Pevar and co-workers were able to digitally simulate cyclic voltammograms for the reduction and loss of CO from $[(\text{Cp})\text{Fe}(\text{CO})_3]^+$ and, comparing them to experimental CVs, determine a $k_{-\text{CO}}$. The difficulty with complex $[\mathbf{2}]^+$ is that not only is its one-electron reduction irreversible but there is also competition between formation of the dimer and formation of the hydride species. Photochemical experiments involving **[1]** have also indicated formation of **[3]** via hydrogen abstraction from the matrix environment, excluding determination of its k_D . Thus, while a relative $k_{-\text{CO}}$ for $[\mathbf{2}]^+$ could be determined, it would be impossible to determine an absolute rate constant.

The results of investigating $[\mathbf{5}]^+$ by cyclic voltammetry were slightly more interesting than those of $[\mathbf{2}]^+$. Since the electrochemical behavior of $[\mathbf{2}]^+$ was similar to that of $[(\text{Cp})\text{Fe}(\text{CO})_3]^+$, it was expected that $[\mathbf{5}]^+$ would act in a similar fashion to $[(\text{Ind})\text{Fe}(\text{CO})_3]^+$. However, at no time was any chemical reversibility apparent on the CV time scale, including lower temperatures and scan rates of 5 V/s; determination of $k_{-\text{CO}}$ for two P-donor ligands, PPh_3 and $\text{P}(\text{O}i\text{Pr})_3$, was thus not possible. The first reduction wave occurred at -0.594 V, followed by a second, more negative reduction at -1.69 V (Figure 5a). The second reduction wave was assigned to compound **[4]**, since bulk electrolysis of $[\mathbf{5}]^+$ at -1.0 V yielded **[4]**.

CVs recorded after the addition of 3 equiv of PPh_3 resulted in the appearance of a second chemically irreversible reduction wave at -1.01 V, due to $[(\text{Ind})\text{Ru}(\text{CO})_2(\text{PPh}_3)]^+$, which was formed in an analogous fashion to $[(\text{Cp})\text{Ru}(\text{CO})_2(\text{PPh}_3)]^+$. There was an almost complete suppression of the $[\mathbf{5}]^+$ wave (Figure 5b); $i(\text{PPh}_3)/i([\mathbf{5}]^+)$ at room temperature was 10.3. These factors indicate an ETC mechanism. It can be inferred that $k_{-\text{CO}}$ is quite

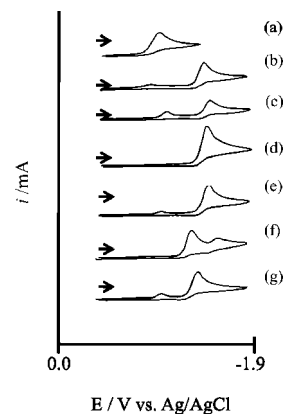


Figure 5. Cyclic voltammograms of 1.0 mM $[\mathbf{5}]^+$ in $\text{CH}_2\text{Cl}_2/0.10$ M TBAPF_6 under N_2 at the indicated temperatures and in the presence of the indicated nucleophiles: (a) $23\text{ }^\circ\text{C}$, none; (b) $23\text{ }^\circ\text{C}$, 3.0 equiv PPh_3 ; (c) $-30\text{ }^\circ\text{C}$, 3.0 equiv PPh_3 ; (d) $23\text{ }^\circ\text{C}$, 30 equiv PPh_3 ; (e) $-30\text{ }^\circ\text{C}$, 30 equiv PPh_3 ; (f) $23\text{ }^\circ\text{C}$, 4.64 equiv $\text{P}(\text{O}i\text{Pr})_3$; (g) $-30\text{ }^\circ\text{C}$, $\text{P}(\text{O}i\text{Pr})_3$. The working electrode was a 1 mm diameter platinum disk, and the scan rate was 0.50 V/s. All potentials are relative to the ferrocene/ferrocenium couple ($E_{1/2} = 0.50$ V).

large, and formation of the 19-electron $[(\text{Ind})\text{Ru}(\text{CO})_2(\text{PPh}_3)]$ is quite fast. Reduction of $[\mathbf{5}]^+$ by $[(\text{Ind})\text{Ru}(\text{CO})_2(\text{PPh}_3)]$ is favored, and the process removes $[\mathbf{5}]^+$ from the vicinity of the electrode surface; the wave due to reduction of $[\mathbf{5}]^+$ is diminished. The ETC mechanism was verified by the IR spectrum recorded after chemical reduction of $[\mathbf{5}]^+$ with 0.1 equiv of CoCp_2 in the presence of a 3 equiv excess of PPh_3 ; there was total conversion to the PPh_3 -substituted product (**S6**). At lower temperature, $i([\mathbf{5}]^+)$ increased and $i(\text{PPh}_3)/i([\mathbf{5}]^+)$ became 2.68 (Figure 5c). Lowering the temperature retarded $k_{-\text{CO}}$, resulting in a diminished concentration of $[(\text{Ind})\text{Ru}(\text{CO})_2(\text{PPh}_3)]$. Since the catalytic source of electrons, $[(\text{Ind})\text{Ru}(\text{CO})_2(\text{PPh}_3)]$, had diminished, the working electrode surface became the new reduction source for $[\mathbf{5}]^+$; $i([\mathbf{5}]^+)$ increased. Addition of 30 equiv of PPh_3 did not noticeably affect a difference in voltammetric response. The extreme excess of PPh_3 did, however, cause the suppression of the $[\mathbf{5}]^+$ reduction wave (Figure 5d); the low-temperature behavior was analogous (Figure 5e). IR spectra recorded after the CVs were recorded indicated no change in the bulk solution.

CVs of $[\mathbf{5}]^+$ in the presence of a 4.64 equiv excess of the weaker nucleophile $\text{P}(\text{O}i\text{Pr})_3$ exhibited behavior similar to that of the PPh_3 substitution. The wave due to reduction of $[\mathbf{5}]^+$ was completely suppressed, while a chemically irreversible wave due to the reduction of $[(\text{Ind})\text{Ru}(\text{CO})_2\text{P}(\text{O}i\text{Pr})_3]^+$ appeared at -0.925 V (Figure 5f). At lower temperature, $k_{-\text{CO}}$ was again sufficiently slow so as to allow the reappearance of the reduction wave for $[\mathbf{5}]^+$ (Figure 5g).

3.4. Density Functional Theory Investigations. Computational investigations at the extended Hückel level of theory were first reported on $[(\text{Cp})\text{Fe}(\text{CO})_3]^+$ and $[(\text{Ind})\text{Fe}(\text{CO})_3]^+$ by Pevar and co-workers.³ In the presence of phosphine and arsine ligands the rate of CO loss, $k_{-\text{CO}}$, for the $[(\text{Cp})\text{Fe}(\text{CO})_3]^+$ complex is much greater than that for the $[(\text{Ind})\text{Fe}(\text{CO})_3]^+$ complex. The difference in rate was explained on the basis of molecular orbital arguments. The LUMO of $[(\text{Cp})\text{Fe}(\text{CO})_3]^+$ is primarily Fe-CO π^* in nature. When $[(\text{Cp})\text{Fe}(\text{CO})_3]^+$ is reduced, CO readily dissociates from the complex. The LUMO of $[(\text{Ind})\text{Fe}(\text{CO})_3]^+$, however, paints a far different picture. While the LUMO of $[(\text{Ind})\text{Fe}(\text{CO})_3]^+$ contains Fe-CO π^* character, it also contains significant indenyl ring character on the benzene moiety. Pevar and co-workers thus rationalized the slower $k_{-\text{CO}}$ in $[(\text{Ind})$

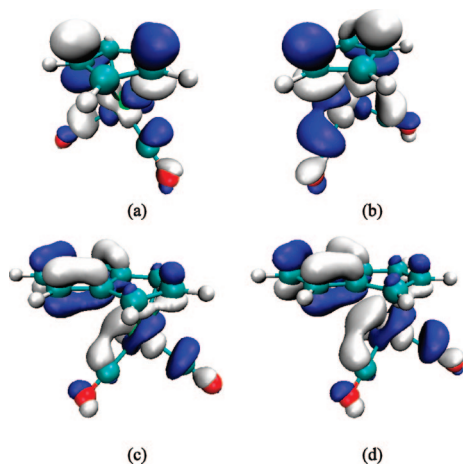


Figure 6. MO isosurfaces of (a) $[(Cp)Fe(CO)_3]^+$; (b) $[2]^+$; (c) $[(Ind)Fe(CO)_3]^+$; and (d) $[5]^+$. All surfaces are shown with a contour value of 0.04.

$Fe(CO)_3]^+$ relative to $[(Cp)Fe(CO)_3]^+$ was due to the ability of the former to accommodate electron density on the benzene moiety.

Our exploration of the Ru analogues $[2]^+$ and $[5]^+$ prompted us to reinvestigate $[(Cp)Fe(CO)_3]^+$ and $[(Ind)Fe(CO)_3]^+$. We have used density functional theory calculations at the B3LYP level of theory to probe the physical and electronic structures of $[(Cp)Fe(CO)_3]^+$, $[(Ind)Fe(CO)_3]^+$, $[2]^+$, and $[5]^+$. Tables TS1 and TS2 in the Supporting Information compares key bond lengths and angles from the X-ray crystal structures of $[(Cp)Fe(CO)_3]^+$,¹⁹ $[(Ind)Fe(CO)_3]^+$,³ $[2]^+$,²⁰ and $[5]^+$ (the current study) with those from our calculations. In each case the calculations agree within an average of 0.042 Å and 1.10° for bond lengths and bond angles, respectively.

Our DFT-calculated LUMOs of both Fe complexes agree with those calculated using extended Hückel theory (Figure 6). A SCPA fragment analysis^{16c} reveals the LUMO of $[(Cp)Fe(CO)_3]^+$ to be 53.20% Fe d-character, 18.64% CO character, and 28.15% cyclopentadienyl ring character. The LUMO of $[(Ind)Fe(CO)_3]^+$ is roughly the same in metal character and CO character, i.e., 57.46% and 20.67%, respectively; however, there is 21.87% of the MO localized on the benzene moiety of the complex. Even though the benzene moiety is *not* coordinated to Fe, the delocalized nature of the ring acts as an “electron sink”, accounting for the less rapid k_{-CO} in $[(Ind)Fe(CO)_3]^+$.

Our investigation into the Ru analogues $[2]^+$ and $[5]^+$ revealed an equivalent trend in the LUMO composition (Figure 6). A SCPA fragment analysis revealed $[2]^+$ to be 19.81% Ru d-character, 46.86% CO character, and 33.33% cyclopentadienyl character. $[5]^+$ is 32.71% Ru d-character, 23.71% CO character, and 43.58% indenyl ring character. The obvious difference between the LUMO compositions of the Fe and Ru complexes is the contribution from the transition metals. There is almost 40% more metal character in the Fe analogues than the Ru ones. The greater Fe character can be attributed to the greater interaction of the Fe 3d-orbitals with symmetry-matched π -orbitals on the indenyl ring. The higher energy Ru 4d-orbitals, however, do not contribute to the LUMOs, since they do not have as great an energetic match with the indenyl π -orbitals.

3.5. A Note on the Source of the Hydride. The most vexing question presented in this study is, “What is the source of the

hydride?” The most obvious answer would be the presence of adventitious water. This possibility, however, was disproved via an IR scale experiment. A sample of $[5]BF_4$ was dissolved in HPLC grade CH_2Cl_2 saturated with deionized water. The ν_{CO} observed were those for $[5]BF_4$, and not $[6]$. On the basis of the aforementioned, we believe water could not be the hydride source.

The literature does provide some clues as to the source of the hydride. A photochemical investigation by Zhang and co-workers showed the dimer $[(Cp)Os(CO)_2]_2$ would undergo Os–Os bond homolysis, followed by hydrogen atom abstraction from excess 1,4-cyclohexadiene in C_6D_6 or THF- d_8 .²¹ This observation leads us to believe there are two potential hydride sources, listed as follows. (1) Since the hydride $[6]$ forms only when $[5]BF_4$ is chemically reduced with Et_3N (Table 2), we cannot rule out Et_3N as a hydrogen source. This comment is lent credibility from an excellent review by Geiger and Connelly on organometallic reducing agents, where it is noted that the reduction products of Et_3N have never been characterized.²² (2) Since the hydride $[3]$ forms from the reduction of $[2]PF_6$ under all reducing conditions tried (Table 2), and since all chemistry for $[2]PF_6$ was carried out in acetonitrile, we cannot rule out acetonitrile as a potential hydrogen source.

3.6. Conclusions. Complexes $[2]^+$ and $[5]^+$ proved to have very different chemistries compared to their Fe analogues. Chemical reductions of $[2]^+$ with NEt_3 and $CoCp_2$, as well as electrochemical reduction via bulk electrolysis, yielded the hydride complex $[3]$. This is remarkably different from chemical reductions with the same reagents, as well as bulk electrolysis, of $[(Cp)Fe(CO)_3]^+$, which yielded only the dimer $[(Cp)Fe(CO)_2]_2$. Determination of k_{-CO} for $[2]$ was impossible due to the irreversible one-electron reduction observed on the CV time scale. The irreversible nature of the CV is attributed to competition between formation of the dimer $[1]$ and formation of the hydride $[3]$ after reduction.

Chemical reduction of $[5]^+$ with NEt_3 yielded the hydride complex $[6]$, while both chemical reduction with $CoCp_2$ and electrochemical reduction via bulk electrolysis yielded the dimer $[4]$. This differs from the Fe complex $[(Ind)Fe(CO)_3]^+$ in that all chemical reductions with the same reagents, as well as bulk electrolysis, yielded the dimer $[(Ind)Fe(CO)_2]_2$. Determination of k_{-CO} for $[5]$ was impossible due to the irreversible one-electron reduction observed on the CV time scale. This differs from $[(Ind)Fe(CO)_3]^+$, whose chemically reversible CV enabled k_{-CO} to be determined. The irreversible nature of the CV for $[5]^+$ is attributed to decomposition of the 19-electron radical formed, most likely to the hydride complex $[6]$. Exploring the mechanism of hydride addition in both $[2]^+$ and $[5]^+$, including the potential source of the hydride, will be the subject of future work.

As previously mentioned, the greatest question remaining in our investigation is the origin of hydride formation from $[2]^+$ and $[5]^+$. The hydride species $[3]$ is known and has been extensively investigated.²³ At least one experiment showed that the formation of $[3]$ could be achieved via photolysis of $[(Cp)Ru(CO)_2(C_2H_6)]$.²⁴ β -Hydride elimination from the coordinated ethyl group resulted in the observed $[(Cp)Ru(CO)H(C_2H_4)]$, which could undergo further CO substitution

(21) Zhang, J.; Grills, D. C.; Huang, K. W.; Fujita, E.; Bullock, R. M. *J. Am. Chem. Soc.* **2005**, *127*, 15684.

(22) Connelly, N. G.; Geiger, W. E. *Chem. Rev.* **1996**, *96*, 877–910.

(23) See, for example: (a) Bullock, R. M.; Song, J.-S. *J. Am. Chem. Soc.* **1994**, *116*, 8602. (b) Pinkes, J. R.; Masi, C. J.; Chiulli, R.; Steffey, B. D.; Cutler, A. R. *Inorg. Chem.* **1997**, *36*, 70. (c) Ellis, D. D.; Jelliss, P. A.; Stone, F. G. A. *Organometallics* **1999**, *18*, 4982.

(19) Gress, M. E.; Jacobson, R. A. *Inorg. Chem.* **1973**, *12*, 1746.

(20) Griffith, C. S.; Koutsantonis, G. A.; Raston, C. L.; Selegue, J. P.; Skelton, B. W.; White, A. H. *J. Organomet. Chem.* **1996**, *518*, 197.

to form [(Cp)Ru(CO)₂H]. The chemical origin of the hydride for the Ru complexes, and the lack thereof in the Fe complexes, will be the subject of a future investigation.

Acknowledgment. This work was supported by startup funds from the College of Letters and Science and the Department of Chemistry at UWSP. J.S.D. and R.S.T. are grateful to Professor A. L. Rheingold at U.C. San Diego for collection of single-crystal X-ray diffraction data. J.S.D. is grateful to Professors M. Zach and J. Lawrence at UWSP for use of equipment to aid in crystal growth and selection, and to Professor N. Bowling for stimulating discussions.

T.A.O. thanks the UWSP College of Letters and Science for a summer stipend provided through a UEI Grant.

Supporting Information Available: CIF file of [5⁺]BF₄; IR spectra of all chemical and electrochemical reductions; tables comparing selected bond lengths and angles of crystal structures to calculated structures; Cartesian coordinates of all geometry-optimized structures. This material is available free of charge via the Internet at <http://pubs.acs.org>.

OM800767G

(24) Mahmoud, K. A.; Rest, A. J.; Alt, H. G. *J. Chem. Soc.* **1985**, 1365–1374.

First Optically Active Phosphapalladacycle Bearing a Phosphorus Atom in an Axially Chiral Environment

Valery V. Dunina,^{*,†} Pavel A. Zykov,^{†,‡} Michail V. Livantsov,[†] Ivan V. Glukhov,[‡]
Konstantin A. Kochetkov,[‡] Igor P. Gloriov,[†] and Yuri K. Grishin^{*,†}

Department of Chemistry, M.V. Lomonosov Moscow State University, 1 Leninskie Gory, 119991 Moscow, Russian Federation, and A.N. Nesmeyanov Institute of Organoelement Compounds, Russian Academy of Sciences, Vavilova Street 28, 119991 Moscow, Russian Federation

Received July 10, 2008

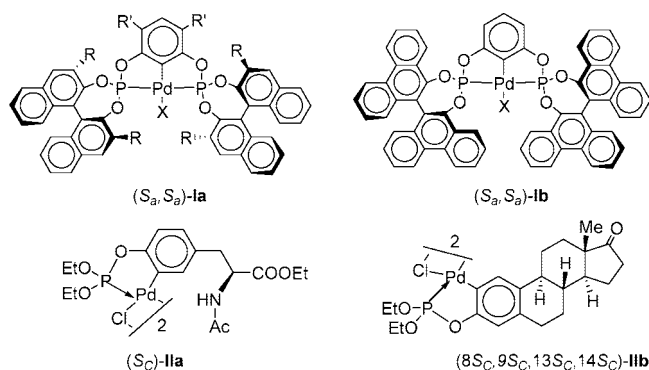
Direct C–H bond activation in the (*S_a*)-BINOL-derived phosphite (**HL**) afforded the dimeric cyclopalladated complex (*S_aS_a*)-{Pd(η^2 -L)(μ -Cl)}₂ (**1**), which is the first optically active phosphapalladacycle bearing a phosphorus atom in an axially chiral environment. The *ortho*-palladated structure of complex **1** was confirmed by spectral (¹H and ³¹P) investigations of mononuclear derivatives and the X-ray diffraction study of the phosphane adduct (η^2 -L)PdCl(PPh₃) (**3**). The enantiomeric purity of the starting ligand remained unchanged in the *PC*-palladacycle under the thermal conditions used for the cyclopalladation (~110 °C); this fact was confirmed by the ³¹P NMR spectroscopy after chiral derivatization of dimer (*S_aS_a*)-**1** with the (*R_c*)-valinate auxiliary ligand. The *trans*(*N,C*)-configuration of the valinate complex (**4**) was supported by DFT calculations. The chirality transfer in the new system was discussed on the basis of X-ray diffraction data for the phosphane adduct *rac*-**3** and DFT calculations performed for both mononuclear derivatives.

Introduction

Coordination complexes of transition metals with mono-¹ or bidentate² *P*-donor ligands bearing elements of axial chirality, including BINOL-derived phosphites³ and phosphoramidites,^{4,5} are well known as very efficient asymmetric catalysts. Participation of the corresponding *PC*-metallacycles in some of the

iridium- and palladium-catalyzed processes was established^{6a,b} or proposed.^{6c} Surprisingly, despite a high catalytic activity of achiral phosphite *PC*-palladacycles⁷ and excellent results achieved in asymmetric catalysis with BINOL-derived phosphite ligands, cyclopalladated compounds (CPCs) obtained from the same type of ligands have remained unknown until now. Recently⁸ several pincer *PCP*-complexes based on bis(phosphites) derived from binaphthol (**1a**) or biphenanthrol (**1b**) were reported. In addition, only two examples of optically active phosphite *PC*-palladacycles (**1a,b**) with rather distant carbon stereocenters⁹ have also been described (Chart 1).

Chart 1



The aim of this work was to study the possibility of direct cyclopalladation of BINOL-derived phosphites as a route to

* Corresponding author. Fax: (495) 932 8846. E-mail: dunina@org.chem.msu.ru.

[†] M.V. Lomonosov Moscow State University.

[‡] A.N. Nesmeyanov Institute of Organoelement Compounds.

(1) (a) Ansell, J.; Wills, M. *Chem. Soc. Rev.* **2002**, *31*, 259. (b) Hayashi, T. *Acc. Chem. Res.* **2000**, *33*, 354. (c) Hayashi, T. *J. Organomet. Chem.* **1999**, *576*, 195.

(2) (a) McCarthy, M.; Guiry, P. J. *Tetrahedron* **2001**, *57*, 3809. (b) Guiry, P. J.; McCarthy, M.; Lacey, P. M.; Saunders, C. P.; Kelly, S.; Connolly, D. *J. Curr. Org. Chem.* **2000**, *4*, 821.

(3) (a) Reetz, M. T.; Mehler, G.; Bondarev, O. *Chem. Commun.* **2006**, 2292. (b) Reetz, M. T.; Meiswinkel, A.; Mehler, G.; Angermund, K.; Graf, M.; Thiel, W.; Mynott, R.; Blackmond, D. G. *J. Am. Chem. Soc.* **2005**, *127*, 10305. (c) Gergely, I. G.; Hegedüs, C.; Gulyás, H.; Scöllösy, A.; Monsees, A.; Riermeier, Th.; Bakos, J. *Tetrahedron: Asymmetry* **2003**, *14*, 1087. (d) Sturla, Sh. J.; Buchwald, St. L. *J. Org. Chem.* **2002**, *67*, 3398. (e) Reetz, M. T.; Mehler, G.; Meiswinkel, A.; Sell, Th. *Tetrahedron Lett.* **2002**, *43*, 7941. (f) Chen, W.; Xiao, J. *Tetrahedron Lett.* **2001**, *42*, 2897. (g) Reetz, M. T.; Mehler, G. *Angew. Chem., Int. Ed.* **2000**, *39*, 3889. (h) Yan, M.; Yang, K.-Y.; Chan, A. S. C. *Chem. Commun.* **1999**, *11*. (i) Yan, M.; Chan, A. S. C. *Tetrahedron Lett.* **1999**, *40*, 6645.

(4) (a) Kurihara, K.; Sugishita, N.; Oshita, K.; Piao, D.; Yamamoto, Ya.; Miyaura, N. *J. Organomet. Chem.* **2007**, *692*, 428. (b) Zhang, A.; RajanBabu, T. V. *J. Am. Chem. Soc.* **2006**, *128*, 54. (c) Zeng, Q.-H.; Hu, X.-P.; Duan, Zh.-Ch.; Liang, X.-M.; Zheng, Zh. *J. Org. Chem.* **2006**, *71*, 393. (d) Vallianatou, K. A.; Kostas, I. D.; Holz, J.; Börner, A. *Tetrahedron Lett.* **2006**, *47*, 7947. (e) Welter, C.; Moreno, R. M.; Streiff, St.; Helmchen, G. *Org. Biomol. Chem.* **2005**, *3*, 3266. (f) de Vries, A. H. M.; Boogers, J. A. F.; van den Berg, M.; Peña, D.; Minnaard, A. J.; Feringa, B. L.; de Vries, J. G. *Pharma Chem.* **2003**, *33*. (g) Zeng, Q.; Liu, H.; Cui, X.; Mi, A.; Jiang, Ya.; Li, X.; Choi, M. C. K.; Chan, A. S. C. *Tetrahedron: Asymmetry* **2002**, *13*, 115. (h) van den Berg, M.; Minnaard, A. J.; Schudde, E. P.; van Esch, J.; de Vries, A. H. M.; de Vries, J. G.; Feringa, B. L. *J. Am. Chem. Soc.* **2000**, *122*, 11539. (i) Feringa, B. L. *Acc. Chem. Res.* **2000**, *33*, 346. (j) Arnold, L. A.; Imbos, R.; Mandoli, A.; de Vries, A. H. M.; Naasz, R.; Feringa, B. L. *Tetrahedron* **2000**, *56*, 2865.

(5) (a) Trost, B. M.; Silverman, St. M.; Stambuli, J. P. *J. Am. Chem. Soc.* **2007**, *129*, 12398. (b) Ohmura, T.; Taniguchi, H.; Suginome, M. *J. Am. Chem. Soc.* **2006**, *128*, 13682. (c) Trost, B. M.; Stambuli, J. P.; Silverman, St. M.; Schwörer, U. *J. Am. Chem. Soc.* **2006**, *128*, 13328. (d) Zhang, A.; RajanBabu, T. V. *J. Am. Chem. Soc.* **2006**, *128*, 5620. (e) Boele, M. D. K.; Kamer, P. C. J.; Lutz, M.; Spek, A. L.; de Vries, J. G.; van Leeuwen, P. W. N. M.; van Strijdonck, G. P. F. *Chem.—Eur. J.* **2004**, *10*, 6232.

enantiopure *PC*-palladacycles and to estimate efficiency of chirality transfer from an axial chiral environment of the phosphorus atom.

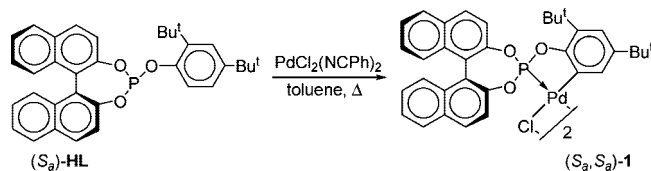
Results and Discussion

Phosphite Cyclopalladation. For steric promotion of an intramolecular C–H bond activation¹⁰ a rather bulky phosphite ligand (*S_a*)-**HL** was chosen for cyclopalladation. Both racemic and enantiopure phosphites **HL** were prepared by a known route^{8d,10c,11} that includes a reaction of the *in situ* obtained BINOL-derived phosphorochloridite^{4j} with 2,4-di-*tert*-butylphenol in the presence of a base. Phosphite **HL** possesses moderate oxidative and hydrolytic stability: keeping a pure sample in a chloroform solution in air for a week resulted in 10% decomposition (³¹P data). To our knowledge, this ligand is a new member¹² of a large group of the BINOL-derived ArO-substituted phosphites.^{3g,i,13–15}

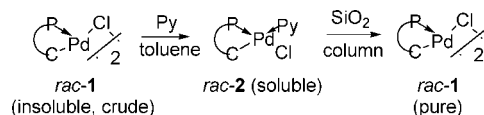
Two protocols were reported for cyclopalladation of achiral phosphite ligands (**HL'**): (i) a two-step procedure through intermediate coordination complex Pd(**HL'**)₂Cl₂^{9a,10b,16,17} and (ii) a one-step synthesis by reaction of PdCl₂ with phosphite **HL'** in a 1:1 ratio at heating.^{10c,11} Typically, the latter method provides a high yield of CPCs from simple triarylphosphites (up to 98%^{10c,18}), which may be decreased to 43–53% in the case of encumbered ligands.^{8d,11}

Cyclopalladation of phosphite **HL** appeared to be a rather difficult task. Thus, our attempts to adopt the aforementioned

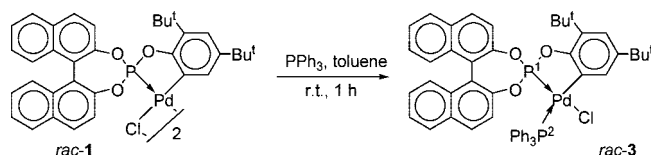
Scheme 1



Scheme 2



Scheme 3



protocols to our system and to use the more electrophilic reagent Pd(OAc)₂ resulted in palladium black precipitation and formation of complex mixtures of coordination complexes. However, the reaction of phosphite **HL** with PdCl₂(NCPh)₂ in refluxing toluene provided racemic and optically active cyclopalladated dimers, *rac-1* and (*S_wS_a*)-**1a**, in 40–43% yield after column chromatography (Scheme 1). In a similar reaction carried out in 1,2-dichloroethane (DCE), the yield of *rac-1* was slightly lower, 37%. Attempts to promote C–H bond activation with Et₃N as a base in DCE (cf. ref 8d) resulted in palladium(II) reduction.

A very low solubility of the racemic dimer **1** complicated its purification. To overcome this obstacle, dimer *rac-1* was converted into its more soluble mononuclear pyridine derivative (**2**) followed by its chromatographic purification (cf. ref 19). Strong *trans*-influence of both carbanionic and phosphorus donor atoms of the *PC*-palladacycle facilitated elimination of the auxiliary pyridine ligand from adduct *rac-2* with formation of the pure dimer *rac-1* (TLC and NMR data; Scheme 2).

Dynamic mobility of dimeric CPCs²⁰ and their existence as mixtures of *syn/anti* and *meso/dl* isomers prevent their use for spectral studies; so we converted the dimer *rac-1* into its mononuclear phosphane derivative *rac-3* by the reaction of chloride bridge cleavage (Scheme 3).

Previously, it was reported that the BINOL-derived bis(phosphites) undergo partial racemization at temperatures above 60 °C.^{8a} This report somewhat contradicts the following data: (i) high optical yields in enantioselective transition metal-catalyzed reactions at 45–120 °C with the BINOL-derived ligands;^{3a,4a,5a,6c,21} (ii) racemization of BINOL²² and its monoacylated derivatives²³

(6) (a) Marković, D.; Hartwig, J. F. *J. Am. Chem. Soc.* **2007**, *129*, 11680. (b) Kiener, Ch. A.; Shu, Ch.; Incarvito, Ch.; Hartwig, J. F. *J. Am. Chem. Soc.* **2003**, *125*, 14272. (c) López, F.; Ohmura, T.; Hartwig, J. F. *J. Am. Chem. Soc.* **2003**, *125*, 3426.

(7) (a) Bedford, R. B.; Betham, M.; Blake, M. E.; Frost, R. M.; Norton, P. N.; Hursthouse, M. B.; López-Nicolás, R.-M. *Dalton Trans.* **2005**, 2774. (b) Bedford, R. B.; Coles, S. J.; Hursthouse, M. B.; Scordia, V. J. M. *Dalton Trans.* **2005**, 991. (c) Bedford, R. B. *Chem. Commun.* **2003**, 1787 (review). (d) Bedford, R. B.; Cazin, C. S. J.; Hazelwood (née Welch), S. M. *Angew. Chem. Int. Ed.* **2002**, *41*, 4120. (e) Bedford, R. B.; Hazelwood (née Welch), S. M.; Limmert, M. E. *Chem. Commun.* **2002**, 2610. (f) Bedford, R. B.; Cazin, C. S. J.; Hazelwood (née Welch), S. M. *Chem. Commun.* **2002**, 2608. (g) Alibisson, D. A.; Bedford, R. B.; Lawrence, S. E.; Scully, P. N. *Chem. Commun.* **1998**, 2095. (h) Alibisson, D. A.; Bedford, R. B.; Scully, P. N. *Tetrahedron Lett.* **1998**, *39*, 9793.

(8) (a) Aydin, J.; Kumar, K. S.; Sayah, M. J.; Wallner, O. A.; Szabó, K. J. *J. Org. Chem.* **2007**, *72*, 4689. (b) Szabó, K. J. *Synlett.* **2006**, 811. (c) Wallner, O. A.; Olsson, V. J.; Eriksson, L.; Szabó, K. J. *Inorg. Chim. Acta* **2006**, *359*, 1767. (d) Baber, R. A.; Bedford, R. B.; Betham, M.; Blake, M. E.; Coles, S. J.; Haddow, M. F.; Hursthouse, M. B.; Orpen, A. G.; Pilarski, L. T.; Pringle, P. G.; Wingad, R. L. *Chem. Commun.* **2006**, 3880.

(9) (a) Sokolov, V. I.; Bulygina, L. A.; Borbulevych, O. Ya.; Shishkin, O. V. *J. Organomet. Chem.* **1999**, *582*, 246. (b) Bulygina, L. A.; Sokolov, V. I. *Russ. Chem. Bull.* **1998**, *47*, 1235.

(10) (a) Dupont, J.; Consorti, C. S.; Spencer, J. *Chem. Rev.* **2005**, *105*, 2527. (b) Dunina, V. V.; Gorunova, O. N. *Russ. Chem. Rev.* **2004**, *73*, 309. (c) Bedford, R. B.; Hazelwood (née Welch), S. M.; Limmert, M. E.; Alibisson, D. A.; Draper, S. M.; Scully, P. N.; Coles, S. J.; Hursthouse, M. B. *Chem.–Eur. J.* **2003**, *9*, 3216.

(11) Bedford, R. B.; Hazelwood, S. M.; Limmert, M. E.; Brown, J. M.; Ramdeehul, Sh.; Cowley, A. R.; Coles, S. J.; Hursthouse, M. B. *Organometallics* **2003**, *22*, 1364.

(12) Despite phosphite **HL**'s use in catalysis being mentioned,^{6c} its synthesis, characteristics, and spectral data were not reported.

(13) Baker, M. J.; Pringle, P. G. *Chem. Commun.* **1991**, 1292.

(14) Fujii, K.; Kinoshita, N.; Tanaka, K.; Kawabata, T. *Chem. Commun.* **1999**, 2289.

(15) Dussault, H. D.; Woller, K. R. *J. Org. Chem.* **1997**, *62*, 1556.

(16) (a) Tune, D. J.; Werner, H. *Helv. Chim. Acta* **1975**, *58*, 2240. (b) Ahmed, N.; Ainscough, E. W.; James, T. A.; Robinson, S. D. *Dalton Trans.* **1973**, 1151.

(17) Albinati, A.; Affolter, S.; Pregosin, P. S. *Organometallics* **1990**, *9*, 379.

(18) (a) Tanase, A. D.; Frey, G. D.; Herdtweck, E.; Hoffmann, St. D.; Herrmann, W. A. *J. Organomet. Chem.* **2007**, *692*, 3316. (b) Bedford, R. B.; Betham, M.; Coles, S. J.; Norton, P. N.; López-Sáez, M.-J. *Polyhedron* **2006**, *25*, 1003.

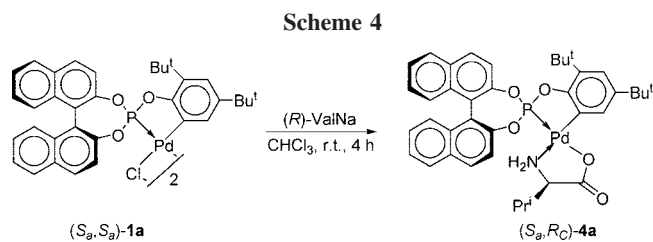
(19) (a) Dunina, V. V.; Razmyslova, E. D.; Gorunova, O. N.; Livantsov, M. V.; Grishin, Yu. K. *Tetrahedron: Asymmetry* **2005**, *16*, 817. (b) Dunina, V. V.; Zalevskaya, O. A.; Potapov, V. M. *Zh. Obshch. Khim. (Russ.)* **1983**, *53*, 468. [*Russ. J. Gen. Chem.* **1983**, *53* (Engl. Transl.)]

(20) (a) Gül, N.; Nelson, J. H. *Organometallics* **2000**, *19*, 91. (b) Herrmann, W. A.; Brossmer, C.; Reisinger, C.-P.; Riermeier, T. H.; Öfele, K.; Beller, M. *Chem.–Eur. J.* **1997**, *3*, 1357. (c) Fuchita, Y.; Nakashima, M.; Hiraki, K.; Kawatani, M.; Ohnuma, K. *Dalton Trans.* **1988**, 785.

(21) Duursma, A.; Lefort, L.; Boogers, J. A. F.; de Vries, A. H. M.; de Vries, J. G.; Minnaard, A. J.; Feringa, B. L. *Org. Biomol. Chem.* **2004**, *2*, 1682.

(22) Meca, L.; Řeha, D.; Havlas, Z. *J. Org. Chem.* **2003**, *68*, 5677, and references therein.

(23) Albrow, V.; Biswas, K.; Crane, A.; Chaplin, N.; Easun, T.; Gladiali, S.; Lygo, B.; Woodward, S. *Tetrahedron: Asymmetry* **2003**, *14*, 2813.



at much higher temperature (220–280 °C); and (iii) reported mechanistic pathways²⁴ for racemization are inapplicable in our case. Consequently, we studied whether palladacycle (S_a)-**1a** kept the enantiopurity of the starting diol after C–H bond activation in boiling toluene (~110 °C).

The enantiopurity of the dimer (S_a, S_a)-**1** was determined by ³¹P NMR spectroscopy after its chiral derivatization *in situ* with the (R_C)-valinate auxiliary ligand (Scheme 4). The ³¹P NMR spectrum of (S_a, R_C)-**4a** contains only one singlet at δ 148.03 ppm, while two singlets at δ 148.07 and 147.73 ppm were found in the spectrum of a mixture of two diastereomers, (S_a, R_C)/R_a, R_C)-**4a, b**, prepared in a similar way from the dimer *rac*-**1**. Thus, the optically active dimer (S_a, S_a)-**1a** completely retained the enantiomeric composition of starting (S_a)-BINOL, confirming the possibility of direct cyclopalladation of chiral BINOL-derived ligands without decrease in their enantiomeric purity.

Spectral Studies of Cyclopalladated Complexes. The signal assignment in the ¹H spectra of ligand **HL** and CPCs **1–4** was performed using homo- and heteronuclear decoupling, COSY and NOE techniques, DFT structure, and ¹H NMR spectra calculations for the complexes **3** and **4a, b**.

The chemical shift value in the ³¹P{¹H} NMR spectra of ligand **HL** (δ 145.1 ppm) is typical for the BINOL-derived mono-^{13,15} and bis-phosphites.^{8c,d,13,25} The ³¹P{¹H} NMR spectra of the dimers *rac*-**1** and (S_a, S_a)-**1a** contain four or two broadened singlets, respectively, which is indicative of their existence as mixtures of *anti* and *syn* isomers. The ³¹P{¹H} NMR spectrum of the mononuclear adduct **3** consists of two doublets at δ 149.9 and 17.66 ppm assigned to the phosphorus atoms of the PC-palladacycle (P¹) and auxiliary phosphane PPh₃ (P²), respectively. The value of the constant ²J_{PP} 45.2 Hz is an unambiguous evidence of its *cis*(P, P)-geometry,²⁶ which is typical for phosphite palladacycles.^{10c,16b,17,18b,27}

The ¹H NMR spectrum of adduct **3** confirms its cyclopalladated structure. The metalation at the *ortho*-C–H bond of the 2,4-di-*tert*-butyl-substituted phenyl ring is supported by the presence of only two one-proton signals at δ 8.57 (ddd) and 7.18 ppm (dd) without a ³J_{HH} coupling constant. Their assignment to H(6'') and H(4'') protons, respectively, was based on the following arguments: (i) the most low-field position of the first signal due to the influence of the adjacent chloride anisotropy [H(6'')...Cl distance is equal to 2.49–2.66 Å, DFT and X-ray data]; (ii) both protons have a spin–spin coupling

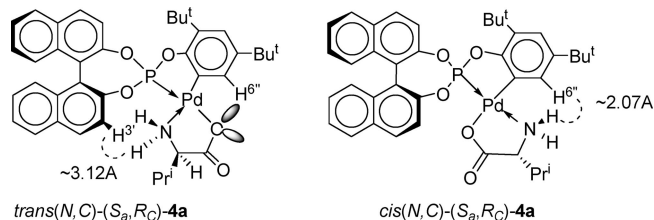


Figure 1. Mutual arrangement of NH and aromatic protons in two geometric isomers of valinate derivative (S_a, R_C)-**4a**.

with the P¹ atom (⁵J_{HP¹} 5.6 and 2.6 Hz, respectively), and (iii) only one of the two protons, H(6''), has a rather large ⁴J_{HP²} constant (8 Hz) with the P² atom of the PPh₃ ligand. The signals of the 1,1'-binaphthyl moiety were identified starting from the ⁴J_{HP¹} constant values for the H(3)/H(3') protons (0.9 and 1.2 Hz, respectively).

The signals at δ 1.69 and 2.10 ppm in the ¹H NMR spectrum of the valinate derivative (S_a, R_C)-**4a** were assigned to the NH^{eq} and NH^{ax} protons using the correlation of the ³J_{HNC^αH} values (4.4 and 7.2 Hz, respectively) with the dihedral angles ∠HNC^αH (+44.67° and +161.84°, respectively, DFT data). The *trans*-(N, C)-configuration of complex **4a** can be supported by the following data: (i) the signal of the H(6'') proton was shifted low-field (δ 7.87 ppm) due to anisotropy of the carboxylate oxygen (Figure 1); it was confirmed by DFT calculation of the chemical shifts and the H(6'')...O(CO) distance (2.31 Å, cf. ref 28); (ii) DFT calculations for both isomers predict significant dipole–dipole interactions due to a short H(6'')...NH^{eq} distance (2.22 Å) only for the alternative *cis*(N, C) isomer (it was not detected); and (iii) the *trans*(N, C)-configuration seems to be preferable with respect to the “*transphobia*” concept.^{27a,29}

DFT calculations were performed for *trans*(N, C) and *cis*(N, C) isomers of (S_a, R_C)-**4a** and (R_a, R_C)-**4b** diastereomers of the valinate derivative (Figure 2, Table 1).³⁰ They provided the following data: (i) for both diastereomers **4a, b** the *trans*(N, C) geometry is more preferable than the *cis*(N, C) (ΔE⁰ 2.33 and 2.57 kcal/mol, respectively); (ii) both diastereomers demonstrate preference for the λ(R_C)-conformation of the valinate N, O-ring;³¹

(28) Bondi, A. J. *Phys. Chem.* **1964**, *68*, 441.

(29) (a) Vicente, J.; Abad, J.-A.; Martínez-Viviente, E. *Organometallics* **2002**, *21*, 4454. (b) Vicente, J.; Arcas, A.; Bautista, D.; de Arellano, M. C. R. *J. Organomet. Chem.* **2002**, *663*, 164. (c) Vicente, J.; Arcas, A.; Bautista, D.; Jones, P. G. *Organometallics* **1997**, *16*, 2127.

(30) The parameters used for discussion of the conformation of the valinate N, O-chelate ring and PC-palladacycle were the same as described below for the X-ray data discussion.

(31) Hawkins, C. J. *Absolute Configuration of Metal Complexes*; Wiley-Interscience: New York, 1971.

(32) Hursthouse, M. B.; Gelbrich, T.; Bedford, R. B. Private communication, 2003 (IPOLUU).

(33) Bedford, R. B.; Betham, M.; Coles, S. J.; Frost, R. M.; Hursthouse, M. B. *Tetrahedron* **2005**, *61*, 9663.

(34) Mahalakshmi, L.; Krishnamurthy, S. S.; Nethaji, M. *Curr. Sci.* **2002**, *83*, 870 (HUXHIR).

(35) Miyazaki, F.; Yamaguchi, K.; Shibasaki, M. *Tetrahedron Lett.* **1999**, *40*, 7379 (GACYUE).

(36) *Nomenclature of Inorganic Chemistry. Recommendations 1990*; International Union of Pure and Applied Chemistry; Leigh, G. J., Ed.; Blackwell Scientific Publications: Oxford, 1990.

(37) Here and later on, the base of the envelope was determined using the minimal value of the intrachelate torsion angle.

(38) (a) Ayscough, A. P.; Costello, J. F.; Davies, S. G. *Tetrahedron: Asymmetry* **2001**, *12*, 1621. (b) Dance, I.; Scudder, M. *Dalton Trans.* **2000**, 1579. (c) Costello, J. F.; Davies, S. G. *J. Chem. Soc., Perkin Trans. 2* **1999**, 465. (d) Costello, J. F.; Davies, S. G. *J. Chem. Soc., Perkin Trans. 2* **1998**, 1683. (e) Garner, S. E.; Orpen, A. G. *J. Chem. Soc., Dalton Trans.* **1993**, 533.

(39) Sharp, J. T.; Gosney, I.; Rowley, A. G. *Practical Organic Chemistry. A student handbook of techniques*; London, 1989.

(24) (a) Juríček, M.; Brath, H.; Kasák, P.; Putala, M. *J. Organomet. Chem.* **2007**, *692*, 5279. (b) Kasák, P.; Brath, H.; Dubovská, M.; Juríček, M.; Putala, M. *Tetrahedron Lett.* **2004**, *45*, 791.

(25) Iní, S.; Oliver, A. G.; Tilley, T. D.; Bergman, R. G. *Organometallics* **2001**, *20*, 3839.

(26) (a) *Phosphorus-31 NMR Spectroscopy in Stereochemical Analysis*; Verkade, J. G.; Quin, J. G., Eds.; VCH: Weinheim, 1987. (b) Pregosin, P. S.; Kunz, R. W. ³¹P and ¹³C NMR of transition metal phosphine complexes. In *NMR Basic Principles and Progress Grundlagen und Fortschritte*, Bd. 16; Diel, P., Fluck, E., Kosfeld, R., Eds.; Springer-Verlag: New York, 1979.

(27) (a) Dunina, V. V.; Gorunova, O. N. *Russ. Chem. Rev.* **2005**, *74*, 871. (b) Albinati, A.; Affolter, S.; Pregosin, P. S. *J. Organomet. Chem.* **1990**, *395*, 231.

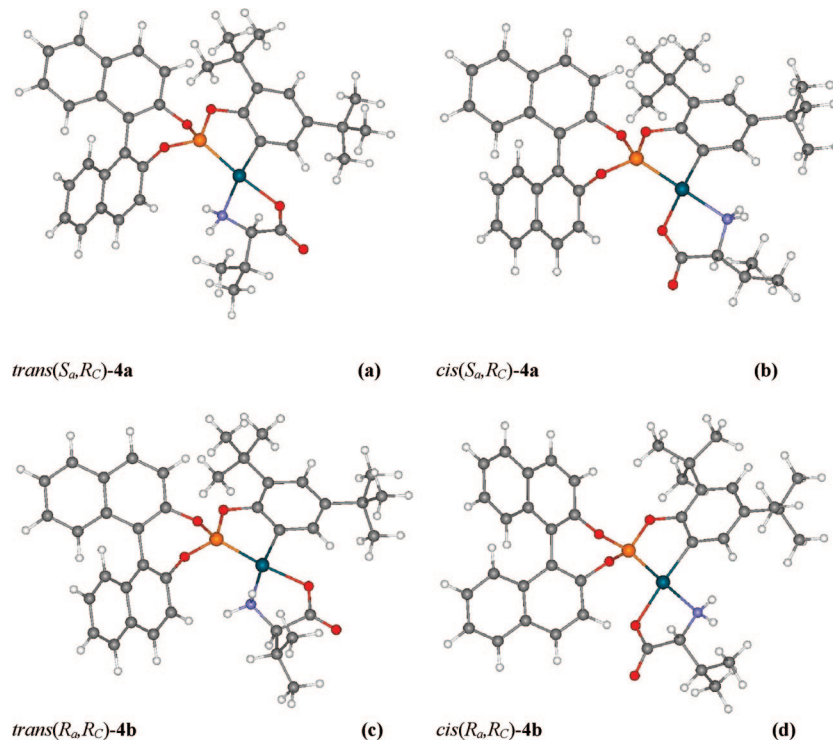


Figure 2. DFT-calculated structures for the more stable conformers of *trans*(*N,C*) (a, c) and *cis*(*N,C*) isomers (b, d) of (*S_aR_C*)-**4a** (a, b) and (*R_aR_C*)-**4b** diastereomers (c, d) in the gas phase.

Table 1. Selected Parameters of Two Geometric Isomers of Each of Diastereomeric Valinate Derivatives (*S_aR_C*)-**4a** and (*R_aR_C*)-**4b** (DFT data).

coordination sphere geometry (<i>N,C</i>)	ΔE^0 , kcal/mol	<i>N,O</i> -chelate ring ^a			<i>PC</i> -palladacycle		
		ϖ_{av}^b	$\angle ONC^cC(O)$	conformation	ϖ_{av}^b	$\angle C^1POC^2$	conformation
diastereomer (<i>S_aR_C</i>)- 4a							
<i>trans</i> - 4a	0.10	18.55°	+10.97°	λ	0.71°	+0.60°	— ^c
<i>cis</i> - 4a	2.43	17.62°	+10.61°	λ	11.93°	+4.64°	λ
diastereomer (<i>R_aR_C</i>)- 4b							
<i>trans</i> - 4b	0.00	16.87°	+10.03°	λ	2.25°	−1.43°	— ^c
<i>cis</i> - 4b	2.57	17.30°	+12.83°	λ	9.52°	−3.62°	δ

^a The *N,O*-chelate ring in all isomers exists in the λ -conformation with equatorial disposition of the *i*-Pr group. ^b The average magnitude of the absolute values of intrachelate torsion angles (ϖ_{av}) was chosen to characterize the nonplanarity extent of the *N,O*-chelate ring or *PC*-palladacycle. ^c The *PC*-palladacycle conformation has to be considered as a nontwisted one.

(iii) the *PC*-palladacycle's nonplanarity is substantial in the complexes *cis*(*N,C*)-**4a,b** ($\varpi_{av} = 11.93^\circ$ and 9.52° , respectively), whereas their *trans*(*N,C*) isomers contain a nearly planar metallacycle ($\varpi_{av} = 0.71^\circ$ and 2.25°); (iv) the *PC*-palladacycles in *cis*(*N,C*) isomers of (*S_aR_C*)-**4a** and (*R_aR_C*)-**4b** exist in opposite envelope-like λ - and δ -conformations, respectively, in accordance with the configuration of the dioxaphosphepine moiety; and (v) the palladium coordination environment is square-planar, with torsion angles $\angle P \cdots C^1 \cdots O \cdots N < 2.6^\circ$.

X-ray Diffraction Study of the Phosphane Adduct *rac*-3**.** The cyclopalladated structure of dimer **1** and the *cis*(*P,P*)-geometry of its mononuclear phosphane derivative *rac*-**3** were

established unambiguously by the X-ray diffraction study of the latter. The molecular structure of complex **3** is presented in Figure 3; selected bond lengths and angles are given in Table 2; its structural and stereochemical peculiarities are discussed using the (*S_a*)-enantiomer as an example. To follow the chirality transfer and to clarify the influence of the bulky 1,3,2-dioxaphosphepine ring, the structure of complex **3** was compared with those of its pincer *PCP*-analogue **1a** (*R* = *R'* = H) and known achiral phosphite *PC*-CPCs (Chart 2).

The Pd–C bond length (2.072 Å) in complex **3** is close to those of known analogues **V** and **VII** with *trans*(*P²,C*)-configuration (2.084–2.064 Å). The length of the *endo*-cyclic Pd–P¹ bond in adduct **3** (2.152 Å) falls in the range 2.142–2.177 Å, typical for other triarylphosphite complexes bearing bridged (**IIIa–d**) or terminal (**V**, **VII**) chloride on the P¹–Pd–Cl diagonal. The Pd–Cl bond in complex **3** (2.381 Å) is weakened to some extent compared to that in mononuclear analogues **V** and **VII** (2.349–2.319 Å); however, it is stronger than the (μ)Cl–Pd bond *trans*-disposed to the phosphite *P*-donor atom in dimers **IIIa–d** and **IIb** (2.390–2.419 Å). The *exo*-cyclic Pd–P² bond length in adduct **3** (2.357 Å) falls in the range of

(40) Mononuclear pyridine adduct **2** partially decomposed on the silica to give the dimer **1** (*R_f* 0.98).

(41) Signal is overlapped with that of the *ortho*-PPh protons.

(42) Partial decomposition of valinate complexes **4a,b** on silica was observed, resulting in formation of dimer **1** (*R_f* 0.90).

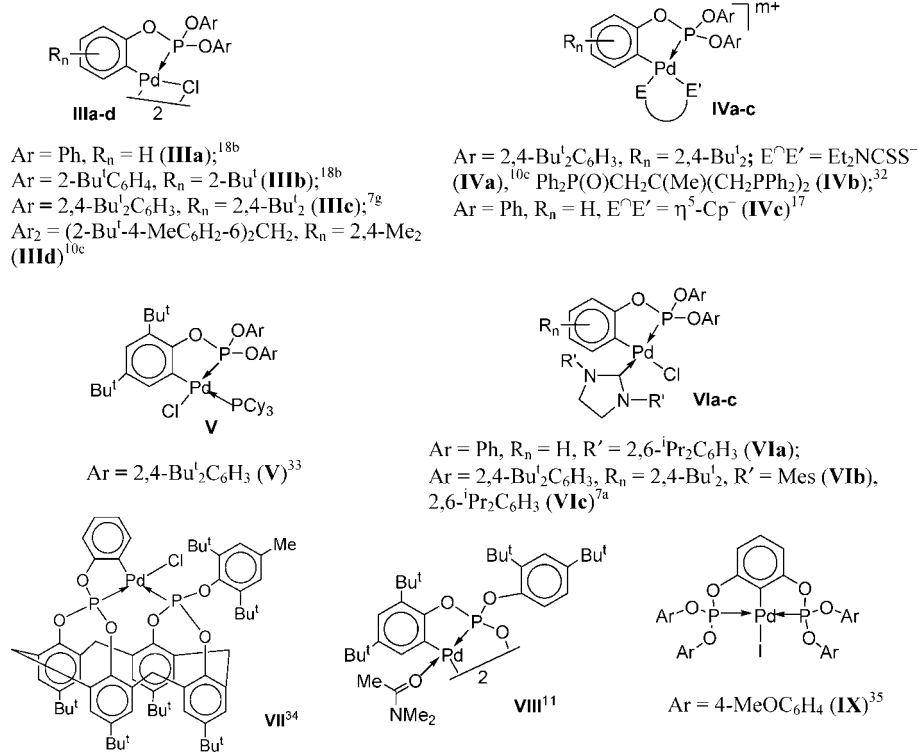
(43) Perdev, J. P.; Burke, K.; Ernzerhof, M. *Phys. Rev. Lett.* **1996**, *77*, 3865.

(44) Laikov, D. N. *Chem. Phys. Lett.* **2005**, *416*, 116.

(45) Stevens, W. J.; Bash, H.; Jasien, P. *Can. J. Chem.* **1992**, *70*, 612.

(46) (a) Schreckenbach, G.; Ziegler, T. *Int. J. Quantum Chem.* **1997**, *61*, 899. (b) Schreckenbach, G.; Ziegler, T. *J. Phys. Chem.* **1995**, *99*, 606.

Chart 2



this parameter's values (2.340–2.405 Å) found for analogues **IVb**, **V**, and **VII** with the $\text{P}^2\text{-Pd-C}$ diagonal.

The square-planar coordination environment of the palladium atom in complex **3** reveals a marked tetrahedral distortion ($\text{C}^1\text{Pd}^1\text{P}^1/\text{Cl}^1\text{Pd}^1\text{P}^2$ 14.83°), which exceeds that for the majority of phosphite PC-CPCs (0.81–5.76°), including those reported for the sterically congested compounds **IIIb,d**, **VIc**, and **VII** (8.36–13.45°). According to the “skew-line convention”³⁶ the configuration of the pseudo-tetrahedron in adduct **3** may be defined as Λ on the basis of the positive sign of the torsion

angle $\angle \text{P}^1 \cdots \text{C} \cdots \text{Cl} \cdots \text{P}^2$ (+15.48°) connecting four metal-bonded donor atoms (Figure 4).

The PC -palladacycle in complex **3** has an envelope-like conformation³⁷ with $\text{P}^1\text{O}^1\text{C}^2\text{C}^1$ atoms coplanar within 0.0344 Å and the palladium atom deviating from their plane by 0.587 Å. The nonplanarity of the PC -palladacycle is rather high, with average absolute values of intrachelate torsion angles (ϖ_{av}) equal to 16.80°. Only three sterically encumbered analogues possess a palladacycle of comparable (**V**) or more pronounced (**III d** and **VIb**) puckering extent ($\varpi_{\text{av}} = 15.19\text{--}21.08^\circ$), while in other CPCs the palladacycle is rather flattened ($\varpi_{\text{av}} = 1.16\text{--}10.29^\circ$). The envelope-like conformation of the palladacycle in adduct **3** is twisted, with the negative torsion angle $\angle \text{C}^1 \cdots \text{P}^1\text{-O}^1\text{-C}^2$ (-5.48°) determining its $\delta(S_a)$ -stereochemistry.³⁶

The (S_a) -BINOL-derived dioxaphosphepine ring in complex **3** is highly puckered ($\varpi_{\text{av}} 42.35^\circ$); it adopts the $\delta(S_a)$ conformation ($\angle \text{O}^3 \cdots \text{O}^3\text{-C}^{26} \cdots \text{C}^{16} = -28.59^\circ$). These characteristics are similar to those reported for phosphepine rings of the PCP -analogue (R_a)-**1a** ($\varpi_{\text{av}} = 44.12^\circ$ and 46.03°) with the same $\lambda(R_a)$ relationship between axial and conformational chirality.

The P -configuration of the PPh_3 propeller in adduct (S_a)-**3** was determined by a known method³⁸ ($\omega_{\text{av}} 38.6^\circ$). The calculated ω_i values for three PPh groups reveal dependence on their disposition regarding the BINOL-derived phosphepine ring: ω_A, ω_B and ω_C values are equal to 66.8°, 33.7°, and 15.4°, respectively.

The comparative analysis of X-ray data for complex **3** and its analogues has shown that the introduction of bulky substituents, including a dioxaphosphepine ring, to the structure of phosphite CPCs results in an increase in the tetrahedral distortion of the coordination sphere and palladacycle's puckering.

DFT Investigation of the Phosphane Adduct (S_a)-3. To estimate the influence of the crystal packing on the structure and stereochemistry of complex **3**, we have performed a DFT study of its (S_a)-enantiomer (Figure 5). The DFT data confirmed the tetrahedral distortion of the metal coordination sphere

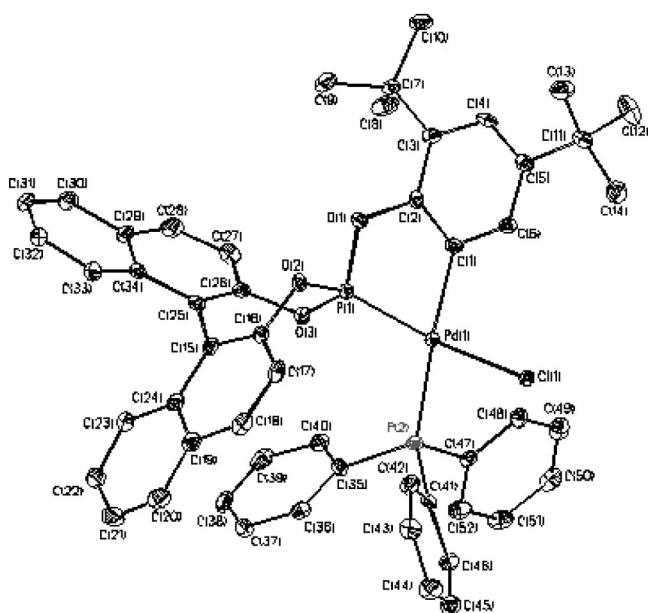


Figure 3. Molecular structure and numbering scheme of the (S_a)-enantiomer of the phosphane derivative *rac*-**3**. The dichloroethane solvate molecules are omitted for clarity; thermal ellipsoids are given for 50% probability.

Table 2. Comparison of the Experimental and DFT-Calculated Values of the Selected Bond Lengths (Å) and Bond Angles (deg) for Phosphane Adduct *rac-3*

bond	bond lengths (<i>l</i>)			angle	bond angles (ϕ)		
	X-ray	DFT	Δl		X-ray	DFT	$\Delta\phi$
Pd(1)–C(1)	2.072(3)	2.097	0.025	C(1)–Pd(1)–P(1)	76.28(9)	77.40	1.12
Pd(1)–P(1)	2.1517(9)	2.180	0.028	C(1)–Pd(1)–P(2)	169.84(9)	173.25	3.41
Pd(1)–P(2)	2.3567(9)	2.409	0.052	P(1)–Pd(1)–P(2)	104.31(3)	105.94	1.63
Pd(1)–Cl(1)	2.3813(8)	2.360	–0.022	C(1)–Pd(1)–Cl(1)	95.22(9)	92.94	–2.28
P(1)–O(3)	1.588(2)	1.635	0.047	P(1)–Pd(1)–Cl(1)	167.02(3)	169.12	2.10
P(1)–O(1)	1.588(2)	1.654	0.066	P(2)–Pd(1)–Cl(1)	85.81(3)	84.20	–1.61
P(1)–O(2)	1.609(2)	1.628	0.019	O(3)–P(1)–O(1)	103.47(12)	103.00	–0.47
O(1)–C(2)	1.421(3)	1.416	–0.005	O(3)–P(1)–O(2)	104.03(11)	101.56	–2.47
O(2)–C(16)	1.406(4)	1.391	–0.015	O(1)–P(1)–O(2)	100.20(12)	98.07	–2.13
O(3)–C(26)	1.414(3)	1.402	0.012	O(3)–P(1)–Pd(1)	120.97(9)	121.93	0.96
C(1)–C(2)	1.387(4)	1.399	0.022	O(1)–P(1)–Pd(1)	111.13(9)	109.67	–1.46
C(1)–C(6)	1.395(4)	1.398	0.003	O(2)–P(1)–Pd(1)	114.56(9)	119.06	4.50
C(2)–C(3)	1.398(4)	1.407	0.009	C(2)–O(1)–P(1)	110.33(18)	110.95	0.62
C(3)–C(4)	1.392(4)	1.401	0.009	C(16)–O(2)–P(1)	115.84(19)	119.32	3.48
C(4)–C(5)	1.391(4)	1.402	0.011	C(26)–O(3)–P(1)	120.15(19)	119.68	–0.47
C(5)–C(6)	1.384(4)	1.400	0.016	C(2)–C(1)–Pd(1)	119.6(2)	118.99	–0.61
				C(6)–C(1)–Pd(1)	123.1(2)	122.96	–0.14

($\angle P^1 \cdots C \cdots Cl \cdots P^2 = +8.69^\circ$) and the same Λ -configuration of the pseudo-tetrahedron (Figure 6a). The calculated nonplanarity extent of the *PC*-palladacycle ($\omega_{av} = 15.41^\circ$) is very close to that found for the crystal with the same δ -conformation ($\angle C^1 \cdots P^1 - O^1 - C^2 = -6.15^\circ$, Figure 6b). The (*S_a*)-dioxaphosphine ring possesses a similar puckering extent ($\omega_{av} 41.58^\circ$) and the same $\delta(S_a)$ -conformation ($\angle O^2 \cdots O^3 - C^{26} \cdots C^{16} = -27.89^\circ$, Figure 6c). The calculated rotameric state of the PPh₃ ligand corresponds to that found for the crystal, with the same

P-configuration of the PPh₃ propeller ($\omega_{av} = 41.20^\circ$) and similar dependence of the phosphine group orientation on their disposition regarding the phosphine ring (ω_A , ω_B , and ω_C values are equal to 68.74° , 35.14° , and 19.73° , respectively, Figure 6d).

From the comparison between the calculated parameters for two derivatives of phosphite *PC*-palladacycle, **3** and **4a**, one can see that bulkiness of the auxiliary ligand has a considerable impact on the overall stereochemistry of the complexes. Thus, phosphane adduct **3** reveals a more pronounced tetrahedral distortion and a more puckered *PC*-palladacycle conformation compared to the less sterically congested valinate adduct **4a**. Such a difference allows one to assume that chirality transfer from the phosphite palladacycle to sterically encumbered auxiliary ligands may be rather efficient due to participation of two additional chirality elements (pseudo-tetrahedron and twisted conformation) in this process.

Conclusions

We have described the preparation of the first optically active *PC*-palladacycle with a phosphorus atom in an axially chiral environment. The possibility of direct C–H bond activation in the (*S_a*)-BINOL-derived phosphite under thermal conditions ($\sim 110^\circ\text{C}$) without decrease its enantiopurity was confirmed by ³¹P NMR spectroscopy after chiral derivatization of dimer (*S_a,S_a*)-**1** with the (*R_C*)-valinate auxiliary ligand. The X-ray diffraction data and DFT calculations performed for the phosphane derivative (*S_a*)-**3** showed that axial chirality of the (*S_a*)-

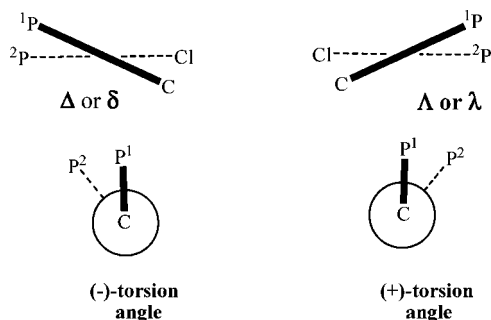


Figure 4. Correlation of the skew-line disposition with torsion angle sign.

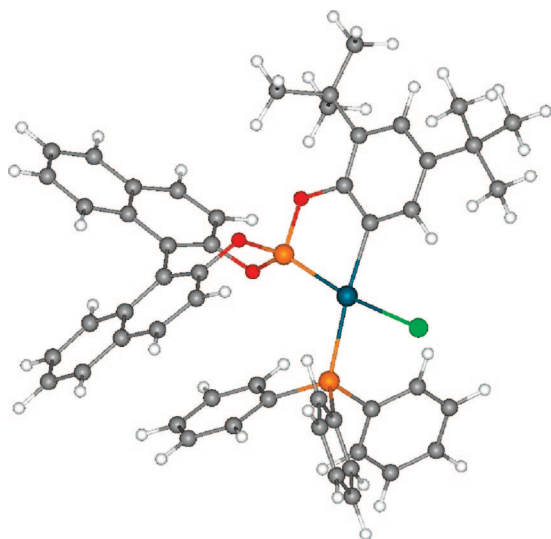


Figure 5. DFT-calculated structure for the phosphane derivative *rac-3* in the gas phase.

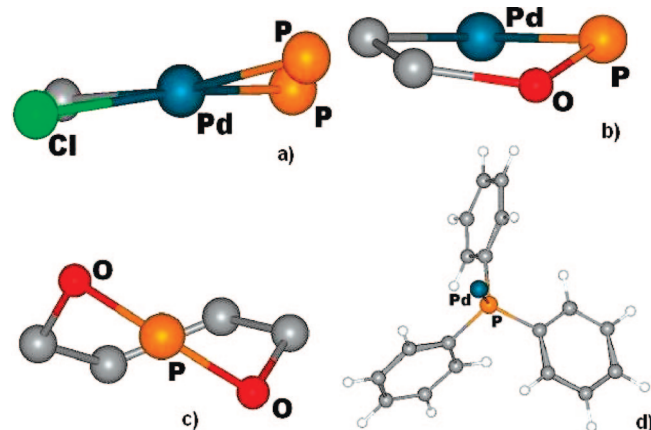


Figure 6. Chirality elements in the phosphane derivative *rac-3*.

BINOL fragment causes both the seven-membered 1,3,2-dioxaphosphepine ring and the five-membered *PC*-palladacycle to adopt the δ -conformation. The (*S_a*)-BINOL moiety in complex (*S_a*)-**3** also triggers both the Λ -configuration of the pseudo-tetrahedral palladium coordination environment and the *P*-rotameric state of the PPh₃ propeller.

Experimental Section

General Procedures. The ¹H and ³¹P NMR spectra were recorded on Varian VXR-400 and Bruker DPX-400 spectrometers operating at the frequencies 400 and 161.9 MHz for ¹H and ³¹P nuclei, respectively. The measurements were carried out at ambient temperature in CDCl₃ solutions (unless otherwise indicated). The chemical shifts are reported in δ -scale in parts per million relative to TMS as an internal standard for ¹H NMR and relative to H₃PO₄ as an external reference for the ³¹P NMR spectra. The signal assignment was based on homo- and heteronuclear decoupling, COSY, and NOE experiments. Optical rotations were measured on a Perkin-Elmer (model 341) polarimeter in 0.5 dm cells at 25 °C. Melting points were measured on an Electrothermal IA 9000 series device in sealed capillaries. All reactions were conducted under argon using TLC control on Silufol. All manipulations with the free phosphite were carried out under dry purified argon in deoxygenated and dried solvents using Schlenk techniques. Compound purification was performed using a short, dry column³⁹ or flash chromatography on silica gel (60, Fluka).

Toluene was dried over CaCl₂, refluxed over Na, and then distilled under argon. Anhydrous MeOH was prepared by distillation from MeONa. Chloroform and dichloromethane were passed through a short Al₂O₃ column and distilled under argon. Hexane and light petroleum ether were distilled from Na under argon. CDCl₃ and CD₂Cl₂ (from Aldrich) were distilled from CaH₂ under argon just before using. Palladium(II) chloride and acetate and (*R_C*)-valine (from Aldrich), Pd(PhCN)₂Cl₂ (from Merck), and (*S_a*)-1,1'-binaphthyl-2,2'-diol (from Fluka) were used as received. PPh₃ and racemic BINOL (from Aldrich) were purified by 2-fold recrystallization from benzene/hexane and acetone, respectively. PCl₃ was distilled under argon. Et₃N was distilled from Na under argon before using. 2,4-Di-*tert*-butylphenol (from Aldrich) was recrystallized two times from light petroleum ether and dried under P₂O₅ and paraffin *in vacuo*.

(*S_a*)-(1,1'-Binaphthyl-2,2'-diyl)(2,4-di-*tert*-butylphenyl)phosphite, (*S_a*)-HL**.** (*S_a*)-**HL** was prepared by a slightly modified known method^{8d,10c,11} and chromatographically purified. [α]_D²⁵ +103.5 (*c* 1.31, CH₂Cl₂). Anal. Calcd for C₃₄H₃₃PO₃: C, 78.43; H, 6.40. Found: C, 78.60; H, 6.48. ³¹P{¹H} NMR: δ 145.07 (s). ¹H NMR: δ 1.32 (s, 9H, Bu¹), 1.37 (s, 9H, Bu²), 7.19 (dd, ³J_{HH} 8.3, ⁴J_{HH} 2.5, 1H, H^{5'}), 7.24 (d, ³J_{HH} 8.3, 1H, H^{6'}), 7.27 (ddd, ³J_{HH} 8.3, ³J_{HH} 7.0, ⁴J_{HH} 1.3, 1H, H⁷/H^{7'}), 7.29 (ddd, ³J_{HH} 8.3, ³J_{HH} 6.9, ⁴J_{HH} 1.5, 1H, H⁷/H^{7'}), 7.39 (d, ⁴J_{HH} 2.5, 1H, H^{3''}), 7.40 (d, ³J_{HH} 8.3, 1H, H⁸/H^{8'}), 7.42 (d, ³J_{HH} 8.3, 1H, H⁸/H^{8'}), 7.43 (ddd, ³J_{HH} 8.3, ³J_{HH} 7.0, ⁴J_{HH} 1.3, 1H, H⁶/H^{6'}), 7.46 (ddd, ³J_{HH} 8.3, ³J_{HH} 6.9, ⁴J_{HH} 1.3, 1H, H⁶/H^{6'}), 7.48 (dd, ³J_{HH} 8.8, ⁴J_{HP} 0.8, 1H, H³/H^{3'}), 7.58 (d, ³J_{HH} 8.8, 1H, H³/H^{3'}), 7.90 (d, ³J_{HH} 8.8, 1H, H⁴/H^{4'}), 7.91 (d, ³J_{HH} 8.3, 1H, H⁵/H^{5'}), 7.95 (d, ³J_{HH} 8.3, 1H, H⁵/H^{5'}), 8.01 (d, ³J_{HH} 8.8, 1H, H⁴/H^{4'}).

Racemic (1,1'-binaphthyl-2,2'-diyl)(2,4-di-*tert*-butylphenyl)phosphite. was obtained similarly.

Racemic Di- μ -chlorobis[(1,1'-binaphthyl-2,2'-diyl)(2,4-di-*tert*-butylphenyl)phosphite-*C,P*]dipalladium(II), *rac*-1**.** A solution of Pd(PhCN)₂Cl₂ (0.0715 g, 0.186 mmol) in 1,2-dichloroethane (3 mL) was added to a phosphite **HL** (0.097 g, 0.186 mmol) and the homogeneous reaction mixture was refluxed for 9 h under stirring. The precipitate formed was filtered and dried *in vacuo* to give the crude dimer **1** in a yield of 57% (0.0707 g, 0.0534 mmol) as a highly insoluble powder. The suspension of the crude dimer *rac*-**1** in dichloromethane (3 mL) was treated with pyridine (0.0085 g,

0.107 mmol) and stirred for 15 min to give the homogeneous solution of the pyridine adduct **2** (*R_f* 0.30; toluene/acetone, 1:1),⁴⁰ which was evaporated. In the course of the complex *rac*-**2** elution through the flash column loaded with silica (*h* = 13 cm, *d* = 2 cm; eluents: toluene/light ligroin, 2:1, then toluene and toluene/acetone, 5:1) the complete decomplexation of auxiliary pyridine ligand took place to afford purified dimer *rac*-**1** in a yield of 43% (0.0533 g, 0.0402 mmol) as a colorless, amorphous powder: mp (dec) 247 °C; *R_f* 0.5 (toluene/hexane, 1:1). Anal. Calcd for C₆₈H₆₄P₂O₆Pd₂Cl₂: C, 61.73; H, 4.89. Found: C, 61.44; H, 5.05. ³¹P{¹H} NMR: δ 138.45 (s) and 138.54 (s) (86%); 140.75 (s) and 140.81 (s) (14%).

(*S_a*,*S_a*)-Di- μ -chlorobis[(1,1'-binaphthyl-2,2'-diyl)(2,4-di-*tert*-butylphenyl)phosphite-*C,P*]dipalladium(II), (*S_a*,*S_a*)-1a**.** A solution of Pd(PhCN)₂Cl₂ (0.0465 g, 0.1212 mmol) and phosphite (*S_a*)-**HL** (0.0631 g, 0.1212 mmol) in toluene (2 mL) was refluxed for 7 h under stirring. The palladium black formed was removed by filtration, and mother liquid was evaporated. The residue was purified using flash-column chromatography (*h* = 13 cm, *d* = 2 cm; eluents: toluene/petroleum ether, 1:1, then toluene, and toluene/acetone, 10:1) to give dimer (*S_a*,*S_a*)-**1a** in a yield of 40% (0.0320 g, 0.0242 mmol) as a colorless, amorphous powder: mp (dec) 230 °C; *R_f* 0.5 (toluene/hexane, 1:1). Anal. Calcd for C₆₈H₆₄P₂O₆Pd₂Cl₂: C, 61.73; H, 4.89. Found: C, 61.49; H, 4.88. ³¹P{¹H} NMR: δ 140.68 (s, 16%), 138.43 (s, 84%). ¹H NMR: δ 1.12 (s, Bu¹), 1.20 (s, Bu²), 7.10 (app. br s), 7.14–7.19 (m), 7.24–7.26 (m), 7.28–7.29 (m), 7.31–7.35 (m), 7.37–7.42 (m), 7.49–7.53 (m), 7.81 (br d), 7.97 (app. br d), 8.06 (br d).

Racemic Chloro[(1,1'-binaphthyl-2,2'-diyl)(2,4-di-*tert*-butylphenyl)phosphite-*C,P*](triphenylphosphane)palladium(II), *rac*-3**.** A suspension of the racemic dimer **1** (0.0182 g, 0.0138 mmol) in toluene (1.5 mL) was treated with triphenylphosphane (0.0072 g, 0.0275 mmol). The reaction mixture was stirred for 30 min at rt under TLC control and evaporated, and the residue was purified using dry column chromatography³⁹ (*h* = 5 cm, *d* = 4 cm; eluents: toluene and then toluene/acetone, 5:1). After 2-fold recrystallization from dichloromethane/hexane mononuclear derivative *rac*-**3** was obtained in a yield of 60% (0.020 g, 0.0216 mmol) as a light-yellow crystalline solid: mp (dec) 225 °C; *R_f* 0.73 (toluene/acetone, 10:1). Anal. Calcd for C₅₂H₄₇P₂O₃PdCl: C, 67.60; H, 5.14. Found: C, 67.43; H, 5.25. The monocrystals for X-ray investigation were grown from 1,2-dichloroethane/pentane using vapor diffusion technique. ³¹P{¹H} NMR (CD₂Cl₂): δ 17.66 (d, ²J_{PP} 45.2), 149.91 (d, ²J_{PP} 45.2). ¹H NMR (CD₂Cl₂): δ 1.14 (s, 9H, Bu¹), 1.40 (s, 9H, Bu²), 7.01–7.08 (m, ⁴J_{HP} 2.0, 6H, *meta*-PPh), 7.10–7.15 (m, ⁵J_{HP} 2.0, 3H, *para*-PPh), 7.17 (dd, ⁵J_{HP} 2.6, ⁴J_{HH} 2.1, 1H, H^{4'}), 7.21 (d, ³J_{HH} 8.6, 1H, H⁸/H^{8'}), 7.22–7.28 (m, 2H, H⁷/H^{7'} and H⁸/H^{8'}), 7.33 (m, 1H, H⁷/H^{7'}), ⁴¹ 7.35–7.41 (m, ³J_{HP} 10.9, 6H, *ortho*-PPh), 7.38 (dd, ³J_{HH} 8.8, ⁴J_{HP} 0.9, 1H, H³/H^{3'}), 7.46 (dd, ³J_{HH} 8.9, ⁴J_{HP} 1.2, 1H, H³/H^{3'}), 7.48–7.52 (m, 1H, H⁶/H^{6'}), 7.50–7.54 (m, 1H, H⁶/H^{6'}), 7.58 (d, ³J_{HH} 8.8, 1H, H⁴/H^{4'}), 7.84 (d, ³J_{HH} 8.2, 1H, H⁵/H^{5'}), 7.98 (d, ³J_{HH} 8.2, 1H, H⁵/H^{5'}), 8.03 (d, ³J_{HH} 8.9, 1H, H⁴/H^{4'}), 8.47 (ddd, ⁴J_{HP} 5.6, ⁴J_{HP} 8.0, ⁴J_{HH} 2.2, 1H, H^{6'}).

{[(*S_a*)-1,1'-Binaphthyl-2,2'-diyl](2,4-di-*tert*-butylphenyl)phosphite-*C,P*]}[(*R_C*)-valinato-*N,O*]palladium(II), (*S_a*,*R_C*)-4a**.** The dimer (*S_a*)-**1a** (0.0062 g, 0.0062 mmol) was added to a solution of excess sodium (*R*)-valinate (0.0028 g, 0.0248 mmol) in chloroform (2 mL), and the reaction mixture was stirred at rt for 4 h, filtered, and evaporated. At this stage ³¹P{¹H} NMR (CDCl₃, δ , ppm): 148.03 (s). After recrystallization of the residue from chloroform/hexane at low temperature diastereomer (*S_a*,*R_C*)-**4a** was obtained in a yield of 93% (0.0083 g, 0.0115 mmol) as a colorless, finely crystalline solid: mp (dec) 228–230 °C, *R_f* 0.48 (toluene/acetone, 1:1).⁴² [α]_D²⁵ +155.6 (*c* 0.25, CHCl₃). Anal. Calcd for C₃₉H₄₂PO₅NPd: C, 63.11; H, 5.72; N 1.89. Found: C, 63.09; H, 5.70; N 1.94. ³¹P{¹H} NMR: δ 148.12 (s). ¹H NMR: δ 0.94 (d, ³J_{HH} 7.1, 3H, Me), 1.16 (d, ³J_{HH} 7.0, 3H, Me), 1.69 (br dd, ²J_{HH} 11.0, ³J_{HNC^{CH}} 4.4, 1H, NH^{eq}), 2.10 (br dd, ²J_{HH} 11.0, ³J_{HNC^{CH}} 7.2, 1H, NH^{ax}), 2.47 (m, 1H, CHMe₂),

3.40 (ddd, $^3J_{\text{HCNH}}$ 7.2, $^3J_{\text{HCNH}}$ 4.4, $^3J_{\text{HCCH}}$ 6.9, 1H, α -CH), 1.27 (s, 9H, Bu¹), 1.33 (s, 9H, Bu²), 7.23 (dd, $^3J_{\text{HP}}$ 3.5, $^4J_{\text{HH}}$ 2.1, 1H, H^{4'}), 7.38–7.43 (m, 2H, H⁷/H^{7'} and H⁸/H^{8'}), 7.46 (ddd, $^3J_{\text{HH}}$ 8.7, $^3J_{\text{HH}}$ 6.9, $^4J_{\text{HH}}$ 1.3, 1H, H⁷/H^{7'}), 7.48 (br d, $^3J_{\text{HH}}$ 8.8, 1H, H³/H^{3'}), 7.53 (d, $^3J_{\text{HH}}$ 8.7, 1H, H⁸/H^{8'}), 7.57 (m, 1H, H⁶/H^{6'}), 7.63 (ddd, $^3J_{\text{HH}}$ 8.3, $^3J_{\text{HH}}$ 6.9, $^4J_{\text{HH}}$ 1.3, 1H, H⁶/H^{6'}), 7.72 (app. d, $^3J_{\text{HH}}$ 8.8, $^4J_{\text{HP}}$ 0.4, 1H, H³/H^{3'}), 7.87 (dd, $^4J_{\text{HP}}$ 7.1, $^4J_{\text{HH}}$ 2.1, 1H, H^{6''}), 8.04 (d, $^3J_{\text{HH}}$ 8.3, 1H, H⁵/H^{5'}), 8.06 (d, $^3J_{\text{HH}}$ 8.3, 1H, H⁵/H^{5'}), 8.09 (d, $^3J_{\text{HH}}$ 8.8, 1H, H⁴/H^{4'}), 8.17 (d, $^3J_{\text{HH}}$ 8.8, 1H, H⁴/H^{4'}).

Diastereomer Mixture of [(1,1'-Binaphthyl-2,2'-diyl)(2,4-di-*tert*-butylphenyl)phosphite-*C,P*][(R_C)-valinato-*N,O*]palladium(II), (S_aR_C)-4a** and (R_aR_C)-**4b**.** Dimer *rac*-**1** (0.0157 g, 0.0118 mmol) was added to a solution of sodium (*R*)-valinate (0.0029 g, 0.0237 mmol) in chloroform (2 mL), and the reaction mixture was stirred at rt for 3 h, filtered, and evaporated. At this stage $^{31}\text{P}\{^1\text{H}\}$ NMR: δ 147.73 (s), 148.07 (s). After recrystallization of the residue from dichloromethane/hexane at low temperature diastereomer mixture **4a,b** was obtained in a yield of 84% (0.0141 g, 0.0197 mmol) as a colorless, finely crystalline solid: mp (dec) 235–237 °C, R_f 0.53 (toluene/acetone, 1:1).⁴² $[\alpha]_{\text{D}}^{25}$ 0.00, $[\alpha]_{\text{D}}^{25}$ 17.0 (*c* 0.19, CHCl₃). Anal. Calcd for C₃₉H₄₂PO₅NPd: C, 63.11; H, 5.72; N 1.89. Found: C, 63.07; H, 5.74; N 1.93. $^{31}\text{P}\{^1\text{H}\}$ NMR: δ 147.73 (s), 148.05 (s).

Computational Details. All DFT calculations were performed for the gas phase at the generalized gradient approximation for the nonempirically constructed PBE functional,⁴³ using the program package in version PRIRODA-6.⁴⁴ The one-electron wave functions were expanded into the extended TZ2P basis sets⁴⁴ including the contracted Gauss functions {311/1} for the hydrogen atoms, {51111/51111/51111} for palladium atom, and {6,11111/411/11} for all other atoms (carbon, nitrogen, oxygen, and phosphorus). The relativistic pseudopotential SBK was used in the known version.⁴⁵ The energy E^0 was calculated taking into account the zero-point vibration energy in harmonic approximation. All structures were fully optimized. Corrections for zero-point energies were calculated in the harmonic approximation. The ^1H NMR spectra were calculated using gauge-including atomic orbitals (GIAO)⁴⁶ in the complete electronic TZ2P basis. The calculated chemical shifts were expressed as the difference between the shielding of the reference (TMS) and the complex to be studied. All calculations were performed on the MVS 15000BM computer cluster at the Joint Supercomputer Center (JSCC, Moscow).

X-ray Diffraction Study of Phosphane Derivative *rac*-3**.** Crystal of adduct **3** (C₅₆H₅₅Cl₅O₃P₂Pd, $M = 1121.59$), triclinic, space group $P\bar{1}$, at 100 K, $a = 12.9201(7)$ Å, $b = 14.3239(8)$ Å, $c = 16.3593(14)$ Å, $\alpha = 111.534(2)^\circ$, $\beta = 106.222(2)^\circ$, $\gamma = 98.2940(10)^\circ$, $V = 2598.8(3)$ Å³, $Z = 2$, $F(000) = 1152$, $d_{\text{calc}} = 1.433$ g·cm⁻³, $\mu = 0.719$ mm⁻¹. Unit cell parameters and intensities of 32 453 reflections were measured with a Bruker SMART APEX2 CCD area detector diffractometer, using graphite-monochromated Mo K α radiation at 100 K, φ - and ω -scan, $\theta_{\text{max}} = 29^\circ$. Reflection intensities were integrated using SAINT software,⁴⁷ and absorption correction was applied semiempirically using the SADABS program. The structure was solved by direct methods and refined by full-matrix least-squares against F^2 in anisotropic approximation for non-hydrogen atoms. All hydrogen atoms were placed in geometrically calculated positions, and their positions were refined in isotropic approximation in a riding model. The crystal of **3** contains two solvate molecules of 1,2-dichloroethane; in one of them the carbon atoms are disordered over two sites with 3:7 occupancies. All calculations were performed using the SHELXTL software.⁴⁸ Final R -factors are equal to $R_1 = 0.0517$ for 9366 reflections with $I > 2\sigma(I)$ and $wR_2 = 0.0749$ for all 14 061 independent reflections. CCDC-677989 contains the supplementary crystallographic data for this paper. These data can be obtained free of charge from the Cambridge Crystallographic Data Centre via www.ccdc.cam.ac.uk/data_request/cif.

Acknowledgment. This research was supported partly by the Presidium Russian Academy of Sciences, grant P1. The authors thank Dr. I. P. Smoliakova for valuable discussions.

Supporting Information Available: Full crystallographic data for complex **3** are available as a cif file. Synthesis of phosphites *rac*-**HL** and (S_a)-**HL**, experimental ^1H and ^{31}P NMR spectra, DFT-calculated ^1H chemical shifts, and structures of complexes **4a,b** (in Decart coordinates) are given. These materials are available free of charge via the Internet at <http://pubs.acs.org>.

OM800654R

(47) SMART V5.051 and SAINT V5.00, Area detector control and integration software; Bruker AXS Inc.: Madison, WI, 1998.

(48) Sheldrick, G. M. *SHELXTL-97*, V5.10; Bruker AXS Inc.: Madison, WI, 1997.

Mechanistic Study of Acetate-Assisted C–H Activation of 2-Substituted Pyridines with $[\text{MCl}_2\text{Cp}^*]_2$ (M = Rh, Ir) and $[\text{RuCl}_2(p\text{-cymene})]_2$

Youcef Boutadla, Omar Al-Duaij, David L. Davies,* Gerald A. Griffith, and Kuldip Singh

University of Leicester, Leicester, U.K., LE1 7RH

Received September 18, 2008

Reactions of 2-substituted pyridines HL with $[\text{MCl}_2\text{Cp}^*]_2$ (M = Ir, Rh) and $[\text{RuCl}_2(p\text{-cymene})]_2$ have been carried out in the presence and absence of sodium acetate. 2-Phenylpyridine (HL1) is cyclometalated easily to form $[\text{MCl}(\text{L1})(\text{ring})] \mathbf{1a-c}$ (M = Rh, Ir, ring = Cp*; M = Ru, ring = *p*-cymene). However, in the case of 2-acetylpyridine (HL2) sp^3 C–H activation occurs cleanly with rhodium to form N,C chelate complex $[\text{RhCl}(\text{L2})\text{Cp}^*] \mathbf{2b}$, but the reactions with iridium and ruthenium give unseparable mixtures of products. The N,C cyclometalated products $[\text{MCl}(\text{L2})(\text{ring})] \mathbf{2a-c}$ (M = Ir, Rh, ring = Cp*; M = Ru, ring = *p*-cymene) have been independently prepared from the lithium enolates of 2-acetylpyridine. Notably, in the absence of acetate, $[\text{RhCl}_2\text{Cp}^*]_2$ shows no reaction with 2-acetylpyridine, whereas $[\text{IrCl}_2\text{Cp}^*]_2$ and $[\text{RuCl}_2(p\text{-cymene})]_2$ react to form equilibrium mixtures of the starting materials and N,O chelate complexes $\mathbf{4a,c}$, respectively. In the presence of KPF_6 the N,O chelate complexes $[\text{MCl}(\text{HL2})(\text{ring})][\text{PF}_6] \mathbf{4a,c,d}$ (M = Ir, ring = Cp*; M = Ru, ring = *p*-cymene, mesitylene) can be isolated. These are not intermediates en route to the N,C cyclometalated products. These results suggest that for C–H activation to occur under these mild conditions acetate must coordinate to the metal prior to coordination of the ligand.

Introduction

Cyclometalation reactions have been known for a long time, the first platinum metal complex being reported in 1965.¹ Since then, cyclometalated complexes have attracted considerable interest for a wide variety of applications.² In recent years C–H activation to form a cyclometalated complex has become an integral part of many catalytic cycles,³ including ruthenium-catalyzed arylation^{4,5} or alkenylation⁶ of 2-phenyl-substituted pyridines or other N-heterocycles. In order to design better catalysts, a detailed understanding of the mechanism of the cyclometalation and factors affecting the C–H activation step are desirable. We have previously reported room-temperature cyclometalation of phenyl-substituted imines, oxazolines, and amines by $[\text{MCl}_2\text{Cp}^*]_2$ (M = Rh, Ir) and $[\text{RuCl}_2(p\text{-cymene})]_2$ in the presence of sodium acetate.⁷ Subsequently in collaboration

with Macgregor we have investigated the mechanism of this reaction⁸ and related acetate-assisted cyclometalations^{9,10} using DFT calculations. These studies have shown that the C–H activation step involves a simultaneous activation of the C–H bond by the metal and intramolecular deprotonation by acetate. This type of mechanism has been proposed for several catalytic cycles with palladium,^{11,12} platinum,¹³ and indeed ruthenium,⁵ and Fagnou has used the term concerted metalation–deprotonation (CMD) to describe this mechanism.¹² We now wish to report experimental observations on cyclometalation of 2-substituted pyridines, which provide further support for the intramolecular nature of the deprotonation and which highlight some of the issues involved in extending these processes from activation of sp^2 C–H bonds to sp^3 C–H bonds.

Results and Discussion

Reactions of 2-phenylpyridine with $[\text{MCl}_2\text{Cp}^*]_2$ (M = Ir, Rh) and $[\text{RuCl}_2(p\text{-cymene})]_2$ in the presence of sodium acetate occur at room temperature to yield the complexes $[\text{MCl}(\text{L1})(\text{ring})] \mathbf{1a-c}$ in good yields. During the course of our work Pfeffer et

* Corresponding author. E-mail: dld3@le.ac.uk.

- (1) Cope, A. C.; Siekman, R. W. *J. Am. Chem. Soc.* **1965**, *87*, 3272–3.
- (2) Dupont, J.; Consorti, C. S.; Spencer, J. *Chem. Rev.* **2005**, *105*, 2527–2571.
- (3) Ghedini, M.; Aiello, I.; Crispini, A.; Golemme, A.; La Deda, M.; Pucci, D. *Coord. Chem. Rev.* **2006**, *250*, 1373–1390.
- (4) Dupont, J.; Pfeffer, M.; Spencer, J. *Eur. J. Inorg. Chem.* **2001**, 1917–1927.
- (5) Bedford, R. B. *Chem. Commun.* **2003**, 1787–1796.
- (6) Kakiuchi, F.; Murai, S. *Acc. Chem. Res.* **2002**, *35*, 826–834.
- (7) Alberico, D.; Scott, M. E.; Lautens, M. *Chem. Rev.* **2007**, *107*, 174–238.
- (8) Oi, S.; Funayama, R.; Hattori, T.; Inoue, Y. *Tetrahedron* **2008**, *64*, 6051–6059.
- (9) Ackermann, L. *Org. Lett.* **2005**, *7*, 3123–3125.
- (10) Ackermann, L.; Althammer, A.; Born, R. *Angew. Chem., Int. Ed.* **2006**, *45*, 2619–2622.
- (11) Ackermann, L.; Born, R.; Alvarez-Bercedo, P. *Angew. Chem., Int. Ed.* **2007**, *46*, 6364–6367.
- (12) Ackermann, L.; Althammer, A.; Born, R. *Tetrahedron* **2008**, *64*, 6115–6124.
- (13) Oi, S.; Sato, H.; Sugawara, S.; Inoue, Y. *Org. Lett.* **2008**, *10*, 1823–1826.
- (14) Ozdemir, I.; Demir, S.; Cetinkaya, B.; Gourlaouen, C.; Maseras, F.; Bruneau, C.; Dixneuf, P. H. *J. Am. Chem. Soc.* **2008**, *130*, 1156–1157.
- (15) Ackermann, L.; Vicente, R.; Althammer, A. *Org. Lett.* **2008**, *10*, 2299–2302.
- (16) Matsuura, Y.; Tamura, M.; Kochi, T.; Sato, M.; Chatani, N.; Kakiuchi, F. *J. Am. Chem. Soc.* **2007**, *129*, 9858–9859.
- (17) Davies, D. L.; Al-Duaij, O.; Fawcett, J.; Giardiello, M.; Hilton, S. T.; Russell, D. R. *Dalton Trans.* **2003**, 4132–4138.

- (8) Davies, D. L.; Donald, S. M. A.; Al-Duaij, O.; Macgregor, S. A.; Polleth, M. *J. Am. Chem. Soc.* **2006**, *128*, 4210–4211.
- (9) Davies, D. L.; Donald, S. M. A.; Macgregor, S. A. *J. Am. Chem. Soc.* **2005**, *127*, 13754–55.
- (10) Davies, D. L.; Donald, S. M. A.; Al-Duaij, O.; Fawcett, J.; Little, C.; Macgregor, S. A. *Organometallics* **2006**, *25*, 5976–5978.
- (11) Garcia-Cuadrado, D.; Braga, A. A. C.; Maseras, F.; Echavarren, A. M. *J. Am. Chem. Soc.* **2006**, *128*, 1066–1067.
- (12) Garcia-Cuadrado, D.; deMendoza, P.; Braga, A. A. C.; Maseras, F.; Echavarren, A. M. *J. Am. Chem. Soc.* **2007**, *129*, 6880–6886.
- (13) Lafrance, M.; Rowley, C. N.; Woo, T. K.; Fagnou, K. *J. Am. Chem. Soc.* **2006**, *128*, 8754–8756.
- (14) Gorelsky, S. I.; Lapointe, D.; Fagnou, K. *J. Am. Chem. Soc.* **2008**, *130*, 10848–10849.
- (15) Ziatdinov, V. R.; Oxgaard, J.; Mironov, O. A.; Young, K. J. H.; Goddard, W. A.; Periana, R. A. *J. Am. Chem. Soc.* **2006**, *128*, 7404–7405.

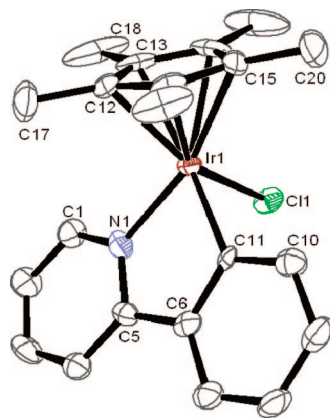


Figure 1. Ortep plot of **1a**. Thermal ellipsoids are drawn at 50% probability level, and hydrogen atoms are omitted for clarity. Selected bond lengths [Å] and bond angles [deg]: Ir(1)–N(1), 2.074(5); Ir(1)–C(11), 2.058(5); Ir(1)–Cl(1), 2.4046(15); C(11)–Ir(1)–N(1), 78.0(2); Ir(1)–C(11)–C(6), 116.2(4); Ir(1)–N(1)–C(5), 116.5(4); C(6)–C(5)–N(1), 113.8(5); C(5)–C(6)–C(11), 115.1(5).

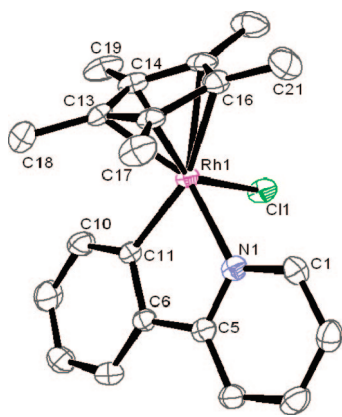
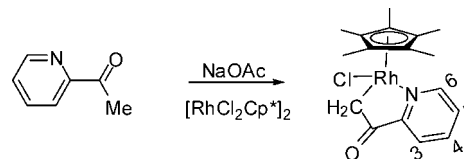


Figure 2. Ortep plot of **1b**. Thermal ellipsoids are drawn at 50% probability level, and hydrogen atoms are omitted for clarity. Selected bond lengths [Å] and bond angles [deg]: Rh(1)–N(1), 2.099(3); Rh(1)–C(11), 2.035(3); Rh(1)–Cl(1), 2.392(1); C(11)–Rh(1)–N(1), 78.7(1); Rh(1)–C(11)–C(6), 115.7(2); Rh(1)–N(1)–C(5), 115.8(2); C(6)–C(5)–N(1), 114.2(3); C(5)–C(6)–C(11), 115.5(3).

al. reported¹⁴ that this method works for cyclometalation of 2-phenylpyridine with $[MCl_2Cp^*]_2$ ($M = Rh, Ir$), while ruthenium complex **1c** has been prepared previously by the same workers by transmetalation with $[L1HgCl]$.¹⁵ The characterization of complexes **1a–c** is in accord with previously published data. The structure of the ruthenium complex has been published;¹⁵ however for rhodium and iridium the only structures are of complexes that have a $Cr(CO)_3$ unit π -coordinated to the cyclometalated phenyl.¹⁴ Hence, we have determined the structures of the rhodium and iridium complexes **1a** and **1b**, and these are shown in Figures 1 and 2, respectively, with selected distances and angles. The chelate bite angle of the cyclometalated ligand is 78.0(2)° and 78.71(12)° in **1a** and **1b**, respectively. The M–N bond in **1a** and **1b** [2.074(2) and 2.099(2) Å, respectively] is longer than the M–C(phenyl) bond

Scheme 1. Reaction of 2-Acetylpyridine with $[RhCl_2Cp^*]_2$ in the Presence of NaOAc



[2.058(5) and 2.035(3) Å, respectively]. These bond lengths are reasonably similar to the corresponding $Cr(CO)_3$ complexes reported earlier.¹⁴ However a notable difference with the $Cr(CO)_3$ complexes is the planarity of the phenylpyridine ligand. The dihedral angle between the phenyl and pyridine rings, C(11)–C(6)–C(5)–N(1), is 5.47° and 2.95° in **1a** and **1b**, respectively, which are much smaller than those, 12.86° and 9.72°, observed for the corresponding $Cr(CO)_3$ complexes, consistent with the large steric effect of the bulky $Cr(CO)_3$ unit as noted previously.¹⁴

Having demonstrated that pyridine could act as a directing group for metalation of a phenyl sp^2 C–H bond in these complexes, we decided to test whether it could also promote activation of an sp^3 C–H bond. To our knowledge there are only two previous examples of cyclometalation of sp^3 C–H bonds with these half-sandwich dimers, both with $[IrCl_2Cp^*]_2$.^{16,17} Our attempts to cyclometalate 2-ethylpyridine with $[MCl_2Cp^*]_2$ ($M = Ir, Rh$) in the presence of sodium acetate failed, the dimers just reacting with acetate, as we have observed previously.⁷ Our mechanistic studies^{8–10} have shown that hydrogen bonding between the C–H bond and acetate is key to the process; hence we decided to test 2-acetylpyridine as a substrate since this has a similar structure, but the methyl C–H bonds will be more acidic, hence more favorable for hydrogen bonding.

Reaction of 2-acetylpyridine (HL2) with $[IrCl_2Cp^*]_2$ in the presence of sodium acetate was monitored by ES mass spectrometry, and after 4 h all the ligand had reacted. Several iridium-containing species were observed, including ions at m/z 569 $[Cp^*Ir(L2)(HL2)]$ and 448 $[Cp^*Ir(L2)]$, suggesting that cyclometalation had occurred. The ¹H NMR spectrum of the crude product showed the presence of more than two Cp^*Ir species and several signals for pyridine protons. Unfortunately it was not possible to isolate any pure products even after attempted chromatography. However, two mutually coupled doublets were observed at δ 2.96 and 3.40, which are consistent with a C–H activation product (see below). It is possible that **2a** is formed and then reacts further with 2-acetylpyridine. Pfeffer et al. have previously reported difficulty in isolating C–H activation products of primary benzylamines due to fast reaction of the initially formed product with unreacted amine.¹⁸

The corresponding reaction with $[RhCl_2Cp^*]_2$ gave **2b** in good yield (Scheme 1). The ¹H NMR spectrum of **2b** showed a signal at δ 1.57 due to the Cp^* and four multiplets in the aromatic region, each integrating to 1H due to the pyridine ring. However, there was no methyl signal; instead two mutually coupled doublets of doublets were observed at δ 2.84 ($J = 7, 1$ Hz) and 3.84 ($J = 7, 1$ Hz) (the smaller coupling is to Rh), assigned to a metal-bound CH_2 . These resonances confirm the expected sp^3 C–H activation, and their inequivalence shows that epimerization at the metal is slow on the NMR time scale. In the ¹³C{¹H}

(14) Scheeren, C.; Maasarani, F.; Hijazi, A.; Djukic, J. P.; Pfeffer, M.; Zanic, S. D.; Le Goff, X. F.; Ricard, L. *Organometallics* **2007**, *26*, 3336–3345.

(15) Djukic, J. P.; Berger, A.; Duquenne, M.; Pfeffer, M.; de Cian, A.; Kyritsakas-Gruber, N. *Organometallics* **2004**, *23*, 5757–5767.

(16) Bauer, W.; Prem, M.; Polborn, K.; Sunkel, K.; Steglich, W.; Beck, W. *Eur. J. Inorg. Chem.* **1998**, 485–493.

(17) Wik, B. J.; Romming, C.; Tilset, M. *J. Mol. Catal. A: Chem.* **2002**, *189*, 23–32.

(18) Sortais, J. B.; Pannetier, N.; Holuigue, A.; Barloy, L.; Sirlin, C.; Pfeffer, M.; Kyritsakas, N. *Organometallics* **2007**, *26*, 1856–1867.

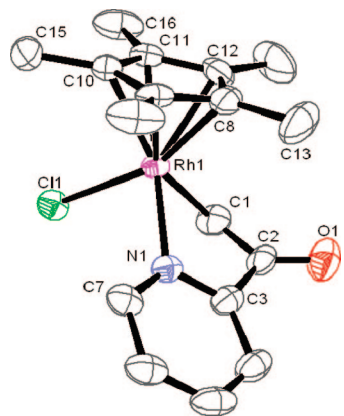


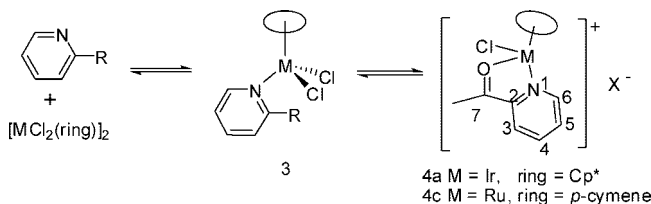
Figure 3. Ortep plot of **2b**. Thermal ellipsoids are drawn at 50% probability level, and hydrogen atoms are omitted for clarity. Selected bond lengths [Å] and bond angles [deg]: Rh(1)–N(1), 2.112(2); Rh(1)–C(1), 2.138(3); Rh(1)–Cl(1), 2.4294(8); O(1)–C(2), 1.224(4); C(1)–Rh(1)–N(1), 77.8(1); Rh(1)–C(1)–C(2), 101.1(2); Rh(1)–N(1)–C(3), 112.2(2); C(2)–C(3)–N(1), 113.0(3); C(1)–C(2)–C(3), 112.7(3).

NMR spectrum, the CH₂ carbon was observed at δ 45.33 as a doublet (J_{RhC} 22 Hz). The FAB mass spectrum of **2b** showed an ion at m/z 393 due to $[\text{M}]^+$ and a fragment ion at m/z 358 due to $[\text{M} - \text{Cl}]^+$. Crystals of **2b** suitable for X-ray diffraction were obtained from dichloromethane/hexane, and the structure is discussed below.

The structure of **2b** is shown in Figure 3, with selected bond distances and angles, and this confirms the activation of an sp^3 C–H bond of a methyl group. Complex **2b** has a pseudo-octahedral geometry about the metal. The Rh–N bond length [2.112(2) Å] is similar to that [2.099(2) Å] in **1b** (*vide supra*); however, the Rh–C(1) bond length [2.138(3) Å] in **2b** is significantly longer than the Rh–C(phenyl) bond [2.035(3) Å] in **1b** (see above), consistent with a bond to an sp^3 carbon rather than an sp^2 one. Indeed, the Rh–C(1) bond length is similar to the Ir–CH₂ bond length [2.165(3) Å] in a Cp* iridium cyclometalated diimine.¹⁷ The C–O bond length is 1.224(4) Å, as expected for a double bond. The presence of the sp^3 -hybridized carbon has a marked effect on the bond angles and conformation of the metallacycle. Thus, the 2-acetylpyridine ligand has a chelate angle of 77.84(11)°, similar to that (78.71(12)°) in **1b**, but the angle at the sp^3 carbon C(1) (Rh–C(1)–C(2) 101.1(2)°) is considerably smaller than 115.7(2)° at the sp^2 carbon in **1b**, with the other angles in the metallacycle (average 112.6°) being slightly reduced from those in **1b** (average 115.2°). As a result, the pyridine and acetyl groups are significantly nonplanar; the dihedral angle C(1)–C(2)–C(3)–N(1) is 26.65°. As found for other cyclometalated Cp* complexes,^{7,14} **2b** shows an η -Cp* coordination with three short Rh–C bonds [2.141(3)–2.160(3) Å] and two longer ones [2.222(3)–2.231(3) Å].

The reaction of 2-acetylpyridine and $[\text{RuCl}_2(p\text{-cymene})_2]$ in the presence of NaOAc, as in the case with iridium, failed to give any pure products, though all the ruthenium complex did react. Hence, in the case of acetylpyridine it seems that sp^3 C–H activation is more successful with rhodium than iridium, or ruthenium. This contrasts with our previous synthetic work for phenyl C–H bond activation, in which C–H activation was superior with iridium.⁷ The reason for this difference may not be related to the C–H activation step. Indeed DFT calculations suggest there is very little difference in activation barrier for acetate-assisted C–H activation with these three metals.¹⁹ To investigate this difference further, we examined the interaction

Scheme 2. Reaction of 2-Acetylpyridine and $[\text{IrCl}_2\text{Cp}^*]_2$ or $[\text{RuCl}_2(p\text{-cymene})_2]$



of 2-acetylpyridine with the dimers $[\text{MCl}_2\text{Cp}^*]_2$ (M = Rh, Ir) and $[\text{RuCl}_2(p\text{-cymene})_2]$ in the absence of acetate.

The coordination of 2-acetylpyridine to $[\text{MCl}_2\text{Cp}^*]_2$ (M = Ir, Rh) and $[\text{RuCl}_2(p\text{-cymene})_2]$ was examined by ¹H NMR spectroscopy at different temperatures (Scheme 2). In the case of $[\text{RhCl}_2\text{Cp}^*]_2$, no coordination of 2-acetylpyridine was observed, even at low temperature (247 K). It is interesting to note that for rhodium even the simple pyridine adduct $[\text{RhCl}_2(\text{C}_5\text{H}_5\text{N})\text{Cp}^*]$ was reported as being unstable in solution in the absence of free pyridine.²⁰ In the case of iridium the ¹H NMR spectrum of a mixture of $[\text{IrCl}_2\text{Cp}^*]_2$ and 2-acetylpyridine (1:2 molar ratio) in CD₂Cl₂ at 300 K showed mainly the presence of both starting materials but with two additional broad signals at δ 1.75 and 3.26 due to a Cp* and an acetyl methyl with some very weak multiplets in the pyridine region. This new species integrated to about 5% of the starting materials and was assigned to the N,O chelate complex salt **4a**, rather than a simple N-coordinated neutral adduct **3**, in equilibrium with starting materials (Scheme 2). As the temperature was lowered, the aromatic pyridine signals of **4a** became well resolved, giving two doublets at δ 8.96 and 9.13 and two triplets at δ 8.66 and 8.13. These were assigned to H⁶, H³, H⁴, and H⁵, respectively, on the basis of ROESY experiments at 270 K, which show correlations between signals for free and coordinated 2-acetylpyridine. The proportion of coordinated 2-acetylpyridine increased as the temperature was lowered, and at 211 K the equilibrium was slow on the NMR time scale and coordinated and free 2-acetylpyridine were present in approximately a 1:1 ratio. Notably, all the signals of the 2-acetylpyridine shifted downfield on coordination, the largest coordination shift (1.04 ppm) being observed for H³ (see below). Further information on the structure of the complex in solution is available from observation of NOEs between H⁶ and the Cp*, and between H³ and the acetyl methyl, suggesting that the carbonyl oxygen is pointing in the same direction as the nitrogen, i.e., toward the metal. Interestingly addition of *d*₄-methanol to the NMR sample (20% by volume) caused a significant shift of the equilibrium position, favoring coordinated 2-acetylpyridine over free 2-acetylpyridine (ratio 3:1 at room temperature), and also slowed the exchange between free and coordinated 2-acetylpyridine. This result suggests the new complex is **4a** rather than **3** since the presence of methanol is likely to have a more significant effect on the stability of the salt than on the neutral species. It seems that in CD₂Cl₂ formation of **4a** is not very favorable due to the formation of chloride anion. Addition of methanol provides better solvation of the chloride and hence displaces the equilibrium toward **4a**. Hence, the large coordination shift (see above) for (H³) may be due to hydrogen bonding with the chloride anion, which is in close contact in CD₂Cl₂.

The reaction of $[\text{RuCl}_2(p\text{-cymene})_2]$ and 2-acetylpyridine (1:2 molar ratio) was also carried out in CD₂Cl₂ in an NMR tube.

(19) Poblador-Bahamonde, A.; Davies, D. L.; Donald, S. M. A.; Macgregor, S. A., unpublished results.

(20) Kang, J. W.; Moseley, K.; Maitlis, P. M. *J. Am. Chem. Soc.* **1969**, *91*, 5970.

After 10 min the ^1H NMR spectrum showed the presence of two new ruthenium species as well as some starting materials. The major new ruthenium species (30%) showed four broad multiplets at δ 9.65, 8.24, 8.14, and 8.08 for the pyridine protons, four multiplets between δ 5.9 and δ 6.22 for the *p*-cymene group, and signals due to acetyl and isopropyl protons. The high frequency of the *p*-cymene aromatic protons is consistent with a cationic species, and their inequivalence agrees with a chiral metal center; therefore we assign these to the N,O chelate complex **4c**. The other new species present had signals due to a Ru(*p*-cymene) fragment but with no additional pyridine signals. These signals have been assigned to the anionic species $[\text{RuCl}_3(\textit{p}\text{-cymene})]^-$, which is formed from the chloride liberated in the formation of the N,O chelate cation. The amount of $[\text{RuCl}_3(\textit{p}\text{-cymene})]^-$ did not match that of the cation of **4c**; hence there was still some free chloride. Note, the complex $\text{Cs}[\text{RuCl}_3(\text{benzene})]$ has been reported previously though it was not fully characterized.²¹ We have independently prepared $[\text{RuCl}_3(\textit{p}\text{-cymene})]^-$ by the addition of Et_4NCl to $[\text{RuCl}_2(\textit{p}\text{-cymene})]_2$ and confirmed the identity of the anion by electrospray mass spectrometry (m/z 343 in CH_2Cl_2), and have shown that the anion and dimer interconvert on the NMR time scale. As in the case of iridium, variable-temperature NMR spectroscopy and ROESY spectra indicated that free and coordinated 2-acetylpyridine were exchanging on the NMR time scale, and hence **4c** is exchanging with $[\text{RuCl}_2(\textit{p}\text{-cymene})]_2$ and $[\text{RuCl}_3(\textit{p}\text{-cymene})]^-$. As the temperature was lowered, the proportion of **4c** increased to 40% at 258 K. The addition of only 10 molar equiv (per ruthenium) of *d*₄-methanol was sufficient to displace the equilibrium still further to approximately 1:1 (coordinated: free 2-acetylpyridine) at room temperature. In order to more fully characterize the N,O chelates and investigate whether they are on the pathway to C–H activation, we attempted to isolate these species as the PF_6 salts.

Reactions of 2-acetylpyridine (HL2) with $[\text{MCl}_2\text{Cp}^*]_2$ ($\text{M} = \text{Ir}, \text{Rh}$) and $[\text{RuCl}_2(\text{arene})]_2$ (arene = *p*-cymene, mesitylene) were carried out in dichloromethane in the presence of KPF_6 . In the case of iridium the N,O chelate complex $[\text{IrCl}\{\text{C}_5\text{H}_4\text{N}-2\text{-C}(=\text{O})\text{CH}_3\text{-K,N,O}\}\text{Cp}^*]\text{PF}_6$ (**4a**) was isolated in 74% yield. The ^1H NMR spectrum of **4a** showed two singlets at δ 3.10 and 1.79 due to the methyl group and Cp^* , respectively. The pyridine protons gave rise to three doublets of doublets at δ 8.91 (H^6), 8.50 (H^3), and 8.05 (H^5) and a doublet of triplets at δ 8.34 (H^4). Thus, in this case with PF_6 as the anion H^3 is more upfield than in the chloride case, reflecting the lack of hydrogen bonding to the anion. The ^{13}C NMR spectrum showed the expected number of carbons, the CO was observed at δ 210.78, and a peak at δ 26.04 was assigned to the acetyl methyl group. The FAB mass spectrum showed ions at m/z 484 due to the cation $[\text{IrCl}(\text{HL2})\text{Cp}^*]^+$. Crystals of this compound were obtained from DCM/hexane and were suitable for X-ray diffraction, and the structure is discussed with a ruthenium analogue below. An attempt to make the corresponding compound with $[\text{RhCl}_2\text{Cp}^*]_2$ under the same conditions failed. The ^1H NMR spectrum showed the free ligand and $[\text{RhCl}_2\text{Cp}^*]_2$ were still present.

The same reaction was attempted with $[\text{RuCl}_2(\textit{p}\text{-cymene})]_2$ and $[\text{RuCl}_2(\text{mes})]_2$. The latter was chosen as a starting material since it has much simpler ^1H NMR signals than $[\text{RuCl}_2(\textit{p}\text{-cymene})]_2$, which makes identification much easier. Reaction of 2-acetylpyridine with $[\text{RuCl}_2(\textit{p}\text{-cymene})]_2$ in the presence of KPF_6 gave **4c** in 58% yield. The ^1H NMR spectrum was very

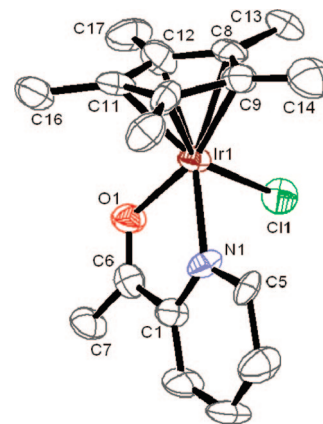


Figure 4. Ortep plot of **4a**. Thermal ellipsoids are drawn at 50% probability level, and hydrogen atoms are omitted for clarity. Selected bond lengths [\AA] and bond angles [deg]: Ir(1)–N(1), 2.101(11); Ir(1)–O(1), 2.154(10); Ir(1)–Cl(1), 2.377(5); O(1)–C(6), 1.235(17); O(1)–Ir(1)–N(1), 76.1(4); Ir(1)–O(1)–C(6), 117.0(9); Ir(1)–N(1)–C(1), 114.8(8); C(6)–C(1)–N(1), 113.8(12); C(1)–C(6)–O(1), 117.5(13).

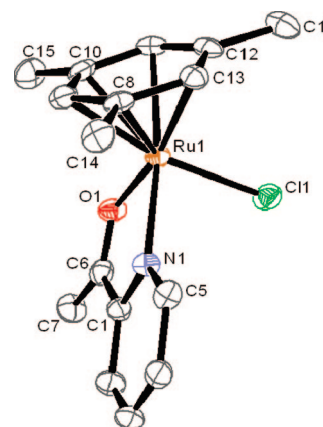


Figure 5. Ortep plot of **4d**. Thermal ellipsoids are drawn at 50% probability level, and hydrogen atoms are omitted for clarity. Selected bond lengths [\AA] and bond angles [deg]: Ru(1)–N(1), 2.106(4); Ru(1)–O(1), 2.105(3); Ru(1)–Cl(1), 2.385(1); O(1)–C(6), 1.234(5); O(1)–Ru(1)–N(1), 75.92(13); Ru(1)–O(1)–C(6), 117.8(3); Ru(1)–N(1)–C(1), 114.9(3); C(6)–C(1)–N(1), 114.0(4); C(1)–C(6)–O(1), 117.3(4).

similar to the spectrum observed in the NMR reaction described previously with minor changes in chemical shifts for some of the pyridine protons presumably due to different interactions with the PF_6 anion rather than chloride, and full details of the characterization are given in the Experimental Section. Reaction of 2-acetylpyridine with $[\text{RuCl}_2(\text{mes})]_2$ and KPF_6 gave **4d** in 87% yield. The ^1H NMR spectrum was similar to **4a,c**, with four signals in the aromatic region due to the pyridine. The most downfield was a doublet at δ 9.21 assigned to H^6 . A singlet for the methyl group was observed at δ 3.01 and two singlets for the mesitylene, one for the methyl groups at δ 2.33 (9H) and one for the aromatic CH at δ 5.37 (3H). The ^{13}C NMR spectrum showed the expected number of carbons, and the acetyl methyl was seen at δ 25.8. The FAB mass spectrum showed ions at m/z 378 due to $[\text{M}]^+$. Crystals of this compound were obtained from DCM/hexane and were suitable for X-ray diffraction.

The structures of **4a** and **4d** with selected bond distances and angles are shown in Figures 4 and 5, respectively. The Ru–N and Ru–O bond lengths, 2.106(4) and 2.105(3) \AA , respectively, are identical in **4d**, but the Ir–O, 2.154(10) \AA , is slightly longer

(21) Robertson, D. R.; Stephenson, T. A.; Arthur, T. J. *Organomet. Chem.* **1978**, *162*, 121–136.

than the Ir–N, 2.101(11) Å, in **4a**. The O–M–N chelate angles are the same (ca. 76°) in both complexes. The other angles in the metallacyclic rings are all between 117.8° and 113.8°, and the acetylpyridine is almost planar in both complexes. The N–C–C–O torsion angle is less than 4° in both complexes.

An important consideration in the reactivity of these complexes is whether the acetyl protons are acidic. We noticed that over time the signals due to the acetyl methyl protons in the ¹H NMR spectra of **4a** and **4d** (in *d*₄-methanol) gradually disappeared though the other signals were unchanged. This disappearance was accelerated by the addition of D₂O, and we assign it to deuterium incorporation via a ket–enol equilibrium and proton exchange with D₂O in the NMR solvent. The amount of enol complex present is presumably very small, as no signals for this species were observed. In an attempt to isolate the enol complex and to assess whether these N,O chelate complexes can be intermediates on the way to C–H-activated N,C complexes, we have attempted deprotonation of the complexes.

Complexes **4a** and **4d** were each treated with NaOAc in dichloromethane; however, no reaction occurred in either case. The ¹H NMR spectra showed only the starting compounds after 4 h. Note the reaction of [RhCl₂Cp*]₂ with 2-acetylpyridine and NaOAc has progressed significantly within this time, suggesting that complexes **4** are not intermediates en route to complexes **2**. We have also tested the reaction of **4d** with a stronger base. Thus, **4d** was reacted with sodium methoxide. The ¹H NMR spectrum showed that a reaction occurred with no starting material remaining; two different sets of mesitylene signals, in a 1:1 ratio, were observed, indicating a possible unsymmetrical dimer with additional signals at δ 1.96 due to a methyl and two single proton signals at δ 3.19 and 6.54, the former of which is assigned as a hydroxyl proton since it exchanges with D₂O. Unfortunately we have not managed to get the compound totally pure; it transforms to further products if left in solution for long periods. However, we have managed to get some crystals from the product, and the structure with selected bond distances and angles is shown in Figure 6.

The structure shows an unsymmetrical dicationic dimer **5**. Each ruthenium is coordinated to an η⁶ mesitylene ring and there is a bridging chloride. The coordination of Ru(1) is completed by an N,O chelated acetylpyridine, the original methyl group of which, C(7), has been deprotonated twice and is bonded to C(8) and Ru(2). There is some contribution from an enol resonance form for C(7)–C(6)–O(1) in the 2-acetylpyridine bonded to Ru(1). Thus, C(7)–C(6) (1.385(14) Å) and Ru(1)–O(1) (1.995(9) Å) are somewhat shorter, and O(1)–C(6) (1.286(12) Å) somewhat longer than the corresponding bonds, 1.481(6), 2.105(3), and 1.234(5) Å, respectively, in the N,O chelate complex **4d**. It would appear that deprotonation of **4d** leads to a very reactive O-bound enolate, which immediately reacts in an aldol-type reaction with the cationic starting material rather than isomerize to an N,C-bound enolate.

The deuterium incorporation results and formation of complex **5** shows that deprotonation of complexes **4** can occur; however the enolate formed is clearly very reactive. The failure of OAc to convert the cationic N–O chelate **4a,d** to N–C complexes **2a,d** suggests these are not intermediates on the pathway to the cyclometalated N,C products. In a further attempt to investigate the stability of C- or O-bound enolates, we attempted the reactions of the dimers [MCl₂Cp*]₂ (M = Rh, Ir) and [RuCl₂(*p*-cymene)]₂ with the preformed enolate of 2-acetylpyridine (Scheme 3).

The lithium enolate was made *in situ* by reaction of 2-acetylpyridine with LiHMDS in THF at –80 °C, and after

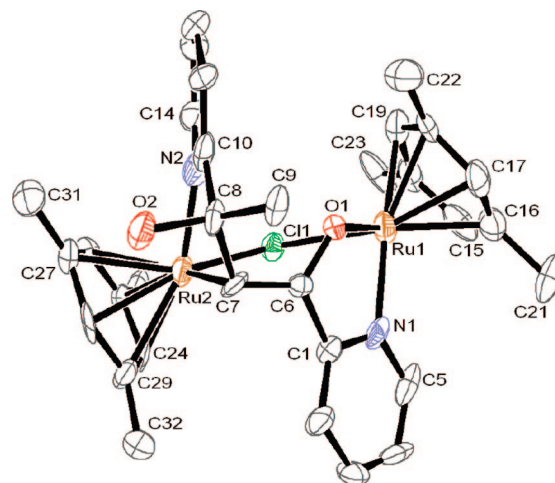
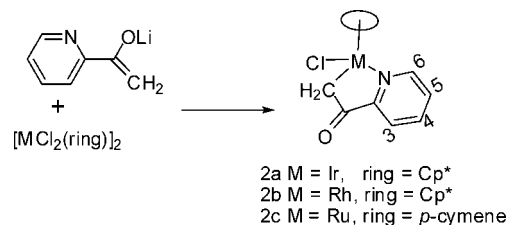


Figure 6. Ortep plot of **5**. Thermal ellipsoids are drawn at 50% probability level, and hydrogen atoms are omitted for clarity. Selected bond lengths [Å] and bond angles [deg]: Ru(1)–N(1), 2.099(10), Ru(1)–O(1), 1.995(9); Ru(1)–Cl(1), 2.442(3); Ru(2)–N(2), 2.080(11), Ru(2)–C(7), 2.203(12); Ru(2)–Cl(1), 2.441(3); O(1)–C(6), 1.286(12); O(2)–C(8), 1.442(13); C(6)–C(7), 1.385(14); C(7)–C(8), 1.540(15); O(1)–Ru(1)–N(1), 77.4(4); Ru(1)–O(1)–C(6), 114.7(7); Ru(1)–N(1)–C(1), 113.1(8); C(6)–C(1)–N(1), 111.7(11); C(1)–C(6)–O(1), 116.1(10); C(7)–Ru(2)–N(2), 75.3(4); Ru(2)–C(7)–C(6), 108.7(8); Ru(2)–N(2)–C(10), 120.3(9); C(8)–C(10)–N(2), 114.9(12); C(7)–C(8)–C(10), 109.7(11).

Scheme 3. Reaction of the Lithium Enolate of 2-Acetylpyridine with [MCl₂Cp*]₂ (M = Ir, Rh) or [RuCl₂(*p*-cymene)]₂



stirring for 1 h the relevant dimer was added. The reaction with [RhCl₂Cp*]₂ gave N,C chelate complex **2b** in 81% yield with identical spectroscopic data to the sample prepared by C–H activation. Similarly, the reaction with [IrCl₂Cp*]₂ gave the iridium C-bound enolate **2a**. The spectrum showed four signals for the pyridine group and a Cp* signal at δ 1.55. There was no methyl signal; instead two mutually coupled doublets were observed at δ 3.41 and 3.00 assigned to the metal-bound CH₂. Hence, the lithium enolate gave the N,C product **2a** rather than an isomeric N,O enolate complex. The inequivalence of the metal-bound CH₂ resonances also shows that epimerization at the metal is slow on the NMR time scale. The ES mass spectrum showed a molecular ion at *m/z* 448 [M – Cl]⁺, a fragment at *m/z* 406 [M – CH₂CO – Cl]⁺, and a peak at *m/z* 569 corresponding to [M – Cl + HL₂]⁺ from the substitution of the chloride by a second 2-acetylpyridine. The complex was also characterized by X-ray diffraction, and the structure is shown in Figure 7.

The structure of **2a** is similar to that of **2b** discussed above. The Ir–N bond length [2.094(6) Å] is similar to the Ir–N bond length [2.074(5) Å] in **1a** (*vide supra*); however, the Ir–C(7) bond, [2.121(8) Å], in **2a** is significantly longer than the Ir–C(11) bond [2.058(5) Å] in **1a** and is similar to the Rh–C bond length [2.138(3) Å] in **2b** but slightly shorter than the Ir–CH₂ bond length [2.165(3) Å] in a Cp*iridium cyclometalated diimine.¹⁷ As in **2b**, the presence of the sp³-hybridized carbon has a marked

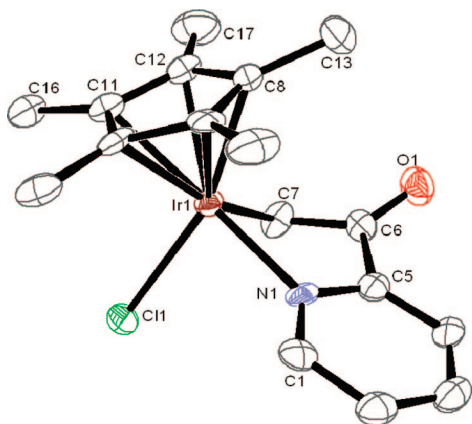


Figure 7. Ortep plot of **2a**. Thermal ellipsoids are drawn at 50% probability level, and hydrogen atoms are omitted for clarity. Selected bond lengths [Å] and bond angles [deg]: Ir(1)—N(1), 2.094(6); Ir(1)—C(7), 2.121(8); Ir(1)—Cl(1), 2.424(2); O(1)—C(6), 1.213(10); C(7)—Ir(1)—N(1), 77.2(3); Ir(1)—C(7)—C(6), 102.1(5); Ir(1)—N(1)—C(5), 114.5(5); C(6)—C(5)—N(1), 111.6(6); C(5)—C(6)—C(7), 112.2(7).

effect on the bond angles and conformation of the metallacycle. Thus, the 2-acetylpyridine ligand has a chelate angle of 77.2(3)° (cf. 77.84(11)° in **2b**), but the angle at the metallated carbon [Ir—C(7)—C(6)] is 102.1(5)° (cf. 101.1(2)° in **2b**) and the average of the other angles in the metallacycle is 112.8°, statistically the same as in **2b**. As a result, the pyridine and acetyl groups are significantly nonplanar; the dihedral angle C(7)—C(6)—C(5)—N(1) is 26.7°, the same as the corresponding angle in **2b**.

The reaction of the lithium enolate with [RuCl₂(*p*-cymene)]₂ was not as clean, and we have failed to isolate the product pure; however the major product could be identified as **2c** from the ¹H NMR spectrum. The spectrum showed the expected signals for a coordinated *p*-cymene and four multiplets for the pyridine (see Experimental Section for details) and two mutually doublets at δ 3.72 and 3.08 as expected for the CH₂ group bonded to the metal.

The formation of the N,C chelates **2a,c** is proof that these compounds are stable and can be made by an alternative route to direct C—H activation of the sp³ bond. The failure of the iridium and ruthenium dimers to give pure **2a,c** by the C—H activation route is therefore not due to thermodynamic instability of the product. These results suggest that if the pyridine coordinates to the chloride dimer before reaction with acetate, then other reaction pathways are opened and acetate-assisted C—H activation may not occur. This is consistent with our mechanism in which the acetate must be coordinated to the metal in the C—H activation step. Ikariya et al. have also reported that [Ir(OAc)₂Cp*] can carry out C—H activation in the absence of added acetate.²² To further investigate the mechanism, we have examined the coordination of 2-ethyl and 2-phenylpyridine with [MCl₂Cp*]₂ (M = Rh, Ir) in the absence of sodium acetate by ¹H NMR spectroscopy at different temperatures.

The ¹H NMR spectrum of 2-ethylpyridine with [IrCl₂Cp*]₂ shows exchange is occurring between the starting materials and a 2-ethylpyridine complex of type **3**. The two Cp* signals are very broad, as are the signals for H⁶ and the CH₂ of the ethyl group. The integration suggests that the major species is the coordinated complex. At 233 K the spectrum shows sharp

signals indicating that exchange is now slow on the NMR time scale. At this point two multiplets are observed for the CH₂ of the ethyl group at δ 2.96 and 3.70, showing that coordination has occurred and that these two protons are inequivalent. This proves that the plane of the pyridine is not perpendicular to the Cp* and there is no mirror plane in the molecule; that is, it is chiral. In the case of the reaction of 2-ethylpyridine with [RhCl₂Cp*]₂ there is no evidence for coordination at room temperature; however, at 247 K the NMR shows broad resonances corresponding to the coordinated 2-ethylpyridine (20%) although it is still exchanging on the NMR time scale. Similar reaction of 2-phenylpyridine with [IrCl₂Cp*]₂ gave no evidence for any coordination of the pyridine even at 247 K.

In conclusion, in the case of 2-phenylpyridine the pyridine does not react until after the dimer has reacted with acetate, consistent with easy C—H activation of this substrate by [MCl₂Cp*]₂ (M = Ir, Rh) and [RuCl₂(*p*-cymene)]₂. In the case of 2-ethylpyridine, even though the reaction with acetate can occur first, there is no subsequent C—H activation. We have noted previously that hydrogen bonding plays an important role in the C—H activation step.¹⁰ The decreased acidity of the proton to be activated in 2-ethylpyridine compared with 2-acetylpyridine may be a factor in the lower reactivity of 2-ethylpyridine. In addition, the need to include another sp³ carbon in the metallacyclic ring may also make cyclometalation of 2-ethylpyridine less favorable. In the case of 2-acetylpyridine with [RhCl₂Cp*]₂ reaction with acetate occurs first, leading to C—H activation product **2b**; however, for iridium and ruthenium the possibility of forming an N,O chelate, **4a,c**, provides an alternative reaction pathway that is competitive with the acetate-assisted C—H activation.

Experimental Section

All reactions were carried out at room temperature under nitrogen; however the workup was carried out in air unless stated otherwise. ¹H, and ¹³C{¹H} NMR spectra were obtained using a Bruker ARX 400 MHz spectrometer, with CDCl₃ as solvent, unless otherwise stated. Chemical shifts were recorded in ppm (on δ scale for ¹H NMR, with tetramethylsilane as internal reference), and coupling constants are reported in Hz. FAB mass spectra were obtained on a Kratos concept mass spectrometer using NOBA as matrix, and electrospray (ES) mass spectra were recorded using a micromass Quattro LC mass spectrometer in acetonitrile. Microanalyses were performed by the Elemental Analysis Service (London Metropolitan University). Starting materials [MCl₂Cp*]₂ (M = Rh, Ir),²³ [RuCl₂(*p*-cymene)]₂,²⁴ and [RuCl₂(mes)]₂²⁴ were made by literature methods; other compounds were obtained from Aldrich and Alfa Aesar.

Preparation of [MCl(C₆H₄-2-C₅H₄N-κ-C,N)(ring)] (1a–c) (M = Rh, Ir, ring = Cp*; M = Ru, ring = *p*-cymene). A mixture of [MCl₂(ring)]₂, 2-phenylpyridine (2.2 equiv), and sodium acetate (2.5 equiv) in CH₂Cl₂ (5 mL) was stirred for 4 h at room temperature. The solution was filtered through Celite and rotary evaporated to dryness. The product was crystallized from CH₂Cl₂/hexane to give **1a–c** (55, 75, 61%, respectively) as orange (Ir, Rh) or brown (Ru) crystals. The spectroscopic data are consistent with the literature.^{14,15}

Preparation of [RhCl(C₅H₄N-2-C(=O)CH₂-κ-C,N)Cp*], 2b. A mixture of NaOAc (58.7 mg, 0.49 mmol), [RhCl₂Cp*]₂ (150 mg, 0.24 mmol), and 2-acetylpyridine (53 mg, 0.44 mmol) was stirred for 20 h at room temperature. The solution was filtered through

(22) Arita, S.; Koike, T.; Kayaki, Y.; Ikariya, T. *Organometallics* **2008**, 27, 2795–2802.

(23) White, C.; Yates, A.; Maitlis, P. M. *Inorg. Synth.* **1992**, 29, 228.
(24) Bennett, M. A.; Smith, A. K. *J. Chem. Soc., Dalton Trans.* **1974**, 233.

Table 1. Crystallographic Data for Complexes 1a,b, 2a,b, 4a,d, and 5

	1a	1b	2a	2b
empirical formula	C ₂₁ H ₂₃ ClIrN	C ₂₁ H ₂₃ ClNRh	C ₁₇ H ₂₁ ClIrNO	C ₁₇ H ₂₁ ClNRh
fw	517.05	427.76	483.00	393.71
temp/K	150(2)	150(2)	150(2)	293(2)
cryst syst	monoclinic	monoclinic	orthorhombic	orthorhombic
space group	<i>P</i> 2(1)/ <i>c</i>	<i>P</i> 2(1)/ <i>n</i>	<i>I</i> ba2	<i>I</i> ba2
<i>a</i> /Å	7.474(2)	7.4528(13)	14.227(3)	14.512(2)
<i>b</i> /Å	14.685(4)	14.780(3)	16.654(3)	16.715(2)
<i>c</i> /Å	16.615(4)	16.956(3)	13.727(3)	13.660(2)
α /deg	90	90	90	90
β /deg	97.304(5)	102.644(3)	90	90
γ /deg	90	90	90	90
<i>U</i> /Å ³	1808.8(8)	1822.5(6)	3252.3(11)	3313.5(9)
<i>Z</i>	4	4	8	8
density(calc)/Mg m ⁻³	1.899	1.559	1.973	1.578
abs coeff/mm ⁻¹	7.531	1.085	8.373	1.190
<i>F</i> (000)	1000	872	1856	1600
cryst size/mm	0.13 × 0.10 × 0.07	0.15 × 0.12 × 0.07	0.21 × 0.11 × 0.03	0.32 × 0.21 × 0.08 mm ³
θ range/deg	1.86 to 26.00	1.85 to 26.00	1.88 to 26.00	1.86 to 26.00
index ranges	−9 ≤ <i>h</i> ≤ 9, −18 ≤ <i>k</i> ≤ 18, −20 ≤ <i>l</i> ≤ 20	−9 ≤ <i>h</i> ≤ 9, −18 ≤ <i>k</i> ≤ 18, −20 ≤ <i>l</i> ≤ 20	−17 ≤ <i>h</i> ≤ 17, −20 ≤ <i>k</i> ≤ 20, −16 ≤ <i>l</i> ≤ 16	−17 ≤ <i>h</i> ≤ 17, −20 ≤ <i>k</i> ≤ 20, −16 ≤ <i>l</i> ≤ 16
no. of reflns collected	13 926	14 041	12 174	12 205
no. of indep collected (<i>R</i> _{int})	3555 [<i>R</i> (int) = 0.0533]	3580 [<i>R</i> (int) = 0.0458]	3162 [<i>R</i> (int) = 0.0621]	3243 [<i>R</i> (int) = 0.0292]
data/restraints/params	3555/0/222	3580/0/222	3162/1/195	3243/1/195
goodness-of-fit, <i>F</i> ²	1.017	1.004	0.994	1.090
final <i>R</i> indices [<i>I</i> > 2 σ (<i>I</i>)]	<i>R</i> 1 = 0.0322, <i>wR</i> 2 = 0.0579	<i>R</i> 1 = 0.0349, <i>wR</i> 2 = 0.0708	<i>R</i> 1 = 0.0327, <i>wR</i> 2 = 0.0713	<i>R</i> 1 = 0.0246, <i>wR</i> 2 = 0.0587
<i>R</i> indices (all data)	<i>R</i> 1 = 0.0431, <i>wR</i> 2 = 0.0604	<i>R</i> 1 = 0.0465, <i>wR</i> 2 = 0.0741	<i>R</i> 1 = 0.0385, <i>wR</i> 2 = 0.0730	<i>R</i> 1 = 0.0255, <i>wR</i> 2 = 0.0592
largest diff. peak and hole/e Å ⁻³	1.220 and −1.001	0.819 and −0.504	2.316 and −1.111	1.292 and −0.263
	4a	4d	7	
empirical formula	C ₁₈ H ₂₃ Cl ₄ F ₆ IrNOP	C ₁₆ H ₁₉ ClF ₆ NOPRu	C ₃₃ H ₃₉ Cl ₃ F ₁₂ N ₂ O ₂ P ₂ Ru ₂	
fw	748.34	522.81	1094.09	
temp/K	150(2)	150(2)	150(2)	
cryst syst	monoclinic	monoclinic	triclinic	
space group	<i>P</i> 2(1)/ <i>c</i>	<i>C</i> 2/ <i>c</i>	<i>P</i> $\bar{1}$	
<i>a</i> /Å	11.915(13)	29.187(4)	8.767(6)	
<i>b</i> /Å	13.452(15)	9.8982(13)	11.659(8)	
<i>c</i> /Å	16.428(18)	15.325(2)	20.804(13)	
α /deg	90	90	92.606(15)	
β /deg	106.67(2)	120.985(2)	100.426(15)	
γ /deg	90	90	107.533(15)	
<i>U</i> /Å ³	2522(5)	3795.6(9)	1983(2)	
<i>Z</i>	4	8	2	
density(calc)/Mg m ⁻³	1.971	1.830	1.832	
abs coeff/mm ⁻¹	5.837	1.114	1.136	
<i>F</i> (000)	1440	2080	1088	
cryst size/mm	0.17 × 0.12 × 0.08	0.15 × 0.10 × 0.06	0.22 × 0.08 × 0.02	
θ range/deg	1.78 to 26.00	1.63 to 26.00	1.84 to 26.00	
index ranges	−14 ≤ <i>h</i> ≤ 14, −16 ≤ <i>k</i> ≤ 16, −19 ≤ <i>l</i> ≤ 20	−35 ≤ <i>h</i> ≤ 35, −12 ≤ <i>k</i> ≤ 12, −18 ≤ <i>l</i> ≤ 18	−10 ≤ <i>h</i> ≤ 10, −14 ≤ <i>k</i> ≤ 14, −25 ≤ <i>l</i> ≤ 25	
no. of reflns collected	19 294	14 542	15 719	
no. of indep collected (<i>R</i> _{int})	4959 [<i>R</i> (int) = 0.1745]	3733 [<i>R</i> (int) = 0.0715]	7700 [<i>R</i> (int) = 0.1649]	
data/restraints/params	4959/0/268	3733/0/248	7700/0/513	
goodness-of-fit, <i>F</i> ²	0.934	0.919	0.860	
final <i>R</i> indices [<i>I</i> > 2 σ (<i>I</i>)]	<i>R</i> 1 = 0.0857, <i>wR</i> 2 = 0.1976	<i>R</i> 1 = 0.0444, <i>wR</i> 2 = 0.0860	<i>R</i> 1 = 0.0898, <i>wR</i> 2 = 0.1557	
<i>R</i> indices (all data)	<i>R</i> 1 = 0.1159, <i>wR</i> 2 = 0.2096	<i>R</i> 1 = 0.0677, <i>wR</i> 2 = 0.0922	<i>R</i> 1 = 0.2097, <i>wR</i> 2 = 0.1949	
largest diff peak and hole/e Å ⁻³	5.542 and −4.648	0.894 and −0.543	2.170 and −0.975	

Celite and rotary evaporated to dryness to give a red solid, which was washed with hexane and diethyl ether to give **2b** (150 mg, 78%). Anal. Calc for C₁₇H₂₁ClNRh: C, 51.86, H, 5.38, N, 3.56. Found: C, 51.82, H, 5.21, N, 3.46. ¹H NMR (300 MHz): δ 1.57 (s, 15H, Cp*), 2.84 (dd, 1H, *J* 7, 1, *CHH'*), 3.84 (dd, 1H, *J* 7, 1, *CHH''*), 7.49 (m, 1H, H⁵), 7.65 (m, 1H, H³), 7.89 (dt, 1H, *J* 7.5, 1.5, H⁴), 8.65 (m, 1H, H⁶). ¹³C NMR: δ 8.82 (C₅Me₅), 45.33 (d, *J*_{RhC} 22, CH₂), 94.36 (d, *J*_{RhC} 7, C₅Me₅), 121.44, 127.44, 138.89, 151.49 (C³, C⁴, C⁵, C⁶), 159.15 (C²), 197.64 (CO). MS (FAB): *m/z* 393 [M]⁺, 358 [M − Cl]⁺.

Preparation of [IrCl{C₅H₄N-2-C(=O)CH₃-K,N,O}Cp*]PF₆ (4a). A mixture of KPF₆ (92 mg, 0.50 mmol), [IrCl₂Cp*]₂ (100 mg, 0.13 mmol), and 2-acetylpyridine (30 mg, 0.25 mmol) in CH₂Cl₂ (10 mL) was stirred for 4 h at room temperature. The solution was filtered through Celite and rotary evaporated to dryness.

The product was crystallized from chloroform to give **4a** (117 mg, 74%) as orange crystals. Anal. Calc for C₁₇H₂₂ClF₆NOPIr: C, 32.46, H, 3.53, N, 2.23. Found: C, 32.47, H, 3.43, N, 2.35. ¹H NMR (CD₂Cl₂, 400 MHz): δ 1.79 (s, 15H, C₅Me₅), 4.00 (s, 3H, COMe), 8.05 (ddd, 1H, *J* 8.0, 5.5, 1.5, H⁵), 8.34 (td, 1H, *J* 8.0, 1.5, H⁴), 8.50 (ddd, 1H, *J* 8.0, 2.0, 1.5, H³), 8.91 (ddd, 1H, *J* 5.5, 1.5, 1.0, H⁶). ¹³C NMR: δ 8.75 (C₅Me₅), 26.04 (COMe), 88.80 (C₅Me₅), 131.43 (C³), 133.17 (C⁵), 140.90 (C⁴), 151.27 (C⁶), 152.19 (C²), 210.78 (CO). MS (FAB): *m/z* 484 [M]⁺.

[RuCl{C₅H₄N-2-C(=O)CH₃-K,N,O}(p-cymene)]PF₆ (4c). A mixture of KPF₆ (60 mg, 0.33 mmol), [RuCl₂(p-cymene)]₂ (50 mg, 0.08 mmol), and 2-acetylpyridine (19.8 mg, 0.16 mmol) in CH₂Cl₂ (5 mL) was stirred for 20 h at room temperature. The solution was filtered through Celite and rotary evaporated to dryness. The product was crystallized from chloroform to give **4c** (51 mg, 58%) as brown

crystals. Anal. Calc for $C_{17}H_{21}ClF_6NOPRu$: C, 38.03, H, 3.94, N, 2.61. Found: C, 37.94, H, 3.85, N, 2.60. 1H NMR: δ 1.38 (d, 3H, *J* 7, CHMeMe'), 1.40 (d, 3H, *J* 7, CHMeMe'), 2.31 (s, 3H, Me), 2.95 (s, 3H, COMe), 2.99 (sept, 1H, *J* 7, CHMeMe'), 5.76 (d, 1H, *J* 6, Cy), 5.82 (d, 1H, *J* 6, Cy), 5.89 (d, 1H, *J* 6, Cy), 6.00 (d, 1H, *J* 6, Cy), 7.87 (ddd, 1H, *J* 7, 5, 1, H^5), 8.18 (td, 1H, *J* 7, 1, H^4), 8.25 (d, 1H, *J* 7, H^3), 9.25 (d, 1H, *J* 5, H^6). ^{13}C NMR: δ 18.30 (Me (Cy)), 22.07, (CHMeMe' (Cy)) 22.51 (CHMeMe' (Cy)), 25.85 (COMe), 31.28 (CHMeMe'), 82.45, 83.29, 83.39, 85.47 ($4 \times CH$, C_6H_4 , (Cy)), 99.61 (C (C_6H_4)), 103.98 (C (C_6H_4)), 130.63 (C^3), 132.07 (C^5), 140.41 (C^4), 151.7 (C^2), 154.77 (C^6), 211.24 (CO). MS (FAB): m/z 392 [$M - PF_6$] $^+$.

[RuCl{C₅H₄N-2-C(=O)CH₃-κN,O}(mes)PF₆(4d). A mixture of KPF₆ (63.2 mg, 0.34 mmol), [RuCl₂(Mes)₂] (50 mg, 0.08 mmol), and 2-acetylpyridine (20.8 mg, 0.17 mmol) in CH₂Cl₂ (5 mL) was stirred for 20 h at room temperature. The solution was filtered through Celite and rotary evaporated to dryness. The product was crystallized from chloroform to give **4d** (78 mg, 87%) as brown crystals. Anal. Calc for $C_{16}H_{19}ClF_6NOPRu$: C, 36.76, H, 3.66, N, 2.68. Found: C, 36.86, H, 3.51, N, 2.66. 1H NMR (CD₂Cl₂): δ 2.33 (s, 9H, $C_6H_3Me_3$), 3.01 (s, 3H, COMe), 5.37 (s, 3H, $C_6H_3Me_3$), 7.94 (ddd, 1H, *J* 7.5, 5.5, 2, H^5), 8.26 (ddd, 1H, *J* 8, 7.5, 1, H^4), 8.30 (d, 1H, *J* 8, H^3), 9.21 (d, 1H, *J* 5.5, H^6). ^{13}C NMR: δ 18.7 ($C_6H_3Me_3$), 25.8 (COMe), 77.0 [CH($C_6H_3Me_3$)], 105.9 [CMe($C_6H_3Me_3$)], 130.1 (C^4), 131.7 (C^5), 140.2 (C^3), 151.7 (C^2), 154.1 (C^6), 211.0 (CO). MS (FAB): m/z 378 [M] $^+$.

Reaction of [RuCl{C₅H₄N-2-C(=O)CH₃-κN,O}(mes)PF₆(4d) with NaOMe. NaOMe (4.1 mg, 0.076 mmol) was added to a solution of complex **4d** (40 mg, 0.076 mmol) in CH₂Cl₂ (5 mL), and the mixture was stirred for 6 days at room temperature. Another equivalent of MeONa (4.14 mg, 0.076 mmol) was added, and the reaction was stirred for a further day. The mixture was filtered through Celite and rotary evaporated to dryness. Attempted crystallization from CH₂Cl₂/hexane gave a black precipitate (25 mg) and a few crystals suitable for X-ray analysis. The 1H NMR spectrum of the crystals was slightly impure, but the peaks for **5** could be assigned as follows. 1H NMR (CD₂Cl₂): δ 1.96 (s, 3H, MeC(OH)), 1.98 (s, 9H, $C_6H_3Me_3$), 2.01 (s, 9H, $C_6H_3Me_3$), 3.19 (s, 1H, OH), 5.05 (s, 3H, $C_6H_3Me_3$), 5.10 (s, 3H, $C_6H_3Me_3$), 6.54 (s, 1H, CHC(OH)), 7.47 (d, 1H, *J* 7.5, Hpyr), 7.62 (dd, 1H, *J* 6.0 Hpyr), 7.68 (dd, 1H, *J* 5.5, Hpyr), 8.00 (t, 1H, *J* 7.5, Hpyr), 8.05 (d, 1H, *J* 7.5, Hpyr), 8.11 (t, 1H, *J* 7.5, Hpyr), 8.66 (d, 1H, *J* 5.5, Hpyr), 9.01 (d, 1H, *J* 5.5, Hpyr). MS (FAB): m/z 719 [$M - H$] $^+$.

Reaction of the Lithium Enolate of 2-Acetylpyridine with [IrCl₂Cp*]₂. 2-Acetylpyridine (21.3 mg, 0.176 mmol) was added to a solution of LiHMDS (0.18 mL, 0.194 mmol) in THF (5 mL) at -78 °C. After being stirred for 1 h at the same temperature, [IrCl₂(Cp*)]₂ (70 mg, 0.088 mmol) was added to the mixture. The mixture was allowed to warm and was stirred for 4 h. The solution was filtered through Celite and evaporated to dryness. The product, **2a**, was isolated as an orange precipitate (58 mg, 68%). Anal. Calc for $C_{17}H_{21}NOClIr$: C, 42.27, H, 4.38, N, 2.90. Found: C, 42.23, H, 4.28, N, 2.81. 1H NMR (CD₂Cl₂, 300 MHz): δ 1.53 (s, 15H, C_5Me_5), 2.96 (d, 1H, *J* 9.5, H^8), 3.40 (d, 1H, *J* 9.5, H^8), 7.36 (ddd, 1H, *J* 8.0, 5.5, 1.5, H^5), 7.54 (ddd, 1H, *J* 8.0, 1.5, 1.0, H^3), 7.86 (td, 1H, *J* 8.0, 1.5, H^4), 8.51 (ddd, 1H, *J* 5.5, 1.5, 1.0, H^6). ^{13}C NMR: δ 7.51 (C_5Me_5), 35.24 (CH₂), 85.56 (C_5Me_5), 120.47 (C^3), 126.79 (C^5), 137.47 (C^4), 150.83 (C^6), 156.54 (C^2), 200.65 (CO). MS (FAB): m/z 483 [M] $^+$, 448 [$M - Cl$] $^+$.

Reaction of the Lithium Enolate of 2-Acetylpyridine with [RhCl₂(Cp*)]₂. 2-Acetylpyridine (27.0 mg, 0.230 mmol) was added to a solution of LiHMDS (0.23 mL, 0.250 mmol) in THF (5 mL)

at -78 °C. After being stirred for 1 h at the same temperature, [RhCl₂(Cp*)]₂ (70 mg, 0.110 mmol) was added to the mixture. The mixture was allowed to warm and stirred for 4 h. The solution was filtered through Celite and evaporated to dryness. Complex **2b** was isolated as an orange precipitate (70 mg, 81%) and was spectroscopically identical to the sample prepared by C–H activation (see above).

Reaction of the Lithium Enolate of 2-Acetylpyridine with [RuCl₂(*p*-cymene)]₂. 2-Acetylpyridine (27.8 mg, 0.228 mmol) was added to a solution of LiHMDS (0.24 mL, 0.236 mmol) in THF (5 mL) -78 °C. After being stirred for 1 h at this temperature, [RuCl₂(*p*-cymene)]₂ (70 mg, 0.114 mmol) was added to the mixture. The mixture was allowed to warm and was stirred for 4 h. The solution was filtered through Celite and evaporated to dryness (70.4 mg). The 1H NMR spectrum showed a mixture, but the peaks due to **2c** can be assigned as follows (CDCl₃, 400 MHz): δ 1.04 (d, 3H, *J* 7.0, CHMeMe'), 1.13 (d, 3H, *J* 7.0, CHMeMe'), 1.77 (s, 3H, Me), 2.57 (sept, 1H, *J* 7.0, CHMeMe'), 3.08 (d, 1H, *J* 8.0, CH₂), 3.72 (d, 1H, *J* 8.0, CH₂), 4.97 (d, 1H, *J* 5.0, Cy), 5.02 (d, 1H, *J* 5.5, Cy), 5.25 (d, 1H, *J* 5.0, Cy), 5.31 (d, 1H, *J* 5.5, Cy), 7.35 (ddd, 1H, *J* 7.0, 5.5, 1.5, H^5), 7.47 (d, 1H, *J* 7.0, H^3), 7.74 (td, 1H, *J* 7.0, 1.0, H^4), 8.91 (d, 1H, *J* 5.5, H^6).

Examination of the Coordination of Substituted Pyridines by 1H NMR Spectroscopy. A mixture of [MCl₂Cp*]₂ (M = Ir, Rh) or [RuCl₂(*p*-cymene)]₂ (15 to 20 mg) and an equimolar amount of the appropriate ligand (2-acetylpyridine, 2-ethylpyridine, or 2-phenylpyridine) was dissolved in CD₂Cl₂ (or CDCl₃). The 1H NMR spectra were recorded using a Bruker DRX (400 MHz) at different temperatures.

X-ray Crystal Structure Determinations. Details of the structure determinations of crystals of **1a,b**, **2a,b**, **4a,d**, and **5** are given in Table 1; those for **4c** are in the Supporting Information. Data were collected on a Bruker Apex 2000 CCD diffractometer using graphite-monochromated Mo K α radiation, $\lambda = 0.7107$ Å. The data were corrected for Lorentz and polarization effects, and empirical absorption corrections were applied. The structures were solved by direct methods and with structure refinement on F^2 employing SHELXTL version 6.10.²⁵ Hydrogen atoms were included in calculated positions (C–H = 0.93–1.00 Å, O–H = 0.84 Å) riding on the bonded atom with isotropic displacement parameters set to 1.5 U_{eq} (O) for hydroxyl H atoms, 1.5 U_{eq} (C) for methyl hydrogen atoms, and 1.2 U_{eq} (C) for all other H atoms. All non-hydrogen atoms were refined with anisotropic displacement parameters without positional restraints. In the cases of **4a** and **5** disordered solvent molecules were removed by using the SQUEEZE option in Platon²⁶ (solvent has been included in all formulas). Figures were drawn using the program ORTEP.²⁷

Acknowledgment. We thank the Saudi Arabian government (O.A.-D.) for a studentship, EPSRC for funding (EP/D055024/1), and Johnson Matthey for a loan of platinum metal salts.

Supporting Information Available: Crystallographic data in CIF format for **1a,b**, **2a,b**, **4a,d**, and **5**. These materials are available free of charge via the Internet at <http://pubs.acs.org>.

OM800909W

(25) Bruker; Version 6.10 ed.; Bruker Inc.: Madison, WI, 1998–2000.

(26) Spek, A. L. *Acta Crystallogr., Sect. A* **1990**, *A46*, C-34.

(27) Farrugia, L. J. *J. Appl. Crystallogr.* **1997**, *30*, 565.

Carbonyl-Amplified Catalyst Performance: Balancing Stability against Activity for Five-Coordinate Ruthenium Hydride and Hydridocarbonyl Catalysts

Nicholas J. Beach, Johanna M. Blacquiere, Samantha D. Drouin, and Deryn E. Fogg*

Centre for Catalysis Research and Innovation, Department of Chemistry, University of Ottawa, Ottawa, Ontario, Canada K1N 6N5

Received August 13, 2008

The activity of RuHCl(H₂)(PCy₃)(L) **2a/b** and RuHCl(CO)(PCy₃)(L) **3a/b** (a: L = PCy₃; b: L = IMes; IMes = 1,3-dimesitylimidazol-2-ylidene) was assessed in hydrogenation of a range of molecular and polymeric olefins and in hydrogenation and isomerization of allylbenzene. Elevated temperatures and/or high H₂ pressures are required for efficient hydrogenation. Under these conditions, **3a/b** outperform their dihydrogen analogues in both total productivity and turnover frequencies, despite theoretical and experimental evidence that the π -acid CO ligand should be deactivating. A thermolysis study reveals that the CO complexes are much less susceptible to deactivation under conditions relevant to catalysis (also, the IMes derivative **2b** is shorter-lived than **2a**). We attribute the superior performance of **3a/b** to their greater stability, which maintains higher concentrations of active catalyst than that possible for their H₂ analogues over the time scale of hydrogenation.

Introduction

The high volume of waste characteristic of fine chemicals and pharmaceutical manufacturing^{1,2} is coming under closer scrutiny in an increasingly stringent economic climate that underscores the correspondence between process costs and the proportion of waste generated per ton of product. Tandem catalysis is of interest for its potential to improve process efficiencies by eliminating unnecessary workup stages and solvent use, two major contributors to waste in pharmaceutical manufacturing.^{1,3} Improved efficiencies in catalyst consumption confer added advantages in reducing direct costs, as well as indirect costs associated with purification of the organic products.

As part of a program of study focusing on tandem catalysis,^{4–6} we have developed efficient⁷ methodologies for tandem ROMP–hydrogenation (ROMP = ring-opening metathesis polymerization).^{8–11} Hydrogenation is important in extending the range of applications for unsaturated ROMP polymers, by reducing their susceptibility to oxidative, thermal, and chemical degradation.¹² Tandem metathesis–hydrogenation methodologies typically rest on the accessibility of five-coordinate Ru hydrides from Grubbs catalysts of type **1** (Scheme 1). We earlier showed¹⁰ that the hydrido-dihydrogen complex **2a** is formed

clearly by hydrogenolysis of **1a** in the presence of base: the corresponding hydridocarbonyl complexes **3** are formed from both **2**⁸ and the alkylidene complexes **1**^{13–15} by reaction with methanol or other primary alcohols, via established^{16–19} alcohol decarbonylation pathways.²⁰ In related work, we found that use of small amounts of methanol as cosolvent dramatically increased hydrogenation efficiency in tandem ROMP–hydrogenation via **1a**, leading us to speculate that formation of **3a**–

(7) Reduction of ROMP polyoctenes was achieved via tandem catalysis at 50–60 °C and as little as 1 atm of H₂; see ref 8. Hydrogenation of polynorbornenes, particularly those bearing bulky substituents, is considerably more demanding; see ref 9. Hydrogen pressures of up to 1000 psi can be required for efficient reduction at these moderate temperatures: the high pressures are preferable to use of higher temperatures, which can trigger competitive thermal cross-linking of the unsaturated polymers. Less satisfactory results have been reported using a range of other catalysts (e.g., Wilkinson's catalyst, RhCl(PPh₃)₃; the Crabtree catalyst, [Ir(COD)(PCy₃)(py)]PF₆, and various supported palladium catalysts), despite their often outstanding performance in reduction of molecular olefins at relatively low H₂ pressures. See, for example, ref 9 and: (a) Lee, L.-B. W.; Register, R. A. *Macromolecules* **2005**, *38*, 1216–1222. (b) Dettmer, C. M.; Gray, M. K.; Torkelson, J. M.; Nguyen, S. T. *Macromolecules* **2004**, *37*, 5504–5512. (c) Lee, B. S.; Mahajan, S.; Clapham, B.; Janda, K. D. *J. Org. Chem.* **2004**, *69*, 3319–3329. (d) Sohn, B. H.; Gratt, J. A.; Lee, J. K.; Cohen, R. E. *J. Appl. Polym. Sci.* **1995**, *58*, 1041. (e) Vargas, J.; Santiago, A. A.; Tlenkopatchev, M. A.; Gavino, R.; Laguna, M. F.; Lopez-Gonzalez, M.; Riande, E. *Macromolecules* **2007**, *40*, 563–570.

(8) Drouin, S. D.; Zamanian, F.; Fogg, D. E. *Organometallics* **2001**, *20*, 5495–5497.

(9) Camm, K. D.; Castro, N. M.; Liu, Y.; Czechura, P.; Snelgrove, J. L.; Fogg, D. E. *J. Am. Chem. Soc.* **2007**, *129*, 4168–4169.

(10) Drouin, S. D.; Yap, G. P. A.; Fogg, D. E. *Inorg. Chem.* **2000**, *39*, 5412–5414.

(11) Related advances in methodology by others: (a) McLain, S. J.; McCord, E. F.; Arthur, S. D.; Hauptman, E.; Feldman, J.; Nugent, W. A.; Johnson, L. K.; Mecking, S.; Brookhart, M. *Proc. PMSE* **1997**, *76*, 246. (b) Watson, M. D.; Wagener, K. B. *Macromolecules* **2000**, *33*, 3196–3201. (c) Bielawski, C. W.; Louie, J.; Grubbs, R. H. *J. Am. Chem. Soc.* **2000**, *122*, 12872–12873. (d) Schmidt, B. *Chem. Commun.* **2004**, 742–743.

(12) Mulhaupt, R. *Macromol. Chem. Phys.* **2003**, *204*, 289–327.

(13) Dinger, M. B.; Mol, J. C. *Organometallics* **2003**, *22*, 1089–1095.

(14) Dinger, M. B.; Mol, J. C. *Eur. J. Inorg. Chem.* **2003**, 2827–2833.

(15) Trnka, T. M.; Morgan, J. P.; Sanford, M. S.; Wilhelm, T. E.; Scholl, M.; Choi, T.-L.; Ding, S.; Day, M. W.; Grubbs, R. H. *J. Am. Chem. Soc.* **2003**, *125*, 2546–2558.

* Corresponding author. E-mail: dfogg@uottawa.ca.

(1) (a) Sheldon, R. A. *Green Chemistry and Catalysis*; Wiley-VCH: Chichester, 2007. (b) Sheldon, R. A. *Green Chem.* **2007**, *9*, 1273–1283.

(2) Constable, D. J. C.; Dunn, P. J.; Hayler, J. D.; Humphrey, G. R.; Leazer, J. L., Jr.; Linderman, R. J.; Lorenz, K.; Manley, J.; Pearlman, B. A.; Wells, A.; Zaks, A.; Zhang, T. Y. *Green Chem.* **2007**, *9*, 411–420.

(3) Constable, D. J. C.; Jimenez-Gonzalez, C.; Henderson, R. K. *Org. Process Res. Dev.* **2007**, *11*, 133–137.

(4) Recent reviews of tandem catalysis: (a) Dragutan, V.; Dragutan, I. *J. Organomet. Chem.* **2006**, *691*, 5129–5147. (b) Wasilke, J.-C.; Obrey, S. J.; Baker, R. T.; Bazan, G. C. *Chem. Rev.* **2005**, *105*, 1001–1020. (c) Fogg, D. E.; dos Santos, E. N. *Coord. Chem. Rev.* **2004**, *248*, 2365–2379.

(5) Dragutan, V.; Dragutan, I.; Delaude, L.; Demonceau, A. *Coord. Chem. Rev.* **2007**, *251*, 765–794.

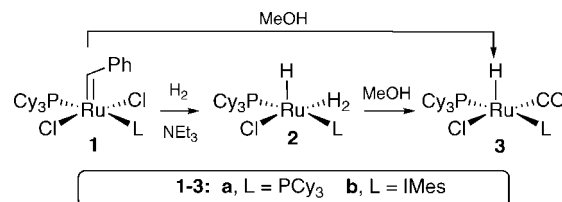
(6) (a) Schmidt, B. *Pure Appl. Chem.* **2006**, *78*, 469–476. (b) Schmidt, B. *Eur. J. Org. Chem.* **2004**, 186, 1865–1880.

inference, a more reactive catalyst than **2a**—could be an important contributing factor.^{8,21}

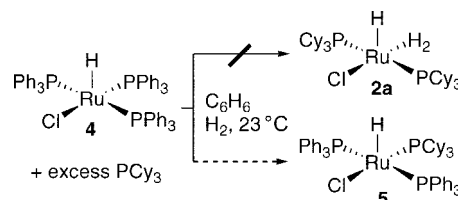
While ample precedents exist for hydrogenation via **3a**,^{13,22–27} catalysis via **2a** has gone less studied,²⁸ and no direct comparison of the hydrogenation activity of the two complexes has been reported. We were intrigued by the possibility that **3a** is the more active, given that much evidence correlates higher hydrogenation activity with a more electron-rich Ru center. Thus, Ru catalysts containing strongly σ -donating alkylphosphine ligands outperform those containing arylphosphines, and incorporation of a CO ligand is known to decrease hydrogenation activity in arylphosphine complexes of Ru, Rh, and Ir.^{26,29–31} The latter behavior is consistent with the inhibiting effect of the π -acid ligand on both phosphine loss (a required step in olefin hydrogenation via **3a**^{22,27} and related polyphosphine³¹ catalysts) and oxidative addition of dihydrogen. Further, in a computational study designed to probe the effect of a σ -donor, versus a π -acid, ancillary ligand in RuHCl(L)(PⁱPr₃)₂ model systems (L = CO, PH₃), we found a systematically more stable reaction profile for the PH₃ species.³² That is, this study revealed no electronic basis for increased hydrogenation activity on the part of the CO complex.

The apparent contradiction between these findings and the tandem catalysis data in the presence of methanol prompted us to undertake a systematic experimental comparison of the hydrogenation activity of the isolated, well-defined dihydrogen and carbonyl complexes. The complexes examined are those accessible from the first- and second-generation Grubbs catalysts, viz., RuHCl(H₂)(L)(PCy₃) (**2a/b**) and RuHCl(CO)(L)(P-

Scheme 1. Hydride Complexes Formed from First- and Second-Generation Grubbs Metathesis Catalysts



Scheme 2. Attempted Synthesis of **2a**^a



^a Dashed arrow indicates incomplete reaction: for details, see text.

Cy₃) (**3a/b**). Here we describe synthesis of the previously unreported **2b**, we demonstrate that the carbonyl derivatives are more efficient hydrogenation catalysts than their dihydrogen analogues, and we show that this effect originates in the greater robustness of the CO complexes, which limits their susceptibility to the deactivation pathways from which their H₂ analogues suffer.

Results and Discussion

Synthesis of RuHCl(H₂)LL' Complexes **2a/b.** We recently reported a clean, high-yield route to the hydridocarbonyl complexes **3a/b**, in which RuHCl(CO)(PPh₃)₃ is warmed with PCy₃ in benzene.³³ The success of this approach led us to attempt synthesis of **2a** by the analogous reaction of RuHCl(PPh₃)₃ **4**. These efforts were thwarted, however, by the poor solubility of **4** in aromatic solvents, which resulted in only partial conversion to RuHCl(PCy₃)(PPh₃)₂ **5** (30% of the soluble portion and an undetermined amount of the suspended material; Scheme 2) over 24 h at room temperature. Complete conversion, moreover, was hindered by the onset of product decomposition on longer reaction, while use of methylene chloride, in which **4** is soluble, is precluded by the susceptibility of the basic alkylphosphine to chlorination by this solvent. We therefore prepared **2a** by established methods, involving hydrogenolysis of **1a**¹⁰ or ligand exchange³⁴ of [RuCl₂(COD)]_n with PCy₃ (in the latter synthesis, we used 2-propanol as a convenient alternative to the original *sec*-butanol solvent,³⁴ and higher pressures of H₂). The identity of **2a** was confirmed by comparison to the reported^{35,36} NMR data, Table 1.

Leitner and co-workers have successfully prepared the dihydride complex RuH₂(H₂)₂(IMes)(PCy₃) by ligand exchange of RuH₂(H₂)₂(PCy₃)₂ with IMes at 55 °C under H₂, the room-temperature reaction failing to yield product.³⁷ We obtained

(16) Chaudret, B. N.; Cole-Hamilton, D. J.; Nohr, R. S.; Wilkinson, G. *J. Chem. Soc., Dalton Trans.* **1977**, 1546–1557.

(17) Jung, C. W.; Garrou, P. E. *Organometallics* **1982**, *1*, 658–666.

(18) Van der Sluys, L. S.; Kubas, G. J.; Caulton, K. G. *Organometallics* **1991**, *10*, 1033–1038.

(19) Chen, Y.-Z.; Chan, W. C.; Lau, C. P.; Chu, H. S.; Lee, H. L.; Jia, G. *Organometallics* **1997**, *16*, 1241–1246.

(20) Complexes **1a** and **1c** (c: L = H₂IMes) have also been transformed into **3a/c** via reaction with H₂C=CHOR (R = Et, SiMe₃), followed by thermolysis of the resulting Fischer carbenes. See: (a) Louie, J.; Grubbs, R. H. *Organometallics* **2002**, *21*, 2153–2164. (b) Arisawa, M.; Terada, Y.; Takahashi, K.; Nakagawa, M.; Nishida, A. *J. Org. Chem.* **2006**, *71*, 4255–4261.

(21) Use of 2-propanol, which does not undergo carbonylation, also led to rate accelerations, albeit smaller than those found for methanol.⁸ The alcohol cosolvent therefore exerts additional favorable effects beyond any arising from formation of **3a**: an increase in the dielectric constant of the reaction medium is almost certainly one relevant factor.

(22) Yi, C. S.; Lee, D. W.; He, Z.; Rheingold, A. L.; Lam, K.-C.; Concolino, T. E. *Organometallics* **2000**, *19*, 2909–2915.

(23) Yi, C. S.; Lee, D. W. *Organometallics* **1999**, *18*, 5152–5156.

(24) Mueller, L. A.; Dupont, J.; De Souza, R. F. *Macromol. Rapid Commun.* **1998**, *19*, 409–411.

(25) De Souza, R. F.; Rech, V.; Dupont, J. *Adv. Syn. Catal.* **2002**, *344*, 153–155.

(26) Martin, P.; McManus, N. T.; Rempel, G. L. *J. Mol. Catal. A* **1997**, *126*, 115–131.

(27) McManus, N. T.; Rempel, G. L. *J. Macromol. Sci., Rev. Macromol. Chem. Phys.* **1995**, *C35*, 239–285.

(28) For a study of **2a** in olefin silylation, see: (a) Lachaize, S.; Sabo-Etienne, S.; Donnadieu, B.; Chaudret, B. *Chem. Commun.* **2003**, 214–215; in dehydrogenative coupling of cyclic amines and alkenes, see: (b) Yi, C. S.; Yun, S. Y.; Guzei, I. A. *Organometallics* **2004**, *23*, 5392–5395. A Dupont patent also records its use in hydrogenation catalysis: (c) Beatty, R. P.; Paciello, R. A. U.S. Patent 5,554,778, 1996.

(29) Clapham, S. E.; Hadzovic, A.; Morris, R. H. *Coord. Chem. Rev.* **2004**, *248*, 2201–2237.

(30) Burk, M. J. *Acc. Chem. Res.* **2000**, *33*, 363–372.

(31) (a) James, B. R. In *Computational Organometallic Chemistry*; Wilkinson, G., Ed.; Pergamon: New York, 1982; Vol. 8, Chapter 51, and references therein. (b) James, B. R. *Homogeneous Hydrogenation*; Wiley: Toronto, 1973.

(32) Rowley, C. N.; Foucault, H. M.; Woo, T. K.; Fogg, D. E. *Organometallics* **2008**, *27*, 1661–1663.

(33) Beach, N. J.; Dharmasena, U. L.; Drouin, S. D.; Fogg, D. E. *Adv. Synth. Catal.* **2008**, *350*, 773–777.

(34) Wilhelm, T. E.; Belderrain, T. R.; Brown, S. N.; Grubbs, R. H. *Organometallics* **1997**, *16*, 3867–3869.

(35) Christ, M. L.; Sabo-Etienne, S.; Chaudret, B. *Organometallics* **1994**, *13*, 3800–3804.

(36) Sabo-Etienne, S.; Chaudret, B. *Coord. Chem. Rev.* **1998**, *178–180*, 381–407.

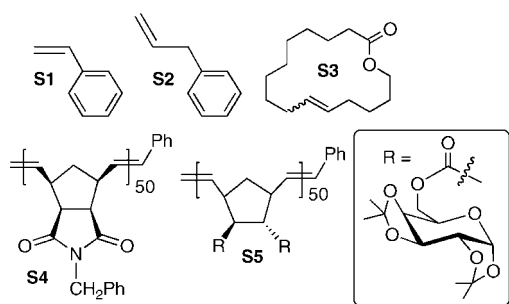
(37) Giunta, D.; Hoelscher, M.; Lehmann, C. W.; Mynott, R.; Wirtz, C.; Leitner, W. *Adv. Synth. Catal.* **2003**, *345*, 1139–1145.

Table 1. Key NMR Data for Ruthenium Hydride Complexes Relevant to This Work (Ar, 298 K)

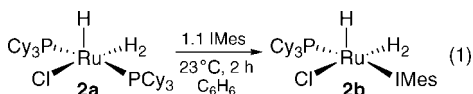
complex	solvent	δ_P (ppm)	δ_H (ppm)	ref
RuHCl(H ₂)(PCy ₃) ₂ , 2a ^a	C ₆ D ₆	54.2 (s)	-16.3 (br s) ^b	10,35
	CD ₂ Cl ₂	52.8 (s)	-16.93 (br s) ^{b,c}	this work
RuHCl(N ₂)(PCy ₃) ₂ , 6a	C ₆ D ₆	43.7 (s)	-27.26 (t, ² J _{PH} = 18.3 Hz)	52
RuHCl(H ₂)(IMes)(PCy ₃), 2b	C ₆ D ₆	56.3 (s)	-16.44 (br s) ^b	this work
RuHCl(N ₂)(IMes)(PCy ₃), 6b	C ₆ D ₆	45.0 (s)	-27.63 (d, ² J _{HP} = 21.4 Hz)	this work
RuHCl(CO)(PCy ₃) ₂ , 3a	C ₆ D ₆	46.9 (s)	-24.21 (t, ² J _{HP} = 18.1 Hz)	33
RuHCl(CO)(IMes)(PCy ₃), 3b	C ₆ D ₆	47.8 (s)	-24.82 (d, ² J _{HP} = 21.2 Hz)	33
RuH ₂ Cl ₂ (PCy ₃) ₂ , 7	C ₆ D ₆ ^a	91.3 (s)	-12.0 (t, ² J _{HP} = 31.5 Hz)	10
	CD ₂ Cl ₂	91.3 (s)	-12.39 (t, ² J _{HP} = 31.6 Hz).	10,54

^a In C₆D₆, the ³¹P{¹H} NMR singlet for RuCl₂(H₂)(PCy₃)₂ **8** is coincident with that for **2a**, but is accompanied by a singlet for the Ru(IV) tautomer **7** (ratio 1:2).¹⁰ The corresponding hydride signals appear at -16.2 ppm (br s, **8**) and -12.0 ppm (t, 31.5 Hz, **7**). In CD₂Cl₂, only **7** is present. ^b The hydride and dihydrogen signals for **2a/b** appear as a single broad peak integrating to 3H. ^c A chemical shift of -16.8 (br t, ²J_{HP} = 11 Hz) was originally reported for **2a** in CD₂Cl₂ (250 MHz).³⁵ The difference may reflect the presence of H₂ in the literature report.

Chart 1. Substrates Employed in Hydrogenation Studies



RuHCl(H₂)(IMes)(PCy₃) **2b** by the corresponding reaction of **2a** under argon: in this case, reaction was complete within 2 h at 23 °C (eq 1). No products other than **2b** and free PCy₃ were evident by NMR analysis, and the 1:1 ratio between the signals for free and bound PCy₃ confirmed clean formation of **2b** (i.e., free of paramagnetic byproducts; see below). Extraction of the free phosphine with hexanes enabled isolation of clean **2b** in ca. 70% yield. Its identity is supported by spectroscopic and elemental analysis.



The NMR features for **2b** correspond well with those for **2a** (Table 1). Thus, a ³¹P{¹H} NMR singlet appears at 56.3 ppm, and the broad singlet due to the hydride/dihydrogen ligands at -16.44 ppm. The $T_{1(\text{min})}$ value for the latter signal, 36.6 ms in C₇D₈ (253 K, 300 MHz), corresponds to a H-H distance of 1.03 Å.³⁸ Both the breadth of this signal and its comparatively long relaxation time are characteristic of η^2 -H₂ perturbed by interaction with *cis*-hydride.³⁸ In comparison, a value of ca. 30 ms was reported for **2a** at 243 K and 250 MHz.³⁵ Averaging of the classical and nonclassical hydrides in **2b** causes their NMR signal to appear ca. 11 ppm downfield from the doublet due to the unperturbed hydride in the corresponding dinitrogen complex **6b**. (The latter complex is discussed in greater detail below.) Well-resolved singlets appear for the IMes methyl, aromatic, and =CHN groups for **2b**, integration of which against the H/H₂ singlet is consistent with the proposed structure.

Catalytic Activity. Hydrogenation studies focused on the substrates shown in Chart 1. In a preliminary assessment of the relative hydrogenation activity of catalysts **2** and **3**, we

established their baseline activity toward styrene, **S1**, at 23 °C. The duration of these experiments was normalized to that required for quantitative formation of ethylbenzene by the most reactive catalyst, **3a** (Figure 1a). The lower activity of the IMes derivative **3b** at room temperature, versus its "first-generation" analogue **3a**, has precedent,³⁹ the data for **2a/b** indicate that this trend is retained for the H₂ complexes. We attribute the drop in activity to the low lability of PR₃ *trans* to an NHC ligand,^{40,41} originally described by the Grubbs group in a seminal paper on olefin metathesis.⁴⁰ Within both the bis(PCy₃) and the IMes-PCy₃ series, the activity of the CO complexes **3** is consistently greater than that of their dihydrogen analogues **2** at the high H₂ pressures required for complete hydrogenation within <24 h.⁴² The implications in terms of process efficiency are manifested most explicitly in the time profile for complete hydrogenation of styrene at a catalyst loading of 0.1 mol % (Figure 1b). Reduction by **3a** under the conditions specified is complete at 1.5 h, while quantitative reduction via **2a** requires 12 h.

We also evaluated the tendency of the more reactive catalysts **2a/3a** to promote competing isomerization, using allylbenzene **S2** as substrate. Hydridocarbonyl **3a** proves considerably more reactive than its H₂ analogue **2a** in both reduction and isomerization (Figure 1a). Of note, hydrogenation is ca. 30 times faster than isomerization for **2a**, but only 15 times faster for **3a**, suggesting that the higher activity of the latter may come at the price of reduced discrimination.

To assess the generality of the trends indicated in Figure 1, we turned to hydrogenation of several additional substrates of broader interest, which present successively greater challenges to reduction (Chart 1; Table 2). Reduction of lactone **S3** affords the musk-odored perfume Exaltolide, while the reduced ROMP polymers are of interest for, respectively, their relevance to well-defined polymer platforms for further functionalization (**S4**)⁴³ or for tissue engineering (**S5**).⁴⁴ Other hydrogenated ROMP polynorbornenes find applications as engineering thermo-

(39) Lee, H. M.; Smith, D. C., Jr.; He, Z.; Stevens, E. D.; Yi, C. S.; Nolan, S. P. *Organometallics* **2001**, *20*, 794–797.

(40) Sanford, M. S.; Love, J. A.; Grubbs, R. H. *J. Am. Chem. Soc.* **2001**, *123*, 6543–6554.

(41) Getty, K.; Delgado-Jaime, M. U.; Kennepohl, P. *J. Am. Chem. Soc.* **2007**, *129*, 15774–15776.

(42) Catalyst **2a** exhibits a complex dependence on H₂ concentration, possibly reflecting the lower activity of its bis(H₂) derivative, as reported for related dihydride catalysts: see ref 35. Borowski, A. F.; Sabo-Etienne, S.; Chaudret, B. *J. Mol. Catal. A* **2001**, *174*, 69–79. Hydrogenation is slow at low H₂ pressures, however, and use of elevated temperatures to accelerate reaction causes decomposition. This behavior is discussed in more detail in the following sections.

(43) Strong, L. E.; Kiessling, L. L. *J. Am. Chem. Soc.* **1999**, *121*, 6193–6196.

(44) Liu, Y.; Fogg, D.; Griffith, M. U.S. Patent 11/442,755, 2006.

(38) (a) Jessop, P. G.; Morris, R. H. *Coord. Chem. Rev.* **1992**, *121*, 155–284. (b) Kubas, G. J. *Metal Dihydrogen and σ -Bond Complexes*; Kluwer/Plenum: Dordrecht, 2001.

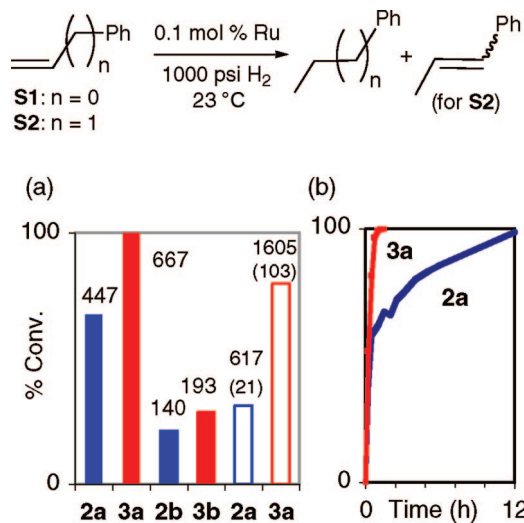


Figure 1. (a) Relative catalyst performance in hydrogenation of styrene (**S1**, 1.5 h, filled bars) and allylbenzene (**S2**, 0.5 h, unfilled), showing turnover frequencies (TOF; mol product · mol catalyst⁻¹ h⁻¹), with isomerization TOF in parentheses. (b) Time for complete hydrogenation of styrene by **2a** vs **3a**. All reactions carried out in benzene at 23 °C under 1000 psi H₂, using 0.1 mol % Ru and 1.0 M styrene or 0.7 M allylbenzene. Average of three trials (±3%).

Table 2. Relative Efficiency of Dihydrogen and Carbonyl Catalysts in Hydrogenation of Various Olefinic Substrates^a

substrate	mol % Ru	time (h)	cat.	TOF (h ⁻¹)	conv (%)
S1	0.1	0.5	2a	1260	63
			3a	1840	92
			2b	540	27
			3b	1520	76
S3	0.1	1	2a	830	83
			3a	960	96
			2b	530	53
			3b	810	81
S4	0.1	1	2a	310	31
			3a	660	66
			2b	310	31
			3b	510	51
S5	0.5 ^b	6	2a	3	10
			3a	7	21
			2b	7	20
			3b	17	50

^a Conditions: 1000 psi H₂, refluxing CH₂Cl₂ (except for **S1**: 23 °C); conversions measured by GC-FID or ¹H NMR analysis. ^b Conversions <10% at 0.1 mol % Ru.

plastics^{12,45} and fluoropolymers,⁴⁶ as polymer supports in synthetic applications,^{7c,47} as nanoporous materials,⁴⁸ and as gradient polymers with potentially programmable thermal properties.^{7b} We recently described tandem ROMP–hydrogenation of **S5** via first-, second-, and third-generation Grubbs catalysts, using protocols that generate **2a/b** and, in the presence of methanol, **3a/b**.⁹

Reduction of these substrates in CH₂Cl₂ follows the trend established above, with the CO complexes **3** outperforming

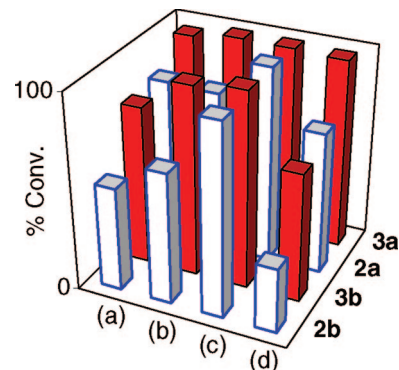


Figure 2. Effect of solvent and additives on hydrogenation of lactone **S3** via catalysts **2** and **3**: (a) CH₂Cl₂ solvent without additives (Table 2); (b) in CH₂Cl₂ with 3 equiv of NEt₃; (c) in 20% MeOH–CH₂Cl₂ with 3 equiv of NEt₃; (d) in C₆H₆ without additives. Conditions: 1000 psi H₂, 0.1 mol % Ru, bath temperature 55 °C, 1 h reaction time.

their H₂ analogues **2** in all cases. Also, the “first-generation” catalysts (**2a**, **3a**) generally outperform the second-generation catalysts (**2b**, **3b**) in reduction of all substrates, with the exception of neoglycopolymer **S5**. The challenging nature of **S5** is illustrated by the low turnover numbers found even at 0.5 mol % Ru (i.e., a catalyst loading 5 times higher than that used for **S1–S4**). While the CO catalysts remain more effective than their H₂ analogues for reduction of this substrate, maximum conversions are found for the IMes derivative **3b**, rather than the bis-PCy₃ complex **3a**. We attribute this to the significant steric bulk present in **S5**, arising from its polymeric nature, the *endo/exo* disubstitution of the repeat unit, the bulk of the galactose groups, and the additional steric pressure exerted by the acetal protecting groups. The unexpectedly higher activity of the IMes catalyst **2b** may reflect the essentially two-dimensional steric bulk of the N-heterocyclic carbene, relative to PCy₃; we presume that one phosphine ligand is replaced by olefin during the hydrogenation cycle as for **2a**; vide supra.

A more detailed study focused on the effect of solvent and additives on hydrogenation of lactone **S3** (Figure 2; for tabulated numerical data, see Supporting Information). Consistently higher conversions are found for reduction in methylene chloride, relative to benzene: the reactivity trends in both solvents follow the norm established above. Addition of base to the reactions in CH₂Cl₂ improves activity slightly, particularly for the IMes derivatives, suggesting some competing chlorination of the hydride catalyst by the chlorocarbon solvent (see later). Finally, the difference in activity between the H₂ and CO series of catalysts is minimized in the presence of MeOH, in which the dihydrogen catalysts undergo carbonylation, as discussed above.

Relative Stability of **2 and **3**.** The data above demonstrate that the carbonyl complexes **3** are more effective hydrogenation catalysts than their dihydrogen analogues **2**. Given the similarly low bulk of the CO and H₂ ligands, we discount a steric origin for this higher activity. However, the DFT study described in the Introduction, which predicts a higher-energy reaction profile for hydrogenation via RuHCl(L)(PR₃)₂ species in which L is CO, versus the σ -donor PH₃, implies that the π -acidity of the CO ligand should be detrimental to hydrogenation activity.³² We speculated that the higher hydrogenation efficiency of **3a/b**, particularly at elevated temperatures, might be largely due to their greater stability relative to **2a/b**, and hence higher

(45) Hatjopoulos, J. D.; Register, R. A. *Macromolecules* **2005**, *38*, 10320–10322.

(46) Feast, W. J.; Gimeno, M.; Khosravi, E. *J. Mol. Catal. A* **2004**, *213*, 9–14.

(47) Barrett, A. G. M.; Hopkins, B. T.; Koebberling, J. *Chem. Rev.* **2002**, *102*, 3301–3323.

(48) Connor, E. F.; Sundberg, L. K.; Kim, H.-C.; Cornelissen, J. J.; Magbitang, T.; Rice, P. M.; Lee, V. Y.; Hawker, C. J.; Volksen, W.; Hedrick, J. L.; Miller, R. D. *Angew. Chem., Int. Ed.* **2003**, *42*, 3785–3788.

concentrations of the catalytically active species over the time scale of hydrogenation.

This hypothesis stemmed in part from the high reactivity characteristic of the related, classic H_2 complex $RuH_2(H_2)_2-(PCy_3)_2$ **9**, a function of the electron-rich character of the metal and the lability of the dihydrogen ligand(s).³⁶ In **9** and cyclohexylphosphine complexes, this reactivity is manifested in C–H bond activation even at ambient temperatures.^{36,49–51} Of interest, Leitner and co-workers have reported that $RuH_2(H_2)_2(IMes)(PCy_3)$ is more reactive than **9** in C–H activation chemistry.³⁷ While this was of value in enabling intermolecular C–H bond activation at room temperature, it may also signify a greater susceptibility to deactivation via intramolecular bond activation.

The ease of H_2-N_2 exchange can afford a preliminary indicator of such lability.^{38a} The relative robustness of the Ru– H_2 interaction in **2a** is suggested by the early comment that this complex resists exchange with 1 atm of N_2 at room temperature.³⁵ We find that exchange does occur to afford **6a**, but slowly (5–15% after 24 h; **6a** identified on the basis of the reported chemical shifts⁵² of –27.26 and 43.7 ppm for the hydride and ^{31}P nuclei, respectively; Table 1). The higher lability of the dihydrogen ligand in **2b** is suggested by observation of ca. 70% conversion to $RuHCl(N_2)(IMes)(PCy_3)$ **6b** after 24 h under N_2 . Complex **6b** is identified from its well-resolved hydride doublet at –27.63 ppm (ca. 11 ppm upfield of the averaged hydride/dihydrogen signal for **2b**), which correlates in HMBC experiments with a new $^{31}P\{^1H\}$ NMR singlet at 45.0 ppm. These chemical shifts agree well with the values for **6a** above.

In related cyclohexylphosphine complexes, loss of a stabilizing H_2 or N_2 ligand is often the entry point to extensive intramolecular bond activation, as noted above.^{36,49–51,53} Under argon at 23 °C, neither **2a/b** or **3a/b** shows evidence of bond activation in C_6D_6 after 24 h, as judged by integration of their $^{31}P\{^1H\}$ NMR signals against an internal standard. (Use of an internal standard in these experiments is important, as the potential paramagnetism of the product(s), and the consequent absence of an NMR “marker”, means that losses can otherwise easily go unnoticed.) In CH_2Cl_2 , however, **2a** undergoes partial conversion to the known⁵⁴ Ru(IV) complex $RuH_2Cl_2(PCy_3)_2$ **7**, with a ca. 1:1 ratio of **2a**:**7** after 16 h. We earlier described the low catalytic activity of coordinatively saturated **7**.⁸ Its assignment was confirmed in the present experiment by HMBC correlation of the $^{31}P\{^1H\}$ NMR singlet at 91.3 ppm with the expected hydride triplet for **7** at –12.39 (t, $^2J_{PH} = 31.6$ Hz; CD_2Cl_2). Chlorination of **2a** is consistent with earlier findings from the Toulouse group, which described the successive conversion of $RuH_2(H_2)_2(PCy_3)_2$ **9** to **2a** and **7** in Freons (mixtures of $CDCl_3$, $CDFCl_2$, and CDF_2Cl) and in neat $CDCl_3$.⁵⁴ In sharp contrast, **2b** undergoes complete decomposition to paramagnetic products in CH_2Cl_2 over 16 h, while **3a/b** is wholly unaffected.

In a more direct probe of the relative susceptibility of **2a/b** and **3a/b** to deactivation under conditions related to catalysis,

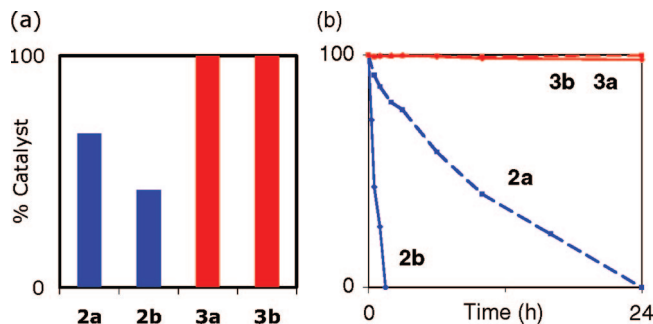


Figure 3. Thermolytic stability of **2** and **3** under 1 atm of H_2 , as indicated by $^{31}P\{^1H\}$ NMR integration against $O=PPh_3$ as internal standard: (a) after 1 h in C_6D_6 at 55 °C; (b) in refluxing CH_2Cl_2 . Dashed lines, L = PCy_3 ; solid lines, L = IMes.

we subjected all four complexes to thermolysis in benzene and methylene chloride under 1 atm of H_2 . Again, the high stability of the carbonyl complexes is notable, little to no change being evident in either solvent. The dihydrogen complexes are less robust: after just 1 h at 55 °C in benzene, the concentration of **2a** has decreased by ca. 30% (Figure 3a). Free PCy_3 is present, accompanied by minor amounts of an unidentified species at ca. δ_P 63 ppm (6%), but the balance of material is either paramagnetic or devoid of ^{31}P nuclei. For **2b**, ca. 60% decomposition occurs over this time, and no new signals are apparent.

In refluxing CH_2Cl_2 , **2a** is completely consumed after 24 h (Figure 3b), and **7** is the only ^{31}P -containing product observed (70%). The coordinative saturation of **7**, while detrimental to catalytic activity (see above), appears to confer some protection against more extensive decomposition. When formation of **7** is suppressed by repeating this reaction in the presence of NEt_3 , the only species observed by $^{31}P\{^1H\}$ NMR is an unidentified product of singlet multiplicity at 36 ppm, which integrates to ca. 40%.

Consistent with the generally greater vulnerability described above, **2b** undergoes near-total conversion to paramagnetic species within 2.5 h in refluxing CH_2Cl_2 (Figure 3b). Unexpectedly, however, a small signal for **2a** is observed within 15 min, which disappears over the next 2 h. A very small signal at 91 ppm (<5% integration) is observable after this time (see Supporting Information). Formation of **2a** from **2b** signifies that the latter undergoes some disproportionation under these conditions, as also reported by the Mol group for thermolysis of a second-generation Ru benzylidene complexes in MeOH at 80 °C.¹⁴ Immediate scavenging of any dissociated IMes by the chlorinated solvent is anticipated, based on Arduengo’s findings;⁵⁵ this, as well as competing chlorination of dissociated PCy_3 , will adversely affect ligand recapture and regeneration of catalytically active Ru complexes.

Conclusions

The foregoing describes a clean, high-yield synthetic route to $RuHCl(H_2)(IMes)(PCy_3)$ **2b** by ligand exchange reactions of $RuHCl(H_2)(PCy_3)_2$ **2a**, although attempts to develop a route to **2a** itself from $RuHCl(PPh_3)_3$ **4** were unsuccessful. Comparison of the olefin hydrogenation activity of **2a/b** with the corresponding carbonyl complexes **3a/b** demonstrates that

(49) Borowski, A. F.; Sabo-Etienne, S.; Christ, M. L.; Donnadieu, B.; Chaudret, B. *Organometallics* **1996**, *15*, 1427–1434.

(50) Christ, M. L.; Sabo-Etienne, S.; Chaudret, B. *Organometallics* **1995**, *14*, 1082–1084.

(51) Leitner, W.; Six, C. *Chem. Ber.* **1997**, *130*, 555–558.

(52) Oliván, M.; Caulton, K. G. *Inorg. Chem.* **1999**, *38*, 566–570.

(53) Amoroso, D.; Yap, G. P. A.; Fogg, D. E. *Can. J. Chem.* **2001**, *79*, 958–963.

(54) Rodríguez, V.; Sabo-Etienne, S.; Chaudret, B.; Thoburn, J.; Ulrich, S.; Limbach, H.-H.; Eckert, J.; Barthelat, J.-C.; Hussein, K.; Marsden, C. J. *Inorg. Chem.* **1998**, *37*, 3475–3485.

(55) Arduengo, A. J.; Davidson, F.; Dias, H. V. R.; Goerlich, J. R.; Khasnis, D.; Marshall, W. J.; Prakasha, T. K. *J. Am. Chem. Soc.* **1997**, *119*, 12742–12749.

replacing the H₂ ligand by CO improves hydrogenation efficiency, particularly at elevated temperatures. Independent thermolysis experiments suggest that this reflects a positive influence on catalyst lifetime associated with the low lability of the CO ligand, as complexes **3a/b** are much more stable than their dihydrogen analogues **2a/b**. The π -acidity of the carbonyl group may also play a part: while this will have detrimental effects on catalyst initiation via ligand loss, as well as oxidative addition of H₂, it offers the advantage of decreasing the susceptibility of the complex to nucleophilic attack. The significantly greater robustness of the CO complexes appears to compensate for their lower activity, by maintaining higher concentrations of active catalyst over the time scale of hydrogenation.

Experimental Section

General Procedures. Reactions were carried out at room temperature (23 °C) under argon, using standard Schlenk or glovebox techniques, unless otherwise stated. Dry, oxygen-free solvents were obtained using a Glass Contour solvent purification system and stored over Linde 4 Å molecular sieves. CDCl₃ and C₆D₆ were degassed by consecutive freeze/pump/thaw cycles and dried over activated sieves (Linde 4 Å). [RuCl₂(COD)]_n,⁵⁶ RuHCl(PPh₃)₃,⁵⁷ RuHCl(CO)(PCy₃) **3a**,³³ RuHCl(CO)(IMes)(PCy₃) **3b**,³³ IMes,⁵⁸ and substrates **S3**,⁵⁹ **S4**,⁹ and **S5**⁹ were prepared according to literature methods. H₂ (UHP grade) was obtained from BOC Gases and used as received. Styrene and allylbenzene (Aldrich) were distilled from CaH₂ under vacuum and stored at -35 °C under Ar in the dark. Tetrahydronaphthalene was distilled from Na metal, freeze-pump-thaw degassed, and stored over Linde 4 Å molecular sieves under Ar. Ethylbenzene (Aldrich) and PCy₃ (Strem) were used as received. NMR spectra were recorded on a Bruker Avance 300 or Avance-500 spectrometer at 298 K, unless otherwise specified. ¹H and ¹³C NMR spectra were referenced to the residual proton and carbon signals of the deuterated solvent. Peaks are reported in ppm, relative to TMS (¹H, ¹³C) or 85% H₃PO₄ (³¹P) at 0 ppm. IR spectra were measured on a Bomem MB100 IR spectrometer. Microanalysis was carried out by Guelph Chemical Laboratories Ltd., Guelph, Ontario.

Synthesis of RuHCl(H₂)(PCy₃)₂ (2a**).** In a modification of a literature method,³⁴ a suspension consisting of [RuCl₂(COD)]_n (400 mg, 1.43 mmol), PCy₃ (850 mg, 3.0 mmol), NEt₃ (199 μ L, 1.43 mmol), and 2-propanol (20 mL) was stirred at 200 psi H₂ and 80 °C for 40 h. The resulting orange precipitate was filtered off, washed with EtOH (3 \times 3 mL) and then cold hexanes (5 \times 4 mL), and dissolved in 15 mL of CH₂Cl₂ under H₂. A bright orange solid was obtained by filtering through Celite to remove a dark, insoluble impurity, concentrating to 0.2 mL, and adding 5 mL of cold hexanes under 1 atm of H₂. The precipitate was filtered off, washed with hexanes (3 \times 3 mL), and reprecipitated from a minimum volume of toluene by adding hexanes under H₂ and chilling at -35 °C for 1 h, and then dried under vacuum. Yield: 0.511 g (73%). ³¹P{¹H} NMR (C₆D₆, Ar): 54.2 (s). ¹H NMR (C₆D₆, Ar): 2.3–0.9 (m, 66 H, Cy), -16.3 (br s, 3H, RuH(H₂)). Under N₂, ca. 10% RuHCl(N₂)-(PCy₃)₂ is observed: δ_P 43.7 (s);⁵² δ_H -27.26 (t, 1 H, RuH, ²J_{PH} = 18.3 Hz).

Synthesis of RuHCl(H₂)(IMes)(PCy₃) (2b**).** Solid IMes (46 mg, 0.15 mmol) was added to orange RuHCl(H₂)(PCy₃)₂ **2a** (100 mg, 0.142 mmol) in 5 mL of benzene. No color change is apparent, but ³¹P{¹H} NMR monitoring indicated complete reaction at 1.5 h at 23 °C: only signals for free phosphine and **2b** (integration 1:1) were observed in an aliquot removed at this time. The solvent was stripped off, and hexanes (2 mL) added. An orange powder was obtained on cooling to -35 °C overnight. This was filtered off, washed with cold hexanes (3 \times 3 mL), and dried under vacuum. Yield: 73 mg (71%); limited by partial solubility in hexanes. ³¹P{¹H} NMR (C₆D₆, Ar): 56.3 (s, PCy₃). ¹H NMR: 6.82 (s, 4H, Mes *m*-CH), 6.16 (s, 2H, NCH=CHN), 2.37 (s, 12H, *o*-CH₃), 2.14 (s, 6H, *p*-CH₃), 1.88–1.10 (m, 33H, PCy₃), -16.44 (s, 3H, RuH(H₂)). Hydride T_{1(min)}: 36.6 ms (C₇D₈, 253 K, 300 MHz; corresponds to a H–H distance of 1.03 Å). ¹³C{¹H} NMR: 196.0 (d, ²J_{PC} = 100 Hz, NCN), 138.1 (s, Mes *p*-C), 137.1 (s, Mes C_i), 136.5 (s, Mes *o*-C), 129.1 (s, Mes *m*-CH), 121.4 (s, NC=CN), 35.3 (d, ²J_{PC} = 17 Hz, Cy), 30.6 (d, ²J_{PC} = 2 Hz, Cy), 28.0 (d, ²J_{PC} = 10 Hz, Cy), 26.9 (s, Cy), 21.1 (s, *p*-CH₃), 19.0 (s, *o*-CH₃). IR (Nujol): ν (Ru–H) 2047 cm⁻¹. Anal. Calcd for C₃₉H₆₀ClN₂PRu: C, 64.66; H, 8.35; N, 3.87. Found: C, 64.63; H, 7.98; N, 3.70. NMR spectra under N₂ (24 h) show ca. 70% RuHCl(N₂)(IMes)(PCy₃) **6b**: δ_P 45.0 (s, PCy₃); δ_H -27.63 ppm (d, RuH, ²J_{HP} = 21.4 Hz).

Attempted Synthesis of RuHCl(H₂)(PCy₃)₂ **2a from RuHCl(PPh₃)₃ **4**: Partial Formation of RuHCl(PCy₃)(PPh₃)₂ **5**.** Solid PCy₃ (31 mg, 0.11 mmol) was added to purple **4** (50 mg, 0.054 mmol) in 10 mL of C₆H₆, and H₂ was bubbled through the suspension. No color change was observed after 3 h, but integration of the ¹H NMR signals against the quartet for **4** at -17.5 ppm indicates 70% unreacted **4** in the soluble portion. Complete conversion was hampered by competing decomposition of the product over a further 20 h reaction. ³¹P{¹H} NMR for **5** (C₆D₆): 73.3 (d, ²J_{PP} = 118 Hz, 2P, PPh₃), 29.1 (t, ²J_{PP} = 118 Hz, 1P, PCy₃). Key ¹H NMR for **5** (C₆D₆): -18.1 (td, ²J_{HP} = 29 and 18 Hz). ¹H–³¹P HMBC correlations between the ³¹P{¹H} NMR doublet and the aromatic ¹H NMR signals support identification of **5** as a bis(PPh₃) complex.

Hydrogenation Reactions. (a) Representative procedure for hydrogenation of molecular substrates. Solid RuHCl(H₂)(PCy₃)₂ **2a** (14 mg, 0.0198 mmol) was added to a glass-lined Parr autoclave containing a solution of styrene (2.083 g, 0.020 mol, 1.0 M) with tetrahydronaphthalene as internal standard (1.322 g, 0.010 mol) in 20 mL of C₆H₆ in the glovebox. The autoclave was sealed, removed from the drybox, purged with H₂, and pressurized to 1000 psi H₂ at 23 °C. Samples were analyzed by GC-FID. Kinetic runs on **S1** were monitored by removing 1 mL samples at set time intervals using the sampler tube. The first 0.5 mL was discarded; from the second half, a 5 μ L aliquot was removed, diluted to 1.00 mL with CH₂Cl₂, and analyzed (GC). Reactions of other substrates were carried out at a bath temperature of 55 °C. Reactions of **S3** were analyzed by GC-FID; of **S2**, by ¹H NMR.

(b) Representative procedure for hydrogenation of polymer substrates. A solution of **S4** (183 mg, 0.722 mmol, 1.0 M in CH₂Cl₂) with 1,3,5-trimethoxybenzene (51 mg, 0.30 mmol, 0.2 M in CH₂Cl₂) as internal standard was subjected to hydrogenation as above (1000 psi H₂, 55 °C). Following reaction, volatiles were removed under reduced pressure and the residues were dissolved in CDCl₃ for ¹H NMR analysis. Conversions were determined through comparison of integrals between olefinic signals (**S4**: br m, 5.58 ppm) and the methoxy singlet of trimethoxybenzene (3.77 ppm). For **S5**, conversions were quantified by comparing the olefinic/galactopyranose CH signal at 5.60–5.30 ppm with the galactopyranose C⁵ CH multiplet at 4.59 ppm.

Thermolysis of **2 and **3**.** In a representative procedure, a solution of **2a** (8 mg, 0.011 mmol) and O=PPh₃ (4 mg, 0.014 mmol) was dissolved in CH₂Cl₂ (0.75 mL, with a 50 μ L spike of C₆D₆ as deuterium lock for shimming) in a J. Young NMR tube. An initial

(56) Genet, J. P.; Pinel, C.; Ratovelomanana-Vidal, V.; Mallart, S.; Pfister, X.; Cano De Andrade, M. C.; Laffitte, J. A. *Tetrahedron: Asymmetry* **1994**, *5*, 665–674.

(57) Schunn, R. A.; Wonchoba, E. R.; Wilkinson, G. *Inorg. Synth.* **1971**, *13*, 131–134.

(58) Arduengo, A. J.; Krafczyk, R.; Schmutzler, R.; Craig, H. A.; Goerlich, J. R.; Marshall, W. J.; Unverzagt, M. *Tetrahedron* **1999**, *55*, 14523–14534.

(59) Fürstner, A.; Langemann, K. *Synthesis* **1997**, 792–803.

$^{31}\text{P}\{^1\text{H}\}$ spectrum was measured to establish the **2a**: $\text{Ph}_3\text{P}=\text{O}$ integration ratio at t_0 . The NMR sample was then freeze–pump–thaw degassed, backfilled with 1 atm of H_2 , and heated.

Acknowledgment. This work was supported by NSERC of Canada and the Canada Foundation for Innovation. N.J.B., J.M.B., and S.D.D. thank NSERC for postgraduate scholarships.

Supporting Information Available: NMR spectra for **2b** and thermolysis experiments in CH_2Cl_2 ; numerical data for Figure 2. This material is available free of charge via the Internet at <http://pubs.acs.org>.

OM800778H

Insertion of Isocyanides, Isothiocyanates, and Carbon Monoxide into the Pd–C Bond of Cyclopalladated Complexes Containing Primary Arylalkylamines of Biological and Pharmaceutical Significance. Synthesis of Lactams and Cyclic Amidinium Salts Related to the Isoquinoline, Benzo[*g*]isoquinoline, and β -Carboline Nuclei

José Vicente,* Isabel Saura-Llamas,* and José-Antonio García-López

Grupo de Química Organometálica, Departamento de Química Inorgánica, Facultad de Química, Universidad de Murcia, Apartado 4021, E-30071 Murcia, Spain

Delia Bautista[†]

SAI, Universidad de Murcia, Apartado 4021, E-30071 Murcia, Spain

Received October 2, 2008

Cyclometalation of 3-(2-naphthyl)-D-alanine methyl ester is achieved by reacting the corresponding hydrochloride salt and Pd(OAc)₂ in a 1:1 molar ratio (acetonitrile, room temperature, 6 days). Although the chloro-bridged dimer (**A**) cannot be isolated in a pure form, addition of RNC to the reaction mixture affords the mononuclear derivatives (*R*)-[Pd{ κ^2 (*C,N*)-C₁₀H₆CH₂CH(CO₂Me)NH₂-2}Cl(CNR)] (R = ^tBu (**1a-^tBu**), Xy (C₆H₃Me₂-2,6) (**1a-Xy**)). Similar complexes (*S*)-[Pd{ κ^2 (*C,N*)-C₈H₅N(CH₂CH(CO₂Me)NH₂-2}Cl(CNR)] (R = ^tBu (**1b-^tBu**), Xy (**1b-Xy**)) are prepared from RNC and a previously reported cyclometalated derivative of L-tryptophan methyl ester, (*S,S*)-[Pd₂{ κ^2 (*C,N*)-C₈H₅N(CH₂CH(CO₂Me)NH₂-2)}₂(μ -Cl)₂] (**B**). Compound **1b-Xy** reacts with XyNC to give the iminoacyl complex (*S*)-[Pd{ κ^2 (*C,N*)-C(=NXy)C₈H₅N(CH₂CH(CO₂Me)NH₂-2}Cl(CNXy)] (**2b**), whose crystal structure has been determined by X-ray diffraction studies. The cyclopalladated dimer **B** or those containing phenethylamine (**C**) or phentermine (**D**; see Chart 1) reacts with RNC (R = ^tBu, Xy) in refluxing chloroform or toluene to render, depending on the reaction conditions, the cyclic amidines (**3c-^tBu**, **3d-Xy**) or the amidinium salts (**4b-^tBu**, **4c-^tBu**, **4c-Xy**, **4d-^tBu**, **4d-Xy**). The amidines **3a-^tBu** and **3a-Xy** and the amidinium salts **4a-^tBu** and **4a-Xy** are synthesized from complexes **1a-^tBu** and **1a-Xy**. When **D** reacts with isothiocyanates RNCS (R = Me, To (C₆H₄Me-4)), the cyclic amidinium salts **4d-Me** and **4d-To** are isolated. Amidinium triflates derived from phentermine with an aryl substituent at the exocyclic nitrogen atom (**4d-Xy**, **4d-To**) present *E/Z* isomerism in CHCl₃ or CH₂Cl₂ solution. CO reacts with **A–D** to give, after depalladation, the corresponding lactams: (*R*)-1-oxo-3-(methoxycarbonyl)-1,2,3,4-tetrahydrobenzo[*g*]isoquinoline (**5a**), (*S*)-1-oxo-3-(methoxycarbonyl)-2,3,4,9-tetrahydro-1*H*-pyrido[3,4-*b*]indole (**5b**), 1-oxo-1,2,3,4-tetrahydroisoquinoline (**5c**), and 1-oxo-3,3-dimethyl-1,2,3,4-tetrahydroisoquinoline (**5d**). The crystal structures of compounds **4b-^tBu**, **4c-^tBu**, **4d-^tBu**, **4d-Xy**, **4d-Me**, **4d-To**, and **5a–d** have been determined by X-ray diffraction studies.

Introduction

It is well-known that carbon monoxide and isocyanides insert into the Pd–C bond of aryl complexes to afford acyl^{1–5} or iminoacyl derivatives.^{4–17} These reactions have been extensively studied, as they are involved in many stoichiometric and catalytic palladium-mediated organic transformations.^{5,10,18–21} Particularly, when ortho-metalated tertiary benzylamines are used as starting materials, depalladation of the organometallic intermediates allows the synthesis of N-heterocycles.²² Nevertheless, only a few examples involving cyclopalladated primary amines have been reported,^{14,21,23–25} probably due to the scarce number of these complexes reported in the literature.^{21,26}

We report in this article (1) the regiospecific cyclopalladation of the non-natural occurring aminoacid derivative 3-(2-naph-

thyl)-D-alanine methyl ester, (2) the insertion reactions of RNC, RNCS, and CO into the Pd–C bond in this cyclopalladated complex as well as in others containing primary arylalkylamines (Chart 1) of biological or/and pharmaceutical relevance such as phenethylamine,²⁷ phentermine,²⁸ or L-tryptophan methyl ester,²⁹ which afford the corresponding lactams or cyclic amidine derivatives related to the isoquinoline, and β -carboline nuclei (Chart 2), and (3) the isomeric equilibria of the amidinium salts derived from phentermine and XyNC or ToNCS.

The 1,2,3,4-tetrahydroisoquinolin-1-one and 2,3,4,9-tetrahydro-1*H*-pyrido[3,4-*b*]indol-1-one (tetrahydro- β -carboline) rings

(1) Dupont, J.; Pfeffer, M. *J. Chem. Soc., Dalton Trans.* **1990**, 3193.

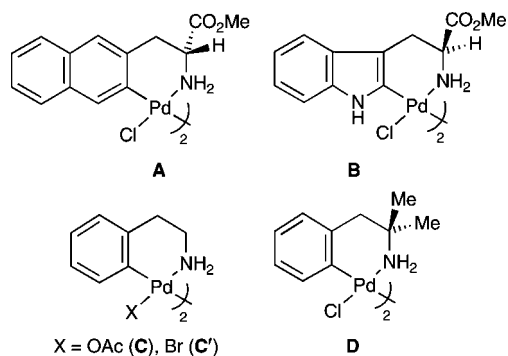
(2) Yamamoto, A.; Tanase, T.; Yanai, T.; Asano, T.; Kobayashi, K. *J. Organomet. Chem.* **1993**, 456, 287.

(3) Hoare, J. L.; Cavell, K. J.; Hecker, R.; Skelton, B. W.; White, A. H. *J. Chem. Soc., Dalton Trans.* **1996**, 2197. Vicente, J.; Abad, J. A.; Frankland, A. D.; Ramírez de Arellano, M. C. *Chem. Commun.* **1997**, 959. Kim, Y.-J.; Song, S.-W.; Lee, S.-C.; Lee, S.-W.; Osakada, K.; Yamamoto, T. *J. Chem. Soc., Dalton Trans.* **1998**, 1775.

* To whom correspondence should be addressed. E-mail: jvs1@um.es (J.V.); ims@um.es (I.S.L.). Web: <http://www.um.es/gqo/>.

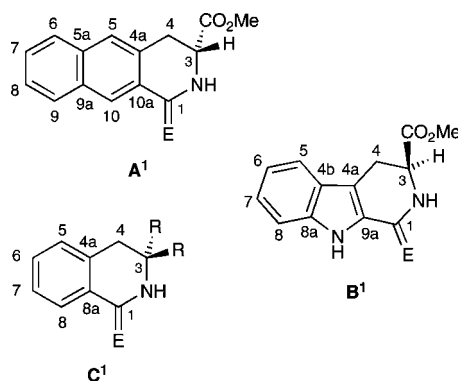
[†] To whom correspondence should be addressed regarding the X-ray diffraction studies. E-mail: dbc@um.es.

Chart 1. Cyclometalated Complexes Derived from 3-(2-Naphthyl)-D-alanine Methyl Ester (A), L-Tryptophan Methyl Ester (B), Phenethylamine (C, C'), and Phentermine (D)^a



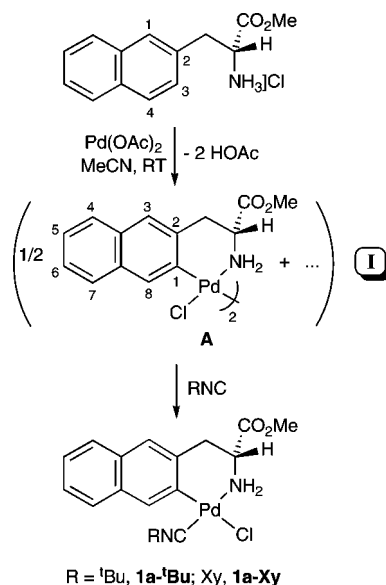
^a See ref 30 for compound numbering.

Chart 2. Lactams (E = O) and Amidines (E = NR) Containing the 3,4-Dihydrobenzo[*g*]isoquinoline (A¹), 2,3,4,9-Tetrahydro- β -carboline (B¹), and 3,4-Dihydroisoquinoline (C¹) Nuclei and Their Numbering Schemes



are structural units found in natural products.³¹ Both nuclei possess significant bioactivities (e.g., central nervous system,³² antiviral,³³ antithrombotic,³⁴ or cytotoxic activity³⁵) and have served as important intermediates for the synthesis of more complex alkaloids and further functionalized polycyclic systems of biological interest.^{36–39} The wide variety of pharmacological activity associated with cyclic amidines has also been very well documented and includes antitumoral,⁴⁰ anticoagulant,⁴¹ antiinflammatory,^{42,43} antihypertensive,⁴⁴ and hypoglycemic activities.⁴⁵

Scheme 1. Synthesis of Cyclometalated Derivatives of D-Naphthylalanine Methyl Ester



In addition, they can act as potent inhibitors of human nitric oxide synthase (NOS)^{46,47} and glycosidases.⁴⁸ Because of this, significant efforts have been made to construct both lactam^{19,49–52} and cyclic amidine skeletons^{41,43,47,53} in recent years.

Results and Discussion

Synthesis and Structure of New Cyclometalated Complexes. When 3-(2-naphthyl)-D-alanine (D-naphthylalanine) methyl ester hydrochloride reacted with Pd(OAc)₂ in a 1:1 molar ratio in acetonitrile for 6 days, the orange solid **I** (Scheme 1) was isolated from the reaction mixture, the ¹H NMR spectrum of which showed very broad signals that could not be easily assigned. Nevertheless, the aromatic region of the spectrum showed signals corresponding to the metalated and nonmetalated naphthyl rings of the starting amino acid derivative. There were also two resonances in the region corresponding to the OMe groups (one very sharp and other very strong and broad), but they overlapped and their relative ratio was difficult to evaluate. In addition, no acetate signals were present. The mixture could not be separated by fractional crystallization or by chromatography, although its reactivity showed that the cyclometalated

(4) Vicente, J.; Saura-Llamas, I.; Turpín, J.; Ramírez de Arellano, M. C.; Jones, P. G. *Organometallics* **1999**, *18*, 2683.

(5) Vicente, J.; Abad, J. A.; López-Serrano, J.; Jones, P. G.; Nájera, C.; Botella-Segura, L. *Organometallics* **2005**, *24*, 5044. Vicente, J.; Abad, J. A.; López-Sáez, M. J.; Förtsch, W.; Jones, P. G. *Organometallics* **2004**, *23*, 4414.

(6) Usón, R.; Forniés, J.; Espinet, P.; Lalinde, E. *J. Organomet. Chem.* **1983**, *254*, 371. Vicente, J.; Abad, J. A.; Förtsch, W.; Jones, P. G.; Fischer, A. K. *Organometallics* **2001**, *20*, 2704. Vicente, J.; Abad, J. A.; López-Serrano, J.; Clemente, R.; Ramírez de Arellano, M. C.; Jones, P. G.; Bautista, D. *Organometallics* **2003**, *22*, 4248. Kim, Y. J.; Chang, X. H.; Han, J. T.; Lim, M. S.; Lee, S. W. *Dalton Trans.* **2004**, 3699. Vicente, J.; Abad, J. A.; Hernández-Mata, F. S.; Rink, B.; Jones, P. G.; Ramírez de Arellano, M. C. *Organometallics* **2004**, *23*, 1292. Yamamoto, Y.; Yamazaki, H. *Synthesis* **1976**, 750.

(7) Dupont, J.; Pfeifer, M.; Daran, J. C.; Jeannin, Y. *Organometallics* **1987**, *6*, 899.

(8) Zografidis, A.; Polborn, K.; Beck, W.; Markies, B. A.; van Koten, G. Z. *Naturforsch., B: Chem. Sci.* **1994**, *49*, 1494.

(9) Kayaki, Y.; Shimizu, I.; Yamamoto, A. *Bull. Chem. Soc. Jpn.* **1997**, *70*, 917.

(10) Vicente, J.; Abad, J. A.; Shaw, K. F.; Gil-Rubio, J.; Ramírez de Arellano, M. C.; Jones, P. G. *Organometallics* **1997**, *16*, 4557.

(11) Vicente, J.; Abad, J. A.; Frankland, A. D.; López-Serrano, J.; Ramírez de Arellano, M. C.; Jones, P. G. *Organometallics* **2002**, *21*, 272.

(12) Vicente, J.; Abad, J. A.; Martínez-Viviente, E.; Jones, P. G. *Organometallics* **2002**, *21*, 4454.

(13) Vicente, J.; Chicote, M. T.; Martínez-Martínez, A. J.; Jones, P. G.; Bautista, D. *Organometallics* **2008**, *27*, 3254.

(14) Vicente, J.; Saura-Llamas, I.; Grünwald, C.; Alcaraz, C.; Jones, P. G.; Bautista, D. *Organometallics* **2002**, *21*, 3587.

(15) Böhm, A.; Polborn, K.; Sünkel, K.; Beck, W. *Z. Naturforsch., B: Chem. Sci.* **1998**, *53*, 448.

(16) Delis, J. G. P.; Aubel, P. G.; Vrieze, K.; van Leeuwen, P. W. N. M.; Veldman, N.; Spek, A.; van Neer, F. J. R. *Organometallics* **1997**, *16*, 2948.

(17) Yamamoto, Y.; Yamazaki, H. *Inorg. Chim. Acta* **1980**, *41*, 229.

(18) Heck, R. F. *Palladium Reagents in Organic Syntheses*; Academic Press: London, 1985. Tsuji, J. *Palladium Reagents and Catalysts*; Wiley: Chichester, U.K., 1995. Gehrig, K.; Klaus, A. J.; Rys, P. *Helv. Chim. Acta* **1983**, *66*, 2603. Albinati, A.; Pregosin, P. S.; Rüedi, R. *Helv. Chim. Acta* **1985**, *68*, 2046. Yamamoto, A. *Bull. Chem. Soc. Jpn.* **1995**, *68*, 433.

Yamamoto, A. *J. Chem. Soc., Dalton Trans.* **1999**, 1027. Lin, Y.-S.; Yamamoto, A. *Organometallics* **1998**, *17*, 3466. Saluste, C. G.; Whitby, R. J.; Furber, M. *Angew. Chem., Int. Ed.* **2000**, *39*, 4156. Curran, D. P.; Du, W. *Org. Lett.* **2002**, *4*, 3215. Carbayo, A.; Cuevas, J. V.; Garcia Herbosa, G. *J. Organomet. Chem.* **2002**, *658*, 15. Vicente, J.; Abad, J. A.; Martínez-Viviente, E.; Jones, P. G. *Organometallics* **2003**, *22*, 1967.

complex (R,R) -[Pd₂{κ²(*C,N*)-C₁₀H₆CH₂CH(CO₂Me)NH₂-2}₂(μ-Cl)₂] (**A**) was the main component (Scheme 1). Thus, this mixture **I** was successfully used as the starting material to synthesize other *D*-naphthylalanine methyl ester derivatives (see below).

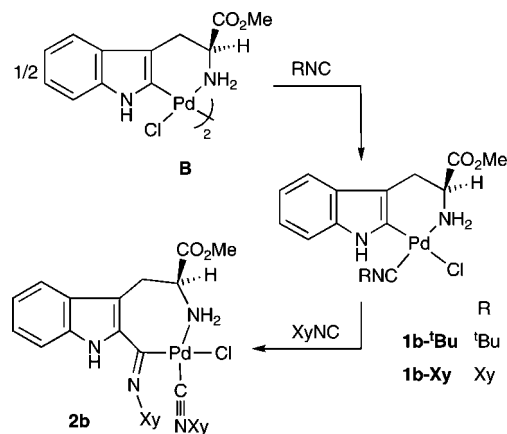
Other reaction conditions (acetonitrile at 80 °C for 4–8 h, or toluene at 60 or 75 °C for 12 h) were tested to cyclopalladate the *D*-naphthylalanine methyl ester hydrochloride. In all cases, decomposition to metallic palladium was observed and the yield of the cyclometalated material **A** in the mixture **I** did not improve (tested by ¹H NMR).

Addition of ^tBuNC or XyNC to a solution of the mixture **I** in CH₂Cl₂ allowed the isolation of the mononuclear isocyanide complex (R) -[Pd{κ²(*C,N*)-C₁₀H₆CH₂CH(CO₂Me)NH₂-2}Cl(CNR)] (R = ^tBu (**1a-^tBu**), Xy (**1a-Xy**); Scheme 1). **I** was assumed to be pure complex **A** in order to calculate the required amount of the isocyanide to prepare these complexes, which means that an excess of the ligands was used.

There are two possible sites for metalation of naphthylalanine methyl ester: the C1 and C3 atoms of the naphthyl ring (see Scheme 1 for numbering diagram). The ¹H and ¹³C NMR spectra of complexes **1a-^tBu** and **1a-Xy** showed only one set of signals; thus, one isomer was formed. This isomer agreed with C–H activation at the C3 position, as the resonance for H3 in the free ligand (7.39 ppm in DMSO-*d*₆) disappeared upon metalation. In addition, the ¹H NMR spectra of complexes **1a-^tBu** and **1a-Xy** showed two sharp singlets in the aromatic region, assigned to the H3 and H8 protons of the cyclometalated ring (**1a-^tBu**, 7.43, 7.70 ppm; **1a-Xy**, 7.47, 7.90 ppm). In the ¹³C NMR spectra of both complexes, the resonances due to C1 (**1a-^tBu**, 140.8 ppm; **1a-Xy**, 140.6 ppm) were deshielded with respect to that of the corresponding free ligand (127.4 ppm in DMSO-*d*₆), as observed in other cyclopalladated complexes.^{21,54}

We could not discard the presence of the other regioisomer (emerging from C–H activation at C1 position of the free ligand) in the mixture **I**, but none of its derivatives was detected, either in the reactions with isocyanides or in the reaction of **I** with CO (see below).

Scheme 2. Reactions of the Cyclopalladated Complexes Derived from Tryptophan Methyl Ester with Isocyanides



Direct palladation of *N,N*-dimethyl-(2-naphthyl)methylamine,⁵⁵ *N,N*-dimethyl(1-(2-naphthyl)ethyl)amine,⁵⁶ and 2-(2'-naphthyl)pyridine⁵⁷ has also been reported to occur regioselectively at the C3 position,⁵⁵ and this fact has been explained in terms of different steric constraints for the 1- and the 3-metalated transition states.⁵⁵

The cyclopalladated *L*-tryptophan methyl ester complex (S,S) -[Pd₂{κ²(*C,N*)-C₈H₅N(CCH₂CH(CO₂Me)NH₂-2)₂(μ-Cl)₂] (**B**; Chart 1)⁵⁸ also reacted in a 1:2 molar ratio with RNC to give (S) -[Pd{κ²(*C,N*)-C₈H₅N(CH₂CH(CO₂Me)NH₂-2}Cl(CNR)] (R = ^tBu (**1b-^tBu**), Xy (**1b-Xy**); Scheme 2). When XyNC was used, a small amount of the aminoacyl complex (S) -[Pd{κ²(*C,N*)-C(=NXy)C₈H₅N(CH₂CH(CO₂Me)NH₂-2}Cl(CNXy)] (**2b**) was isolated from the reaction mixture. Complex **2b** was independently prepared in excellent yield by reaction of the complex **1b-Xy** and XyNC in a 1:1 molar ratio. Under the same conditions, ^tBuNC did not insert into the Pd–C bond, which was not surprising because this reaction becomes more difficult for isocyanides having electron-donating groups.^{16,17} The behavior of **B** is in contrast with that of **A**, which does not insert XyNC even when using an excess of this isocyanide (see below).

The ¹H and ¹³C NMR spectra of complexes **1b-^tBu**, **1b-Xy**, and **2b** are in agreement with the proposed structures. In

- (19) Mori, M.; Chiba, K.; Ban, Y. *J. Org. Chem.* **1978**, *43*, 1684.
 (20) Vicente, J.; Abad, J. A.; López-Serrano, J.; Jones, P. G. *Organometallics* **2004**, *23*, 4711.
 (21) Vicente, J.; Saura-Llamas, I.; García-López, J. A.; Calmuschi-Cula, B.; Bautista, D. *Organometallics* **2007**, *26*, 2768.
 (22) Ryabov, A. D. *Synthesis* **1985**, 233. Omae, I. *Coord. Chem. Rev.* **2004**, *248*, 995. Dupont, J.; Consorti, C. S.; Spencer, J. *Chem. Rev.* **2005**, *105*, 2527. Omae, I. *J. Organomet. Chem.* **2007**, *692*, 2608.
 (23) O'Sullivan, R. D.; Parkins, A. W. *J. Chem. Soc., Chem. Commun.* **1984**, 1165.
 (24) Barr, N.; Bartley, J. P.; Clark, P. W.; Dunstan, P.; Dyke, S. F. *J. Organomet. Chem.* **1986**, *302*, 117.
 (25) Albert, J.; D'Andrea, L.; Granell, J.; Zafrilla, J.; Font-Bardia, M.; Solans, X. *J. Organomet. Chem.* **2007**, *692*, 4895.
 (26) Albert, J.; Cadena, J. M.; Granell, J. *Tetrahedron Asymmetry* **1997**, *8*, 991. Bosque, R.; López, C. *Polyhedron* **1999**, *18*, 135. Dunina, V. V.; Kuzmina, L. G.; Kazakova, M. Y.; Golunova, O. N.; Grishin, Y. K.; Kazakova, E. I. *Eur. J. Inorg. Chem.* **1999**, 1029. Gomez, M.; Granell, J.; Martínez, M. *Eur. J. Inorg. Chem.* **2000**, 217. Calmuschi, B.; Englert, U. *Acta Crystallogr., Sect. C: Cryst. Struct. Commun.* **2002**, *58*, M545. Vicente, J.; Saura-Llamas, I.; Cuadrado, J.; Ramírez de Arellano, M. C. *Organometallics* **2003**, *22*, 5513. Calmuschi, B.; Jonas, A. E.; Englert, U. *Acta Crystallogr., Sect. C: Cryst. Struct. Commun.* **2004**, *60*, M320. Albert, J.; Granell, J.; Müller, G. *J. Organomet. Chem.* **2006**, *691*, 2101. Vicente, J.; Saura-Llamas, I. *Comments Inorg. Chem.* **2007**, *28*, 39.
 (27) *The Merck Index*, 12th ed.; Merck: Rahway, NJ, 1996, p 1244.
 (28) *The Merck Index*, 12th ed.; Merck: Rahway, NJ, 1996, p 1251.
 (29) *The Merck Index*, 12th ed.; Merck: Rahway, NJ, 1996, p 1669.
 (30) Numbers assigned to the synthesized compounds include the letter of their parent complexes. Thus, compounds **1a–5a** are derivatives of cyclopalladated naphthylalanine methyl ester (**A**), compounds **1b–5b** are synthesized from complex **B**, compounds **3c–5c** are synthesized from **C**, and compounds **3d–5d** are synthesized from **D**.

- (31) Karady, S. *J. Org. Chem.* **1962**, *27*, 3720. Doskotch, R. W.; Schiff, P. L.; Beal, J. L. *Tetrahedron* **1969**, *25*, 469. Pettit, G. R.; Gaddamidi, V.; Cragg, G. M.; Herald, D. L.; Sagawa, Y. *J. Chem. Soc., Chem. Commun.* **1984**, 1693. Banwell, M. G.; Cowden, C. J.; Gable, R. W. *J. Chem. Soc., Perkin Trans. 1* **1994**, 3515. Gonzalez, D.; Martinot, T.; Hudlicky, T. *Tetrahedron Lett.* **1999**, *40*, 3077. Chang, Y.-C.; Chang, F.-R.; Khalil, A. T.; Hsieh, P.-W.; Wu, Y.-C. *Z. Naturforsch., C: J. Biosci.* **2003**, *58*, 521. Pettit, G. R.; Melody, N.; Herald, D. L.; Knight, J. C.; Chapuis, J.-C. *J. Nat. Prod.* **2007**, *70*, 417. Yamada, F.; Saida, Y.; Somei, M. *Heterocycles* **1986**, *24*, 2619. Jokela, R.; Lounasmaa, M. *Tetrahedron* **1987**, *43*, 6001. Rama-Rao, A. V.; Kishita-Reddy, K.; Yadav, J. S.; Singh, A. K. *Tetrahedron Lett.* **1988**, *29*, 3991.
 (32) Maeda, H.; Suzuki, M.; Sugano, H.; Yamamura, M.; Ishida, R. *Chem. Pharm. Bull.* **1988**, *36*, 190.
 (33) Gabrielsen, B.; Monath, T. P.; Huggins, J. W.; Kefauver, D. F.; Pettit, G. R.; Groszek, G.; Hollingshead, M.; Kirsj, J. J.; Shannon, W. M.; Schubert, E. M.; Dare, J.; Ugarkar, B.; Ussery, M. A.; Phelan, M. J. *J. Nat. Prod.* **1992**, *55*, 1569. Smith, A. B., III; Cantin, L.-D.; Pasternak, A.; Guise-Zawacki, L.; Yao, W.; Charnley, A. K.; Barbosa, J.; Sprengler, P. A.; Hirschmann, R.; Munshi, S.; Olsen, D. B.; Schleif, W. A.; Kuo, L. C. *J. Med. Chem.* **2003**, *46*, 1831.
 (34) Hutchinson, J. H.; Cook, J. J.; Brashear, K. M.; Breslin, M. J.; Glass, J. D.; Gould, R. J.; Halczenko, W.; Holahan, M. A.; Lynch, R. J.; Sitko, G. R.; Stranieri, M. T.; Hartman, G. D. *J. Med. Chem.* **1996**, *39*, 4583.
 (35) McNulty, J.; Mao, J.; Gibe, R.; Mo, R.; Wolf, S.; Pettit, G. R.; Herald, D. L.; Boyd, M. R. *Bioorg. Med. Chem. Lett.* **2001**, *11*, 169. McNulty, J.; Larichev, V.; Pandey, S. *Bioorg. Med. Chem. Lett.* **2005**, *15*, 5315.

complex **2b**, prevented rotation around the Xy–N bond of the inserted isocyanide fragment, due to steric hindrance, makes the two Me groups inequivalent, as well as the meta protons and carbons and ortho carbons of the xylyl ring, as observed in the ^1H and ^{13}C NMR spectra (^1H NMR: Me, 1.87 and 2.48 ppm; *m*-H, 6.54 and 7.16 ppm. ^{13}C NMR: Me, 18.6 and 20.1 ppm; *o*-C, 126.5 and 127.8 ppm; *m*-CH, 126.9 and 128.8 ppm).

In complex **2b**, the coordinated isocyanide is located in a position trans to the amine group. We propose the same geometry for complexes **1a-Bu**, **1a-Xy**, **1b-Bu**, and **1b-Xy** because this is the normal behavior for benzylamine palladacycles^{1,8,14,15,17} and it is in agreement with the well-established transphobia between C-donor ligands.^{11,12,20,59}

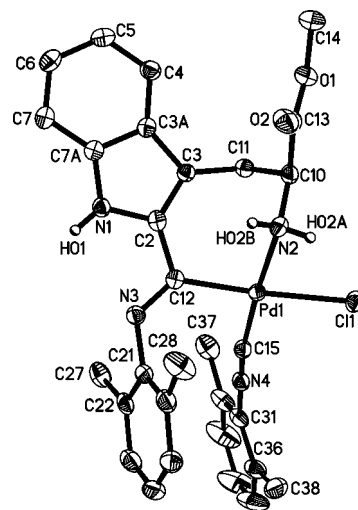


Figure 1. Thermal ellipsoid plot (50% probability) of **2b** along with the labeling scheme. Selected bond lengths (Å) and angles (deg): Pd(1)–Cl(1) = 2.4138(5), Pd(1)–N(2) = 2.1067(16), Pd(1)–C(12) = 2.0154(18), Pd(1)–C(15) = 1.9222(19), C(12)–N(3) = 1.278(2), C(15)–N(4) = 1.151(2); Cl(1)–Pd(1)–N(2) = 86.78(4), N(2)–Pd(1)–C(12) = 91.37(7), C(12)–Pd(1)–C(15) = 92.02(8), C(15)–Pd(1)–Cl(1) = 89.84(6), C(12)–N(3)–C(21) = 124.47(16), Pd(1)–C(15)–N(4) = 171.91(17), C(15)–N(4)–C(31) = 178.8(2).

The crystal structure of complex **2b** has been determined by X-ray diffraction (Figure 1) and shows the palladium atom coordinated to Cl(1), N(2), the terminal carbon atom of the isocyanide ligand (C15), and the carbon atom of the inserted isocyanide (C12) in a square-planar geometry (mean deviation from the plane Pd(1), Cl(1), N(2), C(12), C(15) 0.0324 Å). The seven-membered metallacycle adopts a boat conformation, defined by three planes: (1) C(12)–Pd(1)–N(2), (2) C(2)–C(3)–C(10)–N(2) (mean deviation 0.055 Å), and (3) C(3)–C(11)–C(10).

(36) Pachter, I. J.; Suld, G. *J. Org. Chem.* **1960**, *25*, 1680. Clark, R. D.; Jahangir, *J. Org. Chem.* **1989**, *54*, 1174. Veale, C. A.; Damewood, J. R. J.; Steelman, G. B.; Bryant, C.; Gomes, B.; Williams, J. *J. Med. Chem.* **1995**, *38*, 86. Grunewald, G. L.; Caldwell, T. M.; Li, Q.; Dahanukar, V. H.; McNeil, B.; Criscione, K. R. *J. Med. Chem.* **1999**, *42*, 4351. Grunewald, G. L.; Caldwell, T. M.; Li, Q.; Criscione, K. R. *J. Med. Chem.* **2001**, *44*, 2849. Snow, R. J.; Cardozo, M. G.; Morwick, T. M.; Busacca, C. A.; Dong, Y.; Eckner, R. J.; Jacober, S.; Jakes, S.; Kapadia, S.; Lukas, S.; Panzenbeck, M.; Peet, G. W.; Peterson, J. D.; Prokopowicz, A. S.; Sellati, R.; Tolbert, R. M.; Tschant, M. A.; Moss, N. *J. Med. Chem.* **2002**, *45*, 3394. Moreau, A.; Couture, A.; Deniau, E.; Grandclaude, P. *Eur. J. Org. Chem.* **2005**, 3437. Grunewald, G. L.; Seim, M. R.; Regier, R. C.; Criscione, K. R. *Bioorg. Med. Chem.* **2007**, *15*, 1298. Baruah, B.; Dasu, K.; Vaitilingam, B.; Mamnoor, P.; Venkata, P. P.; Rajagopal, S.; Yeleswarapu, K. R. *Bioorg. Med. Chem.* **2004**, *12*, 1991. Eguchi, S. *ARKIVOC* **2005**, *ii*, 98.

(37) Girard, Y.; Atkinson, J. G.; Bélanger, P. C.; Fuentes, J. J.; Rokach, J.; Rooney, C. S.; Remy, D. C.; Hunt, C. A. *J. Org. Chem.* **1983**, *48*, 3220.

(38) Decker, M. *Eur. J. Med. Chem.* **2005**, *40*, 305.

(39) Bracher, F.; Hildebrand, D.; Häberlein, H. *Nat. Prod. Res.* **2004**, *18*, 391.

(40) Houlihan, W. J.; Munder, P. G.; Handley, D. A.; Cheon, S. H.; Parrino, V. A. *J. Med. Chem.* **1995**, *38*, 234. Kraka, E.; Cremer, D. *J. Am. Chem. Soc.* **2000**, *122*, 8245.

(41) Glushkov, V. A.; Arapov, K. A.; Minova, O. N.; Ismailova, N. G.; Syropaytov, B. Y.; Shklyayev, Y. V. *Pharm. Chem. J.* **2006**, *40*, 363.

(42) Anikina, L. V.; Vikharev, Y. B.; Safin, V. A.; Gorbunov, A. A.; Shklyayev, Y. V.; Karmanov, V. I. *Pharm. Chem. J.* **2002**, *36*, 72.

(43) Glushkov, V. A.; Anikina, L. V.; Vikharev, Y. B.; Feshina, E. V.; Shklyayev, Y. V. *Pharm. Chem. J.* **2005**, *39*, 533.

(44) Diana, G. D.; Hinshaw, W. B.; Lape, H. E. *J. Med. Chem.* **1977**, *20*, 449.

(45) Grisar, J. M.; Claxton, G. P.; Carr, A. A.; Wiech, N. L. *J. Med. Chem.* **1973**, *16*, 679.

(46) Beaton, H.; Hamley, P.; Nicholls, D. J.; Tinkera, A. C.; Wallace, A. V. *Bioorg. Med. Chem. Lett.* **2001**, *11*, 1023.

(47) Guthikonda, R. N.; Shah, S. K.; Pacholok, S. G.; Humes, J. L.; Mumford, R. A.; Grant, S. K.; Chabin, R. M.; Green, B. G.; Tsou, N.; Ball, R.; Fletcher, D. S.; Luell, S.; MacIntyre, D. E.; MacCoss, M. *Bioorg. Med. Chem. Lett.* **2005**, *15*, 1997.

(48) Heck, M.-P.; Vincent, S. P.; Murray, B. W.; Bellamy, F.; Wong, C.-H.; Mioskowski, C. *J. Am. Chem. Soc.* **2004**, *126*, 1971.

(49) Glushkov, V. A.; Shklyayev, Y. V. *Chem. Heterocycl. Compd.* **2001**, *37*, 663. Clark, R. D.; Jahangir, *J. Org. Chem.* **1987**, *52*, 5378. Kawase, M. *J. Chem. Soc., Chem. Commun.* **1990**, 1328. Luis, S. V.; Burguete, M. I. *Tetrahedron* **1991**, *47*, 1737. Davis, F. A.; Andemichael, Y. W. *J. Org. Chem.* **1999**, *64*, 8627. Hanessian, S.; Demont, E.; van Otterlo, W. A. L. *Tetrahedron Lett.* **2000**, *41*, 4999. Dardau, V.; Snieckus, V. *J. Org. Chem.* **2001**, *66*, 1992. Bois-Choussy, M.; De Paolis, M.; Zhu, J. *Tetrahedron Lett.* **2001**, *42*, 3427. Beccalli, E. M.; Brogini, G.; Marchesinia, A.; Rossia, E. *Tetrahedron* **2002**, *58*, 6673. Haro Castellanos, J. A.; Gutiérrez Carillo, A.; Romero Martínez, A.; James Molina, G.; Ramírez Chavarrín, L.; Pérez Yescas, W. *J. Mex. Chem. Soc.* **2002**, *46*, 79. Sapi, J.; Laronze, J.-Y. *ARKIVOC* **2004**, *vii*, 208. Chern, M.-S.; Li, W.-R. *Tetrahedron Lett.* **2004**, *45*, 8323. Chern, M.-S.; Shih, Y.-K.; Dewang, P. M.; Li, W.-R. *J. Comb. Chem.* **2004**, *6*, 855. Liu, C.; Han, X.; Wang, X.; Widenhoefer, R. A. *J. Am. Chem. Soc.* **2004**, *126*, 3700. Bandini, M.; Emer, E.; Tommasi, S.; Umami-Ronchi, A. *Eur. J. Org. Chem.* **2006**, 3527. Morimoto, T.; Fujioka, M.; Fuji, K.; Tsutsumi, K.; Kakiuchi, K. *J. Organomet. Chem.* **2007**, *692*, 625. Liu, C.; Bender, C. F.; Han, X.; Widenhoefer, R. A. *Chem. Commun.* **2007**, 3607.

(50) Wang, X.-J.; Tan, J.; Grozinger, K. *Tetrahedron Lett.* **1998**, *39*, 6609.

(51) Rodríguez, D.; Martínez-Esperón, M. F.; Castedo, L.; Domínguez, D.; Súa, C. *Synlett* **2003**, 1524. Tsai, M.-R.; Hung, T.-C.; Chen, B.-F.; Cheng, C.-C.; Chang, N.-C. *Tetrahedron* **2004**, *60*, 10637.

(52) Orito, K.; Miyazawa, M.; Nakamura, T.; Horibata, A.; Ushito, H.; Nagasaki, H.; Yuguchi, M.; Yamashita, S.; Yamazaki, H.; Tokuda, M. *J. Org. Chem.* **2006**, *71*, 5951.

(53) Moriconi, E. J.; Cevasco, A. A. *J. Org. Chem.* **1968**, *33*, 2109. Christoff, J. J.; Bradley, L.; Miller, D. D.; Lei, L.; Rodriguez, F.; Fraundorfer, P.; Romstedt, K.; Shams, G.; Feller, D. R. *J. Med. Chem.* **1997**, *40*, 85. Yoshida, H.; Fukushima, H.; Ohshita, J.; Kunai, A. *Tetrahedron Lett.* **2004**, *45*, 8659. Hellal, M.; Bihel, F.; Mongeot, A.; Bourguignon, J.-J. *J. Org. Biomol. Chem.* **2006**, *4*, 3142. Chang, S.; Lee, M.; Jung, D. Y.; Yoo, E. J.; Cho, S. H.; Han, S. K. *J. Am. Chem. Soc.* **2006**, *128*, 12366.

(54) Granell, J.; Sáinz, D.; Sales, J.; Solans, X.; Font-Altaba, M. *J. Chem. Soc., Dalton Trans.* **1986**, 1785. Martínez-Viviente, E.; Pregosin, P. S.; Tschoerner, M. *Magn. Reson. Chem.* **2000**, *38*, 23.

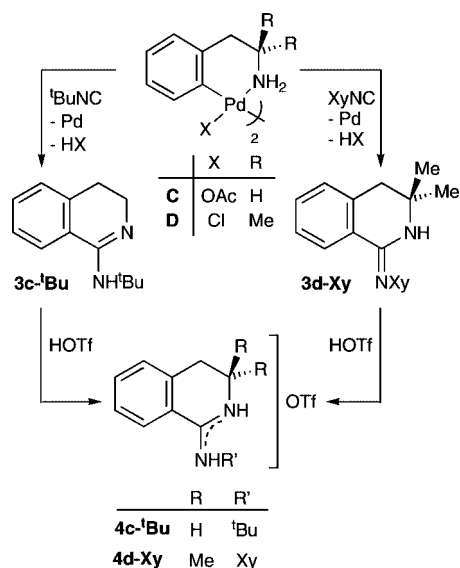
(55) Valk, J.-M.; Maassarani, F.; van der Sluis, P.; Spek, A. L.; Boersma, J.; van Koten, G. *Organometallics* **1994**, *13*, 2320.

(56) Tani, K.; Brown, L. D.; Ahmed, J.; Ibers, J. A.; Nakamura, A.; Otsuka, S.; Yokota, M. *J. Am. Chem. Soc.* **1977**, *99*, 7876.

(57) Ford, A.; Sinn, E.; Woodward, S. *J. Organomet. Chem.* **1995**, *493*, 215.

(58) Vicente, J.; Saura-Llamas, I.; Bautista, D. *Organometallics* **2005**, *24*, 6001.

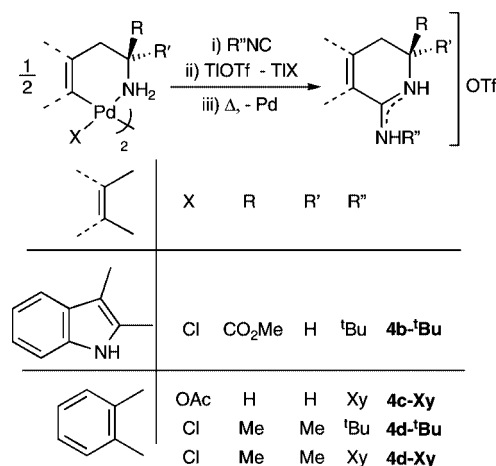
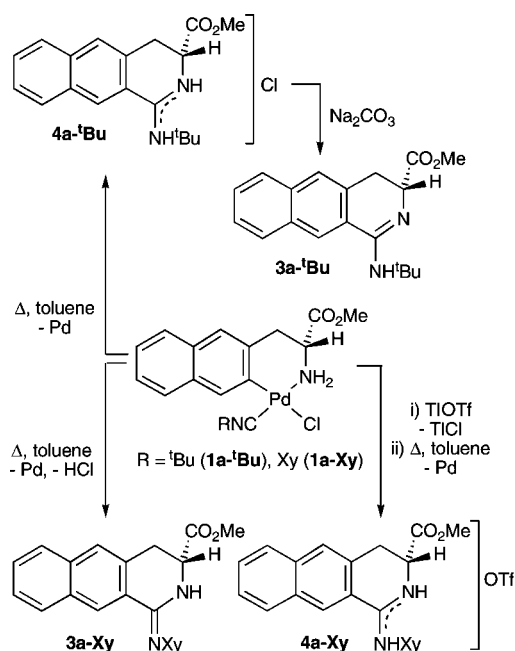
(59) Vicente, J.; Chicote, M.-T.; Rubio, C.; Ramírez de Arellano, M. C.; Jones, P. G. *Organometallics* **1999**, *18*, 2750. Vicente, J.; Abad, J. A.; Frankland, A. D.; Ramírez de Arellano, M. C. *Chem. Eur. J.* **1999**, *5*, 3066. Larraz, C.; Navarro, R.; Urriolabeitia, E. P. *New J. Chem.* **2000**, *24*, 623. Carbayo, A.; Cuevas, J. V.; García-Herbosa, G.; García-Granda, S.; Miguel, D. *Eur. J. Inorg. Chem.* **2001**, 2361. Crespo, M.; Granell, J.; Solans, X.; Font-Bardia, M. *J. Organomet. Chem.* **2003**, *681*, 143. Rodríguez, N.; Cuenca, A.; Ramírez de Arellano, C.; Medio-Simón, M.; Peine, D.; Asensio, G. *J. Org. Chem.* **2004**, *69*, 8070. Vicente, J.; Arcas, A.; Gálvez-López, M. D.; Jones, P. G. *Organometallics* **2006**, *25*, 4247. Vicente, J.; Arcas, A.; Fernández-Hernández, J. M.; Bautista, D. *Organometallics* **2001**, *20*, 2767. Vicente, J.; Abad, J. A.; Hernández-Mata, F. S.; Jones, P. G. *J. Am. Chem. Soc.* **2002**, *124*, 3848. Vicente, J.; Arcas, A.; Bautista, D.; Ramírez de Arellano, M. C. *J. Organomet. Chem.* **2002**, *663*, 164.

Scheme 3. Synthesis and Protonation of Amidines 3c-^tBu and 3d-Xy

The angle between planes 1 and 2 is 69.8°, while that between planes 2 and 3 is 50.6°. Both Xy rings are nearly parallel (dihedral angle between the two Xy rings 15.7°) and nearly perpendicular to the Pd coordination plane (angles of 72.3 and 70.1°, respectively), thus avoiding steric hindrance. Similar features have been observed in related structures.^{11,15,60} Each molecule of complex **2b** is connected to two others through hydrogen bonds (involving the NH group of the indole rings and the chlorine atoms), giving infinite chains along the *a* axis.

Synthesis of Amidines and Amidinium Salts through Insertion of Isocyanides into the Pd–C Bond of Cyclopalladated Complexes. When **C** or **D** was treated with RNC (1:2.2 or 1:2 molar ratio, respectively) in refluxing toluene, formation of Pd(0) was observed and, from the reaction mixture, the crude 3,4-dihydroisoquinoline **3c-^tBu** or **3d-Xy** was isolated as a pale yellow liquid or colorless solid, respectively (Scheme 3). These amidines were very difficult to purify by fractional crystallization, because they were very soluble in organic solvents (including *n*-pentane), or by chromatography, as they were retained even in deactivated silica gel or alumina. The few previous related studies on the reactivity of cyclopalladated primary amines toward isocyanides always reported the synthesis of the corresponding amidinium salts^{14,21,23} or complexes [PdX₂L₂], where L is the amidine.¹⁴

In order to get more easily isolable amidine derivatives, the corresponding salts were obtained by reacting **3c-^tBu** or **3d-Xy** with triflic acid in Et₂O. The cyclic amidinium triflate **4c-^tBu** or **4d-Xy** precipitated in the reaction mixture and was isolated as a colorless powder (Scheme 3). The salt **4d-Xy** was a mixture of two isomers, the nature of which will be discussed in the last part of this section. Whitby et al. have reported the palladium-catalyzed synthesis of cyclic amidines, starting from 2-bromobenzylamine or 2-bromophenethylamine, ^tBuNC, and Cs₂CO₃.⁶¹ Nevertheless, it is necessary to point out the restricted availability of the required 2-haloarenes and the limitations of the process, which seems to give only good yields for *tert*-alkyl isocyanides.

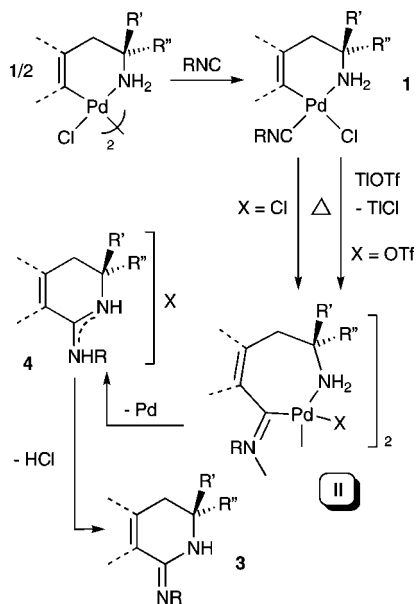
Scheme 4. Synthesis of Cyclic Amidinium Salts Containing the Isoquinoline and β-Carboline Nuclei**Scheme 5. Synthesis of Cyclic Amidines and Amidinium Salts Containing the Benzo[*g*]isoquinoline Nucleus**

Following a method we have previously used with other cyclopalladated derivatives,^{14,21} the amidinium salt **4d-Xy** was also prepared by reacting the ortho-metallated derivative **D** with XyNC and TiOTf (OTf = O₃SCF₃; Scheme 4), but surprisingly, the same method did not afford **4c-^tBu** on starting from **C'**. Instead, an unidentified product was obtained, which showed no ^tBu resonance in its ¹H NMR spectrum. This one-pot synthesis allows us to prepare with moderate to good yields (47–66%) other amidinium salts, **4b-^tBu**, **4c-Xy**, and **4d-^tBu** (Scheme 4), but no **4a** salts using the mixture **I**, because they could not be separated from other products. However, refluxing **1a-^tBu** in toluene yielded the amidinium chloride **4a-^tBu**, along with a small amount of the amidine **3a-^tBu** (Scheme 5), which can be prepared by treatment of the salt **4a-^tBu** with Na₂CO₃. In contrast, when **1a-Xy** was heated in toluene, the amidine **3a-Xy** was isolated instead of the salt **4a-Xy** that was obtained when complex **1a-Xy** was treated with thallium triflate and heated in toluene.

In agreement with the previous studies on the reactivity of cyclopalladated complexes toward isocyanides,^{1,4–6,8–17} we propose that the first step in the synthesis of amidines and their

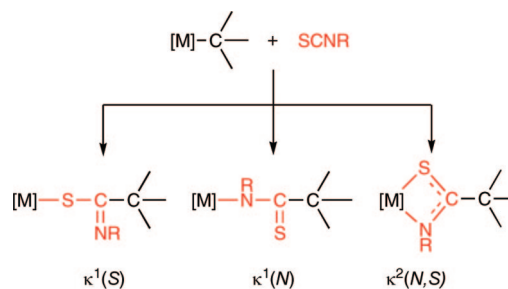
(60) Ma, J.-F.; Kojima, Y.; Yamamoto, Y. *J. Organomet. Chem.* **2000**, *616*, 149.

(61) Saluste, C. G.; Crumpler, S.; Furber, M.; Whitby, R. J. *Tetrahedron Lett.* **2004**, *45*, 6995.

Scheme 6. Proposed Reaction Pathway for the Synthesis of Amidinium Salts through Isocyanide Insertion

salts is the coordination of the isocyanide to afford complexes **1** (Schemes 5 and 6). In fact, complexes **3a-Xy** and **4a-Bu** could be prepared by starting from **1a-Xy** and **1a-Bu**, respectively. Under thermal conditions, insertion of the isocyanide into the Pd–C bond to give the iminoacyl complex **II** is proposed (Scheme 6).^{7,8,13,14} Although such an intermediate has not been isolated, we have reported the synthesis of a related complex by refluxing a solution of [Pd{ $\kappa^2(C,M)$ -C₆H₄CH₂NH₂-2}Br-(CNXy)] in toluene.¹⁴ Depalladation and C–N coupling from the iminoacyl complex **II** will give the corresponding amidinium salt (compounds **4**), which in the case of X = Cl can afford an amidine (compounds **3**) after HCl elimination. The additional use of TlOTf hinders the last step, leading always to amidinium salts. In fact, when **1a-Xy** was refluxed in toluene with or without TlOTf, the salt **4a-Xy** or, respectively, the amidine **3a-Xy** was obtained. However, in contrast to the case for **1a-Xy**, when complex **1a-Bu** was refluxed in toluene the amidinium chloride **4a-Bu** was formed, along with only a small amount of the amidine **3a-Bu** (Scheme 5), which must be attributed to **4a-Xy** having a more acidic character than **4a-Bu**.⁶²

The migration rate of the aryl group to the coordinated isocyanide increases when increasing the electrophilicity of the isocyanide and the nucleophilicity of the carbon atom bonded to palladium(II).¹⁶ Thus, aryl isocyanides react more quickly than alkyl isocyanides. In addition, insertion reactions into the Pd–C bond of the cyclometalated tryptophan derivatives (complexes **b**) should be faster than reactions on cyclometalated phenethyl derivatives, as the indole ring is strongly activated toward electrophilic reagents due to the effect of the lone pair at the nitrogen atom.⁶³ Moreover, the smaller steric requirements of the indole nucleus compared to those of the phenyl ring would also accelerate the reaction. These trends explain the following experimental observations: (1) the preparation of compound **4b-Bu** required milder conditions than for the synthesis of the other amidinium salts, (2) insertion of isocyanide at room temperature was only observed when XyNC and the cyclometalated tryptophan derivative were used, and (3) the amidinium salt derived from tryptophan methyl ester and XyNC was not obtained when the standard procedure (cationic intermediate and refluxing toluene) was used, probably because the insertion reaction is so favored that polyinserted derivatives are formed.^{2,12,64}

Chart 3. Products of the Insertion Reactions of Isothiocyanates into M–C Bonds

tophan derivative were used, and (3) the amidinium salt derived from tryptophan methyl ester and XyNC was not obtained when the standard procedure (cationic intermediate and refluxing toluene) was used, probably because the insertion reaction is so favored that polyinserted derivatives are formed.^{2,12,64}

Synthesis of Amidinium Salts through Insertion of Isothiocyanates into the Pd–C Bond of Cyclopalladated Complexes. There are only a few examples of the insertion of isothiocyanates into a σ M–C bond (M = Mg,⁶⁵ Al,⁶⁶ Zr,⁶⁷ Nb,⁶⁸ Ta,⁶⁸ Re,⁶⁹ Fe,⁷⁰ Co,⁷¹ Ni,⁷² Pd⁷³). In most cases, the heterocumulene inserts to form an N-alkyl or N-aryl thioamidato ligand which binds to the metal in a $\kappa^2(N,S)$ (Chart 3) fashion, although examples of κ^1 bonding through the sulfur or the nitrogen atom have also been reported.

Reactions of RNCS (R = Me, To) with cyclometalated primary arylalkylamines were attempted with **B–D**. The reactions were carried out in a one-pot/two-step process involving addition of TlOTf to an acetone solution (**C**, **D**) or suspension (**B**) of the cyclopalladated complex to generate a cationic derivative, which would be more reactive toward insertion reactions.⁹ After TlCl was removed, RNCS was added, the suspension was refluxed in toluene, and the crystalline black solid formed during the reaction was removed. However, only from **D** could amidinium salts **4d-Me** and **4d-To** be isolated in pure form and in moderate yields (41–67%; Scheme 7). Other reaction conditions were also unsuccessfully attempted with **C** and **D**. The isolated salts **4** would have been the products obtained from insertion of MeNC and ToNC into the C–Pd bond of **D**. To confirm that the formation of the isocyanide fragment does not arise from decomposition of the isothiocyanate prior to the insertion reaction, ToNCS was heated in toluene at 110 °C for 4 h. Unaltered ToNCS was recovered (by ¹H NMR).

(64) Onitsuka, K.; Ogawa, H.; Joh, T.; Takahashi, S.; Yamamoto, Y.; Yamazaki, H. *J. Chem. Soc., Dalton Trans.* **1991**, 1531.

(65) Srinivas, B.; Chang, C.-C.; Chen, C.-H.; Chiang, M. Y.; Chen, I.-T.; Wang, Y.; Lee, G.-H. *J. Chem. Soc., Dalton Trans.* **1997**, 957. Chang, C.-C.; Chen, J.-H.; Srinivas, B.; Chiang, M. Y.; Lee, G.-H.; Peng, S.-M. *Organometallics* **1997**, *16*, 4980.

(66) Horder, J. R.; Lappert, M. F. *J. Chem. Soc. A* **1968**, 2004.

(67) Clarke, J. F.; Fowles, G. W. A.; Rice, D. A. *J. Organomet. Chem.* **1974**, *74*, 417. Erker, G.; Mena, M.; Krüger, C.; Noe, R. *J. Organomet. Chem.* **1991**, *402*, 67.

(68) Wilkins, J. D. *J. Organomet. Chem.* **1974**, *65*, 383.

(69) Adams, R. D.; Chen, L.; Wu, W. *Organometallics* **1993**, *12*, 2404. Adams, R. D.; Chen, L.; Wu, W. *Organometallics* **1993**, *12*, 3812.

(70) Müller, H.; Seidel, W.; Görls, H. *J. Organomet. Chem.* **1994**, *472*, 215.

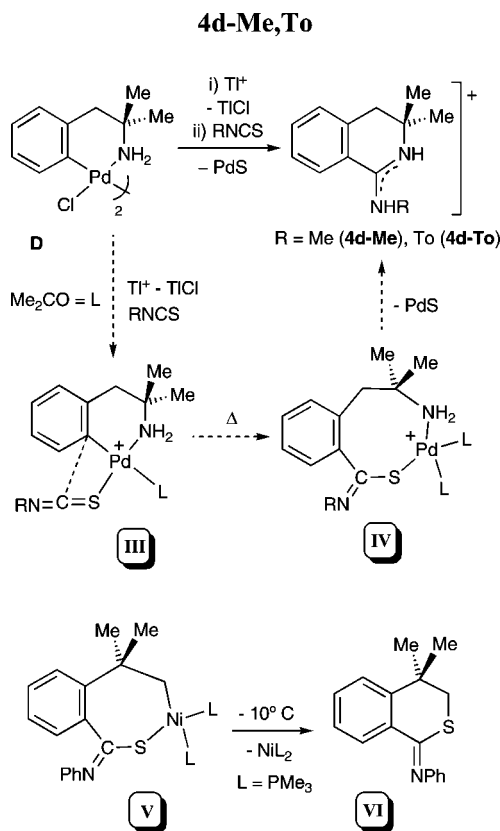
(71) Werner, H.; Strecker, B. *J. Organomet. Chem.* **1991**, *413*, 379.

(72) (a) Sato, F.; Noguchi, J.; Sato, M. *J. Organomet. Chem.* **1976**, *118*, 117. (b) Cámpora, J.; Gutiérrez, E.; Monge, A.; Palma, P.; Poveda, M. L.; Ruiz, C.; Carmona, E. *Organometallics* **1994**, *13*, 1728.

(73) Vicente, J.; Abad, J. A.; Bergs, R.; Ramírez de Arellano, M. C.; Martínez-Viviente, E.; Jones, P. G. *Organometallics* **2000**, *19*, 5597.

(62) Oszczapowicz, J.; Raczynska, E. *J. Chem. Soc., Perkin Trans. 2* **1984**, 1643. Oszczapowicz, J.; Jaroszewska-Manaj, J. *J. Chem. Soc., Perkin Trans. 2* **1991**, 1677.

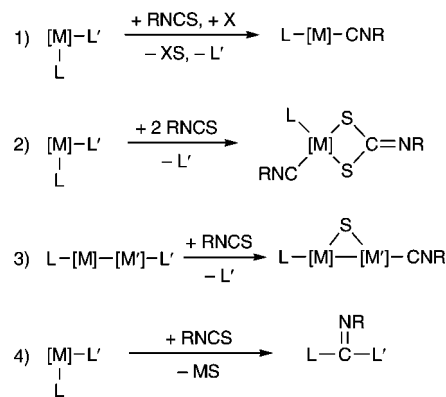
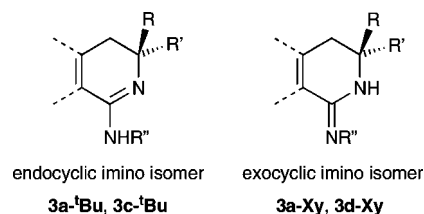
(63) Tollari, S.; Cenini, S.; Tunice, C.; Palmisano, G. *Inorg. Chim. Acta* **1998**, *272*, 18.

Scheme 7. Synthesis and Proposed Reaction Pathway for the Synthesis of Amidinium Salts 4d-Me and 4d-To

The black solid that formed contained C, H, and S (by elemental analysis), did not react with PPh_3 to afford SPPH_3 , and was only partially soluble in aqua regia. When the solid was treated with concentrated HNO_3 , a small fraction of it dissolved. This fraction was diluted with distilled water and treated with AgNO_3 to precipitate a dark gray solid. All these data move us to propose that the black solid is PdS , along with some occluded organic compounds, and is not a mixture of $\text{Pd}(0)$ and sulfur.

The proposed reaction pathway for the synthesis of **4d-Me** and **4d-To** is shown in Scheme 7. Removing the chloro ligand in **D** allows coordination of the isothiocyanate, probably via the sulfur atom (**III**).⁷⁴ Insertion of the isothiocyanate into the $\text{Pd}-\text{C}$ bond affords an unstable eight-membered palladacycle (**IV**) that may be a solvato complex, as shown in Scheme 7, or a dimer, as both the imino N and the endocyclic S atoms support lone pairs. A $\text{Ni}(\text{II})$ intermediate of this type (**V**),^{72b} isolated at -80°C , decomposes at -10°C , rendering the coupling product of the two atoms bonded to palladium (C and S). However, the loss of the metal from our intermediate **IV** does not occur in the same way and the most thermodynamically favored C–N coupling and PdS precipitation are observed.

It has been described that the reactions of metal complexes with isothiocyanates frequently involve the cleavage of the S–C bond to afford products containing the degradation fragments of RNCS .⁷⁵ These reactions normally require the presence of (1) a sulfur abstracting ligand, such as phosphine, to render the metal isocyanide and the corresponding sulfide,⁷⁶ (2) an excess

Scheme 8. Model Reactions for Activation of RNCS through Metal Complexes**Chart 4. Tautomeric Forms for Cyclic Amidines**

of isothiocyanate, to yield, through a disproportionation reaction, an isocyanide and a dithiocarbamate group,⁷⁷ and (3) a bimetallic system, to render an isocyanide ligand and a bridging sulfide group.⁷⁸ None of these routes correspond with the reaction described in this paper (Scheme 8, reaction 4), which seems to be a new path for activation of the S–C bond of isothiocyanates through coordination to metal complexes.

Structures of Amidines and Amidinium Salts. The N,N' -disubstituted amidines $\text{RN}=\text{C}(\text{R}')\text{NHR}''$ can show prototropic tautomerism (Chart 4). This equilibrium is displaced in favor of the tautomer containing the proton at the N atom with the weaker electron-withdrawing group.⁷⁹ In our case, the ^1H NMR and ^{13}C NMR spectra of crude **3a-tBu**, **3a-Xy**, **3c-tBu**, and **3d-Xy** show one set of signals and thus, for each amidine, only one tautomer is observed in solution. For the amidines **3a-tBu** and **3c-tBu** ($\text{R}' = \text{tBu}$), the proton chemical shift of the *tert*-butyl group (**3a-tBu**, 1.54 ppm; **3c-tBu**, 1.46 ppm) shows that the isomer with the endocyclic C=N bond (Chart 4) was formed. Whitby et al. have found that the proton shift of this group in a variety of amidines $\text{ArC}(\text{=N}^t\text{Bu})\text{NR}_2$ and $\text{ArC}(\text{=NR})\text{NH}^t\text{Bu}$ was 1.00–1.26 ppm in the former and 1.41–1.45 ppm in the latter,^{61,80} including **3c-tBu**.⁶¹ For the amidines **3a-Xy** and **3d-Xy** (Chart 4), the resonances corresponding to the *p*-H of the xyllyl group (**3a-Xy**, 6.93 ppm; **3d-Xy**, 6.88 ppm) and *p*-C (**3a-Xy**, 122.8 ppm; **3d-Xy**, 122.2 ppm) appear in their NMR spectra strongly shielded with respect to those of the free isocyanide.

(77) Harris, R. O.; Powell, J.; Walker, A.; Yanoff, P. V. *J. Organomet. Chem.* **1977**, *141*, 217. Ahmed, J.; Itoh, K.; Matsuda, I.; Ueda, F.; Ishii, Y.; Ibers, J. A. *Inorg. Chem.* **1977**, *16*, 620. Thewissen, D. H. M. W.; van Gaal, H. L. M. *J. Organomet. Chem.* **1979**, *172*, 69. Bertleff, W.; Werner, H. *Chem. Ber.* **1982**, *115*, 1012. Brunner, H.; Buchner, H.; Wachter, J.; Bernal, I.; Ries, W. H. *J. Organomet. Chem.* **1983**, *244*, 247. Lee, G. R.; Cooper, N. *J. Organometallics* **1989**, *8*, 1538.

(78) Lee, C.-L.; Hunt, C. T.; Balch, A. L. *Inorg. Chem.* **1981**, *20*, 2498. George, D. S. A.; Hilts, R. W.; McDonald, R.; Cowie, M. *J. Organomet. Chem.* **2000**, *300–302*, 353.

(79) Prevorsek, D. C. *J. Phys. Chem.* **1962**, *66*, 769. Raczynska, E.; Oszczapowicz, J. *Tetrahedron* **1985**, *41*, 5175.

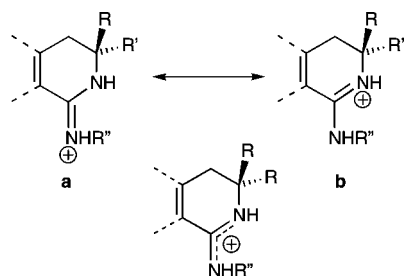
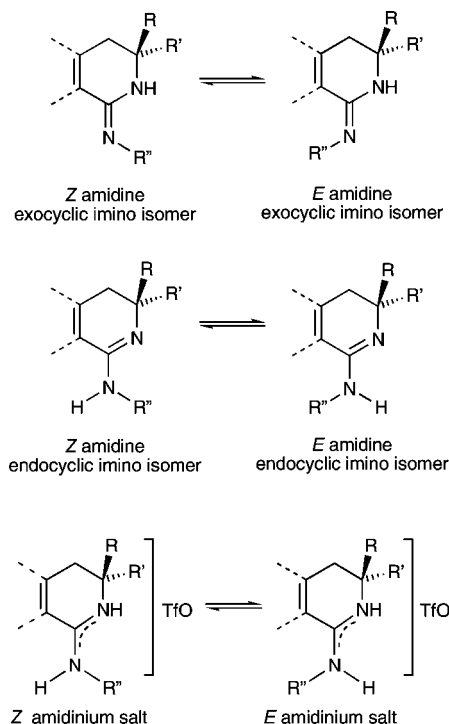
(80) Kishore, K.; Tetala, R.; Whitby, R. J.; Light, M. E.; Hursthouse, M. B. *Tetrahedron Lett.* **2004**, *45*, 6991.

(74) Owen, G. R.; Vilar, R.; White, A. J. P.; Williams, D. J. *Organometallics* **2003**, *22*, 4511.

(75) Gibson, J. A. E.; Cowie, M. *Organometallics* **1984**, *3*, 984.

(76) Werner, H.; Lotz, S.; Heiser, B. *J. Organomet. Chem.* **1981**, *209*, 197.

Chart 5. Resonance Forms for Cyclic Amidinium Salts

Chart 6. *E/Z* Isomerism for Cyclic Amidines and Amidinium Salts

This fact has been used to assign an exocyclic imino tautomeric form to similar amidines.⁸¹

In general, protonation of amidines occurs at the imino nitrogen, rather than the amino nitrogen, because the new cation is thus stabilized by resonance (Chart 5).⁸² Therefore, both tautomeric forms of *N,N'*-disubstituted amidines must lead to only one amidinium tautomer.

Because of the double or partially double character of the exocyclic C–N bond in amidines and amidinium salts, *E/Z* isomerism around this bond is possible (Chart 6). Variable-temperature ¹H NMR spectra of the compounds **4d**-*Bu*, **4d**-*Xy*, **4d**-*Me*, and **4d**-*To* were recorded (CD₂Cl₂, from –80 to 20 °C; CDCl₃, from 20 to 60 °C). The ¹H NMR spectrum of **4d**-*Xy* at –60 °C showed two sets of signals, accounting for two isomers, in the molar ratio 9:1 (determined by the NH integral ratios). Its ¹H–¹⁵N HMQC spectrum confirmed the presence of two sets of two singly protonated, anisochronous nitrogen nuclei, which were assigned to the *E* and *Z* isomers.

The ¹H NMR signals of the *Z* isomer (the major isomer) were easily distinguished by the resonance corresponding to H8 of the isoquinoline nucleus (8.54 ppm), as it showed a NOE to the exocyclic NH signal (*XyNH*). The composition of the mixture was temperature dependent. Thus, at 25 °C in CDCl₃, a 3:1 mixture (*Z*-**4d**-*Xy*:*E*-**4d**-*Xy*) was obtained, while at 60 °C in CDCl₃ the ratio between isomers was 3:2 (*Z*-**4d**-*Xy*:*E*-**4d**-*Xy*). The amidinium salt **4d**-*To* also exhibits dynamic behavior in CDCl₃ solution, although in this case, only at –60 °C is the *E/Z* equilibrium slow enough to allow observation of both isomers. At this temperature, the *Z* isomer was the major component (*Z*-**4d**-*To*:*E*-**4d**-*To* = 7:1), as proved by ¹H NMR (H8, 8.26 ppm).

Above this temperature, all the NH and the aromatic signals became broader, until they nearly disappear at 60 °C. The ¹H NMR spectra of amidinium salts **4d**-*Bu* and **4d**-*Me*, recorded at different temperatures in CD₂Cl₂ or CDCl₃, showed only one set of resonances, assigned to the *Z* isomers (in both cases, H8 of the isoquinoline nucleus showed a NOE to the exocyclic NH signal). The ¹H NMR spectra of amidinium triflates **4d** were also recorded in DMSO-*d*₆ solutions, and they showed exclusively the presence of the *Z* isomer, which proves that the equilibrium observed for **4d**-*Xy* and **4d**-*To* is also solvent dependent, as described for other amidinium salts.⁸³ For the remaining amidinium triflates **4a**-*Bu*, **4a**-*Xy*, **4b**-*Bu*, and **4c**-*Bu* and amidines **3a**-*Bu*, **3a**-*Xy*, **3c**-*Bu*, and **3d**-*Xy*, although no variable-temperature NMR studies have been carried out, the chemical shifts of the only set of signals observed in solution at room temperature correspond to a unique isomer (and not to an average situation emerging from an equilibrium, as observed for **4d**-*To*). We propose a *Z* stereochemistry based on the following facts: (1) this is the geometry showed in the solid state by all the amidinium salts synthesized whose crystal structures have been solved (**4b**-*Bu*, **4c**-*Bu*, **4d**-*Bu*, **4d**-*Xy*, **4d**-*Me*, and **4d**-*To*; see below) and by other aryl amidines similar to **3d**-*Xy*,⁸⁴ (2) this geometry minimizes steric hindrance, as the most bulky substituent at the exocyclic nitrogen and its nearest aromatic hydrogen atom are situated in *trans* positions, (3) for the amidines **3a**-*Bu*, **3a**-*Xy*, **3c**-*Bu*, and **3d**-*Xy*, DFT calculations estimate the difference in stability between the *Z* and *E* isomers (see the Supporting Information) to be around 23 kJ/mol, which is comparable to that in **4d**-*Bu*, **4d**-*Xy*, **4d**-*Me*, and **4d**-*To* (34.8–21.6 kJ/mol).

The different behavior in solution of **4d**-*Xy* and **4d**-*To* (equilibrium between *Z* and *E* isomers) and the other amidinium salts (only *Z* isomers) arises from the nature of the substituents at both nitrogen atoms: in the former the most electron-withdrawing group is bonded to the exocyclic nitrogen atom (*R*' = *To*, *Xy*) and the most electron-releasing group to the endocyclic nitrogen atom (*R* = *R*' = *Me*), which increases the contribution of resonance form **b** (Chart 5). In addition, the lower rotational energy around the exocyclic C–N bond when *R*' = *To* than when *R*' = *Xy* is due to a stronger –I effect and smaller steric demand of *To* compared to that of *Xy*.

Other authors observed *E/Z* isomerism in solution for semicyclic amidinium salts derived from 2-[(2-cyclohexylcyclopentyl)imino]hexahydroazepine⁸³ and attributed the greater amount of *E* isomers in equilibrium to the greater steric demand

(81) Jackman, L. M.; Jen, T. *J. Am. Chem. Soc.* **1975**, *97*, 2811.

(82) Borgarello, M.; Houriet, R.; Raczynska, E. D.; Drapala, T. *J. Org. Chem.* **1990**, *55*, 38. Cunningham, I. D.; Blanden, J. S.; Llor, J.; Muñoz, L.; Sharratt, A. P. *J. Chem. Soc., Perkin Trans. 2* **1991**, 1747. Raczynska, E. D.; Decouzon, M.; Gal, J.-F.; Maria, P.-C.; Taft, R. W.; Anvia, F. *J. Org. Chem.* **2000**, *65*, 4635.

(83) Hartmann, S.; Brecht, V.; Frahm, A. W. *Magn. Reson. Chem.* **1999**, *37*, 69.

(84) Sokol, V. I.; Davydov, V. V.; Shklyayev, Y. V.; Glushkov, V. A.; Sergienko, V. S. *Russ. Chem. Bull.* **1999**, *48*, 957. Sokol, V. I.; Davydov, V. V.; Merkur'eva, N. Y.; Sergienko, V. S.; Ryabov, M. A.; Shklyayev, Y. V.; Egorova, O. A. *Russ. J. Coord. Chem.* **2001**, *27*, 214.

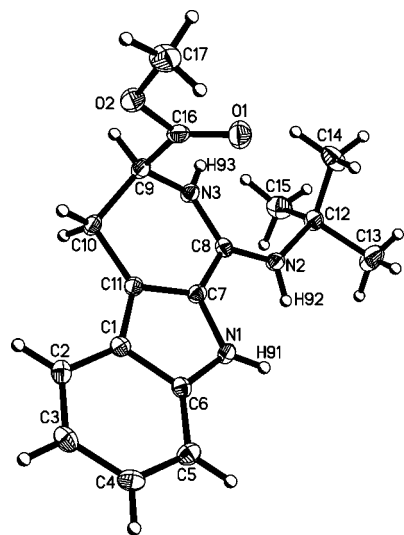


Figure 2. Thermal ellipsoid plot (50% probability) of the cation of **4b-Bu** along with the labeling scheme. Selected bond lengths (Å) and angles (deg): N2–C12 = 1.498(2), N2–C8 = 1.315(2), N3–C8 = 1.339(2), N3–C9 = 1.461(2), C7–C8 = 1.446(2); C8–N2–C12 = 129.49(16), C8–N3–C9 = 121.51(15), N3–C8–N2 = 123.40(16), N3–C8–C7 = 115.41(15), N2–C8–C7 = 121.11(16).

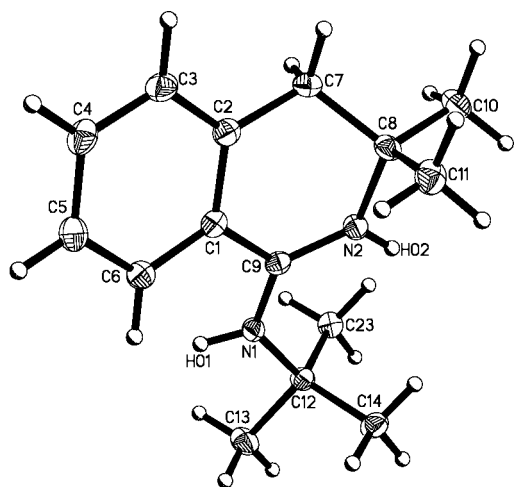


Figure 3. Thermal ellipsoid plot (50% probability) of the cation of **4d-Bu** along with the labeling scheme. Selected bond lengths (Å) and angles (deg): N1–C12 = 1.4943(18), N1–C9 = 1.3225(18), N2–C9 = 1.3249(19), N2–C8 = 1.4952(18), C1–C9 = 1.4835(19); C9–N1–C12 = 128.95(12), C9–N2–C8 = 123.58(12), N2–C9–N1 = 123.71(13), N2–C9–C1 = 117.86(13), N1–C9–C1 = 118.43(13).

of the substituent at the exocyclic nitrogen atom. This is not our case, as isomerization is not observed for the amidinium salt **4d-Bu**, with the largest substituent at the exocyclic nitrogen atom.

The crystal structures of amidinium salts **4b-Bu** (Figure 2), **4c-Bu** (see the Supporting Information), **4d-Bu** (Figure 3), **4d-Xy** (Figure 4), and **4d-Me** and **4d-To** (see the Supporting Information) have been determined by X-ray diffraction. For each salt, the lengths of the $N_{\text{exocyclic}}-C$ and $N_{\text{endocyclic}}-C$ bonds are nearly identical (around 1.32 Å; see the Supporting Information) and the C–C(–N)–N atoms are coplanar. These values indicate delocalized bonding within the amidinium groups. All the crystal structures correspond to *Z* isomers, reflecting the thermodynamic stability of this geometry. For

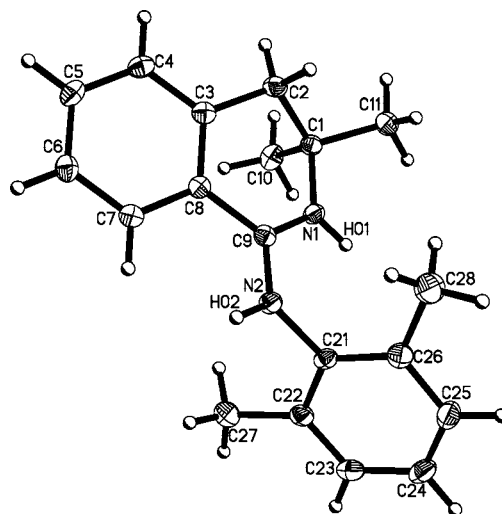


Figure 4. Thermal ellipsoid plot (50% probability) of the cation of **4d-Xy** along with the labeling scheme. Selected bond lengths (Å) and angles (deg): N2–C21 = 1.4413(17), N2–C9 = 1.3227(17), N1–C9 = 1.3182(17), N1–C1 = 1.4897(16), C8–C9 = 1.4785(18); C9–N2–C21 = 125.78(11), C9–N1–C1 = 124.63(11), N1–C9–N2 = 121.13(12), N1–C9–C8 = 119.36(12), N2–C9–C8 = 119.49(12).

compounds **4d-Xy** and **4d-To**, the angles between the Xy or To plane and the plane defined above are 75 and 129°, respectively. All these features are similar to those reported for analogous amidinium triflates.^{14,58}

In all these compounds, the cationic units are connected to the triflate groups through hydrogen bonds (**4b-Bu** and **4d-To**, for each cation, five interactions with three different triflates; **4c-Bu**, three interactions with two different triflates; **4d-Bu** and **4d-Xy**, two interactions with two different triflates; **4d-Me**, three interactions with three different triflates), generating single (**4b-Bu**, **4c-Bu**, **4d-Bu**, **4d-Xy**) or double chains (**4d-Me**, **4d-To**).

Synthesis of Lactams through Insertion of Carbon Monoxide into the Pd–C Bond of Cyclopalladated Complexes. Insertion of CO into the Pd–C bond of cyclopalladated tertiary arylalkylamines and related compounds is a well-known process that,^{22,85} depending on the reaction conditions, allows the synthesis of esters^{63,86} or N-heterocycles.^{7,15,24,87} Palladium complexes have been used to prepare lactams (1) through a catalytic oxidative addition process using bromo or iodo arylalkylamines with CO in the presence of catalytic amounts of Pd(0)¹⁹ or (2) via ortho palladation of the amine. This second way can be a catalytic or stoichiometric process, depending on the nature of the amine. Thus, *N*-alkyl- ω -arylalkylamines react with CO using Pd(OAc)₂ as catalyst and Cu(OAc)₂/O₂ as reoxidant, affording benzolactams;^{52,88} however, primary amines lead to ureas, certainly because ortho palladation of these amines, required to give lactams, does not occur when an excess of the amine is present.^{89,90} Therefore, to prepare lactams from

(85) Thompson, J. M.; Heck, R. F. *J. Org. Chem.* **1975**, *40*, 2667.

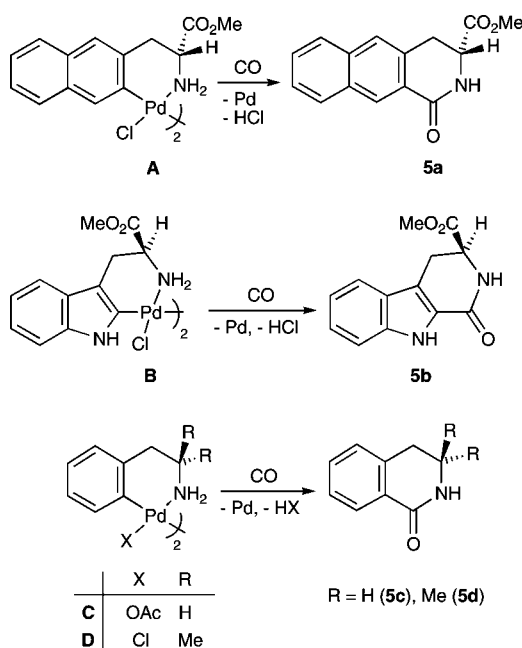
(86) Tollari, S.; Demartin, F.; Cenini, S.; Palmisano, G.; Raimondi, P. *J. Organomet. Chem.* **1997**, *527*, 93.

(87) Spencer, J.; Sharratt, D. P.; Dupont, J.; Monteiro, A. L.; Reis, V. I.; Stracke, M. P.; Rominger, F.; McDonald, I. M. *Organometallics* **2005**, *24*, 5665.

(88) Orito, K.; Horibata, A.; Nakamura, T.; Ushito, H.; Nagasaki, H.; Yaguchi, M.; Yamashita, S.; Tokuda, M. *J. Am. Chem. Soc.* **2004**, *126*, 14342.

(89) Vicente, J.; Saura-Llamas, I.; Palin, M. G.; Jones, P. G. *J. Chem. Soc., Dalton Trans.* **1995**, 2535.

Scheme 9. Synthesis of Lactams 5a–d



primary amines requires the stoichiometric carbonylation of their ortho-palladated derivatives.^{14,21,23,24} Thus, the reaction of **A–C** with CO in CHCl₃ or CH₂Cl₂ at room temperature gave palladium(0) and lactams **5a–c** (Scheme 9). The yield of **5a** (48% with respect to the used D-naphthylalanine methyl ester hydrochloride) proves that the cyclometalated complex [Pd₂{κ²(C,N)-C₁₀H₆CH₂CH(CO₂Me)NH₂-2}₂(μ-Cl)₂] (**A**) is the main component of mixture **I**.

Previous reports on the synthesis of compounds **5b–d** involve (1) the ring closure of isocyanates or isothiocyanates with polyphosphoric acid (PPA; for **5c,d**),^{37,91,92} trifluoroacetic acid (TFA; for **5b**),⁹³ a mixture of HBr and HOAc (for **5b**),⁹⁴ and AlCl₃ (for **5b**),³⁹ (2) cyclization of phenethylcarbamates with PPA (for **5c,d**)^{91,95} and a mixture of P₂O₅ and POCl₃ (for **5c**),^{38,50} and (3) Bischler–Napieralski reactions from ortho-substituted *N*-acyl-2-phenethylamines^{92,96} and subsequent reduction of the imide formed (for **5c**). None of these methods have been successfully applied to the preparation of the three lactams, and in most cases, yields are from low to moderate and several steps are involved in the synthesis. To our knowledge, no synthesis of compound **5a** has been reported, although some derivatives are known.⁵¹

¹H and ¹³C NMR spectra of compounds **5b–d** are in agreement with the reported data.^{39,92,97} For lactam **5a**, the ¹H and ¹³C NMR spectra correspond with the proposed structure. Protons H8 of the isoquinoline nucleus and H10 of the naphthylalanine fragment appear deshielded, probably due to

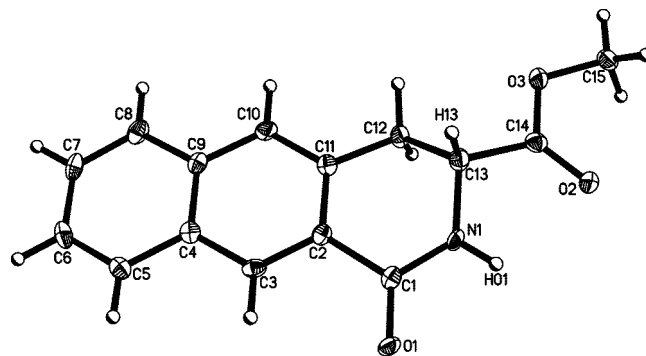


Figure 5. Thermal ellipsoid plot (50% probability) of one of the independent molecules of **5a** along with the labeling scheme. Selected bond lengths (Å) and angles (deg) are given for both independent molecules. For A: C(1)–O(1) = 1.232(3), C(1)–N(1) = 1.339(4), N(1)–C(13) = 1.461(4), C(1)–C(2) = 1.496(4); C(2)–C(1)–O(1) = 121.2(3), C(2)–C(1)–N(1) = 116.9(3), O(1)–C(1)–N(1) = 121.9(3), C(1)–N(1)–C(13) = 123.5(2). For B: C(21)–O(4) = 1.243(3), C(21)–N(2) = 1.343(4), N(2)–C(33) = 1.464(3), C(21)–C(22) = 1.488(4); C(22)–C(21)–O(4) = 121.2(3), C(22)–C(21)–N(2) = 116.8(2), O(4)–C(21)–N(2) = 122.0(3), C(21)–N(2)–C(33) = 122.6(2).

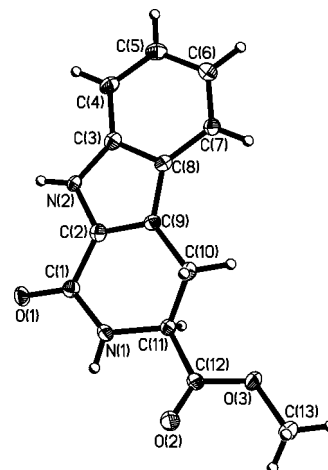


Figure 6. Thermal ellipsoid plot (50% probability) of one of the independent molecules of **5b** along with the labeling scheme. Selected bond lengths (Å) and angles (deg) are given for both independent molecules. For A: C(1)–O(1) = 1.238(3), C(1)–N(1) = 1.363(3), N(1)–C(11) = 1.458(3), C(1)–C(2) = 1.460(3); C(2)–C(1)–O(1) = 124.0(2), C(2)–C(1)–N(1) = 113.5(2), O(1)–C(1)–N(1) = 122.4(2), C(1)–N(1)–C(11) = 122.4(2). For B: C(21)–O(4) = 1.235(3), C(21)–N(3) = 1.356(3), N(3)–C(31) = 1.469(3), C(21)–C(22) = 1.464(3); C(22)–C(21)–O(4) = 123.9(2), C(22)–C(21)–N(3) = 113.2(2), O(4)–C(21)–N(3) = 122.9(2), C(21)–N(3)–C(31) = 122.5(2).

the anisotropic influence of the C=O double bond (**5a**, H10, 8.65 ppm; **5c**, H8, 8.04 ppm; **5d**, H8, 8.07 ppm).

The crystal structures of the lactams **5a–d** have been determined by X-ray diffraction studies (see Figures 5 (**5a**) and 6 (**5b**) and the Supporting Information (**5c,d**)). In all cases, the discrete molecules are associated through hydrogen bonds, giving dimers (**5d**), infinite double chains (**5a,c**), or layers (**5b**). For compounds **5a,b** there are two independent molecules in the asymmetric unit, which are also connected through hydrogen bonds.

Conclusions

Cyclometalation of 3-(2-naphthyl)-D-alanine methyl ester is achieved by reacting the corresponding hydrochloride salt and

(90) Vicente, J.; Saura-Llamas, I.; Palin, M. G.; Jones, P. G.; Ramírez de Arellano, M. C. *Organometallics* **1997**, *16*, 826. Kurzeev, S. A.; Kazankov, G. M.; Ryabov, A. D. *Inorg. Chim. Acta* **2002**, *340*, 192.

(91) Davies, R. V.; Iddon, B.; Suschitzky, H.; Gittos, M. G. *J. Chem. Soc., Perkin Trans. 1* **1978**, 180.

(92) Bailey, D. M.; De Grazia, C. G. *J. Org. Chem.* **1970**, *35*, 4088.

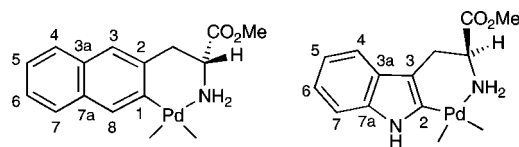
(93) Knölker, H.-J.; Braxmeier, T. *Synlett* **1997**, 925.

(94) Jeannin, L.; Sapi, J.; Vassileva, E.; Renard, P.; Laronze, J.-Y. *Synth. Commun.* **1996**, *26*, 1711.

(95) Lansbury, P. T.; Colson, J. G.; Mancuso, N. R. *J. Am. Chem. Soc.* **1964**, *86*, 5225. Gramain, J. C.; Simonet, N.; Vermeersch, G.; Febvay-Garot, N.; Caplain, S.; Lablache-Combiere, N. *Tetrahedron* **1982**, *38*, 539.

(96) Smith, J. R. L.; Norman, R. O. C.; Rose, M. E.; Curran, A. C. W. *J. Chem. Soc., Perkin Trans. 1* **1979**, 1185.

(97) Koltunov, K. Y.; Prakash, G. K. S.; Rasul, G.; Olah, G. O. *J. Org. Chem.* **2002**, *67*, 8943.

Chart 7. Numbering Schemes for Cyclometalated Fragments Containing (*R*)-Naphthylalanine Methyl Ester and (*S*)-Tryptophan Methyl Ester


$\text{Pd}(\text{OAc})_2$. Regiospecific functionalization of the resulting cyclopalladated complex as well as those derived from other primary arylalkylamines of pharmaceutical and biological relevance (phenethylamine, phentermine, *L*-tryptophan methyl ester) can be achieved through insertion reactions of RNC, RNCS, and CO into the Pd–C bond of these cyclometalated complexes. Thus, isocyanides or isothiocyanates afford the corresponding cyclic amidines or amidinium salts. The reaction with RNCS involves a new path for activation of the S–C bond of isothiocyanates through coordination to metal complexes. *E/Z* isomerism is observed in those amidinium salts supporting an electron-withdrawing group at the exocyclic nitrogen atom and an electron-releasing group at the endocyclic nitrogen atom: that is, amidinium salts derived from phentermine and XyNC or ToNCS . Reactions of the cyclometalated complexes with CO afford 1-oxo-3,4-dihydroisoquinolines and 1-oxo-2,3,4,9-tetrahydro- β -carbolines.

Experimental Section

Caution! Special precautions should be taken when handling thallium(I) compounds because of their toxicity.

General Procedures. Infrared spectra were recorded on a Perkin-Elmer 16F-PC-FT spectrometer. C, H, N, and S analyses, conductance measurements, and melting point determinations were carried out as described elsewhere.⁹⁸ Unless otherwise stated, NMR spectra were recorded in CDCl_3 on Bruker Avance 300, 400, and 600 spectrometers. Chemical shifts are referenced to TMS (^1H and $^{13}\text{C}\{^1\text{H}\}$). Signals in the ^1H and ^{13}C NMR spectra of all compounds were assigned with the help of HMQC and HMBC techniques. Mass spectra and exact masses were recorded on an AUTOSPEC 5000 VG mass spectrometer. Reactions were carried out without special precautions against moisture.

$^i\text{BuNC}$, XyNC , MeNCS (Fluka), ToNCS (Aldrich), and $\text{Pd}(\text{OAc})_2$ (Johnson Matthey) were used as received. 3-(2-Naphthyl)-*D*-alanine (Degussa) was converted to 3-(2-naphthyl)-*D*-alanine methyl ester hydrochloride by treatment with 2,2-dimethoxypropane and concentrated hydrochloric acid (see the Supporting Information), using Rachele's procedure.⁹⁹ (*S,S*)- $[\text{Pd}_2\{\kappa^2(\text{C},\text{N})-\text{C}_8\text{H}_5\text{N}(\text{CH}_2\text{CH}(\text{CO}_2\text{Me})\text{NH}_2)_2\}_2(\mu\text{-Cl})_2]$ (**B**) and $[\text{Pd}_2\{\kappa^2(\text{C},\text{N})-\text{C}_6\text{H}_4\text{CH}_2\text{CMe}_2\text{NH}_2)_2\}_2(\mu\text{-Cl})_2]$ (**D**) were prepared as previously reported.⁵⁸ $[\text{Pd}_2\{\kappa^2(\text{C},\text{N})-\text{C}_6\text{H}_4\text{CH}_2\text{CH}_2\text{NH}_2)_2\}_2(\mu\text{-OAc})_2]$ (**C**) was prepared from $\text{Pd}(\text{OAc})_2$ and phenethylamine (acetonitrile, 78 °C, 6 h) by a procedure similar to that reported for $[\text{Pd}_2\{\kappa^2(\text{C},\text{N})-\text{C}_6\text{H}_4\text{CH}_2\text{CH}_2\text{NH}_2)_2\}_2(\mu\text{-Br})_2]$ (**C'**).⁸⁹ TiOTf was prepared by reaction of Ti_2CO_3 and HO_3SCF_3 (1:2) in water, and recrystallized from acetone/ Et_2O . Charts 2 and 7 give the numbering schemes for the organic compounds and the new palladacycles, respectively.

Ortho Metalation of 3-(2-Naphthyl)-*D*-alanine Methyl Ester. 3-(2-Naphthyl)-*D*-alanine methyl ester hydrochloride (500 mg, 1.88 mmol) was added to a solution of $\text{Pd}(\text{OAc})_2$ (423 mg, 1.88 mmol) in acetonitrile (60 mL), and the resulting solution was stirred at room temperature for 6 days. A small amount of metallic palladium

was formed. The solvent was evaporated, CH_2Cl_2 (15 mL) was added, and the suspension was filtered through a plug of Celite. The filtrate was concentrated to ca. 2 mL, Et_2O (30 mL) was added, and the resulting suspension was filtered, washed with Et_2O (2×3 mL), and air-dried to give mixture **I** (537 mg) as an orange solid. The ^1H NMR of this solid in CDCl_3 showed very broad peaks, difficult to assign, but the analysis of the aromatic region indicated a mixture of the cyclometalated complex $[\text{Pd}_2\{\kappa^2(\text{C},\text{N})-\text{C}_{10}\text{H}_6\text{CH}_2\text{CH}(\text{CO}_2\text{Me})\text{NH}_2)_2\}_2(\mu\text{-Cl})_2]$ (**A**) or other noncyclometalated species such as $[\text{Pd}_2(\mu\text{-Cl})\text{Cl}\{\text{NH}_2\text{CH}(\text{CO}_2\text{Me})\text{CH}_2\text{C}_{10}\text{H}_7\}_2]$ and $[\text{Pd}_2\text{Cl}_2\{\text{NH}_2\text{CH}(\text{CO}_2\text{Me})\text{CH}_2\text{C}_{10}\text{H}_7\}_2]$. This mixture could not be separated either by fractional crystallization or by chromatography.

Mixture **I** was used as the starting material to synthesize complexes **1a**–**1Bu**, **1a**–**Xy**, and **5a**.

Synthesis of (*R*)- $[\text{Pd}\{\kappa^2(\text{C},\text{N})-\text{C}_{10}\text{H}_6\text{CH}_2\text{CH}(\text{CO}_2\text{Me})\text{NH}_2)_2\text{Cl}(\text{CN}^i\text{Bu})]$ (1a**–**1Bu**).** $^i\text{BuNC}$ (80 μL , 0.708 mmol) was added to a solution of mixture **I** (250 mg of the crude product, obtained from 233 mg (0.876 mmol) of *D*-naphthylalanine methyl ester hydrochloride) in CH_2Cl_2 (15 mL). The resulting solution was stirred for 30 min and then concentrated to ca. 1 mL, Et_2O (30 mL) was added, and the suspension was filtered to give a solid, which was washed with Et_2O (2×5 mL) and air-dried to afford complex **1a**–**1Bu** (93 mg, 0.205 mmol) as a yellow solid. The filtrate was cooled to 0 °C, the suspension was filtered, and the solid was washed with Et_2O (2×5 mL) and air-dried to afford a second crop of analytically pure **1a**–**1Bu** (95 mg, 0.210 mmol). Yield: 188 mg, 0.415 mmol, 47%. Mp: 190 °C. Anal. Calcd for $\text{C}_{19}\text{H}_{23}\text{ClN}_2\text{O}_2\text{Pd}$ (453.258): C, 50.35; H, 5.11; N, 6.18. Found: C, 49.90; H, 5.12; N, 6.35. IR (cm^{-1}): $\nu(\text{NH})$ 3105; $\nu(\text{CN})$ 2212; $\nu(\text{CO})$ 1739. ^1H NMR (400 MHz): δ 1.48 (s, 9 H, ^iBu), 3.35 (dd, 1 H, CH_2 , $^2J_{\text{HH}} = 13.8$, $^3J_{\text{HH}} = 5.3$ Hz), 3.59 (dd, 1 H, CH_2 , $^2J_{\text{HH}} = 13.8$, $^3J_{\text{HH}} = 4.4$ Hz), 3.70 (s, 3 H, OMe), 3.76 (m, 1 H, CH), 3.96 (m, 1 H, NH_2), 4.20 (m, 1 H, NH_2), 7.37 (m, 2 H, H5 + H6), 7.43 (s, 1 H, H3), 7.65 (d, 1 H, H7, $^3J_{\text{HH}} = 7.8$ Hz), 7.69–7.70 (m, 2 H, H4 + H8). $^{13}\text{C}\{^1\text{H}\}$ NMR (100.81 MHz): δ 30.0 (s, CMe_3), 45.6 (s, CH_2), 50.8 (s, CH), 53.1 (s, OMe), 58.1 (s, CMe_3), 124.7 (s, CH, C6), 125.4 (s, CH, C5), 125.7 (s, CH, C3), 126.4 (s, CH, C4), 127.2 (s, CH, C7), 130.4 (t, $\text{C}\equiv\text{N}$, $^1J_{\text{CN}} = 19.0$ Hz), 131.7 (s, C3a), 132.2 (s, C7a), 135.5 (s, C2), 136.3 (s, CH, C8), 140.8 (s, C–Pd), 171.8 (s, CO).

Synthesis of (*R*)- $[\text{Pd}\{\kappa^2(\text{C},\text{N})-\text{C}_{10}\text{H}_6\text{CH}_2\text{CH}(\text{CO}_2\text{Me})\text{NH}_2)_2\text{Cl}(\text{CNXy})]$ (1a**–**Xy**).** XyNC (54 mg, 0.411 mmol) was added to a solution of mixture **I** (150 mg of the crude product, obtained from 140 mg (0.527 mmol) of *D*-naphthylalanine methyl ester hydrochloride) in CH_2Cl_2 (20 mL). The resulting solution was stirred for 1 h, then concentrated to ca. 1 mL and Et_2O (20 mL) was added to give a suspension which was filtered, and the solid was washed with Et_2O (2×2 mL) and air-dried to afford analytically pure complex **1a**–**Xy** as a yellow solid. The filtrate was concentrated to ca. 5 mL, *n*-hexane was added and the suspension filtered off, the solid washed with *n*-hexane (2×3 mL) and air-dried to give a second crop of complex **1a**–**Xy**. Yield: 149 mg, 0.297 mmol, 56%. Mp: 158 °C dec. Anal. Calcd for $\text{C}_{23}\text{H}_{23}\text{ClN}_2\text{O}_2\text{Pd}$ (501.302): C, 55.11; H, 4.62; N, 5.59. Found: C, 54.89; H, 4.61; N, 5.86. IR (cm^{-1}): $\nu(\text{NH})$ 3167, 3093; $\nu(\text{CN})$ 2195; $\nu(\text{CO})$ 1738. ^1H NMR (400 MHz): δ 2.39 (s, 6 H, Me, Xy), 3.40 (A part of an ABMXY system, 1 H, CH_2 , $^2J_{\text{AB}} = 13.8$, $^3J_{\text{AM}} = 5.4$ Hz), 3.71 (s, 3 H, OMe), 3.65 (B part of an ABMXY system, 1 H, CH_2 , $^2J_{\text{AB}} = 13.8$, $^3J_{\text{BM}} = 4.4$ Hz), 3.81 (M part of an ABMXY system, 1 H, CH), 4.11 (X part of an ABMXY system, 1 H, NH_2 , $^2J_{\text{XY}} = 11.0$, $^3J_{\text{XM}} = 10.0$ Hz), 4.33 (Y part of an ABMXY system, 1 H, NH_2 , $^2J_{\text{XY}} = 11.0$, $^3J_{\text{YM}} = 4.9$ Hz), 7.06 (d, 2 H, *m*-H, Xy, $^3J_{\text{HH}} = 7.6$ Hz), 7.20 (t, 1 H, *p*-H, Xy, $^3J_{\text{HH}} = 7.5$ Hz), 7.35 (m, 2 H, H5 + H6), 7.47 (s, 1 H, H3), 7.61 (m, 1 H, H4), 7.69 (m, 1 H, H7), 7.90 (s, 1 H, H8). $^{13}\text{C}\{^1\text{H}\}$ NMR (100.81 MHz): δ 18.7 (s, Me, Xy), 45.7 (s, CH_2), 50.9 (s, CH), 53.1 (s, OMe), 124.8 (s, CH, C6), 125.4 (s, CH,

(98) Vicente, J.; Saura-Llamas, I.; Jones, P. G. *J. Chem. Soc., Dalton Trans.* **1993**, 3619.

(99) Rachele, J. R. *J. Org. Chem.* **1963**, *28*, 2898.

Table 1. Crystal Data and Structure Refinement Details for Complex 2b and Lactams 5a–d

	2b	5a	5b	5c	5d
formula	C ₃₀ H ₃₁ ClN ₄ O ₂ Pd	C ₁₅ H ₁₃ NO ₃	C ₁₃ H ₁₂ N ₂ O ₃	C ₉ H ₉ NO	C ₁₁ H ₁₃ NO
fw	621.44	255.26	244.25	147.17	175.22
temp (K)	100(2)	100(2)	100(2)	100(2)	100(2)
cryst syst	orthorhombic	orthorhombic	triclinic	monoclinic	monoclinic
space group	P2 ₁ 2 ₁ 2 ₁	P2 ₁ 2 ₁ 2 ₁	P1	P2 ₁ /c	C2/c
a (Å)	12.9743(10)	6.0656(3)	5.8964(4)	11.3470(11)	19.8437(12)
b (Å)	14.5650(11)	15.6690(8)	8.3010(5)	5.2078(5)	5.5447(3)
c (Å)	15.1878(12)	25.2834(14)	11.9991(8)	13.5158(12)	17.6217(11)
α (deg)	90	90	72.139(2)	90	90
β (deg)	90	90	81.825(2)	113.083(2)	103.851(2)
γ (deg)	90	90	86.683(2)	90	90
V (Å ³)	2870.0(4)	2403.0(2)	553.26(6)	734.74(12)	1882.49(19)
Z	4	8	2	4	8
ρ _{calcd} (Mg m ⁻³)	1.438	1.411	1.466	1.330	1.237
μ(Mo Kα) (mm ⁻¹)	0.773	0.099	0.106	0.088	0.079
F(000)	1272	1072	256	312	752
cryst size (mm)	0.21 × 0.20 × 0.19	0.31 × 0.12 × 0.07	0.43 × 0.17 × 0.10	0.34 × 0.12 × 0.09	0.32 × 0.20 × 0.14
θ range (deg)	1.94–28.26	2.07–28.14	1.80–26.37	1.95–27.10	2.11–28.07
no. of rflns collected	33 299	27 919	6159	5726	10 312
no. of indep rflns	6678	3268	2262	1616	2188
R _{int}	0.0239	0.0728	0.0197	0.0439	0.0221
max, min transmsn	0.867, 0.855				0.989, 0.975
no. of restraints/params	1/360	1/353	3/343	0/104	0/124
goodness of fit on F ²	1.062	1.049	1.068	1.065	1.088
R1 (I > 2σ(I))	0.0218	0.0534	0.0331	0.0636	0.0448
wR2 (all rflns)	0.0545	0.1005	0.0838	0.1787	0.1171
largest diff peak, hole (e Å ⁻³)	0.510, -0.219	0.296, -0.342	0.257, -0.279	0.784, -0.357	0.339, -0.240

Table 2. Crystal Data and Structure Refinement Details for the Amidinium Salts 4b⁻Bu, 4c⁻Bu, 4d⁻Bu, 4d-Xy, 4d-Me, and 4d-To

	4b ⁻ Bu	4c ⁻ Bu	4d ⁻ Bu	4d-Xy	4d-Me	4d-To
formula	C ₁₈ H ₂₂ F ₃ N ₃ O ₅ S	C ₁₄ H ₁₉ F ₃ N ₂ O ₅ S	C ₁₆ H ₂₃ F ₃ N ₂ O ₅ S	C ₂₀ H ₂₃ F ₃ N ₂ O ₅ S	C ₁₃ H ₁₇ F ₃ N ₂ O ₅ S	C ₁₉ H ₂₁ F ₃ N ₂ O ₅ S
fw	449.45	352.37	380.42	428.46	338.35	414.44
temp (K)	100(2)	100(2)	100(2)	100(2)	293(2)	100(2)
cryst syst	orthorhombic	monoclinic	orthorhombic	monoclinic	monoclinic	triclinic
space group	P2 ₁ 2 ₁ 2 ₁	P2 ₁ /c	Pbca	C2/c	P2 ₁ /c	P1
a (Å)	9.436(4)	9.7404(7)	11.5966(5)	15.5438(6)	10.5365(5)	9.2550(6)
b (Å)	10.310(5)	9.1752(7)	15.1252(7)	19.1839(7)	16.8639(8)	10.3129(7)
c (Å)	21.063(10)	18.1889(13)	20.7926(11)	15.5671(6)	8.6326(4)	11.2789(8)
α (deg)	90	90	90	90	90	103.744(2)
β (deg)	90	98.581(2)	90	117.576(2)	102.701(2)	109.012(2)
γ (deg)	90	90	90	90	90	91.426(2)
V (Å ³)	2049.2(16)	1607.3(2)	3647.0(3)	4114.6(3)	1496.36(12)	982.51(12)
Z	4	4	8	8	4	2
ρ _{calcd} (Mg m ⁻³)	1.457	1.456	1.386	1.383	1.502	1.401
μ(Mo Kα) (mm ⁻¹)	0.220	0.248	0.244	0.208	0.236	0.215
F(000)	936	736	1600	1792	704	432
cryst size (mm)	0.29 × 0.22 × 0.09	0.36 × 0.32 × 0.09	0.25 × 0.24 × 0.11	0.34 × 0.14 × 0.12	0.23 × 0.15 × 0.10	0.22 × 0.13 × 0.11
θ range (deg)	1.93–27.11	2.11–26.37	1.96–26.37	1.82–26.37	1.98–26.37	1.98–28.18
no. of rflns collected	12 636	17 044	37 842	22 478	16 171	11 471
no. of indep rflns	4428	3287	3728	4211	3050	4407
R _{int}	0.0412	0.0237	0.0300	0.0237	0.0269	0.0393
max, min transmsn		0.978, 0.916	0.976, 0.946	0.976, 0.933	0.974, 0.942	
no. of restraints/params	5/287	0/219	0/239	11/274	0/210	0/264
goodness of fit on F ²	1.074	1.047	1.068	1.020	1.051	1.026
R1 (I > 2σ(I))	0.0374	0.0348	0.0355	0.0345	0.0334	0.0429
wR2 (all rflns)	0.0932	0.0929	0.0886	0.0910	0.0855	0.1093
largest diff peak, hole (e Å ⁻³)	0.321, -0.338	0.524, -0.253	0.398, -0.336	0.421, -0.322	0.518, -0.314	0.406, -0.335

C5), 126.0 (s, CH, C3), 126.3 (s, CH, C4), 127.2 (s, CH, C7), 128.0 (s, *m*-CH, Xy), 129.7 (s, *p*-CH, Xy), 131.8 (s, C3a), 132.1 (s, C7a), 135.5 (s, C2), 135.9 (s, *o*-C, Xy), 137.0 (s, CH, C8), 140.6 (s, C–Pd), 171.6 (s, CO). The ¹³C NMR resonances corresponding to the *i*-C of Xy and the C≡N group (both carbon atoms bonded to N) were not observed.

Synthesis of (S)-[Pd{κ²(C,N)-C₈H₅N(CH₂CH(CO₂Me)NH₂)-2}Cl(CN⁻Bu)] (1b⁻Bu). ¹BuCN (150 μL, 1.328 mmol) was added to a suspension of the complex (C,S)-[Pd₂{κ²(C,N)-C₈H₅N(CH₂-CH(CO₂Me)NH₂)-2}₂(μ-Cl)₂]·2MeCN (B·2MeCN; 500 mg, 0.625 mmol) in CH₂Cl₂ (20 mL). The mixture was stirred for 45 min and then filtered through a plug of MgSO₄. The filtrate was concentrated to ca. 2 mL, and Et₂O (20 mL) was added to give a suspension which was filtered; the solid was washed with Et₂O (2 × 3 mL) and air-dried to give complex 1b⁻Bu as a

yellow solid. Yield: 385 mg, 0.871 mmol, 70%. Dec pt: 160 °C. Anal. Calcd for C₁₇H₂₂ClN₃O₂Pd (442.235): C, 46.17; H, 5.01; N, 9.50. Found: C, 45.67; H, 5.08; N, 9.49. IR (cm⁻¹): ν(NH) 3294, 3184, 3112; ν(CN) 2214; ν(CO) 1740. ¹H NMR (300 MHz): δ 1.47 (s, 9 H, ¹Bu), 2.77 (dd, 1 H, CH₂, ²J_{HH} = 15.6, ³J_{HH} = 11.1 Hz), 2.98 (m, 1 H, CH), 3.23–3.33 (m, 1 H of CH₂ + 1 H of NH₂), 3.61 (s, 3 H, OMe), 3.65 (br s, 1 H, NH₂), 7.03 (m, 2 H, H5 + H6), 7.31 (dd, 1 H, H7, ³J_{HH} = 8.1, ⁴J_{HH} = 1.2 Hz), 7.37 (dd, 1 H, H4, ³J_{HH} = 8.1, ⁴J_{HH} = 1.2 Hz), 8.35 (s, 1 H, NH, C₈H₅N). ¹³C{¹H} NMR (75.45 MHz): δ 28.9 (s, CH₂), 29.7 (s, CMe₃), 52.7 (s, OMe), 53.2 (s, CH), 59.0 (s, CMe₃), 108.8 (s, C3), 109.8 (s, CH, C7), 116.6 (s, CH, C4), 119.0 (s, CH, C5), 120.3 (s, CH, C6), 126.8 (s, C3a), 127.2 (t, C≡N, ¹J_{CN} = 20.0 Hz), 134.3 (s, C–Pd), 137.1 (s, C7a), 172.0 (s, CO).

Synthesis of (S)-[Pd{ κ^2 (C,N)-C₈H₅N(CH₂CH(CO₂Me)NH₂)-2}Cl(CNXY)] (1b-Xy). XyNC (82 mg, 0.625 mmol) was added to a suspension of the complex (S,S)-[Pd₂{ κ^2 (C,N)-C₈H₅N(CH₂-CH(CO₂Me)NH₂)-2}₂(μ -Cl)] · 2MeCN (**B** · 2MeCN; 250 mg, 0.312 mmol) in CH₂Cl₂ (25 mL). The mixture was stirred for 15 min and then filtered through a plug of MgSO₄. The filtrate was concentrated to ca. 2 mL, Et₂O (25 mL) was added, the suspension was filtered, and the solid was washed with Et₂O (2 × 3 mL) and air-dried to give the yellow complex **1b-Xy**. Yield: 179 mg, 0.365 mmol, 58%. Dec pt: 176 °C. Λ_M (Ω^{-1} cm² mol⁻¹): 0 (8.8 × 10⁻⁴ M). Anal. Calcd for C₂₁H₂₂ClN₃O₂Pd (490.279): C, 51.45; H, 4.52; N, 8.57. Found: C, 51.47; H, 4.55; N, 8.45. IR (cm⁻¹): ν (NH) 3284, 3230; ν (CN) 2196; ν (CO) 1744, 1735. ¹H NMR (400 MHz): δ 2.30 (s, 6 H, Me, Xy), 2.99 (dd, 1 H, CH₂, ²J_{HH} = 15.0, ³J_{HH} = 10.4 Hz), 3.24–3.34 (m, 2 H, CH + 1 H of CH₂), 3.65 (s, 3 H, OMe), 3.73 (br d, 1 H, NH₂, ³J_{HH} = 10.7 Hz), 3.94 (“t”, 1 H, NH₂, ²J_{HH} = ³J_{HH} = 10.9 Hz), 6.82 (td, 1 H, H5, ³J_{HH} = 7.8, ⁴J_{HH} = 0.9 Hz), 6.91 (td, 1 H, H6, ³J_{HH} = 7.1, ³J_{HH} = 1.0 Hz), 7.01 (d, 2 H, *m*-H, Xy, ³J_{HH} = 7.6 Hz), 7.17–7.22 (m, 3 H, H4 + H7 + *p*-H of Xy), 8.36 (s, 1 H, NH, C₈H₅N). ¹³C{¹H} NMR (100.81 MHz): δ 18.7 (s, Me, Xy), 28.6 (s, CH₂), 52.7 (s, OMe), 53.5 (s, CH), 108.9 (s, C3), 109.5 (s, CH, C7), 116.4 (s, CH, C4), 118.9 (s, CH, C5), 120.3 (s, CH, C6), 125.7 (s, *i*-C, Xy), 126.7 (s, C3a), 128.1 (s, *m*-CH, Xy), 129.9 (s, *p*-CH, Xy), 134.3 (s, C–Pd), 135.9 (s, *o*-C, Xy), 137.4 (s, C7a), 140.6 (br s, C≡N), 171.9 (s, CO).

Synthesis of (S)-[Pd{ κ^2 (C,N)-C(=NXy)C₈H₅N(CH₂CHCO₂-Me)NH₂}-2}Cl(CNXY)] (2b). XyNC (42 mg, 0.318 mmol) was added to a suspension of the complex **1b-Xy** (150 mg, 0.306 mmol) in CHCl₃ (30 mL). The mixture was stirred for 18 h and then filtered through a plug of MgSO₄; the filtrate was concentrated to ca. 2 mL, *n*-pentane (25 mL) was added, the suspension was filtered, and the solid was washed with *n*-pentane (2 × 3 mL) and air-dried to give the yellow complex **2b**. Yield: 126.6 mg, 0.204 mmol, 67%. Mp: 213 °C dec. Anal. Calcd for C₃₀H₃₁ClN₄O₂Pd (621.457): C, 57.98; H, 5.03; N, 9.02. Found: C, 57.94; H, 5.16; N, 9.00. IR (cm⁻¹): ν (NH) 3328, 3314, 3272; ν (C≡N) 2199; ν (CO) 1730; ν (C=N) 1577. ¹H NMR (400 MHz): δ 1.87 (s, 3 H, Me, inserted Xy), 2.09 (s, 6 H, Me, coordinated Xy), 2.48 (s, 3 H, Me, inserted Xy), 3.26 (“t”, 1 H, NH₂, ²J_{HH} = ³J_{HH} = 10.6 Hz), 3.52 (m, 1 H, NH₂), 3.70 (s, 3 H, OMe), 3.97 (br d, 1 H, CH₂, ²J_{HH} = 15.0 Hz), 4.47 (m, 1 H, CH), 4.98 (dd, 1 H, CH₂, ²J_{HH} = 15.0, ³J_{HH} = 6.4 Hz), 6.54 (d, 1 H, *m*-H, inserted Xy, ³J_{HH} = 7.4 Hz), 6.82 (t, 1 H, *p*-H, inserted Xy, ³J_{HH} = 7.5 Hz), 7.01 (d, 2 H, *m*-H, coordinated Xy, ³J_{HH} = 7.6 Hz), 7.12 (ddd, 1 H, H5, ³J_{HH} = 8.0, ³J_{HH} = 7.0, ⁴J_{HH} = 0.9 Hz), 7.16 (d, 1 H, *m*-H, inserted Xy, ³J_{HH} = 7.6 Hz), 7.17 (t, 1 H, *p*-H, coordinated Xy, ³J_{HH} = 7.6 Hz), 7.28 (ddd, 1 H, H6, ³J_{HH} = 8.0, ³J_{HH} = 7.0, ⁴J_{HH} = 1.0 Hz), 7.37 (d, 1 H, H7, ³J_{HH} = 8.1 Hz), 7.56 (d, 1 H, H4, ³J_{HH} = 8.1 Hz), 9.25 (s, 1 H, NH, C₈H₅N). ¹³C{¹H} NMR (100.81 MHz): δ 18.6 (s, Me, coordinated + inserted Xy), 20.1 (s, Me, inserted Xy), 30.0 (s, CH₂), 53.0 (s, OMe), 53.6 (s, CH), 111.5 (s, CH, C7), 118.9 (s, CH, C4), 120.0 (s, CH, C5), 123.4 (s, *p*-CH, inserted Xy), 124.9 (s, CH, C6), 125.8 (s, *i*-C, coordinated Xy), 126.5 (s, *o*-C, inserted Xy), 126.9 (s, *m*-CH, inserted Xy), 127.7 (s, *m*-CH, coordinated Xy), 127.8 (s, *o*-C, inserted Xy), 128.8 (s, *m*-CH, inserted Xy), 128.0 (s, C3a), 129.5 (s, *p*-CH, coordinated Xy), 133.1 (s, C2), 135.2 (s, *o*-C, coordinated Xy), 135.5 (s, C7a), 139.0 (br s, C≡N), 151.9 (s, *i*-C, inserted Xy), 164.0 (s, C–Pd), 172.4 (s, CO). The ¹³C NMR resonance corresponding to C3 was not observed.

Single crystals of **2b**, suitable for an X-ray diffraction study, were obtained by slow diffusion of *n*-hexane into a solution of **2b** in CHCl₃.

Synthesis of (R)-1-(tert-Butylamino)-3-(methoxycarbonyl)-3,4-dihydrobenzo[g]isoquinoline (3a^tBu) and (Z)-(R)-1-(tert-Butylamino)-3-(methoxycarbonyl)-3,4-dihydrobenzo[g]isoquinolinium Chloride (4a^tBu). Complex **1a^tBu** (140 mg, 0.309 mmol) was dissolved in toluene (15 mL), and the solution was refluxed for

7 h. Decomposition to metallic palladium was observed. Toluene was evaporated, CH₂Cl₂ (30 mL) was added, and the resulting suspension was filtered through a plug of Celite. The filtrate was concentrated to ca. 2 mL, Et₂O (25 mL) was added, the suspension was filtered, and the solid was washed with Et₂O (2 × 5 mL) and air-dried to give the pale yellow amidinium salt **4a^tBu** (72 mg, 0.207 mmol, 67%). ¹H NMR (400 MHz): δ 1.80 (s, 9 H, ^tBu), 3.39 (m, 2 H, CH₂), 3.65 (s, 3 H, OMe), 5.21 (br s, 1 H, CH), 7.56 (t, 1 H, H8, ³J_{HH} = 7.7 Hz), 7.65 (t, 1 H, H7, ³J_{HH} = 7.9 Hz), 7.70 (s, 1 H, H5), 7.81 (d, 1 H, H6, ³J_{HH} = 8.2 Hz), 8.08 (d, 1 H, H9, ³J_{HH} = 8.2 Hz), 8.33 (br s, 1 H, CHNH), 8.78 (s, 1 H, H10), 10.02 (br s, 1 H, ^tBuNH).

A small amount of the crude amidine **3a^tBu** was isolated after the Et₂O filtrate was concentrated to dryness and the residue was dried under vacuum.

Solid **4a^tBu** (72 mg, 0.207 mmol) was suspended in acetone (15 mL), Na₂CO₃ (150 mg, 1.41 mmol) was added, and the mixture was stirred for 12 h. The suspension was filtered through a plug of MgSO₄ and the solvent evaporated. Et₂O (25 mL) was added, and the suspension was filtered to remove solid impurities. The filtrate was concentrated to dryness to give compound **3a^tBu** as a pale yellow solid. Yield: 34 mg, 0.109 mmol, 53%. Mp: 152 °C. IR (cm⁻¹): ν (NH) 3429; ν (CO) 1735; ν (CN) 1615, 1526. ¹H NMR (300 MHz): δ 1.54 (s, 9 H, ^tBu), 3.04–3.17 (m, 2 H, CH₂), 3.70 (s, 3 H, OMe), 4.35 (m, 1 H, CH), 4.64 (br s, 1 H, CHNH), 7.41–7.52 (m, 2 H, H7 + H8), 7.61 (s, 1 H, H5), 7.76 (m, 1 H, H6), 7.82 (s, 1 H, H10), 7.84 (m, 1 H, H9). ¹³C{¹H} NMR (75.45 MHz): δ 29.0 (s, CMe₃), 30.9 (s, CH₂), 51.4 (s, CMe₃), 51.9 (s, OMe), 58.2 (s, CH), 121.9 (s, CH, C10), 125.6 (s, C10a), 125.8 (s, CH, C8), 126.0 (s, CH, C5), 127.1 (s, CH, C6), 127.2 (s, CH, C7), 128.5 (s, CH, C9), 132.2 (s, C9a), 133.3 (s, C4a + C5a), 154.3 (s, C1), 174.6 (s, CO). FAB⁺-MS: *m/z* 311.0 [(M + 1)⁺]. EI-HRMS: exact mass calcd for C₁₉H₂₂N₂O₂ 310.1681; found 310.1670; Δ = 0.0011.

Synthesis of (R)-1-((2,6-Dimethylphenyl)amino)-3-(methoxycarbonyl)-3,4-dihydrobenzo[g]isoquinoline (3a-Xy). Complex **1a-Xy** (100 mg, 0.199 mmol) was dissolved in toluene (15 mL), and the solution was refluxed for 7 h. Decomposition to metallic palladium was observed. Toluene was evaporated, CH₂Cl₂ (30 mL) was added, and the resulting suspension was filtered through a plug of Celite. The filtrate was concentrated to ca. 1 mL, *n*-pentane (15 mL) was added, and the suspension was filtered. The solid was washed with *n*-pentane (2 × 5 mL) and air-dried to give crude **3a-Xy**. Yield: 40 mg, 0.112 mmol, 56%. Crude **3a-Xy** was dissolved in CH₂Cl₂ (1 mL) and subjected to silica gel preparative TLC. Elution with CH₂Cl₂ gave a yellow band (*R_f* = 0.7), which was collected and extracted with methanol; the solution was filtered through a plug of Celite, and the filtrate was concentrated to dryness to give spectroscopically pure compound **3a-Xy** as a yellow solid (11 mg, 0.031 mmol; purification yield: 28%). Mp: 75 °C. IR (cm⁻¹): ν (NH) 3381; ν (CO) 1743; ν (CN) 1645, 1626. ¹H NMR (400 MHz): δ 2.17 (s, 3 H, Me, Xy), 2.25 (s, 3 H, Me, Xy), 3.36, 3.50 (AB part of an ABMX system, 2 H, CH₂, ²J_{AB} = 15.1, ³J_{AM} = 6.8, ³J_{BM} = 4.8 Hz), 3.64 (s, 3 H, OMe), 4.21 (m, M part of an ABMX system, 1 H, CH), 5.16 (br s, 1 H, NH), 6.93 (t, 1 H, *p*-H, Xy, ³J_{HH} = 7.5 Hz), 7.08 (d, 1 H, *m*-H, Xy, ³J_{HH} = 7.5 Hz), 7.11 (d, 1 H, *m*-H, Xy, ³J_{HH} = 7.5 Hz), 7.46–7.54 (m, 2 H, H7 + H8), 7.67 (s, 1 H, H5), 7.80 (d, 1 H, H6, ³J_{HH} = 8.1 Hz), 7.97 (d, 1 H, H9, ³J_{HH} = 7.9 Hz), 8.98 (s, 1 H, H10). ¹³C{¹H} NMR (100.81 MHz): δ 17.8 (s, Me, Xy), 17.9 (s, Me, Xy), 32.5 (s, CH₂), 52.9 (s, CH), 52.5 (s, OMe), 122.8 (s, *p*-CH, Xy), 126.0 (s, CH, C8), 126.1 (s, CH, C5), 127.0 (s, CH, C6), 127.3 (s, C10a), 127.4 (s, CH, C7 + C10), 128.1 (s, *m*-CH, Xy), 128.3 (s, *m*-CH, Xy), 128.9 (s, *o*-C, Xy), 129.2 (s, CH, H9), 129.3 (s, *o*-C, Xy), 131.0 (s, C4a), 132.5 (s, C9a), 134.3 (s, C5a), 145.9 (s, *i*-C, Xy), 148.6 (s, C1), 171.9 (s, CO). FAB⁺-MS: *m/z* 359.2 [(M + 1)⁺]. EI-HRMS: exact mass calcd for C₂₃H₂₂N₂O₃ 358.1681; found 358.1705; Δ = 0.0024.

Synthesis of 1-(*tert*-Butylamino)-3,4-dihydroisoquinoline (3c-Bu) and (Z)-1-(*tert*-Butylamino)-3,4-dihydroisoquinolinium Triflate (4c-Bu). ^tBuNC (65 μ L, 0.575 mmol) was added to a suspension of the complex $[\text{Pd}_2\{\kappa^2(\text{C},\text{N})\text{-C}_6\text{H}_4\text{CH}_2\text{CH}_2\text{NH}_2\text{-2}\}_2(\mu\text{-OAc})_2]$ (C; 150 mg, 0.262 mmol) in toluene (15 mL), and the mixture was refluxed for 7 h. Decomposition to metallic palladium was observed. The suspension was concentrated to dryness, Et₂O (30 mL) was added, and the suspension was filtered through a plug of Celite. The solvent was evaporated, *n*-pentane (30 mL) was added, and the resulting suspension was filtered to remove solid impurities. The filtrate was concentrated to dryness to give compound **3c-Bu** as a pale yellow liquid. Yield: 98 mg, 0.484 mmol, 92%. ¹H NMR (400 MHz): δ 1.46 (s, 9 H, ^tBu), 2.63 (“t”, 2 H, CH₂Ar, ³J_{HH} = 6.8 Hz), 3.48 (“t”, 2 H, CH₂N, ³J_{HH} = 6.8 Hz), 4.30 (br s, 1 H, NH), 7.17 (br d, 1 H, H5, ³J_{HH} = 7.2 Hz), 7.23–7.32 (m, 3 H, H6 + H7 + H8). ¹³C{¹H} NMR (100.81 MHz): δ 27.7 (s, CH₂Ar), 29.0 (s, CMe₃), 44.8 (s, CH₂N), 50.8 (s, CMe₃), 122.2 (s, CH, C8), 126.4 (s, CH, C7), 127.5 (s, CH, C5), 127.7 (s, C8a), 129.4 (s, CH, C6), 139.8 (s, C4a), 153.9 (s, C1). ESI-MS: *m/z* 203.1 [(M + 1)⁺].

HOTf (0.1 mL, 1.13 mmol) was added to a solution of compound **3c-Bu** (98 mg, 0.484 mmol) in Et₂O (10 mL). The resulting suspension was stirred for 15 min and then filtered off; the solid was washed with *n*-pentane (2 \times 5 mL) and air-dried to give compound **4c-Bu** as a colorless solid. Yield: 78 mg, 0.221 mmol, 46%. Mp: 153 °C. Anal. Calcd for C₁₄H₁₉F₃N₂O₃S (352.375): C, 47.72; H, 5.44; N, 7.95; S, 9.10. Found: C, 47.76; H, 5.62; N, 8.03; S, 8.86. IR (cm⁻¹): ν (NH) 3323 s; ν (CN) 1651, 1575. Λ_M (Ω^{-1} cm² mol⁻¹): 137 (5.11 \times 10⁻⁴ M). ¹H NMR (400 MHz): δ 1.58 (s, 9 H, ^tBu), 2.96 (t, 2 H, CH₂Ar, ³J_{HH} = 6.5 Hz), 3.72 (td, 2 H, CH₂NH, ³J_{HH} = 6.5, ³J_{HH} = 3.5 Hz), 7.32 (d, 1 H, H5, ³J_{HH} = 7.5 Hz), 7.45 (t, 1 H, H7, ³J_{HH} = 7.6 Hz), 7.57 (td, 1 H, H6, ³J_{HH} = 7.6, ⁴J_{HH} = 1.0 Hz), 7.62 (br s, 1 H, ^tBuNH), 7.95 (d, 1 H, H8, ³J_{HH} = 7.7 Hz), 8.37 (br s, 1 H, CH₂NH). ¹³C{¹H} NMR (100.81 MHz): δ 27.3 (s, CH₂Ar), 28.2 (s, CMe₃), 39.7 (s, CH₂NH), 54.6 (s, CMe₃), 120.4 (q, CF₃, ¹J_{CF} = 319.7 Hz), 122.6 (s, C8a), 126.9 (s, CH, C8), 128.2 (s, CH, C7), 128.5 (s, CH, C5), 134.3 (s, CH, C6), 138.3 (s, C4a), 156.3 (s, C1).

Single crystals of **4c-Bu**, suitable for an X-ray diffraction study, were obtained by slow diffusion of *n*-hexane into a solution of **4c-Bu** in CHCl₃.

Synthesis of 1-((2,6-Dimethylphenyl)imino)-3,3-dimethyl-1,2,3,4-tetrahydroisoquinoline (3d-Xy). XyNC (68 mg, 0.518 mmol) was added to a suspension of the complex $[\text{Pd}_2\{\kappa^2(\text{C},\text{N})\text{-C}_6\text{H}_4\text{CH}_2\text{CMe}_2\text{NH}_2\text{-2}\}_2(\mu\text{-Cl})_2]$ (150 mg, 0.258 mmol) in acetone (20 mL), and the mixture was stirred for 10 min. TlOTf (183 mg, 0.518 mmol) was added, and the resulting suspension was further stirred for 15 min and filtered through a plug of Celite. The filtrate was concentrated to dryness, and the residue was suspended in toluene (20 mL) and refluxed for 7 h. Decomposition to metallic palladium was observed. The solvent was evaporated, the residue was taken up in acetone (25 mL), the mixture was filtered through a plug of Celite, and Na₂CO₃ (100 mg, 0.943 mmol) was added to the filtrate. The mixture was stirred for 3 h and then filtered through a plug of Celite. The filtrate was concentrated to dryness, the residue was dissolved in CH₂Cl₂ (2 \times 10 mL), and the mixture was filtered through a plug of Celite. The solvent was evaporated, and the solid was dried under vacuum to give compound **3d-Xy** as a colorless solid. Yield: 118 mg, 0.422 mmol, 82%. Mp: 88–90 °C. Anal. Calcd for C₁₉H₂₂N₂ (278.399): C, 81.97; H, 7.97; N, 10.06. Found: C, 82.16; H, 8.25; N, 10.00. IR (cm⁻¹): ν (NH) 3368; ν (CN) 1628, 1574. ¹H NMR (300 MHz): δ 1.13 (s, 6 H, CMe₂), 2.11 (s, 6 H, Me, Xy), 2.85 (s, 2 H, CH₂), 4.31 (br s, 1 H, NH), 6.88 (t, 1 H, *p*-H, Xy, ³J_{HH} = 7.5 Hz), 7.06 (d, 2 H, *m*-H, Xy, ³J_{HH} = 7.5 Hz), 7.16 (dd, 1 H, H5, ³J_{HH} = 6.6, ⁴J_{HH} = 0.9 Hz), 7.35 (m, 2 H, H6 + H7), 8.43 (dd, 1 H, H8, ³J_{HH} = 7.3, ⁴J_{HH} = 1.6 Hz). ¹³C{¹H} NMR (75.45 MHz): δ 17.8 (s, Me, Xy), 29.0 (s, CMe₂), 42.1 (s, CH₂),

50.7 (s, CMe₂), 122.2 (s, *p*-CH, Xy), 126.5 (s, CH, C7), 126.7 (s, CH, C8), 128.0 (s, CH, C5), 128.0 (s, *m*-CH, Xy), 128.8 (s, *o*-C, Xy), 128.9 (s, C8a), 130.0 (s, CH, C6), 135.8 (s, C4a), 146.2 (s, *i*-C, Xy), 148.7 (s, C1). FAB⁺-MS: *m/z* 279.1 [(M + 1)⁺].

Synthesis of (Z)-(R)-1-((2,6-Dimethylphenyl)amino)-3-(methoxycarbonyl)-3,4-dihydrobenzo[*g*]isoquinolinium Triflate (4a-Xy). Complex **1b** (170 mg, 0.339 mmol) was dissolved in CH₂Cl₂, TlOTf (245 mg, 0.69 mmol) was added, the resulting suspension was stirred for 4 h and filtered through a plug of Celite, and the filtrate was concentrated to dryness. The residue was dissolved in toluene (15 mL), and the solution was refluxed for 7 h. Decomposition to metallic palladium was observed. Toluene was evaporated, CH₂Cl₂ (30 mL) was added, and the resulting suspension was filtered through a plug of Celite. The filtrate was concentrated to ca. 3 mL, Et₂O (15 mL) was added, and the suspension was filtered to remove a black solid. The solvent was evaporated to give crude **4a-Xy**. Yield: 84.0 mg, 0.165 mmol, 49%. Crude **4a-Xy** was dissolved in CH₂Cl₂ (1 mL), and *n*-pentane (20 mL) was added. A colorless suspension formed, which was stirred at 0 °C for 30 min and filtered (17 mg, 0.033 mmol; recrystallization yield: 20%). Mp: 167 °C. Λ_M (cm⁻¹ cm² mol⁻¹): 114 (4.95 \times 10⁻⁴ M). Anal. Calcd for C₂₄H₂₃F₃N₂O₅S (508.515): C, 56.69; H, 4.56; N, 5.51; S, 6.31. Found: C, 56.23; H, 4.75; N, 5.41; S, 6.04. IR (cm⁻¹): ν (NH) 3190; ν (CO) 1747; ν (CN) 1644, 1626. ¹H NMR (400 MHz): δ 2.21 (s, 3 H, Me, Xy), 2.32 (s, 3 H, Me, Xy), 3.41, 3.52 (AB part of an ABX system, 2 H, CH₂, ²J_{AB} = 16.3, ³J_{AX} = 5.7, ³J_{BX} = 5.1 Hz), 3.63 (s, 3 H, OMe), 4.62 (m, X part of an ABX system, 1 H, CH), 7.09 (d, 1 H, *m*-H, Xy, ³J_{HH} = 7.6 Hz), 7.11 (d, 1 H, *m*-H, Xy, ³J_{HH} = 7.2 Hz), 7.18 (t, 1 H, *p*-H, Xy, ³J_{HH} = 7.6 Hz), 7.52 (br d, 1 H, CHNH, ³J_{HH} = 4.0 Hz), 7.56 (t, 1 H, H8, ³J_{HH} = 8.0 Hz), 7.68 (t, 1 H, H7, ³J_{HH} = 8.0 Hz), 7.76 (s, 1 H, H5), 7.83 (d, 1 H, H6, ³J_{HH} = 8.0 Hz), 8.23 (d, 1 H, H9, ³J_{HH} = 8.4 Hz), 9.15 (s, 1 H, H10), 10.92 (s, 1 H, XyNH). ¹³C{¹H} NMR (100.81 MHz): δ 17.4 (s, Me, Xy), 17.7 (s, Me, Xy), 30.9 (s, CH₂), 52.3 (s, CH), 53.3 (s, OMe), 117.9 (s, C10a), 120.3 (q, CF₃, ¹J_{CF} = 317.0 Hz), 127.1 (s, CH, C6), 127.6 (s, CH, C8), 127.7 (s, CH, C5), 128.7 (s, C4a), 129.4 (s, *m*-CH, Xy), 129.5 (s, *m*-CH, Xy), 130.1 (s, *p*-CH, Xy), 130.5 (s, CH, C7), 130.7 (s, CH, C9), 130.8 (s, CH, C10), 135.9 (s, *o*-C, Xy), 136.0 (s, C5a), 136.1 (s, *o*-C, Xy), 132.3 (s, C9a), 158.4 (s, C1), 169.4 (s, CO). The ¹³C NMR resonance corresponding to the *i*-C of Xy was not observed.

Synthesis of (Z)-(S)-1-(*tert*-Butylamino)-3-(methoxycarbonyl)-4,9-dihydro-3*H*- β -carboline-2-ium Triflate (4b-Bu). ^tBuNC (71 μ L, 0.628 mmol) was added to a suspension of the complex (*S,S*)- $[\text{Pd}_2\{\kappa^2(\text{C},\text{N})\text{-C}_8\text{H}_5\text{N}(\text{CH}_2\text{CH}(\text{CO}_2\text{Me})\text{NH}_2\text{-2})_2(\mu\text{-Cl})_2\} \cdot 2\text{CH}_3\text{CN}]$ (**B** · 2MeCN; 250 mg, 0.312 mmol) in acetone (30 mL), and the mixture was stirred for 5 min. TlOTf (220 mg, 0.622 mmol) was added, and the resulting suspension was further stirred for 15 min and then filtered through a plug of Celite. The solvent was evaporated, CHCl₃ (30 mL) was added, and the resulting solution was refluxed for 8 h. Decomposition to metallic palladium was observed. The mixture was filtered through a plug of Celite, the solvent was evaporated, and the oily residue was vigorously stirred in *n*-hexane to give a dark yellow solid, which was filtered, washed with *n*-hexane (2 \times 5 mL), and air-dried. This solid was chromatographed on deactivated silica gel, using Et₂O as eluent and then acetone. The acetone effluent was collected, the solvent was evaporated, and the solid was recrystallized from CH₂Cl₂/Et₂O to give **4b-Bu** as a colorless solid. Yield: 184 mg, 0.493 mmol, 66%. Mp: 187–189 °C. Λ_M (Ω^{-1} cm² mol⁻¹): 121 (5.25 \times 10⁻⁴ M). Anal. Calcd for C₁₈H₂₂F₃N₃O₅S (449.448): C, 48.10; H, 4.93; N, 9.35; S, 7.13. Found: C, 47.94; H, 5.07; N, 9.17; S, 6.87. IR (cm⁻¹): ν (NH) 3304 br, s; ν (CO) 1746; ν (CN) 1636, 1590. ¹H NMR (300 MHz): δ 1.64 (s, 9 H, ^tBu), 3.41, 3.52 (AB part of an ABMX system, 2 H, CH₂, ²J_{AB} = 17.1, ³J_{AM} = 4.4, ³J_{BM} = 7.1 Hz), 3.71 (s, 3 H, OMe), 4.89 (m, M part of an ABMX system, 1 H, CH), 7.16 (td, 1 H, H6, ³J_{HH} = 7.3, ⁴J_{HH} = 0.9 Hz), 7.35 (td, 1 H, H7,

$^3J_{\text{HH}} = 7.2$, $^4J_{\text{HH}} = 1.2$ Hz), 7.52–7.61 (m, 3 H, H5 + H8 + CHNH), 8.32 (s, 1 H, ¹BuNH), 10.88 (s, 1 H, NH, C₆H₅N). $^{13}\text{C}\{^1\text{H}\}$ NMR (75.45 MHz): δ 22.8 (s, CH₂), 28.6 (s, CMe₃), 53.4 (s, OMe), 54.0 (s, CH), 55.3 (s, CMe₃), 113.5 (s, CH, C8), 119.4 (s, C9a), 120.1 (s, C4a), 120.2 (q, CF₃, $^1J_{\text{CF}} = 318.9$ Hz), 120.3 (s, CH, C5), 121.4 (s, CH, C6), 124.3 (s, C4b), 127.6 (s, CH, C7), 139.3 (s, C8a), 151.6 (s, C1), 170.5 (s, CO).

Single crystals of **4b-¹Bu**, suitable for an X-ray diffraction study, were obtained by slow diffusion of *n*-hexane into a solution of **4b-¹Bu** in CH₂Cl₂.

Synthesis of (Z)-1-((2,6-Dimethylphenyl)amino)-3,4-dihydroisoquinolinium Triflate (4c-Xy). XyNC (78 mg, 0.595 mmol) was added to a suspension of the complex [Pd₂{κ²(C,N)-C₆H₄CH₂CH₂NH₂-2}₂(μ-OAc)₂] (**C**; 170 mg, 0.298 mmol) in acetone (20 mL), and the mixture was stirred for 10 min. TlOTf (210 mg, 0.595 mmol) was added, and the mixture was stirred for 15 min. The solvent was evaporated, CH₂Cl₂ (20 mL) was added, and the suspension was filtered through a plug of Celite. The filtrate was concentrated to dryness, toluene (25 mL) was added, and the mixture was refluxed for 7 h. Decomposition to metallic palladium was observed. Toluene was evaporated, CH₂Cl₂ (30 mL) was added, the suspension was filtered through a plug of MgSO₄, the filtrate was concentrated to ca. 2 mL, and Et₂O (30 mL) was added. The suspension was filtered, and the solid was washed with Et₂O (2 × 5 mL) and air-dried to give crude **4c-Xy**. Yield: 112 mg, 0.280 mmol, 47%. An analytically pure sample of the off-white **4c-Xy** was obtained by recrystallization from acetone/Et₂O (38 mg, 0.095 mmol; recrystallization yield: 34%). Mp: 172 °C. Λ_{M} (Ω⁻¹ cm² mol⁻¹): 125 (5.80 × 10⁻⁴ M). Anal. Calcd for C₁₈H₁₉F₃N₂O₃S (400.419): C, 53.99; H, 4.78; N, 6.99; S, 8.01. Found: C, 53.63; H, 4.72; N, 6.82; S, 7.63. IR (cm⁻¹): ν(NH) 3202 br s; ν(CN) 1646, 1572. ¹H NMR (400 MHz): δ 2.17 (s, 6 H, Me, Xy), 2.97 ("t", 2 H, CH₂Ar, $^3J_{\text{HH}} = 6.8$ Hz), 3.53 ("t", 2 H, CH₂NH, $^3J_{\text{HH}} = 6.8$ Hz), 7.07 (d, 2 H, *m*-H, Xy, $^3J_{\text{HH}} = 7.5$ Hz), 7.14 (t, 1 H, *p*-H, Xy, $^3J_{\text{HH}} = 7.5$ Hz), 7.38 (d, 1 H, H5, $^3J_{\text{HH}} = 7.4$ Hz), 7.49 (t, 1 H, H7, $^3J_{\text{HH}} = 7.5$ Hz), 7.57 (br s, 1 H, CH₂NH), 7.65 (td, 1 H, H6, $^3J_{\text{HH}} = 7.6$, $^4J_{\text{HH}} = 1.0$ Hz), 8.36 (d, 1 H, H8, $^3J_{\text{HH}} = 7.6$ Hz), 10.22 (br s, 1 H, XyNH). $^{13}\text{C}\{^1\text{H}\}$ NMR (100.81 MHz): δ 17.6 (s, Me, Xy), 27.3 (s, CH₂Ar), 39.5 (s, CH₂NH), 120.2 (q, CF₃, $^1J_{\text{CF}} = 319.6$ Hz), 121.2 (s, C8a), 127.6 (s, CH, C8), 128.6 (s, CH, C5), 128.6 (s, CH, C7), 129.3 (s, *m*-CH, Xy), 129.7 (s, *p*-CH, Xy), 129.7 (s, *i*-C, Xy), 135.0 (s, CH, C6), 135.8 (s, *o*-C, Xy), 138.3 (s, C4a), 157.6 (s, C1).

Synthesis of (Z)-1-(tert-Butylamino)-3,3-dimethyl-3,4-dihydroisoquinolinium Triflate (4d-¹Bu). ¹BuNC (70 μL, 0.619 mmol) was added to a suspension of the complex [Pd₂{κ²(C,N)-C₆H₄CH₂CH₂Me₂NH₂-2}₂(μ-Cl)₂] (**D**; 180 mg, 0.310 mmol) in acetone (20 mL), and the mixture was stirred for 5 min. TlOTf (220 mg, 0.622 mmol) was added, and the resulting suspension was further stirred for 15 min and filtered through a plug of MgSO₄. The solvent was evaporated, toluene (30 mL) was added, and the mixture was refluxed for 6 h. Decomposition to metallic palladium was observed. The mixture was filtered through a plug of MgSO₄, toluene was evaporated, and the oily residue was vigorously stirred in Et₂O to give a suspension, which was filtered; the solid was washed with Et₂O (2 × 5 mL) and air-dried to give compound **4d-¹Bu** as an off-white solid. Yield: 153.9 mg, 0.402 mmol, 65%. Mp: 137 °C. Λ_{M} (Ω⁻¹ cm² mol⁻¹): 143 (5.33 × 10⁻⁴ M). Anal. Calcd for C₁₆H₂₃F₃N₂O₃S (380.429): C, 50.52; H, 6.09; N, 7.36; S, 8.43. Found: C, 50.35; H, 6.40; N, 7.32; S, 8.35. IR (cm⁻¹): ν(NH) 3353 s, 3315 s; ν(CN) 1636, 1561. ¹H NMR (400 MHz): δ 1.45 (s, 6 H, CMe₂), 1.61 (s, 9 H, ¹Bu), 2.96 (s, 2 H, CH₂), 7.16 (br s, 1 H, CMe₂NH), 7.28 (d, 1 H, H5, $^3J_{\text{HH}} = 7.3$ Hz), 7.47 (t, 1 H, H7, $^3J_{\text{HH}} = 7.5$ Hz), 7.59 (t, 1 H, H6, $^3J_{\text{HH}} = 7.5$ Hz), 7.98 (br s, 1 H, ¹BuNH), 8.08 (d, 1 H, H8, $^3J_{\text{HH}} = 7.9$ Hz). $^{13}\text{C}\{^1\text{H}\}$ NMR (100.81 MHz): δ 27.1 (s, CMe₂), 28.6 (s, CMe₃), 41.0 (s, CH₂), 54.1 (s, CMe₂), 54.9 (s, CMe₃), 120.5 (q, CF₃, $^1J_{\text{CF}} = 320.1$ Hz), 121.5 (s, C8a), 127.4 (s, CH, C8), 128.4

(s, CH, C7), 129.0 (s, CH, C5), 134.7 (s, CH, C6), 136.4 (s, C4a), 156.1 (s, C1).

Single crystals of **4d-¹Bu**, suitable for an X-ray diffraction study, were obtained by slow diffusion of Et₂O into a solution of **4d-¹Bu** in CH₂Cl₂.

Synthesis of (Z)-/(E)-1-((2,6-Dimethylphenyl)amino)-3,3-dimethyl-3,4-dihydroisoquinolinium Triflate (Z-/E-4d-Xy). XyNC (107 mg, 0.816 mmol) was added to a suspension of the complex [Pd₂{κ²(C,N)-C₆H₄CH₂CH₂Me₂NH₂-2}₂(μ-Cl)₂] (**D**; 237 mg, 0.408 mmol) in acetone (15 mL), and the mixture was stirred for 10 min. TlOTf (288 mg, 0.815 mmol) was added, and the resulting suspension was further stirred for 15 min and then filtered through a plug of MgSO₄. The solvent was evaporated, toluene (20 mL) was added, and the mixture was refluxed for 7 h. Decomposition to metallic palladium was observed. Toluene was evaporated, CH₂Cl₂ (25 mL) was added, the suspension was filtered through a plug of Celite, and the filtrate was concentrated to ca. 2 mL. Et₂O (15 mL) was added to give a suspension, which was filtered to afford *Z-/E-4d-Xy* as a colorless solid. Yield: 218 mg, 0.509 mmol, 62%. Λ_{M} (Ω⁻¹ cm² mol⁻¹): 137 (5.13 × 10⁻⁴ M). Anal. Calcd for C₂₀H₂₃F₃N₂O₃S (428.473): C, 56.06; H, 5.41; N, 6.54; S, 7.48. Found: C, 56.25; H, 5.56; N, 6.68; S, 7.03. IR (cm⁻¹): ν(NH) 3192 vs; ν(CN) 1644, 1578. ¹H NMR (25 °C, CDCl₃, 600 MHz): **Z-4d-Xy**, δ 1.31 (s, 6 H, CMe₂), 2.23 (s, 6 H, Me, Xy), 3.03 (s, 2 H, CH₂), 6.30 (br s, 1 H, CMe₂NH), 7.20 (d, 2 H, *m*-H, Xy, $^3J_{\text{HH}} = 7.8$ Hz), 7.28 (t, 1 H, *p*-H, Xy, $^3J_{\text{HH}} = 7.8$ Hz), 7.38 (d, 1 H, H5, $^3J_{\text{HH}} = 7.8$ Hz), 7.58 (t, 1 H, H7, $^3J_{\text{HH}} = 7.8$ Hz), 7.70 (t, 1 H, H6, $^3J_{\text{HH}} = 7.8$ Hz), 8.54 (d, 1 H, H8, $^3J_{\text{HH}} = 7.8$ Hz), 10.77 (br s, 1 H, XyNH); **E-4d-Xy**, δ 1.41 (s, 6 H, CMe₂), 2.15 (s, 6 H, Me, Xy), 3.02 (s, 2 H, CH₂), 6.89 (d, 1 H, CH, $^3J_{\text{HH}} = 7.8$ Hz), 7.02 (t, 1 H, CH, $^3J_{\text{HH}} = 7.8$ Hz), 7.07 (d, 2 H, *m*-H, Xy, $^3J_{\text{HH}} = 7.8$ Hz), 7.19 (t, 1 H, *p*-H, Xy, $^3J_{\text{HH}} = 7.8$ Hz; partially obscured by *m*-H of Xy of Z isomer), 7.34 (d, 1 H, CH, $^3J_{\text{HH}} = 7.8$ Hz), 7.51 (dt, 1 H, CH, $^3J_{\text{HH}} = 7.8$, $^4J_{\text{HH}} = 1.2$ Hz), 9.71 (br s, 1 H, CMe₂NH), 9.99 (br s, 1 H, XyNH). Low-temperature ¹H NMR (-60 °C, CD₂Cl₂, 400 MHz): **Z-4d-Xy**, δ 1.26 (s, 6 H, CMe₂), 2.19 (s, 6 H, Me, Xy), 3.02 (s, 2 H, CH₂), 6.18 (s, 1 H, CMe₂NH), 7.22 (d, 2 H, *m*-H, Xy, $^3J_{\text{HH}} = 7.2$ Hz), 7.32 (t, 1 H, *p*-H, Xy, $^3J_{\text{HH}} = 7.6$ Hz), 7.41 (d, 1 H, H5, $^3J_{\text{HH}} = 7.6$ Hz), 7.53 (t, 1 H, H7, $^3J_{\text{HH}} = 7.6$ Hz), 7.72 (t, 1 H, H6, $^3J_{\text{HH}} = 7.6$ Hz), 8.34 (d, 1 H, H8, $^3J_{\text{HH}} = 8.0$ Hz), 10.51 (s, 1 H, XyNH). ¹H NMR (DMSO-*d*₆, 400 MHz; only the isomer **Z-4d-Xy** was observed): δ 1.23 (s, 6 H, CMe₂), 2.21 (s, 6 H, Me, Xy), 3.09 (s, 2 H, CH₂), 7.29 (br d, 2 H, *m*-H, Xy, $^3J_{\text{HH}} = 7.2$ Hz), 7.36 (dd, 1 H, *p*-H, Xy, $^3J_{\text{HH}} = 8.8$, $^3J_{\text{HH}} = 6.4$ Hz), 7.52 (d, 1 H, H5, $^3J_{\text{HH}} = 7.6$ Hz), 7.61 (t, 1 H, H7, $^3J_{\text{HH}} = 7.6$ Hz), 7.78 (dt, 1 H, H6, $^3J_{\text{HH}} = 7.6$, $^4J_{\text{HH}} = 0.8$ Hz), 8.25 (d, 1 H, H8, $^3J_{\text{HH}} = 7.6$ Hz), 8.92 (s, 1 H, CMe₂NH), 10.91 (s, 1 H, XyNH). $^{13}\text{C}\{^1\text{H}\}$ NMR (DMSO-*d*₆, 100.81 MHz; only the isomer **Z-4d-Xy** was observed): δ 17.44 (s, Me, Xy), 26.6 (s, CMe₂), 39.8 (s, CH₂), 53.1 (s, CMe₂), 121.0 (s, C8a), 126.6 (s, CH, C8), 127.8 (s, CH, C7), 128.9 (s, *m*-CH, Xy), 129.3 (s, CH, C5), 129.5 (s, *p*-CH, Xy), 135.0 (s, CH, C6), 135.8 (s, *o*-C, Xy), 137.8 (s, C4a), 155.7 (s, C1). The ^{13}C NMR resonances corresponding to the *i*-C of Xy and the CF₃ of triflate were not observed.

Single crystals of **Z-4d-Xy**, suitable for an X-ray diffraction study, were obtained by slow diffusion of Et₂O into a solution of **4d-Xy** in CH₂Cl₂.

Synthesis of (Z)-1-(Methylamino)-3,3-dimethyl-3,4-dihydroisoquinolinium Triflate (4d-Me). TlOTf (245 mg, 0.693 mmol) was added to a solution of [Pd₂{κ²(C,N)-C₆H₄CH₂CH₂Me₂NH₂-2}₂(μ-Cl)₂] (**D**; 200 mg, 0.344 mmol) in acetone (15 mL). The resulting suspension was stirred for 15 min and filtered through a plug of Celite. MeNCS (60 mg, 0.820 mmol) was added to the filtrate, and the mixture was stirred for 1 h. The solvent was evaporated, and the residue was suspended in toluene (25 mL) and refluxed for 7 h. Formation of a black solid was observed. Toluene was evaporated, CH₂Cl₂ (30 mL) was added, and the mixture was filtered through a

plug of MgSO₄. The filtrate was concentrated to ca. 2 mL, Et₂O (20 mL) was added, and the suspension was filtered off. The solid was washed with Et₂O (2 × 5 mL) and air-dried to give crude **4d-Me**. Yield: 96 mg, 0.284 mmol, 41%. Crude **4d-Me** was recrystallized from CHCl₃/Et₂O to give analytically pure **4d-Me** as a colorless solid (76 mg, 0.225 mmol, recrystallization yield: 79%). Mp: 131 °C. Λ_M (Ω^{-1} cm² mol⁻¹): 135 (5.09×10^{-4} M). Anal. Calcd for C₁₃H₁₇F₃N₂O₃S (338.348): C, 46.15; H, 5.06; N, 8.28; S, 9.48. Found: C, 46.09; H, 5.24; N, 8.56; S, 9.17. IR (cm⁻¹): ν (NH) 3317 s; ν (CN) 1658, 1556. ¹H NMR (400 MHz): δ 1.43 (s, 6 H, CMe₂), 2.94 (s, 2 H, CH₂), 3.20 (d, 3 H, MeNH, ³J_{HH} = 5.04 Hz), 7.28 (d, 1 H, H5, ³J_{HH} = 7.5 Hz), 7.44 (t, 1 H, H7, ³J_{HH} = 7.5 Hz), 7.58 (td, 1 H, H6, ³J_{HH} = 7.5, ⁴J_{HH} = 1.1 Hz), 8.01 (d, 1 H, H8, ³J_{HH} = 7.9 Hz), 8.10 (br s, 1 H, CMe₂NH), 8.77 (m, 1 H, MeNH). ¹³C{¹H} NMR (100.81 MHz): δ 27.1 (s, CMe₂), 29.1 (s, MeNH), 41.2 (s, CH₂), 53.5 (s, CMe₂), 120.4 (q, CF₃, ¹J_{CF} = 318.7 Hz), 121.2 (s, C8a), 126.3 (s, CH, C8), 128.3 (s, CH, C7), 129.1 (s, CH, C5), 134.5 (s, CH, C6), 136.5 (s, C4a), 157.2 (s, C1).

Single crystals of **4d-Me**, suitable for an X-ray diffraction study, were obtained by slow diffusion of *n*-hexane into a solution of **4d-Me** in CH₂Cl₂.

Synthesis of (Z)-1-(*p*-Tolylamino)-3,3-dimethyl-3,4-dihydroisoquinolinium Triflate (4d-To). TlOTf (194 mg, 0.55 mmol) was added to a solution of [Pd₂{ κ^2 (*C,N*)-C₆H₄CH₂CMe₂NH₂-2}₂(μ -Cl)₂] (**D**; 160 mg, 0.275 mmol) in acetone (15 mL). The mixture was stirred for 15 min and filtered through a plug of Celite. *p*-ToNCS (90 μ L, 0.66 mmol) was added to the filtrate, and the resulting mixture was stirred for 1 h. The solvent was evaporated, and the remaining residue was suspended in toluene (25 mL) and refluxed for 8 h. Formation of a black solid was observed. Toluene was evaporated, CH₂Cl₂ (30 mL) was added, and the mixture was filtered through a plug of Celite. The solvent was concentrated to ca. 2 mL, Et₂O (20 mL) was added, and the suspension was filtered off. The solid was washed with Et₂O (2 × 5 mL) and air-dried to give colorless **4d-To**. Yield: 153 mg, 0.369 mmol, 67%. Mp: 155 °C. Λ_M (Ω^{-1} cm² mol⁻¹): 161 (4.92×10^{-4} M). Anal. Calcd for C₁₉H₂₁F₃N₂O₃S (414.446): C, 55.06; H, 5.11; N, 6.76; S, 7.74. Found: C, 55.00; H, 5.25; N, 6.83; S, 7.56. IR (cm⁻¹): ν (NH) 3242 br, s; ν (CN) 1634, 1574. ¹H NMR (DMSO-*d*₆, 300 MHz): δ 1.24 (s, 6 H, CMe₂), 2.38 (s, 3 H, Me, To), 3.07 (s, 2 H, CH₂), 7.33–5.40 (m, 4 H, *m*-H + *o*-H, To), 7.49 (d, 1 H, H5, ³J_{HH} = 7.5 Hz), 7.57 (t, 1 H, H7, ³J_{HH} = 7.5 Hz), 7.75 (dt, 1 H, H6, ³J_{HH} = 7.5, ⁴J_{HH} = 0.9 Hz), 8.18 (d, 1 H, H8, ³J_{HH} = 7.5 Hz), 9.15 (s, 1 H, CMe₂NH), 11.05 (s, 1 H, ToNH). ¹³C{¹H} NMR (DMSO-*d*₆, 75.45 MHz): δ 20.8 (s, Me, To), 26.3 (s, CMe₂), 53.0 (s, CMe₂), 121.5 (s, C8a), 126.1 (s, *o*-CH, To), 126.7 (s, CH, C8), 127.5 (s, CH, C7), 129.3 (s, CH, C5), 130.5 (s, *m*-CH, To), 131.7 (s, *i*-C, To), 134.8 (s, CH, C6), 137.8 (s, C4a), 138.0 (s, *p*-C, To), 155.9 (s, C1). The resonances corresponding to the CH₂ group (obscured by the DMSO) and the CF₃ of triflate were not observed. Low-temperature NMR data are as follows. ¹H NMR (–60 °C, CDCl₃, 400 MHz): δ 1.40 (s, 6 H, CMe₂), 2.38 (s, 3 H, Me, To), 3.06 (s, 2 H, CH₂), 7.84 (s, 1 H, CMe₂NH), 7.27 (“d”, 2 H, *m*-H, To, ³J_{HH} = 8.3 Hz), 7.33 (“d”, 2 H, *o*-H, To, ³J_{HH} = 9.0 Hz), 7.41 (d, 1 H, H5, ³J_{HH} = 7.6 Hz), 7.55 (t, 1 H, H7, ³J_{HH} = 7.8 Hz), 7.76 (t, 1 H, H6, ³J_{HH} = 7.5 Hz), 8.26 (d, 1 H, H8, ³J_{HH} = 7.9 Hz), 10.75 (s, 1 H, ToNH). ¹³C{¹H} NMR (–60 °C, CDCl₃, 100.81 MHz): δ 21.2 (s, Me, To), 27.1 (s, CMe₂), 40.2 (s, CH₂), 53.3 (s, CMe₂), 119.6 (q, CF₃, ¹J_{CF} = 319.0 Hz), 119.6 (s, C8a), 125.0 (s, *o*-CH, To), 127.3 (s, CH, C8), 128.3 (s, CH, C7), 129.1 (s, CH, C5), 129.1 (s, *i*-C, To), 131.1 (s, *m*-CH, To), 135.4 (s, CH, C6), 136.6 (s, C4a), 139.4 (s, *p*-C, To), 156.8 (s, C1).

Single crystals of **4d-To**, suitable for an X-ray diffraction study, were obtained by slow diffusion of *n*-pentane into a solution of **4d-To** in CHCl₃.

Synthesis of (R)-1-Oxo-3-(methoxycarbonyl)-1,2,3,4-tetrahydrobenzolo[*g*]isoquinoline (5a). CO was bubbled for 10 min through a suspension of 200 mg of the mixture **I** (obtained from 186 mg, (0.700 mmol) of *D*-naphthylalanine methyl ester hydrochloride) in CHCl₃ (15 mL). The resulting mixture was stirred under a CO atmosphere for 12 h. Decomposition to metallic palladium was observed. The mixture was filtered through a plug of Celite, the filtrate was concentrated to ca. 1 mL, and Et₂O (15 mL) was added. The suspension was filtered and the solid washed with Et₂O (2 × 5 mL) and air-dried to afford crude off-white **5a**. Yield: 86 mg, 0.337 mmol, 48%. Crude **5a** was recrystallized from CHCl₃/Et₂O to give pure **5a** as a colorless solid (51 mg, 0.200 mmol; recrystallization yield: 59%). Mp: 183 °C. Anal. Calcd for C₁₅H₁₃NO₃ (255.273): C, 70.58; H, 5.13; N, 5.49. Found: C, 70.19; H, 5.52; N, 5.40. IR (cm⁻¹): ν (NH) 3209; ν (CO) 1745, 1662. ¹H NMR (300 MHz): δ 3.51, 3.36 (AB part of an ABMX system, 2 H, CH₂, ²J_{AB} = 15.4, ³J_{AM} = 9.4, ³J_{BM} = 4.6 Hz), 3.79 (s, 3 H, OMe), 4.47 (m, M part of an ABMX system, 1 H, CH), 6.77 (br s, 1 H, NH), 7.47–7.59 (m, 2 H, H7 + H8), 7.67 (s, 1 H, H5), 7.81 (d, 1 H, H6, ³J_{HH} = 8.2 Hz), 7.95 (d, 1 H, H9, ³J_{HH} = 8.0 Hz), 8.65 (s, 1 H, H10). ¹³C{¹H} NMR (75.45 MHz): δ 31.6 (s, CH₂), 52.9 (s, OMe), 53.2 (s, CH), 126.0 (s, CH, C5), 126.1 (s, C10a), 126.3 (s, CH, C8), 127.2 (s, CH, C6), 128.3 (s, CH, C7), 129.4 (s, CH, C9), 129.5 (s, CH, C10), 131.8 (s, C4a), 132.2 (s, C9a), 135.2 (s, C5a), 165.4 (s, CONH), 170.9 (s, CO₂Me). FAB⁺-MS: *m/z* 256.1 [(M + 1)⁺]. EI-HRMS: exact mass calcd for C₁₅H₁₃NO₃ 255.0895; found 255.0913; Δ = 0.0018.

Single crystals of **5a**, suitable for an X-ray diffraction study, were obtained by slow evaporation of a solution of **5a** in CHCl₃.

Synthesis of (S)-1-Oxo-3-(methoxycarbonyl)-2,3,4,9-tetrahydro-1H-pyrido[3,4-*b*]indole (5b). CO was bubbled through a suspension of the complex (S,S)-[Pd₂{ κ^2 (*C,N*)-C₈H₅N(CH₂CH(CO₂Me)NH₂-2)₂(μ -Cl)₂] · 2CH₃CN (**B** · 2MeCN; 250 mg, 0.312 mmol) in CHCl₃ (30 mL), and the resulting mixture was stirred under a CO atmosphere for 24 h. Decomposition to metallic palladium was observed. The mixture was filtered, the filtrate was concentrated to dryness, CH₂Cl₂ (20 mL) was added, and the resulting suspension was filtered through a plug of MgSO₄. The solvent was evaporated, the residue was vigorously stirred with *n*-pentane, the suspension was filtered, and the solid was washed with *n*-pentane (2 × 2 mL) and air-dried to give compound **5b** as a creamy solid. Yield: 110 mg, 0.448 mmol, 72%. Mp: 178 °C dec (lit.⁹⁴ mp 178–179 °C). IR (cm⁻¹): ν (NH) 3251, 3212; ν (CO) 1732, 1665. ¹H NMR (300 MHz): δ 3.32, 3.46 (AB part of an ABMX system, 2 H, CH₂, ²J_{AB} = 16.1, ³J_{BM} = 9.7, ³J_{AM} = 6.2 Hz), 3.79 (s, 3 H, OMe), 4.58 (M part of an ABMX system, 1 H, CH, ³J_{MX} = 2.1 Hz), 6.65 (s, 1 H, CONH), 7.13 (td, 1 H, H6, ³J_{HH} = 7.8, ⁴J_{HH} = 0.9 Hz), 7.29 (td, 1 H, H7, ³J_{HH} = 8.1, ⁴J_{HH} = 1.2 Hz), 7.49 (d, 1 H, H8, ³J_{HH} = 8.1 Hz), 7.58 (d, 1 H, H5, ³J_{HH} = 8.1 Hz), 10.48 (br s, 1 H, NH, C₈H₅N). ¹³C{¹H} NMR (100.81 MHz): δ 24.0 (s, CH₂), 52.9 (s, OMe), 55.0 (s, CH), 112.9 (s, CH, C8), 117.6 (s, C4a), 120.2 (s, CH, C5), 120.3 (s, CH, C6), 124.9 (s, C4b), 125.4 (s, CH, C7), 125.9 (s, C9a), 137.9 (s, C8a), 162.4 (s, CONH), 171.3 (s, CO₂Me). FAB⁺-MS: *m/z* 245.0 [(M + 1)⁺]. EI-HRMS: exact mass calcd for C₁₃H₁₂N₂O₃ 244.0848; found 244.0850; Δ = 0.0002. Spectroscopic data are in accordance with the data available in the literature (¹H and ¹³C NMR in DMSO-*d*₆).³⁹

Single crystals of **5b**, suitable for an X-ray diffraction study, were obtained by slow diffusion of *n*-hexane into a solution of **5b** in CH₂Cl₂.

Synthesis of 1-Oxo-1,2,3,4-tetrahydroisoquinoline (5c). CO was bubbled through a suspension of the complex [Pd₂{ κ^2 (*C,N*)-C₆H₄CH₂CH₂NH₂-2}₂(μ -OAc)₂] (**C**; 170 mg, 0.298 mmol) in CH₂Cl₂ (20 mL), and the resulting mixture was stirred under a CO atmosphere for 3 h. Decomposition to metallic palladium was observed. The solvent was evaporated, Et₂O (45 mL) was added, and the mixture was filtered through a plug of MgSO₄. The filtrate

was concentrated to dryness to give compound **5c** as a colorless liquid. When stored, thin needles of solid **5c** appeared in the walls of the vial. Yield: 74 mg, 0.502 mmol, 84%. IR (cm⁻¹): $\nu(\text{NH})$ 3242; $\nu(\text{CO})$ 1666. ¹H NMR (200 MHz): δ 2.97 (t, 2 H, CH₂Ar, ³J_{HH} = 6.8 Hz), 3.56 (td, 2 H, CH₂NH, ³J_{HH} = 6.8, ³J_{HH} = 3.0 Hz), 7.21 (d, 1 H, H5, ³J_{HH} = 7.4 Hz), 7.33 (t, 1 H, H7, ³J_{HH} = 7.4 Hz), 7.44 (td, 1 H, H6, ³J_{HH} = 7.4, ⁴J_{HH} = 1.4 Hz), 7.88 (br s, 1 H, NH), 8.04 (dd, 1 H, H8, ³J_{HH} = 7.6, ⁴J_{HH} = 1.4 Hz). ¹³C{¹H} NMR (50.30 MHz): δ 28.5 (s, CH₂Ar), 40.4 (s, CH₂NH), 127.5 (s, CH, C7), 127.7 (s, CH, C5), 128.3 (s, CH, C8), 129.1 (s, C8a), 132.7 (s, CH, C6), 139.4 (s, C4a), 167.8 (s, CO). EI-MS: *m/z* 147.1 [M]. EI-HRMS: exact mass calcd for C₉H₉NO 147.0684; found 147.0682; Δ = 0.0002. Spectroscopic data are in accordance with the data available in the literature (¹H and ¹³C NMR).⁹⁷

Single crystals of **5c**, suitable for an X-ray diffraction study, grew in the vial where compound **5c** was stored.

Synthesis of 1-Oxo-3,3-dimethyl-1,2,3,4-tetrahydroisoquinoline (5d). CO was bubbled through a suspension of the complex [Pd₂{ κ^2 (C,N)-C₆H₄CH₂CMe₂NH₂-2}₂(μ -Cl)₂] (**D**; 200 mg, 0.344 mmol) in CH₂Cl₂ (25 mL), and the resulting mixture was stirred under a CO atmosphere for 2.5 h. Decomposition to metallic palladium was observed. The solvent was evaporated, and acetone (10 mL) and NEt₃ (95 μ L, 0.688 mmol) were added. The resulting suspension was stirred for 15 min, and then acetone was evaporated. Et₂O (10 mL) was added, and the suspension was filtered to remove metallic palladium and NHEt₃Cl. The filtrate was concentrated to dryness to give compound **5d** as a colorless solid. Yield: 118 mg, 0.676 mmol, 98%. Mp: 148 °C (lit.⁹² mp 146–148 °C). IR (cm⁻¹): $\nu(\text{NH})$ 3179, 3043; $\nu(\text{CO})$ 1666. ¹H NMR (300 MHz): δ 1.32 (s, 6 H, Me), 2.92 (s, 2 H, CH₂), 6.58 (br s, 1 H, NH), 7.18 (dd, 1 H, H5, ³J_{HH} = 7.5, ⁴J_{HH} = 0.9 Hz), 7.34 ("t", 1 H, H7, ³J_{HH} = 7.5 Hz), 7.45 (td, 1 H, H6, ³J_{HH} = 7.5, ⁴J_{HH} = 1.5 Hz), 8.07 (dd, 1 H, H8, ³J_{HH} = 7.5, ⁴J_{HH} = 1.5 Hz). ¹³C{¹H} NMR (75.45 MHz): δ 28.8 (s, Me), 41.5 (s, CH₂), 51.9 (s, CMe₂), 126.9 (s, CH, C7), 127.7 (s, CH, C8), 127.8 (s, CH, C5), 127.9 (s, C8a), 132.2 (s, CH, C6), 137.5 (s, C4a), 165.6 (s, CO). FAB⁺-MS: *m/z* 176.1 [(M + 1)⁺]. Spectroscopic data are in accordance with the data available in the literature (¹H NMR).⁹²

Single crystals of **5d**, suitable for an X-ray diffraction study, were obtained by slow diffusion of *n*-pentane into a solution of **5d** in CH₂Cl₂.

X-ray Structure Determinations. X-ray data for compounds **2b**, **4b**-**1Bu**, **4c**-**1Bu**, **4d**-**1Bu**, **4d**-**Xy**, **4d**-**Me**, **4d**-**To**, and **5a**-**d** are summarized in Tables 1 and 2.

a. Data Collection. Crystals were mounted in inert oil on a glass fiber and transferred to a Bruker SMART APEX diffractometer. Data were recorded at low temperature using ω scans. Multiscan absorption corrections were applied for compounds **2b**, **4c**-**1Bu**, **4d**-**1Bu**, **4d**-**Xy**, **4d**-**Me**, and **5d**.

b. Structure Solution and Refinement. Structures were solved by direct methods and refined anisotropically on *F*² using the program SHELX-97.¹⁰⁰ Hydrogen atoms were refined as follows:

(100) Sheldrick, G. M. SHELX-97; University of Göttingen, Göttingen, Germany, 1997.

NH, free; NH₂, free with SADI; methyl, rigid group; all others, riding. *Special features:* complex **2b**, absolute structure (Flack) parameter¹⁰¹ -0.006(16); compound **4b**-**1Bu**, Flack parameter -0.02(6); compounds **5a**, **b**, noncentrosymmetric structures without heavy atoms (just C, H, N, O). With Mo radiation there are usually no significant Friedel differences, and thus the Friedel opposite reflections become exactly equivalent in intensity. Because of that, MERG 3 was used in the refinement of the structures.

Computational Details. Density functional calculations were carried out using the GAUSSIAN-03 program package.¹⁰² The hybrid density functional B3LYP method was applied,¹⁰³ employing 6-31G* as the basis set.¹⁰⁴ After geometry optimizations, analytical frequency calculations were carried out to confirm that all of them correspond with a minimum.

Acknowledgment. We thank the Ministerio de Educación y Ciencia (Spain) and FEDER (CTQ2007-60808/BQU, C-Consolider) for financial support. J.-A.G.-L. is grateful to the Ministerio de Educación y Ciencia and the University of Murcia (Spain) for consecutive research grants.

Supporting Information Available: Text, tables, and figures giving total energies and total energy differences (hartrees/molecule) calculated for the *E/Z* isomers of compounds **3a**-**1Bu**, **3a**-**Xy**, **3c**-**1Bu**, **3d**-**Xy**, **4d**-**1Bu**, **4d**-**Xy**, **4d**-**Me**, and **4d**-**To**, experimental details for 3-(2-naphthyl)-D-alanine methyl ester hydrochloride, ¹H and ¹³C NMR data for the new compounds, details (including symmetry operators) of hydrogen bonds and all refined and calculated atomic coordinates, anisotropic thermal parameters, and bond lengths and angles and CIF files giving crystallographic data for compounds **2b**, **4b**-**1Bu**, **4c**-**1Bu**, **4d**-**1Bu**, **4d**-**Xy**, **4d**-**Me**, **4d**-**To**, and **5a**-**d**. This material is available free of charge via the Internet at <http://pubs.acs.org>.

OM800951K

(101) Flack, H. D. *Acta Crystallogr., Sect. A* **1983**, *39*, 876.

(102) Frisch, M. J.; Trucks, G. W.; Schlegel, H. B.; Scuseria, G. E.; Robb, M. A.; Cheeseman, J. R.; Montgomery, J. A., Jr.; Vreven, T.; Kudin, K. N.; Burant, J. C.; Millam, J. M.; Iyengar, S. S.; Tomasi, J.; Barone, V.; Mennucci, B.; Cossi, M.; Scalmani, G.; Rega, N.; Petersson, G. A.; Nakatsuji, H.; Hada, M.; Ehara, M.; Toyota, K.; Fukuda, R.; Hasegawa, J.; Ishida, M.; Nakajima, T.; Honda, Y.; Kitao, O.; Nakai, H.; Klene, M.; Li, X.; Knox, J. E.; Hratchian, H. P.; Cross, J. B.; Bakken, V.; Adamo, C.; Jaramillo, J.; Gomperts, R.; Stratmann, R. E.; Yazyev, O.; Austin, A. J.; Cammi, R.; Pomelli, C.; Ochterski, J. W.; Ayala, P. Y.; Morokuma, K.; Voth, G. A.; Salvador, P.; Dannenberg, J. J.; Zakrzewski, V. G.; Dapprich, S.; Daniels, A. D.; Strain, M. C.; Farkas, O.; Malick, D. K.; Rabuck, A. D.; Raghavachari, K.; Foresman, J. B.; Ortiz, J. V.; Cui, Q.; Baboul, A. G.; Clifford, S.; Cioslowski, J.; Stefanov, B. B.; Liu, G.; Liashenko, A.; Piskorz, P.; Komaromi, I.; Martin, R. L.; Fox, D. J.; Keith, T.; Al-Laham, M. A.; Peng, C. Y.; Nanayakkara, A.; Challacombe, M.; Gill, P. M. W.; Johnson, B.; Chen, W.; Wong, M. W.; Gonzalez, C.; Pople, J. A. Gaussian 03, revision C.02; Gaussian, Inc., Wallingford, CT, 2004.

(103) Becke, A. D. *J. Chem. Phys.* **1993**, *98*, 5648. Lee, C.; Yang, W.; Parr, R. G. *Phys. Rev. B: Condens. Matter* **1988**, *37*, 785.

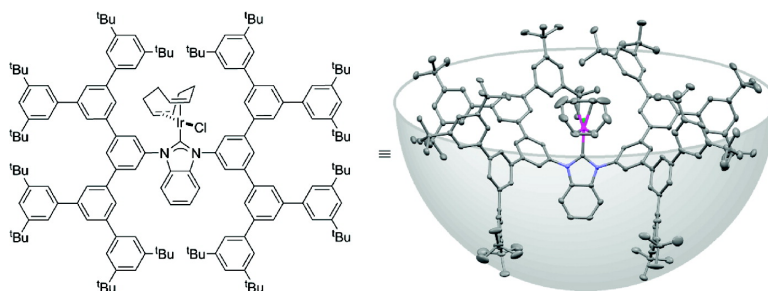
(104) Hariharan, P. C.; Pople, J. A. *Theor. Chim. Acta* **1973**, *28*, 213. Francl, M. M.; Pietro, W. J.; Hehre, W. J.; Binkley, J. S.; Gordon, M. S.; DeFrees, D. J.; Pople, J. A. *J. Chem. Phys.* **1982**, *77*, 3654.

Flexible, Bowl-Shaped N-Heterocyclic Carbene Ligands: Substrate Specificity in Iridium-Catalyzed Ketone Hydrosilylation

Anthony R. Chianese, Allen Mo, and Dibyadeep Datta

Organometallics, 2009, 28 (2), 465-472 • DOI: 10.1021/om800878m • Publication Date (Web): 19 December 2008

Downloaded from <http://pubs.acs.org> on April 10, 2009



More About This Article

Additional resources and features associated with this article are available within the HTML version:

- Supporting Information
- Access to high resolution figures
- Links to articles and content related to this article
- Copyright permission to reproduce figures and/or text from this article

[View the Full Text HTML](#)



ACS Publications
High quality. High impact.

Flexible, Bowl-Shaped N-Heterocyclic Carbene Ligands: Substrate Specificity in Iridium-Catalyzed Ketone Hydrosilylation

Anthony R. Chianese,* Allen Mo, and Dibyadeep Datta

Department of Chemistry, Colgate University, 13 Oak Drive, Hamilton, New York 13346

Received September 9, 2008

A series of benzimidazolium chlorides was synthesized as precursors to N-heterocyclic carbene ligands, with N-substituents varying in size from 3,5-xylyl (**1a**) to first-generation dendritic 3,5-bis(3,5-*tert*-butylphenyl)phenyl (**1b**), to the second-generation 3,5-bis[3,5-bis(3,5-*tert*-butylphenyl)phenyl]phenyl (**1c**). The dendritic side groups of **1b** and **1c** form a flexible, bowl-like cavity. Iridium complexes of **1a–c** were synthesized and were shown to be catalytically active for the hydrosilylation of aryl methyl ketones. The dendritic ligands **1b** and **1c** effect a moderate level of substrate specificity in the competitive hydrosilylation of ketones of varying size. In the competitive hydrosilylation of acetophenone versus 3-(3,5-*tert*-butylphenyl)acetophenone, acetophenone is consumed approximately 3.7 times more quickly using the second-generation ligand **1c**. Using the control ligand **1a**, this ratio is 1.8.

Introduction

A central goal in synthetic chemistry is the development of organic transformations that are simultaneously general and specific. The most widely useful methods offer predictable selectivity for a well-defined class of substrates, ideally tolerating variations in substrate auxiliary functionality and steric size. Homogeneous catalysis is at the center of this effort, as rational and empirical variation of the catalyst structure provides a versatile, cost-effective manifold for optimizing the reaction outcome. Enzymes are known for their often extreme substrate specificity, but Nature has also evolved catalysts with synthetically useful generality, as evidenced by the utility of lipases in kinetic resolutions.¹

Efforts at bridging the gap between traditional synthetic catalysis and the exquisite, superstructure-directed selectivity exhibited by enzymes are challenging, but many successes² motivate continued study. For example, Nolte et al.,³ Gibson and Rebek,⁴ and Crabtree, Brudvig, et al.⁵ have observed substrate recognition in transition metal catalysis using rationally designed, host-like ligands. Breit and co-workers^{6–8} and Reek and co-workers⁹ have employed recognition in ligand self-assembly. Nguyen, Hupp, et al.¹⁰ and Wärnmark et al.¹¹ have employed self-assembled catalysts for specificity, while Ray-

mond, Bergman, et al.^{12,13} have demonstrated selective catalysis inside enclosed self-assembled containers. Mirkin and co-workers^{14,15} have designed allosterically regulated catalysts.

One strategy that mimics some features of enzyme catalysis is to enclose a catalyst in the core of a dendrimer.^{16–22} With higher generations, the reaction microenvironment is defined increasingly by the dendrimer structure rather than the solvent. Interesting and potentially useful effects have been observed, including increased catalyst activity,^{23,24} varied selectivity,^{25–27} and substrate specificity.^{28,29}

This report describes the synthesis of dendritic N-heterocyclic carbene (NHC)³⁰ ligands expected to exhibit a bowl-like topology and their application to iridium-catalyzed ketone hydrosilylation, with an emphasis on discrimination between

* To whom correspondence should be addressed. E-mail: achianese@colgate.edu.

- (1) Turner, N. J. *Curr. Opin. Chem. Biol.* **2004**, *8*, 114–119.
- (2) Das, S.; Brudvig, G. W.; Crabtree, R. H. *Chem. Commun.* **2008**, 413–424.
- (3) Coolen, H. K. A. C.; Meeuwis, J. A. M.; Van Leeuwen, P. W. M. N.; Nolte, R. J. M. *J. Am. Chem. Soc.* **1995**, *117*, 11906–11913.
- (4) Gibson, C.; Rebek, J. *Org. Lett.* **2002**, *4*, 1887–1890.
- (5) Das, S.; Incarvito, C. D.; Crabtree, R. H.; Brudvig, G. W. *Science* **2006**, *312*, 1941–1943.
- (6) Weis, M.; Waloch, C.; Seiche, W.; Breit, B. *J. Am. Chem. Soc.* **2006**, *128*, 4188–4189.
- (7) Breit, B.; Seiche, W. *Angew. Chem., Int. Ed.* **2005**, *44*, 1640–1643.
- (8) Breit, B.; Seiche, W. *J. Am. Chem. Soc.* **2003**, *125*, 6608–6609.
- (9) Kuil, M.; Soltner, T.; van Leeuwen, P.; Reek, J. N. H. *J. Am. Chem. Soc.* **2006**, *128*, 11344–11345.
- (10) Merlau, M. L.; Mejia, M. D. P.; Nguyen, S. T.; Hupp, J. T. *Angew. Chem., Int. Ed.* **2001**, *40*, 4239–4242.
- (11) Jónsson, S.; Odille, F. G. J.; Norrby, P. O.; Wärnmark, K. *Chem. Commun.* **2005**, 549–551.

- (12) Fiedler, D.; Leung, D. H.; Bergman, R. G.; Raymond, K. N. *Acc. Chem. Res.* **2005**, *38*, 349–358.
- (13) Fiedler, D.; Bergman, R. G.; Raymond, K. N. *Angew. Chem., Int. Ed.* **2004**, *43*, 6748–6751.
- (14) Gianneschi, N. C.; Nguyen, S. T.; Mirkin, C. A. *J. Am. Chem. Soc.* **2005**, *127*, 1644–1645.
- (15) Gianneschi, N. C.; Bertin, P. A.; Nguyen, S. T.; Mirkin, C. A.; Zakharov, L. N.; Rheingold, A. L. *J. Am. Chem. Soc.* **2003**, *125*, 10508–10509.
- (16) Brunner, H. *J. Organomet. Chem.* **1995**, *500*, 39–46.
- (17) Smith, D. K.; Diederich, F. *Chem.–Eur. J.* **1998**, *4*, 1353–1361.
- (18) Astruc, D.; Chardac, F. *Chem. Rev.* **2001**, *101*, 2991–3023.
- (19) Oosterom, G. E.; Reek, J. N. H.; Kamer, P. C. J.; van Leeuwen, P. *Angew. Chem., Int. Ed.* **2001**, *40*, 1828–1849.
- (20) Twyman, L. J.; King, A. S. H.; Martin, I. K. *Chem. Soc. Rev.* **2002**, *31*, 69–82.
- (21) Helms, B.; Fréchet, J. M. J. *Adv. Synth. Catal.* **2006**, *348*, 1125–1148.
- (22) Méry, D.; Astruc, D. *Coord. Chem. Rev.* **2006**, *250*, 1965–1979.
- (23) Fujihara, T.; Obora, Y.; Tokunaga, M.; Sato, H.; Tsuji, Y. *Chem. Commun.* **2005**, 4526–4528.
- (24) Müller, C.; Ackerman, L. J.; Reek, J. N. H.; Kamer, P. C. J.; van Leeuwen, P. W. N. M. *J. Am. Chem. Soc.* **2004**, *126*, 14960–14963.
- (25) Ooe, M.; Murata, M.; Mizugaki, T.; Ebitani, K.; Kaneda, K. *J. Am. Chem. Soc.* **2004**, *126*, 1604–1605.
- (26) Oosterom, G. E.; van Haaren, R. J.; Reek, J. N. H.; Kamer, P. C. J.; van Leeuwen, P. W. N. M. *J. Am. Chem. Soc.* **1999**, 1119–1120.
- (27) Sato, H.; Fujihara, T.; Obora, Y.; Tokunaga, M.; Kiyosu, J.; Tsuji, Y. *Chem. Commun.* **2007**, 269–271.
- (28) Bhyrappa, P.; Young, J. K.; Moore, J. S.; Suslick, K. S. *J. Am. Chem. Soc.* **1996**, *118*, 5708–5711.
- (29) Chow, H. F.; Mak, C. C. *J. Org. Chem.* **1997**, *62*, 5116–5127.
- (30) Herrmann, W. A. *Angew. Chem., Int. Ed.* **2002**, *41*, 1290–1309.

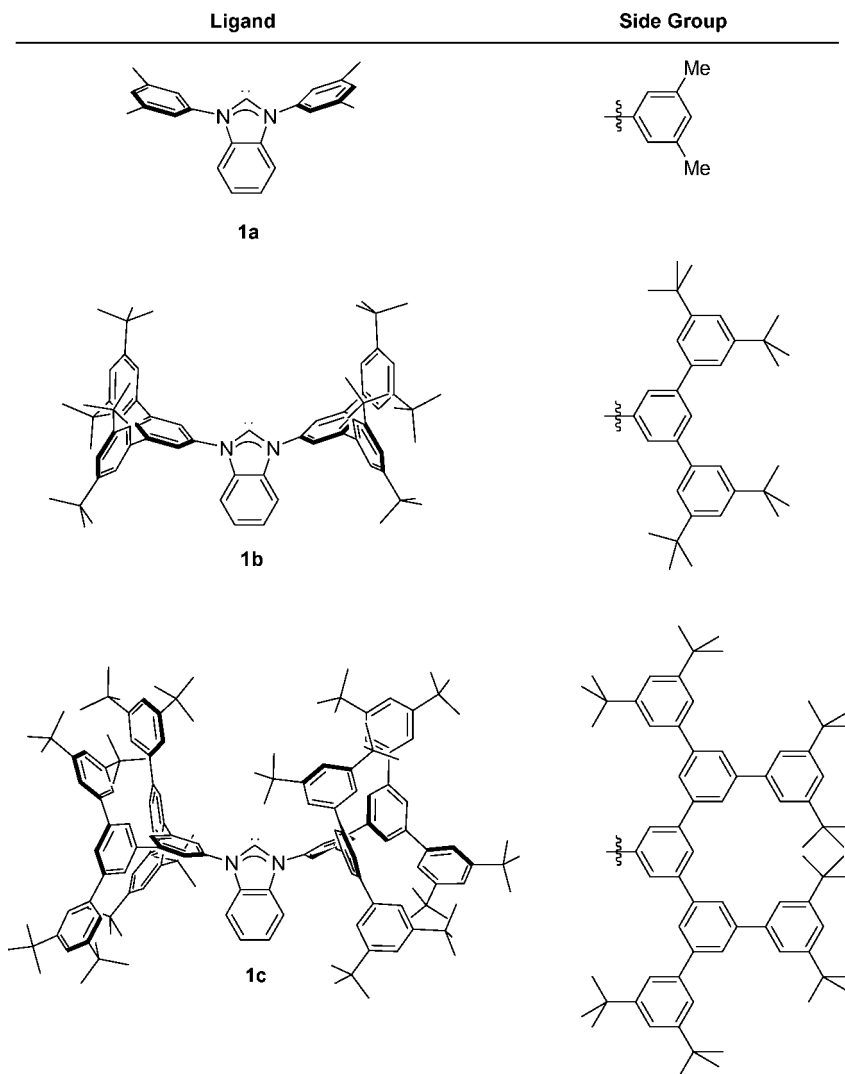


Figure 1. N-Heterocyclic carbene ligands with *m*-phenylene dendritic side groups.

aryl methyl ketone substrates of varying size. Substrate specificity has been explored using competition experiments continuously monitored by NMR spectroscopy. The largest ligand employed, **1c**, exhibits modest specificity for smaller ketone substrates over larger ones, as compared to smaller control ligands **1a** and **1b**. The smallest and largest iridium-NHC precatalysts have been structurally characterized by X-ray crystallography.

Results and Discussion

Ligand Design and Synthesis. Inspection of molecular models indicates that for NHC ligands with dendritic side groups based on a 1,3,5-substituted aromatic monomer unit as shown in Figure 1, the carbene lone pair (or bound metal atom) rests at the bottom of a roughly bowl-shaped cavity. The structure may be highly rigid or semiflexible, depending on hindrance of rotation about the aryl–aryl linkages. Goto and Kawashima have used the same meta-terphenyl framework in the synthesis of bowl-shaped tertiary phosphine ligands, which have an extremely large cone angle, estimated at 206° .^{31,32} Tsuji and

co-workers have employed phosphine ligands of this nature in palladium-catalyzed Suzuki–Miyaura coupling³³ and rhodium-catalyzed ketone hydrosilylation. A significant rate enhancement was observed for the latter reaction, caused by enhanced formation of monophosphine–rhodium species.^{34,35} Ding and co-workers have shown that achiral bowl-shaped phosphine ligands are also useful for Ru-catalyzed asymmetric hydrogenation of ketones.³⁶ Goto and Kawashima have also reported the synthesis of an NHC with meta-terphenyl side groups; a derived Pd⁰ complex exhibited unique reactivity toward CO₂ and O₂.³⁷

Benzimidazolium precursors to **1a–c** were synthesized as shown in Scheme 1. The simplest ligand precursor, **1a·HCl**, was prepared via Buchwald–Hartwig amination^{38,39} of 1,2-

(33) Ohta, H.; Tokunaga, M.; Obora, Y.; Iwai, T.; Iwasawa, T.; Fujihara, T.; Tsuji, Y. *Org. Lett.* **2007**, *9*, 89–92.

(34) Niyomura, O.; Iwasawa, T.; Sawada, N.; Tokunaga, M.; Obora, Y.; Tsuji, Y. *Organometallics* **2005**, *24*, 3468–3475.

(35) Niyomura, O.; Tokunaga, M.; Obora, Y.; Iwasawa, T.; Tsuji, Y. *Angew. Chem., Int. Ed.* **2003**, *42*, 1287–1289.

(36) Jing, Q.; Zhang, X.; Sun, H.; Ding, K. L. *Adv. Synth. Catal.* **2005**, *347*, 1193–1197.

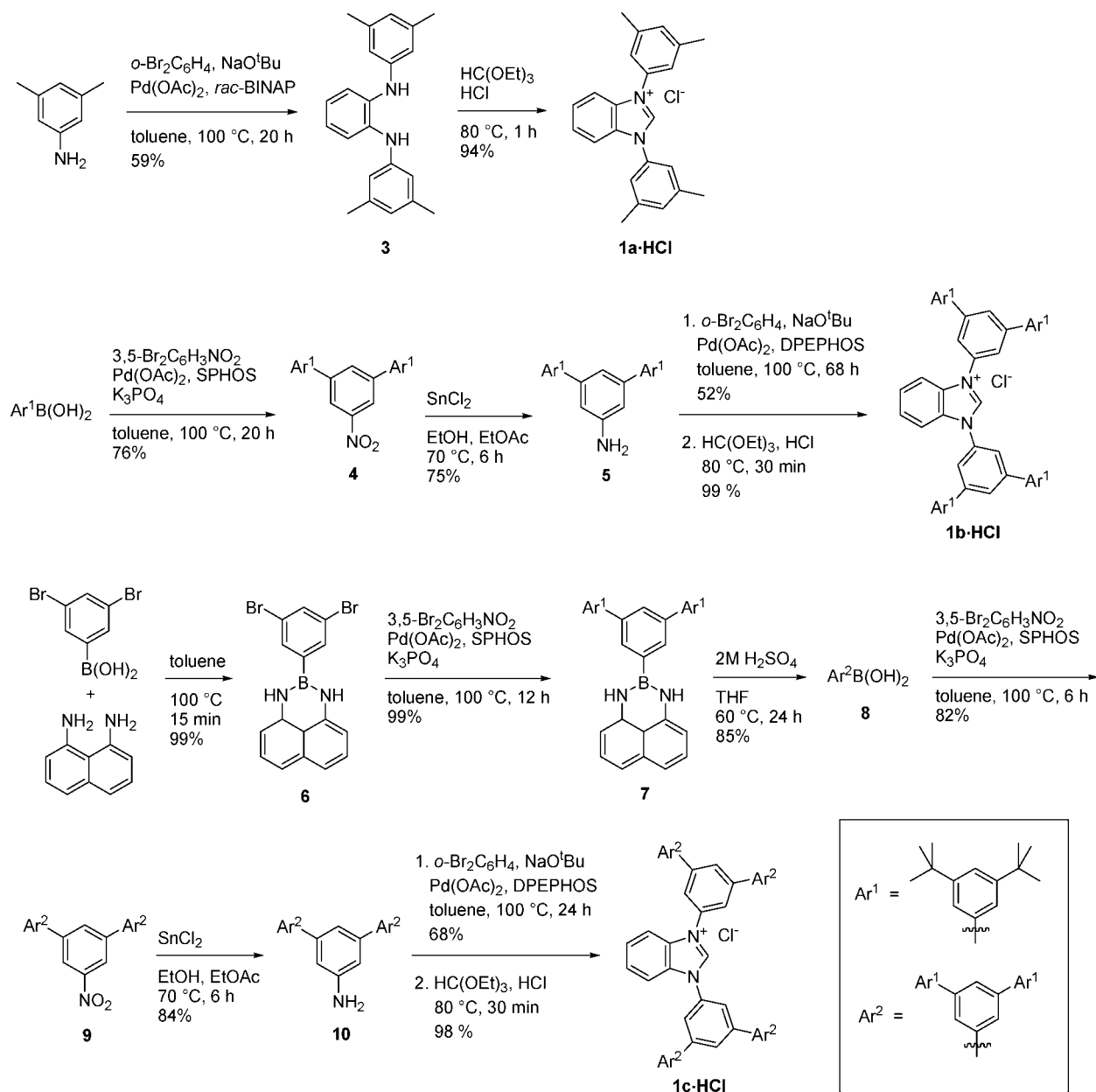
(37) Yamashita, M.; Goto, K.; Kawashima, T. *J. Am. Chem. Soc.* **2005**, *127*, 7294–7295.

(38) Hartwig, J. F.; Kawatsura, M.; Hauck, S. I.; Shaughnessy, K. H.; Alcazar-Roman, L. M. *J. Org. Chem.* **1999**, *64*, 5575–5580.

(39) Sadighi, J. P.; Harris, M. C.; Buchwald, S. L. *Tetrahedron Lett.* **1998**, *39*, 5327–5330.

(31) Ohzu, Y.; Goto, K.; Kawashima, T. *Angew. Chem., Int. Ed.* **2003**, *42*, 5714–5717.

(32) Ohzu, Y.; Goto, K.; Sato, H.; Kawashima, T. *J. Organomet. Chem.* **2005**, *690*, 4175–4183.

Scheme 1. Synthesis of Benzimidazolium Salts **1a–c**·HCl⁴³

dibromobenzene with 3,5-dimethylaniline to give **3**, followed by treatment with triethyl orthoformate and HCl.⁴⁰ To prepare the first-generation dendrimer **1b**·HCl, nitroarene **4** was synthesized by the Suzuki coupling⁴¹ of 3,5-di-*tert*-butylbenzeneboronic acid with 3,5-dibromonitrobenzene. Reduction of the nitro group⁴² then gave the aniline **5**, from which benzimidazolium salt **1b**·HCl was acquired analogously to **1a**·HCl.

To synthesize the second-generation **1c**·HCl, Suginome's procedure for boronic acid masking was employed.⁴⁴ First, 3,5-dibromobenzeneboronic acid was protected with 1,8-diaminonaphthalene to give **6**. Reaction with 3,5-di-*tert*-butylbenzeneboronic acid under Buchwald's optimized conditions for Suzuki

coupling⁴¹ gave **7** in high yield, and deprotection with aqueous acid in THF⁴⁴ yielded boronic acid **8**. Coupling with 3,5-dibromonitrobenzene gave **9**, and nitro-group reduction gave **10**. Palladium-catalyzed amination of 1,2-dibromobenzene followed by treatment with triethyl orthoformate and HCl then gave the desired benzimidazolium chloride **1c**·HCl.

Synthesis and Characterization of Iridium Complexes. Neutral iridium(I) complexes of ligands **1a–c** were synthesized by Lin's method⁴⁵ of transmetalation from intermediate silver(I) complexes **1a–c**·AgCl (Scheme 2). Metalation of the benzimidazolium salts **1a–c**·HCl using Ag_2O was monitored by ¹H NMR spectroscopy, but the silver complexes were not isolated as described by Lin and co-workers. Instead, $[\text{Ir}(\text{cod})\text{Cl}]_2$ (cod = 1,5-cyclooctadiene) was added directly to the dichlo-

(40) Khranov, D. M.; Boydston, A. J.; Bielawski, C. W. *Org. Lett.* **2006**, *8*, 1831–1834.

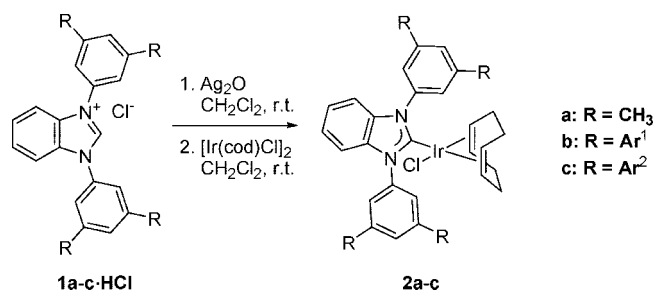
(41) Walker, S. D.; Barder, T. E.; Martinelli, J. R.; Buchwald, S. L. *Angew. Chem., Int. Ed.* **2004**, *43*, 1871–1876.

(42) McDonald, I. M.; Black, J. W.; Buck, I. M.; Dunstone, D. J.; Griffin, E. P.; Harper, E. A.; Hull, R. A. D.; Kalindjian, S. B.; Lilley, E. J.; Linney, I. D.; Pether, M. J.; Roberts, S. P.; Shaxted, M. E.; Spencer, J.; Steel, K. I. M.; Sykes, D. A.; Walker, M. K.; Watt, G. F.; Wright, L.; Wright, P. T.; Xun, W. *J. Med. Chem.* **2007**, *50*, 3101–3112.

(43) Abbreviations: *rac*-BINAP = *rac*-2,2'-bis(diphenylphosphino)-1,1'-binaphthyl; SPHOS = 2-dicyclohexylphosphino-2',6'-dimethoxy-1,1'-biphenyl; DPEPHOS = bis(2-diphenylphosphinophenyl) ether.

(44) Noguchi, H.; Hojo, K.; Suginome, M. *J. Am. Chem. Soc.* **2007**, *129*, 758–759.

(45) Wang, H. M. J.; Lin, I. J. B. *Organometallics* **1998**, *17*, 972–975.

Scheme 2. Synthesis of Iridium Complexes **2a–c**

romethane solutions of **1a–c·AgCl**. Precipitation of silver chloride was observed immediately, but the mixtures were allowed to stir at room temperature for 30 min before workup. Iridium complexes **2a–c** were isolated by silica gel chromatography in 36–58% yield.

The ¹H and ¹³C NMR spectra for **2a–c** are as expected for complexes of the general formula Ir(NHC)(cod)Cl.^{46–50} Cyclooctadiene vinylic hydrogens appear in the range 2.50–2.74 ppm for the alkene moiety trans to chloride; those trans to the NHC ligand appear at 4.49–4.61 ppm, indicative of the larger trans influence of the NHC ligand. The carbene carbon resonates at 192.0–193.3 ppm. For **2a**, the four methyl groups are chemically equivalent by ¹H and ¹³C NMR; the same is true for the ortho-CH groups and the meta-*ipso* carbons. This indicates that rotation about the N–C single bonds is fast on the NMR time scale. For **2b** and **2c**, a broadened resonance is observed for the four hydrogens closest to the benzimidazole ring in the ¹H NMR spectrum; the associated carbon signal is also broad in the ¹³C NMR spectrum. This is consistent with rotation about the N–C bonds near the fast exchange limit.

Complexes **2a** and **2c** were structurally characterized by X-ray crystallography. Figure 2 shows the structure of **2a**. Figure 3 shows the full structure of **2c**, and Figure 4 shows a close-up view of the organometallic fragment. Relevant distances and angles are given in Table 1 (**2a**) and Table 2 (**2c**). The structural parameters for **2a** and **2c** are consistent with previously characterized related complexes.^{47,51,52} The Ir–C_{NHC} distances of 2.007 Å (**2a**) and 2.008 Å (**2c**) are within the expected range. The unsymmetrical binding of cyclooctadiene reflects the larger trans influence of the NHC ligand as compared to chloride: the distance between Ir and the alkene centroid trans to the NHC ligand is 2.063 Å for **2a** and 2.063 for **2c**, while the distance to the alkene centroid trans to chloride is 1.981 Å for **2a** and 1.995 for **2c**. As is generally observed for monodentate NHC ligands, the benzimidazol-2-ylidene ring plane is orthogonal to the iridium coordination plane.

The crystal structure of **2c** confirms what is predicted by molecular models: that NHC ligand **1c** forms a loose pocket around the iridium center, which is expected to impose an

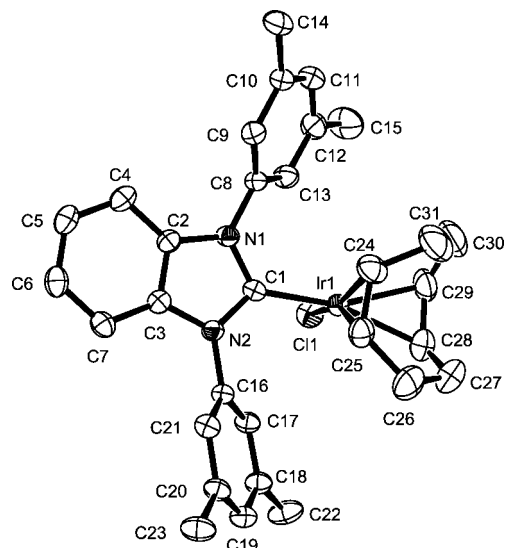


Figure 2. ORTEP diagram of **2a**, showing 50% probability ellipsoids. Hydrogen atoms are omitted for clarity.

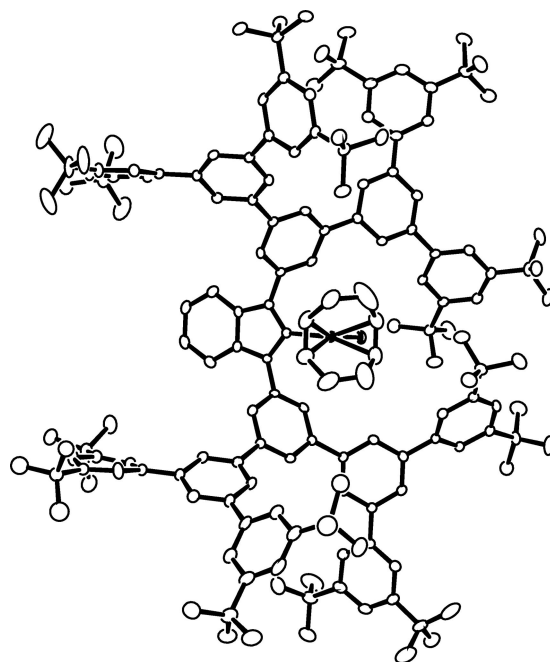


Figure 3. ORTEP diagram of **2c**, showing 50% probability ellipsoids. Hydrogen atoms are omitted for clarity.

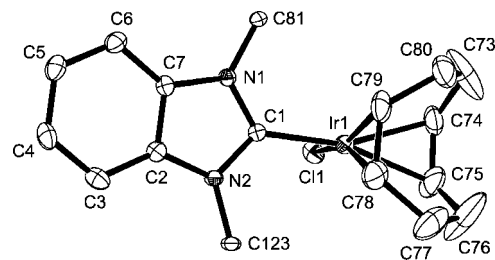


Figure 4. ORTEP diagram of **2c**, showing 50% probability ellipsoids. Side groups attached to C(81) and C(123) are excluded, and hydrogen atoms are omitted for clarity.

energetic cost as the side groups rearrange to accommodate a large incoming substrate.

Ketone Hydrosilylation. The hydrosilylation of carbonyl compounds to give silyl ethers is a useful transformation, as

(46) Herrmann, W. A.; Elison, M.; Fischer, J.; Kocher, C.; Artus, G. R. J. *Chem.–Eur. J.* **1996**, *2*, 772–780.

(47) Chianese, A. R.; Li, X. W.; Janzen, M. C.; Faller, J. W.; Crabtree, R. H. *Organometallics* **2003**, *22*, 1663–1667.

(48) Stylianides, N.; Danopoulos, A. A.; Tsoureas, N. *J. Organomet. Chem.* **2005**, *690*, 5948–5958.

(49) Kelly, R. A.; Clavier, H.; Giudice, S.; Scott, N. M.; Stevens, E. D.; Bordner, J.; Samardjiev, I.; Hoff, C. D.; Cavallo, L.; Nolan, S. P. *Organometallics* **2008**, *27*, 202–210.

(50) Zanardi, A.; Peris, E.; Mata, J. A. *New J. Chem.* **2008**, *32*, 120–126.

(51) Seo, H.; Kim, B. Y.; Lee, J. H.; Park, H. J.; Son, S. U.; Chung, Y. K. *Organometallics* **2003**, *22*, 4783–4791.

(52) Herrmann, W. A.; Baskakov, D.; Herdtweck, E.; Hoffmann, S. D.; Bunlaksanusorn, T.; Rampf, F.; Rodefeld, L. *Organometallics* **2006**, *25*, 2449–2456.

Table 1. Selected Bond Lengths and Angles for 2a

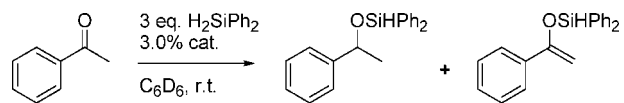
		Bond Lengths (Å)	
Ir(1)—C(1)	2.007(4)	Ir(1)—C(25)	2.106(4)
Ir(1)—Cl(1)	2.384(1)	Ir(1)—C(28)	2.189(5)
Ir(1)—C(24)	2.101(4)	Ir(1)—C(29)	2.165(5)
		Bond Angles (deg)	
N(1)—C(1)—N(2)	105.2(3)	N(2)—C(1)—Ir(1)	128.5(3)
N(1)—C(1)—Ir(1)	126.1(3)	C(1)—Ir(1)—Cl(1)	92.65(10)
		Torsion Angles (deg)	
N(1)—C(1)—Ir(1)—Cl(1)		−92.2(3)	
N(2)—C(1)—Ir(1)—Cl(1)		93.7(3)	

Table 2. Selected Bond Lengths and Angles for 2c

		Bond Lengths (Å)	
Ir(1)—C(1)	2.008(3)	Ir(1)—C(75)	2.179(4)
Ir(1)—Cl(1)	2.3654(8)	Ir(1)—C(78)	2.108(4)
Ir(1)—C(74)	2.169(3)	Ir(1)—C(79)	2.124(3)
		Bond Angles (deg)	
N(1)—C(1)—N(2)	105.4(2)	N(2)—C(1)—Ir(1)	127.3(2)
N(1)—C(1)—Ir(1)	127.20(19)	C(1)—Ir(1)—Cl(1)	92.20(8)
		Torsion Angles (deg)	
N(1)—C(1)—Ir(1)—Cl(1)		−96.1(2)	
N(2)—C(1)—Ir(1)—Cl(1)		87.5(2)	

protected alcohols can be produced directly from ketone or aldehyde precursors. Catalyst systems employing a wide variety of transition metal complexes have been developed, including several highly enantioselective systems for the asymmetric reduction of prochiral ketones.^{53,54} Rhodium complexes are often employed, but the use of less expensive iridium is increasingly common,^{55–62} in one case giving usefully distinct enantioselectivity.^{63,64} Rhodium and iridium complexes of N-heterocyclic carbenes are well known as catalysts for ketone hydrosilylation,^{23,60,65–78} so this reaction is a potentially useful testbed for comparing the steric influence of ligands **1a–c** in catalysis. Iridium complexes **2a–c** proved to be active precatalysts for the hydrosilylation of aryl methyl ketones using diphenylsilane at room temperature. Hydrosilylation of acetophenone **11a**, performed in benzene-*d*₆ with 3.0 equiv of silane and 3 mol % catalyst, reaches full conversion in 3–17 h, depending on the ligand (Table 3). In each case, the major product is the silyl ether **12a**, while 4% of the enol silyl ether **13a**, a product of dehydrogenative silylation, is formed. A slight decrease in the yield (NMR) of **12a** with increasing size of the NHC ligand is observed.

To assess whether ligands that form a bowl-shaped cavity such as **1b** and **1c** can promote substrate specificity based on size and shape, the series of aryl methyl ketones shown in Figure

Table 3. Hydrosilylation of Acetophenone Using Catalysts 2a–c^a

entry	catalyst	time (h)	NMR yield 12a	NMR yield 13a
1	2a	3	92%	4%
2	2b	16	87%	4%
3	2c	17	84%	4%

^a Initial concentration: 0.074 M **11a** in benzene-*d*₆. Yields calculated by ¹H NMR spectroscopy using 1,3,5-trimethoxybenzene as internal standard.

5 was employed. Internal competition experiments were performed for each catalyst **2a–c**, comparing the reactivity of acetophenone (**11a**) with larger ketones **11b–d** of varying size and shape. For each experiment, the conversion of both substrates was monitored continuously by ¹H NMR. For each catalyst and pair of substrates, Figure 6 shows the ratio of

(53) Díez-González, S.; Nolan, S. P. *Org. Prep. Proced. Int.* **2007**, 39, 523–559.

(54) Carpentier, J. F.; Bette, V. *Curr. Org. Chem.* **2002**, 6, 913–936.

(55) Kinting, A.; Kreuzfeld, H. J.; Abicht, H. P. *J. Organomet. Chem.* **1989**, 370, 343–349.

(56) Faller, J. W.; Chase, K. J. *Organometallics* **1994**, 13, 989–992.

(57) Nishibayashi, Y.; Singh, J. D.; Segawa, K.; Fukuzawa, S.; Uemura, S. *J. Chem. Soc., Chem. Commun.* **1994**, 1375–1376.

(58) Nishibayashi, Y.; Segawa, K.; Singh, J. D.; Fukuzawa, S.; Ohe, K.; Uemura, S. *Organometallics* **1996**, 15, 370–379.

(59) Karame, I.; Tommasino, M. L.; Lemaire, M. *J. Mol. Catal. A: Chem.* **2003**, 196, 137–143.

(60) Chianese, A. R.; Crabtree, R. H. *Organometallics* **2005**, 24, 4432–4436.

(61) Cuervo, D.; Díez, J.; Gamasa, M. P.; Gimeno, J.; Paredes, P. *Eur. J. Inorg. Chem.* **2006**, 599–608.

(62) Gómez, M.; Jansat, S.; Muller, G.; Bonnet, M. C.; Breuzard, J. A. J.; Lemaire, M. *J. Organomet. Chem.* **2002**, 659, 186–195.

(63) Nishibayashi, Y.; Segawa, K.; Ohe, K.; Uemura, S. *Organometallics* **1995**, 14, 5486–5487.

(64) Nishibayashi, Y.; Segawa, K.; Takada, H.; Ohe, K.; Uemura, S. *Chem. Commun.* **1996**, 847–848.

(65) Lappert, M. F.; Maskell, R. K. *J. Organomet. Chem.* **1984**, 264, 217–28.

(66) Herrmann, W. A.; Goossen, L. J.; Köcher, C.; Artus, G. R. *J. Angew. Chem., Int. Ed. Engl.* **1996**, 35, 2805–2807.

(67) Enders, D.; Gielen, H.; Breuer, K. *Tetrahedron: Asymmetry* **1997**, 8, 3571–3574.

(68) Enders, D.; Gielen, H.; Runsink, J.; Breuer, K.; Brode, S.; Boehn, K. *Eur. J. Inorg. Chem.* **1998**, 913–919.

(69) Duan, W. L.; Shi, M.; Rong, G. B. *Chem. Commun.* **2003**, 2916–2917.

(70) Rivera, G.; Crabtree, R. H. *J. Mol. Catal. A: Chem.* **2004**, 222, 59–73.

(71) Cesar, V.; Bellemin-Lapponnaz, S.; Wadepohl, H.; Gade, L. H. *Chem.—Eur. J.* **2005**, 11, 2862–2873.

(72) Yiğit, M.; Özdemir, I.; Çetinkaya, B.; Çetinkaya, E. *J. Mol. Catal. A: Chem.* **2005**, 241, 88–92.

(73) Yuan, Y.; Raabe, G.; Bolm, C. *J. Organomet. Chem.* **2005**, 690, 5747–5752.

(74) Chen, T.; Liu, X. G.; Shi, M. *Tetrahedron* **2007**, 63, 4874–4880.

(75) Özdemir, I.; Yiğit, M.; Yiğit, B.; Çetinkaya, B.; Çetinkaya, E. *J. Coord. Chem.* **2007**, 60, 2377–2384.

(76) Sato, H.; Fujihara, T.; Obora, Y.; Tokunaga, M.; Kiyosu, J.; Tsuji, Y. *Chem. Commun.* **2007**, 269–271.

(77) Wolf, J.; Labande, A.; Daran, J. C.; Poli, R. *Eur. J. Inorg. Chem.* **2007**, 5069–5079.

(78) Nonnenmacher, M.; Kunz, D.; Rominger, F. *Organometallics* **2008**, 27, 1561–1568.

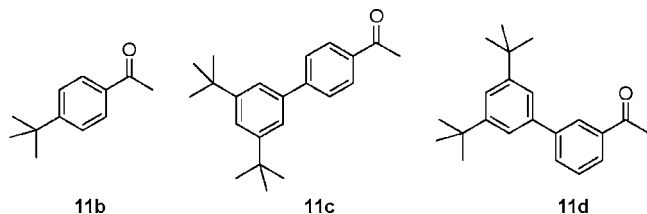


Figure 5. Aryl methyl ketones of varying size and shape.

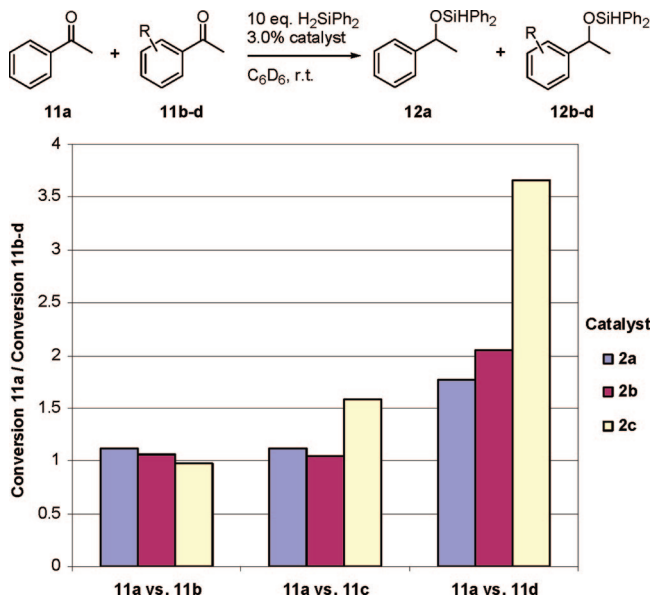


Figure 6. Results of internal competitive hydrosilylation of **11a** versus **11b–d**. The ratio of conversion **11a/11b–d** is reported at 25% conversion of **11a**.

conversion **11a/11b–d**, when **11a** is 25% consumed.⁷⁹ As one might expect, no discrimination is observed between **11a** and **11b** using any catalyst, the only difference being the para *tert*-butyl group of **11b**. For the competitive hydrosilylation of **11a** versus **11c**, which has a large 3,5-di-*tert*-butylphenyl group at the para position, catalyst **2c** exhibits a slight discrimination, while catalysts **2a** and **2b** still show none. For **11a** versus **11d**, where the bulky di-*tert*-butylphenyl group is installed at the meta position, the unsubstituted **11a** is consumed more rapidly using any catalyst, but the second-generation catalyst **2c** shows the largest effect, as **11a** is consumed approximately 3.7 times more quickly than **11d**. Figure 7 shows the time course of competition experiments between **11a** and **11d**.⁷⁹ It is apparent that both substrates are smoothly consumed throughout the course of the experiment and that the discrimination between **11a** and **11d** increases as the size of the NHC ligand is increased. It is also noteworthy that catalyst initiation and/or decomposition do not appear to pose a problem under these conditions.

Conclusion

A series of benzimidazole-based N-heterocyclic carbene ligands was synthesized as the hydrochloride salts, with N-substituents varying in size from a simple 3,5-xylyl group to first- and second-generation meta-phenylene-linked dendrimers that form a flexible, bowl-like cavity. Iridium complexes were synthesized and were shown to be catalytically active for the hydrosilylation of aryl methyl ketones. The largest ligand, **1c**,

affects a moderate level of substrate specificity in the competitive hydrosilylation of ketones of varying size and shape. Current efforts are directed at the development of ligands with conformationally more rigid dendritic side groups, which may improve the level of discrimination between substrates or between different carbonyl groups in the same substrate molecule.

Experimental Section

General Methods. $[\text{Ir}(\text{cod})\text{Cl}]_2$ was prepared as previously described.⁸⁰ All other materials were commercially available and were used as received, unless otherwise noted. All solvents were reagent grade. Synthesis was performed using solvents that were sparged with argon, then passed through columns of activated alumina. Catalytic experiments were performed in benzene-*d*₆, which was dried over activated 3.5 Å molecular sieves, but was not purified further. Isolated yields are given for all products. NMR spectra were recorded on a Bruker spectrometer operating at 400 MHz (¹H NMR) and 100 MHz (¹³C NMR) and referenced to the residual solvent resonance (δ in parts per million, and J in Hz). NMR spectra were recorded at room temperature. Elemental analyses were performed by Robertson Microлит, Madison, NJ.

Iridium Complex 2a. Benzimidazolium salt **1a**·HCl (160 mg, 0.44 mmol) and Ag₂O (56 mg, 0.24 mmol) were combined in a 25 mL Schlenk flask, and 10 mL of dry, degassed dichloromethane was added under argon. After stirring for 30 min, the flask was opened, and $[\text{Ir}(\text{cod})\text{Cl}]_2$ (147 mg, 0.22 mmol) was added. The mixture was stirred for an additional 30 min, opened, and filtered through Celite, washing with dichloromethane. The crude product was purified by flash chromatography on silica gel, first washing with dichloromethane, then eluting the product with 1:1 ethyl acetate/dichloromethane. The product was recrystallized from CH₂Cl₂/pentane. Yield: 170 mg, 58%. ¹H NMR (CDCl₃): δ 7.69 (s, 4H); 7.35 (AA'BB', 2H, ³J_{HH} = 6.2 Hz, ⁴J_{HH} = 3.3 Hz); 7.23 (AA'BB', 2H, ³J_{HH} = 6.2 Hz, ⁴J_{HH} = 3.3); 7.14 (s, 2H); 4.49 (m, 2H); 2.50 (m, 2H); 2.46 (s, 12H); 1.74 (m, 2H); 1.45 (m, 4H); 1.25 (m, 2H). ¹³C NMR (CDCl₃): δ 192.0; 138.6; 137.6; 135.7; 130.0; 125.3; 123.2; 111.2; 84.7; 52.1; 33.1; 29.2; 21.5. Anal. Calcd for C₃₁H₃₄ClIrN₂: C, 56.22; H, 5.17; N, 4.23. Found: C, 56.22; H, 5.18; N, 4.20.

Iridium Complex 2b. Benzimidazolium salt **1b**·HCl (0.146 mmol, 150 mg) and Ag₂O (0.081 mmol, 18.8 mg) were combined in a 25 mL Schlenk flask, and 4 mL of dry, degassed dichloromethane was added under argon. After stirring for 30 min, the flask was opened, and $[\text{Ir}(\text{cod})\text{Cl}]_2$ (0.073 mmol, 48.8 mg) was added; a white precipitate was observed immediately. The mixture was stirred for an additional 30 min and then filtered through Celite. The solvent was evaporated, and the residue was purified by flash chromatography on silica gel, using 2% EtOAc in hexanes as eluent. The product was recrystallized by slow evaporation of a CH₂Cl₂/benzene solution. Yield: 72 mg, 36%. ¹H NMR (CDCl₃): δ 8.33 (4H, br s), δ 8.03 (2H, s), δ 7.70 (8H, s), δ 7.52 (6H, m), δ 7.32 (2H, aa'bb', ³J_{HH} = 6.1 Hz, ⁴J_{HH} = 3.2 Hz), δ 4.58 (2H, m), δ 2.6 (2H, m), δ 1.43 (72H, s), δ 1.66–1.16 (8H, m). ¹³C NMR (CDCl₃): 193.3, 151.7, 143.6, 139.9, 138.3, 135.9, 126.6, 125.6, 123.5, 122.1, 122.1, 111.1, 85.8, 52.7, 35.3, 33.1, 31.7, 29.2. The coincidence at 122.1 ppm was verified by HMQC. Anal. Calcd for C₈₃H₁₀₆ClIrN₂: C, 73.33; H, 7.86; N, 2.06. Found: C, 73.27; H, 8.01; N, 1.96.

Iridium Complex 2c. Compound **1c**·HCl (77.2 μ mol) was dissolved in 5 mL of CH₂Cl₂, and silver(I) oxide (18 mg, 77 μ mol) was added. The mixture was stirred under argon for 1 h, and $[\text{Ir}(\text{cod})\text{Cl}]_2$ (26 mg, 39 μ mol) was added. After stirring for 30 min, the mixture was filtered through Celite. The volatiles were removed, and the residue was purified by flash chroma-

(79) See Supporting Information for conversion data at additional timepoints and additional time course plots.

(80) Lin, Y.; Nomiya, K.; Finke, R. G. *Inorg. Chem.* **1993**, *32*, 6040–6045.

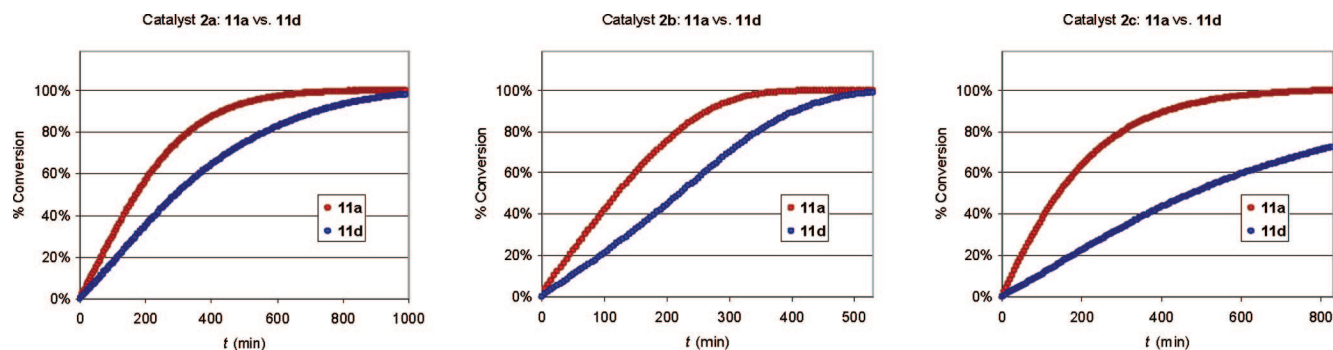


Figure 7. Time course for competition experiments between substrate **11a** and **11d**.

tography on silica gel, eluting with 1% ethyl acetate in hexanes. Some residual hexane was observed even after several days under vacuum at room temperature. Yield: 82 mg, 44%. ^1H NMR (CDCl_3): δ 8.51 (br d, 4H), 8.19 (br t, 2H); 7.95 (d, 8H, $^4J_{\text{HH}} = 1.3$ Hz); 7.81 (t, 4H, $^4J_{\text{HH}} = 1.3$ Hz); 7.58 (aa'bb', 2H, $^3J_{\text{HH}} = 6.1$ Hz, $^4J_{\text{HH}} = 3.2$ Hz); 7.52 (d, 16H, $^4J_{\text{HH}} = 1.6$ Hz); 7.48 (t, 8H, $^4J_{\text{HH}} = 1.6$ Hz); 7.29 (aa'bb', 2H, $^3J_{\text{HH}} = 6.1$ Hz, $^4J_{\text{HH}} = 3.2$ Hz); 4.61 (m, 2H, CH_{cod}); 2.74 (m, 2H, CH_{cod}); 1.7–1.25 (m, 8H, $\text{CH}_2\text{-cod}$); 1.38 (s, 144H). ^{13}C NMR (CDCl_3): δ 193.2, 151.4, 144.2, 143.0, 141.2, 140.9, 138.9, 135.9, 127.2, 126.9, 125.8, 125.6, 123.6, 122.2, 121.9, 111.2, 86.2, 52.9, 35.2, 31.7, 29.9, 22.8. Anal. Calcd for $\text{C}_{163}\text{H}_{202}\text{ClIrN}_2$: C, 81.00; H, 8.42; N, 1.16. Found: C, 80.88; H, 8.40; N, 1.09.

X-ray Structure Determination of 2a. A yellow plate, obtained by slow evaporation of a dichloromethane/pentane solution, was mounted on a Cryoloop with Paratone oil and transferred to a Bruker CCD platform diffractometer. Unit cell determination, data collection, and multiscan absorption correction were performed using the APEX2 program suite. Subsequent calculations were carried out using the SHELXTL⁸¹ program package. The structure was solved by a Patterson projection and refined on F^2 by full-matrix least-squares techniques. All non-hydrogen atoms were refined anisotropically, and hydrogen atoms were placed in calculated positions using a riding model. Details of data collection and refinement are given in Table 4.

X-ray Structure Determination of 2c. A yellow plate, grown by slow evaporation of an ethanol/diethyl ether solution, was mounted on a Cryoloop with Paratone oil and transferred to a Bruker CCD platform diffractometer. Unit cell determination, data collection, and multiscan absorption correction were performed using the APEX2 program suite. Subsequent calculations were carried out using the SHELXTL⁸¹ program package. The structure was solved by direct methods (SHELXS) and refined on F^2 by full-matrix least-squares techniques (SHELXL). In the main residue, a *tert*-butyl group was disordered over two conformations, C(8A)–C(12A) and C(8B)–C(12B); these fragments were restrained using SAME and were refined isotropically. Two diethyl ether molecules were located and included in the model. Correction for residual density of additional disordered solvent was performed using the option SQUEEZE in the program package PLATON.⁸² A total of 79 electrons per unit cell were removed, from a total potential solvent-accessible void of 1441.2 \AA^3 . In the final Fourier difference map, a positive residual density peak of 5.35 $\text{e}/\text{\AA}^3$ was observed, 1.295 \AA from C(78), 1.224 \AA from C(79), and 2.135 \AA from Ir(1). Attempts to account for this density were unsuccessful. All remaining non-hydrogen atoms were refined anisotropically, and hydrogen atoms were placed in calculated positions using a riding model. Details of data collection and refinement are given in Table 4.

Table 4. Crystal Data and Structure Refinement for **2a** and **2c**

	2a	2c
color, shape	yellow, block	yellow, block
empirical formula	$\text{C}_{31}\text{H}_{34}\text{ClIrN}_2$	$\text{C}_{171}\text{H}_{222}\text{ClIrN}_2\text{O}_2$
fw	662.25	2565.32
radiation	Mo $\text{K}\alpha$, 0.71073	Mo $\text{K}\alpha$, 0.71073
temp (K)	100	100
cryst syst	triclinic	triclinic
space group	$P\bar{1}$ (No. 2)	$P\bar{1}$ (No. 2)
unit cell dimens		
<i>a</i> (\AA)	7.9618(18)	20.670(2)
<i>b</i> (\AA)	11.220(3)	21.111(2)
<i>c</i> (\AA)	16.253(4)	21.924(2)
α (deg)	81.661(3)	105.182(1)
β (deg)	83.367(3)	91.662(1)
γ (deg)	70.772(3)	112.457(1)
<i>V</i> (\AA^3)	1352.9(6)	8442.8(14)
<i>Z</i>	2	2
D_{calc} (g cm^{-3})	1.626	1.009
μ (Mo $\text{K}\alpha$) (mm^{-1})	5.055	0.852
cryst size (mm)	$0.30 \times 0.20 \times 0.20$	$0.54 \times 0.51 \times 0.33$
θ range for data coll. (deg)	$1.93 < \theta < 28.76$	$1.55 < \theta < 28.36$
total, unique no. of reflns	9466, 6156	121 184, 38 383
R_{int}	0.339	0.483
no. of params, restraints	321, 0	1645, 64
R , R_w^2 for all data	0.0334, 0.0799	0.0619, 0.1358
R , R_w^2 for $I > 2\sigma$	0.0312, 0.0780	0.0492, 0.1293
GOF	1.074	1.079
resid density (e \AA^{-3})	$-2.66 < 1.73$	$-0.80 < 5.35$

Ketone Hydrosilylation, Table 3. Iridium complex **2a**, **2b**, or **2c** (1.1 μmol) and 1,3,5-trimethoxybenzene (internal standard, 3.1 mg, 18.6 μmol) were weighed into a small vial. C_6D_6 (0.48 mL) was added, followed by diphenylsilane (21 μL , 0.112 mmol) and acetophenone (4.3 μL , 37.2 μmol). The tube was capped and inverted several times, and the reaction was monitored by ^1H NMR spectroscopy until acetophenone was fully consumed. The yield of silyl ether **12a** was calculated by comparing the integration values of the CH_3 doublet and the CH quartet with that of the OCH_3 singlet from the internal standard, 1,3,5-trimethoxybenzene. The yield of the enol silyl ether **13a** was calculated by comparing the integration values of the two vinylic CH doublets with that of the OCH_3 singlet from the internal standard, 1,3,5-trimethoxybenzene.

Competition Experiments, Table 4. Iridium complex **2a**, **2b**, or **2c** (1.1 μmol) and 1,3,5-trimethoxybenzene (internal standard, 3.1 mg, 18.6 μmol) were weighed into a small vial. About 0.3 mL of C_6D_6 was added, followed by diphenylsilane (69 μL , 0.372 mmol). The solution was transferred to an NMR tube, and C_6D_6 was added to bring the total volume to 0.5 mL. The tube was capped and incubated at room temperature for 2 h, during which time a small amount of H_2 was evolved as adventitious water was consumed by iridium-catalyzed silane hydrolysis.⁸³ Acetophenone (**11a**) and ketone **11b**, **11c**, and **11d** were added (37.2 μmol of each), the NMR tube was inverted several times, and the reaction was monitored by ^1H NMR at 23 $^\circ\text{C}$ for ap-

(81) Sheldrick, G. M. *SHELXTL, Version 6.14*; Bruker AXS Inc.: Madison, WI, 2004.

(82) Spek, A. L. *J. Appl. Crystallogr.* **2003**, *36*, 7–13.

proximately 12 h. Conversion of the starting ketones was measured using the $-\text{COCH}_3$ resonance. In all experiments, silyl ethers **12a–d** were the major products; less than 5% yield (NMR) of silyl enol ether from dehydrogenative silylation was observed. Products **12a–d** decompose upon attempts at chromatographic purification and were identified by their ^1H NMR spectra, as observed in individual (noncompetition) hydrosilylation experiments using **2a** as catalyst. The identities of silyl ethers **12c,d** were confirmed by hydrolysis of the siloxy group and full characterization of the resulting alcohols **13c,d**, as described in the Supporting Information. Silyl ethers **12a,b** were identified by hydrolysis and comparison with the known phenethyl alcohols.⁸⁴

Acknowledgment. This work was supported by generous funding from the ACS Petroleum Research Fund (46754-GB3) and Colgate University. The authors would like to thank Bruce Foxman, Paul Williard, and James Golen for

helpful advice on X-ray crystallography, and the Crystallography Summer School hosted by Arnold Rheingold for instruction and use of instrumentation.

Supporting Information Available: Details of the synthesis and characterization of new compounds, including images of ^1H and ^{13}C NMR spectra. Complete data for catalytic experiments. CIF files giving X-ray diffraction data, atomic coordinates, thermal parameters, and complete bond distances and angles. This material is available free of charge via the Internet at <http://pubs.acs.org>.

OM800878M

(83) Lee, Y.; Seomoon, D.; Kim, S.; Han, H.; Chang, S.; Lee, P. H. *J. Org. Chem.* **2004**, *69*, 1741–1743.

(84) Hu, A. G.; Ngo, H. L.; Lin, W. B. *J. Am. Chem. Soc.* **2003**, *125*, 11490–11491.

Deactivation of the Shvo Catalyst by Ammonia: Synthesis, Characterization, and Modeling

Dirk Hollmann,[†] Haijun Jiao,[†] Anke Spannenberg,[†] Sebastian Bähn,[†] Annegret Tillack,[†] Rudy Parton,[‡] Rinke Altink,[‡] and Matthias Beller^{*†}

Leibniz-Institut für Katalyse e.V. an der Universität Rostock, Albert-Einstein-Str. 29a, 18059 Rostock, Germany, and DSM Research Technology & Analysis Geleen, P.O. Box 18, 6160 MD Geleen, The Netherlands

Received September 29, 2008

The novel stable Shvo ammonia complex $[2,3,4,5\text{-Ph}_4(\eta^4\text{-C}_4\text{CO})\text{Ru}(\text{CO})_2(\text{NH}_3)]$ (**6**) has been isolated in high yield in the catalytic alkylation of aniline with hexylamine. It has been characterized by X-ray analysis and density functional theory computation. The thermodynamic stability of Shvo-like ruthenium complexes with primary, secondary, and tertiary amines has been computed and compared. Calculations confirmed the high stability of this ruthenium ammonia complex.

Introduction

Shvo complex $\{[2,3,4,5\text{-Ph}_4(\eta^5\text{-C}_4\text{CO})]_2\text{H}\}\text{Ru}_2(\text{CO})_4(\mu\text{-H})$ (**1**) constitutes an efficient catalyst for numerous hydrogen transfer processes.¹ More specifically, it has been applied successfully in the hydrogenation reactions of alkynes,² carbonyl compounds, and imines^{3,4} and in the oxidation reactions of alcohols^{5,6} and amines,^{7,8} as well as in the dynamic kinetic resolution of secondary alcohols and primary amines in combination with lipases.^{9–15} In addition, tandem catalysis processes are known.¹⁶ On the basis of our ongoing interest in the development of amination methodologies^{17,18} and the synthesis of aliphatic and

aromatic amines,¹⁹ recently we have developed novel alkylation reactions of amines applying the Shvo catalyst (**1**) with mono-, di-, and trialkylamines as selective alkylation reagents.²⁰

Due to its significant catalytic potential, **1** has been the subject of detailed mechanistic investigations by Bäckvall,^{21–26} Casey,^{27–33} and others.³⁴ It is well known that the Shvo complex dissociates into two active species, **2** and **3** (Scheme 1) by

* Corresponding author. E-mail: matthias.beller@catalysis.de.

[†] Leibniz-Institut für Katalyse e.V. an der Universität Rostock.

[‡] DSM Research Technology & Analysis Geleen.

(1) (a) Karvembu, R.; Prabhakaran, R.; Natarajan, N. *Coord. Chem. Rev.* **2005**, *249*, 911–918. (b) Shvo, Y.; Czarkie, D.; Rahamim, Y. *J. Am. Chem. Soc.* **1986**, *108*, 7400–7402. (c) Blum, Y.; Czarkie, D.; Rahamim, Y.; Shvo, Y. *Organometallics* **1985**, *4*, 1459–1461. (d) Shvo, Y.; Laine, R. M. *J. Chem. Soc., Chem. Commun.* **1980**, 753–754.

(2) Shvo, Y.; Goldberg, I.; Czarkie, D.; Reshef, D.; Stein, Z. *Organometallics* **1997**, *16*, 133–138.

(3) Samec, J. S. M.; Mony, L.; Bäckvall, J.-E. *Can. J. Chem.* **2005**, *83*, 909–916.

(4) Samec, J. S. M.; Bäckvall, J.-E. *Chem.–Eur. J.* **2002**, *8*, 2955–2961.

(5) Csajnyik, G.; Éll, A. H.; Fabini, L.; Pugin, B.; Bäckvall, J.-E. *J. Org. Chem.* **2002**, *67*, 1657–1662.

(6) Choi, J. H.; Kim, N.; Shin, Y. J.; Park, J. H.; Park, J. *Tetrahedron Lett.* **2004**, *45*, 4607–4610.

(7) Éll, A. H.; Samec, J. S. M.; Brasse, C.; Bäckvall, J.-E. *Chem. Commun.* **2002**, 1144–1145.

(8) Samec, J. S. M.; Éll, A. H.; Bäckvall, J.-E. *Chem.–Eur. J.* **2005**, *11*, 2327–2337.

(9) Paetzold, J.; Bäckvall, J.-E. *J. Am. Chem. Soc.* **2005**, *127*, 17620–17621.

(10) Pamies, O.; Bäckvall, J.-E. *J. Org. Chem.* **2001**, *66*, 4022–4025.

(11) Pamies, O.; Bäckvall, J.-E. *Chem. Rev.* **2003**, *103*, 3247–3261.

(12) Pamies, O.; Éll, A. H.; Samec, J. S. M.; Hermanns, N.; Bäckvall, J.-E. *Tetrahedron Lett.* **2002**, *43*, 4699–4702.

(13) Strübing, D.; Krumlinde, P.; Piera, J.; Bäckvall, J.-E. *Adv. Synth. Catal.* **2007**, *349*, 1577–1581.

(14) Atuu, M. R.; Hossain, M. M. *Tetrahedron Lett.* **2007**, *48*, 3875–3878.

(15) Leijondahl, K.; Borén, L.; Braun, R.; Bäckvall, J.-E. *Org. Lett.* **2008**, *10*, 2027–2030.

(16) (a) van As, B. A. C.; van Buijtenen, J.; Mes, T.; Palmans, A. R. A.; Meijer, E. W. *Chem.–Eur. J.* **2007**, *13*, 8325–8332. (b) Kanca, Ü.; van Buijtenen, J.; van As, B. A. C.; Korevaar, P. A.; Vekemans, J. A. J. M.; Palmans, A. R. A.; Meijer, E. W. *J. Polym. Sci. A* **2008**, *46*, 2721–2733.

(17) (a) Mobaligh, A.; Buch, C.; Routaboul, L.; Jackstell, R.; Klein, H.; Spannenberg, A.; Beller, M. *Chem.–Eur. J.* **2007**, *13*, 1594–1601. (b) Routaboul, L.; Buch, C.; Klein, H.; Jackstell, R.; Beller, M. *Tetrahedron Lett.* **2005**, *46*, 7401–7405. (c) Mobaligh, A.; Seayad, A.; Jackstell, R.; Beller, M. *J. Am. Chem. Soc.* **2003**, *125*, 10311–10318.

(18) (a) Alex, K.; Tillack, A.; Schwarz, N.; Beller, M. *ChemSusChem* **2008**, *1*, 333–338. (b) Seayad, J.; Tillack, A.; Hartung, C. G.; Beller, M. *Adv. Synth. Catal.* **2002**, *344*, 795–813. (c) Beller, M.; Breindl, C.; Eichberger, M.; Hartung, C. G.; Seayad, J.; Thiel, O.; Tillack, A.; Trauthwein, H. *Synlett* **2002**, 1579–1594. (d) Tillack, A.; Garcia Castro, I.; Hartung, C. G.; Beller, M. *Angew. Chem., Int. Ed.* **2002**, *41*, 2541–2543. (e) Hartung, C. G.; Trauthwein, H.; Tillack, A.; Beller, M. *J. Org. Chem.* **2001**, *66*, 6339–6343. (f) Beller, M.; Breindl, C. *Chemosphere* **2001**, *43*, 21–26. (g) Beller, M.; Thiel, O.; Trauthwein, H.; Hartung, C. G. *Chem.–Eur. J.* **2000**, *6*, 2513–2522. (h) Trauthwein, H.; Tillack, A.; Beller, M. *Chem. Commun.* **1999**, 2029–2030.

(19) (a) Tillack, A.; Hollmann, D.; Mevius, K.; Michalik, D.; Bähn, S.; Beller, M. *Eur. J. Org. Chem.* **2008**, 4745–4750. (b) Tillack, A.; Hollmann, D.; Michalik, D.; Beller, M. *Tetrahedron Lett.* **2006**, *47*, 8881–8885. (c) Hollmann, D.; Tillack, A.; Michalik, D.; Jackstell, R.; Beller, M. *Chem. Asian J.* **2007**, *3*, 403–410.

(20) (a) Bähn, S.; Hollmann, D.; Tillack, A.; Beller, M. *Adv. Synth. Catal.* **2008**, *13*, 2099–2103. (b) Hollmann, D.; Bähn, S.; Tillack, A.; Beller, M. *Chem. Commun.* **2008**, 3199–3201. (c) Hollmann, D.; Bähn, S.; Tillack, A.; Beller, M. *Angew. Chem., Int. Ed.* **2007**, *46*, 8291–8294.

(21) Samec, J. S. M.; Éll, A. H.; Åberg, J. B.; Privalov, T.; Eriksson, L.; Bäckvall, J.-E. *J. Am. Chem. Soc.* **2006**, *128*, 14293–14305.

(22) Samec, J. S. M.; Bäckvall, J.-E.; Andersson, P. G.; Brandt, P. *Chem. Soc. Rev.* **2006**, *35*, 237–248.

(23) Samec, J. S. M.; Éll, A. H.; Bäckvall, J.-E. *Chem. Commun.* **2004**, 2748–2749.

(24) Johnson, J. B.; Bäckvall, J.-E. *J. Org. Chem.* **2003**, *68*, 7681–7684.

(25) Éll, A. H.; Johnson, J. B.; Bäckvall, J.-E. *Chem. Commun.* **2003**, 1652–1653.

(26) Åberg, J. B.; Samec, J. S. M.; Bäckvall, J.-E. *Chem. Commun.* **2006**, 2771–2773.

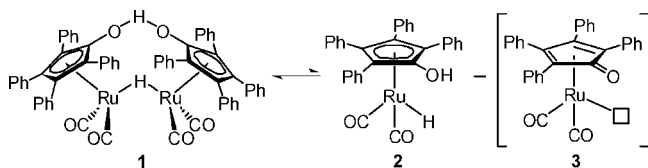
(27) Casey, C. P.; Singer, S. W.; Powell, D. R.; Hayashi, R. K.; Kavana, M. *J. Am. Chem. Soc.* **2001**, *123*, 1090–1100.

(28) Casey, C. P.; Johnson, J. B. *J. Am. Chem. Soc.* **2005**, *127*, 1883–1894.

(29) Casey, C. P.; Johnson, J. B.; Singer, S. W.; Cui, Q. *J. Am. Chem. Soc.* **2005**, *127*, 3100–3109.

(30) Casey, C. P.; Bikzhanova, G. A.; Cui, Q.; Guzei, I. A. *J. Am. Chem. Soc.* **2005**, *127*, 14062–14071.

Scheme 1. Equilibrium between 1 and Active Species 2 and 3



transferring a hydride (bonded to a metal center) and a proton (bonded to a ligand). Despite the known studies on the mechanism of the hydrogen transfer process, it is still speculated whether the respective reaction proceeds concerted without substrate coordination in a solvent cage (Casey) or concerted with substrate coordination and ring slippage of the aromatic ring (Bäckvall). Until now few investigations were performed on the deactivation of the Shvo catalyst **1**.

Previous Shvo Amine Complexes. In 1988, Shvo et al. isolated the crystals of $[2,3,4,5\text{-Ph}_4(\eta^4\text{-C}_4\text{CO})\text{Ru}(\text{CO})_2(\text{NHEt}_2)]$ (**4**) during transalkylation of amines.³⁵ Later, in a joint cooperation Casey, Bäckvall, and Park reinvestigated the structure of the isopropyl alcohol complex $[2,3,4,5\text{-Ph}_4(\eta^4\text{-C}_4\text{CO})\text{Ru}(\text{CO})_2(\text{HOCHMe}_2)]$,³⁶ which turned out to be the stable $[2,3,4,5\text{-Ph}_4(\eta^4\text{-C}_4\text{CO})\text{Ru}(\text{CO})_2(\text{H}_2\text{NCHMe}_2)]$ complex (**5**).³⁷ During their mechanistic investigations on the reduction of imines, Casey^{27–32} and Bäckvall^{4,7,8,23} identified and characterized different ruthenium amine complexes $[2,3,4,5\text{-Ph}_4(\eta^4\text{-C}_4\text{CO})\text{Ru}(\text{CO})_2(\text{R}_2\text{CHNHR})]$.

Herein, we report for the first time the deactivation of the active species **3** by ammonia. The resulting Shvo ammonia complex **6** is structurally characterized by X-ray analysis. Calculations on the thermodynamic stability of amine-substituted cyclopentadienone ruthenium complexes and on the exchange of amines demonstrate that complex **6** is one of the most stable amine complexes known.^{38,39}

Results and Discussion

During our studies on the selective synthesis of monoalkylated arylamines we performed the reaction of alkylamines with

(31) Casey, C. P.; Bikzhanova, G. A.; Guzei, I. A. *J. Am. Chem. Soc.* **2006**, *128*, 2286–2293.

(32) Casey, C. P.; Clark, T. B.; Guzei, I. A. *J. Am. Chem. Soc.* **2007**, *129*, 11821–11827.

(33) Casey, C. P.; Beetner, S. E.; Johnson, J. B. *J. Am. Chem. Soc.* **2008**, *130*, 2285–2295.

(34) Comas-Vives, A.; Ujaque, H.; Lledos, A. *Organometallics* **2007**, *26*, 4135–4144.

(35) Abed, M.; Goldberg, I.; Stein, Z.; Shvo, Y. *Organometallics* **1988**, *7*, 2054–2057.

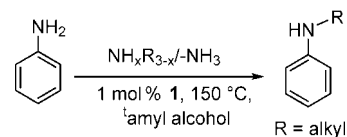
(36) Jung, H. M.; Shin, S. T.; Kim, Y. H.; Kim, M.-J.; Park, J. *Organometallics* **2001**, *20*, 3370–3372.

(37) Casey, C. P.; Bikzhanova, G. A.; Bäckvall, J.-E.; Johansson, L.; Park, J.; Kim, Y. H. *Organometallics* **2002**, *21*, 1955–1959.

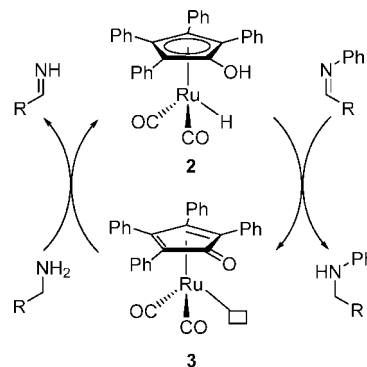
(38) For other transition metal ammonia complexes, see: (a) Derrah, E. J.; Pantazis, D. A.; McDonald, R.; Rosenberg, L. *Organometallics* **2007**, *26*, 1473–1482. (b) Hughes, R. P.; Smith, J. M.; Incarvito, C. D.; Lam, K.-C.; Rhatigan, B.; Rheingold, A. L. *Organometallics* **2004**, *23*, 3362–3362. (c) Braun, T. *Angew. Chem., Int. Ed.* **2005**, *44*, 5012–5014. (d) Fulton, J. R.; Bouwkamp, M. W.; Bergman, R. G. *J. Am. Chem. Soc.* **2000**, *122*, 8799–8800. (e) Magnusson, E.; Moriarty, N. W. *Inorg. Chem.* **1996**, *35*, 5711–5719. (f) Schulz, M.; Milstein, D. *J. Chem. Soc., Chem. Commun.* **1993**, 318–319. (g) Roundhill, D. M. *Chem. Rev.* **1992**, *92*, 1–27. (h) Koelliker, R.; Milstein, D. *Angew. Chem., Int. Ed. Engl.* **1991**, *30*, 707–709. (i) Sakane, H.; Miyanaga, T.; Watanabe, I.; Yokoyama, Y. *Chem. Lett.* **1990**, 9, 1623–1626. (j) Casalnuovo, A. L.; Calabrese, J. C.; Milstein, D. *Inorg. Chem.* **1987**, *26*, 971–973. (k) Lever, F. M.; Powell, A. R. *J. Chem. Soc. A* **1969**, 1477–1482.

(39) For theoretical study of the NH_3 ligand bonding with transition metals, see: Pilme, J.; Silvi, B.; Alkhan, M. E. *J. Phys. Chem. A* **2005**, *109*, 10028–10037. For theoretical study of the oxidative addition of NH_3 to transition metals, see: Macgregor, S. A. *Organometallics* **2001**, *20*, 1860–1874.

Scheme 2. Alkylation of Aniline with Alkylamines



Scheme 3. Coupled Catalytic System for Hydrogenation of Imines and Dehydrogenation of Amines



aryl amines in *tert*-amyl alcohol in the presence of 1 mol % of **1** (Scheme 2). The observed alkyl transfer proceeds by a coupled reaction of hydrogenation and dehydrogenation of the alkylamine (Scheme 3).

After complete conversion, we were able to isolate the desired product along with an unknown white powder. Due to the insolubility of the side-product in methanol, ether, acetone, and water identification and characterization were initially difficult. However, it was soluble in boiling DMSO. After cooling to room temperature crystals suitable for X-ray analysis were obtained. Surprisingly, the side-product was identified as the Shvo ammonia complex $[2,3,4,5\text{-Ph}_4(\eta^4\text{-C}_4\text{CO})\text{Ru}(\text{CO})_2(\text{NH}_3)]$ (**6**) (Figure 1). The detailed crystallographic data and selected bond lengths of **6** are given in Tables 1 and 2, respectively. Apparently, ammonia is stabilized by a weak intramolecular hydrogen bond between H(1) and O(1) of the cyclopentadienone ring (2.28(2) Å) and by a strong intermolecular hydrogen bond between H(2A) and O(1B) of the second cyclopentadienone ring (1.97(2) Å), which is shown in Figure 2 and in the Supporting Information. Such an intermolecular hydrogen bond is not known for any ruthenium Shvo-like complexes with primary or secondary amines. In comparison to **1** with an η^5 -coordination mode, **6** exhibits a C(1)–O(1) bond length of 1.250(2) Å and a Ru(1)–C(1) distance of 2.425(1) Å, which is distinctly elongated compared to the other four ruthenium ring carbon

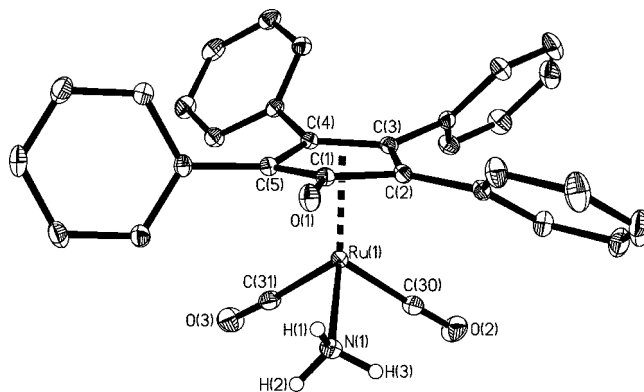


Figure 1. ORTEP diagram of **6**. Thermal ellipsoids are set at the 30% probability level. For clarity H atoms are omitted except H(1), H(2), and H(3).

Table 1. Crystallographic Data of **6**

[2,3,4,5-Ph ₄ (η ⁴ -C ₄ CO)]- Ru(CO) ₂ (NH ₃) (6)	
chemical formula	C ₃₁ H ₂₃ NO ₃ Ru
fw	558.57
cryst syst	monoclinic
space group	P2 ₁ /c
a [Å]	12.656(3)
b [Å]	8.767(2)
c [Å]	22.359(5)
β [deg]	101.79(3)
V [Å ³]	2428.6(8)
Z	4
ρ _{calc} [g·cm ⁻³]	1.528
μ(Mo Kα) [mm ⁻¹]	0.680
T [K]	200(2)
no. of rflns (measd)	38 827
no. of rflns (indep)	5572
no. of rflns (obsd)	4907
no of params	337
R ₁ (I > 2σ(I))	0.0182
wR ₂ (all data)	0.0479

Table 2. Selected Bond Distances [Å] for [2,3,4,5-Ph₄(η⁴-C₄CO)]Ru(CO)₂(NH₃) (**6**)

	X-ray (6)	theory (6)	theory (6')
Ru(1)–C(1)	2.425(1)	2.4668	2.4825
Ru(1)–C(2)	2.236(1)	2.2892	2.2951
Ru(1)–C(3)	2.197(1)	2.2645	2.2435
Ru(1)–C(4)	2.196(1)	2.2485	2.2435
Ru(1)–C(5)	2.214(1)	2.2907	2.2951
Ru(1)–C(30)	1.891(2)	1.9090	1.9077
Ru(1)–C(31)	1.895(2)	1.9052	1.9077
C(1)–O(1)	1.250(2)	1.2483	1.2506
C(30)–O(2)	1.139(2)	1.1600	1.1600
C(31)–O(3)	1.135(2)	1.1604	1.1600
Ru(1)–N(1)	2.155(1)	2.2443	2.2387

intramolecular hydrogen bonds N(1)–H(1)⋯O(1) (Figure 1)

N(1)–H(1)	0.85(2)	1.0345	1.0345
O(1)–H(1)	2.28(2)	1.9944	1.9868
N(1)–O(1)	2.960(2)	2.8884	2.8883

intermolecular hydrogen bonds N(1A)–H(2A)⋯O(1B) (Figure 2)

N(1A)–H(2A)	0.86(2)
H(2A)–O(1B)	1.97(2)
N(1A)–O(1B)	2.828(2)

atom distances (2.196(1)–2.236(1) Å). This suggests that the cyclopentadienone ring is bonded to the Ru in an η⁴-coordination mode.

The formation of **6** is explained by the reaction of ammonia (produced from dealkylation of alkylamines, Scheme 4) with the unsaturated 16-electron compound **3** (Scheme 5).

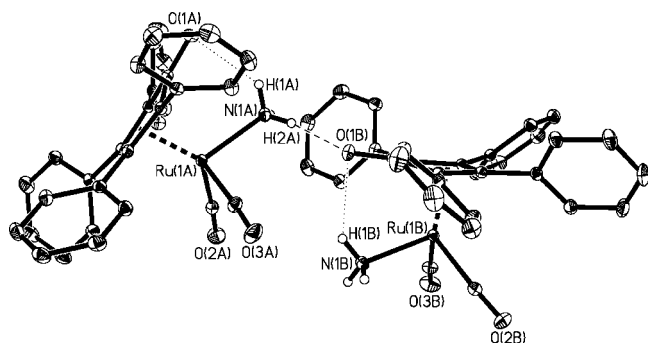
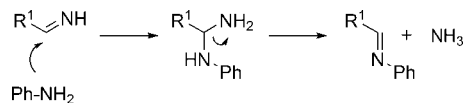
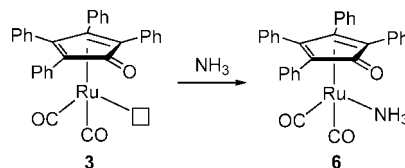


Figure 2. ORTEP diagram of **6** showing intra- and intermolecular hydrogen bond interactions. Thermal ellipsoids are set at the 30% probability level. For clarity H atoms are omitted except hydrogen atoms attached to nitrogen.

Scheme 4. Formation of Ammonia during the Dealkylation of Alkylamines



Scheme 5. Proposed Formation of **6** during the Amination Reaction with Alkylamines



Scheme 6. Synthesis of **6** from **7**

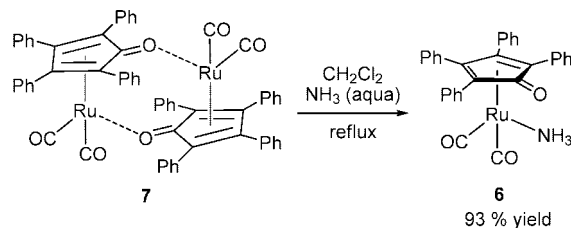


Table 3. Free Energy for the Formation of Shvo Ruthenium–Amine Complexes

entry	amine	formed complex	ΔG [kcal/mol]
1		3	+10.55
2	NH ₃	6	–22.66
3	NH ₂ Me	8	–22.82
4	NHMe ₂	9	–19.28
5	c-HN(C ₄ H ₈)	10	–22.78
6	NMe ₃	11	–4.98
7	NEt ₃	12	+9.56
8	PhNH ₂	13	–11.72
9	PhNHMe	14	–7.46

We assume that under the reaction conditions, complex **3** is in equilibrium with the cyclopentadienone dimer **7**.⁴⁰ Indeed, **6** is generated in 93% yield by treating a dichloromethane solution of **7** with an ammonium hydroxide solution (28% NH₃) under reflux conditions (Scheme 6). Upon heating, a gray precipitate dropped out of the solution. The ATR FTIR spectra of this gray powder exactly correspond with the ATR FTIR spectra of **6**. As stated above, this complex is insoluble in any solvent with the exception of boiling DMSO.

Next, we were interested in the stability of the Ru–N bond and the potential exchange of amines on the ruthenium center. Hence, the thermodynamic properties of the reactions of complex **7** with different amines were calculated at the B3LYP level of density functional theory (Table 3).

As shown in Figure 3, we have computed two ammonia complexes; one has the propeller orientation of the four phenyl groups as found in **6** (Figure 1) and one has C_s symmetry with the phenyl groups in symmetrical orientations (**6'**). The com-

(40) Mays, M. J.; Morris, M. J.; Raithby, P. R.; Shvo, Y.; Czarkie, D. *Organometallics* **1989**, *8*, 1162–1167.

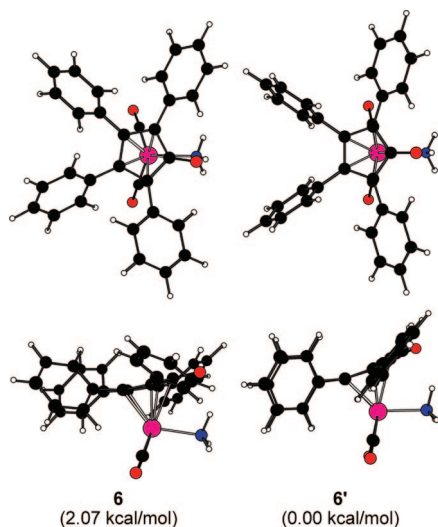


Figure 3. Conformations of the ruthenium ammonia complex.

puted structural parameters are compared with the X-ray data in Table 2, and reasonable agreement has been found between the two methods. In **6** (or **6'**), one N–H bond is directed to the ketone group and the other two N–H bonds are eclipsed by the two CO groups, and the N–H \cdots O=C distance is 1.9944 Å (or 1.9868 Å), which is in the range of hydrogen bonding. As discussed below, this hydrogen bonding is responsible for the enhanced stability of the ammonia complex and complexes with primary and secondary amines. We have also calculated the conformation with NH₃ staggered to the metal fragment, but free optimization resulted in **6** (or **6'**) in eclipsed conformation.

Figure 3 shows that the symmetrical conformation (**6'**) is computed to be more stable than the propeller one (**6**) by 2.07 kcal/mol. This small energy difference indicates equilibrium of the two conformations in the gas phase or solution. The observed propeller conformation of **6** in the solid state is attributed to packing effects.

In addition, we have also computed the complexes of primary, secondary, and tertiary amines. As shown in Figure 4, the complexes **8**, **9**, **10**, **13**, and **14** of primary and secondary amines have the eclipsed conformation of the amine groups with one N–H bond toward the C=O group as found in **6**. They also contain comparable N–H \cdots O= distances. However, the complexes **11** and **12** with tertiary amines have a staggered conformation of the amine group to the metal fragment, and most importantly complexes **11** and **12** do not show hydrogen bonding between the amine and carbonyl group.

Figure 4 also clearly demonstrates the change of the Ru–N distance on amines. From NH₃ and methylamine to trimethylamine, the Ru–N distance increases gradually from 2.229 and 2.244 Å to 2.341 Å, indicating the increased steric effects between amine and metal fragment. Stronger steric effects have been found for the complex with triethylamine (**12**) with a Ru–N distance of 2.408 Å. The changes are associated directly with the relative stability of the respective complex as discussed below.

As shown in Table 3, the direct dissociation of **7** into **3** is computed to be endogonic by 10.55 kcal/mol and disfavored thermodynamically (Table 3, entry 1). However, the formation of most ruthenium amine complexes is exogonic, and the theoretical data correspond well with the experimental observations of Casey and Bäckvall. For example, the reaction of **7** with ammonia to form **6** is thermodynamically favored ($\Delta G_2 = -22.66$ kcal/mol, Table 3, entry 2). In addition, reactions of

primary, secondary, and secondary cyclic aliphatic amines with **7** are also strongly exogonic (Table 3, entries 3–5), revealing the high thermodynamic stability of these compounds, and the driving force of such stability is the formation of the intramolecular hydrogen bonding between NH and the C=O group.

The small difference between the free energy of primary and secondary amine complexes is in agreement with a competition experiment of benzylamine with *N*-methylbenzylamine reported by Casey (Scheme 7).³⁰ During equilibrium a 1:1 ratio of **17** and **18** was observed.

In contrast to ammonia and primary as well as secondary aliphatic amines, tertiary aliphatic amines showed only a low exogonic free energy of -4.98 kcal/mol (trimethylamine, Table 3, entry 6) or even an endogonic free energy of $+9.56$ kcal/mol (triethylamine, Table 3, entry 7). Clearly, tertiary amines cannot form stabilizing intramolecular hydrogen bonding between the amine hydrogen and the carbonyl oxygen of the cyclopentadienone ring on one hand, and on the other hand they have increased steric interaction with the metal fragment.

Next, the formation of ruthenium amine complexes with primary as well as secondary arylamines was calculated. Again reactions are exogonic, but less pronounced with respect to aliphatic amines. The energy difference between primary and secondary arylamines is larger compared with aliphatic amines. Thus, primary arylamine complexes are more stable ($\Delta\Delta G = +4.26$ (arylamines) vs $+3.54$ kcal/mol (alkylamines)). The general stability order of Shvo ruthenium amine complexes is shown in Scheme 8.

Our computed thermodynamic data explains nicely known experimental findings. For example, the rapid displacement of *N*-phenylbenzylamine (**21**) by aniline (**20**) observed by Casey et al.³⁰ as well as competition experiments during equilibrium of aniline (**20**) and *N*-methylaniline (**19**) shown in Scheme 9 are in good agreement with the calculated free energies. The higher stability of ruthenium alkylamine complexes corresponds also with the trapping experiments of Bäckvall (Scheme 10).³⁰ Under equilibrium conditions the kinetic product **23** is converted to the thermodynamically more stable secondary alkylamine **24**.

The relatively small difference of the free energy between the ammonia complex **6** and primary and secondary alkylamine complexes **8**–**10** seemed surprising. Thus, we calculated the exchange reaction of ammonia by other amines. In Table 4 the free energies⁴¹ and the ratios of **3** in % during equilibrium at 25 °C with different amines are displayed.

These results point out that the reaction of **6** with all amines is thermodynamically disfavored, as indicated by positive reaction free energies. Only sterically unhindered aliphatic amines are in equilibrium with **6**. Clearly, if ammonia is present or formed in the reaction of amines, then arylamines and tertiary alkylamines will be completely replaced at the metal center. Notably, in reactions of primary or secondary cyclic amines, a significant amount of the Shvo catalyst will be blocked by ammonia, which is important to understand the catalytic behavior of the Shvo catalysts in amination reactions.

Finally, we were interested in the reactivity of the Shvo ammonia complex **6** in the alkylation of aniline with *n*-hexylamine.¹⁸ To compare complex **6** with the Shvo catalyst **1**, the reactions were performed in the presence of 2 mol % **6** or 1 mol % **1**, *tert*-amyl alcohol as solvent, and 2 equiv of aniline (Scheme 11). Interestingly, with both catalysts *N*-hexylaniline is obtained in an excellent yield of 99 %!

(41) $\Delta G = \Delta H - T\Delta S = -RT \ln(K)$ (during equilibrium)

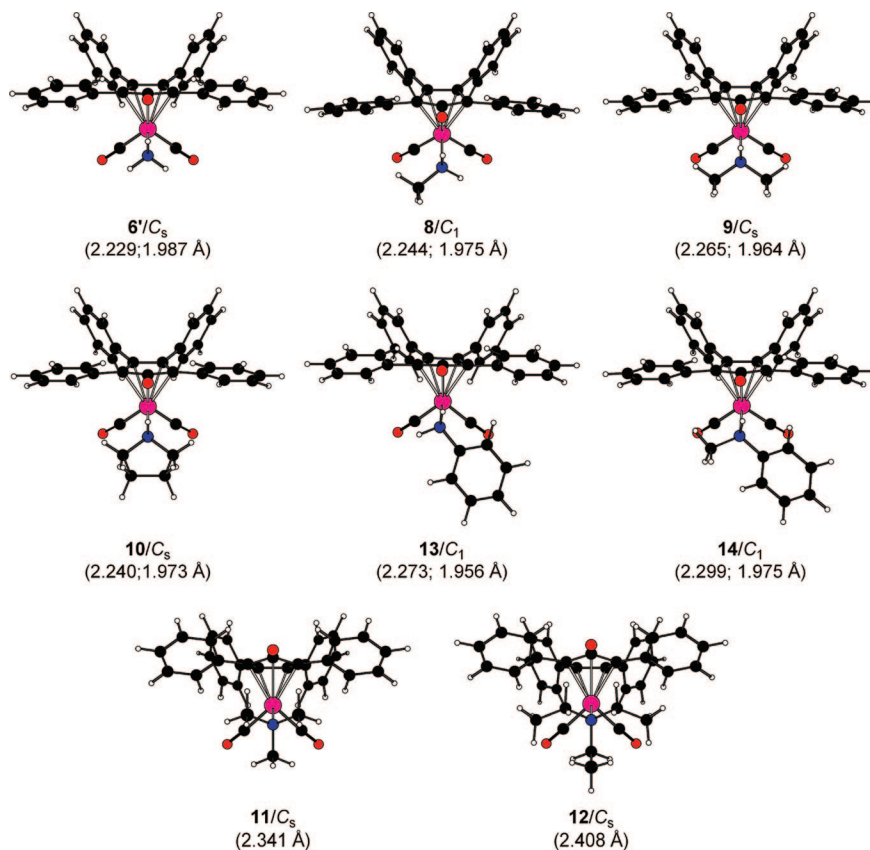
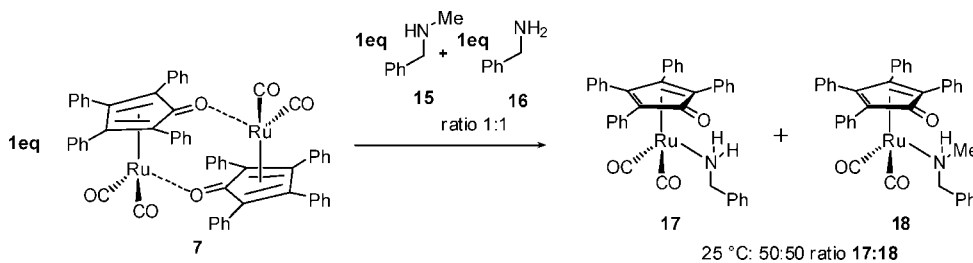
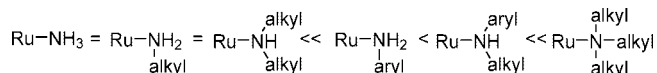


Figure 4. Ruthenium complexes with different amines and the respective Ru–N and N–H···O=C distances

Scheme 7. Competition Experiments of Alkylamines



Scheme 8. Stability Order of Shvo Amine Complexes



Apparently, under the reaction conditions complex **6** is in equilibrium with the corresponding alkylamine complex. However, in agreement with the theoretical calculations complex **6** precipitated after the reaction in 85 % yield and can be reused for catalysis. Hence, the addition of ammonia offers a convenient way to recycle the Shvo catalyst for catalytic aminations and probably other reactions, too.

Summary

In summary, we have synthesized and isolated a new neutral Shvo ammonia complex (**6**). The stabilities of different Shvo amine complexes were calculated and compared. The high stability of the ammonia complex **6** is to be noted. The driving forces of the enhanced stability of **6** are inter- and intramolecular hydrogen bonding interactions between the N–H of the amine and the carbonyl group of the cyclopentadienone ring. Calculation on the exchange of ammonia with other amines demon-

strates that **6** is in equilibrium with primary and secondary cyclic amines but not tertiary amines. The novel complex **6** is shown to be active in the alkylation reaction of aniline with hexylamine. The final precipitation of **6** allows a convenient recycling of Shvo-like ruthenium complexes.

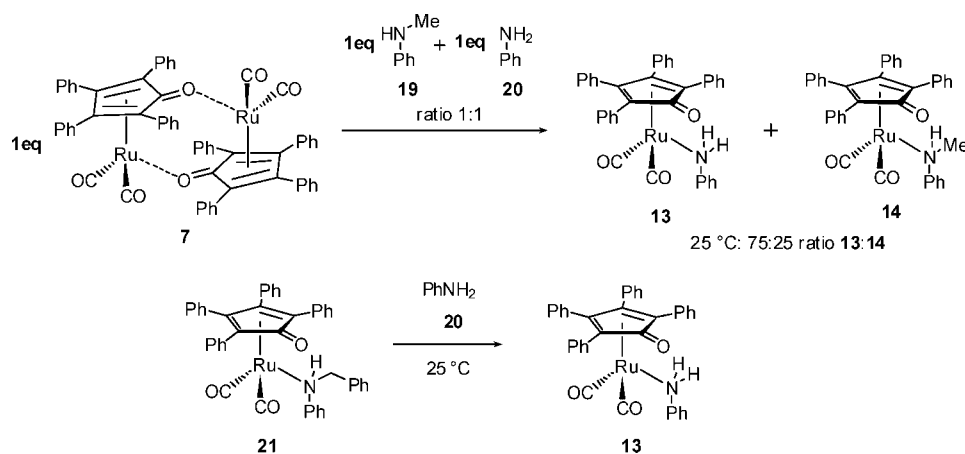
Experimental Section

Computational Details. All structures have been optimized at the B3LYP⁴² level of density functional theory along with the LANL2DZ basis set by adding a set of polarization functions (LANL2DZ(d)).⁴³ Optimized structures were characterized by frequency calculation as energy minima without imaginary frequencies (NImag = 0) or transition states with only one imaginary frequency (NImag = 1) at the same level of theory (B3LYP/

(42) (a) Stevens, P. J.; Devlin, F. J.; Chabrowski, C. F.; Frisch, M. J. *J. Phys. Chem.* **1994**, *98*, 11623–11627. (b) Becke, A. D. *J. Chem. Phys.* **1993**, *98*, 5648–5652.

(43) (a) Hay, P. J.; Wadt, W. R. *J. Chem. Phys.* **1985**, *82*, 299–311. (b) For polarization functions see: Huzinaga, S.; Anzelm, J.; Klobukowski, M.; Radzio-Andzelm, E.; Sakai, Y.; Tatewaki, H. *Gaussian Basis Sets for Molecular Calculations*; Elsevier: Amsterdam, 1984.

Scheme 9. Exchange and Competition Experiments of Arylamines



Scheme 10. Trapping Experiments of Bäckvall

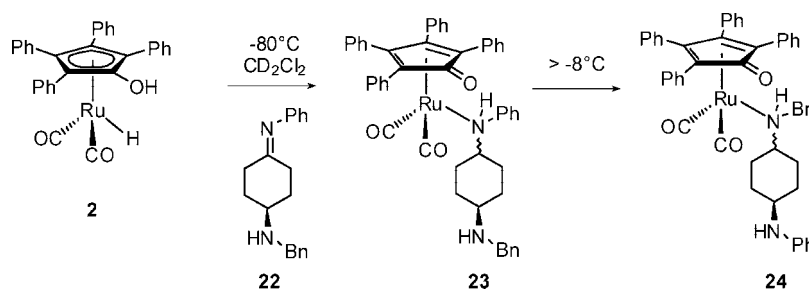
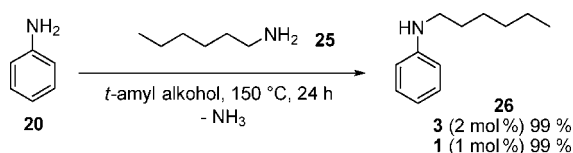


Table 4. Free Energy of the Exchange of Ammonia with Different Amines

entry	amine	formed complex	ΔG [kcal/mol]	ratio of 3 [%]
1	NH ₂ Me	8	+0.42	67
2	NHMe ₂	9	+2.20	97
3	c-HN(C ₄ H ₈)	10	+0.44	68
4	NMe ₃	11	+9.34	100
5	NEt ₃	12	+16.61	100
6	PhNH ₂	13	+5.97	100
7	PhNHMe	14	+8.10	100

Scheme 11. Reactivity of the Shvo Ammonia Complex **3**

LANL2DZ(d)).⁴⁴ The thermal corrections to enthalpy and Gibbs free energies at 298 K from the frequency calculations were added to the total electronic energies for analyzing the relative reaction free energies. All calculations were carried out by using the Gaussian 03 program package.⁴⁵

General Remarks. All reactions were carried out under an inert atmosphere of argon gas by standard Schlenk technique. Chemicals

were purchased from Aldrich, Fluka, Acros, and Strem and unless otherwise noted were used without further purification. Amines were distilled and stored under argon. All compounds were characterized by ¹H NMR, ¹³C NMR, MS, HRMS, and IR spectroscopy. ¹H and ¹³C NMR spectra were recorded on a Bruker AV 400 spectrometer. The ¹H and ¹³C NMR chemical shifts δ reported are relative to SiMe₄. EI mass spectra were recorded on a MAT 95XP spectrometer (70 eV, Thermo Electron Corporation). ESI high-resolution mass spectra were recorded on an Agilent Technologies 6210 TOF LC/MS. FTIR spectra were recorded on a Nicolet 6700 spectrometer and a ATR Smart Endurance (Thermo Electron Corporation) equipment. Elemental analyses were determined by C/H/N/S-Analysator 932 (Leco). X-ray crystallographic study of complex **6**: Data were collected with a STOE-IPDS diffractometer using graphite-monochromated Mo K α radiation. The structure was solved by direct methods [SHELXS-97: Sheldrick, G. M., University of Göttingen, Germany, 1997] and refined by full-matrix least-squares techniques on F^2 [SHELXL-97: Sheldrick, G. M., University of Göttingen, Germany, 1997.] XP (Bruker AXS) was used for structural representations.

Synthesis of [Ru(CO)₂(η^4 -Ph₄C₄CO)(NH₃)] (6**).** Shvo-H₂ complex **7** (520 mg, 0.481 mmol) was suspended in dichloromethane (5 mL) and ammonia–water solution (25% NH₃, 5 mL). The reaction mixture was heated for 10 min under reflux. The color of the precipitate changed from brown to gray. After filtration and washing with acetone (2 \times 5 mL), the gray precipitate was filtered and washed with acetone (2 \times 5 mL) and dichloromethane (5 mL) to yield 499.2 mg (93%) of **6** (gray powder). Crystals were obtained by recrystallization of **6** from dimethylsulfoxide.

¹H NMR (DMSO-*d*₆, 400 MHz): δ 3.06 (s, 3H, NH₃), 7.06–7.16 (m, 16H, Ar), 7.37–7.40 (m, 4H, Ar). ¹³C NMR (DMSO-*d*₆, 100 MHz): δ 82.0 (q, C_{3,4} of Cp), 102.9 (q, C_{2,5} of Cp), 126.0 (CH, Ph), 127.4 (CH, Ph), 127.5 (CH, Ph), 127.6 (CH, Ph), 129.7 (CH, Ph), 130.2 (CH, Ph), 131.8 (CH, Ph), 131.9 (q, Ph), 133.2 (q, Ph), 163.7 (q, C₁ of Cp), 201.2 (q, CO). FTIR (ATR): ν (cm⁻¹) 3349m (N–H), 3229w, 3053m, 1996s, 1942s, 1598m, 1541s, 1498m,

(44) Foresman, J. B., Frisch, E., Eds. *Exploring Chemistry with Electronic Structure Methods: A Guide to Using Gaussian*, 2nd ed.; Gaussian Inc.: Pittsburgh, PA, 1996.

(45) Frisch, M. J.; et al. *Gaussian 03, Revision C.02*; Gaussian Inc.: Wallingford, CT, 2004.

1442m, 1264m (C–N), 1071m, 1029m, 837, 767, 760m, 745m, 730m, 708s, 696s. HRMS(ESI): calcd for $C_{31}H_{23}O_3NRu$ 560.07942, found 560.08012. Anal. Calcd for $C_{31}H_{23}NO_3Ru$ (%): 1/2DCM: C, 62.95; H, 4.02; Cl 5.90. Found: C, 62.75; H, 4.45; Cl, 6.00.

General Amination Procedure. In an ACE pressure tube under an argon atmosphere Shvo ammonia catalyst (**6**, 0.04 mmol) and hexylamine (**25**, 2 mmol) were dissolved in *tert*-amyl alcohol (0.5 mL) and aniline (**20**, 4 mmol). The pressure tube was fitted with a Teflon cap and heated at 150 °C for 24 h in an oil bath. The solvent was removed in vacuo, and the crude product was easily purified by column chromatography with pentane–ethyl acetate (20:1). To recycle the catalyst, the reaction mixture was filtered. The precipitate was washed with ethyl acetate, transferred with ethyl acetate, and

dried in vacuo to give 38.5 mg (85%) of catalyst **6** (for two reactions).

Acknowledgment. This work has been supported by DSM, the BMBF (Bundesministerium für Bildung and Forschung), and the Deutsche Forschungsgemeinschaft (Leibniz-price). We thank Dr. Andreas Koch for excellent analytical support.

Supporting Information Available: Crystallographic information for **6** in cif format, energetic data for calculations, NMR data of **6**, and complete ref 45. This material is available free of charge via the Internet at <http://pubs.acs.org>.

OM8009415

Cationic Rhodium (I) Complexes of *N*-Phosphino-*tert*-butylsulfonamide Ligands: Synthesis, Structure, and Coordination Modes

Thierry Achard, Jordi Benet-Buchholz, Antoni Riera,* and Xavier Verdager*

Unitat de Recerca en Síntesi Asimètrica (URSA-PCB), Institute for Research in Biomedicine (IRB Barcelona) and Departament de Química Orgànica, Universitat de Barcelona, c/Baldiri Reixac 10, E-08028 Barcelona, Spain, and Institute of Chemical Research of Catalonia (ICIQ), Avda. Països Catalans 16, 43007 Tarragona, Spain

Received July 18, 2008

Here we describe the rhodium (I) complexes of *N*-phosphino-*tert*-butylsulfonamide ligands. This novel class of hemilabile ligands (PNSO) can work as either P,O or P,S chelating ligands when attached to the square planar rhodium center. Complexes bearing diene ligands such as [Rh(PNSO)(NBD)][TfO] and [Rh(PNSO)(COD)][TfO] provided P,O coordination, whereas [Rh(PNSO)₂][TfO]-type complexes provided P,S coordination. Ligand exchange experiments with mono and bidentate phosphines afforded evidence of the hemilabile behavior of the PNSO ligands.

Introduction

Bidentate ligands have become the most powerful tool in metal-catalyzed asymmetric processes.¹ Chelation provides the rigidity required to firmly allocate the chiral information around the metal center. Usually, the chirality of these ligands resides in the carbon backbone; however, some have a chiral phosphorus or sulfur center. The synthesis of chiral-phosphorus compounds is complex and difficult. Conversely, chiral-sulfur compounds can be prepared efficiently, and some are commercially available in large scale.^{2–5} Our group has recently reported *N*-phosphino-*tert*-butylsulfonamides (I) as new class of chiral bidentate ligands (PNSO) and their application in the intermolecular asymmetric Pauson-Khand reaction.⁶ In response to dicobalt carbonyl complexes, the PNSO ligand acts as a hemilabile bridging P,S ligand, thereby providing type II complexes (Figure 1).

An essential feature of hemilabile ligands is the presence of at least one labile donor function while the other donor group remains firmly bound to the metal center(s). Hemilabile ligands have the capacity to provide open coordination sites at the metal center during reactions that are “masked” in the ground-state structure and to stabilize reactive intermediates.⁷ PNSO ligands are an unusual class of hemilabile ligands, since the sulfoxide moiety can bind the metal through either sulfur or oxygen, thus enabling the ligand to provide both P,S and P,O chelation (Scheme 1). We have previously shown that PNSO ligands work solely as P,S bridging ligands toward bimetallic cobalt–carbonyl complexes; however, there is no data on the coordination

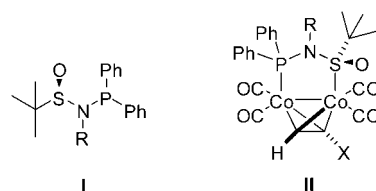
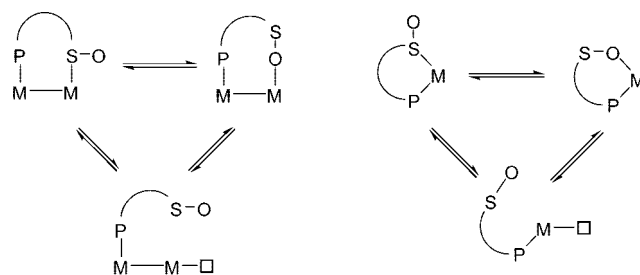


Figure 1

Scheme 1. Possible Coordination Modes of *N*-Phosphino Sulfonamide Ligands with Mono- and Bimetallic Complexes



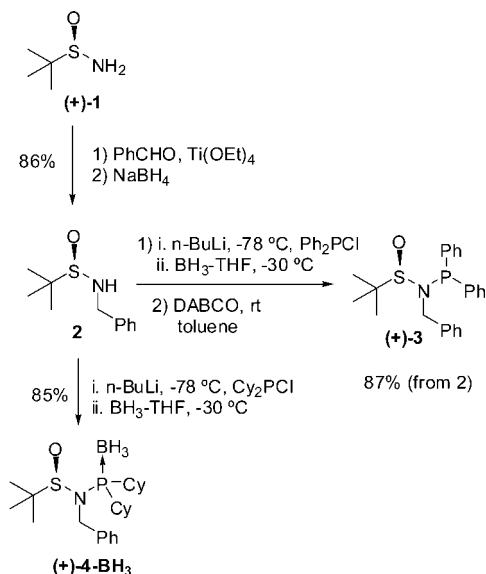
behavior of these ligands toward monometallic systems. Here, we report on the cationic rhodium (I) complexes of *N*-benzyl-*N*-phosphino-*tert*-butylsulfonamide ligands, their structure, coordination modes, and their behavior toward ligand exchange reactions.

Results and Discussion

Synthesis of the Ligands. Chiral PNSO ligands were synthesized from the commercially available *tert*-butylsulfonamide (+)-**1** (Scheme 2). The synthesis of **1** in two steps from the inexpensive starting material *tert*-butyl disulfide has been reported by Ellman and co-workers.⁸ From (+)-**1**, reductive amination protocol with Ti(OEt)₄ in the presence of benzaldehyde produced an intermediate sulfinimine, which was reduced in situ to the corresponding sulfonamide (**2**).⁹ In an optimized

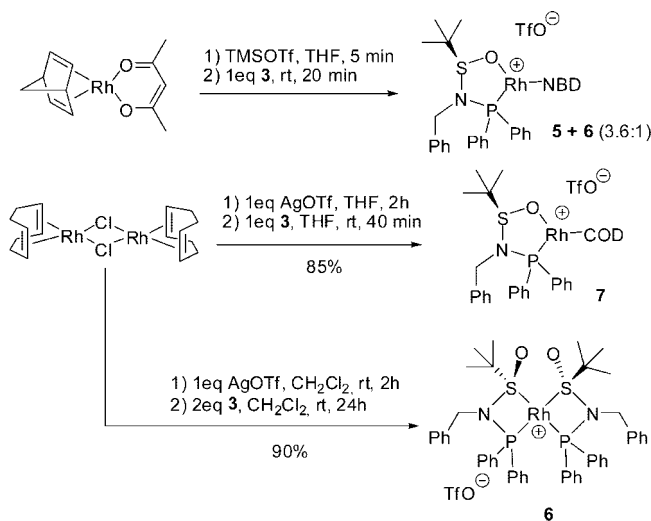
* Corresponding author. E-mail: xavier.verdager@irbbarcelona.org.
 (1) Jacobsen, E. N.; Pfaltz, A.; Yamamoto, H. In *Comprehensive Asymmetric Catalysis*; Springer: Berlin, 1999; Vol. I–III.
 (2) Fernandez, I.; Khair, N. *Chem. Rev.* **2003**, *103*, 3651–3706.
 (3) Pellissier, H. *Tetrahedron* **2006**, *62*, 5559–5601.
 (4) Senanayake, C. H.; Krishnamurthy, D.; Lu, Z.; Han, Z.; Gallou, I. *Aldrichim. Acta* **2005**, *38*, 93–104.
 (5) Mellah, M.; Voituriez, A.; Schulz, E. *Chem. Rev.* **2007**, *107*, 5133–5209.
 (6) Solà, J.; Revés, M.; Riera, A.; Verdager, X. *Angew. Chem., Int. Ed.* **2007**, *46*, 5020–5023. Revés, M.; Achard, T.; Solà, J.; Riera, A.; Verdager, X. *J. Org. Chem.* **2008**, *73*, 7080–7087.
 (7) Braunstein, P.; Naud, F. *Angew. Chem., Int. Ed.* **2001**, *40*, 680–699.

(8) Cogan, D. A.; Liu, G.; Kim, K.; Backes, B. J.; Ellman, J. A. *J. Am. Chem. Soc.* **1998**, *120*, 8011–8019.

Scheme 2. Synthesis of Optically Pure *N*-Phosphino-*N*-benzyl-*tert*-butylsulfonamide Ligands


protocol, anion formation with *n*-BuLi at low temperature followed by the addition of either Ph₂PCL or Cy₂PCL and protection of the phosphine moiety with borane provided the corresponding borane-protected ligands **3**-BH₃ and **4**-BH₃ (Scheme 2). In the case of diphenylphosphine, the borane-free ligand was obtained by deprotection with DABCO at room temperature to afford (+)-**3** as a crystalline solid in good yield. Conversely, borane-free ligand **4** could not be isolated because of the undesired sulfur-to-oxygen migration that leads to the corresponding phosphine oxide.^{10,11} Therefore, the cyclohexylphosphine ligand was used in its borane-protected form, **4**-BH₃, throughout the present study.

***N*-Benzyl-*N*-diphenylphosphino-*tert*-butylsulfonamide (3): Synthesis and Characterization of Its Cationic Rhodium Complexes.** The first attempts to obtain a cationic Rh complex with ligand **3** followed the procedure described by Alcock and co-workers, who reported the synthesis of a phosphine sulfoxide ligand and its Rh^I-NBD complex.¹² In that study, Alcock used (NBD)Rh(acac) as the rhodium source and TMSOTf to remove the acac ligand from the metal. Following this procedure, we treated a solution of (NBD)Rh(acac) in dry THF at room temperature under N₂ with 1 equiv of TMSOTf, followed by 1 equiv of ligand **3** (Scheme 3). After 20 min at room temperature, the mixture was added to a vigorously stirred hexane solution to give a yellow precipitate. ¹H NMR (CDCl₃) of this solid showed both noncoordinated and metal-coordinated NBD and no trace of the corresponding original ligand (*t*-Bu, 0.93 ppm). Two new major metal species were present with resonances at 1.47 and 1.34 ppm for the *t*-Bu group. Consistently, ³¹P NMR showed two doublets at 69.5 and 115.8 ppm, respectively, with a phosphorus–rhodium coupling constant of 141 and 193 Hz, respectively. This mixture was crystallized upon layering a hexane/Et₂O mixture over CH₂Cl₂. This approach produced a few dark orange crystals suitable for X-ray

Scheme 3. Synthesis of Cationic Rhodium (I) Complexes with Ligand 3


analysis. The crystalline compound (**5**) was the corresponding (PNSO)Rh^I(NBD) triflate complex with the PNSO ligand acting as a bidentate P,O ligand (Figure 2). ¹H NMR of pure **5** shows resonances at 1.34 ppm for the *t*-Bu group and two low-field broad doublets for the benzylic PhCH₂N protons at 4.47 and 4.58 ppm. The metal coordinated NBD showed the olefinic protons as a broad resonance centered at 4–5 ppm. Unfortunately, we could obtain only small amounts of pure **5** with this methodology, and its preparation was not consistently reproducible. In addition to this, compound **5** showed limited stability in solution.

Alternatively, the analogous (PNSO)Rh^I(COD) complex was prepared in good yield (85%) using [RhCl(COD)]₂ as a metal source (Scheme 3). Thus, chloride abstraction with AgOTf in dry THF and addition of ligand **3** under N₂ provided the desired compound (**7**) after 40 min at room temperature. This compound was isolated as an air-stable orange solid by layering the reaction mixture with diethyl ether. ¹H NMR of **7** showed the *t*-Bu resonance at 1.54 ppm in CDCl₃ and four signals corresponding to the olefinic protons of the metal-coordinated COD ligand, as would be expected for a complex with no symmetry. Suitable crystals for X-ray analysis were obtained by slow diffusion of Et₂O into a CH₂Cl₂ solution of **7**. The resulting structure revealed that **3** again acts as a P,O bidentate ligand (Figure 2), in analogy to the structure of complex **5**.

Metal–phosphorus and metal–oxygen, as well as oxygen–sulfur distances for **5** and **7** are consistent with the structure of [Ph₂PCH₂S(O)Ph]Rh^I(NBD) reported by Alcock and co-workers (Figure 2).¹² The Rh–O–S–N–P atoms formed a five-member ring with an envelope-like conformation in which the oxygen bonded to rhodium was slightly out of plane (0.44 Å). This observation differs from the structure reported by Alcock, in which it is the central carbon atom of the ligand that is out of plane. A strong trans effect was observed for both structures on the Rh–olefin distances. For example, **5** showed Rh–C (olefinic) distance trans to phosphorus of 2.231(2) and 2.237(2), whereas the Rh–C (olefinic) distance trans to oxygen was 2.093(1) and 2.093(2). The olefinic group placed trans to the most electronegative donor atom presented a shorter and stronger bond to the metal. Alignment of structures **5** and **7** without the olefinic ligands produced an almost perfect fit, except for the *N*-benzyl group (Figure 3). In complex **5**, the benzyl group was perpendicular to the phenyl ring of the phosphine, whereas in complex **7**, it showed a parallel-type disposition. The observed

(9) Tanuwidjaja, J.; Peltier, H. M.; Ellman, J. A. *J. Org. Chem.* **2007**, *72*, 626–629.

(10) Hiroi, K.; Suzuki, Y.; Kawagishi, R. *Tetrahedron Lett.* **1999**, *40*, 715–718.

(11) Vedejs, E.; Meier, G. P.; Powell, D. W.; Mastalerz, H. *J. Org. Chem.* **1981**, *46*, 5253–5254.

(12) Alcock, N. W.; Brown, J. M.; Evans, P. L. *J. Organomet. Chem.* **1988**, *356*, 233–247.

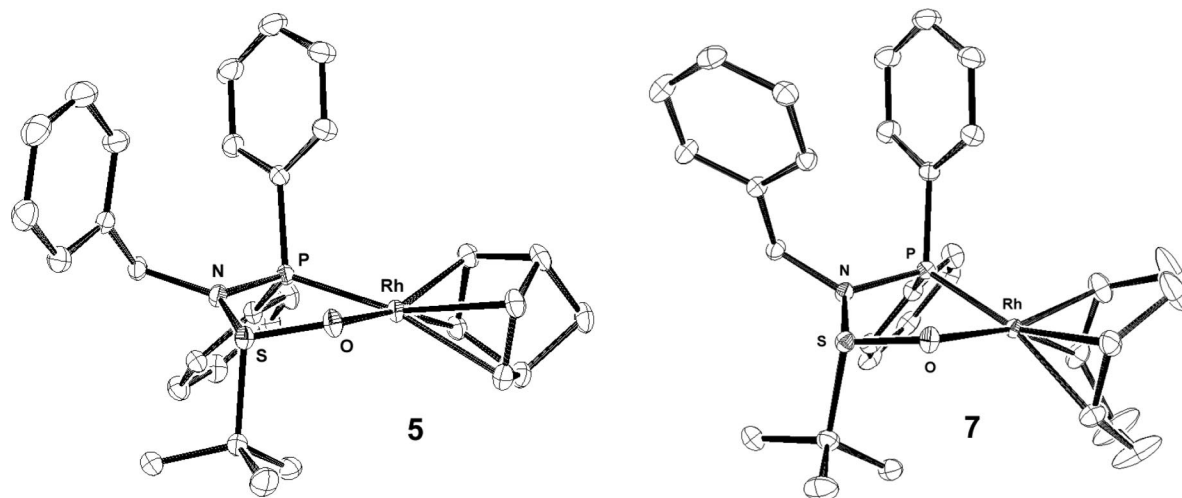


Figure 2. Ortep plot for crystal structures **5** and **7** with thermal ellipsoids shown at 50% probability. Only the metal cations are shown. For **5**, a single molecule of the two independent complexes that form the original unit cell is shown. Selected bond distances (Å) for **5** and **7**, respectively: Rh–O, 2.116(1) and 2.100(1); Rh–P, 2.262(1) and 2.250(1); S–O, 1.527(1) and 1.523(1).

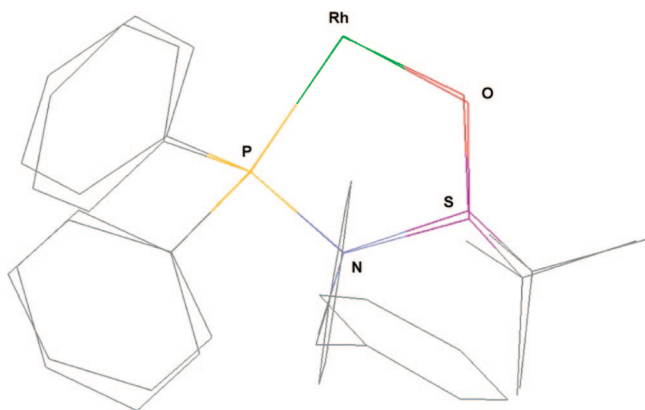


Figure 3. Alignment of Rh–P–N centers for complexes **5** and **7**. NBD and COD ligands are omitted for clarity.

O-bonding mode to the metal led to a considerable lengthening of the S=O bond (1.527(1) and 1.523(1) Å for **5** and **7**, respectively) in comparison with noncoordinated DMSO 1.493(av) Å. O-Coordination could, in principle, be expected in response to a hard cationic-Rh^I center. ³¹P NMR spectra of complexes **5** and **7** showed resonances at 115.8 and 116.5 ppm, respectively, whereas the free ligand **3** displayed the corresponding resonance at 60.0 ppm. In addition, Milstein and co-workers reported a [Rh(COD)(DMSO)₂][BF₄] complex in which both DMSO molecules bind the metal through oxygen.¹³ These findings indicate that the presence of a diolefinic ligand on the metal makes this center more electron-deficient, thereby favoring the O-coordination mode of the PNSO ligand.

We next examined the preparation of rhodium species with two PNSO ligands. With this purpose, [RhCl(COD)]₂ was treated with AgOTf in dichloromethane, and the resulting solution was added to a solution of 2 equiv of ligand **3** and stirred for 24 h at room temperature (Scheme 3). The resulting yellow mixture was poured over stirred Et₂O to provide an air-stable yellow precipitate. Spectroscopic analysis of this solid revealed the presence of a single substance with ¹H NMR resonances at 1.47 ppm (*t*-Bu). ³¹P NMR showed a doublet at 69.5 ppm and coupling constant of 141 Hz, which corresponded

to one of the substances obtained in the initial experiments with (NBD)Rh(acac). Finally, ESI mass spectroscopy confirmed the new substance (**6**) as a *bis*-(PNSO) rhodium (I) triflate. Traditionally, IR spectroscopy is a good tool to distinguish whether O–M or S–M bonding occurs in sulfoxide metal complexes.¹⁴ In our case, although noncoordinated **3** displayed an intense S=O absorption band at 1074 cm⁻¹, no diagnostic bands were observed for complexes **5**, **6**, or **7**.

To elucidate the structure of the dimeric PNSO complex and the coordination mode of the sulfinamide moiety, single crystals for X-ray analysis were obtained by layering Et₂O over a CH₂Cl₂ solution of **6** (Figure 4). The Rh center presented a slightly distorted square-planar geometry, with the two phosphorus atoms (and sulfur) in a *cis* arrangement in close analogy with other reported P–S, P–N, or P–O ligands.^{15–18} The Rh, S, N, and P atoms adopted a planar double diamond disposition in which the metal center was the connection point of two identical four-member rings. The complex showed a C₂ symmetry axis in the coordination plane of the metal. The oxygen atoms and the *t*-Bu groups of the sulfinamide were in anti position to each other to minimize steric and electronic interactions. The PNSO ligand provided bite angle (P–Rh–S) values of 71.33(2) and 71.20(2)°, which fall between dppm (70.80°) and MiniPHOS (72.96°) ligands in analogous Rh^I complexes.^{19,20} The Rh–P (2.251(1) and 2.249(1) Å) and Rh–S (2.289(1) and 2.288(1) Å) distances were quite similar. In this respect, the Rh–S distances observed were in the long range for an S-bonding mode.^{13,14,21} This observation could be attributed to the strong trans effect exerted by the phosphine ligands. Moreover, the occurrence of S-bonding in complex **6** can be reasoned on the

(14) Calligaris, M. *Coord. Chem. Rev.* **2004**, *248*, 351–375.

(15) Dick, D. G.; Stephan, D. W. *Can. J. Chem.* **1986**, *64*, 1870–1875.

(16) Esquiús, G.; Pons, J.; Yanez, R.; Ros, J.; Mathieu, R.; Donnadieu, B.; Lukan, N. *Eur. J. Inorg. Chem.* **2002**, 299, 9–3006.

(17) Kuznetsov, V. F.; Facey, G. A.; Yap, G. P. A.; Alper, H. *Organometallics* **1999**, *18*, 4706–4711.

(18) Braunstein, P.; Chauvin, Y.; Naehring, J.; DeCian, A.; Fischer, J.; Tiripicchio, A.; Ugozzoli, F. *Organometallics* **1996**, *15*, 5551–5567.

(19) Gridnev, I. D.; Yamanoi, Y.; Higashi, N.; Tsuruta, H.; Yasutake, M.; Imamoto, T. *Adv. Synth. Catal.* **2001**, *343*, 118–136.

(20) Fornika, R.; Six, C.; Gorls, H.; Kessler, M.; Kruger, C.; Leitner, W. *Can. J. Chem.* **2001**, *79*, 642–648.

(21) For the structure of a related neutral sulfinamide Rh(I) (COD) complex displaying sulfur coordination, see: (a) Souers, A. J.; Owens, T. D.; Oliver, A. G.; Hollander, F. J.; Ellman, J. A. *Inorg. Chem.* **2001**, *40*, 5299–5301.

(13) Dorta, R.; Rozenberg, H.; Shimon, L. J. W.; Milstein, D. *Chem.–Eur. J.* **2003**, *9*, 5237–5249.

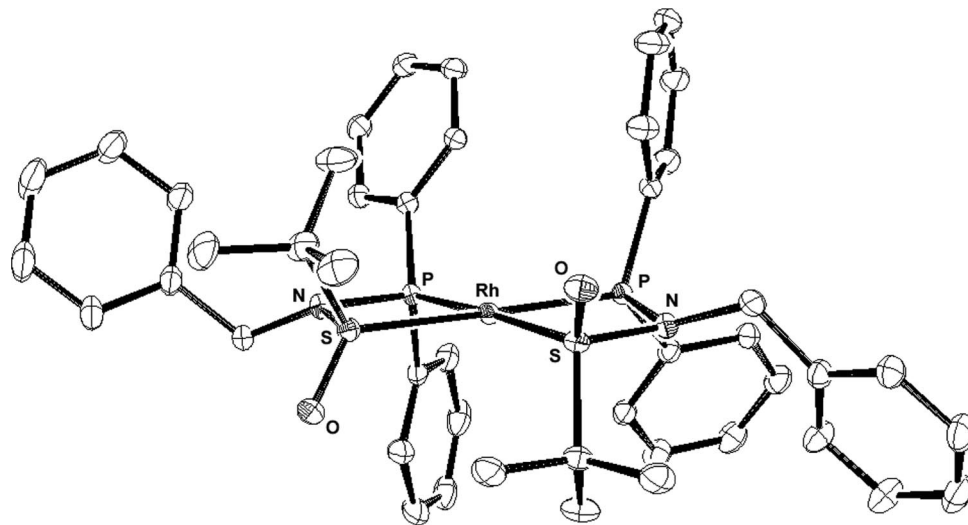
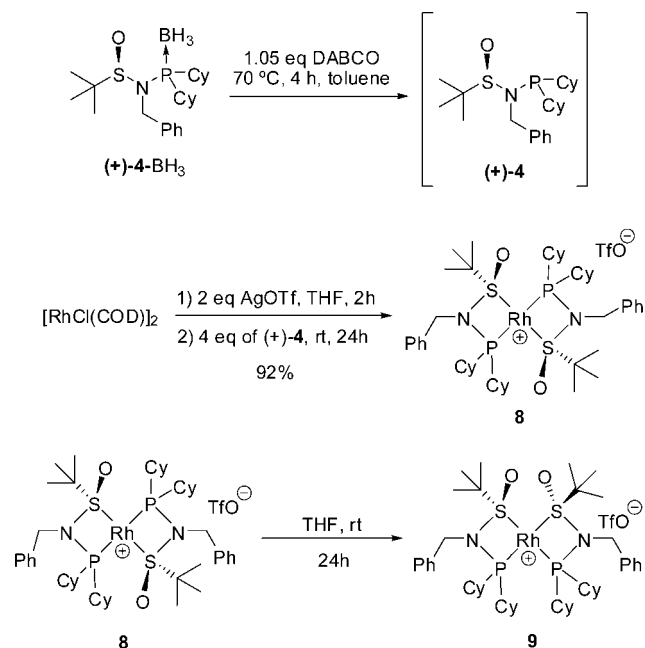


Figure 4. Ortep plot for crystal structure **6** with thermal ellipsoids shown at 50% probability. Only the metal cation is shown. Selected bond distances (Å) and angles (deg): Rh–P, 2.251(1) and 2.249(1); Rh–S, 2.289(1) and 2.288(1); P–Rh–S, 71.33(2) and 71.20(2).

Scheme 4. Synthesis of Cationic Rhodium Complexes with Ligand 4



basis that the metal center, which lacks the bis-olefin ligand, is more electron-rich than complexes **5** and **7** and thus prefers the softer S-coordination mode. This notion is corroborated by the ^{31}P NMR of complex **6** (69.5 ppm), which is very close to that of the free ligand **3** (60.0 ppm).

***N*-Benzyl-*N*-dicyclohexylphosphino-*tert*-butylsulfonamide (4): Synthesis and Characterization of Its Cationic Rh Complexes.** The use of ligand **4** in the preparation of rhodium complexes presented an additional challenge; that is, it could not be isolated pure in its borane-free form. Deprotection of borane-protected PNSO ligands occurs in toluene in the presence of DABCO. Under these conditions in the presence of a base and prior to purification, the ligand preserves its integrity, as determined by ^1H and ^{31}P NMR (Scheme 4). Under these circumstances, we attempted the synthesis of the corresponding bis-PNSO–Rh^I complex. Thus, chloride removal on $[\text{RhCl}(\text{COD})]_2$ with AgOTf, an addition of the resulting solution to deprotected **4**, was left to stir for 24 h at room temperature.

The product was purified by flash chromatography of the reaction mixture on SiO_2 using hexane/acetone mixtures as mobile phase. This approach provided the desired bis PNSO complex **8** in an excellent 92% yield. ^1H NMR revealed a single *t*-Bu resonance at 1.46 ppm and for the benzylic PhCH_2N an AB system coupled to phosphorus at 4.29 and 4.46 ppm. The ^{31}P NMR spectrum displayed a single doublet at 86 ppm with a coupling constant to Rh of 121 Hz. ESI mass spectroscopy confirmed complex **8** as a bis-PNSO–rhodium complex. Again, no concluding information on the coordination mode of the sulfoxide fragment could be drawn from the IR spectra of **8**. Finally, crystallization of **8** in a hexane/THF mixture provided green-yellow plated crystals suitable for X-Ray analysis (Figure 5). In contrast to what we expected, complex **8** showed a trans configuration of the two phosphines and the two sulfonamide groups around the square planar rhodium center. The complex now showed a C_2 axis perpendicular to the Rh coordination plane. This configuration positioned the two *t*-Bu groups on the same face of the complex and caused a distortion of the square planar geometry around the metal. Thus, the P–Rh–P angle was $165.28(1)^\circ$, whereas the analogous S–Rh–S angle was $167.97(1)^\circ$. Longer Rh–P distances were observed (2.312(1) and 2.297(1) Å) for **8** because of the dicyclohexylphosphine residue's being a weaker back-bonding ligand than diphenylphosphine. Like complex **6**, double S-coordination mode was observed for the sulfonamide fragment. The Rh–S distances were 2.251(1) and 2.269(1) Å, again falling in the long-range for this type of bonding. This distance is in agreement with the trans S-bonded DMSO molecules in rhodium complexes reported by Milstein and co-workers and can be explained on the basis that S-bound sulfoxides have a relatively higher trans influence than O-bound sulfoxides.^{13,22}

After some experimentation, we observed that the bis-PNSO–Rh complex **8** was not configurationally stable. Solving **8** in THF provided a distinct PNSO complex. ^1H NMR analysis of the new complex **9** showed a *t*-Bu resonance at 1.63 ppm, and in the benzylic region, the original AB system for **8** changed to a multiplet. Additionally, a new doublet at 95 ppm and $J_{\text{Rh}} = 132$ Hz was observed in the ^{31}P NMR spectrum. Compound **9** crystallized as air-stable yellow needles (THF/hexanes). High-resolution mass spectroscopy (ESI) revealed a composition

(22) Dorta, R.; Rozenberg, H.; Milstein, D. *Chem. Commun.* **2002**, 710–711.

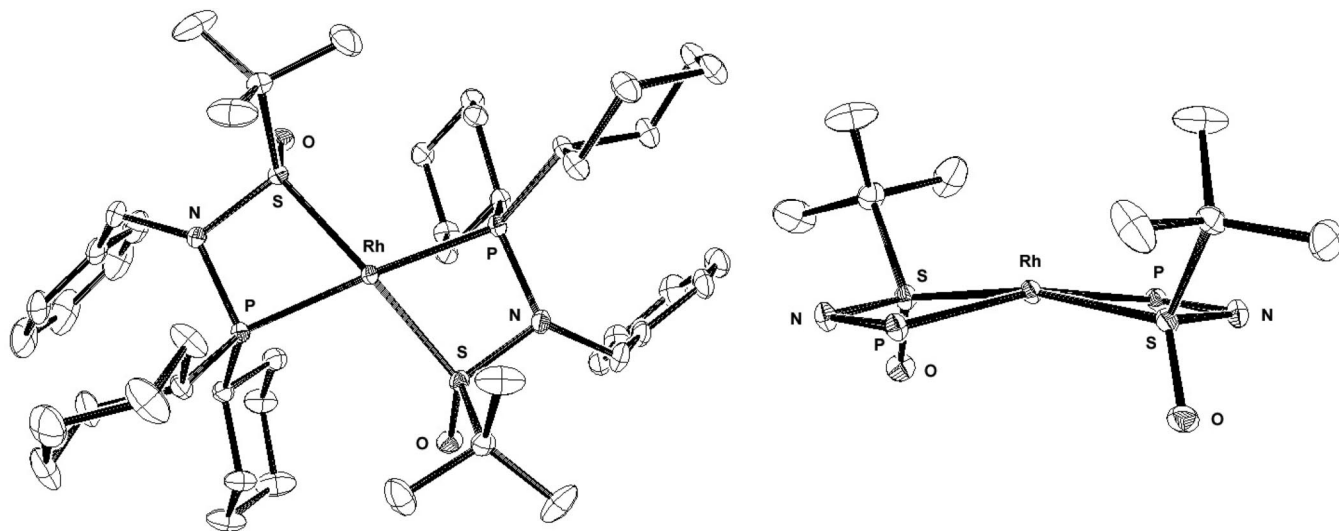
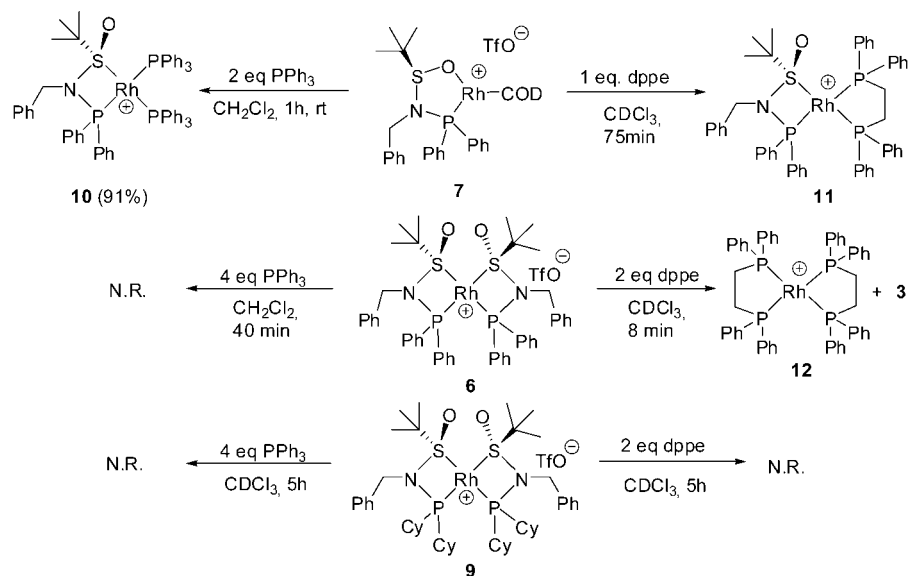


Figure 5. Ortep plot for crystal structure **8** with thermal ellipsoids shown at 50% probability (left). Lateral view of the central coordination core (right). Cyclohexyl and benzyl groups are omitted for clarity. Only the metal cation is shown. Selected bond distances (Å) and angles (deg): Rh–P, 2.312(1) and 2.297(1); Rh–S, 2.251(1) and 2.269(1); P–Rh–P, 165.28(1); S–Rh–S, 167.97(1).

Scheme 5. Reactivity of Rhodium (I) Complexes with Phosphines



identical to that of **8**. Solving **8** in a coordinating solvent such as THF (24 h) and acetonitrile (24 h) provided full conversion to the new complex **9** (Scheme 4). However, no isomerization from **8** to **9** was observed in CDCl_3 or toluene for 24 h. Moreover, the isomerization was not reversible, even when solving **9** in a nonpolar solvent for a long period of time (i.e., toluene). These experimental observations indicated that complex **8** is a kinetic product and **9** is the thermodynamically more stable complex. From the electronic point of view, the similarity of the ^{31}P NMR resonances for **8** and **9** suggests that both are S-bonded complexes. All things considered, the proposed structure for complex **9** is the corresponding S-coordinated cis analog of **8** (Scheme 4). The cis configuration should be the thermodynamically preferred one. In structure **9** the *t*-Bu groups are placed at opposite faces of the complex, thus releasing the steric strain built up in **8** that resulted in a distortion of the square planar geometry.

Reactivity of Rhodium (I) Complexes with Phosphines.

To examine how competent the PNSO ligands were with respect to other phosphines, ligand exchange reactions with PPh_3 and *dppe* were carried out and monitored by ^{31}P NMR (Scheme 5).

Reaction of $[\text{Rh}(\text{PNSO})(\text{COD})][\text{TfO}]$ (**7**) with two equivalents of PPh_3 provided the corresponding $[\text{Rh}(\text{PNSO})(\text{PPh}_3)_2][\text{TfO}]$ complex **10**, which was synthesized and isolated in an excellent 91% yield in preparative scale. Compound **10** showed the characteristic pattern for three nonequivalent phosphorus atoms attached to a square-planar Rh center in the ^{31}P NMR: three resonances with three distinct couplings each, two couplings to phosphorus, and one to rhodium. In an analogous fashion, after 75 min, the reaction of **7** with *dppe* provided the expected $[\text{Rh}(\text{PNSO})(\text{dppe})]$ (**11**) as a major complex, along with smaller amounts of $[\text{Rh}(\text{dppe})_2]$ (**12**) and $[\text{Rh}(\text{PNSO})_2]$ (**6**) in a 16:4:1 ratio (Scheme 5). The reaction spectrum at 8 min (Figure 6) showed two species that disappeared over time: free ligand **3** (s, 60.0 ppm) and the $[\text{Rh}(\text{dppe})(\text{COD})]$ complex **13** (d, 56.5 ppm, $J_{\text{Rh}} = 149$ Hz).²³ The reactivity of **7** with PPh_3 and *dppe* is consistent with **3** being a labile ligand. Thus, the PNSO ligand provided coordination sites for the incoming phosphine to

(23) de Wolf, E.; Spek, A. L.; Kuipers, B. W. M.; Philipse, A. P.; Meeldijk, J. D.; Bomans, P. H. H.; Frederik, P. M.; Deelman, B.; van Koten, G. *Tetrahedron* **2002**, *58*, 3911–3922.

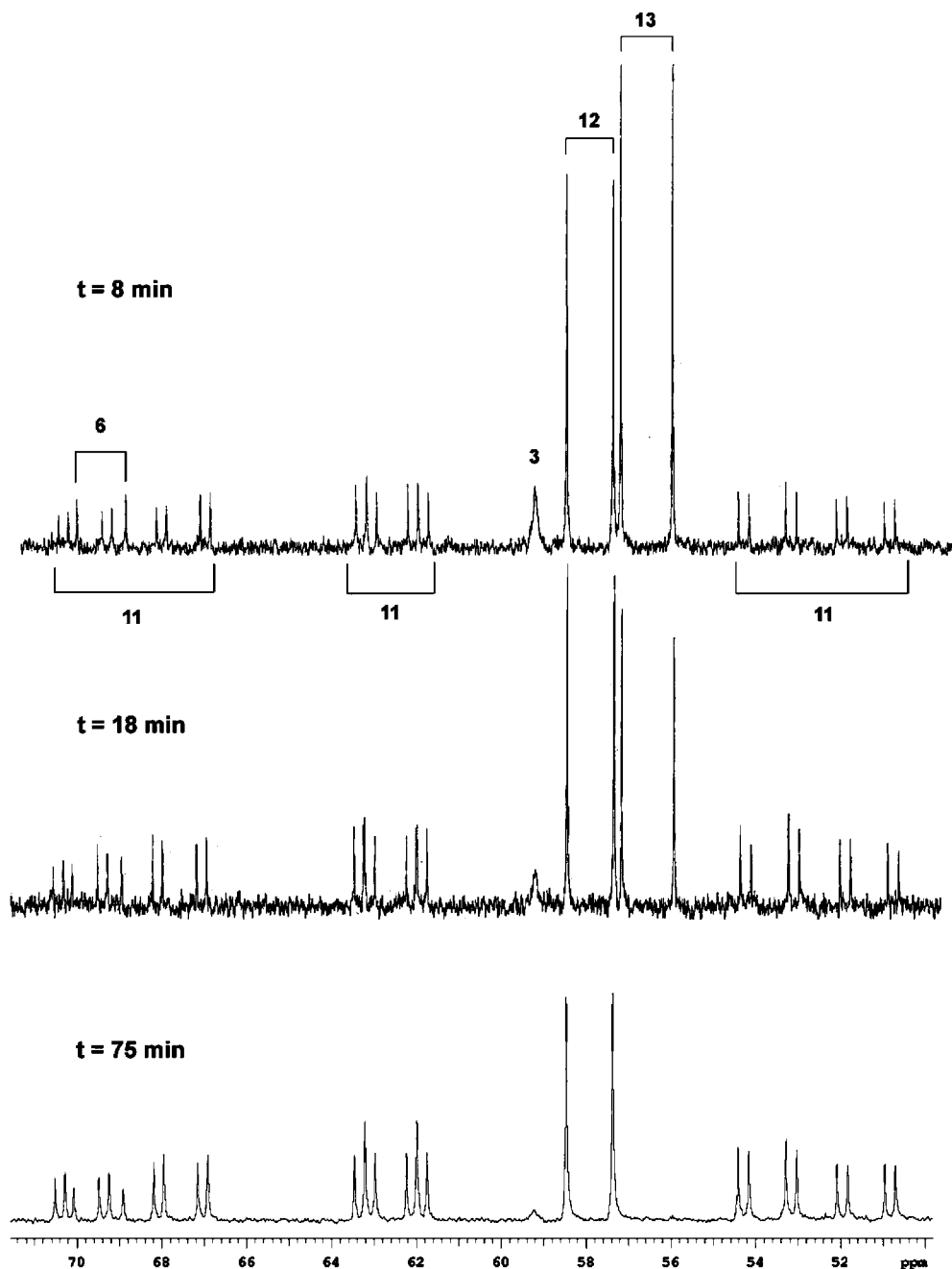


Figure 6. ^{31}P NMR monitoring for the reaction of complex **7** with 1 equiv of dppe in CDCl_3 .

coordinate the metal. This behavior allowed the displacement of the COD ligand with PPh_3 for **7**. It is known that the COD ligand cannot be displaced from $[\text{Rh}(\text{PPh}_3)_2(\text{COD})]$ complex with excess PPh_3 .²⁴ In addition, the emergence of $[\text{Rh}(\text{dppe})(\text{COD})]$ (**13**) and free PNSO ligand at the initial stages of the reaction reveals that dppe preferentially removes the PNSO rather than the COD ligand and that only later does the PNSO displace the COD ligand. With an electron-rich Rh^{I} center, the PNSO ligand in complexes **10** and **11** was presumed to display an S-coordination mode, in concordance with complexes in **6** and **8**.²⁵

Finally, interesting and distinct behaviors were observed when bis-PNSO complexes **6** and **9** were treated with PPh_3 and dppe (Scheme 5). Although **6** and **9** were similarly unreactive toward PPh_3 , they showed a different reaction profile with a diphosphine. Reaction of dppe with **6** produced a complete ligand exchange to yield the corresponding bis-dppe rhodium complex

12 in only 8 min. However, no reaction was observed after 5 h when cyclohexyl PNSO complex **9** was treated with dppe. The reactivity observed allows us to confirm that PNSO ligands are more competent ligands than monophosphines and that they cannot be replaced by PPh_3 . Furthermore, a chelating diphosphine such as dppe can easily replace the diphenylphosphino PNSO ligand **3** from the Rh coordination sphere, but not the cyclohexyl analog **4**.

Conclusions

Here, we report on the first rhodium (I) complexes with PNSO ligands. We have shown that these compounds can work as

(24) Albers, J.; Dinjus, E.; Pitter, S.; Walter, O. *J. Mol. Catal. A* **2004**, *219*, 41–46.

(25) No characteristic absorption bands were identified for the S=O stretch in these complexes; see reference 14.

either P,O or P,S chelating ligands, depending on the electronic environment around the metal center. Thus, *N*-benzyl-*N*-diphenylphosphino-*tert*-butylsulfonamide (**3**) provides P,O coordination when olefin ligands (NBD or COD) are attached to the metal center. Alternatively, rhodium complexes with two PNSO ligands provides P,S coordination. [Rh(PNSO)₂] complexes preferentially show the thermodynamically most stable *cis* configuration. However, we have identified the kinetic *trans* complex with a dicyclohexylphosphino analog of **3**. Finally, ligand exchange experiments with PPh₃ and dppe show that PNSO ligands act as hemilabile ligands by providing coordination sites for the incoming phosphines.

Experimental Section

(+)-(R)-N-Benzyl-N-dicyclohexylphosphino-*tert*-butylsulfonamide Borane (4-BH₃). A 1.3 mL portion of *n*-BuLi 2.5 M in hexane (3.2 mmol) was added dropwise to a cooled ($-78\text{ }^\circ\text{C}$) solution of the corresponding (*R*)-(-)-*N*-benzyl-*tert*-butylsulfonamide (600 mg, 2.8 mmol) in THF (20 mL). After 15 min, 0.72 mL (0.76 g, 3.3 mmol) of chlorodicyclohexylphosphine was added via syringe. The mixture was stirred at $-78\text{ }^\circ\text{C}$ for 1 h, and then the temperature was allowed to rise to $-30\text{ }^\circ\text{C}$. At this point, 0.35 mL (0.28 g, 3.7 mmol) of BH₃-SMe₂ was added via syringe. The mixture was stirred at this temperature for 30 min and then warmed to $0\text{ }^\circ\text{C}$. The reaction was then quenched with 15 mL of water (caution: bubbling occurs) and extracted with Et₂O (30 mL). The organic layer was dried over MgSO₄, filtered, and concentrated under reduced pressure. The crude products were purified by flash column chromatography (SiO₂, hexanes/AcOEt, 80/20) to afford 1.00 g (85%) of the desired ligand as a foamy oil. $[\alpha]_D = +49.3$ (*c* 1.0, CHCl₃). IR (KBr): ν_{max} 2932, 2853, 2390, 1451 cm^{-1} . ¹H NMR (400 MHz, CDCl₃): δ 0.20–0.80 (br s, 3H, BH₃), 1.10 (s, 9H), 1.14–1.38 (m, 6H), 1.50–1.98 (m, 11H), 2.00–2.24 (m, 5H), 4.46 (dd, *J* = 14 and 17 Hz, 1H), 4.68 (dd, *J* = 10 and 17 Hz, 1H), 7.21–7.38 (m, 5H). ¹³C NMR (100 MHz, CDCl₃): δ 24.2 (CH₃), 26.0–26.2 (m, 2 \times CH₂), 26.9–27.3 (m, 4 \times CH₂), 36.2 (d, *J*_P = 36 Hz, CH), 37.2 (d, *J*_P = 27 Hz, CH), 44.2 (d, *J*_P = 3 Hz, CH₂), 60.9 (C), 127.3 (CH), 128.2 (CH), 128.3 (CH), 139.0 (C) ppm. ³¹P NMR (121 MHz, CDCl₃): δ -63.9 (m) ppm. MS (CI, NH₃) *m/e* = 422 ([M + H]⁺, 25%), 421 ([M]⁺, 38%), 420 ([M - H]⁺, 100%), 364 ([M - C₄H₉]⁺, 21%). HRMS (ESI-TOF) *calcd.* for C₂₃H₄₁BNOPS: H, 420.2661; *found*, 420.2656.

(S_R)-[Rh(PNSO)(NBD)][TfO] (5). Me₃SiOSO₂CF₃ (0.062 mL, 0.339 mmol) was added to a yellow solution of (nbd)Rh(acac) (0.1 g, 0.339 mmol) in dry THF (4 mL) under argon. The yellow-orange solution was stirred for 5 min, and (+)-**3** (0.134 g, 0.339 mmol) was then added in one portion. The solution briefly changed to orange, and a yellow precipitate separated to leave an orange liquor. The suspension was stirred at room temperature for 1 h and then added to vigorously stirred hexane (50 mL); a yellow-orange precipitate was formed. Most of the mother liquor was removed by canula and additional hexane (10 mL) was added. The precipitate was filtered off and dried to give a yellow solid (206 mg) as a mixture of complexes. Dark orange crystals of **5**, suitable for X-ray analysis, were obtained upon layering a THF solution of the resulting solid with Et₂O and hexane. IR (KBr): ν_{max} = 1260, 11173, 1035 cm^{-1} . ¹H NMR (400 MHz, CDCl₃): δ 1.34 (s, 9H), 1.62 (br 2), 3.99 (br, 2H), 4.42–4.48 (br m, 1H), 4.55–4.60 (br m, 1H), 6.83 (br, 2H), 7.16–7.20 (br, 4H), 7.42 (br, 3H), 7.51–7.60 (m, 8H), 7.82–7.86 (br, 3H) ppm. ³¹P NMR (121 MHz, CDCl₃): 115.8 (d, *J*_{Rh} = 193 Hz) ppm. MS (ESI, H₂O/CH₃CN (1:1) 1% formic) *m/z*: 893 [100, (2M - OTf - 2NBD)⁺], 590 [92, (M - OTf)⁺]. HRMS (ESI): *calcd.* for C₃₀H₃₄NOPSRh⁺, 590.1153; *found*, 590.1141.

(S_R)-cis-[Rh(PNSO)₂][TfO] (6). [RhCl(COD)]₂ (0.1 g, 0.202 mmol) and AgOTf (0.104 g, 0.404 mmol) were placed in a Schlenk

flask protected from light with aluminum foil. The flask was then purged with N₂, and dry CH₂Cl₂ (2 mL) was added and stirred for 2 h. The resulting white precipitate (AgCl) was removed by filtration over Celite under nitrogen and subsequently washed with extra CH₂Cl₂ (3 \times 2 mL). This orange solution was added dropwise into a Schlenk tube containing a solution of ligand (+)-**3** (0.320 g, 0.808 mmol) in CH₂Cl₂ (2 mL), and the mixture turned yellow. The reaction was stirred for 24 h at room temperature, then the yellow solution was evaporated under vacuum to a small volume (2–3 mL) and poured over vigorously stirred Et₂O (50 mL). The resulting precipitate was filtered, washed with 2 \times 10 mL of Et₂O and dried to give complex **6** as a yellow shiny powder (0.36 g, 90%). Suitable crystals for X-ray analysis were obtained upon layering Et₂O over a CH₂Cl₂ solution of **6**. mp: $177\text{ }^\circ\text{C}$. $[\alpha]_D = +34$ (*c* = 0.1, CHCl₃). IR (KBr): ν_{max} = 1439, 1272, 1149, 1131, 1106, 1062, 1031 cm^{-1} . ¹H NMR (400 MHz, CDCl₃): δ 1.47 (s, 18H), 4.35 (dd, *J* = 11 and 17 Hz, 2H), 4.43 (dd, *J* = 10 and 17 Hz, 2H), 6.66 (d, *J* = 8 Hz, 4H), 6.95–7.02 (m, 8H), 7.06–7.12 (m, 6H), 7.47–7.56 (m, 10H), 7.70 (t, *J* = 8 Hz, 2H) ppm. ¹³C NMR (100 MHz, CDCl₃): δ 24.7 (3 \times CH₃), 49.7 (CH₂), 68.6 (C), 125.5 (C), 128.0 (C), 128.3 (CH), 128.4 (CH), 128.7 (CH), 129.4 (CH), 130.0 (CH), 132.2 (CH), 132.6 (CH), 133.7 (C), 133.9 (CH), 134.2 (CH) ppm. ³¹P NMR (121 MHz, CDCl₃): 69.5 (d, *J* = 141 Hz) ppm. MS (ESI, H₂O/CH₃CN (1:1) 1% formic) *m/z*: 893 [100, (M - OTf)⁺]. HRMS (ESI): *calcd.* for C₄₆H₅₂N₂O₂P₂S₂Rh⁺, 893.1995; *found*, 893.1988. Anal. *calcd.* for C₄₇H₅₂F₃N₂O₃P₂RhS₃: C, 54.12; H, 5.03; N, 2.69. *Found*: C, 54.16; H, 4.93; N, 2.60.

(S_R)-[Rh(PNSO)(COD)][TfO] (7). [RhCl(COD)]₂ (0.2 g, 0.404 mmol) and AgOTf (0.208 g, 0.809 mmol) were placed in a Schlenk flask protected from light with aluminum foil. The flask was then purged with N₂, and dry THF (2 mL) was added and stirred for 2 h. The resulting white precipitate (AgCl) was removed by filtration over Celite under nitrogen, and subsequently washed with extra THF (3 \times 2 mL). The resulting orange solution was transferred into a Schlenk tube, and a solution of ligand **3** (0.320 g, 0.808 mmol) in THF was added dropwise. The reaction was stirred for 40 min at room temperature. Finally, the solvent was removed under vacuum to a small volume (2–3 mL), and Et₂O (10 mL) was layered over the reaction mixture. After one night, this afforded a crop of orange crystals (0.518 g, 85%) of complex **7**. Suitable yellow/orange crystals for X-ray analysis were obtained upon layering Et₂O over a CH₂Cl₂ solution of **7**. $[\alpha]_D = -115$ (*c* = 0.1, CHCl₃); IR (KBr): ν_{max} = 1274, 1223, 1148, 1031 cm^{-1} . ¹H NMR (400 MHz, CDCl₃): δ 1.54 (s, 9H), 2.05–2.52 (br m, 8H), 3.55 (br, 1H), 3.74 (br, 1H), 4.49 (dd, *J* = 15 Hz and *J*_P = 4 Hz, 1H), 4.70 (dd, *J* = 15 Hz and *J*_P = 4 Hz, 1H), 5.37 (br, 1H), 5.68 (br, 1H), 6.69 (d, *J* = 7 Hz, 2H), 7.12–7.19 (m, 3H), 7.37 (br, t, *J* = 10 Hz, 2H), 7.57–7.71 (m, 6H), 8.01 (t, *J* = 8 Hz, 2H) ppm. ¹³C NMR (100 MHz, CDCl₃): δ 22.6 (3 \times CH₃), 27.8 (CH₂), 28.4 (CH₂), 32.0 (CH₂), 33.5 (CH₂), 53.9 (CH₂), 61.9 (C), 70.4 (d, *J*_{Rh} = 14 Hz, CH), 73.8 (d, *J*_{Rh} = 14 Hz, CH), 105.6 (CH), 109.6 (CH), 127.0 (d, *J*_P = 56 Hz, C), 128.5 (C), 128.9 (C), 129.1 (CH), 130.0 (d, *J*_P = 10 Hz, CH), 130.2 (d, *J*_P = 11 Hz, CH), 130.5 (d, *J*_P = 11 Hz, CH), 131.2 (d, *J*_P = 56 Hz, C), 132.7 (d, *J*_P = 3 Hz, CH), 133.8 (CH), 134.4 (C), 135.5 (d, *J*_P = 16 Hz, CH) ppm. ³¹P NMR (121 MHz, CDCl₃): 116.5 (d, *J* = 167 Hz) ppm. MS (ESI, H₂O/CH₃CN (1:1) 1% formic) *m/z*: 893 [100, (2M - OTf - 2COD)⁺], 539 [37, (M + CH₃CN - COD)⁺]. HRMS (ESI): *calcd.* for C₂₄H₂₉N₂OPSRh⁺, 539.0787; *found*, 539.0786. Anal. *calcd.* for C₃₂H₃₈F₃NO₄PRhS₂: C, 50.86; H, 5.07; N, 1.85. *Found* C, 50.59; H, 4.90; N, 1.79.

(S_R)-trans-[Rh(PNSO)₂][TfO] (8). Ligand 4-BH₃ (100 mg, 0.237 mmol, 2 equiv), DABCO (28 mg, 0.249 mmol, 2.1 equiv), and dry toluene (3 mL) were placed in a Schlenk tube under nitrogen. The solution was warmed to $70\text{ }^\circ\text{C}$ for 4 h and then cooled to room temperature. In a separate Schlenk flask, [RhCl(COD)]₂ (29 mg, 0.059 mmol, 0.5 equiv), AgOTf (30 mg, 0.118 mmol, 1 equiv),

and dry THF (2 mL) were stirred at room temperature under nitrogen for 2 h. The resulting suspension was filtered over Celite under nitrogen. The Rh solution was then added to the ligand/DABCO mixture and allowed to stir for 24 h at room temperature. Removal of solvent under vacuum and purification by flash chromatography (acetone/hexanes, 60:40) afforded 116 mg (92%) of complex **8** as an air-stable yellowish solid. Suitable yellow/green crystals for X-ray analysis were obtained upon layering hexanes over a THF solution of **8**. $[\alpha]_D = -34$ ($c = 0.0016$, CHCl_3). IR (KBr): $\nu_{\text{max}} = 2931, 2854, 1450, 1264, 1141, 1057, 1028 \text{ cm}^{-1}$. ^1H NMR (400 MHz, CDCl_3): δ 0.93–1.38 (m, 18H), 1.46 (s, 18H), 1.73–1.86 (m, 18H), 2.06–2.06 (m, 2H), 2.11–2.20 (m, 4H), 2.36–2.48 (m, 2H), 4.29 (dt, $J = 6$ and 16 Hz, 2H), 4.46 (dt, $J = 4$ and 16 Hz, 2H), 7.35–7.46 (m, 10H) ppm. ^{13}C NMR (100 MHz, $\{^3\text{P}\}$, CDCl_3): δ 25.2 ($3 \times \text{CH}_3$), 25.59 (CH_2), 26.64 (CH_2), 26.3 (CH_2), 26.7 (CH_2), 27.4 (CH_2), 27.5 (CH_2), 27.9 (CH_2), 29.8 (CH_2), 30.6 (CH_2), 34.7 (CH), 39.5 (CH), 51.5 (CH_2), 69.5 (C), 128.8 (CH), 129.1 (CH), 129.2 (CH), 135.3 (C) ppm. ^{31}P NMR (121 MHz, CDCl_3): 86.2 (d, $J = 121$ Hz) ppm. MS (ESI, $\text{H}_2\text{O}/\text{CH}_3\text{CN}$ (1:1) 1% formic) m/z : 917.38 [59, (M – OTf) $^+$], 121 [100%]. HRMS (ESI): calcd. for $\text{C}_{46}\text{H}_{76}\text{N}_2\text{O}_2\text{P}_2\text{S}_2\text{Rh}^+$, 917.3878; found, 917.3858.

(S_R)-*cis*-[Rh(PNSO) $_2$][TfO] (**9**). Solid complex **8** was suspended in dry THF under nitrogen and stirred overnight at room temperature. Solvent removal under vacuum afforded pure *cis*-Rh complex **9** as a yellow solid. Suitable crystals for X-ray analysis were obtained by layering hexanes over a solution of **9** in THF. $[\alpha]_D = -43$ ($c = 0.0021$, CHCl_3). IR (KBr): $\nu_{\text{max}} = 2931, 2854, 1450, 1267, 1151, 1123, 1031 \text{ cm}^{-1}$. ^1H NMR (400 MHz, CDCl_3): δ 0.82–1.26 (m, 16H), 1.63 (s, 18H), 1.70–1.81 (m, 20H), 1.96–2.03 (m, 2H), 2.15 (br, 2H), 2.33 (br, 2H), 4.41 (m, 4H), 7.35–7.42 (m, 6H), 7.445–7.48 (m, 4H) ppm. ^{13}C NMR (100 MHz, $\{^3\text{P}\}$, CDCl_3): δ 25.5 (CH_2), 25.72 (CH_2), 25.77 ($3 \times \text{CH}_3$), 26.0 (CH_2), 26.2 (CH_2), 27.0 (CH_2), 28.4 (CH_2), 29.9 (CH_2), 30.2 (CH_2), 35.3 (CH), 39.6 (CH), 51.6 (CH_2), 71.2 (C), 128.9 (CH), 129.2 (CH), 129.4 (CH), 135.1 (C) ppm. ^{31}P NMR (121 MHz, CDCl_3): 95.5 (d, $J = 135$ Hz) ppm. MS (ESI, $\text{H}_2\text{O}/\text{CH}_3\text{CN}$ (1:1) 1% formic) m/z : 918

[51, (MH – OTf) $^+$], 917 [100, (M – OTf) $^+$]. HRMS (ESI): calcd. for $\text{C}_{46}\text{H}_{76}\text{N}_2\text{O}_2\text{P}_2\text{S}_2\text{Rh}^+$, 917.3878; found, 917.3879. Anal. calcd. for $\text{C}_{47}\text{H}_{76}\text{F}_3\text{N}_2\text{O}_5\text{P}_2\text{RhS}_3 + 1/2\text{CH}_2\text{Cl}_2$: C, 51.41; H, 6.99; N, 2.52. Found: C, 51.34; H, 6.97; N, 2.53.

(S_R)-[Rh(PNSO)(PPh $_3$) $_2$][TfO] (**10**). A Schlenk tube containing complex **7** (0.05 g, 0.066 mmol), PPh $_3$ (0.034 g, 0.132 mmol) and dry dichloromethane was stirred under nitrogen for 1 h at room temperature. The resulting yellow-orange solution was poured over vigorously stirred hexane (50 mL), and the precipitate was filtered and washed with hexane (2×10 mL). The yellow solid was dried over high vacuum to provide 0.071 g (91%) of complex **10**. $[\alpha]_D = -16$ ($c = 0.1$, CHCl_3). IR (KBr): $\nu_{\text{max}} = 1436, 1272, 1148, 1093, 1031 \text{ cm}^{-1}$. ^1H NMR (400 MHz, CDCl_3): δ 1.12 (s, 9H), 4.05 (dd, $J = 17$ Hz and $J_P = 12$ Hz, 1H), 4.40 (dd, $J = 17$ Hz and $J_P = 12$ Hz, 1H), 6.40 (d, $J = 7$ Hz, 2H), 6.89–6.95 (m, 7H), 7.02–7.09 (m, 7H), 7.17–7.27 (m, overlap with CDCl_3 peak, 9H), 7.31–7.48 (m, 17H), 7.50–7.61 (m, 2H), 7.64–7.69 (m, 1H) ppm. ^{31}P NMR (121 MHz, CDCl_3): 23.7 (ddd, $J_{\text{PPcis}} = 37.2$, $J_{\text{PRh}} = 138.8$, $J_{\text{PPtrans}} = 279$ MHz), 32.2 (dt, $J_{\text{PPcis}} = 37.2$, $J_{\text{PRh}} = 155.8$), 63.6 (ddd, $J_{\text{PPcis}} = 37.3$, $J_{\text{PRh}} = 127.7$, $J_{\text{PPtrans}} = 278.9$ MHz) ppm. MS (ESI, $\text{H}_2\text{O}/\text{CH}_3\text{CN}$ (1:1) 1% formic) m/z : 760 [26, (M – PPh $_3$) $^+$], 801 [100], 1022 [8, (M) $^+$]. HRMS (ESI): calcd. for $\text{C}_{59}\text{H}_{56}\text{NOP}_3\text{SRh}$, 1022.2345; found, 1022.2341.

Acknowledgment. We thank MEC (CTQ2005-623) and Enantia S. L. for financial support. T.A. thanks Enantia for financial support. We thank Prof. Anton Vidal-Ferran and Dr. Elisenda Reixach (ICIQ) for helpful assistance in ^{31}P decoupled NMR experiments.

Supporting Information Available: General methods and NMR spectra for ligand **4-BH $_3$** and complexes **6**, **7**, **8**, and **9**. X-ray crystal data with a complete numbering scheme, atomic distances and angles for **5**, **7**, **6**, and **8**. This material is available free of charge via the Internet at <http://pubs.acs.org>.

OM8006823

On the Nature of “RuCl(dmsO)₂{HB(mt)₃}” (mt = methimazolyl)

Robyn J. Abernethy, Anthony F. Hill,* Never Tshabang, Anthony C. Willis, and Rowan D. Young

Research School of Chemistry, Institute of Advanced Studies, Australian National University, Canberra, ACT, Australia

Received July 31, 2008

The high-yield product of the reaction of [RuCl₂(dmsO)₄] (dmsO = dimethylsulfoxide) with Na[HB(mt)₃] (mt = methimazolyl) is not, as reported, the complex [RuCl(dmsO)₂{κ³-S,S',S''-HB(mt)₃}] but rather the isomeric [RuCl(dmsO)₂{κ³-H,S,S'-HB(mt)₃}], which features a three-center, two-electron B–H–Ru interaction, as also found for the complex [RuH(PPh₃)₂{κ³-H,S,S'-H₂B(mt)₂}], which results from [RuHCl(PPh₃)₃] and Na[H₂B(mt)₂].

Introduction

Within the growing field of poly(methimazolyl)borate chemistry (Chart 1), three-center, two-electron B–H–metal interactions appear to be a recurrent feature of the binding of these and related ligands to transition metals.¹ It has been suggested that they are important intermediates in the formation of metallaboratrane via B–H activation.^{2,3} Although potentially more far-reaching routes to compounds with B→M dative bonding have now been demonstrated by Bourissou,⁴ the facile B–H activation of poly(methimazolyl)borates by late transition metals remains a remarkably general route.^{2,3} Within scorpionate chemistry, B–H–M interactions are of course not unheard of, the first examples having been encountered for simple dihydrobis(dimethylpyrazolyl)borates of molybdenum some 35

ago.⁵ Nevertheless, evidence continues to accumulate to suggest that such interactions are especially favorable for bis(methimazolyl)borate complexes,¹ presumably a corollary of the increased chelate size that attends replacement of pyrazolyl groups (BNNM) with methimazolyl (BNCSM) bridges. Indeed, we have previously shown that even the HB(mt)₃ ligand may adopt this coordination mode (κ³-H,S,S') in preference to the more commonly observed κ³-S,S',S'' mode, e.g., the complex [RuH(CO)(PPh₃){HB(mt)₃}] (**1**).⁶ The spontaneous reaction of **1** with

* To whom correspondence should be addressed. E-mail: a.hill@anu.edu.au.

(1) (a) Kimblin, C.; Churchill, D. G.; Bridgewater, B. M.; Girard, J. N.; Quarless, D. A.; Parkin, G. *Polyhedron* **2001**, *20*, 1891. (b) Kimblin, C.; Bridgewater, B. M.; Churchill, D. G.; Hascall, T.; Parkin, G. *Inorg. Chem.* **2000**, *39*, 4240. (c) Dodds, C. A.; Garner, M.; Reglinski, J.; Spicer, M. D. *Inorg. Chem.* **2006**, *45*, 2733. (d) Graham, L. A.; Fout, A. R.; Kuehne, K. R.; White, J. L.; Mookherji, B.; Marks, F. M.; Yap, G. P. A.; Zakharov, L. N.; Rheingold, A. L.; Rabinovich, D. *Dalton Trans.* **2005**, 171. (e) Alvarez, H. M.; Tanski, J. M.; Rabinovich, D. *Polyhedron* **2004**, *23*, 395. (f) Alvarez, H. M.; Krawiec, M.; Donovan-Merkert, B. T.; Fouzi, M.; Rabinovich, D. *Inorg. Chem.* **2001**, *40*, 5736. (g) Kuan, S. L.; Leong, W. K.; Goh, L. Y.; Webster, R. D. *J. Organomet. Chem.* **2006**, *691*, 907. (h) Kuan, S. L.; Leong, W. K.; Goh, L. Y.; Webster, R. D. *Organometallics* **2005**, *24*, 4639. (i) Foreman, M. R.; St. J.; Hill, A. F.; Tshabang, N.; White, A. J. P.; Williams, D. J. *Organometallics* **2003**, *22*, 5593. (j) Hill, A. F.; Smith, M. K.; Wagler, J. *Organometallics* **2008**, *27*, 2137. (k) Hill, A. F.; Smith, M. K. *Chem. Commun.* **2005**, 1920. (l) Abernethy, R. J.; Hill, A. F.; Neumann, H.; Willis, A. C. *Inorg. Chim. Acta* **2005**, *358*, 1605. (m) Hill, A. F.; Smith, M. K. *Organometallics* **2007**, *26*, 3900. (n) Crossley, I. R.; Hill, A. F.; Willis, A. C. *Organometallics* **2007**, *26*, 3891. (o) Crossley, I. R.; Hill, A. F.; Humphrey, E. R.; Smith, M. K. *Organometallics* **2006**, *25*, 2242. (p) Foreman, M. R.; St. J.; Hill, A. F.; Smith, M. K.; Tshabang, N. *Organometallics* **2005**, *24*, 5224. (q) Crossley, I. R.; Hill, A. F.; Willis, A. C. *Organometallics* **2005**, *24*, 4889. (r) Abernethy, R. J.; Foreman, M. R. St. J.; Hill, A. F.; Tshabang, N.; Willis, A. C.; Young, R. D. *Organometallics* **2008**, in press. (s) Gennari, M.; Lanfranchi, M.; Marchio, L.; Pellinghelli, M. A.; Tegoni, M.; Cammi, R. *Inorg. Chim. Acta* **2006**, *45*, 3456. (t) Santini, C.; Pettinari, C.; Gioia Lobbia, G.; Spagna, R.; Pellei, M.; Vallorani, F. *Inorg. Chim. Acta* **1999**, *285*, 81. (u) Maria, L.; Moura, C.; Paulo, A.; Santos, I. C.; Santos, I. J. *J. Organomet. Chem.* **2006**, *691*, 4773. (v) Garcia, R.; Xing, Y.-H.; Paulo, A.; Domingos, A.; Santos, I. *J. Chem. Soc., Dalton Trans.* **2002**, 4236. (w) Garcia, R.; Domingos, A.; Paulo, A.; Santos, I.; Alberto, R. *Inorg. Chem.* **2002**, *41*, 2422. (x) Maria, L.; Domingos, A.; Santos, I. *Inorg. Chem.* **2001**, *40*, 6863. (y) Garcia, R.; Paulo, A.; Domingos, A.; Santos, I.; Ortner, K.; Alberto, R. *J. Am. Chem. Soc.* **2000**, *122*, 11240.

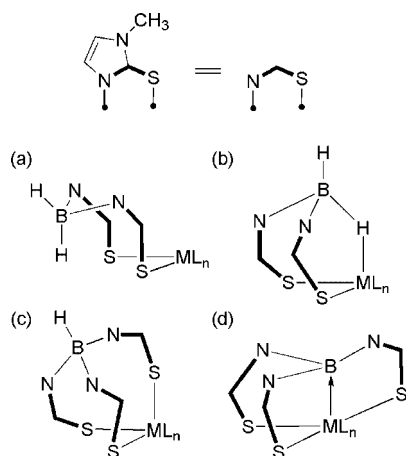
(2) (a) Hill, A. F.; Owen, G. R.; White, A. J. P.; Williams, D. J. *Angew. Chem., Int. Ed.* **1999**, *38*, 2759. (b) Foreman, M. R. St. J.; Hill, A. F.; White, A. J. P.; Williams, D. J. *Organometallics* **2004**, *23*, 913. (c) Crossley, I. R.; Foreman, M. R. St. J.; Hill, A. F.; White, A. J. P.; Williams, D. J. *Chem. Commun.* **2005**, 221. (d) Crossley, I. R.; Hill, A. F.; Humphrey, E. R.; Willis, A. C. *Organometallics* **2005**, *24*, 4083. (e) Crossley, I. R.; Hill, A. F.; Willis, A. C. *Organometallics* **2006**, *25*, 289. (f) Crossley, I. R.; Hill, A. F.; Willis, A. C. *Organometallics* **2005**, *24*, 1062. (g) Crossley, I. R.; Hill, A. F.; Willis, A. C. *Organometallics* **2006**, *25*, 289. (h) Crossley, I. R.; Hill, A. F. *Organometallics* **2004**, *23*, 5656. (i) Crossley, I. R.; Hill, A. F.; Willis, A. C. *Organometallics* **2007**, *26*, 3891. (j) Crossley, I. R.; Hill, A. F. *Dalton Trans.* **2008**, 231. (k) Crossley, I. R.; Hill, A. F.; Willis, A. C. *Organometallics* **2008**, *27*, 312. (l) Crossley, I. R.; Foreman, M. R.; St. J.; Hill, A. F.; Owen, G. R.; White, A. J. P.; Williams, D. J.; Willis, A. C. *Organometallics* **2008**, *27*, 381.

(3) (a) Mihalciak, D. J.; White, J. L.; Tanski, J. M.; Zakharov, L. N.; Yap, G. P. A.; Incarvito, C. D.; Rheingold, A. L.; Rabinovich, D. *Dalton Trans.* **2004**, 1626. (b) Blagg, R. J.; Charmant, J. P. H.; Connelly, N. G.; Haddow, M. F.; Orpen, A. G. *Chem. Commun.* **2006**, 2350. (c) Senda, S.; Ohki, Y.; Yasuhiro, H.; Tomoko, T.; Toda, D.; Chen, J.-L.; Matsumoto, T.; Kawaguchi, H.; Tatsumi, K. *Inorg. Chem.* **2006**, *45*, 9914. (d) Landry, V.; Melnick, J. G.; Buccella, D.; Pang, K.; Ulichny, J. C.; Parkin, G. *Inorg. Chem.* **2006**, *45*, 2588. (e) Figueroa, J. S.; Melnick, J. G.; Parkin, G. *Inorg. Chem.* **2006**, *45*, 7056. (f) Pang, K.; Quan, S. M.; Parkin, G. *Chem. Commun.* **2006**, 5015. (g) Pang, K.; Tanski, J. M.; Parkin, G. *Chem. Commun.* **2008**, 1008.

(4) (a) Bontemps, S.; Gornitzka, H.; Bouhadir, G.; Miqueu, K.; Bourissou, D. *Angew. Chem., Int. Ed.* **2006**, *45*, 1611. (b) Bontemps, S.; Bouhadir, G.; Miqueu, K.; Bourissou, D. *J. Am. Chem. Soc.* **2006**, *128*, 12056. (c) Bontemps, S.; Sircoglou, M.; Bouhadir, G.; Puschmann, H.; Howard, J. A. K.; Dyer, P. W.; Miqueu, K.; Bourissou, D. *Chem.–Eur. J.* **2008**, *14*, 731. (d) Sircoglou, M.; Bontemps, S.; Mercy, M.; Saffon, N.; Takahashi, M.; Bouhadir, G.; Maron, L.; Bourissou, D. *Angew. Chem., Int. Ed.* **2007**, *46*, 8583. (e) Bebbington, M. W. P.; Bouhadir, G.; Bourissou, D. *Eur. J. Org. Chem.* **2007**, 4483. (f) Bontemps, S.; Bouhadir, G.; Gu, W.; Mercy, M.; Chen, C.-H.; Foxman, B. M.; Maron, L.; Ozerov, O. V.; Bourissou, D. *Angew. Chem., Int. Ed.* **2008**, *47*, 1481.

(5) (a) Trofimenko, S. *Scorpionates: The Coordination of Polypyrazolylborate Ligands*; Imperial College Press: London, 1999. (b) Rheingold, A. L.; Liable-Sands, L. M.; Incarvito, C. L.; Trofimenko, S. *Dalton Trans.* **2002**, 2297. (c) Chowdhury, S. K.; Samanta, U.; Puranik, V. G.; Sarkar, A. *Organometallics* **1997**, *16*, 2618. (d) Kosky, C. A.; Ganis, P.; Avitabile, G. *Acta Crystallogr., Sect. B: Struct. Crystallogr. Cryst. Chem.* **1971**, *27*, 1859.

Chart 1. (a) $\kappa^2\text{-S,S}'\text{-Dihydrobis(methimazolyl)borato}$, (b) $\kappa^3\text{-H,S,S}'\text{-Dihydrobis(methimazolyl)borato}$, (c) $\kappa^3\text{-S,S,S}'\text{-Hydrotris(methimazolyl)borato}$, and (d) $\kappa^4\text{-B,S,S,S}'\text{-Tris(methimazolyl)borane}$ ("metallaboratrane") Complexes



ethynylbenzene under ambient conditions to provide styrene and the archetypal metallaboratrane^{7–9} $[\text{Ru}(\text{CO})(\text{PPh}_3)\{\text{B}(\text{mt})_3\}]\text{-}(\text{Ru}\rightarrow\text{B})^8$ would, however, appear to indicate that the B–H–Ru interaction is, in this case, hemilabile.

Against this background, we were intrigued by the report of a complex, $[\text{RuCl}(\text{dmsO})_2\{\text{HB}(\text{mt})_3\}]$ (**2**),¹⁰ obtained as red-orange crystals (19%) from the reaction of $[\text{RuCl}_2(\text{dmsO})_4]$ ¹¹ with $\text{Na}[\text{HB}(\text{mt})_3]$.^{2a} On the basis of an imprecise crystallographic study ($R \approx 0.20$) supported by infrared and ¹H NMR data, **2** was formulated as involving $\kappa^3\text{-S,S,S}'$ coordination of a $\text{HB}(\text{mt})_3$ ligand. Our problem with this formulation was the inconsistency of the limited spectroscopic data with the solid state structure. Specifically, (i) an IR absorption was reported at 2198 cm^{-1} that was attributed to the terminal B–H stretch, while this region corresponds more closely to that typical of a B–H–Ru interaction.^{1,6} (ii) The solid state structure has no element of symmetry due to the intrinsic chirality of the $\text{HB}(\text{mt})_3\text{Ru}$ cage, inversion of which in related ruthenium complexes¹² has been shown to be a high-energy process that does not operate under mild conditions, if at all.¹³ Thus the NMR data, which were claimed to comprise two singlet methyl resonances (δ_{H} ($d_6\text{-dmsO}$) = 2.55 (SCH₃), 3.30 (NCH₃)) for the bulk sample, are not consistent with the molecular structure of **2**, which has seven chemically distinct methyl environments.

(6) Foreman, M. R.; St, J.; Hill, A. F.; Owen, G. R.; White, A. J. P.; Williams, D. J. *Organometallics* **2003**, *22*, 4446.

(7) There is some debate in the literature^{8,9} as to how best to describe the bonding of metallaboratranes. The debate centers on whether the formation of a metal–boron dative bond represents a two-electron oxidation of the metal center and increase in valency and/or oxidation state by two units. Experimental evidence germane to this debate continues to accumulate,⁴ and in the interim we recommend a nomenclature that rises above semantics by following line formulas for metallaboratranes with the $(M\rightarrow B)^n$ notation where n represents the total number of d-electrons, including those involved to some variable extent in the formation of the $M\rightarrow B$ bond.⁸

(8) Hill, A. F. *Organometallics* **2006**, *25*, 4741.

(9) Parkin, G. *Organometallics* **2006**, *25*, 4744.

(10) Bailey, P. J.; Loroño-Gonzales, D. J.; McCormack, C.; Parson, S.; Price, M. *Inorg. Chim. Acta* **2003**, *354*, 61.

(11) Evans, I. P.; Spencer, A.; Wilkinson, G. *J. Chem. Soc., Dalton Trans.* **1973**, 204.

(12) Bailey, P. J.; Dawson, A.; McCormack, C.; Moggach, S. A.; Oswald, D. H.; Parsons, S.; Rankin, D. W. H.; Turner, A. *Inorg. Chem.* **2005**, *44*, 8884.

(13) (a) In other systems it should however be noted that cage inversion may be facile, though a dissociative S–W mechanism has been invoked: (b) Foreman, M. R. St.-J.; Hill, A. F.; White, A. J. P.; Williams, D. J. *Organometallics* **2003**, *22*, 3831.

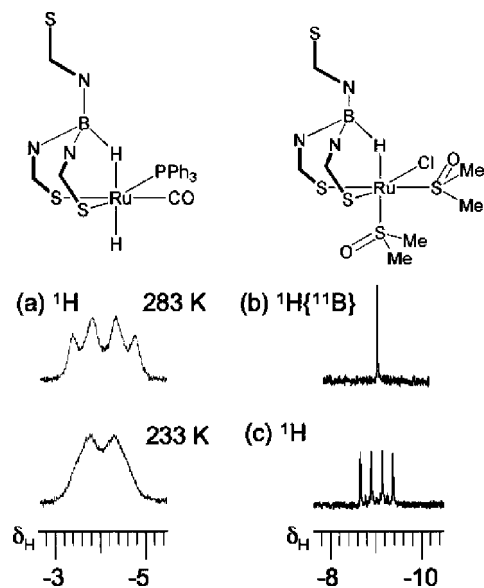
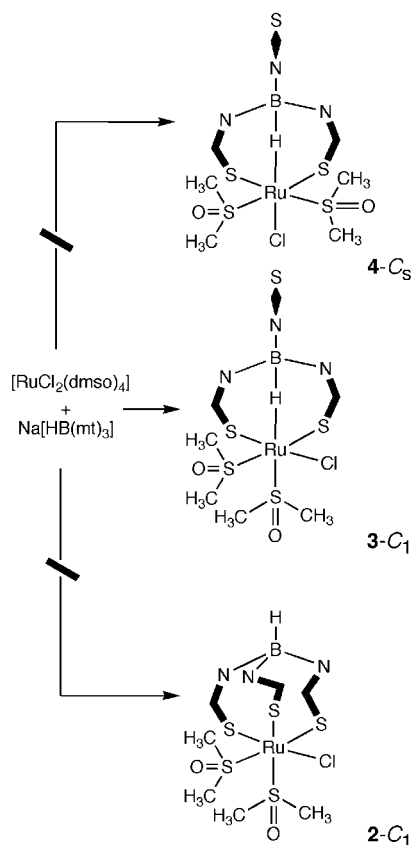


Figure 1. ¹H NMR spectra of B–H–Ru complexes: (a) **1** (¹H);^{2b} (b) **3** (¹H{¹¹B}); and (c) **3** (¹H).

We report herein the full characterization of the major product (up to 92% of the crude material) of the reaction of $[\text{RuCl}_2(\text{dmsO})_4]$ with $\text{Na}[\text{HB}(\text{mt})_3]$, which is in fact the bright orange complex $[\text{RuCl}(\text{dmsO})_2\{\kappa^3\text{-H,S,S}'\text{-HB}(\text{mt})_3\}]$ (**3**). In addition, a further example of a complex adopting the $\kappa^3\text{-H,S,S}'$ coordination mode, $[\text{RuH}(\text{PPh}_3)_2\{\text{H}_2\text{B}(\text{mt})_2\}]$, is reported as evidence in support of the prevalence of this coordination mode.

Results and Discussion

In contrast to the reported reaction of $[\text{RuCl}_2(\text{dmsO})_4]$ with $\text{Na}[\text{HB}(\text{mt})_3]$ in dichloromethane to provide a brown¹⁰ solution we find that combining these reagents anaerobically in tetrahydrofuran results in the formation of a dark orange solution over 3 h. Removal of the solvent in vacuo and measurement of the ¹H NMR spectrum of the bulk sample indicates that it comprises approximately 90–95% of a single compound (vide infra). This composition does not change appreciably if the mixing time is extended to 24 h. Considerable losses however attend purification by extraction and fractional crystallization to remove the salt side product such that yields of the pure isolated, salt-free product range from 40 to 60%. Spectroscopic data for the product are superficially as expected (and distinct from those reported¹⁰) for the solid state structure in that seven methyl resonances are observed in both the ¹H and ¹³C NMR spectra, indicative of a lack of any symmetry element in the complex. However, both the solution (THF: 2226 cm^{-1}) and solid state (Nujol: 2206 cm^{-1}) infrared spectra include absorptions in the region characteristic of B–H–Ru rather than terminal B–H stretches.¹ This prompted us to measure the ¹H NMR spectra to high frequency of SiMe_4 , where a remarkably well-resolved 1:1:1:1 quartet may be found ($\delta_{\text{H}} = -9.02$, $^1J_{\text{BH}} = 71.6\text{ Hz}$, Figure 1) in the region typical of B–H–M interactions. We have often had recourse to this spectroscopic signature, but have never encountered a situation where the boron quadrupole is so effectively decoupled, especially when the boron experiences such an asymmetric electric field gradient. Such sharp lines are typically characteristic of cubic electric fields about boron, e.g., $\text{Na}[\text{BH}_4]$. Indeed the resolution is such that the heptet resonance for the ¹⁰B isotopomer is also discernible, displaying the expected $^1J_{\text{BH}}$ coupling (24.0 Hz , $\nu(^{10}\text{B})/\nu(^{11}\text{B}) = 3.0$). This

Scheme 1. Synthesis of HB(mt)₃ Complexes of Ruthenium

resonance collapses to a singlet in the boron-decoupled spectrum. The ¹¹B NMR spectrum comprises a doublet ($\delta_B = 0.99$ ppm, $^1J_{BH} = 73.2$ Hz), which collapses to a singlet in the ¹¹B{¹H} spectrum.

Thus, the alternative, low-symmetry isomer for **2** must account for these data, indicated as **3** in Scheme 1. The more symmetric isomer **4**, which also involves κ^3 -H,S,S' coordination, may be discarded in that it has overall C_s symmetry and would therefore give rise to four different methyl resonances. The molecular geometry of **3** was confirmed in the solid state by a crystallographic study, the results of which are summarized in Figure 2.

The geometry at ruthenium is essentially octahedral when the constraints of chelation are taken into account. Thus all interligand angles are close to 90°, the smallest of these (Cl1–Ru1–S2 87.91(5)°) being traced to an apparent weak interaction between the B–H–Ru group and two of the protons on C22 (B1H1...HC22 = 2.82, 2.62 Å), though hydrogen positions adjacent to heavy atoms should not be overscrutinized. The protons of dmsO are weakly acidic in nature, and this would be expected to increase upon coordination to Lewis acidic ruthenium(II), while the B–H group is characteristically hydridic in nature. The ¹H NMR spectrum of **3** has one S-CH₃ resonance shifted somewhat upfield of the remainder, and it is this resonance that displays an NOE correlation with the borohydride resonance. It might therefore be inferred that this is not a solid state artifact, but quite possibly persists in solution. There is also an NOE correlation observed between the hydride resonance and one aromatic methimazolyl resonance, which presumably corresponds to the 5-H proton on the unique pendant methimazolyl group (H...H = 3.02 Å). The two dimethylsulfoxide ligands have significantly different (30 esd) Ru–S bond lengths, with that trans to the B–H–Ru interaction being

noticeably shorter. Thus the three-center, two-electron interaction would appear to exert an inverse trans influence, presumably due to the weakness of the H...Ru interaction.

Having established the identity of **3**, the questions as to the nature of “**2**” remain. As noted above, the bulk spectroscopic data reported are inconsistent with the crystallographic data, which perhaps relate to a “rogue” crystal. We have been unable to identify conditions that provide any isomer other than **3** from the reaction of [RuCl₂(dmsO)₄] with Na[HB(mt)₃]. Indeed, repeating the reaction of [RuCl₂(DMSO)₄] with Na[HB(mt)₃] in CD₂Cl₂ under conditions identical to those reported¹⁰ gives primarily (ca. 70%) **3**. Removal of the CD₂Cl₂ and dissolving the entire residue in d₆-dmsO provided a spectrum devoid of the resonances reported for **2**, although it should be noted that the single SCH₃ resonance that was reported (δ_H 2.55) would not have been discernible beneath the broad signal due to residual dmsO. These spectra are provided as Supporting Information.

We have previously noted that ligand fragmentation attends the reaction of Na[HB(mt)₃] with [RuCl₂(PPh₃)₃] such that [Ru(κ^2 -N,S-mt)₂(PPh₃)₂] is the only isolated complex, to date.¹⁴ Furthering our studies of B–H–metal interactions with poly(methimazolyl)borates, we have now investigated the reaction of [RuHCl(PPh₃)₃]·C₆H₅Me¹⁵ with Na[H₂B(mt)₂]¹¹ and find that, in contrast, a clean reaction ensues to provide a hydrido complex formulated as [RuH(PPh₃)₂{H₂B(mt)₂}] (**5**) on the basis of spectroscopic and elemental microanalytical data. The mass spectrum is devoid of an isotopic cluster attributable to a tris(phosphine) complex [RuH(PPh₃)₃{H₂B(mt)₂}], though this is not necessarily definitive. However, the ³¹P{¹H} NMR spectrum shows a single phosphorus environment, which would not be possible for a static tris(phosphine) complex. Thus we were drawn to the conclusion that the complex has only two, chemically equivalent, phosphine ligands and either is coordinatively unsaturated or involves a further example of a B–H–Ru association, viz., [RuH(PPh₃)₂{ κ^3 -H,S,S'-H₂B(mt)₂}]. This conclusion was substantiated by the usual B–H–M spectroscopic signatures ($\delta_H = -5.7$ ppm; $\nu_{BHRu} = 2121$ cm⁻¹) in addition to the triplet multiplicity of the resonance for the terminal ruthenium hydride ($\delta_H = -12.74$, t, $^2J_{HP} = 23$ Hz). The formulation was confirmed by a crystallographic study, the

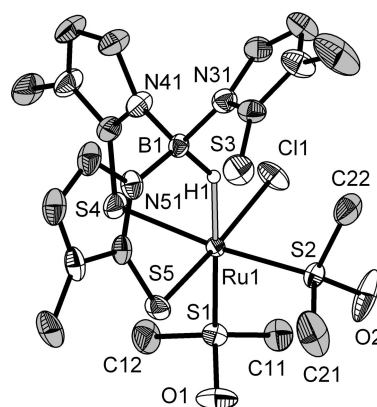


Figure 2. Molecular structure of [RuCl(dmsO)₂{HB(mt)₃}] (**3**) in a crystal of **3**·(CH₂Cl₂)_{0.5} (50% displacement ellipsoids, carbon-bound hydrogen atoms omitted, carbon atoms in gray). Selected distances (Å) and angles (deg): Ru1–Cl1 2.4431(14), Ru1–S1 2.2401(14), Ru1–S2 2.2798(14), Ru1–S4 2.4271(15), Ru1–S5 2.3467(14), Ru1–B1 2.817(6), Ru1–H1 1.84(6), B1–H1 1.14(6), Cl1–Ru1–S1 95.94(5), Cl1–Ru1–S2 87.91(5), S1–Ru1–S2 91.42(5), Cl1–Ru1–S4 87.08(6), S1–Ru1–S4 92.27(5), S1–Ru1–S5 88.41(5), S2–Ru1–S5 93.29(5), S4–Ru1–S5 91.46(6), Ru1–S4–Cl1 104.0(2), Ru1–S5–C51 103.82(19), Ru1–H1–B1 142(4).

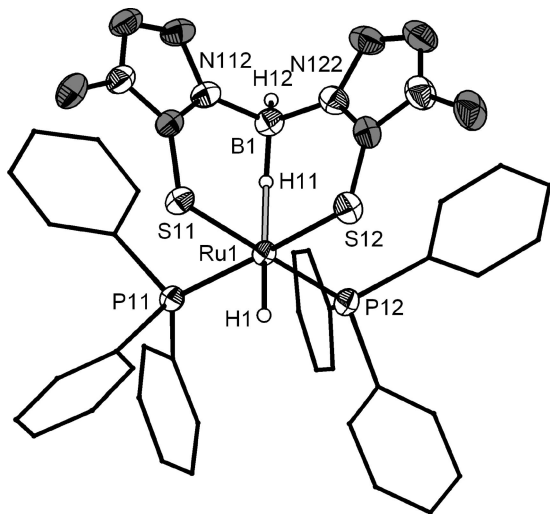


Figure 3. Molecular structure of $[\text{RuH}(\text{PPh}_3)_2\{\text{H}_2\text{B}(\text{mt})_2\}]$ (**5**) in a crystal of $5 \cdot (\text{CH}_2\text{Cl}_2)_2$ (50% displacement ellipsoids, carbon-bound hydrogen atoms omitted, carbon atoms in gray, phenyl groups simplified, one of two crystallographically independent molecules shown). Selected distances (Å) and angles (deg): Ru1–S11 2.4374(7), Ru1–S12 2.4130(7), Ru1–P11 2.2871(7), Ru1–P12 2.2779(7), Ru1–B1 2.774(3), Ru1–H1 1.55(2), Ru1–H11 1.77(2), B1–H11 1.20(2), B1–H12 1.16(2), S11–Ru1–S12 87.64(3), S11–Ru1–P11 82.78(2), S12–Ru1–P12 89.68(3), P11–Ru1–P12 99.71(3), S11–Ru1–B1 79.79(7), S12–Ru1–B1 80.30(7), P11–Ru1–B1 104.81(7), P12–Ru1–B1 101.08(7), S11–Ru1–H1 90(1), S12–Ru1–H1 86(1), P11–Ru1–H1 87(1), P12–Ru1–H1 89(1), S11–Ru1–H11 91.3(8), S12–Ru1–H11 93.0(8), P11–Ru1–H11 94.3(8), P12–Ru1–H11 90.2(8), H1–Ru1–H11 179(1), Ru1–S11–C11 1103.4(1), Ru1–S12–C12 103.7(1), B1–H11–Ru1 138(2).

results of which are summarized in Figure 3, which depicts the approximate (though not crystallographically requisite) C_s symmetry. This symmetry accounts for the chemical equivalence of the two phosphine ligands and the appearance of a single methimazolyl environment in the ^1H and $^{13}\text{C}\{^1\text{H}\}$ NMR spectra. The Ru–S separations of Ru1–S11 2.4374(7) and 2.4130(7) Å are somewhat disparate (35 esd), giving an indication that these are quite flexible in response to crystal packing effects and should therefore in general not be overinterpreted. The chelate bite angle ($87.64(3)^\circ$) is somewhat smaller than that for **3** ($91.46(6)^\circ$), presumably reflecting the increased steric congestion about ruthenium and reduced substitution at boron.

Concluding Remarks

The high-yielding product of the reaction of $[\text{RuCl}_2(\text{dmsO})_4]$ with $\text{Na}[\text{HB}(\text{mt})_3]$ has been shown to involve the less commonly encountered coordination of the $\text{HB}(\text{mt})_3$ ligand through one B–H and two sulfur donors. A remarkable feature to emerge from the spectroscopic characterization of complex **3** is the unusually sharp and well-resolved multiplet ^1H resonance for the B–H–Ru group, for which at present we have no explanation. Although the synthesis of **3** was carried out in tetrahydrofuran, the workup and purification involved crystallization from dichloromethane over a time frame comparable to the originally reported synthesis of **2** executed in dichloromethane. We may therefore surmise that **3** is *not* an intermediate en route to **2** nor in solvent-dependent equilibrium with **2**.

(14) Dewhurst, R. D.; Hansen, A. R.; Hill, A. F.; Smith, M. K. *Organometallics* **2006**, *25*, 5843.

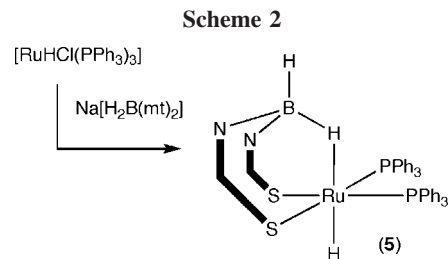
(15) Hallman, P. S.; Evans, D.; Osborn, J. A.; Wilkinson, G. *Chem. Commun.* **1967**, 305.

Experimental Section

General Considerations. All manipulations were carried out under a dry and oxygen-free nitrogen atmosphere using standard Schlenk, vacuum line, and inert atmosphere drybox techniques, with dried and degassed solvents that were distilled from either calcium hydride (CH_2Cl_2) or sodium–potassium alloy and benzophenone (ethers and paraffins). NMR spectra were obtained at 25°C on a Varian Gemini 300BB spectrometer (^1H , 299.945 MHz, ^{13}C , 75.428 MHz, referenced to residual protio-solvent peaks; ^{31}P , 121.420 MHz, ref external 85% H_3PO_4 ; ^{11}B , 96.232 MHz, ref external $\text{BF}_3 \cdot \text{OEt}_2$). Elemental microanalysis was performed by the microanalytical service of the Australian National University. Electrospray (ESI) and FAB mass spectrometry were performed by the Research School of Chemistry mass spectrometry service. Data for X-ray crystallography were collected with a Nonius Kappa CCD diffractometer. The compounds $\text{Na}[\text{HB}(\text{mt})_3]$,^{2a} $\text{Na}[\text{H}_2\text{B}(\text{mt})_2]$,¹¹ $[\text{RuCl}_2(\text{dmsO})_4]$,¹⁰ and $[\text{RuHCl}(\text{PPh}_3)_3] \cdot \text{C}_6\text{H}_5\text{Me}$ ¹⁵ were prepared according to the indicated published procedures. Other reagents were used as received from commercial suppliers.

Synthesis of $[\text{RuCl}(\text{dmsO-S})_2\{\kappa^3\text{-H,S,S'}\text{-HB}(\text{mt})_3\}]$ (3**).** A mixture of $[\text{RuCl}_2(\text{dmsO})_4]$ ¹⁰ (0.20 g, 0.41 mmol) and $\text{Na}[\text{HB}(\text{mt})_3]$ ^{2a} (0.16 g, 0.41 mmol) was stirred in THF (30 mL) at room temperature for 3 (or 24) h, after which time the reaction had changed from bright yellow to yellow-orange. The solvent was removed and the crude mixture was extracted with CH_2Cl_2 (2×10 mL) and filtered through diatomaceous earth. Ethanol (10 mL) was added to the filtrate and the solvent volume reduced (rotary evaporator) until a yellow-orange product precipitated. The product was filtered off, washed with ethanol (10 mL) and hexane (10 mL), and dried in vacuo for 3 h. Yield = 0.16 g (60% based on dichloromethane hemisolvate). IR (Nujol): 2206w ν_{BHRu} , 1648wbr, 1565, 1463s, 1393s, 1364m, 1310, 1266, 1196s, 1132, 1095vs ν_{SO} , 1016 cm^{-1} . IR (THF): 2226 ν_{BHRu} cm^{-1} . ^1H NMR (298 K, CDCl_3): δ -9.02 (q+h, 1H, $^1J(^1\text{B}^1\text{H}) = 71.6$ Hz, $^1J(^{10}\text{B}^1\text{H}) = 24.4$ Hz), 3.15 (NOE with $\delta_{\text{H}} -9.02$), 3.37, 3.38, 3.44 (s \times 4, 3H \times 4, SCH_3), 3.55, 3.63, 3.67 (s \times 3, 3H \times 3, NCH_3), 6.74–6.77 (m, 3H, NCHCH), 6.91, 6.99 (NOE with $\delta_{\text{H}} = -9.02$), 6.70 (s br \times 3, 1H \times 3, NCHCH) ppm. The respective identities of NCH_3 and SCH_3 resonances were confirmed by HSQ correlations with resonances at δ_{C} 33 and 48 ppm, respectively. $^1\text{H}\{^{11}\text{B}\}$ NMR (298 K, CDCl_3): δ -9.07 (s, 1H, B–H–Ru), 3.09, 3.31, 3.32, 3.38 (s \times 4, 3H \times 4, SCH_3), 3.49, 3.56, 3.60 (s \times 3, 3H \times 3, NCH_3), 6.67–6.70 (m, 3H, NCHCH), 6.94, 6.97, 6.98 (s br \times 3, 1H \times 4 NCHCH) ppm. ^{11}B NMR (298 K, d_6 -dmsO): δ 0.99 (d, $^1J_{\text{BH}} = 73.2$ Hz) ppm. $^{11}\text{B}\{^1\text{H}\}$ NMR (278 K, d_6 -dmsO): δ 0.99 ppm. $^{13}\text{C}\{^1\text{H}\}$ NMR (298 K, CDCl_3): δ 165.7(1CS), 163.8(2CS), 122.1(2C), 120.8, 120.2, 119.9, 118.4 (NCHCHN), 47.51, 47.13, 46.67, 46.14(SCH_3), 36.16(1C), 35.01(2C, NCH_3) ppm. FAB(+)-MS (nitrobenzyl alcohol): m/z (%) 545 (10) $[\text{M}-\text{H}]^+$, 566(10) $[\text{HM}-\text{dmsO}]^+$, 530.2(10) $[\text{M}-\text{HCl}-\text{dmsO}]^+$, 452.1(100) $[\text{M}-\text{HCl}-2(\text{dmsO})]^+$. ESI(+)-MS (MeCN): m/z (%) 644(2) $[\text{M}]^+$, 589(3) $[\text{M}+\text{Na}-\text{dmsO}]^+$, 567(28) $[\text{HM}-\text{dmsO}]^+$, 470(100) $[\text{M}+\text{H}_2\text{O}-\text{dmsO}]^+$, 453(92) $[\text{M}-\text{dmsO}]^+$. Anal. Found: C, 28.84; H, 4.33; N, 11.84. Calcd for $\text{C}_{16}\text{H}_{28}\text{BClN}_6\text{O}_2\text{S}_5\text{Ru} \cdot (\text{CH}_2\text{Cl}_2)_{0.5}$: C, 28.87; H, 4.26; N, 12.24 (dichloromethane of solvation established crystallographically and by ^1H NMR integration). Crystals of a dichloromethane hemisolvate $3 \cdot (\text{CH}_2\text{Cl}_2)_{0.5}$ suitable for diffractometry were obtained by slow evaporation of a dichloromethane solution. *Crystal data:* $\text{C}_{16}\text{H}_{28}\text{BClN}_6\text{O}_2\text{RuS}_5 \cdot (\text{CH}_2\text{Cl}_2)_{0.5}$; $M_r = 686.57$; triclinic; $P\bar{1}$ (No. 2); $a = 10.6309(2)$ Å; $b = 10.7378(4)$ Å; $c = 12.8683(4)$ Å; $\alpha = 109.1434(13)^\circ$; $\beta = 93.297(2)^\circ$; $\gamma = 98.6958(18)^\circ$; $V = 1362.72(7)$ Å³; $Z = 2$; $D_c = 1.673$ mg m^{-3} ; $\mu(\text{Mo K}\alpha) = 1.182$ mm^{-1} ; $T = 200(2)$ K, orange plate $0.04 \times 0.05 \times 0.20$ mm; 6226 independent reflections, F^2 refinement, $R_1 = 0.0446$, $wR_2 = 0.1051$ for 30 656 measured reflections; 4319 independent observed absorption-corrected reflections [$|I| > 2\sigma(I)$, $2\theta \leq 55^\circ$], 316 parameters, CCDC 693224.

Synthesis of [RuH(PPh₃)₂{κ³-H,S,S'-H₂B(mt)₂}] (5). In a 100 mL Schlenk flask, [RuHCl(PPh₃)₃]·C₆H₅CH₃¹⁵ (0.25 g, 0.25 mmol) and Na[H₂B(mt)₂]¹¹ (65 mg, 0.25 mmol) were combined in dichloromethane (20 mL). The suspension was stirred at room temperature for 16 h, during which time the reaction mixture changed from a dark purple suspension to a yellow solution with a white precipitate. The solution was filtered through diatomaceous earth and diluted with hexane, and the yellow product precipitated by reduction of the solvent volume by rotary evaporation. The yellow solid was collected on a glass sinter frit and recrystallized from a mixture of dichloromethane and hexane. Yield = 0.16 g (75%). IR (Nujol): 2379 ν_{BH}, 2120 ν_{BHRu}, 1950 ν_{RuH} cm⁻¹. IR (CH₂Cl₂): 2378 ν_{BH}, 2121 ν_{BHRu}, 1956 ν_{RuH} cm⁻¹. ¹H NMR (C₆D₆, 298 K): δ -12.74 (t, ²J_{HP} = 23 Hz, 1H, RuH), -5.7 (s vbr, 1H, B-H-Ru), 2.34 (s, 6H, NCH₃), 5.54, 6.30 (s × 2, 4H, NCH=CH), 6.87–7.86 (m, 30H, C₆H₅) ppm. ¹³C{¹H} NMR (CD₂Cl₂, 298 K): δ 167.4 (CS), 139.1 [d, ¹J_{CP} = 38 Hz, C¹(C₆H₅)], 134.3 [d, ²J_{CP} = 5 Hz, C^{2,6}(C₆H₅)], 127.7 [C⁴(C₆H₅)], 126.5 [d, ³J_{CP} = 5 Hz, C^{3,5}(C₆H₅)], 120.7, 120.3 (s × 2, NCH=CH), 34.01 (NCH₃) ppm. ³¹P{¹H} NMR (C₆D₆, 298 K): δ 65.99 ppm. ESI(+)-MS: *m/z* (%) [assignment]: 865 (30) [M]⁺, 603 (100) [M-PPh₃]⁺. Anal. Found: C, 61.23; H, 5.34; N, 6.74. Calcd for C₄₄H₄₃BN₄P₂RuS₂: C, 61.04; H, 5.01; N, 6.47. Crystals of the bis(dichloromethane) solvate suitable for diffractometry were grown by slow diffusion of hexane into a concentrated dichloromethane solution of the complex at -18 °C. *Crystal data*: C₄₄H₄₃BN₄P₂RuS₂·(CH₂Cl₂)₂; *M_r* = 1035.67; triclinic; *P* $\bar{1}$ (No. 2); *a* = 13.6077(1) Å; *b* = 19.4945(2) Å; *c* = 20.7775(2) Å; α = 105.8160(6)°; β = 100.3594(6)°; γ =



109.6253(5)°; *V* = 4765.85(8) Å³; *Z* = 4; *D_x* = 1.443 mg m⁻³; μ(Mo Kα) = 0.74 mm⁻¹; *T* = 200(2) K, yellow plate 0.08 × 0.26 × 0.30 mm; 104 738 measured reflections, 21 781 independent reflections, *F* refinement, *R*₁ = 0.0424, *wR*₂ = 0.0509 for 15 857 independent absorption-corrected reflections [*l* | *l* | > 3σ(*l* | *l* |), 2θ < 55], 1135 parameters (CCDC 693223).

Acknowledgment. We thank the Australian Research Council (ARC) for financial support (Grant Nos. DP0771497, DP0881692) and the University of Botswana for a studentship (to N.T.).

Supporting Information Available: Full details of the crystal structure determinations of **3**·(CH₂Cl₂)_{0.5} (CCDC 693224) and **5**·(CH₂Cl₂)₂ (CCDC 693223) in CIF format; in situ ¹H NMR spectra of crude reaction mixtures. This material is available free of charge via the Internet at <http://pubs.acs.org>.

OM8007426

Mechanism of the Reaction of Alkynes with a “Constrained Geometry” Zirconaaziridine. PMe_3 Dissociates More Rapidly from the Constrained Geometry Complex than from its Cp_2 Analogue

Kathleen E. Kristian, Masanori Iimura, Sarah A. Cummings, Jack R. Norton,*
Kevin E. Janak, and Keliang Pang

Department of Chemistry, Columbia University, New York, New York 10027

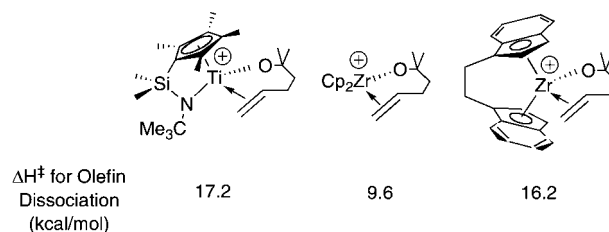
Received October 20, 2008

The “constrained geometry” (cg) zirconaaziridines $\text{Me}_4\text{C}_5\text{SiMe}_2\text{N}(t\text{Bu})\text{Zr}(\eta^2\text{-}[\text{N}(\text{Ph})\text{CH}(\text{Ph})](\text{PMe}_2\text{R}))$ ($\text{R} = \text{Me}, \text{Ph}$) have been synthesized, and the $\text{R} = \text{Ph}$ derivative has been structurally characterized by X-ray crystallography. Treatment of these zirconaaziridines with unsaturated electrophiles such as diphenylacetylene results in insertion. Kinetic data for these irreversible reactions indicate that PMe_3 dissociation must occur prior to insertion and that PMe_3 dissociation from the cg zirconaaziridine **4a** is faster ($k_1 = 0.204(7) \text{ s}^{-1}$) than from the Cp_2 zirconaaziridine **5a** ($k_1' = 0.0013(1) \text{ s}^{-1}$). The reaction of **4a** with diphenylacetylene is several orders of magnitude faster than the reaction of **5a** with diphenylacetylene.

Introduction

In addition to the many developments in metallocene catalysis for olefin polymerization over the past 20 years,¹ there has been great interest in nonmetallocene-mediated olefin polymerization.² Nonmetallocene catalysts can offer increased thermal stability and increased regio- and stereoselectivity. Since Bercaw and co-workers first reported the dimeric “constrained geometry” scandium complex $[(\eta^5\text{-C}_5\text{Me}_4)\text{Me}_2\text{Si}(\eta^1\text{-NCMe}_4)](\text{PMe}_3)\text{ScH}_2$ in 1990,^{3,4} there has been interest in complexes of the “constrained geometry” (cg) ligand, $\text{Me}_4\text{C}_5\text{SiMe}_2\text{N}(t\text{Bu})$,² with Group 4^{5,6} and other early transition metals (Group 3,^{7,8} Group

Chart 1



5,⁹ Ln and An¹⁰). cgTi and cgZr complexes are highly active olefin polymerization catalysts that are particularly good for the copolymerization of ethylene and α -olefins.

Although the polymerization activity of constrained geometry Ti and Zr complexes has been studied widely, the origin of the enhanced reactivity (“constrained geometry effect”) remains unclear. Breitling has suggested that the high activity “most probably results from a more Lewis-acidic transition metal centre”;⁵ Bercaw has characterized cgM complexes as “more acidic and even more electron deficient [than Cp_2M]”.⁸ The enhanced Lewis acidity has been attributed to both electronic factors and steric effects, such as the less crowded coordination sphere and smaller $\text{Cp}_{\text{centroid}}\text{-M-N}$ bite angle in a cgM complex (vs those found in Cp_2M complexes with $\text{M} = \text{Ti}, \text{Zr}$).¹¹

However, quantitative data explaining the enhanced reactivity are scarce. Bercaw and co-workers noted that PMe_3 dissociates readily from the original cgSc dimer,⁸ but did not measure the

* Corresponding author. E-mail: jrn11@columbia.edu.

(1) Alt, H. G.; Koppl, A. *Chem. Rev.* **2000**, *100*, 1205–1222. Angermund, K.; Fink, G.; Jensen, V. R.; Kleinschmidt, R. *Chem. Rev.* **2000**, *100*, 1457–1470. Coates, G. W. *Chem. Rev.* **2000**, *100*, 1223–1252. Fink, G.; Steinmetz, B.; Zechlin, J.; Przybyla, C.; Tesche, B. *Chem. Rev.* **2000**, *100*, 1377–1390. Resconi, L.; Cavallo, L.; Fait, A.; Piemontesi, F. *Chem. Rev.* **2000**, *100*, 1253–1346.

(2) Boffa, L. S.; Novak, B. M. *Chem. Rev.* **2000**, *100*, 1479–1494. Butenschon, H. *Chem. Rev.* **2000**, *100*, 1527–1564. Gibson, V. C.; Spitzmesser, S. K. *Chem. Rev.* **2003**, *103*, 283–316. Hlatky, G. G. *Chem. Rev.* **2000**, *100*, 1347–1376. Ittel, S. D.; Johnson, L. K.; Brookhart, M. *Chem. Rev.* **2000**, *100*, 1169–1204. Siemeling, U. *Chem. Rev.* **2000**, *100*, 1495–1526.

(3) Shapiro, P. J.; Bunel, E.; Schaefer, W. P.; Bercaw, J. E. *Organometallics* **1990**, *9*, 867–869.

(4) Shapiro, P. J.; Schaefer, W. P.; Labinger, J. A.; Bercaw, J. E.; Cotter, W. D. *J. Am. Chem. Soc.* **1994**, *116*, 4623–4640.

(5) Braunschweig, H.; Breitling, F. M. *Coord. Chem. Rev.* **2006**, *250*, 2691–2720.

(6) Brintzinger, H. H.; Fischer, D.; Mulhaupt, R.; Rieger, B.; Waymouth, R. M. *Angew. Chem., Int. Ed. Engl.* **1995**, *34*, 1143–1170. Cano, J.; Kunz, K. *J. Organomet. Chem.* **2007**, *692*, 4411–4423. Lian, B.; Thomas, C. M.; Navarro, C.; Carpentier, J. F. *Organometallics* **2007**, *26*, 187–195. Lian, B.; Thomas, C. M.; Navarro, C.; Carpentier, J. F. *Macromolecules* **2007**, *40*, 2293–2294.

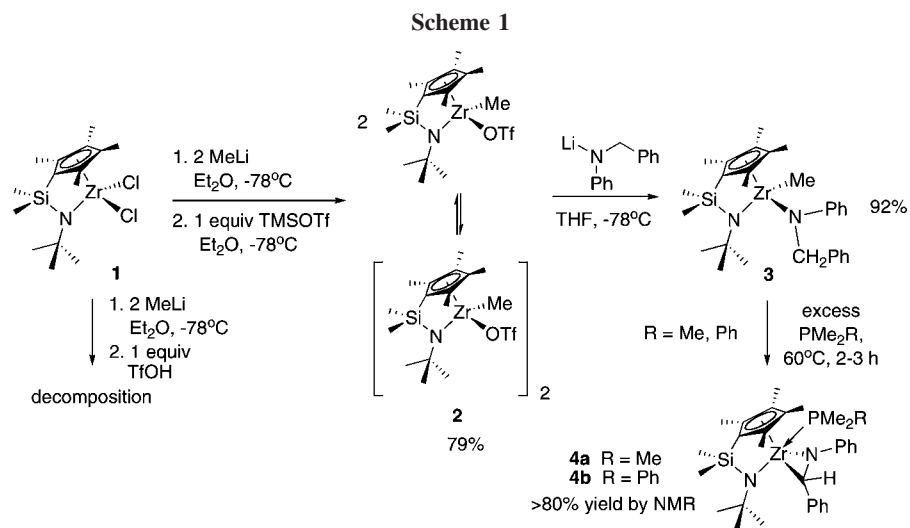
(7) Gromada, J.; Carpentier, J.-F.; Mortreux, A. *Coord. Chem. Rev.* **2004**, *248*, 397–410. Trifonov, A. A.; Spaniol, T. P.; Okuda, J. *Organometallics* **2001**, *20*, 4869–4874. Trifonov, A. A.; Spaniol, T. P.; Okuda, J. *Dalton Trans.* **2004**, 2245–2250.

(8) Shapiro, P. J.; Bunel, E.; Schaefer, W. P.; Bercaw, J. E. *Organometallics* **1990**, *9*, 867–869.

(9) Alcalde, M. I.; Gomez-Sal, M. P.; Royo, P. *Organometallics* **1999**, *18*, 546–554. Alcalde, M. I.; Gomez-Sal, M. P.; Royo, P. *Organometallics* **2001**, *20*, 4623–4631. Postigo, L.; Sanchez-Nieves, J.; Royo, P. *Inorg. Chim. Acta* **2007**, *360*, 1305–1309.

(10) Arredondo, V. M.; McDonald, F. E.; Marks, T. J. *Organometallics* **1999**, *18*, 1949–1960. Li, H. B.; Marks, T. J. *Proc. Natl. Acad. Sci. U.S.A.* **2006**, *103*, 15295–15302. Seyam, A. M.; Stubbart, B. D.; Jensen, T. R.; O’Donnell, J. J.; Stern, C. L.; Marks, T. J. *Inorg. Chim. Acta* **2004**, *357*, 4029–4035. Stubbart, B. D.; Marks, T. J. *J. Am. Chem. Soc.* **2007**, *129*, 4253–4271. Stubbart, B. D.; Marks, T. J. *J. Am. Chem. Soc.* **2007**, *129*, 6149–6167. Stubbart, B. D.; Stern, C. L.; Marks, T. J. *Organometallics* **2003**, *22*, 4836–4838.

(11) Stevens, J. C. *Stud. Surf. Sci. Catal.* **1996**, *101*, 11–20.



rate. Jordan¹² reported activation barriers for the dissociation of pendant olefins in *cg*Ti complexes, finding them to be larger than the barrier to dissociation in a Cp₂Zr complex or a *rac*-(EBI)Zr complex (Chart 1). Petersen¹³ compared the solid-state structures of *cg*TiCl₂ and Cp*(NⁱPr)₂TiCl₂ and concluded that the *cg* ligand is a poorer π donor than separate Cp and amido fragments.

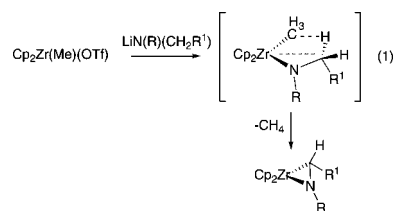
Comparisons of tethered and untethered ligand systems can lend insight into both steric and electronic effects, but directly analogous systems containing identical amido substituents should be employed. Erker¹⁴ utilized a constrained geometry “CpC₁O”Zr dimer for olefin polymerization and found that the dimer, *not* the less sterically encumbered monomer, was the active catalyst. This suggests that steric effects are not responsible for the enhanced reactivity of *cg* complexes relative to the corresponding metallocenes.

Kinetic data for substitution reactions of *cg* and Cp₂ systems should give a clearer picture of the origin of the “constrained geometry effect”. Thus, when our long-standing interest in zirconaaziridine chemistry¹⁵ led us to prepare a *cg* analogue to Cp₂ zirconaaziridines, we decided to compare the substitution kinetics of the *cg* and Cp₂ systems. Herein we report the synthesis of that “constrained geometry” zirconaaziridine, its reactions with unsaturated electrophiles, and comparative kinetic data for the substitution reactions of the *cg* and Cp₂ complexes.

Results and Discussion

Synthesis and Characterization of Constrained Geometry Complexes. Metallocene-derived zirconaaziridines Cp₂Zr(η²-N(R)CH(R'))L¹⁵ are available from the reaction of

Cp₂Zr(Me)(OTf) with a lithiated amine, forming a transient methyl amide complex that spontaneously loses methane to form a zirconaaziridine (eq 1).^{16,17} CH₄ elimination appears to occur via σ-bond metathesis, requiring a syn orientation of the Zr–Me bond and the C–H bond in the benzylamido ligand.



We first attempted the synthesis of a *cg* zirconaaziridine by this method, from the known complex *cg*ZrMe₂.¹⁸ Unfortunately, TfOH protonated the amido portion of the *cg* ligand and led to decomposition (Scheme 1). Treatment of *cg*ZrMe₂ with 1 equiv of TMSOTf, however, gave *cg*Zr(Me)(OTf) (**2**) in excellent yield.

X-ray analysis of *cg*Zr(Me)(OTf) (**2**) (Figure 1) showed that its crystals contain a triflate-bridged dimer. At room temperature the ¹H NMR of **2** showed significant broadening of two methyl resonances, the Zr–Me and one of the four Cp methyl groups, suggesting a monomer–dimer equilibrium in solution.

Treatment of **2** with LiN(Ph)C(H)(Ph) yielded **3**, *cg*Zr(Me)-(N(Ph)CH₂Ph). However, unlike its Cp₂ analogue, **3** did not spontaneously lose CH₄ at room temperature to yield a zirconaaziridine. An NOE study of the *cg* complex **3** explained this lack of reactivity by revealing the nonplanar conformation shown in Figure 2. A NOE was detected between one of the methylene protons on the benzylamido ligand and the remaining

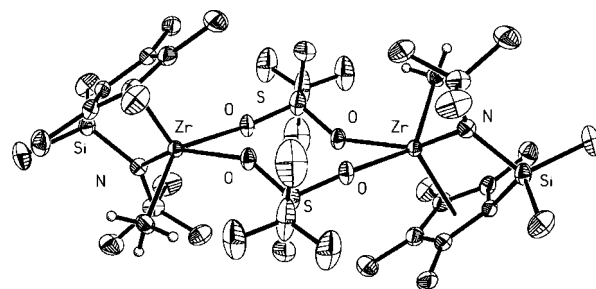


Figure 1. Molecular structure of **2** (20% probability level). Select hydrogen atoms are omitted for clarity.

(12) Carpentier, J. F.; Maryin, V. P.; Luci, J.; Jordan, R. F. *J. Am. Chem. Soc.* **2001**, *123*, 898–909.

(13) Carpenetti, D. W.; Kloppenburg, L.; Kupec, J. T.; Petersen, J. L. *Organometallics* **1996**, *15*, 1572–1581. Kloppenburg, L.; Petersen, J. L. *Organometallics* **1997**, *16*, 3548–3556.

(14) Kunz, K.; Erker, G.; Kehr, G.; Frohlich, R.; Jacobsen, H.; Berke, H.; Blacque, O. *J. Am. Chem. Soc.* **2002**, *124*, 3316–3326.

(15) Cummings, S. A.; Tunge, J. A.; Norton, J. R. Synthesis and Reactivity of Zirconaaziridines. In *New Aspects of Zirconium Containing Organic Compounds*; Marek, I., Ed.; Springer: New York, 2005; pp 1–39.

(16) Buchwald, S. L.; Watson, B. T.; Wannamaker, M. W.; Dewan, J. C. *J. Am. Chem. Soc.* **1989**, *111*, 4486–4494.

(17) Gately, D. A.; Norton, J. R.; Goodson, P. A. *J. Am. Chem. Soc.* **1995**, *117*, 986–996.

(18) Canich, J. M. EP 420436-A1, 1991. Stevens, J. C.; Timmers, F. J.; Wilson, D. R.; Schmidt, G. F.; Nickias, P. N.; Rosen, R. K.; Knight, G. W.; Lai, S. Y. EP 416815-A2, 1991.

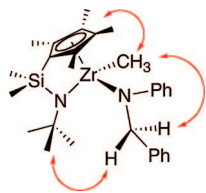


Figure 2. Conformation of **3** supported by NOE experiments. A NOE was observed between the indicated protons.

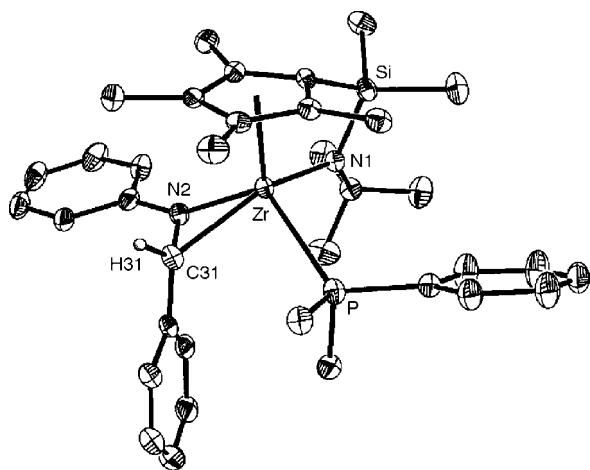


Figure 3. Molecular structure of **4b** (20% probability level). Select hydrogen atoms are omitted for clarity. Selected bond lengths (Å) and angles (deg): Zr–N2 2.056(3), Zr–C31 2.321(5), Zr–N1 2.128(3), Zr–P 2.815(1), C–N2–C31 123.3(4), C–N2–Zr 150.6(3), C31–N2–Zr 81.3(2), N2–Zr–C31 37.5(1), N2–C31–Zr 61.1(2).

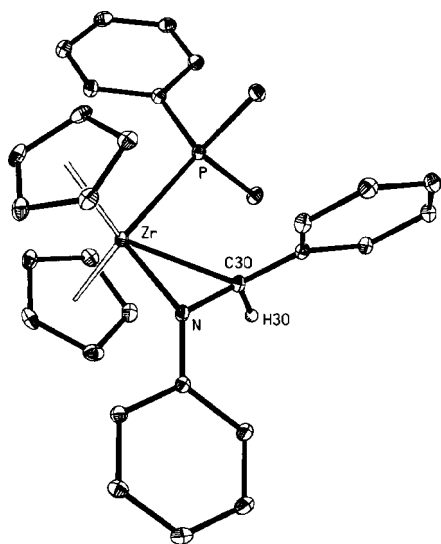


Figure 4. Molecular structure of **5b** (20% probability level). Select hydrogen atoms are omitted for clarity. Selected bond lengths (Å) and angles (deg): Zr–N 2.100(1), Zr–C30 2.377(1), Zr–P 2.7227(3), C–N–C30 124.0(1), C–N–Zr 144.10(8), C30–N–Zr 82.65(7), N–Zr–C30 36.16(4), N–C30–Zr 61.19(6).

methyl group on Zr, and between the other methylene proton and the *t*Bu group in the *cg* ligand (Figure 2).

When heated at 60 °C for 2–3 h a benzene solution of **3** and excess PMe_2R (R = Me, Ph) changed from yellow to bright orange. The ^1H and $^{31}\text{P}\{^1\text{H}\}$ NMR spectra showed the formation of the zirconaaziridines $\text{cgZr}(\eta^2\text{-N}(\text{Ph})\text{CH}(\text{Ph}))\text{PMe}_2\text{R}$ (**4**, Scheme 1). In the ^1H NMR the AB quartet (δ 4.25) corresponding to

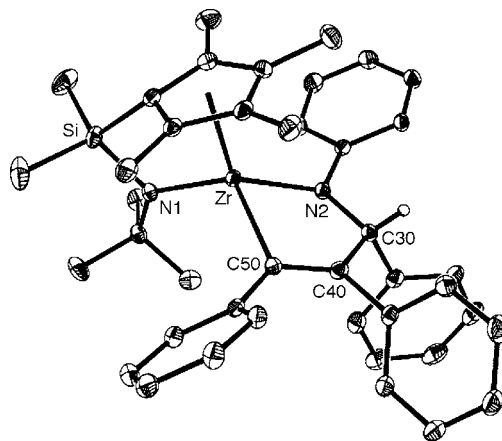
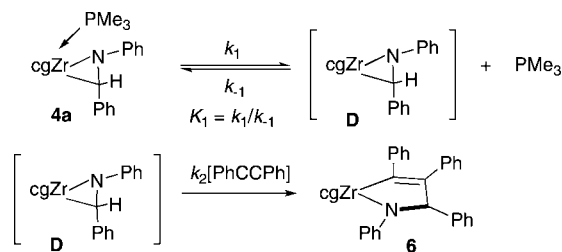


Figure 5. Molecular structure of **6** (20% probability level). Select hydrogen atoms are omitted for clarity. Selected bond lengths (Å): Zr–N2 2.097(2), Zr–C(50) 2.263(3), Zr–N1 2.080(2), C(50)–C(40) 1.338(4).

Scheme 2



the methylene protons in **3** disappeared, with concurrent growth of a ^1H singlet at δ 3.10, which is assigned to the methine proton in **4**. In the $^{31}\text{P}\{^1\text{H}\}$ NMR a peak at δ –27 appeared that can be assigned to coordinated PMe_3 . The zirconaaziridine could not be trapped by weaker donors such as THF or pyridine. The ^1H NMR of **4** indicated the formation of the stereoisomer shown in Scheme 1, along with its enantiomer. A NOE was observed between the methine H and one of the Cp methyl groups but *not* between this H and the *t*Bu group, indicating that the methine H is oriented toward the Cp.

Single crystals of **4b** were obtained from slow diffusion of hexanes into a benzene solution. Their ^1H NMR was identical to that of **4b** formed in solution. X-ray analysis showed the structure in Figure 3.

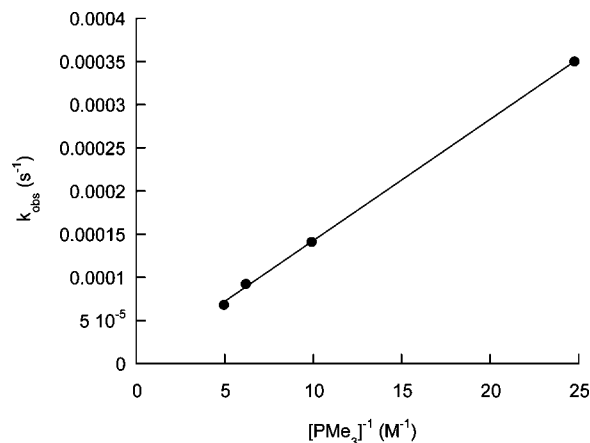


Figure 6. Plot of k_{obs} vs $[\text{PMe}_3]^{-1}$ for the reaction of **4a** (0.02 M) with 10 equiv of PhCCPh at 50 °C in C_6D_6 .

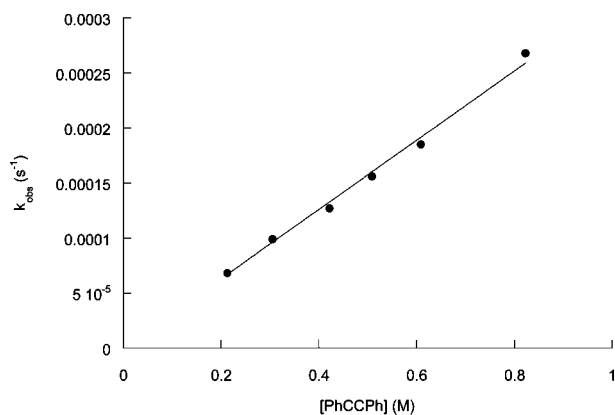
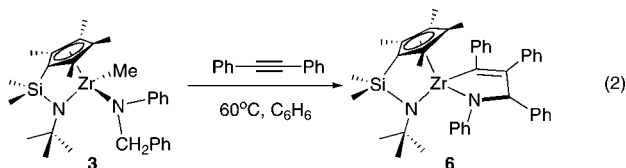


Figure 7. Plot of k_{obs} vs [PhCCPh] for the reaction of **4a** (0.02 M) in the presence of 10 equiv of PMe_3 at 50 °C in C_6D_6 .

For comparison with **4b**, we synthesized $\text{Cp}_2\text{Zr}(\eta^2\text{-N}(\text{Ph})\text{-CH}(\text{Ph}))\text{PMe}_2\text{R}$ (**5a**, R = Me; **5b**, R = Ph) by a modification^{17,19} of Buchwald's procedure.¹⁶ The X-ray structure of **5b** is shown in Figure 4. The bond angles within the three-membered ring in the *cg* zirconaaziridine **4b** are comparable to those in **5b** as well as to those in other Cp_2 zirconaaziridines.¹⁵ The Zr–P bond length in the Cp_2 complex **5b** is 2.7227(3) Å, considerably shorter than the Zr–P bond in the *cg* complex **4b** (2.816(1) Å). However, the Zr–N and Zr–C bonds within the zirconaaziridine ring are slightly longer in **5b** (Zr–N = 2.100(1) Å, Zr–C = 2.377(1) Å) than in **4b** (Zr–N = 2.056(3) Å, Zr–C = 2.321(5) Å). Thus the η^2 imine is slightly closer to the Zr in the *cg* complex **4b**, while the PMe_3 is considerably closer to the Zr in the Cp_2 complex **5b**.

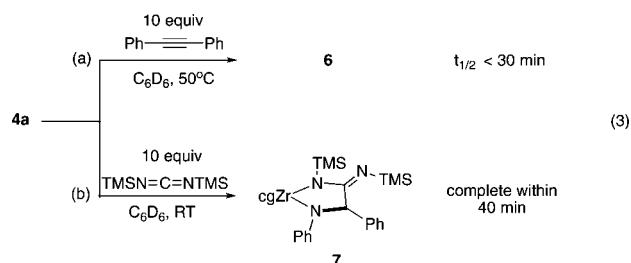
Reactivity of the *cg* Zirconaaziridine **4a and Its Cp_2 Analogue **5a**.** Heating **3** at 60 °C in benzene with diphenylacetylene gave **6**, an azazirconacyclopentene resulting from insertion into the Zr–C bond (eq 2). X-ray analysis of a crystal of **6** confirmed this structure (Figure 5). Compound **6** was also obtained (along with PMe_3) when the PMe_3 adduct **4a** was treated with diphenylacetylene. Heating **6** at 60 °C with excess PMe_3 gave no reaction even after 24 h, indicating that the reaction of **4a** with $\text{PhC}\equiv\text{CPh}$ is irreversible.



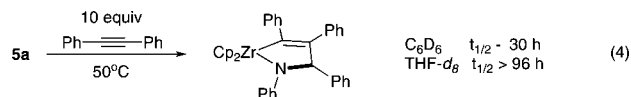
Cp_2 zirconaaziridines form very stable complexes (e.g., **5**) with PMe_3 . Their insertion reactions are slower than those of THF adducts because the dissociation of the PMe_3 is slower than that of THF.^{15,16} Given that “constrained geometry” complexes were purported to be more electron deficient and Lewis acidic than Cp_2 complexes, we suspected that **4a** might dissociate PMe_3 even more slowly than **5a** and that **4a** would therefore insert electrophiles very slowly. However, the reaction of 10 equiv of diphenylacetylene with **4a** proceeded rapidly at 50 °C and even at room temperature to form the insertion product **6** and free PMe_3 (eq 3a).

The reaction of **4a** with 10 equiv of the carbodiimide $(\text{Me}_3\text{Si})\text{NCN}(\text{SiMe}_3)$ at room temperature proceeded even more rapidly. Two products were formed, each of which showed an

upfield shift for the ring methine. By analogy with previously characterized carbodiimide insertion products,²⁰ we believe these products to be the azazirconacyclopentanes resulting from insertion into the Zr–C and Zr–N bonds (the Zr–C insertion product is shown as **7** in eq 3b).



In order to quantify the rate of insertion into a PMe_3 -ligated Cp_2 zirconaaziridine, we treated **5a** with 10 equiv of diphenylacetylene at 50 °C. It was indeed slow, with $t_{1/2} \approx 30$ h in C_6D_6 and >96 h²¹ in THF-*d*₆ (eq 4), more than 60 times slower than the reaction of **4a** with diphenylacetylene.



Mechanisms of the Insertion Reactions. The great disparity between the reaction rates of the Cp_2 complexes **5** and the *cg* complexes **4** led us to consider the mechanisms by which they occur. Previous work had shown that the insertion of carbodiimides into THF-ligated Cp_2 zirconaaziridines required dissociation of the THF and suggested that the same mechanism was operative for the insertion of cyclic carbonates and isocyanates.^{17,20} We therefore expected that insertion into the Zr–C bond of the Cp_2 zirconaaziridine **5a** would require dissociation of the PMe_3 , though we expected PMe_3 dissociation to be slower than THF dissociation. Indeed, mixing **5a** and diphenylacetylene in the presence of 10 equiv of PMe_3 resulted in no reaction even after 36 h at 50 °C, confirming our hypothesis that PMe_3 dissociation must occur prior to insertion.

The *cg* zirconaaziridine **4a** is electronically unsaturated (even with a coordinated PMe_3), and an associative mechanism would seem possible for its insertion reactions. However, the addition of excess PMe_3 to reaction 3a decreased the rate ($t_{1/2}$ increased to approximately 3 h), implying a dissociative mechanism for that insertion.

Such a mechanism (Scheme 2) will obey eq 5 or 6 if either of two different simplifying assumptions is valid.²⁰ If the equilibrium between **4a** and **D** + PMe_3 is rapidly maintained, i.e., if k_1 and $k_{-1}[\text{PMe}_3]$ are $\gg k_2[\text{PhCCPh}]$, the overall rate law will be eq 5. If instead we apply the steady-state approximation to reactive intermediate **D**, i.e., if $k_{-1}[\text{PMe}_3] + k_2[\text{PhCCPh}]$ is $\gg k_1$, the rate law is given by eq 6.

$$\frac{d[\mathbf{6}]}{dt} = \frac{K_1 k_2 [\text{PhCCPh}] [\mathbf{4a}]}{[\text{PMe}_3] + K_1} \quad (5)$$

$$\frac{d[\mathbf{6}]}{dt} = \frac{k_1 k_2 [\text{PhCCPh}] [\mathbf{4a}]}{k_{-1} [\text{PMe}_3] + k_2 [\text{PhCCPh}]} \quad (6)$$

Determining the order in PMe_3 was complicated by the fact that, as reaction 3a proceeds, 1 equiv of PMe_3 is produced and

(19) Tunge, J. A.; Gately, D. A.; Norton, J. R. *J. Am. Chem. Soc.* **1999**, *121*, 4520–4521.

(20) Tunge, J. A.; Czerwinski, C. J.; Gately, D. A.; Norton, J. R. *Organometallics* **2001**, *20*, 254–260.

(21) At 50 °C, decomposition of **5a** began after about 96 h.

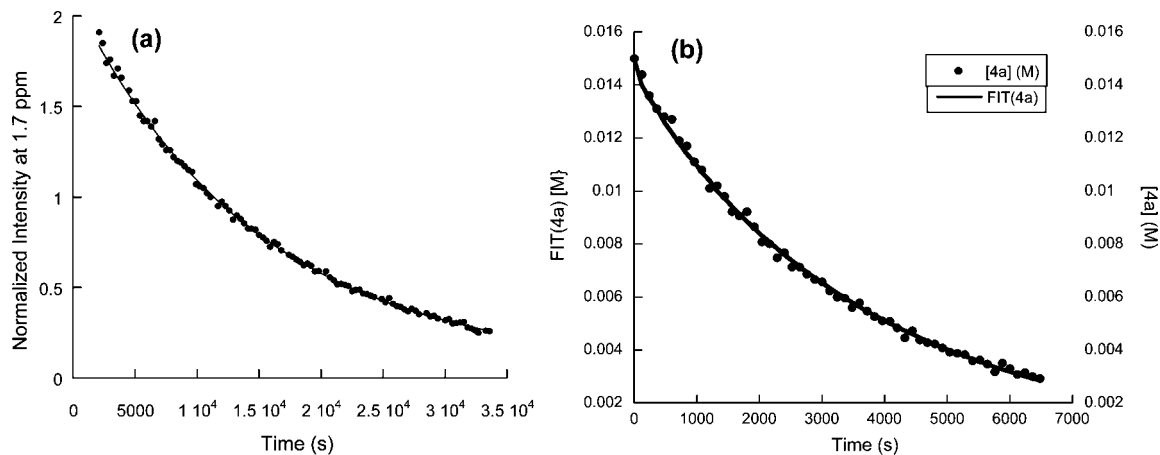


Figure 8. (a) Plot of peak intensity at 1.7 ppm (methyl group in cg ligand of **4a**) vs time (s) for the reaction of **4a** (0.02 M) with 0.202 M PhCCPh in the presence of 10 equiv (0.0404 M) of added PMe_3 at 50 °C. The data are fit with a first-order equation. (b) Plot of the experimental data for the reaction of **4a** (0.02 M) with 0.202 M PhCCPh in the presence of 2 equiv (0.0404 M) of added PMe_3 at 50 °C, and the best fit curve from a Kintecus simulation.

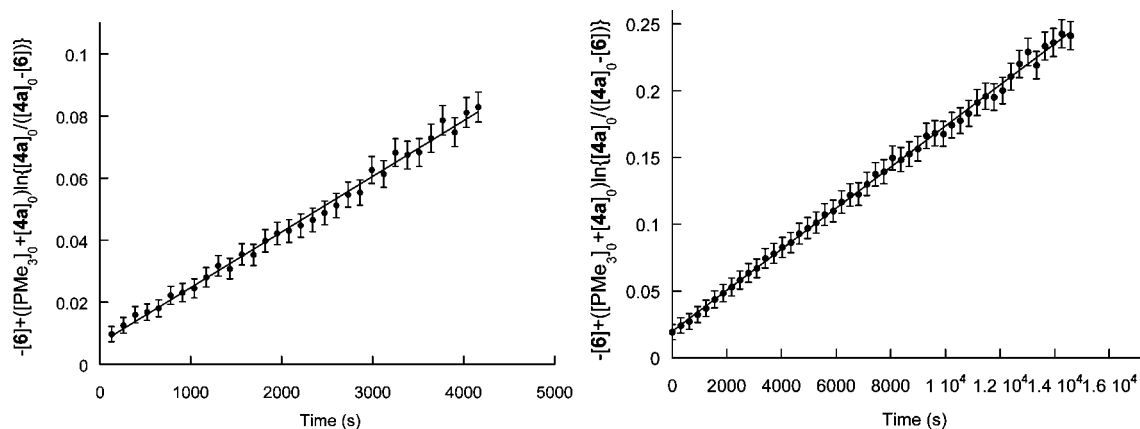


Figure 9. Left-hand side of eq 8 vs time for (a) the reaction of **4a** (0.02 M) with 0.213 M PhCCPh in the presence of 2 equiv of added PMe_3 at 50 °C and (b) the reaction of **4a** (0.02 M) with 0.213 M PhCCPh in the presence of 5 equiv of added PMe_3 at 50 °C.

$[\text{PMe}_3]$ therefore varies with time. The reaction of **4a** with excess PhCCPh *without* added PMe_3 yielded kinetic traces that deviated from first-order behavior, while with *large amounts* of added PMe_3 the reaction was too slow for kinetic measurements to be practical. With *modest amounts* (2–10 equiv) of added PMe_3 we were able to follow the progress of the reaction and determined approximate first-order rate constants k_{obs} for the conversion of **4a** to **6**. A plot of k_{obs} as a function of $1/[\text{PMe}_3]$ (Figure 6, $[\mathbf{4a}] = 0.02 \text{ M}$) proved to be linear over the concentration range 0.040–0.222 M.

We also found k_{obs} to be linear in $[\text{PhCCPh}]$ over the concentration range 0.213–0.823 M (Figure 7, $[\mathbf{4a}] = 0.02 \text{ M}$).

These measurements were made in the presence of excess (10 equiv) PMe_3 to render deviations from first-order behavior negligible.

The linearity of the plots in Figures 6 and 7 suggests the rate of conversion of **4a** \rightarrow **6** is proportional to $[\text{PhCCPh}]/[\text{PMe}_3]$. A rate law with this form (the “equilibrium steady-state” approximation,²² eq 7) can be obtained from either eq 5 or eq 6. Because we cannot observe **D** by ^1H NMR in a solution of **4a**, K_1 must be $\leq 10^{-5} \text{ M}$, and during a kinetics experiment $[\text{PMe}_3] \gg K_1$ and eq 5 reduces to eq 7. Because Figure 7 is linear, with no evidence for saturation behavior, $k_2[\text{PhCCPh}]$ must be $\ll k_{-1}[\text{PMe}_3]$, and eq 6 reduces to eq 7.

$$\frac{d[\mathbf{6}]}{dt} = \frac{K_1 k_2 [\text{PhCCPh}][\mathbf{4a}]}{[\text{PMe}_3]} \quad (7)$$

The validity of the rate law in eq 7 for eq 3a was tested with the kinetic simulation program Kintecus,²³ which calculated the variation of $[\text{PMe}_3]$ during the reaction. We set k_1 and k_{-1} to give a reasonable estimate of K_1 and kept k_1 and k_{-1} fixed as we refined k_2 ; refinements converged to a constant $K_1 k_2$ over a range of these k_1 and k_{-1} estimates (details are given in the Supporting Information). Iteration on data from the reaction of **4a** with excess PhCCPh and 2 equiv of added PMe_3 gave $K_1 k_2$ as $6.4(1) \times 10^{-5} \text{ s}^{-1}$ (Figure 8b), which is indistinguishable

(22) Pyun, C. W. *J. Chem. Educ.* **1971**, *48*, 194–196.

(23) Ianni, J. C. *Kintecus*, Windows Version 3.95, 2008; www.kintecus.com.

(24) We are unaware of any previous report of the integration of such a rate law, with a concentration in the denominator increasing during the reaction.

(25) The K_1 equilibrium in Scheme 2 lies far to the left, i.e., $k_1 \gg k_{-1}$. We cannot observe **D** directly, and only the product $K_1 k_2$ is available from k_{obs} , or from fitting time-dependent data to eq 7 or eq 8. In theory it should be possible to obtain K_1 and k_2 individually from a data set where $[\text{PMe}_3]$ varies a great deal (i.e., the reaction of **4a** with excess PhCCPh when no PMe_3 is added), but we have been unable to refine these parameters separately with Kintecus.

from the value of K_1k_2 ($6.47(6) \times 10^{-5} \text{ s}^{-1}$) obtained with a pseudo-first-order treatment of data from the analogous reaction with 10 equiv of added PMe_3 (Figure 8a). Thus eq 7 adequately describes the kinetics of reaction 3a.

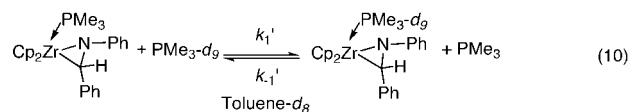
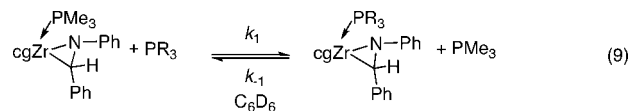
We also ran Kintecus simulations (see Supporting Information) for reaction 3a with 5 equiv and 10 equiv of added PMe_3 . The K_1k_2 values thus obtained ($6.8(1) \times 10^{-5}$ and $6.5(1) \times 10^{-5} \text{ s}^{-1}$ for 5 and 10 equiv, respectively) are in good agreement with both the value from the simulation of the 2 equiv case and the value from pseudo-first-order treatment of the 10 equiv case. The average of the three values of K_1k_2 from Kintecus simulations is $6.6(2) \times 10^{-5} \text{ s}^{-1}$.

If we assume that $[\text{PMe}_3]_t = [\text{PMe}_3]_0 + [6]$, we can integrate eq 7 to eq 8 (the derivation is given in the Supporting Information).²⁴ The function on the left-hand side of eq 8 is indeed linear with time for our data (Figure 9), offering additional evidence that reaction 3a obeys the rate law in eq 7. However, there is only fair agreement (a discrepancy of 27%) between the values of K_1k_2 obtained from the slope of such plots and the values obtained from either (1) iteration with Kintecus or (2) a first-order treatment of the data from a run with 10 equiv of PMe_3 . The discrepancies probably arise from the fact that $[\text{PMe}_3]_t$ is not exactly equal to $[\text{PMe}_3]_0 + [6]$ (details are given in the Supporting Information).

$$-[6] + ([\text{PMe}_3]_0 + [4\mathbf{a}]_0) \log \frac{[4\mathbf{a}]_0}{[4\mathbf{a}]_0 - [6]} = K_1k_2[\text{PhCCPh}]_0 t \quad (8)$$

PMe_3 Dissociation Rate Constants. Although we know the product K_1k_2 for the cg system, we cannot usefully compare that system with the Cp_2 system without determining an individual equilibrium or rate constant for both.²⁵ We have therefore measured k_1 , the rate constant for PMe_3 dissociation from **4a**, and the analogous rate constant k_1' for **5a** (eqs 9 and 10). These rate constants enable us to quantitatively compare directly analogous cg and Cp_2 complexes and may therefore lend insight into the origin of the differences in these systems.

The phosphine exchange equilibria described in eq 9 were established before an NMR spectrum could be obtained, but no broadening was observed in the room-temperature ^1H NMR spectra of **4a**, indicating k_1 to be on the order of 10^{-2} to 10^{-1} s^{-1} . The analogous equilibria for **5a** (eq 10) showed the same behavior in both C_6D_6 and $\text{THF-}d_8$.



A ^1H EXSY spectrum of the cg complex **4a** with added PMe_3 showed exchange cross-peaks for free and coordinated PMe_3 , indicating that k_1 could be measured by a selective population inversion (SPI) experiment.²⁶ Due to the complexity of the ^1H NMR spectrum, we carried out the SPI experiment using $^{31}\text{P}\{^1\text{H}\}$ NMR.²⁷ Figures S-1 through S-4 in the Supporting Information display peak intensity vs mixing time data from these experiments. The rate constant for phosphine dissociation from **4a** (k_1) proved to be $0.204(7) \text{ s}^{-1}$ at 298 K. A ^1H EXSY spectrum of the Cp_2 complex **5a** with added PMe_3 showed that the rate constant k_1' is too small to be quantified by SPI at room temperature. Therefore, we measured k_1' at several temperatures over the range 269.9–287.7 K by monitoring the exchange of PMe_3 and $\text{PMe}_3\text{-}d_9$ described in eq 10. Eyring analysis (Figure S-5) determined k_1' to be $0.0013(1) \text{ s}^{-1}$ at 298 K.

PMe_3 dissociation from the cg zirconaaziridine **4a** is therefore faster than from the Cp_2 zirconaaziridine **5a**, a result consistent with the much longer Zr–P distance in crystalline **4a**. While the relative dissociation rates may not be the same for other ligands (e.g., olefins), our results call into question the idea^{3,5,11} that constrained geometry complexes are better Lewis acids than their Cp_2 counterparts.

Acknowledgment. This work was supported by the National Science Foundation (CHE-0749537). K.E.K. gratefully acknowledges a fellowship from the NSF Graduate Teaching Fellows in K-12 Education (GK-12) Program. The authors are grateful to G. Parkin for assistance with the X-ray structure determinations and to the National Science Foundation (CHE-0619638) for the acquisition of an X-ray diffractometer; to A. D. Bain and R. A. Petros for assistance with CIFIT; to J. Espenson, A. Bakac, and A. Haim for consultation on the kinetics; to Boulder Scientific for gifts of Cp_2ZrCl_2 and $\text{Me}_4\text{C}_5(\text{H})\text{SiMe}_2\text{NH}(t\text{Bu})$; and to A. Voskoboynikov for a gift of $\text{Me}_4\text{C}_5\text{SiMe}_2\text{NH}(t\text{Bu})\text{ZrCl}_2$.

Supporting Information Available: Synthetic procedures and details of the SPI, EXSY, simulations, and other kinetic experiments. This information is available free of charge via the Internet at <http://pubs.acs.org>.

OM801009P

(26) Bain, A. D. *CIFIT*; McMaster University, 2003. Bain, A. D.; Duns, G. J.; Rathgeb, F.; Vanderkloet, J. *J. Phys. Chem.* **1995**, *99*, 17338–17343.

(27) Fischer, A.; Wendt, O. F. *J. Chem. Soc., Dalton Trans.* **2001**, 1266–1268.

Titanium Complexes Bearing Bisaryloxy-N-heterocyclic Carbenes: Synthesis, Reactivity, and Ethylene Polymerization Study

Dao Zhang* and Nan Liu

Department of Chemistry, Fudan University, Shanghai 200433, People's Republic of China

Received July 28, 2008

Reaction of titanium complex $[(L)TiX_2(THF)]$ ($L = \{N,N'-[(5-R-3-tert-Bu-2-O^- -C_6H_2)CH_2]_2(C_3H_2N_2)\}$, $R = tert-Bu$, L^a , $R = Me$, L^b ; $X = Cl$, **1a**, **1b**; $X = Br$, L^a , **2**) with 2.0 equiv of $PhCH_2MgCl$ or $MeLi$ in diethyl ether gave dimethyl complexes $[(L)Ti(CH_2Ph)_2]$ (**3a**, **3b**) and $[(L)Ti(CH_3)_2]$ (**4a**, **4b**) by salt metathesis. Dibenzyl titanium complex $[(L^a)Ti(CH_2Ph)_2]$ (**3a**) absorbs dioxygen gas to afford the oxygen-insertion product $[(L^a)Ti(OCH_2Ph)_2]$ (**5**) in 57% yield. The reduction of $[(L^a)TiBr_2(THF)]$ (**2**) with 1 equiv of $LiBEt_3H$ in toluene gave the titanium(III) species $[(L^a)TiBr(THF)_2]$ (**6**). The molecular structures of **3b**, **4b**, **5**, and **6** have been confirmed by X-ray single-crystal analysis. The solid state structures of these compounds reveal that these hybrid carbene ligands adopt a *transoid* conformation to form a pseudotrigonal-bipyramidal (for **3b**, **4a**, **4b**, and **5**) or octahedral (for **6**) coordination geometry around metal centers. These titanium complexes (**1**, **2**, and **6**) showed high activities up to ca. 97 kg PE/(mol Ti · h · atm) for ethylene polymerization in the presence of MAO as coactylast. The ^{13}C NMR analysis revealed that linear polyethylene with low molecular weight was formed by these NHC titanium complexes. No methyl or other long-chain branch could be observed.

Introduction

N-Heterocyclic carbene (NHC) ligands have been studied intensely recently and are now used widely as strongly basic phosphine analogues, to support early and late transition metal complexes.^{1,2} Unlike the robust late transition metal NHC system, the early transition metal NHC chemistry is difficult to study due to the ease of dissociation of the NHC ligand from the electron-deficient metal center.^{3–9} The overwhelming majority of NHCs are functionalized (with respect to the N and N'

substituents) by incorporating neutral donor or anionic groups such as pyridyl, phosphine, NHC, amide, alkoxide, and cyclopentadienyl. It has been proven that the NHC moiety could be held in proximity of the metal center with the help of such covalent teething.

In our previous study, several aryloxy-modified N-heterocyclic carbenes multidentate hybrid ligands (for example, L^a , Chart 1) have been successfully developed, and some early transition Ti(IV),^{9a} Zr(IV),^{9b} and S-block Mg(II)¹⁰ metal compounds have been synthesized and characterized by X-ray single-crystal analysis. Later we extended this group IV metal-NHC chemistry to binuclear metal systems.¹¹ The NHC ligands $(L^1)^{2-}$ adopt *transoid* conformation in mononuclear complexes but the rare *cisoid* conformation in binuclear complexes. Moreover, for comparison with the aforementioned bisaryloxy-NHC titanium complexes, the reactivity of the corresponding bis(aryloxy) titanium compounds has been carefully investigated.¹² Some unexpected hexacyclic $[Al_3O_2Cl]$ aluminum(III),^{12b} titanium(IV),

* Corresponding author. Fax: +86 21 65641740. E-mail: dao Zhang@fudan.edu.cn.

(1) For recent reviews see: (a) Hahn, F. E. *Angew. Chem., Int. Ed.* **2006**, *45*, 1348. (b) Scott, N. M.; Nolan, S. P. *Eur. J. Inorg. Chem.* **2005**, 1815. (c) Cavell, K. J.; McGuinness, D. S. *Coord. Chem. Rev.* **2004**, *248*, 671. (d) César, V.; Bellemin-Lapinaz, S.; Gade, L. H. *Chem. Soc. Rev.* **2004**, *33*, 619. (e) Crudden, C. M.; Allen, D. P. *Coord. Chem. Rev.* **2004**, *248*, 2247. (f) Kirmse, W. *Angew. Chem., Int. Ed.* **2004**, *43*, 1767. (g) Herrmann, W. A. *Angew. Chem., Int. Ed.* **2002**, *41*, 1290. (h) Arnold, P. L. *Heteroat. Chem.* **2002**, *13*, 534. (i) Bourissou, D.; Guerret, O.; Gabbai, F. P.; Bertrand, G. *Chem. Rev.* **2000**, *100*, 39.

(2) Nolan, S. P. *N-Heterocyclic Carbenes in Synthesis*; Wiley-VCH: Weinheim, 2006.

(3) (a) Arnold, P. L.; Zlatogorsky, S.; Jones, N. A.; Carmichael, C. D.; Liddle, S. T.; Blake, A. J.; Wilson, C. *Inorg. Chem.* **2008**, *47*, 9042. (b) Jones, N. A.; Liddle, S. T.; Wilson, C.; Arnold, P. L. *Organometallics* **2007**, *26*, 755. (c) Arnold, P. L.; Liddle, S. T. *Chem. Commun.* **2006**, 3959. (d) Patel, D.; Liddle, S. T.; Mungur, S. A.; Rodden, M.; Blake, A. J.; Arnold, P. L. *Chem. Commun.* **2006**, 1124. (e) Mungur, S. A.; Blake, A. J.; Wilson, C.; McMaster, J.; Arnold, P. L. *Organometallics* **2006**, *25*, 1861. (f) Liddle, S. T.; Arnold, P. L. *Organometallics* **2005**, *24*, 2597. (g) Arnold, P. L.; Scarisbrick, A. C. *Organometallics* **2004**, *23*, 2519. (h) Arnold, P. L.; Mungur, S. A.; Blake, A. J.; Wilson, C. *Angew. Chem., Int. Ed.* **2003**, *42*, 5981.

(4) (a) Downing, S. P.; Guadano, S. C.; Pugh, D.; Danopoulos, A. A.; Bellabarba, R. M.; Hanton, M.; Smith, D.; Tooze, R. P. *Organometallics* **2007**, *26*, 3762. (b) Downing, S. P.; Danopoulos, A. A. *Organometallics* **2006**, *25*, 1337. (c) Pugh, D.; Wright, J. A.; Freeman, S.; Danopoulos, A. A. *Dalton Trans.* **2006**, 775. (d) Lorber, C.; Vendier, L. *Organometallics* **2008**, *27*, 2774.

(5) (a) Spencer, L. P.; Fryzuk, M. D. *J. Organomet. Chem.* **2005**, *690*, 5788. (b) Spencer, L. P.; Winston, S.; Fryzuk, M. D. *Organometallics* **2004**, *23*, 3372.

(6) (a) Tamm, M.; Randoll, S.; Herdtweck, E.; Kleigrew, N.; Kehr, G.; Erker, G.; Rieger, B. *Dalton Trans.* **2006**, 459. (b) Tamm, M.; Randoll, S.; Bannenberg, T.; Herdtweck, E. *Chem. Commun.* **2004**, 876. (c) Niehues, M.; Erker, G.; Kehr, G.; Schwab, P.; Froehlich, R.; Blacque, O.; Berke, H. *Organometallics* **2002**, *21*, 2905. (d) Tamm, M.; Hahn, F. E. *Coord. Chem. Rev.* **1999**, *182*, 175.

(7) (a) Herrmann, W. A.; Köcher, C. *Angew. Chem., Int. Ed.* **1997**, *36*, 2162. (b) Herrmann, W. A.; Munck, F. C.; Artus, G. R. J.; Runte, O.; Anwander, R. *Organometallics* **1997**, *16*, 682. (c) Herrmann, W. A.; Lobmaier, G. M.; Elison, M. *J. Organomet. Chem.* **1996**, *520*, 231. (d) Herrmann, W. A.; Oefele, K.; Elison, M.; Kuehn, F. E.; Roesky, P. W. *J. Organomet. Chem.* **1994**, *480*, C7–C9.

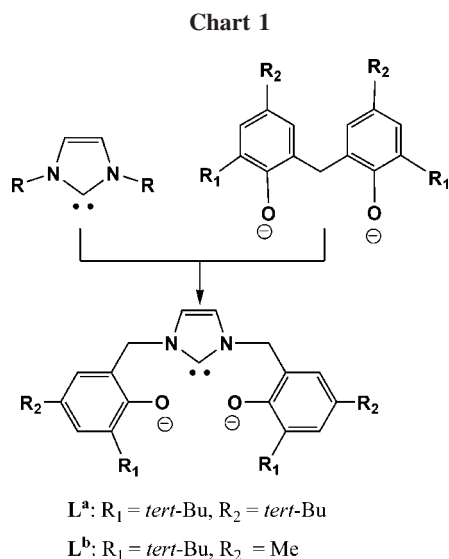
(8) Shukla, P.; Johnson, J. A.; Vidovic, D.; Cowley, A. H.; Abernethy, C. D. *Chem. Commun.* **2004**, 360.

(9) (a) Aihara, H.; Matsuo, T.; Kawaguchi, H. *Chem. Commun.* **2003**, 2204. (b) Zhang, D.; Aihara, H.; Watanabe, T.; Matsuo, T.; Kawaguchi, H. *J. Organomet. Chem.* **2007**, *692*, 234.

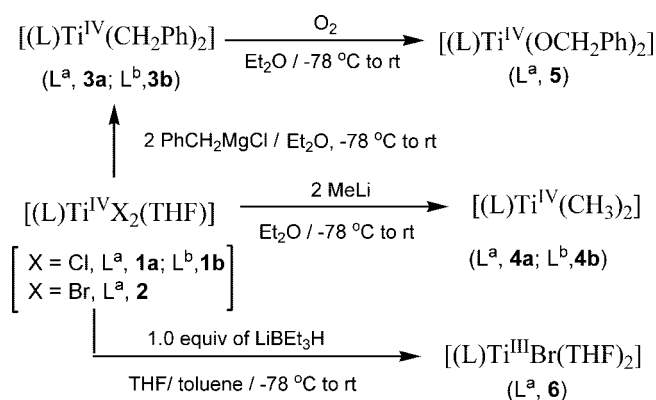
(10) Zhang, D.; Kawaguchi, H. *Organometallics* **2006**, *25*, 5506.

(11) Zhang, D. *Eur. J. Inorg. Chem.* **2007**, 3077.

(12) (a) Zhang, D. *Organometallics* **2007**, *26*, 4072–4075. (b) Zhang, D. *Eur. J. Inorg. Chem.* **2007**, 1570.



Scheme 1. Synthesis of Titanium Complexes



and titanium(III) complexes bearing such bis(phenolato)ligands have been achieved and confirmed by X-ray diffractions.

Herein, we wish to report the synthesis and structural characterization of some novel organotitanium species with such bisaryloxy-modified N-heterocyclic carbene ligands (**L**) (Scheme 1). We also give a full account of their catalytic behavior for ethylene polymerization and the structural characterization of the obtained polymer.

Results and Discussion

Dialkyl Titanium(IV) Complexes. Ligand $[\text{H}_3\text{L}^b]\text{Br}$, titanium complexes $[(L^b)\text{TiX}_2(\text{THF})]$ (**1b** and **2b**), and $[(L^b)\text{Ti}(\text{CH}_2\text{C}_6\text{H}_5)_2]$ (**3b**) were prepared and characterized according to the methods we previously reported.^{9–11} The structure of dibenzyl titanium complex **3b** is similar to that of **3a**^{9a} and the zirconium derivative $[(L^a)\text{Zr}(\text{CH}_2\text{C}_6\text{H}_5)_2]$.^{9b} The geometry at titanium is distorted trigonal bipyramidal with a meridional coordination of the tridentate $(L^a)^-$ ligand. The two aryloxy donors [O(1) and O(2)] occupy the axial positions with a O–Ti–O angle of $164.3(2)^\circ$. The twist angle of the S-shaped ligand in **3b** $[\text{TiC}(8)\text{N}(1)\text{N}(2)/\text{TiC}(8)\text{O}(1)\text{O}(2)]$ is larger than those of **1a**^{9a} and $[(L^a)_2\text{Ti}]$.¹¹ The Ti–C(carbene) distance [$2.165(9) \text{ \AA}$] is shortened relative to those of the six-coordinated NHC complexes of **1a**^{9a} and $[(L^a)_2\text{Ti}]$.¹¹ The Ti–C_α–C_{ipso} angles of $114.3(6)^\circ$ and $119.5(5)^\circ$ indicate η^1 binding of the benzyl groups, and the Ti–C(benzyl) distances of $2.126(8)$ and $2.127(7) \text{ \AA}$ are normal.

Complexes $[(L)\text{Ti}(\text{CH}_3)_2]$ (**4a** and **4b**) were prepared in good yield (>88%) from the dihalide complex **1** or **2** by salt

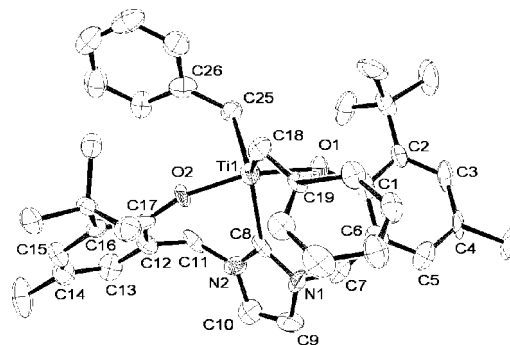


Figure 1. Molecular structure of **3b**. All hydrogen atoms are omitted for clarity. Selected distances (\AA) and angles ($^\circ$): Ti(1)–O(1) = $1.863(6)$, Ti(1)–O(2) = $1.882(6)$, Ti(1)–C(8) = $2.165(9)$, Ti(1)–C(18) = $2.126(8)$, Ti(1)–C(25) = $2.127(7)$, O(1)–Ti(1)–O(2) = $164.3(2)$, O(3)–Ti(1)–C(8) = $81.4(3)$, O(1)–Ti(1)–C(18) = $91.7(3)$, O(1)–Ti(1)–C(25) = $94.9(3)$, O(2)–Ti(1)–C(8) = $83.0(3)$, O(2)–Ti(1)–C(18) = $98.8(3)$, O(2)–Ti(1)–C(25) = $92.5(3)$, C(8)–Ti(1)–C(18) = $128.3(3)$, C(8)–Ti(1)–C(25) = $121.8(3)$, Ti(1)–C(18)–C(19) = $114.3(6)$, Ti(1)–C(25)–C(26) = $119.5(5)$, N(3)–C(39)–N(4) = $106.2(8)$.

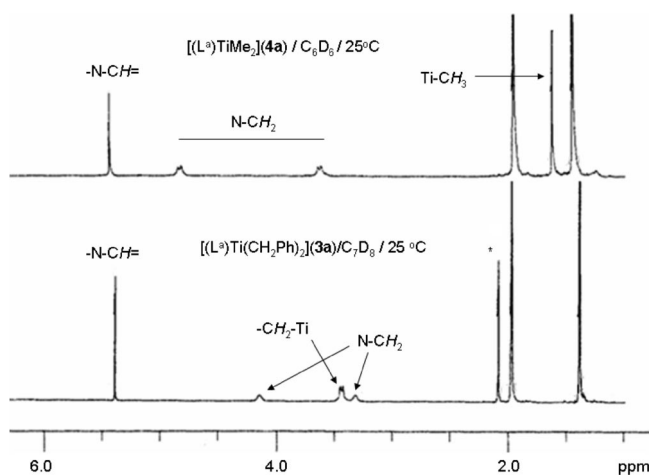


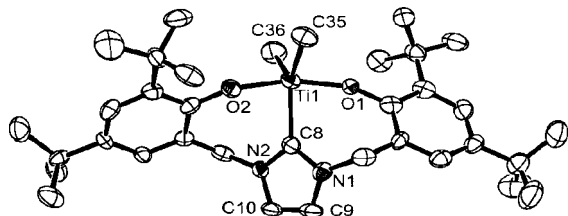
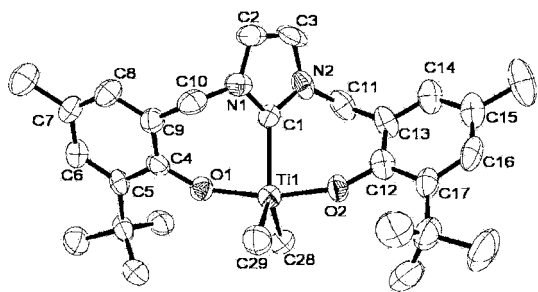
Figure 2. Selected ^1H NMR region of **3a** (below) in C_6D_6 and **4a** (above) in C_7D_8 at 25 and 75°C . The ^1H chemical shifts are reported relative to SiMe_4 and were determined by reference to the residual solvent signal (δ 7.15 ppm for benzene and 2.11 ppm for toluene) at 25°C .

metathesis reactions with 2 equiv of CH_3Li at -78°C in Et_2O solution. Complexes **4a** and **4b** were obtained as orange microcrystalline solids and are air- and moisture-sensitive and soluble in common organic solvents, including benzene, toluene, dimethyl ether, and THF. In benzene- d_6 , the ^{13}C NMR spectrum exhibits a signal at 185.7 ppm for **4a** (186.0 ppm for **4b**) characteristic of an NHC, and the resonances of inequivalent protons of N–CH₂ were observed in its ^1H NMR spectrum, indicating an average C_2 -symmetry at room temperature (Figure 2). Table 1 summarizes the typical NMR data of methylene and alkyl groups of dimethyl complex **4a** and previously reported dibenzyl titanium complex **3a** bearing these hybrid carbene ligands.

X-ray diffraction quality crystals of **4a** and **4b** were obtained by storing their diethyl ether solution at -20°C for a week. The X-ray crystallographic study of **4a** and **4b** shows that they have similar solid state structures, and the coordinated hybrid carbene tridentate ligand adopts a *transoid* conformation to form a pseudotrigonal-bipyramidal coordination geometry around the titanium center (Figures 3 and 4). Two aryloxy oxygen atoms

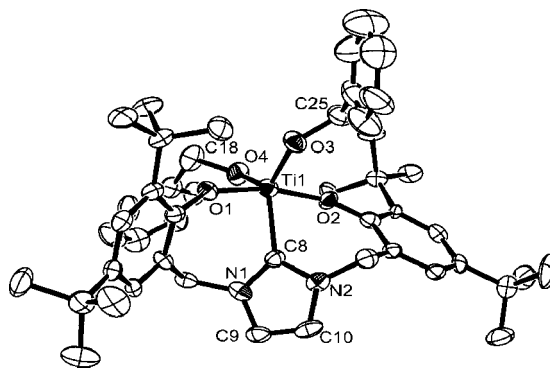
Table 1. Selected NMR Data of Dialkyl Organometal(IV) Complexes^a

compound	¹ H NMR (ppm)			¹³ C NMR (ppm)
	N-CH ₂ -Ar	Ti-CH ₂ -Ph or Ti-CH ₃		C _{carbene}
[(L ^a TiMe ₂) (4a)]	3.60	4.81	1.61	185.7
[(L ^b TiMe ₂) (4b)]	3.52	4.72	1.57	186.0
[(L ^a Ti(CH ₂ C ₆ H ₅) ₂)(3a) ^{9a}]	3.33	4.14	3.43	188.3
[(L ^b Ti(CH ₂ C ₆ H ₅) ₂)(3b)	3.34	4.14	3.38	188.1
[(L ^a Zr(CH ₂ C ₆ H ₅) ₂) ^{9b}]	2.81	3.72	3.26	187.5
[(L ^a Zr(CH ₂ SiMe ₃) ₂) ^{9b}]	3.83	5.24	0.99	185.8

^a Note: benzene-*d*₆, room temperature, ppm.**Figure 3.** Molecular structure of **4a**. All hydrogen atoms are omitted for clarity. Selected distances (Å) and angles (deg): Ti(1)–O(1) = 1.855(6), Ti(1)–O(2) = 1.849(6), Ti(1)–C(8) = 2.175(9), Ti(1)–C(35) = 2.099(8), Ti(1)–C(36) = 2.07(1); O(1)–Ti(1)–O(2) = 164.6(3), O(1)–Ti(1)–C(8) = 83.5(3), O(2)–Ti(1)–C(8) = 81.4(3), C(35)–Ti(1)–C(36) = 110.1(4).**Figure 4.** Molecular structure of **4b**. All hydrogen atoms are omitted for clarity. Selected distances (Å) and angles (deg): Ti(1)–O(1) = 1.872(6), Ti(1)–O(2) = 1.862(6), Ti(1)–C(1) = 2.179(9), Ti(1)–C(28) = 2.104(9), Ti(1)–C(29) = 2.09(1); O(1)–Ti(1)–O(2) = 166.4(3), O(1)–Ti(1)–C(1) = 83.2(3), O(2)–Ti(1)–C(1) = 83.2(3), C(28)–Ti(1)–C(29) = 110.9(4).

occupy the axial positions (O(1)–Ti–O(2) angle $\geq 164.6^\circ$), and three carbon atoms from the carbene and the two methyl groups occupy the equatorial sites, with the C(2)–Ti–C(3) angle (from 106.2° to 110.1°) compressed substantially relative to the C(1)–Ti–C(2) and C(1)–Ti–C(3) angles (from 119.2° to 130.7°). The average Ti(IV)–C_{carbene} distance for complexes in the literature is 2.242 Å (12 instances), although there is a wide range (2.194(7) to 2.313(5) Å).^{3–9} The Ti–C_{carbene} distance of **4a** is 2.175(9) Å, shorter than in other Ti(IV)–NHC complexes, e.g., [(C₅H₅)₂TiMe{C(NPrⁱ)CH₂}][BPh₄] [2.289(2) Å],^{6c} Ti(NMe₂)Cl₂(carbene) (carbene = 1,3-dimesitylimidazol-2-ylidene) [2.313(5) Å],⁷ and *trans*-[(L)Ti(=NBu-*tert*)Cl₂] (L = 2,6-bis(arylimidazol-2-ylidene)pyridine, aryl = 2,6-*i*-Pr₂C₆H₃) [2.281(6) and 2.286(6) Å],^{4b} **1a** [2.200(9) Å],^{9a} and [(L^a)Ti(CH₂C₆H₅)₂] [2.187(3) Å].^{9a}

Oxygen-Insertion Reaction of the Ti–R Bond. The chemical behaviors of **3a**, **3b**, **4a**, and **4b** with small molecules (H₂, CO, and C₂H₄) have been investigated. The proton NMR tube experiments in benzene-*d*₆ show that they do not react with H₂, even at high temperature (60 °C) overnight. Moreover, these alkyl complexes could absorb carbon monoxide gas at room

**Figure 5.** Molecular structure of complex **5**. All solvent molecules and hydrogen atoms are omitted for clarity. Selected bond distances (Å) and angles (deg): Ti(1)–C(8) = 2.170(8), Ti(1)–O(1) = 1.879(4), Ti(1)–O(2) = 1.889(4), Ti(1)–O(3) = 1.809(5), Ti(1)–O(4) = 1.816(6), O(1)–Ti(1)–O(2) = 165.8(2), O(1)–Ti(1)–O(3) = 94.6(2), O(1)–Ti(1)–O(4) = 94.4(2), O(1)–Ti(1)–C(8) = 83.2(2), O(2)–Ti(1)–O(3) = 92.8(2), O(2)–Ti(1)–O(4) = 93.0(2), O(2)–Ti(1)–C(8) = 82.6(2), O(3)–Ti(1)–O(4) = 117.1(3), O(3)–Ti(1)–C(8) = 121.9(3), O(4)–Ti(1)–C(8) = 120.9(3), C(25)–O(3)–Ti(1) = 136.5(5), C(18)–O(4)–Ti(1) = 136.2(5).

temperature or 60 °C but afford unidentified products. However, complexes **3a** and **3b** could absorb dioxygen to afford monomeric oxygen-insertion products. When the solution of **3a** was exposed to either an excess or 1 equiv of dry dioxygen, the corresponding dibenzyloxide titanium compound [(L)Ti(OCH₂Ph)₂] (**5**) was isolated as a light yellow solid in 57% yield. Varying the solvent (toluene, diethyl ether, benzene, and hexane) or excluding light had no discernible effect on either the rate or cleanliness of the oxygenation. Light yellow crystals of **5** are grown from the mother liquor by storage at –30 °C. The molecular structure is shown in Figure 5.

A ¹H NMR tube reaction experiment in C₆D₆ showed the reaction would be complete in about 6 h, which could be seen from the proton NMR shift of the CH₂ group from δ 3.44 ppm for Ti–CH₂–Ph to δ 5.87 ppm for Ti–O–CH₂–Ph (see Supporting Information). Several examples on the insertion reactions of O₂ and “Ti–C” bonds of group 4 metal complexes have been reported.^{12–14} Wolczanski¹³ and Kang¹⁴ et al. have reported the dioxygen activation by monomeric methyl titanium complexes bearing tritor (tritor = ^tBu₃CO[–]) and cyclic silene (cyclic silene = 1,1-bis(butylamido)-1-silacycloalkane) ligands, respectively. The insertion products were all dimeric alkoxy-bridged species, and oxo insertion did not occur when dibenzyl titanium-bearing cyclic silene was used.¹⁴ We also prepared several oxygen-insertion products of titanium compounds by the reactions of alkyl titanium compounds with dioxygen.¹² A possible mechanism is that dioxygen first inserts into the Ti–C bond and then the O–O bond cleaves. This procedure implicates an alkylperoxy alkyl [(L)Ti(η^2 -OOCH₂Ph)(CH₂Ph)] intermediate whose similar compound [Cp₂Ti(OO^tBu)Cl] has been isolated at low temperature and characterized by single-crystal X-ray analysis.¹⁵

Titanium(III) Complex. Low-valent species of metal complexes usually have unique properties. To the best of our

(13) (a) Lubben, T. V.; Wolczanski, P. T. *J. Am. Chem. Soc.* **1987**, *109*, 424. (b) Lubben, T. V.; Wolczanski, P. T. *J. Am. Chem. Soc.* **1985**, *107*, 701.(14) (a) Kim, S.-J.; Jung, I. N.; Yoo, B. R.; Cho, S.; Ko, J.; Kim, S. H.; Kang, S. O. *Organometallics* **2001**, *20*, 1501. (b) Kim, S.-J.; Choi, D.-W.; Lee, Y.-J.; Chae, B.-H.; Ko, J.; Kang, S. O. *Organometallics* **2004**, *23*, 559.(15) DiPasquale, A. G.; Kaminsky, W.; Mayer, J. M. *J. Am. Chem. Soc.* **2002**, *124*, 14534.

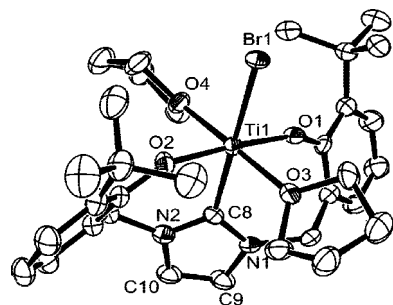


Figure 6. Molecular structure of **6**. All solvent molecules, two *tert*-butyl groups on the 5-position, and hydrogen atoms are omitted for clarity. Selected distances (Å) and angles (deg): Ti(1)–C(8) = 2.18(1), Ti(1)–Br = 2.636(2), Ti(1)–O(1) = 1.912(6), Ti(1)–O(2) = 1.871(5), Ti(1)–O(3) = 2.180(9), Ti(1)–O(4) = 2.170(9); O(1)–Ti(1)–O(2) = 173.1(2), O(1)–Ti(1)–O(3) = 190.2(2), O(1)–Ti(1)–O(4) = 88.8(2), O(1)–Ti(1)–C(8) = 87.1(2), O(1)–Ti(1)–Br(1) = 91.8(2), O(2)–Ti(1)–O(3) = 91.2(2), O(2)–Ti(1)–O(4) = 89.5(2), O(2)–Ti(1)–C(8) = 86.2(2), O(2)–Ti(1)–Br(1) = 94.9(2), O(3)–Ti(1)–O(4) = 177.6(2), O(3)–Ti(1)–C(8) = 89.1(3), O(3)–Ti(1)–Br(1) = 90.7(2), O(4)–Ti(1)–C(8) = 88.7(3), O(4)–Ti(1)–Br(1) = 91.5(2), Br(1)–Ti(1)–C(8) = 178.9(2), N(1)–C(8)–N(2) = 100.8(8).

knowledge, the Ti(III)-NHC complexes are rare, and there are five such examples containing nine Ti(III)–C_{carbene} bonds reported to date.^{3a,b,4a,b,d} For example, The fluorenyl-NHC titanium(III) complex [Ti{C(N[-(CH₂)₂-9-fluorenyl])N[2,6-Prⁱ₂C₆H₃]CH₂)}₂(NMe₂)Cl] was generated by an *in situ* redox reaction between the proligand and Ti(IV).^{4b} The alkoxy-NHC titanium(III) adduct [Ti{OCMe₂CH₂-(1-C[NCHCHNPrⁱ])₃}] was synthesized by treatment of [TiCl₃(THF)₃] with 3 equiv of the potassium alkoxy-carbene.^{3b}

When bromide complex [(L^a)Ti^{IV}Br₂(THF)] **2** was reduced with 1.0 equiv of LiBEt₃H, the titanium compound [(L^a)Ti^{III}Br(THF)₂] (**6**) was obtained as yellow green thin plate crystals from a greenish toluene solution in 25.7–31.1% yield. Addition of 2.0 or more equivalents of LiBEt₃H in THF to a toluene solution of **1a** under the same conditions led to the formation of intractable brown oils. Complex **6** does not react with CO, H₂, or alkynes. Attempts to prepare Ti(III) alkyl complexes of the general formula [(L^a)Ti^{III}R₂] by salt metathesis reaction with RLi (R = Me, CH₂SiMe₃) or PhCH₂MgCl reagents were hindered by the thermal instability of the final products. The initial highly colored solutions formed at low temperature rapidly decomposed upon warming to yield intractable brown oils after workup.

Compound **6** was confirmed by single-crystal X-ray diffraction analysis (Figure 6). Complex **6** features a distorted octahedral metal center with the aryloxy-NHC ligand occupying meridional sites. The two THF molecules are mutually *trans*, and the sixth coordination site is filled by a terminal bromide. The titanium lies close to the plane defined by two oxygen atoms of the aryloxy groups and one carbon atom of the NHC rings (the O–Ti–O angle is 177.1(3)°). The notable merit of this complex is that the bromide lies in a site *trans* to the carbene, possibly in order to minimize interelectronic repulsions. The Ti–C distance [2.181(1) Å] in **6** is significantly shorter than the Ti–C_{carbene} bond length in the other NHCs Ti(III) complexes [Ti^{III}L₂{PrⁱOSiMe₂O} K₂OTi^{IV}(OPrⁱ)₄] (L = OCMe₂CH₂[C(N(CHCH)NPrⁱ)]₂) [2.308(3), 2.306(4) Å],^{3a} [Ti{OCMe₂CH₂(1-C[NCHCHNPrⁱ])₃}] [2.252(4), 2.263(5), 2.299(4) Å], the average Ti–C_{carbene} bond length is 2.279 Å,^{3b} {3-(2,6-Prⁱ₂-C₆H₃)-1-[2-(1-(4,7-Me₂)indeny]ethyl]imidazol-2-ylidene}TiCl₂ [2.196(5) Å],^{4a} [Ti{C(N[-(CH₂)₂-9-fluorenyl])N[2,6-

Prⁱ₂C₆H₃]CH₂)}₂(NMe₂)Cl] [2.221(2) Å],^{4b} and TiCl₂(NMe₂)-(IMes)₂ (Imes = 1,3-dimesitylimidazol-2-ylidene) [2.293(3), 2.297(3) Å].^{4d} The bond angles O(1)–Ti(1)–O(2) [172.6(3)°], O(3)–Ti(1)–O(4) [177.4(3)°], and Br(1)–Ti(1)–C(8) [178.8(2)°] are near 180°.

Cyclotrimerization of Alkyne. In an effort to trap an unequivocal example of titanium (II)-carbene species, the reduction of halide titanium complexes was investigated in the presence of a range of metal reducing agents (such as Na/Hg, Mg, K, C₈K) and alkynes (Me₃SiC≡CH and Me₃SiC≡CSiMe₃) or CO at room temperature in toluene. GC-MS showed that the catalytic cyclotrimerization products 1,3,5-C₆H₃(SiMe₃)₃ and 1,2,4-C₆H₃(SiMe₃)₃ (the molar ratio is ca. 3.8:1) were formed in significant amount only when the reductant was Mg and the alkyne was Me₃SiC≡CH (10 equiv) (Figure 7). Catalytic cyclotrimerization of alkynes is well known for late-transition-metal complexes, but few examples are known with early-transition-metal catalysts,¹⁶ especially for the noncyclopentadienyl ligand.

Despite repeated attempts, we have been unable to isolate the titanium(II) species by the reaction of **1a** with 2 or 3 equiv of Me₃SiC≡CH in the presence of Mg powder.^{16g,i} However, reduction of **1a** in the presence of bis(trimethylsilyl)acetylene resulted in the clear production of a dark brown solid that was supposed to be the titanium low-valence species [(L^a)Ti-(C₂(SiMe₃)₂)] (**7**). The proton NMR spectrum of **7** contains sharp resonances at δ 0.16 and 0.53 attributable to unequal trimethylsilyl groups. The ¹³C NMR spectrum also revealed two different resonance at δ 206.78 and 212.33 ppm for the C≡C moiety. These data were different from those of all other reported analogous titanocenes bearing η²-C₂(SiMe₃)₂.¹⁷ Unfortunately, we could not obtain suitable crystals for X-ray analysis to confirm the exact structure and give the reason for the inequality. According to the above obtained structural information, we supposed that in this complex the carbene-aryloxy ligand shares the U conformation that makes the unequal proton and carbene of Me₃SiC≡CSiMe₃ moiety. Mechanistically, it is suggested that reduction of titanium(IV) dibromide generates transient Ti(II) species, which easily react with alkynes.

Ethylene Polymerization. The catalytic behavior of titanium complexes for ethylene polymerization was systemically studied at low pressure (50 psig) in the presence of MAO as cocatalyst (Table 2). These titanium complexes revealed a similar catalytic activity due to their similar structures (up to ca. 90 kg PE/(mol Ti·h·atm)). The number average molecular weights (*M_n*) of polymer are very low, less than 3830. Moreover, the polyethylene *M_n* seems lower for titanium(III) **6**/MAO than titanium(IV)

(16) (a) Wielstra, Y.; Gambarotta, S.; Meetsma, A.; de Boer, J. L. *Organometallics* **1989**, *8*, 2696. (b) Calderazzo, F.; Marchetti, F.; Pampaloni, G.; Hiller, W.; Antropiusova, H.; Mach, K. *Chem. Ber.* **1989**, *122*, 2229. (c) Calderazzo, F.; Pampaloni, G.; Pallavicini, P.; Strahle, J.; Wurst, K. *Organometallics* **1991**, *10*, 896. (d) van der Linden, A.; Schaverien, C. J.; Meijboom, N.; Ganter, C.; Orpen, A. G. *J. Am. Chem. Soc.* **1995**, *117*, 3008. (e) Hill, J. E.; Fanwick, P. E.; Rothwell, I. P. *Organometallics* **1990**, *9*, 2211. (f) Hill, J. E.; Balaich, G.; Fanwick, P. E.; Rothwell, I. P. *Organometallics* **1993**, *12*, 2911. (g) Ozerov, O. V.; Patrick, B. O.; Ladipo, F. T. *J. Am. Chem. Soc.* **1999**, *121*, 7941. (h) Ozerov, O. V.; Patrick, B. O.; Ladipo, F. T. *J. Am. Chem. Soc.* **2000**, *122*, 6423. (i) Ladipo, F. T.; Sarveswaran, V.; Kingston, J. V.; Huyck, R. A.; Bylikin, S. Y.; Carr, S. D.; Watts, R.; Parkin, S. J. *Organomet. Chem.* **2004**, *689*, 502.

(17) (a) Varga, V.; Mach, K.; Polásek, M.; Sedmera, P.; Hiller, J.; Thewalt, U.; Troyanov, S. I. *J. Organomet. Chem.* **1996**, *506*, 241. (b) Burlakov, V. V.; Polyakov, A. V.; Yanovsky, A. I.; Struchkov, Yu. T.; Shur, V. B.; Vol'pin, M. E.; Rosenthal, U.; Görls, H. J. *Organomet. Chem.* **1994**, *476*, 197, and references therein. (c) Ohff, A.; Pulst, S.; Peulecke, N.; Arndt, P.; Burlakov, V. V.; Rosenthal, U. *Synlett* **1996**, *2*, 111, and references therein.

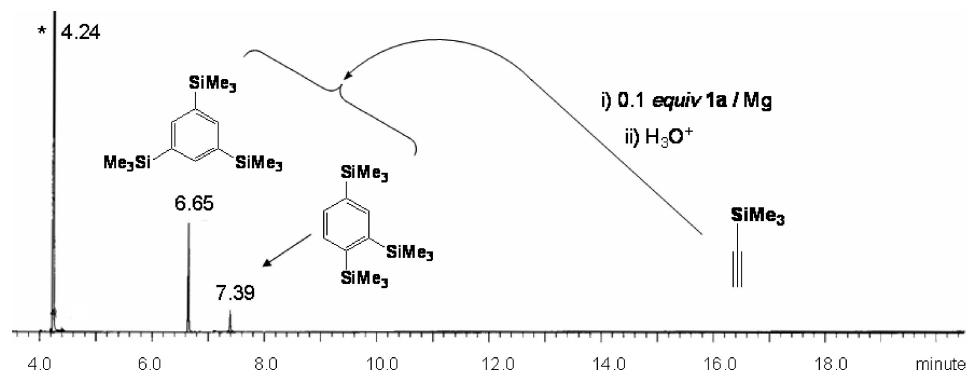


Figure 7. GC spectrum of the reaction product. The asterisk represents the internal standard of 1,3,5-trimethylbenzene at 4.24 min.

Table 2. Results of Polymerization of Ethylene using 1a/MMAO^a

entry	catalyst	mole ratio of [Al]/[Ti]	<i>T</i> (°C)	polymer (g)	activity kg PE/(mol Ti · h · atm)	<i>M_n</i> ^b (g mol ⁻¹)
1	1a	1000	10	0.068	9.71	n.d. ^c
2	1a	1000	30	0.297	42.6	3590
3	1a	1000	50	0.622	88.9	3230
4	1a	1000	70	0.410	58.6	1300
5	1a	300	50	0.196	28.0	n.d. ^c
6	1a	500	50	0.497	71.1	3830
7	1a	1500	50	0.530	75.7	n.d. ^c
8	1a	2000	50	0.406	58.0	1640
9	1a	1000	15–55	0.532	76.0	n.d. ^c
10 ^d	1a	1000	50	1.174	83.9	n.d. ^c
11	1b	1000	50	0.676	96.9	3220
12	2	1000	50	0.596	85.1	3320
13	6	1000	50	0.572	81.7	2460

^a Polymerization conditions: 4 μmol of [Ti] (the concentration of [Ti] is 8×10^{-5} mol/L), MAO as co-catalyst, 50 mL of toluene, 50 psig of ethylene pressure, 30 min. ^b Determined by ¹³C NMR at 120 °C. ^c Not determined. ^d 100 psig of ethylene pressure.

2/MAO. Until now, it is not clear whether MAO activation of **2** and **6** produces different active species with this slightly different olefin polymerization behavior.

Polymerization activity and product properties are determined by a wide range of process parameters. Here we mainly focus on complex **1a** and study the influence of reaction conditions (temperature, ethylene pressure, and the amount of MAO). First, the yield of PE increases significantly as the temperature is raised from 10 to 50 °C but then decreases as the temperature is raised further (Table 2, entries 1–4). This is reflected in the catalyst turnover. The highest catalyst activity is observed at 50 °C, and **1a** showed the highest activity of 88.9 kg PE/(mol Ti · h · atm). Throughout the temperature regime explored, the molecular weight of the polymer decreases from 3590 to 1300. Second, the increase in ethylene pressure (and thereby concentration) has a significant influence on the polymerization reaction. As the ethane pressure is raised from 50 to 100 psig, the yield and catalyst activity increase (Table 2, entries 3 and 10). Finally, the optimized Al/Ti ratio is 1000. One obvious fact is that, with the increase of Al/Ti from 300 to 2000, the number average molecular weight decreases quickly (Table 2, entries 3, 6–8). The transfer process from titanium to aluminum possibly occurs during the polymerization.

The structure of the produced polymers was studied by ¹H and ¹³C NMR spectroscopy (see Supporting Information). The ¹³C NMR spectrum (Figure 8) of polyethylene produced by **1a** (Table 2, entry 3) revealed linear polymer, and no methyl or long -chain branches could be observed. No resonances of terminal (P-CH=CH₂, vinyl end group) and internal (P-CH=CH-CH₃, 2 olefin types) double bonds (P means polymer) could be found in the NMR spectrum.

In summary, the present work demonstrated the synthesis and crystal structures of some novel unique alkyl and low-oxidation titanium complexes bearing N-heterocyclic hybrid carbene ligands. Several points can be concluded. First, the two anionic hybrids sufficiently act as chelate ligands to stabilize Ti(IV)⁻ and Ti(III)⁻ centers. Second, the metal–carbon (carbene) bond distances of these complexes are shorter than those of previously reported monodentate NHC metal complexes, as a result of the rigid tridentate architecture that pulls the carbene donor closer to the metal centers. Finally, these aryloxy-functionalized NHC carbene ligands showed high activities for ethylene polymerization to produce linear polymer with low molecular weight.

Experimental Section

All manipulations were carried out under a dry, oxygen-free argon atmosphere using standard Schlenk techniques. Solvents were dried by refluxing with appropriate drying agents (sodium/benzophenone for toluene, diethyl ether, THF, and hexane; CaH₂ for dichloromethane) and distilled under argon prior to use. CDCl₃ and C₆D₆ were distilled from CaH₂ or K and degassed by three freeze–pump–thaw cycles prior to use. The chemicals LiMe (1.4 M solution in diethyl ether) and LiBEt₃H (1.0 M solution in THF) were obtained commercially and used as received. Ligand [H₃(L^b)]Br and complexes **1a**, **2**, and **3a** were prepared according to the literature.⁹

NMR spectra were recorded on a JEOL Lambda-500 spectrometer. Chemical shifts are reported relative to SiMe₄ and were determined by referenced to the residual ¹H and ¹³C solvent resonances. High-temperature NMR measurements of polymers were obtained as follows. A mixture of polymer and CDCl₂CDCl₂ in an NMR tube was heated to 115 °C, affording a homogeneous solution. The tube was inserted into a preheated NMR probe at 115 °C, and NMR spectra were obtained after a 5 min temperature equilibration period. Chemical shifts are reported relative to the residual ¹H and ¹³C solvents resonances. The number average molecular weight (*M_n*) of polymer can be estimated from ¹H NMR.

Synthesis of [H₃(L^b)]Br. The ligands were synthesized in a similar method to [H₃(L^b)]Br.^{9a} A 500 mL three-necked round flask equipped with a dropping funnel, a reflux condenser, and a magnetic stirring bar was charged with imidazole (4.8 g, 70 mmol), anhydrous sodium hydrogen carbonate (6.2 g, 74 mmol), and THF (50 mL). 2-Bromomethyl-4-methyl-6-*tert*-butylphenol (17.23 g, 67 mmol) in THF (100 mL) was added dropwise to the above refluxing suspension with vigorous stirring. After stirred for 10 h the reaction mixture was cooled to room temperature, then poured into water (100 mL) and extracted with diethyl ether (3 × 40 mL). The extracts were dried with anhydrous sodium sulfate overnight, then evaporated to dryness to give a white powder, *N*-(3-*tert*-butyl-5-methyl-2-salicyl)imidazole, 13.8 g. Yield: 74.8%. ¹H NMR(500 MHz, C₆D₆): 1.65 (s, 9H, C(CH₃)₃), 2.18 (s, CH₃), 4.58 (d, 2H, CH₂),

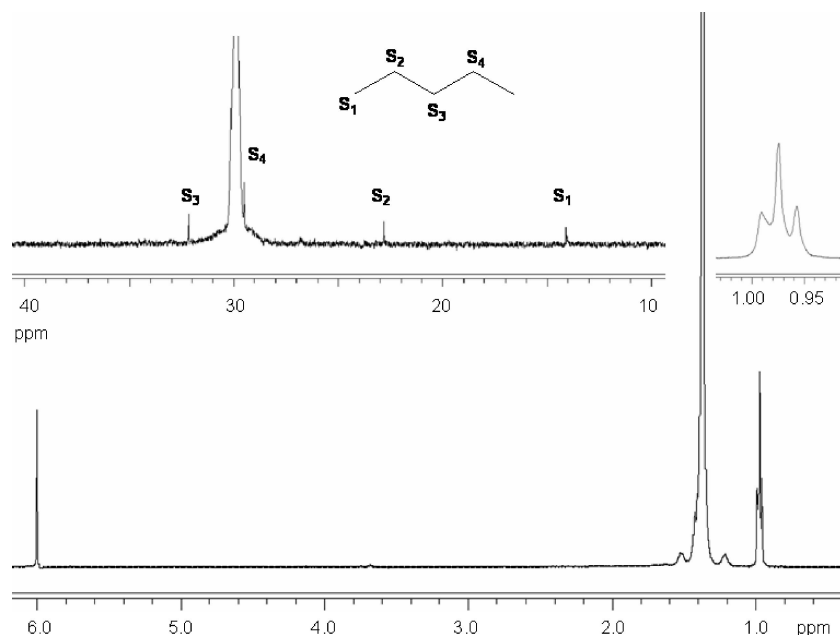


Figure 8. ^1H and ^{13}C NMR spectra of polyethylene produced by titanium catalyst **1a** (entry 5 in Table 2). The chemical shift is in units of δ . NMR conditions: 115 °C in $\text{CDCl}_2\text{CDCl}_2$.

6.30 (s, 1H, H-Ar), 6.30 (s, 1H, N-CH=N), 6.56 (d, 1H, N-CH=C), 6.57 (s, 1H, N-CH=C) 6.69 (s, 1H, H-Ar) 7.25 (d, 1H, H-Ar), 10.40 (br, 1H, -OH). A 500 mL round-bottom flask fitted with a reflux condenser and a dropping funnel was charged with *N*-(3-*tert*-butyl-5-methyl-2-salicyl)imidazole (9.39 g, 35 mmol) and THF (25 mL). 2-Bromomethyl-4-methyl-6-*tert*-butylphenol (9.0 g, 35 mmol) in THF (50 mL) was slowly added to the above refluxing suspension. After stirring for another 12 h the mixture was cooled to room temperature. THF was removed under vacuum, and the crude was washed with toluene (3×10 mL) and hexane (3×10 mL) to give 15.546 g of $[\text{H}_3(\text{L}^b)]\text{Br}$ as an off-white powder. Yield: 88.6%. ^1H NMR (400 MHz, CDCl_3): δ 1.37 (s, 18H, C(CH₃)₃), 2.24 (s, 6H, CH₃), 5.52 (s, 4H, N-CH₂-Ar), 6.68 (brs, 2H, OH), 6.92 (brs, 2H, Ar-H), 7.10 (s, 2H, Ar-H), 7.24 (d, $J = 1.2$ Hz, 2H, =CH_{imidazolium}), 9.39 (br, 1H, CH_{imidazolium}). ^{13}C NMR (127 MHz, CDCl_3): δ 20.95 (*Me*-Ar), 30.32 (*CMe*₃), 34.88 (*CMe*₃), 50.84 (N-CH₂-Ar), 121.95, 122.63 (N-CH=CH-N of imidazolium), 128.44, 128.55, 129.21, 129.68, 130.58, 136.64 (aromatics), 140.25 (N-CH-N of imidazolium), 151.86 (O-C). Anal. Calcd for C₂₇H₃₃BrN₂O₂: C, 64.53; H, 7.62; N, 5.57. Found: C, 63.77; H, 7.39; N, 5.23.

Synthesis of $[(\text{L}^b)\text{TiCl}_2(\text{THF})]$ (1b**).** **1b** was prepared as an orange-red solid in a similar fashion to **1a**.^{9a} Yield: 86.2%. ^1H NMR (500 MHz, CDCl_3): δ 1.50 (s, 18H, *CMe*₃), 1.85 (m, 2H, CH₂THF), 2.25 (s, 6H, Ar-CH₃), 3.76 (m, 2H, CH₂THF), 4.3–6.0 (m, br, 4H, Ar-CH₂-N), 6.83 (brs, 2H, Ar-H), 7.08 (brs, 2H, N-CH=), 7.35 (brs, 2H, Ar-H). ^{13}C NMR (127 MHz, CDCl_3): δ 21.08, 21.68 (Ar-CH₃), 25.83 (CH₂ of THF), 31.50 (*CMe*₃), 34.17, 35.53 (*CMe*₃), 52.55 (N-CH₂-Ar), 68.50 (O-CH₂ of THF), 119.91 (CH of carbene), 125.52, 129.17, 129.27, 138.10, 138.64 (aromatics), 165.62 (Ti-O-C). Anal. Calcd for C₃₁H₄₃Cl₂N₂O₃Ti: C, 60.99; H, 7.10; N, 4.59. Found: C, 60.57; H, 6.89; N, 4.83.

Synthesis of $[(\text{L}^b)\text{Ti}(\text{CH}_2\text{Ph})_2]$ (3b**).** **3b** was obtained as an orange solid in a similar manner to **3a**.^{9a} Yield: 90.1%. ^1H NMR (500 MHz, C₆D₆): δ 1.95 (s, 18H, C(CH₃)₃), 2.29 (s, 6H, CH₃), 3.34 (brs, 2H, N-CH₂-Ar), 3.38 (brs, 2H, CH₂-Ti), 3.44 (brs, 2H, CH₂-Ti), 4.14 (brs, 2H, N-CH₂-Ar), 5.46 (s, 2H, CH=CH), 6.57 (s, 2H H-Ar), 7.38 (s, 2H, H-Ar). ^{13}C NMR (500 MHz, C₆D₆): δ 22.02 (*Me*-Ar), 31.87 (*CMe*₃), 36.74 (*CMe*₃), 53.31 (N-CH₂-Ar), 86.59 (CH₂-Ti), 118.28, 118.82 (CH_{carbene}), 122.55, 127.24, 128.76, 128.80, 129.02, 129.07, 139.02, 146.99 (aromatics), 162.39 (Ti-O-C), 188.06 (C_{carbene}). Anal. Calcd for C₄₁H₄₉N₂O₂Ti: C, 75.79; H, 7.60; N, 4.31. Found: C, 75.64; H, 7.74; N, 4.31.

Synthesis of $[(\text{L}^a)\text{Ti}(\text{CH}_3)_2]$ (4a**).** LiMe (1.2 mL, 1.4 M solution in diethyl ether, 1.68 mmol) was added dropwise to a precooled suspension of **1a** (0.569 g, 0.82 mmol) in Et₂O (30 mL) at -78 °C. The mixture was slowly warmed, and the color of the solution changed from dark red to yellow-brown. After the mixture was stirred for another 4 h at room temperature, the solvent was removed under vacuum, and CH₂Cl₂ (20 mL) was added to the solid residue. The suspension was centrifuged to remove the formed salt, and the upper clear solution was evacuated to dryness, yielding a dark yellow solid, **4a**, 0.437 g. Yield: 91.8%. ^1H NMR (500 MHz, C₆D₆): δ 1.43 (s, 18H, CH₃ of tBu), 1.61 (s, 6H, CH₃-Ti), 1.99 (s, 18H, CH₃ of iBu), 3.59, 3.62 (br, 2H, N-CH₂-Ar), 4.80, 4.82 (br, 2H, N-CH₂-Ar), 5.42 (s, 2H, CH=CH), 6.98 (d, $J = 2.5$ Hz, 2H, H-Ar), 7.69 ppm (d, $J = 2.5$ Hz). $^{13}\text{C}\{^1\text{H}\}$ NMR (127 MHz, C₆D₆): δ 31.46, 32.92 (CH₃ of tBu), 35.39, 36.99 (*CMe*₃), 54.01 (N-CH₂-Ar), 64.00 (CH₃-Ti), 118.30, 118.37 (CH_{carbene}), 124.71, 124.77, 125.24, 126.79, 128.45, 128.50, 128.60, 138.77, 140.80 (aromatics), 162.73 (Ti-O-C), 185.69 ppm (NCN). Anal. Calcd (%) for C₃₅H₅₃N₂O₂Ti: C 72.27, H 9.18, N 4.82. Found: C 72.49, H 9.26, N 4.82.

Synthesis of $[(\text{L}^b)\text{Ti}(\text{CH}_3)_2]$ (4b**).** **4b** was obtained as a dark yellow solid in a similar manner to **4a** using **1b**. Yield: 88.3%. ^1H NMR (500 MHz, C₆D₆): δ 1.57 (s, 6H, CH₃-Ti), 1.91 (s, 18H, C(CH₃)₃), 2.30 (s, 6H, CH₃-Ar), 3.51, 3.53 (br, 2H, N-CH₂-Ar), 4.71, 4.73 (br, 2H, N-CH₂-Ar), 5.55 (s, 2H, CH=CH), 6.64 (d, $J = 2.0$ Hz, 2H, H-Ar), 7.38 (d, $J = 2.0$ Hz). ^{13}C NMR (127 MHz, C₆D₆): δ 22.00, 24.02 (*Me*-Ar), 31.43, 32.86 (*CMe*₃), 36.62 (*CMe*₃), 53.65 (N-CH₂-Ar), 63.91 (CH₃-Ti), 118.31, 118.37 (CH_{carbene}), 127.09, 127.44, 127.68, 128.60, 129.08, 129.11, 139.2 (aromatics), 162.79 (Ti-O-C), 185.98 (C_{carbene}). Anal. Calcd for C₂₉H₄₁N₂O₂Ti · 0.5(C₆H₁₄): C, 71.10; H, 8.95; N, 5.18. Found: C, 70.71; H, 8.76; N, 5.51.

Synthesis of $[(\text{L}^a)\text{Ti}(\text{OCH}_2\text{C}_6\text{H}_5)_2]$ (5**).** **A: NMR Tube Experiment.** The reaction was first monitored using NMR scale experiment in the following way: A J. Young NMR tube was charged with 30 mg (0.04 mmol) of **3a** and 0.5 mL of C₆D₆. The tube was cooled to -40 °C and charged with 1 atm of dried O₂. After the solution was warmed to room temperature, the ^1H NMR spectrum was recorded at different times. **B: Scale-up Experiment.** A stirred solution of **3a** (0.366 g, 0.50 mmol) in diethyl ether (20 mL) was cooled to -78 °C and exposed to 1 atm of pure, dried O₂ by bubbling the gas through it for 30 min. The reaction system was

Table 3. Summary of X-ray Collection Data of 3b, 4a, 4b, 5, and 6

	3b	4a	4b·0.5(C ₆ H ₁₄)	5·0.5(C ₆ H ₁₄)	6·2.5(C ₇ H ₈)
formula	C ₈₂ H ₉₆ N ₄ O ₄ Ti ₂	C ₇₀ H ₁₀₄ N ₄ O ₄ Ti ₂	C ₃₂ H ₄₇ N ₂ O ₂ Ti	C ₅₀ H ₇₀ N ₂ O ₆ Ti	C ₆₂ H ₈₆ N ₂ O ₄ BrTi
M _r	1297.48	1161.42	539.64	871.03	1051.18
cryst syst	triclinic	monoclinic	monoclinic	triclinic	monoclinic
space group	P $\bar{1}$	P2 ₁ /n	P2 ₁ /c	P $\bar{1}$	P2 ₁ /c
a [Å]	14.831(6)	15.013(4)	8.131(4)	12.904(7)	16.537(10)
b [Å]	15.919(7)	17.845(5)	17.610(8)	13.672(8)	21.034(12)
c [Å]	16.986(7)	25.913(7)	22.363(10)	13.941(8)	18.842(12)
α [deg]	110.203(7)	90	90	107.540(4)	90
β [deg]	93.968(5)	97.681(6)	103.952(9)	110.005(7)	115.152(10)
γ [deg]	101.361(6)	90	90	97.782(7)	90
V [Å ³]	3648.6(26)	6879.8(22)	3107.8(24)	2124.1(21)	5932.5(14)
Z	2	4	4	2	4
D _{calcd} [g cm ⁻³]	1.181	1.121	1.153	1.362	1.177
M [mm ⁻¹]	2.70	2.79	3.04	2.59	8.65
data collected	29 338	97 984	24 856	17 032	95 022
unique data	13 317	15 710	6983	8082	13 859
goodness of fit	1.00	1.00	1.00	1.099	1.00
R ₁ /wR ₂	0.092/0.15	0.091/0.228	0.069/0.176	0.090/0.232	0.129/0.349

closed and warmed to room temperature. After the mixture was stirred for another 4 h, the obtained light yellow solution was concentrated to 2 mL and layered with hexane (5 mL) to afford yellow crystals of **5**, 0.218 g. Yield: 57.1%. ¹H NMR (500 MHz, C₆D₆): δ 1.37 (s, 18H, C(CH₃)₃), 1.84 (s, 18H, C(CH₃)₃), 3.62 (brs, 1H, N-CH₂-Ar), 3.65 (brs, 1H, N-CH₂-Ar), 5.00 (brs, 1H, N-CH₂-Ar), 5.03 (brs, 1H, N-CH₂-Ar), 5.43 (s, 2H, CH=CH), 5.88 (q, 4H, CH₂-O-Ti), 6.90 (d, *J* = 3.0 Hz, 2H, H-Ar), 7.08–7.22 (m, 6H, H-Ar), 7.44 (d, *J* = 7.5 Hz, 2H, H-Ar), 7.59 (d, *J* = 7.5 Hz, 2H, H-Ar). ¹³C NMR (500 MHz, C₆D₆): δ 31.59, 32.92 (CMe₃), 35.35, 36.74 (CMe₃), 54.09 (N-CH₂-Ar), 79.80 (CH₂-O-Ti), 118.78 (=CH_{carbene}), 124.00, 125.08, 125.62, 127.14, 127.64, 128.64, 138.85, 143.67 (aromatics), 162.00 (Ti-O-C), 182.02 (C_{carbene}). Anal. Calcd for C₄₇H₆₁N₂O₄Ti: C, 73.71; H, 8.03; N, 3.66. Found: C, 73.23; H, 8.27; N, 3.39.

Synthesis of [(L^a)Ti^{III}Br(THF)₂] (6**).** A toluene solution (10 mL) of **2** (0.348 g, 0.445 mmol) was cooled to −78 °C in a methanol/N₂(liquid) bath. To the solution was added LiBET₃H (0.5 mL, 1.0 M solution in THF, 0.5 mmol) via syringe. The mixture was slowly warmed to room temperature and was stirred for another 4 h. The solution was concentrated to 5 mL and cooled at −29 °C overnight to afford 0.107 g of **6** as yellow-green plate crystals. Yield: 31.1%. Anal. Calcd (%) for C₂₇H₃₃BrN₂O₂·2.5(C₇H₈): C, 69.99; H, 8.49; N, 2.74. Found: C, 69.83; H, 8.15; N, 2.94.

Trimethylsilylacetylene Cyclopolymerization Procedure Using 1a/Mg as Catalyst. A 0.5 mmol amount of **1a**, 5 mmol of Mg powder, and 5 mmol of trimethylsilylacetylene were charged into a Schlenk flask with 25 mL of toluene. Then 5 mmol of trimethylbenzene was added as a standard. The mixture was stirred at room temperature. After a certain time, a small amount of reaction mixture was brought out, diluted with hexane, and quenched with HCl (3 M). The organic solution was subjected to GC-MS analysis.

Synthesis [(L^a)Ti(Me₃SiC≡CSiMe₃)] (7**) (NMR Scale Experiment).** Benzene-*d*₆ (1.0 mL) was added to **1a** (39.1 mg, 0.05 mmol) and Mg powder (12 mg, 0.5 mmol), and the mixture was cooled to −78 °C. Bis(trimethylsilyl)acetylene (11.3 μ L, 0.05 mmol) was then added, and then the mixture was slowly warmed to room temperature and continuously stirred for 48 h. The resultant superclear dark purple solution was directly transferred to an NMR tube for analysis. ¹H NMR (400 MHz, C₆D₆): δ 0.16 (s, 9H, Si(CH₃)₃), 1.40 (s, 18H, C(CH₃)₃), 1.59 (s, 18H, C(CH₃)₃), 2.11 (s, CH₃ of toluene), 3.95, 3.98 (brs, 2H, N-CH₂-Ar), 5.04, 5.07 (brs, 1H, N-CH₂-Ar), 6.18 (brs, 2H, N-CH=), 7.02 (m, H-Ar + H-toluene), 7.50 (d, *J* = 6.4 Hz, 2H, H-Ar). ¹³C NMR (500 MHz, C₆D₆): δ −0.01, 0.58, 1.66 (SiMe₃), 21.47 (CH₃ of toluene), 31.06, 32.05 (CMe₃), 34.43, 35.71 (CMe₃), 53.41 (N-CH₂-Ar), 114.16 (=CH-N), 122.35, 124.80, 125.16, 125.34, 125.69, 128.52, 128.57, 129.33, 136.94, 138.87, 140.77 (aromatics), 162.04 (Zr-O-C), 203.03 (C_{carbene}), 206.78, 212.33 (C≡C).

Ethylene Polymerizations. A 100 mL autoclave was charged with 50 mL of toluene under argon, and a mixture of titanium complex **1a**/MAO (the molar ratio of Al:Ti was 1000) in 10 mL toluene was added. After three ethylene gas exchanges, the ethylene pressure was raised to the desired pressure of ethylene and maintained for 0.5 h. The polymerization was terminated by the addition of methanol and diluted HCl (10%). The solid polyethylene was filtered, washed with methanol, and dried at 40 °C in vacuo.

X-ray Crystallography. A summary of the crystallographic data for compounds **3b**, **4a**, **4b**, **5**, and **6** are given in Table 3. All data sets were collected on a Rigaku CCD area detector diffractometer (Mo K α radiation, λ = 0.710 70 Å) and a Rigaku low-temperature device. Crystals were immersed in mineral oil, mounted on a nylon loop in a random orientation, and transferred directly to the cold N₂ stream of the diffractometer. The data were collected in a hemisphere of data in 720 frames with 20–40 s exposure times. The data sets were collected (4.0° < 2 θ < 45–55°). Data collection and reduction were carried out using the CrystalClear (Rigaku) Processing software packages.¹⁸ Structure solutions were carried out by direct methods using the Crystal Structure (Rigaku) software package¹⁹ or SHELXS.²⁰ In all cases refinement was carried out by full matrix least-squares methods against F² using SHELXL-97.²⁰ In the final cycles of each refinement, all non-hydrogen atoms were assigned anisotropic temperature factors in the absence of disorder data. C–H atom positions were calculated and allowed to ride on the carbon to which they are bonded assuming a C–H bond length of 0.97 Å. The H atom contributions were calculated, but not refined.

Acknowledgment. This work was financially supported by National Natural Science Foundation of China, Grant No. 20671021, SRF for ROCS, SEM, and Shanghai Leading Academic Discipline Project, Project No. B 108. The author is grateful to Dr. H. Kawaguchi for his help at IMS.

Supporting Information Available: Crystal data (CIF files) for complexes **3b**, **4a**, **4b**, **5**, and **6**, and figures of high-temperature ¹H and ¹³C NMR and DSC thermograms for polypropylenes obtained from **1**, **2**, and **6**/MAO catalytic systems. This material is available free of charge via the Internet at <http://pubs.acs.org>.

OM800717H

(18) (a) *CrystalClear* Software Package; Rigaku and Molecular Structure Corp., 1999. (b) Pflugrath, J. W. *Acta Crystallogr.* **1999**, D55, 1718.

(19) *Crystal Structure Analysis* Package; Rigaku and Molecular Structure Corp., 2001.

(20) Sheldrick, G. M. *SHELXL-97* Programs for Crystal Structure Analysis; University of Göttingen: Germany, 1997.

Tricarbonylchromium Complexes of 1,2-Dihydro-1,2-benzazaborines

Jun Pan, Jeff W. Kampf, and Arthur J. Ashe III*

Department of Chemistry, University of Michigan, Ann Arbor, Michigan 48109-1055

Received May 1, 2008

1,2-Dihydro-2-phenyl-1,2-benzazaborine reacts with $\text{Cr}(\text{CO})_3(\text{CH}_3\text{CN})_3$ in THF at 140 °C to form complex **18**, in which the phenyl is η^6 -bound to chromium. 1,2-Dihydro-2-methyl-1,2-benzazaborine reacts with $\text{Cr}(\text{CO})_3(\text{CH}_3\text{CN})_3$ in THF at 60 °C to form complex **23**, in which the benzo ring is η^6 -bound to chromium. Treating **23** with potassium bis(trimethylsilyl)amide in THF forms the corresponding potassium salt **25**, which on heating undergoes haptotropic isomerization to complex **26**, in which the anionic heterocyclic ring is η^6 -bound to the chromium.

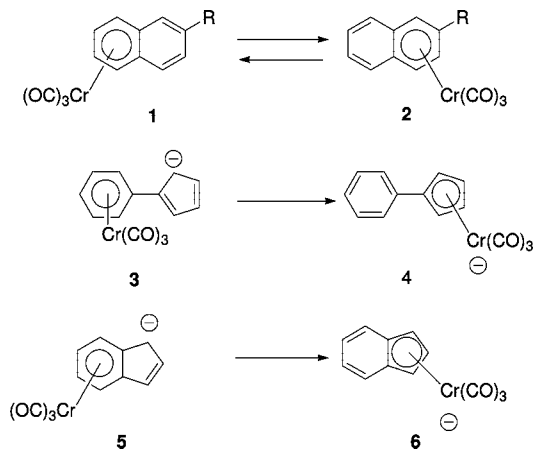
Introduction

Metal complexes of polycyclic aromatic compounds often undergo haptotropic migrations in which the metal migrates from one ring to another.¹ Chromium tricarbonyl complexes of naphthalenes (e.g., **1** and **2**) in which a $\text{Cr}(\text{CO})_3$ group migrates across a ring fusion have been well studied experimentally and computationally.^{1–5} $\text{Cr}(\text{CO})_3$ migration across a single bond between two rings are also known, e.g. **3** → **4**.^{6a} In most cases the migration of an electron withdrawing $\text{Cr}(\text{CO})_3$ group from a neutral to an anionic ring is particularly favorable, e.g. **5** → **6**.^{6,7} See Scheme 1.

We have been interested in haptotropic migrations involving boron–nitrogen analogues of benzocyclic aromatics as shown in Scheme 2. The isomerization of **7** → **8**⁸ is closely analogous to that of **5** → **6**.^{6b} However, reactions of boron–nitrogen heterocycles with acidic NH groups are potentially more complex. Thus, the reaction of 1,2-dihydro-2-phenyl-1,2-azaborine (**9**) with $\text{Cr}(\text{CO})_3(\text{CH}_3\text{CN})_3$ gives complex **10**, which can

be thermally isomerized to **11**. Complex **11** can then be deprotonated to form **12**, which on heating is isomerized to **13**. Protonation of **13** forms **10** again (see Scheme 2).⁹ This cycle of haptotropic migrations and acid/base steps is unique in that the $\text{Cr}(\text{CO})_3$ groups can be switched to either the phenyl or the heterocyclic ring. In order to explore this phenomenon further, we have now examined the corresponding reactions of complexes of 1,2-dihydro-1,2-benzazaborines **15** and **16**, which are ring-fused analogues of **9**.

Scheme 1. Haptotropic Shifts of $\text{Cr}(\text{CO})_3$ Complexes of Selected Carbocyclic Aromatic Compounds



Results and Discussion

2-Chloro-1,2-dihydro-1,2-benzazaborine (**14**) was originally prepared in 1959 by Dewar and Dietz by the reaction of BCl_3 with 2-aminostyrene.¹⁰ The boron-bound chloro group of **14** can be easily replaced by nucleophiles to give **15–17**, as illustrated in eq 1. More recently Paetzold and co-workers have reported on **14**, **16**, and several more highly substituted 1,2-dihydro-1,2-benzazaborines.¹¹ These compounds have now been more thoroughly characterized but are identical with those originally reported.¹⁰ Furthermore, we have obtained a crystal structure of the parent compound **17**, which establishes its structure.

(9) Pan, J.; Kampf, J. W.; Ashe, A. J. *Organometallics* 2006, 25, 197.

(10) Dewar, M. J. S.; Dietz, R. J. *Chem. Soc.* 1959, 2728.

(11) Paetzold, P.; Stanescu, C.; Stubenrauch, J. R.; Bienmüller, M.; Englert, U. *Z. Anorg. Allg. Chem.* 2004, 630, 2632.

* To whom correspondence should be addressed. E-mail: ajashe@umich.edu.

(1) For reviews see: (a) Dötz, K. H.; Wenzel, B.; Jahr, H. C. *Top. Curr. Chem.* 2004, 248, 63. (b) Dötz, K. H.; Jahr, H. C. *Chem. Recl.* 2004, 4, 61. (c) Oprunenko, Y. F. *Russ. Chem. Rev.* 2000, 69, 683. (d) Morris, M. J. In *Comprehensive Organometallic Chemistry II*; Abel, E. W., Stone, F. G. A., Wilkinson, G., Eds.; Pergamon Press: New York, 1995; Vol. 5, p 501. (e) Ustynyuk, N. A. *Metalloorg. Khim.* 1989, 2, 43.

(2) (a) Kirss, R. U.; Treichel, P. M., Jr. *J. Am. Chem. Soc.* 1986, 108, 853. (b) Oprunenko, Y. F.; Malugina, S. G.; Ustynyuk, Y. A.; Ustynyuk, N. A.; Kravtsov, D. N. *J. Organomet. Chem.* 1988, 338, 357.

(3) (a) Jahr, H. C.; Nieger, M.; Dötz, K. H. *Chem. Commun.* 2003, 2866. (b) Dötz, K. H.; Stendel, J.; Müller, S.; Nieger, M.; Ketrat, S.; Dolg, M. *Organometallics* 2005, 24, 3219.

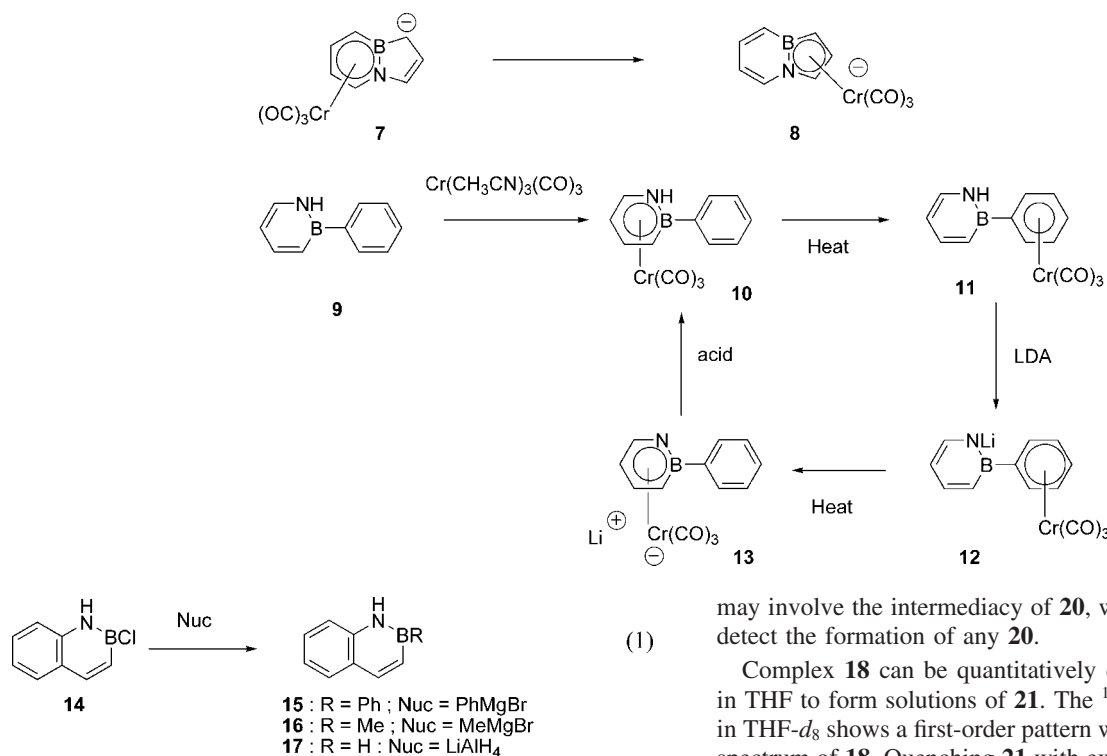
(4) Oprunenko, Y. F.; Akhmedov, N. G.; Laikov, D. N.; Malyugina, S. G.; Mstislavsky, V. I.; Roznyatovsky, V. A.; Ustynyuk, Y. A.; Ustynyuk, N. A. *J. Organomet. Chem.* 1999, 583, 136.

(5) (a) Albright, T. A.; Hofmann, P.; Hoffmann, R.; Lillya, C. P.; Dobosh, P. A. *J. Am. Chem. Soc.* 1983, 105, 3396. (b) Howell, J. A. S.; Ashford, N. F.; Dixon, D. T.; Kola, J. C.; Albright, T. A.; Kang, S. K. *Organometallics* 1991, 10, 1852.

(6) (a) Cecon, A.; Gambaro, A.; Gottardi, F.; Santi, S.; Venzo, A.; Lucchini, V. J. *Organomet. Chem.* 1989, 379, 67. (b) Cecon, A.; Gambaro, A.; Gottardi, F.; Santi, S.; Venzo, A. *J. Organomet. Chem.* 1991, 412, 85.

(7) (a) Ustynyuk, N. A.; Oprunenko, Y. F.; Malyugina, S. G.; Trifonova, O. I.; Ustynyuk, Y. A. *J. Organomet. Chem.* 1984, 270, 185. (b) Thoma, T.; Pleshakov, V. G.; Prostakov, N. S.; Ustynyuk, Y. A.; Nesmeyanov, A. N.; Ustynyuk, N. A. *J. Organomet. Chem.* 1980, 192, 359. (c) Trifonova, O. I.; Galiullin, R. A.; Ustynyuk, Y. A.; Ustynyuk, N. A.; Petrovsky, P. V.; Kravtsov, D. N. *J. Organomet. Chem.* 1987, 328, 321. and other papers in this series.

(8) Pan, J.; Wang, J.; Banazak Holl, M. M.; Kampf, J. W.; Ashe, A. J. *Organometallics* 2006, 25, 3463.

Scheme 2. Haptotropic Shifts of Cr(CO)₃ Complexes of Boron–Nitrogen Heteroaromatic Compounds

The phenyl derivative **15** was of particular interest to us, since it is the benzo-fused analogue of **9**, which we had previously investigated in detail. Heating **15** with Cr(CO)₃(CH₃CN)₃ in THF to 140 °C for 40 h gave complex **18** as the sole product in 50% yield. The ¹H NMR spectrum of **18** in THF-*d*₈ is first order and can be readily assigned by inspection. The signals for the phenyl protons are shifted upfield relative to those of **15**, while those of the 1,2-dihydro-1,2-benzazaborine group are little effected by complexation. Therefore, π -complexation to the phenyl ring is indicated.¹² The regioselectivity of the Cr(CO)₃ complexation was confirmed by obtaining an X-ray structure of **18**, which is illustrated in Figure 1.

The reaction of **15** with Cr(CO)₃(CH₃CN)₃ under milder conditions (25 °C) gave a mixture of **18** and an isomer tentatively identified as **19** in the ratio of 1:3. We have been unable to isolate pure **19** from the mixture, while heating it to 140 °C converted it to pure **18**. The structure of **19** was assigned on the basis of the ¹H NMR spectrum of the mixture. In particular signals for the fused benzocyclic ring of **19** were shifted markedly upfield from those of the uncoordinated ring of **15**. Similar π -coordination shifts are characteristic of Cr(CO)₃-coordinated arene rings.¹² Although the conversion of **19** to **18**

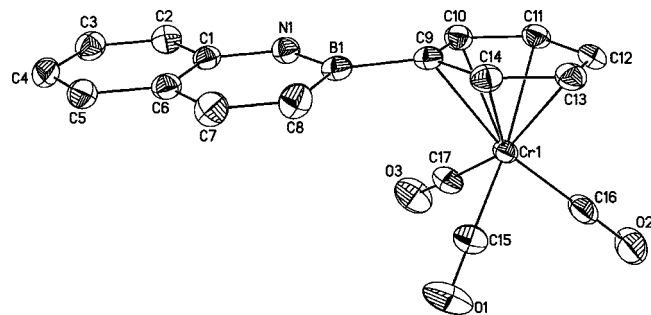


Figure 1. Solid-state structure of **18** (ORTEP). Thermal ellipsoids are given at the 50% probability level. Hydrogen atoms have been omitted for clarity.

may involve the intermediacy of **20**, we have not been able to detect the formation of any **20**.

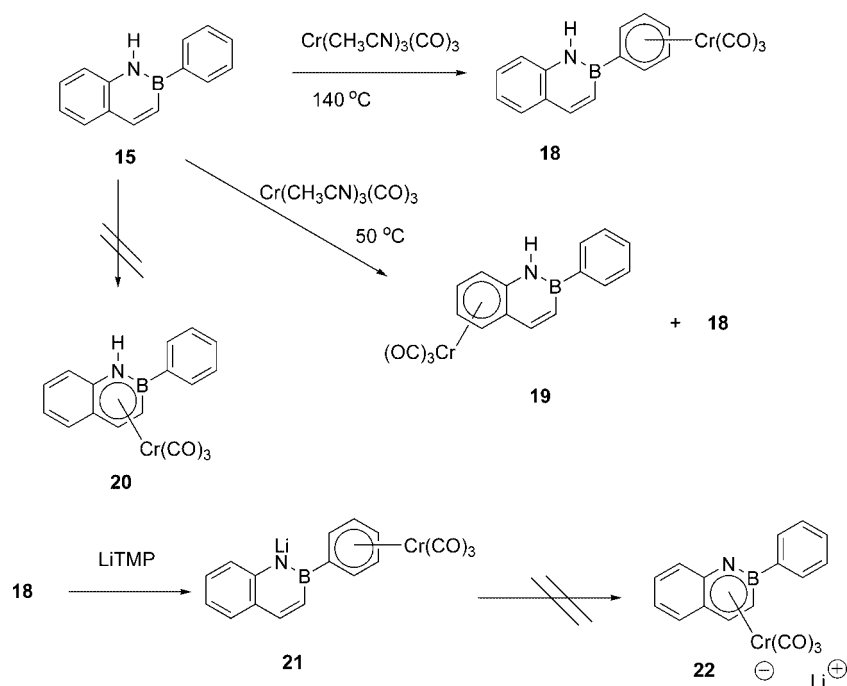
Complex **18** can be quantitatively deprotonated by LiTMP in THF to form solutions of **21**. The ¹H NMR spectrum of **21** in THF-*d*₈ shows a first-order pattern which is distinct from the spectrum of **18**. Quenching **21** with excess D₂O afforded **18-d**, in which the deuterium was exclusively at N(1). Heating anion **21** to 110 °C in THF led to slow decomposition without giving any detectable **22**. This greater thermal lability of **21** relative to that of **12** prevented observation of Cr(CO)₃ migration from phenyl to the anionic heterocyclic ring which had been found for **12**. See Scheme 3.

Our initial goal had been to examine possible “biphenyl-like” haptotropic migrations of complexes of **15** which might be analogous to those illustrated in Scheme 2. Since we were unable to prepare **20** and **22** and no Cr(CO)₃ migrations from **18** or **21** were found, this goal could not be achieved. Therefore, we decided to examine possible “naphthalene-type” migrations between the fused rings of the 1,2-dihydro-1,2-benzazaborine system. In order to limit metal coordination to the fused rings, we have examined the reactions of the methyl derivative **16**.

Treating **16** with Cr(CO)₃(CH₃CN)₃ in THF at 60 °C resulted in formation of complex **23** mixed with excess **16**. On heating to higher temperatures **23** decomposes to give **16** and unidentified chromium-containing materials. No complex **24** could be detected. Pure **23** was isolated in 39% yield using column chromatography on silica gel. The ¹H NMR spectrum of **23** in THF-*d*₈ is first order and can readily be assigned by inspection. The signals for the benzo-ring protons are shifted upfield in comparison with those of **16**, while the signals for the uncomplexed C₄BN ring are little changed. Therefore, π -complexation to the benzo ring is indicated,¹² which was later confirmed by obtaining a crystal structure of **23**, shown in Figure 2.

Neutral complex **23** can be quantitatively deprotonated by treatment with potassium bis(trimethylsilyl)amide in THF to give a solution of potassium salt **25**. The ¹H spectrum of **25** in THF-*d*₈ shows a first-order pattern, which is easily distinguished from that of **23**. Quenching **25** with excess D₂O yielded N-deuterium-labeled **23-d**. Heating **25** in THF-*d*₈ to 90 °C converted it to **26**. Decomposition was approximately 25%. The conversion of **25** to **26** was monitored by ¹H NMR spectroscopy. In comparison to that of **25** the ¹H NMR spectrum of **26** showed that all of the signals of the benzo ring are shifted downfield and all of

Scheme 3. Reactions of 1,2-Dihydro-2-phenyl-1,2-benzazaborines



the signals for the C_4BN ring are shifted upfield. In addition, the ^{11}B NMR spectrum shows that the signal for **26** (δ 24.0) is shifted upfield relative to that of **25** (δ 40.8). This is consistent with a coordination shift of the $\text{Cr}(\text{CO})_3$ group from the benzo ring to the heterocyclic ring.^{12,13}

Quenching **26** with methyl iodide in THF at $25\text{ }^\circ\text{C}$ afforded the uncomplexed *N*-methyl derivative **28**.¹⁰ We suspect that the methyl iodide converted **26** to intermediate **27**, which must be highly labile at room temperature since it rapidly decomplexes to give **28**. See Scheme 4.

The thermal conversion of **25** to **26** and the presumed lability of **27** suggest that the order of ligand strength toward $\text{Cr}(\text{CO})_3$ is the anionic heterocyclic ring of 1,2-benzazaboratabenzene > the benzo ring of 1,2-benzazaboratabenzene > the neutral heterocyclic ring of 1,2-dihydro-1,2-benzazaborine. This order is analogous to that previously found for the monocyclic ring systems **10**–**13**, in which the order of ligand strength was 1,2-azaboratabenzene > *B*-phenyl > 1,2-dihydro-1,2-azaborine. In both sets the anionic heterocyclic ring is the strongest ligand, while the neutral heterocyclic ring is the weakest ligand toward the electron-withdrawing $\text{Cr}(\text{CO})_3$ group. Computational studies have indicated that the π -bonding of 1,2-dihydro-1,2-azaborine

is weaker than that of benzene due to localization of electrons by the B–N bond.¹⁴ This is consistent with the observed lower π -basicity of the heterocyclic ring toward $\text{Cr}(\text{CO})_3$. Apparently deprotonation of NH of 1,2-dihydro-1,2-azaborine greatly enhances its π -basicity so that 1,2-azaboratabenzene is a stronger π -base toward $\text{Cr}(\text{CO})_3$.

Our inability to prepare stable complexes in which the $\text{Cr}(\text{CO})_3$ group is π -bound to the heterocyclic ring of 1,2-dihydro-1,2-benzazaborines implies that this ring system is a poorer ligand than the 1,2-dihydro-1,2-azaborine ring of **10**. Reduction in the π -ligand strength on benzannulation has a precedent in the observation that naphthalene is a poorer ligand than benzene toward $\text{Cr}(\text{CO})_3$.¹⁵

It was of interest to examine the conversion of **25** to **26** in order to compare it with the formally similar $\text{Cr}(\text{CO})_3$ migrations between the rings of η^6 -naphthalene complexes **1** and **2**. The reaction of **25** to give **26** at $60\text{ }^\circ\text{C}$ in $\text{THF-}d_8$ was monitored by ^1H NMR spectroscopy. Unfortunately, heating **25** led to unidentified products as well as **26**. When the reaction was performed in the presence of the good π -donor hexamethylbenzene, no crossover products were observed. These data are consistent with a unimolecular reaction. The first-order rate constant for the loss of **25** was found to be $k = 2.80 \times 10^{-5}\text{ s}^{-1}$ at $60\text{ }^\circ\text{C}$. For comparison the conversion of **1** to **2**, where $\text{R} = \text{Me}$, is 34 times slower with an extrapolated $k = 8.2 \times 10^{-7}\text{ s}^{-1}$ at $60\text{ }^\circ\text{C}$.^{2a} Precise comparison is not warranted because of differences in charge type, solvent, and ring substituents. Nevertheless, the rates are qualitatively similar. It has been proposed that naphthalene– $\text{Cr}(\text{CO})_3$ ring exchange occurs via an intramolecular stepwise decomplexation of the formal double

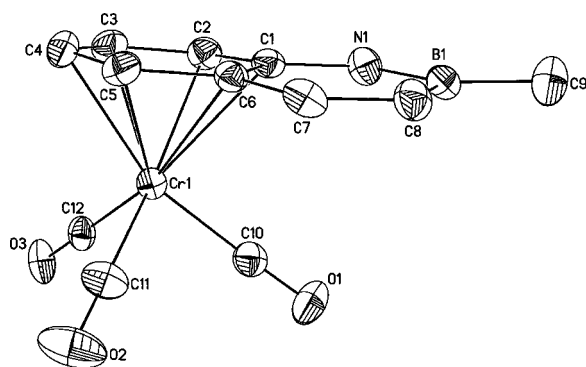


Figure 2. Solid-state structure of **23** (ORTEP). Thermal ellipsoids are given at the 50% probability level. Hydrogen atoms have been omitted for clarity.

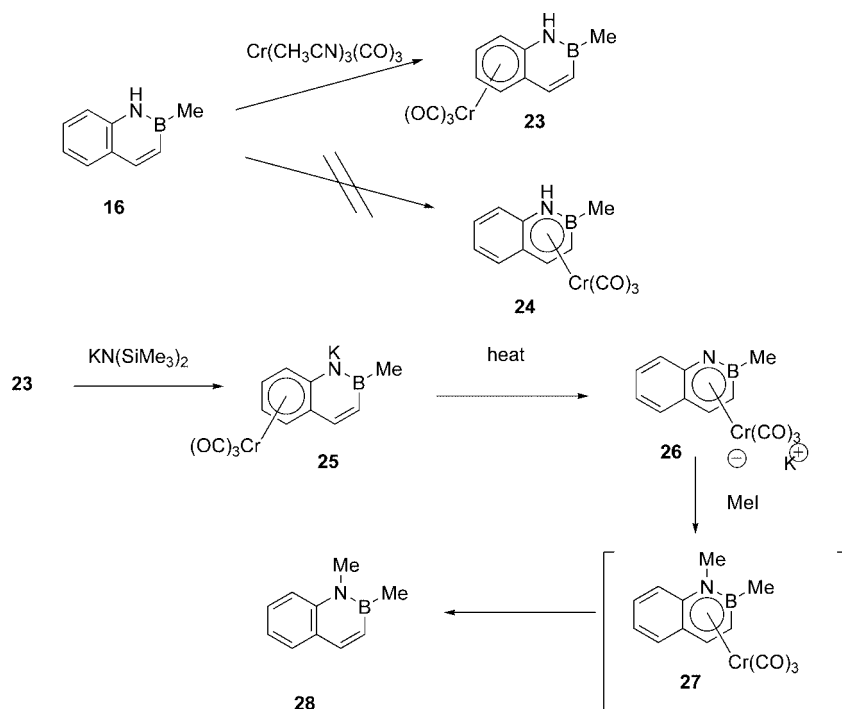
(12) Elschenbroich, C.; Salzer, A. *Organometallics*, 2nd ed.; VCH: Weinheim, Germany, 1991; pp 296–307.

(13) Wrackmeyer, B.; Köster, R. *Methoden der Organischen Chemie*; G. Thieme Verlag: Stuttgart, Germany, 1984; Vol. XIII, Part 3c, p 584.

(14) (a) Kranz, M.; Clark, T. *J. Org. Chem.* **1992**, *57*, 5492. (b) Kar, T.; Elmore, D. E.; Scheiner, S. *J. Mol. Struct.* **1997**, *392*, 65.

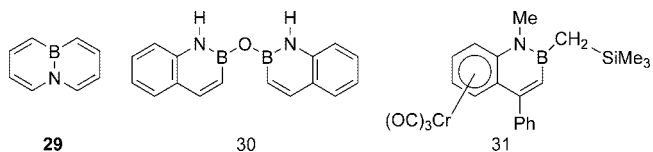
(15) (a) Mukerjee, S. L.; Lang, R. F.; Ju, T.; Kiss, G.; Hoff, C. D. *Inorg. Chem.* **1992**, *31*, 4885. (b) Zhang, S.; Shen, J. K.; Basolo, F.; Ju, T. D.; Lang, R. F.; Kiss, G.; Hoff, C. D. *Organometallics* **1994**, *13*, 3692.

Scheme 4. Reactions of 1,2-Dihydro-2-methyl-1,2-benzazaborines



bonds of one ring concomitant with or followed by complexation of the double bonds of the second ring.^{1–5} It seems most reasonable to propose a similar mechanism for the conversion of **25** to **26**, although a mechanism involving intermediate complexation to the nucleophilic nitrogen cannot be excluded.⁹

Crystal Structures. An X-ray structure determination of **17** (in the Supporting Information) unambiguously identifies the compound. Since **17** is isostructural with naphthalene,¹⁶ the benzocyclic and heterocyclic rings are crystallographically identical. Thus, accurate bond distances could not be obtained. It is worth noting that the isomeric 4a,8a-azoniaboratanaphthalene **29**¹⁷ is also isostructural with naphthalene and that a similar isostructural relationship has been found for other boron–nitrogen heterocyclic compounds with their carbocyclic analogues.¹⁸ It has recently been proposed that this close structural similarity is a general and significant feature of boron–nitrogen heterocycles.¹⁹



The molecular structures of the 1,2-dihydro-1,2-benzazaborine-Cr(CO)₃ complexes **18** and **23** are illustrated in Figures 1 and 2, respectively. Selected bond distances of **18**, **11**, and **23** are compared in Table 1. Structure **18** consists of a near-planar

Table 1. Comparison of Selected Bond Distances (Å) for **18**, **11**,^{a,b} and **23**^c

bond	18	11	23
C(1)–N(1)	1.391(2)	1.368(5)	1.376(4)
N(1)–B(1)	1.422(2)	1.430(5)	1.424(3)
B(1)–C(8)	1.526(2)	1.500(5)	1.534(4)
C(8)–C(7)	1.355(2)	1.370(6)	1.358(15)
C(7)–C(6)	1.439(2)	1.413(7)	1.447(6)
C(6)–C(1)	1.407(2)	1.353(6)	1.427(6)
B(1)–C(9)	1.576(2)	1.575(2)	1.583(5)
C(1)–C(2)	1.405(2)		1.420(4)
C(2)–C(3)	1.384(2)		1.399(12)
C(3)–C(4)	1.399(2)		1.412(3)
C(4)–C(5)	1.379(2)		1.411(11)
C(5)–C(6)	1.408(2)		1.428(4)

^a Reference 9. ^b The atom-numbering scheme for **11** corresponds to that of **18** and **23**. ^c Average for two independent molecules.

uncoordinated 1,2-dihydro-1,2-benzazaborine ring which is bound to a *B*-phenyl, bearing an η^6 -bound Cr(CO)₃ unit. Structure **23** consists of a near planar 1,2-dihydro-2-methyl-1,2-benzazaborine ring which is η^6 -bound to a Cr(CO)₃ unit through the benzo-ring. In both cases the Cr(CO)₃ units are bound in typical piano-stool fashion.

Compound **18** is particularly notable, since it contains a noncoordinated 1,2-dihydro-1,2-benzazaborine group. This group is bound to the *B*-pendant Ph–Cr(CO)₃ unit in the same manner as is the parent 1,2-dihydro-1,2-azaborine ring of complex **11**. Comparison of the boron–nitrogen heterocyclic rings of **18** and **11** shows that the bonds which are α – β to the ring fusion (N(1)–B(1) and C(7)–C(8)) are shorter while the other endocyclic bonds (C(1)–N(1), B(1)–C(8), C(7)–C(6), and C(6)–C(1)) are longer than the corresponding bonds of **11**. Similar differentiation of the C–C bond distances is found for naphthalene¹⁵ vs benzene and generally for linearly fused arenes vs monocyclic arenes.¹⁹ It reflects a localization of π -bonding relative to monocyclic aromatics. However, the B–C bond lengths of **18** suggest that the 1,2-dihydro-1,2-benzazaborine ring has strong endocyclic π -bonding. The endocyclic B–C bond (1.526(2) Å) of **18** is significantly shorter than the exocyclic B–C bond (1.576(2) Å).

(16) (a) Cruickshank, D. W. J.; Sparks, R. A. *Proc. R. Soc. London, Ser. A* **1960**, 258, 270. (b) Brock, C. P.; Dunitz, J. D. *Acta Crystallogr., Sect. B* **1982**, 38, 2218.

(17) Fang, X. D.; Yang, H.; Kampf, J. W.; Banaszak Holl, M. M.; Ashe, A. J. *Organometallics* **2006**, 25, 513.

(18) Pan, J.; Kampf, J. W.; Ashe, A. J. *Organometallics* **2004**, 23, 5626.

(19) (a) Zhou, H.-B.; Nettles, K. W.; Bruning, J. B.; Kim, Y.; Joachimiak, A.; Sharma, S.; Carlson, K. E.; Stossi, F.; Katzenellenbogen, B. S.; Greene, G. L.; Katzenellenbogen, J. A. *Chem. Biol.* **2007**, 14, 659. (b) Marwitz, A. J. V.; Abbey, E. R.; Jenkins, J. T.; Zakharov, L. N.; Liu, S.-Y. *Org. Lett.* **2007**, 9, 4905. Badger, G. M. *Aromatic Character and Aromaticity*; Cambridge University Press: Cambridge, U.K., 1969; p 38.

Table 2. Crystal and Data Collection Parameters for 18 and 23

	18	23
empirical formula	C ₁₇ H ₁₂ BCrNO ₃	C ₁₂ H ₁₀ BCrNO ₃
fw	341.09	279.02
temp, K	123(2)	123(2)
wavelength, Å	0.710 73	0.710 73
cryst syst	monoclinic	monoclinic
space group	<i>P</i> 2 ₁ / <i>n</i>	<i>P</i> 2 ₁ / <i>n</i>
<i>a</i> , Å	11.8163(16)	15.212(4)
<i>b</i> , Å	10.9188(14)	10.730(3)
<i>c</i> , Å	12.0946(16)	16.259(4)
β, deg	104.151(2)	112.855(4)
<i>V</i> , Å ³ ; <i>Z</i>	1513.1(3); 4	2445.6(11); 8
calcd density, Mg/m ³	1.497	1.516
abs coeff, mm ⁻¹	0.768	0.932
<i>F</i> (000)	696	1136
cryst size, mm	0.58 × 0.22 × 0.20	0.36 × 0.32 × 0.22
limiting indices	−15 ≤ <i>h</i> ≤ 15 −14 ≤ <i>k</i> ≤ 14 −16 ≤ <i>l</i> ≤ 16	−20 ≤ <i>h</i> ≤ 20 −14 ≤ <i>k</i> ≤ 14 −21 ≤ <i>l</i> ≤ 21
no. of rflns collected/unique	15 374/3762	39 806/26 502
abs cor	semiempirical from equivalents	
refinement method	full-matrix least squares on <i>F</i> ²	
no. of data/restraints/params	3762/0/208	
GOF on <i>F</i> ²	1.050	1.099
final <i>R</i> indices (<i>I</i> > 2σ(<i>I</i>))	<i>R</i> 1 = 0.0304 w <i>R</i> 2 = 0.0865	<i>R</i> 1 = 0.0583 w <i>R</i> 2 = 0.1559
<i>R</i> indices (all data)	<i>R</i> 1 = 0.0351 w <i>R</i> 2 = 0.0900	<i>R</i> 1 = 0.0716 w <i>R</i> 2 = 0.1627
largest diff peak and hole, e/Å ³	0.392 and −0.291	0.697 and −0.720

It is also interesting to compare the structure of the heterocyclic ring of **18** with that of B–O–B ether **30**, which was reported by Paetzold and co-workers.¹¹ The intra-ring distances of **18** and **30** were virtually identical, which indicates that the pendant oxygen makes only a small perturbation to the π -bonding of the ring. Finally, comparison of the structure of **23** with that of **18** shows that the C–C bonds of the benzocyclic ring expand by an average of 0.02 Å on complexation. This is a normal effect which is a consequence of partial removal of the π electrons by the Cr(CO)₃ group. On the other hand, bond distances in the heterocyclic rings of **23** and **18** differ by an average of only 0.01 Å, indicating that the coordination in **23** has little effect on the adjacent ring. It should also be noted that the corresponding bond distances in the more highly substituted **31**¹¹ are not appreciably different from those of **23**.

Experimental Section

General Considerations. Manipulations of air-sensitive compounds were performed under a nitrogen or argon atmosphere using standard Schlenk techniques or in a nitrogen-filled MBraun drybox. THF, ether, pentanes, and hexanes were dried and deoxygenated by distillation from sodium/benzophenone ketyl. THF-*d*₈ was dried over K/Na alloy before use. ¹H, ¹¹B, and ¹³C NMR spectra were recorded on a Varian Inova 400 or 500 NMR spectrometer operating at ambient temperature. The ¹H and ¹³C NMR chemical shifts were determined relative to internal solvent standards and are referenced to tetramethylsilane. The ¹¹B NMR chemical shifts were referenced to external boron trifluoride diethyl etherate. Combustion analyses were determined using a Perkin-Elmer 240 CHN analyzer by the analytical services department of the Department of Chemistry of the University of Michigan, Ann Arbor, MI.

1,2-Dihydro-2-methyl-1,2-benzazaborine (**16**) and 2-chloro-1,2-dihydro-1,2-benzazaborine (**14**) were prepared by the route of Dietz and Dewar.¹⁰ NMR spectra of **14** and **16** were identical with those reported by Paetzold and co-workers.¹¹

1,2-Dihydro-2-phenyl-1,2-benzazaborine (15). Compound **15** was prepared by the reaction of phenylmagnesium bromide with **14** as described by Dewar and Dietz¹⁰ and was isolated as a white

powder. ¹H NMR (400 MHz, THF-*d*₈): δ 7.12 (t, *J* = 8.1 Hz, 1H, (Benzo)H); 7.24 (d, *J* = 11.4 Hz, 1H, C(3)H); 7.38 (m, 4H, (Benzo)H, ArH); 7.52 (d, *J* = 8.1 Hz, 1H, (Benzo)H); 7.61 (d, *J* = 8.1 Hz, 1H, (Benzo)H); 7.96 (d, *J* = 8.1 Hz, 2H, ArH); 8.10 (d, *J* = 11.4 Hz, 1H, C(4)H); 9.62 (br, 1H, NH). ¹³C NMR (100.6 MHz, CD₂Cl₂): δ 118.8, 121.7, 128.8, 129.0, 129.9, 130.2, 133.2, 146.1; signals for C(ipso), C(3), C(4a), and C(8a) not observed. ¹¹B NMR (160.4 MHz, CD₂Cl₂): δ 33.9. HRMS (EI, *m/z*): calcd for C₁₄H₁₂¹¹BN (M⁺), 205.1063; found, 205.1062. Anal. Calcd for C₁₄H₁₂BN: C, 82.00; H, 5.90; N, 6.83. Found: C, 81.61; H, 5.84; N, 6.71.

1,2-Dihydro-1,2-benzazaborine (17). The reaction of **14** with LiAlH₄ gave **17** as a white powder.¹⁰ ¹H NMR (500 MHz, DMSO-*d*₆): δ 5.02 (br, 1H, BH); 6.92 (d, *J* = 11.2 Hz, 1H, C(3)H); 7.19 (t, *J* = 8.0 Hz, 1H, (Benzo)H); 7.46 (t, *J* = 8.0 Hz, 1H, (Benzo)H); 7.54 (d, *J* = 8.0 Hz, 1H, (Benzo)H); 7.70 (d, *J* = 8.0 Hz, 1H, (Benzo)H); 8.11 (d, *J* = 11.2 Hz, 1H, C(4)H); 10.68 (br, 1H, NH). ¹³C NMR (100.6 MHz, DMSO-*d*₆): δ 118.4, 120.9, 125.2, 128.2, 129.2, 129.4 (br), 140.5, 144.7. ¹¹B NMR (160.4 MHz, DMSO-*d*₆): δ 31.5. HRMS (EI, *m/z*): calcd for C₈H₈¹¹BN (M⁺), 129.0750; found, 129.0747.

Tricarbonyl[1,2-dihydro-2-(η^6 -phenyl)-1,2-benzazaborine]chromium (18). 1,2-Dihydro-2-phenyl-1,2-benzazaborine (**15**) (600 mg, 2.93 mmol) and Cr(CH₃CN)₃(CO)₃ (800 mg, 3.09 mmol) were dissolved in 25 mL of THF. The resulting solution was heated to 140 °C with stirring for 60 h in a Teflon screw-stoppered thick-walled glass reaction tube. After the solvent was removed in vacuo, the residue was washed with hexanes (3 × 30 mL) at 0 °C. The residue was purified by column chromatography on silica gel (25% ethyl acetate in hexanes elution) to give a pure sample of the product (494 mg, 49%) as a yellow powder. IR (benzene film): 1968, 1895 cm⁻¹. ¹H NMR (500 MHz, THF-*d*₈): δ 5.50 (t, *J* = 6.3 Hz, 2H, ArH); 5.70 (t, *J* = 6.3 Hz, 1H, ArH); 6.10 (d, *J* = 6.3 Hz, 2H, ArH); 7.05 (d, *J* = 11.5 Hz, 1H, C(3)H); 7.15 (t, *J* = 8.1 Hz, 1H, (Benzo)H); 7.40 (t, *J* = 8.1 Hz, 1H, (Benzo)H); 7.46 (d, *J* = 8.1 Hz, 1H, (Benzo)H); 7.63 (d, *J* = 8.1 Hz, 1H, (Benzo)H); 8.11 (d, *J* = 11.5 Hz, 1H, C(4)H); 9.60 (br, 1H, NH). ¹³C NMR (100.6 MHz, THF-*d*₈): δ 93.5, 96.1, 99.8, 119.4, 122.1, 127.0 (br), 129.4, 130.3, 146.9; signals for C(ipso), C(4a), C(8a), and CO not observed. ¹¹B NMR (160.4 MHz, THF-*d*₈): δ 32.9. HRMS (EI, *m/z*): calcd for C₁₇H₁₂¹¹BNO₃⁵²Cr (M⁺), 341.0315; found, 341.0327. Anal. Calcd for C₁₇H₁₂BNO₃Cr: C, 59.86; H, 3.55; N, 4.11. Found: C, 60.23; H, 3.49; N, 4.14.

When the starting materials were stirred at 25 °C for 18 h, the ¹H spectrum indicated a mixture of **15**, **18**, and another product tentatively identified as **19**. ¹H NMR for **19** (500 MHz, THF-*d*₈): δ 5.06 (t, *J* = 7 Hz); 5.72 (t, *J* = 7 Hz); 5.88 (d, *J* = 7 Hz); 6.19 (d, *J* = 7 Hz) for the coordinated benzocyclic ring protons. Other peaks were obscured by peaks from **15** and **18**. Heating the mixture to 140 °C converted it to **18**.

Tricarbonyl[1,2-dihydro-1-lithio-2-(η^6 -phenyl)-1,2-benzazaborine]chromium (21). A mixture of LiTMP (6 mg, 0.041 mmol) and **18** (13 mg, 0.038 mmol) was dissolved in 0.75 mL of THF-*d*₈. The ¹H NMR spectrum showed that **21** was formed quantitatively. Quenching the mixture with 10 μL of D₂O resulted in the formation of **18-d**, which was confirmed by ¹H spectroscopy (absence of the NH signal) and HRMS (HRMS (EI, *m/z*): calcd for C₁₇H₁₁²H¹¹BNO₃⁵²Cr (M⁺), 342.0378; found, 342.0376). Heating a sample of **21** in THF-*d*₈ resulted in slow decomposition to unidentified products. Data for **21** are as follows. ¹H NMR (500 MHz, THF-*d*₈): δ 5.38 (t, *J* = 6.3 Hz, 2H, ArH); 5.44 (t, *J* = 6.3 Hz, 1H, ArH); 6.05 (d, *J* = 6.3 Hz, 2H, ArH); 6.76 (t, *J* = 8.0 Hz, 1H, (Benzo)H); 6.88 (d, *J* = 11.1 Hz, 1H, C(3)H); 7.10 (t, *J* = 8.0 Hz, 1H, (Benzo)H); 7.31 (d, *J* = 8.0 Hz, 1H, (Benzo)H); 7.40 (d, *J* = 8.0 Hz, 1H, (Benzo)H); 7.86 (d, *J* = 11.1 Hz, 1H, C(4)H). ¹³C NMR (100.6 MHz, THF-*d*₈): δ 93.9, 94.8, 100.8, 117.0, 125.9,

126.4, 128.0 (br), 130.0, 142.9; signals for C(ipso), C(4a), and C(8a) not observed. ^{11}B NMR (160.4 MHz, THF- d_8): δ 34.8.

Tricarbonyl[(4a,5,6,7,8,8a- η)-1,2-dihydro-2-methyl-1,2-benzazaborine]chromium (23). 1,2-Dihydro-2-methyl-1,2-benzazaborine (**16**; 1.70 g, 11.89 mmol) and $\text{Cr}(\text{CH}_3\text{CN})_3(\text{CO})_3$ (5.80 g, 22.4 mmol) were dissolved in 80 mL of THF. The resulting solution was heated to 60 °C with stirring for 14 h. After the solvent was removed in vacuo, a ^1H NMR spectrum of the residue indicated that it was a mixture of **16** and **23** in a 1:3 ratio. Heating the reaction mixture to higher temperature resulted in the destruction of **23**, but **16** survived. The residue was extracted with ethyl ether (4×20 mL). Ethyl ether was removed in vacuo, and the residue was washed with pentane (3×15 mL). The residue was purified by column chromatography on silica gel (30% CH_2Cl_2 in hexanes elution) to give a pure sample of the product (1.30 g, 39%) as an orange powder. IR (hexanes film): 1975, 1908 cm^{-1} . ^1H NMR (500 MHz, benzene- d_6): δ 0.45 (s, 3H, CH_3); 4.09 (t, $J = 6.3$ Hz, 1H, (Benzo)H); 4.35 (d, $J = 6.3$ Hz, 1H, (Benzo)H); 4.76 (t, $J = 6.3$ Hz, 1H, (Benzo)H); 5.14 (d, $J = 6.3$ Hz, 1H, (Benzo)H); 5.86 (br, 1H, NH); 6.37 (d, $J = 11.5$ Hz, 1H, C(3)H); 6.96 (d, $J = 11.5$ Hz, 1H, C(4)H). ^{13}C NMR (125.7 MHz, benzene- d_6): δ 80.5, 85.9, 94.5, 95.6, 131.6 (br), 144.9; signals for C(ipso), C(4a), C(8a), Me, and CO not observed. ^{11}B NMR (160.4 MHz, benzene- d_6): δ 39.9. HRMS (EI, m/z): calcd for $\text{C}_{12}\text{H}_{10}^{11}\text{BNO}_3^{52}\text{Cr}$ (M^+), 279.0159; found, 279.0152. Anal. Calcd for $\text{C}_{12}\text{H}_{10}\text{BNO}_3\text{Cr}$: C, 51.66; H, 3.61; N, 5.02. Found: C, 51.84; H, 3.73; N, 4.96.

Conversion of 23 to 25. A mixture of KHMDS (8 mg, 0.040 mmol) and **23** (10 mg, 0.036 mmol) was dissolved in 0.75 mL of THF- d_8 . The resulting NMR showed that **25** was formed quantitatively. Quenching the mixture with 10 μL of D_2O resulted in the formation of **23-d**, which was confirmed by HRMS (HRMS (EI, m/z): calcd for $\text{C}_{12}\text{H}_9^2\text{H}^{11}\text{BNO}_3^{52}\text{Cr}$ (M^+), 280.0222; found, 280.0229). Data for **25** are as follows. ^1H NMR (500 MHz, THF- d_8): δ 0.54 (s, 3H, CH_3); 4.92 (t, $J = 6.3$ Hz, 1H, (Benzo)H); 5.51 (t, $J = 6.3$ Hz, 1H, (Benzo)H); 5.59 (d, $J = 6.3$ Hz, 1H, (Benzo)H); 6.05 (d, $J = 6.3$ Hz, 1H, (Benzo)H); 6.48 (d, $J = 11.1$ Hz, 1H, C(3)H); 7.34 (d, $J = 11.1$ Hz, 1H, C(4)H). ^{13}C NMR (100.6 MHz, THF- d_8): δ 84.0, 92.1, 97.4, 100.7, 133.8(br), 142.7; signals for C(ipso), C(4a), C(8a), CO, and Me not observed. ^{11}B NMR (160.4 MHz, THF- d_8): δ 40.8.

Conversion of 25 to 26. A solution of **25** was prepared from **23** (12 mg, 0.043 mmol) and KHMDS (10 mg, 0.05 mmol) in 0.75 mL of THF- d_8 . After the resulting solution was heated to 90 °C

for 4 h, the ^1H NMR spectrum indicated the formation of **26** along with 25% of unidentified products. After the reaction mixture was cooled to room temperature, it was quenched with excess MeI to give **28** and other unidentified materials. The ^1H NMR and mass spectra showed that **28** was identical with previously obtained material.¹⁰ Data for **26** are as follows. ^1H NMR (500 MHz, THF- d_8): δ 0.56 (s, 3H, CH_3); 4.36 (d, $J = 9.5$ Hz, 1H, C(3)H); 6.30 (d, $J = 9.5$ Hz, 1H, C(4)H); 6.95 (t, $J = 7.8$ Hz, 1H, (Benzo)H); 7.13 (d, $J = 7.8$ Hz, 1H, (Benzo)H); 7.22 (t, $J = 7.8$ Hz, 1H, (Benzo)H); 7.47 (d, $J = 7.8$ Hz, 1H, (Benzo)H). ^{13}C NMR (125.7 MHz, THF- d_8): δ 95.0 (br), 110.3, 129.0, 129.9, 133.1, 133.9; signals for C(ipso), C(3), C(4a), C(8a), CO, and C(Me) not observed. ^{11}B NMR (160.4 MHz, THF- d_8): δ 24.0.

Kinetics of the Haptotropic Migration of 25. The reaction was carried out on solutions of **25** prepared as described above and sealed in NMR tubes. The reaction was monitored by ^1H NMR spectroscopy. The integrals of various proton multiplets of **25** were normalized against that of the signal of cyclohexane used as an internal standard. Use of the first-order rate equation gave satisfactory plots ($R^2 = 0.998$) for up to 2 half-lives. The rate constant was found to be $2.80 \times 10^{-5} \text{ s}^{-1}$ at 333 K. No crossover products were found when the reaction was performed in the presence of hexamethylbenzene.

Single-Crystal X-ray Crystallography. Crystals of **17**, **18**, and **23** suitable for X-ray diffraction were obtained by recrystallization at room temperature from pentane/ CH_2Cl_2 , benzene/ethyl acetate, and ethyl acetate, respectively. All crystallographic data for **17** are available in the Supporting Information. Crystallographic and data collection parameters for **18** and **23** are collected in Table 2. ORTEP drawings of **18** and **23** showing the atom-numbering schemes are given in Figures 1 and 2, respectively. Selected bond distances are collected in Table 1. Additional crystallographic data are available in the Supporting Information.

Acknowledgment. Partial support of this research has been provided by the NSF.

Supporting Information Available: CIF files giving X-ray characterization data for **17**, **18**, and **23** and figures giving ^1H NMR spectra. This material is available free of charge via the Internet at <http://pubs.acs.org>.

OM800383V

Reversible Neutral Dissociation of the N–Si Dative Bond in Hexacoordinate Hydrido Complexes of Silicon

Inna Kalikhman,^{*,‡} Evgenia Kertsnus-Banchik,[‡] Boris Gostevskii,[‡] Nikolaus Kocher,[†] Dietmar Stalke,[†] and Daniel Kost^{*,‡}

Department of Chemistry, Ben Gurion University of the Negev, Beer-Sheva 84105, Israel, and Institut für Anorganische Chemie, Universität Göttingen, Göttingen, Germany

Received September 2, 2008

Hexacoordinate silicon dichelates with hydrido and methyl monodentate ligands were prepared by transsilylation. The temperature-dependent ²⁹Si NMR spectra of toluene-*d*₈ or CDCl₃ solutions provide evidence for a reversible, neutral dissociation of the dative N–Si bond, accompanied by a shift of the ²⁹Si resonance from high field (hexacoordinate) to lower field (pentacoordinate) with increasing temperature. When a phenyl group is attached directly to silicon (replacing methyl), the N–Si dissociation is prevented, presumably due to electron withdrawal by the phenyl. Two of the silicon complexes were characterized by crystallographic analysis. Quantum chemical calculations at the RB3LYP/6-31G(d) level confirm the stability of an N–Si dissociated species (1.03 kcal mol⁻¹ lower in energy than the hexacoordinate dichelate) and rule out the alternative possibility of an O–Si zwitterionic dissociation, thus supporting the mechanism suggested by the experimental results.

Introduction

Neutral hexacoordinate silicon dichelates¹ based on hydrazide-derived bidentate ligands² (**1**) show significant structural and chemical flexibility,^{2b} manifest in a variety of properties.^{1–3} It has been shown that such dichelates bearing a halo ligand (Y = Cl, Br, I) generally can interconvert between hexa- and pentacoordination through equilibrium ionic dissociation, driven by hydrogen-bond donor solvents capable of solvating the halide anion (eq 1).⁴ Changes in the coordination number of silicon complexes have also been reported resulting from various intramolecular rearrangements and other reactions: photochemical conversion of tetra- to pentacoordinate compounds,^{5,6} as well

as chemical increase of the silicon coordination number from five to six by reaction with KF;⁷ migration of a silicon ligand from silicon to an adjacent C=N double bond;⁸ as well as carbon-ligand migration^{9–11} and a case of intramolecular hydrosilylation by migration of a hydrido ligand from silicon to an adjacent imino carbon.¹² Recently we have reported a case of a hexacoordinate silicon dichelate (**3**) in which neutral dissociation of the N–Si dative bond took place,¹³ rather than the ionic dissociation reported previously.⁴ In this unique case (eq 2) neutral dissociation was forced by two factors: the presence of a bulky cyclohexyl ligand bound to silicon and the effect of the electron-withdrawing CF₃ ring substituent. Bulky monodentate ligands have previously been shown to enhance ionic dissociation, whereas powerful electron-withdrawing chelate-ring substituents have the opposite effect: prevention of ionic dissociation.⁴ The combination of the two factors resulted in nonionic dissociation of the N–Si bond, satisfying both the steric repulsion, by getting the bulky dimethylamino ligand out of the way, and the electron demand by the ring substituent, avoiding accumulation of positive charge at the silicon atom.¹³

* Corresponding authors. E-mail: kostd@bgu.ac.il.

[‡] Ben Gurion University of the Negev.

[†] Universität Göttingen.

(1) For recent reviews on hypercoordinate silicon compounds see: (a) Bassindale, A. R.; Glin, S. J.; Taylor, P. G. In *The Chemistry of Organic Silicon Compounds*, vol. 2; Rappoport, Z.; Apeloig, Y., Eds.; Wiley: Chichester, U.K., 1998; pp 495–511. (b) Kost, D.; Kalikhman, I. In *The Chemistry of Organic Silicon Compounds*, vol. 2; Rappoport, Z.; Apeloig, Y., Eds.; Wiley: Chichester, U.K., 1998; pp 1339–1445. (c) Chuit, C.; Corriu, R. J. P.; Reyé, C. In *The Chemistry of Hypervalent Compounds*; Akiba, K.-y., Ed.; Wiley-VCH: Weinheim, Germany, 1999; pp 81–146. (d) Kira, M.; Zhang, L. C. In *The Chemistry of Hypervalent Compounds*; Akiba, K.-y., Ed.; Wiley-VCH: Weinheim, Germany, 1999; pp 147–169. (e) Tacke, R.; Pülm, M.; Wagner, B. *Adv. Organomet. Chem.* **1999**, *44*, 221–273. (f) Brook, M. A. *Silicon in Organic, Organometallic, and Polymer Chemistry*; Wiley: New York, 2000; pp 97–114. (g) Tacke, R.; Seiler, O. In *Silicon Chemistry, From the Atom to Extended Systems*; Jutzi, P.; Schubert, U., Eds.; Wiley-VCH: Weinheim, Germany, 2003; pp 324–337.

(2) (a) Kost, D.; Kalikhman, I. *Adv. Organomet. Chem.* **2004**, *50*, 1–106. (b) Kost, D.; Kalikhman, I. *Acc. Chem. Res.* **2008**, in press.

(3) For latest publications on hypercoordinate silicon see: (a) Metz, S.; Burschka, C.; Tacke, R. *Eur. J. Inorg. Chem.* **2008**, *28*, 4433–4439. (b) Haga, R.; Burschka, C.; Tacke, R. *Organometallics* **2008**, *27*, 4395–4400. (c) Yamamura, M.; Kano, N.; Kawashima, T.; Matsumoto, T.; Harada, J.; Ogawa, K. *J. Org. Chem.* **2008**, *73*, 8244–8249. (d) Lippe, K.; Gerlach, D.; Kroke, E.; Wagler, J. *Inorg. Chem. Commun.* **2008**, *11*, 492–496.

(4) Kost, D.; Kingston, V.; Gostevskii, B.; Ellern, A.; Stalke, D.; Walfort, B.; Kalikhman, I. *Organometallics* **2002**, *21*, 2293–2305.

(5) Kano, N.; Komatsu, F.; Yamamura, M.; Kawashima, T. *J. Am. Chem. Soc.* **2006**, *128*, 7097–7109.

(6) Yamamura, M.; Kano, N.; Kawashima, T. *Tetrahedron Lett.* **2007**, *48*, 4033–4036.

(7) Kano, N.; Yamamura, M.; Kawashima, T. *J. Am. Chem. Soc.* **2004**, *126*, 6250–6251.

(8) Wagler, J.; Böhme, U.; Roewer, G. *Organometallics* **2004**, *23*, 6066–6069.

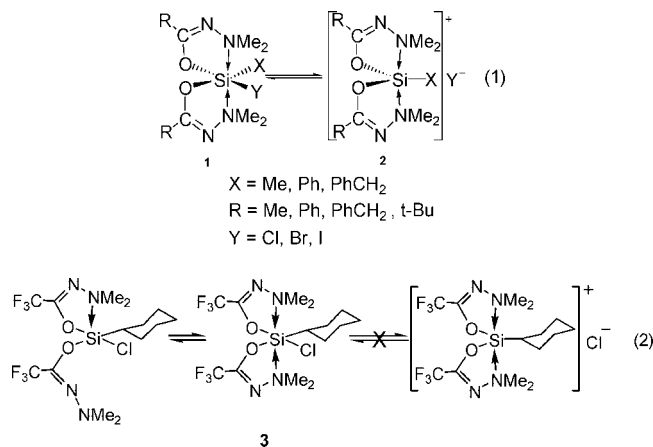
(9) Wagler, J.; Doert, T.; Roewer, G. *Angew. Chem., Int. Ed.* **2004**, *43*, 2441–2444.

(10) Yamamura, M.; Kano, N.; Kawashima, T. *J. Organomet. Chem.* **2007**, *692*, 313–325.

(11) Kalikhman, I.; Gostevskii, B.; Kertsnus, E.; Botoshansky, M.; Tessier, C. A.; Youngs, W. J.; Deuerlein, S.; Stalke, D.; Kost, D. *Organometallics* **2007**, *26*, 2652–2658.

(12) Kertsnus-Banchik, E.; Kalikhman, I.; Gostevskii, B.; Deutsch, Z.; Botoshansky, M.; Kost, D. *Organometallics* **2008**, *27*, 5286–5294.

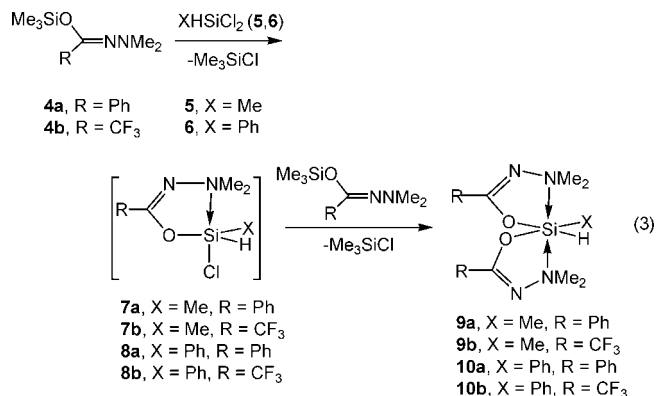
(13) (a) Gostevskii, B.; Silbert, G.; Adear, K.; Sivaramakrishna, A.; Stalke, D.; Deuerlein, S.; Kocher, N.; Voronkov, M. G.; Kalikhman, I.; Kost, D. *Organometallics* **2005**, *24*, 2913–2920. (b) Gostevskii, B.; Adear, K.; Sivaramakrishna, A.; Silbert, G.; Stalke, D.; Kocher, N.; Kalikhman, I.; Kost, D. *Chem. Commun.* **2004**, 1644–1645.



It was of interest to investigate whether N–Si dissociation was a special case, driven by the unique steric and electronic factors described above, or whether it was general enough for additional cases to be discovered. The present report describes the preparation of four new hexacoordinate hydrosilicon complexes, their characterization by elemental analysis, NMR spectroscopy, and X-ray crystallography (for two of them), and the study of their reversible N–Si dissociation by means of NMR spectroscopy.

Results and Discussion

Compounds **9** and **10** were prepared from the *O*-trimethylsilyl hydrazide derivatives (**4**) and methyl- or phenyldichlorosilane (**5** and **6**, respectively) by transsilylation, as shown in eq 3. The compounds were characterized by elemental analysis and by their ²⁹Si, ¹H, and ¹³C NMR spectra. The relatively high field ²⁹Si chemical shifts clearly place all four compounds in the hexacoordinate silicon category at or below room temperature. In addition, the presence of the hydrido ligand is immediately evident through the large one-bond ²⁹Si–¹H coupling constant observed in the ²⁹Si NMR spectrum. For two of the compounds (**10a,b**) the structure was further verified by single-crystal X-ray diffraction analysis, leading to the molecular geometries depicted, respectively, in Figures 1 and 2. Selected bond lengths and angles are listed in Table 1, and crystallographic details are given in Table 2.



The monochelate intermediates **7a,b** and **8b** reacted further rapidly and were not isolated. **7a** and **7b** were identified by their ²⁹Si NMR spectra: **7a**, ²⁹Si (CDCl₃, 300 K) δ –51.1 (d, ¹J_{Si–H} = 309 Hz); **7b**, ²⁹Si (CDCl₃, 300 K) δ –37.2 (d, ¹J_{Si–H} = 320 Hz). **8a** was isolated, fully characterized, and reported previ-

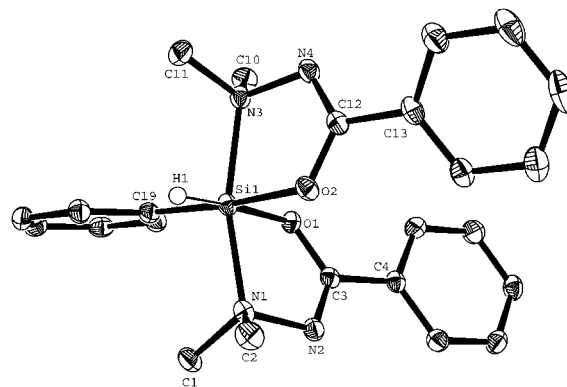


Figure 1. Molecular structure of **10a** in the crystal, at the 50% probability level. Hydrogen atoms are omitted, except the hydrido ligand.

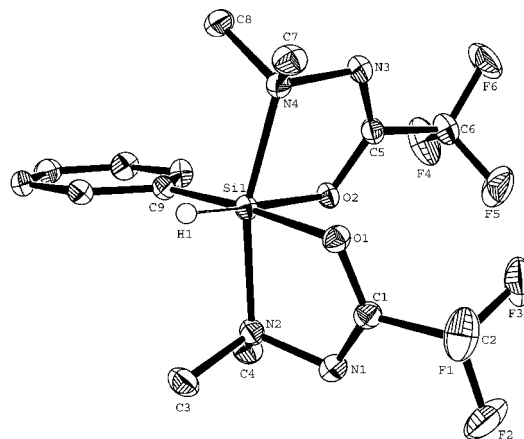


Figure 2. Molecular structure of **10b** in the crystal, at the 50% probability level. Hydrogen atoms are omitted, except the hydrido ligand.

Table 1. Selected Crystallographic Bond Lengths and Angles for **10a** and **10b**^a

10a		10b	
Bond Lengths, Å			
Si–O(1)	1.7965(9)	Si–O(1)	1.8590(9)
Si–O(2)	1.8212(9)	Si–O(2)	1.8214(9)
Si–C(19)	1.9212(13)	Si–C(9)	1.9082(13)
Si–N(1)	2.0141(12)	Si–N(4)	2.0233(12)
Si–N(3)	2.0319(12)	Si–N(2)	2.0255(12)
Si–H(1)	1.507(16)	Si–H(1)	1.441(16)
N(1)–N(2)	1.4634(14)	N(1)–N(2)	1.4684(15)
N(2)–C(3)	1.2855(17)	N(1)–C(1)	1.2757(18)
O(1)–C(3)	1.3153(15)	O(1)–C(1)	1.2948(16)
Angles, deg			
O(1)–Si–O(2)	85.70(4)	O(1)–Si–O(2)	84.50(4)
O(1)–Si–C(19)	94.13(5)	O(2)–Si–C(9)	93.19(5)
O(2)–Si–C(19)	175.40(5)	O(1)–Si–C(9)	174.41(5)
N(1)–Si–N(3)	164.44(5)	N(4)–Si–N(2)	162.68(5)
O(1)–Si–H(1)	170.9(6)	O(2)–Si–H(1)	170.3(6)
C(19)–Si–H(1)	93.2(6)	C(9)–Si–H(1)	95.5(6)
N(3)–Si–H(1)	95.3(6)	N(2)–Si–H(1)	96.5(6)

^a Note that atoms are not equally labeled in **10a** and **10b**: O(1) is *trans* to the hydrido ligand in **10a**, but *cis* in **10b**.

ously, including a single-crystal X-ray analysis.¹⁴ **8a** was used for a study of spin–spin interactions across the N–Si dative bond, as well as a first determination of the Si–N dative-bond

(14) Kalikhman, I.; Gostevskii, B.; Kingston, V.; Krivonos, S.; Stalke, D.; Walford, B.; Kottke, T.; Kocher, N.; Kost, D. *Organometallics* **2004**, *23*, 4828–4835.

Table 2. Experimental Crystallographic Data for 10a and 10b

	10a	10b
CCDC number	700715	700716
empirical formula	C ₂₄ H ₂₈ N ₄ O ₂ Si	C ₁₄ H ₁₈ F ₆ N ₄ O ₂ Si
form mass, g mol ⁻¹	432.59	416.41
collection T, K	100(2)	100(2)
cryst syst	monoclinic	monoclinic
space group	P2(1)/n	P2(1)/n
a, Å	8.9891(7)	14.9337 (9)
b, Å	17.0629(14)	7.8090 (5)
c, Å	14.9778(12)	17.1515 (10)
α, deg	90	90
β, deg	103.867(1)	115.0130(10)
γ, deg	90	90
V, Å ³	2230.30(30)	1812.57(19)
Z	4	4
ρ _{calc} , Mg/m ³	1.288	1.526
F(000)	920	856
θ range, deg	1.84–26.40	1.52–26.38
no. of coll rflns	23 298	19 375
no. of indep rflns	4561	3700
R _{int}	0.028	0.0186
no. of rflns used	4561	3700
no. params	288	252
goodness-of-fit	1.050	1.044
R1, wR2 [I > 2σ(I)]	0.0356, 0.0950	0.0326, 0.0851
R1, wR2 (all data)	0.0399, 0.0988	0.0348, 0.0869
max./min. res electron dens, e Å ⁻³	0.443/–0.275	0.383/–0.265

dissociation barrier (14.6 kcal/mol⁻¹ at 310 K).¹⁴ **8b** reacted further too fast to be identified by NMR.

²⁹Si NMR spectra were measured for **9** and **10** in toluene-*d*₈ and CDCl₃ solutions, respectively, over a significant temperature range. **9a** and **9b** showed rather dramatic temperature dependencies of their ²⁹Si NMR chemical shifts, plotted in Figures 3 and 4, respectively. Over a range of ca. 170 °C, the ²⁹Si chemical shifts of **9a** and **9b** changed by close to 40 ppm. Interestingly, the one-bond ¹J_{H–Si} coupling constants follow almost exactly the temperature dependence patterns of the corresponding chemical shifts. This is evidence that both of the observations represent the same chemical phenomenon. The fact that in both **9a** and **9b** the ²⁹Si resonances shift toward lower field as the sample temperature is increased, i.e., dissociation of hexa- to pentacoordinate silicon species takes place with increasing temperature, contrasts with ionic dissociation, in which the trend is reversed: ionic dissociation is enhanced as the temperature is decreased.⁴ This is, of course, in line with the absence of an easily ionizable halo ligand and in agreement with neutral dissociation of the N–Si dative bond (eq 4), as observed previously in the case shown in eq 2.¹³ It is thus demonstrated

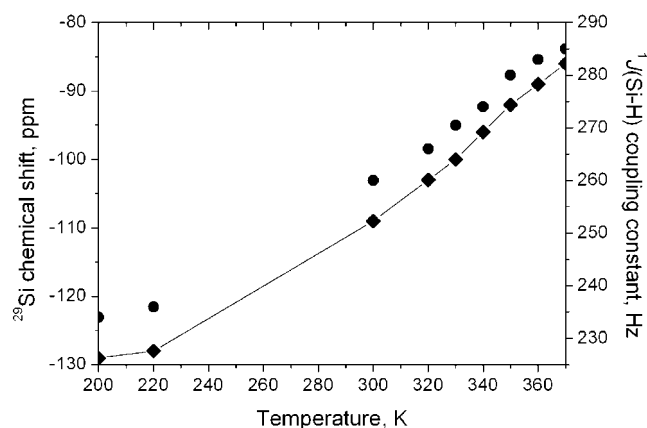


Figure 3. Plot of the ²⁹Si chemical shift (◆) and one-bond ¹H–²⁹Si coupling constant (●) for **9a** in toluene-*d*₈ solution as functions of temperature.

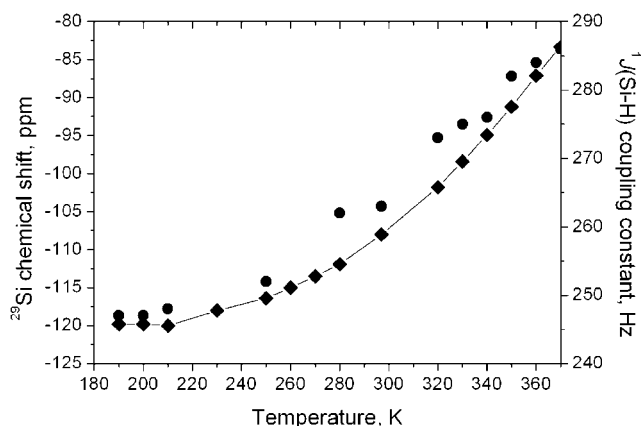
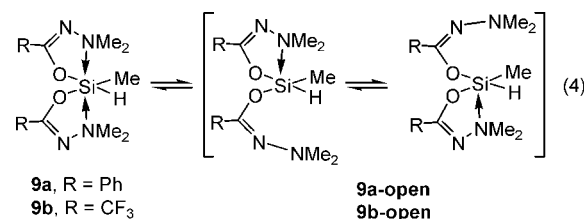


Figure 4. Plot of the ²⁹Si chemical shift (◆) and one-bond ¹H–²⁹Si coupling constant (●) for **9b** in toluene-*d*₈ solution as functions of temperature.

that N–Si dissociation can be general, as long as the monodentate ligands are not strongly electron-withdrawing (i.e., no halogeno ligand).



Surprisingly, replacement of the methyl ligand (**9**) by a phenyl group (**10**) was sufficient to completely suppress N–Si dissociation under similar conditions: the ²⁹Si chemical shifts of **10a** (–121.6) and **10b** (–116.5 ppm) are essentially independent of temperature, within NMR measurement limits. It follows that the stronger electron-withdrawing property of the phenyl ligand relative to methyl is sufficient to make the silicon electron deficient and, hence, more susceptible to hexacoordination and less likely to lose one of the N–Si dative bonds by dissociation.

One may wonder why in **9a** and **9b** neutral N–Si dissociation is observed, while in numerous previously studied dichelates ionic dissociation prevails. Obviously, ionic dissociation is excluded in the present compounds, in the absence of a halogeno ligand. But this alone may not cause and does not explain the observed N–Si dissociation. In order for N–Si dissociation to take place, the dative bonds have to be relatively weak; this is caused by two factors: strong electron withdrawal by the ring substituent R and weak electron withdrawal by the monodentate ligands.¹³ Electron withdrawal by the substituent R reduces electron density at the nitrogen donor atom (through double-bond conjugation) and makes it a weaker donor, more likely to allow N–Si dissociation. On the other hand, electron withdrawal by the monodentate ligands attached to silicon reduce electron density at the silicon atom and make it more susceptible to coordination and, hence, less likely to allow dative-bond dissociation.⁴

Thus, initially the compounds under investigation (**9**, **10**) had a reasonable chance to show N–Si dissociation, since the chloro ligand, present in most of the previously studied dichelate complexes, has been replaced by the less electron withdrawing hydrido ligand. On the chelate ring side, the powerful electron-withdrawing group (EWG) CF₃ in **9b** causes sufficient reduction in donor strength and hence in N–Si bond strength to facilitate neutral dissociation, as was also observed previously in **3** (eq

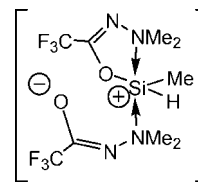
2).¹³ However, the present results show that even the weaker EWG, R = phenyl, is sufficient to allow N–Si dissociation, as observed in **9a**. On the other hand, *neither* R = Ph nor R = CF₃ was strong enough as EWG in **10a** and **10b**, respectively, because the methyl ligand in **9** has now been replaced by a phenyl ligand (**10**), which, evidently, causes the silicon to be electrophilic enough to hold on to the nitrogen donor and prevent N–Si dissociation.

Despite the fact that the temperature-dependent NMR spectra for **10a** and **10b** showed no N–Si dissociation (essentially invariant ²⁹Si NMR chemical shift), they did show conformational dynamics, observable on the NMR time scale. The diastereotopic N-methyl groups appeared as four distinct singlets at 265 K and below, in the ¹H NMR spectra (500 MHz, in CDCl₃ solution), and upon warming, the signals broadened until near room temperature coalescence was observed of all four signals to one. This type of conformational exchange was reported previously for similar hexacoordinate complexes.^{15,16} The N-methyl signals coalesced *pairwise* in two consecutive rate processes, which were attributed to intramolecular exchange of adjacent ligands through a bicapped tetrahedral intermediate or transition state.¹⁶ In the present case both processes took place simultaneously, such that only one combined coalescence of all four signals was observed.

The N-methyl exchange observed in the NMR spectra of **10a** and **10b** occurs between 270 and 320 K. In contrast, the N-methyl signals for **9a** and **9b** appear as one sharp singlet in both the ¹H and ¹³C NMR spectra, down to temperatures as low as 240 K, with line broadening and splitting to four singlets only near 220 K. This suggests that in **9a** and **9b** the N-methyl groups are diastereotopic only in the hexacoordinate form and become equivalent as soon as a significant concentration of the pentacoordinate species is present, presumably by a rapid “flip-flop” type exchange as shown in eq 4 or by a rapid Berry pseudorotation type exchange characteristic of pentacoordinate silicon compounds.¹⁷

Computational Support. Ideally one would seek mechanistic evidence by isolation and characterization of one of the pentacoordinate species **9a**- and **9b-open** (eq 4). However, in the absence of crystallographic evidence, computational support was sought.^{13,18} Three isomeric molecular structures were subjected to quantum chemical calculations: **9b**, **9b-open**, and **11**, the hypothetical O–Si-dissociated analogue of **9b-open**. Full geometry optimizations, as well as harmonic frequencies and zero-point vibrational energies, were calculated using restricted density functional theory (DFT) at the B3LYP level^{19a,b} and employing the polarized 6-31G(d)^{19c,d} basis set using the GAUSSIAN-03w software system.²⁰

The rationale for choosing **11** as a possible intermediate comes from the well-established ionic dissociation of similar



11

chloro complexes:⁴ in the absence of a halogen ligand, it is not unlikely to expect O–Si ionic dissociation, in analogy to Cl–Si ionic dissociation. However, the O–Si-dissociated zwitterionic **11** did not converge to a minimum point on the potential energy hypersurface and, hence, is not a stable species in the gas phase. Upon geometry optimization, starting with one of the chelate rings wide open (N–Si distance 3.5 Å), while bond-angle strain is relieved by relaxing the corresponding dihedral angles, the molecular geometry collapsed to that of **9b**. On the other hand, the N–Si-bond-dissociated **9b-open** converged to a minimum, evidence of its intrinsic stability. The total energies of **9b** and **9b-open**, corrected for zero-point vibrational energies, differ by only 1.03 kcal mol⁻¹, in favor of the ring-opened **9b-open**. This indicates that the open and closed chelate compounds can reasonably be in equilibrium in solution and very likely are the two experimentally observed species.

The fact that **11** is not a minimum point seems to rule it out as a reasonable component in the equilibrium mixture. However, it should be noted that polar species are substantially stabilized in polar solvent solutions, and hence the calculation, in the absence of solvent, is only an indication of its instability and not absolute evidence. In view of the proven stability of **9b-open** relative to **9b**, it remains most likely that the observed NMR spectral phenomena result from the neutral N–Si dissociation of **9b** to **9b-open**, and by analogy also **9a** to **9a-open**.

Experimental Section

The reactions were carried out under dry argon using Schlenk techniques. Solvents were dried and purified by standard methods. NMR spectra were recorded on a Bruker Avance DMX-500 spectrometer operating at 500.13, 125.76, and 99.36 MHz, respectively, for ¹H, ¹³C, and ²⁹Si spectra. Spectra are reported in δ (ppm) relative to TMS, as determined from standard residual solvent proton (or carbon) signals for ¹H and ¹³C and directly from TMS for ²⁹Si. Melting points were measured in sealed capillaries using a Büchi melting point instrument and are uncorrected. Elemental analyses were performed by Mikroanalytisches Laboratorium Beller, Göttingen, Germany. Single-crystal X-ray diffraction patterns were measured on a Bruker Smart Apex CCD diffractometer at low temperature using oil-coated shock-cooled crystals²¹ using Mo Kα radiation at 0.71073 Å. The structures were solved by direct

(15) Kost, D.; Kalikhman, I.; Raban, M. *J. Am. Chem. Soc.* **1995**, *117*, 11512–11522.

(16) Kost, D.; Kalikhman, I.; Krivonos, S.; Stalke, D.; Kottke, T. *J. Am. Chem. Soc.* **1998**, *120*, 4209–4214.

(17) (a) Berry, R. S. *J. Chem. Phys.* **1960**, *32*, 933. (b) Holmes, R. R.; Deiters, J. A. *J. Am. Chem. Soc.* **1977**, *99*, 3318–3326.

(18) Previous calculations on N–Si-coordinated complexes: (a) Nakash, M.; Goldvaser, M. *J. Am. Chem. Soc.* **2004**, *126*, 3436. (b) Kocher, N.; Henn, J.; Gostevskii, B.; Kost, D.; Kalikhman, I.; Engels, B.; Stalke, D. *J. Am. Chem. Soc.* **2004**, *126*, 5563. (c) Timoshkin, A. Yu.; Sevast'yanova, T. N.; Davidova, E. I.; Suvorov, A. V.; Schaefer, H. F., III *Russ. J. Gen. Chem.* **2002**, *72*, 1911.

(19) (a) Becke, A. D. *J. Chem. Phys.* **1993**, *98*, 5648. (b) Stevens, P. J.; Devlin, F. J.; Chablowski, C. F.; Frisch, M. J. *J. Phys. Chem.* **1994**, *98*, 11623. (c) Hariharan, P. C.; Pople, J. A. *Theor. Chim. Acta* **1973**, *28*, 213. (d) Francl, M. M.; Petro, W. J.; Hehre, W. J.; Binkley, J. S.; Gordon, M. S.; DeFrees, D. J.; Pople, J. A. *J. Chem. Phys.* **1982**, *77*, 3654.

(20) Frisch, J.; Trucks, G. W.; Schlegel, H. B.; Scuseria, G. E.; Robb, M. A.; Cheeseman, J. R.; Zakrzewski, V. G.; Montgomery, J. A., Jr.; Stratmann, R. E.; Burant, J. C.; Dapprich, S.; Millam, J. M.; Daniels, A. D.; Kudin, K. N.; Strain, M. C.; Farkas, O.; Tomasi, J.; Barone, V.; Cossi, M.; Cammi, R.; Mennucci, B.; Pomelli, C.; Adamo, C.; Clifford, S.; Ochterski, J.; Petersson, G. A.; Ayala, P. Y.; Cui, Q.; Morokuma, K.; Malick, D. K.; Rabuck, A. D.; Raghavachari, K.; Foresman, J. B.; Cioslowski, J.; Ortiz, J. V.; Stefanov, B. B.; Liu, G.; Liashenko, A.; Piskorz, P.; Komaromi, I.; Gomperts, R.; Martin, R. L.; Fox, D. J.; Keith, T.; Al-Laham, M. A.; Peng, C. Y.; Nanayakkara, A.; Gonzalez, C.; Challacombe, M.; Gill, P. M. W.; Johnson, B.; Chen, W.; Wong, M. W.; Andres, J. L.; Gonzalez, C.; Head-Gordon, M.; Replogle, E. S.; Pople, J. A. *Gaussian 03W*, Rev. E.01; Gaussian Inc.: Pittsburgh, PA, 1998.

(21) (a) Kottke, T.; Stalke, D. *J. Appl. Crystallogr.* **1993**, *26*, 615. (b) Kottke, T.; Lagow, R. J.; Stalke, D. *J. Appl. Crystallogr.* **1996**, *29*, 465. (c) Stalke, D. *Chem. Soc. Rev.* **1998**, *27*, 171.

methods using SHELXS 97.²² The structures were refined by full-matrix least-squares procedures on F^2 , using SHELXL 97.²³ The silicon-bonded hydrogen atom positions were located from the final Fourier difference map and refined freely without application of any restraints.

Bis[*N*-(dimethylamino)benzimidato-*N'*,*O*]hydridomethylsilicon(IV) (9a). A mixture of 1.22 g (5.15 mmol) of **4a**²⁴ and 0.266 g (2.31 mmol) of MeHSiCl₂ (**5**) in 5 mL of trichloromethane was stirred at room temperature for 2 h. The volatiles were removed under reduced pressure (0.1 mmHg), and the white solid residue was recrystallized from 15 mL of *n*-hexane; 0.654 g was obtained (76%). Mp: 85–86 °C. ¹H NMR (toluene-*d*₈, 296 K): δ 0.24 (s, 3H, SiCH₃), 2.11 (s, 3H, CCH₃), 2.62 (s, 12H, NCH₃), 4.94 (s, 1H, SiH), 7.08–8.09 (m, 10H, Ph). ¹³C NMR (toluene-*d*₈, 296 K): δ 7.1 (SiCH₃), 49.5 (NCH₃), 124.9–137.4 (Ph), 164.4 (C=N). ²⁹Si NMR (toluene-*d*₈): δ (200 K) –128.7 (d, ¹*J*_{Si-H} = 234 Hz); δ (300 K) –108.8 (d, ¹*J*_{Si-H} = 266 Hz); δ (370 K) –85.9 (d, ¹*J*_{Si-H} = 285 Hz). Anal. Calcd for C₁₉H₂₆N₄O₂Si: C, 61.59; H, 7.07; N, 15.12. Found: C, 61.35; H, 6.90; N, 15.21.

Bis[*N*-(dimethylamino)trifluoroacetimidato-*N'*,*O*]hydridomethylsilicon(IV) (9b). A mixture of 1.12 g (4.92 mmol) of **4b**²⁵ and 0.265 g (2.31 mmol) of **5** in 5 mL of trichloromethane was stirred at room temperature for 24 h. The volatiles were removed under reduced pressure (0.1 mmHg), and the white solid residue was recrystallized from 15 mL of *n*-hexane; 0.603 g was obtained (74%). Mp: 71–72 °C. ¹H NMR (toluene-*d*₈, 296 K): δ 0.06 (s, 3H, SiCH₃), 2.32 (s, 12H, NCH₃), 4.60 (s, 1H, SiH). ¹³C NMR (toluene-*d*₈, 296 K): δ 5.5 (SiCH₃), 48.1 (NCH₃), 117.4 (q, ¹*J*_{CF} = 277 Hz, CF₃), 156.6 (q, ²*J*_{CF} = 37 Hz, C=N). ²⁹Si NMR (toluene-*d*₈): δ (200 K) –114.1 (d, ¹*J*_{Si-H} = 246 Hz); δ (300 K) –106.8 (d, ¹*J*_{Si-H} = 262 Hz); δ (370 K) –83.0 (d, ¹*J*_{Si-H} = 290 Hz). Anal. Calcd for C₉H₁₆F₆N₄O₂Si: C, 30.51; H, 4.55; N, 15.81. Found: C, 30.38; H, 4.44; N, 15.71.

(22) Sheldrick, G. M. *Acta Crystallogr.* **1990**, *A46*, 467.

(23) Sheldrick, G. M. *SHELXL-97, Program for Crystal Structure Refinement*; University of Göttingen: Germany, 1997.

(24) Kalikhman, I. D.; Bannikova, O. B.; Volkova, L. I.; Gostevskii, B. A.; Yushmanova, T. I.; Lopirev, V. A.; Voronkov, M. G. *Bull. Akad. Nauk. SSSR* **1988**, 460. *Chem. Abstr.* **1989**, *110*, 75608c.

(25) Kalikhman, I. D.; Medvedeva, E. N.; Bannikova, O. B.; Fabina, N. G.; Larin, M. F.; Lopirev, V. A.; Voronkov, M. G. *Zh. Obshch. Khim.* **1984**, *54*, 477. *Chem. Abstr.* **1984**, *101*, 55158.

Bis[*N*-(dimethylamino)benzimidato-*N'*,*O*]hydridophenylsilicon(IV) (10a). A mixture of 0.892 g (3.77 mmol) of **4a**²⁴ and 0.311 g (1.76 mmol) of PhHSiCl₂ (**6**) in 5 mL of trichloromethane was stirred at room temperature for 24 h. The volatiles were removed under reduced pressure (0.1 mmHg), and the resulting viscous liquid was crystallized from 10 mL of *n*-hexane. The white solid was washed twice with *n*-hexane and dried to yield 0.605 g (79%). Mp: 160.5–162 °C. A single crystal for X-ray analysis was grown from a diethyl ether solution. ¹H NMR (CDCl₃, 300 K): δ 2.18–3.17 (br, 12H, NCH₃), 5.22 (s, 1H, SiH), 7.30–7.97 (m, 15H, Ph). ¹H NMR (CDCl₃, 243 K): 2.17, 2.64, 2.73, 3.19 (4s, 12H, NCH₃), 5.20 (s, 1H, SiH), 7.22–8.00 (m, 10H, Ph). ¹³C NMR (CDCl₃, 300 K): δ 51.0 (br, NCH₃), 127.3–149.2 (Ph), 165.5 (C=N). ¹³C NMR (CDCl₃, 243 K): 49.5, 50.0, 51.8, 52.8 (NCH₃), 127.0–149.0 (Ph), 165.3, 165.6 (C=N). ²⁹Si NMR (CDCl₃, 300 K): δ –121.6 (d, ¹*J*_{Si-H} = 249.4 Hz). Anal. Calcd for C₂₄H₂₈N₄O₂Si: C, 66.64; H, 6.52; N, 12.95. Found: C, 66.36; H, 6.50; N, 12.76.

Bis[*N*-(dimethylamino)trifluoroacetimidato-*N'*,*O*]hydridophenylsilicon(IV) (10b). **10b** was prepared like **10a** from 0.681 g (2.98 mmol) of **4b**²⁵ and 0.250 g (1.41 mmol) of **6**. The yield of crystalline **10b** was 0.444 g (76%). Mp: 111 °C, from *n*-hexane. ¹H NMR (CDCl₃, 300 K): δ 2.50 (br, 12H, NCH₃), 4.96 (s, 1H, SiH), 7.37–7.64 (m, 5H, Ph). ¹H NMR (CDCl₃, 253 K): δ 2.13, 2.72, 2.72, 3.05 (3s, 12H, NCH₃), 5.08 (s, 1H, SiH), 7.51–7.82 (m, 5H, Ph). ¹³C NMR (CDCl₃, 300 K): δ 50.1 (NCH₃), 117.1 (q, ¹*J*_{CF} = 277 Hz, CF₃), 127.9–145.0 (Ph), 157.0 (q, ²*J*_{CF} = 37 Hz, C=N). ¹³C NMR (CDCl₃, 230 K): δ 48.9, 49.5, 50.9, 52.5 (NCH₃), 117.1 (q, ¹*J*_{CF} = 277 Hz, CF₃), 127.9–144.8 (Ph), 157.8, 158.1 (2q, ²*J*_{CF} = 37 Hz, C=N). ²⁹Si NMR (CDCl₃, 300 K): δ –116.5 (d, ¹*J*_{Si-H} = 268 Hz). Anal. Calcd for C₁₄H₁₈F₆N₄O₂Si: C, 40.38; H, 4.36; N, 13.46. Found: C, 40.32; H, 4.24; N, 13.56.

Acknowledgment. Financial support by the Israel Science Foundation, grant no. ISF-139/05, is gratefully acknowledged.

Supporting Information Available: Crystallographic data for **10a** and **10b** in CIF format and details of the calculations for **9b** and **9b-open** in Gaussian archive format. This material is available free of charge via the Internet at <http://pubs.acs.org>.

OM8008487

1,2-Azaboroly-Ligated Half-Sandwich Complexes of Scandium(III) and Lutetium(III): Synthesis, Structures, and Syndiotactic Polymerization of Styrene[†]

Xiangdong Fang,^{*,‡} Xiaofang Li,[§] Zhaomin Hou,^{*,§} Jalil Assoud,^{‡,⊥} and Rui Zhao[‡]

Department of Chemistry, University of Waterloo, Ontario N2L 3G1, Canada, and Organometallic Chemistry Laboratory, RIKEN (The Institute of Physical and Chemical Research), Hirosawa 2-1, Wako, Saitama 351-0198, Japan

Received July 31, 2008

Half-sandwich Sc(III) and Lu(III) complexes with ancillary trisubstituted 1,2-azaboroly (Ab) ligands have been conveniently prepared via the reaction of the corresponding anionic Ab ligands with cationic Sc(III) and Lu(III) dialkyl species in good yields and characterized crystallographically. In the solid-state molecular structures of the half-sandwich mono-Ab Sc(III) complexes **5** and **6**, the interaction between the Sc metal center and Ab ligand is strongly influenced by the exocyclic B substituent, whereas in the analogous Lu(III) system **8** this interaction becomes much less prominent, as indicated by a relatively shorter Lu–B bond distance along with an attenuated exocyclic B–N bond interaction. Upon activation, the Sc(III) complexes **5** and **7** were found to be highly active in the syndiospecific polymerization of styrene.

Introduction

Cyclopentadienyl (Cp)-based half-sandwich group III rare-earth metal dialkyl complexes (Figure 1, **A**) have attracted a tremendous amount of current research interest in selective organic transformations and homogeneous polymerization catalysis, due to their unique bonding and structural features.¹ For example, the coordination site in half-sandwich group III metal Cp complexes becomes generally more accessible to the substrate and the metal center is more electronically unsaturated, which furnishes the complexes with significantly higher reactivity with respect to their metallocene analogues (Figure 1, **B**). On the other hand, this sterically and electronically unsaturated character of **A** also hampers its synthesis, mainly because of the thermodynamics-driven ligand redistribution reaction that prefers to yield relatively more stabilized metallocene analogues **B** as the product. Thus, the synthetic strategies used to stabilize these considerably labile half-sandwich group III metal complexes and to avoid the occurrence of ligand redistribution involve either sterically demanding Cp ligands such as pentamethylcyclopentadienyl (Cp*) or Cp derivatives bearing a chelate structure, as utilized in constrained geometry catalysts (CGC). Despite the great success in the Cp chemistry, a myriad of useful Cp surrogate ligands have been synthesized and studied with an aim to provide new possibilities relative to more readily

available Cp derivatives.² In particular, as the isoelectronic and isolobal Cp analogues,^{3,4,6,7} 1,2-azaboroly (Ab) ligands have been observed to be more electron-donating than the Cp counterparts by Fu and co-workers,^{4,7c} which is also supported by the DFT calculation results.⁵ One additional advantage of Ab over Cp ligands has been noted for easy modulation of the electronic nature of the Ab ligand in the complexes being studied.⁴ Ab ligands also merit from their unique ring geometry, which may provide a coordination environment different from that of Cp.⁶ Surprisingly, in sharp contrast to the rapid development of Cp-containing half-sandwich group III metal complexes, no example even exists in the literature concerning analogous Ab-ligated half-sandwich transition-metal alkyl complexes.^{7,8} We have recently reported the syntheses and characterization of multiply substituted Ab ligands and demonstrated that these Ab ligands can serve as good supporting ancillary ligands in group IV transition-metal complexes.⁶ These results provide further incentives for the study of half-sandwich transition-metal complexes based on Ab ligands in a broad sense. In this contribution we describe a novel synthesis and structural comparison of mono-Ab dialkyl complexes of Sc(III) and Lu(III), the first examples of Ab-ligated half-sandwich group

* To whom correspondence should be addressed. Tel: 01-519-888-4567, ext. 36229 (X.F.). Fax: 01-519-746-0435 (X.F.). E-mail: xdfang@uwaterloo.ca (X.F.); hou@riken.jp (Z.H.).

[†] The design, syntheses, and structural determination of Sc complexes **5–7**, Lu complex **8**, and initial polymerization study were carried out independently at the University of Waterloo; the polymerization study of **5–7** and elemental analyses of **5–7** were performed at RIKEN.

[‡] University of Waterloo.

[§] RIKEN.

[⊥] X-ray crystallographer.

(1) For reviews on Cp-ligated half-sandwich rare-earth-metal complexes, see: (a) Arndt, S.; Okuda, J. *Chem. Rev.* **2002**, *102*, 1953. (b) Hou, Z.; Luo, Y.; Li, X. *J. Organomet. Chem.* **2006**, *691*, 3114. (c) Okuda, J. *Dalton Trans.* **2003**, 2367.

(2) Edlmann, F. T.; Freckmann, D. M. M.; Schumann, H. *Chem. Rev.* **2002**, *102*, 1851.

(3) Ashe, A. J., III; Fang, X. *Org. Lett.* **2000**, *2*, 2089.

(4) Liu, S.-Y.; Lo, M. M. C.; Fu, G. C. *Angew. Chem., Int. Ed.* **2002**, *41*, 174.

(5) Orian, L. *Rev. Roum. Chim.* **2007**, *52*, 551.

(6) Fang, X.; Assoud, J. *Organometallics* **2008**, *27*, 2408.

(7) There are a few scattered examples of Ab-ligated half-sandwich late-transition-metal non-alkylated complexes (e.g. Cr/Co/Rh); see: (a) Schmid, G. In *Comprehensive Heterocyclic Chemistry II*; Shinkai, I., Ed.; Elsevier: Oxford, U.K., 1996; Chapter 3.17. (b) Schmid, G.; Schütz, M. *Organometallics* **1992**, *11*, 1789. (c) Liu, S.-Y.; Hills, I. D.; Fu, G. C. *Organometallics* **2002**, *21*, 4323.

(8) Half-sandwich rare-earth-metal dialkyl complexes bearing pyrrolyl and phospholyl ligands were reported recently. See: (a) Nishiura, M.; Mashiko, T.; Hou, Z. *Chem. Commun.* **2008**, 2019. (b) Jaroschik, F.; Shima, T.; Li, X.; Mori, K.; Ricard, L.; Le Goff, X.-F.; Nief, F.; Hou, Z. *Organometallics* **2007**, *26*, 5654. (c) Roux, E. L.; Nief, F.; Jaroschik, F.; Törnroos, K. W.; Anwender, R. *Dalton Trans.* **2007**, 4866.

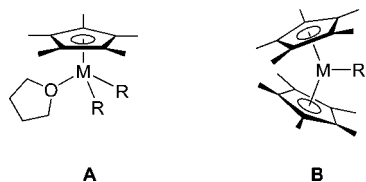
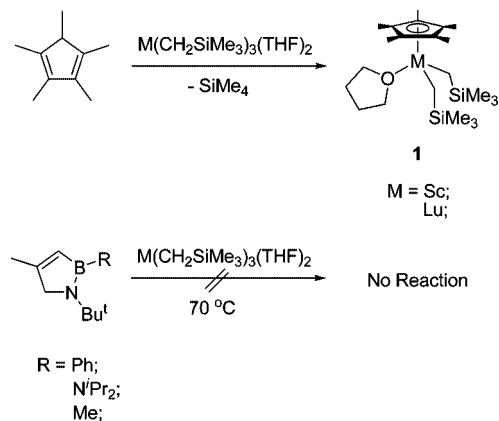


Figure 1. Cp-based rare-earth-metal complexes (M = Sc; Y; lanthanide metals. R = alkyl group).

Scheme 1



III rare-earth metal complexes. Upon activation with trityl cation and AlⁱBu₃, these complexes show interesting catalytic activity in the syndiospecific polymerization of styrene.

Results and Discussion

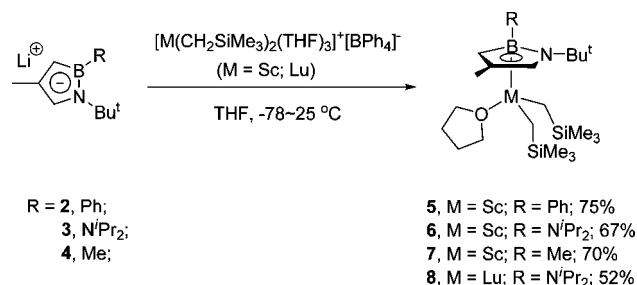
In analogy to the Cp chemistry,⁹ our initial synthetic approach involved the reaction of M(CH₂SiMe₃)₃(THF)₂ (M = Sc, Lu) with the conjugate acids of the anionic Ab ligands, as shown in Scheme 1. Unfortunately, the expected Sc or Lu adducts such as complexes **5–8** were not observed, as monitored by ¹H NMR spectroscopy, even after prolonged reaction time at 70 °C. Admittedly, this observation was completely consistent with the fact that the conjugate acids of Ab ligands were less acidic than those of Cp ligands, due to the less aromatic nature of the Ab ligands, relative to their Cp analogues. Therefore, the chemistry of Ab ligands did not necessarily follow that of Cp congeners, which prompted us to find other synthetic routes for the preparation of the intended mono-Ab group III metal dialkyl complexes **5–8**.

In 2005, Okuda et al. reported that some THF-coordinated rare-earth-metal (Sc/Y/Lu) dialkyl cations and monoalkyl dicationic species can be conveniently prepared in excellent yields via the reaction of the corresponding trialkyl species with a weak protic acid such as [Ph₂NMeH]⁺[BPh₄]⁻.¹⁰ We reasoned that, unlike lithium halides that might form “ate” types of bimetallic complexes by bridging two electron-deficient metal centers (rare-earth metal and lithium) via a halide group, noncoordinating salts such as Li⁺[BPh₄]⁻ had no lone pair of electrons to share with the metal centers and thus were ideal candidates for the preparation of salt-free half-sandwich group III metal complexes

(9) (a) Evans, W. J.; Brady, J. C.; Ziller, J. W. *J. Am. Chem. Soc.* **2001**, *123*, 7711. (b) Hultsch, K. C.; Spaniol, T. P.; Okuda, J. *Angew. Chem., Int. Ed.* **1999**, *38*, 227. (c) Cameron, T. M.; Gordon, J. C.; Scott, B. L. *Organometallics* **2004**, *23*, 2995. (d) Cui, D. M.; Nishiura, M.; Hou, Z. M. *Macromolecules* **2005**, *38*, 4089.

(10) (a) Elvidge, B. R.; Arndt, S.; Zeimentz, P. M.; Spaniol, T. P.; Okuda, J. *Inorg. Chem.* **2005**, *44*, 6777. (b) Arndt, S.; Okuda, J. *Adv. Synth. Catal.* **2005**, *347*, 339.

Scheme 2



through a salt elimination pathway. We further envisioned that Okuda's cationic species can serve as the precursors for the direct preparation of THF-coordinated half-sandwich rare-earth-metal dialkyl complexes such that the synthetic difficulty encountered above can be easily resolved (Scheme 2). Thus, a simple reaction of [M(CH₂SiMe₃)₂(THF)₃]⁺[BPh₄]⁻ (M = Sc, Lu) with the corresponding trisubstituted Ab ligands **2–4**⁶ in THF afforded the desired half-sandwich Sc/Lu complexes as air- and moisture-sensitive colorless crystals in good yields, which appeared to be much more soluble in hydrocarbon solvents such as pentane and hexane. The colorless block single crystals of complexes **5–8** suitable for X-ray diffraction experiments were grown slowly in pentane at -35 °C. In contrast, the reaction of less substituted Ab ligands such as 1-*tert*-butyl-2-phenyl-1,2-azaborolyl with the above Sc/Lu cationic species yielded uncharacterizable products, and attempts to prepare a yttrium analogue of complexes **5–8** with a disubstituted Ab ligand afforded only [(Ab)₂Y(CH₂SiMe₃)(THF)], presumably as a result of facile ligand redistribution.¹¹ These observations underline the importance of multiply substituted Ab ligands in the synthesis of Ab-ligated half-sandwich metal complexes.

The solid-state molecular structures of Sc (**5** and **6**) and Lu (**8**) complexes along with the selected bond lengths and angles are summarized in Figures 2–4, respectively. With the exception of Sc complex **7**, whose structural parameters could not be refined, the other two Sc complexes (**5**, *B*-Ph; **6**, *B*-NⁱPr₂) similarly show a typical three-legged piano-stool coordination geometry around the Sc center. In both cases, the Ab ligands coordinate to the Sc centers in an unsymmetric way such that Sc atoms tend to slip away from boron (Sc–B (Å): **5**, 2.664(2); **6**, 2.715(2))¹² and become more tightly affiliated with intraring C (Sc–C (Å): **5**, 2.443(2)–2.512(2); **6**, 2.411(2)–2.453(2)) and N (Sc–N (Å): **5**, 2.505(2); **6**, 2.459(2)), while the Ab ligands adopt a slight envelope-like structure. Therefore, the Sc coordination modes can be best depicted as η⁴. Interestingly, the exocyclic B substituent seems to dictate the coordination mode of the metal center, because this metal slippage away from boron becomes much more intensified when a more electron-donating group such as -NⁱPr₂ is utilized, as seen in complex **6**. Notably, in the case of complex **6**, this coordination slippage makes the Sc atom even more tightly bound to an intraring N that bears a more sterically demanding *tert*-butyl group. Thus, it is likely that the above slippage is induced electronically by the exocyclic B substituent rather than the steric effect. As a consequence, the Sc–C(Ab) and Sc–N(Ab) bond lengths in **6** are much shorter than those observed in **5** (vide supra). In

(11) Fang, X.; Deng, Y.; Xie, Q.; Moingeon, F. *Organometallics* **2008**, *27*, 2892.

(12) Shorter Sc–B bond distances (1.50–1.55 Å) were recorded in a dinuclear [(Cp*(C₂B₉H₁₁)ScH)₂]²⁻ dianionic species; see: Bazan, G. C.; Schaefer, W. P.; Bercaw, J. E. *Organometallics* **1993**, *12*, 2126.

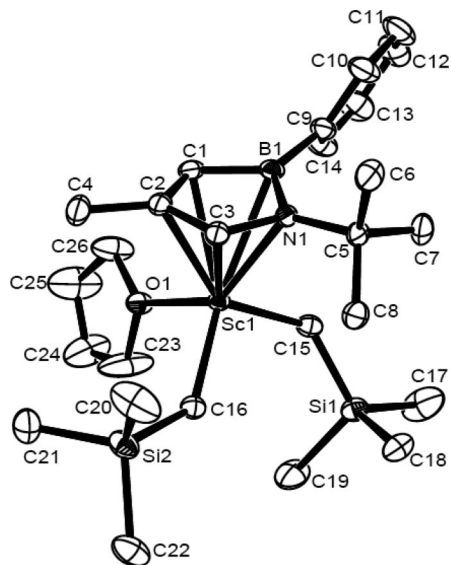


Figure 2. ORTEP drawing of Sc complex **5**. Hydrogen atoms are omitted for clarity, and thermal ellipsoids are drawn at the 30% probability level. Selected bond lengths (Å) and bond angles (deg): Sc1–B1 = 2.664(2), Sc1–C1 = 2.512(2), Sc1–C2 = 2.490(2), Sc1–C3 = 2.443(2), Sc1–N1 = 2.505(2), B1–N1 = 1.480(3), B1–C3 = 1.503(3); \angle O1–Sc1–C15 = 98.1(1), \angle O1–Sc1–C16 = 98.2(1), \angle C15–Sc1–C16 = 103.6(1).

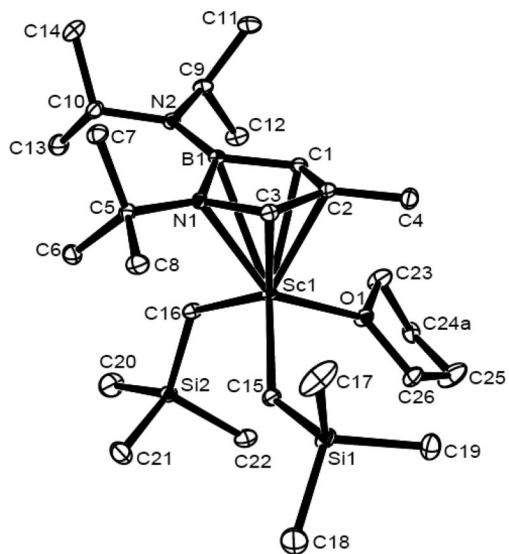


Figure 3. ORTEP drawing of Sc complex **6**. Hydrogen atoms are omitted for clarity, and thermal ellipsoids are drawn at the 30% probability level. Selected bond lengths (Å) and bond angles (deg): Sc1–B1 = 2.715(2), Sc1–C1 = 2.453(2), Sc1–C2 = 2.441(2), Sc1–C3 = 2.411(2), Sc1–N1 = 2.459(2), B1–N1 = 1.525(3), B1–N2 = 1.440(3), B1–C1 = 1.532(3); \angle O1–Sc1–C15 = 96.5(1), \angle O1–Sc1–C16 = 97.0(1), \angle C15–Sc1–C16 = 108.0(1).

addition, the Sc–O(THF) and Sc–C(alkyl) bond distances in complex **6** are all relatively longer than the corresponding bond distances in complex **5**, consistent with a weaker interaction between Sc and non-Ab groups in **6**, as a result of the stronger electron-donating character of the *B*-diisopropylamino Ab ligand vs that of the *B*-phenyl Ab ligand. It is also worth noting that the bonding interaction between Sc and the Ab ligand in **6** may be even stronger than that in the comparable Cp*Sc(CH₂SiMe₃)₂(THF) complex **1**,¹³ as evi-

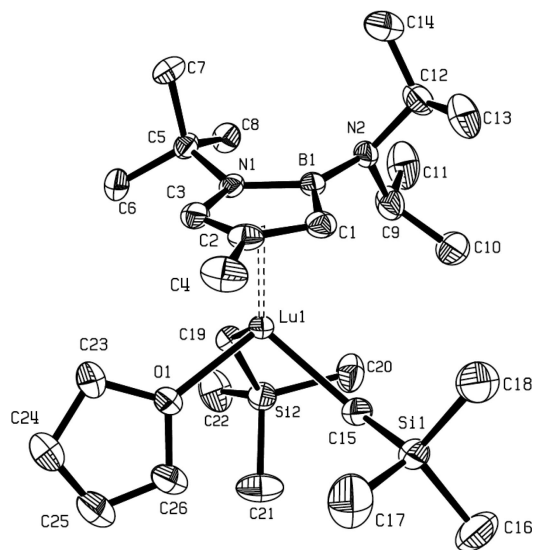


Figure 4. ORTEP drawing of Lu complex **8**. Hydrogen atoms are omitted for clarity, and thermal ellipsoids are drawn at the 30% probability level. Selected bond lengths (Å) and bond angles (deg): Lu1–B1 = 2.775(3), Lu1–N1 = 2.643(2), Lu1–C1 = 2.601(3), Lu1–C2 = 2.592(3), Lu1–C3 = 2.567(3), Lu1–O1 = 2.269(2), Lu1–C15 = 2.331(3), Lu1–C19 = 2.323(4), B1–N2 = 1.471(4), B1–C1 = 1.506(4), B1–N1 = 1.498(4), C1–C2 = 1.422(4), C2–C3 = 1.363(4), C3–N1 = 1.414(3); \angle B1–N2–C9 = 116.1(2), \angle B1–N2–C12 = 119.5(2), \angle C9–N2–C12 = 116.2(2), \angle O1–Lu1–C15 = 97.59(10), \angle O1–Lu1–C19 = 94.29(10), \angle C15–Lu1–C19 = 103.09(11).

denced by a relatively shorter average Sc–C(Ab) bond length (**6**: 2.45 Å) vs average Sc–C(Cp*) bond length (**1**: 2.50 Å).

It is of great interest to compare the X-ray structures of **6** and **8**, as they only differ in the metal atoms. First, complexes **6** and **8** share some structural similarities, as the metal centers in both cases are pseudotetrahedrally coordinated to give the complexes a typical three-legged piano-stool geometry, in which only one Ab ring is allowed to ligate the η^4 -metal center that is shifted away from B (**6**, vide supra; **8**, Lu–B = 2.775(3) Å, Lu–C/N = 2.567(3)–2.643(3) Å). Second, both **6** and **8** differ from each other. In a closer examination, one can tell that the slippage away from B becomes relatively less prominent in the Lu complex **8**, as the observed metrical difference between Lu–B and Sc–B bond lengths (2.77 vs 2.71 Å) is noticeably smaller than that of normal Lu–B and Sc–B covalent bonds (2.42 vs 2.26 Å).¹⁴ In addition, the exocyclic B–N bond of the Ab ligand in **8** is attenuated with less double bond character. For example, the elongation of the exocyclic B–N bond length in **8** (**6**, 1.441(3) Å; **8**, 1.471(3) Å) has been noted, and the diisopropylamino group is twisted away from being coplanar with the Ab ring such that the diisopropylamino N in **8** turns pyramidal (sum of the three bond angles around N (in deg): **6**, 360; **8**, 352). Another notable structural difference is that upon switching the metal center from Sc to Lu, the metrical values of intraring bond lengths of the Ab ligand in the Lu complex **8** fall short of those of Sc analogue **6**, and the Ab ring in complex **8** is almost planar, in contrast to an η^4 -coordinated envelope-like Ab structure of complex **6**. Perhaps this structural discrepancy of complexes **6** and **8** cannot be simply ascribed to the different ionic radii of Sc (0.88 Å) and Lu (1.00 Å),¹⁴ because

(13) Li, X.; Baldamus, J.; Hou, Z. *Angew. Chem., Int. Ed.* **2005**, *44*, 962.

(14) *Lange's Handbook of Chemistry*, 13th ed.; Dean, J. A., Ed.; McGraw-Hill: New York, 1985.

in analogous bis-Ab yttrium alkyl complexes, the Ab ligands were observed to coordinate to the Y atom with a larger ionic radius (1.04 Å)¹⁴ in a way much similar to that in complex **6**,¹⁵ which clearly does not sustain the above ionic-radius assumption. In view of the electropositive nature and limited radial extension of the 4f orbital configuration generally associated with lanthanide metals,¹⁶ we expect that the electrostatic interaction between the lanthanide metal center (e.g., Lu) and ligand (e.g., Ab) becomes important. As a result, the Lu–Ab interaction possesses more ionic character, which drives the Ab ligand to keep its original aromatic identity. Nonetheless, further studies are needed to provide a conclusive explanation for the above observations.

The ¹H and ¹³C NMR spectroscopic investigations were carried out in benzene-*d*₆ or toluene-*d*₈ to gain insight into their solution-phase behavior. The NMR data of all Sc and Lu complexes in hydrocarbon solution are consistent with their monomeric structures. For example, the ring H resonances appeared as two doublets ranging from 3.9 to 6.8 ppm in all four cases. In particular, the ambient-temperature NMR spectrum suggests the slow B–N rotation in complexes **6** and **8**, as indicated by diastereotopic ¹Pr groups. Upon heating up to 100 °C in toluene-*d*₈, no coalescence of two signals corresponding to the ¹Pr methyl groups (**6**, δ 25.0, 24.8 ppm; **8**, 24.8, 24.7 ppm) in the ¹³C NMR spectra has been observed, which implies a fairly strong B–N π bond with a rotational barrier of Δ*G*[‡] > 19.2 ± 0.5 kcal mol⁻¹ in both cases.¹⁷ This result agrees well with the strongly electron deficient nature of the metal centers that effectively withdraws electron density away from the Ab ligand and makes boron interact with its electron-rich exocyclic substituent, as evidenced by short exocyclic B–N bond lengths (**6**, 1.440(3) Å; **8**, 1.471(4) Å). It should be pointed out that the presence of a bulky *N*-Bu group also helps to increase the free energy of the B–N bond rotational barrier.

At the beginning of the preliminary polymerization study, we were intrigued by the role of Ab ligand as a strong electron donor in stabilizing electron-deficient cationic metal species, the catalytically active species responsible for the chain growth in syndiospecific styrene polymerization processes.^{1b,18} It is expected that this relatively more stabilized cationic Ab-ligated metal species, relative to the Cp analogues, may have an increased life span and essentially contribute to a more efficient catalyst system. In fact, when activated by 1 equiv of [Ph₃C]⁺[B(C₆F₅)₄]⁻ in the presence of AlⁱBu₃, Sc complexes **5**–**7** showed high activity for the syndiospecific polymerization of styrene to yield polystyrene with syndioselectivity of >99% (*rrrr*). Some representative results are summarized in Table 1. In the case of complexes **5** and **7**, 2000 equiv of styrene monomer could be quantitatively polymerized within 10 min, yielding unimodal syndiotactic polystyrenes with moderate molecular weight distributions (*M*_w/*M*_n = 2.2–2.5), consistent with the predominance of a single homogeneous catalytic species (Table 1, entries 1 and 5). Under the same conditions ([M]/[Sc] = 2000), Sc complex **6** showed lower activity and afforded polystyrene with a bimodal molecular weight distribution,

Table 1. Syndiospecific Polymerization of Styrene^a

entry	cat.	amt of Al ⁱ Bu ₃ (equiv)	[M]/[Sc]	yield (%)	<i>s</i> PS ^b (%)	10 ⁵ <i>M</i> _n ^c	<i>M</i> _w / <i>M</i> _n ^c	<i>T</i> _m ^d (°C)
1	5	2	2000	100	100	6.8	2.2	270
2	5	2	2500	100	100	9.1	2.1	270
3	5	2	3000	94	100	13.5	1.9	270
4	6	2	2000	27	100	31.2/2.2	1.5/2.5	271
5	7	2	2000	100	100	5.7	2.5	271
6	7	2	2500	100	100	10.5	1.7	271
7	7	2	3000	95	100	16.3	1.5	271
8	7	5	3000	100	100	4.1	3.1	271
9	7	10	3000	100	100	1.9	3.5	270
10	8	1	500	20	100	0.38	2.6	270
11	8	2	500	16	100	0.30	1.8	271
12	8	5	500	10	100	0.10	1.5	270
13	8	1	1000	22	100	0.36	2.6	270

^a Conditions: Sc, 25 μmol; [Sc]/[B] = 1/1 (mol/mol); 30 mL of toluene; *t* = 10 min, *T* = 25 °C; Lu, 25 μmol; [Lu]/[B] = 1/1 (mol/mol); 30 mL of toluene; *t* = 10 h, *T* = 25 °C. ^b Determined by ¹³C NMR. Solvent fractionation showed no presence of atactic polystyrene. ^c Determined by Tosoh HLC-8121GPC/HT in 1,2-dichlorobenzene or Varian PL GPC-220 with Wyatt HELEOS MALS in 1,2,4-trichlorobenzene at 145 °C against polystyrene standard. ^d Determined by DSC.

suggesting the presence of two active species in this system (Table 1, entry 4). Similarly, Lu complex **8** showed lower yet steady activity that could last at least for 10 h, and its polymerization was unaffected by the relative monomer-to-catalyst ratio (Table 1, entries 10 and 13) but was significantly influenced by the amount of AlⁱBu₃ added in the polymerization process, as the increase of the AlⁱBu₃ addition resulted in lower molecular weight and smaller *M*_w/*M*_n (Table 1, entries 11 and 12). Complexes **5** and **7** were then further examined under various monomer-to-catalyst ratios (2000–3000) (Table 1, entries 1–3 and 5–7). In both systems, the molecular weight of the resultant polymers has been significantly increased with decreased polydispersity as the monomer-to-catalyst ratio is raised. In the case of [M]/[Sc] = 3000, syndiotactic polystyrene with an *M*_n value as high as 1.6 × 10⁶ and *M*_w/*M*_n controlled at 1.5 can be obtained (Table 1, entries 3 and 7). The addition of AlⁱBu₃ also showed great influence on the present catalyst system.¹⁹ In the case of 7/[Ph₃C]⁺[B(C₆F₅)₄]⁻, the use of more AlⁱBu₃ led to a higher yield of polystyrene (Table 1, entries 7 and 8). On the other hand, an increase of the [Al]/[Sc] ratio resulted in lower molecular weight and broader molecular weight distribution of the resulting polymers (Table 1, entries 7–9), suggesting that the chain-transfer reaction to AlⁱBu₃ could occur more frequently at a higher AlⁱBu₃ feed. Nevertheless, the present catalyst systems yield syndiotactic polystyrene with molecular weight much higher than that produced in the case of the Cp-ligated analogous systems, albeit in the presence of AlⁱBu₃.

Conclusions

In summary, we have developed an efficient synthesis for novel half-sandwich Sc and Lu dialkyl complexes **5**–**8**, the first examples of Ab-ligated half-sandwich group III metal complexes. Our synthesis has the advantage of being general. The interaction between the Sc metal center and Ab ligand is strongly

(15) Two bis-Ab yttrium alkyl complexes with B-substituted diisopropylamino groups have been prepared and crystallographically characterized. In both cases, the diisopropylamino N atoms are sp² hybridized and the exocyclic B–N bond lengths are in an appropriate range for a moiety with substantial double-bond character (unpublished work).

(16) Evans, W. J. *Inorg. Chem.* **2007**, *46*, 3435.

(17) Friebolin, H. *Basic One- and Two-Dimensional NMR Spectroscopy*, 3rd ed.; Wiley-VCH: New York, 1998; p 307.

(18) (a) Luo, Y.; Baldamus, J.; Hou, Z. *J. Am. Chem. Soc.* **2004**, *126*, 13910. (b) Zhang, H.; Luo, Y.; Hou, Z. *Macromolecules* **2008**, *41*, 1064.

(19) In the absence of AlⁱBu₃, 7/[Ph₃C]⁺[B(C₆F₅)₄]⁻ alone showed much lower activity and gave a bimodal polymer under the same conditions, which was in contrast with case for the Cp-ligated analogues.

influenced by the exocyclic B substituent, whereas in the analogous Lu(III) system, this interaction becomes much less prominent, as revealed by the X-ray diffraction experiments. When treated with 1 equiv of $[\text{Ph}_3\text{C}]^+[\text{B}(\text{C}_6\text{F}_5)_4]^-$ in the presence of Al^iBu_3 , these Ab-ligated half-sandwich metal complexes demonstrate moderate-to-high catalytic activity in producing syndiotactic polystyrene with molecular weight higher than that for the corresponding Cp systems. Further studies toward the preparation of the analogous half-sandwich complexes based on other group III rare-earth metals and the copolymerization of CO_2 and epoxides are in progress.

Experimental Section

General Method and Instrumentation. All operations involving organometallic compounds were carried out under an atmosphere of pure dinitrogen by means of standard Schlenk techniques and an MBraun Unilab 1200/780 glovebox. The oxygen and moisture in the atmosphere of the MBraun Unilab glovebox were constantly monitored by both oxygen and moisture analyzers to ensure $\text{O}_2/\text{H}_2\text{O}$ concentrations below 0.1 ppm. Et_2O and THF were distilled under nitrogen prior to use from sodium/benzophenone ketyl and CH_2Cl_2 from CaH_2 . Pentane, hexane, and toluene were distilled from Na/K alloy. *n*-BuLi (2.5 M in hexanes) and MeMgBr (3.0 M in Et_2O) were purchased from Sigma-Aldrich and used as received. The deuterated NMR solvents were obtained from Cambridge Isotope Laboratories. THF- d_6 was degassed and dried over Na/K alloy. C_6D_6 and CDCl_3 were distilled from CaH_2 and degassed prior to use. 1,2-Azaboroly ligands⁶ and $[\text{M}(\text{CH}_2\text{SiMe}_3)_2(\text{THF})_3]^+[\text{BPh}_4]^-$ ($\text{M} = \text{Sc}; \text{Lu}$)¹⁰ were prepared using the literature procedures. Styrene (99%, Sigma-Aldrich) was dried by stirring with CaH_2 for 2 days and was purified by distillation and vacuum transfer prior to use. All other materials were commercially available and used without further purification. All B-containing samples for NMR spectroscopic measurements were prepared in the glovebox. NMR spectra were recorded on a Bruker Avance 300 spectrometer. ^1H and ^{13}C NMR spectra were calibrated using the signals from the solvents referenced to Me_4Si . The ^{11}B NMR spectra were referenced to external $\text{BF}_3 \cdot \text{OEt}_2$. Chemical shifts (δ) are reported in parts per million (ppm). The combustion, differential scanning calorimeter (DSC), and gel permeation chromatography (GPC) analyses were performed at the facility of Organometallic Chemistry Laboratory of RIKEN (Japan), the University of Michigan, or the University of Waterloo. The X-ray diffraction experiments were carried out at the X-ray facility center, Department of Chemistry, University of Waterloo (Canada).

The GPC analyses were performed using Tosoh HLC-8121GPC/HT or Varian PL GPC-220 with Wyatt HELEOS MALS systems maintained at 145 °C. 1,2-Dichlorobenzene (Tosoh) or 1,2,4-trichlorobenzene (Varian) was used as an eluant with a flow rate at 1.0 mL/min. M_w , M_n , and M_w/M_n values were obtained against polystyrene standard or with MALS. The DSC measurement for the melting temperatures (T_m) of polystyrene samples were obtained with an SII Nanotechnology EXSTAR6220 instrument at a heating rate of 10 °C/min under a helium atmosphere.

Synthesis and Characterization of Scandium Complex 5. A typical procedure for the synthesis of Ab-ligated half-sandwich scandium(III) and lutetium(III) dialkyl complexes is given as follows. A solution of lithium salt **2** (0.350 g, 1.59 mmol) in 5 mL of THF was added dropwise into a colorless solution of $[\text{Sc}(\text{CH}_2\text{SiMe}_3)_2(\text{THF})_3]^+[\text{BPh}_4]^-$ (1.20 g, 1.59 mmol) in 7 mL of THF at -78 °C. The mixture was stirred for 2 h at -78 °C and then for 20 min at 25 °C. After solvent removal, the pale yellow residue was extracted with 20 mL of hexane. The mixture was filtered to remove LiBPh_4 . The filtrate was further concentrated and crystallized at -35 °C to give compound **5** as colorless block crystals (0.60 g, 1.18 mmol, 75% yield). Other complexes such as

6 and **7** can be prepared analogously. ^1H NMR (300 MHz, C_6D_6): δ 7.85 (d, $J = 2$ Hz, 2H, ArH), 7.31 (t, $J = 2$ Hz, 2H, ArH), 7.19 (t, $J = 2$ Hz, 1H, ArH), 6.76 (d, $J = 2.6$ Hz, 1H), 4.50 (d, $J = 2.6$ Hz, 1H), 3.65 (br, 4H, THF), 2.00 (s, 3H, AbMe), 1.43 (s, 9H, ^iBu), 1.07 (br, 4H, THF), 0.33 (s, 18 H, SiMe₃), 0.16 (dd, $J = 27.2$ and 11.5 Hz, 2H, CH_2Si), -0.13 (s, 2H, CH_2Si). ^{13}C NMR (75.5 MHz, C_6D_6): δ 134.5, 132.7, 127.3, 126.7, 109.9, 72.3, 57.3, 32.4, 24.7, 16.5, 4.2, 4.0. ^{11}B NMR (96.3 MHz, C_6D_6): δ 33.0. Anal. Calcd for $\text{C}_{26}\text{H}_{49}\text{BNOScSi}_2$: C, 62.01; H, 9.81; N, 2.78. Found: C, 62.37; H, 9.68; N, 2.59.

Synthesis and Characterization of Scandium Complex 6. A solution of lithium salt **3** (0.385, 1.59 mmol) in 5 mL of THF was treated with a solution of $[\text{Sc}(\text{CH}_2\text{SiMe}_3)_2(\text{THF})_3]^+[\text{BPh}_4]^-$ (1.20 g, 1.59 mmol) in 7 mL of THF to yield complex **6** as colorless block crystals (0.56 g, yield 67%). ^1H NMR (300 MHz, C_6D_6): δ 6.40 (d, $J = 2.8$ Hz, 1H, AbH), 3.93 (d, $J = 2.8$ Hz, 1H, AbH), 3.75 (br, 4H, THF), 3.70 (sept, $J = 6.6$ Hz, 2H, NCH), 1.87 (s, 3H, C(4)Me), 1.59 (s, 9H, ^iBu), 1.27 (d, $J = 6.6$ Hz, 6H, NCHCH₃), 1.17 (br, 4H, THF), 0.33 (s, 18 H, SiMe₃), 0.24 (d, $J = 11.2$ Hz, 1H, CH_2SiMe_3), -0.20 (dd, $J = 26.2$, 11.5 Hz, 2H, CH_2SiMe_3), -0.32 (s, $J = 11.2$ Hz, 1H, CH_2SiMe_3). ^{13}C NMR (75.5 MHz, C_6D_6): δ 131.0, 125.6, 106.1, 72.4, 55.7, 47.8, 32.2, 24.8(CH(CH₃)₂), 24.7(CH(CH₃)₂), 23.9, 16.1, 4.31, 4.08. ^{11}B NMR (96.3 MHz, C_6D_6): δ 31.8. Anal. Calcd for $\text{C}_{26}\text{H}_{58}\text{BN}_2\text{OScSi}_2$: C, 59.29; H, 11.10; N, 5.32. Found: C, 59.54; H, 10.90; N, 5.68.

Synthesis and Characterization of Scandium Complex 7. A solution of lithium salt **4** (0.250, 1.59 mmol) in 5 mL of THF was treated with a solution of $[\text{Sc}(\text{CH}_2\text{SiMe}_3)_2(\text{THF})_3]^+[\text{BPh}_4]^-$ (1.20 g, 1.59 mmol) in 7 mL of THF to yield complex **7** as colorless block crystals (0.50 g, yield 72%). ^1H NMR (300 MHz, C_6D_6): δ 6.65 (d, $J = 2.9$ Hz, 1H, AbH), 4.41 (d, $J = 2.9$ Hz, 1H, AbH), 3.67 (br, 4H, THF), 1.91 (s, 3H, C(4)Me), 1.43 (s, 9H, ^iBu), 1.12 (br, 4H, THF), 1.07 (s, 3H, BMe), 0.30 (s, 18H, SiMe₃), 0.12 (d, $J = 10.2$ Hz, 1H, CH_2SiMe_3), -0.14 (d, $J = 11.2$ Hz, 1H, CH_2SiMe_3), -0.32 (dd, $J = 11.2$ and 10.2 Hz, 2H, CH_2SiMe_3). ^{13}C NMR (75.5 MHz, C_6D_6): δ 130.9, 109.4, 71.9, 56.4, 31.7, 24.8, 15.9, 4.3, 4.1. ^{11}B NMR (96.3 MHz, C_6D_6): δ 33.7. Anal. Calcd for $\text{C}_{21}\text{H}_{47}\text{BNOScSi}_2$: C, 57.12; H, 10.73; N, 3.17. Found: C, 56.72; H, 10.38; N, 3.31.

Synthesis and Characterization of Lutetium Complex 8. A solution of lithium salt **3** (0.22 g, 0.90 mmol) in 5 mL of THF was treated with a solution of $[\text{Lu}(\text{CH}_2\text{SiMe}_3)_2(\text{THF})_3]^+[\text{BPh}_4]^-$ (0.80 g, 0.90 mmol) in 7 mL of THF to yield complex **8** as colorless block crystals (0.37 g, yield 52%). ^1H NMR (300 MHz, C_6D_6): δ 6.39 (d, $J = 3.0$ Hz, 1H, AbH), 3.93 (d, $J = 3.0$ Hz, 1H, AbH), 3.79 (b, 4H, THF), 3.74 (sep, $J = 6.0$ Hz, 2H, NCHMe₂), 1.86 (s, 3H, $\text{CH}_3(\text{Ab})$), 1.58 (s, 9H, ^iBu), 1.33 (d, $J = 6.0$ Hz, 6H, $\text{CH}_3(\text{Pr})$), 1.27 (d, $J = 6.0$ Hz, 6H, $\text{CH}_3(\text{Pr})$), 1.18 (b, 4H, THF), 0.31 (s, 18H, SiMe₃), 0.22 (d, $J = 12$ Hz, 1H, CH_2Si), -0.16 (d, $J = 12$ Hz, 1H, CH_2Si), -0.25 (d, $J = 12$ Hz, 1H, CH_2Si), -0.32 (d, $J = 12$ Hz, 1H, CH_2Si). ^{13}C NMR (75.5 MHz, C_6D_6): δ 131.0 (C₄(Ab)), 106.1 (C₅(Ab)), 96.1 (b, C₃(Ab)), 72.4, 55.7, 47.8, 41.1 (b), 37.6 (b), 32.2, 24.8 (CH(CH₃)₂), 24.7 (CH(CH₃)₂), 23.9, 16.7, 4.3, 4.1, -2.5 . ^{11}B NMR (96.3 MHz, C_6D_6): δ 31.6. Anal. Calcd for $\text{C}_{26}\text{H}_{58}\text{BN}_2\text{OSi}_2\text{Lu}$: C, 47.55; H, 8.90; N, 4.27. Found: C, 47.91; H, 9.12; N, 4.20.

Polymerization Procedures. A typical procedure for styrene polymerization using **7**/ $[\text{Ph}_3\text{C}][\text{B}(\text{C}_6\text{F}_5)_4]/\text{Al}^i\text{Bu}_3$ (Table 1, entry 5) is as follows. In a glovebox, a solution of $[\text{Ph}_3\text{C}][\text{B}(\text{C}_6\text{F}_5)_4]$ (23 mg, 25 μmol) in 15 mL of toluene was added to a solution of **7** (11 mg, 25 μmol) in 15 mL of toluene in a 100 mL flask. The mixture was stirred at room temperature for a few minutes, and 2 equiv of Al^iBu_3 (50 μL , 50 μmol) was added into the above mixture with stirring, followed by styrene (5.2 g, 50 mmol) within 2 min. The magnetic stirring was stopped within a few seconds due to the increased viscosity. After ca. 10 min, methanol (2 mL) was added to terminate the polymerization. The flask was then taken out from

the glovebox and the mixture was poured into methanol (400 mL) to precipitate the polymer. The white polymer powder was collected by filtration, washed with methanol, and dried under vacuum at 60 °C to a constant weight (5.2 g, 100%).

Crystallographic Data. The single crystals of complexes **5**, **6** and **8** were immersed in FOMBLIN Y oil (HVAC 140/13, Sigma-Aldrich), mounted on a glass fiber, and examined on a Bruker AXS SMART-CCD 1K detector diffractometer equipped with a Cryostream N₂ cooling device using graphite-monochromated Mo K α radiation ($\lambda = 0.71073 \text{ \AA}$) at 173 K, respectively. The determination of crystal class and unit cell was carried out by the SMART program package.²⁰ The raw frame data were processed using SAINT²¹ and SADABS²² to yield the reflection data file. The structures were solved using the SHELXTL program.²³ Refinement was performed on F^2 anisotropically for all the non-hydrogen atoms by full-matrix least-squares methods. Analytical scattering factors for neutral atoms were used throughout the analysis.

Crystal data for **5**: C₂₆H₄₉BNOScSi₂, $M_w = 503.61$, monoclinic, $P2_1/n$, $a = 11.3970(5) \text{ \AA}$, $b = 18.2738(8) \text{ \AA}$, $c = 15.0873(7) \text{ \AA}$, $\alpha = 90^\circ$, $\beta = 95.8040(10)^\circ$, $\gamma = 90^\circ$, $V = 3126.1(2) \text{ \AA}^3$, $D_c = 1.070$

g/cm^3 , $Z = 4$, $R1 = 0.0449$, $wR2 = 0.0979$, for 301 parameters and 7567 reflections ($I > 2\sigma(I)$).

Crystal data for **6**: C₂₆H₅₈BN₂OScSi₂, $M_w = 526.69$, triclinic, $P\bar{1}$, $a = 10.4194(7) \text{ \AA}$, $b = 12.5772(8) \text{ \AA}$, $c = 14.1792(9) \text{ \AA}$, $\alpha = 75.5220(10)^\circ$, $\beta = 76.1870(10)^\circ$, $\gamma = 66.6320(10)^\circ$, $V = 1631.07(18) \text{ \AA}^3$, $D_c = 1.072 \text{ g/cm}^3$, $Z = 2$, $R1 = 0.0555$, $wR2 = 0.0999$, for 308 parameters and 9170 reflections ($I > 2\sigma(I)$).

Crystal data for **8**: C₂₆H₅₈BLuN₂OSi₂, $M_w = 656.70$, triclinic, $P\bar{1}$, $a = 9.2953(6) \text{ \AA}$, $b = 10.4744(7) \text{ \AA}$, $c = 19.1047(12) \text{ \AA}$, $\alpha = 94.948(1)^\circ$, $\beta = 97.502(1)^\circ$, $\gamma = 111.509(1)^\circ$, $V = 1697.5(2) \text{ \AA}^3$, $T = 296(2) \text{ K}$, $Z = 2$, $D_c = 1.285$, 22 005 measured reflections, 9799 unique reflection ($R_{\text{int}} = 0.0186$), 298 refined parameters, $R1(I > 2\sigma(I)) = 0.0288$, $wR2(F^2) = 0.0611$.

Acknowledgment. Financial support to X.F. from the Natural Sciences and Engineering Council of Canada (NSERC), the Canadian Foundation for Innovation (CFI), the Ontario Innovation Trust (OIT), and the University of Waterloo is gratefully acknowledged.

Supporting Information Available: CIF files giving crystallographic data for complexes **5**, **6**, and **8**. This material is available free of charge via the Internet at <http://pubs.acs.org>.

OM800734V

(20) *SMART Software Users Guide, version 4.21*; Bruker AXS, Inc.: Madison, WI, 1997.

(21) SAINT+, Version 6.02; Bruker AXS, Inc., Madison, WI, 1999.

(22) Sheldrick, G. M. SADABS; Bruker AXS, Inc., Madison, WI, 1998.

(23) Sheldrick, G. M. SHELXTL, Version 5.1; Bruker AXS, Inc., Madison, WI, 1998.

Structure and Reactivity of Rhodium(I) Complexes Based on Electron-Withdrawing Pyrrolyl-PCP-Pincer Ligands

Elizaveta Kossoy,[†] Boris Rybtchinski,[†] Yael Diskin-Posner,[‡] Linda J. W. Shimon,[‡] Gregory Leitus,[‡] and David Milstein^{*†}

Department of Organic Chemistry and Chemical Research Support,
Weizmann Institute of Science Rehovot, 76100 Israel

Received August 17, 2008

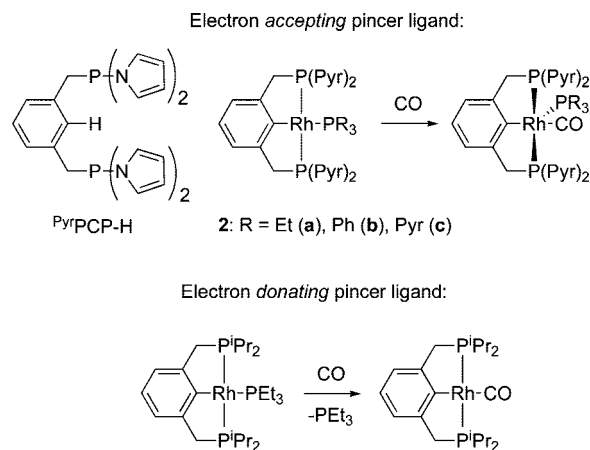
Rhodium complexes based on the electron-withdrawing PCP-type pincer ligand dipyrrolylphoshoxylylene (DPyPX, ^{Pyr}PCP) were synthesized and their reactivity was studied. Reaction of Rh^I(^{Pyr}PCP)PR₃ (**2**) (R = Et (**a**); Ph (**b**); Pyr (pyrrolyl, NC₄H₄) (**c**); Pyd (pyrrolyldinyl, NC₄H₈) (**d**)) with MeI was strongly dependent on the sterics and nucleophilicity of PR₃. Complex **2a** (PET₃ cone angle, Θ°, 132°) reacted with MeI to give isomers of Rh^{III}(^{Pyr}PCP)Me(I)PET₃, **3**. Reaction of **2b** (Θ°_{PR₃} = 145°, R = Pyd (**2d**), Ph (**2b**), Pyr (**2c**)) with MeI was accompanied by release of PPh₃ and is thought to proceed via the 14e intermediate Rh^I(^{Pyr}PCP). While the PPyd₃ complex **2d** reacted with MeI to give [Rh^{III}(^{Pyr}PCP)Me(I)₂][MePPy₃], **4a**, the PPy₃ complex **2c** did not react, owing to steric hindrance around Rh^I and the low nucleophilicity of PPy₃. The aptitude of complexes **2** toward activation of H₂ was also examined. Our results support the involvement of 14e intermediates in the olefin hydrogenation process. The ancillary ligand substitution at the Rh^I center of **2** was found to proceed by an associative mechanism. ML₅ d⁸ intermediates were clearly detected by ³¹P{¹H} NMR at 213 K during equilibrium between **2a** and **2c**.

Introduction

Since the pioneering work of Moulton and Shaw¹ pincer-type ligands have attracted much scientific interest.² Late transition metal complexes based on pincer ligands of the PCP type were found to be active in a variety of important catalytic processes^{2a} and in the activation of strong bonds.^{2b,c} They were also invaluable for mechanistic studies and for the stabilization of unusual structures,^{2d} and useful as functional materials.^{2e} Although PCP ligands with a variety of electron-donating phosphine substituents have been widely explored, electron-accepting substituents were introduced only recently.^{3–5}

^{Pyr}PCP-H (Scheme 1) was the first reported highly electron accepting PCP-type pincer ligand.^{3,4} Its synthesis was inspired by the work of Molloy and Petersen,⁶ who demonstrated that N-pyrrolyl phosphines possess exceptional electron-accepting

Scheme 1. ^{Pyr}PCP-H and the Coordination Mode of ^{Pyr}PCP-Based Rhodium(I) Complexes



* Corresponding author. E-mail: david.milstein@weizmann.ac.il.

[†] Department of Organic Chemistry.

[‡] Chemical Research Support.

(1) Moulton, C. J.; Shaw, B. L. *J. Chem. Soc., Dalton Trans.* **1976**, 11, 1020–1024.

(2) (a) van der Boom, M. E.; Milstein, D. *Chem. Rev.* **2003**, 103, 1759–1792. (b) Rybtchinski, B.; Milstein, D. *Angew. Chem., Int. Ed.* **1999**, 28, 870–883. (c) Rybtchinski, B.; Milstein, D. *ACS Symp. Ser.* **2004**, 885, 70–85. (d) Vigalok, A.; Milstein, D. *Acc. Chem. Res.* **2001**, 34, 798–807. (e) Albrecht, M.; van Koten, G. *Angew. Chem., Int. Ed.* **2001**, 40, 3750–3781. (f) Singleton, J. T. *Tetrahedron* **2003**, 59, 1837–1857. (g) Milstein, D. *Pure Appl. Chem.* **2003**, 75, 445–460. (h) Jensen, C. M. *Chem. Commun.* **1999**, 24, 2443–2449. (i) Morales-Morales, D.; Jensen, C. M. *The Chemistry of Pincer Compounds*; Elsevier: Amsterdam, 2007.

(3) Kossoy, E.; Iron, M. A.; Rybtchinski, B.; Ben-David, Y.; Shimon, L. J. W.; Konstantinovskii, L.; Martin, J.; Milstein, D. *Chem.–Eur. J.* **2005**, 11, 2319–2326.

(4) Another electron-withdrawing pincer ligand of PCP type with perfluorophenyl substituents was reported a short time after our report about ^{Pyr}PCP-H: Chase, P. A.; Gagliardo, M.; Lutz, M.; Spek, A. L.; van Klink, G. P. M.; van Koten, G. *Organometallics* **2005**, 24, 2016–2019.

(5) Adams, J. J.; Lau, A.; Arulsamy, N.; Roddick, D. M. *Inorg. Chem.* **2007**, 46, 11328–11334.

properties. The π-accepting ability of trispyrrolylphosphine, PPy₃, was found to be similar to that of P(C₆F₅)₃ and to exceed those of phosphites such as P(OPh)₃. Contrary to many perfluoroalkyl moieties, pyrrole-like precursors are readily available and easily amenable to structural variations.

The high electron-accepting ability of the pyrrolyl moieties in ^{Pyr}PCP and the rigidity and synergetic effects typical of pincer-type ligands² are combined in order to create electron-deficient and structurally well-defined metal centers. We have reported that ^{Pyr}PCP-based rhodium(I) complexes possess significantly different coordination chemistry from those of Rh^I complexes based on electron-donating pincer-type ligands.³ Namely, the π-accepting nature of the ^{Pyr}PCP ligand disfavors formation of

(6) Molloy, K. G.; Petersen, J. L. *J. Am. Chem. Soc.* **1995**, 117, 7696–7710.

the coordinately unsaturated ML_4 complexes, leading to formation of the first stable $d^8 ML_5$ PCP complexes (Scheme 1).

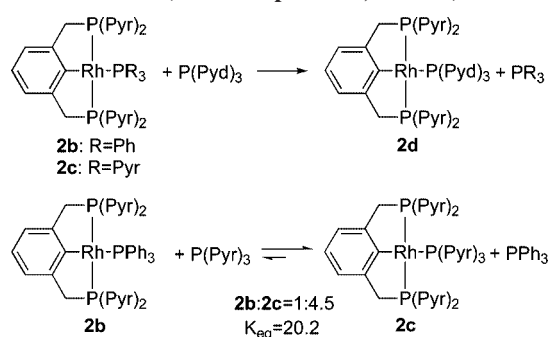
We present here a study of the reactivity of $Rh^I(P^{yr}PCP)PR_3$ ($R = Et, Ph, Pyr, Pyd$) complexes. Understanding the effect of the electron-accepting $P^{yr}PCP$ pincer ligand on the reactivity of the rhodium(I) center is essential for the development of catalytic applications of this type of complexes.

Results and Discussion

Preparation of $Rh^I(P^{yr}PCP)PR_3$ ($R = Et, Ph, Pyr$) Complexes. PCP-based rhodium(III) compounds are easily prepared by oxidative addition of the Ar–H bond of α, α' -diphosphine-*m*-xylenes to rhodium(I) metal centers.^{1,7} Similarly, the compounds $Rh^{III}(P^{yr}PCP)H(PR_3)Cl$ (**1a**, $R = Et$; **1b**, $R = Ph$) were obtained by the reaction of equivalent amounts of $P^{yr}PCP-H$, $[Rh^I(COE)_2\mu Cl]_2$, and PR_3 ($R = Et, Ph$) in THF at 65 °C.⁸ Subsequent reaction of **1a, b** with KO^tBu resulted in deprotonation of the hydride ligand and formation of the rhodium(I) complexes $Rh^I(P^{yr}PCP)PR_3$ (**2a**, $R = Et$; **2b**, $R = Ph$), respectively, as previously described.³ However, $Rh^{III}(P^{yr}PCP)H(PPyr_3)Cl$, bearing the electron-accepting ancillary ligand $PPyr_3$, could not be prepared either via oxidative addition of the Ar–H bond of $P^{yr}PCP-H$ to rhodium(I) (cyclometalation) or by direct reaction of $Rh^I(P^{yr}PCP)PPyr_3$,³ **2c**, with HCl. The latter reaction resulted in decomposition of **2c**. It appears that in the $P^{yr}PCP/PPyr_3/Rh$ system coordination of three highly electron accepting pyrrolylic moieties to the rhodium center retards oxidative addition of the Ar–H bond or protonation of the rhodium(I) metal center. Complex **2c** was prepared by adding 1 equiv of $PPyr_3$ to the PPh_3 complex **2b** followed by 1 equiv of MeOTf to precipitate the displaced PPh_3 as its phosphonium salt.³ Indeed, the metal center of **2c** has a significantly lower electron density than in the case of **2a, b**, as reflected by its low back-donation ability to carbon monoxide. Thus, the CO stretch in the IR spectrum of $Rh^I(P^{yr}PCP)PPyr_3(CO)$ appears at a significantly higher frequency (2007 cm^{-1}) than in the case of $Rh^I(P^{yr}PCP)PPh_3(CO)$ (1987 cm^{-1}) or $Rh^I(P^{yr}PCP)PEt_3(CO)$ (1975 cm^{-1}).³ The synthetic route toward **2c** described above took advantage of its low oxidative addition reactivity, enabling removal of the displaced PPh_3 with MeOTf without affecting the metal center.

Ancillary Ligand Exchange in Complexes 2a–d. Ligand substitution reactions at rhodium(I) centers were reported to follow both associative⁹ and dissociative¹⁰ mechanisms. In our previous report³ we considered $d^8 ML_5$ rhodium $Rh^I(P^{yr}PCP)PR_3(CO)$ compounds (Scheme 1) as “arrested intermediates”

Scheme 2. Ancillary Ligand Exchange of Complexes 2b–d (room temperature, toluene)



in associative ancillary ligands exchange. In the current work we studied exchange between monodentate phosphines coordinated to the $P^{yr}PCP$ -based rhodium(I) center.

The phosphines $PPyr_3$, PPh_3 , and PPy_3 (trispyrrolidinylphosphine) were reported as isosteric, possessing the same cone angle of 145°.⁶ Reaction of 1 equiv of PPy_3 with either $Rh^I(P^{yr}PCP)PPh_3$, **2b**, or $Rh^I(P^{yr}PCP)PPyr_3$, **2c**, at room temperature (r.t.) resulted in phosphine exchange to form the complex $Rh^I(P^{yr}PCP)PPy_3$, **2d**, accompanied by release of 1 equiv of either PPh_3 or $PPyr_3$, respectively (Scheme 2). However, addition of either 1 equiv of $PPyr_3$ to **2b** or 1 equiv of PPh_3 to **2c** resulted in equilibrium between **2b** and **2c**, strongly shifted toward formation of **2c** at 295 K ($K_{eq} = 20.2$) (Scheme 2).

Orange crystals of **2c** were obtained at room temperature by slow diffusion of hexane into a concentrated THF solution. Yellow crystals of **2d** were obtained from a saturated pentane solution. The single-crystal X-ray structures of **2b**,³ **2c**, and **2d** reveal distorted square-planar geometries (Table 1; Figure 1). Counterintuitively, despite the electron-withdrawing pincer ligand, the $Rh-P_{ancillary}$ bond was found to be remarkably shorter for the electron-withdrawing $PPyr_3$, $Rh-PPyr_3$ being 2.244 Å, as compared with $Rh-PPh_3$ (2.315 Å) and $Rh-PPy_3$ (2.320 Å) (Table 1). It should be mentioned that the single-crystal X-ray structures of **2b**³ and **2c** (Figure 1, left) did not reveal any pronounced $\pi-\pi$ interactions between $P^{yr}PCP$ and either $PPyr_3$ or PPh_3 , which might have affected their coordination. Moreover, the smallest sum of $C_{ipso}-Rh$ and $Rh-P_{ancillary}$ bond lengths was found for **2c** (4.351(4) Å), while the largest was for **2d** (4.433(4) Å). Therefore, it is likely that the ancillary ligand coordination to the $P^{yr}PCP$ -based Rh^I is governed by the *trans* influences between the $P^{yr}PCP$ and the ancillary ligands, despite the overall reduction in electron density caused by chelation of $P^{yr}PCP$.

However, our results indicate that coordination of PPy_3 is thermodynamically more favorable than coordination of either PPh_3 or $PPyr_3$, leading to complete substitution of $PPh_3/PPyr_3$ with 1 equiv of PPy_3 . A possible reason for stabilization of the PPy_3 adduct may be interaction of a C–H bond with the rhodium center. We found that the distance between H39B and rhodium in **2d** (Figure 1, right; Table 1) is relatively short, 2.82(3) Å, compared to the hydrogen atoms closest to rhodium in the compounds **2b** ($Rh-H42C$, 2.94(3) Å) and **2c** ($Rh-H53A$, 2.97(3) Å) (Table 1). Such M–H(C) bonds in square-planar d^8 complexes¹¹ are usually described as anagostic, largely elec-

(7) (a) Nemeh, S.; Jensen, C.; Binamira-Soriaga, E.; Kaska, W. C. *Organometallics* **1983**, *2*, 1442–1447. (b) Weisman, A.; Gozin, M.; Kraatz, H.-B.; Milstein, D. *Inorg. Chem.* **1996**, *35*, 1792. (c) Liou, S.-Y.; Gozin, M.; Milstein, D. *J. Chem. Soc., Chem. Commun.* **1995**, 1965. (d) van der Boom, M. E.; Zubkov, T.; Shukla, A. D.; Rytchinski, B.; Shimon, L. J. W.; Rozenberg, H.; Ben-David, Y.; Milstein, D. *Angew. Chem., Int. Ed.* **2004**, *43* (44), 5961–5963.

(8) Synthesis of **1a, b** by cyclometalation required heating of the reaction mixture to 65 °C. Therefore, preparation of $Rh^{III}(P^{yr}PCP)H(PPy_3)Cl$ was not possible using this procedure because of the thermal instability of PPy_3 . Compound **2d** was prepared by synthesis of $Rh^I(P^{yr}PCP)$ (norbornene) with subsequent norbornene substitution with PPy_3 .

(9) (a) Garrou, P. E.; Hartwell, G. E. *Inorg. Chem.* **1976**, *15*, 646–650. (b) Leipoldt, J. G.; Lamprecht, G. J.; Steynberg, E. C. *J. Organomet. Chem.* **1990**, *397*, 239–244. (c) Leipoldt, J. G.; Lamprecht, G. J.; Steynberg, E. C. *J. Organomet. Chem.* **1991**, *402*, 259–263. (d) Alonso, M. A.; Casares, J. A.; Espinet, P.; Soulantica, K. *Angew. Chem., Int. Ed.* **1999**, *38*, 533–535.

(10) (a) Crociani, B.; Antonaroli, S.; Di Vona, M. L.; Licocchia, S. *J. Organomet. Chem.* **2001**, *631*, 117–124. (b) Bossio, R. E.; Hoffman, N. W.; Cundari, T. R.; Marshall, A. G. *Organometallics* **2004**, *23*, 144–148.

(11) In $[RhCl(PPh_3)_3]$: (a) Bennet, M. J.; Donaldson, P. B.; Hitchcock, P. B.; Mason, R. *Inorg. Chim. Acta* **1975**, *12*, L9–L10. (b) Bennett, M. J.; Donaldson, P. B. *Inorg. Chem.* **1977**, *16*, 655–660. In $d^8 Ni, Pd$, and Pt compounds: (c) Mukhopadhyay, A.; Pal, S. *Eur. J. Inorg. Chem.* **2006**, *23*, 4879–4887.

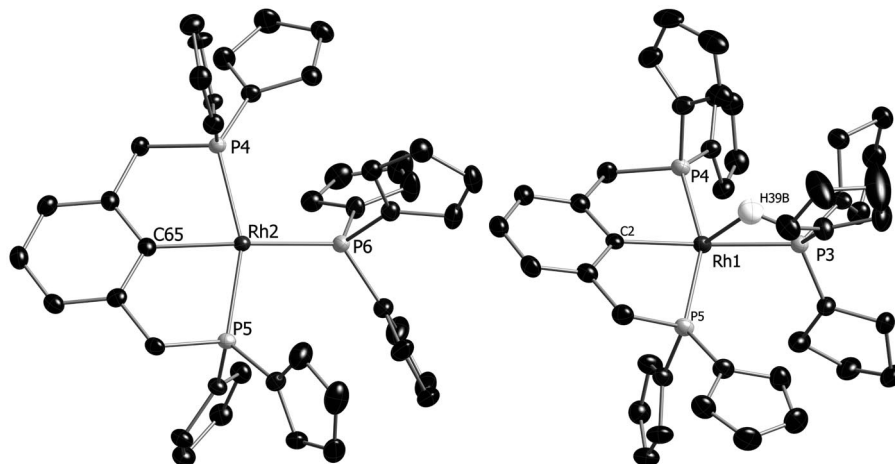


Figure 1. ORTEP diagrams of molecules of complexes **2c** (left) and **2d** (right) at the 50% probability level. Hydrogen atoms, except H39B, were omitted for clarity.

Table 1. Selected Bond Lengths (Å) and Angles (deg) of **2b**,³ **2c**, and **2d**

Rh(^{Pyr} PCP)PPy ₃ , 2d		Rh(^{Pyr} PCP)PPh ₃ , 2b		Rh(^{Pyr} PCP)PPy ₃ , 2c	
Rh1–C2 _{ipso}	2.113(3)	Rh1–C1 _{ipso}	2.079(3)	Rh2–C65 _{ipso}	2.107(3)
Rh1–P4	2.212(1)	Rh1–P2	2.228(1)	Rh2–P4	2.266(1)
Rh1–P5	2.257(1)	Rh1–P3	2.229(1)	Rh2–P5	2.236(1)
Rh1–P3 _{ancillary}	2.320(1)	Rh1–P4 _{ancillary}	2.315(1)	Rh2–P6 _{ancillary}	2.244(1)
C2–Rh1–P4	79.24(7)	C1–Rh1–P2	80.98(8)	C65–Rh2–P4	79.06(9)
C2–Rh1–P5	77.05(7)	C1–Rh1–P3	77.88(7)	C65–Rh2–P5	78.16(9)
C2–Rh1–P3	173.12(7)	C1–Rh1–P4	172.43(7)	C65–Rh2–P6	171.83(8)
P4–Rh1–P5	155.14(3)	P2–Rh1–P3	154.12(3)	P4–Rh2–P5	157.10(3)
Rh1–H39B	2.82(3)	Rh1–H42C	2.94(3)	Rh2–H53A	2.97(3)

trostatic interactions.¹² Structural characteristics of the Rh–H39B bond in **2d** meet those anagostic interactions observed for several square-planar d⁸ complexes. Namely, the Rh–H distance of 2.82(3) Å and the Rh–H–C angle of 116° fall within the range of ca. 2.3–2.9 Å and ca. 110–170°, respectively.¹²

It is worthwhile to mention the stronger *trans* influence of PPy₃ as compared to PPh₃. While the Rh–PPh₃ and Rh–PPy₃ bond lengths are similar, 2.315 and 2.320 Å, respectively, the C_{ipso}–Rh bond of **2d** (2.113 Å) is longer than that of **2b** (2.079 Å), as a result of coordination of the stronger electron donor, PPy₃, *trans* to the *ipso* carbon.

Next we studied exchange with PEt₃. Reaction of 1 equiv of PEt₃ (cone angle 132°¹³) with Rh^I(^{Pyr}PCP)PPh₃, **2b**, at room temperature resulted in formation of Rh^I(^{Pyr}PCP)PEt₃, **2a**, accompanied by release of 1 equiv of PPh₃ (Scheme 3). However, reaction of either 1 equiv of PEt₃ with Rh^I(^{Pyr}PCP)-PPy₃, **2c**, or 1 equiv of PPy₃ with **2a** resulted in equilibrium between **2a** and **2c**, which was strongly shifted toward formation of **2a** at 295 K (*K*_{eq} = 12.2) (Scheme 3). At 295 K, the ³¹P{¹H} NMR spectrum showed broad signals at chemical shifts similar to those of **2a** and **2c**. Upon cooling to 213 K, the ³¹P{¹H} NMR spectrum showed signals that could be attributed to pentacoordinate compounds of the type d⁸ ML₅, Rh(^{Pyr}PCP)(PEt₃)PPy₃, **2a'**, **2c'**, with both monodentate phosphines coordinated to the rhodium center (Scheme 3, Table 2). Relying on the ³¹P{¹H} NMR (213 K) spectrum of compounds **2a'** and **2c'** (Table 2) we can conclude that **2a'** and **2c'** are two stereoisomers that differ by the position of the monodentate phosphines: PEt₃ is bound in the *apical* position in **2a'** (double quartet at 8.1, ¹J_{RhP} = 93 Hz, ²J_{PP} = 42 Hz) and in an equatorial position in **2c'**

Scheme 3. Ancillary Ligand Exchange of Complexes **2a–c** (room temperature, toluene)

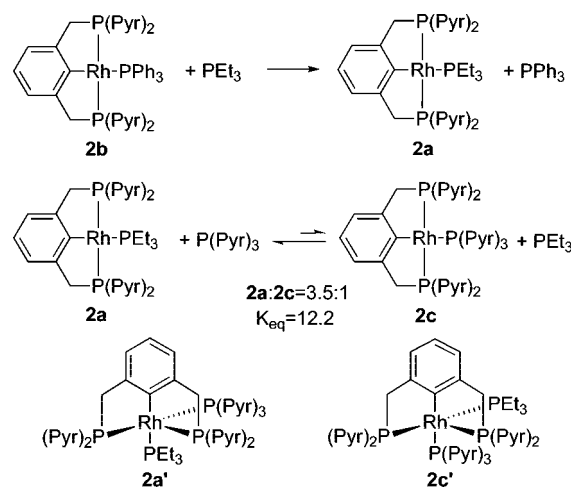


Table 2. Signals of **2a'** and **2c'** in ³¹P{¹H} NMR (213 K, tol-*d*₈) Spectrum

P atom	chemical shift	multiplicity	coupling constants
2a' - ^{Pyr} PCP	120.3	ddd	² J _{PP} = 312 Hz, ¹ J _{RhP} = 192 Hz, ² J _{PP} = 44 Hz
2a' -PPy ₃	98.9	m	
2a' -PEt ₃	8.1	dq	¹ J _{RhP} = 93 Hz, ² J _{PP} = 42 Hz
2c' - ^{Pyr} PCP	112.46	ddd	² J _{PP} = 201 Hz, ¹ J _{RhP} = 191 Hz, ² J _{PP} = 42 Hz
2c' -PPy ₃	obscured by other peaks		
2c' -PEt ₃	1.4	tdd	² J _{PP} = 202 Hz, ¹ J _{RhP} = 142 Hz, ² J _{PP} = 44 Hz

(triple doublet of doublets at 1.4, ²J_{PP} = 202 Hz, ¹J_{RhP} = 142 Hz, ²J_{PP} = 44 Hz). X-ray diffraction study of the compound Rh^I(^{Pyr}PCP)PEt₃CO₃ points out the possibility of *cisoid* coordination of ^{Pyr}PCP.

(12) (a) Zhang, Y.; Lewis, J. C.; Bergman, R. G.; Ellman, J. A.; Oldfield, E. *Organometallics* **2006**, *25*, 3515–3519. (b) Brookhart, M.; Green, M. L. H.; Parkin, G. *Proc. Natl. Acad. Sci.* **2007**, *104*, 6908–6914.

(13) Tolman, C. A. *Chem. Rev.* **1977**, *77*, 313.

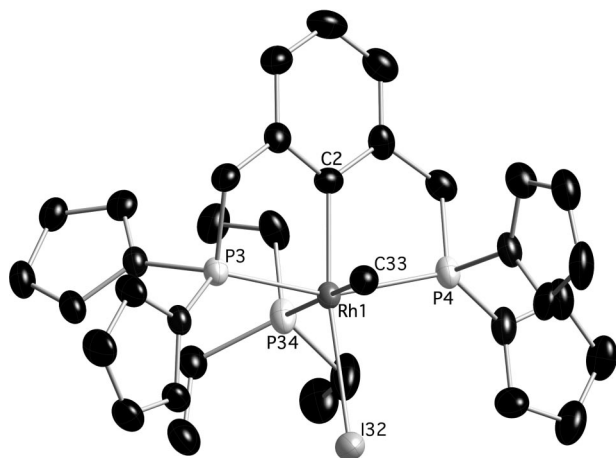


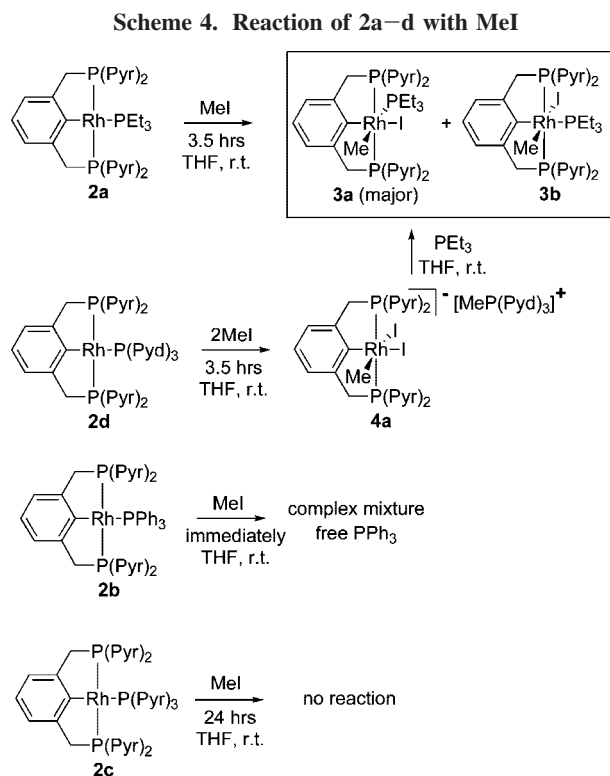
Figure 2. ORTEP diagram of a molecule of complex **3a** at the 50% probability level. Hydrogen atoms were omitted for clarity.

The equilibrium between **2a** and **2c** is a clear example of associative ancillary ligand exchange of a square-planar d^8 ML_4 metal center. Associative ligand exchange is likely to be more suitable for electron-deficient metal centers. This is due to two facts: first, the dissociative pathway demands formation of highly electron deficient $14e$ species; second, filled–filled orbital repulsions between HOMO orbitals of a d^8 ML_4 compound (d_{z^2}) and an incoming ligand are less pronounced for electron-deficient d^8 ML_4 complexes, because of overall reduction in the energy of the metal d -orbitals.³

H₂ Activation by 2a–d. Although no reaction was observed when 1 equiv of hydrogen gas was added to **2a–d**, activation of H_2 was evident from the ability of complexes **2a–d** to catalyze the hydrogenation of styrene to ethyl benzene. In a typical experiment, a 1 mL toluene- d_8 solution containing 0.029 mmol of the complex and 30 equiv of styrene was stirred at room temperature under H_2 (25 psi) and analyzed after 30 min, for the purpose of comparison between complexes **2a–d**. The conversion to ethyl benzene after that period was **2b** (22%), **2a** (9.4%), **2d** (1.7%), and **2c** (0.5%). However, some decomposition was observed in the cases of **2c,d**, rendering comparison impossible in these cases. No decomposition was observed with **2a,b** under the same reaction conditions. The higher catalytic activity of **2b** for styrene hydrogenation as compared with **2a** might be due to PPh_3 being more loosely bound than PEt_3 , suggesting that $14e$ intermediates are the active species during olefin hydrogenation¹⁴ with ^{Pyr}PCP -rhodium(I).

Reaction of 2a–d with MeI. The nucleophilicity of **2** was examined using MeI as an electrophile. Oxidative addition of alkyl halides to transition metals is a process of much interest since it is involved in important catalytic processes, such as carbonylation of alkyl¹⁵ and aryl¹⁶ halides and the iodide-promoted methanol carbonylation to acetic acid.¹⁷

Reaction of **2a** with 1 equiv of MeI in THF was complete after 3.5 h at room temperature (Scheme 4), leading to formation of three new compounds, **3a–c**. Multinuclear NMR analysis revealed the geometries of the main products **3a** (80% yield by $^{31}P\{^1H\}$ NMR) and **3b** (15% NMR yield). However, we could not establish the geometry of the very minor product (5%), **3c**.



All three products are Rh^{III} complexes based on $^1J_{RhP}$ coupling constants. Namely, the $^{31}P\{^1H\}$ NMR spectrum of **3a** revealed a doublet of doublets at δ 113.8 ppm with $^1J_{RhP} = 144.5$ Hz and $^2J_{PP} = 24.1$ Hz and a doublet of triplets at δ -14.4 ppm with $^1J_{RhP} = 74.8$ Hz (**3b,c** showed similar signals to those of **3a** in the $^{31}P\{^1H\}$ NMR). PEt_3 is coordinated *trans* to the CH_3 group in **3a**, as deduced from the $^{13}C\{^1H\}$ NMR spectrum, which revealed a doublet of doublets of triplets at δ -3.32 with $^2J_{PC, trans} = 72.7$ Hz, $^1J_{RhC} = 15.5$ Hz, and $^2J_{PC, cis} = 6.6$ Hz for $Rh-CH_3$. In complex **3b** PEt_3 is bound *cis* to CH_3 , which appeared in the $^{13}C\{^1H\}$ NMR spectrum as a doublet of quartets at δ -4.8 with $^1J_{RhC} = 15.8$ Hz and $^2J_{PC, cis} = 5.3$ Hz. The geometry of **3a** was also revealed by a single-crystal X-ray study (Figure 2, Table 3). Yellow prismatic crystals of **3a** were obtained at room temperature from a concentrated MeOH solution of a mixture of complexes **3**. Complex **3a** exhibits a distorted octahedral coordination geometry, with a ligand arrangement consistent with the multinuclear NMR data.

Reaction of **2d** with 2 equiv of MeI was complete after 3.5 h at room temperature, resulting in quantitative formation of $[Rh(^{Pyr}PCP)Me(I)_2][MePPy_3]$, **4a** (Scheme 4). When 1 equiv of MeI was used, only half the amount of **2d** was consumed to give **4a**, the other half of **2d** remaining unreacted. The $^{31}P\{^1H\}$ NMR spectrum of **4a** showed a doublet at δ 113.5 ppm with $^2J_{RhP} = 151.3$ Hz for ^{Pyr}PCP and a singlet at δ 43.86 ppm for $[MePPy_3]^+$. The aryl *ipso* carbon, $C_{ipso-Rh}$, appeared as a doublet of triplets at δ 169.1 ppm with $^1J_{RhC} = 34.0$ Hz (unresolved triplet) in the $^{13}C\{^1H\}$ NMR. The methyl group, $Rh-CH_3$, appeared in the 1H NMR spectrum as a triplet of doublets at δ 0.116 ppm with $^3J_{PH} = 6.3$ Hz and $^2J_{RhH} = 1.92$ Hz, and in the $^{13}C\{^1H\}$ NMR spectrum it gave rise to a doublet of triplets at δ -0.233 ppm with $^1J_{RhC} = 22.3$ Hz and $^2J_{PC} = 4.7$ Hz. Reaction of **4a** with 1 equiv of PEt_3 resulted in formation of **3a** and **3b** (90% and 10% yield by $^{31}P\{^1H\}$ NMR, respectively) accompanied by precipitation of $[MePPy_3]I$ (Scheme 4). The prevailing formation of **3a** indicates a stronger *trans* influence of the methyl ligand compared to the aryl ligand. The *trans* influence is reflected by the weaker binding of the iodide *trans*

(14) Daniel, C.; Koga, N.; Han, J.; Fu, X. Y.; Morokuma, K. *J. Am. Chem. Soc.* **1988**, *110*, 3773–87, and references therein.

(15) Ellis, P. R.; Pearson, J. M.; Haynes, A.; Adams, H.; Bailey, N. A.; Maitlis, P. M. *Organometallics* **1994**, *13*, 3215–26.

(16) Mizuno, T.; Alper, H. *J. Mol. Catal. A: Chem.* **1997**, *123*, 21–24.

(17) Maitlis, P. M.; Haynes, A.; Sunley, G. J.; Howard, M. J. *J. Chem. Soc., Dalton Trans.* **1996**, 2187–2196.

Table 3. Selected Bond Lengths (Å) and Angles (deg) of **3a**, **4b**, and **2e**

Rh ^{(PyrPCP)Me(I)PEt₃, 3a}		[Rh ^{(PyrPCP)Me(I)₂][NBu₄], 4b}		Rh ^{(PyrPCP)CO, 2e}	
Rh1–C2 _{ipso}	2.068(5)	Rh1–C2 _{ipso}	2.048(6)	Rh1–C1 _{ipso}	2.094(2)
Rh1–P3	2.274(2)	Rh1–P3	2.268(2)	Rh1–P1	2.249(1)
Rh1–P4	2.280(2)	Rh1–P4	2.287(2)	Rh1–P2	2.270(1)
Rh1–C33	2.156(5)	Rh1–C34	2.115(5)	Rh1–C25	1.884(3)
Rh1–I32	2.791(1)	Rh1–I32	2.784(1)	C25–O1	1.147(3)
Rh1–P34 _{ancil.}	2.434(2)	Rh1–I33	2.815(1)	C1–Rh1–P1	78.10(8)
C2–Rh1–C33	86.4(2)	C2–Rh1–C34	91.4(3)	C1–Rh1–P2	78.70(7)
C2–Rh1–P34	95.3(2)	C2–Rh1–I33	88.7(2)	P1–Rh1–P2	156.75(3)
C2–Rh1–I32	169.7(2)	C2–Rh1–I32	179.8(2)	C1–Rh1–C25	174.3(1)
P34–Rh1–I32	93.7(1)			Rh1–C25–O1	175.8(2)

to the methyl group in **4b** (Figure 3 and Table 3 describe the single-crystal X-ray study of **4b** (*vide infra*)). Addition of an excess of PEt₃ did not result in further reaction.

Addition of 1 equiv of MeI to Rh^I(PyrPCP)PPh₃, **2b**, resulted in immediate formation of an inseparable complex product mixture. However, based on the ³¹P{¹H} NMR spectrum (doublets at 114–116 ppm, ¹J_{RhP} = 148–150 Hz) one can conclude that oxidative addition of MeI to rhodium(I) took place, accompanied by dissociation of PPh₃.

Remarkably, no reaction was observed during more than 24 h after addition of MeI to Rh^I(PyrPCP)PPyr₃, **2c**.

It seems that the reaction of **2** with MeI strongly depends on the sterics and nucleophilicity of the ancillary ligand bound to PyrPCP-Rh^I. The remarkable stability of **2c** toward oxidative addition of MeI can arise from low nucleophilicity of the metal center as well as from the steric hindrance caused by the relatively bulky PPyr₃. Unlike PPyr₃, dissociation of PPyr₃ from the rhodium center cannot be promoted by formation of its phosphonium iodide salt, since PPyr₃ is not nucleophilic enough to react with MeI. This quaternization reaction drives the dissociation equilibrium of PPyr₃ to the right and also generates the iodide anion, which might also affect the oxidative addition reaction.

In order to explore the iodide effect on the oxidative addition of MeI, complex **2c** was reacted with 1 equiv of MeI in the presence of 1 equiv of the iodide salt [NBu₄]I. Interestingly, as opposed to the lack of reaction in the absence of iodide, the reaction was complete after 2.5 h, leading to formation of **4b**

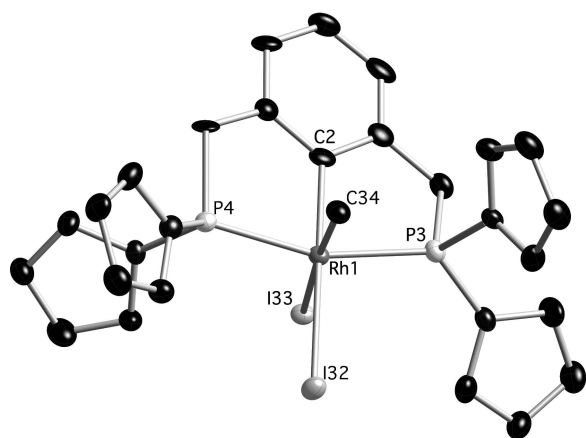
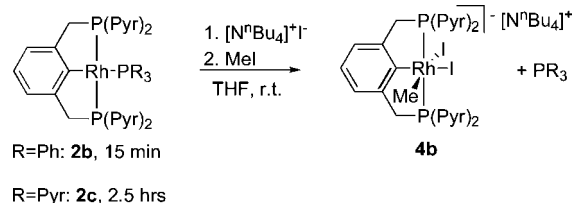


Figure 3. ORTEP diagram of a molecule of complex **4b** at the 50% probability level. Hydrogen atoms and counteranion [NBu₄]⁺ were omitted for clarity.

Scheme 5. Effect of Iodide on the Reaction of **2b,c** with MeI



accompanied by release of PPyr₃ (Scheme 5).¹⁸ Colorless prismatic crystals of **4b** were obtained from a 1:1 THF/pentane solution. The single-crystal X-ray structure of **4b** revealed a distorted octahedral geometry with *cis* arrangement of the iodide ligands (Figure 3). As mentioned above, the stronger *trans* influence of the methyl ligand as compared with the aryl ligand results in weaker binding of the iodide *trans* to the methyl group, than to the aryl, as reflected in the bond lengths: 2.815 and 2.784 Å, respectively.

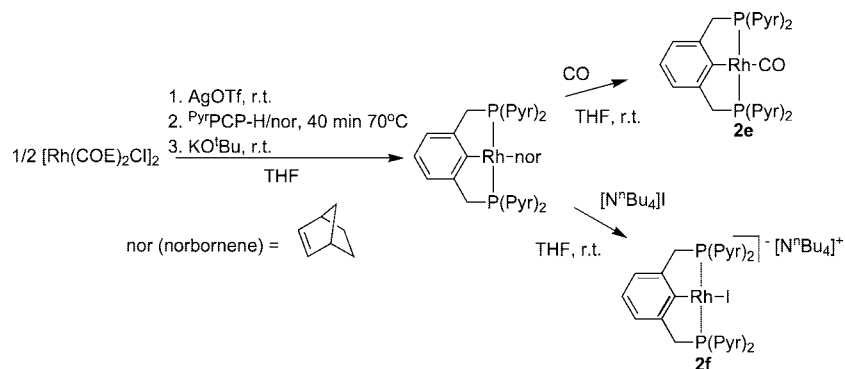
In order to examine the impact of steric hindrance on the lack of reactivity of **2c** with MeI, we explored the reaction of Rh^I(PyrPCP)CO, **2e**, with MeI. Unlike **2c**, complex **2e** has a strongly π -accepting, but sterically undemanding ancillary ligand (CO).

The synthesis of **2e** is summarized in the Scheme 6. The cationic rhodium(I) precursor [Rh(COE)₂(THF)_n](OTf)¹⁹ was prepared *in situ* by adding 2 equiv of AgOTf to [Rh^I(COE)₂μCl]₂ in THF at room temperature. Then 2 equiv of PyrPCP-H and an excess of norbornene were added, and the reaction mixture was heated in THF at 70 °C for 40 min. Subsequent addition of KO^tBu resulted in formation of the rhodium(I) complex Rh^I(PyrPCP)(nor) (nor = norbornene), which was stable only in the presence of excess norbornene, making impossible its purification and full characterization. The ³¹P{¹H} NMR spectrum of Rh^I(PyrPCP)(nor) revealed a doublet at 132 ppm with ¹J_{RhP} = 201 Hz, which is characteristic of PyrPCP-Rh^I complexes. The methylene protons of the PyrPCP appeared in the ¹H NMR spectrum at 4.29 ppm as a virtual triplet with ²J_{PH} = 3.6 Hz, indicating the C_{2v} symmetry of the complex. Bubbling of CO through the crude solution of Rh^I(PyrPCP)(nor) resulted in formation of **2e**. The ³¹P{¹H} NMR spectrum of **2e** exhibited a doublet at 119.8 ppm (¹J_{RhP} = 194.4 Hz). The methylene protons of the PyrPCP gave rise to a virtual triplet at 4.49 ppm with ²J_{PH} = 4.7 Hz in ¹H NMR, thus indicating the C_{2v} symmetry of the complex. The *ipso* carbon, C_{ipso}-Rh, appeared as a doublet of

(18) ³¹P{¹H} NMR (THF) showed a significant broadening of the spectrum of **2c** in the presence of [NBu₄]I: full width at half-height (fwhh) was equal to 25 Hz in the presence of 1 equiv of [NBu₄]I and 7 Hz for pure **2c**. No compound, other than **2c**, was observed at low temperature (down to 213 K). The same shapes of signals were observed at a certain temperature, whether reached by cooling or heating.

(19) (a) Osborn, J. A.; Schrock, R. R. *J. Am. Chem. Soc.* **1971**, *93*, 3089–3091. (b) Gandelman, M.; Konstantinovskii, L.; Rozenberg, H.; Milstein, D. *Chem.–Eur. J.* **2003**, *9*, 2595–2602.

Scheme 6. Synthesis of Complexes 2e,f



triplets at 172.16 ppm ($^1J_{\text{RhC}} = 28.2$ Hz, $^2J_{\text{PC}} = 9.25$ Hz) in the $^{13}\text{C}\{^1\text{H}\}$ NMR spectrum. The carbonyl group gave rise to a doublet of triplets at 196.62 ppm ($^1J_{\text{RhC}} = 55.3$ Hz, $^2J_{\text{PC}} = 14.2$ Hz) in the $^{13}\text{C}\{^1\text{H}\}$ NMR spectrum and exhibited a strong IR absorption band at 1969 cm^{-1} . Yellow crystals of **2e** were obtained by slow diffusion of pentane into a concentrated THF solution of **2e**. The single-crystal X-ray structure of **2e** exhibits a distorted square-planar geometry (Figure 4, Table 3), in agreement with the multinuclear NMR spectra.

Reaction of **2e** with MeI resulted in C–C bond formation with the *ipso* carbon to give η^2 -($\text{Py}^*\text{PCP-Me}$) $\text{Rh}^{\text{I}}\text{CO(I)}$, **5** (Scheme 7). The reaction was complete after 2 weeks at ambient temperature (38% and 78% spectral conversions were observed after 3 and 7 days, respectively). The $^{31}\text{P}\{^1\text{H}\}$ NMR spectrum of **5** exhibited a doublet at 102.4 ppm ($^1J_{\text{RHP}} = 154.6$ Hz). The methylene groups of the Py^*PCP ligand appeared at 4.84 ppm as a broad singlet in the ^1H NMR spectrum and as a virtual triplet at 38.89 ppm ($^1J_{\text{PC}} = 16.7$ Hz) in the $^{13}\text{C}\{^1\text{H}\}$ NMR spectrum. The carbonyl group gave rise to a doublet of triplets at 181.5 ppm ($^1J_{\text{RhC}} = 76$ Hz, $^2J_{\text{PC}} = 14$ Hz) in the $^{13}\text{C}\{^1\text{H}\}$ NMR spectrum, and in the IR spectrum it gave rise to a strong absorption band at 2008 cm^{-1} . The $^{31}\text{P}\{^1\text{H}\}$ NMR spectrum of the phosphines and the $^{13}\text{C}\{^1\text{H}\}$ NMR spectrum of the methylene and the carbonyl groups revealed the *trans* coordination of the phosphines. No signal was detected for the aryl carbon bound to the rhodium center. The methyl group gave rise to a singlet at 1.42 ppm in the ^1H NMR spectrum and a singlet at 14.61 ppm in the $^{13}\text{C}\{^1\text{H}\}$ NMR spectrum, as confirmed by C–H correlation. The methylated Py^*PCP pincer ligand ($\text{Py}^*\text{PCP-Me}$) was released from the metal center by its substitution with P^iPr_3 and was purified and characterized separately (Scheme 7).

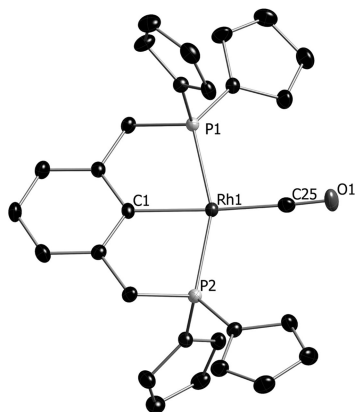


Figure 4. ORTEP diagram of a molecule of complex **2e** at the 50% probability level. Hydrogen atoms were omitted for clarity.

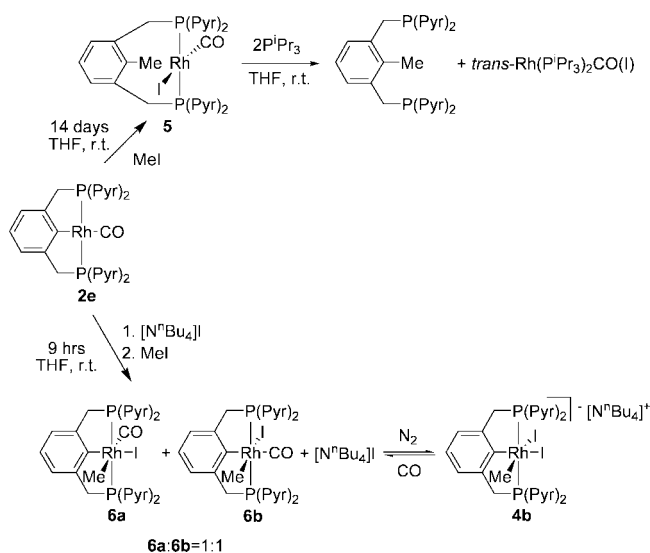
The reaction of **2e** with MeI, in contrast to the remarkable stability of **2c** toward MeI, highlights the impact of steric hindrance on reactivity of the metal center. It is important to mention that MeI attack is likely to proceed on the rhodium center of **2e**, rather than directly on the *ipso* carbon of the aryl ring; otherwise **2c** would be expected to react in a similar way to **2e**, since the *ipso* carbon is not strongly affected by sterics of an ancillary ligand, as can be seen from the single-crystal X-ray studies of the compounds **2b–e**. Consequently, addition of MeI to **2e** probably proceeds by an $\text{S}_{\text{N}}2$ mechanism.²⁰ Thus, nucleophilic attack of rhodium on the methyl group results in formation of an electron-deficient cationic rhodium(III) species, $[\text{Rh}^{\text{III}}(\text{Py}^*\text{PCP})\text{CO}(\text{Me})]^+$, which undergoes C–C reductive elimination to give **5**. Square-planar d^8 rhodium complexes usually react easily with methyl iodide to afford octahedral d^6 compounds.²¹ However, the electron density around the metal center plays a key role in the addition of MeI. For example, as published by our group, $\text{Rh}^{\text{I}}(\text{P}^i\text{Pr}_3)_2\text{-}\eta^2\text{-OTf}$ showed remarkable stability toward MeI addition, unlike $\text{Rh}^{\text{I}}(\text{PET}_3)_3\text{Cl}$.²² Although coordination of the electron-accepting Py^*PCP and PPyr_3 to rhodium(I) resulted in reduction of the electron density on the metal center, it is more likely that the stability of **2c** toward oxidative addition of MeI in the absence of added iodide, I^- , is due to steric hindrance at the metal center and low nucleophilicity of PPyr_3 (*vide infra*).

Although reaction of **2e** with MeI resulted in the demetalated rhodium(I) product **5**, and no $\text{Rh}^{\text{III}}(\text{Py}^*\text{PCP})\text{Me(I)CO}$ was detected, this fact does not exclude the possibility of existence of $\text{Rh}^{\text{III}}(\text{Py}^*\text{PCP})\text{Me(I)CO}$. Indeed, reaction of **4** with CO in THF resulted in formation of $\text{Rh}^{\text{III}}(\text{Py}^*\text{PCP})\text{Me(I)CO}$, **6a** and **6b** (1:1), accompanied by dissociation of the corresponding iodide salt, as either $[\text{NBu}_4]\text{I}$ or $[\text{MePPy}_3]\text{I}$ (Scheme 7). In the presence of an equivalent amount of $[\text{NBu}_4]\text{I}$ or $[\text{MePPy}_3]\text{I}$, CO binds reversibly to the rhodium center of **6a,b** and can be easily removed by bubbling N_2 through the reaction mixture. The $^{31}\text{P}\{^1\text{H}\}$ NMR spectrum of **6a,b** showed doublets at δ 120.5 ($^1J_{\text{RHP}} = 133.6$ Hz) and 111.8 ($^1J_{\text{RHP}} = 135.4$ Hz). The methyl groups, Rh-CH_3 , appeared in the ^1H NMR spectrum as triplets of doublets at δ 0.303 ($^3J_{\text{PH}} = 8.16$ Hz, $^2J_{\text{RHH}} = 1.81$ Hz) and 0.014 ($^3J_{\text{PH}} = 6.04$ Hz, $^2J_{\text{RHH}} = 2.1$ Hz) and in the $^{13}\text{C}\{^1\text{H}\}$ NMR spectrum as doublets of triplets at δ -2.78 ($^1J_{\text{RhC}} = 15.5$ Hz, $^2J_{\text{PC}} = 5.9$ Hz) and -6.9 ($^1J_{\text{RhC}} = 20.47$ Hz, unresolved

(20) Chauby, V.; Daran, J.-C.; Serra-Le Berre, C.; Malbosc, F.; Kalck, P.; Gonzales, O. D.; Haslam, C. E.; Haynes, A. *Inorg. Chem.* **2002**, *41*, 3280–3290.

(21) (a) Sharp, P. R. In *Comprehensive Organometallic Chemistry II*; Abel, E. W., Stone, F. G. A., Wilkinson, G., Atwood, J. D., Eds.; Pergamon, 1995; Vol. 8, pp 190–200. (b) Aullon, G.; Alvarez, S. *Inorg. Chem.* **1996**, *35*, 3137–44.

(22) Goikhman, R.; Milstein, D. *Angew. Chem., Int. Ed.* **2001**, *40*, 1119–1122.

Scheme 7. Reaction of **2e** with MeI

triplet). The carbonyl groups appeared at δ 189.5 and 180.9 ppm, and the aryl *ipso* carbons, C_{ipso} -Rh, appeared at 166.1 and 161.0 ppm in the $^{13}\text{C}\{^1\text{H}\}$ NMR spectrum.

Interestingly, formation of **6a,b** was also observed during reaction of **2e** with MeI in the presence of 1 equiv of $[\text{NBu}_4]\text{I}$. It was complete after 9 h, leading to the formation of **4b**, **6a**, and **6b** (9:1:1, respectively). The reaction was also examined at earlier stages, e.g., 4 h after adding MeI, and $^{31}\text{P}\{^1\text{H}\}$ NMR showed that ca. 70% of **2e** had reacted to give **4b**:**6a**:**6b** \approx 4:1:1. Obviously, **4b** was formed after CO dissociation from **6a,b** in the presence of $[\text{NBu}_4]\text{I}$. No interaction was observed between **2e** and $[\text{NBu}_4]\text{I}$ at room temperature by $^{31}\text{P}\{^1\text{H}\}$ NMR, and $[\text{Rh}^{\text{I}}(\text{Pyr}^{\text{PCP}})\text{I}][\text{NBu}_4]$, **2f**, was not observed after 3 days of stirring at room temperature. To confirm this, complex **2f** was prepared separately by reaction of $\text{Rh}^{\text{I}}(\text{Pyr}^{\text{PCP}})(\text{nor})$ with $[\text{NBu}_4]\text{I}$ (Scheme 6). $^{31}\text{P}\{^1\text{H}\}$ NMR of **2f** exhibited a doublet at 108.2 ppm ($^1J_{\text{RhP}} = 221.27$ Hz). The methylene protons of the Pyr^{PCP} appeared at 3.96 ppm as a virtual triplet with $^2J_{\text{PH}} = 4.2$ Hz in the ^1H NMR spectrum, thus indicating the C_{2v} symmetry of the complex. The *ipso* carbon, C_{ipso} -Rh, appeared as a doublet of triplets at 173.49 ppm ($^1J_{\text{RhC}} = 41.1$ Hz, $^2J_{\text{PC}} = 8.6$ Hz) in the $^{13}\text{C}\{^1\text{H}\}$ NMR spectrum.

In the presence of $[\text{NBu}_4]\text{I}$ C–C reductive elimination is prevented during the reaction of **2e** with MeI. This indicates that C–C reductive elimination probably proceeds by a dissociative mechanism, involving prior iodide dissociation to form the coordinatively unsaturated 16e cationic $[\text{Rh}^{\text{III}}(\text{Pyr}^{\text{PCP}})\text{Me}(\text{CO})]^+$ species. The requirement for ligand dissociation prior to C–H and C–C reductive elimination of octahedral rhodium(III) complexes was reported.²³

Since PPy_3 and PPy_3 are isosteric, the rhodium center of **2d**, similarly to that of **2c**, seems to be too sterically hindered for a direct attack on MeI. The reaction proceeds via formation of $[\text{MePPy}_3]\text{I}$ (Scheme 4). Once formed, $[\text{MePPy}_3]\text{I}$ may be involved in the addition of MeI to the rhodium center. Indeed, in the presence of 1 equiv of $[\text{NBu}_4]\text{I}$ the reaction proceeded faster and was completed after 2 h. Nevertheless, almost 2 equiv of MeI were required to complete the reaction.

As concluded from the results described in the previous sections, the Rh– PPh_3 bond is the weakest among the examined Rh– PR_3 (R = Et, Pyd, Ph, Pyr). The reaction of $\text{Rh}^{\text{I}}(\text{PCP})\text{PPh}_3$,

2b, with MeI is fast. Although we did not succeed in separating the products, it is important to note that only 1 equiv of MeI was required to complete the reaction, which was accompanied by dissociation of PPh_3 . These observations suggest involvement of 14e $\text{Rh}^{\text{I}}(\text{Pyr}^{\text{PCP}})$ species in the reaction of **2b** with MeI. MeI addition to the highly electron deficient 14e species may proceed either by a three-centered mechanism²⁴ or by addition of iodide prior to methyl addition.²⁵ Dissociation of PPh_3 results in liberation of $\text{Rh}^{\text{I}}(\text{Pyr}^{\text{PCP}})$ 14e species, which is likely to be more reactive toward MeI than PPh_3 . Therefore, the amount of the phosphonium salt $[\text{MePPh}_3]\text{I}$, which can play the role of the iodide donor, like $[\text{MePPy}_3]\text{I}$, is insufficient. Indeed, upon addition of 1 equiv of $[\text{NBu}_4]\text{I}$ the reaction of **2b** with 1 equiv of MeI was complete after 15 min, leading to quantitative formation of **4b** (Figure 3, Table 3) accompanied by release of PPh_3 (Scheme 5).²⁶ Addition of 1 equiv of TIPF_6 to **4b** in the presence of 1 equiv of PPh_3 resulted in formation of the same complex mixture as during reaction of **2b** with 1 equiv of MeI.

Acceleration of oxidative addition reactions by halide ions has been reported.²⁷ For example, the catalytic action of Pd^0L_2 complexes in cross-coupling of aryl halides with nucleophiles and in the Heck reaction was found to depend on the concentration of an additive anion, e.g., Cl^- , thus indicating involvement of a trivalent anionic complex, $[\text{Pd}^0\text{L}_2\text{Cl}]^-$, in the catalytic cycle, which makes the latter more efficient.²⁸ $[\text{NBu}_4]\text{I}$ can affect either the transition or ground state of the reaction of **2b,c** with MeI. Concerning its effect on the ground state, the much faster reaction of **2b**, compared to **2c**, points at $[\text{Rh}^{\text{I}}(\text{Pyr}^{\text{PCP}})\text{I}][\text{NBu}_4]$ as a reactive specie, since the Rh– PPh_3 bond is weaker than Rh– PPy_3 . Indeed, $[\text{Rh}^{\text{I}}(\text{Pyr}^{\text{PCP}})\text{I}][\text{NBu}_4]$ immediately reacted with MeI to give **4b**.

Conclusions

The reactivity of rhodium(I) complexes based on the recently reported strongly electron accepting PCP-pincer ligand dipyrrolylphosphinoxylene (Pyr^{PCP}) was investigated. Complexes of the type $\text{Rh}^{\text{I}}(\text{Pyr}^{\text{PCP}})\text{PR}_3$ (R = Et, Ph, Pyr, PPyd) (**2**) were synthesized.

The ancillary ligand coordination is governed by *trans* effect, rather than by the overall reduction in electron density at the rhodium center caused by Pyr^{PCP} chelation.

The ancillary ligand substitution process at the Pyr^{PCP} -based rhodium(I) center proceeds via an associative mechanism. An associative, contrary to dissociative, ligand exchange mechanism is likely to be more suitable for electron-deficient metal centers due to avoiding formation of electron-deficient 14e species and due to overall stabilization of the metal d-orbitals,³ which leads

(24) Venter, J. A.; Leipoldt, J. G.; van Eldik, R. *Inorg. Chem.* **1991**, *30*, 2207–2209.

(25) (a) Louw, W. J.; de Waal, D. J. A.; Chapman, J. E. *Chem. Commun.* **1977**, 845–846. (b) Ashworth, T. V.; Singleton, J. E.; de Waal, D. J. A.; Louw, W. J.; Singleton, E.; van der Stok, E. *J. Chem. Soc., Dalton Trans.* **1978**, 340–347. (c) Crabtree, R. H.; Quirk, J. M.; Fillebeen-Khan, T.; Morris, G. E. *J. Organomet. Chem.* **1979**, *181*, 203–212. (d) Crabtree, R. H.; Quirk, J. M. *J. Organomet. Chem.* **1980**, *199*, 99–106.

(26) $^{31}\text{P}\{^1\text{H}\}$ NMR (THF) showed a slight broadening of the spectrum of **2b** in the presence of $[\text{NBu}_4]\text{I}$: fwhh was equal to 8 Hz in the presence of 1 equiv of $[\text{NBu}_4]\text{I}$ and 4.3 Hz for a pure **2b**. No compound, other than **2b**, was observed at low temperature (down to 213 K). The same shapes of signals were observed at a certain temperature, whether reached by cooling or heating.

(27) Fairlamb, I. J. S.; Taylor, R. J. K.; Serrano, J. L.; Sanchez, G. *New J. Chem.* **2006**, *30*, 1695–1704.

(28) (a) Amatore, C.; Jutand, A. *J. Organomet. Chem.* **1999**, *576*, 254–278. (b) Amatore, C.; Jutand, A. *Acc. Chem. Res.* **2000**, *33*, 314–321. (c) Kozuch, S.; Amatore, C.; Jutand, A.; Shaik, S. *Organometallics* **2005**, *24*, 2319–2330.

(23) (a) Milstein, D. *J. Am. Chem. Soc.* **1982**, *104*, 5227–5228. (b) Milstein, D. *Acc. Chem. Res.* **1984**, *17*, 221–226.

to reduced filled–filled orbital repulsions between HOMO orbitals of a d^8 ML_4 compound (d_z^2) and an incoming ligand.

Complexes **2** catalyze styrene hydrogenation to ethyl benzene. Comparison between the reactivities of **2a** and **2b** suggests, although does not prove, that a $14e$ intermediate is the active species in this process.

The ability of **2** to oxidatively add MeI depends on the sterics, nucleophilicity, and binding strength of the ancillary ligand to the rhodium center. The complexes $Rh^I(PyrPCP)L$ are thought to follow a two-step S_N2 mechanism when the metal center is not sterically hindered, e.g., $L = PET_3$ (**2a**), CO (**2e**). Coordination of relatively bulky PR_3 ($R = Pyd, Ph, Pyr$; cone angle 145°) to the rhodium(I) sterically hinders nucleophilic attack by d^8 RhL_4 on MeI.

Reaction of $Rh^I(PyrPCP)PPh_3$, **2b**, with MeI is thought to proceed via the $Rh^I(PyrPCP)$ 14-electron species, owing to the relatively weak $Rh-PPh_3$ bond.

The inertness of $Rh^I(PyrPCP)PPyr_3$, **2c**, toward oxidative addition of MeI is due to a number of factors: steric hindrance at the metal center, $Rh-PPyr_3$ bond strength, and the low nucleophilicity of $PPyr_3$. Steric hindrance disfavors an S_N2 mechanism; strong binding of $PPyr_3$ to the rhodium center disfavors intermediacy of a 14-electron species; low nucleophilicity of $PPyr_3$ disfavors a reaction involving formation of $[MePPyr_3]I$, unlike the case of $Rh^I(PyrPCP)PPy_3$, **2d**.

Experimental Section

General Procedures. All experiments with metal complexes and phosphine ligands were carried out under an atmosphere of purified nitrogen in a Vacuum Atmospheres glovebox equipped with a MO 40-2 inert gas purifier or using standard Schlenk techniques. All solvents were reagent grade or better. All nondeuterated solvents were refluxed over sodium/benzophenone ketyl and distilled under argon atmosphere. Deuterated solvents were used as received. All the solvents were degassed with argon and kept in the glovebox over 4 Å molecular sieves. Commercially available reagents were used as received. $[Rh^I(COE)_2\mu Cl]_2$,²⁹ **1a,b**, and **2a–c** were prepared according to a literature procedure.

1H , ^{13}C , ^{31}P , and ^{19}F NMR spectra were recorded at 400, 100, 162, and 376 MHz, respectively, using a Bruker AMX-400 NMR spectrometer. All spectra were recorded at 295 K, unless otherwise noted. 1H NMR and $^{13}C\{^1H\}$ NMR chemical shifts are reported in ppm downfield from tetramethylsilane and referenced to the residual signals of an appropriate deuterated solvent. ^{31}P NMR chemical shifts are reported in ppm downfield from H_3PO_4 and referenced to an external 85% solution of phosphoric acid in D_2O . ^{19}F NMR chemical shifts are reported in ppm downfield from $CFCl_3$ and referenced to an external solution of C_6F_6 ($\delta = -163$ ppm) in $CDCl_3$.

Elemental analyses were performed by H. Kolbe, Mikroanalytisches Laboratorium, Muelheim, Germany.

Synthesis of $Rh^I(PyrPCP)PPy_3$ (**2d**).

Synthesis of $Rh^I(PyrPCP)$ norbornene. AgOTf (14.3 mg, 0.056 mmol) in THF (1 mL) was added dropwise to $[Rh^I(COE)_2\mu Cl]_2$ (20 mg, 0.028 mmol) in THF (1.5 mL). A gray precipitate appeared immediately. The resulting mixture was left at r.t. for 10 min while stirring, and then it was filtered through a Celite column (2 cm long, in a Pasteur pipette). To the resulting deep yellow solution was added dropwise the ligand $PyrPCP-H$ (24 mg, 0.056 mmol) in THF (0.5 mL) and norbornene (80 mg, 0.85 mmol). The mixture was heated at 70 °C for 40 min. To the resulting brown solution was added dropwise KO^tBu (6.2 mg, 0.056 mmol) in THF (0.5

mL) while stirring. The reaction mixture became dark brown immediately. The yield of $Rh^I(PyrPCP)$ norbornene was 60% by $^{31}P\{^1H\}$ NMR integration. The complex was not stable to vacuum and was stabilized only in the presence of excess norbornene, making impossible its purification and full characterization.

$^{31}P\{^1H\}$ NMR (THF- H_8): 132 (d, $^1J_{RhP} = 201$ Hz). 1H NMR (THF- H_8): 7.04 (br s, Py, 8 $HC-N$, 8H), 6.31 (br s, Py, 8 $HC-HC-N$, 8H), 4.29 (vt, $^2J_{PH} = 3.6$ Hz, 2 Ar- H_2C-P , 4H).

Synthesis of **2d from $Rh^I(PyrPCP)$ norbornene.** To a crude solution of $Rh^I(PyrPCP)$ norbornene (made from 50 mg of $[Rh^I(COE)_2\mu Cl]_2$) was added PPy_3 (30.5 μL , 0.133 mmol), resulting in formation of **2d**. The product was dried by vacuum, extracted with pentane, dried, washed with a small amount of pentane (0.5 mL), and dried again to give 81.7 mg (76%) of **2d** as a yellow solid.

$^{31}P\{^1H\}$ NMR (C_6D_6): 122.4 (dd, $^1J_{RhP} = 214.4$ Hz, $^2J_{PP} = 44.1$ Hz, 2P), 110.6 (dt, $^1J_{RhP} = 147.4$ Hz, 1P). 1H NMR (C_6D_6): 7.13 (m, Pyr, $HC-N$, 8H), 6.95 (m, Ar), 6.26 (m, Pyr, $HC-HC-N$, 8H), 3.82 (vt, $^2J_{PH} = 3$ Hz, Ar- CH_2-P , 4H), 2.92 (m, Pyd, H_2C-N , 12H), 1.37 (m, Pyd, H_3C-H_2C-P , 12H). $^{13}C\{^1H\}$ NMR (C_6D_6): 173.6 (ddt, $^2J_{PC,trans} = 87.4$ Hz, $^1J_{RhC} = 27.9$ Hz, $^2J_{PC,cis} = 10.2$ Hz, $C_{ipso-Rh}$, 1C), 144.05 (vt, $^2J_{PC} = 12.3$ Hz, Ar, C-C-Rh, 2C), 125.51 (s, Ar, CH-CH-C-C-Rh, 1C), 124.42 (vt, $^2J_{PC} = 3.4$ Hz, Pyr, CH-N-P, 8C), 122.2 (vtd, $^3J_{PC} = 10.5$ Hz, $J = 3.8$ Hz, Ar, CH-C-C-Rh, 2C), 111.73 (br s, Pyr, CH-CH-N-P, 8C), 53.61 (vtt, $^1J_{PC} = 16.5$ Hz, $J = 5.2$ Hz, Ar- CH_2-P , 2C), 47.85 (d, $^2J_{PC} = 8.85$ Hz, Pyd, CH_2-N-P , 6C), 25.95 (d, $^3J_{PC} = 6.18$ Hz, Pyd, CH_2-CH_2-N-P , 6C). Anal. (%) Found (Calc): C 56.08 (55.89), H 6.07 (6.12).

Synthesis of $Rh^I(PyrPCP)CO$ (2e**).** CO was bubbled for 30 min through a brown crude solution of $Rh^I(PyrPCP)$ norbornene (made from 100 mg of $[Rh^I(COE)_2\mu Cl]_2$); as described in the procedure for the synthesis of **2d**), resulting in formation of **2e**. The solvent was removed under vacuum, and the residue was washed with toluene (3×3 mL), dried under vacuum, redissolved in CH_2Cl_2 , and filtered. The solvent was removed under vacuum to give 92 mg (59%) of **2e** as a yellow solid.

$^{31}P\{^1H\}$ NMR (THF- d_8): 119.76 (d, $^1J_{RhP} = 194.42$ Hz). 1H NMR (THF- d_8): 7.26 (m, Pyr, $HC-N$, 8H), 7.1 (d, $^3J_{HH} = 7.47$ Hz, Ar, *meta* to Rh, 2H), 6.97 (t, $^3J_{HH} = 7.47$ Hz, Ar, *para* to Rh, 1H), 6.28 (m, Pyr, $HC-HC-N$, 8H), 4.49 (vt, $^2J_{PH} = 4.7$ Hz, Ar- CH_2-P , 4H). $^{13}C\{^1H\}$ NMR (THF- d_8): 196.62 (dt, $^1J_{RhC} = 55.3$ Hz, $^2J_{PC} = 14.2$ Hz, C=O, 1C), 172.16 (dt, $^1J_{RhC} = 28.2$ Hz, $^2J_{PC} = 9.25$ Hz, $C_{ipso-Rh}$, 1C), 147.61 (vtd, $^2J_{PC} = 14.9$ Hz, $^2J_{RhC} = 2.1$ Hz, Ar, C-C-Rh, 2C), 128.37 (s, Ar, CH-CH-C-C-Rh, 1C), 124.76 (vt, $^2J_{PC} = 4.46$ Hz, Pyr, CH-N-P, 8C), 123.13 (vt, $^3J_{PC} = 12.7$ Hz, Ar, CH-C-C-Rh, 2C), 113.40 (vt, $^3J_{PC} = 3.23$ Hz, Pyr, CH-CH-N-P, 8C), 50.0 (vtd, $^1J_{PC} = 19.1$ Hz, $^2J_{RhC} = 4.1$ Hz, Ar- CH_2-P , 2C). IR (film): $\nu_{CO} = 1969$ cm^{-1} . Anal. (%) Found (Calc): C 53.43 (53.59), H 4.11 (4.14).

Reaction of $Rh^I(PyrPCP)PPh_3$ (2b**) with PPy_3 .** PPy_3 (neat, 6.3 μL , 0.027 mmol) was added to a toluene (0.7 mL) solution of **2b** (21.9 mg, 0.027 mmol), resulting in formation of **2d** accompanied by release of 1 equiv of free PPh_3 , as detected by $^{31}P\{^1H\}$ NMR.

Reaction of $Rh^I(PyrPCP)PPyr_3$ (2c**) with PPy_3 .** To a toluene (1 mL) solution of **2c** (23.5 mg, 0.031 mmol) was added PPy_3 (neat, 7.1 μL , 0.031 mmol), resulting in formation of **2d** accompanied by release of 1 equiv of free $PPyr_3$, as detected by $^{31}P\{^1H\}$ NMR.

Reaction of $Rh^I(PyrPCP)PPh_3$ (2b**) with PET_3 .** PET_3 (neat, 3.4 μL , 0.025 mmol) was added to a toluene (0.7 mL) solution of **2b** (19.7 mg, 0.025 mmol), resulting in formation of **2a** accompanied by release of 1 equiv of free PPh_3 , as detected by $^{31}P\{^1H\}$ NMR.

Equilibrium between $Rh^I(PyrPCP)PET_3$ (2a**) and $Rh^I(PyrPCP)PPyr_3$ (**2c**).** Addition of either 1 equiv of $PPyr_3$ (8.8 mg, 0.038 mmol) to **2a** (25.0 mg, 0.038 mmol) or 1 equiv of PET_3 (neat, 4.5 μL , 0.033 mmol) to **2c** (25.5 mg, 0.033 mmol) in toluene (1 mL) resulted in equilibrium between **2a** and **2c** (**2a:2c** = 3.5:1).

(29) Hofmann, P.; Meier, C.; Englert, U.; Schmidt, M. U. *Chem. Ber.* **1992**, *125*, 353–365.

$^{31}\text{P}\{^1\text{H}\}$ NMR (tol- d_8 , 295 K): 126.9 (br s, PCP-**2a**, 2P), 121.4 (br dd, $^1J_{\text{RhP}} = 197.5$ Hz, $^2J_{\text{PP}} = 45$ Hz, PCP-**2c**, 2P), 111.3 (br d, $^1J_{\text{RhP}} = 165.6$ Hz, PPy₃-**2c**, 1P), 83.4 (br s, free PPy₃), 18.7 (br s, PEt₃-**2a**, 1P), -7.8 (s, free PEt₃). ^1H NMR (tol- d_8 , 295 K): 7.2–5.9 (Ar and Pyr of **2a**, **2c** and free PPy₃), 3.75 (br s, **2c**, Ar- H_2 C-P, 4H), 3.70 (br s, **2a**, Ar- H_2 C-P, 4H), 1.47(m, free PEt₃, H_2 C-P, 6H), 1.08 (m, PEt₃-**2a**, H_2 C-P, 6H), 0.97 (m, free PEt₃, H_3 C- H_2 C-P, 9H), 0.83 (m, PEt₃-**2a**, H_3 C- H_2 C-P, 9H). $^{31}\text{P}\{^1\text{H}\}$ NMR (tol- d_8 , 213 K): 120.3 (ddd, $^2J_{\text{PP}} = 312$ Hz, $^1J_{\text{RhP}} = 192$ Hz, $^2J_{\text{PP}} = 44$ Hz, PCP-**2a'**, 2P), 112.46 (ddd, $^2J_{\text{PP}} = 201$ Hz, $^1J_{\text{RhP}} = 191$ Hz, $^2J_{\text{PP}} = 42$ Hz, PCP-**2c'**, 2P), 98.9 (m, PPy₃-**2a'**, 1P), 8.1 (dq, $^1J_{\text{RhP}} = 93$ Hz, $^2J_{\text{PP}} = 42$ Hz, PEt₃-**2a'**, 1P), 1.4 (tdd, $^2J_{\text{PP}} = 202$ Hz, $^1J_{\text{RhP}} = 142$ Hz, $^2J_{\text{PP}} = 44$ Hz, PEt₃-**2c'**, 1P), the signal of the ancillary PPy₃ of **2c'** is obscured by other peaks. ^1H NMR (tol- d_8 , 213 K): 7.2–5.9 (Ar and Pyr of **2a'** and **2c'**), 4.05 (br d, AB pattern, $^2J_{\text{HH}} = 15$ Hz, **2c'**, Ar- H (H)C-P, 2H), 3.82 (br d, AB pattern, $^2J_{\text{HH}} = 15$ Hz, **2c'**, Ar- H (H)C-P, 2H), 3.44 (br d, AB pattern, $^2J_{\text{HH}} = 15.4$ Hz, **2a'**, Ar- H (H)C-P, 2H), 3.34 (br d, AB pattern, $^2J_{\text{HH}} = 15.4$ Hz, **2c'**, Ar- H (H)C-P, 2H), 1.43 (m, Et-**2c'**, H_2 C-P, 6H), 1.36 (br s, Et-**2a'**, H_2 C-P, 6H), 0.92 (m, Et-**2c'**, H_3 C- H_2 C-P, 9H), 0.61 (m, Et-**2a'**, H_3 C- H_2 C-P, 9H).

Equilibrium between Rh^I(PyrPCP)PPh₃ (2b**) and Rh^I(PyrPCP)PPy₃ (**2c**).** Addition of either 1 equiv of PPy₃ (6.6 mg, 0.029 mmol) to **2b** (22.8 mg, 0.029 mmol) or 1 equiv of PPh₃ (7.7 mg, 0.029 mmol) to **2c** (22.5 mg, 0.029 mmol) in toluene (1 mL) resulted in equilibrium between **2b** and **2c** (**2b**:**2c** = 1:4.5).

Reaction of Rh^I(PyrPCP)PR₃ (R = Et (a**); Ph (**b**); Pyr (**c**); Pyd (**d**)) with H₂.** In a typical experiment a toluene- d_8 solution (1 mL, final volume) of catalyst (0.029 mmol) was incubated with styrene (0.87 mmol) under H₂ (25 psi) in an 80 mL glass pressure tube during 30 min at room temperature. No significant decrease in H₂ pressure was detected for **2a,c,d**, while the pressure decreased to 22.5 psi for **2b**. Percents of conversion were estimated by ^1H NMR spectroscopy, revealing reduction of styrene to ethyl benzene: **2a** 9.4%, **2b** 22%, **2c** 0.5%, **2d** 1.7%. Slight decay of **2c** (5–10%) and **2d** (up to 10%) was observed by $^{31}\text{P}\{^1\text{H}\}$ NMR.

Reaction of 2a with MeI. To a solution of **2a** (30.4 mg, 0.047 mmol) in toluene (1 mL) was added MeI (3 μL , 0.048 mmol), resulting in a deep red solution. $^{31}\text{P}\{^1\text{H}\}$ NMR showed no starting material left after incubation at RT for 1.5 h and formation of three products (**3**) in the ratio (estimated by $^{31}\text{P}\{^1\text{H}\}$ NMR) **3a**:**3b**:**3c** = 10:2:2.

$^{31}\text{P}\{^1\text{H}\}$ NMR (toluene- d_8) **3a**: 113.8 (dd, $^1J_{\text{RhP}} = 144.5$ Hz, $^2J_{\text{PP}} = 24.1$ Hz, 2P), -14.4 (dt, $^1J_{\text{RhP}} = 74.8$ Hz, 1P); **3c**: 116.0 (dd, $^1J_{\text{RhP}} = 144.4$ Hz, $^2J_{\text{PP}} = 25.9$ Hz, 2P), -8.0 (dt, $^1J_{\text{RhP}} = 74.2$ Hz, 1P); **3b**: 121.1 (dd, $^1J_{\text{RhP}} = 141.0$ Hz, $^2J_{\text{PP}} = 31.3$ Hz, 2P), -9.6 (dt, $^1J_{\text{RhP}} = 80.3$ Hz, 1P). ^1H NMR (toluene- d_8) **3a**: 7.3–6.8 (Ar, *meta* and *para* to Rh, 3H; Pyr, $HC-N$, 8H), 6.15 (m, Pyr, $HC-HC-N$, 4H), 6.13 (m, Pyr, $HC-HC-N$, 4H), 3.90 (dvt, ABX₂, $^2J_{\text{HH}} = 16.7$ Hz, $^2J_{\text{PH}} = 5.3$ Hz, Ar- CH (H)-P, 2H), 3.69 (dvt, ABX₂, $^2J_{\text{HH}} = 16.7$ Hz, $^2J_{\text{PH}} = 3.8$ Hz, Ar- CH (H)-P, 2H), 1.12 (m, H_2 C-P, 6H), 0.57 (m, H_3 C- H_2 C-P, 9H), 0.07 (br q, $^3J_{\text{PH}} = 6.4$ Hz, H_3 C-Rh, 3H). $^{13}\text{C}\{^1\text{H}\}$ NMR (C₆D₆) **3a**: 164.9 (ddt, $^1J_{\text{RhC}} = 32$ Hz, $^2J_{\text{C-PEt3}} = 5$ Hz, $^2J_{\text{C-PPyr2}} = 4$ Hz, C_{ipso}-Rh, 1C), 141.95 (vtd, $^2J_{\text{PC}} = 11.2$ Hz, $J = 1.5$ Hz, Ar, C-C-Rh, 2C), 124.45 (s, Pyr, CH-N-P, 8C), 123.7 (s, Ar, CH-CH-C-C-Rh, 1C), 123.32 (vt, $^3J_{\text{PC}} = 11.0$ Hz, Ar, CH-C-C-Rh, 2C), 112.74 (vt, $^3J_{\text{PC}} = 2.46$ Hz, Pyr, CH-CH-N-P, 4C), 112.37 (vt, $^3J_{\text{PC}} = 3.1$ Hz, Pyr, CH-CH-N-P, 4C), 49.43 (vtd, $^1J_{\text{PC}} = 18.8$ Hz, $^2J_{\text{RhC}} = 3.55$ Hz, Ar- CH_2 -P, 2C), 18.24 (d, $^1J_{\text{PC}} = 18.0$ Hz, Et, P- CH_2 , 3C), 9.65 (d, $^2J_{\text{PC}} = 5.6$ Hz, Et, P- CH_2 -CH₃, 3C), -3.32 (ddt, $^2J_{\text{PC}}$, $trans = 72.7$ Hz, $^1J_{\text{RhC}} = 15.5$ Hz, $^2J_{\text{PC}}$, *cis* = 6.6 Hz, Rh-CH₃, 1C).

Reaction of 2d with MeI. A solution of **2d** (33 mg, 0.043 mmol) in THF (1 mL) was precooled to -25 °C. Then a MeI solution precooled to -25 °C (neat, 5.3 μL , 0.085 mmol) was added. The reaction mixture was left stirring at ambient temperature for 3.5 h, resulting in quantitative formation of **4a**. Since slight decomposition

of **4a** occurred under reduced pressure, the product was precipitated at -25 °C with pentane, the upper solution was decanted, and the pale solid was dried to give 26 mg (58%) of the product.

$^{31}\text{P}\{^1\text{H}\}$ NMR (THF- d_8 , 273 K): 113.5 (d, $^1J_{\text{RhP}} = 151.3$ Hz, PPy₃, 2P), 43.86 (s, [MePPy₃]⁺, 1P). ^1H NMR (THF- d_8 , 273 K): 7.58 (br s, Pyr, $HC-N$, 4H), 7.27 (br s, Pyr, $HC-N$, 4H), 7.10 (d, $^3J_{\text{HH}} = 7.4$ Hz, Ar, *meta* to Rh, 2H), 6.83 (t, $^3J_{\text{HH}} = 7.4$ Hz, Ar, *para* to Rh, 1H), 6.08 (m, Pyr, $HC-HC-N$, 8H), 4.59 (dvt, $^2J_{\text{HH}} = 16.9$ Hz, $^2J_{\text{PH}} = 5.4$ Hz, Ar- CH (H)-P, 2H), 4.40 (dvt, $^2J_{\text{HH}} = 16.9$ Hz, $^2J_{\text{PH}} = 5.3$ Hz, Ar- CH (H)-P, 2H), 3.22 (m, [MePPy₃]⁺, P-N-CH₂, 12H), 2.02 (d, $^2J_{\text{PH}} = 14.6$ Hz, [MePPy₃]⁺, P-CH₃, 3H), 1.87 (m, [MePPy₃]⁺, P-N-CH₂-CH₂, 12H), 0.116 (td, $^3J_{\text{PH}} = 6.3$ Hz, $^2J_{\text{RhH}} = 1.92$ Hz, Rh-CH₃, 3H). $^{13}\text{C}\{^1\text{H}\}$ NMR (THF- d_8 , 273 K): 169.1 (dt, $^1J_{\text{RhC}} = 34.0$ Hz, unresolved t, C_{ipso}-Rh, 1C), 142.66 (vt, $^2J_{\text{PC}} = 11.9$ Hz, Ar, C-C-Rh, 2C), 126.33 (s, Pyr, CH-N-P, 4C), 124.79 (s, Pyr, CH-N-P, 4C), 123.94 (s, Ar, CH-CH-C-C-Rh, 1C), 122.85 (vt, $^3J_{\text{PC}} = 11.7$ Hz, Ar, CH-C-C-Rh, 2C), 111.24 (s, CH-CH-N-P, 4C), 110.76 (s, Pyr, CH-CH-N-P, 4C), 48.58 (vtd, $^1J_{\text{PC}} = 17.9$ Hz, $^2J_{\text{RhC}} = 3.1$ Hz, Ar- CH_2 -P, 2C), 47.9 (d, $^3J_{\text{PC}} = 4.41$ Hz, [MePPy₃]⁺, P-N-CH₂-CH₂, 6C), 27.19 (d, $^2J_{\text{PC}} = 7.88$ Hz, [MePPy₃]⁺, P-N-CH₂, 6C), -0.233 (dt, $^1J_{\text{RhC}} = 22.3$ Hz, $^2J_{\text{PC}} = 4.7$ Hz, Rh-CH₃, 1C). Confirmed by DEPT. Anal. (%) Found (Calc): C 43.04 (43.16); H 4.96 (5.05).

Reaction of 4a with PEt₃. PEt₃ (neat, 4.6 μL , 0.034 mmol) was added to **4a** (35.5 mg, 0.034 mmol) in THF (1 mL), resulting in formation of **3a**:**3b** = 10:1. The solvent was removed under vacuum to give a brown, viscous solid. The products were recrystallized from MeOH (0.7 mL) during overnight at room temperature. The brown MeOH solution was decanted, and the resulting yellow crystals were rinsed with a small amount of MeOH (0.2 mL) and dried under vacuum, yielding the isomers (17.2 mg, 65%) as a yellow solid.

The *cis* to aryl coordination of the methyl group was confirmed by NOE. Anal. (%) Found (Calc): C 47.20 (46.99); H 5.18 (5.22).

Reaction of 2e with MeI. To a solution of **2e** (30 mg, 0.054 mmol) in THF (3 mL) was added MeI (neat, 3.5 μL , 0.056 mmol) while stirring. The resulting reaction mixture was left stirring at ambient temperature. The reaction was complete after 14 days, resulting in formation of **5** (38% and 78% conversions were observed by NMR after 3 and 7 days, respectively) together with some minor products, which gave $^{31}\text{P}\{^1\text{H}\}$ NMR spectra similar to **5**. No formation of **6a,b** was observed at any stage of the reaction. We were unable to isolate **5**, which was characterized in solution.

Upon addition of 2 equiv of PⁱPr₃ to the reaction mixture, *trans*-Rh(PⁱPr₃)₂CO(I)³⁰ was formed accompanied by release of ⁱPyrPCP-Me. The solvent was evaporated, and the yellow residue was washed with a small amount of pentane to remove *trans*-Rh(PⁱPr₃)₂CO(I) (yellow solution). The remaining pale residue was treated with a small amount of Et₂O and recrystallized at -25 °C to give pure ⁱPyrPCP-Me as a pale solid, 16 mg (67%).

Spectral Data for 5. $^{31}\text{P}\{^1\text{H}\}$ NMR (THF- d_8): 102.4 (d, $^1J_{\text{RhP}} = 154.6$ Hz). ^1H NMR (THF- d_8): 8.46 (d, $^3J_{\text{HH}} = 7.6$ Hz, Ar, *meta* to Rh, 2H), 7.60 (t, $^3J_{\text{HH}} = 7.6$ Hz, Ar, *para* to Rh, 1H), 6.87 (br s, Pyr, $HC-N$, 8H), 6.22 (s, Pyr, $HC-HC-N$, 8H), 4.84 (br s, Ar- CH_2 -P, 4H), 1.42 (s, Ar-CH₃, 3H). $^{13}\text{C}\{^1\text{H}\}$ NMR (THF- d_8): 181.5 (dt, $^1J_{\text{RhC}} = 76$ Hz, $^2J_{\text{PC}} = 14$ Hz, CO, 1C), 141.15 (s, Ar, C-CH₃, 1C), 132.18 (s, Ar, C-C-CH₃, 2C), 131.0 (s, Ar, CH-C-C-CH₃, 2C), 125.76 (s, Ar, CH-CH-C-C-CH₃, 1C), 125.08 (br s, Pyr, CH-N-P, 8C), 113.27 (s, Pyr, CH-CH-N-P, 8C), 38.89 (vt, $^1J_{\text{PC}} = 16.7$ Hz, Ar- CH_2 -P, 2C), 14.61 (s, Ar-CH₃, 1C). Confirmed by DEPT and HMQC. IR (film): $\nu_{\text{CO}} = 2008$ cm⁻¹.

Spectral Data for ⁱPyrPCP-Me. $^{31}\text{P}\{^1\text{H}\}$ NMR (CDCl₃): 66.74 (s). ^1H NMR (CDCl₃): 6.97 (m, Pyr, $HC-N$, 8H), 6.73 (t, $^3J_{\text{HH}} = 7.7$ Hz, Ar, *para* to Rh, 1H), 6.523 (d, $^3J_{\text{HH}} = 7.7$ Hz, Ar, *meta* to

(30) Moigno, D.; Kiefer, W.; Callejas-Gaspar, B.; Gil-Rubio, J.; Werner, H. *New J. Chem.* **2001**, 25, 1389–1397.

Rh, 2H), 6.28 (m, Pyr, HC-HC-N, 8H), 3.72 (d, $^2J_{\text{PH}} = 2.47$ Hz, Ar-CH₂-P, 4H), 2.25 (s, Ar-CH₃, 3H). $^{13}\text{C}\{^1\text{H}\}$ NMR (CDCl₃): 135.14 (t, unresolved, Ar, C-CH₃, 1C), 132.2 (dd, $^2J_{\text{PC}} = 10.44$ Hz, $^4J_{\text{PC}} = 2.36$ Hz, Ar, C-C-CH₃, 2C), 129.0 (dd, Ar, $^3J_{\text{PC}} = 6.4$ Hz, $^5J_{\text{PC}} = 3.5$ Hz, CH-C-C-CH₃, 2C), 126.23 (t, $^4J_{\text{PC}} = 2.7$ Hz, Ar, CH-CH-C-C-CH₃, 1C), 123.5 (d, $^2J_{\text{PC}} = 13.9$ Hz, Pyr, CH-N-P, 8C), 112.14 (d, $^3J_{\text{PC}} = 4.1$ Hz, Pyr, CH-CH-N-P, 8C), 37.2 (d, $^1J_{\text{PC}} = 14.5$ Hz, Ar-CH₂-P, 2C), 15.99 (t, $^4J_{\text{PC}} = 5.4$ Hz, Ar-CH₃, 1C). Confirmed by DEPT.

Synthesis of 6a,b. CO was bubbled through a THF-*d*₈ (1 mL) solution of **4a** (20 mg, 0.019 mmol) for a few minutes, resulting in formation of **6a:6b** = 1:1, accompanied by precipitation of [MePPy₃]I. The complexes **6a,b** were not isolated because of slow decomposition to form **5**.

$^{31}\text{P}\{^1\text{H}\}$ NMR (THF-*d*₈): 120.5 (d, $^1J_{\text{RHP}} = 133.6$ Hz), 111.8 (d, $^1J_{\text{RHP}} = 135.4$ Hz), 45.1 (s, I[MePPy₃]). ^1H NMR (THF-*d*₈): 7.44 (m, Pyr, HC-N, 4H), 7.40 (m, Pyr, HC-N, 4H), 7.38–7.06 (Ar, *meta* and *para* to Rh), 7.02 (m, Pyr, HC-N, 4H), 6.85 (m, Pyr, HC-N, 4H), 6.32 (br s, Pyr, HC-HC-N, 4H), 6.28 (br s, Pyr, HC-HC-N, 8H), 6.25 (br s, Pyr, HC-HC-N, 4H), 4.86 (dvt, ABX₂, $^2J_{\text{HH}} = 16.7$ Hz, $^2J_{\text{PH}} = 5.8$ Hz, Ar-CH(H)-P, 2H), 4.71 (dvt, ABX₂, $^2J_{\text{HH}} = 18.2$ Hz, $^2J_{\text{PH}} = 5.8$ Hz, Ar-CH(H)-P, 2H), 4.65 (dvt, ABX₂, $^2J_{\text{HH}} = 16.8$ Hz, $^2J_{\text{PH}} = 5.7$ Hz, Ar-CH(H)-P, 2H), 4.57 (dvt, ABX₂, $^2J_{\text{HH}} = 18.1$ Hz, $^2J_{\text{PH}} = 5.3$ Hz, Ar-CH(H)-P, 2H), 3.36 (m, P-N-CH₂, PPy₃), 2.32 (d, $^2J_{\text{RH}} = 14.9$ Hz, P-CH₃, I[MePPy₃]), 1.92 (m, P-N-CH₂-CH₂, I[MePPy₃]), 1.59 (m, P-N-CH₂-CH₂, I[MePPy₃]), 0.303 (td, $^3J_{\text{PH}} = 8.16$ Hz, $^2J_{\text{RH}} = 1.81$ Hz, H₃C-Rh, 3H), 0.014 (td, $^3J_{\text{PH}} = 6.04$ Hz, $^2J_{\text{RH}} = 2.1$ Hz, H₃C-Rh, 3H). $^{13}\text{C}\{^1\text{H}\}$ NMR (THF-*d*₈): 189.5 (m, unresolved, Rh-CO, 1C), 180.9 (m, unresolved, Rh-CO, 1C), 166.1 (dt, $^1J_{\text{RhC}} = 25.0$ Hz, unresolved triplet, C_{ipso}-Rh, 1C), 161.0 (d, $^1J_{\text{RhC}} = 31.33$ Hz, C_{ipso}-Rh, 1C), 142.78 (vt, $^2J_{\text{PC}} = 11.8$ Hz, Ar, C-C-Rh, 2C), 142.28 (vt, $^2J_{\text{PC}} = 11.0$ Hz, Ar, C-C-Rh, 2C), 125.15 (m, Pyr, CH-N-P, 4C), 125.06 (m, Pyr, CH-N-P, 4C), 124.80 (m, Pyr, CH-N-P, 4C), 124.20 (m, Pyr, CH-N-P, 4C), 114.06 (m, Pyr, CH-CH-N-P, 4C), 113.80 (m, Pyr, CH-CH-N-P, 4C), 113.40 (m, Pyr, CH-CH-N-P, 8C), 50.1 (vtd, $^1J_{\text{PC}} = 20.3$ Hz, $^2J_{\text{RhC}} = 2.8$ Hz, Ar-CH₂-P, 2C), 48.3 (vtd, $^1J_{\text{PC}} = 19.3$ Hz, $^2J_{\text{RhC}} = 3.2$ Hz, Ar-CH₂-P, 2C), 48.1 (d, $^3J_{\text{PC}} = 4.4$ Hz, P-N-CH₂-CH₂, I[MePPy₃]), 27.2 (d, $^2J_{\text{PC}} = 7.8$ Hz, P-N-CH₂, I[MePPy₃]), 6C), -2.78 (dt, $^1J_{\text{RhC}} = 15.5$ Hz, $^2J_{\text{PC}} = 5.9$ Hz, Rh-CH₃, 1C), -6.9 (dt, $^1J_{\text{RhC}} = 20.47$ Hz, unresolved triplet, Rh-CH₃, 1C). Confirmed by DEPT.

Reaction of 2b with MeI at the Presence of [NBu₄]I. A THF (1 mL) solution of **2b** (20 mg, 0.025 mmol) was added to a THF (0.5 mL) suspension of [NBu₄]I (9.3 mg, 0.025 mmol), resulting in a yellow suspension. MeI (neat, 1.6 μL , 0.026 mmol) was added. The solution became clear yellow after 15 min stirring at r.t. $^{31}\text{P}\{^1\text{H}\}$ NMR showed quantitative formation of **4b** accompanied by PPh₃. The product was precipitated with pentane (6 volumes) at -25 °C. The soluble fraction was decanted, giving 19 mg (72%) of **4b** as pale brown crystals.

$^{31}\text{P}\{^1\text{H}\}$ NMR (C₆D₆): 115.6 (d, $^1J_{\text{RHP}} = 151.1$ Hz). ^1H NMR (C₆D₆): 7.90 (br s, Pyr, HC-N, 4H), 7.51 (br s, Pyr, HC-N, 4H), 7.3 (br s, Ar, *para* to Rh, 1H), 7.1 (m, Ar, *meta* to Rh, 2H), 6.46 (m, Pyr, HC-HC-N, 4H), 6.35 (m, Pyr, HC-HC-N, 4H), 4.65 (dvt, $^2J_{\text{HH}} = 16.8$ Hz, $^2J_{\text{PH}} = 5.4$ Hz, Ar-CH(H)-P, 2H), 4.24 (dvt, $^2J_{\text{HH}} = 16.8$ Hz, $^2J_{\text{PH}} = 5.2$ Hz, Ar-CH(H)-P, 2H), 2.99 (m, NBu₄, N-CH₂, 8H), 1.37 (m, NBu₄, N-CH₂-(CH₂)₂, 16H), 1.03 (t, $^3J_{\text{HH}} = 6.9$ Hz, NBu₄, N-(CH₂)₃-CH₃, 12H), 0.795 (td, $^3J_{\text{PH}} = 6.3$ Hz, $^2J_{\text{RH}} = 1.8$ Hz, Rh-CH₃, 3H). $^{13}\text{C}\{^1\text{H}\}$ NMR (C₆D₆): 167.9 (dt, $^1J_{\text{RhC}} = 34.1$ Hz, unresolved t, C_{ipso}-Rh, 1C), 142.06 (vt, $^2J_{\text{PC}} = 11.8$ Hz, Ar, C-C-Rh, 2C), 126.21 (vt, $^2J_{\text{PC}} = 2.34$ Hz, Pyr, CH-N-P, 4C), 124.56 (s, Pyr, CH-N-P, 4C), 124.01 (s, Ar, CH-CH-C-C-Rh, 1C), 122.73 (vt, $^3J_{\text{PC}} = 11.6$ Hz, Ar, CH-C-C-Rh, 2C), 111.44 (vt, unresolved t, Pyr, CH-CH-N-P, 4C), 110.83 (vt, $^3J_{\text{PC}} = 2.69$ Hz, Pyr, CH-CH-N-P, 4C), 58.68 (s, NBu₄, N-CH₂, 4C), 49.11 (vtd, $^1J_{\text{PC}} = 17.5$ Hz, $^2J_{\text{RhC}} = 3.5$ Hz, Ar-CH₂-P, 2C), 24.31 (s, NBu₄,

N-CH₂-CH₂, 4C), 19.95 (s, NBu₄, N-(CH₂)₂-CH₂, 4C), 14.06 (s, NBu₄, N-(CH₂)₃-CH₃, 4C), -0.07 (dt, $^1J_{\text{RhC}} = 22.1$ Hz, $^2J_{\text{PC}} = 4.9$ Hz, Rh-CH₃, 1C). Confirmed by DEPT and HSQC. Anal. (%) Found (Calc): C 47.29 (47.19); H 6.01 (5.99).

Reaction of 2c with MeI in the Presence of [NBu₄]I. A THF (2 mL) solution of **2c** (15.6 mg, 0.021 mmol) was added to a THF (2 mL) suspension, of [NBu₄]I (7.6 mg, 0.021 mmol), resulting in a yellow suspension. MeI (neat, 1.3 μL , 0.021 mmol) was added. The solution became clear yellow after 2.5 h stirring at r.t. $^{31}\text{P}\{^1\text{H}\}$ NMR showed quantitative formation of **4b** accompanied by PPy₃. The product was precipitated with pentane (6 volumes) at -25 °C overnight. The soluble fraction was decanted, and the light brown solid was dried to give 19 mg (89%) of **4b**.

Reaction of 2e with MeI in the Presence of [NBu₄]I. To a suspension of [NBu₄]I (6.6 mg, 0.018 mmol) and **2e** (10 mg, 0.018 mmol) in THF (2 mL) was added MeI (neat, 1.1 μL , 0.018 mmol). The reaction was complete during 9 h stirring at ambient temperature. $^{31}\text{P}\{^1\text{H}\}$ NMR showed formation of **4b:6a:6b** = 9:1:1. The solution was left stirring at room temperature for 2 days, resulting in formation of **4b**.

Synthesis of [Rh^I(P^{yr}PCP)]NBu₄ (2f). To a brown crude solution of Rh^I(P^{yr}PCP)norborene (made from 50 mg of [Rh^I(COE)₂μCl]₂ as described in the procedure for the synthesis of **2d**) was added [NBu₄]I (51.5 mg, 0.139 mmol). The resulting reaction mixture was stirred for 24 h at rt, resulting in formation of [Rh^I(P^{yr}PCP)]NBu₄. We were not able to purify the product either on a Florisil column or by extractions. The yield was estimated as at least 60% by $^{31}\text{P}\{^1\text{H}\}$ NMR spectrum integration.

$^{31}\text{P}\{^1\text{H}\}$ NMR (THF-*d*₈): 108.2 (d, $^1J_{\text{RHP}} = 221.27$ Hz). ^1H NMR (THF-*d*₈): 7.64 (m, Pyr, HC-N, 8H), 6.79 (d, $^3J_{\text{HH}} = 7.31$ Hz, Ar, *meta* to Rh, 2H), 6.65 (t, $^3J_{\text{HH}} = 7.31$ Hz, Ar, *para* to Rh 1H), 6.05 (m, Pyr, HC-HC-N 8H), 3.96 (vt, $^2J_{\text{HP}} = 4.2$ Hz, Ar-H₂C-P, 4H), 3.24 (m, NBu₄, H₂C-N, 8H), 1.64 (m, NBu₄, H₂C-CH₂-N, 8H), 1.37 (m, NBu₄, CH₂-CH₂-CH₂-N, 8H), 0.96 (t, $^3J_{\text{HH}} = 7.4$ Hz, NBu₄, CH₃-CH₂-CH₂-CH₂-N, 12H). ^{13}C NMR (THF-*d*₈): 173.49 (dt, $^1J_{\text{RhC}} = 41.1$ Hz, $^2J_{\text{PC}} = 8.6$ Hz, C_{ipso}-Rh, 1C), 146.11 (vtd, $^2J_{\text{PC}} = 15.2$ Hz, $^2J_{\text{RhC}} = 2.2$ Hz, Ar, C-C-Rh, 2C), 125.68 (vt, $^2J_{\text{PC}} = 3.8$ Hz, Pyr, CH-N-P, 8C), 121.83 (vt, $^3J_{\text{PC}} = 12.3$ Hz, Ar, CH-C-C-Rh, 2C), 121.42 (s, Ar, CH-CH-C-C-Rh, 1C), 110.53 (unresolved vt, Pyr, CH-CH-N-P, 8C), 59.19 (s, NBu₄, CH₂-N, 4C), 50.79 (vtd, $^1J_{\text{PC}} = 16.5$ Hz, $^2J_{\text{RhC}} = 5.4$ Hz, Ar-CH₂-P, 2C), 24.74 (s, NBu₄, CH₂-CH₂-N, 4C), 20.54 (s, NBu₄, CH₂-CH₂-CH₂-N, 4C), 14.05 (s, NBu₄, CH₃-CH₂-CH₂-N, 4C).

Reaction of [Rh^I(P^{yr}PCP)]NBu₄ with MeI. To a crude solution of [Rh^I(P^{yr}PCP)]NBu₄ (prepared from 50 mg of [Rh^I(COE)₂μCl]₂) was added MeI (neat, 8.7 μL , 0.139 mmol). $^{31}\text{P}\{^1\text{H}\}$ NMR (THF-H₈) showed formation of **4b** after 5 min at rt (about 70% spectral yield). The product was dried, extracted with toluene, dried, and quickly washed with Et₂O (2 × 5 mL). The remaining brown solid was dried, giving 101 mg (69%) of **4b**.

General Information for X-ray Analysis of the Structures 2c–e, 3a, and 4b. Data were collected with a Nonius KappaCCD diffractometer at 120(2) K, Mo K α ($\lambda = 0.71073$ Å), graphite monochromator. The data were processed with Denzo-Scalepack. Structures were solved by direct methods with SHELXS-97 and refined with full matrix least-squares refinement based on F^2 by SHELXL-97.

X-ray Analysis of the Structure of Rh^I(P^{yr}PCP)PPy₃ (2c). Orange needles of **2c** were obtained by slow diffusion of hexane into a concentrated solution of **2c** in THF, in a 5 mm NMR tube, at room temperature.

Crystal data: 2C₃₆H₃₅N₇P₃Rh + 1/2(C₆H₁₄), 0.40 × 0.05 × 0.05 mm³, triclinic, $P\bar{1}$, $a = 9.180(0)$ Å, $b = 17.938(4)$ Å, $c = 22.503(5)$ Å, $\alpha = 79.923(3)^\circ$, $\beta = 78.612(1)^\circ$, $\gamma = 82.986(1)^\circ$, $T = 120(2)$ K, $V = 3562.4(12)$ Å³, $Z = 2$, $fw = 1566.15$, $D_c = 1.460$ Mg m⁻³, $\mu = 0.653$ mm⁻¹.

Data collection and processing: $0 \leq h \leq 11$, $-22 \leq k \leq 23$, $-28 \leq l \leq 29$, frame scan width = 1.0° , scan speed 1.0° per 320 s, typical peak mosaicity 0.47° , 59 988 reflections collected, 16 144 independent reflections ($R_{\text{int}} = 0.049$).

Solution and refinement: 863 parameters with 0 restraints, final $R_1 = 0.0427$ (based on F^2) for data with $I > 2\sigma(I)$ and $R_1 = 0.0630$ on 16 137 reflections, goodness-of-fit on $F^2 = 1.016$, largest electron density peak = $2.488 \text{ e } \text{Å}^{-3}$.

X-ray Analysis of the Structure of $\text{Rh}^{\text{I}}(\text{PyrPCP})\text{PPy}_3$ (2d). A saturated pentane solution of **2d** was put in a 20 mL vial, twice concentrated by evaporation under reduced pressure, and left overnight at room temperature in a closed evaporator without normalizing the pressure. Yellow chunks of **2d** were obtained.

Crystal data: $\text{C}_{36}\text{H}_{47}\text{N}_7\text{P}_3\text{Rh}$, $0.18 \times 0.1 \times 0.09 \text{ mm}^3$, monoclinic, $P2_1/n$, $a = 16.7698(2) \text{ Å}$, $b = 12.2296(3) \text{ Å}$, $c = 18.4779(3) \text{ Å}$, $\beta = 112.219(1)^\circ$, $T = 120(2)\text{K}$, $V = 3508.1(1) \text{ Å}^3$, $Z = 4$, fw = 773.63, $D_c = 1.465 \text{ Mg m}^{-3}$, $\mu = 0.661 \text{ mm}^{-1}$.

Data collection and processing: $-22 \leq h \leq 20$, $0 \leq k \leq 16$, $0 \leq l \leq 24$, frame scan width = 1.0° , scan speed 1.0° per 70 s, typical peak mosaicity 0.411° , 45 263 reflections collected, 8732 independent reflections ($R_{\text{int}} = 0.104$).

Solution and refinement: 430 parameters with no restraints, final $R_1 = 0.0416$ (based on F^2) for data with $I > 2\sigma(I)$ and $R_1 = 0.0742$ on 8331 reflections, goodness-of-fit on $F^2 = 0.980$, largest electron density peak = $0.932 \text{ e } \text{Å}^{-3}$.

X-ray Analysis of the Structure of $\text{Rh}^{\text{I}}(\text{PyrPCP})\text{CO}$ (2e). Yellow prism crystals of **2e** were obtained by slow diffusion of pentane into a concentrated solution of **2e** in THF, in a 5 mm NMR tube, at room temperature.

Crystal data: $\text{C}_{25}\text{H}_{23}\text{N}_4\text{OP}_2\text{Rh}$, $0.5 \times 0.3 \times 0.2 \text{ mm}^3$, triclinic, $P\bar{1}$, $a = 9.385(2) \text{ Å}$, $b = 10.736(2) \text{ Å}$, $c = 12.812(3) \text{ Å}$, $\alpha = 107.29(3)^\circ$, $\beta = 106.06(3)^\circ$, $\gamma = 99.08(3)^\circ$, $T = 120(2)\text{K}$, $V = 1143.2(4) \text{ Å}^3$, $Z = 2$, fw = 560.32 g/mol, $D_c = 1.628 \text{ Mg m}^{-3}$, $\mu = 0.914 \text{ mm}^{-1}$.

Data collection and processing: 25 507 reflections collected, $0 \leq h \leq 12$, $-13 \leq k \leq 13$, $-16 \leq l \leq 15$, frame scan width = 1.0° , scan speed 1.0° per 20 s, typical peak mosaicity 0.381° , 5602 independent reflections ($R_{\text{int}} = 0.061$).

Solution and refinement: 298 parameters with 0 restraints, final $R_1 = 0.0325$ (based on F^2) for data with $I > 2\sigma(I)$ and $R_1 = 0.0396$ on 5194 reflections, goodness-of-fit on $F^2 = 1.095$, largest electron density peak = $1.926 \text{ e } \text{Å}^{-3}$.

X-ray Analysis of the Structure of $\text{Rh}^{\text{I}}(\text{PyrPCP})\text{Me}(\text{I})\text{PEt}_3$ (3a). Yellow prism crystals were obtained at room temperature from a concentrated MeOH solution of the mixture of **3**.

Crystal data: $\text{C}_{31}\text{H}_{41}\text{IN}_4\text{P}_3\text{Rh}$, $0.25 \times 0.07 \times 0.07 \text{ mm}^3$, orthorhombic, $Pca2_1$, $a = 16.2351(2) \text{ Å}$, $b = 10.6516(4) \text{ Å}$, $c = 19.0486(2) \text{ Å}$, $T = 120(2)\text{K}$, $V = 3294.2(1) \text{ Å}^3$, $Z = 4$, fw = 792.4 g/mol, $D_c = 1.598 \text{ Mg m}^{-3}$, $\mu = 1.628 \text{ mm}^{-1}$.

Data collection and processing: $0 \leq h \leq 21$, $0 \leq k \leq 13$, $0 \leq l \leq 24$, frame scan width = 1.0° , scan speed 1.0° per 60 s, typical peak mosaicity 0.551° , 31 184 reflections collected, 4251 independent reflections ($R_{\text{int}} = 0.093$).

Solution and refinement: 366 parameters with one restraint, final $R_1 = 0.0322$ (based on F^2) for data with $I > 2\sigma(I)$ and $R_1 = 0.0460$ on 3899 reflections, goodness-of-fit on $F^2 = 1.078$, largest electron density peak = $0.855 \text{ e } \text{Å}^{-3}$.

X-ray Analysis of the Structure of $[\text{Rh}^{\text{I}}(\text{PyrPCP})\text{Me}(\text{I})_2]\text{[NBu}_4\text{]}$ (4b). Colorless prism crystals of **4b** were obtained from a THF/pentane (1:1) solution of **4b** in a 5 mm NMR tube. The crystals appeared after 3 days at room temperature.

Crystal data: $\text{C}_{25}\text{H}_{26}\text{I}_2\text{N}_4\text{P}_2\text{Rh} + \text{C}_{16}\text{H}_{36}\text{N} + \text{C}_4\text{H}_8\text{O}$, $0.25 \times 0.25 \times 0.15 \text{ mm}^3$, monoclinic, $P2_1$, $a = 13.2256(2) \text{ Å}$, $b = 15.7831(3) \text{ Å}$, $c = 13.3389(2) \text{ Å}$, $\beta = 119.5274(7)^\circ$, $T = 120(2) \text{ K}$, $V = 2422.8(1) \text{ Å}^3$, $Z = 2$, fw = 1115.71 g/mol, $D_c = 1.529 \text{ Mg m}^{-3}$, $\mu = 1.730 \text{ mm}^{-1}$.

Data collection and processing: $-16 \leq h \leq 14$, $0 \leq k \leq 20$, $0 \leq l \leq 17$, frame scan width = 1.0° , scan speed 1.0° per 30 s, typical peak mosaicity 0.411° , 30 712 reflections collected, 6177 independent reflections ($R_{\text{int}} = 0.059$).

Solution and refinement: 511 parameters with one restraint, final $R_1 = 0.0317$ (based on F^2) for data with $I > 2\sigma(I)$ and $R_1 = 0.0424$ on 5522 reflections, goodness-of-fit on $F^2 = 1.142$, largest electron density peak = $2.943 \text{ e } \text{Å}^{-3}$.

Acknowledgment. This work was supported by the Israel Science Foundation, by the DIP program for German-Israeli cooperation, and by the Helen and Martin Kimmel Center for Molecular Design. D.M. is the Israel Matz Professor of Organic Chemistry.

Supporting Information Available: CIF files containing X-ray crystallographic data for compounds **2c**, **2d**, **2e**, **3a**, and **4b**. This material is available free of charge via the Internet at <http://pubs.acs.org>.

OM800792Y

Synthesis and Crystal Structures of the First Stable Mononuclear Dihydrogermyl(hydrido) Platinum(II) Complexes

Norio Nakata, Shun Fukazawa, and Akihiko Ishii*

Department of Chemistry, Graduate School of Science and Engineering, Saitama University, Shimo-okubo, Sakura-ku, Saitama, 338-8570, Japan

Received August 20, 2008

The first stable dihydrogermyl(hydrido) platinum(II) complex *cis*-(Ph₃P)₂Pt(H)(GeH₂Trip) (**2**) was synthesized by the oxidative addition reaction of an overcrowded trihydrogermane, TripGeH₃ (**1**, Trip = 9-triptycyl), with (Ph₃P)₂Pt(η²-C₂H₄) in toluene. The reaction of **1** with (dppe)PtCl₂ in the presence of NaBH₄ afforded the corresponding hydrido complex (dppe)Pt(H)(GeH₂Trip) (**3**) together with bis(germyl) platinum(II) complex (dppe)Pt(GeH₂Trip)₂ (**4**). In addition, the ligand exchange reaction of complex **2** with free Cy₂PCH₂CH₂PCy₂ in toluene resulted in the formation of (dcpe)Pt(H)(GeH₂Trip) (**5**) in moderate yield. The structures of complexes **2–5** were fully determined on the basis of their NMR and IR spectra and elemental analyses. Moreover, the low-temperature X-ray crystallography of **2**, **3**, and **5** revealed that the platinum center has a distorted square-planar environment, probably due to the steric requirement of the *cis*-coordinated phosphine ligands and the bulky 9-triptycyl group on the germanium atom. Furthermore, the thermal rearrangement of bis(germyl) complex **4** in toluene at 60 °C gave digermyl(hydrido) complex (dppe)Pt(H)[Ge(HTrip)GeH₂Trip] (**6**) in high yield without irreversible reductive elimination of tetrahydrogermane.

Introduction

Oxidative additions of Si–H bonds to the metal center of low-valent transition metal complexes have been proposed as the key elementary steps to generate active intermediates for catalytic reactions such as hydrosilylation.¹ While many reactions of hydrosilanes with platinum(0) complexes affording mono(silyl), bis(silyl), and silyl-bridged multinuclear platinum complexes^{2,3} have been reported so far, the reactivity of Ge–H bonds toward platinum(0) complexes has been investigated for only a few cases of tertiary and secondary hydrogermanes.^{4–6} Recently, Braddock-Wilking et al. have described the syntheses

of hydrido(germyl) complex *cis*-(Ph₃P)₂Pt(H)(GeHMes₂) and symmetrical dinuclear complex [(Ph₃P)Pt(μ-η²-H-GePh₂)₂] by the reactions of the corresponding secondary hydrogermanes with (Ph₃P)₂Pt(η²-C₂H₄) and their characterization.⁴ Osakada et al. also have reported that the reaction of Ph₂GeH₂ with (Cy₃P)₂Pt afforded the corresponding *cis*- and *trans*-(Cy₃P)₂Pt(H)-(GeHPh₂) as the kinetic and thermodynamic products.⁵ In the reactions of tertiary hydrogermanes such as (HPh₂Ge)₂(SiMe₂)_n (*n* = 1, 2) with (Ph₃P)₂Pt(η²-C₂H₄), Mochida et al. have reported an unexpected formation of germylene-bridged dinuclear complex [(Ph₃P)Pt]₂(μ-GePh₂)₂ through the corresponding germasilaplatinacycles.⁵ Quite recently, they have also reported that the reactions of primary hydrogermane MesGeH₃ with (Ph₃P)₂Pt(η²-C₂H₄) produced unsymmetrical diplatinum complex [(Ph₃P)₃Pt₂(μ-η²-H-GeHMes₂)], symmetrical diplatinum complex [(Ph₃P)Pt(μ-η²-H-GeHMes)₂], and bis(germyl)platinum complex *cis*-(Ph₃P)₂Pt-(GeH₂Mes)₂, respectively.⁷ However, there are no structural characterizations of dihydrogermyl(hydrido) platinum(II) complexes, which are anticipated as the initial products in the Ge–H bond activation reactions of primary hydrogermanes with platinum(0) complexes.

Meanwhile, we have recently succeeded in the first isolation of stable hydrido(selenolato) platinum(II) complex *cis*-(Ph₃P)₂Pt(H)(SeTrip)⁸ using a bulky substituent, the 9-triptycyl group (Trip = 9-triptycyl).⁹ On the basis of this result, we envisioned

* To whom correspondence should be addressed. E-mail: ishiiaki@chem.saitama-u.ac.jp.

(1) (a) Marciniak, B. *Comprehensive Handbook on Hydrosilylation*; Pergamon Press: Oxford, 1992. (b) Ojima, I.; Li, Z.; Zhu, J. Recent Advances in Hydrosilylation and Related Reactions. In *The Chemistry of Organic Silicon Compounds*; Patai, S., Rappoport, Z., Eds.; John Wiley and Sons: New York, 1998; p 1687.

(2) For recent reviews, see: (a) Eisen, M. S. In *The Chemistry of Organic Silicon Compounds*; Rappoport, Z., Apeloig, Y., Eds.; Wiley: New York, 1998; Vol. 2, Part 3, Chapter 35. (b) Ogino, H.; Tobita, H. *Adv. Organomet. Chem.* **1998**, *42*, 223–290. (c) Corey, J. Y.; Braddock-Wilking, J. *Chem. Rev.* **1999**, *99*, 175–292. (d) Osakada, K.; Tanabe, M. *Bull. Chem. Soc. Jpn.* **2005**, *78*, 1887–1898. (e) Shimada, S.; Tanaka, M. *Coord. Chem. Rev.* **2006**, *250*, 991–1011.

(3) For recent works on (silyl) platinum complexes, see: (a) Braddock-Wilking, J.; Corey, J. Y.; Trankler, K. A.; Xu, H.; French, L. M.; Praingam, N.; White, C.; Rath, N. P. *Organometallics* **2006**, *25*, 2859–2871. (b) Shimada, S.; Li, Y.-H.; Rao, M. L. N.; Tanaka, M. *Organometallics* **2006**, *25*, 3796–3798. (c) Braddock-Wilking, J.; Corey, J. Y.; French, L. M.; Choi, E.; Speedie, V. J.; Rutherford, M. F.; Yao, S.; Xu, H.; Rath, N. P. *Organometallics* **2006**, *25*, 3974–3988. (d) Tanabe, M.; Ito, D.; Osakada, K. *Organometallics* **2007**, *26*, 459–462. (e) Arai, H.; Takahashi, M.; Noda, A.; Nanjo, M.; Mochida, K. *Organometallics* **2008**, *27*, 1929–1935. (f) Tanabe, M.; Ito, D.; Osakada, K. *Organometallics* **2008**, *27*, 2258–2267.

(4) (a) Braddock-Wilking, J.; Corey, J. Y.; White, C.; Xu, H.; Rath, N. P. *Organometallics* **2005**, *24*, 4113–4115. (b) White, C. P.; Braddock-Wilking, J.; Corey, J. Y.; Xu, H.; Redekop, E.; Sedinkin, S.; Rath, N. P. *Organometallics* **2007**, *26*, 1996–2004.

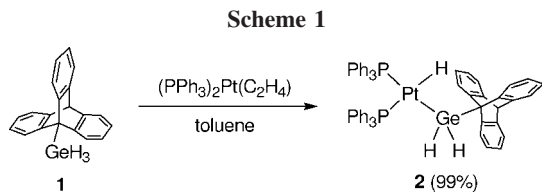
(5) Tanabe, M.; Ishikawa, N.; Osakada, K. *Organometallics* **2006**, *25*, 796–798.

(6) Usui, Y.; Hosotani, S.; Ogawa, A.; Nanjo, M.; Mochida, K. *Organometallics* **2005**, *24*, 4337–4339.

(7) Arai, H.; Nanjo, M.; Mochida, K. *Organometallics* **2008**, *27*, 4147–4151.

(8) Ishii, A.; Nakata, N.; Uchiumi, R.; Murakami, K. *Angew. Chem., Int. Ed.* **2008**, *47*, 2661–2664.

(9) For applications of the Trip group, see: (a) Ishii, A.; Matsubayashi, S.; Takahashi, T.; Nakayama, J. *J. Org. Chem.* **1999**, *64*, 1084–1084. (b) Ishii, A.; Takahashi, T.; Nakayama, J. *Heteroat. Chem.* **2001**, *12*, 198–203. (c) Ishii, A.; Takahashi, T.; Tawata, A.; Furukawa, A.; Oshida, H.; Nakayama, J. *Chem. Commun.* **2002**, 2810–2811. (d) Ishii, A.; Mori, Y.; Uchiumi, R. *Heteroat. Chem.* **2005**, *16*, 525–528.



that the introduction of the 9-triptycyl group onto a germanium atom that should coordinate to a platinum center would be useful for the preparation of novel classes of germyl(hydrido) complexes. Herein, we present the synthesis, characterization, and properties of the first stable dihydrogermyl(hydrido) platinum(II) complexes, having Ph_3P , dppe [bis(1,2-diphenylphosphino)ethane], and dcpe [bis(1,2-dicyclohexylphosphino)ethane] ligands by the reactions of an overcrowded primary germane, TripGeH_3 (**1**), with platinum(0) complexes or ligand exchange reaction of a dihydrogermyl(hydrido) platinum(II) complex.

Results and Discussion

The reaction of TripGeH_3 (**1**)¹⁰ with $(\text{Ph}_3\text{P})_2\text{Pt}(\eta^2\text{-C}_2\text{H}_4)$ in toluene at room temperature proceeded efficiently to form *cis*- $(\text{Ph}_3\text{P})_2\text{Pt}(\text{H})(\text{GeH}_2\text{Trip})$ (**2**) in 99% yield as colorless crystals (Scheme 1). In the ^1H NMR spectrum of **2**, characteristic signals due to the platinum hydride were observed as a doublet of doublets around $\delta -3.23$ ($^2J_{\text{P-H}} = 168, 18, ^1J_{\text{Pt-H}} = 894$ Hz). The Ge-H protons appeared as a multiplet signal at 4.43 ppm. The $^{31}\text{P}\{^1\text{H}\}$ NMR spectrum for **2** showed two nonequivalent doublet signals ($^2J_{\text{P-P}} = 13$ Hz) at $\delta 31.2$ and 31.6 with similar $^{195}\text{Pt}-^{31}\text{P}$ coupling constants, 2317 and 2252 Hz. The former signal is assigned to the phosphorus *trans* to the platinum hydride on the basis of NMR data reported for *cis*- $(\text{Ph}_3\text{P})_2\text{Pt}(\text{H})(\text{GeHMes}_2)$ [$\delta 29.5$ ($^1J_{\text{Pt-P}} = 2350$ Hz), 33.3 ($^1J_{\text{Pt-P}} = 2137$ Hz)].^{4b} In the IR spectrum for **2**, the Ge-H and Pt-H stretching vibrations were observed at 1953 and 2063 cm^{-1} , respectively. Complex **2** is thermally stable in the solid state (mp 127 °C) or in solution, and no dimerization or dissociation of phosphine ligands was observed. The molecular structure of **2** was confirmed unambiguously by X-ray analysis, as depicted in Figure 1. The X-ray crystallographic analysis of **2** revealed that the platinum center has a distorted square-planar environment, probably due to the steric requirement of the *cis*-coordinated PPh_3 ligands and the bulky 9-triptycyl group on the germanium atom. The Pt-Ge bond length [2.4135(7) Å] is slightly shorter than those of previously reported mononuclear germyl(hydrido) platinum(II) complexes, *cis*- $(\text{Ph}_3\text{P})_2\text{Pt}(\text{H})(\text{GeHMes}_2)$ [2.4285(5) Å],^{4b} *cis*- $(\text{Ph}_3\text{P})_2\text{Pt}(\text{H})(\text{GePh}_3)$ [2.4400(4) Å],¹¹ and *cis*- $(\text{Ph}_3\text{P})_2\text{Pt}(\text{H})(\text{GeHMesGeH}_2\text{Mes})$ [2.4348(8) Å].⁷ Both of the Pt-P bond lengths [Pt1-P1 2.3030(16), Pt1-P2 2.2941(16) Å] are almost the same, indicating that the *trans* influence of the germanium atom is close to that of the hydride in this complex.

As part of a program geared to exploring the synthesis of new types of dihydrogermyl(hydrido) platinum(II) complexes, we next focused our attention on the bidentate phosphine ligands such as dppe and dcpe. Thus, the reaction of **1** with 1 equiv with (dppe)Pt, which was generated in situ by the reduction of (dppe)PtCl₂ with an excess amount of NaBH₄ in ethanol,¹² afforded the corresponding dihydrogermyl(hydrido) complex (dppe)Pt(H)(GeH₂Trip) (**3**) together with bis(germyl) complex (dppe)Pt(GeH₂Trip)₂ (**4**) in 36% and 16% yields, respectively, while the reaction of **1** with a half-equivalent of (dppe)Pt in

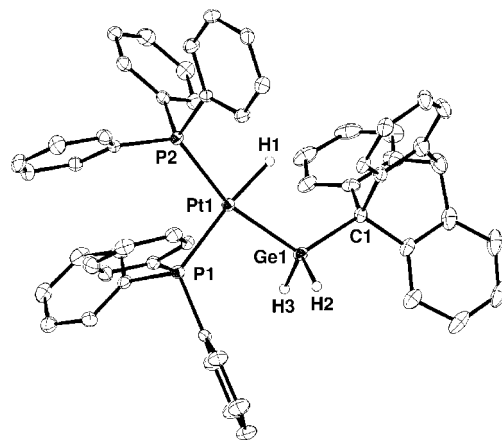
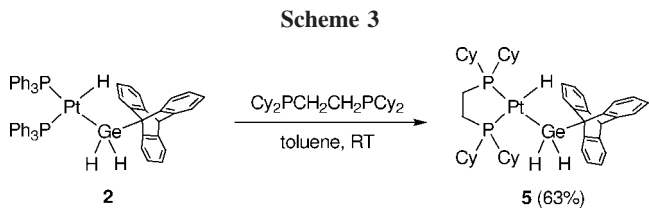
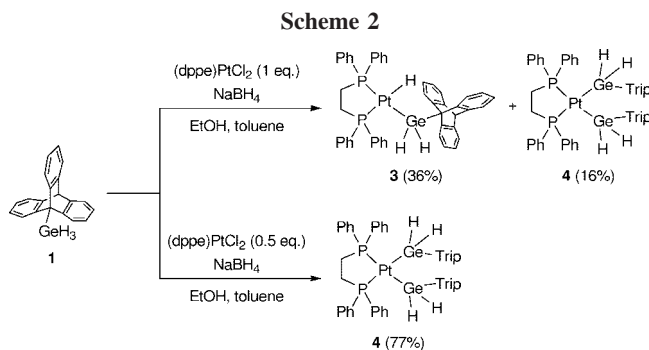


Figure 1. ORTEP drawing of *cis*- $(\text{Ph}_3\text{P})_2\text{Pt}(\text{H})(\text{GeH}_2\text{Trip})$ (**2**) (30% thermal ellipsoids, three CH_2Cl_2 molecules and hydrogen atoms except H1, H2, and H3 were omitted for clarity). Selected bond lengths (Å): Pt1-Ge1 = 2.4135 (7), Pt1-P1 = 2.3030(16), Pt1-P2 = 2.2941(16), Pt1-H1 = 1.64(7), Ge1-C1 = 1.998(6). Selected bond angles (deg): P1-Pt1-P2 = 100.93(6), Ge1-Pt1-P1 = 96.97(6), Ge1-Pt1-H1 = 77(3), P2-Pt1-H1 = 85(3), Ge1-Pt1-P2 = 162.04(4), P1-Pt1-H1 = 174(3).



toluene produced only complex **4** in 77% yield (Scheme 2). The formation of bis(germyl) complex **4** was verified by the reaction of **1** in toluene at room temperature for 3 days to give a 1:1 mixture of **3** and **4** (judged from ^1H NMR). By sharp contrast, complex **2** did not react with **1** under similar conditions, indicating that the steric hindrance due to a tied-back dppe ligand is smaller than that due to two Ph_3P ligands.

On the other hand, dihydrogermyl(hydrido) platinum(II) complex (dcpe)Pt(H)(GeH₂Trip) (**5**) was synthesized by the ligand exchange reaction of complex **2** with free dcpe in toluene at ambient temperature in 63% isolated yield (Scheme 3). The structures of **3-5** were confirmed by NMR and IR spectroscopies and elemental analyses. In the ^1H NMR spectrum of

(10) Brynda, M.; Geoffroy, M.; Bernardinelli, G. *Chem. Commun.* **1999**, 961-962.

(11) Haberer, T.; Nöth, H. *Appl. Organomet. Chem.* **2003**, *17*, 525-538.

(12) The generation of (dppe)Pt species was identified by ^1H and $^{31}\text{P}\{^1\text{H}\}$ NMR spectra. ^1H NMR (400 MHz, C_6D_6): δ 2.12 (br s, 4 H), 6.90-6.98 (m, 12 H), 7.53 (br s, 8 H). $^{31}\text{P}\{^1\text{H}\}$ NMR (162 MHz, C_6D_6): δ 31.2 (s, $^1J_{\text{P-Pt}} = 3729$ Hz). These NMR results are obviously different from those of the related hydrido-(dppe)Pt complexes [(dppe)PtH]₂ [$^{31}\text{P}\{^1\text{H}\}$ NMR: δ 70.9 (s, $^1J_{\text{P-Pt}} = 2201$ Hz)],^{13a} [(dppe)₂Pt₂H₂] [$^{31}\text{P}\{^1\text{H}\}$ NMR: δ -68.1 (s, $^1J_{\text{P-Pt}} = 2201$ Hz)],^{13b} and [(dppe)₃Pt₃H₃]⁺ [$^{31}\text{P}\{^1\text{H}\}$ NMR: δ -82.2 (s, $^1J_{\text{P-Pt}} = 2834$ Hz)].^{13b}

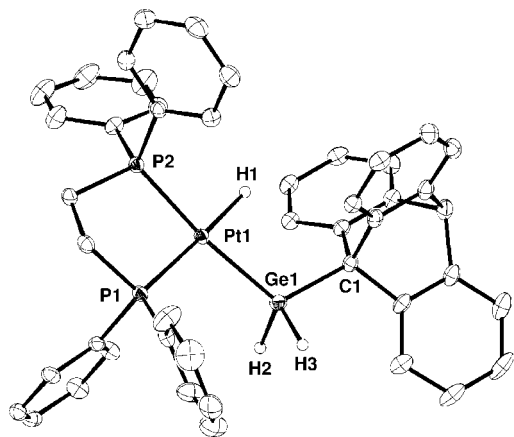


Figure 2. ORTEP drawing of $(dppe)Pt(H)(GeH_2Trip)$ (**3**) (30% thermal ellipsoids, a CH_2Cl_2 molecule and hydrogen atoms except H1, H2, and H3 were omitted for clarity). Selected bond lengths (Å): Pt1–Ge1 = 2.4207(7), Pt1–P1 = 2.2867(15), Pt1–P2 = 2.2534(16), Pt1–H1 = 1.61(8), Ge1–C1 = 2.001(6). Selected bond angles (deg): P1–Pt1–P2 = 86.06(6), Ge1–Pt1–P1 = 103.61(4), Ge1–Pt1–H1 = 80(2), P2–Pt1–H1 = 91(2), Ge1–Pt1–P2 = 169.89(4), P1–Pt1–H1 = 177(2).

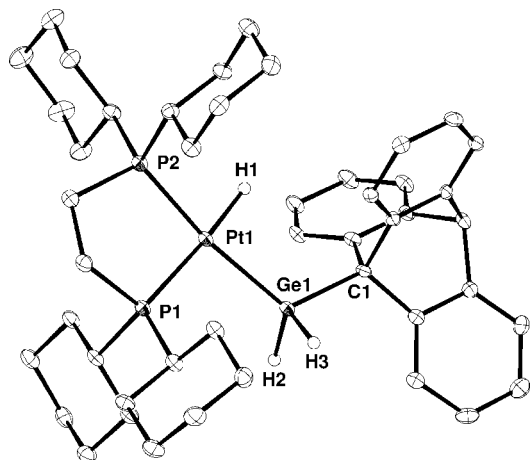
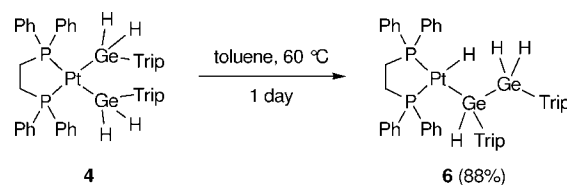


Figure 3. ORTEP drawing of $(dcpe)Pt(H)(GeH_2Trip)$ (**5**) (30% thermal ellipsoids, two CH_2Cl_2 , a toluene molecule, and hydrogen atoms except H1, H2, and H3 were omitted for clarity). Selected bond lengths (Å): Pt1–Ge1 = 2.4162(4), Pt1–P1 = 2.2875(9), Pt1–P2 = 2.2635(10), Pt1–H1 = 1.55(4), Ge1–C1 = 2.017(3). Selected bond angles (deg): P1–Pt1–P2 = 87.63(3), Ge1–Pt1–P1 = 99.63(3), Ge1–Pt1–H1 = 84.0(16), P2–Pt1–H1 = 88.9(16), Ge1–Pt1–P2 = 171.95(3), P1–Pt1–H1 = 175.3(15).

3 and **5**, the hydride resonated as a doublet of doublets at δ -0.58 ($^2J_{P-H} = 180, 10$, $^1J_{Pt-H} = 1034$ Hz) for **3** and -0.85 ($^2J_{P-H} = 172, 12$, $^1J_{Pt-H} = 956$ Hz) for **5**, which are shifted downfield relative to that of complex **2**. The $^{31}P\{^1H\}$ NMR spectra exhibited two singlets with ^{195}Pt satellites at δ 54.1 ($^1J_{Pt-P} = 1802$ Hz) and 61.3 ($^1J_{Pt-P} = 2144$ Hz) for **3** and δ 69.4 ($^1J_{Pt-P} = 1793$ Hz) and 83.2 ($^1J_{Pt-P} = 2161$ Hz) for **5**, which were assigned to the phosphorus atoms lying *trans* to a hydride and a germyl ligand, respectively. By contrast, the $^{31}P\{^1H\}$ NMR chemical shift of **4** was δ 55.1 ($^1J_{Pt-P} = 2027$ Hz). The molecular structures of **3** and **5** are determined by X-ray crystallography, as shown in Figures 2 and 3. Distortions from square-planar geometry at the platinum centers were observed, similarly to the case of **2**, which were due to the steric repulsion between dppe or dcpe ligands and each 9-triptycyl group. The Pt–Ge bond lengths [2.4212(5) Å for **3**, 2.4162(4) Å for **5**] are relatively similar to that observed in complex **2**. The Pt1–P1

Scheme 4



bond lengths [2.2897(11) Å for **3**, 2.2875(9) Å for **5**] are slightly longer than the Pt1–P2 bond length [2.2546(11) Å for **3**, 2.2635(10) Å for **5**], suggesting the lower *trans* influence of the germanium atom compared to that of the hydride.

Banaszak-Holl and co-workers reported thermal rearrangement of bis(germyl) complex *trans*-(Et_3P) $_2Pt(GeAr_2H)_2$ (Ar = 3,5-(CF_3) $_2C_6H_3$), which was prepared by the reaction of secondary hydrogermane Ar_2GeH_2 with $(Et_3P)_2PtGe[N(SiMe_3)_2]_2$, to give digermyl(hydrido) complex *cis*-(Et_3P) $_2Pt(H)(GeAr_2GeAr_2H)$.¹⁴ Very recently, Mochida et al. also reported that bis(germyl) complex *cis*-(Ph_3P) $_2Pt(GeH_2Mes)_2$ was converted to digermyl(hydrido) complex *cis*-(Ph_3P) $_2Pt(H)(GeHMesGeH_2Mes)$, involving the 1,2-migration of a germyl group at room temperature.⁷ Thus, we examined the thermal reaction of *cis*-bis(germyl) derivative **4** (Scheme 4). Heating a toluene solution of **4** at 60 °C for 1 day efficiently gave the corresponding digermyl(hydrido) complex $(dppe)Pt(H)[Ge(HTrip)GeH_2Trip]$ (**6**) in 88% yield. The 1H NMR spectrum of **6** displayed characteristic Ge–H and Pt–H signals at δ 5.57, 5.21, and -0.37 ($^2J_{P-H} = 179, 8$, $^1J_{Pt-H} = 1019$ Hz), respectively. The $^{31}P\{^1H\}$ NMR spectrum of **6** showed two singlets with ^{195}Pt satellites at δ 52.8 ($^1J_{Pt-P} = 1834$ Hz) and 57.3 ($^1J_{Pt-P} = 2182$ Hz). The formation mechanism of **6** can be explained by the formation of a germylene-platinum complex as formal platinum(IV) intermediate **7** or the reductive elimination of digermene **8** from **4**, followed by an oxidative addition of the Ge–H bond in **8**, to generate the $(dppe)Pt$ complex (Scheme 5).¹⁵ Tilley has reported that 1,2-migrations in four-coordinated Pt–Si complexes to produce platinum-silylene complexes without prior ligand dissociation are not favorable and that the metal center must be unsaturated for the α -migration to be favorable.¹⁶ In our system, the dissociation of chelating dppe ligand in **4** is not likely. Therefore, the pathway via reductive elimination may be more preferable.

Conclusion

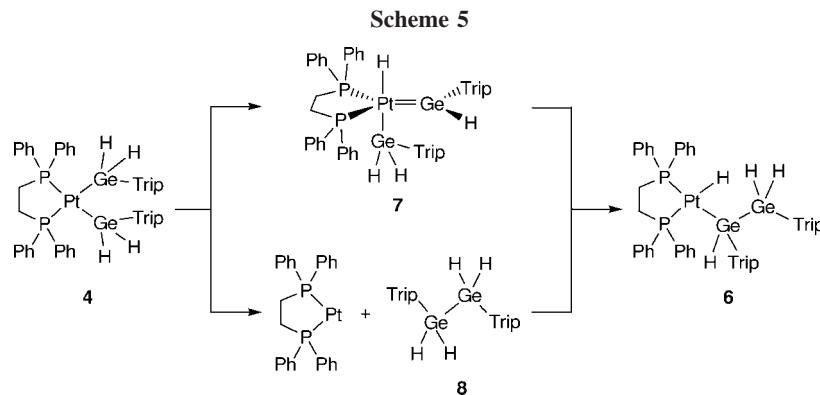
The oxidative addition of an overcrowded trihydrogermane, $TripGeH_3$ (**1**), to Pt(0) precursors such as $(Ph_3P)_2Pt(\eta^2-C_2H_4)$ or $(dppe)Pt$ resulted in the successful isolations of dihydrogermyl(hydrido) platinum(II) complexes *cis*-(Ph_3P) $_2Pt(H)(GeH_2Trip)$ (**2**) or $(dppe)Pt(H)(GeH_2Trip)$ (**3**), respectively. Additionally, the ligand exchange reaction between complex **1** and dcpe smoothly proceeded at room temperature to give the corresponding hydrido complex $(dcpe)Pt(H)(GeH_2Trip)$, **5**. The molecular structures of the hydrido complexes were revealed

(13) (a) Knobler, C. B.; Kaesz, H. D.; Minghetti, G.; Bandini, A. L.; Banditelli, G.; Bonati, F. *Inorg. Chem.* **1983**, *22*, 2324–2331. (b) Carmichael, D.; Hitchcock, P. B.; Nixon, J. F.; Pidcock, A. P. *J. Chem. Soc., Chem. Commun.* **1988**, 1554–1556.

(14) Bender, J. E.; Litz, K. E.; Giarikos, D.; Wells, N. J.; Banaszak-Holl, M. M.; Kampf, J. W. *Chem.–Eur. J.* **1997**, *3*, 1793–1796.

(15) We confirmed the production of (digermyl) complex **6** by the oxidative addition of tetrahydrodigermene ($TripH_2Ge$) $_2$ with $(Ph_3P)_2Pt(\eta^2-C_2H_4)$ in toluene (29% yield).

(16) (a) Mitchell, G. P.; Tilley, T. D. *Angew. Chem., Int. Ed.* **1998**, *37*, 2524–2526. (b) Feldman, J. D.; Mitchell, G. P.; Nolte, J.-O.; Tilley, T. D. *Can. J. Chem.* **2003**, *81*, 1127–1136.

**Table 1. Crystallographic Data and Details of Refinement for 2, 3, and 5**

	2	3	5
formula	C ₃₉ H ₅₂ Cl ₆ GeP ₂ Pt	C ₄₇ H ₄₂ Cl ₂ GeP ₂ Pt	C ₅₅ H ₇₆ Cl ₄ GeP ₂ Pt
fw	1303.33	1007.33	1208.58
color	colorless	colorless	colorless
cryst size/mm	0.30 × 0.20 × 0.20	0.43 × 0.40 × 0.25	0.30 × 0.30 × 0.30
temp/K	123	103	103
cryst syst	triclinic	monoclinic	monoclinic
space group	P1	P2 ₁ /n	P2 ₁ /c
a/Å	11.8284(9)	11.2374(4)	16.2932(6)
b/Å	12.1690(9)	20.0320(7)	19.9960(7)
c/Å	21.1183(16)	19.0101(7)	17.0506(6)
α/deg	102.190(2)	90	90
β/deg	93.663(2)	105.2000(10)	104.4760(10)
γ/deg	114.777(2)	90	90
V/Å ³	2657.6(3)	4129.6(3)	5378.7(3)
Z	2	4	4
D _{calcd} /g cm ⁻³	1.629	1.620	1.492
no. of unique data	10 351	7682	11 138
no. of params	626	490	635
no. of restraints	0	1	29
R ₁ (I > 2σ(I))	0.0480	0.0329	0.0340
wR ₂ (all data)	0.1322	0.0855	0.0852
GOF	1.035	1.023	1.036

by the spectroscopic data and by X-ray crystallography. These results present the first examples of stable dihydrogermyl(hydrido) platinum(II) complexes, which are proposed as the initial products in the oxidative additions of primary trihydrogermanes to platinum(0) complexes.

Experimental Section

General Procedure. All experiments were performed under an argon atmosphere unless otherwise noted. Solvents were dried by standard methods and freshly distilled prior to use. ¹H, ¹³C{¹H}, and ³¹P{¹H} NMR spectra were recorded on a Bruker DPX-400 or DRX-400 (400, 100.7, and 162 MHz, respectively) spectrometer using CDCl₃ or C₆D₆ as the solvent at room temperature. IR spectra were obtained on a Perkin-Elmer System 2000 FT-IR spectrometer. Elemental analyses were carried out at the Molecular Analysis and Life Science Center of Saitama University. All melting points were determined on a Mel-Temp capillary tube apparatus and are uncorrected. Preparative thin-layer chromatography (PTLC) was performed with Merck Kieselgel 60 PF254. 9-Triptycyltrihydrogermane (**1**)¹⁰ and (Ph₃P)₂Pt(η²-C₂H₄)¹⁷ were prepared according to the reported procedures.

[cis-(Ph₃P)₂Pt(H)(GeH₂Trip)] (2). A mixture of **1** (31.3 mg, 0.095 mmol) and (Ph₃P)₂Pt(η²-C₂H₄) (75.8 mg, 0.101 mmol) in dry toluene (3 mL) was stirred at room temperature for 1 h to form a pale yellow solution. After removal of the solvent in vacuo, the residual colorless solid was purified by washing three times with hexane (ca. 3 mL) to give **2** (100 mg, 99%) as colorless crystals. Mp: 127 °C (dec). ¹H NMR (400 MHz, CDCl₃): δ -3.23 (dd, 1 H, ²J_{H-P(trans)} = 168, ²J_{H-P(cis)} = 18, ¹J_{Pt-H} = 894 Hz, Pt-H), 4.43 (m,

2 H, Ge-H), 5.28 (s, 1 H), 6.80–6.90 (m, 6 H), 7.01–7.05 (m, 6 H), 7.14–7.30 (m, 21 H), 7.45–7.49 (m, 6 H), 7.77–7.79 (d, 3 H, J = 7.1 Hz). ¹³C{¹H} NMR (101 MHz, CDCl₃): δ 55.3, 122.7, 123.8, 126.5, 127.7, 127.8, 129.4, 129.6, 134.1, 134.1, 134.2, 134.3, 148.3, 149.8. ³¹P{¹H} NMR (162 MHz, CDCl₃): δ 31.2 (d, ²J_{P-P} = 13, ¹J_{P-Pt} = 2317 Hz, *trans* to Ge), 31.6 (d, ²J_{P-P} = 13, ¹J_{P-Pt} = 2252 Hz, *trans* to H). IR (KBr) (ν, cm⁻¹): 1953 (Ge-H), 2063 (Pt-H). Anal. Calcd for C₅₆H₄₆GeP₂Pt: C, 64.13; H, 4.42. Found: C, 63.87; H, 4.32.

Reaction of 1 with 1 equiv of (dppe)Pt. A solution of **1** (20.0 mg, 0.061 mmol) in dry toluene (2 mL) was added to the ethanol (2 mL) solution of (dppe)Pt, which was prepared via reduction of (dppe)PtCl₂ (42.8 mg, 0.064 mmol) with NaBH₄ (8.4 mg, 0.221 mmol) at room temperature for 10 min. The reaction mixture was stirred at room temperature for 3 h. The solution was filtered through Celite and rinsed with CH₂Cl₂. After removal of the solvent in vacuo, the residue was purified by PTLC (CH₂Cl₂/hexane, 1:1) to give [(dppe)Pt(H)(GeH₂Trip)] (**3**) (20.3 mg, 36%) and [(dppe)Pt(GeH₂Trip)₂] (**4**) (5.7 mg, 16%) as colorless crystals. **3**: mp 155 °C (dec). ¹H NMR (400 MHz, CDCl₃): δ -0.58 (dd, 1 H, ²J_{H-P(trans)} = 180, ²J_{H-P(cis)} = 10, ¹J_{Pt-H} = 1034 Hz, Pt-H), 2.43 (m, 4 H), 5.02–5.26 (m, 2 H, Ge-H), 5.34 (s, 1 H), 6.83–6.93 (m, 6 H), 7.31–7.34 (m, 8 H), 7.43–7.45 (m, 6 H), 7.70–7.80 (m, 9 H), 7.89–7.91 (d, 3 H, J = 7 Hz). ¹³C{¹H} NMR (100.6 MHz, C₆D₆): δ 27.8 (dd, ¹J_{C-P} = 31, ²J_{C-P} = 17 Hz), 30.5 (dd, ¹J_{C-P} = 32, ²J_{C-P} = 19 Hz), 51.1 (m, 1 C), 56.1, 123.3, 124.3, 124.3, 127.5, 128.3, 128.7–128.9 (m), 130.6 (d, ⁴J_{C-P} = 2 Hz), 130.7 (d, ⁴J_{C-P} = 2 Hz), 133.0 (d, ¹J_{C-P} = 44 Hz), 133.0 (d, ¹J_{C-P} = 44 Hz), 133.3–133.4 (m), 150.0, 150.8. ³¹P{¹H} NMR (162 MHz, CDCl₃): δ 54.1 (s, ¹J_{P-Pt} = 1802 Hz, *trans* to H), 61.3 (s, ¹J_{P-Pt} = 2144 Hz, *trans* to Ge). IR (KBr) (ν, cm⁻¹): 1941 (Ge-H), 2032 (Pt-H). Anal. Calcd for C₄₆H₄₀GeP₂Pt: C, 59.89; H, 4.37. Found: C, 59.53; H, 4.49. **4**: mp 185 °C (dec). ¹H NMR (400 MHz, CDCl₃): δ 2.00–2.05 (m, 4 H), 4.86–5.05 (m, 4 H, Ge-H), 5.17 (s, 2 H), 6.48–6.52 (m, 6 H), 6.73–6.77 (m, 6 H), 7.10–7.24 (m, 18 H), 7.62–7.73 (m, 14 H). ¹³C{¹H} NMR (100.7 MHz, CDCl₃): δ 32.0–32.5 (m, 2 C), 52.2 (dd, ³J_{C-P} = 5, 5 Hz, Ge-C), 55.2, 122.4, 123.6, 123.9, 127.3, 128.2 (d, ³J_{C-P} = 5 Hz), 128.2 (d, ³J_{C-P} = 5 Hz), 129.5 (d, ³J_{C-P} = 47 Hz), 130.9, 133.7 (d, ³J_{C-P} = 6 Hz), 133.8 (d, ³J_{C-P} = 6 Hz), 147.2, 149.4. ³¹P{¹H} NMR (162 Hz, CDCl₃): δ 55.1 (s, ³J_{P-Pt} = 2027 Hz). IR (KBr) (ν, cm⁻¹): 1976 (Ge-H). Anal. Calcd for C₆₆H₅₄Ge₂P₂Pt: C, 63.45; H, 4.36. Found: C, 63.46; H, 4.47.

Reaction of 1 with 0.5 equiv of (dppe)Pt. A solution of **1** (247.3 mg, 0.751 mmol) in dry toluene (5 mL) was added to the ethanol (5 mL) solution of 0.5 equiv of (dppe)Pt (0.373 mmol). The reaction mixture was stirred at room temperature for 13 h. The solution was filtered through Celite and rinsed with CH₂Cl₂. After removal of the solvent in vacuo, the residue was purified by PTLC (CH₂Cl₂/hexane, 1:1) to give complex **4** (358.8 mg, 77%).

[(dcpe)Pt(H)(GeH₂Trip)] (5). A mixture of **2** (60.5 mg, 0.058 mmol) and Cy₂PCH₂CH₂PCy₂ (24.8 mg, 0.059 mmol) in dry toluene (5 mL) was stirred at room temperature for 30 min to form a clear solution. After removal of the solvent in vacuo, the residual colorless

solid was purified by PTLC (CH₂Cl₂/hexane, 1:2) to give complex **5** (34.3 mg, 63%) as colorless crystals. Mp: 182 °C (dec). ¹H NMR (400 MHz, CDCl₃): δ -0.85 (dd, 1 H, ²J_{H-P(trans)} = 172, ²J_{H-P(cis)} = 12, ¹J_{Pt-H} = 956 Hz, Pt-H), 1.16–1.37 (m, 20 H), 1.64–1.86 (m, 24 H), 2.15–2.18 (m, 2 H), 2.34–2.39 (m, 2 H), 5.25 (dd, 2 H, ²J_{H-H} = 15, ³J_{H-P(trans)} = 5, ²J_{Pt-H} = 72 Hz, Ge-H), 5.33 (s, 1 H), 6.81–6.91 (m, 6 H), 7.30–7.32 (d, 3 H, *J* = 7.0 Hz), 7.90–7.92 (d, 3 H, *J* = 7.0 Hz). ¹³C{¹H} NMR (101 MHz, CDCl₃): δ 23.5 (dd, ³J_{C-P} = 23, 16 Hz, PCH₂), 25.1 (dd, ³J_{C-P} = 24, 18 Hz, PCH₂), 26.2 (d, ³J_{C-P} = 14 Hz, PCy), 26.6 (d, ³J_{C-P} = 13 Hz, PCy), 26.8–27.1 (m, PCy × 2), 28.8 (m, PCy), 29.1 (m, PCy), 29.6 (m, PCy), 35.1–35.8 (m, PCy × 2), 49.9, 55.4, 122.7, 123.6, 123.7, 127.1, 149.4, 150.5. ³¹P{¹H} NMR (162 MHz, CDCl₃): δ 69.4 (s, ¹J_{P-Pt} = 1793 Hz, *trans* to H), 83.2 (s, ¹J_{P-Pt} = 2161 Hz, *trans* to Ge). IR (KBr) (ν, cm⁻¹): 1929 (Ge-H), 2024 (Pt-H). Anal. Calcd for C₄₆H₆₄GeP₂Pt: C, 58.36; H, 6.81. Found: C, 58.63; H, 6.81.

{(dpe)Pt(H)[Ge(HTrip)GeH₂Trip]} (**6**). **4** (17.9 mg, 0.014 mmol) was heated to 60 °C in toluene (3 mL) for 1 day. After removal of the solvent in vacuo, the residual colorless solid was purified by washing three times with hexane (ca. 3 mL) to give **6** (15.8 mg, 88%) as colorless crystals. Mp: 205 °C (dec). ¹H NMR (400 MHz, C₆D₆): δ -0.37 (dd, 1 H, ²J_{H-P(trans)} = 179, ²J_{H-P(cis)} = 8, ¹J_{Pt-H} = 1019 Hz, Pt-H), 1.65 (br s, 1 H), 1.89–2.13 (m, 3 H), 5.22 (br, 1 H, Ge-H), 5.22 (s, 1 H), 5.26 (s, 1 H), 5.31–5.32 (m, 1 H, Ge-H), 5.54–5.61 (m, 1 H, Ge-H), 6.39 (dd, 3 H, *J* = 7.2, *J* = 7.6 Hz), 6.73 (dd, 3 H, *J* = 7.2, *J* = 7.6 Hz), 6.80–7.25 (m, 24 H), 7.48–7.69 (m, 8 H), 7.90 (d, *J* = 7.6 Hz, 3 H), 8.27 (br s, 2 H), 9.11 (br s, 1 H). ³¹P{¹H} NMR (162 MHz, C₆D₆): δ 52.8 (s, ¹J_{P-Pt} = 1834 Hz, *trans* to H), 57.3 (s, ¹J_{P-Pt} = 2182 Hz, *trans* to Ge). IR (KBr) (ν, cm⁻¹): 1934 (br), 2002 (br). Anal. Calcd for C₆₆H₅₄Ge₂P₂Pt: C, 63.45; H, 4.36. Found: C, 63.37; H, 4.34. We were unable to obtain a ¹³C{¹H} NMR spectrum due to the poor solubility of this complex in CDCl₃ or C₆D₆.

X-ray Crystallographic Analyses of 2, 3, and 5. Colorless single crystals of **2** and **3** were grown by the slow evaporation of its saturated CH₂Cl₂ and hexane solution, and single crystals of **5** were grown by the slow evaporation of its saturated toluene, CH₂Cl₂, and hexane solution. The intensity data were collected at 123 K for **2** and 103 K for **3** and **5** on a Bruker AXS SMART diffractometer employing graphite-monochromatized Mo Kα radiation (λ = 0.71073 Å). The structures were solved by direct methods and refined by full-matrix least-squares procedures on *F*² for all reflections (SHELX-97).¹⁸ Hydrogen atoms, except for the PtH hydrogen of **2** and PtH and GeH hydrogens of **3** and **5**, were located by assuming ideal geometry and were included in the structure calculations without further refinement of the parameters. Crystallographic data and details of refinement for **2**, **3**, and **5** are summarized in Table 1.

Acknowledgment. This work was supported by a Grant-in-Aid for Scientific Research (Nos. 18750026 and 19027014) from the Ministry of Education, Science, Sports, and Culture of Japan. We are grateful to Professor Kohtaro Osakada and Dr. Makoto Tanabe of Tokyo Institute of Technology for their useful discussions and suggestions.

Supporting Information Available: Crystallographic data for **2**, **3**, and **5** as CIF files. This material is available free of charge via the Internet at <http://pubs.acs.org>.

OM800809N

(17) (a) Cook, C. D.; Jauhal, G. S. *J. Am. Chem. Soc.* **1968**, *90*, 1464–1467. (b) Ugo, R.; Calciati, F.; LaMonica, G. *Inorg. Synth.* **1968**, *11*, 106.

(18) Sheldrick, G. M. *SHELXL-97*, Program for Crystal Structure Refinement; University of Göttingen: Germany, 1997.

Bi- and Trinuclear Complexes of Group 4 Metal and Palladium Bridged by OPPh₂ Groups: Synthesis and High Catalytic Activities in Double Hydrophosphinylation of 1-Octyne

Tsutomu Mizuta,* Chihiro Miyaji, Takafumi Katayama, Jun-ichi Ushio, Kazuyuki Kubo, and Katsuhiko Miyoshi

Department of Chemistry, Graduate School of Science, Hiroshima University, Kagamiyama 1-3-1, Higashi-Hiroshima, Hiroshima 739-8526, Japan

Received August 26, 2008

The early–late heterobinuclear complexes Cp₂M(μ-OPPh₂)₂PdMe₂ (M = Ti (**1**), Zr (**2**), and Hf (**3**)) were synthesized by the reaction of PdMe₂(tmeda) (tmeda = Me₂NCH₂CH₂NMe₂) with respective metallocene diphosphinite ligands Cp₂M(OPPh₂)₂ prepared from Cp₂MCl₂ (M = Ti, Zr, and Hf) and LiOPPh₂. The complexes **1–3** catalyzed the addition (hydrophosphinylation) of HP(O)Ph₂ to 1-octyne to give mainly not the single-addition product *n*-Hex-CH=CHP(O)Ph₂ (**4a**) or *n*-Hex-C{P(O)Ph₂}=CH₂ (**4b**) but the double-addition product *n*-Hex-CH{P(O)Ph₂}CH₂P(O)Ph₂ (**5**) at 40 °C in low yields. The yield of **5** was, however, substantially improved to >95% for **2** and **3** when tertiary phosphine PR₃ such as PMePh₂ was added to the catalytic system. The stoichiometric reaction of the complexes **1–3** with the phosphorus substrate HP(O)Ph₂ and PMePh₂ afforded in situ the trinuclear complexes H(PMePh₂)Pd(μ-OPPh₂)₃M(μ-OPPh₂)₃PdH(PMePh₂), which were found to exhibit the high catalytic activities similar to those of their parent complexes **1–3** in the presence of PR₃ and were thus proposed to be a practical catalyst. On the basis of the above findings, simple mixtures of mononuclear Cp₂MCl₂ and PdMe₂(tmeda) complexes together with PMePh₂ could be used successfully as precatalysts for the double hydrophosphinylation of 1-octyne with HP(O)Ph₂ to give satisfactory results comparable to those attained with the preorganized binuclear complexes **2** and **3** with PMePh₂ added.

Introduction

Early–late heterobinuclear complexes have long been recognized to have new and valuable reactivities brought about through the combination of different properties that respective metal centers assume.^{1,2} Lewis-acidic early-transition-metal and electron-rich late-transition-metal catalysts are both well-established mononuclear systems used widely for conjugate additions and coupling reactions, respectively, in organic synthesis.^{3,4} Hence, their combinations have been believed to exhibit a promising cooperative catalytic activity, and actually dramatic effects on the reactivity were demonstrated simply by using these two different types of catalysts together.⁵ If early- and late-transition-metal catalysts are intentionally linked in advance so as to interact cooperatively with a substrate, the resulting preorganized heterobinuclear complex would exhibit a higher efficiency and/or novel function in catalytic reactions. However, a fairly limited number of systems have attained outstanding catalytic activities so far.^{1,6}

A Pd-catalyzed hydrophosphinylation of terminal alkynes was first reported by Tanaka's group in 1996.⁷ Since then, it has been intensively investigated by several research groups and has become a useful synthetic method to give monohydrophosphinylated alkene, i.e., a single addition product, under mild reaction conditions.^{8–10} However, the second addition to give the double-addition product proceeded to a limited extent, because the steric demand of the single-addition product prevents its alkene part from coordinating to the Pd center of the catalyst. It is only under enforcing conditions (above 100 °C) that the double-addition product was obtained in

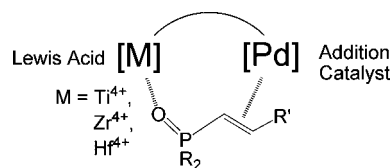


Figure 1. Cooperative interaction of group 4 metal–Pd binuclear complexes with olefin bearing a hard functional group.

a good yield.¹¹ Thus, development of a metal catalyst that promotes the double addition “under mild conditions” is an important subject in view of the delicate tuning of catalyst–substrate interactions.

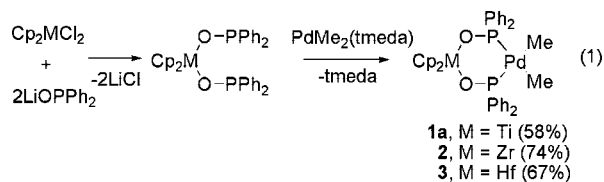
On the other hand, as a part of our ongoing research on heterobinuclear complexes,¹² we have recently obtained a bidentate Cp₂Ti(OPPh₂)₂ metallo ligand having two OPPh₂ arms as P-donor groups, which allowed us to synthesize a bifunctional Ti–Pd binuclear complex to catalyze the hydrophosphinylation. Since the hard Ti(IV) center of the preorganized binuclear complex is expected to hold firmly the single-addition product bearing a hard O=P group through the concurrent interaction as illustrated in Figure 1, otherwise inaccessible double addition would be promoted. With this expectation in mind, we examined the hydrophosphinylation of 1-octyne with the M–Pd (M = Ti, Zr, Hf) binuclear complexes as catalysts.

Results and Discussion

Preparation of Binuclear Complexes. The binuclear complexes **1a**, **2**, and **3** were prepared according to eq 1, in which metallocene diphosphinite ligands Cp₂M(OPPh₂)₂ were obtained in advance from Cp₂MCl₂ (M = Ti, Zr, Hf) and LiOPPh₂, according to a method similar to that reported for the analogue

* To whom correspondence should be addressed. Fax: +81-82-424-0729. E-mail: mizuta@sci.hiroshima-u.ac.jp.

(1) (a) Stephan, D. W. *Coord. Chem. Rev.* **1989**, *95*, 41–107. (b) Wheatley, N.; Kalck, P. *Chem. Rev.* **1999**, *99*, 3379–3419.



$\text{Cp}_2\text{Zr}(\text{CH}_2\text{PPh}_2)_2$, having CH_2PPh_2 arms.^{13,14} The formation of these metallo ligands was confirmed by the appearance of ^{31}P NMR signals at 126.7, 114.1, and 112.2 ppm for the Ti, Zr, and Hf ligands, respectively. Out of these, $\text{Cp}_2\text{Ti}(\text{OPPh}_2)_2$ was found to decompose gradually to give an arm-coupling product $\text{Ph}_2\text{P}(\text{O})\text{-PPh}_2$ in addition to a white precipitate, which was probably a polymeric species $(\text{Cp}_2\text{TiO})_n$. Hence the Ti ligand prepared in situ was immediately used for the subsequent

reaction with $\text{PdMe}_2(\text{tmeda})$ ($\text{tmeda} = \text{Me}_2\text{NCH}_2\text{CH}_2\text{NMe}_2$), which gave $\text{Cp}_2\text{Ti}(\mu\text{-OPPh}_2)_2\text{PdMe}_2$ (**1a**) in a moderate yield. On the other hand, the Zr and Hf ligands were stable at ambient temperature to give the corresponding M–Pd (M = Zr **2** and Hf **3**) complexes in better yields. For the Ti–Pd complex, the analogue $\text{Cp}'_2\text{Ti}(\mu\text{-OPPh}_2)_2\text{PdMe}_2$ (**1b**), having $\text{C}_3\text{H}_4\text{Me}$ (Cp') in place of Cp, was also prepared in hopes of its increased solubility (vide infra). The characterization of the binuclear complexes was carried out by $^{31}\text{P}\{^1\text{H}\}$, ^1H , and $^{13}\text{C}\{^1\text{H}\}$ NMR as well as X-ray crystal structure analysis, as follows. The $^{31}\text{P}\{^1\text{H}\}$ NMR signals of **1a**, **1b**, **2**, and **3** were observed at 166.7, 164.1, 151.2, and 149.2 ppm, respectively, which were all at a lower field by ca. 40 ppm than those of the corresponding

(9) (a) Alnasleh, B. K.; Sherrill, W. M.; Rubin, M. *Org. Lett.* **2008**, *10*, 3231–3234. (b) Dobashi, N.; Fuse, K.; Hoshino, T.; Kanada, J.; Kashiwabarara, T.; Kobata, C.; Nune, S. K.; Tanaka, M. *Tetrahedron Lett.* **2007**, *48*, 4669–4673. (c) Nune, S. K.; Tanaka, M. *Chem. Commun.* **2007**, *27*, 2858–2860. (d) Stockland, R. A.; Lipman, A. J.; Bawiec, J. A.; Morrison, P. E.; Guzei, I. A.; Findeis, P. M.; Tamblin, J. F. *J. Organomet. Chem.* **2006**, *691*, 4042–4053. (e) Van Rooy, S.; Cao, C.; Patrick, B. O.; Lam, A.; Love, J. A. *Inorg. Chim. Acta* **2006**, *359*, 2918–2923. (f) Montchamp, J.-L. *J. Organomet. Chem.* **2005**, *690*, 2388–2406. (g) Stockland, R. A. J.; Taylor, R. I.; Thompson, L. E.; Patel, P. B. *Org. Lett.* **2005**, *7*, 851–853. (h) Deprele, S.; Montchamp, J.-L. *J. Am. Chem. Soc.* **2002**, *124*, 9386–9387. (i) Deprele, S.; Montchamp, J.-L. *J. Am. Chem. Soc.* **2002**, *124*, 9386–9387. (j) Levine, A. M.; Stockland, R. A. J.; Clark, R.; Guzei, I. *Organometallics* **2002**, *21*, 3278–3284. (k) Zhao, C.-Q.; Han, L.-B.; Tanaka, M. *Organometallics* **2000**, *19*, 4196–4198. (l) Han, L.-B.; Hua, R.; Tanaka, M. *Angew. Chem., Int. Ed.* **1998**, *37*, 94–96.

(10) (a) Kondoh, A.; Yorimitsu, H.; Oshima, K. *Bull. Chem. Soc. Jpn.* **2008**, *81*, 502–505. (b) Niu, M.; Fu, H.; Jiang, Y.; Zhao, Y. *Chem. Commun.* **2007**, *3*, 272–274. (c) Ribiere, P.; Bravo-Altamirano, K.; Antczak, M. I.; Hawkins, J. D.; Montchamp, J.-L. *J. Org. Chem.* **2005**, *70*, 4064–4072. (d) Han, L.-B.; Zhao, C.-Q.; Onozawa, S.; Goto, M.; Tanaka, M. *J. Am. Chem. Soc.* **2002**, *124*, 3842–3843. (e) Han, L.-B.; Zhao, C.-Q.; Tanaka, M. *J. Org. Chem.* **2001**, *66*, 5929–5932. (f) Zhao, C.-Q.; Han, L.-B.; Goto, M.; Tanaka, M. *Angew. Chem., Int. Ed.* **2001**, *40*, 1929–1932. (g) Reichwein, J. F.; Patel, M. C.; Pagenkopf, B. L. *Org. Lett.* **2001**, *3*, 4303–4306.

(11) (a) Han, L.-B.; Ono, Y.; Shimada, S. *J. Am. Chem. Soc.* **2008**, *130*, 2752–2753. (b) Dobashi, N.; Fuse, K.; Hoshino, T.; Kanada, J.; Kashiwabarara, T.; Kobata, C.; Nune, S. K.; Tanaka, M. *Tetrahedron Lett.* **2007**, *48*, 4669–4673. (c) Stone, J. J.; Stockland, R. A.; Reyes, J. M.; Kovach, J.; Goodman, C. C.; Tillman, E. S. *J. Mol. Catal. A. Chem.* **2005**, *226*, 11–21. (d) Allen, A. J.; Ma, L.; Lin, W. *Tetrahedron Lett.* **2002**, *43*, 3707–3710. (e) Allen, A. J.; Manke, D. R.; Lin, W. *Tetrahedron Lett.* **2000**, *41*, 151–154.

(12) (a) Mizuta, T.; Nakazono, T.; Miyoshi, K. *Angew. Chem., Int. Ed.* **2002**, *41*, 3897–3898. (b) Imamura, Y.; Kubo, K.; Mizuta, T.; Miyoshi, K. *Organometallics* **2006**, *25*, 2301–2307. (c) Mizuta, T.; Iwakuni, Y.; Nakazono, T.; Kubo, K.; Miyoshi, K. *J. Organomet. Chem.* **2007**, *692*, 184–193. (d) Kubo, K.; Akimoto, T.; Mizuta, T.; Miyoshi, K. *Chem. Lett.* **2008**, *37*, 166–167.

(13) (a) Schore, N. E.; Hope, H. *J. Am. Chem. Soc.* **1980**, *102*, 4251–4253. (b) Schore, N. E.; Young, S. J.; Olmstead, M.; Hofmann, P. *Organometallics* **1983**, *2*, 1769–1780. (c) Etienne, M.; Choukroun, R.; Gervais, D. *J. Chem. Soc., Dalton Trans.* **1984**, *5*, 915–917. (d) Choukroun, R.; Gervais, D.; Rifai, C. E. *J. Organomet. Chem.* **1989**, *368*, C11–C14. (e) Cuenca, T.; Flores, J. C.; Royo, P.; Larssonneur, A. M.; Choukroun, R.; Dahhan, F. *Organometallics* **1992**, *11*, 777–780. (f) Tuetting, D. R.; Olmstead, M. M.; Schore, N. E. *Organometallics* **1992**, *11*, 2235–2241. (g) Cuenca, T.; Flores, J. C.; Royo, P. *J. Organomet. Chem.* **1993**, *462*, 191–201.

(14) (a) Choukroun, R.; Gervais, D. *J. Organomet. Chem.* **1984**, *266*, C37–C40. (b) Karsch, H. H.; Muller, G.; Kruger, C. *J. Organomet. Chem.* **1984**, *273*, 195–212. (c) Senocq, F.; Randrianalimanana, C.; Thorez, A.; Kalck, P.; Choukroun, R.; Gervais, D. *J. Chem. Soc., Chem. Commun.* **1984**, *20*, 1376–1377. (d) Senocq, F.; Randrianalimanana, C.; Thorez, A.; Kalck, P.; Choukroun, R.; Gervais, D. *J. Mol. Catal.* **1986**, *35*, 213–219. (e) Choukroun, R.; Gervais, D.; Jaud, J.; Kalck, P.; Senocq, F. *Organometallics* **1986**, *5*, 67–71. (f) Choukroun, R.; Iraqi, A.; Gervais, D. *J. Organomet. Chem.* **1986**, *311*, C60–C62. (g) Choukroun, R.; Iraqi, A.; Gervais, D.; Daran, J. C.; Jeannin, Y. *Organometallics* **1987**, *6*, 1197–1201. (h) Choukroun, R.; Gervais, D.; Kalck, P.; Senocq, F. *J. Organomet. Chem.* **1987**, *335*, C9–C12. (i) Choukroun, R.; Iraqi, A.; Rifai, C.; Gervais, D. *J. Organomet. Chem.* **1988**, *353*, 45–52. (j) Choukroun, R.; Gervais, D.; Rifai, C. *Polyhedron* **1989**, *8*, 1760–1761. (k) Choukroun, R.; Dahhan, F.; Gervais, D.; Rifai, C. *Organometallics* **1990**, *9*, 1982–1987. (l) Trzeciak, A. M.; Ziolkowski, J. J.; Choukroun, R. *J. Organomet. Chem.* **1991**, *420*, 353–358. (m) Trzeciak, A. M.; Ziolkowski, J. J.; Choukroun, R. *J. Mol. Catal. A. Chem.* **1996**, *110*, 135–139.

(2) Selected recent examples: (a) Edelmann, F. T.; Blaurock, S.; Lorenz, V.; Chivers, T. Z. *Anorg. Allg. Chem.* **2008**, *634*, 413–415. (b) Arashiba, K.; Iizuka, H.; Matsukawa, S.; Kuwata, S.; Tanabe, Y.; Iwasaki, M.; Ishii, Y. *Inorg. Chem.* **2008**, *47*, 4264–4274. (c) Hernandez-Gruel, M. A. F.; Dobrinovitch, I. T.; Lahoz, F. J.; Oro, L. A.; Perez-Torrente, J. J. *Organometallics* **2007**, *26*, 6437–6446. (d) Packheiser, R.; Lang, H. *Inorg. Chem. Commun.* **2007**, *10*, 580–582. (e) Hernandez-Gruel, M. A. F.; Lahoz, F. J.; Dobrinovitch, I. T.; Modrego, F. J.; Oro, L. A.; Perez-Torrente, J. J. *Organometallics* **2007**, *26*, 2616–2622. (f) Sisak, A.; Halmos, E. J. *Organomet. Chem.* **2007**, *692*, 1817–1824. (g) Kuwabara, J.; Takeuchi, D.; Osakada, K. *Chem. Commun.* **2006**, *36*, 3815–3817. (h) Arashiba, K.; Matsukawa, S.; Kuwata, S.; Tanabe, Y.; Iwasaki, M.; Ishii, Y. *Organometallics* **2006**, *25*, 560–562. (i) Alvarez-Vergara, M. C.; Casado, M. A.; Martin, M. L.; Lahoz, F. J.; Oro, L. A.; Perez-Torrente, J. J. *Organometallics* **2005**, *24*, 5929–5936. (j) Comte, V.; Le Gendre, P.; Richard, P.; Moiese, C. *Organometallics* **2005**, *24*, 1439–1444. (k) Cornelissen, C.; Erker, G.; Kehr, G.; Froehlich, R. *Organometallics* **2005**, *24*, 214–225. (l) Cornelissen, C.; Erker, G.; Kehr, G.; Fröhlich, R. *Dalton Trans.* **2004**, *405*, 9–4063. (m) Braunstein, P.; Morise, X.; Benard, M.; Rohmer, M.-M.; Welter, R. *Chem. Commun.* **2003**, *5*, 610–611. (n) Takeuchi, D.; Kuwabara, J.; Osakada, K. *Organometallics* **2003**, *22*, 2305. (o) Hernandez-Gruel, M. A. F.; Perez-Torrente, J. J.; Ciriano, M. A.; Rivas, A. B.; Lahoz, F. J.; Dobrinovitch, I. T.; Oro, L. A. *Organometallics* **2003**, *22*, 1237–1249. (p) Lang, H.; Meichel, E.; Stein, T.; Weber, C.; Kralik, J.; Rheinwald, G.; Pritzkow, H. *J. Organomet. Chem.* **2002**, *664*, 150–160. (q) Back, S.; Stein, T.; Kralik, J.; Weber, C.; Rheinwald, G.; Zsolnai, L.; Huttner, G.; Lang, H. *J. Organomet. Chem.* **2002**, *664*, 123–129. (r) Kuwata, S.; Nagano, T.; Matsubayashi, A.; Ishii, Y.; Hidai, M. *Inorg. Chem.* **2002**, *41*, 4324–4330. (s) Fong, S.-W. A.; Yap, W. T.; Vittal, J. J.; Henderson, W.; Hor, T. S. A. *J. Chem. Soc., Dalton Trans.* **2002**, *8*, 1826–1831. (t) Meichel, E.; Stein, T.; Kralik, J.; Rheinwald, G.; Lang, H. *J. Organomet. Chem.* **2002**, *649*, 191–198. (u) Kato, H.; Seino, H.; Mizobe, Y.; Hidai, M. *J. Chem. Soc., Dalton Trans.* **2002**, 1494–1499. (v) Wenzel, B.; Loennecke, P.; Stender, M.; Hey-Hawkins, E. J. *Chem. Soc., Dalton Trans.* **2002**, *4*, 478–480. (w) Ikada, T.; Mizobe, Y.; Hidai, M. *Organometallics* **2001**, *20*, 4441–4444. (x) Lutz, M.; Haukka, M.; Pakkanen, T. A.; Gade, L. H. *Organometallics* **2001**, *20*, 2631. (y) Mokuolu, Q. F.; Avent, A. G.; Hitchcock, P. B.; Love, J. B. *J. Chem. Soc., Dalton Trans.* **2001**, *18*, 2551–2553. (z) Takayama, C.; Yamaguchi, Y.; Mise, T.; Suzuki, N. *J. Chem. Soc., Dalton Trans.* **2001**, *94*, 8–953.

(3) For recent reviews, see: (a) Krause, N.; Hoffmann-Roder, A. *Synthesis* **2001**, *2*, 171–196. (b) Christoffers, J.; Korielly, G.; Rosiak, A.; Roessle, M. *Synthesis* **2007**, *9*, 1279–1300.

(4) (a) *Handbook of Organopalladium Chemistry for Organic Synthesis*; Negishi, E., Ed.; Wiley-Interscience: New York, 2002; Vols. 1 and 2. (b) Tsuji, J. *Palladium Reagents and Catalysts: New Perspectives for the 21st Century*; John Wiley & Sons: Chichester, 2004. (c) Harrington, P. J. In *Comprehensive Organometallic Chemistry II*; Abel, E. W., Stone, F. G. A., Wilkinson, G., Eds.; Pergamon: Oxford, 1995; Vol. 12, Chapter 8.2, pp 798–903.

(5) (a) Lou, S.; Westbrook, J. A.; Schaus, S. E. *J. Am. Chem. Soc.* **2004**, *126*, 11440–11441. (b) Poli, G.; Giambastiani, G.; Mordini, A. *J. Org. Chem.* **1999**, *64*, 2962–2965. (c) Shen, Q.; Hartwig, J. F. *J. Am. Chem. Soc.* **2007**, *129*, 7734–7735. (d) Nakao, Y.; Yada, A.; Ebata, S.; Hiyama, T. *J. Am. Chem. Soc.* **2007**, *129*, 2428–2429.

(6) Handa, S.; Gnanadesikan, V.; Matsunaga, S.; Shibasaki, M. *J. Am. Chem. Soc.* **2007**, *129*, 4900–4901.

(7) (a) Han, L.-B.; Tanaka, M. *J. Am. Chem. Soc.* **1996**, *118*, 1571–1572. (b) Han, L.-B.; Choi, N.; Tanaka, M. *Organometallics* **1996**, *15*, 3259–3261.

(8) (a) Tanaka, M. *Top. Curr. Chem.* **2004**, *232*, 25–54. (b) Alonso, F.; Beletskaya, I. P.; Yus, M. *Chem. Rev.* **2004**, *104*, 3079–3159.

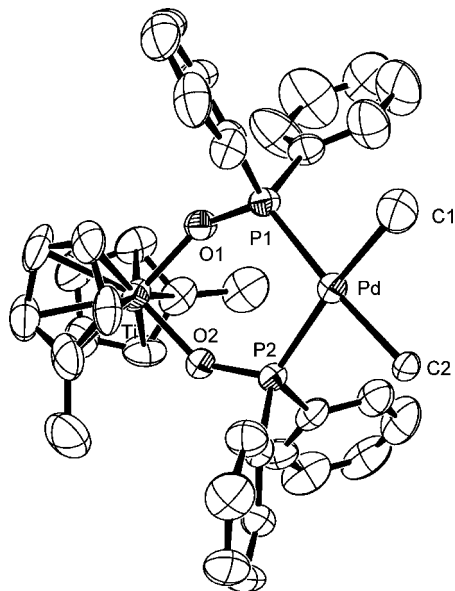


Figure 2. Molecular structure of $\text{Cp}'_2\text{Ti}(\mu\text{-OPPh}_2)_2\text{PdMe}_2$ (**1b**) with thermal ellipsoids given at the 50% probability level.

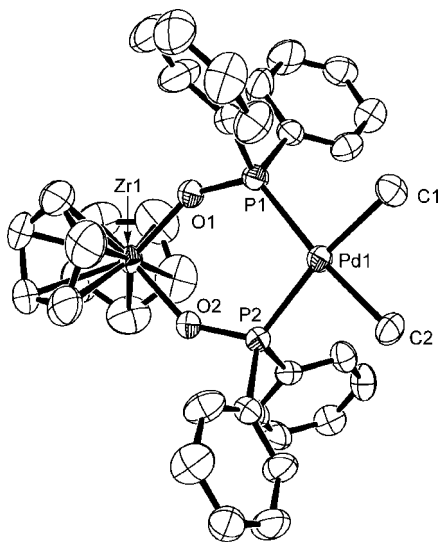


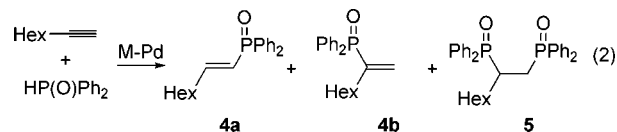
Figure 3. Molecular structure of $\text{Cp}_2\text{Zr}(\mu\text{-OPPh}_2)_2\text{PdMe}_2$ (**2**) with thermal ellipsoids given at the 50% probability level. Note that only one of two crystallographically independent molecules per asymmetric unit is shown.

free ligands. The Me groups on the Pd centers of all the complexes showed multiplet ^1H NMR signals at ca. 0.9 ppm and double-doublet $^{13}\text{C}\{^1\text{H}\}$ NMR signals coupled with both cis and trans phosphorus nuclei.

The molecular structures determined by X-ray analysis are shown in Figures 2–4 for **1b**, **2**, and **3**, respectively, where each metallocene diphosphinite ligand coordinates to a PdMe_2 fragment to form a standard square-planar geometry. The selected geometric parameters are summarized in Table 1. The average Pd–P bond distances are 2.287(2), 2.283(1), and 2.282(1) Å for **1b**, **2**, and **3**, respectively, which are slightly smaller than those of the corresponding $[\text{PdMe}_2\text{L}_2]$ -type ($\text{L} = \text{PRPh}_2$) complexes, e.g., 2.324(1) Å in *cis*- $[\text{PdMe}_2(\text{PMePh}_2)_2]$ and 2.304(3) Å in $[\text{PdMe}_2(\text{dppp})]$ ($\text{dppp} = 1,3\text{-bis}(\text{diphenylphosphino})\text{propane}$).^{15,16} The shorter Pd–P bonds observed for **1b**, **2**, and **3** are in line with the observation that the usual phosphinite ($\text{P}(\text{OR})\text{Ar}_2$) forms a shorter Pd–P bond than does

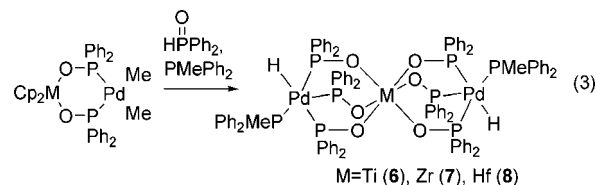
the corresponding phosphine (PRAr_2).¹⁷ In addition, the P–Pd–P bite angles of the metallocene chelates forming six-membered rings are 97.15(8)°, 98.44(4)°, and 98.28(4)° for **1b**, **2**, and **3**, respectively, which are somewhat greater than 93.18(9)° of dppp in $[\text{PdMe}_2(\text{dppp})]$, having a similar six-membered chelate ring. The wider bite angles adopted are attributable both to longer M–O bonds (1.93–1.99 Å) in **1b**, **2**, and **3** than C–C bonds in dppp and to the considerably wide P–O–M angles (140.7–145.3°), leading to favorable π -donation from O to M.

Catalytic Double-Hydrophosphinylation Reaction. The M–Pd complexes **1–3** were used as catalysts for hydrophosphinylation (eq 2) of 1-octyne with $\text{HP}(\text{O})\text{Ph}_2$. The results obtained are summarized in Table 2. In these reactions, the complexes **2** (Zr) and **3** (Hf) were dissolved completely in the reaction mixture, whereas the Ti complexes **1a** and **1b** had to



be used as a suspension owing to their low solubilities. After the reaction mixtures were kept at 40 °C for 20 h, the Ti (**1b**), Zr (**2**), and Hf (**3**) complexes all gave the double-addition product **5** as a main product, with the yield increasing in the order $\text{Hf} > \text{Zr} > \text{Ti}$ (entries 2–4). The poorest activity of **1a** (entry 1) is probably due to its much lower solubility. The same holds more or less for **1b**. In each reaction, 1-octyne was used in excess, since use of its stoichiometric amount lowered the reaction rate, resulting in the decreased yield. All these complexes work rather poorly under the present mild conditions; the yields in entries 2–4 are at an unsatisfactory level. However, we fortunately found that addition of tertiary phosphine such as PMePh_2 brought about much better results (entries 5, 7, and 11). For the Zr (**2**) and Hf (**3**) complexes, in particular, the yields of **5** as well as the required reaction times were significantly improved; the yields were >95% for 1 h at 40 °C. Similar effects were also observed when related phosphines were used as an additive (entries 6–14).¹⁸ In this way, the present double hydrophosphinylation of 1-octyne with $\text{HP}(\text{O})\text{Ph}_2$ became highly efficient by using the preorganized heterobinuclear M–Pd complexes **1–3** with tertiary phosphines added. The role of the phosphine added will be mentioned later.

Catalytically Active Trinuclear Complex. To obtain information about the catalytically active species promoting the present double addition, the reaction was monitored with $^{31}\text{P}\{^1\text{H}\}$ NMR. Complex **1a** was selected, because its catalytic reaction with added PMePh_2 proceeded slowly, and thus it was easy to follow. After 10 h, new transient signals different from those of the substrate and the final products were observed at 8.0 and 112.9 ppm as a mutually coupled quartet and doublet ($J_{\text{P-P}} = 114$ Hz), respectively. These peculiar signals were observed with much higher intensities when a stoichiometric amount of **1a** was treated similarly with $\text{HP}(\text{O})\text{Ph}_2$ and PMePh_2 (eq 3). The product of this stoichiometric reaction was isolated



and characterized by X-ray analysis to be the Pd–Ti–Pd trinuclear complex **6**, shown in Figure 5, in which the six OPPh_2

Table 1. Selected Bond Distances (Å) and Bond Angles (deg)

	1b	2		3	
		molecule 1	molecule 2	molecule 1	molecule 2
Pd–C1	2.13(5)	2.130(5)	2.124(4)	2.114(4)	2.114(3)
Pd–C2	2.169(6)	2.126(5)	2.135(4)	2.117(4)	2.111(4)
Pd–P1	2.2955(19)	2.2895(12)	2.2802(10)	2.2867(10)	2.2793(8)
Pd–P2	2.278(2)	2.2718(13)	2.2900(10)	2.2733(10)	2.2893(9)
M–O1	1.927(5)	1.987(3)	2.012(3)	1.975(3)	2.002(2)
M–O2	1.925(5)	2.005(3)	2.001(3)	1.982(3)	1.988(2)
P1–O1	1.573(5)	1.596(3)	1.592(3)	1.594(3)	1.590(2)
P2–O2	1.574(5)	1.589(3)	1.586(3)	1.596(3)	1.590(3)
C1–Pd–C2	85.2(14)	83.4(2)	84.69(18)	83.94(18)	85.33(16)
P1–Pd–P2	97.15(8)	98.10(4)	98.78(4)	97.95(4)	98.61(3)
O1–M–O2	91.6(2)	90.36(14)	90.90(11)	90.95(11)	91.66(10)
O1–P1–Pd	117.4(2)	119.40(14)	117.98(11)	119.47(11)	118.07(9)
O2–P2–Pd	119.1(2)	118.73(14)	119.45(11)	118.68(11)	119.81(10)
P1–O1–M	143.2(3)	145.3(2)	141.05(17)	144.98(18)	140.70(15)
P2–O2–M	143.8(3)	145.2(2)	142.54(18)	145.05(17)	141.71(15)

Table 2. Hydrophosphinylation of 1-Octyne with HP(O)Ph₂^a

entry	catalyst	phosphine (mol %)	time (h)	yield (%) ^b	
				4 ^c	5
1	1a		20		trace
2	1b		20		7
3	2		20		27
4	3		20		36
5	1b	5 (PMePh ₂)	20	7	19
6	2	5 (PMe ₂ Ph)	2		>99
7	2	5 (PMePh ₂)	1	4	95
8	2	5 (PPh ₃)	9	2	97
9	3	5 (PMe ₃)	5	3	97
10	3	5 (PMe ₂ Ph)	1	3	99
11	3	5 (PMePh ₂)	1	2	97
12	3	5 (PPh ₃)	5	2	98
13	3	2.5 (PMePh ₂)	2	3	97
14	3	10 (PMePh ₂)	1	3	97
15	[Ti] + [Pd] ^d	5 (PMePh ₂)	20		76
16	[Zr] + [Pd] ^d	5 (PMePh ₂)	3	7	88
17	[Hf] + [Pd] ^d	5 (PMePh ₂)	1	4	94

^a Conditions: toluene solution of HP(O)Ph₂ (0.5 M) and 1-octyne (0.5 M), 5 mol % catalyst, 40 °C. ^b Yields are based on intensities of ³¹P NMR signals of the crude reaction mixture. ^c Total yield of 4a and 4b. ^d [Ti] = Cp₂TiCl₂, [Zr] = Cp₂ZrCl₂, [Hf] = Cp₂HfCl₂, [Pd] = PdMe₂(tmeda).

arms bridge the Ti center with the two terminal Pd atoms. Each Pd center has the added tertiary phosphine PMePh₂ coordinated, which is responsible for ³¹P{¹H} NMR signals observed at 8.0 ppm. The remaining signal at 112.9 ppm is thus assigned to the bridging OPPh₂ ligands. Each Pd center has, in addition to these four phosphorus groups, a hydride ligand, which was found on a difference Fourier map and was refined isotropically, to form a pentacoordinate [Pd(H)P₄]⁺-type complex,¹⁹ which is characterized by X-ray analysis for the first time. Selected geometric parameters for 6 are given in Table 3.

The Pd–H bond lengths of Pd1 and Pd2 centers are 1.50(5) and 1.67(8) Å, respectively. Though their standard deviations are large, they are close to 1.58 Å, estimated by a QM/MM calculation for [PdH(dppe)₂]⁺ (dppe = 1,2-bis(diphenylphosphino)ethane) having a similar [Pd(H)P₄]⁺ coordination

(15) Ledford, J.; Shultz, C. S.; Gates, D. P.; White, P. S.; DeSimone, J. M.; Brookhart, M. *Organometallics* **2001**, *20*, 5266–5276.

(16) Wisner, J. M.; Bartczak, T. J.; Ibers, J. A. *Organometallics* **1986**, *5*, 2044–2050.

(17) Trzeciak, A. M.; Bartosz-Bechowski, H.; Ciunik, Z.; Niesyty, K.; Ziolkowski, J. J. *Can. J. Chem.* **2001**, *79*, 752–759.

(18) We used PMePh₂ mainly, because liquid phosphine (usually a few mg) was easy to measure out using a microsyringe in a glovebox.

Table 3. Selected Bond Distances (Å) and Bond Angles (deg) for 6

Pd1–P1	2.3309(11)	Pd2–P5	2.3434(12)
Pd1–P2	2.3715(11)	Pd2–P6	2.3463(12)
Pd1–P3	2.4594(12)	Pd2–P7	2.5031(13)
Pd1–P4	2.3055(12)	Pd2–P8	2.3176(13)
Pd1–H1	1.50(5)	Pd2–H2	1.67(8)
Ti1–O1	1.960(3)	Ti1–O4	1.949(3)
Ti1–O2	1.966(3)	Ti1–O5	1.961(3)
Ti1–O3	1.924(3)	Ti1–O6	1.919(3)
P1–O1	1.555(3)	P5–O4	1.564(3)
P2–O2	1.568(3)	P6–O5	1.564(3)
P3–O3	1.576(3)	P7–O6	1.582(3)
P1–Pd1–P2	87.32(4)	P5–Pd2–P6	90.53(4)
P1–Pd1–P3	92.60(4)	P5–Pd2–P7	91.62(4)
P1–Pd1–P4	101.90(4)	P5–Pd2–P8	102.28(5)
P2–Pd1–P3	88.69(4)	P6–Pd2–P7	87.70(4)
P2–Pd1–P4	142.14(5)	P6–Pd2–P8	142.05(5)
P3–Pd1–P4	126.81(4)	P7–Pd2–P8	126.81(5)
P1–Pd1–H1	178(2)	P5–Pd2–H2	173(2)
O1–Ti1–O6	177.47(13)	O2–Ti1–O4	176.64(13)
O3–Ti1–O5	176.95(13)		

sphere.^{19g} Each of the hydride ligands H1 and H2 occupies the position trans to one of the three OPPh₂ groups with the P1–Pd1–H1 and P5–Pd2–H2 angles of 178(2)° and 173(2)° close to 180°, respectively. Other noteworthy bond angles are P2–Pd1–P4 and P6–Pd2–P8, which are 142.14(5)° and 142.14(5)°, respectively. Since they are in an intermediate range between 120° for an equatorial bond angle of a trigonal bipyramid and 180° for a trans bond angle of a square pyramid, the geometry around each Pd center can be understood to be an intermediate between a trigonal bipyramid with the hydride in an axial position and a square pyramid with P3 or P7 in an apical position for the Pd1 or Pd2 center, respectively. For the Ti(IV) center, its geometry is an almost ideal octahedron with the three trans O–Ti–O angles all close to 180° but the Ti–O3 and Ti–O6 bonds somewhat shorter than other Ti–O bonds.

For 6, several tautomeric structures are conceivable, but only tautomers having cationic or neutral Pd centers are depicted in

(19) (a) Nimlos, M. R.; Chang, C. H.; Curtis, C. J.; Miedaner, A.; Pilath, H. M.; DuBois, D. L. *Organometallics* **2008**, *27*, 2715–2722. (b) Qi, X.-J.; Fu, Y.; Liu, L.; Guo, Q.-X. *Organometallics* **2007**, *26*, 4197–4203. (c) Kovacs, G.; Papai, I. *Organometallics* **2006**, *25*, 820–825. (d) Aresta, M.; Dibenedetto, A.; Papai, I.; Schubert, G.; MacChioni, A.; Zuccaccia, D. *Chem.–Eur. J.* **2004**, *10*, 3708–3716. (e) Raebiger, J. W.; Miedaner, A.; Curtis, C. J.; Miller, S. M.; Anderson, O. P.; DuBois, D. L. *J. Am. Chem. Soc.* **2004**, *126*, 5502–5514. (f) Curtis, C. J.; Miedaner, A.; Raebiger, J. W.; DuBois, D. L. *Organometallics* **2004**, *23*, 511–516. (g) Aresta, M.; Dibenedetto, A.; Amodio, E.; Papai, I.; Schubert, G. *Inorg. Chem.* **2002**, *41*, 6550–6552. (h) Aresta, M.; Quaranta, E. J. *Organomet. Chem.* **2002**, *662*, 112–119. (i) Miedaner, A.; DuBois, D. L.; Curtis, C. J.; Haltiwanger, R. C. *Organometallics* **1993**, *12*, 299–303. (j) Brueggeller, P. *Inorg. Chem.* **1990**, *29*, 1742–1750.

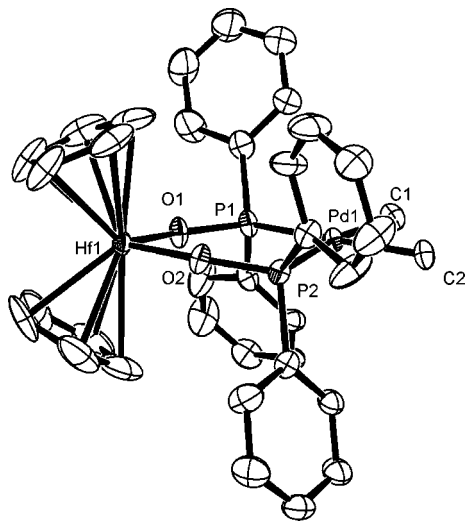


Figure 4. Molecular structure of $\text{Cp}_2\text{Hf}(\mu\text{-OPPh}_2)_2\text{PdMe}_2$ (**3**) with thermal ellipsoids given at the 50% probability level. Note that only one of two crystallographically independent molecules per asymmetric unit is shown.

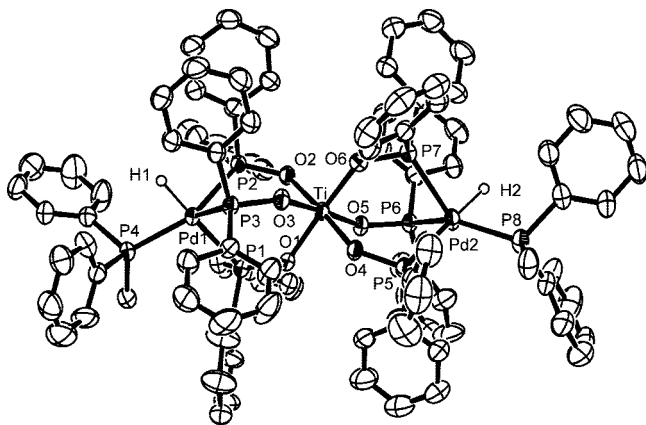


Figure 5. Molecular structure of $(\text{PMePh}_2)(\text{H})\text{Pd}(\mu\text{-OPPh}_2)_3\text{Ti}(\mu\text{-OPPh}_2)_2\text{Pd}(\text{H})(\text{PMePh}_2)$ (**6**) with thermal ellipsoids given at the 50% probability level. Hydrogen atoms except those on Pd centers are omitted for clarity.

Figure 6, because a number of cationic and neutral five-coordinate Pd(II) complexes are known to be thermodynamically stable, while only a few anionic five-coordinate Pd(II) complexes have been described so far.²⁰ In Figure 6, **6a** (left) is a zwitterion form in which the six $\text{O}^-\text{-PPh}_2$ groups are all monoanionic trivalent phosphorus ligands. Each half of them bridges the Ti(IV) with each Pd(II) center triply to leave the dianionic Ti and monocationic Pd centers to which each $\text{O}^-\text{-PPh}_2$ coordinates as an anionic O- and neutral P-donor, respectively. The other tautomer **6b** (right) is different from **6a** in that two of the six groups adopt a pentavalent form, $\text{O}=\text{PPh}_2^-$, which coordinates to the Ti center as a neutral O-donor, but as an anionic P-donor to the Pd center, leading overall to the neutral Ti and Pd centers. If the trivalent OPPh_2 group bridges the Ti and Pd centers, the resulting three bonds in the $\text{Ti}-\text{O}-\text{P}-\text{Pd}$ sequence should be shorter–longer–longer, respectively, than the corresponding three bonds in the $\text{Ti}-\text{O}=\text{P}-\text{Pd}$ sequence formed by the pentavalent form, because a covalent bond formed by an anionic

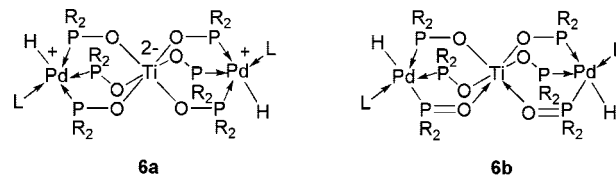


Figure 6. Two tautomeric forms of the trinuclear complex **6**, where dative bonds are indicated by arrows: a zwitterion form (left **6a**) and a neutral form with two $\text{O}=\text{PPh}_2$ groups (right **6b**).

O- or P-donor is generally shorter than a dative bond formed by the corresponding neutral donor and also because an O–P single bond is no doubt longer than an O=P double bond. Detailed comparison of the bond lengths given in Table 3 shows that the three bonds in the $\text{Ti}-\text{O}_3-\text{P}_3-\text{Pd}_1$ and $\text{Ti}-\text{O}_6-\text{P}_7-\text{Pd}_2$ sequences are somewhat but definitely shorter–longer–longer, respectively, than those in the other four sequences $\text{Ti}-\text{O}_1-\text{P}_1-\text{Pd}_1$, $\text{Ti}-\text{O}_2-\text{P}_2-\text{Pd}_1$, $\text{Ti}-\text{O}_4-\text{P}_5-\text{Pd}_2$, and $\text{Ti}-\text{O}_5-\text{P}_6-\text{Pd}_2$, suggesting that the former two sequences are comprised of the trivalent form. This inference is supported by a close similarity of their Ti–O and O–P distances to those of the metallo ligand in **1b**, where the OPPh_2 groups are apparently the trivalent forms (Figure 2 and Table 1), and it is reasonable that the weakly coordinating neutral P3 and P7 atoms occupy the equatorial (trigonal bipyramid) or apical (square pyramid) position around the d^8 Pd(II) center.

The remaining four sequences have the opposite bond-length trend to the above, indicating appreciable contribution of the pentavalent form to these four sequences. If these four OPPh_2 groups all adopt the pentavalent form $\text{O}=\text{PPh}_2^-$, each five-coordinate Pd center would carry an anionic charge (and the Ti center a dicationic one), which is unlikely as mentioned above. Therefore, only two of the four groups are depicted as the pentavalent form in **6b** (Figure 6). However, which group adopts the pentavalent form cannot be settled, because the four groups actually have comparable bond lengths owing to a possible conjugation between the trivalent and pentavalent forms, but the pentavalent form obviously contributes to the opposite trend observed. In short, the tautomer **6b** plays an important role in the present bridging system.

On the other hand, the three OPPh_2 groups on each Pd center were observed as equivalent in ^{31}P NMR (vide supra), indicating a dynamic exchange between PMePh_2 and hydride in solution through a turnstile rotation or pseudorotation, that is, an accompanying complete averaging of the six Ti–O–P–Pd sequences. In accordance with the exchange, the hydride signal in the ^1H NMR was observed at -8.50 ppm as a doublet of quartets due to couplings with phosphorus centers of both PMePh_2 and three now equivalent OPPh_2 groups.

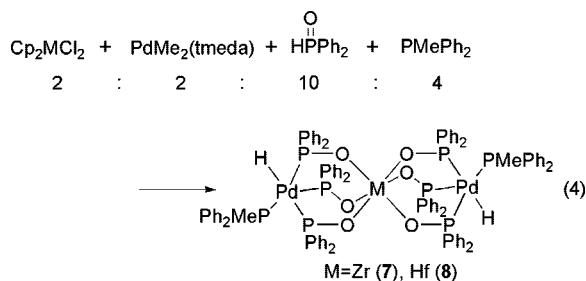
In the course of the reaction in eq 3, the Ti center has lost Cp rings as CpH, which was detected when the reaction was monitored with ^1H NMR. Marks et al. reported similar liberation of Cp from Cp_2TiCl_2 under acidic conditions.²¹ Since $\text{HP}(\text{O})\text{Ph}_2$ added in eq 3 is known to isomerize partially to its tautomer $\text{P}(\text{OH})\text{Ph}_2$, the proton dissociated from this phosphinous acid might attack Cp^- ligands on Ti to liberate CpH. The vacant sites thus left were probably occupied by OPPh_2^- . In addition, formation of the trinuclear complex implies disproportionation of the starting 1:1 Ti–Pd complex having taken place, but the fate of the remaining half of the Ti species is not known at present.

(20) (a) Vendilo, A. G.; Dyatlova, N. M.; Fridman, A. Y. *Zh. Neorg. Khim.* **1987**, *32*, 3006–3010. (b) Parthasarathy, V.; Joergensen, C. K. *Chimia* **1975**, *29*, 210–212. (c) Gonzalez Garcia, S.; Gonzalez Vilchez, F. *An. Quim.* **1970**, *66*, 875–890.

(21) Toney, J. H.; Marks, T. J. *J. Am. Chem. Soc.* **1985**, *107*, 947–953.

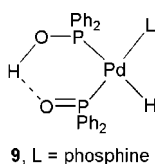
When the Zr (or Hf)–Pd complex in place of the Ti–Pd complex **1a** was treated similarly (eq 3), the corresponding Zr or Hf trinuclear complex **7** or **8**, respectively, was also formed in situ, as confirmed by the characteristic doublet and quartet observed in the $^{31}\text{P}\{^1\text{H}\}$ NMR as for **6**. These reaction mixtures were found to have a high catalytic activity comparable to those of the starting Zr–Pd and Hf–Pd binuclear complexes with PMePh_2 as an additive. These results suggest that the preorganized binuclear complexes must have been converted to their corresponding trinuclear complexes with the aid of the added tertiary phosphine in the reaction mixture so as to exhibit a practical catalytic activity.

Since each of the trinuclear complexes in eq 3 was obtained from the binuclear M–Pd complex prepared in advance according to eq 1, the direct preparation of the trinuclear complex was tried using Cp_2MCl_2 (M = Zr, Hf) and $\text{PdMe}_2(\text{tmeda})$ as the starting materials. The reaction of a 2:2 equiv mixture of these two metal complexes with $\text{HP}(\text{O})\text{Ph}_2$ (10 equiv) and PMePh_2 (2 equiv) gave successfully the corresponding trinuclear complex **7** or **8** as a major product after initial formation of the binuclear complex **2** or **3**, respectively (eq 4). These results prompted us to examine the double addition using a simple mixture of Cp_2MCl_2 (M = Zr, Hf) and



$\text{PdMe}_2(\text{tmeda})$ as the metal sources. The results (entries 16 and 17 in Table 2) demonstrate that satisfactory yields are obtained with the combination of these non-elaborately designed early- and late-metal complexes. In addition, the yield obtained with Cp_2TiCl_2 (entry 15) is also improved substantially compared to that given in entry 5, where the preorganized Ti–Pd catalyst **1b** was used. A homogeneous reaction mixture attained for the former case is probably responsible for the better yield, while a limited amount of **1b** was dissolved for the latter case. In this way, we need not procure either the preorganized binuclear complexes or the trinuclear complexes prepared therefrom.

Reaction Mechanism of Double Hydrophosphinylation. It is worth noting that the trinuclear complexes **6–8** possess structural similarities to the mononuclear Pd complex **9**, which has been reported as an active catalyst for the single-addition



reaction;^{7b} complex **9** has one hydride, one phosphine ligand, and two OPPh_2 groups linked with a proton. These structural features are common also to the trinuclear complexes **6–8**, though the proton in the chelate-like part of **9** is replaced with the group 4 metals and the third OPPh_2 group coordinates additionally to the Pd center to form the five-coordinate structure. The hydrophosphinylation catalyzed by complex **9** has been reported to proceed via insertion of terminal alkyne

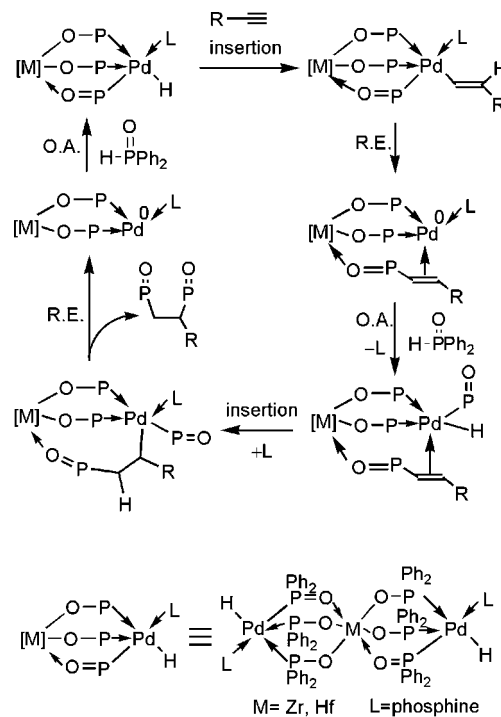


Figure 7. Catalytic cycle proposed for the double hydrophosphinylation catalyzed by trinuclear complexes **7** and **8**. [M] denotes the remaining half of the starting trinuclear complex, as shown at the bottom of the figure, and all Ph groups of the complexes are eliminated for clarity.

to the Pd–H bond and succeeding reductive elimination of the vinyl group with the $\text{O}=\text{PPh}_2$ moiety, followed by regeneration of **9** by oxidative addition of $\text{HP}(\text{O})\text{Ph}_2$ to the Pd(0) center.⁸ Judging from the common structural features between **9** and the present catalysts, it is reasonable to assume a similar mechanism in the present catalysis. Actually, a preliminary cross experiment using the Zr–Pd binuclear complex **2** and $\text{HP}(\text{O})(p\text{-Tol})_2$ as a substrate gave the double-addition products having not only the $\text{P}(\text{O})(p\text{-Tol})_2$ but also the $\text{P}(\text{O})\text{Ph}_2$ groups. Therefore, it is highly plausible that the OPPh_2 bridges incorporated into the catalyst are transferred to 1-octyne to give the double-addition product. In addition, when these reactions were monitored with $^{31}\text{P}\{^1\text{H}\}$ NMR, consumption of $\text{HP}(\text{O})\text{Ph}_2$ was observed with the growth of the two doublets due to the double-addition product **5**. Notably, even at the early stage of the reaction, the signals assigned to the single addition products **4a** and **4b** were much smaller in intensity. This reveals that both **4a** and **4b** once formed undergo promptly the second addition reaction to give **5**, indicating that the present catalysts add $\text{HP}(\text{O})\text{Ph}_2$ preferentially to phosphinoalkene **4** rather than to intact 1-octyne, probably through the cooperative interaction assumed in Figure 1. Details of the reaction mechanism are not clear at this stage, but a tentative one is given in Figure 7. The reaction starts from the top left of the figure, where one of the three OPPh_2 groups is depicted as the pentavalent form ($\text{O}=\text{P}$) as in **6b** (Figure 6), since the OPPh_2 group transferred to 1-octyne is eventually the pentavalent form. Before the insertion of alkyne, one of the phosphorus ligands, particularly L in the figure, dissociates from the Pd center to incorporate alkyne onto the Pd center. After a usual insertion followed by a reductive elimination, the monophosphinoalkene **4** formed does not leave the catalyst but is firmly held on both the Zr(IV) (or Hf(IV)) and Pd(0) centers via $\text{O}=\text{P}$ and alkene groups, respectively, as shown in the middle of the right side. Even if partial dissociation

of **4** takes place here, dissociated **4** recoordinates to the catalyst much more readily than 1-octyne present in excess coordinates to it, probably because the strong attractive interaction between the group 4 metal and the O=P group of **4** prevails over the steric repulsion between the catalyst and the bulky P(O)Ph₂ group of **4**. Then, the subsequent oxidative addition of HP(O)Ph₂ followed by insertion leads to the second addition, to liberate the double-addition product by reductive elimination. Finally, the second oxidative addition of HP(O)Ph₂ regenerates the starting catalyst.

In conclusion, the double addition of HP(O)Ph₂ to 1-octyne was accomplished under mild conditions using the Zr (or Hf)–Pd heterobinuclear system, while mononuclear Pd complexes such as **9** reported so far gave the double-addition product only under enforcing conditions. The present reaction is catalyzed by the trinuclear Zr (or Hf)–Pd₂ complexes formed in situ through the reaction of the preorganized Zr (or Hf)–Pd binuclear complexes with HP(O)Ph₂ and PMePh₂ or through the direct self-assembling of the simple Cp₂MCl₂ (M = Zr, Hf) and PdMe₂(tmeda) complexes in the presence of HP(O)Ph₂ and PMePh₂. Concurrent interactions of the group 4 metal and Pd centers with the O=P and alkene groups, respectively, are proposed to play a key role in the catalytic cycle, which effects the unusually facile double hydrophosphinylation of 1-octyne with HP(O)Ph₂.

Experimental Section

General Remarks. All reactions were carried out under an atmosphere of dry nitrogen using Schlenk tube techniques or an MBraun Labmaster 130 glovebox. All solvents were dried and distilled from sodium (for hexane) or sodium/benzophenone (for benzene, ether, THF, and toluene). These purified solvents were stored under an N₂ atmosphere. Cp₂TiCl₂ was purified by vacuum sublimation. Cp₂HfCl₂,²² HP(O)Ph₂,²³ PMe₃,²⁴ PMe₂Ph,²⁵ and PMePh₂²⁶ were prepared according to literature methods. Other reagents were used as received.

NMR spectra were recorded on JEOL LA-300 and LA-500 spectrometers. ¹H and ¹³C NMR chemical shifts were reported relative to Me₄Si and were determined by reference to the residual solvent peaks. ³¹P NMR chemical shifts were reported relative to H₃PO₄ (85%) used as an external reference. Elemental analyses were performed with a Perkin-Elmer 2400CHN elemental analyzer.

Preparation of Cp₂Ti(μ-OPPh₂)₂PdMe₂, **1a.** To a THF (10 mL) solution of HP(O)Ph₂ (560 mg, 2.78 mmol) in a Schlenk tube was added BuLi (1.60 M in hexane; 1.74 mL, 2.78 mmol) at –78 °C. The yellow solution was stirred for 4 h with warming gradually to room temperature. The LiOPPh₂ solution thus obtained was added to a THF (10 mL) solution of Cp₂TiCl₂ (346 mg, 1.39 mmol). After stirring for 5 min, the formation of Cp₂Ti(OPPh₂)₂ was confirmed with a ³¹P{¹H} NMR spectrum, and then PdMe₂(tmeda) (351 mg, 1.39 mmol) dissolved in THF (10 mL) was added dropwise to the solution containing Cp₂Ti(OPPh₂)₂. After the solution was stirred for 2 h, THF was removed under reduced pressure, and the residue was dried in vacuo. This residue was extracted repeatedly with benzene (10 mL × 5), until the benzene solution became colorless. After the extract obtained was filtered, benzene was removed under reduced pressure, and then the residue was washed with ether (5

mL × 6) and dried in vacuo to give a reddish-orange powder of **1a**. Yield: 580 mg (58%). ¹H NMR (300.5 MHz, C₆D₆): δ 0.96 (m, 6H, Pd–CH₃), 5.67 (s, 10H, Cp), 7.15–7.25 (m, 12H, Ph), 8.07 (dd, 8H, Ph). ¹³C{¹H} NMR (75.6 MHz, C₆D₆): δ 117.2 (s, Cp), 130.3 (s, Ph), 133.6 (t, J_{C–P} = 7.2 Hz, Ph). Owing to the poor solubility of the sample, other carbons did not have signal intensities enough to be observed. ³¹P{¹H} NMR (121.7 MHz, C₆D₆): δ 166.7 (s). The elemental analysis of **1a** did not give satisfactory and reproducible results, because its low solubility precluded complete purification.

Preparation of (C₅H₄Me)₂Ti(μ-OPPh₂)₂PdMe₂, **1b.** Preparation of **1b** was carried out in a manner similar to that described for **1a** starting with Cp′₂TiCl₂ (300 mg, 1.08 mmol), HP(O)Ph₂ (438 mg, 2.17 mmol), BuLi (1.60 M in hexane; 1.30 mL, 2.17 mmol), and PdMe₂(tmeda) (274 mg, 1.08 mmol). An orange powder of **1b** (469 mg, 58%) was obtained. ¹H NMR (300.5 MHz, C₆D₆): δ 0.92 (m, 6H, Pd–CH₃), 1.49 (s, 6H, C₅H₄–CH₃), 5.55–5.64 (m, 8H, C₅H₄), 7.10–7.21 (m, 12H, Ph), 8.10 (dd, 8H, Ph). ¹³C{¹H} NMR (75.6 MHz, C₆D₆): δ 6.2 (dd, J_{C–P} = 14 Hz, J_{C–P} = 121 Hz, Pd–CH₃), 15.8 (s, C₅H₄–CH₃), 115.9 (s, Cp), 119.1 (s, Cp), 128.5 (m, Ph), 130.1 (s, Ph), 133.9 (m, Ph), 142.6 (m, *ipso*-Ph). ³¹P{¹H} NMR (121.7 MHz, C₆D₆): δ 164.1 (s). Anal. Calcd for C₃₈H₄₀O₂P₂PdTi · 2/3LiCl: C, 59.03; H, 5.21. Found: C, 58.73; H, 5.03.

Preparation of Cp₂Zr(μ-OPPh₂)₂PdMe₂, **2.** Preparation of **2** was carried out in a manner similar to that described for **1a** starting with Cp₂ZrCl₂ (219 mg, 0.75 mmol), HP(O)Ph₂ (303 mg, 1.50 mmol), BuLi (1.6 M in hexane; 0.93 mL, 1.50 mmol), and PdMe₂(tmeda) (189 mg, 0.75 mmol). A pale pink powder of **2** (423 mg, 74%) was obtained. ¹H NMR (300.5 MHz, C₆D₆): δ 0.87 (m, 6H, Pd–CH₃), 5.67 (s, 10H, Cp), 7.11–7.21 (m, 12H, Ph), 7.98 (dd, 8H, Ph). ¹³C{¹H} NMR (75.6 MHz, C₆D₆): δ 6.3 (dd, J_{C–P} = 16 Hz, J_{C–P} = 122 Hz, Pd–CH₃), 114.4 (s, Cp), 128.5 (m, Ph), 130.2 (s, Ph), 133.4 (m, Ph), 142.2 (m, *ipso*-Ph). ³¹P{¹H} NMR (121.7 MHz, C₆D₆): δ 151.2 (s). Anal. Calcd for C₃₆H₃₆O₂P₂PdZr · 2/3LiCl: C, 54.83; H, 4.60. Found: C, 55.06; H, 4.39.

Preparation of Cp₂Hf(μ-OPPh₂)₂PdMe₂, **3.** Preparation of **3** was carried out in a manner similar to that described for **1a** starting with Cp₂HfCl₂ (300 mg, 0.79 mmol), HP(O)Ph₂ (320 mg, 1.58 mmol), BuLi (1.6 M in hexane; 0.99 mL, 1.58 mmol), and PdMe₂(tmeda) (200 mg, 0.79 mmol). A pale pink powder of **3** (447 mg, 67%) was obtained. ¹H NMR (300.5 MHz, C₆D₆): δ 0.86 (m, 6H, Pd–CH₃), 5.63 (s, 10H, Cp), 7.11–7.21 (m, 12H, Ph), 7.99 (dd, 8H, Ph). ¹³C{¹H} NMR (75.6 MHz, C₆D₆): δ 6.4 (dd, J_{C–P} = 16 Hz, J_{C–P} = 123 Hz, Pd–CH₃), 113.2 (s, Cp), 128.5 (m, Ph), 130.3 (s, Ph), 133.4 (m, Ph), 142.2 (m, *ipso*-Ph). ³¹P{¹H} NMR (121.7 MHz, C₆D₆): δ 149.2 (s). Anal. Calcd for C₃₆H₃₆O₂P₂PdHf: C, 51.02; H, 4.28. Found: C, 50.80; H, 4.00.

Preparation and Isolation of the Pd–Ti–Pd Complex **6 from **1a**.** The complex **1a** (200 mg, 0.28 mmol), HP(O)Ph₂ (112 mg, 0.56 mmol), PMePh₂ (52 μL, 0.28 mmol), and toluene (10 mL) were put in a vial. The suspension was stirred for 17 h at 40 °C. The dark red reaction mixture was filtered to remove a small amount of the remaining Ti–Pd complex, then the solvent was removed under reduced pressure. The residue was washed with hexane (5 mL × 3) and ether (5 mL × 10) and dried in vacuo to give (PMePh₂)(H)Pd(μ-OPPh₂)₂Ti(μ-OPPh₂)₂Pd(H)(PMePh₂) (**6**). Yield: 123 mg (49%). ¹H NMR (300.5 MHz, C₆D₆): δ –8.50 (dq, 2H, ²J_{H–P} = 9.7, 76.3 Hz), 1.45 (d, 6H, PMe), 6.91–7.85 (m, 80H, Ph). ³¹P{¹H} NMR (121.7 MHz, C₆D₆): δ 8.0 (q, 2P, ²J_{P–P} = 114 Hz, PMePh₂), 112.7 (d, 6P, ²J_{P–P} = 114 Hz, OPPh₂). Anal. Calcd for C₉₈H₈₈O₆P₈Pd₂Ti · 1/2LiCl: C, 62.23; H, 4.69. Found: C, 62.23; H, 4.59.

Preparation of the Pd–Zr–Pd Complex **7 from **2**.** The Zr–Pd complex **2** (20 mg, 0.026 mmol), HP(O)Ph₂ (22 mg, 0.109 mmol), PMePh₂ (4.9 μL, 0.026 mmol), and toluene (0.5 mL) were put in an NMR tube and kept at 40 °C. After 3 h, the ³¹P{¹H} NMR spectrum recorded (Figure S2) showed major signals of (PMePh₂)–

(22) Druce, P. M.; Kingston, B. M.; Lappert, M. F.; Spalding, T. R.; Srivastava, R. C. *J. Chem. Soc., A* **1969**, 2106.

(23) Hunt, B. B.; Saunders, B. C. *J. Chem. Soc.* **1957**, 2413–14.

(24) Luetkens, M. L.; Sattelberger, A. P.; Murray, H. H.; Basil, J. D.; Fackler, J. P. *Inorg. Synth.* **1989**, *26*, 7–12.

(25) Benn, F. R.; Briggs, J. C.; McAuliffe, C. A. *J. Chem. Soc., Dalton Trans.* **1984**, 293–295.

(26) Mikolajczyk, M.; Graczyk, P. P. *J. Org. Chem.* **1995**, *60*, 5190–208.

Table 4. Crystallographic Data

	1b	2	3	6
formula	C _{43.7} H _{45.1} Cl _{0.3} O ₂ P ₂ PdTi	C ₃₆ H ₃₆ O ₂ P ₂ PdZr	C ₃₆ H ₃₆ HfO ₂ P ₂ Pd	C ₁₀₅ H ₉₆ O ₆ P ₈ Pd ₂ Ti
cryst color, habit	dark red, cubic	pale pink, plate	pale pink, plate	pale pink, plate
cryst syst	monoclinic	monoclinic	monoclinic	triclinic
space group	<i>P</i> 2 ₁ / <i>a</i> (No. 14)	<i>P</i> 2 ₁ / <i>a</i> (No. 14)	<i>P</i> 2 ₁ / <i>a</i> (No. 14)	<i>P</i> 1̄ (No. 2)
<i>a</i> /Å	19.889(1)	19.9260(2)	19.8990(1)	13.4700(1)
<i>b</i> /Å	10.1284(6)	10.2770(1)	10.2630(1)	15.2910(1)
<i>c</i> /Å	20.030(1)	32.4970(3)	32.4220(1)	24.5460(1)
α /deg	90.00	90.00	90.00	95.029(1)
β /deg	102.708(2)	93.170(1)	93.088(1)	102.054(1)
γ /deg	90.00	90.00	90.00	107.525(2)
<i>V</i> /Å ³	3936.0(4)	6644.5(1)	6611.72(8)	4652.9(2)
<i>Z</i>	4	8	8	2
temp/K	293	200	200	200
μ (Mo K α)/mm ⁻¹	0.797	0.981	3.809	0.659
no. of rflns measd	8987	15 216	15 644	19 971
obsd (<i>I</i> > 2.00 σ (<i>I</i>), 2 θ < 55°)	5180	12 905	14 605	14 723
R1 (<i>I</i> > 2 σ (<i>I</i>))	0.0975	0.0521	0.0310	0.0623
wR2	0.1822	0.1507	0.0807	0.1809
GOF	1.154	1.054	1.040	1.027
<i>ab</i> ^a	0.0310/18.1773	0.0820/21.2224	0.0387/27.6883	0.1035/6.2869

$$^a \text{wR2} = \{\sum[w(F_o^2 - F_c^2)^2]/\sum[w(F_o^2)^2]\}^{1/2}; w = 1/[\sigma^2(F_o^2) + (ap)^2 + bp]; p = (F_o^2 + 2F_c^2)/3.$$

(H)Pd(μ -OPPh₂)₃Zr(μ -OPPh₂)₃Pd(H)(PMePh₂) (**7**) as well as those of remaining HP(O)Ph₂ and PMePh₂. ³¹P{¹H} NMR (121.7 MHz, toluene): δ 7.4 (q, 2P, ²*J*_{P-P} = 117 Hz, PMePh₂), 116.4 (d, 6P, ²*J*_{P-P} = 116 Hz, OPPh₂).

Preparation of the Pd–Hf–Pd Complex 8 from 3. The Hf–Pd complex **3** (40 mg, 0.047 mmol), HP(O)Ph₂ (28 mg, 0.14 mmol), PMePh₂ (8.8 μ L, 0.047 mmol), and toluene (2.0 mL) were put in an NMR tube and kept at 40 °C. After 3 h, the ³¹P{¹H} NMR spectrum recorded (Figure S3) showed major signals of (PMePh₂)₃(H)Pd(μ -OPPh₂)₃Hf(μ -OPPh₂)₃Pd(H)(PMePh₂) (**8**) as a major product as well as those of remaining HP(O)Ph₂ and PMePh₂ and some unidentified products. ³¹P{¹H} NMR (121.7 MHz, toluene): δ 7.3 (q, 2P, ²*J*_{P-P} = 117 Hz, PMePh₂), 101.9 (d, 6P, ²*J*_{P-P} = 117 Hz, OPPh₂).

Preparation of 7 from Cp₂ZrCl₂ and PdMe₂(tmeda). Cp₂ZrCl₂ (5.8 mg, 0.020 mmol), PdMe₂(tmeda) (5.0 mg, 0.020 mmol), HP(O)Ph₂ (20 mg, 0.099 mmol), PMePh₂ (7.4 μ L, 0.040 mmol), and toluene (0.5 mL) were put in an NMR tube and kept at 40 °C. After 23 h, the ³¹P{¹H} NMR spectrum recorded (Figure S4) showed major signals of **7** as well as those of remaining HP(O)Ph₂ and PMePh₂.

Preparation of 8 from Cp₂HfCl₂ and PdMe₂(tmeda). Cp₂HfCl₂ (7.5 mg, 0.020 mmol), PdMe₂(tmeda) (5.0 mg, 0.020 mmol), HP(O)Ph₂ (20 mg, 0.099 mmol), PMePh₂ (7.4 μ L, 0.040 mmol), and toluene (0.5 mL) were put in an NMR tube and kept at 40 °C. After 5 h, the ³¹P{¹H} NMR spectrum recorded (Figure S5) showed major signals of **8** as well as those of remaining PMePh₂ and some unidentified products.

Catalysis. The catalyst **1**, **2**, or **3** (0.014 mmol), HP(O)Ph₂ (56.6 mg, 0.280 mmol), 1-octyne (41.1 μ L, 0.280 mmol), toluene (0.5 mL), and phosphine (its amount is given in Table 1) were all put in an NMR tube and kept at 40 °C. After the reaction time specified in Table 2, the reaction mixture was mixed with CHCl₃ (2 mL) to quench the reaction and then extracted with ether (5 mL \times 5). The extracts were combined, and the solvents were removed under reduced pressure. The residue thus obtained was redissolved in CHCl₃ (0.50 mL), and the amounts of the phosphorus compounds were estimated by ³¹P{¹H} NMR spectra. Similar procedures were applied when the mixture of Cp₂MCl₂ and PdMe₂(tmeda) was used as a catalyst.

X-ray Crystallography. Suitable crystals of **1b**, **2**, **3**, and **6** were mounted separately on glass fibers. The measurements were made on a Rigaku SCXmini at room temperature for **1b** and on a Mac Science

DIP2030 imaging plate area detector at 200 K for **2**, **3**, and **6**. Cell parameters and intensities for the reflections were estimated using the program packages of CrystalClear for **1b** and HKL for **2**, **3**, and **6**.^{27,28} The structures were solved by direct methods and expanded using Fourier techniques. Non-hydrogen atoms were refined anisotropically. Hydrogen atoms except the hydrides of **6** were located at ideal positions, while the hydride ligands of **6** were located on a difference Fourier map and refined isotropically. All calculations were performed using a SHELXL-97 crystallographic software package.²⁹ After several cycles of least-squares refinement for the crystal structure of **1b**, the crystal analyzed was found to be mixed with a PdClMe analogue, Cp'₂Ti(μ -OPh₂)₂PdClMe. Thus one of the two Me groups on the Pd atom of **1b** was treated as a disordered group with a chloride anion in a 70:30 occupancy ratio. For crystal structures of **2** and **3**, each asymmetric unit was comprised of two independent molecules. In the crystal of **6**, considerably disordered solvent molecules were refined as molecules having rigid ideal structures. The molecular structures are depicted in Figures 2–5 for **1b**, **2**, **3**, and **6**, respectively. Details of data collection and refinement for these crystals are listed in Table 4 and CIF files, which include bond distances and angles, atomic coordinates, and anisotropic thermal parameters.

Acknowledgment. This work was supported by Grants-in-Aid for Scientific Research (Nos. 19350032, 19550066, and 19550067) from the Ministry of Education, Culture, Sports, Science, and Technology, Japan. We thank the Natural Science Center for Basic Research and Development (N-BARD), Hiroshima University, for the measurement of NMR.

Supporting Information Available: ³¹P{¹H} NMR spectra of complexes **6**, **7**, and **8**, and CIF files giving full crystallographic data for complexes **1b**, **2**, **3**, and **6**. This material is available free of charge via the Internet at <http://pubs.acs.org>.

OM8008298

(27) *CrystalClear 1.3.6*; Rigaku/MXC, Inc.: The Woodlands, TX, 2004.

(28) Otwinowski, Z.; Minor, W. In *Processing of X-ray Diffraction Data Collected in Oscillation Mode*; Carter, C. W., Jr., Sweet, R. M., Eds.; Academic Press: New York, 1997; Vol. 276 (Macromolecular Crystallography, Part A), pp 307–326.

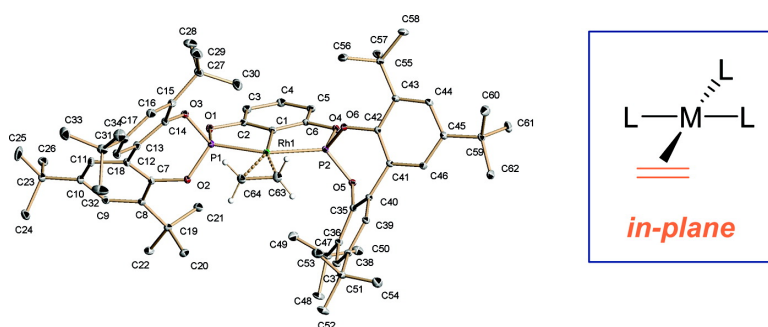
(29) Scheldrick, G. M. *SHELX-97: Programs for Crystal Structure Analysis*; University of Göttingen: Germany, 1997.

Rhodium Complexes with Pincer Diphosphite Ligands. Unusual Olefin in-Plane Coordination in Square-Planar Compounds

Miguel Rubio, Andre#s Sua#rez, Diego del R#o, Agust#n Galindo, Eleuterio A#lvarez, and Antonio Pizzano

Organometallics, 2009, 28 (2), 547-560 • DOI: 10.1021/om800830w • Publication Date (Web): 24 December 2008

Downloaded from <http://pubs.acs.org> on April 10, 2009



More About This Article

Additional resources and features associated with this article are available within the HTML version:

- Supporting Information
- Access to high resolution figures
- Links to articles and content related to this article
- Copyright permission to reproduce figures and/or text from this article

[View the Full Text HTML](#)



ACS Publications
High quality. High impact.

Rhodium Complexes with Pincer Diphosphite Ligands. Unusual Olefin in-Plane Coordination in Square-Planar Compounds[†]

Miguel Rubio,[‡] Andrés Suárez,[‡] Diego del Río,^{‡,§} Agustín Galindo,^{*,‡} Eleuterio Álvarez,[‡] and Antonio Pizzano^{*,‡}

Instituto de Investigaciones Químicas, Consejo Superior de Investigaciones Científicas, and Universidad de Sevilla, Avda Américo Vespucio no. 49, Isla de la Cartuja, 41092 Sevilla, Spain, and Departamento de Química Inorgánica, Universidad de Sevilla, Apto 1203, 41071 Sevilla, Spain

Received August 26, 2008

A family of rhodium complexes bearing pincer diphosphite (PCP) and neutral L (L = PPh₃, CO, CNXy, C₂H₄) ligands has been prepared and characterized. Reactions between Rh(Cl)(PPh₃)₃ and the diphosphites **2** lead to the chloro hydrides Rh(H)(Cl)(PCP)(PPh₃) (**4**), which can be deprotonated to yield the complexes Rh(PCP)(PPh₃) (**5**). In the latter, the PPh₃ ligand is labile and can be exchanged by CO, CNXy, and C₂H₄ to give derivatives **6–8**. Most noteworthy is the fact that ethylene complexes **8a,b** show a remarkable in-plane (*ip*) conformation in the solid state. Solution NMR studies for these complexes show fast olefin rotation in all the temperature ranges, while solution and solid-state ¹³C{¹H} NMR experiments give practically superimposable spectra, also indicating the prevalence of the *ip* conformer in solution. Complementary detailed DFT calculations performed with models of compounds **8** indicate that the olefin conformational preference is due to a dual combination of steric effects arising from the reduction of the P–Rh–P angle from 180°, caused by pincer ligand chelation and by the nature of the phosphite substituents, which in the case of *t*-Bu groups perfectly outline a cavity for an *ip* coordination of the olefin.

Introduction

The orientation of a coordinated olefin is an aspect of fundamental interest in organometallic chemistry, and it is of great importance in relation to the stereochemistry of reactions involving alkene transformation.¹ The preferred conformation for a metal-bonded olefin is explained by the Chatt–Dewar–Duncanson model^{2,3} and, more specifically, by the existence of a back-bonding component from a metal-centered orbital to the π* olefin orbital. As a result, the orientation of the olefin depends on the geometry of the complex.⁴ For the important class of square-planar compounds, in-plane (*ip*) and upright (*u*) olefin orientations are electronically of similar energy. However, steric effects between the olefin and cis coligands L_c are lower in the

u orientation.⁵ This steric preference is marked indeed, and a perusal of the structures of square-planar olefin complexes described in the literature indicates that the *u* conformation has almost exclusively been observed. However, two cases can be considered exceptions to this general behavior. The first regards Pt and Pd cationic complexes of the formulation [M(alkene)-(allyl)(phosphine)]⁺ (**A**). These complexes display different olefin orientations depending on the nature of this ligand, including several cases of *ip* conformation. Due to the small bite angle of the allyl ligand, the definition of their structure is not unambiguous and they have either been assigned as square-planar⁶ or planar-trigonal complexes,⁷ which in turn have a clear preference for an in-plane conformation.⁴ The second pertinent case is constituted by the complexes of the methylene cycloheptene diolefin (**B**), which due to the perpendicularity between the two olefinic bonds forces an *ip* conformation of one of the alkene fragments.⁸ In view of these precedents, there is not a clear-cut case of a square-planar complex in which, the two conformations being accessible, *ip* is preferred.



* To whom correspondence should be addressed. E-mail: galindo@us.es (A.G.); pizzano@iiq.csic.es (A.P.).

[†] This article is dedicated to Prof. Ernesto Carmona on the occasion of his 60th birthday.

[‡] Instituto de Investigaciones Químicas.

[§] Present address: SRI International, 333 Ravenswood Avenue, Menlo Park, CA 94065.

[†] Universidad de Sevilla.

(1) For some representative studies of olefin reactivity considering orientation, see: (a) Musaev, D. G.; Svensson, M.; Morokuma, K.; Strömberg, S.; Zetterberg, K.; Siegbahn, P. E. M. *Organometallics* **1997**, *16*, 1933. (b) Gridnev, I. D.; Yasutake, M.; Higashi, N.; Imamoto, T. *J. Am. Chem. Soc.* **2001**, *123*, 5268. (c) Carbó, J. J.; Lledós, A.; Vogt, D.; Bo, C. *Chem. Eur. J.* **2006**, *12*, 1457. (d) Adlhart, C.; Chen, P. *J. Am. Chem. Soc.* **2004**, *126*, 3496. (e) Sakaki, S.; Mizoe, N.; Sugimoto, M.; Musashi, Y. *Coord. Chem. Rev.* **1999**, *190*, 933.

(2) (a) Chatt, J.; Duncanson, L. A. *J. Chem. Soc.* **1953**, 2939. (b) Dewar, M. J. S. *Bull. Chem. Soc. Chim. Fr.* **1951**, C71.

(3) Recent studies of the metal–olefin bond: (a) Frenking, G.; Fröhlich, N. *Chem. Rev.* **2000**, *100*, 717. (b) Price, D. W.; Drew, M. G. B.; Hii, K. K.; Brown, J. M. *Chem. Eur. J.* **2000**, *6*, 4587. (c) Tshipis, A. C. *Organometallics* **2008**, *27*, 3701.

(4) Albright, T. A.; Hoffmann, R.; Thibeault, J. C.; Thorn, D. L. *J. Am. Chem. Soc.* **1979**, *101*, 3801.

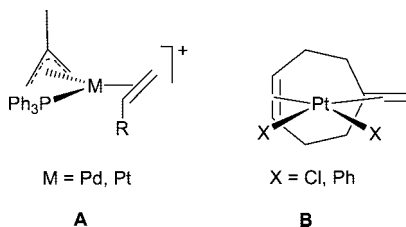
(5) (a) Hay, P. J. *J. Am. Chem. Soc.* **1981**, *103*, 1390. (b) Ziegler, T.; Rauk, A. *Inorg. Chem.* **1979**, *18*, 1558. (c) Senn, H. M.; Blöchl, P. E.; Togni, A. *J. Am. Chem. Soc.* **2000**, *122*, 4098.

(6) (a) Miki, K.; Kai, Y.; Kasai, N.; Kurosawa, H. *J. Am. Chem. Soc.* **1983**, *105*, 2482. (b) Kurosawa, H.; Miki, K.; Kasai, N.; Ikeda, I. *Organometallics* **1991**, *10*, 1607.

(7) Musco, A.; Pontellini, R.; Grassi, M.; Sironi, A.; Meille, S. V.; Rügger, H.; Ammann, C.; Pregosin, P. S. *Organometallics* **1988**, *7*, 2130.

(8) Rakowsky, M. H.; Woolcock, J. C.; Wright, L. L.; Green, D. B.; Rettig, M. F.; Wing, R. M. *Organometallics* **1987**, *6*, 1211.

On the other hand, pincer ligands are also of great interest, due to their marked ability to stabilize transition-metal complexes.⁹ Among them, those possessing two donor phosphine fragments constitute a prominent group. Otherwise, pincer accepting ligands have largely remained unexplored and only recently have attracted the attention of researchers. Thus, new ligands based on fluorophosphines,¹⁰ *N*-pyrrolyl phosphines,¹¹ and phosphites¹² have recently been described.



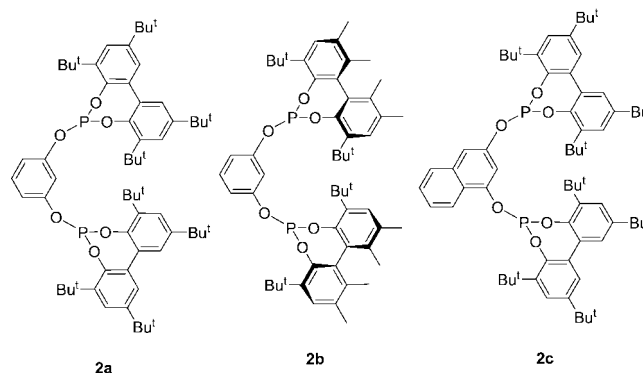
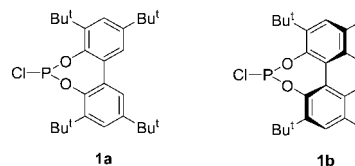
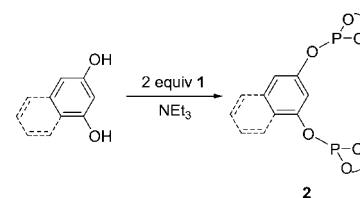
In this contribution we describe a group of novel diphosphites and their incorporation into rhodium complexes, these being the first examples of rhodium–pincer diphosphite complexes. These pincer ligands outline a spatial distribution of steric hindrance which differs from that exhibited by a fragment ML₃, which makes possible a preferred ethylene in-plane coordination in square-planar complexes. These olefinic derivatives have been studied in detail by both structural and theoretical methods. The results have been completed with the synthesis and characterization of isocyanide and carbonyl derivatives which provide information about the acceptor character of these pincer ligands. Part of this work has been communicated in a preliminary form.¹³

Results and Discussion

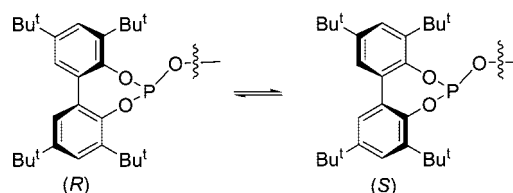
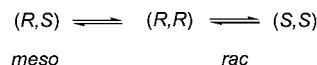
Ligand Synthesis. Diphosphites **2** have been prepared by a condensation between resorcinol or 1,3-naphthalenediol and the appropriate chlorophosphite **1** in the presence of a base in good yields (Scheme 1). NMR spectroscopic characterization reflects the differences in symmetry and conformational flexibility among compounds **2**. Thus, **2a** exhibits in the ³¹P{¹H} NMR spectrum one singlet in the typical region of phosphites, while in the ¹H and ¹³C{¹H} experiments we observe the equivalence of the halves of each biphenyl, as well as the other phosphite fragments. This behavior can be explained by a fast interconversion between *rac* and *meso* isomers (Scheme 2). Otherwise, the presence of the naphthyl backbone in compound **2c** renders two phosphite fragments inequivalent, as shown by two singlets in the ³¹P{¹H} NMR spectrum. Moreover, rapid isomerization makes two aryl fragments of each biaryl equivalent in the ¹³C{¹H} and ¹H NMR experiments. Finally, the atropisomeric diphosphite **2b** exhibits spectra which account for its C₂ symmetry. Therefore, the two ³¹P nuclei are equivalent, but two types of biphenyl aryl rings appear in the ¹H and ¹³C{¹H} NMR spectra, those of each inequivalent biphenyl.

- (9) van der Boom, M. E.; Milstein, D. *Chem. Rev.* **2003**, *103*, 1759.
 (10) Chase, P. A.; Gagliardo, M.; Lutz, M.; Spek, A. L.; van Klink, G. P. M.; van Koten, G. *Organometallics* **2005**, *24*, 2016.
 (11) Kossov, E.; Iron, M. A.; Rybtchinski, B.; Ben-David, Y.; Shimon, L. J. W.; Konstantinovski, L.; Martín, J. M. L.; Milstein, D. *Chem. Eur. J.* **2005**, *11*, 2319.
 (12) (a) Barber, R. A.; Bedford, R. B.; Betham, M.; Blake, M. E.; Coles, S. J.; Haddow, M. F.; Hursthouse, M. B.; Orpen, A. G.; Pilarski, L. T.; Pringle, P. G.; Wingad, R. L. *Chem. Commun.* **2006**, 3880. (b) Miyazaki, F.; Yamaguchi, K.; Shibasaki, M. *Tetrahedron Lett.* **1999**, *40*, 7379.
 (13) Rubio, M.; Suárez, A.; del Río, D.; Galindo, A.; Álvarez, E.; Pizzano, A. *Dalton Trans.* **2007**, 407.

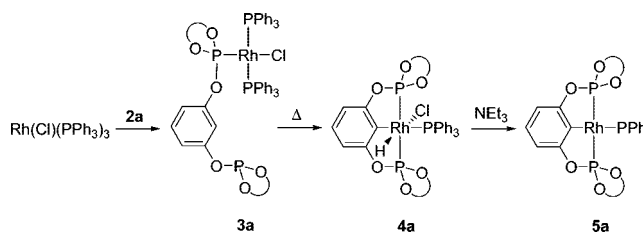
Scheme 1



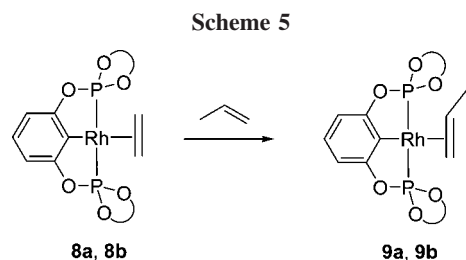
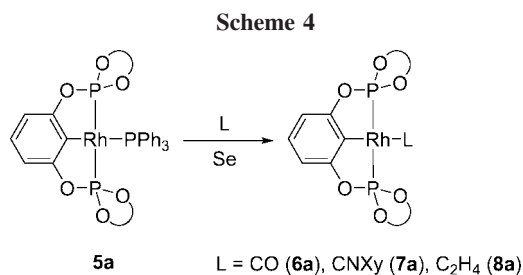
Scheme 2



Scheme 3



Preparation and Characterization of PPh₃ Derivatives. In order to incorporate diphosphites **2** as pincer ligands in Rh complexes, the reaction between **2a** and RhCl(PPh₃)₃ has been studied (Scheme 3). Interaction at room temperature, monitored by ³¹P{¹H} NMR, indicates the formation of the species **3a** characterized by three signals: a singlet at δ 139.9 indicative of an uncoordinated phosphite, a doublet of doublets of doublets (δ 128.4, *J*_{RhP} = 336 Hz, *J*_{PP} = 47, 41 Hz) in the coordinated phosphite region, and finally, an AB system doubly split by phosphorus and rhodium couplings centered at 36.0 ppm (*J*_{AB} = 356 Hz, *J*_{RhP} = 138 Hz), due to two inequivalent PPh₃ groups. Subsequent heating of the solution produces the activation of the central C–H bond and the displacement of another molecule of PPh₃, thus generating chloro hydride **4a**, which incorporates



a pincer diphosphite ligand (PCP^a).¹⁴ The presence of a hydride ligand in the latter complex is characterized in the IR spectrum by a band at 2112 cm⁻¹ due to $\nu(\text{Rh}-\text{H})$ and in the ¹H NMR experiment by a doublet of quartets at $\delta -14.8$. In the latter, coincident couplings of 12 Hz are observed with the three ³¹P and the ¹⁰³Rh nuclei. These values are in good accord with the hydride coordinated in a cis position with respect to the three phosphorus ligands. The ³¹P{¹H} NMR spectrum is characterized by a doublet of doublets for the two diphosphite ³¹P nuclei at 149.9 ppm ($J_{\text{RhP}} = 178$ Hz, $J_{\text{PP}} = 35$ Hz) and a doublet of triplets at 13.7 ppm ($J_{\text{RhP}} = 87$ Hz) for a coordinated PPh₃. The value of J_{RhP} is similar to those found in compounds with chloride and hydride ligands occupying mutually trans positions.^{15,16} This arrangement has been definitively ascertained by an X-ray diffraction study (see the Supporting Information).

Heating the solution of compound **3a** also produces a small amount of complex **5a**, which results from the loss of HCl from chloro hydride **4a**. Subsequent addition of an excess of NEt₃ facilitates this step and results in the isolation of **5a** in good yield. NMR spectra for complex **5a** show the expected signals for the pincer and PPh₃ ligands. Interestingly, the equivalence of the four aryl biphenyls is observed in the ¹H and ¹³C{¹H} spectra at room temperature, indicative of a fast interconversion between *rac* and *meso* conformers. Derivatives Rh(PCP^b)(PPh₃) (**5b**) and Rh(PCP^c)(PPh₃) (**5c**) have been prepared by following the procedure described for **5a**.

Synthesis and Characterization of the Complexes Rh(PCP)L (L = CO, CNXy, H₂C=CH₂, H₃CCH=CH₂). The PPh₃ ligand in compound **5a** is labile and can be replaced by other L ligands. Thus, exposing **5a** to an atmosphere of CO readily produces compound **6a** (Scheme 4). However, the released phosphine interferes in the purification of the carbonyl product, as solvent evaporation during the workup procedure is accompanied by regeneration of the phosphine derivative **4a**. Addition of Se to the reaction mixture quenches the phosphine as P(Se)Ph₃, which can be easily removed from the mixture.¹⁷ This procedure has also been used in the synthesis of the isocyanide compound **7a**. NMR characterization of these complexes shows signals for the pincer and the L ligands. Most meaningful of the presence of the latter is a low-field doublet of triplets in the ¹³C{¹H} spectrum for Rh-CO ($J_{\text{RhC}} = 58$ Hz, $J_{\text{PC}} = 16$ Hz) and Rh-CNXY ($J_{\text{RhP}} = 56$ Hz, $J_{\text{PP}} = 18$ Hz). As in the case of the phosphine derivative **5a**, these complexes also show fluxional behavior in solution resulting from a fast isomerization of phosphite fragments.

(14) In the article the pincer ligands generated by deprotonation of diphosphites **2a-c** will be denoted PCP^a, PCP^b, and PCP^c, respectively, while PCP will be used to generally refer to them.

(15) The magnitude of J_{PRh} depends markedly on the ligand situated in a position trans respect to the P ligand: Naaktgeboren, A. J.; Nolte, R. J. M.; Drenth, W. *J. Am. Chem. Soc.* **1980**, *102*, 3350.

(16) Liou, S.-Y.; Gozin, M.; Milstein, D. *J. Am. Chem. Soc.* **1995**, *117*, 9774.

(17) For alternative quenchers for this reaction, see: (a) Gorla, F.; Venanzi, L. M.; Albinati, A. *Organometallics* **1994**, *13*, 43. (b) Reference 11.

An interesting feature of these pincer-type diphosphite ligands is its acceptor character due to the π -acidity of the phosphite groups. This characteristic has been investigated by IR spectroscopy on complexes **6a** and **7a**, as the magnitudes of $\nu(\text{CO})$ and $\nu(\text{CN})$ have diagnostic value. Thus, the carbonyl gives the corresponding band at 2017 cm⁻¹,¹⁸ considerably shifted to higher energy from that of analogous derivatives of diphosphinite (1962 cm⁻¹)¹⁹ or aryldiphosphine (1955 cm⁻¹) pincer complexes.²⁰ The isonitrile derivative reinforces this observation,²¹ as the band for $\nu(\text{CN})$ appears at 2099 cm⁻¹, only 15 cm⁻¹ lower than in the free isonitrile and considerably higher than the value of 2048 cm⁻¹ observed in *trans*-RhCl(CNXy)(P-Prⁱ)₂.²²

The ethylene complex Rh(PCP^a)(C₂H₄) (**8a**) has also been prepared according to Scheme 4, but this transformation is slow compared with those of CO or CNXY and requires heating of the reaction mixture to 40 °C for 4 days under 4 atm of ethylene to get a good yield. Under similar conditions the derivatives Rh(PCP^b)(C₂H₄) (**8b**) and Rh(PCP^c)(C₂H₄) (**8c**) have also been obtained.²³ Analytical and spectroscopical data for complexes **8** are in good accord with the proposed formulation. Thus, the NMR experiments show, in addition to the signals of the PCP ligand, the pertinent resonances for a coordinated ethylene. For instance, in the ¹³C{¹H} NMR spectrum a relatively broad signal at ca. 60 ppm due to the olefinic carbons is observed, while the ¹H NMR spectra show the corresponding signals for ethylenic protons. For compounds **8a,c**, which possess conformationally flexible phosphite fragments, the four protons appear as a broad signal at 2.8 ppm, while for atropisomeric **8b** the olefinic protons appear as two doublets, with an intensity of two protons for each signal, at 2.3 and 3.0 ppm. These observations account for the fluxional behavior of **8a,c**, which will be discussed below. Moreover, ethylene complexes are capable of exchanging this olefin with propylene, by stirring under an atmosphere of this alkene, to yield complexes **9** (Scheme 5). NMR data for these derivatives show only one group of signals, indicating a fluxional behavior (see below). In addition to the resonances for the PCP fragment, NMR spectra display the expected signals for a propene ligand. For instance, in the ¹H spectrum for **9a** the methyl substituent appears as a doublet at δ 1.06 ($J_{\text{HH}} = 5.4$ Hz), while a broad multiplet is observed at δ 4.39 for the

(18) For comparative purposes, see: Serron, S.; Nolan, S. P.; Moloy, K. G. *Organometallics* **1996**, *15*, 4301.

(19) Salem, H.; Ben-David, Y.; Shimon, L. J. W.; Milstein, D. *Organometallics* **2006**, *25*, 2292.

(20) Weisman, A.; Gozin, M.; Kraatz, H.-B.; Milstein, D. *Inorg. Chem.* **1996**, *35*, 1792.

(21) Conejo, M. M.; Parry, J. S.; Carmona, E.; Schultz, M.; Brennan, J. G.; Beshouri, S. M.; Andersen, R. A.; Rogers, R. D.; Coles, S.; Hurthouse, M. *Chem. Eur. J.* **1999**, *5*, 3000.

(22) Jones, W. D.; Hessel, E. T. *Organometallics* **1990**, *9*, 718.

(23) For other ethylene derivatives with pincer ligands, see: (a) Zhao, J.; Goldman, A. S.; Hartwig, J. F. *Science* **2005**, *307*, 1080. (b) Hahn, C.; Sieler, J.; Taube, R. *Chem. Ber.* **1997**, *130*, 939. (c) Vignalok, A.; Ben-David, Y.; Milstein, D. *Organometallics* **1996**, *15*, 1839. (d) Nemeš, S.; Jensen, C.; Binamira-Soriaga, E.; Kaska, W. C. *Organometallics* **1983**, *2*, 1442. (e) Reference 19.

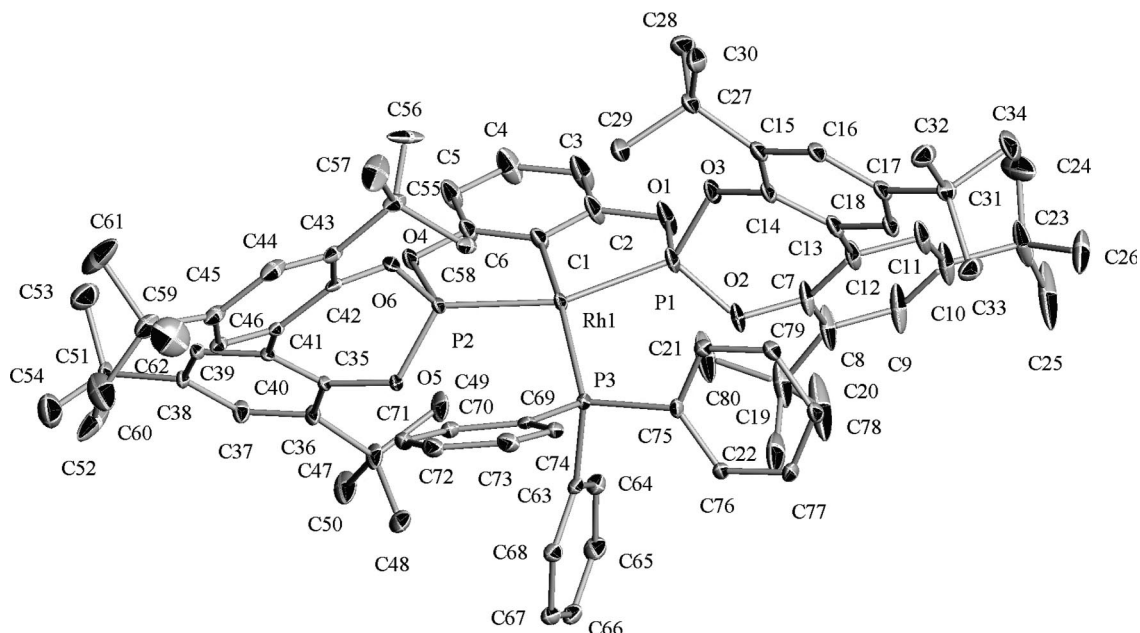


Figure 1. ORTEP perspective of complex **5a**.

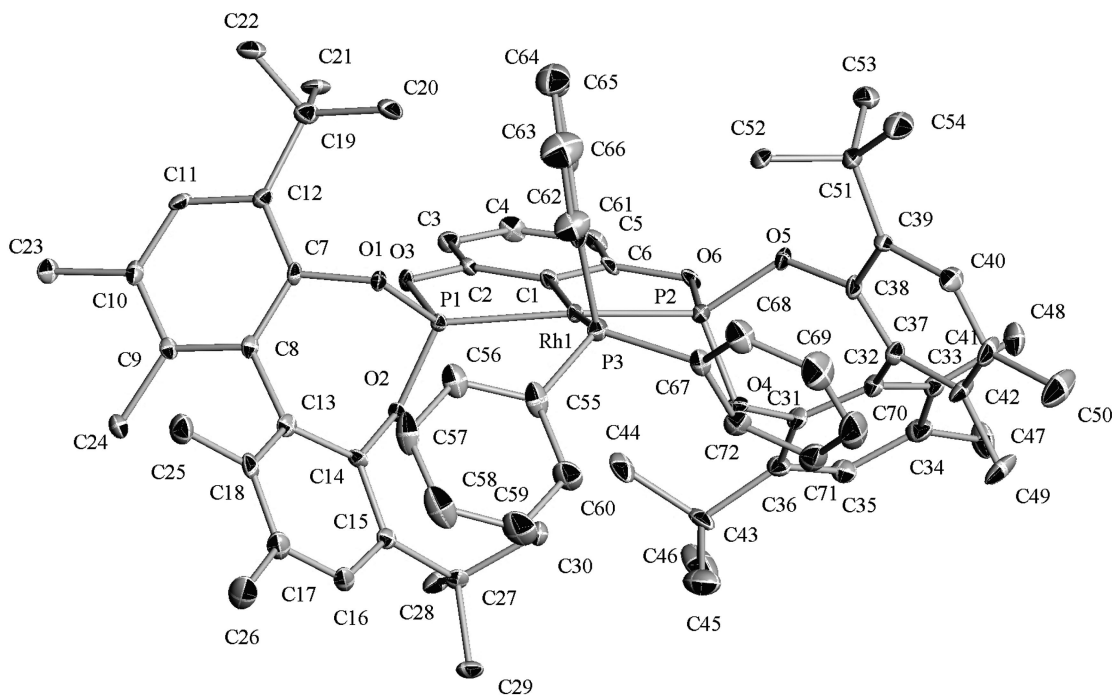


Figure 2. Structure of complex **5b**.

methyne group. Finally, broad doublets at 2.51 ($J_{\text{HH}} = 8.7$ Hz) and 3.29 ppm ($J_{\text{HH}} = 12.3$ Hz) are observed for the methylenic protons.

Structural Characterization of Pincer Complexes. The observation of an ethylene *ip* coordination in **8a,b** has prompted us to perform a detailed structural study of them, focused at investigating the olefin coordination, using X-ray crystallographic, NMR, and computational techniques.

(a) Crystallographic Studies. Complexes **5a–8a**, **5b**, and **8b** have been characterized by single-crystal X-ray crystallography. The corresponding ORTEP diagrams are depicted in Figures 1–6, while in Table 1 are compiled some selected distances and angles for comparative purposes. A comparison of these data indicates that the fragments composed of the metal

and the atoms of the pincer ligand bonded to it are practically superimposable. Moreover, a comparative overview of the structures draws more interesting coincidences among them. First, the magnitude of the angle P–Rh–P lies in the range 153–157°; this angle is substantially smaller than the mean value of ca. 164° found for complexes derived from pincer diphosphines.²⁴ However, values similar to those found here have also been described in the literature. For instance, a value of 154° has been reported for an *N*-pyrrolyl derivative.¹¹ Analogously, Ir complexes with diphosphinite pincer ligands

(24) Cambridge Structural Database System, Cambridge Crystallographic Data Centre, 12 Union Road, Cambridge, CB2 1EZ, UK. For QUEST3D search details see the Experimental Section.

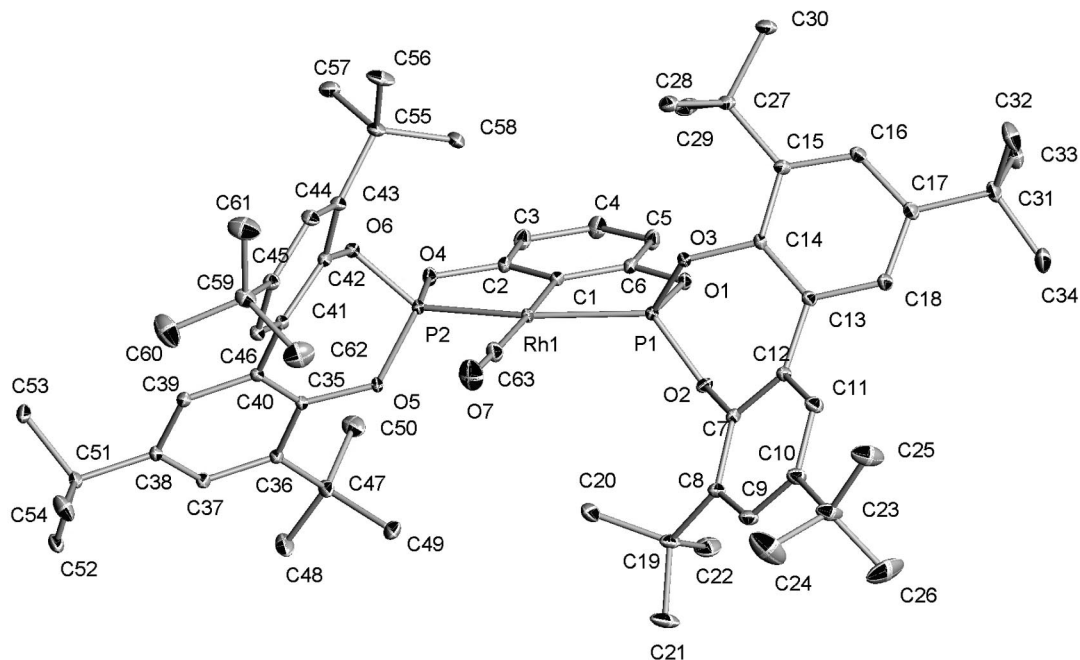


Figure 3. ORTEP view of complex 6a.

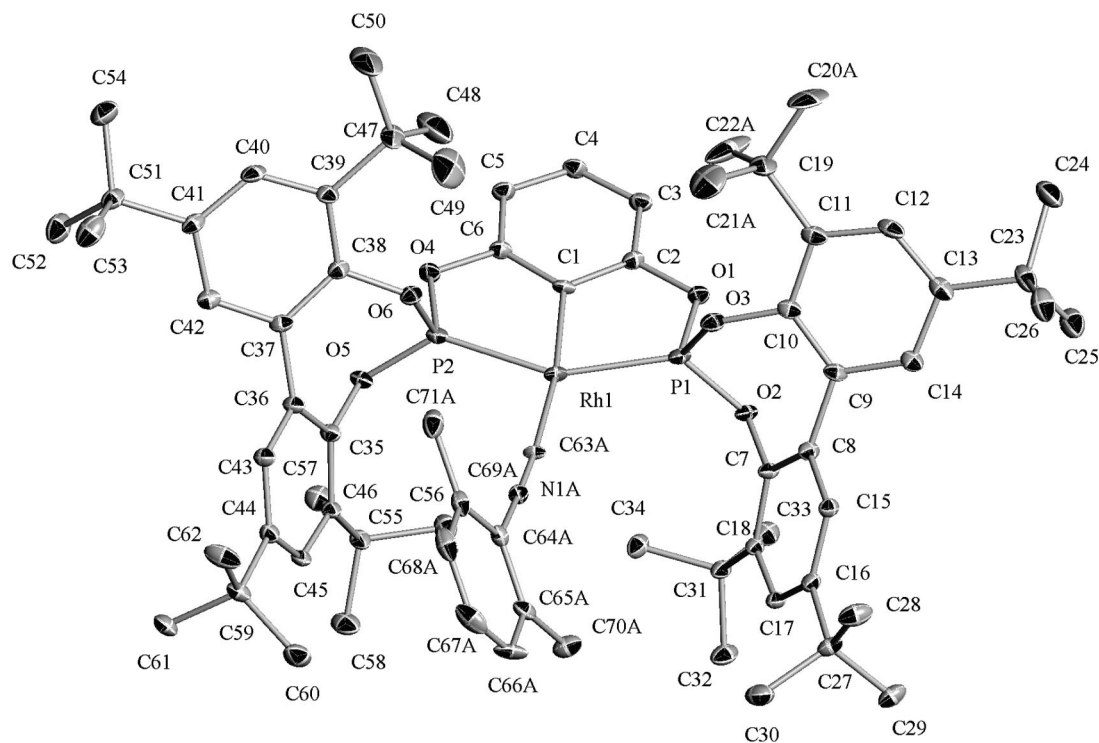


Figure 4. ORTEP perspective of compound 7a.

display similar values of this parameter.^{19,25} Another remarkable feature of the Rh–PCP fragment along the series is its planarity, which is in contrast with the puckered structures usually

produced by pincer diphosphines.²⁶ This backbone planarity seems to be caused by the presence of oxygen atoms in the backbone, as other complexes described in the literature derived

(25) (a) Götter-Schnetmann, I.; White, P.; Brookhart, M. *J. Am. Chem. Soc.* **2004**, *126*, 1804. (b) Götter-Schnetmann, I.; White, P.; Brookhart, M. *Organometallics* **2004**, *23*, 1766. (c) Sykes, A. C.; White, P.; Brookhart, M. *Organometallics* **2006**, *25*, 1644. (d) Kuklin, S. A.; Sheloumov, A. M.; Dolgushin, F. M.; Ezernitskaya, M. G.; Peregudov, A. S.; Petrovskii, P. V.; Koridze, A. A. *Organometallics* **2006**, *25*, 5466. (e) Denney, M. C.; Pons, V.; Hebden, T. J.; Heinekey, D. M.; Goldberg, K. I. *J. Am. Chem. Soc.* **2006**, *128*, 12048.

(26) For representative examples see: (a) Kraatz, H.-B.; Milstein, D. *J. Organomet. Chem.* **1995**, *488*, 223. (b) Cámpora, J.; Palma, P.; del Río, D.; Alvarez, E. *Organometallics* **2004**, *23*, 1652.

(27) Backbone planarity is not exclusive for oxygen in the backbone, and it also has been observed in pincer bisphosphoramidite complexes. For examples see: (a) Benito-Garagorri, D.; Becker, E.; Wiedermann, J.; Lackner, W.; Pollak, M.; Mereiter, K.; Kisala, J.; Kirchner, K. *Organometallics* **2006**, *25*, 1900. (b) Benito-Garagorri, D.; Bocokic, D.; V.; Mereiter, K.; Kirchner, K. *Organometallics* **2006**, *25*, 3817.

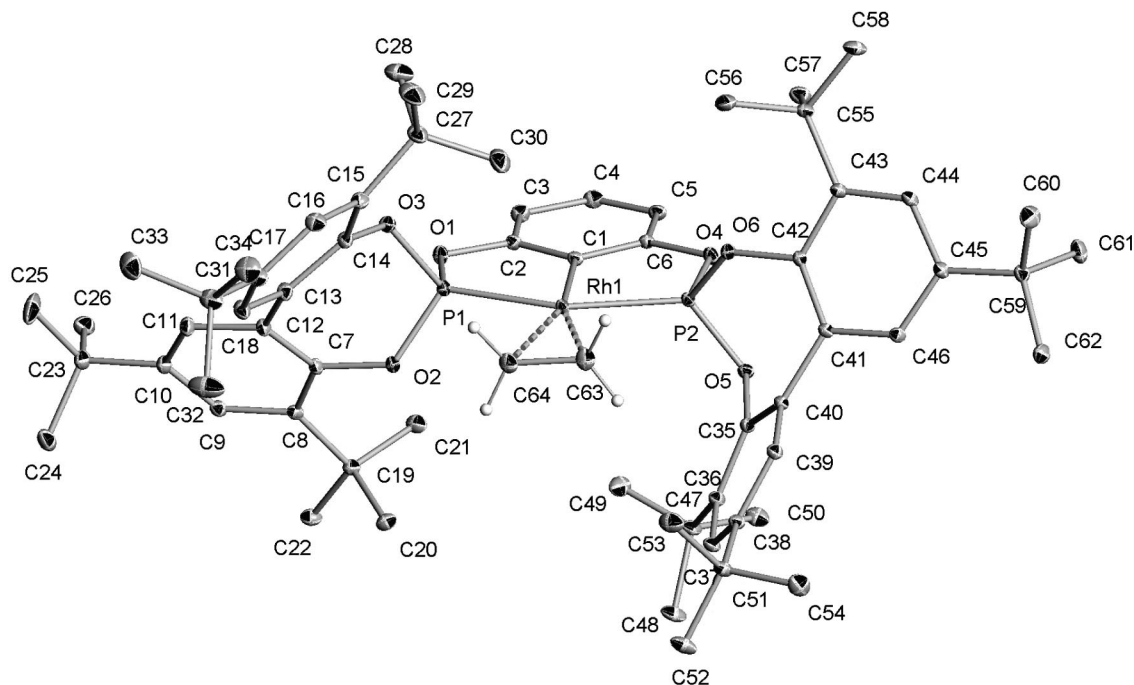


Figure 5. ORTEP view of complex **8a**.

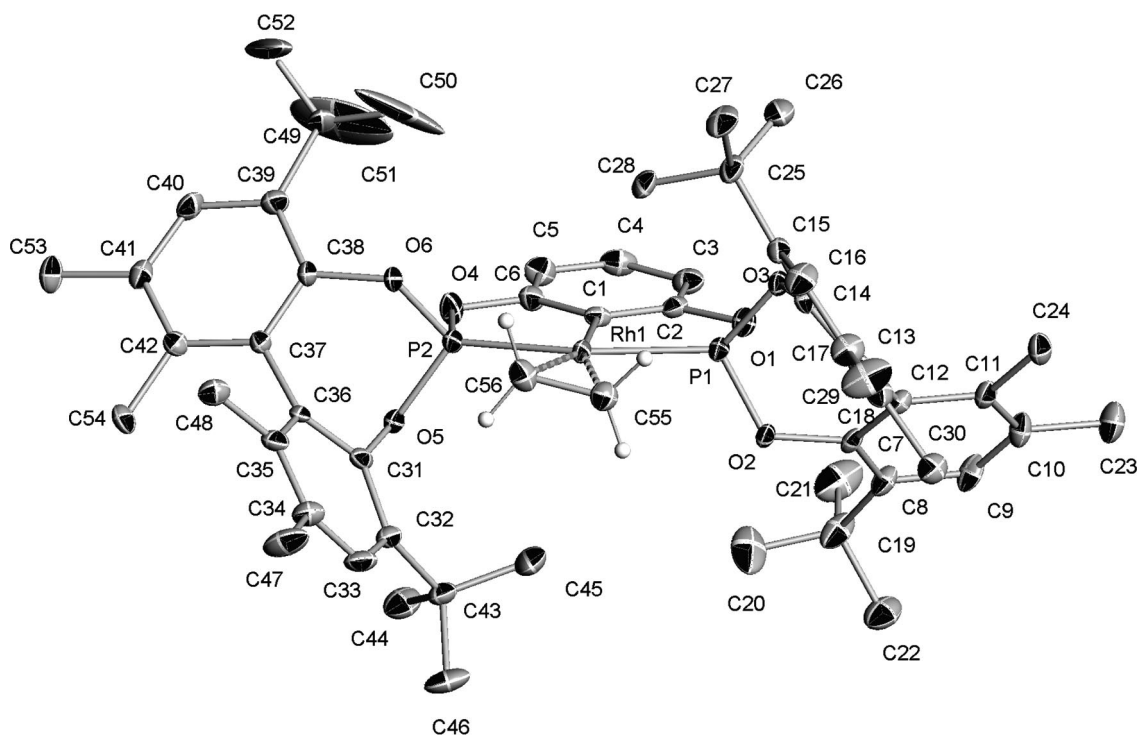


Figure 6. ORTEP view of complex **8b**.

from phosphites or phosphinites also show a planar structure of the bridge.^{12,25,27}

Another interesting aspect of these structures involves the shape and size of the cavity drawn by the pincer ligand. The first observation is with regard to the conformation of the biphenyls. Complexes derived from the conformationally flexible pincer PCP^a can adopt a *rac* (corresponding to two enantiomeric C₂-symmetric Rh-PCP^a fragments with *S,S* or *R,R* configuration) or a *meso* type conformation, which is characterized by a symmetry plane. Upon these considerations it can be concluded that complexes **6a** and **8a**, which bear the smaller CO and C₂H₄ ligands, adopt a *rac* conformation. This arrange-

ment is characterized by similar values of α angles (Figure 7, Table 2) above and below the equatorial plane (i.e. α_1 and α_2 vs α_3 and α_4 , respectively). Otherwise, the magnitude of these parameters is dissimilar in the case of *meso* structures, observed in complexes **5a** and **7a**. Thus, α_1 and α_2 amount for the latter around 31°, while α_3 and α_4 have values around 74°. Moreover, for a *rac* conformation similar values of distances $d(1-2)$ and $d(3-4)$ are observed, while these parameters differ in the case of *meso* structures. Therefore, it is apparent that the *meso* conformation is preferred in the case of sterically encumbered compounds. Steric hindrance should be particularly pronounced in complex **5a**, since the ligand PPh₃ is significantly raised over

Table 1. Selected Structural Parameters of Pincer Complexes^a

compd	Rh–P		Rh–C _{ipso}	Rh–L	P–Rh–P
4a	2.2705(11)	2.2759(10)	2.033(4)	2.3959(10) ^b	154.55(4)
5a	2.2233(11)	2.2470(11)	2.039(4)	2.3360(11)	155.04(4)
5b	2.2275(12)	2.2629(14)	2.040(5)	2.3572(14)	152.15(5)
6a	2.2245(4)	2.2475(4)	2.0338(16)	1.9069(19)	156.378(16)
7a^c	2.2206(9)	2.2207(10)	2.034(3)	1.991(7)	152.89(3)
				1.949(13)	
8a	2.2076(3)	2.2165(3)	2.0233(12)	2.2184(14)	155.490(13)
				2.2353(14)	
8b	2.2237(7)	2.2096(7)	2.019(3)	2.228(3)	155.37(3)
				2.230(3)	

^a Angles in deg and distances in Å. ^b L = PPh₃. ^c Distances for two conformers, modeled due to isonitrile ligand disorder, are given.

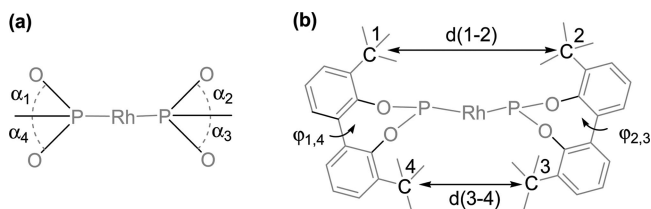


Figure 7. Parameters used to compare metal–ligand cavity dimensions: (a) α_1 – α_4 angles defined between the P–O bond and the best plane defined by Rh and metal-bonded P and C atoms; (b) torsion angles between biphenyl aryls and distances between quaternary carbons of the *t*-Bu substituents (other aryl substituents have been omitted for clarity).

Table 2. Cavity Parameters for Rh(PCP)L Complexes^a

compd	<i>d</i> (1–2)	<i>d</i> (3–4)	α_1	α_2	α_3	α_4	$\varphi_{1,4}$	$\varphi_{2,3}$
4a	7.7	10.0	60.5	55.3	45.6	38.4	48.1	46.9
5a	8.0	9.5	59.6	60.1	41.1	44.5	45.4	47.3
5b	10.2	7.8	32.0	32.6	74.8	76.5	60.4	63.1
6a	8.0	8.8	45.2	49.8	53.4	57.6	45.9	51.6
7a	7.5	8.7	32.5	31.3	75.3	73.1	51.4	50.9
8a	8.0	8.4	48.6	48.8	53.0	52.1	51.6	53.6
8b	8.9	8.2	47.6	48.7	53.8	54.6	62.7	63.5

^a Angles in deg and distances in Å.

the coordination plane, giving a C(1)–Rh–P(3) angle of 163.2°. It is next interesting to consider complexes **5b** and **8b** derived from enantiopure diphosphite **2b**. Ideally, the corresponding pincer ligand should generate a C_2 -symmetric Rh(PCP^b) fragment. Indeed, this is observed in the case of ethylene derivative **8b** and similar values of *d*(1–2) (8.9 Å) and *d*(3–4) (8.2 Å) are observed. Otherwise, steric hindrance introduced by PPh₃ in **5b** cannot be released by a *meso* structure and a significant distortion from the C_2 structure is observed. Thus, the cavity is significantly more opened above the plane (*d*(1–2) = 10.2 Å) than below (*d*(3–4) = 7.8 Å) to accommodate the axial phenyl group. Finally, it is interesting to highlight the differences in torsion angles φ of biphenyls of two types of ligands. Thus, this magnitude amounts to between 40 and 45° for the flexible ligand, while for the chiral ligand, due to the presence of methyl substituents in 6,6'-positions, this angle increases to values of 60 and 63° for **5b** and **8b**, respectively.

Structures of Rh(PCP)L compounds are also of interest due to the magnitude of the Rh–L distance. The distances of the carbonyl and the isonitrile bound to the metal are 1.91 and 1.97 Å, respectively. These distances are longer than those found in related compounds (e.g. 1.86 Å in *trans*-Rh(*p*-tolyl)(CO)-(PPh₃)₂,^{28a} 1.82 Å in *trans*-RhCl(CO)(PPh₃)₂,^{28b} or 1.83 Å in *trans*-RhCl(CNXY)(PPrⁱ)₂).²² Overall, the lengthening of the Rh–L bond can be attributed to the concurrence of two factors, the trans influence exerted by the pincer aryl ligand and a

reduced back-bonding ability of the metal center, caused by the π -acidity of the phosphite groups.

Most noteworthy is the fact that coordinated ethylene shows an unexpected in-plane conformation in complexes **8a,b**, with a small angle of 7.4 (**8a**) and 13.0° (**8b**) between planes defined by Rh–PCP and Rh– η^2 -(C₂H₄) fragments. The C=C bond length is similar for **8a** (1.38 Å), while slightly lower for **8b** (1.35 Å), as compared to the mean value observed in other rhodium ethylene derivatives (1.38–1.39 Å).²⁴ The distance between the ethylene carbons and the Rh atom is 2.23 Å, which is higher than the mean value of 2.13 Å found for rhodium ethylene derivatives and parallels the lengthening of the Rh–L bond observed in complexes **6a** and **7a**.

(b) NMR Studies of the Olefinic Complexes. In order to get information about the structural features of the olefinic complexes in solution, we have also studied them by NMR techniques. It has been mentioned above that derivatives of the PCP^a ligand are fluxional due to an interconversion between *rac* and *meso* conformers; therefore, it is pertinent to consider first the more simple atropisomeric complex **8b**. This compound shows in the ¹H NMR spectrum two filled-in doublets at 2.98 and 2.28 ppm indicative of an AA'XX' spin system for the protons of the ethylene ligand. These signals broaden somewhat on cooling but do not split at the lowest temperature investigated (180 K). Likewise, in the ¹³C{¹H} NMR experiment a slightly broad doublet at 58.6 ppm ($J_{\text{CRh}} = 4$ Hz) is observed at room temperature for the coordinated olefin. This signal broadens somewhat at lower temperatures. An examination of the 2D NOESY spectrum allows us to differentiate between *t*-Bu groups oriented to the backbone (i.e. those denoted by C(49) and C(19) in Figure 6) and those closer to the olefin. It is worth noting that NOE contacts have been observed between the latter and all ethylene protons.

The C_2 symmetry of complex **8b** does not allow us to distinguish between the existence of a single ethylene conformer (*ip* or *u*) or a fast olefin rotation. For that purpose, the less symmetric complex **9b** has also been studied.²⁹ In this particular case, if the olefin is frozen, the four *tert*-butyl substituents will be nonequivalent, while if there is a fast rotation, according to the NMR time scale, an averaged C_2 symmetry is reached and, accordingly, two types of *t*-Bu groups should be observed. Indeed, the latter behavior is observed in both the ¹H and ¹³C{¹H} NMR spectra in the entire temperature range, which is consistent with fast olefin rotation even at 190 K. Therefore, ethylene rotation should also occur in complexes **8**. Upon this assumption, spectra of complexes **8a,c** can be interpreted in terms of an exchange between *rac* and *meso* conformers. Thus, analysis of compound **8a** by ³¹P{¹H} NMR spectroscopy shows at room temperature a doublet at 177.3 ppm ($J_{\text{PRh}} = 253$ Hz), while cooling of the sample leads to the appearance of a second doublet at 179.2 ppm ($^1J_{\text{RHP}} = 250$ Hz) due to a minor species, at a ca. 20:1 rate. On the other hand, in the ¹H NMR region characteristic for a coordinated ethylene, one broad singlet at 2.82 ppm for four protons is observed at room temperature. Upon cooling, this signal splits into two broad signals of equal intensity (e.g. ca. 3.3 and 2.3 ppm at 220 K), while further cooling produces the appearance of an additional broad minor signal at 3.1 ppm. It is interesting to compare these observations with data provided by compound **8c**, which has lower symmetry by virtue of its asymmetric naphthyl backbone. Thus, at room

(28) (a) Krug, C.; Hartwig, J. F. *J. Am. Chem. Soc.* **2002**, *124*, 1674. (b) Rheingold, A. L.; Geib, S. J. *Acta Cryst C* **1987**, *43*, 784.

(29) Cavallo, L.; Cucciolito, M. E.; De Martino, A.; Giordano, F.; Orabona, I.; Vitagliano, A. *Chem. Eur. J.* **2000**, *6*, 1127.

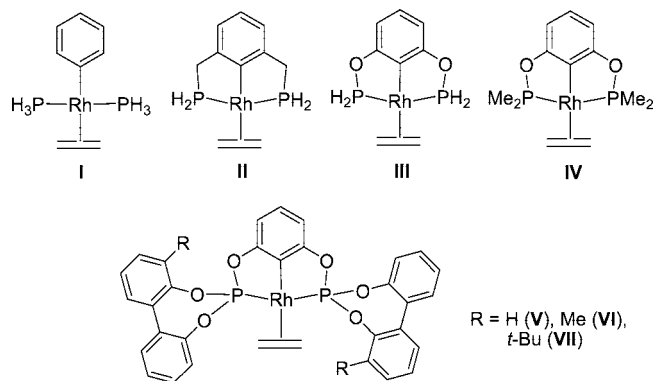


Figure 8. Calculated model complexes.

temperature a broad signal corresponding to all olefinic protons is also observed. However, cooling of the sample produces scission into signals for a major product at 2.2 and 3.2 ppm, while the minor species appears in this case as two broad signals at 2.9 and 3.0 ppm. These observations are in accord with a *rac*-*meso* exchange in which the *rac* isomer is preferred. The *meso* isomer should give one type of ethylene protons for **8a**, due to the symmetry plane perpendicular to the coordination plane. This plane is absent in **8c**, and accordingly, two types of protons are observed.

These studies demonstrate a facile olefin rotation for complexes **8** in solution. Further support for this phenomenon is provided by theoretical calculations (see below). However, in view of the preferred *ip* conformation detected in the solid state, we have also been interested in providing information about the preferred conformation in solution. For that purpose we have obtained a $^{13}\text{C}\{^1\text{H}\}$ CP-MAS spectrum of complex **8b**.³⁰ Interestingly, the spectrum is practically coincident with that obtained in solution (see the Supporting Information). It is worth noting that the olefinic carbons appear in the solid state at 58.6 ppm, while in CD_2Cl_2 solution they appear at δ 58.6 (300 K) or 56.8 (190 K). The similarity is also extended to the phosphorus experiments, as the phosphite groups appear at 175.7 ppm in the ^{31}P CP-MAS experiment and as a doublet centered at 175.1 ppm ($J_{\text{RhP}} = 253$ Hz) in the $^{31}\text{P}\{^1\text{H}\}$ spectrum in solution. These observations indicate an important similarity between the structure of the compound in solution and that in the solid state and suggest that, despite olefin rotation, this ligand is also predominantly located in plane in solution.

(c) Theoretical Studies. In order to understand the factors governing olefin conformation in compounds **8**, we have performed DFT calculations (see the Experimental Section for details) on conformers *u* and *ip* of the model complexes **I–VII** (Figure 8). The set of models has been designed with a growing complexity in order to investigate the factors that control the ethylene orientation. Molecules range from the simplest one, **I**, based on monodentate phosphine and phenyl ligands, to the more realistic **VII**, which only differs from complex **8a** in the absence of *t*-Bu groups at the 5- and 5'-positions of the biphenyls, removed for computer limitations. Thus, the significance of the electronic factors has principally been studied by changing the nature of the phosphorus coordinating group in the phosphine (**II**) and phosphinite (**III**, **IV**) models. Alternatively, the influence of steric effects has been scrutinized by modulating the R group at the biphenyl groups (models **V–VII**). Moreover, selected structural parameters for all model complexes have been collected in Tables 3 and 4.

Table 3. Selected Bond Distances and Angles for Compounds **I–IV**^a

compd	Rh–C _{ethylene}	C–C _{ethylene}	Rh–P	P–Rh–P	$\alpha(\pi_1/\pi_2)^b$
<i>ip</i> - I	2.335	1.363	2.326	174.6	0
<i>u</i> - I	2.239	1.386	2.308	176.9	90
<i>ip</i> - II	2.260	1.377	2.283	158.5	14.8
<i>u</i> - II	2.249	1.380	2.288	162.6	76.3
<i>ip</i> - III	2.250	1.383	2.260	155.4	0
<i>u</i> - III	2.255	1.379	2.273	157.1	90
<i>ip</i> - IV	2.233	1.387	2.284	156.1	0
<i>u</i> - IV	2.242	1.383	2.291	158.4	90

^a Angles in deg and distances in Å. ^b Angle between π_1 (defined by Rh and pincer ligand atoms bonded to it) and π_2 (defined by Rh and ethylene carbons).

Table 4. Selected Bond Distances and Angles for Compounds **V–VII** and **8**^a

compd	Rh–C _{ethylene}	C–C _{ethylene}	Rh–P	P–Rh–P	$\alpha(\pi_1/\pi_2)^b$
<i>ip</i> - V	2.286	1.374	2.259	155.1	4.1
<i>u</i> - V	2.282	1.372	2.265	156.9	82.7
<i>ip</i> - VI	2.288	1.374	2.259	155.0	8.8
<i>u</i> - VI	2.284	1.372	2.266	157.9	86.9
<i>ip</i> - VII	2.285	1.373	2.259	155.1	7.9
8a	2.2184(14)	1.377(2)	2.2076(3)	155.490(13)	7.4
	2.2353(14)		2.2165(3)		
8b	2.228(3)	1.353(4)	2.2237(7)	155.37(3)	13.0
	2.230(3)		2.2096(7)		

^a Angles in deg and distances in Å. ^b Angle between π_1 (defined by Rh and pincer ligand atoms bonded to it) and π_2 (defined by Rh and ethylene carbons).

Table 5. Relative Energy (kcal mol⁻¹) between Isomers of Model Complexes **I–VII**^a

compd	rel energy ^a
RhPh(PH ₃) ₂ (C ₂ H ₄) (I)	+10.8
Rh{C ₆ H ₃ (CH ₂ PH ₂) ₂ }(C ₂ H ₄) (II)	+1.0
Rh{C ₆ H ₃ (OPH ₂) ₂ }(C ₂ H ₄) (III)	-0.9
Rh{C ₆ H ₃ (OPMe ₂) ₂ }(C ₂ H ₄) (IV)	-0.8
Rh{C ₆ H ₃ (OP(OC ₆ H ₄ -OC ₆ H ₄) ₂)}(C ₂ H ₄) (V)	-0.1
Rh{C ₆ H ₃ (OP(OC ₆ H ₃ Me-OC ₆ H ₄) ₂)}(C ₂ H ₄) (VI)	-0.6
Rh{C ₆ H ₃ (OP(OC ₆ H ₃ - <i>t</i> -Bu-OC ₆ H ₄) ₂)}(C ₂ H ₄) (VII)	<i>b</i>

^a A negative value for the relative energy indicates that the *ip* conformer is the most stable. ^b *u* conformation cannot be optimized.

As a starting point, the simplest model, RhPh(PH₃)₂(C₂H₄) (**I**), was computed to confirm in our model system the well-known preference for a *u* orientation of an olefin coordinated to a d⁸-ML₃ fragment and, in addition, to quantify the relative stability between its conformers. As expected, the *u* ethylene conformation is not only preferred but is considerably more stable (10.8 kcal mol⁻¹, Table 5) than the *ip* conformation.

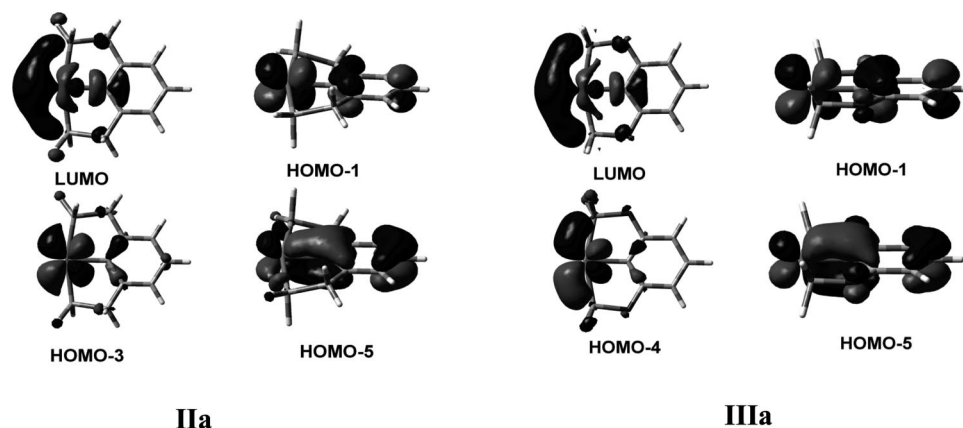
We have next analyzed the effect of formally including a bridge between the phenyl and P ligands to compute model complexes **II–IV**. For the phosphine model **II**, the *u* conformation is, as expected, more stable than the *ip* conformation, but only by 1 kcal mol⁻¹. Thus, the energy difference has significantly decreased in comparison with model **I**. This effect can be ascribed to the mitigation of the steric pressure produced by a lower P–Rh–P angle in **II** (158.5 and 162.6° for *ip* and *u* conformers, respectively), compared with **I** (174.6 and 176.9° for the *ip* and *u* conformers, respectively). Thus, for the latter, the higher steric pressure exerted by the *cis* coligands in the ethylene *ip* conformer significantly destabilizes it with respect to the *u* conformer.⁴ For model complexes **III** and **IV**, in which the P–Rh–P angles are similar to those of **II**, but slightly smaller, the energy difference is also small, although in these cases the *ip* conformation is found to be more stable by about 1 kcal mol⁻¹. Interestingly, the presence of O atoms has an important influence on the structure of the metallacycle. As was mentioned, pincer diphosphine ligands are characterized by

(30) Quan, R. W.; Li, Z.; Jacobsen, E. N. *J. Am. Chem. Soc.* **1996**, *118*, 8156.

Table 6. Summary of Crystallographic Data and Structure Refinement Results from Single-Crystal X-ray Diffraction

	4a	5a	5b	6a	7a	8a	8b
formula	C ₈₀ H ₉₉ O ₆ P ₃ Rh · C ₆ H ₁₄	C ₈₀ H ₉₈ O ₆ P ₃ Rh · 0.5C ₆ H ₁₄	2(C ₇₂ H ₈₂ O ₆ P ₃ Rh) · C ₄ H ₁₀ O	2(C ₆₃ H ₈₃ O ₇ P ₂ Rh) · C ₆ H ₁₄ · C ₅ H ₁₂	2(C ₇₁ H ₉₂ NO ₆ P ₂ Rh) · CHCl ₃ · CH ₂ Cl ₂	C ₆₄ H ₈₇ O ₆ P ₂ Rh · C ₅ H ₁₂	C ₅₆ H ₇₁ O ₆ P ₂ Rh
fw	1474.03	1394.49	2552.51	2392.61	2644.91	1189.33	1004.98
cryst syst	triclinic	triclinic	monoclinic	monoclinic	triclinic	monoclinic	orthorhombic
space group	<i>P</i> $\bar{1}$	<i>P</i> $\bar{1}$	<i>C</i> 2	<i>P</i> 2 ₁ / <i>c</i>	<i>P</i> $\bar{1}$	<i>P</i> 2 ₁ / <i>c</i>	<i>P</i> 2 ₁ 2 ₁
<i>a</i> , Å	13.4989(8)	14.4920(18)	24.7253(9)	12.3963(2)	12.6244(9)	17.2239(5)	10.4092(11)
<i>b</i> , Å	16.7201(9)	17.417(2)	12.9836(4)	19.8113(4)	18.5218(15)	19.2234(6)	18.8544(18)
<i>c</i> , Å	19.3595(11)	19.351(2)	21.7178(6)	27.2608(6)	18.850(2)	20.3456(6)	26.636(3)
α , deg	110.784(3)	65.484(5)	90	90	106.614(3)	90	90
β , deg	96.741(3)	69.097(5)	99.008(2)	95.0850(10)	108.221(3)	97.7050(10)	90
γ , deg	97.170(3)	70.040(5)	90	90	107.806(2)	90	90
cell vol, Å ³	3991.2(4)	4042.7(8)	6885.9(4)	6668.5(2)	3614.0(6)	6675.6(3)	5227.6(9)
<i>Z</i>	2	2	2	2	1	4	4
ρ_{calcd} , Mg/m ³	1.227	1.146	1.231	1.192	1.215	1.183	1.277
cryst color	yellow	orange	yellow	yellow	yellow	orange	orange
μ , mm ⁻¹	0.358	0.318	0.368	0.353	0.421	0.351	0.436
<i>F</i> (000)	1568	1482	2692	2552	1396	2544	2120
no. of measd rflns	49 365	117 604	49 957	110 399	56 585	153 626	45 841
no. of indep rflns	24 502	18 888	16 411	20 357	21 952	20 381	11 402
no. of params	874	865	783	732	917	719	602
R1(<i>F</i>) (<i>F</i> ² > 2 σ (<i>F</i> ²)) ^a	0.0589	0.0613	0.0711	0.0373	0.0680	0.0311	0.0352
wR2(<i>F</i> ²) ^b (all data)	0.1651	0.1788	0.1561	0.0934	0.2169	0.0797	0.0717
<i>S</i> ^c (all data)	1.016	1.020	1.047	1.056	1.043	1.052	1.019
Flack param			0.03(3)				-0.018(17)

^a $R1(F) = \sum(F_o - F_c)/\sum F_o$ for the observed reflections ($F^2 > 2\sigma(F^2)$). ^b $wR2(F^2) = \{\sum[w(F_o^2 - F_c^2)^2]/\sum w(F_o^2)^2\}^{1/2}$. ^c $S = \{\sum[w(F_o^2 - F_c^2)^2]/(n - p)\}^{1/2}$ (n = number of reflections, p = number of parameters).

Figure 9. Selected 3D isosurfaces corresponding to the MOs of fragments **IIa** and **IIIa**.

puckered structures, while pincer diphosphite complexes described here possess a planar structure. This difference is well reproduced in the series of models **II**–**IV**. Thus, phosphinite models **III** and **IV** (as well as **V**–**VII**, see below) describe planar structures, while a puckered arrangement is evident in the structures of isomers of model **II**.

With the aim of rationalizing the effect caused by the formal substitution of a CH₂ group by an O atom, we have analyzed the MOs of the rhodium–pincer ligand fragments of **II** and **III**, namely **IIa** and **IIIa**, respectively. The two interactions between the ethylene ligand and the metallic fragment are well-known: (i) donation from ethylene to the LUMO of the fragment (the typical empty hybrid of a d⁸-ML₃ FMO, Figure 9) and (ii) back-donation from d_{xy} or from d_{xz} orbitals for the *ip* and *u* isomers (the coordination plane is *xy*), respectively. Concerning the donation, the involvement of Rh in the LUMO in the fragments **IIa** and **IIIa** is the same (47%), but the contribution from the P atoms to the LUMO is higher in **IIIa** (39%) than in **IIa** (31%). Thus, the resulting lobes of the LUMO in **IIIa** are to some extent better adapted, in terms of overlap, for receiving the donation of the occupied ethylene orbital if the in-plane conformation is attained than those of **IIa**. Concerning the back-donation, there are two orbitals that are appropriate for such an interaction, one

for the in-plane conformer (HOMO-3 in **IIa** and HOMO-4 in **IIIa**) and the other for the *u* species (HOMO-1 for both **IIa** and **IIIa**). HOMO-5 corresponds to the bonding combination of the d_{xz} orbital with the p orbitals of the aromatic ring. The back-donation in fragment **IIa** is favored for the *u* isomer, with respect to **IIIa**, because the participation of the Rh d_{xz} orbital in HOMO-1 is 78%, higher than the Rh character of 58% found in the HOMO-1 of **IIIa**. In contrast, in fragment **IIIa** HOMO-4 is formed mainly by the Rh d_{xy} orbital (75% Rh character) with an important participation from the P atoms (21%). This contribution expands the lobes of the orbital on the appropriate way to favor the back-donation in the in-plane isomer. This situation is somewhat disfavored for **IIa**, where the analogous orbital, HOMO-3, presents an 83% Rh character, with a small contribution (6%) from the P atoms. Summarizing, there is a subtle electronic effect associated with the formal substitution of a CH₂ group by an O atom. On the basis of the Rh contributions to the frontier FMOs and their corresponding topologies, we can expect a better preference for the *ip* conformer in **IIIa** than in **IIa**.

Interestingly, the analysis of the rotational barrier of the ethylene ligand in compounds **II** and **III** (see the Supporting Information) corroborates the above discussion. The barrier is

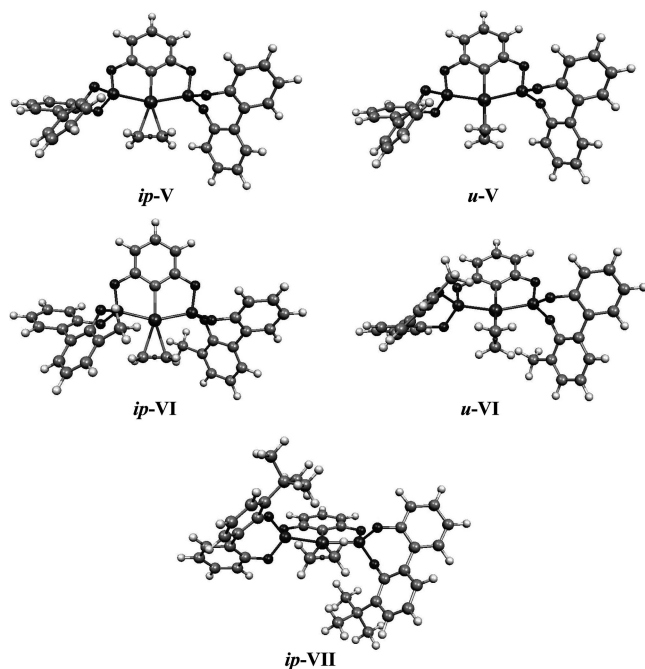


Figure 10. Optimized structures of conformers of the model complexes **V–VII**.

small in both cases (ca. 1 kcal mol⁻¹), in good agreement with a relatively minor π contribution to the Rh–ethylene bond, which would facilitate the rotation of the olefin.

The importance of steric factors produced by the substituents of the biphenyl ring has been studied by calculating the model complexes Rh{C₆H₃(OP(OC₆H₃R-OC₆H₄)₂)(C₂H₄) (R = H (**V**), Me (**VI**), *t*-Bu (**VII**)). For models **V** and **VI**, both *u* and *ip* conformations have been located as stationary points (Figure 10). The computed energies for isomers of **V** and **VI** are quite similar (Table 5). For model **VI** the *ip* conformation is more stable with respect to the *u* isomer by only 0.6 kcal mol⁻¹, while for **V** the *ip* conformation is more stable by no more than 0.1 kcal mol⁻¹. For complex **VII**, although different conformations for the ethylene ligand were explored as starting geometries, the only conformation that appears to be a stationary point corresponds to the *ip* isomer. All our attempts of optimization of the *u* conformer converged into the *ip* conformer. Interestingly, the structural parameters of the computed model **VII** are in good agreement with the experimental data of compound **8a**. For instance, the calculated parameters around the Rh–C₂H₄ moiety (Rh–C = 2.285 Å and C–C = 1.373 Å) agree well with the experimental values (Rh–C = 2.235(2) and 2.218(2) Å and C–C = 1.377(2) Å). Likewise, there is a good accord in the values of the P–Rh–P angle (experimental, 155.5°; computed, 155.1°). The calculations are also capable of describing the small deviation of the Rh–C₂H₄ plane with respect to the Rh–PCP plane (experimental, 7.4°; computed, 7.9°). Finally, the calculation reproduces well the planarity of the Rh–PCP fragment of **8a**.

From comparison of models **V–VII** it appears that the bulky *t*-Bu groups have a decisive role in destabilizing the *u* conformer. This effect can be readily seen using space-filling models of *u*-**VI**, *ip*-**VI**, and *ip*-**VII** complexes (see the Supporting Information). A comparison of conformers of **VI** show that the cavity generated by the metal and the pincer ligand is practically superimposable and can allocate the ethylene in either conformation without distortion. Otherwise, the presence of *t*-Bu groups in **VII** does not increase encumbrance in the coordination

plane but offers an important steric hindrance in a perpendicular direction to this plane. Thus, an ethylene ligand can be easily coordinated in a *ip* fashion, but a *u* orientation would require a distortion of the cavity. This fact is apparently in contradiction with the observed olefin rotation process. However, comparison of structures of complexes **5b** and **8b** reveal the ability of the pincer ligand to distort and generate a more opened cavity which will be able to accommodate transiently the ethylene in a *u* conformation.

Conclusions

A series of rhodium complexes derived from pincer diphosphite and neutral L ligands has been prepared and characterized. IR studies of the carbonyl (**6a**) and isonitrile (**7a**) complexes show the π -acceptor ability of the pincer diphosphite ligand. Comparison of structures of complexes **5a–8a**, **5b**, and **8b** indicate very similar parameters for the Rh–PCP fragment in the coordination plane. In addition, in the series of derivatives of the conformationally flexible ligand PCP^a, it has been observed that the conformation of the biphenyl groups is determined by the size of the L ligand. Thus, a *rac* conformation has been observed for less demanding groups, while the *meso* structure is preferred for larger L ligands. Moreover, *rac–meso* isomerization has been observed for these complexes in solution. Most noteworthy, X-ray structural determination of complexes **8** indicate a rare in-plane conformation of the ethylene ligand. NMR studies indicate that olefin complexes (**8** and **9**) have a fluxional behavior caused by a olefin rotation process, which could not be frozen at the lower temperature investigated. Moreover, ¹³C{¹H} NMR spectra of **8b** in solution and in the solid state practically match, thus indicating an important coincidence between solid-state and solution structures for this complex.

To complete the experimental studies, detailed computational investigations of *u* and *ip* conformers of a set of model complexes **I–VII** have been performed. An investigation of electronic effects indicates that the nature of the P-fragments (phosphine vs phosphinite) do not play an important role in altering the relative stabilities of both types of conformers. Otherwise, steric effects play a decisive influence on olefin conformation. Two different effects have been identified. First, the reduction of the P–Rh–P angle, as compared with the ideal for two trans-coordinated ligands, causes the reduction of hindrance toward the remaining coordination position. The second is with regard to the size of the R substituents at the 3- and 3'-positions of the biphenyl fragments. Thus, while for H and Me derivatives both conformers are of similar energy, the cavity outlined by the *t*-Bu-substituted pincer ligand in model **VII** significantly reduces the available space above and below the coordination plane, favoring the *ip* conformation.

Experimental Section

General Comments. All reactions and manipulations were performed under nitrogen or argon, either in a Braun Labmaster 100 glovebox or using standard Schlenk-type techniques. All solvents were distilled under nitrogen using the following desiccants: sodium benzophenone ketyl for benzene, diethyl ether (Et₂O), and tetrahydrofuran (THF), sodium for petroleum ether and toluene, CaH₂ for dichloromethane (CH₂Cl₂), and NaOMe for methanol (MeOH). Chlorophosphites **1**³¹ and the complex Rh(Cl)(PPh₃)₃³²

(31) (a) Buisman, G. J. H.; Kamer, P. C. J.; van Leeuwen, P. W. N. M. *Tetrahedron: Asymmetry* **1993**, *4*, 1625. (b) Suárez, A.; Méndez-Rojas, M. A.; Pizzano, A. *Organometallics* **2002**, *21*, 4611.

were prepared according to literature procedures. NMR spectra were obtained on Bruker DPX-300, DRX-400, and DRX-500 spectrometers. $^{31}\text{P}\{^1\text{H}\}$ NMR shifts were referenced to external 85% H_3PO_4 , while $^{13}\text{C}\{^1\text{H}\}$ and ^1H shifts were referenced to the residual signals of deuterated solvents. All data are reported in ppm downfield from Me_4Si . HRMS data were obtained using a Jeol JMS-SX 102A mass spectrometer at the Analytical Services of the Universidad de Sevilla (CITIUS). Elemental analyses were run by the Analytical Service of the Instituto de Investigaciones Químicas.

μ -1,3-Phenylenebis[1,1'-(3,3',5,5'-tetra-*tert*-butyl)biphen-2,2'-diyl]diphosphite (2a). Over a solution of phosphorochloridite **1a** (4.74 g, 10 mmol) and NEt_3 (1.5 mL, 11 mmol) in THF (40 mL) was slowly added a resorcinol (0.55 g, 5 mmol) solution in the same solvent (40 mL). After the mixture was stirred for 16 h, the solvent was evaporated, the residue treated with Et_2O (350 mL), and this mixture filtered through a pad of neutral alumina. Removal of the solvent yielded compound **2a** as a white foamy solid (4.29 g, 87%). ^1H NMR (CDCl_3 , 400 MHz): δ 1.36 (s, 36H, 4 CMe_3), 1.48 (s, 36H, 4 CMe_3), 6.80 (dd, $^3J_{\text{HH}} = 8.4$ Hz, $^4J_{\text{HH}} = 2.5$ Hz, 2H, 2 H arom), 6.92 (m, 1H, H arom), 7.16 (t, $^3J_{\text{HH}} = 8.4$ Hz, 1H, H arom), 7.20 (d, $^4J_{\text{HH}} = 2.4$ Hz, 4H, 4 H arom), 7.45 (d, $^4J_{\text{HH}} = 2.4$ Hz, 4H, 4 H arom). $^{31}\text{P}\{^1\text{H}\}$ NMR (CDCl_3 , 202.4 MHz): δ 137.9 (s). $^{13}\text{C}\{^1\text{H}\}$ NMR (CDCl_3 , 100.6 MHz): δ 31.3 (br s, 4 CMe_3), 31.5 (s, 4 CMe_3), 34.7 (4 CMe_3), 35.5 (4 CMe_3), 112.8 (t, $J_{\text{PC}} = 8$ Hz, CH arom), 115.8 (d, $J_{\text{PC}} = 9$ Hz, 2 CH arom), 124.4 (s, 4 CH arom), 126.6 (s, 4 CH arom), 130.0 (s, CH arom), 132.8 (d, $J_{\text{PC}} = 2$ Hz, 4 C_q arom), 140.3 (s, 4 C_q arom), 145.3 (d, $J_{\text{PC}} = 6$ Hz, 4 C_q arom), 146.8 (s, 4 C_q arom), 153.2 (d, $J_{\text{PC}} = 7$ Hz, 2 C_q arom). HRMS (FAB): m/z 986.5755, $[\text{M}]^+$ (exact mass calcd for $\text{C}_{62}\text{H}_{84}\text{O}_6\text{P}_2$ 986.5743).

(*R,R*)- μ -1,3-phenylenebis[1,1'-(3,3'-di-*tert*-butyl-5,5',6,6'-tetramethyl)biphen-2,2'-diyl]diphosphite (2b). Compound **2b** has been obtained as a white solid as described for **2a** but starting from chlorophosphite **1b** (1.70 g, 78%). $[\alpha]_{\text{D}}^{20} = -347$ (c 1.0, THF). ^1H NMR (CDCl_3 , 500 MHz): δ 1.41 (s, 18H, 2 CMe_3), 1.42 (s, 18H, 2 CMe_3), 1.82 (s, 6H, 2 Me), 1.83 (s, 6H, 2 Me), 2.23 (s, 6H, 2 Me), 2.26 (s, 6H, 2 Me), 6.80 (m, 3H, 3 H arom), 7.14 (t, $J_{\text{HH}} = 7.5$ Hz, 1H, H arom), 7.16 (s, 4H, 4 H arom). $^{31}\text{P}\{^1\text{H}\}$ NMR (CDCl_3 , 121.5 MHz): δ 132.6 (s). $^{13}\text{C}\{^1\text{H}\}$ NMR (CDCl_3 , 75.5 MHz): δ 16.9 (s, 2 Ar-Me), 17.1 (s, 2 Ar-Me), 20.7 (s, 4 Ar-Me), 31.5 (s, CMe_3), 31.5 (s, CMe_3), 32.0 (s, 2 CMe_3), 34.9 (s, 2 CMe_3), 35.1 (s, 2 CMe_3), 112.6 (t, $J_{\text{PC}} = 9$ Hz, CH arom, C°), 115.6 (d, $J_{\text{PC}} = 10$ Hz, 2 CH arom), 128.1 (s, 2 CH arom), 128.5 (s, 2 CH arom), 130.2 (s, CH arom), 130.7 (br s, 2 C_q arom), 132.3 (m, 2 C_q arom), 132.4 (s, 2 C_q arom), 133.2 (s, 2 C_q arom), 134.7 (s, 2 C_q arom), 135.5 (s, 2 C_q arom), 137.7 (s, 2 C_q arom), 138.5 (br s, 2 C_q arom), 144.7 (d, $J_{\text{PC}} = 6$ Hz, 2 C_q arom), 144.8 (s, 2 C_q arom), 153.6 (d, $J_{\text{PC}} = 9$ Hz, 2 C_q arom). HRMS (FAB): m/z 875.4586, $[\text{M} + \text{H}]^+$ (exact mass calcd for $\text{C}_{54}\text{H}_{69}\text{O}_6\text{P}_2$ 875.4569).

μ -1,3-Naphthalenediylbis[1,1'-(3,3',5,5'-tetra-*tert*-butyl)biphen-2,2'-diyl]diphosphite (2c). Over a solution of phosphorochloridite **1a** (1.48 g, 3.1 mmol) and NEt_3 (0.5 mL, 3.1 mmol) in THF (25 mL) was slowly added a 1,3-dihydroxynaphthalene (0.250 g, 1.6 mmol) solution in the same solvent (15 mL). After the mixture was stirred for 16 h, the solvent was evaporated and the residue was extracted with Et_2O (3 \times 20 mL) and filtered through a pad of neutral alumina. Removal of the solvent yielded compound **2c** as a white foamy solid (1.46 g, 90%). ^1H NMR (CDCl_3 , 400 MHz): δ 1.35 (s, 18H, 2 CMe_3), 1.36 (s, 18H, 2 CMe_3), 1.39 (s, 18H, 2 CMe_3), 1.50 (s, 18H, 2 CMe_3), 7.09 (s, 1H, H arom), 7.21 (d, $^4J_{\text{HH}} = 2.4$ Hz, 2H, 2 H arom), 7.22 (d, $^4J_{\text{HH}} = 2.4$ Hz, 2H, 2 H arom), 7.24 (s, 1H, H arom), 7.28 (m, 1H, H arom), 7.41 (m, 1H, H arom), 7.44 (d, $^4J_{\text{HH}} = 2.4$ Hz, 2H, 2 H arom), 7.46 (d, $^4J_{\text{HH}} = 2.4$ Hz, 2H, 2 H arom), 7.61 (d, $^3J_{\text{HH}} = 8.0$ Hz, 1H, H arom), 7.97 (d, $^3J_{\text{HH}}$

$= 9.3$ Hz, 1H, H arom). $^{31}\text{P}\{^1\text{H}\}$ NMR (CDCl_3 , 162.1 MHz): δ 136.9 (s), 138.9 (s). $^{13}\text{C}\{^1\text{H}\}$ NMR (CDCl_3 , 125.8 MHz): δ 31.2 (s, 2 CMe_3), 31.3 (s, 2 CMe_3), 31.6 (s, 4 CMe_3), 34.7 (s, 4 CMe_3), 35.4 (s, 2 CMe_3), 35.5 (s, 2 CMe_3), 110.7 (dd, $J_{\text{CP}} = 13$ Hz, $J_{\text{CP}} = 5$ Hz, CH arom), 112.3 (d, $J_{\text{CP}} = 12$ Hz, CH arom), 122.9 (s, CH arom), 124.4 (s, 2 CH arom), 124.5 (s, 2 CH arom), 124.8 (s, CH arom), 126.7 (s, 4 CH arom), 127.0 (s, CH arom), 127.3 (s, CH arom), 132.8 (s, 5 C_q), 134.7 (s, C_q), 140.3 (s, 2 C_q), 140.4 (s, 2 C_q), 145.5 (s, 4 C_q), 146.8 (s, 2 C_q), 146.9 (s, 2 C_q), 149.3 (d, $J_{\text{CP}} = 12$ Hz, C_q), 149.5 (d, $J_{\text{PC}} = 12$ Hz, C_q). HRMS (FAB): m/z 1059.5857, $[\text{M} + \text{Na}]^+$ (exact mass calcd for $\text{C}_{66}\text{H}_{86}\text{O}_6\text{P}_2\text{Na}$: 1059.5797).

Rh(H)(Cl)(PCP^a)(PPh₃) (4a). Although this compound was first observed in the reaction between $\text{Rh}(\text{Cl})(\text{PPh}_3)_3$ and **2a**, it is more conveniently obtained by protonation of **5a**. Over a solution of **5a** (0.11 g, 0.081 mmol) in THF (10 mL) was added HCl (0.2 mL, 1.0 M in Et_2O). The mixture was stirred vigorously for 24 h, the solvent evaporated, and the remaining residue extracted with *n*-hexane (3 \times 10 mL). Solvent evaporation yields **4a** as a yellow solid (0.09 g, 80%). IR (Nujol mull, cm^{-1}): 2112 (m, ν_{RH}). ^1H NMR (CDCl_3 , 500 MHz): δ -15.63 (dq, $J_{\text{HRh}} = J_{\text{HPo}} = J_{\text{HP}} = 12$ Hz, 1H, Rh-H), 1.22 (s, 18H, 2 CMe_3), 1.27 (s, 18H, 2 CMe_3), 1.32 (s, 18H, 2 CMe_3), 1.42 (s, 18H, 2 CMe_3), 6.63 (dd, $J_{\text{HH}} = 8$ Hz, $J_{\text{RH}} = 2$ Hz, 2H, 2 H arom), 6.84 (m, 6H, 6 H arom, PPh_3), 6.85 (m, 2H, 2 H arom), 6.91 (d, $J_{\text{HH}} = 2$ Hz, 2H, 2 H arom), 6.95 (t, $J_{\text{HH}} = 8$ Hz, 1H, H arom), 6.98 (t, $J_{\text{HH}} = 7.5$ Hz, 3H, 3 H arom, PPh_3), 7.17 (dd, $J_{\text{HH}} = 7.5$ Hz, $J_{\text{HP}} = 10$ Hz, 6H, 6 H arom, PPh_3), 7.33 (m, 2H, 2 H arom), 7.37 (d, $J_{\text{HH}} = 2$ Hz, 2H, 2 H arom). $^{31}\text{P}\{^1\text{H}\}$ NMR (C_6D_6 , 162.1 MHz): δ 14.7 (dt, $J_{\text{PRh}} = 87$ Hz, $J_{\text{PP}} = 35$ Hz, P-C), 148.9 (dd, $J_{\text{PRh}} = 178$ Hz, P-O). $^{13}\text{C}\{^1\text{H}\}$ NMR (CDCl_3 , 75.5 MHz): δ 31.6 (s, 2 CMe_3), 31.6 (s, 2 CMe_3), 31.7 (s, 2 CMe_3), 32.0 (s, 2 CMe_3), 34.8 (s, 4 CMe_3), 35.7 (s, 2 CMe_3), 36.1 (s, 2 CMe_3), 106.8 (t, $J_{\text{PC}} = 7$ Hz, 2 CH arom), 124.6 (s, 2 CH arom), 125.0 (s, 2 CH arom), 126.8 (s, CH arom), 127.3 (s, 2 CH arom), 127.8 (d, $J_{\text{PC}} = 9$ Hz, 6 CH arom, PPh_3), 128.3 (s, 2 CH arom), 129.1 (s, 3 CH arom), 129.9 (s, 2 C_q arom), 131.6 (s, 2 C_q arom), 133.4 (d, $J_{\text{PC}} = 12$ Hz, 6 CH arom), 134.6 (d, $J_{\text{PC}} = 35$ Hz, 3 C_q arom), 136.5 (m, C_q arom), 139.7 (s, 2 C_q arom), 141.2 (s, 2 C_q arom), 145.6 (br s, 2 C_q arom), 146.4 (s, 2 C_q arom), 146.8 (s, 2 C_q arom), 147.4 (t, $J_{\text{PC}} = 7$ Hz, 2 C_q arom), 156.0 (t, $J_{\text{PC}} = 11$ Hz, 2 OC_q arom). Anal. Calcd for $\text{C}_{80}\text{H}_{99}\text{ClO}_6\text{P}_3\text{Rh}$: C, 69.2; H, 7.2. Found: C, 69.3; H, 7.6.

Rh(PCP^a)(PPh₃) (5a). Over a suspension of $\text{RhCl}(\text{PPh}_3)_3$ (0.46 g, 0.5 mmol) in THF (5 mL) was added diphosphite **2a** (0.49 g, 0.5 mmol) dissolved in THF (10 mL). The mixture was heated over 24 h at 70 °C. An excess of NEt_3 (0.1 mL) was added and the mixture vigorously stirred for 24 h. Solvent was removed under reduced pressure, and the resulting solid was purified by column chromatography on silica gel (AcOEt:Hex 1:20), yielding **3a** as an orange solid (0.58 g, 85%). ^1H NMR (CDCl_3 , 400 MHz): δ 1.20 (s, 36H, 4 CMe_3), 1.38 (s, 36H, 4 CMe_3), 6.42 (d, $^3J_{\text{HH}} = 8$ Hz, 2H, 2 H arom), 6.71 (t, $^3J_{\text{HH}} = 7$ Hz, 6H, 6 H arom), 6.84 (t, 1H, $^3J_{\text{HH}} = 8$ Hz, H arom), 6.97 (t, $^3J_{\text{HH}} = 7$ Hz, 3H, 3 H arom), 7.10 (br s, 4H, 4 H arom), 7.33 (br s, 4H, 4 H arom), 7.35 (d, $^3J_{\text{HH}} = 7$ Hz, 6H, 6 H arom). $^{31}\text{P}\{^1\text{H}\}$ NMR (CDCl_3 , 162.1 MHz): δ 28.6 (td, $J_{\text{PRh}} = 129$ Hz, $J_{\text{PP}} = 44$ Hz, P-C), 171.5 (dd, $J_{\text{PRh}} = 265$ Hz, P-O). $^{13}\text{C}\{^1\text{H}\}$ NMR (CDCl_3 , 75.5 MHz): δ 31.8 (s, 4 CMe_3), 31.9 (s, 4 CMe_3), 35.0 (s, 4 CMe_3), 35.8 (s, 4 CMe_3), 105.3 (t, $J_{\text{PC}} = 8$ Hz, 2 CH arom), 124.6 (s, 4 CH arom), 126.0 (s, CH arom), 127.6 (s, 4 CH arom), 128.0 (d, $J_{\text{PC}} = 9$ Hz, 6 CH arom), 129.0 (s, 3 CH arom), 131.4 (s, 4 C_q arom), 134.0 (d, $J_{\text{PC}} = 13$ Hz, 6 CH arom), 137.7 (d, $J_{\text{PC}} = 36$ Hz, 3 C_q arom), 140.1 (s, 4 C_q arom), 140.7 (ddd, $J_{\text{PC}} = 58$, 14 Hz, $J_{\text{RHC}} = 28$ Hz, C_q arom), 146.6 (s, 4 C_q arom), 147.4 (t, $J_{\text{PC}} = 5$ Hz, 4 OC_q arom), 159.5 (t, $J_{\text{PC}} = 13$ Hz, 2 OC_q arom). Anal. Calcd for $\text{C}_{80}\text{H}_{98}\text{O}_6\text{P}_3\text{Rh}$: C, 71.1; H, 7.3. Found: C, 70.6; H, 7.4.

Rh(PCP^b)(PPh₃) (5b). Over a suspension of RhCl(PPh₃)₃ (0.473 g, 0.54 mmol) in THF (5 mL) was added diphosphite **2b** (0.500 g, 0.54 mmol) dissolved in THF (5 mL). The mixture was heated over 16 h at 60 °C. An excess of NEt₃ (0.1 mL) was added and the mixture vigorously stirred for 24 h at 60 °C. Solvent was removed under reduced pressure, and the resulting solid was purified by column chromatography on silica gel (AcOEt:hexane, 1:20), yielding **5b** as an orange solid (0.474 g, 71%). ¹H NMR (CD₂Cl₂, 500 MHz): δ 1.13 (s, 18H, 2 CMe₃), 1.42 (s, 18H, 2 CMe₃), 1.76 (s, 6H, 2 Ar-Me), 1.82 (s, 6H, 2 Ar-Me), 2.23 (s, 6H, 2 Ar-Me), 2.32 (s, 6H, 2 Ar-Me), 6.41 (d, ³J_{HH} = 7.5 Hz, 2H, 2 H arom), 6.62 (s, 2H, 2 H arom), 6.90 (m, 7H, 7 H arom), 7.10 (t, ³J_{HH} = 7.5 Hz, 3H, 3 H arom), 7.24 (s, 2H, 2 H arom), 7.42 (dd, ³J_{HP} = 9.0 Hz, ³J_{HH} = 9.0 Hz, 6H, 6 H arom). ³¹P{¹H} NMR (CD₂Cl₂, 202.4 MHz): δ 25.5 (dt, J_{PRh} = 127 Hz, J_{PP} = 43 Hz, P-C), 165.6 (dd, J_{PRh} = 266 Hz, P-O). ¹³C{¹H} NMR (CD₂Cl₂, 125.8 MHz): δ 16.7 (s, 2 Ar-Me), 17.0 (s, 2 Ar-Me), 20.4 (s, 2 Ar-Me), 20.6 (s, 2 Ar-Me), 32.1 (s, 4 CMe₃), 34.8 (s, 2 CMe₃), 35.2 (s, 2 CMe₃), 104.8 (dd, J_{CRh} = 7 Hz, J_{CP} = 7 Hz, 2 CH arom), 126.5 (s, CH arom), 127.6 (d, J_{CP} = 9 Hz, 6 CH arom), 128.2 (s, 2 CH arom), 128.3 (s, 2 CH arom), 128.7 (s, 3 CH arom), 129.0 (s, 2 C_q), 130.6 (s, 2 C_q), 132.1 (s, 2 C_q), 133.3 (s, 2 C_q), 134.7 (d, J_{CP} = 13 Hz, 6 CH arom), 134.8 (s, 2 C_q), 135.3 (s, 2 C_q), 136.8 (s, 2 C_q), 138.4 (s, 2 C_q), 138.5 (d, J_{CP} = 31 Hz, 3 C_q), 140.4 (ddt, J_{CP} = 59, 14 Hz, J_{CRh} = 27 Hz, C_q), 146.5 (s, 2 C_q), 146.7 (s, 2 C_q), 159.4 (dd, J_{CRh} = 13 Hz, J_{CP} = 13 Hz, 2 C_q). Anal. Calcd for C₇₂H₈₂O₆P₃Rh: C, 69.8; H, 6.7. Found: C, 70.0; H, 6.9.

Rh(PCP^c)(PPh₃) (5c). Over a solution of RhCl(PPh₃)₃ (0.200 g, 0.22 mmol) and diphosphite **2c** (0.224 g, 0.22 mmol) in THF (10 mL) was added an excess of NEt₃ (0.3 mL). The mixture was heated over 24 h at 70 °C. Solvent was removed under reduced pressure, and the resulting solid was purified by column chromatography on silica gel (AcOEt:hexane, 1:20), yielding **5c** as a yellow-orange solid (0.150 g, 49%). ¹H NMR (CDCl₃, 400 MHz): δ 1.15 (s, 18H, 2 CMe₃), 1.25 (s, 18H, 2 CMe₃), 1.42 (s, 18H, 2 CMe₃), 1.43 (s, 18H, 2 CMe₃), 6.76 (t, ³J_{HH} = 7.6 Hz, 6H, 6 H arom), 6.87 (s, 1H, H arom), 7.03 (m, 4H, 4 H arom), 7.14 (m, 2H, 2 H arom), 7.21 (m, 3H, 3 H arom), 7.32 (d, ³J_{HH} = 8.4 Hz, 1H, H arom), 7.37 (m, 4H, 4 H arom), 7.43 (m, 6H, 6 H arom), 7.56 (d, ³J_{HH} = 8.0 Hz, 1H, H arom). ³¹P{¹H} NMR (CDCl₃, 162.1 MHz): δ 28.7 (dt, J_{PRh} = 128 Hz, J_{PP} = 44 Hz, P-C), 168.1 (ddd, J_{PP} = 694 Hz, J_{PRh} = 265 Hz, J_{PP} = 44 Hz, P-O), 173.1 (ddd, J_{PP} = 694 Hz, J_{PRh} = 265 Hz, J_{PP} = 44 Hz, P-O). ¹³C{¹H} NMR (CDCl₃, 125.8 MHz): δ 31.2 (s, 2 CMe₃), 31.5 (s, 2 CMe₃), 31.6 (s, 4 CMe₃), 34.7 (s, 2 CMe₃), 34.7 (s, 2 CMe₃), 35.5 (s, 2 CMe₃), 35.6 (s, 2 CMe₃), 110.1 (d, J_{CP} = 13 Hz, CH arom), 118.1 (d, J_{CP} = 13 Hz, C_q), 122.3 (s, CH arom), 122.7 (s, CH arom), 124.3 (s, 2 CH arom), 124.4 (s, 3 CH arom), 126.6 (s, CH arom), 127.3 (s, 2 CH arom), 127.4 (s, 2 CH arom), 127.8 (d, J_{CP} = 9 Hz, 6 CH arom), 128.5 (m, C_q), 128.7 (s, 3 CH arom), 131.0 (s, 2 C_q), 131.2 (s, 2 C_q), 133.8 (d, J_{CP} = 13 Hz, 6 CH arom), 133.9 (s, 2 C_q), 137.4 (d, J_{CP} = 36 Hz, 3 C_q), 139.8 (d, J_{CP} = 5 Hz, 2 C_q), 139.9 (ddt, J_{CP} = 59, 14 Hz, J_{CRh} = 28 Hz, C_q), 146.4 (s, 4 C_q), 147.1 (d, J_{CP} = 10 Hz, 2 C_q), 147.3 (d, J_{CP} = 10 Hz, 2 C_q), 153.9 (d, J_{CP} = 20 Hz, C_q), 157.7 (d, J_{CP} = 19 Hz, C_q). Anal. Calcd for C₈₄H₁₀₀O₆P₃Rh: C, 72.0; H, 7.2. Found: C, 72.1; H, 7.3.

Rh(PCP^a)(CO) (6a). To a solution of compound **3a** (0.04 g, 0.03 mmol) in THF (10 mL) was added an excess of elemental selenium (0.005 g, 0.06 mmol). The mixture was introduced in a Fischer–Porter vessel and charged with 2 atm of CO. After 1 h the reactor was vented and solvent removed. The solution was concentrated until turbidity and filtered. After the mixture stood for 24 h, compound **4a** was collected as yellow crystals (0.020 g, 60%). IR (Nujol mull, cm⁻¹): 2017 (ν_{CO}). ¹H NMR (CDCl₃, 500 MHz): δ 1.33 (s, 36H, 4 CMe₃), 1.40 (s, 36H, 4 CMe₃), 6.64 (d, ³J_{HH} = 8 Hz, 2H, 2 H arom), 7.05 (t, ³J_{HH} = 8 Hz, 1H, H arom), 7.20 (d, ⁴J_{HH} = 2 Hz, 4H, 4 H arom), 7.45 (d, ⁴J_{HH} = 2 Hz, 4H, 4 H arom). ³¹P{¹H}

NMR (CDCl₃, 162.1 MHz): δ 167.3 (d, J_{PRh} = 256 Hz). ¹³C{¹H} NMR (CDCl₃, 125.8 MHz): δ 31.5 (s, 4 CMe₃), 31.7 (s, 4 CMe₃), 34.7 (4 CMe₃), 35.7 (4 CMe₃), 106.1 (t, J_{PC} = 8 Hz, 2 CH arom), 125.0 (s, 4 CH arom), 126.6 (s, 4 CH arom), 129.5 (s, CH arom), 131.6 (s, 4 C_q arom), 140.2 (m, C_q arom), 140.3 (s, 4 C_q arom), 145.1 (s, 4 OC_q arom), 147.6 (s, 4 C_q arom), 160.4 (t, J_{PC} = 14 Hz, 2 OC_q arom), 191.8 (dt, J_{RhC} = 58 Hz, J_{PC} = 16 Hz, CO). Anal. Calcd for C₆₃H₈₃O₇P₂Rh: C, 67.7; H, 7.5. Found: C, 67.9; H, 7.9.

Rh(PCP^a)(CNXy) (7a). A mixture of **5a** (0.04 g, 0.03 mmol), elemental Se (4 mg, 0.05 mmol), and CNXy (0.004 g, 0.03 mmol) in THF was vigorously stirred for 30 min. Solvent was removed under reduced pressure, and the obtained residue was extracted with *n*-pentane (3 × 10 mL). The solution was concentrated until turbidity appeared and then filtered. The resulting solution was left to stand for 24 h, and then compound **7a** appeared as yellow crystals (0.035 g, 95%). IR (Nujol mull, cm⁻¹): 2099 (s, ν_{CN}). ¹H NMR (CDCl₃, 500 MHz): δ 1.31 (s, 36H, 4 CMe₃), 1.40 (br s, 36H, 4 CMe₃), 1.55 (s, 6H, 2 Me), 6.59 (d, ³J_{HH} = 7.5 Hz, 2H, 2 H arom), 6.75 (d, ³J_{HH} = 7.5 Hz, 2H, 2 H arom), 6.92 (t, ³J_{HH} = 7.5 Hz, 1H, H arom), 6.95 (t, ³J_{HH} = 7.5 Hz, 1H, H arom), 7.18 (d, ⁴J_{HH} = 2.5 Hz, 4H, 4 H arom), 7.40 (d, ⁴J_{HH} = 2.5 Hz, 4H, 4 H arom). ³¹P{¹H} NMR (CDCl₃, 162.1 MHz): δ 170.1 (d, J_{PRh} = 265 Hz). ¹³C{¹H} NMR (CDCl₃, 125.8 MHz): δ 18.2 (s, 2 Ar-Me), 31.5 (s, 4 CMe₃), 31.8 (s, 4 CMe₃), 34.7 (s, 4 CMe₃), 35.7 (s, 4 CMe₃), 105.6 (t, 2 CH arom), 124.7 (s, 4 CH arom), 126.5 (s, 4 CH arom), 127.1 (s, CH arom), 127.2 (s, 2 CH arom), 131.6 (s, 2 C_q arom), 132.0 (s, 4 C_q arom), 134.7 (s, CH arom), 140.6 (s, 4 C_q arom), 142.1 (dt, J_{RhC} = 25 Hz, J_{PC} = 15 Hz), 143.8 (s, C_q arom), 145.3 (s, 4 OC_q arom), 146.9 (s, 4 C_q arom), 160.4 (t, J_{PC} = 15 Hz, 2 OC_q arom), 163.0 (dt, J_{RhC} = 56 Hz, J_{PC} = 18 Hz, CN). Anal. Calcd for C₇₁H₉₂NO₆P₂Rh · 0.5CH₂Cl₂: C, 68.0; H, 7.4; N, 1.1. Found: C, 68.4; H, 7.4; N, 1.2.

Rh(PCP^a)(η²-C₂H₄) (8a). In a Fischer–Porter vessel compound **3a** (0.108 g, 0.08 mmol) and Se (0.010 g, 0.13 mmol) were added to THF (10 mL). The reactor was charged with 4 atm of C₂H₄ and heated at 40 °C. Reaction completion was observed after 4 days. Solvent was removed under reduced pressure and the remaining solid extracted with *n*-pentane (3 × 10 mL). Further filtration and concentration yielded **5a** as orange crystals (0.040 g, 45%). ¹H NMR (CD₂Cl₂, 400 MHz): δ 1.30 (s, 36H, 4 CMe₃), 1.39 (s, 36H, 4 CMe₃), 2.82 (br s, 4H, C₂H₄), 6.68 (d, ³J_{HH} = 8 Hz, 2H, 2 H arom), 7.01 (t, ³J_{HH} = 8 Hz, 1H, H arom), 7.28 (d, ⁴J_{HH} = 2.5 Hz, 4H, 4 H arom), 7.50 (d, ⁴J_{HH} = 2.5 Hz, 4H, 4 H arom). ³¹P{¹H} NMR (CD₂Cl₂, 162.1 MHz): δ 177.3 (d, J_{PRh} = 253 Hz). ¹³C{¹H} NMR (CDCl₃, 75.5 MHz): δ 31.5 (s, 4 CMe₃), 31.5 (s, 4 CMe₃), 34.7 (s, 4 CMe₃), 35.6 (s, 4 CMe₃), 58.8 (br s, C₂H₄), 105.7 (t, J_{PC} = 9 Hz, 2 CH arom), 124.8 (s, 4 CH arom), 125.2 (s, CH arom), 126.7 (s, 4 CH arom), 131.6 (s, 4 C_q arom), 139.9 (dt, J_{RhC} = 29 Hz, J_{PC} = 16 Hz, C_q arom), 140.1 (s, 4 C_q arom), 145.5 (br s, 4 OC_q arom), 147.4 (s, 4 C_q arom), 158.8 (t, J_{PC} = 16 Hz, 2 OC_q arom). Anal. Calcd for C₆₄H₈₇O₆P₂Rh: C, 68.8; H, 7.8. Found: C, 69.0; H, 8.2.

Rh(PCP^b)(η²-C₂H₄) (8b). In a Fischer–Porter vessel compound **5b** (0.100 g, 0.08 mmol) and Se (0.007 g, 0.09 mmol) were added to THF (5 mL). The reactor was charged with 4 atm of C₂H₄ and heated at 65 °C for 5 days. Solvent was removed under reduced pressure and the remaining solid purified by chromatography on a silica gel column (CH₂Cl₂:hexane, 1:10). Compound **8b** was obtained as a yellow solid (0.045 g, 56%). ¹H NMR (CD₂Cl₂, 400 MHz): δ 1.19 (s, 18H, 2 CMe₃), 1.37 (s, 18H, 2 CMe₃), 1.88 (s, 6H, 2 Ar-Me), 1.96 (s, 6H, 2 Ar-Me), 2.28 (d, J_{app} = 10 Hz, 2H, C₂H₄), 2.33 (s, 6H, 2 Ar-Me), 2.36 (s, 6H, 2 Ar-Me), 2.98 (d, J_{app} = 10 Hz, 2H, C₂H₄), 6.64 (d, ³J_{HH} = 8.0 Hz, 2H, 2 H arom), 6.97 (t, ³J_{HH} = 8.0 Hz, 1H, H arom), 7.18 (s, 2H, 2 H arom), 7.33 (s, 2H, 2 H arom). ³¹P{¹H} NMR (CD₂Cl₂, 162.1 MHz): δ 175.1 (d, J_{PRh} = 253 Hz). ¹³C{¹H} NMR (CD₂Cl₂, 75.5 MHz): δ 16.7 (s, 2 Ar-Me), 16.8 (s, 2 Ar-Me), 20.5 (s, 2 Ar-Me), 20.6 (s, 2 Ar-Me),

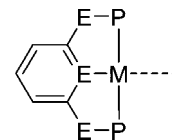
31.8 (s, 2 CMe₃), 32.0 (s, 2 CMe₃), 35.2 (s, 4 CMe₃), 58.6 (br d, J_{CP} = 4 Hz, C₂H₄), 105.9 (dd, J_{CRh} = 9 Hz, J_{CP} = 9 Hz, 2 CH arom), 125.5 (s, CH arom), 128.9 (s, 2 CH arom), 129.2 (s, 2 CH arom), 130.4 (s, 2 C_q), 130.7 (s, 2 C_q), 133.6 (s, 2 C_q), 133.6 (s, 2 C_q), 135.4 (s, 2 C_q), 135.8 (s, 2 C_q), 137.9 (s, 2 C_q), 138.0 (s, 2 C_q), 140.0 (dt, J_{CRh} = 29 Hz, J_{CP} = 16 Hz, C_q), 145.3 (dd, J_{CRh} = 5 Hz, J_{CP} = 5 Hz, 2 C_q), 145.6 (s, 2 C_q), 159.4 (dd, J_{CRh} = 16 Hz, J_{CP} = 16 Hz, 2 C_q). Anal. Calcd for C₅₆H₇₁O₆P₂Rh: C, 66.9; H, 7.1. Found: C, 66.5; H, 7.3.

Rh(PCP^a)(η²-C₂H₄) (8c). In a Fischer–Porter vessel compound **5c** (0.200 g, 0.14 mmol) and Se (0.014 g, 0.18 mmol) were added to THF (5 mL). The reactor was charged with 4 atm of C₂H₄ and heated at 50 °C for 3 days. Solvent was removed under reduced pressure and the remaining solid extracted with *n*-pentane (3 × 10 mL) and purified by chromatography on a silica gel column (hexane). Compound **8c** was obtained as a yellow solid (0.075 g, 46%). ¹H NMR (CD₂Cl₂, 500 MHz): δ 1.27 (s, 36H, 4 CMe₃), 1.35 (s, 18H, 2 CMe₃), 1.36 (s, 18H, 2 CMe₃), 2.80 (br s, 4H, C₂H₄), 7.08 (s, 1H, H arom), 7.21 (m, 1H, H arom), 7.28 (m, 5H, 5 H arom), 7.48 (s, 4H, 4 H arom), 7.65 (d, ³J_{HH} = 8.0 Hz, 1H, H arom), 7.83 (d, ³J_{HH} = 7.6 Hz, 1H, H arom). ³¹P{¹H} NMR (CD₂Cl₂, 202.4 MHz): δ 174.6 (dd, J_{PP} = 590 Hz, J_{PRh} = 253 Hz, P–O), 178.0 (dd, J_{PP} = 590 Hz, J_{PRh} = 252 Hz, P–O). ¹³C{¹H} NMR (CD₂Cl₂, 125.8 MHz): δ 31.5 (s, 2 CMe₃), 31.6 (s, 6 CMe₃), 35.0 (s, 4 CMe₃), 35.8 (s, 2 CMe₃), 35.9 (s, 2 CMe₃), 59.5 (br s, C₂H₄), 101.6 (d, J_{CP} = 13 Hz, CH arom), 118.8 (d, J_{CP} = 12 Hz, C_q), 122.3 (s, CH arom), 124.0 (s, CH arom), 125.0 (s, CH arom), 125.4 (s, 4 CH arom), 127.1 (s, 2 CH arom), 127.1 (s, 2 CH arom), 127.3 (s, CH arom), 131.9 (s, 2 C_q), 131.9 (s, 2 C_q), 133.7 (s, C_q), 139.5 (m, C_q), 140.5 (s, 2 C_q), 140.6 (s, 2 C_q), 145.9 (m, 4 C_q), 148.2 (s, 4 C_q), 153.6 (dd, J_{CP} = 23 Hz, J_{CRh} = 9 Hz, C_q), 157.6 (dd, J_{CP} = 23 Hz, J_{CRh} = 9 Hz, C_q). Anal. Calcd for C₆₈H₈₉O₆P₂Rh: C, 70.0; H, 7.7. Found: C, 69.7; H, 7.9.

Rh(PCP^a)(η²-MeC₂H₃) (9a). In a Fischer–Porter vessel compound **8a** (0.100 g, 0.09 mmol) was added to THF (5 mL). The reactor was charged with 1 atm of propene at room temperature and stirred for 5 days, with the propene atmosphere replaced every 24 h. Solvent was removed under reduced pressure, yielding compound **9a**, accompanied by a minor amount of **8a** (< 3%), as a yellow solid (0.100 g, quantitative). All attempts to further purify compound **9a** were unsuccessful. ¹H NMR (CD₂Cl₂, 300 MHz): δ 1.06 (d, ³J_{HH} = 5.4 Hz, 3H, MeCH=CH₂), 1.31 (s, 18H, 2 CMe₃), 1.38 (s, 18H, 2 CMe₃), 1.39 (s, 18H, 2 CMe₃), 1.41 (s, 18H, 2 CMe₃), 2.51 (br d, ³J_{HH} = 8.7 Hz, 1H, MeCH=CH₂), 3.29 (br d, ³J_{HH} = 12.3 Hz, 1H, MeCH=CH₂), 4.39 (br m, 1H, MeCH=CH₂), 6.66 (d, ³J_{HH} = 7.8 Hz, 2H, 2 H arom), 7.00 (t, ³J_{HH} = 8.1 Hz, 1H, H arom), 7.25 (d, ⁴J_{HH} = 2.4 Hz, 2H, 2 H arom), 7.32 (d, ⁴J_{HH} = 2.4 Hz, 2H, 2 H arom), 7.48 (d, ⁴J_{HH} = 2.1 Hz, 2H, 2 H arom), 7.55 (d, ⁴J_{HH} = 2.4 Hz, 2H, 2 H arom). ³¹P{¹H} NMR (CD₂Cl₂, 121.5 MHz): δ 171.6 (d, J_{PRh} = 259 Hz). ¹³C{¹H} NMR (CD₂Cl₂, 75.5 MHz): δ 19.5 (s, MeCH=CH₂), 31.5 (s, 2 CMe₃), 31.7 (s, 4 CMe₃), 32.0 (s, 2 CMe₃), 35.1 (s, 4 CMe₃), 35.9 (s, 4 CMe₃), 65.0 (s, MeCH=CH₂), 78.2 (s, MeCH=CH₂), 106.0 (dd, J_{CRh} = 9 Hz, J_{CP} = 9 Hz, 2 CH arom), 125.2 (s, 2 CH arom), 125.3 (s, 2 CH arom), 125.8 (s, CH arom), 126.9 (s, 2 CH arom), 127.2 (s, 2 CH arom), 131.7 (s, 2 C_q), 132.2 (s, 2 C_q), 139.3 (dt, J_{CRh} = 30 Hz, J_{CP} = 17 Hz, C_q), 140.6 (s, 4 C_q), 145.6 (s, 2 C_q), 146.1 (s, 2 C_q), 147.9 (s, 2 C_q), 148.3 (s, 2 C_q), 159.3 (dd, J_{CRh} = 15 Hz, J_{CP} = 15 Hz, 2 C_q).

Rh(PCP^b)(η²-MeC₂H₃) (9b). In a Fischer–Porter vessel compound **8b** (0.020 g, 0.02 mmol) was added to THF (3 mL), and the reactor was charged with 1 atm of propene and stirred for 9 days, with the propene atmosphere renewed every 24 h. Solvent was removed under reduced pressure. Compound **9b** was obtained as a yellow solid, contaminated with minor amounts of **8b** (< 5%) (0.020 g, quantitative). All attempts to further purify compound **9b** were unsuccessful. ¹H NMR (CD₂Cl₂, 500 MHz): δ 1.03 (d,

Chart 1



³J_{HH} = 4.0 Hz, 3H, MeCH=CH₂), 1.22 (s, 18H, 2 CMe₃), 1.35 (s, 18H, 2 CMe₃), 1.84 (s, 6H, 2 Ar-Me), 1.94 (s, 6H, 2 Ar-Me), 2.33 (s, 6H, 2 Ar-Me), 2.37 (s, 6H, 2 Ar-Me), 2.38 (br d, ³J_{HH} = 9.0 Hz, 1H, MeCH=CH₂), 3.83 (br d, ³J_{HH} = 13.5 Hz, 1H, MeCH=CH₂), 3.86 (br m, 1H, MeCH=CH₂), 6.58 (d, ³J_{HH} = 8.0 Hz, 2H, 2 H arom), 6.93 (t, ³J_{HH} = 8.0 Hz, 1H, H arom), 7.17 (s, 2H, 2 H arom), 7.29 (s, 2H, 2 H arom). ³¹P{¹H} NMR (CD₂Cl₂, 202.4 MHz): δ 169.5 (d, J_{PRh} = 258 Hz). ¹³C{¹H} NMR (CD₂Cl₂, 125.8 MHz): δ 16.6 (s, 2 Ar-Me), 16.6 (s, 2 Ar-Me), 18.9 (s, MeCH=CH₂), 20.4 (s, 2 Ar-Me), 20.6 (s, 2 Ar-Me), 31.7 (s, 2 CMe₃), 32.0 (s, 2 CMe₃), 35.1 (s, 2 CMe₃), 35.2 (s, 2 CMe₃), 64.5 (s, MeCH=CH₂), 76.9 (s, MeCH=CH₂), 105.8 (dd, J_{CRh} = 9 Hz, J_{CP} = 9 Hz, 2 CH arom), 125.2 (s, CH arom), 128.6 (s, 2 CH arom), 129.0 (s, 2 CH arom), 130.4 (s, 2 C_q), 130.9 (s, 2 C_q), 133.4 (s, 2 C_q), 133.5 (s, 2 C_q), 135.3 (s, 2 C_q), 135.7 (s, 2 C_q), 137.9 (s, 2 C_q), 138.3 (s, 2 C_q), 139.5 (m, C_q), 145.5 (dd, J_{CRh} = 5 Hz, J_{CP} = 5 Hz, 2 C_q), 145.6 (s, 2 C_q), 159.2 (dd, J_{CRh} = 16 Hz, J_{CP} = 16 Hz, 2 C_q).

QUEST3D Search Details. The QUEST3D searches commented in the text have been carried out on the Cambridge Structural Database (updated Nov 2007) and have the following details. (a) For the analysis of the P–M–P angles in square-planar transition-metal complexes containing a pincer ligand (see see Chart 1, E is any atom), the CSD search with restrictions (not disordered, no errors, R ≤ 0.075) gave a mean value of 164° (89 fragments, 71 hits). (b) For the analysis of the C–C distance of ethylene rhodium complexes, the CSD search without any restriction gave a mean value of 1.39 Å (146 fragments, 70 hits). A similar value (1.38 Å for 121 fragments, 57 hits) was obtained with restrictions (not disordered, no errors, R ≤ 0.075). In this case the Rh–C mean value is 2.13 Å.

Computational Details. The electronic structures and geometries of the model complexes **I–VII** were computed within the density functional theory at the B3LYP level.³³ The Rh atom was described with the Stuttgart Relativistic Small Core ECP basis set³⁴ and a polarization function. In all cases the atoms corresponding to the pincer ligand are described using a TZVP basis set. For the more complex models **IV–VII**, the biphenyl groups are described using a DZVP basis set. All the calculations were performed using the Gaussian03 package.³⁵ Figures were drawn using Molekel.³⁶ XYZ coordinates of all optimized complexes are available upon request.

(33) (a) Becke, A. D. *J. Chem. Phys.* **1993**, *98*, 5648. (b) Lee, C. T.; Yang, W. T.; Parr, R. G. *Phys. Rev. B* **1988**, *37*, 785.

(34) Dolg, M.; Stoll, H.; Preuss, H.; Pitzer, R. M. *J. Phys. Chem.* **1993**, *97*, 5852.

(35) Frisch, M. J.; Trucks, G. W.; Schlegel, H. B.; Scuseria, G. E.; Robb, M. A.; Cheeseman, J. R.; Montgomery, Jr., J. A.; Vreven, T.; Kudin, K. N.; Burant, J. C.; Millam, J. M.; Iyengar, S. S.; Tomasi, J.; Barone, V.; Mennucci, B.; Cossi, M.; Scalmani, G.; Rega, N.; Petersson, G. A.; Nakatsuji, H.; Hada, M.; Ehara, M.; Toyota, K.; Fukuda, R.; Hasegawa, J.; Ishida, M.; Nakajima, T.; Honda, Y.; Kitao, O.; Nakai, H.; Klene, M.; Li, X.; Knox, J. E.; Hratchian, H. P.; Cross, J. B.; Bakken, V.; Adamo, C.; Jaramillo, J.; Gomperts, R.; Stratmann, R. E.; Yazyev, O.; Austin, A. J.; Cammi, R.; Pomelli, C.; Ochterski, J. W.; Ayala, P. Y.; Morokuma, K.; Voth, G. A.; Salvador, P.; Dannenberg, J. J.; Zakrzewski, V. G.; Dapprich, S.; Daniels, A. D.; Strain, M. C.; Farkas, O.; Malick, D. K.; Rabuck, A. D.; Raghavachari, K.; Foresman, J. B.; Ortiz, J. V.; Cui, Q.; Baboul, A. G.; Clifford, S.; Cioslowski, J.; Stefanov, B. B.; Liu, G.; Liashenko, A.; Piskorz, P.; Komaromi, I.; Martin, R. L.; Fox, D. J.; Keith, T.; Al-Laham, M. A.; Peng, C. Y.; Nanayakkara, A.; Challacombe, M.; Gill, P. M. W.; Johnson, B.; Chen, W.; Wong, M. W.; Gonzalez, C.; Pople, J. A. *Gaussian 03, Revision C.02*; Gaussian, Inc., Wallingford, CT, 2004.

(36) Portmann, S.; Luthi, H. P. *Chimia* **2000**, *54*, 766.

X-ray Structure Determinations. Crystallographic data were collected on a Bruker-Nonius X8Apex-II CCD diffractometer at 100(2) K using graphite-monochromated Mo K α_1 radiation ($\lambda = 0.71073 \text{ \AA}$). The data were reduced (SAINT)³⁷ and corrected for Lorentz–polarization and absorption effects by a multiscan method (SADABS).³⁸ Structures were solved by direct methods (SIR-2002)³⁹ and refined against all F^2 data by full-matrix least-squares techniques (SHELXTL-6.12).⁴⁰ All the non-hydrogen atoms were refined with anisotropic displacement parameters. The hydrogen atoms were included from calculated positions and refined riding on their respective carbon atoms with isotropic displacement parameters. A summary of cell parameters and data collection, structure solution, and refinement details is given in Table 6.

Solid-State NMR. Single-pulse MAS NMR spectra were recorded on a Bruker DRX400 spectrometer with a magnetic field of 9.36 T and equipped with a multinuclear probe. Powdered samples were packed in 4 mm zirconia rotors and spun at 10 KHz. ³¹P MAS

NMR spectra were acquired at a frequency of 161.98 MHz, using a $\pi/4$ pulse width of $3.58 \mu\text{s}$ and a pulse space of 0.1 s. The ¹³C MAS NMR spectrum was recorded at 104.26 MHz with proton decoupling, a pulse width of $2.5 \mu\text{s}$ ($\pi/2$ pulse length $7.5 \mu\text{s}$), and a delay time of 2 s. The chemical shifts are reported in ppm from tetramethylsilane for ¹H and ¹³C and from 87% solutions of H₃PO₄ for ³¹P.

Acknowledgment. We gratefully acknowledge Dr. M. D. Alba (ICMSE) for acquiring solid-state NMR spectra. The Ministerio de Educación y Ciencia (CTQ2006-05527, FED-ER support, and CONSOLIDER-INGENIO, CSD2007-00006) and Junta de Andalucía are also thanked for financial support. M.R. thanks the Ministerio de Educación y Ciencia for a FPU fellowship and D.d.R. the 6th FP of the EU for a MC-OIF.

Supporting Information Available: Figures giving selected NMR spectra and graphics for olefin rotation barriers and CIF files giving crystallographic details. This material is available free of charge via the Internet at <http://pubs.acs.org>.

OM800830W

(37) SAINT 6.02; Bruker-AXS, Inc., Madison, WI 53711-5373, 1997–1999.

(38) Sheldrick, G. SADABS; Bruker AXS, Inc., Madison, WI, 1999.

(39) Burla, M. C.; Camalli, M.; Carrozzini, B.; Cascarano, G. L.; Giacovazzo, C.; Polidori, G.; Spagna, R. *J. Appl. Crystallogr.* **2003**, *36*, 1103.

(40) SHELXTL 6.14; Bruker AXS, Inc. Madison, WI, 2000–2003.

Water-Soluble Triisopropylphosphine Complexes of Ruthenium(II): Synthesis, Equilibria, and Acetonitrile Hydration

Marta Martín,[†] Henrietta Horváth,[†] Eduardo Sola,^{*†} Ágnes Kathó,[‡] and Ferenc Joó^{*‡}

Departamento de Química de Coordinación y Catálisis Homogénea, Instituto de Ciencia de Materiales de Aragón, Universidad de Zaragoza-CSIC, E-50009 Zaragoza, Spain, Research Group of Homogeneous Catalysis, Hungarian Academy of Sciences, Debrecen, Hungary, and Institute of Physical Chemistry, University of Debrecen, H-4010 Debrecen, Hungary

Received September 3, 2008

The complex $[\text{RuCl}(\text{NCMe})_4(\text{PiPr}_3)]\text{BF}_4$ (**1**) and its water-soluble dicationic products of chloride replacement by PiPr_3 (**2**), $\text{P}(\text{OMe})_3$ (**3**), Hpz (**4**), MeOH (**5**), and H_2O (**6**) have been prepared and characterized. The chloride dissociation constant of **1** in water ($K_d = 2.0 \text{ M}$) and the $\text{p}K_a$ (10.5) for the deprotonation of the water ligand of **6** have been determined by NMR methods. The conjugate base of **6**, $[\text{Ru}(\text{OH})(\text{NCMe})_4(\text{PiPr}_3)]^+$ (**7**), has been observed to isomerize into an amidate complex in route to acetonitrile hydration. Consistently, **6** has been found to catalyze the selective hydration of acetonitrile to acetamide in aqueous solution at pH 10.5 and 353 K, with initial TOF about 50 h^{-1} .

Introduction

Water-soluble and aquo organometallics attract attention in the context of catalysis mainly because of the technological advantages that could result from their operation in aqueous–organic biphasic media,^{1,2} but also due to remaining challenges concerning the selectivity of certain catalytic hydrations.^{3,4} Most compounds investigated within this context are versions of catalysts that have already been successful in organic solvents, turned water-soluble through the use of ligands with solubilizing groups, such as water-soluble phosphines.⁵ However, less attention is paid to the catalytic properties of other complexes that are water-soluble as a consequence of their ionic nature or due to the ions generated in aqueous media after dissociation of charged ligands, generally halides.⁶ Nevertheless, such charged metal complexes are ubiquitous, and the aquation processes that could dissolve them in water can become very favorable due to the strong solvent coordination and the high

solvation energies of the resulting ions.⁷ Furthermore, such phenomena may generate in aqueous solution compounds with reactivities and catalytic properties very different from those of the precursor complexes in organic solvents⁸ and possibly also more suitable for green catalytic technologies.⁹ This type of chemistry is described in the following for the new cationic complex $[\text{RuCl}(\text{NCMe})_4(\text{PiPr}_3)]\text{BF}_4$ (**1**), a precursor of a variety of water-soluble complexes that do not contain any solubilizing phosphine but contain the hydrophobic PiPr_3 .

Results and Discussion

The complex $[\text{RuCl}(\text{NCMe})_4(\text{PiPr}_3)]\text{BF}_4$ (**1**) has been prepared in a one-pot process starting from the conventional ruthenium precursor $[\text{RuCl}_2(\text{cod})]_n$ ($\text{cod} = 1,5\text{-cyclooctadiene}$), by reaction with 1 equiv of the phosphonium salt $[\text{HPiPr}_3]\text{BF}_4$ in refluxing acetonitrile under a dihydrogen atmosphere (eq 1).¹⁰ The compound has been isolated as a pale yellow solid in 65% yield. A compound with a related cation, $[\text{RuCl}(\text{NCMe})_4(\text{PPh}_3)]\text{BF}_4$, has been reported to result from the reaction of the polymeric compound $[\text{Ru}_2\text{Cl}(\text{O}_2\text{CC}_6\text{H}_4\text{-}p\text{-OMe})_4]_n$ with PPh_3 and acetonitrile, although it is formed in very poor yield.¹¹

Figure 1 displays the structure of the cation of **1** determined by X-ray diffraction. The symmetry of the structure is compatible with the simple $^{13}\text{C}\{^1\text{H}\}$ and ^1H NMR spectra obtained from the solutions of **1** in CDCl_3 . The Ru–N distances corresponding to the four equatorial acetonitriles are similar to those in other Ru(II) complexes with mutually trans acetonitrile

* Corresponding author. E-mail: sola@unizar.es.

[†] Instituto de Ciencia de Materiales de Aragón.

[‡] Hungarian Academy of Sciences and Institute of Physical Chemistry.

(1) (a) Cornils, B.; Herrmann, W. A.; Horváth, I. T.; Leitner, W.; Mecking, S.; Olivier-Bourbigou, H.; Vogt, D., Eds. *Multiphase Homogeneous Catalysis*; Wiley-VCH: Weinheim, 2005. (b) Adams, D. J.; Dyson, P. J.; Tavener, S. T. *Chemistry in Alternative Reaction Media*; Wiley: Chichester, 2004. (c) Behr, A. *Angewandte homogene Katalyse*; Wiley-VCH: Weinheim, 2008.

(2) (a) Joó, F. *Aqueous Organometallic Catalysis*; Kluwer: Dordrecht, 2001. (b) Cornils, B.; Herrmann, W. A., Eds. *Aqueous-Phase Organometallic Catalysis*, 2nd ed.; Wiley-VCH: Weinheim, 2004.

(3) (a) Borman, S. *Chem. Eng. News* **2004**, 82, 42–43. (b) Grotjahn, D. B. *Chem.–Eur. J.* **2005**, 11, 7146–7153. (c) Richard, C. J.; Parkins, A. W. *New J. Chem.* **2008**, 32, 151–158.

(4) Kukushkin, V. Y.; Pombeyro, A. J. L. *Inorg. Chim. Acta* **2005**, 358, 1–21.

(5) (a) Phillips, A. D.; Gonsalvi, L.; Romerosa, A.; Vizza, F.; Peruzzini, M. *Coord. Chem. Rev.* **2004**, 248, 955–993. (b) Horváth, I. T.; Lantos, D. In *Comprehensive Organometallic Chemistry*, 3rd ed.; Mingos, D. M. P., Crabtree, R. H., Eds.; Elsevier, 2007; Vol. 1, pp 823–845.

(6) Representative examples and leading references: (a) Wu, X.; Li, X.; Zanotti-Gerosa, A.; Pettman, A.; Liu, J.; Mills, A. J.; Xiao, J. *Chem.–Eur. J.* **2008**, 14, 2209–2222. (b) Li, C.-J. *Chem. Rev.* **2005**, 105, 3095–3165. (c) Breno, K. L.; Pluth, M. D.; Landorf, C. W.; Tyler, D. R. *Organometallics* **2004**, 23, 1738–1746. (d) Russell, M. J. H.; Murrer, B. A. *US Patent 4,517,390*, 1985.

(7) Helm, L.; Merbach, A. E. *Chem. Rev.* **2005**, 105, 1923–1959.

(8) For examples, see: (a) Ohnishi, Y.; Nakao, Y.; Sato, H.; Sakaki, S. *Organometallics* **2006**, 25, 3352–3363. (b) Kovács, G.; Ujaque, G.; Lledós, A.; Joó, F. *Eur. J. Inorg. Chem.* **2007**, 287, 9–2889. (c) Joubert, J.; Delbecq, F. *Organometallics* **2006**, 25, 854–861. (d) Papp, G.; Horváth, H.; Kathó, Á.; Joó, F. *Helv. Chim. Acta* **2005**, 88, 566–573.

(9) Sheldon, R. A.; Arends, I.; Hanefeld, U. *Green Chemistry and Catalysis*; Wiley-VCH: Weinheim, 2007.

(10) The same synthetic procedure has allowed us to prepare closely related iridium complexes: Sola, E.; Navarro, J.; López, J. A.; Lahoz, F. J.; Oro, L. A.; Werner, H. *Organometallics* **1999**, 18, 3534–3546.

(11) Das, B. K.; Chakravarty, A. R. *Inorg. Chem.* **1992**, 31, 1395–1400.

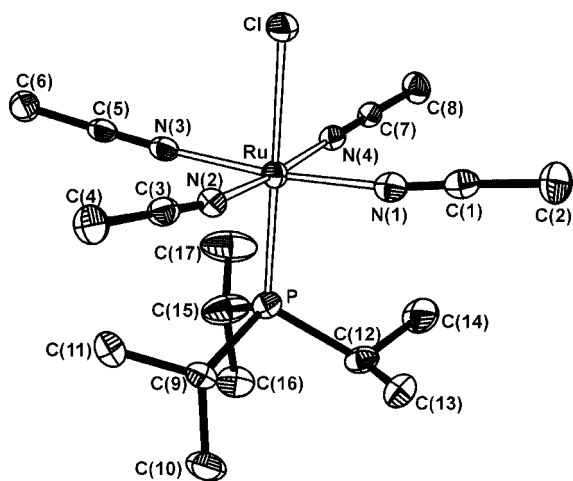
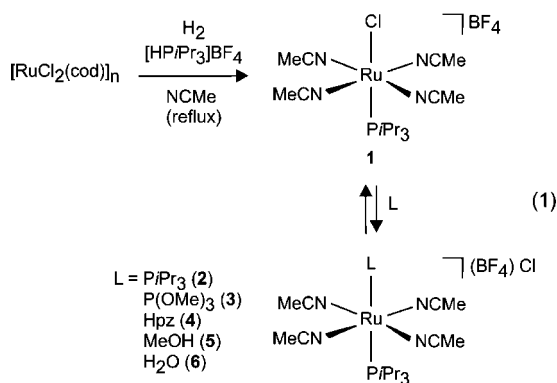


Figure 1. Molecular structure of the cation of **1**. Selected bond distances (Å) and angles (deg): Ru–Cl 2.4713(8), Ru–P 2.3253(8), Ru–N(1) 2.011(2), Ru–N(2) 2.019(2), Ru–N(3) 2.025(2), Ru–N(4) 2.026(2); P–Ru–Cl 179.67(3), N(1)–Ru–N(3) 173.11(9), P–Ru–N(1) 94.84(7).



triles¹² and clearly shorter than those typical in ruthenium compounds with labile acetonitrile ligands (2.1 Å or longer).¹³ In agreement with this, the substitution of these acetonitriles has not been observed even in the presence of an excess of good ligands such as phosphines.

On the contrary, substitution of the chloride ligand of **1** to form dicationic complexes has been found to be an easy process (eq 1). The quantitative chloride replacement by triisopropylphosphine (**2**), trimethylphosphite (**3**), or pyrazol (**4**) requires just 1 equiv of these reactants, whereas weaker ligands such as methanol (**5**) or water (**6**) must be present in large excess. In fact, in the case of methanol, quantitative formation of the substitution product requires the removal of chloride with a silver salt since, even in methanol-*d*₄ solution, the equilibrium still contains 50% of compound **1**. Due to this, the methanol complex **5** has been isolated only as the bis-tetrafluoroborate salt, [Ru(MeOH)(NCMe)₄(PiPr₃)](BF₄)₂, denoted as **5-BF₄**.

In the case of water as solvent, the aquation of the chloride ligand to form [Ru(H₂O)(NCMe)₄(PiPr₃)]²⁺ (**6**) is essentially

(12) For example: (a) Ryabov, A. D.; Le Lagadec, R.; Estevez, H.; Toscano, R. A.; Hernandez, S.; Alexandrova, L.; Kurova, V. S.; Fischer, A.; Sirlin, C.; Pfeffer, M. *Inorg. Chem.* **2005**, *44*, 1626–1634. (b) Widegren, J. A.; Weiner, H.; Miller, S. M.; Finke, R. G. *J. Organomet. Chem.* **2000**, *610*, 112–117. (c) Appelbaum, L.; Heinrichs, C.; Demtschuk, J.; Michman, M.; Oron, M.; Schäfer, H. J.; Schumann, H. *J. Organomet. Chem.* **1999**, *592*, 240–250. (d) Katayama, H.; Ozawa, F. *Organometallics* **1998**, *17*, 5190–5196.

(13) Allen, F. H. The Cambridge Structural Database: a quarter of a million crystal structures and rising. *Acta Crystallogr.* **2002**, *B58*, 380–388.

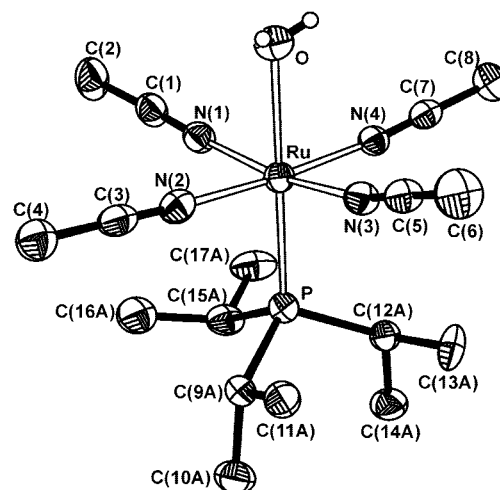
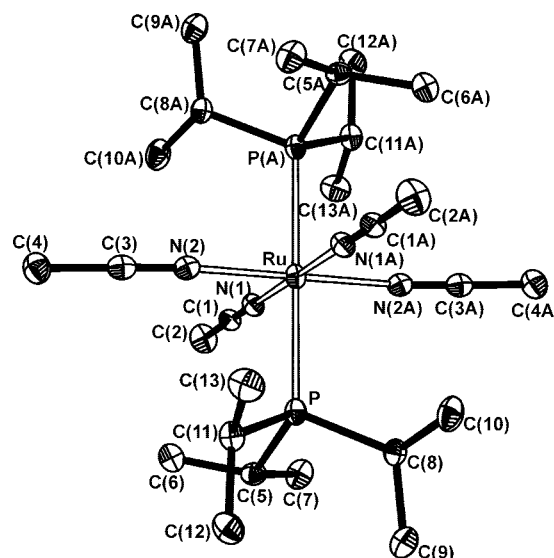


Figure 2. Molecular structures of the cations of **2-BF₄** (above) and **6-BF₄** (below). Selected bond distances (Å) and angles (deg): **2-BF₄**: “A-labeled” atoms are generated by the $-x + 1, -y, -z + 1$ symmetry transformation; Ru–P 2.4440(9), Ru–N(1) 2.019(3), Ru–N(2) 2.013(3); P–Ru–P(A) 180.00(3), P–Ru–N(1) 90.79(8), N(1)–Ru–N(2) 87.74(11). **6-BF₄**: Ru–O 2.217(3), Ru–P 2.3028(11), Ru–N(1) 2.003(3), Ru–N(2) 2.012(4), Ru–N(3) 2.017(3), Ru–N(4) 2.013(3); P–Ru–O 178.76(11), N(1)–Ru–N(3) 167.96(13), O–Ru–N(1) 83.64(13).

complete (by NMR). The equilibrium constant for chloride ligand dissociation ($K_d = [6][Cl^-]/[1]$) has been evaluated in aqueous solutions with excess chloride (ca. 25 equiv). Around room temperature, the exchange between **1** and **6** is slow on the NMR time scale, so that the ³¹P NMR resonance corresponding to each complex can be integrated separately. The value obtained for K_d at 298 K, 2.0 M, is 20 times higher than that found for the related cationic complex [RuHCl(CO)(*m*tppps)₃]₂BF₄ under the same conditions (9.8×10^{-2} M at 298 K, *m*tppps = *m*-diphenylphosphinobenzenesulfonic acid, Na salt).^{8d}

Figure 2 shows the structures of the PiPr₃ derivative **2** and the aquo-complex **6**. In both cases, the diffraction experiment has been carried out on bis-tetrafluoroborate salts, which seem to crystallize easier and better. The equatorial plane of both octahedra is very similar and almost equal to that of the precursor complex (Figure 1). The only noticeable difference among the three structures is in the Ru–P distance, which, as expected, increases by increasing the σ -donor capability of the

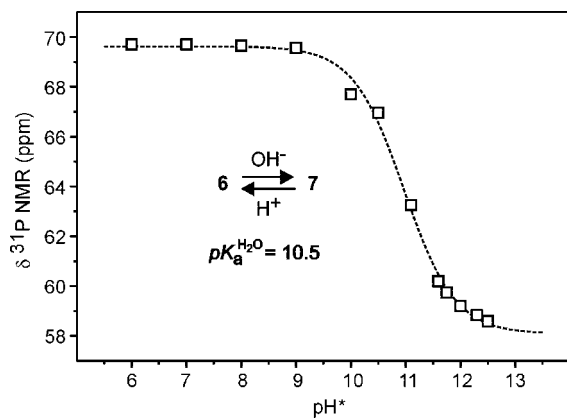
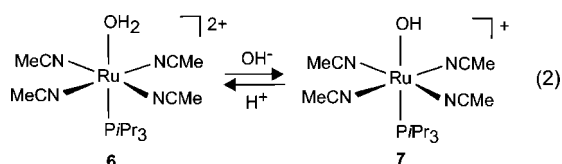


Figure 3. ^{31}P NMR spectroscopic titration of the equilibrium between **6** and **7**: $[\mathbf{6}\text{-BF}_4]_0 = 0.03\text{ M}$, $T = 298\text{ K}$. pH^* is the pH meter reading in D_2O .

trans ligand,¹⁴ irrespective of the cation charge. A complex closely related to **6**, with the NHC ligand IMes instead of PiPr_3 , has been reported to result from degradation of a second-generation Grubbs catalyst, in acetonitrile/water as solvent.¹⁵ In this latter compound, the $\text{Ru}\text{-OH}_2$ distance is slightly shorter than in **6**: 2.199(4) vs 2.217(3) Å.

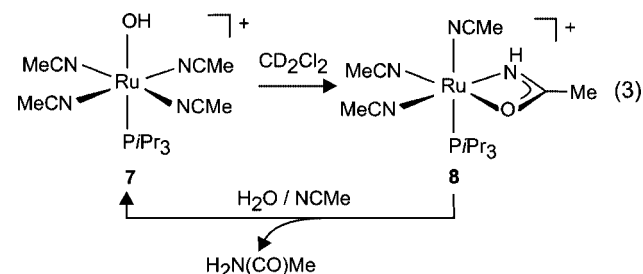
In aqueous solution, the aquo complex **6** behaves as an acid, in equilibrium with the conjugate base $[\text{Ru}(\text{OH})(\text{NCMe})_4(\text{PiPr}_3)]^+$ (**7**) (eq 2). This new species has been isolated as a tetrafluoroborate salt after treatment of **6** with 1 equiv of aqueous KOH in dichloromethane. The IR spectrum of **7** in KBr displays a characteristic $\nu(\text{O}\text{-H})$ stretching mode at 3365 cm^{-1} , while the ^1H NMR resonance attributable to the OH proton appears in CD_2Cl_2 at $\delta -1.11$, as a doublet with a J_{HP} coupling constant of 1.5 Hz. As in all previous compounds, the NMR spectra also indicate four equivalent acetonitrile ligands, confirming that **7** retains the structure of its dicationic precursor **6**.



Consistently with the latter conclusion, the equilibrium between **6** and **7** is fast on the NMR time scale at room temperature, giving rise to exchange-averaged NMR resonances that shift as the equilibrium position changes. The chemical shift of the ^{31}P NMR resonance in D_2O , which changes about 11 ppm on going from **6** to **7**, has been used to evaluate the equilibrium position at different pH and determine the acid dissociation constant of **6**. As can be seen in Figure 3, the cation $[\text{Ru}(\text{H}_2\text{O})(\text{NCMe})_4(\text{PiPr}_3)]^{2+}$ (**6**) is a weak acid showing appreciable deprotonation only above pH 9. Analysis of the δ versus pH data results in a value for the $\text{p}K_{\text{a}}^{\text{H}_2\text{O}}$ of 10.5 at 298 K. The value is significantly higher than those common for related aquo Ru(II) dicationic species, for which a high $\text{p}K_{\text{a}}$ constitutes an advantage.¹⁶ Some orientative examples are the cations

$[\text{Ru}(\text{CO})_3(\text{H}_2\text{O})_3]^{2+}$ ($\text{p}K_{\text{a}} = -0.14$ at 262 K),¹⁷ $[\text{Ru}(\text{tpa})(\text{H}_2\text{O})_2]^{2+}$ ($\text{p}K_{\text{a}} = 2.1$, tpa = tris(2-pyridylmethyl)amine),¹⁸ and $[\text{Ru}(\eta^6\text{-benzene})(\text{en})(\text{H}_2\text{O})]^{2+}$ ($\text{p}K_{\text{a}} = 7.7$).¹⁶ Since the acidity of coordinated water depends on the metal ion and the other ligands in the coordination sphere, the unusually high $\text{p}K_{\text{a}}$ value of species **6** should be attributed to the high basicity of the alkyl phosphine, an unusual ligand in aqueous chemistry.

The hydroxo complex **7** is stable in basic aqueous solution at room temperature, but it has been observed to slowly evolve in dichloromethane as solvent. The initial product of this evolution, an isomeric amidate complex $[\text{Ru}\{\text{NH}(\text{CO})\text{Me}\}(\text{NCMe})_3(\text{PiPr}_3)]\text{BF}_4$ (**8**), could be characterized by NMR spectroscopy in CD_2Cl_2 . The ^1H spectrum of the compound shows the signals expected for an acetamido ligand—a NH broad signal at $\delta 4.24$ and singlet at $\delta 1.97$ for the methyl group—while the $^{13}\text{C}\{^1\text{H}\}$ spectrum shows a singlet at a chemical shift characteristic of a carbonyl function, $\delta 182.93$. The spectra, however, are less explicit for the rest of the structure of **8**, which should be considered with caution. At room temperature, the NMR signals suggest a *C_s* structure in which the symmetry plane contains the phosphorus atom and relates two acetonitrile ligands. The remaining acetonitrile produces broad signals in both the $^{13}\text{C}\{^1\text{H}\}$ and ^1H NMR spectra. Upon cooling of the sample to 233 K, these latter signals progressively narrow to eventually allow for the observation of a $^{13}\text{C}\{^1\text{H}\}$ doublet at $\delta 119.39$ with a J_{CP} coupling constant of 15.1 Hz, attributable to an acetonitrile quaternary carbon trans to phosphorus. In turn, the signals corresponding to the other acetonitriles progressively broaden, suggesting that they could decoalesce at lower temperature. Nevertheless, a general broadening of the spectra below 230 K, probably related to the slow motion of the phosphine substituents, hid this proposed decoalescence. In light of the spectroscopic information available, the most likely structure for **8** is that of eq 3, in which dissociation of the acetonitrile trans to phosphine seems to trigger the facile fluxional rearrangement of the resulting five-coordinate moiety at room temperature.



Amidate complexes such as **8** have been often postulated as intermediates in nitrile hydrations,^{4,19} although only in a few instances have such intermediates been detected and character-

(17) Meier, U. C.; Scopelliti, R.; Solari, E.; Merbach, A. E. *Inorg. Chem.* **2000**, *39*, 3816–3822.

(18) Hirai, Y.; Kojima, T.; Mizutani, Y.; Shiota, Y.; Yoshizawa, K.; Fukuzumi, S. *Angew. Chem., Int. Ed.* **2008**, *47*, 5772–5776.

(19) (a) Ahmad, T. J.; Zakharov, L. N.; Tyler, D. R. *Organometallics* **2007**, *26*, 5179–5187. (b) Crestani, M. G.; Arévalo, A.; García, J. J. *Adv. Synth. Catal.* **2006**, *348*, 732–742. (c) Breno, K. L.; Pluth, M. D.; Tyler, D. R. *Organometallics* **2003**, *22*, 1203–1211.

(14) Coe, B. J.; Glenwright, S. J. *Coord. Chem. Rev.* **2000**, *203*, 5–80.

(15) Kim, M.; Eum, M.-S.; Jin, M. Y.; Jun, K.-W.; Lee, C. W.; Kuen, K. A.; Kim, C. H.; Chin, C. S. *J. Organomet. Chem.* **2004**, *689*, 3535–3540.

(16) Wang, F.; Chen, H.; Parsons, S.; Oswald, I. D. H.; Davidson, J. E.; Sadler, P. J. *Chem.—Eur. J.* **2003**, *9*, 5810–5820.

ized.²⁰ Among the various different mechanistic proposals to explain their formation, the intramolecular nucleophilic attack of hydroxide onto a cis nitrile ligand seems the alternative that better fits the characteristics of the reaction leading to **8**. Also, it is conceivable that such nucleophilic attack could be relatively disfavored in aqueous solution due to the stabilization of the coordinated OH⁻ by hydrogen bonding to surrounding water.²¹

Although **8** could not be isolated due to its limited stability, it could be reacted in the NMR tube with ca. 1 equiv of a mixture acetonitrile/water, to regenerate **7** and produce acetamide (NMR and GC-MS). In agreement with the cycle of stoichiometric reactions of eq 3, the aquo complex **6-BF₄** has been found to catalyze the selective hydration of acetonitrile to acetamide in aqueous solutions at basic pH. Working at pH 10.5 and 353 K, and using a NCMe/H₂O/Ru ratio 10 000/10 000/1, the initial turnover frequencies (TOF) reach values of about 50 h⁻¹, an activity that compares well to that reported for other transition metal catalysts.^{4,19c,22} No direct (uncatalyzed) hydration of acetonitrile has been observed under these working conditions, and hydrolysis products other than acetamide have not been detected by GC. The only species detectable by ³¹P{¹H} NMR in concentrated samples mimicking the catalytic solutions (acetonitrile-*d*₃:D₂O 1:1 at 353 K) are those of the equilibrium in eq 2, either in the active reactions at basic pH, where **7** is the major species, or in inactive acid samples, where the equilibrium is totally shifted to **6**.

In summary, we have prepared and characterized the complex [RuCl(NCMe)₄(PiPr₃)₂](BF₄), which due to its labile chloride ligand constitutes a convenient precursor for the synthesis of water-soluble complexes containing the PiPr₃ ligand. The high basicity of this phosphine, very unusual in aqueous chemistry, seems to favor chloride ligand dissociation (*K*_d = 2.0 M) and diminish the acidity of the aquation product [Ru(H₂O)(NCMe)₄(PiPr₃)₂]²⁺ (*pK*_a = 10.5), thus conferring relatively unusual properties to these compounds. The conjugate base of this aquation product, [Ru(OH)(NCMe)₄(PiPr₃)₂]⁺, can extensively form only at basic pH, but seems to play a key role in the catalytic hydration of acetonitrile to acetamide, through its isomerization into an amidate complex.

Experimental Section

Equipment. C, H, N analyses were carried out in a Perkin-Elmer 2400 CHNS/O analyzer. MS data were recorded on a VG Autospec double-focusing mass spectrometer operating in the positive mode; ions were produced with the Cs⁺ gun at ca. 30 kV, and 3-nitrobenzyl alcohol (NBA) was used as the matrix. Infrared spectra were recorded in KBr using a FT-IR Perkin-Elmer Spectrum One spectrometer. NMR spectra were recorded on Bruker Avance 400 or 300 MHz spectrometers. ¹H (400.13 or 300.13 MHz) and ¹³C (100.6 or 75.5 MHz) NMR chemical shifts were measured relative to partially deuterated solvent peaks, but are reported in ppm relative

to tetramethylsilane. ³¹P (162.0 or 121.5 MHz) chemical shifts were measured relative to H₃PO₄ (85%). Coupling constants, *J*, are given in hertz. Generally, spectral assignments were achieved by ¹H COSY, ¹³C DEPT, and ¹H/¹³C-HSQC experiments. X-ray data were collected at 100.0(2) K on a Bruker SMART APEX CCD diffractometer with graphite-monochromated Mo K α radiation (λ = 0.71073 Å) using ω scans (0.3°). Data were collected over the complete sphere by a combination of four sets and corrected for absorption using a multiscan method applied with the SADABS program.²³ The structures were solved by the Patterson method. Refinement by full-matrix least-squares on *F*² using SHELXL97²⁴ was similar for all complexes including isotropic and subsequently anisotropic displacement parameters for all non-hydrogen non-disordered atoms.

Synthesis. All manipulations were carried out under argon by standard Schlenk techniques. Solvents were purified by known methods and distilled under argon before use. Complex [RuCl₂(cod)]_{*n*} was prepared as previously reported.²⁵

Synthesis of [RuCl(NCMe)₄(PiPr₃)₂](BF₄) (1**).** [HPiPr₃](BF₄) (884.6 mg, 3.57 mmol) was added to a suspension of [RuCl₂(cod)]_{*n*} (1.00 g, 3.57 mmol for *n* = 1) in 40 mL of acetonitrile, and the mixture was refluxed under dihydrogen (*P* = 1 bar) for 40 h. The resulting yellow solution was filtered through Celite, concentrated under vacuum to ca. 0.5 mL, cooled in ice, and treated with diethyl ether to give a pale yellow solid. The solid was separated by decantation, washed with diethyl ether, and dried in vacuo: yield 1.27 g (65%). Anal. Calcd for C₁₇H₃₃BClF₄N₄PRu: C, 37.28; H, 6.07; N, 10.23. Found: C, 36.79; H, 6.29; N, 10.01. MS (FAB⁺, *m/z* (%)): 461 (50) [M⁺], 420 (38) [M⁺ - NCMe], 379 (100) [M⁺ - 2NCMe]. IR (KBr, cm⁻¹): 2285 ν (N≡C), 1060 ν (BF₄). ¹H NMR (CDCl₃, 293 K): δ 1.22 (dd, *J*_{HP} = 13.2, *J*_{HH} = 6.9, 18H, PCHCH₃), 2.41 (m, 3H, PCHCH₃), 2.43 (s, 12H, NCCH₃). ³¹P{¹H} NMR (CDCl₃, 293 K): δ 59.77 (s). ¹³C{¹H} NMR (CDCl₃, 293 K): δ 4.57 (s, NCCH₃), 19.19 (s, PCHCH₃), 25.33 (d, *J*_{CP} = 22.4, PCHCH₃), 125.20 (s, NCCH₃). Crystals suitable for the X-ray diffraction study were obtained by slow diffusion of diethyl ether into a dichloromethane solution of the complex at 253 K.

Synthesis of [Ru(NCMe)₄(PiPr₃)₂](BF₄)(Cl) (2**).** A solution of **1** (90.5 mg, 0.17 mmol) in dichloromethane (5 mL) was treated with tris(isopropyl)phosphine (52 μ L, 0.28 mmol) and allowed to react at room temperature for 4 h. The resulting solution was evaporated to dryness, and the residue was cooled to 213 K and washed with diethyl ether to afford a pale yellow solid, which was separated by decantation and dried in vacuo: yield 69.7 mg (60%). Anal. Calcd for C₂₆H₅₄BClF₄N₄P₂Ru: C, 44.11; H, 7.69; N, 7.91. Found: C, 44.31; H, 7.52; N, 7.70. MS (FAB⁺, *m/z* (%)): 586 (35) [M⁺], 545 (50) [M⁺ - NCMe], 504 (100) [M⁺ - 2NCMe]. IR (KBr, cm⁻¹): 2286 ν (N≡C), 1036 ν (BF₄). ¹H NMR (CD₂Cl₂, 293 K): δ 1.39 (dvt, *N* = 13.5, *J*_{HH} = 6.6, 18H, PCHCH₃), 2.54 (s, 12H, NCCH₃), 2.56 (m, 3H, PCHCH₃). ³¹P{¹H} NMR (CD₂Cl₂, 293 K): δ 27.09 (s). ¹³C{¹H} NMR (CD₂Cl₂, 293 K): δ 4.87 (s, NCCH₃), 19.42 (s, PCHCH₃), 24.13 (vt, *N* = 18.9, PCHCH₃), 130.99 (s, NCCH₃).

Synthesis of [Ru(NCMe)₄(PiPr₃)₂](BF₄)₂ (2-BF₄**).** A solution of **6-BF₄** (vide infra, 95.0 mg, 0.15 mmol) in 20 mL of dichloromethane was treated with tris(isopropyl)phosphine (47 μ L, 0.25 mmol), and the resulting mixture was stirred under argon for 30 min. The mixture was evaporated to dryness, and the product was washed with 5 \times 3 mL of diethyl ether to afford a white solid: yield 85.4 mg (75%). Anal. Calcd for C₂₆H₅₄B₂F₈N₄P₂Ru: C, 41.12; H, 7.17; N, 7.38. Found: C, 41.32; H, 7.00; N, 7.17. Crystals for

(20) (a) Leung, Ch. W.; Zheng, W.; Wang, D.; Ng, S. M.; Yeung, Ch. H.; Zhou, Z.; Lin, Z.; Lau, Ch. P. *Organometallics* **2007**, *26*, 1924–1933. (b) Hetterscheid, D. G. H.; Kaiser, J.; Reijerse, E.; Peters, T. P. J.; Thewissen, S.; Block, A. N. J.; Smits, J. M. M.; de Gelder, R.; Bruin, B. *J. Am. Chem. Soc.* **2005**, *127*, 1895–1905. (c) Yi, Ch. S.; He, Z.; Guzei, I. A. *Organometallics* **2001**, *20*, 3641–3643. (d) Tellers, D. M.; Ritter, J. C. M.; Bergman, R. G. *Inorg. Chem.* **1999**, *38*, 4810–4818. (e) Kim, J. H.; Britten, J.; Chin, J. *J. Am. Chem. Soc.* **1993**, *115*, 3618–3622.

(21) (a) Roesky, H. W.; Singh, S.; Yussuf, K. K. M.; Maguire, J. A.; Hosmane, R. S. *Chem. Rev.* **2006**, *106*, 3813–3843. (b) Burn, M. J.; Fickes, M. G.; Hartwig, J. F.; Hollander, F. J.; Bergman, R. G. *J. Am. Chem. Soc.* **1993**, *115*, 5875–5876. (c) Zinn, P. J.; Sorrell, T. N.; Powell, D. R.; Day, V. W.; Borovik, A. S. *Inorg. Chem.* **2007**, *46*, 10120–10132.

(22) Cadierno, V.; Francos, J.; Gimeno, J. *Chem.—Eur. J.* **2008**, *14*, 6601–6605.

(23) Blessing, R. H. *Acta Crystallogr.* **1995**, *A51*, 33–38. SADABS: Area-detector absorption correction; Bruker-AXS, Madison, WI, 1996.

(24) SHELXTL Package v. 6.10; Bruker-AXS: Madison, WI, 2000. Sheldrick, G. M. SHELXS-86 and SHELXL-97; University of Göttingen: Göttingen, Germany, 1997.

(25) Albers, M. O.; Ashworths, T.; Oosthuizen, H. E.; Singleton, E. *Inorg. Synth.* **1989**, *26*, 69.

Table 1. Summary of Crystallographic Data for **1**, **2-BF₄**, and **6-BF₄**

	1	2-BF₄	6-BF₄
formula	C ₁₇ H ₃₃ BClF ₄ N ₄ PRu	C ₂₆ H ₅₄ B ₂ F ₈ N ₄ P ₂ Ru · 2CHCl ₃	C ₁₇ H ₃₅ B ₂ F ₈ N ₄ OPRu
description, color	irregular block, colorless	irregular block, colorless	prism, colorless
<i>M</i>	547.77	997.74	617.15
cryst size [mm ³]	0.24 × 0.16 × 0.12	0.16 × 0.08 × 0.06	0.14 × 0.10 × 0.08
cryst syst	monoclinic	monoclinic	monoclinic
space group	<i>P</i> 2(1)/ <i>c</i> (No. 14)	<i>P</i> 2(1)/ <i>n</i> (No. 14)	<i>P</i> 2(1)/ <i>n</i> (No. 14)
<i>a</i> [Å]	14.1734 (11)	10.9787 (9)	9.7534 (5)
<i>b</i> [Å]	11.8002 (9)	17.9817 (14)	15.2583 (8)
<i>c</i> [Å]	16.4097 (13)	11.5691 (9)	18.3284 (10)
β [deg]	113.9240 (10)	106.9210 (10)	95.9070 (10)
<i>V</i> [Å ³]	2508.7 (3)	2185.0 (3)	2713.2 (2)
<i>Z</i>	4	2	4
ρ _{calcd} [g cm ⁻³]	1.450	1.517	1.511
μ [mm ⁻¹]	0.835	0.859	0.708
2θ range [deg]	3.1 ≤ 2θ ≤ 57.8	4.3 ≤ 2θ ≤ 57.5	3.5 ≤ 2θ ≤ 57.8
index ranges	-19 ≤ <i>h</i> ≤ 18 -15 ≤ <i>k</i> ≤ 15 -21 ≤ <i>l</i> ≤ 22	-14 ≤ <i>h</i> ≤ 14 -23 ≤ <i>k</i> ≤ 23 -15 ≤ <i>l</i> ≤ 15	-13 ≤ <i>h</i> ≤ 13 -20 ≤ <i>k</i> ≤ 20 -23 ≤ <i>l</i> ≤ 24
reflins collected	28 249	20 201	31 427
indep reflins	6185 [<i>R</i> _{int} = 0.0661]	5285 [<i>R</i> _{int} = 0.0730]	6699 [<i>R</i> _{int} = 0.0739]
obsd data [<i>I</i> ≥ 2σ(<i>I</i>)]	3858	3521	4076
refinement method		full matrix least-squares on <i>F</i> ²	
absorption corr		multiscan (SADABS)	
data/restraints/params	6185/0/272	5285/0/240	6699/152/453
final <i>R</i> indices [<i>R</i>]	<i>R</i> ₁ = 0.035, <i>wR</i> ₂ = 0.056	<i>R</i> ₁ = 0.0474, <i>wR</i> ₂ = 0.0718	<i>R</i> ₁ = 0.0497, <i>wR</i> ₂ = 0.0934
goodness of fit on <i>F</i> ²	0.726	0.866	0.888
largest diff peak [e Å ⁻³]	0.725	0.936	0.980

the X-ray diffraction experiment were obtained by slow evaporation of chloroform solutions at room temperature.

Synthesis of [Ru(NCMe)₄(P(OMe)₃)(PiPr₃)](BF₄)(Cl) (3**).** The compound was prepared as described for **2**, using **1** (90.5 mg, 0.17 mmol) and trimethylphosphite (32 μL, 0.28 mmol): yield 57.1 mg (50%). Anal. Calcd for C₂₀H₄₂BClF₄N₄O₃P₂Ru: C, 35.76; H, 6.30; N, 8.34. Found: C, 36.16; H, 6.29; N, 8.45. MS (FAB+, *m/z* (%)): 550 (10) [M⁺]. IR (KBr, cm⁻¹): 2291 ν(N≡C), 1034 ν(BF₄). ¹H NMR (acetone-*d*₆, 293 K): δ 1.42 (dd, *J*_{HP} = 13.0, *J*_{HH} = 7.2, 18H, PCHCH₃), 2.66 (s, 12H, NCCH₃), 2.71 (m, 3H, PCHCH₃), 3.99 (d, *J*_{HP} = 10.7, 9H, POCH₃). ³¹P{¹H} NMR (acetone-*d*₆, 293 K): δ 28.55 (d, *J*_{PP} = 455.0, PiPr₃), 120.53 (d, *J*_{PP} = 455.0, P(OMe)₃). ¹³C{¹H} NMR (acetone-*d*₆, 293 K): δ 2.99 (s, NCCH₃), 18.69 (s, PCHCH₃), 23.53 (dd, *J*_{CP} = 19.9, *J*_{CP} = 3.5, PCHCH₃), 53.04 (d, *J*_{CP} = 6.9, POCH₃), 129.57 (s, NCCH₃).

Synthesis of [Ru(NCMe)₄(P(OMe)₃)(PiPr₃)](BF₄)₂ (3-BF₄**).** Trimethylphosphite (15 μL, 0.18 mmol) was slowly added at 273 K to a solution of **6-BF₄** (vide infra, 90.0 mg, 0.14 mmol) in 10 mL of dichloromethane, and the resulting mixture was stirred under argon for 30 min. The solution was evaporated to dryness under vacuum, and the residue was washed with diethyl ether to afford a white solid: yield 68.8 mg (68%). Anal. Calcd for C₂₀H₄₂B₂F₈N₄O₃P₂Ru: C, 33.22; H, 5.85; N, 7.75. Found: C, 33.26; H, 5.41; N, 7.92.

Synthesis of [Ru(Hpz)(NCMe)₄(PiPr₃)](BF₄)(Cl) (4**).** The compound was prepared as detailed for **2**, using **1** (90.5 mg, 0.17 mmol) and pyrazole (18.1 mg, 0.27 mmol): yield 73.3 mg (70%). IR (KBr, cm⁻¹): 3418 ν(NH), 2289 ν(N≡C), 1050 ν(BF₄). Anal. Calcd for C₂₀H₃₇BClF₄N₆PRu: C, 39.00; H, 6.06; N, 13.65. Found: C, 38.92; H, 6.30; N, 13.55. MS (FAB+, *m/z* (%)): 493 (36) [M⁺ - H], 452 (58) [M⁺ - H - NCMe] 411 (100) [M⁺ - H - 2NCMe]. ¹H NMR (CDCl₃, 293 K): δ 1.29 (dd, *J*_{HP} = 13.2, *J*_{HH} = 7.0, 18H, PCHCH₃), 2.39 (m, 3H, PCHCH₃), 2.55 (s, 12H, NCCH₃), 6.49, 7.90, 8.10 (all br, 1H each, CH), 14.18 (br, 1H, NH). ³¹P{¹H} NMR (CDCl₃, 293 K): δ 53.78. ¹³C{¹H} NMR (CDCl₃, 293 K): δ 4.95 (s, NCCH₃), 19.21 (d, *J*_{CP} = 6.0, PCHCH₃), 24.87 (d, *J*_{CP} = 22.0, PCHCH₃), 106.70 (d, *J*_{CP} = 2.3, CH), 127.23 (s, NCCH₃), 132.1 (d, *J*_{CP} = 1.9, CH), 141.87 (s, CH).

Synthesis of [Ru(Hpz)(NCMe)₄(PiPr₃)](BF₄)₂ (4-BF₄**).** The compound was prepared as detailed for **2-BF₄**, using **6-BF₄** (vide infra, 50.0 mg, 0.08 mmol) and pyrazole (5.4 mg, 0.08 mmol):

yield 43.8 mg (82%). Anal. Calcd for C₂₀H₃₇B₂F₈N₆PRu: C, 36.00; H, 5.99; N, 12.60. Found: C, 35.91; H, 5.31; N, 12.90.

[Ru(CD₃OD)(NCMe)₄(PiPr₃)](BF₄)(Cl) (5**).** The NMR spectra of compound **1** (10.0 mg, 0.02 mmol) in methanol-*d*₄ (0.5 mL) obtained at 293 K indicated the presence of a ca. 1:1 mixture of compounds **1** and **5**. The signals corresponding to **5** were assigned by comparison with those of **5-BF₄**. Data for **5**: ¹H NMR (methanol-*d*₄, 293 K): δ 1.27 (dd, *J*_{HP} = 13.7, *J*_{HH} = 7.1, 18H, PCHCH₃), 2.35 (m, 3H, PCHCH₃), 2.54 (s, 12H, NCCH₃). ³¹P{¹H} NMR (methanol-*d*₄, 293 K): δ 69.80 (s).

Synthesis of [Ru(MeOH)(NCMe)₄(PiPr₃)](BF₄)₂ (5-BF₄**).** A solution of **1** (250.0 mg, 0.45 mmol) in 20 mL of methanol was treated with AgBF₄ (89.0 mg, 0.45 mmol) and stirred in the dark at room temperature for 1.5 h. The resulting suspension was filtered through Celite and concentrated in vacuo. The residue was cooled in liquid nitrogen, and diethyl ether was added to precipitate a solid. The solvent was removed by decantation, and the residue was washed with 4 × 5 mL of diethyl ether to afford a pale yellow solid: yield 232.6 mg (81%). IR (KBr, cm⁻¹): 3420 ν(OH), 2287 ν(N≡C), 1049 ν(BF₄). Anal. Calcd for C₁₈H₃₇B₂F₈N₄OPRu: C, 34.25; H, 5.91; N, 8.88. Found: C, 33.89; H, 5.75; N, 9.04. ¹H NMR (CD₂Cl₂, 293 K): δ 1.28 (dd, *J*_{HP} = 13.8, *J*_{HH} = 7.2, 18H, PCHCH₃), 2.36 (m, 3H, PCHCH₃), 2.55 (s, 12H, NCCH₃), 3.70 (d, *J*_{HH} = 4.2, 3H, CH₃OH), 4.93 (q, *J*_{HH} = 4.2, 1H, CH₃OH). ³¹P{¹H} NMR (CD₂Cl₂, 293 K): δ 70.25 (s). ¹³C{¹H} NMR (CD₂Cl₂, 293 K): δ 4.03 (s, NCCH₃), 18.92 (s, PCHCH₃), 25.63 (d, *J*_{CP} = 25.3, PCHCH₃), 52.72 (s, CH₃OH), 127.32 (s, NCCH₃).

[Ru(D₂O)(NCMe)₄(PiPr₃)](BF₄)(Cl) (6**).** The spectra of compound **1** in D₂O obtained at 293 K indicated the quantitative formation of a new compound, the data of which agree with those obtained from a sample of solid **6-BF₄** (vide infra). Data for **6**: ¹H NMR (D₂O, 293 K): δ 1.20 (dd, *J*_{HP} = 13.4, *J*_{HH} = 7.1, 18H, PCHCH₃), 2.28 (m, 3H, PCHCH₃), 2.48 (s, 12H, NCCH₃). ³¹P{¹H} NMR (D₂O, 293 K): δ 69.70 (s).

Synthesis of [Ru(H₂O)(NCMe)₄(PiPr₃)](BF₄)₂ (6-BF₄**).** The complex was prepared as described for **5-BF₄** in a mixture of acetone (20 mL) and water (0.5 mL). Pale yellow solid: yield 233.1 mg (83%). IR (KBr, cm⁻¹): 3434 ν(OH), 2284 ν(N≡C), 1059 ν(BF₄). Anal. Calcd for C₁₇H₃₅B₂F₈N₄OPRu: C, 33.09; H, 5.72; N, 9.08. Found: C, 32.84; H, 5.67; N, 9.09. ¹H NMR (CDCl₃, 293 K): δ 1.21 (dd, *J*_{HP} = 13.8, *J*_{HH} = 7.5, 18H, PCHCH₃), 2.29 (m, 3H,

PCHCH₃), 2.49 (s, 12H, NCCH₃), 5.11 (br, 2H, H₂O). ³¹P{¹H} NMR (CDCl₃, 293 K): δ 72.20 (s). ¹³C{¹H} NMR (CDCl₃, 293 K): δ 3.67 (s, NCCH₃), 18.81 (s, PCHCH₃), 25.34 (d, J_{CP} = 24.8, PCHCH₃), 127.05 (s, NCCH₃). The crystals for the X-ray diffraction experiment were obtained from dichloromethane solutions layered with diethyl ether.

Synthesis of [Ru(OH)(NCMe)₄(P*i*Pr₃)](BF₄) (7). A solution of **6-BF₄** (101.4 mg, 0.16 mmol) in 10 mL of dichloromethane at 258 K was treated with KOH (31 μL, 0.18 mmol; 5.9 N in H₂O) and stirred for 20 min. The resulting suspension was filtered through Celite and evaporated to dryness. The residue was dissolved in 5 mL of dichloromethane at 258 K, filtered again through Celite, and concentrated to ca. 0.5 mL. Addition of diethyl ether at 233 K caused the precipitation of a white solid, which was washed with diethyl ether and dried in vacuo: yield 33.8 mg (63%). IR (KBr, cm⁻¹): 3365 ν(OH), 2284 ν(N≡C), 1059 ν(BF₄). Anal. Calcd for C₁₇H₃₄BF₄N₄OPRu: C, 38.57; H, 6.47; N, 10.59. Found: C, 38.13; H, 6.14; N, 10.48. ¹H NMR (CD₂Cl₂, 233 K): δ -1.11 (d, J_{HP} = 1.5, 1H, OH), 1.27 (dd, J_{HP} = 12.7, J_{HH} = 7.1, 18H, PCHCH₃), 2.37 (br m, 3H, PCHCH₃), 2.56 (s, 12H, NCCH₃). ³¹P{¹H} NMR (CD₂Cl₂, 233 K): δ 55.30 (s). ¹³C{¹H} NMR (CD₂Cl₂, 233 K): δ 4.16 (s, NCCH₃), 18.99 (s, PCHCH₃), 25.67 (br, PCHCH₃), 125.68 (s, NCCH₃).

[Ru{HN(CO)Me}(NCMe)₃(P*i*Pr₃)](BF₄) (8). A solution of **7** in CD₂Cl₂ was monitored by ¹H and ³¹P{¹H} NMR at 273 K. After 40 min the spectra indicated the quantitative formation of **8**. ¹H NMR (CD₂Cl₂, 233 K): δ 1.21 (br dd, J_{HP} = 12.4, J_{HH} = 7.2, 18H, PCHCH₃), 1.97 (s, 3H, CH₃), 2.28 (br m, 3H, PCHCH₃), 2.46 (br, 6H, NCCH₃), 2.49 (s, 3H, NCCH₃), 4.24 (br, 1H, NH). ³¹P{¹H} NMR (CD₂Cl₂, 233 K): δ 64.98 (s). ¹³C{¹H} NMR (CD₂Cl₂, 233 K): δ 4.62 (br, NCCH₃), 4.78 (s, NCCH₃), 18.96 (br, PCHCH₃), 24.90 (br, PCHCH₃), 27.20 (s, CH₃), 119.39 (d, J_{CP} = 15.1, NCCH₃), 125.68 (br, NCCH₃), 182.93 (s, C).

pK_a Determination. The NMR samples were prepared dissolving 13.0 mg of **6-BF₄** in 0.5 mL of D₂O. The pH's were adjusted to the desired value using NaOH and directly measured in the NMR tube with a pH meter. The values read by the pH meter in D₂O

(pH*) were transformed into pH using the relation pH = 0.929pH* + 0.41.²⁶ The pK_a^{H₂O}, which characterizes the acid dissociation of **6** in H₂O solution, was calculated using the ³¹P{¹H} chemical shift and pH data by means of the general computational program for determining stability constants, PSEQUAD.²⁷

Catalytic Acetonitrile Hydration. The complex **6-BF₄** (6.17 mg, 0.01 mmol) was dissolved under argon in a mixture of acetonitrile (4.1 g, 5.22 mL, 100 mmol) and water (1.8 g, 100 mmol), previously deoxygenated. The pH of the resulting solution was adjusted to 10.5 by addition of aqueous KOH (22.0 μL of a 0.10 N solution). The resulting solution was transferred into a 25 mL flask provided with a magnetic stirrer and a PTFE stopcock. The flask was closed and immersed into a thermostated bath, where the reaction was stirred at 353 K. The reaction was periodically stopped and opened to take samples of ca. 1 μL, which were analyzed by GC-MS on an Agilent 6890 Series GC System provided with a 5973 Network mass selective detector. The column used was a HP-5MS (cross-linked methyl silicone gum, 30 m × 0.25 mm × 0.25 μm film thickness). Data: time (h)/(%) conversion: 2/1.1; 4/2.0; 6/3.0; 10/4.8; 20/8.0; 48/11.0; 120/15.2.

Acknowledgment. This work was supported by the Spanish MEC/FEDER (grant CTQ2006-01629/BQU and Consolider Ingenio 2010, grant INTECAT CSD2006-0003) and the Hungarian National Research and Technology Office, National Research Fund (NKTH-OTKA K 68482). The work has been carried out within a bilateral collaboration of CSIC and the Hungarian Academy of Sciences.

Supporting Information Available: X-ray crystallographic file for the complexes **1**, **2-BF₄**, and **6-BF₄** in CIF format. This material is available free of charge via the Internet at <http://pubs.acs.org>.

OM8008553

(26) Krezel, A.; Bal, W. *J. Inorg. Biochem.* **2004**, *98*, 161–166.

(27) Zékány, L.; Nagypál, I. In *Computational Methods for the Determination of Stability Constants*; Leggett, D., Ed.; Plenum: New York, 1985.

Stable Cationic and Neutral Ruthenabenzene

George R. Clark, Tamsin R. O’Neale, Warren R. Roper,* Deborah M. Tinei, and L. James Wright*

Department of Chemistry, The University of Auckland, Private Bag 92019, Auckland, New Zealand

Received September 4, 2008

Reversible protonation of the purple ruthenabenzofuran (or tethered ruthenacyclohexadiene) $\text{Ru}[\text{C}_5\text{H}_2(\text{CO}_2\text{Me}-2)(\text{CO}_2\text{Me}-4)(\text{CHCO}_2\text{Me}-5)](\text{CO})(\text{PPh}_3)_2$ (**1**) with $\text{HBF}_4 \cdot \text{OEt}_2$ gives the structurally characterized stable cationic tethered ruthenabenzene $[\text{Ru}[\text{C}_5\text{H}_2(\text{CO}_2\text{Me}-2)(\text{CO}_2\text{Me}-4)(\text{CH}_2\text{CO}_2\text{Me}-5)](\text{CO})(\text{PPh}_3)_2][\text{BF}_4]_2\text{H}$ (**2**), while the thermal reaction of **1** with HCl forms the stable neutral tethered ruthenabenzene $\text{Ru}[\text{C}_5\text{H}_2(\text{CO}_2\text{Me}-2)(\text{CO}_2\text{Me}-4)(\text{CH}_2\text{CO}_2\text{Me}-5)]\text{Cl}(\text{PPh}_3)_2$ (**3**) as the major product. The cyclopentadienyl complex $\text{Ru}(\eta^5\text{-C}_5\text{H}_2(\text{CH}_2\text{CO}_2\text{Me}-1)(\text{CO}_2\text{Me}-2)(\text{CO}_2\text{Me}-4)\text{Cl}(\text{CO})(\text{PPh}_3))$ (**4**), which is formed in this reaction as a minor product, can be separated from **3** by chromatography. Treatment of the ruthenabenzene **3** with CNR (R = *p*-tolyl) gives the purple ruthenabenzofuran (or tethered ruthenacyclohexadiene) complex $\text{Ru}[\text{C}_5\text{H}_2(\text{CO}_2\text{Me}-2)(\text{CO}_2\text{Me}-4)(\text{CHCO}_2\text{Me}-5)](\text{CNR})(\text{PPh}_3)_2$ (**5**), which is the isocyanide analogue of **1**.

Introduction

Metallabenzene is now a well-established class of organometallic compounds, and considerable attention has been directed toward developing synthetic routes and studying the reaction chemistry of these compounds.¹ In addition, important fundamental information has been provided by a number of computational studies that have explored aspects of the syntheses, reactivity, decomposition pathways, and aromatic character of these materials.^{1,2} Despite this scrutiny, nearly all of the reported metallabenzene derivatives that are stable under ambient conditions are confined to derivatives of the third-row transition metals osmium, iridium, and platinum. Metallabenzene or metallabenzene derivatives of the first- or second-row transition metals iron,³ chromium,⁴ and ruthenium^{5,6} have been proposed as reactive intermediates, and the ruthenabenzene $\text{Ru}[\text{C}(\text{Ph})\text{CH}(\text{CH}_2\text{C}(\text{Ph})\text{C}(\text{OEt}))(\text{CO})\text{Cp}]$, a related ruthenaphenoxide, and a ruthenaphenanthrene oxide have been detected spectroscopically at low temperatures.⁶ However, it was not until 2006 that the first stable metallabenzene of a second-row transition metal was isolated. In that year Jia, Xia, and co-workers reported the synthesis and study of the ruthenabenzene $[\text{Ru}[\text{CHC}(\text{PPh}_3)\text{CHC}(\text{PPh}_3)\text{CH}]\text{Cl}_2(\text{PPh}_3)_2]\text{Cl}$.⁷ This remarkable compound remains mostly unchanged after heating in the solid state in air at 100 °C for 5 h. It was proposed that the two bulky triphenylphosphonium substituents on the ruthenabenzene ring play an important role in stabilizing this compound as well as the other related ruthenabenzene derivatives that were subse-

quently obtained by ligand substitution at ruthenium.⁸ These compounds remain the only simple metallabenzene derivatives that involve a metal from the second transition series that are stable under ambient conditions.

In this paper we now report (i) the synthesis of the stable blue cationic tethered ruthenabenzene $[\text{Ru}[\text{C}_5\text{H}_2(\text{CO}_2\text{Me}-2)(\text{CO}_2\text{Me}-4)(\text{CH}_2\text{CO}_2\text{Me}-5)](\text{CO})(\text{PPh}_3)_2][\text{BF}_4]_2\text{H}$ (**2**) through protonation of the ruthenabenzofuran (or tethered ruthenacyclohexadiene) $\text{Ru}[\text{C}_5\text{H}_2(\text{CO}_2\text{Me}-2)(\text{CO}_2\text{Me}-4)(\text{CHCO}_2\text{Me}-5)](\text{CO})(\text{PPh}_3)_2$ (**1**) with $\text{HBF}_4 \cdot \text{OEt}_2$; (ii) the synthesis of the stable green neutral tethered ruthenabenzene $\text{Ru}[\text{C}_5\text{H}_2(\text{CO}_2\text{Me}-2)(\text{CO}_2\text{Me}-4)(\text{CH}_2\text{CO}_2\text{Me}-5)]\text{Cl}(\text{PPh}_3)_2$ (**3**) through reaction of **1** with HCl in benzene/methanol solution heated under reflux; (iii) isolation of the cyclopentadienyl complex $\text{Ru}(\eta^5\text{-C}_5\text{H}_2(\text{CH}_2\text{CO}_2\text{Me}-1)(\text{CO}_2\text{Me}-2)(\text{CO}_2\text{Me}-4)\text{Cl}(\text{CO})(\text{PPh}_3))$ (**4**) as a byproduct from the thermal reaction of **1** with HCl; (iv) the conversion of **3** to the ruthenabenzofuran (or tethered ruthenacyclohexadiene) complex $\text{Ru}[\text{C}_5\text{H}_2(\text{CO}_2\text{Me}-2)(\text{CO}_2\text{Me}-4)(\text{CHCO}_2\text{Me}-5)](\text{CNR})(\text{PPh}_3)_2$ (**5**) through treatment with *p*-tolylisocyanide, and (v) the crystal structures of **2**, **4**, and **5**.

Results and Discussion

In a recent paper we described the synthesis and some reaction chemistry of the osmabenzofuran $\text{Os}[\text{C}_7\text{H}_2\text{O}(\text{OMe}-7)(\text{CO}_2\text{Me}-4)(\text{Ph}-1)(\text{Ph}-2)](\text{CS})(\text{PPh}_3)_2$.⁹ The case for considering this compound as an osmabenzofuran with delocalized bonding was developed on the basis of spectroscopic, structural, and reactivity data. One of the important reactions this compound undergoes is protonation of C6 in the osmabenzofuran ring to form the cationic, tethered osmabenzene $[\text{Os}[\text{C}_5\text{H}(\text{CH}_2\text{CO}_2\text{Me}-5)(\text{CO}_2\text{Me}-4)(\text{Ph}-1)(\text{Ph}-2)](\text{CS})(\text{PPh}_3)_2]^+$ (see Chart 1).⁹ A ruthenium complex, $\text{Ru}[\text{C}_5\text{H}_2(\text{CO}_2\text{Me}-2)(\text{CO}_2\text{Me}-4)(\text{CHCO}_2\text{Me}-5)](\text{CO})(\text{PPh}_3)_2$ (**1**), that has the same basic metallabicyclic skeleton as this osmabenzofuran and can also be considered as a ruthenabenzofuran⁹ (see Chart 2 and discussion below) has been reported to form through reaction

* Corresponding authors. E-mail: lj.wright@auckland.ac.nz; w.roper@auckland.ac.nz.

(1) For example see: (a) Bleeker, J. R. *Chem. Rev.* **2001**, *101*, 1205. (b) Landorf, C. W.; Haley, M. M. *Angew. Chem., Int. Ed.* **2006**, *45*, 3914. (c) Wright, L. J. *J. Chem. Soc., Dalton Trans.* **2006**, 1821, and references therein.

(2) (a) Fernández, I.; Frenking, G. *Chem.–Eur. J.* **2007**, *13*, 5873. (b) Zhu, J.; Jia, G.; Lin, Z. *Organometallics* **2007**, *26*, 1986.

(3) Ferde, R.; Allison, N. T. *Organometallics* **1983**, *2*, 463.

(4) Sivavec, T. M.; Katz, T. J. *Tetrahedron Lett.* **1985**, *26*, 2159.

(5) Yang, J.; Yin, J.; Abboud, K. A.; Jones, W. M. *Organometallics* **1994**, *13*, 971.

(6) Yang, J.; Jones, W. M.; Dixon, J. K.; Allison, N. T. *J. Am. Chem. Soc.* **1995**, *117*, 9776.

(7) Zhang, H.; Xia, H.; He, G.; Wen, T.; Gong, L.; Jia, G. *Angew. Chem., Int. Ed.* **2006**, *45*, 2920.

(8) Zhang, H.; Feng, L.; Gong, L.; Wu, L.; He, G.; Wen, T.; Yang, F.; Xia, H. *Organometallics* **2007**, *26*, 2705.

(9) Clark, G. R.; Johns, P. M.; Roper, W. R.; Wright, L. J. *Organometallics* **2006**, *25*, 1771.

Chart 1

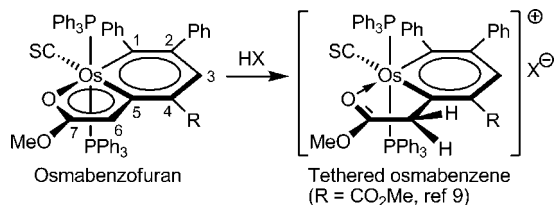
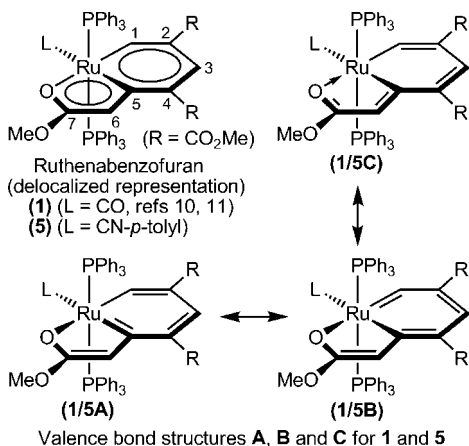
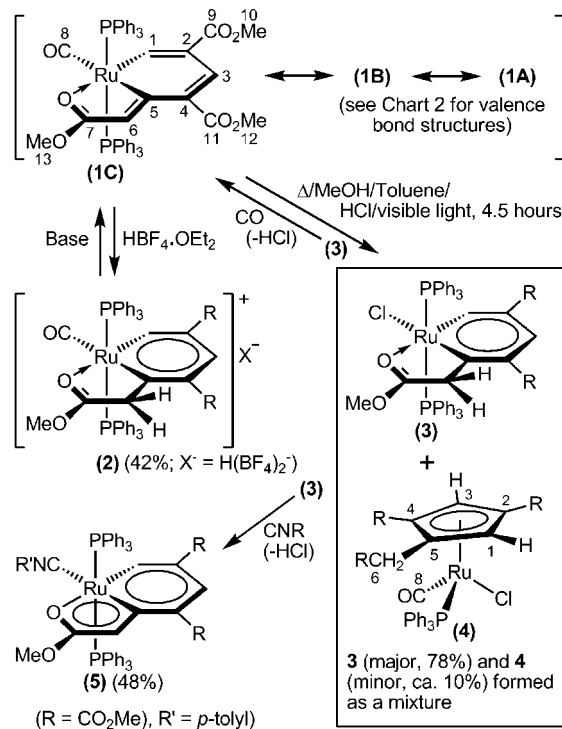


Chart 2



between RuH₂(CO)(PPh₃)₃ and methyl propiolate.^{10,11} We therefore investigated the reactions of **1** with acid to determine whether a related protonation reaction would occur at C6 in the ruthenafuran ring, thereby leading to the formation of a tethered ruthenabenzene.

On treatment of a toluene solution of purple Ru[C₅H₂(CO₂Me-2)(CO₂Me-4)(CHCO₂Me-5)](CO)(PPh₃)₂ (**1**) with HBF₄·OEt₂, the solution immediately turns dark blue, and dark blue crystals of the cationic, tethered ruthenabenzene [Ru[C₅H₂(CO₂Me-2)(CO₂Me-4)(CH₂CO₂Me-5)](CO)(PPh₃)₂[(BF₄)₂H] (**2**) are deposited from solution (see Scheme 1). Although **2** can be successfully recrystallized from dichloromethane/toluene, this protonation reaction is readily reversed, and addition of bases such as NEt₃ to dichloromethane solutions of this product causes immediate reversion back to **1**. Complex **2**, which is stable in solution at 25 °C for days, has been thoroughly characterized, including by a crystal structure determination (see below). Characterizing data for **2** as well as **3–5** are collected in the Experimental Section, and the numbering scheme used for the NMR assignments is given in Scheme 1. In the ¹H NMR spectrum of **2**, H1 appears as a doublet (⁴J_{H1H3} = 2.4 Hz) at 14.97 ppm. Resonances in this downfield region are typically observed for protons attached to the metal-bound carbon atoms of metallabenzene,¹ and the signal for the two equivalent RuCH atoms in the stable ruthenabenzene [Ru[CHC(PPh₃)CHC(PPh₃)CH]Cl₂(PPh₃)₂]Cl appears at 17.5 ppm.⁷ H3 (8.83 ppm) in **2** appears in the aromatic region, and the two protons attached to C6 are observed at 2.73 ppm (cf. 6.06 ppm in **1**), consistent with saturation of this ring carbon atom. In the ¹³C NMR spectrum of **2**, C1 and C5 appear as triplets at 290.8 (²J_{CP} = 6.1 Hz) and 283.6 (²J_{CP} = 7.7 Hz) ppm, respectively, positions that are very similar to that reported for the two equivalent RuC atoms in the ruthenabenzene [Ru[CHC(PPh₃)CHC(PPh₃)CH]Cl₂(PPh₃)₂]Cl (284.3 ppm).⁷ C6 is observed at 52.3 ppm (cf. 119 ppm in **1**), again consistent with saturation of this carbon atom.

Scheme 1. Synthesis of the Tethered Metallabenzenes **2** and **3** and Formation of the Ruthenabenzofuran **5**

The crystal structure of complex **2** was determined, and the structure of the cationic ruthenium complex is shown in Figure 1 (crystal data for **2** as well as for **4** and **5** are given in the Supporting Information). The geometry about Ru is approximately octahedral, and the six atoms of the ruthenabenzene ring (Ru, C1–C5) and the three atoms of the tethering arm (C6, C7, and O6) are all essentially coplanar (maximum deviation from the mean plane through all nine atoms is 0.072 Å). The Ru–C1 and Ru–C5 distances are 1.933(4) and 2.045(5) Å, respectively. The *trans*-influence of the CO ligand is probably the main factor responsible for the greater length of the Ru–C5 bond. The C–C distances within the ruthenabenzene ring of **2** (C1–C2, 1.404(6); C2–C3, 1.383(7); C3–C4, 1.413(7); C4–C5,

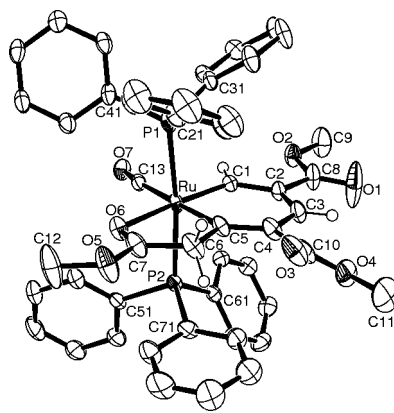


Figure 1. Molecular structure of the ruthenium cation of **2** with thermal ellipsoids at the 50% probability level. Selected distances [Å]: Ru–C1 1.933(4), Ru–C5 2.045(5), Ru–C13 1.941(5), Ru–O6 2.216(3), C1–C2 1.404(6), C2–C3 1.383(7), C3–C4 1.413(7), C4–C5 1.374(7), C5–C6 1.518(7), C6–C7 1.504(8), O6–C7 1.231(7).

(10) Yamazaki, H.; Aoki, K. *J. Organomet. Chem.* **1976**, *122*, C54.

(11) Bruce, M. I.; Hall, B. C.; Skelton, B. W.; Tiekink, E. R. T.; White, A. H.; Zaitseva, N. N. *Aust. J. Chem.* **2000**, *53*, 99.

1.374(7) Å) are close to those found in benzene (1.390 Å)¹² and show relatively little alternation. The C5–C6 and C6–C7 distances (1.518(7) and 1.504(8) Å, respectively) in **2** are significantly longer than the corresponding distances in **1** (1.384(8) and 1.41(1) Å), consistent with saturation of C6. The counteranion in the crystal is comprised of the very unusual [(BF₄)₂H][−] ion. The fluorine atoms in one of the [BF₄][−] groups (the one involving B2) in this counteranion are disordered between two slightly different positions, and the half-weighted sets of atoms used in the refinement are labeled F5a–F8a and F5b–F8b. In each orientation of the disordered BF₄[−] unit one fluorine atom (F8a or F8b) makes a close approach to F4 of the other ordered BF₄[−] (B1) unit, with F4⋯F8a = 2.597 Å and F4⋯F8b = 2.750 Å. Both these distances are longer than the F–H⋯F distance of 2.49 Å in crystalline hydrogen fluoride,¹³ but both are considerably shorter than the sum of the van der Waals radii for two fluorine atoms (ca. 2.94 Å)¹⁴ and are therefore consistent with a hydrogen bond between F4 and F8a/b. Furthermore, the B1–F4 distance (1.428(10) Å) is longer than the other three B1–F distances (B1–F1, 1.361(9); B1–F2, 1.366(8); B1–F3, 1.379(9) Å), and likewise the B2–F8a and B2–F8b distances are longer than the other B2–F distances. In the difference Fourier map there is a peak between F4 and the disordered atoms F8a and F8b. However, the position of this peak was not sufficiently reliable to justify its inclusion as a hydrogen atom in the least-squares refinement. Although this putative hydrogen atom was not located in the crystal structure determination, its presence can be inferred from the structural features noted above. In the ¹⁹F NMR spectrum of **2** only one sharp resonance at −154.49 ppm is observed, indicating that in solution equilibration of the positions of all fluorine atoms occurs rapidly on the NMR time scale.

In an attempt to prepare a neutral ruthenabenzene, the reaction of **1** with HCl was investigated. It was found that on heating **1** under reflux for 4.5 h in benzene/methanol that contains a small amount of trimethylsilyl chloride (a convenient way of introducing nonaqueous HCl to the system) while irradiating the mixture with visible light, the solution slowly changes color from purple to bright green. After purification of the reaction products by column chromatography two products were obtained, the green neutral ruthenabenzene Ru[C₅H₂(CO₂Me-2)(CO₂Me-4)-(CH₂CO₂Me-5)]Cl(PPh₃)₂ (**3**), in 78% yield, and the yellow cyclopentadienyl complex Ru(η⁵-C₅H₂(CH₂CO₂Me-1)-(CO₂Me-2)(CO₂Me-4)Cl(CO)(PPh₃)) (**4**) in ca. 10% yield (see Scheme 1). The ruthenabenzene **3** is remarkably stable in solutions that contain traces of HCl, even at elevated temperatures, as is indicated by the synthetic procedure described above. We were not able to obtain the crystal structure of **3** because of the difficulty in obtaining single crystals suitable for X-ray diffraction studies; however, the spectroscopic and analytical data confirm the ruthenabenzene formulation. In the ¹H NMR spectrum of **3**, H1 appears as a doublet of triplets at 16.45 ppm (⁴J_{HH} = 2.7, ³J_{HP} = 3.0 Hz), H3 is observed as a doublet at 8.76 ppm (⁴J_{HH} = 2.4 Hz), and the two protons on C6 appear as a singlet at 3.19 ppm. In the ¹³C NMR spectrum the two metal-bound carbon atoms again appear as triplets at characteristically low field values (C1, 287.8 (²J_{CP} = 12.6 Hz); C5, 289.3 (²J_{CP} = 10.6 Hz) ppm), and the other ruthenabenzene ring carbon atoms have resonances in the aromatic region. The methylene carbon C6 is observed at 56.2 ppm, and in the ³¹P

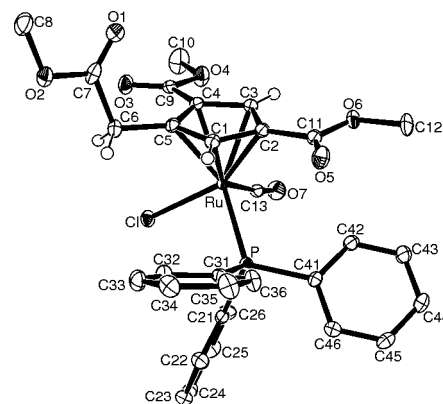


Figure 2. Molecular structure of **4** with thermal ellipsoids at the 50% probability level. Selected distances [Å]: Ru–C13 1.8729(18), Ru–C1 2.2942(17), Ru–C2 2.2069(17), Ru–C3 2.1808(17), Ru–C4 2.2222(16), Ru–C5 2.3113(16), Ru–P 2.3260(4), Ru–Cl 2.3914(4), C5–C6 1.499(2), C6–C7 1.528(3).

NMR spectrum a singlet at 21.55 ppm is observed for the two equivalent phosphorus atoms.

The other product formed during the synthesis of **3** from **1** was the cyclopentadienyl complex Ru(η⁵-C₅H₂(CH₂CO₂Me-1)(CO₂Me-2)(CO₂Me-4)Cl(CO)(PPh₃)) (**4**) (see Scheme 1). If the reaction conditions described above were changed so that the acid used was concentrated aqueous HCl and the solution was not irradiated with visible light, the ratio of **3** to **4** in the crude product was close to 1.0 (as estimated by NMR spectroscopy). We do not have any direct evidence relating to the mechanism by which **3** and **4** are formed from **1**, but a plausible sequence involves protonation of C6 in **1** followed either by (i) loss of CO from the resulting cationic intermediate and coordination of chloride to give **3** (irradiation with visible light could facilitate CO dissociation leading to increased yields of **3**) or (ii) the coupling of C1 and C5 in the cationic intermediate to give an η¹-cyclopentadienyl complex, which then rearranges with coordination of chloride to give the η⁵-cyclopentadienyl complex **4**. There is ample evidence for the transformation of metallabenzene into cyclopentadienyl complexes,¹ and this metallabenzene decomposition route has been studied by computational methods.¹⁵

The characterizing spectroscopic data relating to **4** are collected in the Experimental Section and are mostly unremarkable. In the ¹H NMR spectrum the two inequivalent protons on C6 are observed as doublets at 2.88 and 3.91 ppm, with geminal HH coupling constants of 17.8 Hz. In the ¹³C NMR spectrum the saturated carbon atom C6 appears at 32.6 ppm. The crystal structure of **4** was determined, and the molecular structure is shown in Figure 2. The carbon atoms C2–4 of the π-bound cyclopentadienyl ligand make slightly closer approaches to ruthenium than C1 and C5. The atoms C6 and C7 that formed part of the five-membered ruthenacyclic ring in **1** are found within the CH₂CO₂Me substituent on the cyclopentadienyl ring in **4**.

Although the ruthenabenzene **3** is very stable in solutions that contain traces of HCl, addition of the base NEt₃ or 1,8-diazabicyclo[5.4.0]undec-7-ene (DBU) results in the complete conversion of **3** to intractable mixtures of products. In contrast, treatment of a dichloromethane solution of **3** with CO (1 atm pressure, ambient temperature) rapidly results in the regeneration of **1** (see Scheme 1). The overall outcome of this reaction is

(12) Piermarini, G. J.; Mighell, A. D.; Weir, C. E.; Block, S. *Science* **1969**, *165*, 1250.

(13) Greenwood, N. N.; Earnshaw, A. *Chemistry of the Elements*; Pergamon Press, 1989; ISBN 0-08-022057-6.

(14) Bondi, A. J. *Phys. Chem.* **1964**, *68*, 441.

(15) Iron, M. A.; Lucassen, A. C. B.; Cohen, H.; van der Boom, M. E.; Martin, J. M. L. *J. Am. Chem. Soc.* **2004**, *126*, 11699.

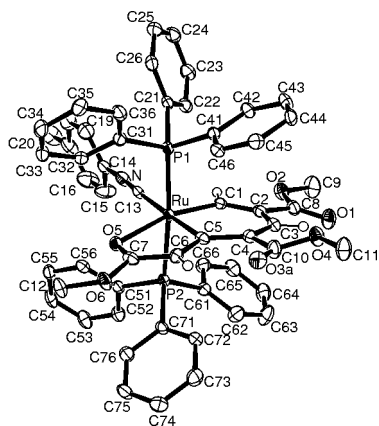


Figure 3. Molecular structure of **5** with thermal ellipsoids at the 50% probability level. Selected distances [Å]: Ru–C1 1.986(3), Ru–C5 2.092(4), Ru–C13 1.954(4), Ru–O5 2.266(2), C1–C2 1.368(5), C2–C3 1.437(5), C3–C4 1.376(5), C4–C5 1.475(5), C5–C6 1.376(5), C6–C7 1.437(5), O5–C7 1.242(4).

that the chloride ligand is substituted by CO and one of the protons on C6 is lost in a process that is formally the reverse of the reaction in which **3** is formed from **1**. We do not have any evidence that indicates whether substitution of chloride by CO occurs before or after the proton is lost from C6 during the reaction in which **1** is regenerated from **3**. In an analogous manner, treatment of **3** with *p*-tolylisocyanide gives the purple isocyanide-containing ruthenabenzofuran (or tethered ruthenacyclohexadiene) Ru[C₅H₂(CO₂Me-2)(CO₂Me-4)(CHCO₂Me-5)]-(CNR)(PPh₃)₂ (**5**) (see Scheme 1). In the IR spectrum of **5** ν (CN) is observed at 2060 cm⁻¹. As might be expected, the ¹H and ¹³C NMR spectra of **5** are similar to the corresponding spectra obtained for **1**. In the ¹H NMR spectrum of **5** H1 is observed at the low field position of 12.40 ppm (cf. 11.67 ppm in **1**), H6 is observed at 6.17 ppm (cf. 6.08 in **1**), and H3 is obscured by the PPh₃ resonances (7.26–7.46 ppm), as is the case for H3 in **1**. In the ¹³C NMR spectrum of **5**, C1 and C5 are observed at the low field positions of 245.0 and 232.8 ppm, respectively (cf. 232.9 and 227.0, respectively, in **1**). The resonances of the other carbon atoms in the six-membered metallacyclic ring all appear in the aromatic region at 127.8 (C2), 147.4 (C3), and 121.1 (C4) ppm (cf. 128.5, 147.3, and 122.2 ppm, respectively, in **1**). The resonance for C6 (117.1 ppm) also falls in the aromatic region (cf. 119.1 ppm in **1**). It is noteworthy that the chemical shifts of H1 and C1/5 in **5** (and **1**) (ca. 12 and 235 ppm, respectively) are midway between the chemical shifts of the corresponding atoms in the ruthenabenzenes **2**, **3**, and [Ru{CHC(PPh₃)CHC(PPh₃)CH}Cl₂(PPh₃)₂]Cl⁷ (ca. 16 and 280 ppm, respectively) and the chemical shifts of the corresponding atoms in simple, nonconjugated vinyl derivatives of ruthenium that bear bis(triphenylphosphine) and carbonyl or isocyanide ligands (ca. 8 and 175 ppm, respectively).¹⁶

The crystal structure of **5** was determined, and the molecular structure is shown in Figure 3. The same fused five- and six-membered bicyclic ring system with Ru at a bridgehead position that is present in **1** is also clearly evident in the structure of **5**. The atoms in the six-membered ruthenacyclic ring (Ru, C1–C5) are essentially coplanar, with the maximum displacement from the mean plane through these atoms being 0.064 Å. The atoms in the five-membered ring (Ru, C5–C7, O5) are also coplanar (maximum displacement from the mean plane through these five atoms is 0.037 Å). The bicyclic ring system is folded slightly

about the Ru–C5 vector, and the angle between the two mean planes is 9.6°.

The Ru–C1 (1.986(3) Å) and Ru–C5 (2.092(4) Å) distances in **5** are both slightly longer than the corresponding distances in the cationic tethered ruthenabenzene **2** (1.933(4) and 2.045(5) Å, respectively), and the *trans*-influence of the CNR ligand is probably mostly responsible for the longer Ru–C(5). The C–C distances within the six-membered ruthenacyclic ring of **5** show considerably more alternation in length (C1–C2, 1.368(5); C2–C3, 1.437(5); C3–C4, 1.376(5); C4–C5, 1.475(5) Å) than do the corresponding distances in **2**. Nevertheless, the first three distances still all fall within the range observed for other metallabenzenes,¹ although the C4–C5 distance is closer to values normally associated with C–C single bonds. The C5–C6 (1.376(5) Å) and C6–C7 (1.437(5) Å) distances are also close to those commonly observed in aromatic systems. The bonding in the bicyclic ring system of **5** can be discussed in terms of the three valence bond structures **5A**–**5C** depicted in Chart 2. Three corresponding valence bond structures were used to discuss the bonding in the related osmabenzofuran Os[C₇H₂O-(OMe-7)(CO₂Me-4)(Ph-1)(Ph-2)](CS)(PPh₃)₂.⁹ The alternation of the C–C distances in the ruthenabicyclic ring system of **5** points to a major contribution from valence bond structure **5C**. However, the C–C distances involving C1–4 and C5–7, which all fall within the normal aromatic range, indicate some contribution from **5A** and **5B**. This is supported by the ¹H and ¹³C NMR chemical shifts of the ring atoms, which are consistent with a degree of delocalization within the ruthenabicyclic system. Accordingly, we favor a delocalized ruthenabenzofuran description for the bonding in **5** (and **1**⁹) rather than an alternative tethered ruthenacyclohexadiene description with localized double bonds.

Concluding Remarks

Tethered ruthenabenzene is accessible through protonation of C6 in the five-membered ruthenacyclic ring of Ru[C₅H₂(CO₂Me-2)(CO₂Me-4)(CHCO₂Me-5)](CO)(PPh₃)₂ (**1**). Thus, treatment of **1** with HBF₄·OEt₂ yields the blue cationic tethered ruthenabenzene [Ru[C₅H₂(CO₂Me-2)(CO₂Me-4)(CH₂CO₂Me-5)]-(CO)(PPh₃)₂[(BF₄)₂H] (**2**), while treatment with HCl gives the green neutral tethered ruthenabenzene Ru[C₅H₂(CO₂Me-2)(CO₂Me-4)(CH₂CO₂Me-5)]Cl(PPh₃)₂ (**3**). Both these ruthenabenzene are stable in solution, and remarkably, **3** survives mostly unchanged on heating under reflux for several hours in a toluene/methanol solution that contains traces of HCl. Since calculations have shown that the coupling of the two metal-bound carbon atoms in simple metallabenzene models to give cyclopentadienyl ligands is a relatively low energy process for second-row transition metal derivatives,¹⁵ the tethering arms and/or the methyl ester ring substituents in **2** and **3** probably provide important stabilizing effects.

Treatment of **3** with CN-*p*-tolyl causes HCl to be lost, and the isocyanide-containing compound Ru[C₅H₂(CO₂Me-2)(CO₂Me-4)(CHCO₂Me-5)](CNR)(PPh₃)₂ (**5**) is formed. This is the isocyanide analogue of compound, **1**. On the basis of the structural and spectroscopic data for **5** (and **1**) some delocalization of the bonding within the fused ruthenabicyclic rings is apparent, and we therefore favor the description of these compounds as “ruthenabenzofurans”.

Experimental Section

General Comments. Standard laboratory procedures were followed, as have been described previously.¹⁶ The compound

(16) Maddock, S. M.; Rickard, C. E. F.; Roper, W. R.; Wright, L. J. *Organometallics* **1996**, *15*, 1793.

$\text{Ru}[\text{C}_5\text{H}_2(\text{CO}_2\text{Me-2})(\text{CO}_2\text{Me-4})(\text{CHCO}_2\text{Me-5})](\text{CO})(\text{PPh}_3)_2$ (**1**) was prepared according to the literature method.¹⁰

Infrared spectra ($4000\text{--}400\text{ cm}^{-1}$) were recorded as Nujol mulls between KBr plates on a Perkin-Elmer Paragon 1000 spectrometer. NMR spectra were obtained on a Bruker DRX 400 at $25\text{ }^\circ\text{C}$. ^1H , ^{13}C , ^{19}F , and ^{31}P NMR spectra were obtained operating at 400.1 (^1H), 100.6 (^{13}C), 376.5 (^{19}F), and 162.0 (^{31}P) MHz, respectively. Resonances are quoted in ppm and ^1H NMR spectra referenced to either tetramethylsilane (0.00 ppm) or the proteo-impurity in the solvent (7.25 ppm for CHCl_3). ^{13}C NMR spectra were referenced to CDCl_3 (77.0 ppm), ^{19}F NMR spectra to CFCl_3 (0.00 ppm), and ^{31}P NMR spectra to 85% orthophosphoric acid (0.00 ppm) as an external standard. Elemental analyses were obtained from the Microanalytical Laboratory, University of Otago.

$[\text{Ru}[\text{C}_5\text{H}_2(\text{CO}_2\text{Me-2})(\text{CO}_2\text{Me-4})(\text{CH}_2\text{CO}_2\text{Me-5})](\text{CO})(\text{PPh}_3)_2][\text{BF}_4\cdot\text{H}](\text{2})$. $\text{Ru}[\text{C}_5\text{H}_2(\text{CO}_2\text{Me-2})(\text{CO}_2\text{Me-4})(\text{CHCO}_2\text{Me-5})](\text{CO})(\text{PPh}_3)_2$ (**1**) (0.100 g) was dissolved in toluene (5 mL) at room temperature, giving a purple solution. $\text{HBF}_4\cdot\text{Et}_2\text{O}$ (0.3 mL, 54% w/w solution) was then slowly added, causing the formation of a dark blue precipitate. This product was collected by filtration and recrystallized from dichloromethane/toluene to give pure **2** as dark blue crystals (0.042 g, 42%). Anal. Calc for $\text{C}_{49}\text{H}_{44}\text{O}_7\text{P}_2\text{RuB}_2\text{F}_8\cdot(0.5\text{CH}_2\text{Cl}_2)\cdot(2.4\text{H}_2\text{O})$: C, 50.93; H, 4.31. Found: C, 50.88; H, 4.21% (NMR spectroscopy showed the presence of ca. 0.5 molar equiv of CH_2Cl_2 of crystallization as well as ca. 2 molar equiv of water in the analytical sample. The crystal grown for X-ray structural analysis contained 0.3 molar equiv of CH_2Cl_2 , 2.4 molar equiv of H_2O , and 0.5 molar equiv of toluene). IR (cm^{-1}): 1988 $\nu(\text{CO})$; 1711, 1631 (CO_2CH_3). ^1H NMR (CDCl_3 , δ): 2.73 (s, 2H, H6), 3.73 (s, 3H, H10), 3.83 (s, 3H, H12), 3.99 (s, 3H, H13), 7.15–7.54 (m, 30H, *PPh*₃), 8.83 (d, $^4J_{\text{HH}} = 2.2\text{ Hz}$, 1H, H3), 14.97 (d, $^4J_{\text{HH}} = 2.4\text{ Hz}$, 1H, H1). ^{13}C NMR (CDCl_3 , δ): 52.0 (s, C12), 52.3 (s, C10), 53.2 (s, C6), 56.6 (s, C13), 129.1 (t' , $^{16,24}J_{\text{CP}} = 10.3\text{ Hz}$, *o-PPh*₃), 129.4 (t' , $^{1,3}J_{\text{CP}} = 48.9\text{ Hz}$, *i-PPh*₃), 129.6 (s, C2), 130.8 (s, C4), 131.9 (s, *p-PPh*₃), 133.0 (t' , $^{3,5}J_{\text{CP}} = 11.3\text{ Hz}$, *m-PPh*₃), 156.6 (s, C3), 163.9 (s, C9), 164.8 (s, C11), 185.9 (s, C7), 199.7 (t, $^2J_{\text{CP}} = 14.4\text{ Hz}$, C8), 283.6 (t, $^2J_{\text{CP}} = 7.7\text{ Hz}$, C5), 290.8 (t, $^2J_{\text{CP}} = 6.1\text{ Hz}$, C1). ^{31}P NMR (CDCl_3 , δ): –154.49.

$\text{Ru}[\text{C}_5\text{H}_2(\text{CO}_2\text{Me-2})(\text{CO}_2\text{Me-4})(\text{CH}_2\text{CO}_2\text{Me-5})]\text{Cl}(\text{PPh}_3)_2$ (**3**). $\text{Ru}[\text{C}_5\text{H}_2(\text{CO}_2\text{Me-2})(\text{CO}_2\text{Me-4})(\text{CHCO}_2\text{Me-5})](\text{CO})(\text{PPh}_3)_2$ (**1**) (0.200 g) was heated under reflux in a solution of benzene (50 mL), methanol (12 mL), and trimethylsilyl chloride (0.180 mL) contained in a Pyrex flask illuminated with a 1000 W tungsten halogen lamp positioned 15 cm away from the flask. After 2 h more trimethylsilyl chloride (0.01 mL) was added to the flask, and the heating and illumination continued for a further 2.5 h. Over the course of the reaction the deep purple solution became bright green in color. The solvent was removed under reduced pressure, and the residue was dissolved in a minimum of the solvent mixture dichloromethane/ethanol/trimethylsilyl chloride (100:2:0.05). This solution was then purified by column chromatography on silica gel using a solution of dichloromethane/ethanol/trimethylsilyl chloride (100:2:0.05) as eluant. The band that appeared dark brown on the column but eluted as a bright green solution was collected, and on removal to the solvent **3** was obtained as a green solid (0.157 g, 78%). MS (m/z , FAB^+ , NBA): calcd for $\text{C}_{48}\text{H}_{43}^{35}\text{ClO}_6\text{P}_2^{102}\text{Ru}$, 914.12669 and $\text{C}_{48}\text{H}_{43}^{35}\text{ClO}_6\text{P}_2^{101}\text{Ru}$, 913.12792, found 914.12554, and 913.12946, respectively. Satisfactory elemental analysis could not be obtained, probably because of the small amounts of HCl that were required to be present in solution to stabilize this product and the poor crystallinity of solid samples. IR (cm^{-1}): 1720, 1586 (CO_2CH_3). ^1H NMR spectrum (CDCl_3 , δ): 3.19 (s, 2H, H6), 3.59 (s, 3H, H13), 3.63 (s, 3H, H12), 3.67 (s, 3H, H10), 7.20–7.38 (m, 30H, *PPh*₃), 8.76 (d, $^4J_{\text{HH}} = 2.4\text{ Hz}$, 1H, H3), 16.45 (dt, $^4J_{\text{HH}} = 2.7$, $^3J_{\text{HP}} = 3.0\text{ Hz}$, 1H, H1). ^{13}C NMR (CDCl_3 , δ): 50.6 (s, C12), 51.3 (s, C10), 53.5 (s, C13), 56.2 (s, C6), 124.3 (s, C4), 126.2 (s, C2), 127.4 (t' ,

$^{2,4}J_{\text{CP}} = 9.5\text{ Hz}$, *o-PPh*₃), 129.6 (s, *p-PPh*₃), 131.4 (t' , $^{1,3}J_{\text{CP}} = 43.4\text{ Hz}$, *i-PPh*₃), 133.8 (t' , $^{3,5}J_{\text{CP}} = 10.7\text{ Hz}$, *m-PPh*₃), 150.7 (s, C3), 165.2 (s, C9), 166.1 (s, C11), 182.6 (s, C7), 287.8 (t, $^2J_{\text{CP}} = 12.6\text{ Hz}$, C1), 289.3 (t, $^2J_{\text{CP}} = 10.6\text{ Hz}$, C5). ^{31}P NMR (CDCl_3 , δ): 21.55.

$\text{Ru}[\eta^5\text{-C}_5\text{H}_2(\text{CO}_2\text{Me-2})(\text{CO}_2\text{Me-4})(\text{CH}_2\text{CO}_2\text{Me-5})]\text{Cl}(\text{CO})(\text{PPh}_3)$ (**4**). Compound **4** can be obtained in low yield (ca. 10%) from a fast moving band eluted from the column described in the synthesis of **3** above. A higher yielding synthesis is as follows: $\text{Ru}[\text{C}_5\text{H}_2(\text{CO}_2\text{Me-2})(\text{CO}_2\text{Me-4})(\text{CHCO}_2\text{Me-5})](\text{CO})(\text{PPh}_3)_2$ (**1**) (0.200 g) and concentrated aqueous HCl (0.5 mL) were heated under reflux in a mixture of benzene (25 mL) and methanol (6 mL) for 5 h. After removal of the solvent under vacuum, the remaining crude solid (a mixture of unchanged **1**, **3**, and **4** in approximately equal amounts as determined by NMR spectroscopy) was dissolved in dichloromethane and a small amount of ethanol added. Upon removal of the dichloromethane under reduced pressure, **1** crystallized from solution and was removed by filtration. Excess hexane was added to the filtrate and the resulting solution left to stand for 16 h. During this time yellow crystals were deposited, and these were collected by filtration. Recrystallization from dichloromethane/hexane gave pure **4** as yellow crystals (0.030 g, 20%). Anal. Calc for $\text{C}_{31}\text{H}_{28}\text{ClO}_7\text{PRu}$: C, 54.75; H, 4.16. Found: C, 54.49; H, 4.37. MS (m/z , FAB^+ , NBA): calcd for $\text{C}_{31}\text{H}_{28}^{35}\text{ClO}_7\text{P}^{102}\text{Ru}$, 680.03047 and $\text{C}_{31}\text{H}_{28}^{37}\text{ClO}_7\text{P}^{102}\text{Ru}$, 682.02752, found 680.03035 and 682.02890, respectively. IR (cm^{-1}): 1971 $\nu(\text{CO})$; 1726, 1688, 1664 (CO_2CH_3). ^1H NMR (CDCl_3 , δ): 2.88 (d, 1H, $^2J_{\text{HH}} = 17.8\text{ Hz}$, H6), 3.31 (s, 3H, H10/H12/H13), 3.67 (s, 3H, H10/H12/H13), 3.78 (s, 3H, H10/H12/H13), 3.91 (d, 1H, $^2J_{\text{HH}} = 17.8\text{ Hz}$, H6), 4.81 (d, 1H, $^4J_{\text{HH}} = 1.3\text{ Hz}$, H1), 6.21 (d, 1H, $^4J_{\text{HH}} = 1.3\text{ Hz}$, H3), 7.19 – 7.54 (m, 15H, *PPh*₃). ^{13}C NMR (CDCl_3 , δ): 32.6 (s, C6), 51.8 (s, C10/C12/C13), 52.09 (s, C10/C12/C13), 52.1 (s, C10/C12/C13), 79.4 (s, C2/C4/C5), 82.3 (d, $^2J_{\text{CP}} = 9.1\text{ Hz}$, C2/C4/C5), 88.1 (s, C3), 99.1 (s, C1), 112.4 (s, C2/C4/C5), 128.4 (d, $^2J_{\text{CP}} = 10.8\text{ Hz}$, *o-PPh*₃), 130.6 (d, $^1J_{\text{CP}} = 51.1\text{ Hz}$, *i-PPh*₃), 133.2 (s, *p-PPh*₃), 133.5 (d, $^3J_{\text{CP}} = 10.5\text{ Hz}$, *m-PPh*₃), 164.6 (s, C11/C9/C7), 165.4 (s, C11/C9/C7), 170.4 (s, C11/C9/C7), 200.7 (d, $^2J_{\text{CP}} = 21.7\text{ Hz}$, C8). ^{31}P NMR (CDCl_3 , δ): 47.16.

$\text{Ru}[\text{C}_5\text{H}_2(\text{CO}_2\text{Me-2})(\text{CO}_2\text{Me-4})(\text{CHCO}_2\text{Me-5})](\text{CN-}p\text{-tolyl})(\text{PPh}_3)_2$ (**5**). A solution of *p*-tolyl isocyanide (0.013 g) in dichloromethane (3 mL) was added with stirring to a solution of $\text{Ru}[\text{C}_5\text{H}_2(\text{CO}_2\text{Me-2})(\text{CO}_2\text{Me-4})(\text{CH}_2\text{CO}_2\text{Me-5})]\text{Cl}(\text{PPh}_3)_2$ (**3**) (0.100 g) in dichloromethane (5 mL) at room temperature. The color of the mixture turned instantly from green to dark purple-brown. After 5 min the solvent was removed under reduced pressure and the residue subjected to column chromatography on silica gel using dichloromethane/ethanol (100:2) as eluant. The major purple band was collected and a purple solid obtained by removal of the dichloromethane under reduced pressure. This was recrystallized from dichloromethane/ethanol to yield pure **5** as purple crystals (0.048 g, 48%). Anal. Calc for $\text{C}_{56}\text{H}_{49}\text{NO}_6\text{P}_2\text{Ru}\cdot(0.25\text{CH}_2\text{Cl}_2)$: C, 66.48; H, 4.91; N, 1.38. Found: C, 66.53; H, 4.88; N, 1.34. MS (m/z , FAB^+ , NBA): calcd for $\text{C}_{56}\text{H}_{49}\text{NO}_6\text{P}_2^{102}\text{Ru}$, 995.20786 and $\text{C}_{56}\text{H}_{49}\text{NO}_6\text{P}_2^{104}\text{Ru}$, 997.20894, found 995.20793 and 997.20918, respectively. IR (cm^{-1}): 2060 $\nu(\text{CNR})$; 1714, 1577 (CO_2CH_3). ^1H NMR (CDCl_3 , δ): 2.27 (s, 3H, $\text{CNC}_6\text{H}_4\text{CH}_3$), 3.20 (s, 3H, H13), 3.53 (s, 3H, H12), 3.66 (s, 3H, H10), 5.95 (d, $^3J_{\text{HH}} = 8.3\text{ Hz}$, 2H, H14b), 6.17 (t, $^4J_{\text{HP}} = 2.7\text{ Hz}$, 1H, H6), 6.86 (d, $^3J_{\text{HH}} = 8.2\text{ Hz}$, 2H, H14c), 7.26 – 7.46 (m, 31H, *PPh*₃, and H3), 12.40 (dt, $^4J_{\text{HH}} = 1.8$, $^3J_{\text{HP}} = 1.7\text{ Hz}$, 1H, H1). ^{13}C NMR (CDCl_3 , δ): 21.1 (s, C15), 50.3 (s, C10), 50.6 (s, C12), 51.3 (s, C13), 117.1 (s, C6), 121.1 (s, C4), 124.8 (s, C14b), 127.4 (t' , $^{2,4}J_{\text{CP}} = 9.1\text{ Hz}$, *o-PPh*₃), 127.6 (s, C14a), 127.8 (s, C2), 129.1 (s, C14c), 129.3 (s, *p-PPh*₃), 133.1 (t' , $^{1,3}J_{\text{CP}} = 41.2\text{ Hz}$, *i-PPh*₃), 134.2 (t' , $^{3,5}J_{\text{CP}} = 11.1\text{ Hz}$, *m-PPh*₃), 136.3 (s, C14d), 147.4 (s, C3), 164.2 (s, C11), 168.6 (s, C9), 171.5 (t, $^2J_{\text{CP}} = 15.1\text{ Hz}$, C8), 178.8 (s, C7), 232.8 (t, $^2J_{\text{CP}} = 11.6\text{ Hz}$, C5), 245.0 (t, $^2J_{\text{CP}} = 11.6\text{ Hz}$, C1). ^{31}P NMR (CDCl_3 , δ): 43.22.

Acknowledgment. We thank the Foundation for Research, Science and Technology for supporting this work through a postdoctoral fellowship to D.M.T.

Supporting Information Available: Crystal and refinement data in CIF format for compounds **2**, **4**, and **5** are available free of charge

via the Internet at <http://pubs.acs.org> and from the Cambridge Crystallographic Data Centre (fax: +44-1223-336-033; e-mail: deposit@ccdc.cam.ac.uk or <http://www.ccdc.cam.ac.uk>) as supplementary publication nos. CCDC 699174–699176, respectively.

OM800857K

General Preparation of $(N_3N)ZrX$ ($N_3N = N(CH_2CH_2NSiMe_3)_3^{3-}$) Complexes from a Hydride Surrogate

Andrew J. Roering,[†] Annalese F. Maddox,[†] L. Taylor Elrod,[†] Stephanie M. Chan,[†] Michael B. Ghebream,[†] Kyle L. Donovan,[†] Jillian J. Davidson,[†] Russell P. Hughes,[§] Tamila Shalumova,[‡] Samantha N. MacMillan,^{‡,⊥} Joseph M. Tanski,[‡] and Rory Waterman^{*†}

Department of Chemistry, University of Vermont, Burlington, Vermont 05405, Department of Chemistry, Dartmouth College, Hanover, New Hampshire 03755, and Department of Chemistry, Vassar College, Poughkeepsie, New York 12604

Received September 5, 2008

A homoleptic triamidoamine zirconium complex featuring a metalated trimethylsilyl substituent, $[\kappa^5-(Me_3SiNCH_2CH_2)_2NCH_2CH_2NSiMe_2CH_2]Zr$ (**1**), was synthesized by reaction of $Zr(CH_2Ph)_4$ with $N(CH_2CH_2NHSiMe_3)_3$ followed by sublimation. Complex **1** is a general precursor to a family of complexes with the formulation $(N_3N)ZrX$ ($N_3N = N(CH_2CH_2NSiMe_3)_3^{3-}$, $X =$ anionic ligand) by reactions that parallel expected reactivity of a hydride derivative. Treatment of **1** with phosphines, amines, thiols, alkynes, and phenol resulted in the formation of new, pseudo- C_{3v} -symmetric $(N_3N)ZrX$ complexes ($X =$ phosphido, amido, alkynyl, thiolate, or phenoxide) via element–H bond activation. Thus, the reactivity of complex **1** is that best described as a *hydride surrogate*. For example, complex **1** reacted with $PhPH_2$ at ambient temperature to provide $(N_3N)ZrPPh$ (**2**) in 86% yield. Density functional theory studies and X-ray crystal structures provide a general overview of the bonding in these complexes, which appears to be highly ionic. In general, there is little evidence for ligand-to-metal π -bonding for the pseudoaxial X ligand in these complexes except for strongly π -basic terminal amido ligands. The limited π -bonding appears to be the result of competitive π -donation by the pseudoequatorial amido arms of the triamidoamine ancillary ligand. Thus, the relative Zr– X bond energies are governed by the basicity of the anionic ligand X . Solid-state structures of phosphido (**3**, **4**, **5**), amido (**10**), and thiolate (**15**) complexes support the computational results.

Introduction

Metal-catalyzed element–element bond formation has garnered increased attention because of the main-group small molecules, polymers, and materials that have already been realized.^{1–5} Thus, simple, readily prepared metal catalysts have become increasingly desirable for this chemistry. The commercially available triamidoamine ligand has been used extensively in early transition-metal chemistry. In particular, these ligands have seen substantial application in supporting group 5 and 6 metals featuring multiply bonded ligands.^{6,7} Despite the well-established value of triamidoamine ligands in synthetic inorganic chemistry, these ligands have seen far less use in catalysis.⁸

Recently however, triamidoamine-supported zirconium complexes have demonstrated reactivity in element–element bond-forming reactions. These complexes affected the catalytic dehydrocoupling of phosphines and, under appropriate conditions, selectively forming diphosphine products.⁹ Similarly, these complexes engaged in the catalytic dehydrocoupling of arsines, and for sterically encumbered primary arsines, evidence for α -arsinidene elimination was observed.¹⁰ Furthermore, these zirconium species catalyzed the heterodehydrocoupling of primary phosphines with silanes or germanes to provide P–E ($E = Si, Ge$) bonds.¹¹ Recently, these complexes have facilitated the synthesis of a phosphalkene with perfect atom economy.¹²

The reported preparation of primary phosphido complexes $(N_3N)ZrPHR$ ($N_3N = N(CH_2CH_2NSiMe_3)_3^{3-}$; $R = Ph$, **2**; Cy , **3**)⁹ began with the synthesis of $(N_3N)ZrNMe_2$, discovered by Verkade and co-workers,¹² and utilized elements of the preparations of highly related $(N'_3N)ZrX$ complexes ($N'_3N = N(CH_2CH_2NSi^iBuMe_2)_3^{3-}$; $X =$ monoanionic ligand) reported by Scott.^{13,14} This synthesis, though effective, was time-consuming and provided an overall yield of less than 50% of

* Corresponding author. E-mail: rory.waterman@uvm.edu.

[†] University of Vermont.

[§] Dartmouth College.

[‡] Vassar College.

[⊥] Current address: Department of Chemistry, Massachusetts Institute of Technology.

(1) Herbert, D. E.; Mayer, U. F. J.; Manners, I. *Angew. Chem., Int. Ed.* **2007**, *46*, 5060–5081.

(2) Clark, T. J.; Lee, K.; Manners, I. *Chem.–Eur. J.* **2006**, *12*, 8634–8648.

(3) Masuda, J. D.; Hoskin, A. J.; Graham, T. W.; Beddie, C.; Fermin, M. C.; Etkin, N.; Stephan, D. W. *Chem.–Eur. J.* **2006**, *12*, 8696–8707.

(4) Waterman, R. *Curr. Org. Chem.* **2008**, *12*, 1322–1339.

(5) Gauvin, F.; Harrod, J. F.; Woo, H. G. *Adv. Organomet. Chem.* **1998**, *42*, 363–405.

(6) Balazs, G.; Gregoriades, L. J.; Scheer, M. *Organometallics* **2007**, *26*, 3058–3075.

(7) Schrock, R. R. *Acc. Chem. Res.* **1997**, *30*, 9–16.

(8) Schrock, R. R. *Acc. Chem. Res.* **2005**, *38*, 955–962.

(9) Waterman, R. *Organometallics* **2007**, *26*, 2492–2494.

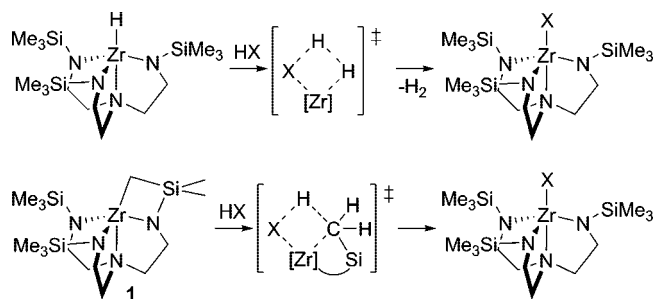
(10) Roering, A. J.; MacMillan, S. N.; Tanski, J. M.; Waterman, R. *Inorg. Chem.* **2007**, *46*, 6855–6857.

(11) Roering, A. J.; Davidson, J. J.; MacMillan, S. N.; Tanski, J. M.; Waterman, R. *Dalton Trans.* **2008**, 4488–4498.

(12) MacMillan, S. N.; Tanski, J. M.; Waterman, R. *Chem. Commun.* **2007**, 4172–4174.

(13) Duan, Z.; Naiini, A. A.; Lee, J.-H.; Verkade, J. G. *Inorg. Chem.* **1995**, *34*, 5477–5482.

(14) Morton, C.; Munslow, I. J.; Sanders, C. J.; Alcock, N. W.; Scott, P. *Organometallics* **1999**, *18*, 4608–4613.

Scheme 1. Metalated Complex 1 Acting As a Hydride Surrogate


the desired phosphido derivatives **2** or **3**. Given the value of these zirconium complexes as catalysts,^{9–11} a simplified preparation of the metal complexes was sought. A zirconium hydride complex, $(N_3N)ZrH$, would be an ideal precursor. However, $(N_3N)MH$ ($M =$ group 4 metal) complexes are exceedingly rare. Schrock and co-workers have reported the observation of $(N_3N)TiH$, but this complex was not isolable due to a cyclometalation process involving a trimethylsilyl substituent.^{15,16} In related $(N'_3N)Zr$ complex chemistry, a hydride ligand was not observed, and only a cyclometalated product was isolated. Facile H/D exchange at the methyl substituents of the Si^tBuMe_2 groups with D_2 provided strong evidence for the importance of such a hydride complex.¹⁴ Later, Scott successfully thwarted this metalation process by replacing the trialkylsilyl substituents with aryl groups on the triamidoamine ligand framework. Unfortunately, these new derivatives did not yield an isolable zirconium hydride.¹⁷ Likewise, it was observed that any putative $(N_3N)ZrH$ complex readily metalated to give $[κ^5-N,N,N,N,C-(Me_3Si-NCH_2CH_2)_2NCH_2CH_2NSiMe_2CH_2]Zr$ (**1**) as the exclusive product. The discovery that **1** is important in the dehydrocoupling of phosphines suggested that this compound may provide a route to $(N_3N)ZrX$ complexes.⁹

It was our hypothesis that the cyclometalated complex **1** would be a general synthetic precursor to $(N_3N)ZrX$ species by acting as a *hydride surrogate* (Scheme 1). The inability to isolate $(N_3N)ZrH$ makes complex **1** the closest accessible chemical species, and it has been observed that $(N_3N)ZrH$ is unstable with respect to cyclometalation to form **1** and H_2 .⁹ Furthermore, complex **1** is important in the catalytic dehydrocoupling of phosphines as the likely precursor to Zr-phosphido complexes. A hydride complex would be expected to react with polar element–hydrogen bonds ($H-X$) to afford $(N_3N)ZrX$ and liberate H_2 as the driving force (Scheme 1). Complex **1** may also react with $H-X$ bonds to form $(N_3N)ZrX$ and restore the trimethylsilyl substituent. The latter reactivity would rely on the strength of the resultant $Zr-X$ bond and the methyl $C-H$ bond, which would presumably be a reasonable driving force.

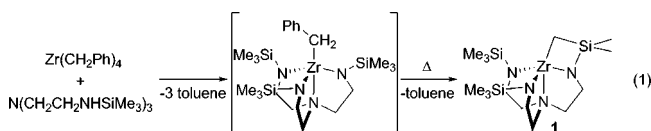
Herein, we report a new preparation of the metalated complex **1** based on methodology described by Scott and co-workers⁷ and demonstrate that complex **1** is a general precursor to $(N_3N)ZrX$ complexes, where X can be an alkynyl, amido, phenoxide, phosphido, or thiolate ligand. This reactivity of complex **1** is best described as a that of a hydride surrogate, affording Zr-products that would be expected from reaction of $(N_3N)ZrH$ with HX . Theoretical studies and solid-state data on

the family of $(N_3N)ZrX$ complexes suggest that the bonding in these complexes is highly ionic and that there is little π -bonding character from most pseudoaxial X ligands with the exception of strong π -bases such as amido ligands. The limited π -interaction may explain the high reactivity of the $Zr-X$ bond already seen in stoichiometric and catalytic reactions.^{9–12}

Results and Discussion

Preparation of Metalated Complex 1. Reaction of $Zr(CH_2Ph)_4$ with 1 equiv of $N(CH_2CH_2NHSiMe_3)_3$ resulted in liberation of toluene to give an oily brown solution. Monitoring the reaction by 1H NMR spectroscopy (benzene- d_6) revealed a mixture of products including starting material as well as a new pseudo- C_3 -symmetric complex. This complex was tentatively assigned as $(N_3N)Zr(\eta^1-CH_2Ph)$ based partly on a diagnostic methylene resonance at δ 2.44. Efforts to isolate or crystallize this benzyl complex from a variety of solvents such as hexane, toluene, and Et_2O were ineffective, and only a mixture of products including $[κ^5-N,N,N,N,C-(Me_3SiNCH_2CH_2)_2NCH_2CH_2NSiMe_2CH_2]Zr$ (**1**) was obtained. A highly related zirconium benzyl complex, $(N'_3N)Zr(\eta^1-CH_2Ph)$, was isolated by the group of Scott, and this complex displayed very similar 1H NMR spectroscopic data.¹⁴

Heating the aforementioned reaction mixture under reduced pressure followed by sublimation at temperatures greater than $100^\circ C$ resulted in the isolation of **1** as a colorless solid in 73% yield (eq 2). Complex **1** can be similarly prepared by heating isolated $(N_3N)ZrMe$; however, the preparation of this complex requires three synthetic steps from $N(CH_2CH_2NHSiMe_3)_3$.⁹



Interestingly, complex **1** prepared by this method exhibited increased resolution in the 1H NMR spectrum. For example, the zirconium methylene resonance at δ 0.314 could be distinguished from the trimethylsilyl methyl resonances at δ 0.274. Otherwise, spectroscopic data for **1** was identical to authentic samples prepared by the literature route.⁹ Sublimed samples of **1** from the literature route gave the same spectroscopic data as this preparation. Attempts to hydrogenate either the putative benzyl complex or **1** to observe or isolate a zirconium hydride complex have thus far been unsuccessful.

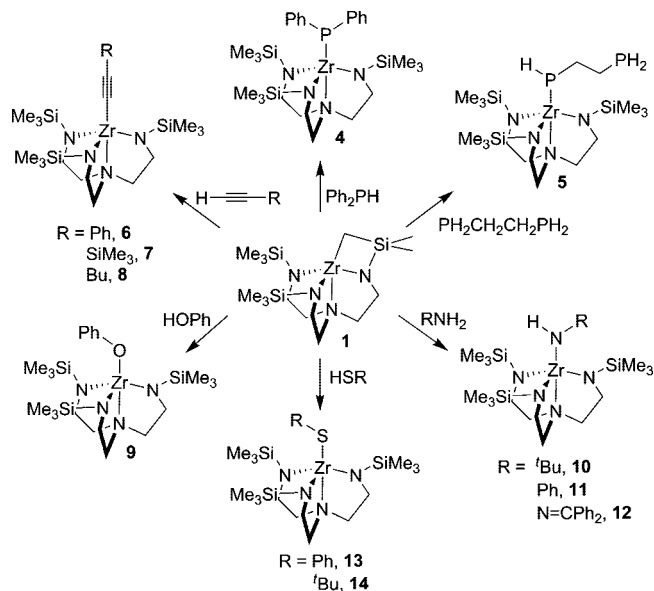
Hydride Surrogate Reactivity of Complex 1. Complex **1** was first observed in the preparation of primary phosphido derivatives $(N_3N)ZrPHR$ ($R = Ph, Cy$) by reaction of RPH_2 with $(N_3N)ZrMe$. These studies suggested that **1** may be a general precursor to $(N_3N)ZrX$ complexes with overall reactivity that would parallel a hydride complex.⁹

Treatment of **1** with either phenyl- or cyclohexylphosphine in Et_2O at ambient temperature afforded of the corresponding phosphido complex $(N_3N)ZrPHR$ ($R = Ph, 2$; $R = Cy, 3$) in 86 and 89% isolated yield, respectively (eq 2). Monitoring the reaction by 1H and ^{31}P NMR spectroscopy (benzene- d_6) showed quantitative conversion to the phosphido complex products. Compounds **2** and **3** gave identical spectral data to authentic samples prepared by the known method.⁹ Starting from metalated complex **1**, the new preparation of these phosphido compounds was more efficient than previously reported. The overall yield of phenylphosphido complex **2** was 64% from commercially available $Zr(CH_2Ph)_4$. This is a significant improvement over the 48% overall yield for **2** starting from

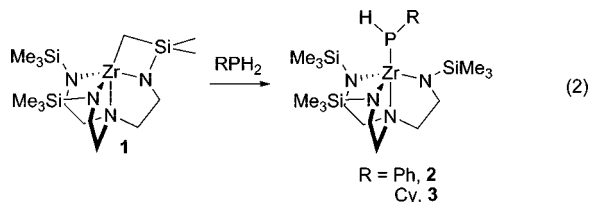
(15) Cummins, C. C.; Schrock, R. R.; Davis, W. M. *Organometallics* **1992**, *11*, 1452–1454.

(16) Schrock, R. R.; Cummins, C. C.; Wilhelm, T.; Lin, S.; Reid, S. M.; Kol, M.; Davis, W. M. *Organometallics* **1996**, *15*, 1470–1476.

(17) Morton, C.; Gillespie, K. M.; Sanders, C. J.; Scott, P. *J. Organomet. Chem.* **2000**, *606*, 141–146.

Scheme 2. General Preparation of (N₃N)ZrX Derivatives from Compound 1

commercially available Zr(NMe₂)₄ by the published route.^{9,13} This increased efficiency is due to the synthetic steps saved by use of complex 1 as a “(N₃N)Zr” synthon. Thus, phosphido complexes were prepared in a single step by the addition of phosphine to complex 1.



The use of complex 1 as a hydride surrogate in the preparation of (N₃N)ZrX complexes is general. Reaction of diphenylphosphine with 1 in benzene at ambient temperature afforded analytically pure, bright red crystals of (N₃N)ZrPPh₂ (4) in 80% yield (Scheme 2). Complex 4 displayed pseudo-C₃-symmetry with respect to the triamidoamine ligand in the ¹H NMR spectrum as well as a characteristic zirconium phosphido ³¹P NMR resonance at δ 85.3.^{9,18,19} Free rotation of P–C and Zr–P bonds was evident by the equivalent phenyl resonances in the ¹H and ¹³C NMR spectra. Confirmation of the solution structure of complex 4 came from a single-crystal X-ray diffraction study. Single crystals of 4 were obtained by slow evaporation of Et₂O solvent over a period of ca. 2 h. The solid-state structure of 4 (Figure 1) features a trigonal-bipyramidal zirconium center (τ = 1.0)²⁰ with Zr–P = 2.7061(4) Å and a long Zr–N_{amine} bond, Zr–N = 2.523(1) Å (Table 1), and an approximately pyramidal phosphorus atom (Σ∠ at P ≈ 341°). Other terminal zirconium phosphido complexes display similar structures and Zr–P bond lengths in the solid state.^{10,19,21–23}

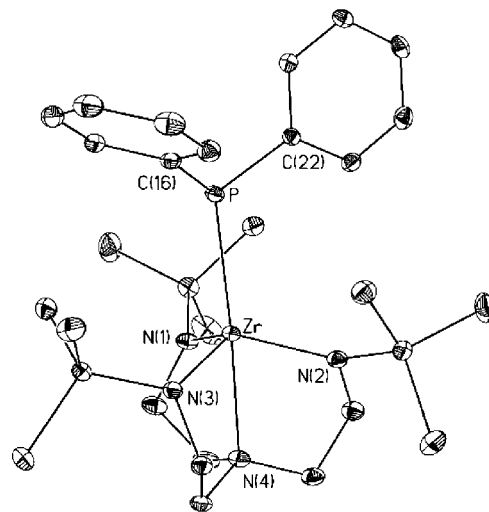


Figure 1. Molecular structure of (N₃N)ZrPPh₂ (4) with thermal ellipsoids drawn at the 35% level. Hydrogen atoms are omitted for clarity.

Table 1. Selected Bond Lengths (Å) and Angles (deg) for (N₃N)ZrPPh₂ (4)

Table 1. Selected Bond Lengths (Å) and Angles (deg) for (N ₃ N)ZrPPh ₂ (4)			
Zr–P	2.7061(4)	Zr–N(1)	2.071(1)
P–C(16)	1.835(1)	Zr–N(2)	2.083(1)
P–C(22)	1.820(1)	Zr–N(3)	2.045(1)
		Zr–N(4)	2.523(1)
Zr–P–C(16)	119.06(5)	N(1)–Zr–P	102.58(4)
Zr–P–C(22)	118.49(5)	N(2)–Zr–P	110.06(3)
C(16)–P–C(22)	103.74(6)	N(3)–Zr–P	106.47(3)
		N(4)–Zr–P	175.87(3)

Treatment of 1 with 1 equiv of 1,2-diphosphinoethane in ethereal solution at ambient temperature gave analytically pure, light orange crystals of (N₃N)ZrPCH₂CH₂PH₂ (5) in 76% yield (Scheme 2). Spectroscopic data (¹H, ¹³C NMR and IR) of complex 5 were consistent with the formulation given. The ³¹P NMR spectrum of 5 revealed two phosphorus environments, one for the zirconium-bound phosphido ligand at δ –72.4 and the other for the free phosphine at δ –133. Single crystals of 5 were obtained by cooling a concentrated Et₂O solution of 5 at –30 °C for extended periods. The molecular structure of 5, shown in Figure 2, was found to be trigonal bipyramidal at the zirconium center (τ = 1.1) with a Zr–P = 2.7185(7) Å (Table 2). The τ value greater than unity reflects the fact that the zirconium center lies above the trigonal plane formed by the amido nitrogen substituents of the N₃N ligand. Though it is greater than 1, the τ parameter indicates that complex 5 is much closer to a trigonal-bipyramidal geometry than square-based pyramid.

Zirconium–carbon bonds can be formed using hydride surrogate 1 (Scheme 2). Terminal alkynes reacted rapidly with 1 to provide analytically pure, colorless microcrystals of alkyne derivatives (N₃N)ZrC_αC_βR (R = Ph, 6; SiMe₃, 7; Bu, 8) in 74–84% isolated yield. Complexes 6, 7, and 8 gave expected spectroscopic data for terminal alkyne complexes, and diagnostic features of these complexes are summarized in Table 3.

Reaction of 1 with phenol in Et₂O at ambient temperature afforded analytically pure, colorless microcrystals of (N₃N)ZrOPh (9) in 85% yield (Scheme 2). Complex 9 gave expected and unremarkable spectroscopic data. Attempts to synthesize alkoxide complexes have met with limited success. In reactions of 1 with alcohols or water, a mixture of products was obtained that appeared to contain the desired (N₃N)ZrOR (R = alkyl, H), but pure complexes have not yet been isolated.

(18) Roddick, D. M.; Santarsiero, B. D.; Bercaw, J. E. *J. Am. Chem. Soc.* **1985**, *107*, 4670–4678.

(19) Vaughan, G. A.; Hillhouse, G. L.; Rheingold, A. L. *Organometallics* **1989**, *8*, 1760–1765.

(20) Addison, A. W.; Rao, T. N.; Reedijk, J.; Rijn, J. v.; Verschoor, G. C. *J. Chem. Soc., Dalton Trans* **1984**, *134*, 9–1356.

(21) Hey-Hawkins, E. *Chem. Rev.* **1994**, *94*, 1661–1717.

(22) Stephan, D. W. *Angew. Chem., Int. Ed.* **2000**, *39*, 315–329.

(23) Urnezis, E.; Klippenstein, S. J.; Protasiewicz, J. D. *Inorg. Chim. Acta* **2000**, *297*, 181–190.

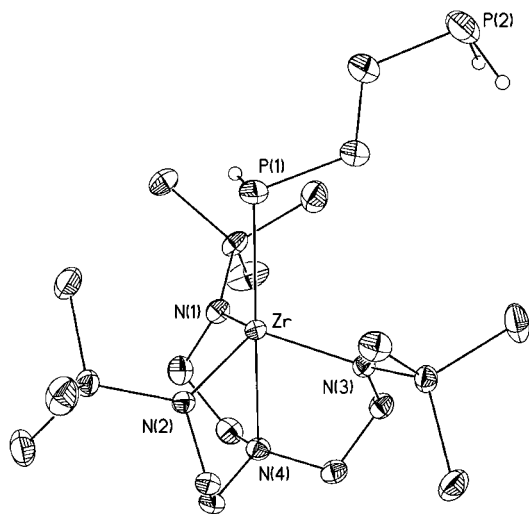


Figure 2. Molecular structure of $(N_3N)ZrPHCH_2CH_2PH_2$ (**5**) with thermal ellipsoids drawn at the 35% level. Hydrogen atoms except those located on P(1) and P(2) are omitted for clarity.

Table 2. Selected Bond Lengths (Å) and Angles (deg) for $(N_3N)ZrPHCH_2CH_2PH_2$ (**5**)

Zr–P(1)	2.7185(7)	Zr–N(1)	2.055(1)
P(1)–C(16)	1.883(3)	Zr–N(2)	2.060(1)
Zr–N(4)	2.540(1)	Zr–N(3)	2.061(1)
C(16)–P(1)–Zr	107.21(8)	N(1)–Zr–P(1)	106.15(5)
C(16)–P(1)–H(1)	99.40(1)	N(2)–Zr–P(1)	107.11(5)
Zr–P(1)–H(1)	88.40(1)	N(3)–Zr–P(1)	106.79(5)
		N(4)–Zr–P(1)	179.47(4)

Table 3. Selected ^{13}C NMR^a and IR^b Spectroscopic Data for Compounds **6**, **7**, and **8**

	6	7	8
C_α	131.77	113.49	107.74
C_β	147.36	169.97	138.43
ν_{cc}	2076	2029	2081

^a In ppm. ^b In cm^{-1} .

Complex **1** provides a facile route to terminal amido complexes (Scheme 2). Treatment of **1** with 1 equiv of *tert*-butyl amine in benzene at ambient temperature gave analytically pure, colorless crystals of $(N_3N)ZrNH^tBu$ (**10**) in 73% yield. Key spectroscopic data for complex **10** include an NH resonance at δ 3.856 in the 1H NMR spectrum and $\nu_{NH} = 3210\text{ cm}^{-1}$ in the infrared. Single crystals of **10** were grown from a concentrated Et_2O solution kept at $-30\text{ }^\circ C$ for extended periods and were subject to a single-crystal X-ray study. The molecular structure of **10**, shown in Figure 3, is truly C_{3v} -symmetric with respect to the triamidoamine ligand. The complex was found to be trigonal bipyramidal at zirconium ($\tau = 0.94$) and planar at the amido nitrogen, N(3). The planar amido nitrogen is consistent with ligand-to-metal π -donation, a structural feature that has been seen for $(N_3N)ZrNMe_2$.¹⁴

Similarly, reaction of **1** with aniline and in benzene at ambient temperature afforded analytically pure, colorless crystals of $(N_3N)ZrNHPh$ (**11**) in 92% yield (Scheme 2). Complex **11** showed pseudo- C_{3v} -symmetry with respect to the triamidoamine ligand and showed typical 1H and ^{13}C NMR resonances with diagnostic features $NH = \delta$ 5.962 in the 1H NMR spectrum and $\nu_{NH} = 3244\text{ cm}^{-1}$ in the infrared.

Other Zr-amido complexes can also be prepared by this route. Treatment of benzophenone hydrazone with **1** in Et_2O at ambient temperature afforded analytically pure, yellow crystals of

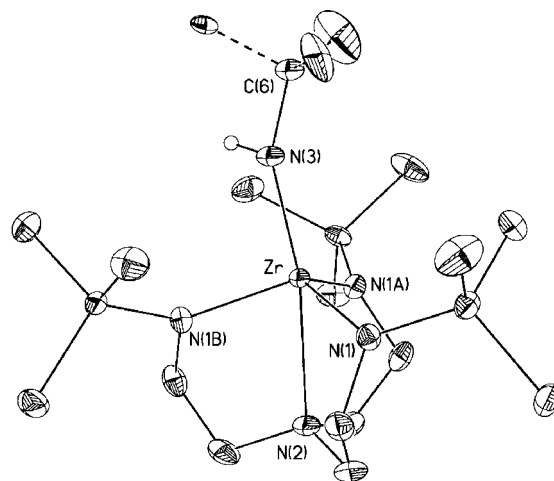
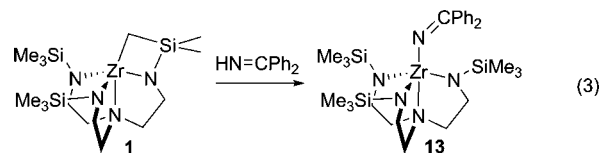


Figure 3. Molecular structure of $(N_3N)ZrNH^tBu$ (**10**) with thermal ellipsoids drawn at the 35% level. Hydrogen atoms except for H(3), located on N(3), are omitted for clarity. Selected bond lengths (Å): Zr–N(3) = 2.071(3), Zr–N(1) = 2.088(1), Zr–N(2) = 2.552(2), N(3)–C(6) = 1.492(3).

$(N_3N)ZrNHN=CPh_2$ (**12**) in 25% yield (Scheme 2). Diagnostic features of the N–H moiety include δ 8.068 in the 1H NMR spectrum and $\nu_{NH} = 3299\text{ cm}^{-1}$ in the infrared for **12**. Complex **1** reacted rapidly with 1 equiv of benzophenone imine to give $(N_3N)ZrN=CPh_2$ (**13**) as an analytically pure, orange powder in 82% yield (eq 3). Spectroscopic features for the iminido ligand included δ 174.8 in the ^{13}C NMR spectrum and $\nu_{CN} = 1641\text{ cm}^{-1}$ in the infrared.



Thiols reacted readily with **1** to form Zr–S bonds (Scheme 2). Treatment of **1** with benzenethiol or *tert*-butylthiol in Et_2O at ambient temperature gave analytically pure, colorless crystals of $(N_3N)ZrSPh$ (**14**) or $(N_3N)ZrS^tBu$ (**15**) in 44% and 64% yield, respectively. Spectroscopic data (1H , ^{13}C NMR and IR) for **14** and **15** supported the formulation given. Single crystals of **15** were grown from concentrated 20:1 toluene/hexane solvent mixture cooled to $-30\text{ }^\circ C$. The molecular structure of **15** (Figure 4) features trigonal-bipyramidal geometry at the zirconium center ($\tau = 0.94$) with Zr–S = 2.5154(4) Å (Table 4, 5). The crystal structure also revealed sulfur displaying bent geometry with a Zr–S–C = 127.74(4) $^\circ$. Other zirconium *tert*-butyl thiolate complexes possess similar bond angles. For $Cp_2Zr(S^tBu)_2$, Zr–S–C = 123 $^\circ$ was observed, while arylthiolates $Cp_2Zr(SPh)_2$ and $Cp_2Zr[S(p-C_6H_4Cl)]_2$ displayed Zr–S–C angles of 119 $^\circ$ and 109 $^\circ$, respectively.^{24–26} It appears that the nature of the organothiol substituent has a great impact on the Zr–S–C bond angle.

It is important to note that while the isolated yields of $(N_3N)ZrX$ complexes varied, in all cases, monitoring the reaction of **1** with any of these HX reagents by NMR spectroscopy

(24) Ashby, M. T.; Alguindigue, S. S.; Khan, M. A. *Inorg. Chim. Acta* **1998**, *270*, 227–237.

(25) Howard, W. A.; Trnka, T. M.; Parkin, G. *Inorg. Chem.* **1995**, *34*, 5900–5909.

(26) Yam, V. W.-W.; Qi, G.-Z.; Cheung, K.-K. *J. Organomet. Chem.* **1997**, *548*, 289–294.

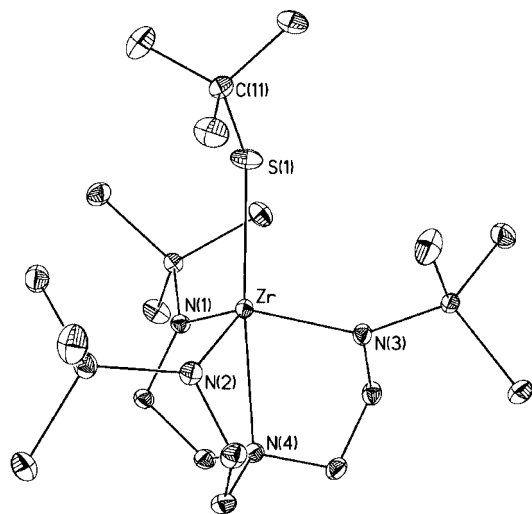


Figure 4. Molecular structure of $(N_3N)ZrS'Bu$ (**15**) with thermal ellipsoids drawn at the 35% level. Hydrogen atoms omitted for clarity.

Table 4. Selected Bond Lengths (Å) and Angles (deg) for $(N_3N)ZrS'Bu$ (**15**)

Zr–S	2.5154(4)	Zr–N(1)	2.066(1)
S–C(16)	1.848(1)	Zr–N(2)	2.076(1)
Zr–N(4)	2.530(1)	Zr–N(3)	2.079(1)
Zr–S–C(16)	127.74(4)	N(3)–Zr–S	102.02(3)
N(1)–Zr–S	101.67(3)	N(4)–Zr–S	170.73(3)
N(2)–Zr–S	115.95(3)		

Table 5. Selected Bond Lengths (Å) and Angles (deg) for $(N_3N)ZrPHCy$ (**3**)

Zr–P	2.734(1)	Zr–N(1)	2.071(1)
P–C(21)	1.890(4)	Zr–N(2)	2.061(1)
Zr–N(4)	2.532(1)	Zr–N(3)	2.066(1)
C(21)–P–Zr	118.0(1)	N(1)–Zr–P	98.02(6)
C(21)–P–H(1)	99(2)	N(2)–Zr–P	112.30(6)
Zr–P–H(1)	100(2)	N(3)–Zr–P	109.24(5)
		N(4)–Zr–P	171.06(6)

(benzene- d_6) showed quantitative conversion to the desired $(N_3N)ZrX$ product. The variety of complexes that can be prepared by using **1** as a hydride surrogate (*vide supra*) suggests that any moderate acidic HX reagent or reactive H–X bond could yield a $(N_3N)ZrX$ complex.

Bonding. The bonding and electronic structure of these complexes, key considerations for any catalytic reaction, were investigated by DFT calculations performed at the B3LYP/LACV3P**++ level of theory using the Jaguar program suite. In these calculations, optimized gas-phase structures of complexes **1–3** were obtained. Similarly structures of the hydride $(N_3N)ZrH$, a model alkynyl complex $(N_3N)ZrC\equiv CH$, and the known, structurally characterized methyl derivative $(N_3N)ZrCH_3$ (**16**)²⁷ were optimized. These optimized structures compared very favorably with X-ray crystallographic structures for complexes **2**, **3**, and **16**. An X-ray diffraction study of **3** was performed on single crystals grown from a concentrated ethereal solution cooled to -30 °C, and a perspective view of the molecular structure can be found in Figure 5. A comparison of the bond lengths and angles for the solid-state structures of **2** and **3** with the gas-phase DFT calculation can be found in Table 6. The tabulated data show strong agreement between the calculations and solid-state structures.

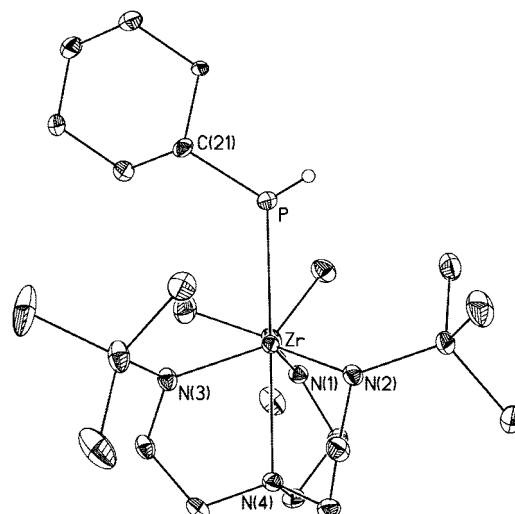


Figure 5. Molecular structure of $(N_3N)ZrPHCy$ (**3**) with thermal ellipsoids drawn at the 35% level. The 65% occupancy model for the 2-fold cyclohexyl disorder is shown here with hydrogen atoms except for H(1), located on P(1), omitted for clarity.

Table 6. Selected Bond Lengths (Å) and angles (deg) for the Solid-State and Minimized Structures of **2** and **3**

bond	$(N_3N)ZrPPh$ (2)		$(N_3N)ZrPHCy$ (3)	
	calc	X-ray	calc	X-ray ^a
Zr–P	2.739	2.7254(6)	2.696	2.734(1)
P–C	1.839	1.830(2)	1.892	1.890(4)
Zr–N _{amine}	2.633	2.526(2)	2.631	2.532(1)
Zr–N _{amido} ^b	2.104	2.059(5)	2.110	2.066(5)
Zr–P–C	118.0	111.50(7)	124.0	118.0(1)
N _{amine} –Zr–P	175.6	175.44(4)	173.2	171.06(6)
N _{amido} –Zr–P ^b	107.7	106.3	107.5	106.5
Σ∠ at P ^c	316.4	305.7	326.2	317

^a Data from one of two orientations of the Cy moiety in the crystal.

^b Simple average of the three amido substituents. ^c Sum of the angles at phosphorus.

A detailed picture of the bonding in these molecules was obtained by natural bond order (NBO) and related natural resonance theory (NRT) and natural population analyses (NPA) of the molecules. From this set of calculations several general trends regarding the bonding in these complexes have emerged. First, there is a high degree of polarization resulting from very ionic bonding between the amido arms of the triamidoamine ligand and the zirconium center. The same is true for the pseudoaxial X ligand, where X is amido, phosphido, hydride, methide, or acetylide in these calculations. For example, in the methide complex **16**, the Zr–CH₃ σ -bond is strongly polarized, with ~16% of the electron density on Zr and ~84% on C. Likewise, the Zr bonds to the amido arms have σ - and π -components, with both components even more strongly polarized compared to the Zr–C bond. The electron density in the σ -component is only ~10% on Zr and ~90% on N, compared to ~6% on Zr and 94% on N in its π -counterpart.

Second, the bond between the axial amine nitrogen of the triamidoamine ligand and zirconium is quite weak. This weak bond is evident in the solid-state structures of these $(N_3N)ZrX$ complexes by the Zr–N_{amine} bond length of ca. 2.53 Å (Zr–N(4) = 2.523(1)–2.540(1) Å, *vide supra*). This weak bonding to the fifth neutral ligand appears to promote a more tetrahedral-like electronic structure at zirconium. This weak bond may also be part of the reason that three amido arms of the N_3N ligand are not coplanar with Zr, as seen in the minimized structures and in the solid-state data. NBO analysis reveals that the lone

(27) MacMillan, S. N.; Tanski, J. M.; Waterman, R. *Acta Crystallogr.* **2008**, E64, m477.

pair on the axial N in **16** is rather localized on the N (occupancy = 1.85 electrons) with only slight stabilization (~15 kcal/mol) by delocalization into the Zr–C σ^* orbital (giving a weak three-center/four-electron bond). The use of second-order perturbative NBO analysis for estimating such stabilization energies from the off-diagonal Fock matrix element expressed in the NBO basis has been thoroughly described and is now well established.^{28–30}

Third, the amido substituents of the N₃N ligand display strong π -donation to the zirconium center, resulting in a significant, though ionic, π -bonding component to the interaction. This insight is also reflected in the solid-state data. The amido arms are planar at nitrogen and have short Zr–N bonds of ca. 2.07 Å (2.045(1)–2.083(1) Å, *vide supra*). A simple orbital analysis on an idealized trigonal-bipyramidal complex suggests that three π -bonds in the equatorial plane is symmetry forbidden. A more tetrahedral-like geometry at zirconium, with the weakened bond between zirconium and the amine nitrogen of the N₃N ligand, would relax the symmetry requirements of a trigonal-bipyramidal structure and allow for more ligand-to-metal π -donation from the amido nitrogen atoms.

The degree of π -bonding from the N₃N ligand likely limits π -donation from the pseudoaxial X ligand to only the most π -basic ligands. Therefore, all structurally characterized phosphido complexes have pyramidal phosphorus centers, and in the two structurally characterized amido complexes, **10** and (N₃N)ZrNMe₂,¹³ the nitrogen centers are planar. In the calculations, the phosphido ligands did not display any significant π -bonding. It would be expected that the axial ligands that display little π -donation may have weak M–X bonds and be reactive. Indeed, the zirconium phosphido and arsenido derivatives have exhibited substantial reactivity.^{9,11}

While cognizant of the caveats,³¹ careful application of DFT does provide an opportunity to compute bond dissociation enthalpies (BDEs), and the B3LYP functional coupled with the LACV3P**++ basis set have been used to compute a large number of such values for idealized transition metal compounds.³² Consequently, the same techniques were applied to evaluating BDE values for the Zr–X bonds in representative (N₃N)ZrX compounds. Values appear in Table 7, and correspond to ΔH_{298} for the gas-phase homolytic process (eq 4),



for which zero-point energy corrected values of H_{298} were calculated for all three components in their fully optimized and unconstrained structures; radicals were treated using unrestricted methods with the assumption of doublet ground states in all cases. The “universal” B3LYP correction (addition of 2 kcal mol^{−1} to the computed values of H_{298})³³ was made for all radical species. Inclusion of this correction gave excellent agreement between benchmark computational and experimental³⁴ (in parentheses) BDE values (kcal mol^{−1}) for H₂P–H [82.3 (83.9

(28) Leyssens, T.; Peeters, D.; Orpen, A. G.; Harvey, J. N. *Organometallics* **2007**, *26*, 2637–2645.

(29) Leyssens, T.; Peeters, D. *J. Org. Chem.* **2008**, *73*, 2725–2730.

(30) Leyssens, T.; Peeters, D.; Orpen, A. G.; Harvey, J. N. *New J. Chem.* **2005**, *29*, 1424–1430.

(31) Cundari, T. R., Crabtree, R., Mingos, M., Eds. *The Application of Modern Computational Chemistry Methods to Organometallic Systems*. In *Comprehensive Organometallic Chemistry III*; Elsevier Ltd., 2007; Vol. 1, pp 639–669.

(32) Uddin, J.; Morales, C. M.; Maynard, J. H.; Landis, C. R. *Organometallics* **2006**, *25*, 5566–5581.

(33) Wright, J. S.; Rowley, C. N.; Chepelev, L. L. *Mol. Phys.* **2005**, *103*, 815–823.

(34) Luo, Y.-R. *Comprehensive Handbook of Chemical Bond Energies*; CRC Press: Boca Raton, FL, 2007.

Table 7. Bond Dissociation Energies (BDEs) for Gas-Phase Minimized Structures of Triamidoamine-Supported Zirconium Complexes^a

compound	BDE ^b
(N ₃ N)ZrH	81.7
(N ₃ N)ZrCH ₃ (16)	72.4
(N ₃ N)ZrPPh (2)	55.4
(N ₃ N)ZrPHCy (3)	56.2
(N ₃ N)ZrC≡CH	126.0
(N# ₃ N)ZrH	78.1
(N# ₃ N)ZrCH ₃	71.8
(N# ₃ N)ZrNH ₂	102.8
(N# ₃ N)ZrPH ₂	65.3
(N# ₃ N)ZrPPh	56.5
(N# ₃ N)ZrPHCy	58.5

^a N[#]₃N ligand (N[#]₃N = N(CH₂CH₂NSiH₃)₃[−]) was used in some cases to simplify the computation. ^b BDEs (ΔH_{298}) in kcal mol^{−1} with estimated errors of 1–2 kcal mol^{−1}.

± 0.5), H₂N–H [106.7 (107.57 ± 0.06)], (CH₃)HP–H [80.4 (77.0 ± 3.0)], H₃C–H [105.0 (105.0 ± 0.09)], and HC≡C–H [135.4 (133.32 ± 0.07)]. While it not clear whether such a correction is required for transition-metal radicals, the same correction was applied to the zirconium radicals to be consistent. Because the zirconium radical is the same in a particular series of BDE values, the *trends* in BDEs should be real, even if absolute values may require further refinement. Though there are no experimental BDE values with which to compare computed numbers for this system, there is a decreasing order of BDE for X = [−]C≡CH > [−]H > [−]CH₃, in agreement with previously published work.³² Zirconium–phosphido bonds ([−]PH₂, [−]PPh, and [−]PHCy) are significantly weaker than corresponding bonds to [−]NH₂, perhaps due to the increased basicity of amido over phosphide and consistent with the greater observed reactivity of the Zr–P linkage.^{4,10,12}

In the original report of complexes **2** and **3**, it was observed that reaction of a zirconium precursor, such as **16**, with an excess of a 1-to-1 mixture of PhPH₂ and CyPH₂ gave exclusively **2**.⁹ Now, with the solid-state structure of both complexes known, it is clear that these complexes are isomorphous. The optimized gas-phase structures of these two molecules are reported herein, and the Zr–P BDEs for the two molecules are essentially identical (Table 7). None of these new data allow a reasonable hypothesis to be made as to the preferential formation of **2**. It seems likely that there are solution effects that are not being accounted for in this analysis that may explain the observed reactivity. Further study to understand the exact nature of the bonding is clearly warranted for the potential impact on catalyst design.

Conclusion

Complexes of the form (N₃N)ZrX can be synthesized by reaction of **1** with HX reagents. It appears that this reaction is general, and it mimics the Zr products that would be expected from reaction of (N₃N)ZrH with HX. These zirconium complexes have highly ionic bonding based on DFT calculations. Solid-state and theoretical data on these complexes support little ligand-to-metal π -donation except for amido derivatives where significant π -bonding to the metal center can be observed. This bonding is attributed to the greater π -basicity of the amido ligand. The lack of strong π -bonding interactions between zirconium and phosphido (and arsenido) ligands may give rise to the observed reactivity.

Experimental Details

All manipulations were performed under a nitrogen atmosphere with dry, oxygen-free solvents using an M. Braun glovebox or using

standard Schlenk techniques. Benzene- d_6 was purchased from Cambridge Isotope Laboratory, then degassed and dried over NaK alloy. Celite-454 was heated to a temperature greater than 180 °C under dynamic vacuum for at least 8 h. Elemental analyses were performed by Desert Analytics, Tucson, AZ. NMR spectra were recorded with either a Bruker AXR or Varian 500 MHz spectrometer in benzene- d_6 and are reported with reference to residual solvent resonances (δ 7.16 and 128.0) or external 85% H_3PO_4 (δ 0.0). Infrared spectra were collected on a Perkin-Elmer System 2000 FT-IR spectrometer at a resolution of 1 cm^{-1} . Starting materials $Zr(CH_2Ph)_4$ and $N(CH_2CH_2NHSiMe_3)_3$ were prepared according to literature procedures.^{35,36} All other chemicals were obtained from commercial suppliers and dried by appropriate means.

Preparation of $[(\kappa^5-N,N,N,N,C-(Me_3SiNCH_2CH_2)_2NCH_2-CH_2NSiMe_2CH_2)Zr]$ (1**).** A Schlenk tube was charged with $Zr(PhCH_2)_4$ (1.25 g, 2.75 mmol), $N(CH_2CH_2NHSiMe_3)_3$ (0.997 g, 2.75 mmol), and ca. 5 mL of toluene and fitted with a coldfinger. The reaction was allowed to stir for ca. 3 h. Following removal of the solvent under reduced pressure, the Schlenk tube was heated in an oil bath under reduced pressure. After the residue reached ca. 80 °C, the coldfinger was charged with a dry ice/acetone slurry. Heating was continued to ca. 110 °C until sublimation deposited **1** as a colorless solid on the coldfinger (0.991 g, 2.20 mmol, 73%). 1H NMR (500.1 MHz): δ 3.600 (t, 2 H) 3.126 (m, 4 H), 2.344 (m, 6 H), 0.437 (s, 6 H, C H_3), 0.314 (s, 2 H, ZrC H_2), 0.274 (s, 18 H, C H_3). Complete data for complex **1** have been reported.⁹

Preparation of $(N_3N)ZrPPh$ (2**).** A 50 mL round-bottom flask was charged with **1** (100 mg, 0.222 mmol) and ca. 5 mL of benzene. A 5 mL benzene solution of phenylphosphine (24.4 mg, 0.222 mmol) was added dropwise to the solution of **1**, whereupon the mixture immediately changed from colorless to red. After stirring the red solution for 30 min, the solution was frozen and lyophilized to give the title compound as an orange powder (1.068 g, 0.191 mmol, 86%). Spectroscopic data for **2** were identical to those previously reported.⁹

Preparation of $(N_3N)ZrPHCy$ (3**).** A 50 mL round-bottom flask was charged with **1** (0.921 g, 2.00 mmol), and ca. 5 mL of benzene. Cyclohexylphosphine (0.255 g, 2.20 mmol) was added dropwise. The solution turned from colorless to yellow upon the addition of PH_2Cy . The solution was stirred for ca. 10 min. The solution was then frozen and lyophilized, yielding yellow crystals of the title compound (1.031 g, 1.780 mmol, 89%). Spectroscopic data for **3** were identical to those previously reported.⁹

Preparation of $(N_3N)ZrPPH_2$ (4**).** A 50 mL round-bottom flask was charged with **1** (0.400 g, 0.889 mmol) and ca. 5 mL of benzene. PH_2PH (0.166 g, 0.889 mmol) in ca. 5 mL of benzene was added to the flask containing **1**. The benzene solution turned from colorless to red gradually over 10 min. The solution was allowed to stir for an additional 2 h, then frozen and lyophilized to give a red powder of **4** (0.452 g, 0.771 mmol, 80%). 1H NMR (500.1 MHz): δ 7.732 (t, C_6H_5 , 4 H), 7.173 (partially obscured by solvent), 6.932 (m, C_6H_5 , 2 H), 3.312 (t, CH_2 , 6 H) 2.256 (t, CH_2 , 6 H), 0.209 (s, 27 H, C H_3). $^{13}C\{^1H\}$ NMR (125.8 MHz): δ 142.03 (s, Ph), 134.71 (d, $J_{PC} = 13.8$ Hz, Ph), 128.35 (d, $J_{PC} = 8.8$ Hz, Ph), 125.58 (s, Ph), 64.37 (s, CH_2), 47.57 (s, CH_2) 1.56 (s, CH_3). ^{31}P NMR (202.4 MHz): δ 85.37 (s). IR (KBr, Nujol): 1578 s, 1560 m, 1432 m, 1333 m, 1299 w, 1264 s, 1243 s, 1143 m, 1047 s, 1026 s, 927 s, 898 s, 835 s, 780 s, 734 s, 696 s, 683 s, 565 m, 461 $w\ cm^{-1}$. Anal. Calcd for $C_{27}H_{29}N_4PSi_3Zr$: C, 50.98; H, 7.76; N, 8.81. Found: C, 50.75; H, 7.57; N, 8.95.

Preparation of $(N_3N)ZrPHC_2H_4PH_2$ (5**).** A scintillation vial was charged with **1** (0.198 g, 0.440 mmol) and 2 mL of Et_2O . To the ethereal solution of **1**, 1,2-diphosphinoethane (0.041 g, 0.440 mmol) in 2 mL of Et_2O was added, resulting in an immediate color

change from colorless to pale yellow. The solution was stirred at ambient temperature for 30 min followed by partial removal of solvent under reduced pressure. The solution was filtered through Celite and concentrated until incipient crystallization. The solids were redissolved with gentle warming, and the homogeneous solution was cooled to -30 °C to afford light orange crystals of **5** (0.182 g, 0.334 mmol, 76%). 1H NMR (500.1 MHz): δ 3.230 (t, CH_2 , 6 H), 2.243 (t, CH_2 , 6 H), 2.730 (ddt, $J_{PH} = 186$ Hz, $J_{HH} = 7.0$ Hz, $J_{HH} = 2.2$ Hz, PH), 2.97 (dt, $J_{PH} = 211$ Hz, $J_{HH} = 6.8$ Hz, PH_2), 2.33 (m, CH_2), 1.86 (m, CH_2), 0.315 (s, CH_3 , 27 H). $^{13}C\{^1H\}$ NMR (125.8 MHz): δ 63.03 (s, CH_2), 47.31 (s, CH_2), 20.63 (m, CH_2), 22.49 (pseudo d, CH_2), 1.31 (s, CH_3). $^{31}P\{^1H\}$ NMR (202.46 MHz): δ -72.4 (s, PH), -133 (s, PH_2). IR (KBr, Nujol): 2349 s, 2340 s, 2283 m, 1411 m, 1376 s, 1335 s, 1261 s, 1245 s, 1144 s, 1052 w, 1024 m, 928 s, 897 m, 837 w, 782 s, 735 m, 678 s, 664 s, 624 s, 565 s, 453 m, 426 $m\ cm^{-1}$. Anal. Calcd for $C_{17}H_{46}N_4P_2Si_3Zr$: C, 37.53; H, 8.52; N, 10.30. Found: C, 37.61; H, 8.45; N, 10.26.

Preparation of $(N_3N)ZrC\equiv CPh$ (6**).** A 50 mL round-bottom flask was charged with **1** (300 mg, 0.667 mmol), phenylacetylene (68 mg, 0.667 mmol), and ca. 5 mL of benzene solvent. After stirring the solution for 12 h the mixture was frozen, then lyophilized, yielding **6** as a colorless powder (310 mg, 0.560 mmol, 84%). 1H NMR (500.1 MHz): δ 7.6159 (d, C_6H_5 , 2 H), 6.920-6.994 (m, C_6H_5 , 3 H), 3.275 (t, CH_2 , 6 H), 2.217 (t, CH_2 , 6 H), 0.421 (s, CH_3 , 27 H). $^{13}C\{^1H\}$ NMR (125.8 MHz): δ 147.36 (s, C_β) 131.77 (s, C_α), 128.10 (s, CH), 127.09 (s, CH), 124.97 (s, CH) 106.54 (s CH), 62.16 (s, CH_2), 47.47 (s, CH_2) 1.32 (s, CH_3). IR (KBr, Nujol): 2076 s (ν_{CC}), 1594 w, 1485 s, 1377 w, 1260 s, 1244 s, 1204 m, 1143 m, 1061 s, 1022 m, 930 s, 903 m, 837 s, 782 s, 756m, 736 s, 679 w, 563 m, 538 m, 459 $w\ cm^{-1}$. Anal. Calcd for $C_{23}H_{44}N_4Si_3Zr$: C, 50.04; H, 8.03; N, 10.15. Found: C, 50.51; H, 8.14; N, 10.15.

Preparation of $(N_3N)ZrC\equiv CSiMe_3$ (7**).** A 50 mL round-bottom flask was charged with **1** (300 mg, 0.667 mmol), trimethylsilylacetylene (65.5 mg, 0.667 mmol), and ca. 5 mL of Et_2O solvent. After stirring for 2 h Et_2O was removed under reduced pressure, and the residue extracted into hexanes. The solution was filtered through Celite, and the volume was reduced until incipient crystallization. The solids were redissolved with gentle warming, and the homogeneous solution was cooled to -30 °C, which yielded colorless microcrystals of **7** (276 mg, 0.500 mmol, 75%). 1H NMR (500.1 MHz): δ 3.225 (t, CH_2 , 6 H), 2.173 (t, CH_2 , 6 H), 0.396 (s, CH_3 , 27H), 0.2623 (s, CH_3 , 9 H). $^{13}C\{^1H\}$ NMR (125.8 MHz): δ 169.97 (s, C_β), 113.49 (s, C_α), 62.52 (s, CH_2), 47.70 (s, CH_2), 1.62 (s, CH_3), 0.37 (s, CH_3). IR (KBr, Nujol): 2029 w (ν_{CC}), 1959 w, 1602 m, 1401 m, 1334 s, 1244 s, 1144 s, 1061 s, 1018 s, 930 s, 841 $s\ cm^{-1}$.

Preparation of $(N_3N)ZrC\equiv CBu$ (8**).** A 50 mL round-bottom flask was charged with **1** (0.200 g, 0.444 mmol), 1-hexyne (0.037 g, 0.444 mmol), and ca. 10 mL of Et_2O . After stirring the solution for 24 h, the solvent was removed under reduced pressure until incipient crystallization. The solution was warmed to ambient temperature, and then the homogeneous solution was cooled to -30 °C, which yielded colorless crystals of **8** (0.190 g, 0.355 mmol, 80%). 1H NMR (500.1 MHz): δ 3.245 (t, CH_2 , 6 H), 2.120 (t, CH_2 , 6 H), 2.135 (t, CH_2 , 2 H), 1.433 (m, CH_2 , 4 H), 0.837 (t, CH_3 , 3 H), 0.407 (s, CH_3 , 27 H). ^{13}C NMR (125.8 MHz): δ 138.43 (s, C_β), 107.74 (s, C_α), 62.41 (s, CH_2), 47.68 (s, CH_2), 31.49 (s, CH_2), 22.31 (s, CH_2), 19.88 (s, CH_2), 13.78 (s, CH_3), 1.69 (s, CH_3). IR (KBr, Nujol): 2081 (s, ν_{CC}), 1372 m, 1330 w, 1270 s, 1239 s, 1144 m, 1080 s, 928 m, 836 m, 779 w, 735 $w\ cm^{-1}$. Anal. Calcd for $C_{21}H_{48}N_4Si_3Zr$: C, 47.40; H, 9.09; N, 10.53. Found: C, 47.47; H, 8.15; N, 10.63.

Preparation of $(N_3N)ZrOPh$ (9**).** A 50 mL round-bottom flask was charged with **1** (0.100 g, 0.222 mmol), phenol (0.021 g, 0.222 mmol), and ca. 5 mL of Et_2O . The resulting solution was stirred for 2.5 h, whereupon the solvent was removed under reduced pressure until incipient crystallization. The solution was warmed

(35) Covert, K. J.; Mayol, A.-R.; Wolczanski, P. T. *Inorg. Chim. Acta* **1997**, *263*, 263-278.

(36) Gudat, D.; Verkade, J. G. *Organometallics* **1989**, *8*, 2772-2779.

to ambient temperature and placed in a $-30\text{ }^{\circ}\text{C}$ freezer, yielding **9** as colorless microcrystals. The mother liquor was reduced further to produce a second batch of crystals (103 mg, 0.189 mmol, 85%). ^1H NMR (500.1 MHz): δ 7.191–7.210 (m, C_6H_5 , 4 H), 6.810 (m, C_6H_5 , 1 H), 3.231 (t, CH_2 , 6 H), 2.3476 (t, CH_2 , 6 H), 0.236 (s, CH_3 , 27 H). ^{13}C NMR (125.8 MHz): δ 129.53 (s, CH), 128.28 (s, CH), 121.11 (s, CH), 120.29 (s, C), 61.33 (s, CH_2), 46.85 (s, CH_2), 1.50 (s, CH_3). IR (KBr, Nujol): 1590 m, 1493 m, 1480 s, 1281 s, 1244 s, 1162 w, 1061 m, 1022 w, 933 s, 906 m, 864 m, 837 s, 784 m, 757 m, 692 w, 625 w, 563 w cm^{-1} . Anal. Calcd for $\text{C}_{21}\text{H}_{44}\text{N}_4\text{OSi}_3\text{Zr}$: C, 46.36; H, 8.15; N, 10.30. Found: C, 46.06; H, 8.10; N, 10.15.

Preparation of $(\text{N}_3\text{N})\text{NH}^t\text{Bu}$ (10**).** A scintillation vial was charged with **1** (0.049 g, 0.108 mmol) and ca. 2 mL of benzene. To the solution of **1** was added a 2 mL benzene solution of $^t\text{BuNH}_2$ (0.009 g, 0.122 mmol), and the resulting solution stirred at ambient temperature for 30 min. The solution was dried under reduced pressure to give **10** as a colorless powder (0.021 g, 0.040 mmol, 73%). ^1H NMR (500.1 MHz): δ 3.856 (bs, NH, 1 H), 3.196 (t, CH_2 , 6 H), 2.324 (t, CH_2 , 6 H), 1.451 (s, CH_3 , 9 H), 0.156 (s, CH_3 , 27 H). $^{13}\text{C}\{^1\text{H}\}$ NMR (125.8 MHz): 63.64 (s, CH_2), 35.12 (s, CH_2), 25.59 (s, C), 22.78 (s, CH_3), 14.20 (s, CH_3). IR (KBr, Nujol): 3210 s (ν_{NH}), 2923 s, 2849 s, 1462 s, 1244 s cm^{-1} . Anal. Calcd for $\text{C}_{19}\text{H}_{49}\text{N}_5\text{Si}_3\text{Zr}$: C, 43.62; H, 9.44; N, 13.39. Found: C, 43.90; H, 9.88; N, 13.44.

Preparation of $(\text{N}_3\text{N})\text{ZrNHP}$ (11**).** A round-bottom flask was charged with **1** (0.726 g, 1.61 mmol) and 2 mL of benzene. A solution of aniline (0.151 g, 1.62 mmol) in 3 mL of benzene was added to the Zr solution, and the resulting homogeneous solution was stirred for 30 min before lyophilization. The resulting solid was washed with pentane and decanted. The remaining colorless solid was redissolved in benzene and filtered before being lyophilized to give **11** as a colorless powder (806 mg, 1.48 mmol, 92%). ^1H NMR (500.1 MHz): δ 7.203 (t, C_6H_5 , 2 H), 6.902 (d, C_6H_5 , 2 H), 6.744 (d, C_6H_5 , 1 H), 5.962 (NH, 1 H), 3.252 (t, CH_2 , 6 H), 2.312 (t, CH_2 , 6 H), 0.221 (s, CH_3 , 27 H). $^{13}\text{C}\{^1\text{H}\}$ NMR (125.8 MHz): δ 153.2 (s, $\text{C}=\text{N}$), 129.1 (s, Ph), 119.4 (s, Ph), 117.9 (s, Ph), 61.79 (s, CH_2), 47.07 (s, CH_2), 1.48 (s, CH_3). IR (KBr, Nujol): 3294 (s, ν_{NH}), 2921 s, 2341 s, 1597 s, 1489 s cm^{-1} . Anal. Calcd for $\text{C}_{21}\text{H}_{45}\text{N}_5\text{Si}_3\text{Zr}$: C, 46.44; H, 8.35; N, 12.90. Found: C, 47.06; H, 8.49; N, 13.03.

Preparation of $(\text{N}_3\text{N})\text{ZrNHN}=\text{CPh}_2$ (12**).** A round-bottom flask was charged with **1** (0.052 g, 0.116 mmol), benzophenone hydrazone (0.023 g, 0.117 mmol), and 2 mL of Et_2O . The resulting bright yellow solution was stirred for 30 min at ambient temperature. The volume of the solution was reduced until a solid appeared, and then the solution was gently warmed to ambient temperature. The homogeneous solution was cooled to $-30\text{ }^{\circ}\text{C}$, yielding yellow microcrystals of **12** (0.019 g, 0.029 mmol, 25%). ^1H NMR (500.1 MHz): δ 8.068 (s, NH, 1 H), 7.820 (d, C_6H_5 , 2 H), 7.604 (d, C_6H_5 , 2 H), 7.290 (m, C_6H_5 , 4 H), 7.146 (t, C_6H_5 , 2 H), 3.508 (t, CH_2 , 6 H), 2.658 (t, CH_2 , 6 H), 0.2686 (s, CH_3 , 27 H). $^{13}\text{C}\{^1\text{H}\}$ NMR (125.8 MHz): δ 148.10 (s, $\text{C}=\text{N}$), 137.72 (s, Ph), 132.20 (s, Ph), 127.26 (s, Ph), 125.60 (s, Ph), 58.86 (s, CH_2), 40.16 (s, CH_2), 0.22 (s, CH_3). IR (KBr, Nujol): 3299 s (ν_{NH}), 2923 s, 2853 s, 1457 s, 1259 s cm^{-1} . Anal. Calcd for $\text{C}_{28}\text{H}_{50}\text{N}_6\text{Si}_3\text{Zr}$: C, 52.04; H, 7.80; N, 13.00. Found: C, 52.20; H, 7.52; N, 12.45.

Preparation of $(\text{N}_3\text{N})\text{ZrN}=\text{CPh}_2$ (13**).** A solution of benzophenone imine (0.009 g, 0.052 mmol) in 2 mL of benzene was added to a 2 mL solution of **1** (26 mg, 0.058 mmol) in benzene at ambient temperature, whereupon the colorless solution immediately changed to orange. The clear orange solution was stirred for 2 h, then lyophilized to an orange powder (0.027 g, 0.042 mmol, 82%). ^1H NMR (500.1 MHz): δ 7.297 (m, C_6H_5 , 4 H), 7.114 (m, C_6H_5 , 6 H), 3.488 (t, CH_2 , 6 H), 2.577 (t, CH_2 , 6 H), 0.256 (s, CH_3 , 27 H). $^{13}\text{C}\{^1\text{H}\}$ NMR (125.8 MHz): δ 174.81 (s, $\text{C}=\text{N}$), 142.08 (s, C_6H_5), 133.91 (s, C_6H_5), 129.30 (s, C_6H_5), 128.45 (s, C_6H_5), 61.42 (s, CH_2),

47.12 (s, CH_2), 1.43 (s, CH_3). IR (KBr, Nujol): 1641 (s, ν_{CN}), 1595 w, 1463 s, 1378 m, 1258 s, 1242 s, 1080 s, 1020 m, 931 s, 901 m, 837 s, 784 s, 741 m, 701 m, 631 m, 564 m, 478 w, 451 w cm^{-1} . Anal. Calcd for $\text{C}_{28}\text{H}_{49}\text{N}_5\text{Si}_3\text{Zr}$: C, 53.28; H, 7.82; N, 11.10. Found: C, 52.98; H, 7.74; N, 11.18.

Preparation of $(\text{N}_3\text{N})\text{ZrSPh}$ (14**).** A 50 mL round-bottom flask was charged with **1** (0.106 g, 0.236 mmol) and 5 mL of Et_2O , and the solution was cooled to $-30\text{ }^{\circ}\text{C}$. A cold 5 mL ethereal solution of benzenethiol (0.026 g, 0.236 mmol) was added to the zirconium solution. The resulting pale yellow solution was stirred for 24 h. Volatile materials were removed under reduced pressure, and the residue was redissolved in Et_2O and filtered through Celite. The solvent was removed again under reduced pressure, and the residue was extracted into hexanes. The solution was concentrated, then cooled to give colorless crystals of **14** (0.058 mg, 0.103 mmol, 44%). ^1H NMR (500.1 MHz): δ 7.703 (d, CH, 2 H), 7.094 (m, CH, 2 H), 7.079 (m, CH, 1 H), 3.256 (t, CH_2 , 6 H), 2.233 (t, CH_2 , 6 H), 0.2832 (s, CH_3 , 27 H). $^{13}\text{C}\{^1\text{H}\}$ NMR (125.8 MHz): δ 133.7 (s, Ph), 128.7 (s, Ph), 128.2 (s, Ph), 124.3 (s, Ph), 63.72 (s, CH_2), 47.64 (s, CH_2), 1.463 (s, CH_3). IR (KBr, Nujol): 1578 m, 1377 s, 1245 s, 1143 w, 1085 w, 1056 m, 1024 m, 929 s, 900 sm, 837 s, 782 m, 737 m, 694 m, 563 s cm^{-1} . Anal. Calcd for $\text{C}_{21}\text{H}_{44}\text{N}_4\text{Si}_3\text{Zr}$: C, 45.03; H, 7.92; N, 10.00. Found: C, 44.57; H, 7.90; N, 9.77.

Preparation of $(\text{N}_3\text{N})\text{ZrS}^t\text{Bu}$ (15**).** A 50 mL round-bottom flask was charged with **1** (0.100 g, 0.222 mmol) and 5 mL of Et_2O , and the solution was cooled to $-30\text{ }^{\circ}\text{C}$. A cold 5 mL Et_2O solution of *tert*-butylthiol (0.020 g, 0.222 mmol) was added to the zirconium solution. The resulting pale yellow solution was stirred for 24 h. Volatile materials were removed under reduced pressure, and the residue was redissolved in Et_2O and filtered through Celite. The solvent was removed again under reduced pressure, and the residue was extracted into a toluene/hexanes solvent mixture (20:1). The solution was concentrated, then cooled to give colorless crystals of **15** (0.077 mg, 0.142 mmol, 64%). ^1H NMR (500.1 MHz): δ 3.194 (t, CH_2 , 6 H), 2.296 (t, CH_2 , 6 H), 1.724 (s, CH_3 , 9 H), 0.389 (s, CH_3 , 27 H). $^{13}\text{C}\{^1\text{H}\}$ NMR (125.8 MHz): δ 64.67 (s, CH_2), 50.25 (s, $\text{C}(\text{CH}_3)_3$), 47.81 (s, CH_2), 37.32 (s, CH_3), 1.94 (s, CH_3). IR (KBr, Nujol): 1376 s, 1360 s, 1335 m, 1300 w, 1260 s, 1244 s, 1147 m, 1056 s, 1023 m, 930 s, 838 s, 783 m, 736 m, 674 s, 623 s, 587 s, 564 s cm^{-1} . Anal. Calcd for $\text{C}_{19}\text{H}_{48}\text{N}_4\text{Si}_3\text{Zr}$: C, 42.25, H, 8.96, N, 10.37. Found: C, 42.07; H, 8.91, N, 10.75.

DFT Computations. Gas-phase structures were optimized using the hybrid B3LYP functional^{37,38} and the triple- ζ LACV3P**++ basis set,^{39–42} which uses extended core potentials on heavy atoms and a 6-311G**++ basis for other atoms, as implemented in the Jaguar⁴³ suite of programs. Natural bond orbital (NBO), natural resonance theory (NRT), and natural population analyses (NPA)^{44–49} are also integrated with the Jaguar program and were run on B3LYP/LACV3P**++ optimized structures. Radical species were

(37) Becke, A. D. *J. Chem. Phys.* **1993**, *98*, 5648–5652.

(38) Becke, A. D. *J. Chem. Phys.* **1993**, *98*, 1372–1377.

(39) Dunning, T. H.; Hay, P. J. *Modern Theoretical Chemistry*, Vol. 4: *Applications of Electronic Structure Theory*; Plenum: New York, 1977; p 461.

(40) Hay, P. J.; Wadt, W. R. *J. Chem. Phys.* **1985**, *82*, 270–283.

(41) Hay, P. J.; Wadt, W. R. *J. Chem. Phys.* **1985**, *82*, 299–310.

(42) Wadt, W. R.; Hay, P. J. *J. Chem. Phys.* **1985**, *82*, 284–298.

(43) *Jaguar*, version 7.0; Schrödinger, LLC: New York, 2007.

(44) Weinhold, F.; Landis, C. R. *Valency and Bonding: A Natural Bond Orbital Donor-Acceptor Perspective*, 1st ed.; Cambridge University Press: Cambridge, 2005.

(45) Reed, A. E.; Curtiss, L. A.; Weinhold, F. *Chem. Rev.* **1988**, *88*, 899–926.

(46) Reed, A. E.; Weinstock, R. B.; Weinhold, F. *J. Chem. Phys.* **1985**, *83*, 735–746.

(47) Foster, J. P.; Weinhold, F. *J. Am. Chem. Soc.* **1980**, *102*, 7211–7218.

(48) Reed, A. E.; Weinhold, F. *J. Chem. Phys.* **1983**, *78*, 4066–4073.

(49) Glendening, E. D.; Badenhoop, J. K.; Reed, A. K.; Carpenter, J. E.; Bohmann, J. A.; Morales, C. M.; Weinhold, F. *NBO 5.0*; Theoretical Chemistry Institute, University of Wisconsin: Madison, 2001.

Table 8. Crystal Data and Structure Refinement Parameters for **3**, **4**, **5**, **10**, and **15**

	3	4	5	10	15
formula	C ₂₁ H ₅₁ N ₄ PSi ₃ Zr	C ₂₇ H ₄₉ N ₄ PSi ₃ Zr	C ₁₇ H ₄₆ N ₄ P ₂ Si ₃ Zr	C ₁₉ H ₄₉ N ₅ Si ₃ Zr	C ₁₉ H ₄₈ N ₄ SSi ₃ Zr
<i>M</i>	566.12	636.16	544.01	523.12	540.16
cryst syst	orthorhombic	monoclinic	orthorhombic	trigonal	monoclinic
color	yellow	orange	orange	colorless	colorless
<i>a</i> /Å	16.8829(9)	10.7744(7)	17.0290(9)	11.9522(6)	11.8438(5)
<i>b</i> /Å	17.589(1)	16.648(1)	17.1007(9)	11.9522(6)	20.1540(8)
<i>c</i> /Å	20.347(1)	19.357(1)	20.194(1)	11.6463(5)	12.0195(5)
α /deg	90	90	90	90	90
β /deg	90	102.495(1)	90	90	95.389(1)
γ /deg	90	90	90	120	90
unit cell vol/Å ³	6042.1(6)	3389.9(4)	5880.6(5)	1440.83(12)	2856.4(2)
space group	<i>Pbca</i>	<i>P2₁/n</i>	<i>Pbca</i>	<i>P3₁/c</i>	<i>P2₁/n</i>
<i>Z</i>	8	4	8	2	4
θ range/deg	1.95 to 30.46	1.63 to 28.28	1.97 to 26.62	2.63 to 28.24	1.98 to 28.70
μ /mm ⁻¹	0.551	0.499	0.615	0.520	0.596
<i>N</i>	81714	43983	64367	18203	38319
<i>N</i> _{ind}	8889	8406	6160	2393	7374
<i>R</i> _{int}	0.0610	0.0314	0.0430	0.0207	0.0248
<i>R</i> ₁ ^a (<i>I</i> > 2 σ (<i>I</i>))	0.0320	0.0250	0.0283	0.0144	0.0212
<i>wR</i> ₂ ^b (<i>I</i> > 2 σ (<i>I</i>))	0.0649	0.0586	0.0640	0.0381	0.0548
$\Delta\rho_{\max}$; $\Delta\rho_{\min}$ /e Å ³	0.436; -0.378	0.401; -0.280	0.388; 0.543	0.197; -0.188	0.371; -0.282
GoF on <i>R</i> ₁	1.007	1.045	1.054	1.068	1.045

$$^a R_1 = |F_o| - |F_c|/\sum|F_o|, \quad ^b wR_2 = \{\sum[w(F_o^2 - F_c^2)^2]/\sum[w(F_o^2)]\}^{1/2}.$$

optimized as doublets using unrestricted occupancy methods, and the absence of significant spin contamination was confirmed by checking the values of *S*² against the expected doublet values of 0.750. All computed structures were confirmed as energy minima by calculating the vibrational frequencies by second-derivative analytic methods and confirming the absence of imaginary frequencies. Thermodynamic quantities were calculated assuming an ideal gas and are zero-point energy corrected. The “universal” B3LYP correction³³ was made for all radical species.³⁴

X-ray Structure Determinations. X-ray diffraction data were collected on a Bruker APEX 2 CCD platform diffractometer (Mo K α , λ = 0.71073 Å) at 125 K. Suitable crystals of each complex were mounted in a nylon loop with Paratone-N cryoprotectant oil. The structures were solved using direct methods and standard difference map techniques and were refined by full-matrix least-squares procedures on *F*² with SHELXTL (version 6.14).⁵⁰ All non-hydrogen atoms were refined anisotropically. Hydrogen atoms on carbon were included in calculated positions and were refined using a riding model. The hydrogen atom on the phosphorus of **3**, H(1), and all hydrogen atoms on phosphorus atoms of **5**, H(1), H(2), and H(3), were located in the Fourier difference map and refined freely. The hydrogen atom on the nitrogen of **10**, H(1), was located in the Fourier difference map and refined semifreely with the help of a distance restraint. Crystal data and refinement details are presented in Table 8. The cyclohexyl phosphido ligand of **3** exhibited a 2-fold disorder that was modeled successfully, refining freely to 65/35

occupancy. The ^tBu amido of **10** exhibited disorder about the crystallographic 3-fold axis that was modeled as a perfect 3-fold disorder and refined with the help of distance restraints (SADI), similarity restraints on displacement parameters (SIMU), and rigid bond restraints on 1–2 and 1–3 distances and anisotropic displacement parameters (DELU).

Acknowledgment. This work was supported by the U.S. National Science Foundation (CHE-0747612 to R.W. and CHE-0518170 to R.P.H.), the American Chemical Society Petroleum Research Fund (466669-G3 to R.W.), and the University of Vermont (UVM). Summer support for S.M.C. was provided by the American Chemical Society (ACS) Project SEED and the Green Mountain ACS Local Section. Research support for J.J.D. was provided by a UVM Undergraduate Research Endeavors Competitive Award. X-ray crystallographic facilities were provided by the U.S. National Science Foundation (CHE-0521237 to J.M.T.). R.P.H. also thanks Professor Clark Landis (University of Wisconsin) for valuable discussions.

Supporting Information Available: Crystallographic data for complexes **3**, **4**, **5**, **10**, and **15** (CIF) and tables of computational results (pdf). These materials are available free of charge via the Internet at <http://pubs.acs.org>.

(50) Sheldrick, G. M. *Acta Crystallogr.* **2008**, *A64*, 112–122.

Hydrosilylation of Aldehydes and Ketones Catalyzed by Nickel PCP-Pincer Hydride Complexes

Sumit Chakraborty, Jeanette A. Krause, and Hairong Guan*

Department of Chemistry, University of Cincinnati, P.O. Box 210172, Cincinnati, Ohio 45221-0172

Received October 1, 2008

Nickel PCP-pincer hydride complexes catalyze chemoselective hydrosilylation of C=O bonds of aldehydes and ketones in the presence of other functional groups. The mechanism involves C=O insertion into a nickel–hydrogen bond, followed by cleavage of the newly formed Ni–O bond with a silane.

Nickel hydride complexes are of great importance in the research areas of homogeneous catalysis, coordination chemistry, and enzymatic reaction mechanisms. They are often postulated as key intermediates in a variety of nickel-catalyzed organic transformations.^{1–10} These hypothesized nickel hydrides are usually too reactive to allow direct observation of reaction intermediates or thorough investigation of reaction mechanisms.

* To whom correspondence should be addressed. E-mail: hairong.guan@uc.edu.

(1) Isomerization of compounds bearing C=C bonds: (a) Gosser, L. W.; Parshall, G. W. *Tetrahedron Lett.* **1971**, *12*, 2555–2558. (b) Bontempelli, G.; Fiorani, M.; Daniele, S.; Schiavon, G. *J. Mol. Catal.* **1987**, *40*, 9–21. (c) Raje, A. P.; Datta, R. *J. Mol. Catal.* **1992**, *72*, 97–116. (d) Frauenrath, H.; Brethauer, D.; Reim, S.; Maurer, M.; Raabe, G. *Angew. Chem., Int. Ed.* **2001**, *40*, 177–179. (e) Cuperly, D.; Petrignet, J.; Crévisy, C.; Grée, R. *Chem. Eur. J.* **2006**, *12*, 3261–3274.

(2) Cycloisomerization of enynes: Tekavec, T. N.; Louie, J. *Tetrahedron* **2008**, *64*, 6870–6875.

(3) Reductive cyclization of 1,3-diene and organic carbonyl moieties: (a) Sato, Y.; Takimoto, M.; Hayashi, K.; Katsuhara, T.; Takagi, K.; Mori, M. *J. Am. Chem. Soc.* **1994**, *116*, 9771–9772. (b) Sato, Y.; Takimoto, M.; Mori, M. *J. Am. Chem. Soc.* **2000**, *122*, 1624–1634.

(4) Dimerization or oligomerization of olefins: (a) Maruya, K.-i.; Mizoroki, T.; Ozaki, A. *Bull. Chem. Soc. Jpn.* **1972**, *45*, 2255–2259. (b) Peuckert, M.; Keim, W. *Organometallics* **1983**, *2*, 594–597. (c) Müller, U.; Keim, W.; Krüger, C.; Betz, P. *Angew. Chem., Int. Ed. Engl.* **1989**, *28*, 1011–1013. (d) Keim, W. *Angew. Chem., Int. Ed. Engl.* **1990**, *29*, 235–244. (e) Bertozzi, S.; Iannello, C.; Barretta, G. U.; Vitulli, G.; Lazzaroni, R.; Salvadori, P. *J. Mol. Catal.* **1992**, *77*, 1–6. (f) Fan, L.; Krzywicki, A.; Somogyvari, A.; Ziegler, T. *Inorg. Chem.* **1994**, *33*, 5287–5294. (g) Fan, L.; Krzywicki, A.; Somogyvari, A.; Ziegler, T. *Inorg. Chem.* **1996**, *35*, 4003–4006. (h) Brown, J. M.; Hughes, G. D. *Inorg. Chim. Acta* **1996**, *252*, 229–237. (i) Wiencko, H. L.; Kogut, E.; Warren, T. H. *Inorg. Chim. Acta* **2003**, *345*, 199–208. (j) Kogut, E.; Zeller, A.; Warren, T. H.; Strassner, T. *J. Am. Chem. Soc.* **2004**, *126*, 11984–11994. (k) Wang, K.; Patil, A. O.; Zushma, S.; McConnachie, J. M. *J. Inorg. Biochem.* **2007**, *101*, 1883–1890.

(5) Polymerization of ethylene: (a) Hicks, F. A.; Jenkins, J. C.; Brookhart, M. *Organometallics* **2003**, *22*, 3533–3545. (b) Jenkins, J. C.; Brookhart, M. *J. Am. Chem. Soc.* **2004**, *126*, 5827–5842.

(6) Hydrovinylolation of styrene: Hölscher, M.; Franciò, G.; Leitner, W. *Organometallics* **2004**, *23*, 5606–5617.

(7) Hydrocyanation of butadiene: Tolman, C. A.; McKinney, R. J.; Seidel, W. C.; Druliner, J. D.; Stevens, W. R. *Adv. Catal.* **1985**, *33*, 1–46.

(8) Alcoholysis of silanes: Barber, D. E.; Lu, Z.; Richardson, T.; Crabtree, R. H. *Inorg. Chem.* **1992**, *31*, 4709–4711.

(9) Reductive cleavage of S–C or Se–C bonds: (a) Back, T. G.; Birss, V. I.; Edwards, M.; Krishna, M. V. *J. Org. Chem.* **1988**, *53*, 3815–3822. (b) Back, T. G.; Yang, K.; Krouse, H. R. *J. Org. Chem.* **1992**, *57*, 1986–1990. (c) Back, T. G.; Baron, D. L.; Yang, K. *J. Org. Chem.* **1993**, *58*, 2407–2413.

(10) Reduction or hydrogenation of C=C, C≡C, and C=O bonds: (a) Brunet, J. J.; Mordenti, L.; Loubinoux, B.; Caubere, P. *Tetrahedron Lett.* **1977**, *18*, 1069–1072. (b) Brunet, J. J.; Mordenti, L.; Caubere, P. *J. Org. Chem.* **1978**, *43*, 4804–4808. (c) Chow, Y. L.; Li, H. *Can. J. Chem.* **1986**, *64*, 2229–2231. (d) Sakai, M.; Hirano, N.; Harada, F.; Sakakibara, Y.; Uchino, N. *Bull. Chem. Soc. Jpn.* **1987**, *60*, 2923–2926. (e) Chow, Y. L.; Li, H.; Yang, M. S. *J. Chem. Soc., Perkin Trans. 2* **1990**, 17–24.

Details of their existence during catalytic processes largely rely on computational studies.^{4f,g,5b} In contrast, a number of discrete and stable nickel hydride complexes have been prepared and many stoichiometric transformations involving these hydrides have been reported.^{4c,11–15} However, very few of these complexes are catalytically competent; of the known well-defined catalytic systems, nickel hydride complexes are solely used as catalysts for olefin isomerization and oligomerization.^{15f,16} This has prompted us to study new reactivity of nickel hydride complexes and to explore their potential as relatively inexpensive metal catalysts for various organic reactions.

We have focused our initial studies on nickel hydrides supported by pincer ligands. Such a ligand set has great flexibility in terms of steric and electronic modifications. In addition, square-planar d⁸ metals with pincer ligands have shown numerous applications in organic synthesis, polymerization, and

(11) Use of [(ⁱPr₂PCH₂)₂NiH]₂ as Ni(0) precursor for C–S, C–C, and C–H bond activation reactions: (a) Vivic, D. A.; Jones, W. D. *J. Am. Chem. Soc.* **1997**, *119*, 10855–10856. (b) Vivic, D. A.; Jones, W. D. *Organometallics* **1998**, *17*, 3411–3413. (c) Edelbach, B. L.; Vivic, D. A.; Lachicotte, R. J.; Jones, W. D. *Organometallics* **1998**, *17*, 4784–4794. (d) Vivic, D. A.; Jones, W. D. *J. Am. Chem. Soc.* **1999**, *121*, 7606–7617. (e) Garcia, J. J.; Jones, W. D. *Organometallics* **2000**, *19*, 5544–5545. (f) Garcia, J. J.; Brunkan, N. M.; Jones, W. D. *J. Am. Chem. Soc.* **2002**, *124*, 9547–9555. (g) Brunkan, N. M.; Brestensky, D. M.; Jones, W. D. *J. Am. Chem. Soc.* **2004**, *126*, 3627–3641. (h) Garcia, J. J.; Arévalo, A.; Brunkan, N. M.; Jones, W. D. *Organometallics* **2004**, *23*, 3997–4002. (i) Ateşin, T. A.; Li, T.; Lachaize, S.; Brennessel, W. W.; Garcia, J. J.; Jones, W. D. *J. Am. Chem. Soc.* **2007**, *129*, 7562–7569. (j) Swartz, B. D.; Reinartz, N. M.; Brennessel, W. W.; García, J. J.; Jones, W. D. *J. Am. Chem. Soc.* **2008**, *130*, 8548–8554.

(12) Studies on hydride donor ability of [HNi(diphosphine)₂]⁺: (a) Miedaner, A.; DuBois, D. L.; Curtis, C. J.; Haltiwanger, R. C. *Organometallics* **1993**, *12*, 299–303. (b) Berning, D. E.; Noll, B. C.; DuBois, D. L. *J. Am. Chem. Soc.* **1999**, *121*, 11432–11447. (c) Berning, D. E.; Miedaner, A.; Curtis, C. J.; Noll, B. C.; DuBois, M. C. R.; DuBois, D. L. *Organometallics* **2001**, *20*, 1832–1839. (d) Curtis, C. J.; Miedaner, A.; Ellis, W. W.; DuBois, D. L. *J. Am. Chem. Soc.* **2002**, *124*, 1918–1925. (e) Curtis, C. J.; Miedaner, A.; Ciancanelli, R.; Ellis, W. W.; Noll, B. C.; DuBois, M. R.; DuBois, D. L. *Inorg. Chem.* **2003**, *42*, 216–227. (f) Curtis, C. J.; Miedaner, A.; Raebiger, J. W.; DuBois, D. L. *Organometallics* **2004**, *23*, 511–516. (g) Frazee, K.; Wilson, A. D.; Appel, A. M.; DuBois, M. R.; DuBois, D. L. *Organometallics* **2007**, *26*, 3918–3924. (h) Nimlos, M. R.; Chang, C. H.; Curtis, C. J.; Miedaner, A.; Pilath, H. M.; DuBois, D. L. *Organometallics* **2008**, *27*, 2715–2722.

(13) Studies on protonation of [HNi(diphosphine)₂]⁺: (a) James, T. L.; Cai, L.; Muetterties, M. C.; Holm, R. H. *Inorg. Chem.* **1996**, *35*, 4148–4161. (b) Wilson, A. D.; Shoemaker, R. K.; Miedaner, A.; Muckerman, J. T.; DuBois, D. L.; DuBois, M. R. *Proc. Natl. Acad. Sci. U.S.A.* **2007**, *104*, 6951–6956.

(14) The dinickel bridging hydride [(diphosphine)₂Ni₂(μ-H)]: (a) Vivic, D. A.; Anderson, T. J.; Cowan, J. A.; Schultz, A. J. *J. Am. Chem. Soc.* **2004**, *126*, 8132–8133. (b) Tyree, W. S.; Vivic, D. A.; Piccoli, P. M. B.; Schultz, A. J. *Inorg. Chem.* **2006**, *45*, 8853–8855.

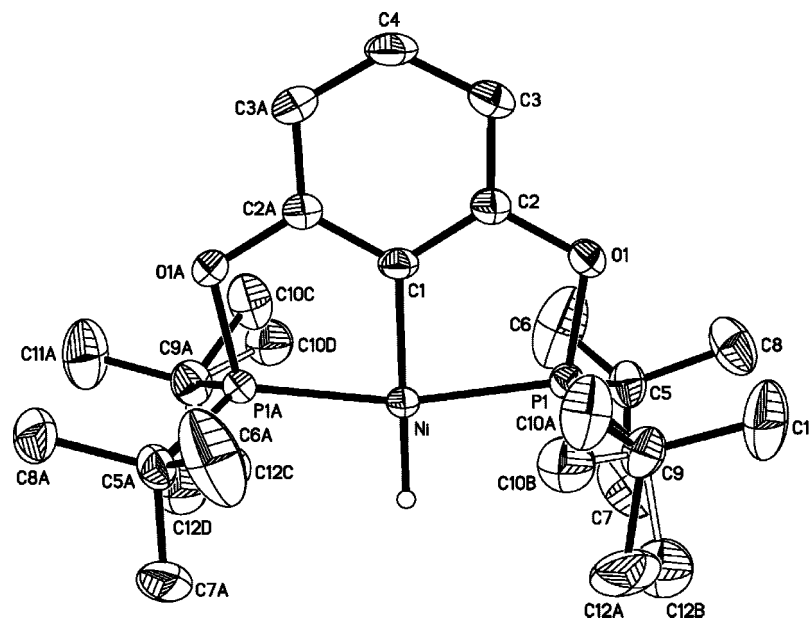


Figure 1. Structure of $[2,6-(t\text{Bu}_2\text{PO})_2\text{C}_6\text{H}_3]\text{NiH}$ (**3b**) (50% probability level). Selected bond lengths (\AA) and angles (deg): Ni–H = 1.37(3), Ni–C1 = 1.892(3), Ni–P1 or Ni–P1A = 2.1160(5); P1–Ni–P1A = 166.26(3), C1–Ni–H = 180.000(9), P1–Ni–C1 or P1A–Ni–C1 = 83.132(17).

molecular sensing.¹⁷ The first synthesis of a nickel pincer hydride complex, specifically $[2,6-(t\text{Bu}_2\text{PCH}_2)_2\text{C}_6\text{H}_3]\text{NiH}$, was reported by Shaw in 1976, although it was not fully characterized.¹⁸ Recently, the Ozerov group¹⁵ⁱ and the Liang group^{15k,m} have independently isolated nickel hydride complexes with amido diphosphine (PNP-pincer) ligands. Liang and co-workers have also demonstrated that this class of compounds is capable of activating arene C–H bonds intermolecularly^{15k} and undergoes C=C bond insertion.^{15m} In any case, we are not aware of any reactions catalyzed by nickel pincer hydride complexes. Herein we describe our preliminary results on the reactivity of new nickel pincer hydrides that led to the discovery of efficient nickel catalysts for hydrosilylation of aldehydes and ketones. To the best of our knowledge, this catalytic system represents

one of the very few examples of nickel-catalyzed hydrosilylation of carbonyl compounds.^{19,20}

Results and Discussion

Encouraged by the excellent reactivity seen in Pd-catalyzed cross-coupling²¹ and Ir-catalyzed alkane dehydrogenation reactions,²² we chose diphosphinites **1a–c** as the pincer ligands for the synthesis of nickel hydrides. First, nickel chlorides **2a,c** were prepared, as reported in the literature,²³ through cyclometalation of the diphosphinites with NiCl_2 . Nickel chloride **2b** was synthesized similarly and characterized by ^1H NMR, ^{31}P NMR, elemental analysis, and X-ray crystallography (see the Supporting Information). The desired nickel hydrides **3a,b** were isolated as yellow-orange solids in good isolated yields from treatment of nickel chlorides with LiAlH_4 (Scheme 1). The ^1H NMR spectra of **3a,b** in C_6D_6 revealed characteristic hydride resonances as triplets at $\delta = -7.89$ ($J_{\text{HP}} = 55.2$ Hz) and $\delta = -7.96$ ($J_{\text{HP}} = 53.2$ Hz), respectively. The hydride ligand in **3b** was also located by X-ray diffraction of its single crystal (Figure 1).²⁴

(15) Other well-defined nickel hydride systems: (a) Srivastava, S. C.; Bigorgne, M. *J. Organomet. Chem.* **1969**, *18*, P30–P32. (b) Green, M. L. H.; Saito, T. *Chem. Commun.* **1969**, 208. (c) Schunn, R. A. *Inorg. Chem.* **1970**, *9*, 394–395. (d) Tolman, C. A. *J. Am. Chem. Soc.* **1970**, *92*, 4217–4222. (e) Nesmeyanov, A. N.; Isaeva, L. S.; Lorens, L. N. *J. Organomet. Chem.* **1977**, *129*, 421–427. (f) Rigo, P.; Bressan, M.; Basato, M. *Inorg. Chem.* **1979**, *18*, 860–863. (g) Darensbourg, D. J.; Darenbourg, M. Y.; Goh, L. Y.; Ludvig, M.; Wiegrefe, P. *J. Am. Chem. Soc.* **1987**, *109*, 7539–7540. (h) Chen, W.; Shimada, S.; Tanaka, M.; Kobayashi, Y.; Saigo, K. *J. Am. Chem. Soc.* **2004**, *126*, 8072–8073. (i) Ozerov, O. V.; Guo, C.; Fan, L.; Foxman, B. M. *Organometallics* **2004**, *23*, 5573–5580. (j) Clement, N. D.; Cavell, K. J.; Jones, C.; Elsevier, C. *J. Angew. Chem., Int. Ed.* **2004**, *43*, 1277–1279. (k) Liang, L.-C.; Chien, P.-S.; Huang, Y.-L. *J. Am. Chem. Soc.* **2006**, *128*, 15562–15563. (l) She, L.; Li, X.; Sun, H.; Ding, J.; Frey, M.; Klein, H.-F. *Organometallics* **2007**, *26*, 566–570. (m) Liang, L.-C.; Chien, P.-S.; Lee, P.-Y. *Organometallics* **2008**, *27*, 3082–3093.

(16) (a) Tolman, C. A. *J. Am. Chem. Soc.* **1970**, *92*, 6777–6784. (b) Green, M. L. H.; Munakata, H. *J. Chem. Soc., Dalton Trans.* **1974**, 269–272.

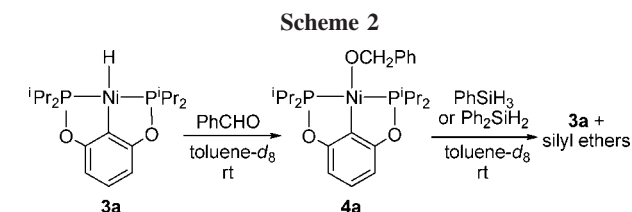
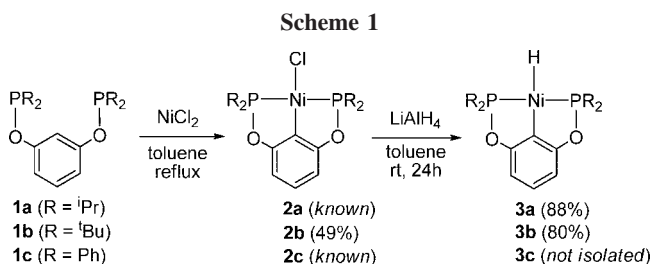
(17) (a) Gossage, R. A.; van de Kuil, L. A.; van Koten, G. *Acc. Chem. Res.* **1998**, *31*, 423–431. (b) Albrecht, M.; van Koten, G. *Angew. Chem., Int. Ed.* **2001**, *40*, 3750–3781. (c) Singleton, J. T. *Tetrahedron* **2003**, *59*, 1837–1857. (d) van der Boom, M. E.; Milstein, D. *Chem. Rev.* **2003**, *103*, 1759–1792. (e) Liang, L.-C. *Coord. Chem. Rev.* **2006**, *250*, 1152–1177. (f) Nishiyama, H. *Chem. Soc. Rev.* **2007**, *36*, 1133–1141.

(18) Moulton, C. J.; Shaw, B. L. *J. Chem. Soc., Dalton Trans.* **1976**, 1020–1024.

(19) A comprehensive review covering transition metal-catalyzed hydrosilylation of carbonyl compounds and imines: Díez-González, S.; Nolan, S. P. *Org. Prep. Proced. Int.* **2007**, *39*, 523–559.

(20) NiCl_2 /additive-catalyzed hydrosilylation of carbonyls accompanied by dehydrogenative hydrosilylation and other side reactions: (a) Frainnet, E.; Martel-Siegfried, V.; Brousse, E.; Dedier, J. *J. Organomet. Chem.* **1975**, *85*, 297–310. (b) Frainnet, E.; Bourhis, R.; Simonin, F.; Moulines, F. *J. Organomet. Chem.* **1976**, *105*, 17–31. Hydrosilylation of both carbonyls and alkenes (thus non-selective hydrosilylation) catalyzed by activated nickel metal: (c) Lee, S. J.; Kim, T. Y.; Park, M. K.; Han, B. H. *Bull. Korean Chem. Soc.* **1996**, *17*, 1082–1085. A brief description of ketone hydrosilylation catalyzed by (indenyl) $\text{Ni}(\text{PPh}_3)^+$: (d) Fontaine, F.-G.; Nguyen, R.-V.; Zargarian, D. *Can. J. Chem.* **2003**, *81*, 1299–1306. Hydrosilylation of mixtures of ketones catalyzed by $\text{Ni}(\text{COD})_2/\text{DIOP}$: (e) Irrgang, T.; Schareina, T.; Kempe, R. *J. Mol. Catal. A: Chem.* **2006**, *257*, 48–52. Hydrosilylation of carbonyls with 1,1'-bis(dimethylsilyl)ferrocene catalyzed by $\text{Ni}(\text{PET}_3)_4$: (f) Kong, Y. K.; Kim, J.; Choi, S.; Choi, S.-B. *Tetrahedron Lett.* **2007**, *48*, 2033–2036.

(21) (a) Bedford, R. B.; Draper, S. M.; Scully, P. N.; Welch, S. L. *New J. Chem.* **2000**, *24*, 745–747. (b) Morales-Morales, D.; Grause, C.; Kasaoka, K.; Redón, R.; Cramer, R. E.; Jensen, C. M. *Inorg. Chim. Acta* **2000**, 300–302, 958–963.



The attempted synthesis of **3c** (R = Ph) from the reduction of **2c** with LiAlH₄, NaBH₄, or LiEt₃BH gave intractable products.

Nickel hydride **3a** appeared inert toward C=C and C≡C bond insertion; no appreciable insertion product was detected when a solution of **3a** in toluene-*d*₈ was treated with 1-hexene, *trans*-3-hexene, styrene, 3-hexyne, 2,3-dimethyl-1,3-butadiene, or methyl methacrylate at room temperature. On the other hand, fast C=O insertion of PhCHO into the same nickel hydride was observed under similar conditions (Scheme 2). ¹H NMR spectroscopy showed the formation of nickel benzyloxide **4a**; the intensity of a new resonance at δ 4.88 (singlet) increased as the intensities of both hydride **3a** (δ -7.90) and PhCHO (δ 9.62) decreased. The insertion reaction was complete within 30 min and provided **4a** in >95% NMR yield. Complex **4a** was also independently generated from the metathesis between **2a** and PhCH₂ONa, although the isolation of compound **4a** in an analytically pure form was unsuccessful. Nevertheless, the reaction shown in Scheme 2 is the first directly observed insertion of an organic carbonyl group into a nickel–hydrogen bond.²⁵ The reverse step of aldehyde insertion, β-hydride elimination of a metal alkoxide, is more commonly observed for late transition metals.²⁶ It is possible that the insertion of PhCHO into **3a** is reversible, with an equilibrium favoring the nickel benzyloxide **4a**.²⁷ As expected, ketones were less reactive than PhCHO, as the resulting secondary alkoxides are more

(22) Götter-Schnettmann, I.; White, P.; Brookhart, M. *J. Am. Chem. Soc.* **2004**, *126*, 1804–1811.

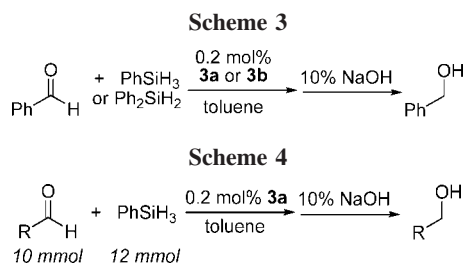
(23) Synthesis of nickel chloride **2a**: (a) Pandarus, V.; Zargarian, D. *Organometallics* **2007**, *26*, 4321–4334. **2c**: (b) Gómez-Benítez, V.; Baldivino-Pantaleón, O.; Herrera-Álvarez, C.; Toscano, R. A.; Morales-Morales, D. *Tetrahedron Lett.* **2006**, *47*, 5059–5062.

(24) The ¹Bu groups show some disorder. A disorder model is presented for C10 and C12. See the Supporting Information for details.

(25) For direct observation of C=O insertion into a metal–hydrogen bond, see the following examples. Ta–H: (a) Weinert, C. S.; Fanwick, P. E.; Rothwell, I. P. *Organometallics* **2005**, *24*, 5759–5766. W–H: (b) van der Zeijden, A. A. H.; Berke, H. *Helv. Chim. Acta* **1992**, *75*, 513–522. (c) Furno, F.; Fox, T.; Schmalte, H. W.; Berke, H. *Organometallics* **2000**, *19*, 3620–3630. Mo–H: (d) Liang, F.; Jacobsen, H.; Schmalte, H. W.; Fox, T.; Berke, H. *Organometallics* **2000**, *19*, 1950–1962. (e) Liang, F.; Schmalte, H. W.; Fox, T.; Berke, H. *Organometallics* **2003**, *22*, 3382–3393. (f) Zhao, Y.; Schmalte, H. W.; Fox, T.; Blacque, O.; Berke, H. *Dalton Trans.* **2006**, *7*, 3–85. (g) Cugny, J.; Schmalte, H. W.; Fox, T.; Blacque, O.; Alfonso, M.; Berke, H. *Eur. J. Inorg. Chem.* **2006**, *54*, 0–552. Re–H: (h) Du, G.; Fanwick, P. E.; Abu-Omar, M. M. *J. Am. Chem. Soc.* **2007**, *129*, 5180–5187. Ru–H: (i) Baratta, W.; Ballico, M.; Esposito, G.; Rigo, P. *Chem. Eur. J.* **2008**, *14*, 5588–5595. Pt–H: (j) van Leeuwen, P. W. N. M.; Roobeek, C. F.; Orpen, A. G. *Organometallics* **1990**, *9*, 2179–2181.

(26) Bryndza, H. E.; Tam, W. *Chem. Rev.* **1988**, *88*, 1163–1188.

(27) Experiments designed to elucidate the reversibility of aldehyde insertion will be reported later.



likely to undergo β-hydride elimination than primary alkoxides. When a solution of hydride **3a** in C₆D₆ was treated with an equimolar amount of PhCOCH₃ at room temperature for 24 h, the insertion product consisted of only 17 mol % of all nickel species. Reaction with PhCOPh under similar conditions did not yield any alkoxide species. To complete a catalytic cycle, complex **4a** was mixed with various silanes to re-form hydride **3a**. Both PhSiH₃ and Ph₂SiH₂ were identified as excellent silyl reagents for the nickel benzyloxide; complete regeneration of **3a** and release of the silyl ether product were seen within a few minutes (Scheme 2). Other silanes such as (EtO)₃SiH and poly(methylhydrosiloxane) (PMHS) regenerated hydride **3a** after longer reaction times (> 1 h), while Et₃SiH showed no reaction with complex **4a**.

Having established the protocols of aldehyde insertion and hydride regeneration, we set out to investigate the catalytic activity of hydrides **3a,b** for the hydrosilylation of benzaldehyde (Scheme 3). With PhSiH₃ or Ph₂SiH₂ as the silyl reagents, hydride **3a** catalyzed the hydrosilylation reaction efficiently; the reaction was complete within 2 h at room temperature with catalyst loading as low as 0.2 mol %. Consistent with the stoichiometric experiments, catalytic reactions with (EtO)₃SiH, PMHS, and Et₃SiH were much slower than those with PhSiH₃ and Ph₂SiH₂.²⁸ A control experiment in the absence of the nickel hydride **3a** showed no significant hydrosilylation, even at 60 °C for 5 days. Hydride **3b** also catalyzed the hydrosilylation reaction, albeit with a slower rate.²⁹

The scope of this catalytic system was studied using 0.2 mol % of **3a** in the presence of a slight excess of PhSiH₃, and the reduction products were isolated as alcohols following basic hydrolysis of the silyl ethers (Scheme 4). As shown in Table 1, the hydrosilylation reaction was tolerant of many functional groups, including OMe (entry 2), NMe₂ (entry 3), Cl (entry 4), NO₂ (entry 5), and CN (entry 10). It would be difficult to rationalize the electronic effect of substituents on the relative hydrosilylation rates, since both the aldehyde with an electron-donating group (entry 2) and the one with an electron-withdrawing group (entry 4) are less reactive than the unsubstituted benzaldehyde (entry 1). An explanation of these results will require more detailed kinetic studies on individual steps of the potential catalytic cycle for each substrate. These studies will be reported in due course. For α,β-unsaturated aldehydes (entries 9 and 12), only the 1,2-addition products were obtained. These results are in contrast to other Ni-catalyzed³⁰ or Cu-catalyzed³¹ hydrosilylations of α,β-unsaturated carbonyl com-

(28) Partial hydrosilylation was seen with (EtO)₃SiH (80% conversion with 2.0 mol % catalyst) when the reaction was quenched after 2 h of stirring at room temperature. Reaction with Et₃SiH or PMHS under similar conditions afforded no hydrosilylation product.

(29) When 0.2 mol % of **3b** was used as the catalyst, 38 mol % of PhCHO was converted after 2 h of reaction.

(30) (a) Boudjouk, P.; Choi, S.-B.; Hauck, B. J.; Rajkumar, A. B. *Tetrahedron Lett.* **1998**, *39*, 3951–3952. (b) Kim, S. O.; Rhee, S.; Lee, S. H. *Bull. Korean Chem. Soc.* **1999**, *20*, 773–774.

(31) Jurkauskas, V.; Sadighi, J. P.; Buchwald, S. L. *Org. Lett.* **2003**, *5*, 2417–2420.

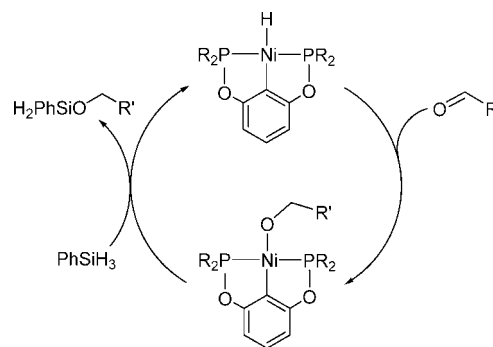
Table 1. Hydrosilylation of Aldehydes Catalyzed by Nickel Pincer Hydride

entry	substrate	product	temperature	time	isolated yield
1			rt	2 h	79%
2			rt	24 h	77%
3			rt	2 h	89%
4			70°C	24 h	92%
5			70°C	24 h	72%
6			60°C	1 h	75%
7			rt	2 h	67%
8			rt	24 h	84%
9			60°C	24 h	71%
10			rt	3 h	30%+60% (5) (6)
11			rt	24 h	85%
12			60°C	24 h	91%
13			rt	4 h	64%

pounds, where only the 1,4-addition products were isolated. The high selectivity for C=O over C=C hydrosilylation was also observed for aldehydes with isolated C=C bonds (entry 13). In addition to substituted benzaldehydes, other aromatic (entries 6–8) and aliphatic (entries 11–13) aldehydes were viable substrates for hydrosilylation. In each reaction studied, no side products such as enoxysilanes and disiloxanes were observed, making our nickel system superior to other nickel systems reported in the literature.^{20a,b} An aldehyde bearing a cyano group on the ortho position (entry 10) gave a mixture of two products: the expected 2-cyanobenzyl alcohol **5** and the lactone **6**. Compound **6** resulted from cyclization of **5** under the hydrolysis conditions. Ketones were much less reactive catalytically. Only partial hydrosilylation was observed for acetophenone (18%), cyclohexanone (60%), and benzophenone (6%), even at an elevated temperature (70 °C, 24 h) using a higher catalyst loading (1 mol %).

In view of the stoichiometric experiments shown in Scheme 2, a catalytic cycle was proposed for the current hydrosilylation system (Scheme 5). A similar mechanism has also been proposed by Nolan in his Cu(I)/carbene-catalyzed hydrosilylation reactions.³² Alternatively, nickel hydrides **3a,b** might activate the silanes prior to their interaction with the carbonyl groups. Such a process would resemble the well-known

Scheme 5. Catalytic Cycle for the Hydrosilylation of Aldehydes



Chalk–Harrod mechanism³³ for alkene hydrosilylation, and it has been proposed for Rh-catalyzed hydrosilylation of carbonyl substrates.³⁴ In addition, oxidative addition of silanes or Si–H σ -bond coordination to a nickel center has been reported.^{15h,35}

(32) (a) Kaur, H.; Zinn, F. K.; Stevens, E. D.; Nolan, S. P. *Organometallics* **2004**, *23*, 1157–1160. (b) Díez-González, S.; Kaur, H.; Zinn, F. K.; Stevens, E. D.; Nolan, S. P. *J. Org. Chem.* **2005**, *70*, 4784–4796. (c) Díez-González, S.; Scott, N. M.; Nolan, S. P. *Organometallics* **2006**, *25*, 2355–2358. (d) Díez-González, S.; Stevens, E. D.; Scott, N. M.; Petersen, J. L.; Nolan, S. P. *Chem. Eur. J.* **2008**, *14*, 158–168. (e) Díez-González, S.; Nolan, S. P. *Acc. Chem. Res.* **2008**, *41*, 349–358.

(33) Chalk, A. J.; Harrod, J. F. *J. Am. Chem. Soc.* **1965**, *87*, 16–21.

However, the mechanism involving initial silane activation is less likely to be operating in our nickel catalytic system. We found no reaction when **3a** was treated with PhSiH₃ in toluene-*d*₈ at room temperature or 60 °C for 24 h.

In conclusion, we have disclosed a nickel hydride system where the insertion of carbonyl groups into nickel–hydrogen bonds has been directly observed. The resulting nickel alkoxides react with silanes to release the silyl ether products and reform the nickel hydrides. More detailed mechanistic studies pertaining to the carbonyl insertion step, electronic influence on the turnover-limiting step of the catalytic cycle, and the development of more reactive nickel catalysts for ketone hydrosilylation are the subjects of ongoing research in our laboratory.

Experimental Section

All the air-sensitive compounds were prepared and handled under an argon atmosphere using standard Schlenk and inert-atmosphere box techniques. All aldehyde and ketone substrates were purchased from commercial sources and were used without further purification. Dry and oxygen-free solvents were collected from an Innovative Technology solvent purification system and used throughout all the experiments. Toluene-*d*₈ and C₆D₆ were distilled from Na and benzophenone under argon. Both ¹H NMR and ³¹P{¹H} NMR spectra were recorded on a Bruker Avance-400 MHz NMR spectrometer. Chemical shift values in ¹H NMR spectra were referenced internally to the residual solvent resonances (δ 7.26 for CDCl₃, δ 7.15 for C₆D₆, and δ 2.09 for toluene-*d*₈). The ³¹P{¹H} NMR spectra were referenced to an external 85% H₃PO₄ sample (δ 0). Column chromatography was performed with silica gel and solvents of commercial grade. All isolated alcohol products were known compounds and characterized by ¹H NMR spectroscopy. The NMR data obtained for all compounds were consistent with the literature values. 1,3-(^tBu₂PO)₂C₆H₄ (**1b**),²² [2,6-(ⁱPr₂PO)₂-C₆H₃]NiCl (**2a**),^{23a} and [2,6-(Ph₂PO)₂C₆H₃]NiCl (**2c**)^{23b} were prepared as described in the literature.

Synthesis of [2,6-(^tBu₂PO)₂C₆H₃]NiCl (2b**).** Under an argon atmosphere 50 mL of toluene was added to a mixture of 1,3-(^tBu₂PO)₂C₆H₄ (1.20 g, 3.0 mmol) and anhydrous NiCl₂ (389 mg, 3.0 mmol), giving an orange suspension. While the solution was being boiled for 18 h, a brown precipitate formed, which was removed by filtration after the mixture was cooled to room temperature. The volume of the orange filtrate was reduced to 5 mL, and then Et₂O was added to cause precipitation. The product was collected by filtration, washed with Et₂O, and dried under vacuum to give an orange-green powder of **2b** (725 mg, 49% yield). X-ray-quality crystals were grown by allowing a layer of pentane to slowly diffuse into a saturated CH₂Cl₂ solution of the nickel chloride. ¹H NMR (400 MHz, CDCl₃): δ 1.49 (virtual triplet, PC(CH₃)₃, *J*_{P-H} = 6.8 Hz, 36H), 6.38 (d, *Ar*, *J*_{H-H} = 8.0 Hz, 2H), 6.92 (t, *Ar*, *J*_{H-H} = 8.0 Hz, 1H). ³¹P{¹H} NMR (162 MHz, CDCl₃): δ 187.20 (s). Anal. Calcd for C₂₂H₃₉ClO₂P₂Ni: C, 53.75; H, 8.00; Cl, 7.21. Found: C, 54.11; H, 8.09; Cl, 7.25.

Synthesis of [2,6-(ⁱPr₂PO)₂C₆H₃]NiH (3a**).** Under an argon atmosphere the suspension of LiAlH₄ (872 mg, 23 mmol) and **2a** (500 mg, 1.15 mmol) in 60 mL of toluene was stirred at room temperature for 24 h. The resulting mixture was filtered through a short plug of Celite to give a yellow solution. After the solvent

was evaporated under vacuum, the desired hydride **3a** was isolated as an orange-yellow crystalline solid (405 mg, 88% yield). ¹H NMR (400 MHz, toluene-*d*₈): δ -7.90 (t, NiH, *J*_{P-H} = 55.2 Hz, 1H), 1.08–1.17 (m, PCH(CH₃)₂, 24H), 2.05–2.11 (m, PCH(CH₃)₂, 4H), 6.74 (d, *Ar*, *J*_{H-H} = 8.0 Hz, 2H), 6.97 (t, *Ar*, *J*_{H-H} = 8.0 Hz, 1H). ³¹P{¹H} NMR (162 MHz, toluene-*d*₈): δ 206.56 (s). Anal. Calcd for C₁₈H₃₂O₂P₂Ni: C, 53.90; H, 8.04. Found: C, 53.88; H, 8.17.

[2,6-(^tBu₂PO)₂C₆H₃]NiH (3b**).** This compound was prepared in 80% yield by a procedure similar to that used for **3a**. X-ray-quality crystals were grown by layering CH₃OH on a saturated THF solution of the hydride at -35 °C and slowly allowing it to diffuse. ¹H NMR (400 MHz, C₆D₆): δ -7.96 (t, NiH, *J*_{P-H} = 53.2 Hz, 1H), 1.30 (virtual triplet, PC(CH₃)₃, *J*_{P-H} = 6.8 Hz, 36H), 6.85 (d, *Ar*, *J*_{H-H} = 7.6 Hz, 2H), 7.02 (t, *Ar*, *J*_{H-H} = 7.6 Hz, 1H). ³¹P{¹H} NMR (162 MHz, C₆D₆): δ 219.35 (s). Anal. Calcd for C₂₂H₄₀O₂P₂Ni: C, 57.80; H, 8.82. Found: C, 57.65; H, 8.85.

Synthesis of [2,6-(ⁱPr₂PO)₂C₆H₃]NiOCH₂Ph (4a**).** **Method A.** To a solution of **3a** (40 mg, 0.10 mmol) in 5 mL of toluene was added degassed benzaldehyde (10 μ L, 0.10 mmol) under an argon atmosphere, and the resulting mixture was stirred at room temperature for 1 h. Evaporating the solvent under vacuum yielded an orange oil, and the NMR spectra of the crude product were recorded (see the Supporting Information). ¹H NMR (400 MHz, toluene-*d*₈): δ 1.18–1.29 (m, PCH(CH₃)₂, 12H), 1.32–1.41 (m, PCH(CH₃)₂, 12H), 2.09–2.15 (m, PCH(CH₃)₂, 4H), 4.88 (s, OCH₂Ph, 2H), 6.50 (d, *Ar*, *J*_{H-H} = 8.0 Hz, 2H), 6.84 (t, *Ar*, *J*_{H-H} = 8.0 Hz, 1H), 7.00–7.56 (m, CH₂Ph, 5H). ³¹P{¹H} NMR (162 MHz, toluene-*d*₈): δ 176.59 (s). Attempts to further purify **4a** via recrystallization led to decomposition of the product.

Method B. Under an argon atmosphere, a suspension of **2a** (87 mg, 0.2 mmol) and sodium benzyloxide (39 mg, 0.3 mmol) in 10 mL of toluene was stirred at room temperature for 24 h. The resulting mixture was passed through a short plug of Celite to remove NaCl, and the filtrate was concentrated under vacuum. Again, an orange oil was obtained and its NMR spectra matched the data above, although further purification of **4a** led to decomposition of the product.

General Procedures for Hydrosilylation. To a flame-dried Schlenk flask was added a solution of nickel **3a** (8.0 mg, 20 μ mol) in toluene (6 mL) and an aldehyde substrate (10 mmol) under an argon atmosphere. The resulting mixture was stirred at room temperature for 5–10 min, after which PhSiH₃ (1.48 mL, 12 mmol) was added via a gastight syringe. The reaction mixture was stirred at room temperature or at a higher temperature until there was no aldehyde left (monitored by withdrawing aliquots and analyzing their ¹H NMR spectra). The reaction was then quenched by a 10% aqueous solution of NaOH (about 10 mL) with vigorous stirring for more than 12 h. The solution containing the alcohol product was extracted with diethyl ether three times, dried over anhydrous Na₂SO₄, and concentrated under vacuum. The desired alcohol was further purified by flash column chromatography.

Acknowledgment. We are grateful for financial support from the University of Cincinnati. X-ray data were collected on a Bruker SMART6000 diffractometer which was funded by an NSF-MRI grant (No. CHE-0215950).

Supporting Information Available: Spectroscopic characterization data for compound **4a** and the alcohol products shown in Table 1, as well as crystallographic data (CIF and PDF) for **2b** and **3b**. This material is available free of charge via the Internet at <http://pubs.acs.org>.

OM800948F

(34) Ojima, I.; Kogure, T.; Kumagai, M.; Horiuchi, S.; Sato, T. *J. Organomet. Chem.* **1976**, *122*, 83–97.

(35) Steinke, T.; Gemel, C.; Cokoja, M.; Winter, M.; Fischer, R. A. *Angew. Chem., Int. Ed.* **2004**, *43*, 2299–2302.

Five- and Seven-Membered Metallacycles in [C,N,N'] and [C,N] Cycloplatinated Compounds

Raquel Martín and Margarita Crespo*

Departament de Química Inorgànica, Universitat de Barcelona, Diagonal 647, 08028 Barcelona, Spain

Mercè Font-Bardia and Teresa Calvet

Departament de Cristal·lografia, Mineralogia i Dipòsits Minerals, Universitat de Barcelona, Martí i Franquès s/n, 08028 Barcelona, Spain

Received September 5, 2008

The reactions of *cis*-[Pt(4-C₆H₄Me)₂(μ-SEt₂)₂] with ligands ArCH=NCH₂CH₂NMe₂ (Ar = 4-ClC₆H₄ (**1a**); 2-BrC₆H₄ (**1b**); 2,6-Cl₂C₆H₃ (**1c**); C₆F₅ (**1d**)) and ArCH=NCH₂(4-ClC₆H₄) (Ar = 4-ClC₆H₄ (**1e**); 2-BrC₆H₄ (**1f**); 2,6-Cl₂C₆H₃ (**1g**); C₆F₅ (**1h**)) were studied. Several types of compounds were formed including (i) [N,N'] coordination compounds (**2a**, **2c**, **2d**), (ii) [C,N,N'] platinum(IV) (**3b**, **3c**), [C,N,N'] platinum(II) (**4a**), and [C,N] platinum(II) (**4e**) cyclometalated compounds with a five-membered metallacycle, and (iii) [C,N,N'] platinum(II) (**5c**) and [C,N] platinum(II) (**5f**, **5g**) cyclometalated compounds with a seven-membered metallacycle. The reactions of the obtained cyclometalated compounds with triphenylphosphine were studied, and the new compounds were fully characterized including structure determinations for **4a**, **5c**, **5g**, and the phosphine derivative **7 g'**. The ease of formation of seven-membered metallacycles is discussed on the basis of the structure of the ligand (terdentate versus bidentate) and the C–X bond to be activated.

Introduction

Palladium and platinum cyclometalated compounds with nitrogen donor ligands attract a great deal of interest due to their numerous applications in several fields, such as organic and organometallic synthesis, the design of new metallomolecules, and biologically active compounds.¹ An interesting feature of platinum derivatives is that, in addition to square-planar platinum(II) compounds, octahedral platinum(IV) complexes may also be obtained; this fact has stimulated the development of electron-rich platinum precursors such as [Pt₂Me₄(SMe₂)₂],² which are able to produce either platinum(II) or platinum(IV) compounds.

Several diarylplatinum(II) compounds have also been tested as metalating agents and shown to produce different types of reactions. A process involving intramolecular C–H activation and loss of 1 equiv of the corresponding arene has been reported

for adequate N-donor ligands when *cis*-[PtPh₂(dmsO)₂],³ *cis*-[PtPh₂(SMe₂)₂],^{4,5} *cis*-[Pt(3,5-R₂C₆H₃)₂(dmsO)₂] (R = Me, CF₃),⁶ or *trans*-[Pt(2,4,6-Me₃C₆H₂)₂(dmsO)₂]⁷ is used. On the other hand, reactions involving intramolecular C–Br activation and elimination of 4,4'-bitolyl have been reported as a convenient method for the synthesis of [N,C,N] cyclometalated platinum(II) compounds⁸ when substrate *cis*-[Pt(4-C₆H₄Me)₂(μ-SEt₂)₂] was used. Finally, processes leading to elimination of 1 equiv of benzene along with formal insertion of one phenyl ligand in the metallacycle have been reported upon reaction of *cis*-[PtPh₂(SMe₂)₂] with N-donor ligands for which C–Br or C–Cl bond activation is possible.⁴ The latter process leads to formation of seven-membered metallacycles (see method **a** in Scheme 1), and it is interesting to point out that this type of metallacycle has also been obtained in a process using *cis*-[PtCl₂(dmsO)₂] as metalating agent and involving intermolecular

* Corresponding author. Phone: +34934039132. Fax: +34934907725. E-mail: margarita.crespo@qi.ub.es.

(1) (a) Ryabov, A. D. *Synthesis* **1985**, 233. (b) Dupont, J.; Pfeiffer, M.; Spencer, J. *Eur. J. Inorg. Chem.* **2001**, 1917. (c) Dupont, J.; Consorti, C. S.; Spencer, J. *Chem. Rev.* **2005**, *105*, 2527. (d) Omae, I. *Coord. Chem. Rev.* **2004**, *248*, 995. (e) Espinet, P.; Esteruelas, M. A.; Oro, L. A.; Serrano, J. L.; Sola, E. *Coord. Chem. Rev.* **1992**, *117*, 215. (f) Navarro-Ranninger, C.; López-Solera, I.; Pérez, J. M.; Masaguer, J. R.; Alonso, C. *Appl. Organomet. Chem.* **1993**, *7*, 57. (g) Albrecht, M.; van Koten, G. *Angew. Chem., Int. Ed.* **2001**, *40*, 3750.

(2) (a) Anderson, C. M.; Crespo, M.; Jennings, M. C.; Lough, A. J.; Ferguson, G.; Puddephatt, R. J. *Organometallics* **1991**, *10*, 2672. (b) Crespo, M.; Martínez, M.; Sales, J.; Solans, X.; Font-Bardia, M. *Organometallics* **1992**, *11*, 1288. (c) Crespo, M.; Martínez, M.; Sales, J. *Organometallics* **1993**, *12*, 4297. (d) Crespo, M.; Solans, X.; Font-Bardia, M. *Organometallics* **1995**, *14*, 355. (e) Baar, C. R.; Jenkins, H. A.; Vittal, J. J.; Yap, G. P. A.; Puddephatt, R. J. *Organometallics* **1998**, *17*, 2805. (f) Baar, C. R.; Hill, G. S.; Vittal, J. J.; Puddephatt, R. J. *Organometallics* **1998**, *17*, 32.

(3) (a) Minghetti, G.; Stoccoro, S.; Cinellu, M. A.; Soro, B.; Zucca, A. *Organometallics* **2003**, *22*, 4770. (b) Zucca, A.; Doppiu, A.; Cinellu, M. A.; Stoccoro, S.; Minghetti, G.; Manassero, M. *Organometallics* **2002**, *21*, 783.

(4) (a) Crespo, M.; Font-Bardia, M.; Solans, X. *Organometallics* **2004**, *23*, 1708. (b) Font-Bardia, M.; Gallego, C.; Martínez, M.; Solans, X. *Organometallics* **2002**, *21*, 3305. (c) Gallego, C.; Martínez, M.; Safont, V. S. *Organometallics* **2007**, *26*, 527.

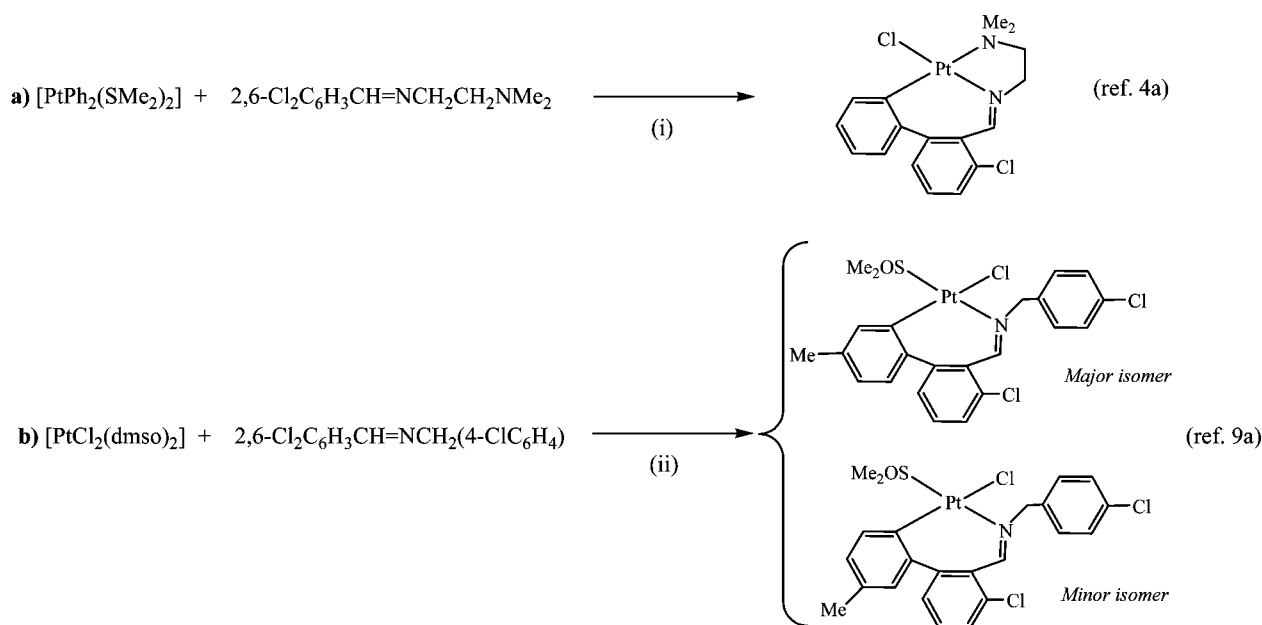
(5) Crespo, M.; Font-Bardia, M.; Solans, X. *J. Organomet. Chem.* **2006**, *691*, 1897.

(6) Yagyu, T.; Ohashi, J.; Maeda, M. *Organometallics* **2007**, *26*, 2383.

(7) Sarkar, B.; Schurr, T.; Hartenbach, I.; Schleid, T.; Fiedler, J.; Kaim, W. *J. Organomet. Chem.* **2008**, *693*, 1703.

(8) (a) Rodríguez, G.; Albrecht, M.; Schoenmaker, J.; Ford, A.; Lutz, M.; Spek, A. L.; van Koten, G. *J. Am. Chem. Soc.* **2002**, *124*, 5127. (b) Albrecht, M.; Rodríguez, G.; Schoenmaker, J.; van Koten, G. *Org. Lett.* **2000**, *2*, 3461. (c) Canty, A. J.; Patel, J.; Skelton, B. W.; White, A. H. *J. Organomet. Chem.* **2000**, *599*, 195. (d) Slagt, M. Q.; Gebbink, R. J. M. K.; Lutz, M.; Spek, A. L.; van Koten, G. *J. Chem. Soc., Dalton Trans.* **2002**, 2591.

Scheme 1



(i) Refluxing toluene, 4h; (ii) + $\text{Na}(\text{CH}_3\text{CO}_2)/\text{MeOH}$, toluene, 90°C , 48h.

activation of toluene used as a solvent,⁹ as shown in method **b** in Scheme 1. These reactions involve formation of a C–C bond leading to a biaryl linkage, which is an important process in organic synthesis.¹⁰

In order to gain insight into the different processes that might take place when diarylplatinum compounds are used as metalating substrates, the study of the reactions of *cis*- $[\text{Pt}(4\text{-C}_6\text{H}_4\text{Me})_2(\mu\text{-SEt}_2)_2]$ with imines of general formulas $\text{ArCH}=\text{NCH}_2\text{CH}_2\text{NMe}_2$ and $\text{ArCH}=\text{NCH}_2(4\text{-ClC}_6\text{H}_4)$ in which the aryl group Ar may contain either Br, Cl, H, or F in the *ortho* positions was envisaged. The aim of this work is to evaluate how both the nature of the *ortho* C–X bonds and the different structure of the ligands, containing either two or one nitrogen atoms, influence the obtained results. Dinuclear compound *cis*- $[\text{Pt}(4\text{-C}_6\text{H}_4\text{Me})_2(\mu\text{-SEt}_2)_2]$, previously used as metalating agent as stated above,⁸ was selected for this study since the presence of an electron-donor methyl substituent in the aryl ring facilitates the activation of the *ortho* C–X bonds⁶ as well as the spectral characterization of the products by means of NOE interactions in which the methyl is involved. In addition, a comparison with the compounds arising from intermolecular activation of toluene⁹ could be drawn, thus allowing for a better understanding of these processes.

Results and Discussion

Reactions with Ligands $\text{ArCH}=\text{NCH}_2\text{CH}_2\text{NMe}_2$ (Ar = 4-ClC₆H₄ (1a**); 2-BrC₆H₄ (**1b**); 2,6-Cl₂C₆H₃ (**1c**); C₆F₅ (**1d**)).** The reactions of *cis*- $[\text{Pt}(4\text{-C}_6\text{H}_4\text{Me})_2(\mu\text{-SEt}_2)_2]$ with ligands **1a**, **1c**, or **1d** in toluene at room temperature produced compounds $[\text{Pt}(4\text{-C}_6\text{H}_4\text{Me})_2(\text{Me}_2\text{NCH}_2\text{CH}_2\text{NCHAr})]$ (**2a**, **2c**, **2d**) containing a bidentate [N,N'] ligand as yellow solids (see Scheme 2). ¹H–¹H NOESY experiments indicated an *E*

conformation across the C=N bond since a cross-peak signal between the imine and the methylene protons was observed. *E* to *Z* isomerization in solution was followed by ¹H NMR spectroscopy at room temperature for compounds **2a** and **2c**, as shown in Scheme 3. For **2a**, after 96 h, the ratio of the isomers was *E:Z* = 1:1.9. For **2c**, the process was more complex since, in addition to *E*–*Z* isomerization, cyclometalated platinum(IV) compound $[\text{PtCl}(4\text{-MeC}_6\text{H}_4)_2\{2\text{-ClC}_6\text{H}_3\text{CHNCH}_2\text{CH}_2\text{NMe}_2\}]$ (**3c**) arising from intramolecular C–Cl oxidative addition and containing a terdentate [C,N,N'] ligand was formed. In this case, after 24 h, the ¹H NMR spectrum indicated disappearance of the *E* isomer and the presence of both the *Z* isomer and compound **3c** as the main product. After 120 h, conversion to compound **3c** was complete.

The reaction of *cis*- $[\text{Pt}(4\text{-C}_6\text{H}_4\text{Me})_2(\mu\text{-SEt}_2)_2]$ with ligand **1b** in toluene at room temperature produced compound $[\text{PtBr}(4\text{-MeC}_6\text{H}_4)_2\{4\text{-ClC}_6\text{H}_3\text{CHNCH}_2\text{CH}_2\text{NMe}_2\}]$ (**3b**) as a white solid, in an analogous process to that described for **3c**, which involves coordination of the ligand, followed by intramolecular oxidative addition of a C–Br bond. In this case, the corresponding coordination compound could not be isolated, or even detected in solution, and this fact is consistent with the higher reactivity of a C–Br versus C–Cl or C–H bond.^{4a,11}

In an attempt to obtain cyclometalated platinum(II) compounds, coordination precursors **2a** and **2c** were treated in toluene under reflux for 6 h to produce, respectively, compounds $[\text{Pt}(4\text{-MeC}_6\text{H}_4)_2\{4\text{-ClC}_6\text{H}_3\text{CHNCH}_2\text{CH}_2\text{NMe}_2\}]$ (**4a**) and $[\text{PtCl}\{(\text{MeC}_6\text{H}_3)(\text{ClC}_6\text{H}_3\text{CHNCH}_2\text{CH}_2\text{NMe}_2)\}]$ (**5c**). The proposed structures, shown in Scheme 2, contain a terdentate [C,N,N'] ligand. The former arises from intramolecular C–H bond activation and elimination of a toluene molecule to yield a five-membered metallacycle, while the latter is formed in a more complex process involving formation of a C–C bond between two aryl rings and formation of a seven-membered platinacycle.⁴

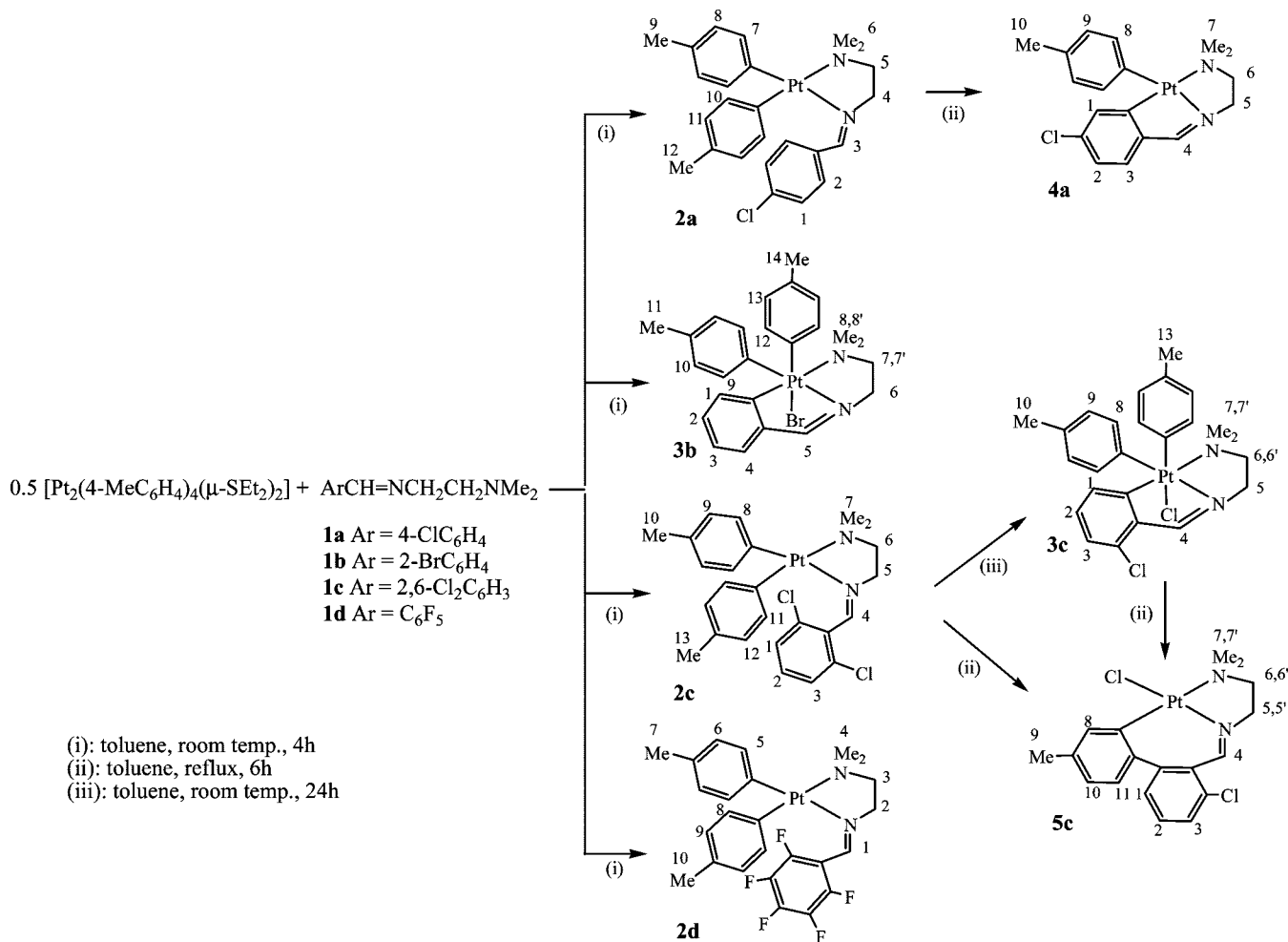
Under analogous conditions, no reaction was observed for ligand $\text{C}_6\text{F}_5\text{CH}=\text{NCH}_2\text{CH}_2\text{NMe}_2$ (**1d**), which can be related to the combined effects of the inertness of the C–F bond and the

(9) (a) Capapé, A.; Crespo, M.; Granell, J.; Vizcarro, A.; Zafrilla, J.; Font-Bardía, M.; Solans, X. *Chem. Commun.* **2006**, 4128. (b) Capapé, A.; Crespo, M.; Granell, J.; Font-Bardía, M.; Solans, X. *Dalton Trans.* **2007**, 2030.

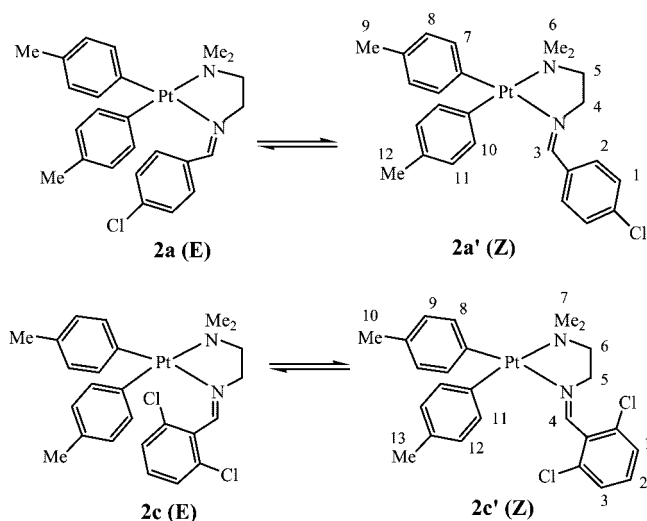
(10) (a) Nicolaou, K. C.; Bulger, P. G.; Sarlah, D. *Angew. Chem., Int. Ed.* **2005**, *44*, 4442. (b) Bedford, R. B. *Chem. Commun.* **2003**, 1787. (c) Bedford, R. B.; Cazin, C. S. J.; Holder, D. *Coord. Chem. Rev.* **2004**, *248*, 2283. (d) Godula, K.; Sames, D. *Science* **2006**, *312*, 67.

(11) Benson, S. W. *Thermochemical Kinetics*; Wiley: New York, 1976.

Scheme 2



Scheme 3



unfavorable steric effects of the tolyl groups. Although the C–F bond has been activated upon reaction of analogous ligands with platinum substrate [Pt₂Me₄(μ-SMe₂)₂],¹² no reaction has been observed when *cis*-[PtPh₂(SMe₂)₂] was used.^{4a}

In order to prove whether the formation of platinum(IV) compounds is involved in the mechanism of formation of seven-

membered metallacycles such as compound **5c**, the behavior of compound [PtCl(4-MeC₆H₄)₂{2-ClC₆H₃CHNCH₂CH₂NMe₂}] (**3c**) in refluxing toluene was also studied. It was confirmed that compound **5c** can be obtained from compound **3c**, although along with some decomposition leading to metallic platinum and lower yields than for the direct synthesis from **2c**. Under the same reaction conditions, compound **3b** reacted very slowly, and concomitant decomposition processes prevented isolation of the corresponding seven-membered derivative.

The new compounds were characterized by elemental analyses, ESI mass spectra, and NMR spectroscopy, and compounds **4a** and **5c** were also characterized crystallographically. In most cases, {¹H–¹H} COSY and NOESY NMR spectra were taken and allowed for a full assignment of the ¹H NMR signals.

For compounds **2**, the *J*(H–Pt) value for the imine is higher for the *E* (ca. 40–50 Hz) than for the *Z* (ca. 26 Hz) isomers, in agreement with the *trans* arrangement for the former.^{5,13} The *ortho* hydrogen atoms in the tolyl ligands are also coupled to platinum, and the *J*(H–Pt) values are smaller for the group *trans* to the imine, in agreement with the higher *trans* influence of imine versus amine.

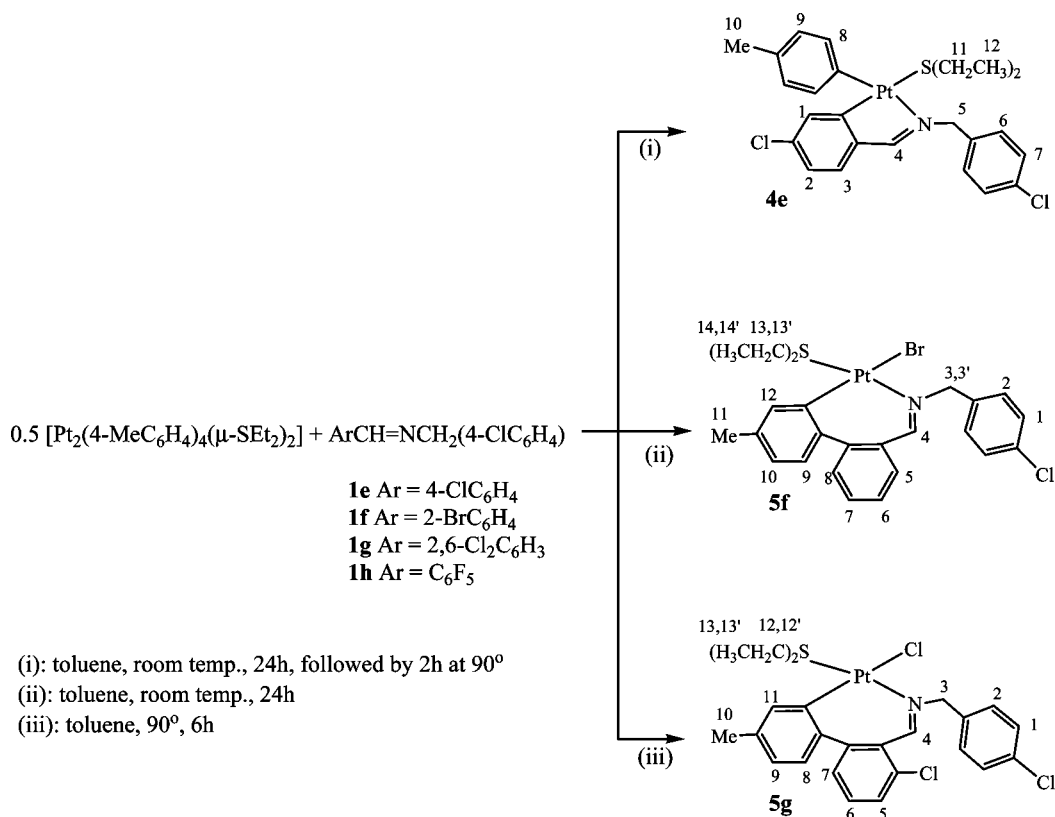
For octahedral platinum(IV) compounds **3**, distinct features are observed. As expected, the *J*(H–Pt) values observed for the imine and the tolyl *ortho* hydrogen atoms decrease when compared to related platinum(II) compounds.¹⁴ As a result of

(12) (a) Anderson, C. M.; Crespo, M.; Ferguson, G.; Lough, A. J.; Puddephatt, R. J. *Organometallics* **1992**, *11*, 1177. (b) López, O.; Crespo, M.; Font-Bardia, M.; Solans, X. *Organometallics* **1997**, *16*, 1233.

(13) Crespo, M.; Font-Bardia, M.; Granell, J.; Martínez, M.; Solans, X. *Dalton Trans.* **2003**, 3763.

(14) Crespo, M.; Puddephatt, R. J. *Organometallics* **1987**, *6*, 2548.

Scheme 4



the lack of symmetry plane, the methyl and methylene groups of the coordinated ligand are nonequivalent. Resonances of the tolyl ligands were assigned on the basis of the 2D-NOESY experiment carried out for **3b**, in which the *ortho* hydrogen atoms of the equatorial tolyl display cross-peaks with both methyl groups of the dimethylamino moiety, while the axial tolyl with only one of them.

For platinum(II) derivatives **4a** and **5c**, both the imine and the aromatic hydrogen adjacent to the metalation site are coupled to platinum. The remarkably different $J(\text{H}-\text{Pt})$ values for the imine are consistent with the presence of a tolyl (**4a**, $J(\text{H}-\text{Pt}) = 56.0$ Hz) or a chloro (**5c**, $J(\text{H}-\text{Pt}) = 147.7$ Hz) ligand in a *trans* position. For **5c**, as reported for related compounds with a seven-membered metallacycle,⁴ the methyl and methylene groups of the coordinated ligand are nonequivalent. The $\{^1\text{H}-^{13}\text{C}\}$ -heterocorrelation spectra of **4a** and **5c** show respectively five and six cross-peaks in the aromatic region, which is consistent with the proposed structures. For both **2a** and **4a**, the position of the ^{195}Pt resonance within the range expected for a [C, C, N, N] set of ligands¹⁵ confirms the proposed structures.

Reactions with Ligands ArCH=NCH₂(4-ClC₆H₄) (Ar = 4-ClC₆H₄ (1e**); 2-BrC₆H₄ (**1f**); 2,6-Cl₂C₆H₃ (**1g**); C₆F₅ (**1h**)).** In order to complete the present study, the reactions of *cis*-[Pt(4-C₆H₄Me)₂(μ-SEt₂)₂] with ligands **1e**, **1f**, **1g**, and **1h** containing only one nitrogen were also studied (see Scheme 4). Previous work using *N*-benzylidenebenzylamines with other metalating agents such as [Pt₂Me₄(SMe₂)₂] indicate that, although coordination of the ligand is postulated as a previous step to the intramolecular C–X bond activation, the corresponding coordination compounds are not usually isolated.^{2b,c,16}

Initially, the reactions were carried out in toluene at room temperature for 24 h. Under these conditions, imine **1f** gave compound **5f**, which contains a seven-membered metallacycle, while imines **1e** and **1g** gave mixtures of compounds, which when submitted to more drastic conditions, evolved to compounds **4e** and **5g**, respectively. Compound **5g** was best obtained when the platinum substrate and imine **1g** were treated in toluene at 90 °C for 6 h. Compounds **4e**, **5f**, and **5g** contain a bidentate [C,N] ligand. Compound [Pt(4-MeC₆H₄){4-ClC₆H₃CHNCH₂(4-ClC₆H₄)}SEt₂] (**4e**), which contains a five-membered metallacycle, arises from intramolecular C–H bond activation with elimination of a molecule of toluene. Compounds [PtBr{(MeC₆H₃)C₆H₄CHNCH₂(4-ClC₆H₄)}SEt₂] (**5f**) and [PtCl{(MeC₆H₃)(ClC₆H₃)CHNCH₂(4-ClC₆H₄)}SEt₂] (**5g**) are formed in processes involving C–X (X = Br or Cl) oxidative addition, formation of a C–C bond between the metalated phenyl and a tolyl ligand, and elimination of one molecule of toluene. No reaction, other than decomposition and imine hydrolyses when more drastic conditions were used, was observed for ligand **1h**. As previously indicated for ligand **1d**, the lack of reactivity can be related to the low reactivity of the C–F bond;¹⁷ in addition, the presence of only one nitrogen and the electron-withdrawing effect of the pentafluoro group prevent the formation of a coordination compound.

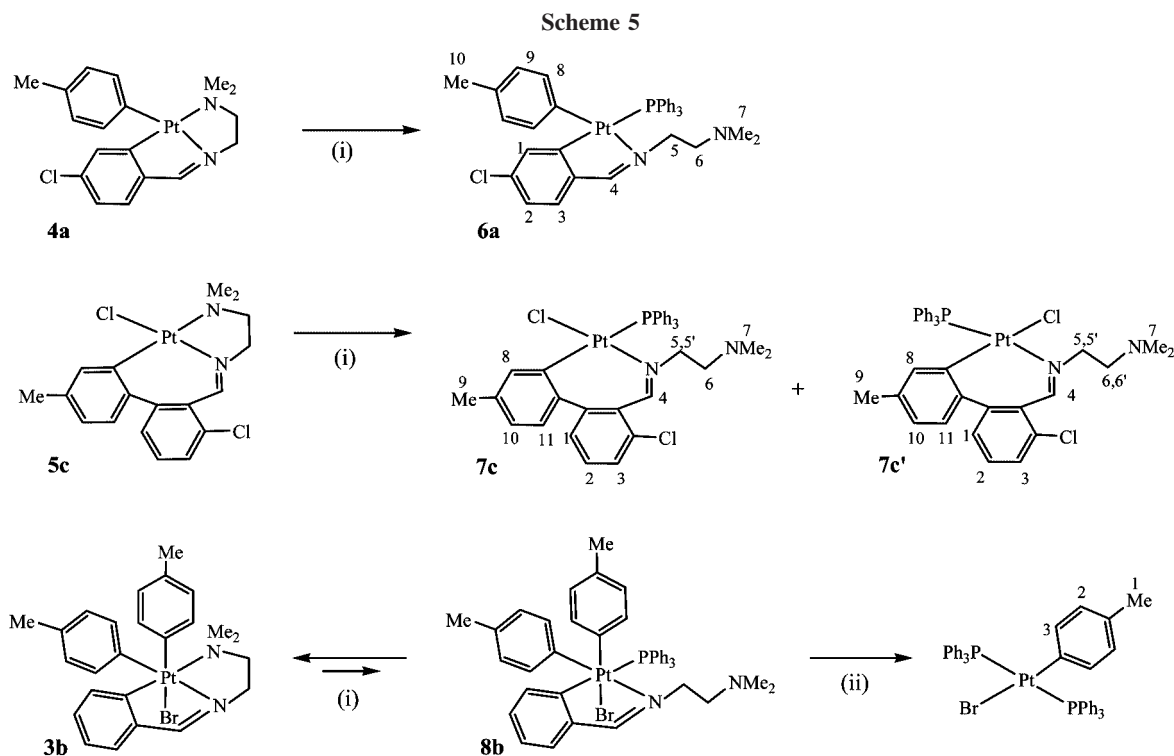
The new compounds were characterized by elemental analyses, ESI mass spectra, and NMR spectroscopy, and compounds **5g** was also characterized crystallographically.

In spite of the presence of a bidentate [C,N] ligand and a diethylsulfide in the coordination sphere of the compounds described in this section versus a tridentate [C,N,N'] in those

(15) Pregosin, P. S. *Coord. Chem. Rev.* **1982**, *44*, 247.

(16) Crespo, M.; Solans, X.; Font-Bardia, M. *J. Organomet. Chem.* **1996**, *518*, 105.

(17) (a) Burdeniuc, J.; Jedlicka, B.; Crabtree, R. H. *Chem. Ber. Recl.* **1997**, *130*, 145. (b) Bosque, R.; Clot, E.; Fantacci, S.; Maseras, F.; Eisenstein, O.; Perutz, R. N.; Renkema, K. B.; Caulton, K. G. *J. Am. Chem. Soc.* **1998**, *120*, 12634.



(i): + PPh₃ (1:1), acetone, room temp., 2h; (ii): + PPh₃ (2:1), acetone, room temp., 2h

described above, common features are observed for five-membered metallacycles (**4a** and **4e**) on one side and seven-membered metallacycles (**5c**, **5f**, and **5g**) on the other. As for **4a** and **5c**, both the imine and the aromatic hydrogen adjacent to the metalation site are coupled to platinum in compounds **4e**, **5f**, and **5g**. For **5f** and **5g**, the $J(\text{H}-\text{Pt})$ values for the imine are lower (ca. 120 Hz) than that observed for **5c** ($J(\text{H}-\text{Pt}) = 147.7$ Hz), in agreement with the presence of a diethylsulfide ligand in a *trans* position. For **5f** and **5g**, the methylene groups of the coordinated ligand are nonequivalent. The $\{^1\text{H}-^{13}\text{C}\}$ -heterocorrelation spectra of **4j**, **5f**, and **5g** show respectively seven, nine, and eight cross-peaks in the aromatic region, which is consistent with the proposed structures.

Reactions with Triphenylphosphine. The reactions of compounds **3b**, **4a**, **4e**, **5c**, **5f**, and **5g** with triphenylphosphine were carried out in acetone at room temperature (see Schemes 5 and 6).

For compounds **4a** and **4e**, the PPh₃ replaces either the dimethylamino moiety or the diethylsulfide ligand in the coordination sphere of platinum to yield, respectively, compounds **6a** and **6e**. An analogous process was observed for compound **5c**; however, in this case, two isomers in a 1:1 ratio were formed as reaction products. This result arises from the fact that replacement of NMe₂ for PPh₃ yields compound **7c** with the PPh₃ *trans* to a tolyl group, and this compound isomerizes to **7c'**, in which the PPh₃ is *trans* to the imine, a more stable situation according to the *transphobia*¹⁸ and the *trans-choice*¹⁹ models. In agreement with the higher stability of isomer **7c'**, after 18 h in solution the ratio **7c'**:**7c** is 3:1. As for **5f** and **5g**, the SET₂ ligand is *trans* to the N atom, in agreement with the *transphobia* and the *trans-choice* models,

and the reactions with triphenylphosphine indicate that the entering ligand is initially placed *trans* to the metalated carbon to yield **7f** and **7g**, respectively, which later isomerize to the more stable **7f'** and **7g'**, in which the phosphine is *trans* to the N atom. For **5f**, the reaction produced initially isomer **7f** only, which later isomerizes in solution to **7f'**. The reaction of **5g** with triphenylphosphine was monitored by NMR spectroscopy, and it was observed that before the replacement of the SET₂ ligand was complete, both isomers **7g** and **7g'** were formed. Within 4 h, the substitution process was complete and the ratio of isomers **7g**:**7g'** was 2.3:1.0; after 140 h in solution, the ratio was 0.7:1.0. Isomer **7g'** crystallized in dichloromethane–methanol. The obtained results suggest that although steric effects of the bulky triphenylphosphine might be responsible for the initial formation of compounds **7f** and **7g**, these isomerize to the more stable species according to the *transphobia* model.

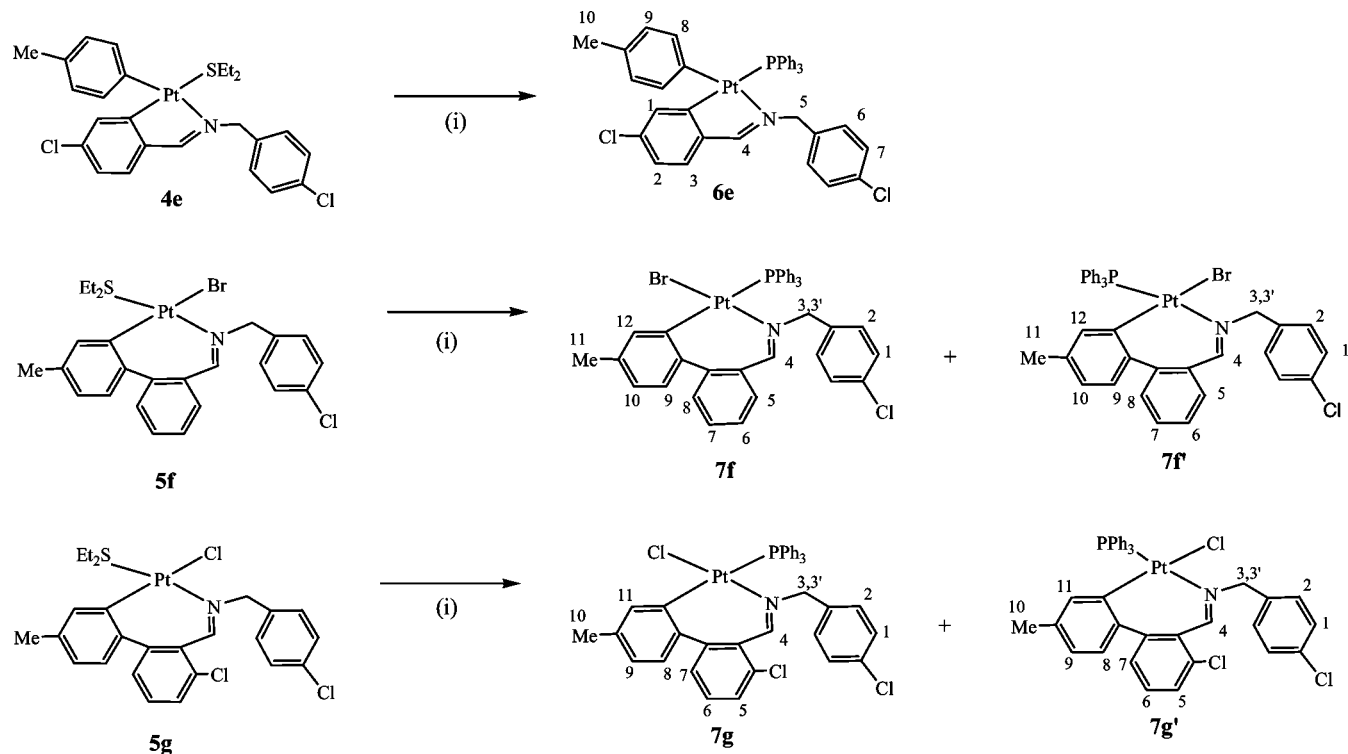
Under the same conditions, compound **3b** led to nearly quantitative recovery of the initial compound. A new signal observed in the ¹H NMR spectra of the crude product is consistent with formation of compound **8b**, which was formed in a very small extension, indicating a high stability of the terdentate [C,N,N'] platinum(IV) compound. In an attempt to displace the reaction, a PPh₃:**3b** = 2:1 ratio was used; however under these conditions compound *trans*-[PtBr(4-CH₃C₆H₄)-(PPh₃)₂] was formed.

Phosphine derivatives were characterized by ¹H and ³¹P NMR spectra; in order to achieve a full assignment $\{^1\text{H}-^1\text{H}\}$ COSY and NOESY experiments were also carried out for **7c** and **7c'**. For compounds **6**, the imine proton is a singlet coupled to platinum and the $J(\text{H}-\text{Pt})$ values are very similar to those observed for the parent compounds **4**. The $J(\text{P}-\text{Pt})$ values (ca. 2200 Hz) indicate that the PPh₃ is *trans* to the aryl group rather

(18) Vicente, J.; Abad, J. A.; Martínez-Viviente, E.; Jones, P. G. *Organometallics* **2002**, *21*, 4454.

(19) Cuevas, J. V.; García-Herbosa, G.; Miguel, D.; Muñoz, A. *Inorg. Chem. Commun.* **2002**, *5*, 340.

Scheme 6



(i): + PPh₃, acetone, room temp., 2h

than to the nitrogen atom.²⁰ Isomers **7** and **7'** show distinct features in both the ¹H and ³¹P NMR spectra. The imine appears as a singlet with a coupling to platinum of ca. 140 Hz for compounds **7** and as a doublet—due to coupling with the phosphorus atom—with a reduced *J*(H–Pt) value (ca. 88 Hz) for compounds **7'**. These data as well as the different *J*(P–Pt) values observed in the ³¹P NMR spectra (ca. 1860 Hz for compounds **7** and ca. 4300 Hz for compounds **7'**) are consistent with the position of the phosphine *trans* either to the metalated carbon or to the nitrogen atoms.²⁰

For compounds **6** and **7**, the NMR spectra did not show the presence of compounds with two coordinated phosphine ligands, even when an excess of the phosphine was present. This fact suggests that both the five-membered and the seven-membered metallacycles are stable and not easily cleaved upon reaction with phosphines.

Crystal Structures. Suitable crystals of compounds **4a**, **5c**, **5g**, and **7g'** were grown from dichloromethane–methanol at room temperature.

The crystal structures are composed of discrete molecules separated by van der Waals distances. Compound **5c** crystallizes with one molecule of CH₂Cl₂. The structures are shown in Figures 1, 2, 3, and 4, and selected molecular dimensions are listed in Table 1. Compound **4a** displays disorder in the positions of atoms C(16) and C(17).

The molecular structures confirm the geometries predicted from spectroscopic data. Square-planar coordination of the platinum(II) is achieved with a terdentate [C,N,N'] and a tolyl (**4a**) or a chloro (**5c**) ligand, or with a bidentate [C,N], a chloro, and a diethylsulfide (**5g**) or a triphenylphosphine (**7g'**) ligand.

For **5c**, **5g**, and **7g'** the metallacycle consists of a nonplanar seven-membered system in which the imine functionality and

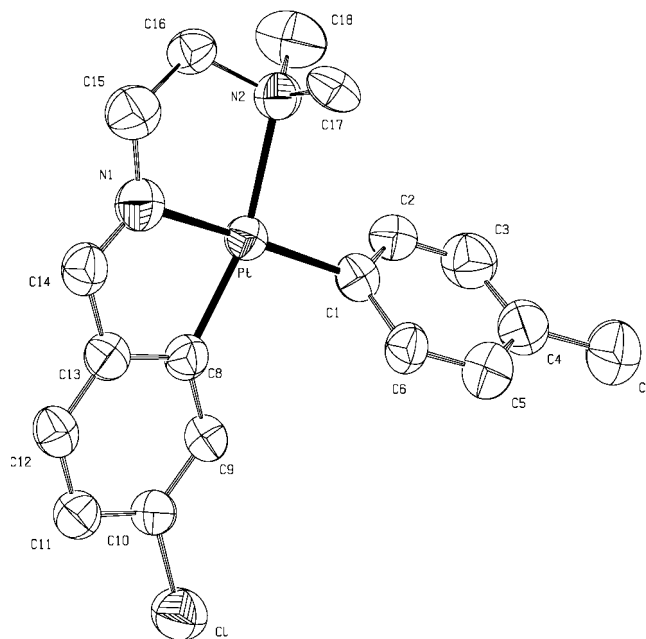


Figure 1. Molecular structure of compound **4a**.

two aryl rings tilted 50.6(2)° (**5c**), 55.2(2)° (**5g**), or 51.9(2)° (**7g'**) from each other are included. For **4a**, the five-membered metallacycle contains the imine functionality and the sum of internal angles is 540.0°, which suggest a planar arrangement for the *endo*-metallacycle.²¹ The dihedral angle between the mean planes of the metallacycle and the coordination plane is 3.9(2)°, and the tolyl ligand is tilted from the coordination plane by 59.8(3)°.

(20) Pregosin, P. S.; Kunz, R. W. *In* ³¹P and ¹³C NMR of Transition Metal Phosphine Complexes; Diehl, P., Fluck, E., Kosfeld, R., Eds.; Springer-Verlag: Berlin, 1979.

(21) Klein, H. F.; Camadanli, S.; Beck, R.; Leukel, D.; Flörke, U. *Angew. Chem., Int. Ed.* **2005**, *44*, 975.

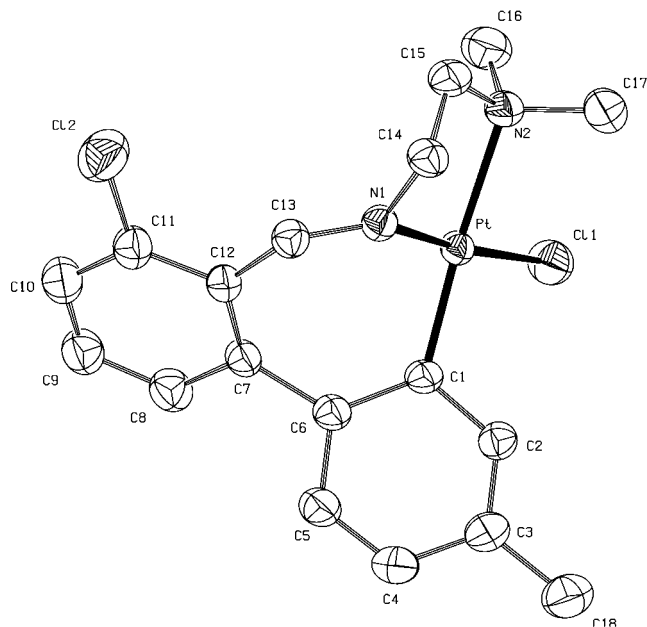


Figure 2. Molecular structure of compound **5c**.

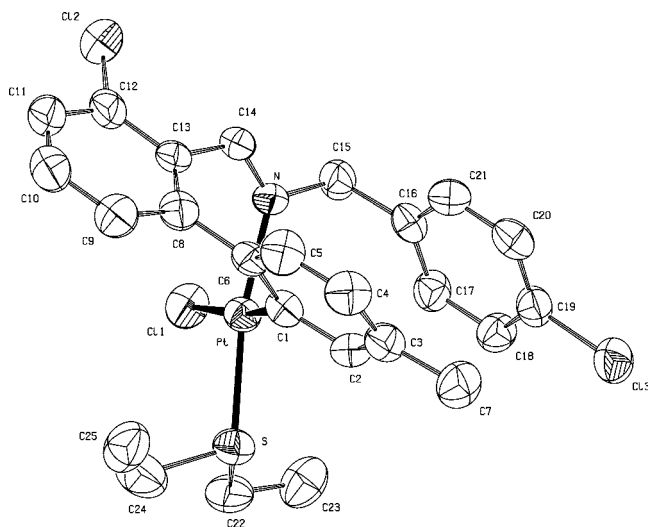


Figure 3. Molecular structure of compound **5g**.

Bond lengths and angles are well within the range of values obtained for analogous compounds. In particular, the Pt–C bonds are in the range of values found for other aryl complexes of platinum(II)^{4,9} and the Pt–amine distances are larger (2.177 and 2.204 Å) than platinum–imine distances (1.959–2.082 Å), consistent with the weaker ligating ability of amines for platinum.²² The Pt–Cl bond in **5c** (2.315 Å) is shorter than in **5g** (2.414 Å) and **7g'** (2.399 Å), in agreement with the presence of either a nitrogen or a carbon atom in a *trans* position. Most bond angles at platinum are close to the ideal value of 90°, and the smallest angles correspond to N(2)–Pt–N(1) (82.31(14)° for **5c** and 81.4(2)° for **4a**) and to the metallacycle (C(8)–Pt–N(1) = 81.3(2)° for **4a**, C(1)–Pt–N = 85.40(16)° for **5g**, and C(1)–Pt–N = 86.53(15)° for **7g'**). For [C,N,N'] compounds, the metallacycle angle is larger for seven- than for five-membered metallacycles (92.90(15)° for **5c** versus 81.3(2)° for **4a**).

(22) Capapé, A.; Crespo, M.; Granell, J.; Font-Bardia, M.; Solans, X. *J. Organomet. Chem.* **2005**, *690*, 4309.

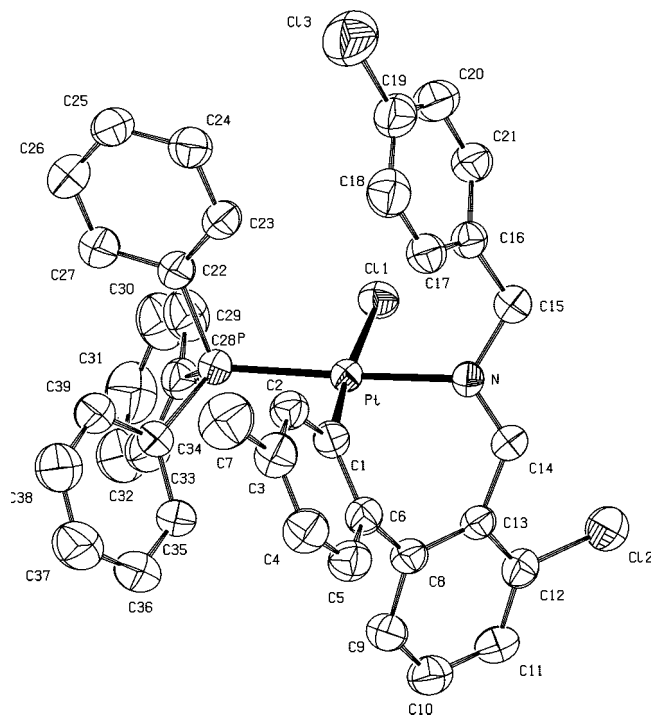


Figure 4. Molecular structure of compound **7g'**.

Conclusions

Previous work using *cis*-[Pt(4-C₆H₄Me)₂(μ-SEt₂)₂] as metalating agent involved oxidative addition to give a platinum(IV) compound, followed by reductive elimination of 4,4'-bitolyl, consistent with the expected instability of triarylplatinum(IV) systems.⁸ However, this process or the also plausible aryl-halogen elimination²³ was not observed in the present study. In addition to [N,N'] coordination compounds (**2a**, **2c**, **2d**), cyclometalated compounds with a five-membered metallacycle (such as [C,N,N'] platinum(IV) (**3b**, **3c**) and platinum(II) (**4a**) as well as [C,N] platinum(II) (**4e**) complexes) or with a seven-membered metallacycle (such as [C,N,N'] platinum(II) (**5c**) and [C,N] platinum(II) (**5f**, **5g**) complexes) were obtained.²⁴ A general scheme showing the processes leading to such compounds is presented (Scheme 7) for potentially tridentate ligands. Analogous processes in which the diamine moiety is replaced by a SEt₂ ligand should take place for the bidentate ligand.

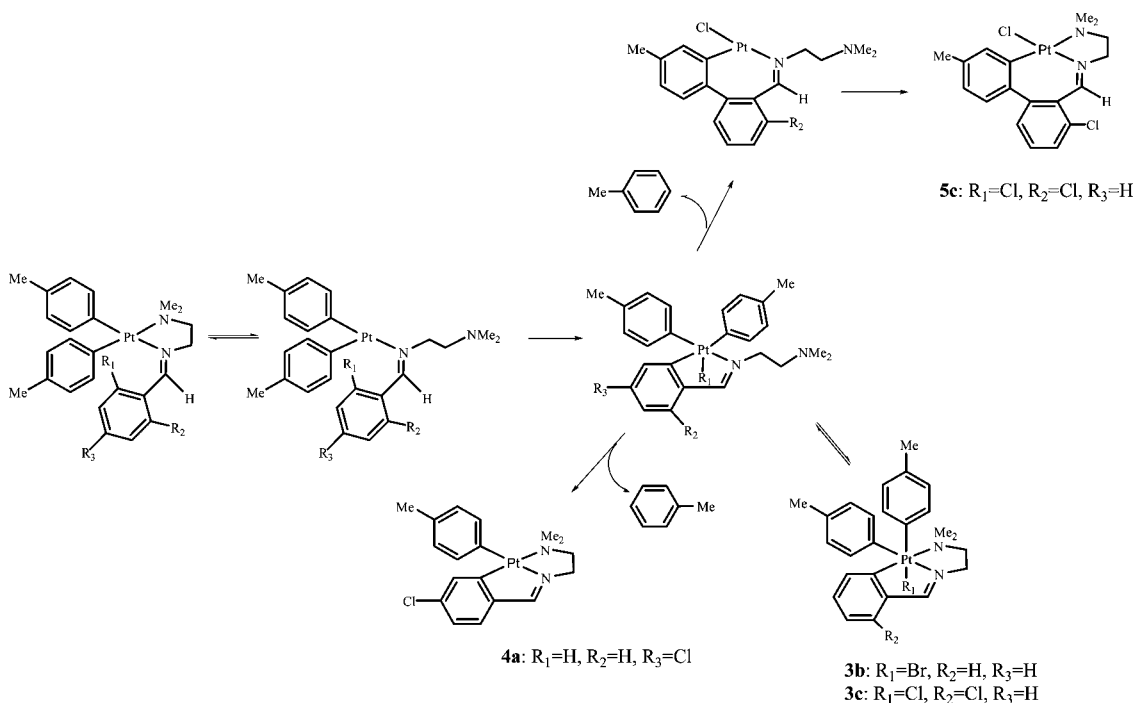
Five-membered rings are the most commonly formed in cyclometalation reactions due to their high stability. The seven-membered rings are novel examples of a recently reported process⁴ involving formal aryl insertion into the metallacycle with reductive elimination of an arene molecule in a process in which a C–C bond is formed. The results here reported support that formation of seven-membered metallacycles may arise from both C–Br and C–Cl intramolecular activation in both potentially tridentate or bidentate ligands. For ligand **1c**, the corresponding platinum(IV) compound **3c** was shown to be an intermediate in the formation of compound **5c**. On the basis of the observation that **5f** and **5g** were easily formed, we may conclude that the process is more facile for bidentate than for tridentate ligands. Assuming that a vacant site in the coordination

(23) (a) Vignalok, A. *Chem.–Eur. J.* **2008**, *14*, 5102. (b) Yahav-Levi, A.; Goldberg, I.; Vignalok, A.; Vedernikov, A. N. *J. Am. Chem. Soc.* **2008**, *130*, 724.

(24) In order to rule out the possibility that the tolyl groups in the products could arise from the toluene used as a solvent, the syntheses of **4a** and **5f** were also carried out successfully in benzene.

Table 1. Selected Bond Lengths (Å) and Angles (deg.) for Compounds 4a, 5c, 5g, and 7g' with Estimated Standard Deviations

compound 4a		compound 5c		compound 5g		compound 7g'	
Pt–C(8)	1.976(5)	Pt–C(1)	1.978(4)	Pt–C(1)	2.004(4)	Pt–C(1)	2.017(4)
Pt–C(1)	2.026(6)	Pt–Cl(1)	2.315(3)	Pt–Cl(1)	2.4144(14)	Pt–Cl(1)	2.3993(12)
Pt–N(2)	2.177(5)	Pt–N(2)	2.204(3)	Pt–N	2.031(3)	Pt–N	2.082(3)
Pt–N(1)	2.014(5)	Pt–N(1)	1.959(4)	Pt–S	2.2719(14)	Pt–P	2.2417(11)
C(8)–Pt–C(1)	97.6(2)	C(1)–Pt–Cl(1)	92.46(12)	C(1)–Pt–N	85.40(16)	C(1)–Pt–N	86.53(15)
C(8)–Pt–N(1)	81.3(2)	Cl(1)–Pt–N(2)	92.55(11)	C(1)–Pt–S	88.33(13)	C(1)–Pt–P	92.69(12)
C(1)–Pt–N(2)	99.7(2)	C(1)–Pt–N(1)	92.90(15)	N–Pt–Cl(1)	88.95(11)	N–Pt–Cl(1)	87.71(9)
N(2)–Pt–N(1)	81.4(2)	N(2)–Pt–N(1)	82.31(14)	S–Pt–Cl(1)	97.77(5)	P–Pt–Cl(1)	93.07(4)

Scheme 7

sphere of platinum is required for the process leading to compounds **5**, the higher lability of the SEt_2 should favor the process. Conversely, the failure to transform easily **3b** into a seven-membered metallacycle can be related to the low tendency of the chelate dinitrogen ligand to dissociate. This is also evidenced from the fact that compound **3b** is reluctant to react with PPh_3 . When an excess of phosphine was used, the reaction yielded compound *trans*-[PtBr(4- $CH_3C_6H_4$)(PPh_3) $_2$], which is analogous to that reported for a reductive elimination process taking place from octahedral platinum(IV) compound [PtPh $_2$ -Br($C_6H_4CH=NCH_2Ph$)SMe $_2$] 4b .

For both potentially tridentate or bidentate ligands, seven-membered metallacycles were not formed from intramolecular C–H or C–F bond activation. The former gave five-membered metallacycles with loss of 1 equiv of toluene, while the stronger C–F bond could not be activated.

The methyl substituent in the tolyl group remains *para* to the platinum in coordination compounds **2** or in cyclometalated platinum(IV) or platinum(II) compounds (**3** and **4**, respectively). However, for compounds **5** the methyl group is now *para* to the formed C–C bond and *meta* to the platinum center. This is evidenced from the 1H NMR spectra of compound **5**, in which a singlet coupled to platinum ($J(H-Pt)$ ca. 53 Hz) was observed and further confirmed in the molecular structures of compounds **5c**, **5g**, and **7g'**. It is interesting to point out that the same position of the methyl substituent has been observed in the major isomer formed in the process described in Scheme 1b for intermolecular toluene activation. The position of the methyl

group is consistent with a process involving C–C coupling between the carbon atoms bound to platinum of the metalated aryl ring and the *para*-tolyl ligand, as expected for a biaryl reductive elimination from a platinum(IV) compound.

Experimental Section

General Procedures. Microanalyses were performed by the Servei de Recursos Científics i Tècnics de la Universitat Rovira i Virgili (Tarragona). Mass spectra were performed at the Servei d'Espectrometria de Masses (Universitat de Barcelona). Electro-spray mass spectra were carried out in a LC/MSD-TOF spectrometer using H_2O-CH_3CN (1:1) to introduce the sample. NMR spectra were performed at the Unitat de RMN d'Alt Camp de la Universitat de Barcelona using Bruker DRX-250 (^{195}Pt , 54 MHz), Varian Unity 300 (1H , 300 MHz; $^{31}P\{^1H\}$, 121.4 MHz), Mercury-400 (1H , 400 MHz; $^1H-^1H$ -NOESY, $^1H-^1H$ -COSY, $^1H-^{13}C$ -gHSQC), and Varian Inova DMX-500 (1H , 500 MHz; $^1H-^1H$ -NOESY, $^1H-^1H$ -COSY, $^1H-^{13}C$ -gHSQC) spectrometers, and referenced to SiMe $_4$ (1H , ^{13}C), H_3PO_4 (^{31}P), and H_2PtCl_6 in D_2O (^{195}Pt). δ values are given in ppm and J values in Hz. Abbreviations used: s = singlet; d = doublet; t = triplet; m = multiplet; br = broad; NMR labeling is as shown in Schemes 2–6.

Preparation of the Compounds. *cis*-[Pt(4- C_6H_4Me) $_2(\mu-SEt_2)]_2$ 25 and ligands **1a–1j** 2a,b,9,26 were prepared as reported elsewhere.

(25) Steele, B. R.; Vrieze, K. *Trans. Met. Chem.* **1977**, *2*, 140.

(26) Crespo, M.; Martín, R.; Calvet, T.; Font-Bardía, M.; Solans, X. *Polyhedron* **2008**, *27*, 2603.

Compound [Pt(4-MeC₆H₄)₂{4-ClC₆H₄CHNCH₂CH₂NMe₂}] (**2a**) was obtained from 45 mg (0.22 mmol) of imine **1a** and 100 mg (0.11 mmol) of compound [Pt₂(4-MeC₆H₄)₂(μ-SEt₂)₂] in toluene. The mixture was stirred for 4 h at room temperature. The solvent was removed in a rotary evaporator, and the residue was treated with ether. The solid was filtered and dried *in vacuo*. Yield: 87 mg (67%). ¹H NMR (400 MHz, CDCl₃): δ 8.74 [s, ³J(Pt-H³) = 42.4, 1H, H³]; 7.88 [d, ³J(H¹-H²) = 8.5, 2H, H¹]; 7.30 [d, ³J(Pt-H⁷) = 68.8, ³J(H⁷-H⁸) = 7.92, 2H, H⁷]; 6.89 [d, ³J(H¹-H²) = 8.5, 2H, H²]; 6.75 [d, ³J(H⁷-H⁸) = 7.5, 2H, H⁸]; 6.73 [d, ³J(H¹⁰-H¹¹) = 8.0, ³J(Pt-H¹⁰) = 73.4, 2H, H¹⁰]; 6.22 [d, ³J(H¹⁰-H¹¹) = 7.5, 2H, H¹¹]; 4.15 [m, ³J(H⁴-H⁵) = 5.4, 2H, H⁴]; 2.76 [m, ³J(H⁴-H⁵) = 5.4, 2H, H⁵]; 2.64 [s, ³J(Pt-H⁶) = 18.3, 6H, H⁶]; 2.19 [s, 3H, H⁹], 1.93 [s, 3H, H¹²]. ¹⁹⁵Pt NMR (54 MHz, CDCl₃): δ -3438.14. ESI-MS, *m/z*: 588.18 [M + H]⁺, 496.11 [M - C₇H₇]⁺. Anal. Found (calc for C₂₅H₂₉ClN₂Pt): C: 51.1 (51.06); H: 5.2 (4.97); N: 4.5 (4.76). After standing in solution for 48 h, compound **2a'** was formed: ¹H NMR (400 MHz, CDCl₃): δ 8.43 [s, ³J(Pt-H³) = 26.0, 1H, H³]; 7.40 [d, ³J(H⁷-H⁸) = 8.5, 2H, H⁷]; 7.31 [d, ³J(H¹-H²) = 8.7, 2H, H²]; 7.29 [d, ³J(H⁷-H⁸) = 8.2, 2H, H⁸]; 7.20 [d, ³J(H¹⁰-H¹¹) = 8.0, 2H, H¹⁰]; 6.75 [d, ³J(H¹-H²) = 8.7, 2H, H¹]; 6.71 [d, ³J(H¹⁰-H¹¹) = 8.1, 2H, H¹¹]; 3.97 [m, 2H, H⁴]; 2.75 [m, 2H, H⁵]; 2.63 [s, br, 6H, H⁶]; 2.17 [s, 3H, H⁹], 2.13 [s, br, 3H, H¹²].

Compound [Pt(4-MeC₆H₄)₂{2,6-Cl₂C₆H₃CHNCH₂CH₂NMe₂}] (**2c**) was obtained using the same procedure as that described above from 57 mg (0.23 mmol) of imine **1c** and 104 mg (0.11 mmol) of compound [Pt₂(4-MeC₆H₄)₂(μ-SEt₂)₂]. Yield: 97 mg (71%). ¹H NMR (400 MHz, CDCl₃): δ 8.69 [s, br, ³J(Pt-H⁴) = 53.5, 1H, H⁴]; 7.24 [d, ³J(H⁸-H⁹) = 7.9, ³J(Pt-H⁸) = 59.3, 2H, H⁸]; 6.90 [s, 3H, H^{1,2,3}]; 6.74 [d, ³J(H¹¹-H¹²) = 7.9, 2H, H¹¹]; 6.68 [d, ³J(H⁸-H⁹) = 7.4, 2H, H⁹]; 6.16 [d, ³J(H¹¹-H¹²) = 7.4, 2H, H¹²]; 4.17 [td, ³J(H⁵-H⁶) = 5.6, ⁴J(H⁴-H⁵) = 1.5, 2H, H⁵]; 2.79 [d, ³J(H⁵-H⁶) = 5.5, 2H, H⁶]; 2.62 [s, br, 6H, H⁷]; 2.13 [s, 3H, H¹⁰], 1.91 [s, 3H, H¹³]. ¹³C NMR (400 MHz, CDCl₃): δ 160.2 [C⁴]; 137.8 [C⁸]; 137.2 [C¹¹]; 130.4 [C²]; 128.1 [C⁹]; 127.7 [C^{1,3}]; 126.8 [C¹²]; 64.5 [C⁵]; 65.4 [C⁶]; 49.5 [C⁷]; 21.0 [C¹⁰]; 20.6 [C¹³]. ESI-MS, *m/z*: 639.14 [M + NH₄]⁺, 622.14 [M + H]⁺, 530.07 [M - C₇H₇]⁺. Anal. Found (calc for C₂₅H₂₈Cl₂N₂Pt·CH₂Cl₂): C: 44.7 (44.14); H: 4.2 (4.27); N: 4.0 (3.96). After standing in solution for a few hours, compound **2c'** was formed: ¹H NMR (400 MHz, CDCl₃): δ 8.36 [t, ⁴J(H⁴-H⁵) = 2.2, ³J(Pt-H⁴) = 26.8, 1H, H⁴]; {7.31 [d, ³J(H-H) = 7.6, 2H]; 7.26 [d, ³J(H-H) = 7.9, 2H]; 6.97 [d, ³J(H-H) = 7.9, 2H]; 6.96 [d, ³J(H-H) = 7.9, 2H]; 6.77 [dd, ³J(H-H) = 8.6, ⁴J(H-H) = 0.7, 1H]; 6.72 [dd, ³J(H-H) = 8.2, ⁴J(H-H) = 0.5, 1H]; H^{1,3,8,9,11,12}}; 4.34-4.32 [m, 2H, H⁵]; 3.64-3.60 [m, 2H, H⁶]; 2.63 [s, ³J(Pt-H⁷) = 19.3, 6H, H⁷]; 2.18 [s, 3H, H¹⁰], 2.13 [s, 3H, H¹³].

Compound [Pt(4-MeC₆H₄)₂{C₆F₅CHNCH₂CH₂NMe₂}] (**2d**) was obtained using the same procedure as that described above from 59 mg (0.22 mmol) of imine **1d** and 101 mg (0.11 mmol) of compound [Pt₂(4-MeC₆H₄)₂(μ-SEt₂)₂]. Yield: 95 mg (67%). ¹H NMR (400 MHz, CDCl₃): δ 8.67 [s, ³J(Pt-H¹) = 48.4, 1H, H¹]; 7.19 [d, ³J(H⁵-H⁶) = 7.9, ³J(Pt-H⁵) = 71.0, 2H, H⁵]; 6.81 [d, ³J(H⁸-H⁹) = 7.9, ³J(Pt-H⁸) = 76.8, 2H, H⁸]; 6.7 [d, ³J(H⁵-H⁶) = 7.5, 2H, H⁶]; 6.35 [d, ³J(H⁸-H⁹) = 7.6, 2H, H⁹]; 4.09 [td, ³J(H²-H³) = 5.1, ⁴J(H¹-H²) = 1.5, 2H, H²]; 2.75 [m, 2H, H³]; 2.61 [s, ³J(Pt-H⁴) = 18.7, 6H, H⁴]; 2.14 [s, 3H, H⁷], 1.99 [s, 3H, H¹⁰]. ¹³C NMR (400 MHz, CDCl₃): δ 152.1 [C¹]; 137.5 [C⁵]; 137.4 [C⁸]; 127.5 [C⁶]; 126.8 [C⁹]; 65.4 [C³]; 64.6 [C²]; 49.5 [C⁴]; 20.8 [C⁷]; 20.4 [C¹⁰]. ESI-MS, *m/z*: 661.18 [M + NH₄]⁺, 644.18 [M + H]⁺, 552.10 [M - C₇H₇]⁺. Anal. Found (calc for C₂₅H₂₅F₅N₂Pt): C: 46.3 (46.66); H: 4.1 (3.92); N: 4.1 (4.35).

Compound [PtBr(4-MeC₆H₄)₂{C₆H₄CHNCH₂CH₂NMe₂}] (**3b**) was obtained using the same procedure as that described above from 57 mg (0.22 mmol) of imine **1b** and 102 mg (0.11 mmol) of compound [Pt₂(4-MeC₆H₄)₂(μ-SEt₂)₂]. Yield: 90 mg (65%). ¹H

NMR (500 MHz, CDCl₃): δ 8.59 [s, ³J(Pt-H⁵) = 45.6, 1H, H⁵]; 7.56 [d, ³J(H⁹-H¹⁰) = 7.6, ³J(Pt-H⁹) = 33.8, 2H, H⁹]; 7.35 [dd, ³J(H³-H⁴) = 7.5, ⁴J(H²-H⁴) = 1.5, 1H, H⁴]; 7.33 [d, ³J(H¹-H²) = 8.0, 1H, H¹]; 7.09 [td, ³J(H²-H^{1,3}) = 7.7, ⁴J(H²-H⁴) = 1.6, 1H, H²]; 7.00 [td, ³J(H³-H^{2,4}) = 7.4, ⁴J(H¹-H³) = 1.0, 1H, H³]; 6.94 [d, ³J(H⁹-H¹⁰) = 7.7, 2H, H¹⁰]; 6.63 [m, ³J(Pt-H) = 20.4, 4H, H^{12,13}]; 4.40-4.33 [m, 1H, H⁷]; 4.31-4.23 [m, 2H, H⁶]; 2.97 [s, ³J(Pt-H⁸) = 10.4, 3H, H⁸]; 2.81-2.79 [m, 1H, H⁷]; 2.47 [s, ³J(Pt-H⁸) = 14.8, 3H, H⁸]; 2.34 [s, 3H, H¹¹]; 2.14 [s, 3H, H¹⁴]. ¹³C NMR (400 MHz, CDCl₃): δ 170.0 [C⁵]; 137.2 [C⁹]; 133.8 [C¹²]; 132.3 [C¹]; 132.2 [C²]; 129.9 [C⁴]; 127.8 [C¹⁰]; 127.7 [C¹³]; 124.3 [C³]; 65.8 [C⁷]; 52.4 [C⁶]; 50.6 [C⁸]; 48.1 [C⁸]; 20.7 [C¹¹]; 20.3 [C¹⁴]. ESI-MS, *m/z*: 650.14 [M + NH₄]⁺, 633.12 [M + H]⁺, 552.20 [M - Br]⁺. Anal. Found (calc for C₂₅H₂₉BrN₂Pt): C: 47.1 (47.47); H: 4.5 (4.62); N: 4.5 (4.43).

Compound [PtCl(4-MeC₆H₄)₂{2-ClC₆H₃CHNCH₂CH₂NMe₂}] (**3c**) was obtained when a solution of compound **2c** was stirred in CH₂Cl₂ at room temperature for 24 h. ¹H NMR (300 MHz, CDCl₃): δ 9.04 [d, ⁴J(H⁴-H⁵) = 1.7, ³J(Pt-H⁴) = 46.6, 1H, H⁴]; 7.47 [d, ³J(H⁸-H⁹) = 7.8, ³J(Pt-H⁸) = 33.7, 2H, H⁸]; 7.32 [dd, ³J(H²-H³) = 6.9, ⁴J(H¹-H³) = 0.7, 1H, H³]; 7.21 [dd, ³J(H¹-H²) = 7.5, 1H, H¹]; 7.02 [t, ³J(H²-H^{1,3}) = 7.8, 1H, H²]; 6.95 [d, ³J(H⁸-H⁹) = 8.3, 2H, H⁹]; 6.72 [d, ³J(H¹¹-H¹²) = 8.3, 2H, H¹¹]; 6.65 [d, ³J(H¹¹-H¹²) = 8.3, 2H, H¹²]; 4.46-4.39 [m, 1H, H⁶]; 4.32-4.23 [m, 2H, H⁵]; 2.83 [s, ³J(Pt-H⁷) = 11.2, 3H, H⁷]; 2.79-2.75 [m, 1H, H⁶]; 2.52 [s, ³J(Pt-H⁷) = 16.2, 3H, H⁷]; 2.33 [s, 3H, H¹⁰], 2.16 [s, 3H, H¹³].

Compound [Pt(4-MeC₆H₄)₂{4-ClC₆H₃CHNCH₂CH₂NMe₂}] (**4a**) was obtained from 50 mg (0.09 mmol) of compound **2a** after reaction in toluene at 90 °C for 6 h. The solvent was removed and the residue was treated with ether to produce a solid, which was filtered and dried *in vacuo*. Yield: 26 mg (62%). ¹H NMR (500 MHz, CDCl₃): δ 8.45 [d, ⁴J(H⁴-H⁵) = 1.4, ³J(Pt-H⁴) = 56.0, 1H, H⁴]; 7.40 [d, ³J(H⁸-H⁹) = 7.8, ³J(Pt-H⁸) = 57.2, 2H, H⁸]; 7.16 [d, ³J(H²-H³) = 8.1, 1H, H³]; 7.08 [d, ³J(Pt-H¹) = 69.4, ³J(H¹-H²) = 2.1, 1H, H¹]; 6.96 [d, ³J(H⁸-H⁹) = 7.5, 2H, H⁹]; 6.93 [dd, ³J(H²-H³) = 8.0, ⁴J(H¹-H²) = 2.1, 1H, H²]; 4.03 [td, ³J(H⁵-H⁶) = 6.0, ⁴J(H⁴-H⁵) = 1.3, 2H, H⁵]; 3.18 [t, ³J(H⁵-H⁶) = 6.0, 2H, H⁶]; 2.76 [s, ³J(Pt-H⁷) = 20.9, 6H, H⁷]; 2.30 [s, 3H, H¹⁰]. ¹³C NMR (400 MHz, CDCl₃): δ 168.5 [C⁴]; 137.0 [C⁸]; 135.7 [C¹]; 129.0 [C³]; 128.0 [C⁹]; 122.5 [C²]; 67.1 [C⁶]; 52.3 [C⁵]; 49.0 [C⁷]; 20.8 [C¹⁰]. ¹⁹⁵Pt NMR (54 MHz, CDCl₃): δ -3580.76. ESI-MS, *m/z*: 899.15 [2M - C₇H₇]⁺, 496.11 [M + H]⁺, 404.05 [M - C₇H₇]⁺. Anal. Found (calc for C₁₈H₂₁ClN₂Pt): C: 43.9 (43.60); H: 4.3 (4.27); N: 5.3 (5.65).

Compound [PtCl{(MeC₆H₃)ClC₆H₃CHNCH₂CH₂NMe₂}] (**5c**) was obtained from 100 mg (0.16 mmol) of compound **2c** after reaction in refluxing toluene for 6 h. The solvent was removed and the residue was treated with ether to produce a yellow solid, which was filtered and dried *in vacuo*. Yield: 58 mg (68%). ¹H NMR (500 MHz, CDCl₃): δ 9.22 [s, ³J(Pt-H⁴) = 147.7, 1H, H⁴]; 7.49 [t, ³J(H²-H^{1,3}) = 7.5, 1H, H²]; 7.44 [s, br, ³J(Pt-H⁸) = 53.4, 1H, H⁸]; 7.35 [dd, ³J(H^{1,3}-H²) = 8.1, ³J(H¹-H³) = 0.9, 2H, H^{1,3}]; 6.87 [d, ³J(H¹⁰-H¹¹) = 7.8, 1H, H¹¹]; 6.80 [dd, ³J(H⁸-H⁹) = 8.0, ⁴J(H⁸-H¹⁰) = 1.3, 1H, H¹⁰]; 4.52 [m, ²J(H⁵-H⁶) = 11.9, ³J(H⁵-H⁶) = 3.9, ⁴J(H⁴-H⁵) = 1.2, 1H, H⁵]; 3.97 [dd, ²J(H⁵-H⁶) = 11.7, ³J(H⁵-H⁶) = 3.8, ³J(Pt-H⁵) = 59.9, 1H, H⁵]; 3.08 [s, 3H, H⁷]; 2.73 [s, 3H, H⁷]; 2.73 [m, 1H, H⁶]; 2.60 [td, ²J(H⁶-H⁶) = 12.9, ³J(H⁵-H⁶) = 4.0, 1H, H⁶]; 2.31 [s, 3H, H⁹]. ¹³C NMR (400 MHz, CDCl₃): δ 162.7 [C⁴]; 139.7 [C⁸]; 132.4 [C¹]; 132.1 [C²]; 129.1 [C¹¹]; 127.3 [C³]; 124.8 [C¹⁰]; 66.9 [C⁵]; 65.13 [C⁶]; 50.5 [C⁷]; 47.8 [C⁷]; 21.0 [C⁹]. ESI-MS, *m/z*: 530.07 [M + H]⁺. Anal. Found (calc for C₁₈H₂₀Cl₂N₂Pt): C: 41.5 (40.76); H: 3.7 (3.80); N: 5.3 (5.28).

Compound [Pt(4-MeC₆H₄)₂{4-ClC₆H₃CHNCH₂(4-ClC₆H₄)SEt₂}] (**4e**) was obtained from 70 mg (0.26 mmol) of imine **1e** and 124 mg (0.13 mmol) of compound [Pt₂(4-MeC₆H₄)₂(μ-SEt₂)₂] in toluene.

The mixture was stirred for 24 h at room temperature and then was heated at 90 °C for 2 h to complete the reaction. The solvent was removed in a rotary evaporator and the residue was treated with ether. The yellow solid was filtered and dried *in vacuo*. Yield: 115 mg (69%). ^1H NMR (400 MHz, CDCl_3): δ 8.45 [s, $^3J(\text{Pt}-\text{H}^4)$ = 52.0, 1H, H^4]; 7.34 [d, $^3J(\text{H}^6-\text{H}^7)$ = 8.5, 1H, H^7]; 7.30–7.26 [m, 3H, $\text{H}^{3,6,8}$]; 7.00 [dd, $^3J(\text{H}^2-\text{H}^3)$ = 8.0, $^4J(\text{H}^1-\text{H}^2)$ = 2.1, 1H, H^2]; 6.87 [d, $^3J(\text{H}^8-\text{H}^9)$ = 7.4, 2H, H^9]; 6.81 [d, $^3J(\text{Pt}-\text{H}^1)$ = 54.4, $^4J(\text{H}^1-\text{H}^2)$ = 2.1, 1H, H^1]; 5.12 [s, 2H, H^5]; 2.31 [m, $^3J(\text{H}^{11}-\text{H}^{12})$ = 7.4, 4H, H^{11}]; 2.27 [s, 3H, H^{10}]; 1.06 [t, $^3J(\text{H}^{11}-\text{H}^{12})$ = 7.4, 6H, H^{12}]. ^{13}C NMR ($^1\text{H}-^{13}\text{C}$ -gHSQC, 400 MHz, CDCl_3): δ 176.4 [C^4]; 136.3 [C^3]; 136.3 [C^6]; 136.1 [C^1]; 129.1 [C^8]; 128.8 [C^7]; 128.8 [C^9]; 123.7 [C^2]; 61.8 [C^5]; 28.7 [C^{11}]; 20.8 [C^{10}]; 13.0 [C^{12}]. ESI-MS, m/z : 548.03 [$\text{M} - \text{SEt}_2$] $^+$. Anal. Found (calc for $\text{C}_{25}\text{H}_{27}\text{Cl}_2\text{NPtS}$): C: 46.7 (46.95); H: 4.2 (4.26); N: 2.4 (2.19); S: 3.8 (5.01).

Compound $[\text{PtBr}\{\text{(MeC}_6\text{H}_5)_3\text{C}_6\text{H}_4\text{CHNCH}_2(4\text{-ClC}_6\text{H}_4)\text{SEt}_2\}]$ (**5f**) was obtained from 68 mg (0.22 mmol) of imine **1e** and 100 mg (0.11 mmol) of compound $[\text{Pt}_2(4\text{-MeC}_6\text{H}_4)_2(\mu\text{-SEt}_2)_2]$ in toluene. The mixture was stirred for 24 h at room temperature. The solvent was removed in a rotary evaporator and the residue was treated with ether. The yellow solid was filtered and dried *in vacuo*. Yield: 98 mg (65%). ^1H NMR (400 MHz, CDCl_3): δ 8.61 [s, $^3J(\text{Pt}-\text{H}^4)$ = 119.4, 1H, H^4]; 7.50–7.46 [m, 1H, H^7]; 7.38–7.34 [m, 3H, $\text{H}^{5,6,8}$]; 7.20 [d, $^3J(\text{H}^1-\text{H}^2)$ = 8.4, 1H, H^1]; 7.15 [d, $^3J(\text{H}^1-\text{H}^2)$ = 8.3, 1H, H^2]; 6.82 [d, $^3J(\text{H}^9-\text{H}^{10})$ = 7.6, 1H, H^9]; 6.71 [d, $^3J(\text{H}^9-\text{H}^{10})$ = 7.3, 1H, H^{10}]; 6.22 [s, $^3J(\text{Pt}-\text{H}^{12})$ = 54.4, 1H, H^{12}]; 5.73 [dd, $^2J(\text{H}^3-\text{H}^3')$ = 12.7, $^4J(\text{H}^3-\text{H}^4)$ = 1.5, 1H, H^3]; 4.88 [d, $^2J(\text{H}^3-\text{H}^3')$ = 12.8, $^3J(\text{Pt}-\text{H}^3')$ = 56.9, 1H, H^3']; 3.03 [s, br, 1H, H^{13a}]; 2.66 [s, br, 2H, H^{13}]; 2.36 [s, br, 1H, H^{13b}]; 2.16 [s, 3H, H^{11}]; 1.59 [s, br, 3H, H^{14}]; 0.96 [s, br, 3H, H^{14}]. ^{13}C NMR ($^1\text{H}-^{13}\text{C}$ -gHSQC, 400 MHz, CDCl_3): δ 165.68 [C^4]; 136.6 [C^{12}]; 131.6 [C^1]; 131.0 [C^7]; 130.2 [C^5]; 128.8 [C^8]; 128.6 [C^2]; 127.9 [C^9]; 126.3 [C^6]; 124.3 [C^{10}]; 68.3 [C^3]; 20.9 [C^{11}]. ESI-MS, m/z : 603.12 [$\text{M} - \text{Br}$] $^+$. Anal. Found (calc for $\text{C}_{25}\text{H}_{27}\text{BrClINPtS}$): C: 43.7 (43.90); H: 3.8 (3.98); N: 2.1 (2.05). S: 4.0 (4.69).

Compound $[\text{PtCl}\{\text{(MeC}_6\text{H}_5)_3\text{(ClC}_6\text{H}_3)\text{CHNCH}_2(4\text{-ClC}_6\text{H}_4)\text{SEt}_2\}]$ (**5g**) was obtained as a yellow solid from 66 mg (0.22 mmol) of imine **1g** and 101 mg (0.11 mmol) of compound $[\text{Pt}_2(4\text{-MeC}_6\text{H}_4)_2(\mu\text{-SEt}_2)_2]$ using an analogous procedure to that for **5f** in toluene at 90 °C for 6 h. Yield: 126 mg (85%). ^1H NMR (400 MHz, CDCl_3): δ 8.70 [d, $^3J(\text{Pt}-\text{H}^4)$ = 120.4, $^4J(\text{H}^3-\text{H}^4)$ = 1.2, 1H, H^4]; 7.41 [t, $^3J(\text{H}^6-\text{H}^{5,7})$ = 7.7, 1H, H^6]; 7.37 [dd, $^3J(\text{H}^5-\text{H}^6)$ = 8.0, $^4J(\text{H}^5-\text{H}^7)$ = 1.5, 1H, H^5]; 7.24 [dd, $^3J(\text{H}^6-\text{H}^7)$ = 7.3, $^4J(\text{H}^5-\text{H}^7)$ = 1.5, 1H, H^7]; 7.20 [d, $^3J(\text{H}^1-\text{H}^2)$ = 8.4, 1H, H^1]; 7.12 [d, $^3J(\text{H}^1-\text{H}^2)$ = 8.4, 1H, H^2]; 6.82 [d, $^3J(\text{H}^8-\text{H}^9)$ = 7.7, 1H, H^8]; 6.70 [dd, $^3J(\text{H}^8-\text{H}^9)$ = 7.7, $^4J(\text{H}^9-\text{H}^{11})$ = 1.11, 1H, H^9]; 6.27 [s, $^3J(\text{Pt}-\text{H}^{11})$ = 53.0, 1H, H^{11}]; 5.57 [dd, $^2J(\text{H}^3-\text{H}^3')$ = 13.0, $^4J(\text{H}^3-\text{H}^4)$ = 1.8, 1H, H^3]; 4.95 [d, $^2J(\text{H}^3-\text{H}^3')$ = 12.9, $^3J(\text{Pt}-\text{H}^3')$ = 54.6, 1H, H^3']; 3.04 [s, br, 1H, H^{12}]; 2.62 [s, br, 2H, H^{12}]; 2.38 [s, br, 1H, H^{12a}]; 2.15 [s, 3H, H^{10}]; 1.26 [s, br, 1H, H^{13}]; 0.93 [s, br, 2H, H^{13}]. ^{13}C NMR ($^1\text{H}-^{13}\text{C}$ -gHSQC, 400 MHz, CDCl_3): δ 163.7 [C^4]; 137.2 [C^{11}]; 131.8 [C^2]; 131.8 [C^6]; 128.9 [C^1]; 128.9 [C^7]; 128.0 [C^8]; 127.4 [C^5]; 124.4 [C^9]; 67.6 [C^3]; 21.0 [C^{10}]; 12.5 [C^{13}]; 12.5 [C^{13}]. ESI-MS, m/z : 601.03 [$\text{M} - \text{SEt}_2 + \text{NH}_4$] $^+$. Anal. Found (calc for $\text{C}_{25}\text{H}_{26}\text{Cl}_3\text{NPtS}$): C: 44.9 (44.55); H: 3.6 (3.89); N: 2.2 (2.08). S: 3.7 (4.76).

Compound $[\text{Pt}(4\text{-MeC}_6\text{H}_4)\{4\text{-ClC}_6\text{H}_3\text{CHNCH}_2\text{CH}_2\text{NMe}_2\}\text{PPh}_3]$ (**6a**) was prepared from 25 mg (0.05 mmol) of compound **4a** and 13 mg (0.05 mmol) of triphenylphosphine, which were dissolved in 30 mL of acetone and allowed to react at room temperature for 2 h. The solvent was removed and the residue was washed with ether and dried *in vacuo*. Yield: 15 mg (39%). ^1H NMR (300 MHz, CDCl_3): δ 8.52 [s, $^3J(\text{Pt}-\text{H}^4)$ = 51.0, 1H, H^4]; 7.56–7.49 [m, 6H, PPh_3]; 7.37–7.23 [m, 9H, PPh_3]; 6.99 [m, 2H, $\text{H}^{1,3}$]; 6.92 [d, $^3J(\text{H}^8-\text{H}^9)$ = 7.2, 2H, H^8]; 6.87 [dd, $^3J(\text{H}^2-\text{H}^3)$ = 5.8, $^4J(\text{H}^1-\text{H}^2)$ = 2.1, 1H, H^2]; 6.43 [d, $^3J(\text{H}^8-\text{H}^9)$ = 7.6, 2H, H^9]; 3.12 [t,

$^3J(\text{H}^5-\text{H}^6)$ = 6.0, 2H, H^5]; 2.09 [s, 3H, H^{10}]; 1.89 [m, 8H, $\text{H}^{6,7}$]. ^{31}P NMR (121 MHz, CDCl_3): δ 28.06 [s, $^1J(\text{Pt}-\text{P})$ = 2197.8].

Compound $[\text{Pt}(4\text{-MeC}_6\text{H}_4)\{4\text{-ClC}_6\text{H}_3\text{CHNCH}_2(4\text{-ClC}_6\text{H}_4)\}\text{PPh}_3]$ (**6e**) was prepared from 40 mg (0.06 mmol) of compound **4e** and 17 mg (0.06 mol) of triphenylphosphine using an analogous procedure to that for **6a**. Yield: 39 mg (80%). ^1H NMR (300 MHz, CDCl_3): δ 8.18 [s, $^3J(\text{Pt}-\text{H}^4)$ = 50.4, 1H, H^4]; {7.49–7.42 [m, 6H]; 7.36–7.30 [m, 6H]; 7.24–7.19 [m, 7H] PPh_3 , H^8 , H^9 }; 7.14 [d, $^3J(\text{H}^6-\text{H}^7)$ = 8.4, 2H, H^7]; 6.99 [dd, $^3J(\text{H}^2-\text{H}^3)$ = 7.9, $^4J(\text{H}^1-\text{H}^2)$ = 2.1, 1H, H^2]; 6.89 [m, 1H, H^1]; 6.68 [d, $^3J(\text{H}^6-\text{H}^7)$ = 8.4, 2H, H^6]; 6.43 [d, $^3J(\text{H}^2-\text{H}^3)$ = 7.7, 1H, H^3]; 4.08 [s, br, 2H, H^5]; 2.09 [s, br, 3H, H^{10}]. ^{31}P NMR (121 MHz, CDCl_3): δ 27.59 [s, $^1J(\text{Pt}-\text{P})$ = 2200.6]. ESI-MS, m/z : 811.14 [$\text{M} + \text{H}$] $^+$.

Compound $[\text{PtCl}\{\text{(MeC}_6\text{H}_4)_3(\text{ClC}_6\text{H}_3)\text{CHNCH}_2\text{CH}_2\text{NMe}_2\}\text{PPh}_3]$ (**7c/7c'**) was prepared from 40 mg (0.08 mmol) of compound **5c** and 20 mg (0.08 mol) of triphenylphosphine using an analogous procedure to that for **6a**. Yield: 27 mg (42%). ^1H NMR (300 MHz, CDCl_3): **7c**: δ 8.26 [s, $^3J(\text{Pt}-\text{H}^4)$ = 140.0, 1H, H^4]; 7.65–7.59 [m, 6H, H^{ar}]; 7.50–7.32 [m, 15H, H^{ar}]; 6.96 [dd, $^3J(\text{H}^{10}-\text{H}^{11})$ = 7.6, $^4J(\text{H}^8-\text{H}^{10})$ = 2.5, 1H, H^{10}]; 6.78 [d, $^3J(\text{H}^{10}-\text{H}^{11})$ = 7.8, 1H, H^{11}]; 3.18 [m, 1H, H^5]; 3.03 [m, 1H, H^5]; 2.45 [m, 2H, H^6]; 2.31 [s, 3H, H^9]; 1.78 [m, 6H, H^7]. **7c'**: δ 8.63 [s, $^3J(\text{Pt}-\text{H}^4)$ = 84.7, $^3J(\text{P}-\text{H}^4)$ = 11.25, 1H, H^4]; 7.42–7.17 [m, 17H, H^{ar}]; 7.11 [dd, $^3J(\text{H}^1-\text{H}^2)$ = 7.6, $^4J(\text{H}^1-\text{H}^3)$ = 0.9, 1H, H^1]; 6.70 [d, $^3J(\text{H}^{10}-\text{H}^{11})$ = 7.7, 1H, H^{11}]; 6.47 [dd, $^3J(\text{H}^{10}-\text{H}^{11})$ = 7.6, $^4J(\text{H}^8-\text{H}^{10})$ = 0.9, 1H, H^{10}]; 6.40 [s, 1H, H^8]; 4.77 [m, 1H, H^5]; 3.95 [m, 1H, H^5]; 2.93 [m, 2H, H^6]; 2.77 [m, 2H, H^6]; 2.08 [s, 3H, H^7]; 1.76 [m, 6H, H^9]. ^{31}P NMR (121 MHz, CDCl_3) **7c**: δ 18.64 [s, $^1J(\text{Pt}-\text{P})$ = 1866.5]. **7c'**: δ 15.19 [s, $^1J(\text{Pt}-\text{P})$ = 4305.1].

Compound $[\text{PtBr}\{\text{(MeC}_6\text{H}_5)_3(\text{C}_6\text{H}_4)\text{CHNCH}_2(4\text{-ClC}_6\text{H}_4)\}\text{PPh}_3]$ (**7f/7f'**) was prepared from 40 mg (0.06 mmol) of compound **5f** and 17 mg (0.06 mol) of triphenylphosphine using an analogous procedure to that for **6a**. Yield: 35 mg (68%). **7f**: ^1H NMR (300 MHz, CDCl_3): δ 8.24 [s, $^3J(\text{Pt}-\text{H}^4)$ = 140.9, 1H, H^4]; {7.66–7.56 [m, 8H] PPh_3 , H^{ar} }; 7.54–7.52 [m, 1H, H^7]; {7.42–7.36 [m, 10H] PPh_3 , H^{ar} }; 7.13 [d, $^3J(\text{H}^1-\text{H}^2)$ = 8.3, 1H, H^2]; 7.06 [d, $^3J(\text{H}-\text{H})$ = 7.4, 1H, H^{ar}]; 6.85 [dd, $^3J(\text{H}^9-\text{H}^{10})$ = 7.6, $^4J(\text{H}^{10}-\text{H}^{12})$ = 2.5, 1H, H^{10}]; 6.72 [d, $^3J(\text{H}^1-\text{H}^2)$ = 8.4, 2H, H^1]; 6.67 [s, $^3J(\text{H}-\text{H})$ = 8.9, 1H, H^{ar}]; 4.21 [d, $^2J(\text{H}^3-\text{H}^3')$ = 13.3, 1H, H^3]; 4.13 [d, $^2J(\text{H}^3-\text{H}^3')$ = 13.4, 1H, H^3]; 2.18 [s, br, 3H, H^{11}]. ^{31}P NMR (121 MHz, CDCl_3): δ 17.76 [s, $^1J(\text{Pt}-\text{P})$ = 1862.2]. **7f'**: ^1H NMR (300 MHz, CDCl_3): δ 8.64 [d, $^3J(\text{Pt}-\text{H}^4)$ = 87.7, $^4J(\text{P}-\text{H}^4)$ = 11.1, $^4J(\text{H}^3-\text{H}^4)$ = 1.5, 1H, H^4]; {7.44–7.36 [m, 2H]; 7.31–7.27 [m, 9H]; 7.16–7.21 [m, 10H] PPh_3 , H^{ar} }; 6.61 [d, $^3J(\text{H}^9-\text{H}^{10})$ = 7.7, 1H, H^9]; 6.39 [d, $^3J(\text{H}^9-\text{H}^{10})$ = 7.4, 1H, H^{10}]; 5.84 [d, $^3J(\text{H}^3-\text{H}^3')$ = 12.4, 1H, H^3]; 5.52 [s, $^3J(\text{Pt}-\text{H}^{12})$ = 59.5, 1H, H^{12}]; 4.88 [dd, $^3J(\text{Pt}-\text{H}^3)$ = 48.5, $^3J(\text{H}^3-\text{H}^3')$ = 12.3, $^4J(\text{P}-\text{H}^3)$ = 5.2, 1H, H^3]; 1.65 [s, br, 3H, H^{11}]. ESI-MS, m/z : 775.16 [$\text{M} - \text{Br}$] $^+$.

Compound $[\text{PtCl}\{\text{(MeC}_6\text{H}_5)_3(\text{ClC}_6\text{H}_3)\text{CHNCH}_2(4\text{-ClC}_6\text{H}_4)\}\text{PPh}_3]$ (**7g/7g'**) was prepared from 40 mg (0.06 mmol) of compound **5g** and 17 mg (0.06 mol) of triphenylphosphine using an analogous procedure to that for **6a**. Yield: 23 mg (46%). **7g**: ^1H NMR (300 MHz, CDCl_3): δ 8.48 [d, $^3J(\text{Pt}-\text{H}^4)$ = 138.9, $^4J(\text{H}^3-\text{H}^4)$ = 1.0, 1H, H^4]; {7.70–7.63 [m, 8H]; 7.48–7.44 [m, 4H]; 7.40–7.43 [m, 6H]; PPh_3 , H^{ar} }; 7.12 [d, $^3J(\text{H}^1-\text{H}^2)$ = 8.4, 2H, H^1]; 6.86 [dd, $^3J(\text{H}-\text{H})$ = 7.8, $^4J(\text{H}-\text{H})$ = 2.3, 1H, H^{ar}]; 6.71–6.67 [m, 2H, H^{ar}]; 6.69 [d, $^3J(\text{H}^1-\text{H}^2)$ = 8.4, 2H, H^2]; 4.18 [d, $^3J(\text{H}^3-\text{H}^3')$ = 13.5, $^3J(\text{Pt}-\text{H}^3)$ = 66.97, 1H, H^3]; 3.95 [dd, $^3J(\text{H}^3-\text{H}^3')$ = 13.2, $^4J(\text{H}^3-\text{H}^4)$ = 1.2, 1H, H^3]; 2.19 [s, br, 3H, H^{10}]. ^{31}P NMR (121 MHz, CDCl_3): δ 18.54 [s, $^1J(\text{Pt}-\text{P})$ = 1856.5]. **7g'**: ^1H NMR (300 MHz, CDCl_3): δ 8.74 [dd, $^3J(\text{Pt}-\text{H}^4)$ = 87.1, $^4J(\text{P}-\text{H}^4)$ = 11.1, $^4J(\text{H}^3-\text{H}^4)$ = 1.6, 1H, H^4]; {7.41 [dd, $^3J(\text{H}-\text{H})$ = 8.1, $^4J(\text{H}-\text{H})$ = 1.3, 1H]; 7.37–7.26 [m, 14H]; 7.22–7.17 [m, 6H]; 7.11 [dd, $^3J(\text{H}-\text{H})$ = 7.5, $^4J(\text{H}-\text{H})$ = 1.2, 1H]; PPh_3 , H^{ar} }; 6.60 [d, $^3J(\text{H}^8-\text{H}^9)$ = 7.6, 1H, H^8]; 6.38 [dd, $^3J(\text{H}^8-\text{H}^9)$ = 7.6, $^4J(\text{H}^9-\text{H}^{11})$ = 1.1, 1H, H^9]; 5.72 [d, $^3J(\text{H}^3-\text{H}^3')$ = 12.2, 1H, H^3]; 5.55 [s, $^3J(\text{Pt}-\text{H}^{11})$ = 54.5, 1H, H^{11}]; 4.93 [dd, $^3J(\text{Pt}-\text{H}^3)$ =

Table 2. Crystallographic and Refinement Data for Compounds 4a, 5c, 5g, and 7g'

	compound 4a	compound 5c	compound 5g	compound 7g'
formula	C ₁₈ H ₂₁ ClN ₂ Pt	C ₁₈ H ₂₀ Cl ₂ N ₂ Pt·CH ₂ Cl ₂	C ₂₅ H ₂₆ Cl ₃ NPtS	C ₃₉ H ₃₁ Cl ₃ NPPt
fw	495.91	615.28	673.97	846.06
temp, K	293(2)	293(2)	293(2)	293(2)
wavelength, Å	0.71073	0.71073	0.71073	0.71073
cryst syst	monoclinic	triclinic	monoclinic	monoclinic
space group	<i>P</i> 2 ₁ / <i>c</i>	<i>P</i> $\bar{1}$	<i>P</i> 2 ₁ / <i>c</i>	<i>P</i> 2 ₁ / <i>a</i>
<i>a</i> , Å	10.683(4)	8.043(8)	10.998(5)	11.748(4)
<i>b</i> , Å	14.836(6)	11.709(2)	8.346(3)	15.925(4)
<i>c</i> , Å	15.174(6)	11.828(6)	27.121(10)	18.487(4)
α , deg	90	90.50(3)	90	90
β , deg	114.29(10)	109.26(6)	91.43(2)	97.46(2)
γ , deg	90	91.57(4)	90	90
<i>V</i> , Å ³ ; <i>Z</i>	1732.1(12); 4	1051.0(12); 2	2488.6(17); 4	3429.4(16); 4
<i>d</i> (calcd), Mg/m ³	1.902	1.944	1.799	1.639
abs coeff, mm ⁻¹	8.253	7.190	6.058	4.401
<i>F</i> (000)	952	592	1312	1664
rfins coll./unique	3829/3829 [<i>R</i> (int) = 0.0562]	6114/6114 [<i>R</i> (int) = 0.0399]	23 534/7270	31 396/9622
data/restraint/params	3829/0/221	6114/2/236	7270/1/280	9622/2/ 407
GOF on <i>F</i> ²	1.118	1.075	1.115	1.146
<i>R</i> ₁ (<i>I</i> > 2 σ (<i>I</i>))	0.0462	0.0360	0.0399	0.0374
<i>wR</i> ₂ (all data)	0.1259	0.0866	0.1074	0.0859
peak and hole, e Å ⁻³	0.756 and -0.646	0.947 and -0.829	0.744 and -0.579	0.510 and -0.614

58.6, ³*J*(H³-H^{3'}) = 12.9, ⁴*J*(P-H^{3'}) = 5.3, 1H, H^{3'}]; 1.64 [s, br, 3H, H¹⁰]. ³¹P NMR (121 MHz, CDCl₃): δ 14.82 [s, ¹*J*(Pt-P) = 4363.5]. ESI-MS, *m/z*: 850.14 [M - Cl + CH₃CN]⁺, 809.12 [M - Cl]⁺.

Preparation of compound [PtBr(4-MeC₆H₄)₂{C₆H₄CHNCH₂-CH₂NMe₂}PPh₃] (**8b**) was attempted from 54 mg (0.09 mmol) of compound **3b** and 25 mg (0.09 mol) of triphenylphosphine using an analogous procedure to that for **6a**. According to the ¹H NMR (300 MHz, CDCl₃) of the crude reaction mixture, the main product was starting material **3b**; a new imine resonance was observed (δ 8.37 [d, ³*J*(Pt-H) = 40.30, ⁴*J*(P-H) = 8.40, 1H, H]) and assigned to **8b**. Addition of a further equivalent of PPh₃ in order to facilitate the reaction resulted in formation of compound *trans*-[PtBr(4-CH₃C₆H₄)(PPh₃)₂]: ¹H NMR (300 MHz, CDCl₃): δ 7.56-7.50 [m, 15H, PPh₃]; 7.34-7.20 [m, 15H, PPh₃]; 6.47 [d, ³*J*(Pt-H³) = 56.1, ³*J*(H²-H³) = 8.0, 2H, H³]; 5.95 [d, ³*J*(H²-H³) = 7.7, 2H, H²]; 1.94 [s, 3H, H¹]. ³¹P NMR (121 MHz, CDCl₃): δ 24.48 [s, ¹*J*(Pt-P) = 3141.8]. ESI-MS: 907.16 [M + NH₄]⁺, 851.23 [M - Br + CH₃CN]⁺, 810.20 [M - Br]⁺.

X-Ray Structure Analysis. Prismatic crystals were selected and mounted on an Enraf-Nonius CAD4 four-circle (**5c**) or on a MAR345 (**4a**, **5g**, and **7g'**) diffractometer with an image plate

detector. Intensities were collected with graphite-monochromatized Mo K α radiation. The structures were solved by direct methods using the SHELXS computer program²⁷ and refined by the full-matrix least-squares method with the SHELXL97 computer program using 3829 (**4a**), 6114 (**5c**), 23 524 (**5g**), and 31 396 (**7g'**) reflections (very negative intensities were not assumed). **5c**, **5g**, and **7g'** were refined with a rigid model restraint for some distances around the platinum center. Further details are given in Table 2.

Acknowledgment. This work was supported by the Ministerio de Ciencia y Tecnología (project CTQ2006-02007/BQU).

Supporting Information Available: X-ray crystallographic data in CIF format for the structure determinations of **4a**, **5c**, **5g**, and **7g'**. This material is available free of charge via the Internet at <http://pubs.acs.org>.

OM800864F

(27) Sheldrick, G. M. *SHELXS97, A Computer Program for Crystal Structure Determination*; University of Göttingen: Germany, 1997.

Cyclopenta[*l*]phenanthrenyl and Cyclopenta[*a*]acenaphthylenyl Half-Sandwich Complexes of Ruthenium as Racemization Catalysts for Secondary Alcohols

Denys Mavrynsky,[†] Reijo Sillanpää,[‡] and Reko Leino^{*†}

Laboratory of Organic Chemistry, Åbo Akademi University, FI-20500 Åbo, Finland, and Department of Chemistry, University of Jyväskylä, FI-40351 Jyväskylä, Finland

Received September 27, 2008

Several half-sandwich complexes of ruthenium with cyclopenta[*l*]phenanthrenyl and cyclopenta[*a*]acenaphthylenyl ligands containing fused aromatic ring substituents on the cyclopentadienyl ring were prepared and characterized by NMR and X-ray crystallography. Activities of the complexes as racemization catalysts for secondary alcohols were preliminarily screened by using (*S*)-phenylethanol as the substrate. The catalytic activities of the fused-ring complexes depend strongly on the number of other substituents in the five-membered ring and are inferior to those reported earlier for chlorodicarbonyl(pentaphenylcyclopentadienyl)ruthenium, currently considered as the best catalyst candidate for dynamic kinetic resolution of secondary alcohols by combined enzyme/metal catalysis.

Introduction

Dynamic kinetic resolution (DKR) of secondary alcohols based on combined enzyme and metallocene catalysis was originally developed more than 10 years ago.¹ The use of efficient organometallic catalysts for racemization allows one to perform the resolutions under sufficiently mild conditions required for enzyme functioning. In recent years, this approach has been extensively investigated. Predominantly, pentasubstituted monocyclopentadienyl complexes of ruthenium have been utilized as racemization catalysts for alcohols.² Only a few examples based on indenyl³ and aryl⁴ ruthenium complexes have been described.

For further structural tuning as well as improvements in activities and stabilities of the racemization catalysts, the screening of new ligand modifications is desirable. Here, the indenyl ligand platform provides a number of opportunities for structural variation. Examples of transition metal complexes containing fused-ring, polycyclic indenyl-type ligands, such as cyclopenta[*l*]phenanthrenyl⁵ and cyclopenta[*a*]acenaphthylenyl,⁶ are relatively scarce, but have been, in the context of catalytic α -olefin polymerization (mainly $M = Zr$),^{5b,c} shown to result in enhanced catalyst properties. To our knowledge, ruthenium complexes containing cyclopenta[*l*]phenanthrenyl ligands have

been reported in one case only: Hagiwara and co-workers recently utilized the 1,2,3-triphenyl cyclopenta[*l*]phenanthrenyl moiety as a ligand in their catalyst design for Suzuki–Miyara coupling.⁷

In the present paper we describe our initial results in the use of cyclopenta[*l*]phenanthrenyl and cyclopenta[*a*]acenaphthylenyl ligands as structural motifs for alcohol racemization catalysts with potential applications in DKR in combination with enzymes. The resulting monocyclopentadienyl ruthenium complexes combine the elements of the previously reported metallocene racemization catalysts containing polysubstituted Cp ligands with a flat polycyclic part. The specific purpose of the work was to investigate the relationships between the structures and catalytic activities of such half-sandwich metallocene complexes.

Results and Discussion

Synthesis and Characterization of the Catalysts and Ligand Precursors. The substituted cyclopenta[*l*]phenanthrenyl ligand precursors **4a** and **4b** and the triphenyl-substituted cyclopenta[*a*]acenaphthylenyl ligand precursor **7** were prepared according to previously reported procedures.^{5a,8} The *tert*-butyldimethylsiloxy-substituted ligand **4d** was synthesized by

* Corresponding author. E-mail: reko.leino@abo.fi.

[†] Åbo Akademi University.

[‡] University of Jyväskylä.

(1) (a) Larsson, A. L. E.; Persson, B. A.; Bäckvall, J.-E. *Angew. Chem., Int. Ed. Engl.* **1997**, *36*, 1211. For reviews, see: (b) Pàmies, O.; Bäckvall, J.-E. *Chem. Rev.* **2003**, *103*, 3247. (c) Martín-Matute, B.; Bäckvall, J.-E. *Curr. Opin. Chem. Biol.* **2007**, *11*, 226.

(2) (a) Leijondahl, K.; Borén, L.; Braun, R.; Bäckvall, J.-E. *Org. Lett.* **2008**, *10*, 2027. (b) Kim, M. J.; Choi, K. Y.; Kim, S.; Kim, D.; Han, K.; Ko, S.-B.; Park, J. *Org. Lett.* **2008**, *10*, 1295. (c) Eckert, M.; Brethon, A.; Li, Y.-X.; Sheldon, R. A.; Arends, I. W. C. E. *Adv. Synth. Catal.* **2007**, *349*, 2603. (d) Choi, J. H.; Choi, Y. K.; Kim, Y. H.; Park, E. S.; Kim, E. J.; Kim, M. J.; Park, J. *J. Org. Chem.* **2004**, *69*, 1972.

(3) (a) Koh, J. H.; Jung, H. M.; Kim, M. J.; Park, J. *Tetrahedron Lett.* **1999**, *40*, 6281. (b) Xi, Q.; Zhang, W.; Zhang, X. *Synlett* **2006**, 945.

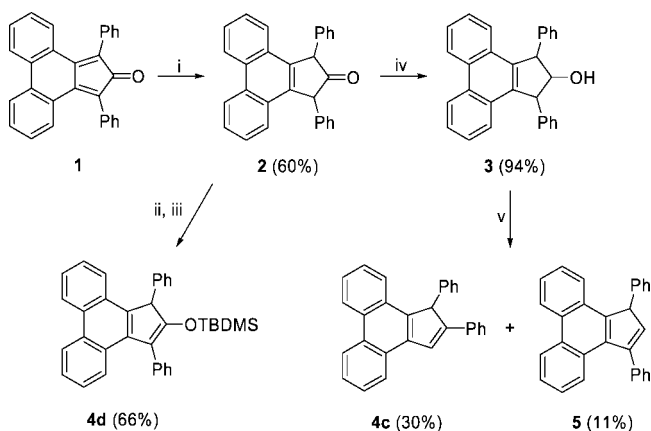
(4) (a) Lee, D.; Huh, E. A.; Kim, J. M.; Jung, H. M.; Koh, J. H.; Park, J. *Org. Lett.* **2000**, *2*, 2377. (b) Dijkstra, A.; Elzinga, J. M.; Li, Y.-X.; Arends, I. W. C. E.; Sheldon, R. A. *Tetrahedron: Asymmetry* **2002**, *13*, 879.

(5) (a) Schneider, N.; Proscenc, M.-H.; Brintzinger, H.-H. *J. Organomet. Chem.* **1997**, *545–546*, 291. (b) Schneider, N.; Huttenloch, M. E.; Stehling, U.; Kirsten, R.; Schaper, F.; Brintzinger, H. H. *Organometallics* **1997**, *16*, 3413. (c) Schneider, N.; Schaper, F.; Schmidt, K.; Kirsten, R.; Geyer, A.; Brintzinger, H. H. *Organometallics* **2000**, *19*, 3597. (d) Luttikhedde, H. J. G.; Leino, R.; Wilén, C.-E.; Näsmän, J. H. *Polym. Prepr. (Am. Chem. Soc., Div. Polym. Chem.)* **1998**, *39* (1), 229. (e) Rigby, S. S.; Decken, A.; Bain, A. D.; McGlinchey, M. J. *J. Organomet. Chem.* **2001**, *637–639*, 372. (f) Sun, J.; Berg, D. J.; Twamley, B. *Organometallics* **2008**, *27*, 683.

(6) (a) Repo, T.; Jany, G.; Hakala, K.; Klinga, M.; Polamo, M.; Leskelä, M.; Rieger, B. *J. Organomet. Chem.* **1997**, *549*, 177. (b) Aitola, E.; Hakala, K.; Byman-Fagerholm, H.; Leskelä, M.; Repo, T. *J. Polym. Sci., Part A: Polym. Chem.* **2008**, *46*, 373.

(7) Hoshi, T.; Nakazawa, T.; Saitoh, I.; Mori, A.; Suzuki, T.; Sakai, J.-i.; Hagiwara, H. *Org. Lett.* **2008**, *10*, 2063.

(8) (a) Eliasson, B.; Nouri-Sorkhabi, M. H.; Trogen, L.; Sethson, I.; Edlund, U.; Sygula, A.; Rabinovitz, M. *J. Org. Chem.* **1989**, *54*, 171. (b) Komatsu, K.; Fujiura, R.; Okamoto, K. *Chem. Lett.* **1988**, 265.

Scheme 1. Synthesis of the Ligand Precursors 4c and 4d^a

^a Conditions: (i) Zn/AcOH, reflux. (ii) NaH, THF, RT. (iii) TBDMSCl, THF, RT. (iv) NaBH₄, dioxane, reflux. (v) P₂O₅, benzene, reflux.

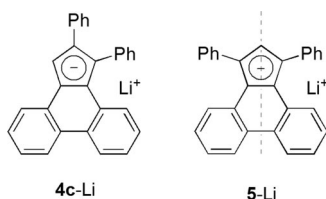


Figure 1. Lithium salts of the cyclopenta[1]phenanthrenyl ligand precursors 4c and 5.

silylation of the corresponding enolized ketone in a manner similar to that reported earlier for 1,3-dihydro-2-oxocyclopenta[1]phenanthrene,^{5d} 2-indanone, and its analogues (Scheme 1).⁹ The preparation of the diphenyl-substituted ligand precursor 4c is likewise illustrated in Scheme 1. A similar transformation has been described earlier,¹⁰ where the authors claimed the formation of the symmetrical 1,3-(diphenyl)cyclopenta[1]phenanthrene 5. In our work, however, we observed a rearrangement taking place leading to a mixture of the 1,3- and 1,2-substituted products 5 and 4c in 1:3 ratio. A similar rearrangement in the case of a trisubstituted analogue under acidic conditions has been described earlier.¹¹

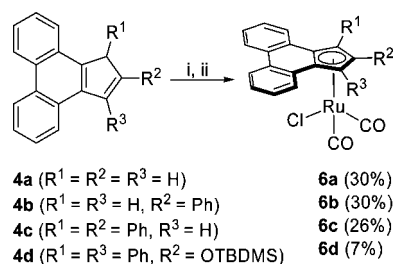
Structures of the compounds isolated here were also confirmed by NMR analysis of the corresponding anions. Upon deprotonation with *n*-BuLi in THF-*d*₈, compound 5 produced a highly symmetrical anion, while compound 4c gave an unsymmetrical structure (Figure 1). The position of the double bond in 4c was likewise confirmed by NMR spectroscopy. The two protons of the C₅ ring give rise to two doublets (⁴*J* = 1.1 Hz) in the ¹H NMR spectrum at 5.42 and 7.81 ppm, respectively. In addition, a weak interaction (typical for allyl or *W*-coupling) between these protons was observed in the COSY spectrum, while a geminal coupling typical for a CH₂ group was absent.

Next, the new ruthenium complexes 6a–d and 8 containing cyclopenta[1]phenanthrenyl and cyclopenta[*a*]acenaphthylenyl

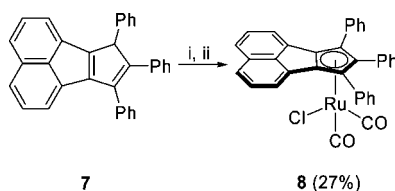
(9) See for example: (a) Leino, R.; Luttkhedde, H.; Wilén, C.-E.; Sillanpää, R.; Näsmän, J. H. *Organometallics* **1996**, *15*, 2450. (b) Leino, R.; Luttkhedde, H. J. G.; Lehtonen, A.; Sillanpää, R.; Penninkangas, A.; Strandén, J.; Mattinen, J.; Näsmän, J. H. *J. Organomet. Chem.* **1998**, *558*, 171. (c) Leino, R.; Luttkhedde, H. J. G.; Långstedt, L.; Penninkangas, A. *Tetrahedron Lett.* **2002**, *43*, 4149.

(10) Kreicberga, J.; Neilands, O.; Kampars, V. *Zh. Org. Khim.* **1975**, *11*, 1941.

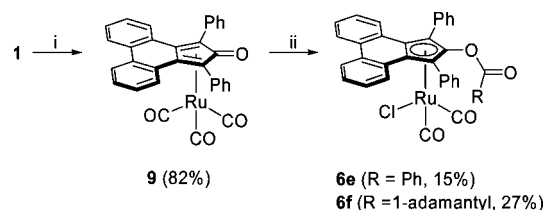
(11) Dennis, G. D.; Edward-Davis, D.; Field, L. D.; Masters, A. F.; Maschmeyer, T.; Ward, A. J.; Buys, I. E.; Turner, P. *Aust. J. Chem.* **2006**, *59*, 135.

Scheme 2. Synthesis of the Ruthenium Complexes 6a–d^a

^a Conditions: (i) *n*-BuLi/THF, –78 °C to RT. (ii) [Ru(CO)₃Cl₂]₂, RT.

Scheme 3. Synthesis of the Ruthenium Complex 8^a

^a Conditions: (i) *n*-BuLi/THF, –78 °C to RT. (ii) [Ru(CO)₃Cl₂]₂, RT.

Scheme 4. Synthesis of the Ruthenium Complexes 6e and 6f^a

^a Conditions: (i) Ru₃(CO)₁₂, mesitylene, 150 °C. (ii) RCOCl, toluene, 90 °C.

ligands were prepared by reactions of dichlorotricarbonylruthenium dimer with the corresponding ligand precursors deprotonated with butyllithium (Schemes 1 and 2). The fairly low yields obtained represent the nonoptimized reaction conditions for metalation. In all cases significant amounts of starting ligand precursor were recovered during the reaction workup. Complex 6a is unstable, decomposing rapidly in solutions and slowly in the solid state during storage at ambient temperature. All other polysubstituted complexes are stable when stored in air.

The synthesis of the trisubstituted cyclopenta[1]phenanthrenyl ruthenium complexes 6e and 6f containing an acyl substituent in position 2 of the C₅ ring commenced, in turn, from the phenylcyclopenta[1]phenanthrene precursor 1 followed by oxidative acylation of the Ru(0) diene complex 9 with the corresponding acyl chlorides (Scheme 4).

In the ¹H NMR spectra of 6d and 6f two kinds of *o*- and *m*-protons and carbons were observed indicating restricted rotation of the phenyl rings. This rotation remained blocked in VT NMR experiments at 50 °C. The lithium salt of 4d obtained by deprotonation with *n*-BuLi, however, showed in the ¹H NMR spectrum time-averaged symmetry with only one type of *o*- and *m*-protons and carbons (Figures 2 and 3). This observation may be due to rapid rotation of the phenyl rings in solution at ambient temperature, resulting in coinciding resonances. Another explanation, however, is the potential lability of the ionically bound lithium cation: a rapid exchange of Li⁺ transiently bound on

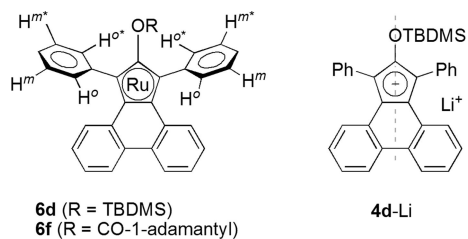


Figure 2. Top views of **6d**, **6f**, and **4d-Li**. Carbonyls and chlorine are omitted for clarity.

one side of the ligand and the other (even being located in the solvent independently from the anion) may also result in time-averaging of the NMR signals without rotation about the C–Ph bond.

X-ray Structures of Ruthenium Complexes. The molecular structures of the ruthenium complexes **6b**, **8**, and **9** were determined by X-ray crystallography and are elucidated, together with selected bond lengths and angles, in Figures 4–6. The ruthenium metal is η^5 -coordinated in complexes **6b** and **8** (with similar Ru–C bond distances to all carbon atoms of the five-membered ring and η^4 -coordinated in complex **9** with the longest Ru–C distance to the carbonyl carbon of the C₅ ring. The Ru–CO bond lengths are similar in all three complexes. In the η^5 -coordinated complexes **6b** and **8** the cyclopenta[*l*]phenanthrenyl and cyclopenta[*a*]acenaphthylenyl moieties are nearly planar. A small distortion from planarity for the terminal C₆ ring of **6b** is observed, possibly due to repulsion of the partial negative charge on the ligand and the electronegative chlorine atom. In the η^4 -diene complex **9** the ligand plane is significantly distorted, with one terminal C₆ ring tilted and the coordinated C₅ ring showing envelope geometry. The formal oxidation states +2 for **6b** and **8** and 0 for **9** are in good accordance with the elongated Ru–carbonyl and Ru–C₅ centroid distances in the latter complex. The Ru–C₅, Ru–carbonyl, and Ru–Cl distances are similar to those in analogous complexes containing (pentaphenyl)cyclopentadienyl¹² and (triphenyl)indenyl^{2d} ligands.

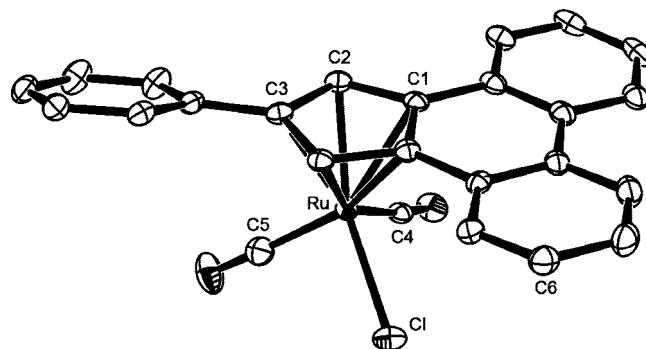


Figure 4. Molecular structure of **6b** (hydrogen atoms excluded for clarity, 50% probability ellipsoids). Selected distances (Å): Ru–C1 2.281(3), Ru–C2 2.196(3), Ru–C3 2.253(3), Ru–C4 1.898(3), Ru–C5 1.889(3), Ru–Cl 2.3988(7), Ru–Ct 1.899, C6–P11 0.078. Ct is the C₅ ring centroid. P11 is the plane calculated for the C₅ ring and two other C₆ rings.

Racemization of (*S*)-Phenylethanol. All ruthenium complexes prepared from **6a–f** and **8** were screened as catalysts for the racemization of (*S*)- α -phenylethanol **10**, a standard reference substrate utilized for initial investigation of catalytic activities in alcohol racemization and DKR (Scheme 5). The racemization reactions were carried out in toluene at ambient temperature by following the procedure described earlier by Bäckvall and co-workers.¹²

The unsubstituted cyclopenta[*l*]phenanthrenyl complex **6a** was found to be inefficient as a catalyst for the racemization reaction. With this complex, the racemization stops at 70% ee after 2 days. Somewhat better activities were obtained with the mono- and disubstituted complexes **6b** and **6c**. The racemization remained, however, fairly low, with 50% ee reached only after 4 and 2 days of reaction, respectively. Only in the case of the fully substituted complexes **6d** and **8** were acceptable activities obtained. The results are summarized in Figure 7.

The proposed mechanism for the racemization of secondary alcohols catalyzed by monoCp-ruthenium complexes has been

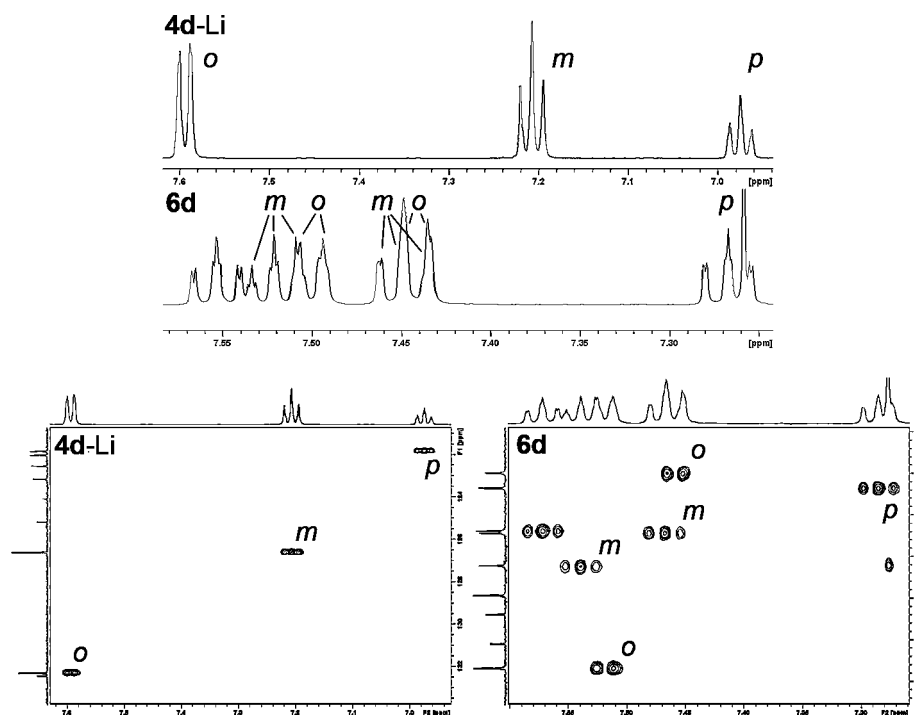


Figure 3. ¹H and HSQC-NMR of **6d** and **4d-Li**.

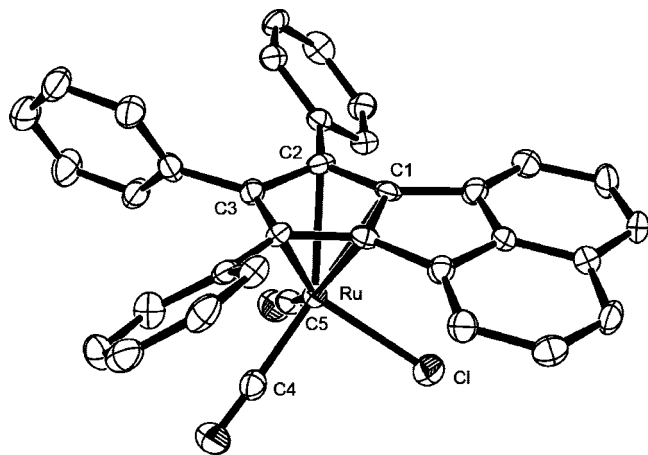


Figure 5. Molecular structure of **8** (hydrogen atoms excluded for clarity, 50% probability ellipsoids). Selected distances (Å): Ru–C1 2.293(4), Ru–C2 2.284(4), Ru–C3 2.204(3), Ru–C4 1.874(5), Ru–C5 1.902(5), Ru–Cl 2.4030(10), Ru–Ct 1.904. Ct is the closest C₅ ring centroid.

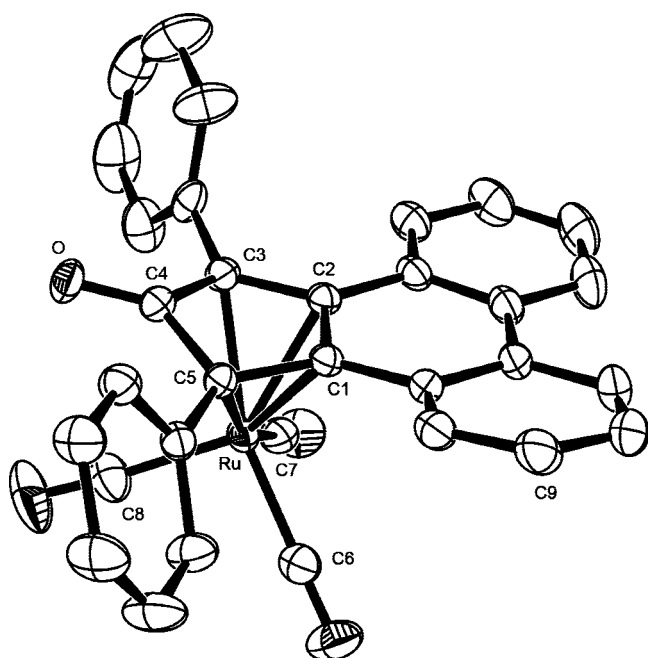
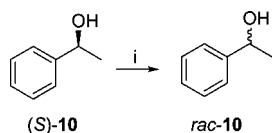


Figure 6. Molecular structure of **9** (hydrogen atoms excluded for clarity, 50% probability ellipsoids). Selected distances (Å): Ru–C1 2.2673(17), Ru–C2 2.2139, Ru–C3 2.2186, Ru–C4 2.4896(18), Ru–C5 2.220(7), Ru–C6 1.932(2), Ru–C7 1.936(2), Ru–C8 1.928(2), C4–O 1.227(2), Ru–Ct 1.919, C9–P11 0.493. Selected angles (deg): P12–P13 17.96. Ct is the C₅ ring centroid. P11 is the plane calculated for the two flat C₆ rings; P12 for C1, C2, C3, C4; P13 for C3, C4, C5, O.

Scheme 5. Racemization of (*S*)-Phenylethanol^a



^a Conditions: (i) Catalyst **6a–f** or **8** 1 mol %, *t*-BuOK 3 mol %, toluene, RT.

elucidated earlier by Bäckvall and co-workers (Scheme 6). The reaction involves a shift of hydrogen from the alcohol to ruthenium accompanied by ring slippage of the Cp ring from

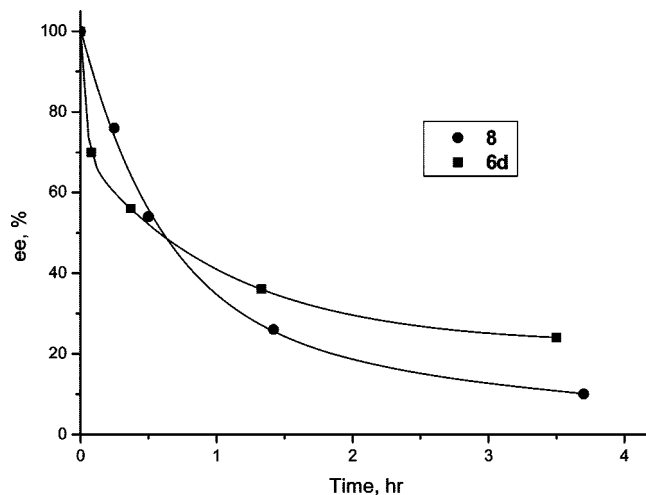
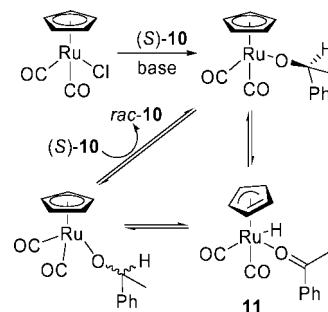


Figure 7. Racemization of (*S*)-phenylethanol catalyzed by **6d** and **8** (1 mol %).

Scheme 6. Racemization of (*S*)-Phenylethanol



η^5 to η^3 . It is well known that the stabilities of Cp complexes generally increase with the increasing amount of substituents.¹³ It is conceivable that in the case of the less substituted complexes **6a–c** the η^3 -coordinated intermediate of type **10** (Scheme 6) might undergo further ring slippage and dissociation via η^1 -coordination, leading to full decomposition of the catalyst. The low stability of **6a** in solution and the decomposition of **6b** and **6c** during the racemization reaction further support this hypothesis. The complexes prepared can be arranged in a series according to their phenylethanol racemization activities as **6a** < **6b** < **6c** \ll **6d**, **8**, clearly demonstrating increasing activities with increasing number of C₅ ring substituents. Only the fully substituted complexes show acceptable activities. Accordingly, our attention next turned to the bulkier catalyst variants **6e** and **6f** of this type.

Both complexes **6e** and **6f** show activities similar to **6d** and **8** in the racemization of (*S*)-phenylethanol (Figure 8). The 2-benzoyl-substituted complex **6e** performs better when compared to its more congested adamantyl analogue **6f**, indicating that steric factors cannot be the only reason governing the catalytic activities. It might be speculated that the pendant phenyl functionality of the 2-benzoyl substituent may have a through-space stabilizing, coordinative interaction with the ruthenium metal center. Similar intramolecular arene coordination is well known for Ti- and Zr-based mono(cyclopentadienyl) olefin polymerization catalysts.¹⁴

The racemization rates obtained with **6e** are, however, slower than those reported for the (pentaphenyl)cyclopentadienyl-based complex **12** (0.5 mol % of catalyst, 50% ee reached after ca. 5 min), currently considered as the lead catalyst structure, under similar reaction conditions.¹² On the other hand, complex **13**, structurally similar to **6e**, was by Park and co-workers reported

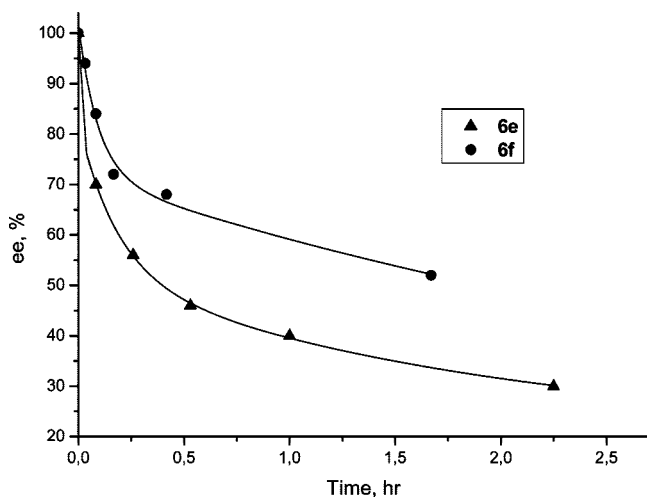


Figure 8. Racemization of (*S*)-phenylethanol catalyzed by **6e** and **6f** (1 mol %).

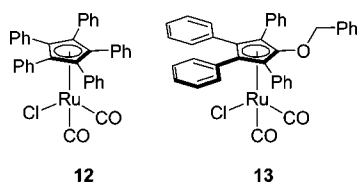


Figure 9. Structures of complexes **12** and **13** (structural analogues of **6e**).

to provide similar activities at 4 mol % concentration¹⁵ to those observed here for **6e** at 1 mol % loading (for structures of **12** and **13**, see Figure 9).

The results obtained here may nevertheless be considered promising, clearly demonstrating variable racemization performance as a function of the ligand sterics, providing structure/reactivity trends to aid in future catalyst design.

Summary and Conclusions

To summarize, a series of half-sandwich ruthenium complexes with substituted cyclopenta[*l*]phenanthrenyl and cyclopenta[*a*]acenaphthylenyl ligands were prepared and characterized by NMR and in three cases by X-ray crystallography. The catalytic activities of the complexes in racemization of (*S*)-phenylethanol were investigated and were shown to depend strongly on the substitution pattern of the ligand framework. Acceptable racemization results were obtained with fully substituted complexes only. The racemization activities were, however, lower than those reported for chlorodicarbonyl(pentaphenyl)cyclopentadienylruthenium (**12**), currently considered as the best-performance catalyst for secondary alcohol racemization in DKR applications with enzymes. For this reason,

(12) Martín-Matute, B.; Edin, M.; Bogár, K.; Kaynak, B.; Bäckvall, J.-E. *J. Am. Chem. Soc.* **2005**, *127*, 8817.

(13) (a) Heeg, M. J.; Janiak, C.; Zuckerman, J. J. *J. Am. Chem. Soc.* **1984**, *106*, 4529. (b) Bercaw, J. E.; Marvich, R. H.; Bell, L. G.; Brintzinger, H. H. *J. Am. Chem. Soc.* **1972**, *94*, 1219. (c) Miller, E. J.; Landon, S. J.; Brill, T. B. *Organometallics* **1985**, *4*, 533. (d) Calabro, D. C.; Hubbard, J. L.; Blevins, C. H.; Campbell, A. C.; Lichtenberger, D. L. *J. Am. Chem. Soc.* **1981**, *103*, 6839.

(14) (a) Sassmannshausen, J.; Powell, A. K.; Anson, C. E.; Wocadlo, S.; Bochmann, M. *J. Organomet. Chem.* **1999**, *592*, 84. (b) Deckers, P. J. W.; Hessen, B.; Teuben, J. H. *Angew. Chem.* **2001**, *40*, 2516. (c) Deckers, P. J. W.; Hessen, B.; Teuben, J. H. *Organometallics* **2002**, *21*, 5122.

(15) Kim, N.; Ko, S.-B.; Kwon, M. S.; Kim, M.-J.; Park, J. *Org. Lett.* **2005**, *7*, 4523.

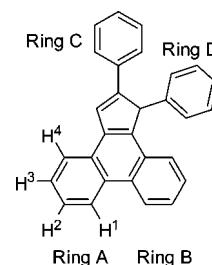


Figure 10. Labeling of substituted cyclopenta[*l*]phenanthrenyl fragments in the NMR spectral data.

neither extended investigations with other secondary alcohols nor attempts to pursue dynamic kinetic resolutions in combination with enzymes were carried out with these catalysts. In the present work, best performance was observed with a ligand structure containing a pendant aromatic moiety (benzoyloxy). Detailed NMR studies were carried out on a number of complexes and their cyclopenta[*l*]phenanthrenyl ligand anion lithium salts. Restricted rotation of phenyl substituents in the ligand five-membered rings was observed in some cases when moving from the lithium salts to transition metal coordination.

Experimental Section

General Remarks. All manipulations with air- and moisture-sensitive compounds were performed under an inert atmosphere of argon using standard Schlenk techniques. Solvents were purchased from standard vendors and dried by standard procedures (THF, benzene, toluene were redistilled from Na/benzophenone ketyl, DCM was redistilled from calcium hydride, and pentane, hexane, heptane were redistilled from sodium). NMR spectra were recorded on a Bruker Avance 600 MHz spectrometer. Assignment of NMR signals is based on 1D TOCSY, NOE-diff, COSY, and HSQC experiments. Chiral GC analyses were performed on a HP 5890 series II gas chromatograph equipped with a Varian capillary column CP7502. Phencyclone (**1**) was prepared according to a literature procedure.^{11,16} Solutions of anions of **4c,d** and **5** in THF-*d*₈ were prepared directly in NMR tubes from the corresponding cyclopentadienes and *n*-BuLi using syringe-septum techniques. (*S*)- α -Phenylethanol was obtained by enzymatic kinetic resolution of the racemate and purified by column chromatography. Commercially available (*S*)- α -phenylethanol (Aldrich, 97%) yielded unreproducible results. Potassium *tert*-butoxide, required for activation of the racemization catalyst, should be freshly sublimated in order to obtain reproducible results.

The following labeling of the cyclopenta[*l*]phenanthrene derivatives was applied in the assignment of NMR signals (Figure 10):

General Procedures for Preparation of the Complexes 6a–d and 8. A solution of ligand precursor **1a–d** or **3** (0.5 mmol) in 3 mL of THF was cooled to -78 °C followed by addition of 0.31 mL (0.5 mmol) of a 1.6 M solution of *n*-BuLi in hexane via syringe. The reaction mixture was stirred for 15 min at -78 °C and allowed to warm to RT. Next, a solution of tricarbonyldichlororuthenium(II) dimer (128 mg, 0.25 mmol) in 2 mL of THF was added via syringe. The mixture was stirred for 2 h at RT, then evaporated with silica and purified by column chromatography using DCM–hexane as eluent. All products were obtained as yellow (**6a–d**) or brown (**8**) microcrystalline powders. Yields: **6a** 30%, **6b** 30%, **6c** 26%, **6d** 7%, **8** 27%.

Chlorodicarbonyl(η^5 -cyclopenta[*l*]phenanthryl)ruthenium(II) (6a**).** ¹H NMR (CDCl₃, 600.13 MHz): δ 5.82 (t, ³J = 2.7 Hz 1H, Cp-H), 5.95 (d, ³J = 2.7 Hz, 2H, Cp-H), 7.66 (dd, ³J = 7.2, 7.9 Hz, 2H, 3-H), 7.72 (ddd, 2H, ³J = 8.4, 7.2, ⁴J = 1.4, 2-H), 7.98 (dd, 2H, ³J

(16) Wooi, G. Y.; White, J. M. *Org. Biomol. Chem.* **2005**, *3*, 972.

= 7.9, $^4J = 1.4$ Hz, 4-*H*), 8.54 (d, $^3J = 8.4$ Hz, 1-*H*). ^{13}C NMR (CDCl_3 , 150.9 MHz): δ 72.34 (Cp), 89.59 (Cp), 107.30, 124.28, 125.02, 125.42, 128.26, 129.35, 131.15, 195.76 (C=O). MS: exact mass calcd. for $\text{C}_{19}\text{H}_{11}^{102}\text{Ru}^{35}\text{ClO}_2$ 407.9491, found 407.9490; 380 ($\text{M}^+ - \text{CO}$), 352 ($\text{M}^+ - 2\text{CO}$).

Chlorodicarbonyl(η^5 -2-phenylcyclopenta[*l*]phenanthryl)ruthenium(II) (6b). ^1H NMR (CDCl_3 , 600.13 MHz): δ 6.34 (s, 2H, Cp-*H*), 7.46 (dd, $^3J = 8.0$, 6.6 Hz, 2H, *m*-Ph), 7.47 (t, $^3J = 6.6$ Hz, 1H, *p*-Ph), 7.66 (d, $^3J = 8.0$ Hz, 2H, *o*-Ph), 7.68 (dd, $^3J = 7.8$, 7.7 Hz, 2H, 3-*H*), 7.72 (ddd, $^3J = 8.0$, 7.7 Hz, $^4J = 1.1$ Hz, 2H, 2-*H*) 8.06 (dd, $^3J = 7.8$, $^4J = 1.1$ Hz, 2H, 4-*H*), 8.54 (d, $^3J = 8.0$ Hz, 2H, 1-*H*). ^{13}C NMR (CDCl_3 , 150.9 MHz): δ 69.46 (Cp-C), 106.01, 113.69, 124.31 (1-C), 125.19, 125.34 (4-C), 126.82 (*o*-C), 128.25 (2-C), 129.18 (*p*-C), 129.25 (3-C), 130.05, 130.28 (*m*-C), 131.10, 195.60 (C=O). MS: exact mass calcd for $\text{C}_{25}\text{H}_{15}^{102}\text{Ru}^{35}\text{ClO}_2$ 483.9804, found 483.9600; 455.97 ($\text{M}^+ - \text{CO}$), 427.97 ($\text{M}^+ - 2\text{CO}$).

Chlorodicarbonyl(η^5 -1,2-diphenylcyclopenta[*l*]phenanthryl)ruthenium(II) (6c). ^1H NMR (CDCl_3 , 600.13 MHz): δ 7.22 (ur, 1H, Ph), 7.23 (d, $^3J = 7.0$ Hz, 1H, *o*-Ph(c)), 7.26–7.30 (m, 3H, Ph), 7.27 (d, $^3J = 7.0$ Hz, 1H, *o*-Ph (c)), 7.35 (d, $^3J = 8.0$ Hz, 1H, *o*-Ph (d)), 7.40 (ur, 1H, Ph), 7.43 (d, $^3J = 8.0$ Hz, 1H, *o*-Ph (d)), 7.52 (dd, $^3J = 7.6$, 7.6 Hz, 1H, 2b- or 3b-*H*), 7.60 (ur, 1H, Ph), 7.61 (dd, $^3J = 7.6$, 7.6 Hz, 1H, 2b- or 3b-*H*), 7.70 (dd, $^3J = 7.8$, 7.8 Hz, 1H, 2a- or 3a-*H*), 7.73 (dd, $^3J = 7.8$, 7.8 Hz, 1H, 2a- or 3a-*H*), 7.97 (d, $^3J = 7.6$ Hz, 1H, 4b-*H*), 8.12 (d, $^3J = 7.8$ Hz, 1H, 4a-*H*), 8.54 (d, $^3J = 7.6$ Hz, 1H, 1b-*H*), 8.55 (d, $^3J = 7.8$, 1H, 1a-*H*). ^{13}C NMR (CDCl_3 , 150.9 MHz): δ 70.94 (Cp), 95.68 (Cp), 103.32, 105.72, 116.06, 124.16 (1a-C), 124.18 (1b-C), 125.05, 125.36 (4a-C), 125.89, 126.52 (*o*-Ph), 127.64 (Ph), 128.23 (2a- or 3a-C), 128.35 (2 carbons, *o*-Ph), 128.80 (Ph), 128.99 (Ph), 129.12 (2b- or 3b-C), 129.22 (2a- or 3a-C), 129.25 (*o*-Ph), 129.45 (Ph), 129.76 (2b- or 3b-C), 129.98, 131.11, 131.25 (*o*-Ph), 131.72, 132.18, 134.71 (4b-C), 196.04 (C=O), 196.29 (C=O). MS: exact mass calcd for $\text{C}_{31}\text{H}_{19}^{102}\text{Ru}^{35}\text{ClO}_2(+\text{Na})$ 583.0015, found 583.0010; exact mass calcd for $\text{C}_{31}\text{H}_{19}^{102}\text{Ru}^{35}\text{ClO}_2(+\text{K})$ 598.9754, found 598.9727.

Chlorodicarbonyl(η^5 -2-*tert*-butyldimethylsiloxy)-1,3-diphenylcyclopenta[*l*]phenanthryl)ruthenium(II) (6d). ^1H NMR (CDCl_3 , 600.13 MHz): δ -0.55 (s, 6H, Si- CH_3), 0.46 (s, 9H, *t*-Bu), 7.27 (t, $^3J = 7.7$ Hz, 2H, *p*-Ph), 7.44 (d, $^3J = 8.5$ Hz, 2H, *o*-Ph), 7.45 (dd, $^3J = 7.7$, 8.5 Hz, 2H, *m*-Ph), 7.50 (d, $^3J = 8.5$, 2H, *o*-Ph), 7.51 (dd, $^3J = 7.7$, 8.5 Hz, 2H, *m*-Ph), 7.55 (dd, $^3J = 8.1$, 7.6 Hz, 2H, 2-*H*), 7.62 (dd, $^3J = 7.6$, 7.6 Hz, 2H, 3-*H*), 8.01 (d, $^3J = 7.6$ Hz, 2H, 4-*H*), 8.49 (d, $^3J = 8.1$ Hz, 2H, 1-*H*). ^{13}C NMR (CDCl_3 , 150.9 MHz): δ -4.65 (Si- CH_3), 18.01 ($\text{C}(\text{CH}_3)_3$), 24.87 ($\text{C}(\text{CH}_3)_3$), 86.00, 123.86 (1-C), 125.62, 126.99 (*o*-Ph), 127.35 (*p*-C), 128.39 (2-C), 128.44 (*m*-Ph), 129.22 (*m*-Ph), 129.93 (3-C), 130.39, 131.10, 131.68 (*o*-Ph), 135.42 (4-C), 196.49 (C=O). MS: exact mass calcd for $\text{C}_{37}\text{H}_{33}^{102}\text{Ru}^{35}\text{ClO}_3(+\text{Na})$ 713.0829, found 713.0802; exact mass calcd for $\text{C}_{37}\text{H}_{33}^{102}\text{Ru}^{35}\text{ClO}_3(+\text{Na} - \text{CO})$ 685.0880, found 685.0860.

Chlorodicarbonyl(η^5 -1,2,3-triphenylcyclopenta[*a*]acenaphthylenyl)ruthenium(II) (8). ^1H NMR (CDCl_3 , 600.13 MHz): δ 7.17 (ur, 2H, Ph), 7.24–7.27 (m, 1H, Ph), 7.35–7.39 (m, 6H, Ph), 7.54 (dd, $^3J = 7.1$, 8.1 Hz, 2H, 2-*H*) 7.55–7.57 (m, 4H), 7.79 (d, $^3J = 7.1$ Hz, 2H, 3-*H*), 7.89 (d, $^3J = 8.1$ Hz, 2H, 1-*H*). ^{13}C NMR (CDCl_3 , 150.9 MHz): δ 100.38 (Cp), 106.77 (Cp), 108.06, 123.19 (3-C), 128.00 (1-C), 128.15 (Ph), 128.20 (2-C), 128.48 (Ph), 128.65 (Ph), 129.11 (Ph), 129.66, 129.90, 130.26, 130.68 (Ph), 130.77, 132.21 (Ph), 138.53, 197.03 (C=O). MS: exact mass calcd for $\text{C}_{35}\text{H}_{21}^{102}\text{Ru}^{35}\text{ClO}_2(+\text{Na})$ 633.0171, found 633.0167; exact mass calcd for $\text{C}_{35}\text{H}_{21}^{102}\text{Ru}^{35}\text{ClO}_2(+\text{K})$ 648.9911, found 648.9892.

Tricarboxyl(η^4 -1,3-diphenylcyclopenta[*l*]phenanthren-2-one)ruthenium(0) (9). A mixture of 0.76 g (2 mmol) of phencyclone (**5**), 0.32 g (0.5 mmol) of triruthenium dodecacarbonyl, and 5 mL of mesitylene was heated to 150 °C with stirring for 24 h. The reaction mixture was cooled to RT, and argon was bubbled through the mixture to remove the carbon monoxide released followed by heating at the same temperature for an additional 4 h. After cooling

to RT, the mixture was diluted with 5 mL of hexane. The precipitate was separated by filtration, redissolved in 10 mL of toluene, and separated from a small amount of insoluble byproduct **2** by filtration. Finally, 0.7 g (82%) of **9** was obtained as a greenish microcrystalline solid. ^1H NMR (CDCl_3 , 600.13 MHz): δ 7.26 (dd, $^3J = 8.2$, 7.6 Hz, 2H, 3-*H*), 7.45 (d, $^3J = 8.2$ Hz, 2H, 4-*H*), 7.48 (dd, $^3J = 8.2$, 8.0 Hz, 2H, *m*-Ph), 7.49 (dd, $^3J = 8.2$, 7.5 Hz, 2H, *m*-Ph), 7.54 (d, $^3J = 8.0$ Hz, 2H, *o*-Ph), 7.55 (d, $^3J = 7.5$ Hz, 2H, *o*-Ph), 7.57 (dd, $^3J = 8.2$, 7.6 Hz, 2H, 2-*H*), 7.58 (t, $^3J = 8.2$ Hz, 2H, *p*-Ph), 8.52 (d, $^3J = 8.2$ Hz, 2H, 1-*H*). ^{13}C NMR (CDCl_3 , 150.9 MHz): δ 82.14 (cyclopentadienone), 97.54 (cyclopentadienone), 124.06 (1-C), 126.00, 126.50 (4-*H*), 127.87 (3-*H*), 128.34 (*m*-Ph), 128.86 (*m*-Ph), 128.92 (1-*H*), 129.42 (*p*-Ph), 130.94, 131.33 (*o*-Ph), 132.83, 134.75 (*o*-Ph), 177.58 (=C-CO-C=), 193.64 (C=O). MS: exact mass calcd for $\text{C}_{32}\text{H}_{19}^{102}\text{RuO}_4(+\text{H})$ 569.0327, found 569.0330; exact mass calcd for $\text{C}_{32}\text{H}_{19}^{102}\text{RuO}_4(+\text{H} - \text{CO})$ 541.0378, found 541.0394; exact mass calcd for $\text{C}_{32}\text{H}_{19}^{102}\text{RuO}_4(+\text{H} - 2\text{CO})$ 513.0429, found 513.0410.

General Procedures for Preparation of the Complexes 6e and 6f. A mixture of 57 mg (0.1 mmol) of **9**, 0.1 mmol of the corresponding acyl chloride, and 2 mL of toluene was heated at 90 °C for 12 h. The solvent was evaporated and the residue purified by column chromatography using DCM–hexane as eluent. The products were obtained as yellow microcrystalline solids. Yields: **6e** 15%, **6f** 27%.

Chlorodicarbonyl(η^5 -2-benzoyloxy-1,3-diphenylcyclopenta[*l*]phenanthryl)ruthenium(II) (6e). ^1H NMR (CDCl_3 , 600.13 MHz): δ 7.30 (dd, $^3J = 8.1$, 7.5 Hz, 2H, *m*-Bz), 7.33 (dd, $^3J = 7.5$, 7.8 Hz, 2H, 3-*H*), 7.37 (dd, $^3J = 8.2$, 8.0 Hz, 2H, *m*-Ph), 7.41 (dd, $^3J = 8.2$, 7.6 Hz, 2H, *m*-Ph), 7.49 (t, $^3J = 8.0$ Hz, 2H, *p*-Ph), 7.49 (t, $^3J = 7.5$ Hz, 2H, *p*-Bz), 7.59 (d, $^3J = 8.2$ Hz, 2H, *o*-Ph), 7.59 (d, $^3J = 7.5$ Hz, 2H, *o*-Ph) 7.62 (dd, $^3J = 8.2$, 7.8 Hz, 2H, 2-*H*), 7.70 (d, $^3J = 7.9$ Hz, 2H, *o*-Bz), 7.92 (d, $^3J = 7.5$ Hz, 2H, 4-*H*), 8.54 (d, $^3J = 8.2$ Hz, 2H, 1-*H*). ^{13}C NMR (CDCl_3 , 150.9 MHz): δ 89.31 (Cp), 99.06 (Cp), 124.09 (1-C), 125.06, 126.91 (*o*-Ph), 127.69 (3-C), 128.51 (*m*-Bz), 128.63 (*m*-Ph), 128.78, 129.01 (2-C), 129.29 (*m*-Ph), 129.38 (*p*-Ph), 129.97 (*o*-Bz), 131.40 (*o*-Ph), 131.58, 133.35, 133.57 (4-C), 134.16 (*p*-Bz), 163.24 (Ph-C=O), 195.61 (C=O). MS: exact mass calcd for $\text{C}_{38}\text{H}_{23}^{102}\text{Ru}^{35}\text{ClO}_4(+\text{Na})$ 703.0226, found 703.0227.

Chlorodicarbonyl(η^5 -2-adamantanoyloxy-1,3-diphenylcyclopenta[*l*]phenanthryl)ruthenium(II) (6f). ^1H NMR (CDCl_3 , 600.13 MHz): δ 1.28 (d, $^3J = 2.5$ Hz, 6H, α -adamantyl-*H*), 1.46 (d, $^2J = 12.5$ Hz, 3H, equatorial δ -adamantyl-*H*), 1.57 (d, $^2J = 12.5$ Hz, 3H, axial δ -adamantyl-*H*), 1.80 (t, $^3J = 2.5$ Hz, 3H, β -adamantyl-*H*), 7.32 (dd, $^3J = 8.2$, 7.5 Hz, 2H, 2-*H*), 7.42 (t, $^3J = 7.2$ Hz, *p*-Ph), 7.50 (dd, $^3J = 8.1$, 7.2 Hz, 2H, *m*-Ph), 7.51 (d, $^3J = 8.1$, 2H, *o*-Ph), 7.56 (dd, $^3J = 8.1$, 7.2, 2H, *m*-Ph), 7.60 (d, $^3J = 8.1$ Hz, 2H, *o*-Ph), 7.61 (dd, $^3J = 7.5$, 7.5 Hz, 2H, 3-*H*), 7.84 (d, $^3J = 7.5$ Hz, 2H, 4-*H*), 8.54 (d, $^3J = 8.2$ Hz, 2H, 1-*H*). ^{13}C NMR (CDCl_3 , 150.9 MHz): δ 27.39 (β -adamantyl-C), 35.98 (δ -adamantyl-C, a,e), 37.85 (α -adamantyl-C), 40.52 (γ -adamantyl-C), 88.97 (Cp), 99.68 (Cp), 124.06 (1-C), 125.07, 126.93 (*o*-Ph), 127.65 (1-C), 128.51 (*p*-Ph), 128.89, 128.95 (4-C), 129.22 (2 carbons, *m*-Ph), 131.66 (*o*-Ph), 131.58, 133.22, 133.78 (3-C), 174.12 (Ad-C=O), 195.55 (C=O). MS: exact mass calcd for $\text{C}_{42}\text{H}_{33}^{102}\text{Ru}^{35}\text{ClO}_4(+\text{Na})$ 761.1009, found 761.0999, exact mass calcd for $\text{C}_{42}\text{H}_{33}^{102}\text{Ru}^{35}\text{ClO}_4(+\text{K})$ 777.0748, found 777.0728.

1,3-Dihydro-1,3-diphenyl-2*H*-cyclopenta[*l*]phenanthren-2-one (2,5-dihydrophencyclone) (2). A suspension of 1.91 g (5 mmol) of phencyclone **1** and 0.98 g (15 mmol) of zinc powder in 50 mL of glacial acetic acid was refluxed until the green color of **5** disappeared (ca. 2 h). The mixture was evaporated, and the residue boiled with 200 mL of xylene and filtered hot from zinc powder. Xylene was evaporated, the residue was suspended in a small amount of DCM, and the precipitate was separated by filtration giving fraction A, enriched in the *cis*-isomer. The filtrate was

evaporated, the residue was suspended in a small amount of acetone, and the precipitate formed was separated by filtration, giving fraction B, enriched in the *trans*-isomer. Configurational assignment of the NMR spectra has been reported earlier.¹⁷ *trans*-**2** was obtained as a mixture with *cis*-**2** with some NMR signals overlapping. Total yield: 1.14 g (60%). *cis*-**2** ¹H NMR (CDCl₃, 600.13 MHz): δ 5.20 (s, 2H, Ph-CH), 7.17–7.27 (m, 8H, Ph), 7.49 (dd, ³J = 8.1, 7.0, 2H phenanthrene-H), 7.58 (d, ³J = 8.1 Hz, 2H, phenanthrene-H), 7.68 (dd, ³J = 8.4, 7.0, 2H, phenanthrene-H), 8.82 (d, ³J = 8.4 Hz, 2H, phenanthrene-H). ¹³C NMR (CDCl₃, 150.9 MHz): δ 58.93, 123.38, 126.52, 126.95, 127.12, 127.27, 128.17, 128.56, 128.76, 131.21, 135.53, 137.37, 210.55. *trans*-**2** ¹H NMR (CDCl₃, 600.13 MHz): δ 5.26 (s, 2H, Ph-CH), 7.14–7.29 (m, 8H, Ph-H), 7.49 (ur, 2H), 7.58 (d, ³J = 8.0 Hz, 2H), 7.69 (ur, 2H), 8.79 (d, ³J = 8.4 Hz, 2H).

2-(tert-Butyldimethylsiloxy)-(1,3-diphenyl)cyclopenta[*l*]phenanthrene (4d) and 2-(tert-Butyldimethylsiloxy)(1,3-diphenyl)cyclopenta[*l*]phenanthrenyllithium (4d-Li). A suspension of 100 mg (0.26 mmol) of **2** (mixture of isomers) and 40 mg (1 mmol) of 60% sodium hydride in mineral oil in 3 mL of THF was stirred overnight. Then 75 mg (0.5 mmol) of TBDMSCl was added, and the obtained clear solution was stirred for 24 h. The reaction mixture was distributed between chloroform and water, the organic phase was separated, dried over sodium sulfate, and evaporated, and the residue was purified by column chromatography (eluent DCM–hexane). **4d** (85 mg, 66%) was obtained as an oil, solidifying upon storage. ¹H NMR (CDCl₃, 600.13 MHz): δ -0.34 (s, 3H, Si-CH₃), -0.11 (s, 3H, Si-CH₃), 0.66 (s, 9H, tBu), 4.80 (s, 1H, Cp-H), 7.19–7.22 (m, 1H), 7.26–7.28 (m, 5H), 7.37 (ur, 1H), 7.40–7.55 (m, 8H), 7.72 (d, ³J = 8.3 Hz, 2H, 4-H), 8.64 (d, ³J = 8.2 Hz, 1H, 1-H), 8.72 (d, ³J = 8.2 Hz, 1H, 1-H). ¹³C NMR (CDCl₃, 150.9 MHz): δ -4.62 (Si-CH₃), -4.23 (Si-CH₃), 18.08 (Si-C(CH₃)₃), 25.40 (Si-C(CH₃)₃), 56.01 (Cp, C–O–Si), 122.42, 123.20, 123.24, 123.38, 124.32, 125.44, 125.49, 125.59, 126.58, 126.98, 127.33, 127.84, 128.56, 128.76, 128.90, 131.06, 134.34, 136.31, 138.41, 138.71, 162.72.

4d-Li. ¹H NMR (THF-*d*₈, 600.13 MHz, aromatic part): δ 6.83δ6.86 (m, 4H, 2- and 3-H), 6.97 (t, ³J = 7.3 Hz, 2H, *p*-Ph), 7.21 (dd, ³J = 7.9, 7.3 Hz, 4H, *m*-Ph), 7.59 (d, ³J = 7.9 Hz, 4H, *o*-Ph), 8.20–8.22 (m, 2H, 4-H), 8.33–8.35 (m, 2H, 1-H). ¹³C NMR (THF-*d*₈, 150.9 MHz, aromatic part): δ 105.50, 113.58, 116.91(2- or 3-C), 121.84 (*p*-Ph), 122.02 (1-C), 122.52 (2- or 3-C), 123.15 (4-C), 124.07, 125.17, 126.61 (*m*-Ph), 132.29 (*o*-Ph), 132.43, 143.67.

2,3-Dihydro-1,3-diphenyl-1H-cyclopenta[*l*]phenanthren-2-ol (3). Sodium borohydride (0.4 g, 10 mmol) was added to a boiling suspension of 0.5 g (1.3 mmol) of **2** (mixture of isomers) in dioxane. The mixture was refluxed for 1 h, cooled to RT, quenched with 5% HCl, and evaporated. The residue was treated with DCM, and the insoluble portion was filtered off. The filtrate was evaporated. **3** (0.47 g, 94%; mixture of stereoisomers) was obtained as a white powder. ¹H NMR (CDCl₃, 600.13 MHz): δ 4.77–4.82 (m, 1H), 5.20–5.22 (m, 1.5H), 5.35–5.39 (m, 0.5 H), 7.14–7.21 (m, 7H), 7.29–7.33 (m, 2H), 7.38–7.42 (m, 2H), 7.46–7.55 (m, 2H), 7.61–7.66 (m, 3H), 8.76 (d, ³J = 8.3 Hz, 1H), 8.80 (d, ³J = 8.3 Hz, 1H).

1,2-Diphenylcyclopenta[*l*]phenanthrene (4c), 1,2-diphenylcyclopenta[*l*]phenanthrenyllithium (4c-Li), 1,3-diphenylcyclopenta[*l*]phenanthrene (5), and 1,3-diphenylcyclopenta[*l*]phenanthrenyllithium (5-Li). Phosphorus pentoxide (0.3 g, 2 mmol) was added to a boiling solution of 0.3 g (0.78 mmol) of **3** in 30 mL of benzene. The mixture was refluxed for 5 min, cooled to RT, washed with water, and evaporated. The residue was purified by column chromatography (eluent DCM–hexane). Two fractions were iso-

lated: 30 mg (11%) of **5** (first band, dark blue in UV) and 85 mg (30%) of **4c** (second band, bright blue in UV) as white solids. **4c** ¹H NMR (CDCl₃, 600.13 MHz): δ 5.37 (d, ⁴J = 1.1 Hz, Cp-H), 7.07 (t, ³J = 7.3 Hz, 1H, *p*-Ph), 7.14 (dd, ³J = 7.9, 7.3 Hz, 2H, *m*-Ph), 7.18 (t, ³J = 7.3 Hz, 1H, *p*-Ph), 7.20 (d, ³J = 7.9 Hz, 2H, *o*-Ph), 7.29 (dd, ³J = 8.4, 7.3 Hz, 2H, *m*-Ph), 7.38 (dd, ³J = 8.0, 7.5 Hz, 1H, 3b-H), 7.46 (dd, ³J = 8.3, 7.5 Hz, 1H, 2b-H), 7.61 (d, ³J = 8.4 Hz, 1H, *o*-Ph), 7.66 (dd, ³J = 7.8, 8.0 Hz, 1H, 2a-H), 7.69 (dd, ³J = 7.8, 8.3 Hz, 1H, 3a-H), 7.76 (d, ⁴J = 1.1 Hz, 1H, Cp-H), 7.83 (d, ³J = 8.0 Hz, 1H, 4b-H), 8.28 (s, ³J = 8.0 Hz, 1H, 4a-H), 8.64 (d, ³J = 8.3 Hz, 1H, 1b-H), 8.71 (d, ³J = 8.3 Hz, 1H, 1a-H). ¹³C NMR (CDCl₃, 150.9 MHz): δ 57.42 (Cp-CH), 123.38 (1a-C), 123.44 (1b-C), 123.86 (4b-C), 124.63 (4a-C), 124.69 (Cp-CH), 125.25 (2b-C), 126.20 (2a-C), 126.59 (*o*-Ph), 126.63 (3a-C), 126.70 (*p*-Ph), 126.73 (3b-C), 127.35 (*p*-Ph), 128.50 (*m*-Ph), 128.52 (*o*-Ph), 128.84 (*m*-Ph), 128.86, 129.44, 130.76, 135.15, 138.96, 139.48, 143.13, 153.20. Due to complexity of the spectrum, one signal corresponding to a quaternary carbon atom is not visible.

Compound **4c-Li:** ¹H NMR (THF-*d*₈, 600.13 MHz): δ 6.71 (t, ³J = 7.3 Hz, 1H, *p*-Ph), 6.79 (dd, ³J = 8.1, 7.4 Hz, 1H, 3b-H), 6.83 (dd, ³J = 8.1, 7.4 Hz, 1H, 2b-H), 6.85 (s, 1H, Cp-H), 6.91 (dd, ³J = 8.1, 7.4 Hz, 1H, 2a-H), 6.91 (dd, ³J = 8.2, 7.3 Hz, 2H, *m*-Ph), 7.10 (t, ³J = 7.3 Hz, 1H, *p*-Ph), 7.15 (dd, ³J = 8.1, 7.4 Hz, 1H, 3a-H), 7.18 (d, ³J = 8.2 Hz, 2H, *o*-Ph), 7.20 (dd, ³J = 8.0, 7.3 Hz, 2H, *m*-Ph), 7.37 (d, ³J = 8.0 Hz, 2H, *o*-Ph), 7.78 (d, ³J = 8.1 Hz, 1H, 4b-H), 8.07 (d, ³J = 8.1 Hz, 1H, 4a-H), 8.26 (d, ³J = 8.1 Hz, 1H, 1a-H), 8.27 (d, ³J = 8.1 Hz, 1H, 1b-H). ¹³C NMR (THF-*d*₈, 150.9 MHz): δ 98.74 (Cp-CH), 115.24, 117.62 (2b-C), 117.93 (2a-C), 120.64 (*p*-Ph), 121.33, 121.37 (4a-C), 122.17 (1b-C), 122.23 (1a-C), 122.79 (4b-C), 123.00 (*p*-Ph), 123.37 (3b-C), 124.06, 124.18 (3a-C), 124.96, 125.94, 126.59 (*m*-Ph), 127.11 (*m*-Ph), 127.63, 127.75 (*o*-Ph), 132.39 (*o*-Ph), 133.01, 133.74.

Compound **5:** ¹H NMR (CDCl₃, 600.13 MHz): δ 5.09 (d, ³J = 1.8 Hz, 1H, Cp-H), 6.58 (d, ³J = 1.8 Hz, 1H, Cp-H), 7.16 (ur, 2H), 7.20 (ur, 1H), 7.26 (ur, 2H), 7.34 (ur, 1H), 7.40–7.48 (m, 4H), 7.58 (ur, 1H), 7.75 (d, ³J = 8.2 Hz, 1H, 4-H), 7.86 (d, ³J = 8.2 Hz, 1H, 4-H), 8.71 (d, ³J = 8.2 Hz, 1H, 1-H), 8.76 (d, ³J = 8.2 Hz, 1H, 1-H). ¹³C NMR (CDCl₃, 150.9 MHz): δ 55.70 (Cp-CH), 123.25, 123.34, 124.86, 125.33, 125.55, 125.75, 125.88, 126.67, 126.79, 127.55, 128.03, 128.12, 128.32, 128.84, 128.97, 129.66, 131.21, 138.27, 138.73, 139.14, 140.73, 143.25, 145.15. Due to complexity of the spectrum, one signal corresponding to a quaternary carbon atom is not visible.

Compound **5-Li:** ¹H NMR (THF-*d*₈, 600.13 MHz): δ 6.39 (s, 1H, Cp-H), 6.90 (ur, 2H, 2-H), 6.91 (t, ³J = 7.0 Hz, 2H, *p*-Ph), 6.92 (ur, 2H, 3-H), 7.16 (dd, ³J = 7.0, 7.4 Hz, 4H, *m*-Ph), 7.58 (d, ³J = 7.4 Hz, 4H, *o*-Ph), 8.32 (d, ³J = 7.7 Hz, 2H, 4-H), 8.33 (d, ³J = 7.7 Hz, 2H, 1-H). ¹³C NMR (THF-*d*₈, 150.9 MHz): δ 117.86, 117.87, 117.89 (2-C), 121.29 (*p*-Ph), 122.23 (1-C + Cp-CH), 123.09 (3-C), 123.20 (4-C), 126.02, 126.87 (*m*-Ph), 128.57 (*o*-Ph), 133.25, 145.72.

General Procedure for the Racemization Reactions. Potassium *tert*-butoxide (0.7 mg, 6 μmol) and 2 μmol of complex (**6a–f** or **8**) were mixed in 1 mL of toluene. The mixture was stirred for 5 min at RT. Then a solution of 24 mg (200 μmol) of (*S*)-α-phenylethanol **10** in 1 mL of toluene was added. Derivatization of samples (propionic anhydride in the presence of pyridine and DMAP) was performed in order to achieve a better resolution and to stop the racemization process. The ratio of the enantiomers formed was determined by chiral GC (oven temperature 100 °C, retention times 10.13 min (*S*) and 11.30 min (*R*)).

Acknowledgment. Financial support from the Finnish Funding Agency for Technology and Innovation (Technology Programme SYMBIO Project #40168/07: Developing New Chemoenzymatic Methods and Biocatalysts) is gratefully acknowledged. The authors thank Prof. Liisa Kanerva and

(17) Schuster, I. I.; Cracium, L.; Ho, D. M.; Pascal, R. A., Jr. *Tetrahedron* **2002**, *58*, 8875.

Mari Päiviö (University of Turku) for fruitful discussions and for providing the (*S*)- α -phenylethanol utilized in the racemization experiments. Markku Reunanen is thanked for recording the HRMS analyses. We also thank the reviewers of this paper for their valuable suggestions and comments on improving the manuscript.

Supporting Information Available: X-ray diffraction data for complexes **4b**, **8**, and **9** in CIF format and copies of NMR spectra of the complexes prepared. This material is available free of charge via the Internet at <http://pubs.acs.org>.

OM8009393

Group 4 Metal Complexes of Fluorous (Di)alkoxide-(Di)imino Ligands: Synthesis, Structure, Olefin Polymerization Catalysis, and Decomposition Pathways

Nicolas Marquet,[†] Evgueni Kirillov,[†] Thierry Roisnel,[†] Abbas Razavi,[#] and Jean-François Carpentier^{*,†}

Catalysis and Organometallics, UMR 6226 Sciences Chimiques de Rennes, CNRS-University of Rennes 1, 35042 Rennes Cedex, France, and Total Petrochemicals Research, Zone Industrielle C, 7181 Feluy, Belgium

Received September 29, 2008

The coordination chemistry of fluorous (di)alkoxide-(di)imino ligands onto Ti(IV), Zr(IV), and Hf(IV) centers has been studied. The diimino-diol [(CF₃)₂C(OH)CH₂C(Me)=NCH₂–]₂ ({ON^{Et}NO}H₂) reacts selectively with Ti(OiPr)₂Cl₂ and Zr(CH₂Ph)₄ to give the corresponding complexes {ON^{Et}NO}TiCl₂ (**1**) and {ON^{Et}NO}Zr(CH₂Ph)₂ (**2**), with concomitant alcohol and alkane elimination, respectively. Reactions of the imino-alcohols (CF₃)₂C(OH)CH₂C(R¹)=NR² ({ON^{R¹,R²}}H; R¹ = Me, Ph; R² = Ph, CH₂Ph) with Ti(OiPr)₄ and M(CH₂Ph)₄ (M = Zr, Hf) gave the corresponding complexes Ti(OiPr)₂{ON^{R¹,R²}}₂ (**3a,b**) and M(CH₂Ph)₂{ON^{R¹,R²}}₂ (M = Zr, **7a,b,c**; M = Hf, **8a,b**). Dibenzyl complexes **7** and **8** decompose above –30 °C by abstraction of a hydrogen from the methylene ligand backbone by a benzyl group to give M(CH₂Ph){ON^{R¹,R²}} {ON^{–R¹,R²}} complexes (M = Zr, **9a–c**; M = Hf, **10a**), in which a ligand unit ({ON^{–R¹,R²}}) has been transformed to an α,β-unsaturated amido-alkoxy dianionic moiety. A slightly different process was observed for the pentafluorophenyl system Zr(CH₂Ph)₂{ON^{Me,ArF}}₂ (ArF = C₆F₅; **7d**), which ultimately yielded the benzyl-free complex Zr{ON^{Me,ArF}}₂{ON^{–Me,ArF}} (**11**). Single-crystal X-ray diffraction studies revealed that complexes **1**, **3a**, **7a**, **7b**, **7d**, **8a**, and **11** are mononuclear in the solid state and adopt either C₁- or mostly C_{2v}-symmetric, distorted octahedral structures with planar coordination of the (di)imino-di(alkoxide) ligands. Multinuclear NMR studies indicate that most of the complexes adopt also a C_{2v}-symmetric structure in solution. Dichloride complexes ZrCl₂{ON^{R¹,R²}}₂ (R¹ = Me, Ph; R² = Ph, C₆F₅; **12a–c**) were prepared by alkane elimination or salt metathesis. When activated by MAO, **3a,b** and **12a–c** lead to active but very unstable ethylene polymerization catalysts that afford very high molecular weight linear polyethylenes.

Introduction

Alkoxides are hard, electronegative π-donor ligands, which are quite attractive because they offer strong metal–oxygen bonds that are expected to stabilize complexes of a variety of electropositive metals.¹ Also, considerable variation in steric and electronic properties is possible thanks to the great variety of these ligands conveniently obtained from alcohols. These features have given alkoxides a key place in modern coordination chemistry of early transition and main group metals (groups 3–5, 13), in particular in the recent search for new-generation polymerization catalysts.² The synthetic chemistry of early transition metal complexes based on simple alkoxides proved to be, however, often complicated.¹ This is largely due to the high tendency of the relatively more basic alkoxide ligands (as compared to aryloxides) to act as bridging ligands, eventually resulting in (highly) agglomerated structures. The use of highly stable fluorous tertiary alcohol ligands affords an efficient

strategy to overcome this difficulty. Introduction of electron-withdrawing CF₃ groups α to the alkoxide generates intra- and intermolecular repulsions, as well as a less basic alkoxide O-atom, and as a result, a less distinct bridging tendency is observed.^{1,3} Following this line, we have described some bi- and tetradentate fluorous (di)alkoxide-(di)amino ligand systems that proved to be effective for preparing well-defined complexes of oxophilic metal centers such as Y(III), Zr(IV), and Al(III), and in turn developing valuable applications in polymerization catalysis.⁴ Recently, we launched another class of bi- and tetradentate fluorous (di)alkoxide-(di)imino ligands,^{5,6} which are

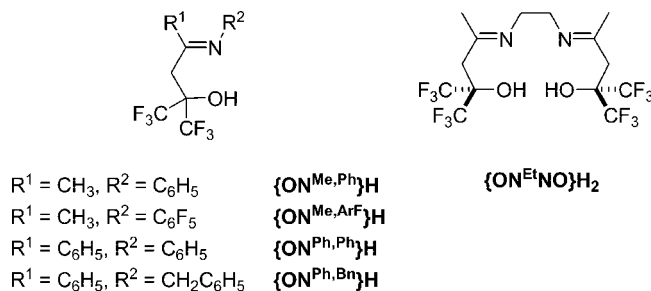
* Corresponding author. Fax: (+33)(0)223-236-939. E-mail: jean-francois.carpentier@univ-rennes1.fr.

[†] CNRS-University of Rennes 1.

[#] Total Petrochemicals Research.

(1) (a) Bradley, D. C.; Mehrotra, R. M.; Rothwell, I. P.; Singh, A. *Alkoxo and Aryloxo Derivatives of Metals*; Academic Press: London, 2001. (b) Mehrotra, R. M.; Singh, A. *Prog. Inorg. Chem.* **1997**, *46*, 239. (c) Hubert-Pfalzgraf, L. G. *Coord. Chem. Rev.* **1998**, *178–180*, 967. (d) Piers, W. E.; Emslie, D. J. H. *Coord. Chem. Rev.* **2002**, *131*, 233–234. (e) Edelmann, F. T.; Freckmann, D. M. M.; Schumann, H. *Chem. Rev.* **2002**, *102*, 1851.

(2) For reviews and leading articles on “post-metallocene” complexes of groups 3–5 and the lanthanides related to polymerization, see: (a) Britovsek, G. J. P.; Gibson, V. C.; Wass, D. F. *Angew. Chem., Int. Ed.* **1999**, *38*, 428. (b) Edelmann, F. T.; Freckmann, D. M. M.; Schumann, H. *Chem. Rev.* **2002**, *102*, 1851. (c) Gibson, V. C.; Spitzmesser, S. K. *Chem. Rev.* **2003**, *103*, 283. (d) Gromada, J.; Mortreux, A.; Carpentier, J.-F. *Coord. Chem. Rev.* **2004**, *248*, 397. (e) Corradini, P.; Guerra, G.; Cavallo, L. *Acc. Chem. Res.* **2004**, *37*, 231. (f) Kol, M.; Tshuva, E. Y.; Goldschmidt, Z. *ACS Symp. Ser.* **2003**, *857*, 62. (g) Kol, M.; Segal, S.; Groysman, S. In *Stereoselective Polymerization with Single-Site Catalysts*; CRC Press LLC: Boca Raton, FL, 2008; pp 345–361. (h) Gueta-Neyroud, T.; Tumanskii, B.; Kapon, M.; Eisen, M. S. *Macromolecules* **2007**, *40*, 5261. (i) Okuda, J. *Stud. Surf. Sci. Catal.* **2007**, *172*, 11. (j) Matsugi, T.; Fujita, F. *Chem. Soc. Rev.* **2008**, *37*, 1264. (k) Coates, G. W.; Husted, P. D.; Reinartz, S. *Angew. Chem., Int. Ed.* **2002**, *41*, 2236. (l) Domski, G. J.; Rose, J. M.; Coates, G. W.; Bolig, A. D.; Brookhart, M. *Prog. Polym. Sci.* **2007**, *32*, 30. (m) Chan, M. C. W.; Kui, S. C. F.; Cole, J. M.; McIntyre, G. J.; Matsui, S.; Zhu, N.; Tam, K. H. *Chem.–Eur. J.* **2006**, *12*, 2607.

Chart 1. $\{\text{ON}^{\text{R}^1, \text{R}^2}\}\text{H}$ and $\{\text{ON}^{\text{EtNO}}\}\text{H}_2$ Pro-ligands Used in This Study

structurally reminiscent of aryloxide-bearing salen⁷ and phenoximine^{2j,8,9} ligands. Those $\{\text{ON}^{\text{R}^1, \text{R}^2}\}^-$ and $\{\text{ON}^{\text{EtNO}}\}^{2-}$ ligands (Chart 1) enabled the preparation of discrete complexes of trivalent metals such as Y(III), La(III),¹⁰ and Al(III),¹¹ conferring a high electrophilicity to the metal centers, that proved to be useful in the controlled ring-opening polymerization of cyclic esters.

We report in this article the preparation, structural characterization, and reactivity of tetravalent group 4 metal complexes supported by $\{\text{ON}^{\text{R}^1, \text{R}^2}\}^-$ and $\{\text{ON}^{\text{EtNO}}\}^{2-}$ ligands. Preliminary studies on the catalytic performances of such discrete complexes in ethylene polymerization are also reported, and discussed in connection with some decomposition pathways.

Results and Discussion

Several routes to Ti, Zr, and Hf complexes based on a variety of bidentate monoanionic $\{\text{ON}^{\text{R}^1, \text{R}^2}\}^-$ ligands, as well as on the tetradentate dianionic $\{\text{ON}^{\text{EtNO}}\}^{2-}$ ligand, have been explored: (a) σ -bond metathesis (alcoholysis) reactions between the alcohol/diol pro-ligands $\{\text{ON}^{\text{R}^1, \text{R}^2}\}\text{H}$ and $\{\text{ON}^{\text{EtNO}}\}\text{H}_2$ and an appropriate homo- or heteroleptic metal precursor, enabling either alkane or alcohol elimination; (b) salt elimination reactions between $\{\text{ON}^{\text{R}^1, \text{R}^2}\}\text{M}$ alkali metal salts, either preliminary prepared or *in situ*-generated, and a $\text{MCl}_4(\text{THF})_n$ precursor. These results are discussed hereafter and summarized in Schemes 1–7. The prepared neutral complexes are all air- and

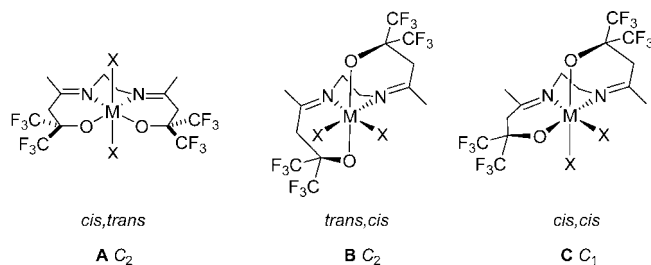


Figure 1. Possible isomers for octahedral $\{\text{ON}^{\text{EtNO}}\}\text{MX}_2$ complexes. The *cis/trans* descriptors refer to the arrangement of alkoxide and X ligands, respectively. Note that the imino ligands must be *cis*. Only one of the possible enantiomers (Λ , Δ , depending on the absolute configuration of the metal)¹⁴ is depicted.

moisture-sensitive¹² and were characterized in the solid state by elemental analysis and X-ray diffraction studies for some of them, and in solution by variable-temperature ¹H, ¹³C, and ¹⁹F NMR spectroscopy.

Synthesis and Structures of Neutral $\{\text{ON}^{\text{EtNO}}\}\text{MX}_2$ Complexes. First investigations were carried out using the tetradentate ligand $\{\text{ON}^{\text{EtNO}}\}^{2-}$. Assuming an ideal octahedral arrangement and flexibility of the $\{\text{ON}^{\text{EtNO}}\}^{2-}$ ligand framework, three $\{\text{ON}^{\text{EtNO}}\}\text{MX}_2$ isomeric structures are possible (A–C, Figure 1), which differ in the arrangement (*cis vs trans*) of the pairs of alkoxide and X ligands.¹³

The 1:1 reaction between diol $\{\text{ON}^{\text{EtNO}}\}\text{H}_2$ and $\text{Ti}(\text{OiPr})_2\text{Cl}_2$, *in situ*-generated from TiCl_4 and $\text{Ti}(\text{OiPr})_4$,¹⁵ proceeded selectively at room temperature to yield $\{\text{ON}^{\text{EtNO}}\}\text{TiCl}_2$ (**1**), as is

(7) (a) Jacobsen, E. N. *Catalytic Asymmetric Synthesis*; Ojima, I., Ed.; VCH: Weinheim, 1993; p 159. (b) Jacobsen, E. N. *Comprehensive Organometallic Chemistry II*; Wilkinson, G.; Stone, F. G. A.; Abel, E. W.; Hegedus, L. S., Eds.; Pergamon Press: New York, 1995; Vol. 12, Chapter 11.1. (c) Larow, J. F.; Jacobsen, E. N. *Top. Organomet. Chem.* **2004**, *6*, 123. (d) Cozzi, P. G. *Chem. Soc. Rev.* **2004**, *33*, 410. (e) Katsuki, T. *Chem. Soc. Rev.* **2004**, *33*, 437. (f) Atwood, D. A.; Harvey, M. J. *Chem. Rev.* **2001**, *101*, 37.

(8) (a) Makio, H.; Fujita, T. *Macromol. Rapid Commun.* **2007**, *28*, 698. (b) Terao, H.; Ishii, S.; Saito, J.; Matsuura, S.; Mitani, M.; Nagai, N.; Tanaka, H.; Fujita, T. *Macromolecules* **2006**, *39*, 8584. (c) Nakayama, Y.; Saito, J.; Bando, H.; Fujita, T. *Chem.–Eur. J.* **2006**, *12*, 7546. (d) Saito, J.; Suzuki, Y.; Makio, H.; Tanaka, H.; Onda, M.; Fujita, T. *Macromolecules* **2006**, *39*, 4023. (e) Mitani, M.; Nakano, T.; Fujita, T. *Chem.–Eur. J.* **2003**, *9*, 2396. (f) Mitani, M.; Furuyama, R.; Mohri, J.; Saito, J.; Ishii, S.; Terao, H.; Nakano, T.; Tanaka, H.; Fujita, T. *J. Am. Chem. Soc.* **2003**, *125*, 4293. (g) Makio, H.; Kashiwa, N.; Fujita, T. *Adv. Synth. Catal.* **2002**, *344*, 477. (h) Mitani, M.; Furuyama, R.; Mohri, J.; Saito, J.; Ishii, S.; Terao, H.; Kashiwa, N.; Fujita, T. *J. Am. Chem. Soc.* **2002**, *124*, 7888. (i) Mitani, M.; Mohri, J.; Yoshida, Y.; Saito, J.; Ishii, S.; Tsuru, K.; Matsui, S.; Furuyama, R.; Nakano, T.; Tanaka, H.; Kojoh, S.; Matsugi, T.; Kashiwa, N.; Fujita, T. *J. Am. Chem. Soc.* **2002**, *124*, 3327. (j) Saito, J.; Mitani, M.; Mohri, J.; Yoshida, Y.; Matsui, S.; Ishii, S.; Kojoh, S.; Kashiwa, N.; Fujita, T. *Angew. Chem., Int. Ed.* **2001**, *40*, 2918. (k) Matsui, S.; Mitani, M.; Saito, J.; Tohii, Y.; Makio, H.; Matsukawa, N.; Takagi, Y.; Tsuru, K.; Nitabaru, M.; Nakano, T.; Tanaka, H.; Kashiwa, N.; Fujita, T. *J. Am. Chem. Soc.* **2001**, *123*, 6847.

(9) (a) Mason, A. F.; Coates, G. W. *J. Am. Chem. Soc.* **2004**, *126*, 10798. (b) DeRosa, C.; Circelli, T.; Auriemma, F.; Mathers, R. T.; Coates, G. W. *Macromolecules* **2004**, *37*, 9034. (c) Mason, A. F.; Coates, G. W. *J. Am. Chem. Soc.* **2004**, *126*, 16326. (d) Reinartz, S.; Mason, A. F.; Lobkovsky, E. B.; Coates, G. W. *Organometallics* **2003**, *22*, 2542. (e) Hustad, P. D.; Tian, J.; Coates, G. W. *J. Am. Chem. Soc.* **2002**, *124*, 3614. (f) Tian, J.; Coates, G. W. *Angew. Chem., Int. Ed.* **2000**, *39*, 3626.

(10) Grunova, E.; Kirillov, E.; Roisnel, T.; Carpentier, J.-F. *Organometallics* **2008**, *27*, 5691.

(11) Bouyahyi, M.; Grunova, E.; Marquet, N.; Kirillov, E.; Thomas, C. M.; Roisnel, T.; Carpentier, J.-F. *Organometallics* **2008**, *27*, 5815–5825.

(12) Benzyl complexes of zirconium and hafnium proved also to be sensitive when exposed to light, as solutions in hydrocarbons.

(13) Sanz, M.; Cuenca, T.; Cuomo, C.; Grassi, A. *J. Organomet. Chem.* **2006**, *691*, 3816, and references therein.

(14) Purcell, K. F.; Kotz, J. C. In *Inorganic Chemistry*; Saunders Co.: Philadelphia, 1977; pp 368–648.

(15) Gothelf, K. V.; Jorgensen, K. A. *J. Org. Chem.* **1994**, *59*, 5687.

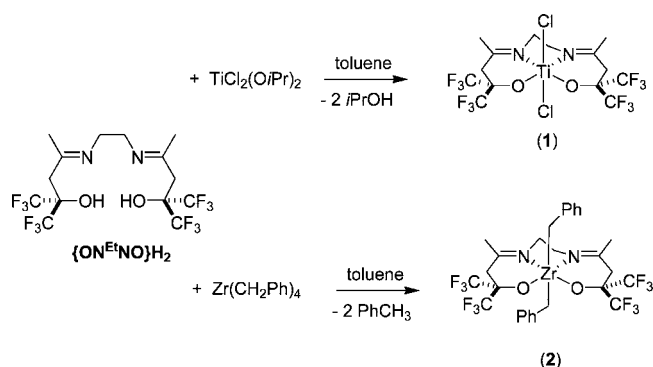
(3) For selected examples of early transition metal complexes bearing fluorous alkoxide ligands: (a) Bradley, D. C.; Chudzynska, H.; Hursthouse, M. B.; Motevalli, M. *Polyhedron* **1994**, *12*, 1907. (b) Bradley, D. C.; Chudzynska, H.; Hursthouse, M. B.; Motevalli, M. *Polyhedron* **1994**, *13*, 7. (c) Samuels, J. A.; Lobkovsky, E. B.; Streib, W. E.; Foltling, K.; Huffman, J. C.; Zwanziger, J. W.; Caulton, K. G. *J. Am. Chem. Soc.* **1993**, *115*, 5093. (d) Tsukuhara, T.; Swenson, D. C.; Jordan, R. F. *Organometallics* **1997**, *16*, 3303. (e) Fujimura, O.; Grubbs, R. J. *J. Am. Chem. Soc.* **1996**, *118*, 2499. (f) Fujimura, O.; De la Mata, F. J.; Grubbs, R. H. *Organometallics* **1996**, *15*, 1865.

(4) (a) Lavanant, L.; Chou, T.-Y.; Chi, Y.; Lehmann, C. W.; Toupet, L.; Carpentier, J.-F. *Organometallics* **2004**, *23*, 5450. (b) Amgoune, A.; Lavanant, L.; Thomas, C. M.; Chi, Y.; Welter, R.; Dagorne, S.; Carpentier, J.-F. *Organometallics* **2005**, *24*, 6279. (c) Kirillov, E.; Lavanant, L.; Thomas, C. M.; Roisnel, T.; Chi, Y.; Carpentier, J.-F. *Chem.–Eur. J.* **2007**, *13*, 923.

(5) Marquet, N.; Grunova, E.; Kirillov, E.; Bouyahyi, M.; Thomas, C. M.; Carpentier, J.-F. *Tetrahedron* **2008**, *64*, 75.

(6) Fluorous alkoxy-imino ligands were first prepared in the coordination sphere of metals ions, i.e., Cu^{2+} , Ni^{2+} , Co^{2+} , Ce^{3+} , Ce^{4+} by the template condensation of primary (di)amines with the fluorous β -ketol $\text{MeC}(=\text{O})\text{CH}_2\text{C}(\text{CF}_3)_2\text{OH}$; see: (a) Martin, J. W. L.; Willis, C. J. *Can. J. Chem.* **1977**, *55*, 2459. (b) Konefal, E.; Loeb, S. J.; Stephan, D. W.; Willis, C. J. *Inorg. Chem.* **1984**, *23*, 538, and references therein.

Scheme 1



common of simple exchange reactions between titanium alkoxide complexes and alcohols.¹ Similarly, the dibenzyl complex $\{\text{ON}^{\text{Et}}\text{NO}\}\text{Zr}(\text{CH}_2\text{Ph})_2$ (**2**) was prepared by alcoholysis of $\text{Zr}(\text{CH}_2\text{Ph})_4$ (Scheme 1). Both complexes are sparingly soluble in aliphatic hydrocarbons (pentane, hexanes) but readily soluble in aromatic hydrocarbons (benzene, toluene) and chlorinated solvents (CH_2Cl_2), in which they are stable for at least weeks at room temperature.

Crystals of **1** suitable for X-ray diffraction were obtained from a toluene solution. The solid-state structure of **1** (Figure 2) features a monomeric molecule with a six-coordinated metal center and equatorial coordination of the $\{\text{ON}^{\text{Et}}\text{NO}\}^{2-}$ ligand, in a Salen-like fashion, that is a type **A** structure (Figure 1). We have observed a similar planar coordination mode when exploring the aluminum chemistry of this ligand, although the square-pyramidal (sqp) geometry structures of these Al complexes are more distorted toward a trigonal-bipyramidal (tbp) geometry.^{7f,11} However, the most worthy and meaningful structural comparison for these new diimino-diolate complexes is undoubtedly with group 4 metal salen (i.e., diimino-bisphenolate) complexes, since both incorporate similar ligand frameworks. In fact, the metrical data in **1**, i.e., bond distances Ti–O (1.819(3)–1.822(3) Å), Ti–N (2.173(4)–2.182(4) Å), and Ti–Cl (2.3368(14)–2.3372(15) Å) and the corresponding bond angles O–Ti–O (108.61(14)°), N–Ti–N (76.63(13)°), and Cl–Ti–Cl (165.00(6)°) (Figure 1), compare very well with those observed in related ethylene- and 1,2-cyclohexylene-bridged-Salen dichlorotitanium complexes [Ti–O (1.816–1.844 Å), Ti–N (2.121–2.171 Å), Ti–Cl (2.326–2.370 Å), O–Ti–O (110.05–113.27°), N–Ti–N (75.29–78.91°), Cl–Ti–Cl (168.21–171.42°)].¹⁶ The Ti, O, O, N, N atoms are almost perfectly coplanar (maximum deviation from mean plane: 0.022 Å). Also, the six-membered metallacycles involving the imino-alkoxide ligand in **1** appear quite planar (deviation from the mean plane Ti–N–C–C–O: Ti(1), –0.076; O(11), +0.059, C(11), +0.204; C(14), –0.314; C(15), +0.072; N(17), +0.154 Å). These data indicate that substitution of a phenoxide group for a bis(trifluoromethyl)alkoxide group did not affect significantly the coordination mode, although there is no more conjugation with the imino moiety in complex **1**. On the other hand, the solid-state structure of **1** differs dramatically from that observed for the related fluoros dialkoxide-diamino complex $\{\text{CH}_2\text{NMeCH}_2\text{C}(\text{CF}_3)_2\text{O}\}_2\text{TiCl}_2$ and $\{\text{CH}_2\text{NMeCH}_2\text{C}(\text{CF}_3)_2\text{O}\}_2\text{Zr}(\text{CH}_2\text{Ph})_2$.^{4a} In fact, the latter complexes adopt also a distorted octahedral geometry but in which the oxygen atoms of the dialkoxide ligand are *trans* and the X ligands (X = Cl, CH_2Ph , respectively) are *cis*; that is a type **B** structure (Figure 1). This observation suggests that substitution of an amino for an imino group is more crucial in terms of ligand framework flexibility than the aforementioned modification (substitution of

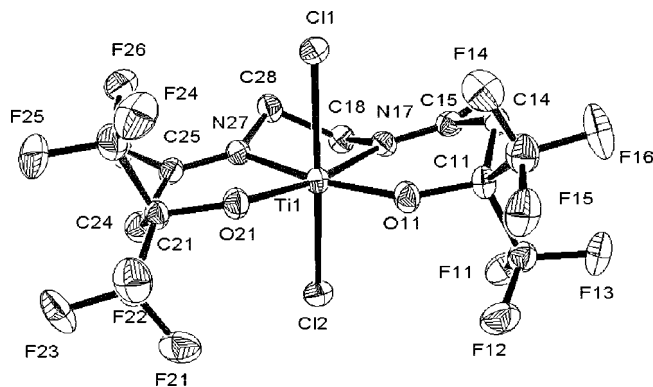


Figure 2. ORTEP view of $\{\text{ON}^{\text{Et}}\text{NO}\}\text{TiCl}_2$ (**1**) (ellipsoids drawn at the 50% probability level; all hydrogen atoms have been omitted for clarity). Selected bond lengths (Å) and angles (deg): Ti(1)–O(21), 1.819(3); Ti(1)–O(11), 1.822(3); Ti(1)–N(17), 2.173(4); Ti(1)–N(27), 2.182(4); Ti(1)–Cl(1), 2.3368(14); Ti(1)–Cl(2), 2.3372(15); O(21)–Ti(1)–O(11), 108.61(14); O(21)–Ti(1)–N(17), 163.85(14); O(11)–Ti(1)–N(17), 87.36(14); O(21)–Ti(1)–N(27), 87.38(13); O(11)–Ti(1)–N(27), 163.99(13); N(17)–Ti(1)–N(27), 76.63(13); O(21)–Ti(1)–Cl(1), 93.35(11); O(11)–Ti(1)–Cl(1), 93.36(11); N(17)–Ti(1)–Cl(1), 83.07(10); N(27)–Ti(1)–Cl(1), 84.84(11); O(21)–Ti(1)–Cl(2), 95.41(11); O(11)–Ti(1)–Cl(2), 95.35(11); N(17)–Ti(1)–Cl(2), 85.15(10); N(27)–Ti(1)–Cl(2), 83.42(11); Cl(1)–Ti(1)–Cl(2), 165.00(6).

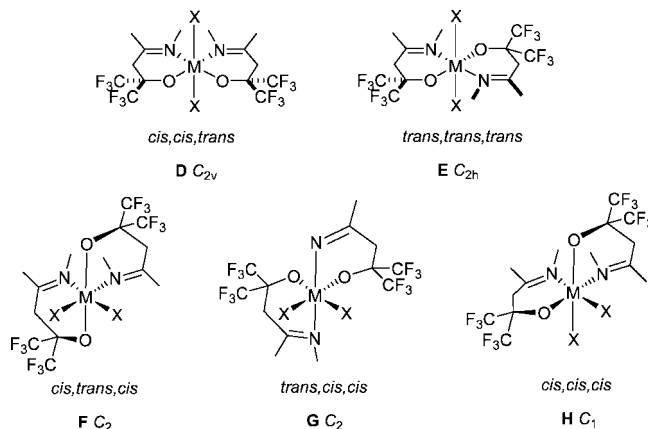


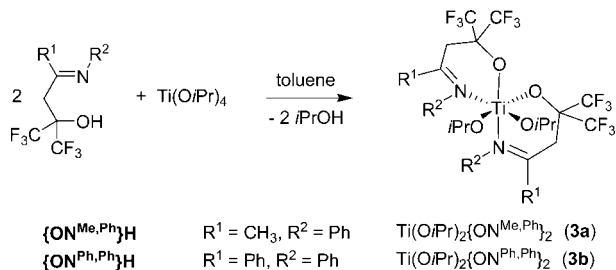
Figure 3. Possible isomers for octahedral $\{\text{ON}^{\text{R}1,\text{R}2}\}\text{MX}_2$ complexes. The *cis/trans* descriptors refer to the arrangement of imino, alkoxide, and X ligands, respectively. Enantiomers of C_2 - and C_1 -symmetric isomers are not depicted. R^1 and R^2 substituents are not shown for the sake of clarity.

a phenoxide group for a bis(trifluoromethyl)alkoxide group) and does not induce significant constraint within the six-membered N–M–O metallacycles.

In agreement with the structure observed in the solid state, the ^1H , ^{13}C , and ^{19}F NMR data for **1** in CD_2Cl_2 at room temperature contain a single set of resonances, consistent with an average C_{2v} -symmetric type **A** structure retained in solution. In particular, the ^1H NMR spectrum contains three singlet resonances for the CH_3 , $\text{CH}_2\text{C}=\text{N}$, and NCH_2 groups, respectively, while only one singlet resonance is observed for the $\text{OC}(\text{CF}_3)_2$ moieties in the $^{19}\text{F}\{^1\text{H}\}$ NMR spectrum.¹⁷ No fluxional dynamic process associated with possible isomerization of the ligand backbone in **1** was observed by VT ^1H NMR in the temperature range –60 to 60 °C.

Single crystals of **2** suitable for X-ray diffraction studies could not be obtained, and this complex was characterized in solution by NMR spectroscopy. The ^1H , ^{13}C , and ^{19}F NMR data for **2** in

Scheme 2



CD_2Cl_2 at room temperature are very similar to those observed for **1** and include a sharp singlet resonance in the $^{19}\text{F}\{^1\text{H}\}$ NMR spectrum, as well as three singlets in the ^1H spectrum for the ligand hydrogens. In addition, the benzyl groups appear as a single singlet resonance in both the ^1H and ^{13}C NMR spectra. These data are consistent with an average C_{2v} -symmetric type **A** structure, with equatorial coordination of the $\{\text{ON}^{\text{Et}}\text{NO}\}^{2-}$ ligand, as observed for **1**.¹⁷

Synthesis, Structures, and Reactivity of Neutral $\{\text{ON}^{\text{R}, \text{R}}\}\text{MX}_2$ Complexes. We turned our attention next to the coordination of monoanionic bidentate ligands $\{\text{ON}^{\text{R}^1, \text{R}^2}\}^-$. In this case, up to five isomeric structures (without considering enantiomers) can be envisaged (Figure 3).¹³

Isopropoxide and Chloride Complexes of Titanium. Due to easiness of alcohol elimination processes¹ and their efficiency demonstrated in the above-mentioned formation of $\{\text{ON}^{\text{Et}}\text{NO}\}-\text{TiCl}_2$ (**1**), this route was also explored to prepare related diisopropoxide titanium complexes based on monoanionic bidentate ligands $\{\text{ON}^{\text{R}^1, \text{R}^2}\}^-$. In fact, alcoholysis of $\text{Ti}(\text{O}i\text{Pr})_4$ with 2 equiv of fluorinated alcohol-imines $\{\text{ON}^{\text{R}^1, \text{R}^2}\}\text{H}$ ($\text{R}^1 = \text{CH}_3, \text{Ph}$; $\text{R}^2 = \text{Ph}$) proceeds fast and selectively, at room temperature in toluene or benzene, to afford the corresponding $\text{Ti}(\text{O}i\text{Pr})_2\{\text{ON}^{\text{R}^1, \text{R}^2}\}_2$ complexes **3a** and **3b**, with concomitant release of 2 equiv of 2-propanol (Scheme 2). Complexes **3a** and **3b** were isolated in 63% and 64% yields, respectively, and are both colorless compounds, readily soluble in most common organic solvents, and thermally stable both in solution and in the solid state in the absence of air.

Crystals of **3a** suitable for X-ray diffraction were grown from a toluene/hexane solution. The molecular structure of **3a** (Figure 4) features a monomeric complex in a distorted octahedral geometry, with a *cis, cis, cis* arrangement of the nitrogen ligand atoms, oxygen ligand atoms, and isopropoxide groups, which is a type **H** structure (Figure 3). The Ti–O (1.894–1.974(1) Å) and Ti–N (2.279–2.374(2) Å) bonds involving the ligand atoms in **3a** are significantly longer than those observed in **1** (*vide supra*; Figure 2) and in related titanium–Salen complexes.^{16,18}

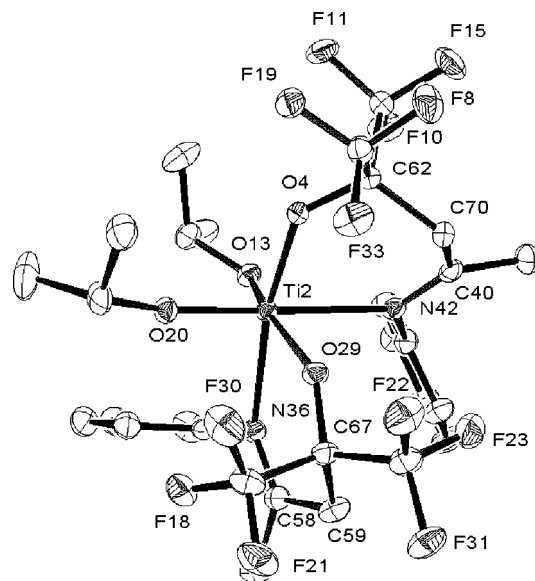
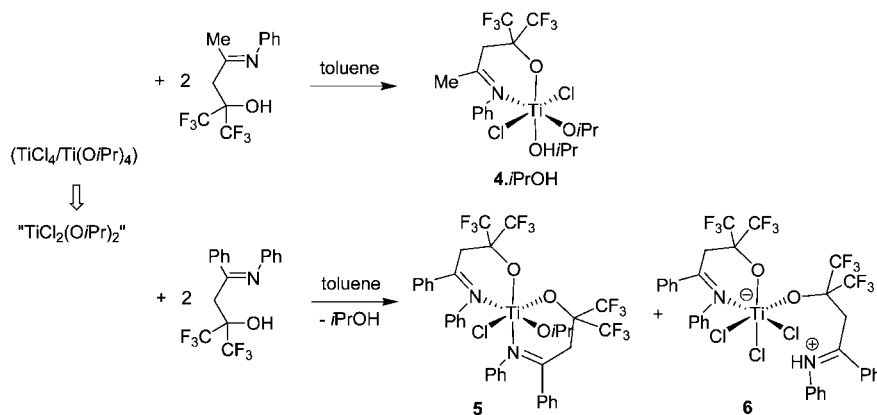


Figure 4. ORTEP view of $\text{Ti}(\text{O}i\text{Pr})_2\{\text{ON}^{\text{Me}, \text{Ph}}\}_2$ (**3a**) (ellipsoids drawn at the 50% probability level; all hydrogen atoms have been omitted for the sake of clarity; only one (#2) of the two independent molecules found in the unit cell is depicted). Selected bond lengths (Å) and angles (deg) [data in square brackets refer to the second independent molecule (#1)]: Ti(2)–O(13), 1.7791(14) [1.8066(14)]; Ti(2)–O(20), 1.8337(13) [1.8128(13)]; Ti(2)–O(4), 1.8947(13) [1.9109(13)]; Ti(2)–O(29), 1.9537(13) [1.9741(13)]; Ti(2)–N(36), 2.2817(17) [2.2794(16)]; Ti(2)–N(42), 2.3428(17) [2.3744(17)]; O(20)–Ti(2)–O(13), 96.88(6) [94.40(6)]; O(20)–Ti(2)–O(4), 96.77(6) [94.49(6)]; O(13)–Ti(2)–O(4), 98.37(6) [99.58(6)]; O(20)–Ti(2)–O(29), 98.92(6) [95.85(6)]; O(13)–Ti(2)–O(29), 160.54(6) [163.49(6)]; O(4)–Ti(2)–O(29), 90.99(6) [92.49(5)]; O(20)–Ti(2)–N(36), 91.75(6) [97.71(6)]; O(13)–Ti(2)–N(36), 86.91(6) [84.22(6)]; O(4)–Ti(2)–N(36), 169.34(6) [166.91(6)]; O(29)–Ti(2)–N(36), 81.34(6) [81.61(5)]; O(20)–Ti(2)–N(42), 177.95(6) [175.93(5)]; O(13)–Ti(2)–N(42), 81.20(6) [84.13(6)]; O(4)–Ti(2)–N(42), 82.84(6) [82.04(6)]; O(29)–Ti(2)–N(42), 83.10(6) [86.46(5)]; N(36)–Ti(2)–N(42), 88.86(6) [85.93(6)].

Also, the O–Ti–N angles (81.34(6)–82.84(6)°) in the six-membered metallacycles of **3a** are smaller than those in **1** (87.36(14)–87.38(13)°). Those differences in metrical data probably reflect, in main part, the influence of the bridging unit in between the two alkoxy-imino moieties and possibly the *trans* influence of ligands as well. On the other hand, these bond distances and bond angles in **3a** compare well with those found in diisopropoxide and other dialkoxide titanium complexes supported by phenoxy-imine ligands (Ti–O, 1.895–1.975 Å; Ti–N, 2.228–2.340 Å; O–Ti–N, 79.73–82.34°).¹⁹ Both the

Scheme 3



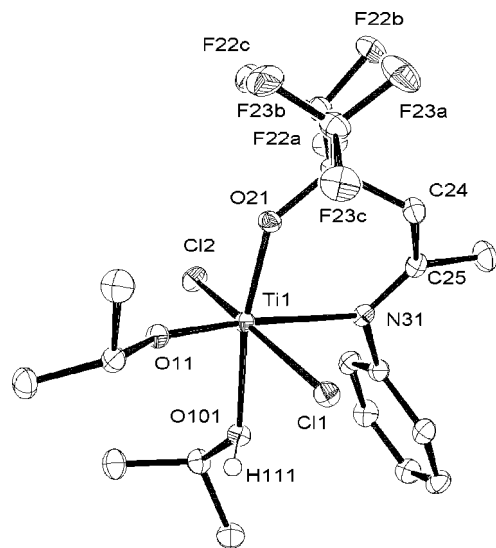


Figure 5. ORTEP view of $\text{TiCl}_2(\text{OiPr})\{\text{ON}^{\text{Me,Ph}}\} \cdot i\text{PrOH}$ (**4** · *iPrOH*) (ellipsoids drawn at the 50% probability level; all hydrogen atoms except H(111) have been omitted for the sake of clarity). Selected bond lengths (Å) and angles (deg): Ti(1)–O(11), 1.7440(11); Ti(1)–O(21), 1.8411(11); Ti(1)–O(101), 2.1338(12); Ti(1)–N(31), 2.2967(13); Ti(1)–Cl(2), 2.3206(5); Ti(1)–Cl(1), 2.4179(5); O(11)–Ti(1)–O(21), 96.81(5); O(11)–Ti(1)–O(101), 93.06(5); O(21)–Ti(1)–O(101), 169.32(5); O(11)–Ti(1)–N(31), 170.38(5); O(21)–Ti(1)–N(31), 83.90(5); O(101)–Ti(1)–N(31), 85.68(5); O(11)–Ti(1)–Cl(2), 101.71(4); O(21)–Ti(1)–Cl(2), 94.38(4); O(101)–Ti(1)–Cl(2), 87.54(3); N(31)–Ti(1)–Cl(2), 87.78(4); O(11)–Ti(1)–Cl(1), 90.48(4); O(21)–Ti(1)–Cl(1), 94.94(4); O(101)–Ti(1)–Cl(1), 80.90(3); N(31)–Ti(1)–Cl(1), 79.90(3); Cl(2)–Ti(1)–Cl(1), 163.654(18).

six-membered metallacycles appear rather planar, apart from the “central” CH_2 carbon that deviates significantly from the mean plane $\text{Ti}–\text{N}–\text{C}–\text{C}–\text{O}$ (C(70), 0.154 Å; C(59), 0.265 Å; all other deviations in the range 0.003–0.117 Å).

The ^1H , ^{13}C , and ^{19}F NMR data for **3a** and **3b**, in C_6D_6 or CD_2Cl_2 at room temperature, are very similar. For both complexes, a single sharp singlet resonance in the $^{19}\text{F}\{^1\text{H}\}$ NMR spectrum as well as three singlets in the ^1H NMR spectrum for the CH_3 , $\text{CH}_2\text{C}=\text{N}$, and NCH_2 hydrogens in the ligand are observed. No change is observed in the low-temperature (–50 °C) ^1H NMR spectrum of **3a** and **3b** in CD_2Cl_2 . These features, which are confirmed in the ^{13}C NMR spectra, are consistent with the existence of a single C_{2v} -symmetric structure on the NMR time scale¹⁷ (type **D**, Figure 3) and indicate that the solid-state structure observed for **3a** is not retained in solution.

Similar alcoholysis reactions were investigated using *in situ*-generated $\text{Ti}(\text{OiPr})_2\text{Cl}_2$ instead of $\text{Ti}(\text{OiPr})_4$ in an attempt to prepare the corresponding dichloride complexes.²⁰ However, in contrast with the clean formation of **1** and **3a,b**, those reactions proved to be not as selective as expected. The reaction of 2 equiv of $\{\text{ON}^{\text{Me,Ph}}\}\text{H}$ with $\text{Ti}(\text{OiPr})_2\text{Cl}_2$ led to the immediate precipitation of the adduct $\text{TiCl}_2(\text{OiPr})\{\text{ON}^{\text{Me,Ph}}\} \cdot i\text{PrOH}$ (**4** · *iPrOH*), which results obviously from the alcoholysis of a single isopropoxide group (Scheme 3). Once isolated and dried under vacuum, this complex rapidly loses its coordinated 2-propanol molecule to give **4**, as confirmed by NMR spectroscopy. Change of the reaction conditions (prolonged heating, solvent) did not allow accessing the targeted $\text{TiCl}_2\{\text{ON}^{\text{Me,Ph}}\}_2$ complex. On the other hand, repeated reactions of 2 equiv of $\{\text{ON}^{\text{Ph,Ph}}\}\text{H}$ with $\text{Ti}(\text{OiPr})_2\text{Cl}_2$ led systematically to complex mixtures of compounds (as judged by ^1H and ^{19}F NMR). Recrystallization of crude products afforded only small amounts of crystals, which

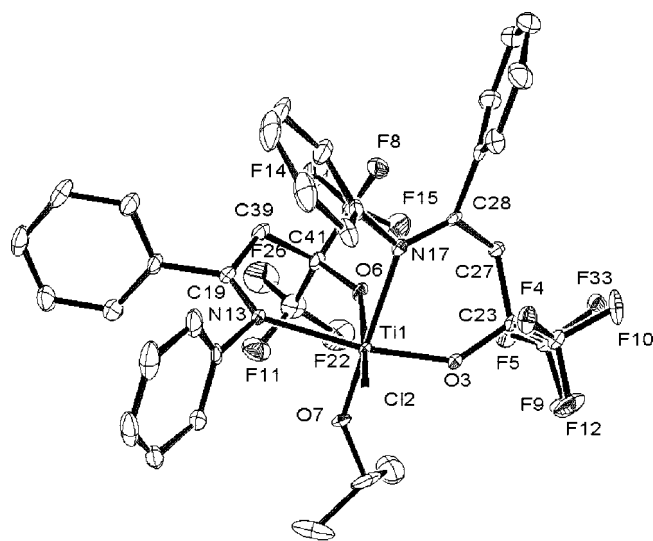


Figure 6. ORTEP view of $\text{TiCl}(\text{OiPr})\{\text{ON}^{\text{Ph,Ph}}\}_2$ (**5**) (ellipsoids drawn at the 50% probability level; all hydrogen atoms have been omitted for the sake of clarity). Selected bond lengths (Å) and angles (deg): Ti(1)–O(7), 1.749(2); Ti(1)–O(3), 1.8519(19); Ti(1)–O(6), 1.884(2); Ti(1)–N(13), 2.260(2); Ti(1)–Cl(2), 2.3428(9); Ti(1)–N(17), 2.376(2); O(7)–Ti(1)–O(3), 96.31(9); O(7)–Ti(1)–O(6), 99.16(9); O(3)–Ti(1)–O(6), 93.49(8); O(7)–Ti(1)–N(13), 91.99(9); O(3)–Ti(1)–N(13), 171.32(9); O(6)–Ti(1)–N(13), 82.65(9); O(7)–Ti(1)–Cl(2), 95.03(8); O(3)–Ti(1)–Cl(2), 92.62(6); O(6)–Ti(1)–Cl(2), 163.82(7); N(13)–Ti(1)–Cl(2), 89.17(7); O(7)–Ti(1)–N(17), 179.61(10); O(3)–Ti(1)–N(17), 83.36(8); O(6)–Ti(1)–N(17), 80.67(8); N(13)–Ti(1)–N(17), 88.34(8); Cl(2)–Ti(1)–N(17), 85.18(6).

turned out to be mixtures of the mixed chloride-isopropoxide complex $\text{TiCl}(\text{OiPr})\{\text{ON}^{\text{Ph,Ph}}\}_2$ (**5**)²¹ and the zwitterionic complex $[\text{TiCl}_3\{\text{ON}^{\text{Ph,Ph}}\}\{\text{ONH}^{\text{Ph,Ph}}\}]$ (**6**) (Scheme 3). In the latter complex, one of the two ligand units is coordinated by a single σ -alkoxide group, while its imino function has been protonated.

Complexes **4** · *iPrOH*, **5**, and **6** were structurally characterized by X-ray diffraction studies (Figures 5–7 Table 1). The main $\text{Ti}–\{\text{ON}^{\text{R}_1\text{R}_2}\}$, $\text{Ti}–\text{OiPr}$, and $\text{Ti}–\text{Cl}$ bond distances and related angles in these three complexes are quite similar to those discussed above for complexes **1** and **3a**. As in the case of **3a**, complex **5** features a type **H** structure. Peculiarities in **4** · *iPrOH*

(16) (a) Tararov, V. I.; Hibbs, D. E.; Hursthouse, M. B.; Ikonnikov, N. S.; Malik, K. M. A.; North, M.; Orizu, C.; Belokon, Y. N. *Chem. Commun.* **1998**, 387. (b) Gilli, G.; Cruickshank, D. W. J.; Beddoes, R. L.; Mills, O. S. *Acta Crystallogr., B Struct. Crystallogr. Cryst. Chem.* **1972**, 28, 1889. (c) Repo, T.; Klinga, M.; Leskela, M.; Pietikainen, P.; Brunow, G. *Acta Crystallogr. C: Cryst. Struct. Commun.* **1996**, 52, 2742. (d) Kim, I.; Ha, Y. S.; Zhang, D. F.; Ha, C.-S.; Lee, U. *Macromol. Rapid Commun.* **2004**, 25, 1319. (e) Choudhary, N. F.; Hitchcock, P. B.; Leigh, G. J. *Inorg. Chim. Acta* **2000**, 306, 24. (f) Kelly, D. G.; Toner, A. J.; Walker, N. M.; Coles, S. J.; Hursthouse, M. B. *Polyhedron* **1996**, 15, 4307.

(17) In a C_2 -symmetric environment such as in structure **B** (Figure 1), **D**, or **E** (Figure 3), two doublets are expected for the diastereotopic hydrogens of the *CHH* ligand unit adjacent, as well as for the diastereotopic hydrogens of *CHHPh* groups in dibenzyl complexes **7** and **8**. Also, the ^{19}F NMR spectrum would feature two quartets for the nonequivalent $\text{C}(\text{CF}_3)(\text{CF}_3)$ groups; see refs 4a,b.

(18) Gregson, C. K. A.; Blackmore, I. J.; Gibson, V. C.; Long, N. J.; Marshall, E. L.; White, A. J. P. *Dalton Trans.* **2006**, 3134.

(19) (a) Fleischer, R.; Wunderlich, H.; Braun, M. *Eur. J. Org. Chem.* **1998**, 1063. (b) Braun, M.; Hahn, A.; Engelmann, M.; Fleischer, R.; Frank, W.; Krysch, C.; Haremza, S.; Kurschner, K.; Parker, R. *Chem.–Eur. J.* **2005**, 11, 3405. (c) Flores-Lopez, L. Z.; Parra-Hake, M.; Somanathan, R.; Walsh, P. J. *Organometallics* **2000**, 19, 2153. (d) Davidson, M. G.; Johnson, A. L.; Jones, M. D.; Lunn, M. D.; Mahon, M. F. *Eur. J. Inorg. Chem.* **2006**, 4449. (e) Johnson, A. L.; Davidson, M. G.; Lunn, M. D.; Mahon, M. F. *Eur. J. Inorg. Chem.* **2006**, 3088.

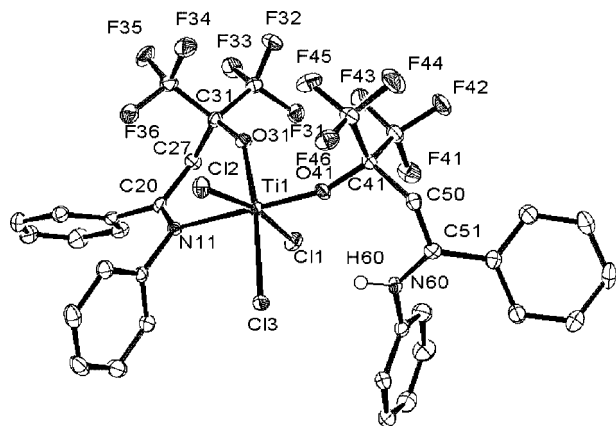
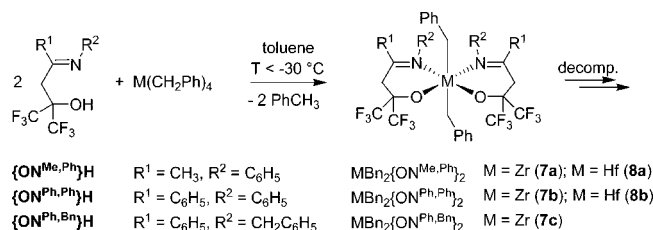


Figure 7. ORTEP view of $[\text{TiCl}_3\{\text{ON}^{\text{Ph,Ph}}\}\{\text{ONH}^{\text{Ph,Ph}}\}]$ (**6**) (ellipsoids drawn at the 50% probability level; all hydrogen atoms have been omitted for the sake of clarity, except the one on the protonated imino function). Selected bond lengths (Å) and angles (deg): Ti(1)–O(41), 1.8298(16); Ti(1)–O(31), 1.8358(16); Ti(1)–N(11), 2.3020(19); Ti(1)–Cl(2), 2.3394(7); Ti(1)–Cl(1), 2.3608(8); Ti(1)–Cl(3), 2.3873(7); O(41)–Ti(1)–O(31), 96.80(7); O(41)–Ti(1)–N(11), 178.84(7); O(31)–Ti(1)–N(11), 82.69(7); O(41)–Ti(1)–Cl(2), 94.80(5); O(31)–Ti(1)–Cl(2), 92.78(6); N(11)–Ti(1)–Cl(2), 86.27(5); O(41)–Ti(1)–Cl(1), O(31)–Ti(1)–Cl(1), 92.64(6); N(11)–Ti(1)–Cl(1), 83.98(5); Cl(2)–Ti(1)–Cl(1), 168.15(3); O(41)–Ti(1)–Cl(3), 91.71(5); O(31)–Ti(1)–Cl(3), 171.33(6); N(11)–Ti(1)–Cl(3), 88.77(5); Cl(2)–Ti(1)–Cl(3), 88.13(3); Cl(1)–Ti(1)–Cl(3), 84.95(3).

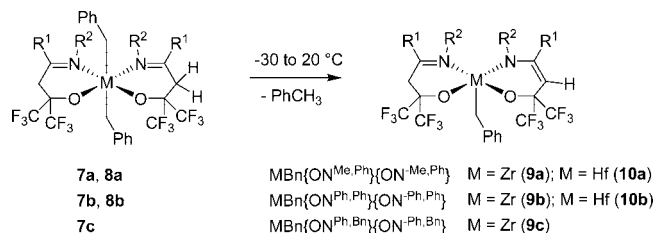
involve an expectedly longer Ti–OH*i*Pr bond distance (2.134(1) Å) (as compared to Ti–O*i*Pr, 1.744(1) Å) and a more acute Ti–O–C bond angle (131.68(9)° vs 151.31(11)°, respectively). The presence of the 2-propanol molecule also likely accounts for the reduced *trans* Ti–O(ligand) bond distance of 1.841(1) Å, as compared to that of 1.954(1) Å for the Ti–O(ligand) *trans* to an isopropoxide group in complex **3a**. In zwitterionic complex **6**, there is a short Cl(3)⋯H(60)–N(60) contact of 2.439 Å.

Dibenzyl Complexes of Zirconium and Hafnium. Dibenzyl complexes of zirconium and hafnium based on monoanionic bidentate ligands $\{\text{ON}^{\text{R}^1,\text{R}^2}\}^-$ were prepared by alcoholysis of $\text{Zr}(\text{CH}_2\text{Ph})_4$ and $\text{Hf}(\text{CH}_2\text{Ph})_4$ with 2 equiv of fluorous alcohol-imines $\{\text{ON}^{\text{R}^1,\text{R}^2}\}\text{H}$. These reactions proceed very fast and selectively, in toluene at low temperature (< -30 °C), to afford the corresponding $\text{M}(\text{CH}_2\text{Ph})_2\{\text{ON}^{\text{R}^1,\text{R}^2}\}_2$ complexes ($\text{M} = \text{Zr}$, **7**; $\text{M} = \text{Hf}$, **8**), with concomitant release of 2 equiv of toluene (Scheme 4). However, these compounds subsequently decompose at higher temperature ($-30 < T$ (°C) < 20), within minutes to days depending on the nature of the ligand and the metal, by abstraction of a hydrogen from the methylene ligand backbone by a benzyl group.^{12,20,22} This process is rather selective [main or only decomposition process observed; see Experimental Section] and eventually results in the release of a toluene molecule and the formation of $\text{M}(\text{CH}_2\text{Ph})\{\text{ON}^{\text{R}^1,\text{R}^2}\}\{\text{ON}^{-\text{R}^1,\text{R}^2}\}$ complexes ($\text{M} = \text{Zr}$, **9**; $\text{M} = \text{Hf}$, **10**) in which a ligand unit ($\{\text{ON}^{-\text{R}^1,\text{R}^2}\}$) now acts as an α,β -unsaturated amido-alkoxy dianionic moiety (Scheme 5). This process differs fundamentally from the one observed in related Schiff base zirconium alkyls, which decompose via migration (1,2-migratory insertion or radical) of an alkyl group to imine.²³ In the present case, abstraction of a hydrogen by a nucleophilic benzyl group can be accounted for by the high acidity of the methylene group,²⁴ due to its substitution by electron-withdrawing α -imino and β -CF₃ groups. We cannot, however, rule out other pathways (e.g., radical)¹² at this stage. More detailed investigations, including

Scheme 4



Scheme 5



computations, are underway to further explore the origin and mechanism of this decomposition and, on the other hand, account for the thermal stability of dibenzyl complex **2** (*vide supra*).^{25,26}

This facile decomposition process hampered the isolation of large amounts of analytically pure dibenzyl complexes **7** and **8**. Nonetheless, suitable crystals for X-ray diffraction of zirconium complexes **7a** and **7b** and of hafnium complex **8a** could be collected from syntheses performed at low temperature. The solid-state structures of **7a**, **7b**, and **8a** are shown in Figures 8–10. The three compounds adopt a distorted octahedral geometry with the two $\{\text{ON}^{\text{R}^1,\text{R}^2}\}^-$ ligand units located in the equatorial plane in a *cis*-N,N/*cis*-O,O fashion

(20) Repeated attempts under various conditions to obtain $\text{TiCl}_2\{\text{ON}^{\text{R}^1,\text{R}^2}\}_2$ complexes by regular salt metathesis of TiCl_4 (or $\text{TiCl}_4(\text{THF})_2$) with the Li^+ (*in situ* generated), Na^+ , or K^+ (isolated; see Experimental Section) salts of $\{\text{ON}^{\text{Me,Ph}}\}^-$ and $\{\text{ON}^{\text{Ph,Ph}}\}^-$ led to intractable mixtures of compounds that could not be separated nor unambiguously identified. Only in one case could small amounts of crystals be isolated, which proved by X-ray diffraction to be $\text{TiCl}_2\{\text{ON}^{\text{Ph,Ph}}\}\{\text{OO}^{\text{Ph}}\}$, where $\{\text{OO}^{\text{Ph}}\}^-$ is the aldolate ligand $[(\text{CF}_3)_2\text{C}(\text{OH})\text{CH}_2\text{C}(\text{=O})\text{Ph}]^-$, i.e., the decomposition product of the initial ligand. Similarly, all attempts to prepare dibenzyl complexes of titanium by alcoholysis of $\text{Ti}(\text{CH}_2\text{Ph})_4$ with 2 equiv of fluorous alcohol-imines $\{\text{ON}^{\text{R}^1,\text{R}^2}\}\text{H}$ led to intractable mixtures of compounds. We assume that the latter difficulties reflect the versatile redox chemistry of Ti, combined with the identified decomposition pathways of dibenzyl-metal (Zr, Hf) complexes of these new ligands. It is noteworthy that, to our knowledge, there is no dibenzyl-titanium complex of “regular” phenoxyimine ligands reported thus far; see refs 8 and 9.

(21) We observed that the reaction of 2 equiv of the aldol $(\text{CF}_3)_2\text{C}(\text{OH})\text{CH}_2\text{C}(\text{=O})\text{CH}_3$ ($\{\text{OO}^{\text{Me}}\}\text{H}$) (ref 5) with $\text{Ti}(\text{O}i\text{Pr})_2\text{Cl}_2$ also leads to the mixed chloride-isopropoxide complex $\text{Ti}(\text{O}i\text{Pr})\text{Cl}\{\text{OO}^{\text{Me}}\}_2$, as the main isolable product (see Experimental Section).

(22) For selected examples of decomposition pathways of early transition metal complexes involving hydrogen abstraction, see: (a) Bernskoetter, W. H.; Pool, J. A.; Lobkovsky, E.; Chirik, P. J. *Organometallics* **2006**, *25*, 1092, and references therein. (b) Schock, L. E.; Brock, C. P.; Marks, T. J. *Organometallics* **1987**, *6*, 232, and references therein. (c) Knight, L. K.; Piers, W. E.; Fleurat-Lessard, P.; Parvez, M.; McDonald, R. *Organometallics* **2004**, *23*, 2087. (d) Pattiasina, J. W.; Hissink, C. E.; de Boer, J. L.; Meetsma, A.; Teuben, J. H. *J. Am. Chem. Soc.* **1985**, *107*, 1158. (e) Skvortsov, G. G.; Fukin, G. K.; Trifonov, A. A.; Noor, A.; Doring, C.; Kempe, R. *Organometallics* **2007**, *26*, 5770.

(23) (a) Knight, P. D.; Clarkson, G.; Hammond, M. L.; Kimberley, B. S.; Scott, P. J. *Organomet. Chem.* **2005**, *690*, 5125. (b) Knight, P. D.; O’Shaughnessy, P. N.; Munslow, I. J.; Kimberley, B. S. *J. Organomet. Chem.* **2003**, *683*, 103. (c) Woodman, P. R.; Alcock, N. W.; Munslow, I. J.; Sanders, C. J.; Scott, P. *Dalton Trans.* **2000**, 3340.

(24) Reaction of $\{\text{ON}^{\text{Me,Ph}}\}\text{H}$ with 2 equiv of KH readily leads to the formation of the $\{\text{ON}^{-\text{Me,Ph}}\}_2$, via proton abstraction from the OH and CHH groups; see Experimental Section.

Table 1. Summary of Crystal and Refinement Data for Complexes 1, 3a, 4, 5, 6, 7a, 7b, 7d, 8a, and 11

	1	3a	4 · iPrOH	5	6
empirical formula	C ₁₄ H ₁₄ C ₁₂ F ₁₂ N ₂ O ₂ Ti	C ₃₀ H ₃₄ F ₁₂ N ₂ O ₄ Ti	C ₁₈ H ₂₅ C ₁₂ F ₆ NO ₃ Ti	C ₃₇ H ₃₁ C ₁₁ F ₁₂ N ₂ O ₃ Ti	C ₃₄ H ₂₅ C ₁₃ F ₁₂ N ₂ O ₂ Ti · C ₇ H ₈
fw	589.07	762.49	536.19	862.99	967.94
cryst syst	orthorhombic	monoclinic	triclinic	monoclinic	monoclinic
space group	<i>P</i> 2 ₁ 2 ₁ 2 ₁	<i>P</i> 2 ₁ / <i>a</i>	<i>P</i> 1̄	<i>P</i> 2 ₁ / <i>n</i>	<i>P</i> 2 ₁ / <i>c</i>
<i>a</i> , Å	11.5983(6)	19.910(4)	10.2267(9)	9.1162(9)	11.44850(10)
<i>b</i> , Å	13.5379(10)	16.379(4)	11.4449(11)	12.2176(12)	14.96840(10)
<i>c</i> , Å	13.592(9)	20.634(4)	14.0137(12)	33.617(3)	24.8484(2)
α, deg	90	90	112.483(4)	90	90
β, deg	90	95.938(10)	106.534(4)	92.780(3)	98.7700(10)
γ, deg	90	90	116.075(4)	90	90
volume, Å ³	2134.2(14)	6693(2)	1140.98(18)	3739.8(6)	4208.38(6)
Z	4	8	2	4	4
density, Mg m ⁻³	1.833	1.513	1.561	1.533	1.528
abs coeff, mm ⁻¹	0.770	0.360	0.677	0.400	0.486
<i>F</i> (000)	1168	3120	548	1752	1960
cryst size, mm	0.05 × 0.06 × 0.16	0.55 × 0.60 × 0.70	0.12 × 0.27 × 0.70	0.18 × 0.35 × 0.55	0.07 × 0.09 × 0.25
θ range, deg	2.76 to 26.49	2.4 to 27.25	2.26 to 27.43	2.43 to 27.55	2.5 to 25.74
limiting indices	-14 ≤ <i>h</i> ≤ 14, -16 ≤ <i>k</i> ≤ 16, -16 ≤ <i>l</i> ≤ 16	-25 ≤ <i>h</i> ≤ 25, -21 ≤ <i>k</i> ≤ 16, -26 ≤ <i>l</i> ≤ 26	-13 ≤ <i>h</i> ≤ 13, -14 ≤ <i>k</i> ≤ 14, -18 ≤ <i>l</i> ≤ 18	-11 ≤ <i>h</i> ≤ 5, -15 ≤ <i>k</i> ≤ 15, -42 ≤ <i>l</i> ≤ 43	-14 ≤ <i>h</i> ≤ 14, -11 ≤ <i>k</i> ≤ 19, -31 ≤ <i>l</i> ≤ 32
reflns collected	18 411	72 912	22 572	24 893	45 695
reflns unique [<i>I</i> > 2σ(<i>I</i>)]	4385 (3204)	15 161 (11 450)	5146 (4451)	8531 (7106)	9605 (6430)
data/restraints/params	4385/0/298	15 161/0 /883	5146/0/283	8531/0/505	9605/0/613
goodness-of-fit on <i>F</i> ²	1.002	1.039	1.043	1.141	1.013
<i>R</i> ₁ [<i>I</i> > 2σ(<i>I</i>)] (all data)	0.0458 (0.0756)	0.0429 (0.0641)	0.0304 (0.0375)	0.0642 (0.079)	0.0459 (0.0863)
<i>wR</i> ₂ [<i>I</i> > 2σ(<i>I</i>)] (all data)	0.1031 (0.1147)	0.0974 (0.1074)	0.0722 (0.0755)	0.1346 (0.141)	0.0819 (0.0943)
largest diff, e Å ⁻³	0.520 and -0.361	0.347 and -0.512	0.368 and -0.425	0.707 and -0.653	0.677 and -0.352
	7a	7b	7d	8a	11
empirical formula	C ₃₈ H ₃₄ F ₁₂ N ₂ O ₂ Zr · 2(C ₂ H ₅ Cl ₂)	C ₄₈ H ₃₈ F ₁₂ N ₂ O ₂ Zr · 1.5(C ₇ H ₈)	C ₃₈ H ₂₄ F ₂₂ N ₂ O ₂ Zr	C ₃₈ H ₃₄ F ₁₂ HfN ₂ O ₂ · 2(C ₇ H ₈)	C ₃₆ H ₁₄ F ₃₃ N ₃ O ₃ Zr
fw	1039.74	1132.23	1049.81	1141.43	1254.72
cryst syst	monoclinic	triclinic	monoclinic	monoclinic	monoclinic
space group	<i>C</i> 2/ <i>c</i>	<i>P</i> 1̄	<i>P</i> 2 ₁ / <i>n</i>	<i>C</i> 2/ <i>c</i>	<i>P</i> 2 ₁ / <i>a</i>
<i>a</i> , Å	19.4235(16)	9.12390(8)	10.1292(5)	27.555(2)	18.6550(13)
<i>b</i> , Å	12.3987(13)	11.97510(10)	19.7931(9)	12.0391(10)	11.5244(10)
<i>c</i> , Å	18.8797(18)	24.35250(16)	19.9920(9)	17.9936(14)	22.4943(19)
α, deg	90	96.3176(4)	90	90	90
β, deg	109.048(3)	96.7064(5)	102.105(2)	127.787(2)	22.4943(19)
γ, deg	90	100.2415(5)	90	90	90
volume, Å ³	4297.8(7)	2577.04(7)	3919.0(3)	4717.4(6)	4461.7(6)
Z	4	2	4	4	4
density, Mg m ⁻³	1.607	1.459	1.779	1.607	1.868
abs coeff, mm ⁻¹	0.595	0.302	0.425	2.302	0.426
<i>F</i> (000)	2096	1158	2080	2288	2448
cryst size, mm	0.20 × 0.20 × 0.20	0.04 × 0.20 × 0.25	0.25 × 0.30 × 0.30	0.26 × 0.37 × 0.44	0.04 × 0.20 × 0.20
θ range, deg	3.29 to 27.4	2.55 to 27.59	2.8 to 27.53	2.73 to 27.52	2.57 to 27.60
limiting indices	-23 ≤ <i>h</i> ≤ 22, -15 ≤ <i>k</i> ≤ 11, -14 ≤ <i>l</i> ≤ 24	-11 ≤ <i>h</i> ≤ 11, -15 ≤ <i>k</i> ≤ 16, -27 ≤ <i>l</i> ≤ 31	-13 ≤ <i>h</i> ≤ 13, -25 ≤ <i>k</i> ≤ 25, -25 ≤ <i>l</i> ≤ 22	-35 ≤ <i>h</i> ≤ 35, -15 ≤ <i>k</i> ≤ 15, -22 ≤ <i>l</i> ≤ 23	-23 ≤ <i>h</i> ≤ 22, -14 ≤ <i>k</i> ≤ 14, -29 ≤ <i>l</i> ≤ 29
reflns collected	8203	22 178	38 611	35 640	84 939
reflns unique [<i>I</i> > 2σ(<i>I</i>)]	4230 (3502)	11 757 (6543)	8952 (7468)	5407 (5298)	10 190 (7995)
data/restraints/params	4230/0/276	11 757/0/687	8952/0/586	5407/0/313	10 190/0/685
goodness-of-fit on <i>F</i> ²	1.055	1.041	1.041	1.049	1.071
<i>R</i> ₁ [<i>I</i> > 2σ(<i>I</i>)] (all data)	0.0337 (0.0445)	0.0852 (0.1587)	0.0285 (0.0387)	0.0154 (0.0159)	0.0713 (0.0852)
<i>wR</i> ₂ [<i>I</i> > 2σ(<i>I</i>)] (all data)	0.0762 (0.0811)	0.2043 (0.2403)	0.0691 (0.0742)	0.0386 (0.0389)	0.2059 (0.2115)
largest diff, e Å ⁻³	0.476 and -0.478	3.035 and -0.917	0.573 and -0.41	0.44 and -0.689	1.894 and -0.884

and the two benzyl groups at the axial positions, which is a type **D** structure (Figure 3). This generates a global *C*_{2v}-symmetric environment around the metal center, and a crystallographic inversion center is actually observed in **7a** and **8a**. The Zr–O (2.001(4)–2.016(2) Å) and Zr–N (2.436(2)–2.483(4) Å) bond distances compare well with

those observed in Zr(IV)–Salen^{23b,27} (1.962–2.030 and 2.359–2.425 Å, respectively) and Zr(IV) bis(phenoxyimine) compounds (1.964–2.022 and 2.316–2.391 Å, respectively),^{8k,23a,28} as well as in the related fluoros dialkoxide-diamino complex {CH₂NMeCH₂C(CF₃)₂O}₂Zr(CH₂Ph)₂.^{4a} The Zr–C bonds in this latter complex (2.266(1)–2.271(1) Å)^{4a} are just slightly

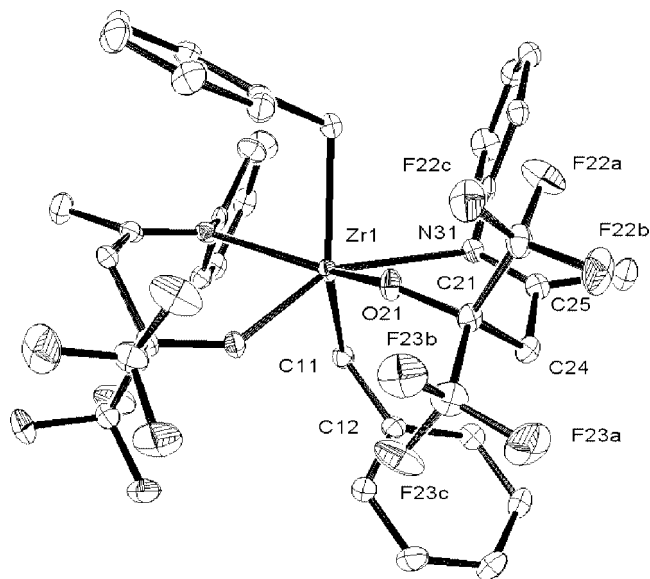


Figure 8. ORTEP view of $\text{Zr}(\text{CH}_2\text{Ph})_2(\text{ON}^{\text{Me,Ph}})_2$ (**7a**) (ellipsoids drawn at the 50% probability level; all hydrogen atoms have been omitted for the sake of clarity; Zr(1) is an inversion center and atoms obtained by this symmetry operation are named hereafter with "#"). Selected bond lengths (Å) and angles (deg): Zr(1)–O(21), 2.0163(15); Zr(1)–C(11), 2.310(2); Zr(1)–N(31), 2.4360(18); O(21)#1–Zr(1)–O(21), 86.83(9); O(21)–Zr(1)–C(11)#1, 91.01(7); O(21)–Zr(1)–C(11), 123.51(7); C(11)#1–Zr(1)–C(11), 133.81(12); O(21)#1–Zr(1)–N(31), 149.24(6); O(21)–Zr(1)–N(31), 75.43(6); C(11)#1–Zr(1)–N(31), 82.37(7); C(11)–Zr(1)–N(31), 78.74(7); N(31)–Zr(1)–N(31)#1, 130.55(9); C(12)–C(11)–Zr(1), 109.07(14).

shorter than those observed in **7a** and **7b** (2.297(6)–2.310(2) Å). Both the benzyl ligands in **7a** and **7b** have a normal structure (C(12)–C(11)–Zr(1), 109.0(4)–111.0(4)°; Zr(1)⋯C(12), 3.128–3.349 Å), indicative of no significant Zr⋯Ph interaction. Overall, **7a**, **7b**, and **8a** are best described as 16-electron species, counting the alkoxides as four-electron (σ , π) donors.^{4a}

The most stable dibenzyl complexes could also be characterized in solution by NMR techniques. All ¹H and ¹⁹F NMR data of the complexes **7a,b** and **8a** (as well as ¹³C NMR for **7a**) in toluene-*d*₈ or CD₂Cl₂ indicate the presence of a single highly symmetric species on the NMR time scale. In each case, a single

(25) To prevent this decomposition pathway, the use of *gem*-dimethyl-substituted pro-ligand analogues was attempted. Surprisingly, fluorous (di)imino-(di)ols such as $\text{HOC}(\text{CF}_3)_2\text{CMe}_2\text{C}(\text{iPr})=\text{N}(\text{iPr})$ and $[\text{HOC}(\text{CF}_3)_2\text{CMe}_2\text{C}(\text{iPr})=\text{NCH}_2-]_2$ were found not to react with $\text{M}(\text{CH}_2\text{Ph})_4$ (M = Ti, Zr, Hf) in toluene up to 60–80 °C, temperatures at which the latter precursors start decomposing at a significant rate. Reasons for this absence of reactivity, while no obvious steric and electronic effects can be accounted for, remain obscure. To date, such *gem*-dimethyl-substituted pro-ligands could be installed only at aluminum centers, under conditions much more drastic than those used for the parent unsubstituted pro-ligands; see ref 11.

(26) The reactions of $\text{Zr}(\text{CH}_2\text{Ph})_4$ with 1 equiv of $\{\text{ON}^{\text{Me,Ph}}\}\text{H}$ or $\{\text{ON}^{\text{Ph,Ph}}\}\text{H}$ were attempted to potentially access the corresponding $\text{Zr}(\text{CH}_2\text{Ph})_2\{\text{ON}^{\text{R}_1\text{R}_2}\}$ complexes. However, in both cases, NMR monitoring showed that these reactions led to ca. 1:1 mixtures of $\text{Zr}(\text{CH}_2\text{Ph})_4$ and $\text{Zr}(\text{CH}_2\text{Ph})_2\{\text{ON}^{\text{R}_1\text{R}_2}\}_2$, which further evolve by decomposition of the latter species into $\text{Zr}(\text{CH}_2\text{Ph})\{\text{ON}^{\text{R}_1\text{R}_2}\}\{\text{ON}^{\text{R}_1\text{R}_2}\}$. Those observations indicate that disproportionation of the putative intermediate species $[\text{Zr}(\text{CH}_2\text{Ph})_2\{\text{ON}^{\text{R}_1\text{R}_2}\}]$ or consecutive reaction of the latter species with $\{\text{ON}^{\text{Ph,Ph}}\}\text{H}$ (to form in both cases $\text{Zr}(\text{CH}_2\text{Ph})_2\{\text{ON}^{\text{R}_1\text{R}_2}\}_2$) is faster than abstraction of a hydrogen atom from the ligand backbone.

(27) Clarkson, G. J.; Gibson, V. C.; Goh, P. K. Y.; Hammond, M. L.; Knight, P. D.; Scott, P.; Smit, T. M.; White, A. J. P.; Williams, D. J. *Dalton Trans.* **2006**, 5484.

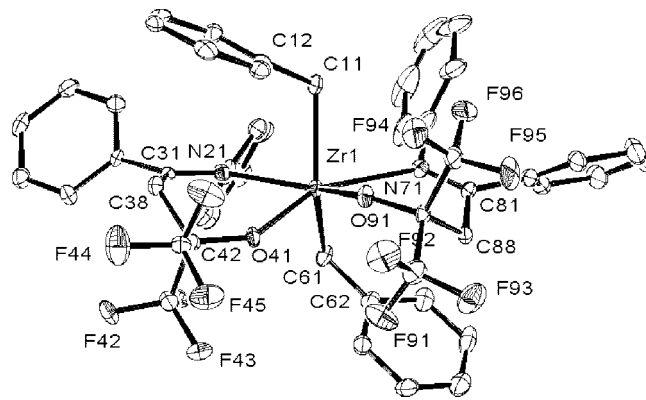


Figure 9. ORTEP view of $\text{Zr}(\text{CH}_2\text{Ph})_2(\text{ON}^{\text{Ph,Ph}})_2$ (**7b**) (ellipsoids drawn at the 50% probability level; all hydrogen atoms have been omitted for the sake of clarity). Selected bond lengths (Å) and angles (deg): Zr(1)–O(91), 2.001(4); Zr(1)–O(41), 2.006(4); Zr(1)–C(61), 2.297(6); Zr(1)–C(11), 2.305(6); Zr(1)–N(21), 2.462(5); Zr(1)–N(71), 2.483(4); O(91)–Zr(1)–O(41), 83.31(16); O(91)–Zr(1)–C(61), 121.2(2); O(41)–Zr(1)–C(61), 95.4(2); O(91)–Zr(1)–C(11), 93.9(2); O(41)–Zr(1)–C(11), 120.89(19); C(61)–Zr(1)–C(11), 132.9(2); O(91)–Zr(1)–N(21), 151.67(16); O(41)–Zr(1)–N(21), 75.17(16); C(61)–Zr(1)–N(21), 79.63(19); C(11)–Zr(1)–N(21), 81.91(19); O(91)–Zr(1)–N(71), 74.33(16); O(41)–Zr(1)–N(71), 150.80(17); C(61)–Zr(1)–N(71), 80.90(19); C(11)–Zr(1)–N(71), 79.83(18); N(21)–Zr(1)–N(71), 131.52(16); C(12)–C(11)–Zr(1), 109.0(4); C(62)–C(61)–Zr(1), 111.0(4).

sharp singlet resonance is observed in the ¹⁹F{¹H} NMR spectrum, and the CH₂C=N and M-CH₂ hydrogens appear as singlets in the ¹H spectrum. These features are consistent with the C_{2v}-symmetric structures observed in the solid state being retained in solution.¹⁷

In the absence of suitable crystals for X-ray diffraction, the identity and structure of decomposition products **9a–c** and **10a,b** were established on the basis of elemental analysis and NMR spectroscopy. Key data include four quartets in the ¹⁹F NMR spectra for the nonequivalent CF₃ groups. In the ¹H spectra, two doublets of an AB spin pattern are observed for both the diastereotopic *CHH*-Ph and (CF₃)₂C*CHH* units of the “unaffected” ligand backbone, while the R¹C=CH of the “affected” ligand appears as a distinctive singlet at δ 4.51–5.29 ppm (CD₂Cl₂, toluene-*d*₈).²⁴ ¹³C NMR data confirm these features.

As for the systems discussed above, reaction of $\{\text{ON}^{\text{Me,ArF}}\}\text{H}$ with $\text{Zr}(\text{CH}_2\text{Ph})_4$ at –30 °C afforded $\text{Zr}(\text{CH}_2\text{Ph})_2\{\text{ON}^{\text{Me,ArF}}\}_2$ (**7d**) (Scheme 6). Crystals of this compound suitable for X-ray diffraction could be isolated at low temperature. In contrast with **7a**, **7b**, and **8a**, the solid-state structure of **7d** features a Zr center in a distorted octahedral geometry, with approximate (noncrystallographic) C₂-symmetry, in which the nitrogen ligand atoms, oxygen ligand atoms, and benzyl groups are arranged in a *cis,trans,cis* fashion (Figure 11), which is a type **F** structure (Figure 3). The Zr–N bond distances in **7d** (2.523(1)–2.552(1)

(28) (a) Ivanchev, S. S.; Truno, V. A.; Rybakov, V. B.; Al'bov, D. V.; Rogozin, D. G. *Dokl. Akad. Nauk. SSSR* **2005**, *404*, 57. (b) Strauch, J.; Warren, T. H.; Erker, G.; Frohlich, R.; Saarenketo, P. *Inorg. Chim. Acta* **2000**, *300*, 810. (c) Said, M.; Hughes, D. L.; Bochmann, M. *Inorg. Chim. Acta* **2006**, *359*, 3467. (d) Bott, R. K. J.; Hughes, D. L.; Schormann, M.; Bochmann, M.; Lancaster, S. J. *J. Organomet. Chem.* **2005**, *665*, 135. (e) Lambert, M.; Gliubizzi, R.; Mazzeo, M.; Tedesco, C.; Pellecchia, C. *Macromolecules* **2004**, *37*, 276. (f) Marsh, R. E. *Acta Crystallogr., Sect. B: Struct. Sci.* **2004**, *60*, 252. (g) Chen, S.; Zhang, X.; Ma, H.; Lu, Y.; Zhang, Z.; Li, H.; Lu, Z.; Cui, N.; Hu, Y. *J. Organomet. Chem.* **2005**, *690*, 4184. (h) Woodman, P. R.; Munslow, I. J.; Hitchcock, P. B.; Scott, P. *J. Chem. Soc., Dalton Trans.* **1999**, 4069. (i) Woodman, P.; Hitchcock, P. B.; Scott, P. *Chem. Commun.* **1996**, 2735.

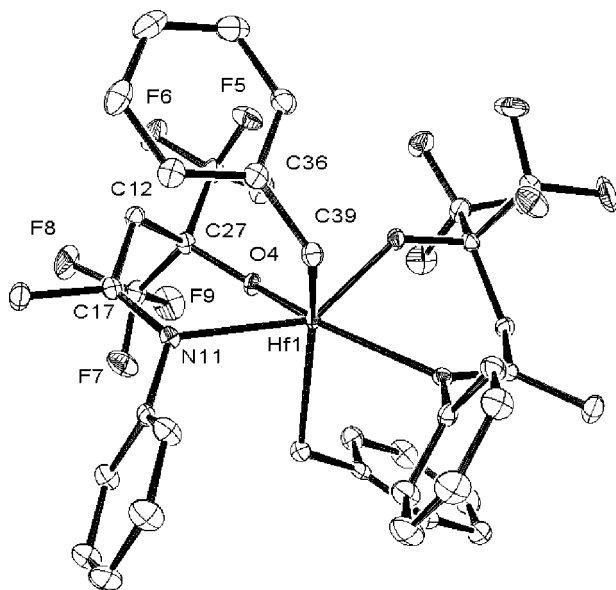


Figure 10. ORTEP view of $\text{Hf}(\text{CH}_2\text{Ph})_2\{\text{ON}^{\text{Me,Ph}}\}_2$ (**8a**) (ellipsoids drawn at the 50% probability level; all hydrogen atoms have been omitted for the sake of clarity; Hf(1) is an inversion center and atoms obtained by this symmetry operation are named hereafter with "#"). Selected bond lengths (Å) and angles (deg): N(11)–Hf(1), 2.3795(12); O(4)–Hf(1), 2.0100(10); C(39)–Hf(1), 2.2951(14); O(4)–Hf(1)–O(4)#1, 84.01(6); O(4)–Hf(1)–C(39), 126.42(5); O(4)#1–Hf(1)–C(39), 89.56(5); C(39)–Hf(1)–C(39)#1, 133.55(8); O(4)–Hf(1)–N(11), 76.33(4); O(4)#1–Hf(1)–N(11), 144.37(4); C(39)–Hf(1)–N(11), 79.08(5); C(39)#1–Hf(1)–N(11), 83.31(5); N(11)–Hf(1)–N(11)#1, 134.35(6); C(36)–C(39)–Hf(1), 113.14(10).

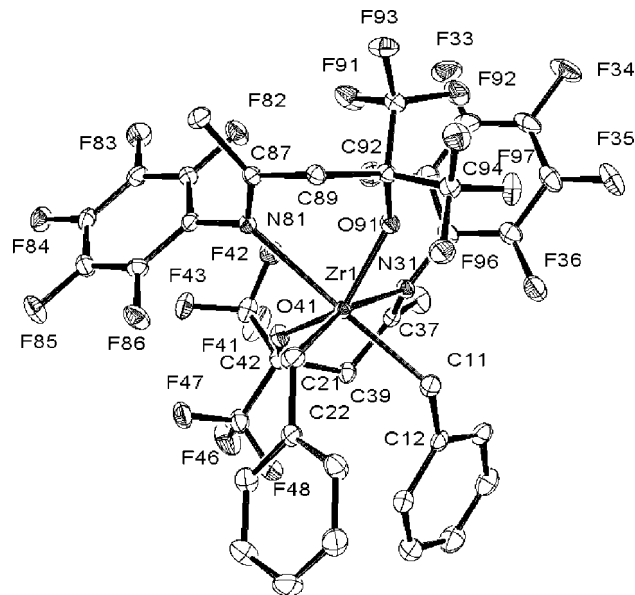
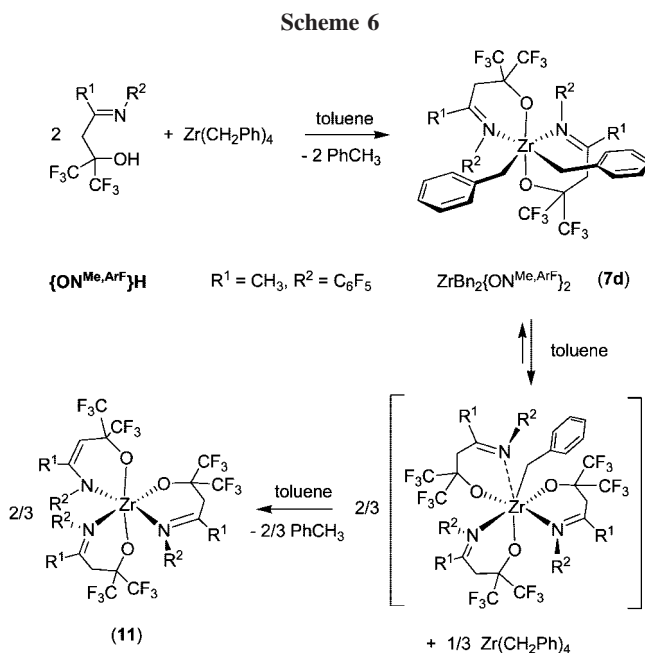


Figure 11. ORTEP view of $\text{Zr}(\text{CH}_2\text{Ph})_2\{\text{ON}^{\text{Me,ArF}}\}_2$ (**7d**) (ellipsoids drawn at the 50% probability level; all hydrogen atoms have been omitted for the sake of clarity). Selected bond lengths (Å) and angles (deg): Zr(1)–O(41), 1.9848(12); Zr(1)–O(91), 2.0017(12); Zr(1)–C(21), 2.2927(18); Zr(1)–C(11), 2.3014(18); Zr(1)–N(31), 2.5229(15); Zr(1)–N(81), 2.5515(14); O(41)–Zr(1)–O(91), 135.40(5); O(41)–Zr(1)–C(21), 103.59(6); O(91)–Zr(1)–C(21), 107.43(6); O(41)–Zr(1)–C(11), 115.12(6); O(91)–Zr(1)–C(11), 99.01(6); C(21)–Zr(1)–C(11), 84.81(7); O(41)–Zr(1)–N(31), 76.45(5); O(91)–Zr(1)–N(31), 80.83(5); C(21)–Zr(1)–N(31), 165.78(6); C(11)–Zr(1)–N(31), 82.42(6); O(41)–Zr(1)–N(81), 82.62(5); O(91)–Zr(1)–N(81), 73.70(5); C(21)–Zr(1)–N(81), 77.79(6); C(11)–Zr(1)–N(81), 157.83(6); N(31)–Zr(1)–N(81), 116.08(5); C(12)–C(11)–Zr(1), 119.36(12).

Å) are longer than those in **7a** and **7b** (2.436(2)–2.483(4) Å), which likely reflects the *trans* influence of the benzyl groups. The latter groups are somewhat more bent than in **7a** and **7b** (C(12)–C(11)–Zr(1), 119.36(12)°; C(12)⋯Zr(1), 3.302 Å). Otherwise, the Zr–O and Zr–C bond distances compare well with those in **7a** and **7b**. On the other hand, the ^1H and ^{19}F NMR data for **7d** in toluene- d_8 solution appear strictly similar to those for **7a**, **7b**, and **8a**; that is, the type **F** structure observed



in the solid state is not retained in solution but transformed to a C_{2v} -symmetric structure of type **D**. This observation indicates that coordination of the $\{\text{ON}^{\text{R}^1, \text{R}^2}\}^-$ fragments onto group 4 metals is rather labile, although it most often leads to the observation of a single species.

The decomposition pathway of **7d** was found to proceed in a somehow different way than for **7a**, **7b**, and **8a**. When a toluene solution of **7d** was kept at room temperature, complete decomposition took place within a few hours, leaving colorless crystals of $\text{Zr}\{\text{ON}^{\text{Me,ArF}}\}_2\{\text{ON}^{-\text{Me,ArF}}\}$ (**11**) (Scheme 6). An X-ray diffraction study and multinuclear NMR spectroscopy of these crystals indicated that there is no more benzyl group in this compound, but three $\{\text{ON}^{\text{Me,ArF}}\}$ ligand units including one $\{\text{ON}^{-\text{Me,ArF}}\}$ that acts as an α, β -unsaturated amido-alkoxy dianionic moiety. We can reasonably assume that compound **11** arises from a ligand redistribution in **7d**, to generate a transient intermediate $\text{Zr}(\text{CH}_2\text{Ph})\{\text{ON}^{\text{Me,ArF}}\}_3$ (not observed by NMR), which further undergoes rapid abstraction of a hydrogen from the methylene ligand backbone by the benzyl group (Scheme 6).

The X-ray diffraction study of **11** revealed a mononuclear structure with the Zr center in a slightly distorted octahedral environment (Figure 12). As a result of the formation of an amido ligand, the Zr–N bond in the “affected” ligand unit (2.179(4) Å) is significantly shorter than the two other Zr–N(imino) bond distances (2.378(5)–2.393(5) Å), while the Zr–O bond distances are essentially all identical to those observed in **7a, b, d**. The ^1H and ^{19}F NMR data for **11** in benzene- d_6 show expectedly two sets of resonances in a 2:1 ratio for the

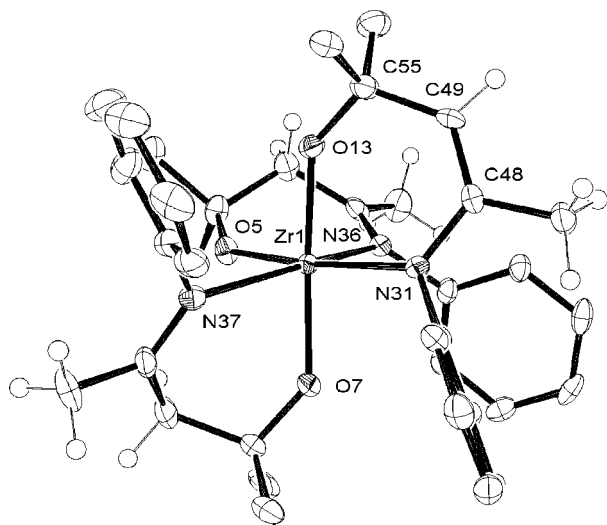


Figure 12. ORTEP view of $\text{Zr}\{\text{ON}^{\text{Me,ArF}}\}_2\{\text{ON}^{-\text{Me,ArF}}\}$ (**11**) (ellipsoids drawn at the 50% probability level; all fluorine atoms have been omitted for the sake of clarity). Selected bond lengths (Å) and angles (deg): Zr(1)–O(13), 1.999(4); Zr(1)–O(7), 2.011(4); Zr(1)–O(5), 2.016(4); Zr(1)–N(31), 2.179(4); Zr(1)–N(36), 2.378(5); Zr(1)–N(37), 2.393(5); O(13)–C(55), 1.371(7); C(49)–C(55), 1.508(8); C(48)–C(49), 1.344(8); N(31)–C(48), 1.416(7); O(13)–Zr(1)–O(7), 166.46(16); O(13)–Zr(1)–O(5), 94.49(16); O(7)–Zr(1)–O(5), 96.73(16); O(13)–Zr(1)–N(31), 81.63(16); O(7)–Zr(1)–N(31), 88.54(16); O(5)–Zr(1)–N(31), 169.58(16); O(13)–Zr(1)–N(36), 92.85(16); O(7)–Zr(1)–N(36), 97.08(15); O(5)–Zr(1)–N(36), 76.76(15); N(31)–Zr(1)–N(36), 93.71(16); O(13)–Zr(1)–N(37), 95.61(16); O(7)–Zr(1)–N(37), 77.84(15); O(5)–Zr(1)–N(37), 85.19(15); N(31)–Zr(1)–N(37), 104.76(16); N(36)–Zr(1)–N(37), 160.60(16).

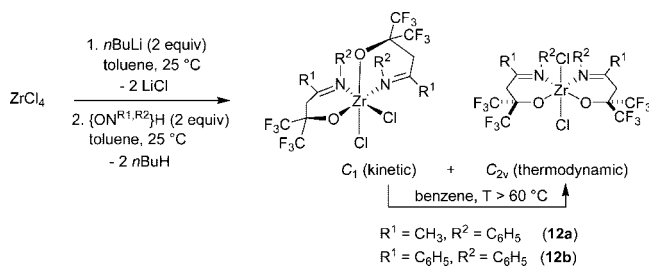
two “unaffected” and the “affected” ligand units, respectively (see Experimental Section).

Dichloride Complexes of Zirconium. Efforts have also been made to access dichlorozirconium complexes, potentially useful for polymerization catalysis. $\text{ZrCl}_2\{\text{ON}^{\text{Me,Ph}}\}_2$ (**12a**) and $\text{ZrCl}_2\{\text{ON}^{\text{Ph,Ph}}\}_2$ (**12b**) could be obtained in moderate yields, in a one-pot procedure, by generating first “ $\text{Zr}(n\text{Bu})_2\text{Cl}_2$ ” from ZrCl_4 and $n\text{BuLi}$ ²⁹ and then adding 2 equiv of the corresponding pro-ligand $\{\text{ON}^{\text{R}^1,\text{R}^2}\}\text{H}$ to perform an alkane elimination (Scheme 7).^{4a,30} Both compounds are moderately soluble in aromatic solvents (toluene, benzene) and sparingly soluble in aliphatic hydrocarbons (hexanes). NMR data in benzene- d_6 of the crude products recovered following this procedure showed that these are mixtures of a C_{2v} -symmetric and a C_1 -symmetric isomer (**12a**, 70:30; **12b**, 30:70). When heated above 60 °C in benzene- d_6 , these (kinetic) mixtures slowly isomerize to yield the C_{2v} -symmetric (thermodynamic) isomer. Also, C_1 -**12a,b** proved to be much less soluble than C_{2v} -**12a,b** and could be selectively isolated by washing the (kinetic) crude mixtures with hot hexanes (see Experimental Section). C_{2v} -**12a,b** show the same NMR features as those discussed above for complexes **3**, **7**, and **8**. The C_1 -symmetric isomers of **12a,b** are characterized by four quartets of equal intensity in the ¹⁹F NMR spectrum (these quartets are broadened and two of them overlap in the case of **12b**) and a complete set of resonances for each individual nonaromatic hydrogen in the ¹H NMR spectrum.

(29) (a) Eisch, J. J.; Owuor, F. A.; Shi, X. *Organometallics* **1999**, *18*, 1583. (b) Eisch, J. J.; Owuor, F. A.; Otieno, P. O. *Organometallics* **2001**, *20*, 4132.

(30) Lavanant, L.; Silvestru, A.; Fauchoux, A.; Toupet, L.; Jordan, R. F.; Carpentier, J.-F. *Organometallics* **2005**, *24*, 5604.

Scheme 7



Repeated attempts under various conditions to obtain such complexes by regular salt metathesis of ZrCl_4 (or $\text{ZrCl}_4(\text{THF})_2$) with the Li^+ (*in situ*-generated), Na^+ , or K^+ (isolated; see Experimental Section) salt of $\{\text{ON}^{\text{Me,Ph}}\}^-$ and $\{\text{ON}^{\text{Ph,Ph}}\}^-$ led to intractable mixtures of compounds that could not be separated nor unambiguously identified.²⁰ A similar approach from $\{\text{ON}^{\text{Me,ArF}}\}\text{Li}$ (*in situ* generated) or $\{\text{ON}^{\text{Me,ArF}}\}\text{K}$ (isolated; see Experimental Section) afforded $\text{ZrCl}_2\{\text{ON}^{\text{Me,ArF}}\}_2$ (**12c**) in poor yield, but this compound features so poor solubility in all common organic solvents that it could be authenticated only on the basis of microanalysis.

Ethylene Polymerization. The complexes based on bidentate ligands were briefly investigated in ethylene polymerization.³¹ Neutral isopropoxide and chloride complexes were activated with MAO or a combination of $[\text{Ph}_3\text{C}][\text{B}(\text{C}_6\text{F}_5)_4]$ and $\text{Al}(i\text{Bu})_3$,³² while $[\text{Ph}_3\text{C}][\text{B}(\text{C}_6\text{F}_5)_4]$ was used to generate *in situ* cationic benzyl-hafnium species from the relatively stable dibenzyl complex **8a**. The results are summarized in Table 2.

Two general characteristics can be drawn from these preliminary investigations. First, all systems show relatively high activity in the early stages of the polymerizations but rapidly deactivate over a 0.1–10 min time period, after which no ethylene uptake is noticed.³³ In fact, in some cases, all of the polyethylene is formed within the first 10 s of the experiment. As a consequence, the activity data reported in Table 2, which were calculated over the whole 10 min time period of the experiments, barely reflect the real behavior of the catalyst systems. These apparent activities, which are usually in the range 100–200 kg PE $\text{mol}^{-1} \text{h}^{-1}$, no matter the nature of the metal and ligand, are of the same order of magnitude as those reported for related catalysts based on discrete zirconium precursors having amino-alkoxide or amino-dialkoxide ligands³⁴ and somewhat lower than those observed for systems based on sulfur-bridged dialkoxide ligands,^{30,35} although direct comparisons are difficult due to differences in polymerization time and conditions.

High initial activities and fast deactivation in ethylene polymerizations have been also reported with group 4 metal catalysts supported by sulfur-bridged dialkoxide $\{\text{OSO}\}^{2-}$ ligands.³⁰ In this case, ligand transfer between group 4 metal

(31) Complexes **1** and **2** were also briefly investigated in polymerization catalysis, although no valuable performance was expected, considering the equatorial coordination of the tetradentate ligand and the anticipated absence of *cis* vacant sites in the resulting cationic species. As a matter of fact, for instance, when complex **1** was activated with MAO (1000 equiv, toluene solution), no polymerization activity was observed (1 atm ethylene, 25 °C).

(32) (a) Chien, J. C. W.; Xu, B. *Makromol. Chem. Rapid Commun.* **1993**, *14*, 109. (b) Chien, J. C. W.; Tsai, W. M. *Makromol. Chem. Macromol. Symp.* **1993**, *66*, 141. (c) Chen, Y. X.; Rausch, M. D.; Chien, J. C. W. *Organometallics* **1994**, *13*, 748. (d) Chien, J. C. W.; Rausch, M. D. *J. Polym. Sci. Part A: Polym. Chem.* **1994**, *32*, 2387. (e) Song, F. S.; Cannon, R. D.; Lancaster, S. J.; Bochmann, M. *J. Mol. Catal. A* **2004**, *218*, 21.

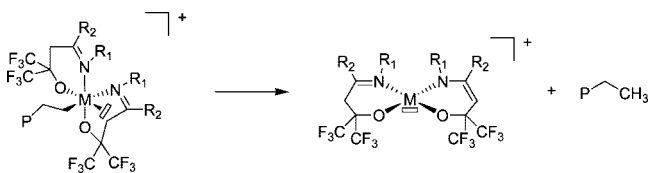
(33) In these experiments, polyethylene was recovered in virtually the same amount as that of ethylene consumed; oligomers (if any) were therefore negligible.

Table 2. Ethylene Polymerization Data^a

entry	catalyst precursor	activator/scavenger (equiv vs metal)	yield (g)	activity ^b (kg PE mol ⁻¹ h ⁻¹)	M_w^c (10 ³ g mol ⁻¹)	M_w/M_n^c	T_m^d (°C)
1	Ti(O <i>i</i> Pr) ₂ {ON ^{Me,Ph} } ₂ (3a)	MAO (1500)	0.429	195	insoluble ^e		135
2	Ti(O <i>i</i> Pr) ₂ {ON ^{Ph,Ph} } ₂ (3b)	MAO (1450)	0.344	174	427	2.7	136
3	TiCl ₂ (O <i>i</i> Pr){ON ^{Me,Ph} } ₂ (4)	MAO (1100)	0.476	201	399	4.7	137
4	TiCl(O <i>i</i> Pr){ON ^{Ph,Ph} } ₂ (5/6 ^f)	MAO (1250)	0.460	222	375	4.4	136
5	ZrCl ₂ {ON ^{Me,Ph} } ₂ (12a)	MAO (1350)	0.387	159	680	8.2	140
6	ZrCl ₂ {ON ^{Ph,Ph} } ₂ (12b)	MAO (1200)	0.285	132	insoluble ^e		133
7	ZrCl ₂ {ON ^{Ph,Ph} } ₂ (12b)	[Ph ₃ C][B(C ₆ F ₅) ₄] (3)/Al(<i>i</i> Bu) ₃ (40)	0.009	4	insoluble ^e		133
8	ZrCl ₂ {ON ^{Me,ArF} } ₂ (12c)	MAO (1300)	0.430	213	insoluble ^e		141
9	ZrCl ₂ {ON ^{Me,ArF} } ₂ (12c)	[Ph ₃ C][B(C ₆ F ₅) ₄] (2)/Al(<i>i</i> Bu) ₃ (100)	0.520	99	insoluble ^e		144
10	Hf(CH ₂ Ph) ₂ {ON ^{Me,Ph} } ₂ (8a)	[Ph ₃ C][B(C ₆ F ₅) ₄] (2.2)/Al(<i>i</i> Bu) ₃ (48)	0	0			

^a Unless otherwise stated, all polymerization experiments were conducted at 50 °C under 7–8 atm of ethylene for 10 min, using 12–32 μmol of catalyst precursor in 50–60 mL of toluene; the results shown for each entry are representative of at least two reproducible runs. ^b Average activity calculated over the whole polymerization time (10 min). ^c Determined by GPC in 1,2,4-trichlorobenzene at 150 °C. ^d Determined by DSC (first heating). ^e PE could not be solubilized in 1,2,4-trichlorobenzene at 160 °C. ^f A mixture of complexes **5** and **6** was used.

Scheme 8. Proposed Deactivation Pathway in Ethylene Polymerizations Catalyzed by M-{ON^{R1,R2}}/Activator Systems (P stands for the growing polyethylenyl chain)



and Al centers was suggested as a possible origin of the catalyst decay. No direct evidence could be found for such a process in the present M-{ON^{R1,R2}}/MAO systems.³⁶ The similar catalyst behavior (decay) observed with quite different activators (MAO³⁷ vs [Ph₃C][B(C₆F₅)₄] with Al(*i*Bu)₃; compare entries 8 and 9, Table 2) suggests that another deactivation pathway may be operative in the present systems. Based on the aforementioned observation of hydrogen abstraction by a benzyl group in neutral Zr(CH₂Ph)₂{ON^{R1,R2}}₂ species (*vide supra*), we assume that a similar process may take place in related cationic species (Scheme 8). Hydrogen abstraction from the ligand backbone by the growing polyethylenyl chain would eventually result in the formation of an alkyl-free, inactive species. In this regard, it is noteworthy that no polymerization at all was noticed when dibenzyl complex **8a** was used as the catalyst precursor (Table 2, entry 10).

The second general feature of these polymerizations concerns the nature of the polymers obtained. All the polyethylenes produced with the [M-{ON^{R1,R2}}] systems under the conditions used have a melting temperature in the range 133–144 °C, indicative of essentially linear long-chain microstructures. The few polymers that proved to be soluble in 1,2,4-trichlorobenzene at 160 °C (and thus analyzable by GPC) showed high molecular

weight. Many polyethylenes could not be solubilized, calling for even higher molecular weights. Polyethylenes that could be analyzed by GPC had broad molecular weight distributions, although most of them feature monomodal shapes with long tailing on low³³ and high molecular weights (see the Supporting Information).

Conclusions

The preparation of discrete group 4 metal complexes based on Schiff base bi- and tetradentate fluoros (di)imino-(di)alkoxide ligands {ON^{R1,R2}}⁻ and {ON^{Et}NO}²⁻ has been studied. Diisopropoxide-Ti(IV) and dibenzyl-Zr(IV) and -Hf(IV) complexes have been obtained using straightforward procedures; the preparation of dichloride-Ti(IV) and -Zr(IV) complexes based on bidentate ligands proved to be somewhat more difficult. Despite the flexibility of the {ON^{R1,R2}}⁻ and {ON^{Et}NO}²⁻ ligands (the bis(trifluoromethyl)alkoxide is not conjugated with the imino group, in contrast to phenoxy-imine and salen ligands) and the lability of their coordination onto group 4 metals (two different stereoisomers of a given compound are sometimes observed in the solid state and in solution), the formation of a single stereoisomer is most often observed, usually with equatorial coordination of the (di)imino-(di)alkoxide functions. This coordination behavior contrasts with that adopted by related fluoros diamino-dialkoxide ligands [helicoidal wrapping of the ligand around the metal center, with both alkoxides located at apical positions, which is a type **B** structure].^{4a} This confirms that imino groups reduce flexibility of the ligand framework.

Another interesting feature revealed in this study is the rapid decomposition of dibenzyl-Zr(IV) and -Hf(IV) complexes, via abstraction of a hydrogen from the ligand framework by a benzyl group. This phenomenon, which is observed only for M(CH₂Ph)₂{ON^{R1,R2}}₂ complexes based on bidentate ligands, while Zr(CH₂Ph)₂{ON^{Et}NO} is stable, provides a reasonable rational basis for the observed rapid deactivation of putative [M(alkyl){ON^{R1,R2}}]⁺ catalytic species during ethylene polymerization.

The many possibilities to tune such fluoros (di)alkoxide-(di)imino ligands⁵ open avenues for designing and preparing new series of group 4 metal complexes. Results of ongoing studies on the coordination chemistry of these original ligands with oxophilic metal centers, the origin of deactivation pathways, and the application of these discrete complexes in catalysis will be reported in due course.

Experimental Section

General Procedures. All experiments were carried out under purified argon using standard Schlenk techniques or in a glovebox.

(34) Zr(CH₂Ph)₂{RN[CH₂CH₂C(O)R']₂}/MAO (1:500) gave at 50 °C, 5 atm, 136–384 kg PE mol⁻¹ h⁻¹ with $M_w = 143$ –452,000, $M_w/M_n = 3.4$ –5.7; see: (a) Shao, P.; Gendron, R. A. L.; Berg, D. J.; Bushnell, G. W. *Organometallics* **2000**, *19*, 509–520. (b) Zr(CH₂Ph)₂{PyC(CF₃)₂O}₂/MAO (1:1000) gave at 30 °C, 8 atm, 10 kg PE mol⁻¹ h⁻¹ with $M_w = 375$ 000, $M_w/M_n = 28$; Zr(CH₂Ph)₂{PyC(CF₃)₂O}₂/B(C₆F₅)₃ (1:1) gave at 40 °C, 3 atm, 96 kg PE mol⁻¹ h⁻¹ with $M_w = 16$ 000, $M_w/M_n = 2.6$; see ref 3d. (c) Berg and Kress observed insignificant or no ethylene polymerization activity with Zr(CH₂Ph)₂{RN[CH₂CH₂C(O)R']₂}/B(C₆F₅)₃ and Zr(CH₂Ph)₂(2,6-bis(menthoxy)pyridyl)/B(C₆F₅)₃ combinations, respectively, and attributed it to the formation of tight ion pairs; see ref 34a and: Gauvin, R. M.; Osborn, J. A.; Kress, J. *Organometallics* **2000**, *19*, 2944.

(35) Eisen and co-workers have reported that the TiCl₂[Py(CPh₂O)₂]/MAO combination exhibits modest ethylene polymerization activity (20 °C, 1 atm); see: Mack, H.; Eisen, M. *J. Chem. Soc., Dalton Trans.* **1998**, 917.

(36) For transfer a phenoxyimino ligand from a Zr to Al center: Makio, H.; Fujita, T. *Macromol. Symp.* **2004**, *213*, 221.

Hydrocarbon solvents, diethyl ether, and tetrahydrofuran were distilled from Na/benzophenone; toluene and pentane were distilled from Na/K alloy under nitrogen and degassed by freeze–vacuum–thaw cycles prior to use. Chlorinated solvents were distilled from calcium hydride. Deuterated solvents (>99.5% D, Eurisotop) were freshly distilled from the appropriate drying agent under argon and degassed prior to use. Pro-ligands $\{\text{ON}^{\text{Et}}\text{NO}\}_2$ and $\{\text{ON}^{\text{R}^1\text{R}^2}\}_2$ were synthesized according to the reported procedures.⁵ Zirconium and hafnium precursors $\text{Zr}(\text{CH}_2\text{Ph})_4$ and $\text{Hf}(\text{CH}_2\text{Ph})_4$ ³⁸ were prepared following literature procedures. ZrCl_4 , TiCl_4 , and $\text{Ti}(\text{OiPr})_4$ were purchased from Strem Chemicals and used as received. $[\text{Ph}_3\text{C}]\text{B}(\text{C}_6\text{F}_5)_4$ (Boulder), $\text{Al}(\text{iBu})_3$ (Aldrich), and MAO (30 wt % solution in toluene, Albermale; contains ca. 10 wt % of free AlMe_3) were used as received.

NMR spectra were recorded in Teflon-valved NMR tubes on Bruker AC-200, AC-300, and AM-500 spectrometers at 20 °C unless otherwise stated. ^1H and ^{13}C NMR chemical shifts were determined using residual solvent resonances and are reported versus SiMe_4 . Assignment of signals was made from 2D ^1H – ^1H COSY and ^1H – ^{13}C HMQC and HMBC NMR experiments. ^{19}F chemical shifts were determined by external reference to an aqueous solution of NaBF_4 . All coupling constants are given in hertz. Elemental analyses (C, H, N) were performed using a Flash EA1112 CHNS Thermo Electron apparatus and are the average of two independent determinations.

Reaction of $\text{TiCl}_2(\text{OiPr})_2$ with $\{\text{ON}^{\text{Et}}\text{NO}\}_2$: Synthesis of $\text{TiCl}_2\{\text{ON}^{\text{Et}}\text{NO}\}$ (1). A solution of diol $\{\text{ON}^{\text{Et}}\text{NO}\}_2$ (100 mg, 0.21 mmol) in toluene (4 mL) was added to a solution of TiCl_4 (20.1 mg, 0.106 mmol) and $\text{Ti}(\text{OiPr})_4$ (30.1 mg, 0.106 mmol) in toluene (4 mL) at -30 °C. The reaction mixture was kept at -30 °C overnight; afterward colorless crystals precipitated. The crystals were separated from the supernatant, washed with a minimal amount of toluene, and dried under vacuum to give **1** as colorless crystals (70 mg, 56%); suitable crystals for X-ray diffraction studies were obtained from this batch. ^1H NMR (500 MHz, CD_2Cl_2 , 298 K): δ 2.37 (s, 6H, CH_3), 3.62 (s, 4H, $\text{CH}_2\text{C}=\text{N}$), 4.16 (s, 4H, NCH_2). $^{13}\text{C}\{^1\text{H}\}$ NMR (125 MHz, CD_2Cl_2 , 298 K): δ 23.6 (CH_3), 41.8 ($\text{CH}_2\text{C}=\text{N}$), 46.7 (NCH_2), 85.3 ($\text{C}(\text{CF}_3)_2$), 122.2 (q, $^1J_{\text{CF}} = 285.3$, CF_3), 173.9 ($\text{N}=\text{C}(\text{CH}_3)$). $^{19}\text{F}\{^1\text{H}\}$ NMR (188 MHz, CD_2Cl_2 , 298 K): δ -76.2 (s, 12F). Anal. Calcd for $\text{C}_{14}\text{H}_{14}\text{Cl}_2\text{F}_{12}\text{N}_2\text{O}_2\text{Ti}$: C, 28.55; H, 2.40; N, 4.76. Found: C, 28.9; H, 2.6; N, 4.7.

Reaction of $\{\text{ON}^{\text{Et}}\text{NO}\}_2$ with $\text{Zr}(\text{CH}_2\text{Ph})_4$: Synthesis of $\text{Zr}(\text{CH}_2\text{Ph})_2\{\text{ON}^{\text{Et}}\text{NO}\}$ (2). NMR-scale synthesis: A Teflon-valved NMR tube was charged with diol $\{\text{ON}^{\text{Et}}\text{NO}\}_2$ (25.7 mg, 54.4 μmol) and $\text{Zr}(\text{CH}_2\text{Ph})_4$ (24.8 mg, 54.4 μmol), and dry toluene- d_8 (ca. 0.5 mL) was vacuum-transferred in at -78 °C. The tube was kept for 3–4 h at -30 °C, and NMR was recorded at room temperature, revealing the formation of **2** in 95% yield, as determined by ^1H NMR spectroscopy. Preparative synthesis: A solution of $\text{Zr}(\text{CH}_2\text{Ph})_4$ (0.41 g, 0.89 mmol) in toluene (3 mL) precooled at -30 °C was added under vigorous stirring to a solution of $\{\text{ON}^{\text{Et}}\text{NO}\}_2$ (0.42 g, 0.86 mmol) in toluene (4 mL) at -30 °C. The reaction mixture was kept at -30 °C overnight, after which **2** precipitated as a yellow crystalline solid, which was separated and dried *in vacuo* (0.25 g, 38%). ^1H NMR (500 MHz, CD_2Cl_2 , 298 K): δ 2.09 (s, 4H, CH_2Ph), 2.12 (s, 6H, CH_3), 2.85 (s, 4H, $\text{CH}_2\text{C}=\text{N}$), 3.62 (s, 4H, NCH_2), 6.64 (d, $^3J_{\text{HH}} = 7.5$, 4H, *o*-Ph), 6.71 (t, $^3J_{\text{HH}} = 7.5$, 2H, *p*-Ph), 7.00 (m, $^3J_{\text{HH}} = 7.5$, 4H, *m*-Ph). $^{13}\text{C}\{^1\text{H}\}$ NMR (125 MHz, CD_2Cl_2 , 298 K): δ 21.1 (CH_2Ph), 24.0 (CH_3), 40.6 ($\text{CH}_2\text{C}=\text{N}$), 51.3 (NCH_2), 79.5 ($\text{C}(\text{CF}_3)_2$), 119.9 (*p*-Ph), 123.8 (CF_3), 125.5 (*o*-Ph), 127.6 (*m*-Ph), 151.1 (*i*-Ph), 177.5 ($\text{N}=\text{C}(\text{CH}_3)$). $^{19}\text{F}\{^1\text{H}\}$ NMR (188 MHz, CD_2Cl_2 , 298 K): δ -76.9

(s, 12F). Anal. Calcd for $\text{C}_{28}\text{H}_{28}\text{F}_{12}\text{N}_2\text{O}_2\text{Zr}$: C, 45.22; H, 3.79; N, 3.77. Found: C, 45.8; H, 3.8; N, 3.7.

Reaction of $\{\text{ON}^{\text{Me,Ph}}\text{H}\}$ with $\text{Ti}(\text{OiPr})_4$: Synthesis of $\text{Ti}(\text{OiPr})_2\{\text{ON}^{\text{Me,Ph}}\}_2$ (3a). A solution of $\text{Ti}(\text{OiPr})_4$ (0.240 g, 0.844 mmol) in toluene (ca. 2.5 mL) was added dropwise at -25 °C to a solution of $\{\text{ON}^{\text{Me,Ph}}\text{H}\}$ (0.510 g, 1.704 mmol). The mixture was stirred until it reached room temperature, and volatiles were removed under vacuum. The solid residue was washed with cold pentane (ca. 5 mL) and dried under vacuum to give **3a** as a white solid (0.410 g, 63%). Crystals of **3a** suitable for X-ray diffraction studies were obtained by recrystallization from a mixture of toluene and hexane. ^1H NMR (500 MHz, benzene- d_6 , 298 K): δ 1.14 (d, $^3J_{\text{HH}} = 6.1$, 12H, $\text{CH}(\text{CH}_3)_2$), 1.25 (s, 6H, CH_3), 3.10 (s, 4H, CH_2), 4.85 (hept, $^3J_{\text{HH}} = 6.1$, 2H, $\text{CH}(\text{CH}_3)_2$), 6.53 (d, $^3J_{\text{HH}} = 7.5$, 4H, *o*-Ph), 6.94 (t, $^3J_{\text{HH}} = 7.2$, 2H, *p*-Ph), 7.03 (t, $^3J_{\text{HH}} = 7.6$, 4H, *m*-Ph). $^{13}\text{C}\{^1\text{H}\}$ NMR (125 MHz, benzene- d_6 , 298 K): δ 24.8 (CH_3), 37.9 (CH_2), 80.2 (CH), 81.5 (hept, $^2J_{\text{CF}} = 28.0$, $\text{C}(\text{CF}_3)_2$), 122.4 (*o*-Ph), 124.5 (q, $^1J_{\text{CF}} = 293.0$, CF_3), 125.1 (*p*-Ph), 128.3 (*m*-Ph), 150.1 (*i*-Ph), 175.6 ($\text{C}=\text{N}$). $^{19}\text{F}\{^1\text{H}\}$ NMR (188 MHz, benzene- d_6 , 298 K): δ -76.6 (s, 12F). Anal. Calcd for $\text{C}_{30}\text{H}_{34}\text{F}_{12}\text{N}_2\text{O}_4\text{Ti}$: C, 47.26; H, 4.49; N, 3.67. Found: C, 47.2; H, 4.6; N, 3.7.

Reaction of $\{\text{ON}^{\text{Ph,Ph}}\text{H}\}$ with $\text{Ti}(\text{OiPr})_4$: Synthesis of $\text{Ti}(\text{OiPr})_2\{\text{ON}^{\text{Ph,Ph}}\}_2$ (3b). This compound was prepared following a similar procedure to the one described above for **3a**, starting from $\text{Ti}(\text{OiPr})_4$ (34.9 mg, 122.8 μmol) and $\{\text{ON}^{\text{Ph,Ph}}\text{H}\}$ (88.7 mg, 245.5 μmol). Compound **3b** was obtained as a pale yellow solid (70.0 mg, 64%). ^1H NMR (300 MHz, benzene- d_6 , 298 K): δ 1.24 (d, $^4J_{\text{HH}} = 6.1$, 12H, $\text{CH}(\text{CH}_3)_2$), 3.70 (s, 4H, CH_2), 5.00 (hept, $^3J_{\text{HH}} = 6.1$, 2H, $\text{CH}(\text{CH}_3)_2$), 6.71–6.85 (m, 20H, Ph). ^1H NMR (300 MHz, CD_2Cl_2 , 298 K): δ 1.06 (d, $^4J_{\text{HH}} = 6.0$, 12H, $\text{CH}(\text{CH}_3)_2$), 3.55 (s, 4H, CH_2), 4.75 (hept, $^3J_{\text{HH}} = 6.0$, 2H, $\text{CH}(\text{CH}_3)_2$), 6.67–7.31 (m, 20H, Ph). $^{13}\text{C}\{^1\text{H}\}$ NMR (75 MHz, benzene- d_6 , 298 K): δ 24.9 ($\text{CH}(\text{CH}_3)_2$), 39.2 (CH_2), 80.7 ($\text{CH}(\text{CH}_3)_2$), 82.0 (m, $\text{C}(\text{CF}_3)_2$), 124.7 (q, $^1J_{\text{CF}} = 292.0$, CF_3), 124.4, 124.9, 126.6, 127.6, 128.0, 128.9 (*o*-, *m*-, *p*-Ph), 139.7 (*i*-Ph from $\text{N}=\text{C}$ -Ph), resonances for the other two *ipso*-Ph carbons were not observed, 175.7 ($\text{C}=\text{N}$). $^{19}\text{F}\{^1\text{H}\}$ NMR (188 MHz, benzene- d_6 , 298 K): δ -76.2 (s, 12F). $^{19}\text{F}\{^1\text{H}\}$ NMR (188 MHz, CD_2Cl_2 , 298 K): δ -76.9 (s, 12F). Anal. Calcd for $\text{C}_{40}\text{H}_{38}\text{F}_{12}\text{N}_2\text{O}_4\text{Ti}$: C, 54.19; H, 4.32; N, 3.16. Found: C, 53.9; H, 4.5; N, 3.4.

Reaction of $\{\text{ON}^{\text{Me,Ph}}\text{H}\}$ with $\text{TiCl}_2(\text{OiPr})_2$: Synthesis of $\text{TiCl}_2(\text{OiPr})\{\text{ON}^{\text{Me,Ph}}\}$ (4). A solution of $\text{Ti}(\text{OiPr})_4$ (24.0 mg, 84.4 μmol) in toluene (1 mL) was added to a solution of TiCl_4 (16.0 mg, 84.4 μmol) in toluene (1 mL). The mixture was stirred for 30 min at room temperature and then cooled to -30 °C. A solution of $\{\text{ON}^{\text{Me,Ph}}\text{H}\}$ (100 mg, 334 μmol , 2 equiv vs Ti) in hexane (2 mL), precooled at -30 °C, was then added dropwise to the previous solution. A precipitate immediately formed (65 mg, 37%). The solid was separated from solution by cannula, dried under vacuum, and recrystallized from dichloromethane at -30 °C to yield colorless crystals of **4**·*i*PrOH, which proved suitable for X-ray diffraction studies (30 mg, 17%). Anal. Calcd for $\text{C}_{18}\text{H}_{25}\text{Cl}_2\text{F}_6\text{NO}_3\text{Ti}$: C, 40.32; H, 4.70; N, 2.61. Found: C, 40.1; H, 4.6; N, 2.8. These crystals lose the coordinated 2-propanol molecule upon prolonged drying under vacuum to give **4**. ^1H NMR (300 MHz, CD_2Cl_2 , 298 K): δ 1.15 (d, $^3J_{\text{HH}} = 5.8$, 6H, $\text{OCH}(\text{CH}_3)_2$), 1.98 (s, 3H, CH_3), 3.21 (br s, 2H, CH_2), 4.54 (br m, 1H, $\text{OCH}(\text{CH}_3)_2$), 6.94 (br s, 2H, *o*-Ph), 7.24 (t, $^3J_{\text{HH}} = 7.6$, 1H, *p*-Ph), 7.40 (t, $^3J_{\text{HH}} = 7.6$, 2H, *m*-Ph). $^{13}\text{C}\{^1\text{H}\}$ NMR (75 MHz, CD_2Cl_2 , 298 K): δ 24.0 ($\text{CH}(\text{CH}_3)_2$), 24.2 (CH_3), 39.6 (CH_2), 84.3 ($\text{CH}(\text{CH}_3)_2$), 121.7 (*o*-Ph), 125.9 (*p*-Ph), 129.0 (*m*-Ph), 147.7 (*i*-Ph), 174.6 ($\text{C}=\text{N}$). $^{19}\text{F}\{^1\text{H}\}$ NMR (188 MHz, CD_2Cl_2 , 298 K): δ -77.6 (br s, 6F).

Reaction of $\{\text{ON}^{\text{Ph,Ph}}\text{H}\}$ with $\text{TiCl}_2(\text{OiPr})_2$: Isolation of $\text{TiCl}(\text{OiPr})\{\text{ON}^{\text{Ph,Ph}}\}_2$ (5) and $[\text{TiCl}_3\{\text{ON}^{\text{Ph,Ph}}\}\{\text{ONH}^{\text{Ph,Ph}}\}]$ (6). A solution of $\text{Ti}(\text{OiPr})_4$ (10.0 mg, 35.2 μmol) in toluene (1 mL) was added to a solution of TiCl_4 (7.0 mg, 36.9 μmol) in toluene (1 mL). The mixture was stirred for 4 h at room temperature and then

(37) Similar catalytic behavior was observed upon using commercial MAO and DMAO (dried MAO from which most of the AlMe_3 has been removed).

(38) Zucchini, U.; Albizzati, E.; Giannini, U. *J. Organomet. Chem.* **1971**, *26*, 357.

cooled to $-30\text{ }^{\circ}\text{C}$. A solution of $\{\text{ON}^{\text{Ph,Ph}}\}\text{H}$ (50 mg, $138\text{ }\mu\text{mol}$) in hexane (4 mL), precooled at $-30\text{ }^{\circ}\text{C}$, was then added dropwise to the previous solution. The reaction mixture was gently warmed to room temperature overnight, after which time period colorless crystals appeared that proved suitable for X-ray diffraction studies (8.0 mg); the latter studies revealed that these crystals are a mixture of **5** and **6**. The ^1H and ^{19}F NMR spectra of this mixture showed many resonances that could not be assigned.

Reaction of $(\text{CF}_3)_2\text{C}(\text{OH})\text{CH}_2\text{C}(\text{=O})\text{CH}_3$ ($\{\text{OO}^{\text{Me}}\}\text{H}$) with $\text{TiCl}_2(\text{O}i\text{Pr})_2$: Synthesis of $\text{TiCl}(\text{O}i\text{Pr})\{\text{OO}^{\text{Me}}\}_2$. A solution of $\text{Ti}(\text{O}i\text{Pr})_4$ (145 mg, $510\text{ }\mu\text{mol}$) in toluene (3 mL) was added to a solution of TiCl_4 (97.0 mg, $511\text{ }\mu\text{mol}$) in toluene (3 mL). The mixture was stirred for 30 min at room temperature and then cooled to $-30\text{ }^{\circ}\text{C}$. A solution of $(\text{CF}_3)_2\text{C}(\text{OH})\text{CH}_2\text{C}(\text{=O})\text{CH}_3$ ($\{\text{OO}^{\text{Me}}\}\text{H}$) (445 mg, 1.99 mmol , 2 equiv vs Ti) in toluene (2 mL), precooled at $-30\text{ }^{\circ}\text{C}$, was then added dropwise to the previous solution. The reaction mixture was gently warmed to room temperature overnight, volatiles were removed under vacuum, and the solid residue was washed with pentane ($2 \times 3\text{ mL}$) and finally dried under vacuum to give $\text{TiCl}(\text{O}i\text{Pr})\{\text{OO}^{\text{Me}}\}_2$ as a white powder (280 mg, 48%). ^1H NMR (300 MHz, benzene- d_6 , 298 K): δ 1.29 (d, $^3J_{\text{HH}} = 6.0$, 6H, $\text{OCH}(\text{CH}_3)_2$), 1.49 (s, 6H, 2 CH_3), 2.75 (d, $^2J_{\text{HH}} = 16.0$, 2H, CHH), 2.99 (br d, $^2J_{\text{HH}} = 16.0$, 2H, CHH), 5.08 (hept, $^3J_{\text{HH}} = 6.0$, 1H, $\text{OCH}(\text{CH}_3)_2$). $^{13}\text{C}\{^1\text{H}\}$ NMR (75 MHz, benzene- d_6 , 298 K): δ 23.6 ($\text{CH}(\text{CH}_3)_2$), 31.5 (CH_3), 39.8 (CH_2), 87.6 ($\text{CH}(\text{CH}_3)_2$). $^{19}\text{F}\{^1\text{H}\}$ NMR (188 MHz, benzene- d_6 , 298 K): δ -77.8 (br m, 6F), -77.5 (br s, 6F). Anal. Calcd for $\text{C}_6\text{H}_5\text{Cl}_2\text{F}_6\text{O}_2\text{Ti}$: C, 21.08; H, 1.47. Found: C, 21.5; H, 1.8.

Reaction of $\{\text{ON}^{\text{Me,Ph}}\}\text{H}$ with $\text{Zr}(\text{CH}_2\text{Ph})_4$: Synthesis of $\text{Zr}(\text{CH}_2\text{Ph})_2\{\text{ON}^{\text{Me,Ph}}\}_2$ (7a**) and $\text{Zr}(\text{CH}_2\text{Ph})\{\text{ON}^{\text{Me,Ph}}\}\{\text{ON}^{\text{Me,Ph}}\}$ (**9a**).** A solution of $\{\text{ON}^{\text{Me,Ph}}\}\text{H}$ (200 mg, $668\text{ }\mu\text{mol}$) in toluene (ca. 1 mL) precooled at $-30\text{ }^{\circ}\text{C}$ was added to a solution of $\text{Zr}(\text{CH}_2\text{Ph})_4$ (152 mg, $334\text{ }\mu\text{mol}$) in toluene at $-30\text{ }^{\circ}\text{C}$. The mixture was kept standing in the freezer at $-30\text{ }^{\circ}\text{C}$ until some precipitate appeared. The supernatant solution was removed by pipet, and the solid residue was dried under vacuum to give **7a** as a yellow powder (182 mg, 29%). Suitable crystals for X-ray diffraction were grown from CD_2Cl_2 at $-10\text{ }^{\circ}\text{C}$. ^1H NMR (500 MHz, CD_2Cl_2 , 298 K): δ 1.81 (s, 6H, CH_3), 1.83 (s, 4H, CH_2), 1.92 (br s, 4H, CH_2Ph), 6.73–7.32 (m, 20H, Ph). $^{19}\text{F}\{^1\text{H}\}$ NMR (188 MHz, CD_2Cl_2 , 298 K): δ -77.0 (s, 12F). $^{13}\text{C}\{^1\text{H}\}$ NMR (125 MHz, CD_2Cl_2 , 298 K): δ 26.5 (CH_3), 36.8 (CH_2), 69.1 ($\text{CH}_2\text{-Ph}$), 178.6 ($\text{C}=\text{N}$); resonances for aromatic carbons were not assigned due to the presence of decomposition products (essentially **9a**, *vide infra*) that formed during data acquisition; resonances for quaternary carbons and CF_3 were not observed. Microanalysis of this compound was not possible due to its slow decomposition at room temperature in the solid state.

Decomposition of **7a** in toluene solution proceeded slowly at room temperature and was completed after one week, yielding **9a** as the major product (68% according to ^1H NMR). ^1H NMR (500 MHz, CD_2Cl_2 , 298 K): δ (ppm) 1.80 (s, 3H, CH_3), 1.84 (s, 3H, CH_3), 2.00 (d, $^2J_{\text{HH}} = 11.7$, 1H, CHH-Ph), 2.17 (d, $^2J_{\text{HH}} = 11.7$, 1H, CHH-Ph), 2.66 (d, $^2J_{\text{HH}} = 16.2$, 1H, CHH), 2.82 (d, $^2J_{\text{HH}} = 16.2$, 1H, CHH), 4.56 (s, 1H, CH), from 6.53 to 7.45 (m, 15H, Ph). $^{19}\text{F}\{^1\text{H}\}$ NMR (188 MHz, CD_2Cl_2 , 298 K): δ (ppm) -79.3 (br q, 3F), -78.9 (br q, 3F), -77.7 (br q, 3F), -77.5 (br q, 3F). $^{13}\text{C}\{^1\text{H}\}$ NMR (125 MHz, CD_2Cl_2 , 298 K): δ 25.2 (CH_3), 25.9 (CH_3), 39.4 (CH_2), 66.6 (CH_2Ph), 94.4 (CH), 181.0 ($\text{C}=\text{N}$); for the same reasons as for **7a**, other resonances for **9a** could not be attributed or were not observed.

Reaction of $\{\text{ON}^{\text{Ph,Ph}}\}\text{H}$ with $\text{Zr}(\text{CH}_2\text{Ph})_4$: Synthesis of $\text{Zr}(\text{CH}_2\text{Ph})_2\{\text{ON}^{\text{Ph,Ph}}\}_2$ (7b**) and $\text{Zr}(\text{CH}_2\text{Ph})\{\text{ON}^{\text{Ph,Ph}}\}\{\text{ON}^{\text{Ph,Ph}}\}$ (**9b**).** NMR-scale reaction. In the glovebox, a Teflon-valved NMR tube was charged with pro-ligand $\{\text{ON}^{\text{Ph,Ph}}\}\text{H}$ (21.0 mg, $58.0\text{ }\mu\text{mol}$) and $\text{Zr}(\text{CH}_2\text{Ph})_4$ (13.0 mg, $28.5\text{ }\mu\text{mol}$). CD_2Cl_2 (ca. 0.5 mL) was vacuum-transferred in at low temperature, and the tube was kept at $-20\text{ }^{\circ}\text{C}$ for a few minutes until NMR was run immediately at

room temperature. ^1H NMR spectroscopy showed quantitative and selective conversion of the reagents into **7b**. Repeated NMR data acquisitions after a short time period showed the appearance of resonances characteristic for the decomposition compound **9b** and toluene. Complete and selective decomposition of **7b** into **9b** was observed after 10 min. Preparation of X-ray suitable single crystals of **7b**: In the glovebox, a solution of $\{\text{ON}^{\text{Ph,Ph}}\}\text{H}$ (40.0 mg, $110\text{ }\mu\text{mol}$) in toluene (ca. 1 mL) precooled at $-30\text{ }^{\circ}\text{C}$ was added to a solution of $\text{Zr}(\text{CH}_2\text{Ph})_4$ (25.0 mg, $54.9\text{ }\mu\text{mol}$) in toluene (ca. 1 mL) at $-30\text{ }^{\circ}\text{C}$. The mixture was kept standing in the freezer at $-30\text{ }^{\circ}\text{C}$ until crystals of **7b** appeared on the walls of the vial and were collected for X-ray data diffraction studies. $\text{Zr}(\text{CH}_2\text{Ph})_2\{\text{ON}^{\text{Ph,Ph}}\}_2$ (**7b**): ^1H NMR (300 MHz, CD_2Cl_2 , 298 K): δ 2.05 (br s, 8H, CH_2), 6.75–7.26 (m, 30H, Ph). $^{19}\text{F}\{^1\text{H}\}$ NMR (188 MHz, CD_2Cl_2 , 298 K): δ -76.5 (s, 12F). $^{19}\text{F}\{^1\text{H}\}$ NMR (188 MHz, toluene- d_8 , 298 K): δ -80.9 (s, 12F). ^{13}C NMR and microanalysis of this compound were not possible due to its slow decomposition in solution as well as in the solid state. $\text{Zr}(\text{CH}_2\text{Ph})\{\text{ON}^{\text{Ph,Ph}}\}\{\text{ON}^{\text{Ph,Ph}}\}$ (**9b**): ^1H NMR (300 MHz, CD_2Cl_2 , 298 K): δ 1.91 (d, $^2J_{\text{HH}} = 11.8$, 1H, CHH-Ph), 2.21 (d, $^2J_{\text{HH}} = 11.8$, 1H, CHH-Ph), 3.22 (d, $^2J_{\text{HH}} = 17.3$, 1H, CHH), 3.32 (d, $^2J_{\text{HH}} = 17.3$, 1H, CHH), 5.09 (s, 1H, CH), 6.63–7.26 (m, 25H, Ph). ^1H NMR (500 MHz, toluene- d_8 , 298 K): δ 2.08 (d, $^2J_{\text{HH}} = 12.0$, 1H, CHHPh), 2.33 (d, $^2J_{\text{HH}} = 12.0$, 1H, CHHPh), 2.98 (s, 2H, CH_2), 5.36 (s, 1H, CH), 6.71–7.13 (m, 25H, Ph). $^{19}\text{F}\{^1\text{H}\}$ NMR (188 MHz, CD_2Cl_2 , 298 K): δ -79.2 (q, $^4J_{\text{FF}} = 9.2$, 3F), -78.5 (q, $^4J_{\text{FF}} = 9.2$, 3F), -78.3 (q, $^4J_{\text{FF}} = 10.3$, 3F), -76.9 (q, $^4J_{\text{FF}} = 10.3$, 3F). $^{19}\text{F}\{^1\text{H}\}$ NMR (188 MHz, toluene- d_8 , 298 K): δ -83.8 (q, $^1J_{\text{FF}} = 9.4$, 3F), -83.0 (2q overlapping, 6F), -81.5 (q, $^4J_{\text{FF}} = 9.4$, 3F). Anal. Calcd for $\text{C}_4\text{H}_{30}\text{F}_{12}\text{N}_2\text{O}_2\text{Zr}$: C, 54.60; H, 3.35; N, 3.11. Found: C, 54.3; H, 3.4; N, 3.0.

NMR-Scale Reaction of $\{\text{ON}^{\text{Ph,Bn}}\}\text{H}$ with $\text{Zr}(\text{CH}_2\text{Ph})_4$: Synthesis of $\text{Zr}(\text{CH}_2\text{Ph})\{\text{ON}^{\text{Ph,Bn}}\}\{\text{ON}^{\text{Ph,Bn}}\}$ (9c**).** A Teflon-valved NMR tube was charged with $\{\text{ON}^{\text{Ph,Bn}}\}\text{H}$ (20.0 mg, $53.3\text{ }\mu\text{mol}$) and $\text{Zr}(\text{CH}_2\text{Ph})_4$ (12.1 mg, $26.5\text{ }\mu\text{mol}$), and CD_2Cl_2 (ca. 0.5 mL) was vacuum-transferred in at $-78\text{ }^{\circ}\text{C}$. The tube was kept at low temperature until NMR was recorded at room temperature, which showed complete conversion of the reagents to **9c** (resonances for **7c** were not observed). ^1H NMR (300 MHz, CD_2Cl_2 , 298 K): δ 1.71 (d, $^2J_{\text{HH}} = 10.8$, 1H, Zr-CHHPh), 2.05 (d, $^2J_{\text{HH}} = 10.8$, 1H, Zr-CHHPh), 3.10 (d, $^2J_{\text{HH}} = 17.4$, 1H, CHHC=N), 3.25 (d, $^2J_{\text{HH}} = 17.4$, 1H, CHHC=N), 4.36 (d, $^2J_{\text{HH}} = 17.0$, 1H, NCHHPh), 4.60 (d, $^2J_{\text{HH}} = 17.0$, 1H, NCHHPh), 4.60 (s, 1H, CH), 4.78 (d, $^2J_{\text{HH}} = 13.8$, 1H, NCHHPh), 5.17 (d, $^2J_{\text{HH}} = 13.8$, 1H, NCHHPh), 6.81–7.45 (m, 25H, Ph). $^{19}\text{F}\{^1\text{H}\}$ NMR (188 MHz, CD_2Cl_2 , 298 K): δ -78.4 (q, $^4J_{\text{FF}} = 9.4$, 3F), -77.9 (2q overlapping, 6F), -77.2 (q, $^1J_{\text{FF}} = 9.4$, 3F). Anal. Calcd for $\text{C}_{43}\text{H}_{34}\text{F}_{12}\text{N}_2\text{O}_2\text{Zr}$: C, 55.54; H, 3.69; N, 3.01. Found: C, 55.1; H, 3.9; N, 2.8.

Reaction of $\{\text{ON}^{\text{Me,Ph}}\}\text{H}$ with $\text{Hf}(\text{CH}_2\text{Ph})_4$: Synthesis of $\text{Hf}(\text{CH}_2\text{Ph})_2\{\text{ON}^{\text{Me,Ph}}\}_2$ (8a**) and $\text{Hf}(\text{CH}_2\text{Ph})\{\text{ON}^{\text{Me,Ph}}\}\{\text{ON}^{\text{Me,Ph}}\}$ (**10a**).** A Schlenk flask was charged with $\{\text{ON}^{\text{Me,Ph}}\}\text{H}$ (101.5 mg, 0.34 mmol) and $\text{Hf}(\text{CH}_2\text{Ph})_4$ (93.0 mg, 0.17 mmol), and toluene (ca. 5 mL) was vacuum-transferred in at $-78\text{ }^{\circ}\text{C}$. The reaction mixture was stirred at room temperature for 1 h, over which time period some precipitate formed. The supernatant solution was removed by cannula, and the solid residue was dried under the vacuum, giving **8a** as an off-white solid (85 mg, 52%). The NMR tube was charged with this solid, and toluene- d_8 was vacuum-transferred in (ca. 0.5 mL). Crystals of **8a** suitable for X-ray diffraction studies were obtained by recrystallization from toluene. ^1H NMR (200 MHz, toluene- d_8 , 298 K): δ 1.14 (s, 6H, CH_3), 1.43 (s, 4H, CH_2), 1.84 (br s, 4H, CH_2Ph), 6.48–7.10 (m, 20H, Ph). $^{19}\text{F}\{^1\text{H}\}$ NMR (188 MHz, toluene- d_8 , 298 K): δ -76.5 (s, 12F). Anal. Calcd for $\text{C}_{38}\text{H}_{34}\text{F}_{12}\text{HfN}_2\text{O}_2$: C, 47.68; H, 3.58; N, 2.93. Found: C, 47.3; H, 3.4; N, 2.7. When a toluene- d_8 solution of **8a** was kept for 10 days at room temperature, the complex decomposed to form mainly **10a** (ca. 65%, as determined by ^1H NMR), as well as other minor (ca. 35%) unidentified secondary products. ^1H NMR

(200 MHz, CD₂Cl₂, 298 K): δ 1.48 (s, 3H, CH₃), 1.80 (d, $^2J_{\text{HH}} = 9.4$, 1H, CHHPPh), 1.98 (s, 3H, CH₃), 2.00 (d, $^2J_{\text{HH}} = 9.4$, 1H, CHHPPh), 2.67 (d, $^2J_{\text{HH}} = 16.5$, 1H, CHH), 2.87 (d, $^2J_{\text{HH}} = 16.5$, 1H, CHH), 4.51 (s, 1H, CH), 6.57–7.48 (m, 15H, Ph). $^{19}\text{F}\{^1\text{H}\}$ NMR (188 MHz, CD₂Cl₂, 298 K): δ -79.6 (q, $^4J_{\text{FF}} = 9.4$, 3F), -79.1 (q, $^4J_{\text{FF}} = 9.4$, 3F), -78.1 (q, $^4J_{\text{FF}} = 9.4$, 3F), -77.6 (q, $^4J_{\text{FF}} = 9.4$, 3F).

NMR-Scale Reaction of {ON^{Ph,Ph}}H with Hf(CH₂Ph)₄: Generation of Hf(CH₂Ph)₂{ON^{Ph,Ph}}₂ (8b) and Hf(CH₂Ph){ON^{Ph,Ph}}{ON^{Ph,Ph}} (10b). A Teflon-valved NMR tube was charged with {ON^{Ph,Ph}}H (30.0 mg, 83.0 μmol) and Hf(CH₂Ph)₄ (22.5 mg, 41.4 μmol), and toluene-*d*₈ (ca. 0.5 mL) was vacuum-transferred in at -78 °C. The tube was kept at -78 °C until NMR spectroscopy was recorded at room temperature. ^1H NMR spectroscopy recorded after 1 min at this temperature revealed that all reagents were consumed and that transient **8b** quantitatively decomposed into **10b** and toluene. ^1H NMR (500 MHz, benzene-*d*₆, 298 K): δ 2.19 (d, $^2J_{\text{HH}} = 12.9$, 1H, CHHPPh), 2.39 (d, $^2J_{\text{HH}} = 12.9$, 1H, CHHPPh), 3.04 (s, 2H, CH₂), 5.46 (s, 1H, CH), 6.78–7.27 (m, 25H, Ph). ^1H NMR (200 MHz, toluene-*d*₈, 298 K): δ 2.02 (d, $^2J_{\text{HH}} = 12.9$, 1H, CHHPPh), 2.22 (d, $^2J_{\text{HH}} = 12.9$, 1H, CHHPPh), 2.94 (s, 2H, CH₂), 5.29 (s, 1H, CH), 6.71–7.13 (m, 25H, Ph). $^{19}\text{F}\{^1\text{H}\}$ NMR (188 MHz, toluene-*d*₈, 298 K): δ -79.0 (q, $^1J_{\text{FF}} = 9.4$, 3F), -78.2 (2 q overl., $^1J_{\text{FF}} = 9.4$, 6F), -76.5 (q, $^1J_{\text{FF}} = 9.4$, 3F). $^{19}\text{F}\{^1\text{H}\}$ NMR (188 MHz, benzene-*d*₆, 298 K): δ -78.9 (q, $^4J_{\text{FF}} = 9.4$, 3F), -78.2 (q, $^4J_{\text{FF}} = 9.4$, 3F), -78.1 (q, $^4J_{\text{FF}} = 9.4$, 3F), -76.5 (q, $^4J_{\text{FF}} = 9.4$, 3F).

Reaction of {ON^{Me,ArF}}H with Zr(CH₂Ph)₄: Synthesis of Zr(CH₂Ph)₂{ON^{Me,ArF}}₂ (7d) and Zr{ON^{Me,ArF}}₂{ON^{Me,ArF}} (11). A Teflon-valved NMR tube was charged with {ON^{Me,ArF}}H (68.3 mg, 175.5 μmol) and Zr(CH₂Ph)₄ (40.0 mg, 87.8 μmol), and toluene-*d*₈ (ca. 0.5 mL) was vacuum-transferred in at -78 °C. The tube was kept for 3–4 h at -30 °C, and afterward NMR spectroscopy was recorded at room temperature. The formation of **7d** proceeded in ca. 80% yield according to ^1H NMR. Green-yellow crystals of **7d** suitable for X-ray diffraction studies were obtained by cooling the solution at -30 °C for 20 h (10 mg, 11% yield). ^1H NMR (500 MHz, toluene-*d*₈, 298 K): δ 1.19 (s, 6H, CH₃), 2.38 (s, 4H, CH₂Ph), 2.74 (s, 4H, CH₂), 6.86–7.09 (m, 10H, Ph). $^{19}\text{F}\{^1\text{H}\}$ NMR (188 MHz, toluene-*d*₈, 298 K): δ -167.2 (m, 4F, *m*-F), -162.7 (t, 2F, *p*-F), -151.9 (br s, 4F, *o*-F), -82.3 (s, 12F, CF₃). Due to the instability of **7d** at room temperature in toluene solution, ^{13}C NMR and HETCOR spectra were not recorded. The toluene solution of **7d** was kept in the glovebox at ambient temperature for one day, after which time period pale-yellow crystals of **11** suitable for X-ray diffraction studies were recovered (36.3 mg, 33% yield). ^1H NMR (500 MHz, benzene-*d*₆, 298 K): δ 1.02 (s, 3H, CH₃), 1.04 (s, 6H, CH₃), 3.16 (s, 4H, CH₂), 4.82 (s, 1H, CH). $^{13}\text{C}\{^1\text{H}\}$ NMR (125 MHz, benzene-*d*₆, 298 K): δ 22.3 (CH₃), 26.0 (CH₃), 39.8 (CH₂), 81.3 (C(CF₃)₂), 99.3 (CH), 150.0 (CH=C(CH₃)N), 193.3 (C=N); the remaining resonances were not observed by HMQC and HMBC methods. $^{19}\text{F}\{^1\text{H}\}$ NMR (188 MHz, benzene-*d*₆, 298 K): δ -165.5 (m, 2F, *p*-F), -161.9 (m, 5F, *m*- and *p*-F), -155.9 (m, 2F, *m*-F), -149.2–-146.7 (br m, 6F, *o*-F), -78.0 (s, 6F, CF₃), -77.5 (s, 12F, CF₃). Anal. Calcd for C₃₆H₁₄F₃₃N₃O₃Zr: C, 34.46; H, 1.12; N, 3.35. Found: C, 35.10; H, 1.50; N, 3.3.

Synthesis of ZrCl₂{ON^{Me,Ph}}₂ (12a). A slurry of ZrCl₄ (192 mg, 0.824 mmol) in toluene (30 mL) was cooled at -78 °C, and *n*BuLi (0.66 mL of a 2.5 M solution in hexanes, 1.65 mmol, 2 equiv) was added dropwise. After 25 min of stirring at room temperature, the light brown solution was cooled at -50 °C, and a solution of {ON^{Me,Ph}}H (496 mg, 1.66 mmol) in toluene (10 mL) was added dropwise. The reaction mixture was stirred at room temperature overnight and then filtered. The clear filtrate was concentrated under vacuum, and the resulting sticky residue was washed with dry hexane (ca. 5 mL) and dried under vacuum to give **12a** as a white powder (245 mg, 39%). Anal. Calcd for C₂₄H₂₀Cl₂F₁₂N₂O₂Zr: C,

38.00; H, 2.66; N, 3.69. Found: C, 38.1; H, 2.8; N, 3.6. NMR revealed that this product is a 70:30 mixture of two isomers: the major one is C_{2v}-symmetric and the minor one is C₁-symmetric. Heating of this mixture at 70 °C for 48 h in benzene-*d*₆ led to a 77:23 mixture of C_{2v}- and C₁-**12b**, as monitored by ^1H NMR. When this mixture of isomers was extracted in hot hexanes, the insoluble powder left after filtration was shown to be exclusively the C₁-symmetric isomer. C_{2v}-**12a**: ^1H NMR (500 MHz, benzene-*d*₆, 298 K): δ (ppm) 1.09 (s, 6H, CH₃), 3.03 (s, 4H, CH₂), 6.82 (d, $^3J_{\text{HH}} = 7.6$ Hz, 4H, *o*-Ph), 6.95 (t, $^3J_{\text{HH}} = 7.6$ Hz, 2H, *p*-Ph), 7.07 (t, $^3J_{\text{HH}} = 7.6$ Hz, 4H, *m*-Ph). $^{13}\text{C}\{^1\text{H}\}$ NMR (125 MHz, benzene-*d*₆, 298 K): δ 25.1 (CH₃), 40.0 (CH₂), 81 (m, C(CF₃)₂), 123.1 (*o*-Ph), 123.6 (q, $^1J_{\text{CF}} = 303.7$, CF₃), 127.1 (*p*-Ph), 129.4 (*m*-Ph), 146.6 (*i*-Ph), 183.2 (C=N). $^{19}\text{F}\{^1\text{H}\}$ NMR (188 MHz, benzene-*d*₆, 298 K): δ -76.5 (s, 12F). C₁-**12a**: ^1H NMR (500 MHz, benzene-*d*₆, 298 K): δ 1.15 (s, 3H, CH₃), 1.53 (s, 3H, CH₃), 2.70 (d, $^2J_{\text{HH}} = 15.0$, 1H, CHH), 3.17 (d, $^2J_{\text{HH}} = 15.8$, 1H, CHH), 3.55 (d, $^2J_{\text{HH}} = 15.0$, 1H, CHH), 4.27 (d, $^2J_{\text{HH}} = 15.8$, 1H, CHH), 5.37 (br d, $^3J_{\text{HH}} = 7.2$, 1H, *o*-Ph), 6.63–7.25 (m, 8H, Ph), 8.19 (br d, $^3J_{\text{HH}} = 7.5$, 1H, *o*-Ph). $^{19}\text{F}\{^1\text{H}\}$ NMR (188 MHz, benzene-*d*₆, 298 K): δ -79.1 (br s, 3F), -77.8 (br s, 3F), -75.5 (q, $^1J_{\text{FF}} = 10.3$, 3F), -75.1 (br s, 3F). $^{13}\text{C}\{^1\text{H}\}$ NMR (125 MHz, benzene-*d*₆, 298 K): δ 25.6 (CH₃), 26.6 (CH₃), 39.0 (CH₂), 40.3 (CH₂), 80.5 (m, C(CF₃)₂), 81.4 (m, C(CF₃)₂), 120.7 (*o*-Ph), 123.0 (*o*-Ph), 124.7 (q, $^1J_{\text{CF}} = 297.1$, CF₃), 124.8 (q, $^1J_{\text{CF}} = 312.4$, CF₃), 125.4 (*o*-Ph), 125.9 (*p*-Ph), 126.0 (*o*-Ph), 126.4 (*p*-Ph), 129.0 (*m*-Ph), 129.3 (2 *m*-Ph), 130.0 (*m*-Ph), 148.4 (*i*-Ph), 149.5 (*i*-Ph), 177.4 (C=N), 182.8 (C=N).

Synthesis of ZrCl₂{ON^{Ph,Ph}}₂ (12b). This compound was prepared following a procedure similar to the one described above for **12a**, starting from ZrCl₄ (161 mg, 0.691 mmol) and {ON^{Ph,Ph}}H (500 mg, 1.384 mmol). Compound **12b** was obtained as a white powder (170 mg, 28%), which proved to be a 30:70 mixture of a C_{2v}-symmetric and a C₁-symmetric isomer. Heating of this mixture at 70 °C for 2.5 days in benzene-*d*₆ led to the complete and selective transformation to C_{2v}-**12b**, as monitored by ^1H NMR. Extraction of the C_{2v}/C₁-mixture with hot hexanes left a residue that proved to be analytically pure C₁-**12b**. C_{2v}-**12b**: ^1H NMR (300 MHz, benzene-*d*₆, 298 K): δ 3.66 (s, 4H, CH₂), 6.46–7.42 (m, 20H, Ph). $^{19}\text{F}\{^1\text{H}\}$ NMR (188 MHz, benzene-*d*₆, 298 K): δ -76.5 (s, 12F). C₁-**12b**: ^1H NMR (500 MHz, benzene-*d*₆, 298 K): δ 3.42 (d, $^2J_{\text{HH}} = 15.5$, 1H, CHH), 3.94 (d, $^2J_{\text{HH}} = 17.0$, 1H, CHH), 4.32 (d, $^2J_{\text{HH}} = 15.5$, 1H, CHH), 5.01 (d, $^2J_{\text{HH}} = 17.0$, 1H, CHH), 5.44 (br d, 1H, *o*-Ph), 6.3 (br t, 1H, *m*-Ph), 6.54 (m, 1H, Ph), 6.60–6.68 (m, 10H, Ph), 6.84 (t, $^3J_{\text{HH}} = 7.9$, 2H, Ph), 7.21 (br t, 1H, *m*-Ph), 7.46 (m, 3H, Ph), 8.77 (br d, 1H, *o*-Ph). $^{19}\text{F}\{^1\text{H}\}$ NMR (188 MHz, benzene-*d*₆, 298 K): δ (ppm) -78.8 (br m, 3F), -77.7 (br m, 3F), -74.8 (2 m overl., 6F). Anal. Calcd for C₃₄H₂₄Cl₂F₁₂N₂O₂Zr: C, 46.26; H, 2.74; N, 3.17. Found: C, 46.5; H, 2.9; N, 3.3.

Synthesis of ZrCl₂{ON^{Me,ArF}}₂ (12c). To a solution of {ON^{Me,ArF}}H (0.70 g, 1.80 mmol) in Et₂O (30 mL) kept at -78 °C was added dropwise *n*BuLi (0.72 mL of a 2.5 M solution in hexanes, 1.80 mmol). The reaction mixture was stirred for 3 h at -78 °C and then allowed to warm to room temperature over 1 h. Volatiles were removed under vacuum, and solid ZrCl₄ (0.21 g, 0.90 mmol) was added to the mixture in the glovebox. Et₂O (30 mL) was vacuum-transferred to the reaction mixture, and the latter was stirred for 12 h at room temperature. Volatiles were removed under vacuum, and dichloromethane (30 mL) was vacuum-transferred onto the solid residue. The resulting solution was filtered off, the pale pink solution was concentrated to ca. 5–7 mL, hexane (5 mL) was added, and the solution was left at -30 °C. After 10 h, a pink microcrystalline solid precipitated out. This was separated and dried under vacuum to give **12c** as a white solid (0.100 g, 12%). This compound featured extremely poor solubility in all common solvents, which hampered characterization by NMR. Anal. Calcd for C₂₄H₁₀Cl₂F₂₂N₂O₂Zr: C, 30.72; H, 1.07; N, 2.99. Found: C, 30.5; H, 1.0; N, 3.1.

Reaction of {ON^{R1,R2}}H with Na: Synthesis of {ON^{R1,R2}}Na. {ON^{Ph,Ph}}Na: In a typical experiment, in the glovebox, a Schlenk flask was charged with {ON^{Ph,Ph}}H (514 mg, 1.42 mmol) and Na powder (32.7 mg, 1.42 mmol). Dry THF (ca. 10 mL) was vacuum-transferred in at -78 °C, and the mixture was stirred overnight at room temperature. Volatiles were removed under vacuum, and the solid residue was washed with hexane (ca. 5 mL) and dried under vacuum to give {ON^{Ph,Ph}}Na as a white powder (355 mg, 65%). ¹H NMR (200 MHz, benzene-*d*₆, 298 K): δ 3.21 (s, 2H, CH₂), 6.78–7.05 (m, 10H, Ph). ¹⁹F{¹H} NMR (188 MHz, benzene-*d*₆, 298 K): δ -78.5 (s, 6F, CF₃). Anal. Calcd for C₁₇H₁₂F₆NNaO: C, 53.27; H, 3.16; N, 3.65. Found: C, 53.4; H, 3.3; N, 3.6. Synthesis of {ON^{Me,Ph}}Na: This compound was prepared following a similar procedure to the one described above for {ON^{Ph,Ph}}Na, starting from {ON^{Me,Ph}}H (500 mg, 1.67 mmol) and Na powder (38.5 mg, 1.67 mmol). {ON^{Me,Ph}}Na was obtained as a white powder (370 mg, 69%). ¹H NMR (500 MHz, THF-*d*₈, 298 K): δ 1.79 (s, 3H, CH₃), 2.64 (s, 2H, CH₂), 6.60 (br d, 2H, *o*-Ph), 7.00 (t, ³J_{HH} = 7.8, 1H, *p*-Ph), 7.22 (m, 2H, *m*-Ph). ¹⁹F{¹H} NMR (188 MHz, THF-*d*₈, 298 K): δ -81.0 (s, 6F, CF₃). Anal. Calcd for C₁₂H₁₀F₆NNaO: C, 44.87; H, 3.14; N, 4.36. Found: C, 45.0; H, 3.2; N, 4.2.

Reaction of {ON^{R1,R2}}H with KH: Synthesis of {ON^{R1,R2}}K and {ON^{-R1,R2}}K₂. (a) {ON^{Me,ArF}}K. This compound was prepared following a similar procedure to the one described above for {ON^{Ph,Ph}}Na, starting from {ON^{Me,ArF}}H (120 mg, 0.308 mmol) and KH (13.0 mg, 0.324 mmol). {ON^{Me,Ph}}K was obtained as a white powder (80 mg, 61%). ¹H NMR (500 MHz, THF-*d*₈, 298 K): δ 2.04 (s, 3H, CH₃), 2.81 (s, 2H, CH₂). ¹⁹F{¹H} NMR (188 MHz, THF-*d*₈, 298 K): δ -167.4 (t, ³J_{CF} = 20.7, 1F, *p*-CF), -166.5 (t, ³J_{CF} = 20.7, 2F, *m*-CF), -154.7 (d, ³J_{CF} = 20.7, 2F, *o*-CF), -79.2 (s, 6F, CF₃).

(b) {ON^{Me,Ph}}K. This compound was prepared following a similar procedure to the one described above for {ON^{Ph,Ph}}Na, starting from {ON^{Me,Ph}}H (99.0 mg, 0.331 mmol) and KH (13.2 mg, 0.331 mmol). The reaction time was 1 h, and {ON^{Me,Ph}}K was obtained as an off-white powder (72 mg, 65%). ¹H NMR (500 MHz, THF-*d*₈, 298 K): δ 1.82 (s, 3H, CH₃), 2.65 (s, 2H, CH₂), 6.61 (d, ³J_{HH} = 7.9, 2H, *o*-Ph), 6.96 (t, ³J_{HH} = 7.9, 1H, *p*-Ph), 7.21 (t, ³J_{HH} = 7.9, 2H, *m*-Ph). ¹⁹F{¹H} NMR (188 MHz, THF-*d*₈, 298 K): δ -78.8 (s, 6F, CF₃).

(c) {ON^{-Me,Ph}}K₂. This compound was prepared as described above, starting from {ON^{Me,Ph}}H (100 mg, 0.334 mmol) and KH (26.7 mg, 0.667 mmol) and leaving the reaction overnight. {ON^{-Me,Ph}}K₂ was obtained as an off-white powder (86 mg, 69%). ¹H NMR (500 MHz, THF-*d*₈, 298 K): δ 1.68 (s, 3H, CH₃), 4.87 (s, 1H, =CH), 6.63 (d, ³J_{HH} = 7.6, 2H, *o*-Ph), 6.85 (t, ³J_{HH} = 7.6, 1H, *p*-Ph), 7.16 (t, ³J_{HH} = 7.6, 2H, *m*-Ph). ¹⁹F{¹H} NMR (188 MHz, THF-*d*₈, 298 K): δ -75.6 (s, 6F, CF₃). Anal. Calcd for C₁₂H₉F₆K₂NO: C, 38.39; H, 2.42; N, 3.73. Found: C, 38.1; H, 2.5; N, 3.7.

Crystal Structure Determinations. As stated above, suitable crystals for X-ray diffraction analysis of **1**, **3a**, **4**, **5**, **6**, **7a**, **7b**, **7d**, **8a**, and **11** were obtained by recrystallization of purified products or in the course of synthetic reactions. Diffraction data were collected at 100 K using a Bruker APEX CCD diffractometer with graphite-monochromated Mo K α radiation ($\lambda = 0.71073$ Å). A combination of ω and ϕ scans was carried out to obtain at least a unique data set. The crystal structures were solved by means of the Patterson method; remaining atoms were located from difference Fourier synthesis followed by full-matrix least-squares refinement based on F^2 (programs SHELXS-97 and SHELXL-97).³⁹ Many hydrogen atoms could be found from the Fourier difference analysis. Carbon-bound hydrogen atoms were placed at calculated positions

and forced to ride on the attached atom. The hydrogen atom contributions were calculated but not refined. All non-hydrogen atoms were refined with anisotropic displacement parameters. The locations of the largest peaks in the final difference Fourier map calculation as well as the magnitude of the residual electron densities were of no chemical significance. In **5**, one trifluoromethyl group was found to be disordered and accordingly modeled. Crystals of **6** and **11** were found to contain lattice disordered solvent molecules (toluene), which could not be sufficiently modeled in the refinement cycles. These molecules were removed using the SQUEEZE procedure⁴⁰ implemented in the PLATON package.⁴¹ Crystal data and details of data collection and structure refinement for the different compounds are given in Table 1. Crystallographic data are also available as cif files (see the Supporting Information).

Ethylene Polymerization. Polymerization experiments (Table 2) were performed in a 320 mL high-pressure glass reactor equipped with a mechanical stirrer and externally heated with a double mantle with a circulating water bath as desired. The reactor was filled with toluene (50 mL) and MAO (30 wt % solution in toluene, 3.0–3.8 mL, 1100–1500 equiv) or Al(*i*Bu)₃ (0.5–3.2 mL, 40–100 equiv) and [Ph₃C][B(C₆F₅)₄] (25–60 mg, 2–3 equiv) and pressurized at 7–8 atm of ethylene (Air Liquide, 99.99%). The reactor was thermally equilibrated at the desired temperature for 1 h. Ethylene pressure was decreased to 1 atm, and the catalyst precursor (12–32 μ mol) in toluene (ca. 1 mL) was added by syringe. The ethylene pressure was immediately increased to 7–8 atm, and the solution was stirred for the desired time. Ethylene consumption was monitored using an electronic manometer connected to a secondary 100 mL ethylene tank, which feeds the reactor by maintaining constant the total pressure. The polymerization was stopped by venting of the vessel and quenching with a 10% HCl solution in methanol (ca. 3 mL). The polymer was precipitated in methanol (ca. 200 mL), and 35% aqueous HCl (ca. 1 mL) was added to dissolve possible catalyst residues. The polymer was collected by filtration, washed with methanol (ca. 200 mL), and dried under vacuum overnight.

Melting temperatures of PE samples were determined on a Perkin-Elmer Pyris 1 differential scanning calorimeter (10 °C/min, nitrogen flow, first pass). Gel permeation chromatography (GPC) analyses were performed at the University of Chicago on a Polymer Laboratories PL-GPC 220 instrument using 1,2,4-trichlorobenzene as solvent (stabilized with 125 ppm BHT) at 150 °C. A set of three PLgel 10 μ m Mixed-B or Mixed-B LS columns was used. Samples were prepared at 160 °C and filtered through 2 or 5 μ m stainless steel frits prior to injection. Molecular weights were determined versus polystyrene standards and are reported relative to polyethylene standards, as calculated by the universal calibration method using Mark–Houwink parameters ($K = 17.5 \times 10^{-5}$, $\alpha = 0.670$ for polystyrene; $K = 40.6 \times 10^{-5}$, $\alpha = 0.725$ for polyethylene).

Acknowledgment. This work was financially supported in part by Agence Nationale de la Recherche (grant ANR-06-BLAN-0213) and Total Co. (Ph.D. grant to N.M.; postdoctoral fellowship to E.K.). We are most grateful to Prof. R. F. Jordan (Univ. Chicago) for HT-GPC analyses. J.F.C. thanks the Institut Universitaire de France for a Junior IUF fellowship (2005–2009).

Supporting Information Available: Crystallographic data for **1**, **3a**, **4**, **5**, **6**, **7a**, **7b**, **7d**, **8a**, and **11** as CIF files; representative GPC traces and DSC profiles of PEs prepared. This material is available free of charge via the Internet at <http://pubs.acs.org>.

OM8009409

(39) (a) Sheldrick, G. M. *SHELXS-97*, Program for the Determination of Crystal Structures; University of Goettingen: Germany, 1997. (b) Sheldrick, G. M. *SHELXL-97*, Program for the Refinement of Crystal Structures; University of Goettingen: Germany, 1997.

(40) van der Sluis, P.; Spek, A. L. *Acta Crystallogr.* **1990**, *A46*, 194.

(41) Spek, A. L. *Acta Crystallogr.* **1990**, *A46*, C-34.

Hypercoordinate Organosilicon Complexes of an ONN'O' Chelating Ligand: Regio- and Diastereoselectivity of Rearrangement Reactions in Si–Salphen Systems

Katrin Lippe, Daniela Gerlach, Edwin Kroke, and Jörg Wagler*

Institut für Anorganische Chemie, Technische Universität Bergakademie Freiberg, Leipziger Strasse 29, D-09596 Freiberg, Germany

Received October 30, 2008

Reactions of various organochlorosilanes with the salphen-like tetradentate (ONN'O') ligand *o*-HO-*p*-MeO-C₆H₃C(Ph)=N(*o*-C₆H₄)N=CHC₆H₄-*o*-OH, bearing two chemically and sterically different imine moieties, provided insights into the regio- and diastereoselectivity of various rearrangement reactions. Whereas thermally driven allyl- and UV-induced phenyl-shift reactions from the Si to an imine carbon atom yield one diastereomer, hydride-shift reactions were found to be less diastereoselective; however, only the sterically less demanding salicylaldimine site was attacked in all these rearrangement reactions.

Introduction

The coordination number of the silicon atom in various silicon complexes¹ exerts great influence on both the reactivity and electronic properties² of these compounds. Examples include a broad range of Si–X bond activation by hypercoordination: e.g.,

* To whom correspondence should be addressed. Tel.: (+49) 3731 39 3556 or (+49) 3731 39 4343. Fax: (+49) 3731 39 4058. E-mail: joerg.wagler@chemie.tu-freiberg.de.

(1) Selected reviews on hypercoordinate silicon compounds: (a) Chuit, C.; Corriu, R. J. P.; Reye, C.; Young, J. C. *Chem. Rev.* **1993**, *93*, 1371. (b) Tacke, R.; Pülm, M.; Wagner, B. *Adv. Organomet. Chem.* **1999**, *44*, 221. (c) Kost, D.; Kalikhman, I. *Adv. Organomet. Chem.* **2004**, *50*, 1. (d) Voronkov, M. G.; Trofimova, O. M.; Bolgova, Yu. I.; Chernov, N. F. *Russ. Chem. Rev.* **2007**, *76*, 825. Selected recent publications dealing with hypercoordinate silicon compounds: (e) Fester, G. W.; Wagler, J.; Brendler, E.; Böhme, U.; Roewer, G.; Kroke, E. *Chem. Eur. J.* **2008**, *14*, 3164. (f) Haga, R.; Burschka, C.; Tacke, R. *Organometallics* **2008**, *27*, 4394. (g) Theis, B.; Burschka, C.; Tacke, R. *Chem. Eur. J.* **2008**, *14*, 4618. (h) González-García, G.; Gutiérrez, J. A.; Cota, S.; Metz, S.; Bertermann, R.; Burschka, C.; Tacke, R. *Z. Anorg. Allg. Chem.* **2008**, *634*, 1281. (i) Negrebetsky, V. V.; Taylor, P. G.; Kramarova, E. P.; Shipov, A. G.; Pogozhikh, S. A.; Ovchinnikov, Yu. E.; Korlyukov, A. A.; Bowden, A.; Bassindale, A. R.; Baukov, Yu. I. *J. Organomet. Chem.* **2008**, *693*, 1309. (j) Seiler, O.; Burschka, C.; Fenske, T.; Troegel, D.; Tacke, R. *Inorg. Chem.* **2007**, *46*, 5419. (k) Yamamura, M.; Kano, N.; Kawashima, T. *J. Organomet. Chem.* **2007**, *692*, 313. (l) Malhotra, R.; Mehta, J.; Puri, J. K. *CEJC* **2007**, *5*, 858. (m) Wagler, J.; Roewer, G. *Inorg. Chim. Acta* **2007**, *360*, 1717. (n) Gerlach, D.; Brendler, E.; Heine, T.; Wagler, J. *Organometallics* **2007**, *26*, 234. (o) Gerlach, D.; Wagler, J. *Inorg. Chem. Commun.* **2007**, *10*, 952. (p) Wagler, J.; Gerlach, D.; Roewer, G. *Inorg. Chim. Acta* **2007**, *360*, 1935. (q) Sergani, S.; Kalikhman, I.; Yakubovich, S.; Kost, D. *Organometallics* **2007**, *26*, 5799. (r) Wagler, J.; Gerlach, D.; Roewer, G. *Chem. Heterocycl. Compd.* **2006**, *42*, 1557. (s) Korlyukov, A. A.; Lysenko, K. A.; Antipin, M. Yu.; Shipov, A. G.; Kramarova, E. P.; Murasheva, T. P.; Negrebetskii, V. V.; Ovchinnikov, Yu. E.; Pogozhikh, S. A.; Yakovlev, I. P.; Baukov, Yu. I. *Chem. Heterocycl. Compd.* **2006**, *42*, 1592. (t) Voronkov, M. G.; Trofimova, O. M.; Chernov, N. F.; Bolgova, Yu. I.; Albanov, A. I.; Chipanina, N. N.; Zolotarev, E. A. *Heteroat. Chem.* **2006**, *17*, 567. (u) Maaranen, J.; Andell, O. S.; Vanne, T.; Mutikainen, I. *J. Organomet. Chem.* **2006**, *691*, 240. (v) Couzijn, E. P. A.; Ehlers, A. W.; Schakel, M.; Lammertsma, K. *J. Am. Chem. Soc.* **2006**, *128*, 13634. (2) (a) Yamamura, M.; Kano, N.; Kawashima, T.; Matsumoto, T.; Harade, J.; Ogawa, K. *J. Org. Chem.* **2008**, *73*, 8244. (b) Liu, Y.; Steiner, S. A., III; Spahn, C. W.; Guzei, I. A.; Touloukhonova, I. S.; West, R. *Organometallics* **2007**, *26*, 1306. (c) Wagler, J.; Gerlach, D.; Böhme, U.; Roewer, G. *Organometallics* **2006**, *25*, 2929. (d) Yamaguchi, S.; Akiyama, S.; Tamao, K. *J. Organomet. Chem.* **2002**, *652*, 3. (e) Mugeruma, C.; Koga, N.; Hatanaka, Y.; El-Sayed, I.; Mikami, M.; Tanaka, M. *J. Phys. Chem. A* **2000**, *104*, 4928. (f) El-Sayed, I.; Hatanaka, Y.; Onozawa, S.; Tanaka, M. *J. Am. Chem. Soc.* **2001**, *123*, 3597.

nucleophile-catalyzed hydrolysis of alkoxy-silanes,³ base-catalyzed trans-silylation reactions,⁴ disproportionation of disilanes,⁵ ionic dissociation of Si–halogen bonds,⁶ and even activation of Si–C bonds for allyl shift reactions between allyl silanes and aldehydes,⁷ Si–C bond cleavage by hydroxylic chelating ligands,⁸ Pd-catalyzed cross-coupling reactions with arylsilanes,⁹ ring-opening reactions of silacyclobutanes,¹⁰ and the thermal rearrangement of silicon-bound silyl groups.¹¹ Furthermore, the tendency of silanes to increase the coordination

(3) (a) Corriu, R. J. P.; Leclercq, D.; Vioux, A.; Pauthe, M.; Phalippou, J. In *Ultrastructure Processing of Advanced Ceramics*; Mackenzie, J. D., Ulrich, D. R., Eds.; Wiley: New York, 1988; p 113. (b) Corriu, R. J. P.; Leclercq, D. *Angew. Chem., Int. Ed.* **1996**, *35*, 1420.

(4) (a) Nahar-Borchert, S.; Kroke, E.; Corriu, R. J. P.; Boury, B.; Riedel, R. *J. Organomet. Chem.* **2003**, *686*, 127. (b) Riedel, R.; Kroke, E.; Greiner, A.; Gabriel, A. O.; Ruwisch, L.; Nicolich, J.; Kroll, P. *Chem. Mater.* **1998**, *10*, 2964.

(5) (a) Trommer, K.; Herzog, U.; Schulze, N.; Roewer, G. *Main Group Met. Chem.* **2001**, *24*, 425. (b) Herzog, U.; Schulze, N.; Trommer, K.; Roewer, G. *Main Group Met. Chem.* **1999**, *22*, 19.

(6) (a) Schley, M.; Wagler, J.; Roewer, G. *Z. Anorg. Allg. Chem.* **2005**, *631*, 2914. (b) Wagler, J.; Böhme, U.; Brendler, E.; Roewer, G. *Z. Naturforsch. B* **2004**, *59*, 1348. (c) Kalikhman, I.; Krivonos, S.; Lameyer, L.; Stalke, D.; Kost, D. *Organometallics* **2001**, *20*, 1053. (d) Kost, D.; Kingston, V.; Gostevskii, B.; Ellern, A.; Stalke, D.; Walfort, B.; Kalikhman, I. *Organometallics* **2002**, *21*, 2293.

(7) (a) Sato, K.; Kira, M.; Sakurai, H. *J. Am. Chem. Soc.* **1989**, *111*, 6429. (b) Aoyama, N.; Hamada, T.; Manabe, K.; Kobayashi, S. *J. Org. Chem.* **2003**, *68*, 7329. (c) Kobayashi, S.; Ogawa, C.; Konishi, H.; Sugiura, M. *J. Am. Chem. Soc.* **2003**, *125*, 6610. (d) Chemler, S. R.; Roush, W. R. *J. Org. Chem.* **2003**, *68*, 1319. (e) Kira, M.; Zhang, L. C.; Kabuto, C.; Sakurai, H. *Organometallics* **1998**, *17*, 887. For related reactions see: (f) Yamamura, M.; Kano, N.; Kawashima, T. *J. Organomet. Chem.* **2007**, *692*, 313. (g) Kano, N.; Yamamura, M.; Kawashima, T. *J. Am. Chem. Soc.* **2004**, *126*, 6250.

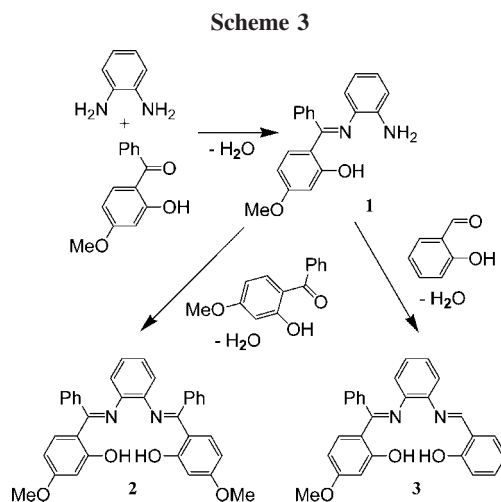
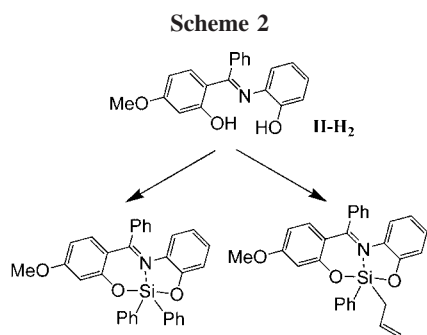
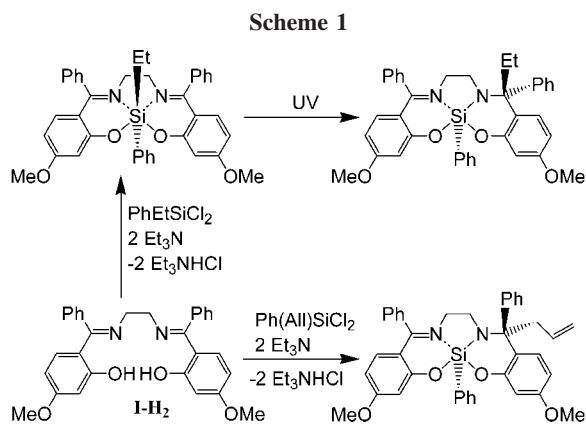
(8) (a) Richter, I.; Penka, M.; Tacke, R. *Organometallics* **2002**, *21*, 3050. (b) Tacke, R.; Heermann, J.; Pülm, M.; Richter, I. *Organometallics* **1998**, *17*, 1663.

(9) (a) Wolf, C.; Lerebours, R. *Org. Lett.* **2004**, *6*, 1147. (b) Seganish, W. M.; DeShong, P. *J. Org. Chem.* **2004**, *69*, 1137. (c) Mowery, M. E.; DeShong, P. *J. Org. Chem.* **1999**, *64*, 3266.

(10) Gostevskii, B.; Kalikhman, I.; Tessier, C. A.; Panzner, M. J.; Youngs, W. J.; Kost, D. *Organometallics* **2005**, *24*, 5786.

(11) (a) Wagler, J.; Böhme, U.; Roewer, G. *Organometallics* **2004**, *23*, 6066. (b) Kummer, D.; Chaudhry, S. C.; Depmeier, W.; Mattern, G. *Chem. Ber.* **1990**, *123*, 2241.

(12) (a) Wagler, J.; Hill, A. F. *Organometallics* **2008**, *27*, 6579. (b) Wagler, J.; Hill, A. F. *Organometallics* **2007**, *26*, 3630. (c) Metz, S.; Burschka, C.; Tacke, R. *Eur. J. Inorg. Chem.* **2008**, 4433. (d) Metz, S.; Burschka, C.; Platte, D.; Tacke, R. *Angew. Chem., Int. Ed.* **2007**, *46*, 7006.



Results and Discussion

As reported by Atkins et al.,¹⁷ the reaction of *o*-phenylenediamine and 2-hydroxybenzophenones in the presence of triethyl orthoformate and piperidine gives rise to *N*-(*o*-aminophenyl)-2-hydroxybenzophenoneimines, which can be converted into ONNO ligand systems by a second equivalent of the hydroxybenzophenone and into ONN'O' ligand systems by reaction with 2-hydroxybenzaldehydes. These procedures allowed the syntheses of compounds **1**,¹⁸ **2**, and **3** (Scheme 3). Single-crystal X-ray diffraction analyses of **2** and **3** (Tables 1 and 2) already reveal some differences between these symmetric and nonsymmetric ONNO and ONN'O' chelators, respectively.

In contrast to the ethylene-bridged salen-type ONNO ligands, which often exhibit an inverse symmetric arrangement,¹⁹ the rigid *o*-phenylene bridge of these salphen-type ligands **2** and **3** forces the *o*-iminomethylphenol moieties to remain in closer proximity to one another. In contrast with the only slight distortions of the two ON chelates out of an idealized tetradentate ONNO plane (together with the almost planar *o*-phenylenediimine moiety) in some symmetric salicylaldimine-derived salphen ligands,²⁰ the sterically more demanding benzophenoneimine moiety of **2** and **3** forces these ligands to a more pronounced distortion. In the case of the ONNO ligand **2** both benzophenoneimine moieties express the same steric requirements, which results in a C_2 -symmetric shape of the ligand (straddling a 2-fold axis in the crystal structure, space group $P2/c$). The noticeably different ON chelates of compound **3** allow for an almost planar ONN' chelate arrangement of the salicylaldimine moiety together with the benzophenoneimine nitrogen atom, whereas the idealized plane of the hydroxybenzophenoneimine (ON) chelate is still twisted out of the *o*-phenylenediimine plane as in compound **2**. Despite these distortions both compounds maintain the O—H—N hydrogen bridge within each ON chelate.

The reaction of **3** with dichlorodiphenylsilane yielded the hexacoordinate Si complex **4** (Scheme 4, Figure 1), which

number of the Si atom may also activate Si-bonded heterocycles.¹² However, diminished reactivity due to the higher coordination number of the Si center may also be observed, as shown by Kawashima et al.¹³

From our investigations of hexa- and pentacoordinate silicon complexes bearing tetradentate ONNO and tridentate ONO' *o*-iminomethylphenolato ligands **I** and **II**, respectively, we reported UV-initiated rearrangement reactions¹⁴ and thermal rearrangement of allyl groups¹⁵ (Scheme 1). These shift reactions have been observed with the ONNO tetradentate ligand system **I**, which generally gives rise to the formation of hexacoordinate silicon complexes. We have also shown that these reactivity patterns may be due to either Si hexacoordination in precursors (or intermediates) or Si pentacoordination in the rearrangement products, since they were not observed in complexes with the related tridentate ONO' ligand **II** (Scheme 2).¹⁶

The 1,3-shift reactions between the ONNO ligand **I** and various silanes (Scheme 1) were found to occur with high diastereoselectivity with regard to the relative configuration of the Si atom and the attacked (former imine) C atom in the rearrangement products, and alkyl vs aryl selectivity regarding the UV-initiated Si—C bond cleavage in hexacoordinate diorganosilanes was also observed. However, the symmetric ONNO ligand system **I** does not allow for regioselectivity studies with respect to two chemically different imine moieties within one tetradentate ligand backbone. Herein we report the synthesis of a new tetradentate (ONN'O') ligand bearing two chemically and sterically different imine moieties and its reactions with various chlorosilanes.

(13) Kobayashi, J.; Ishida, K.; Kawashima, T. *Silicon Chem.* **2002**, *1*, 351.

(14) Wagler, J.; Doert, Th.; Roewer, G. *Angew. Chem., Int. Ed.* **2004**, *43*, 2441.

(15) Wagler, J.; Roewer, G. *Z. Naturforsch., B* **2006**, *61*, 1406.

(16) (a) Wagler, J. *Organometallics* **2007**, *26*, 155. (b) Wagler, J.; Brendler, E. *Z. Naturforsch., B* **2007**, *62*, 225.

(17) Atkins, R.; Brewer, G.; Kokot, E.; Mockler, G. M.; Sinn, E. *Inorg. Chem.* **1985**, *24*, 127.

(18) Lippe, K.; Gerlach, D.; Kroke, E.; Wagler, J. *Inorg. Chem. Commun.* **2008**, *11*, 492.

(19) (a) Darensbourg, D. J.; Billodeaux, D. R. *Inorg. Chem.* **2005**, *44*, 1433. (b) Plitt, P.; Pritzkow, H.; Oeser, T.; Krämer, R. *J. Inorg. Biochem.* **2005**, *99*, 1230.

(20) (a) Kabak, M.; Elmali, A.; Elerman, Y.; Durlu, T. N. *J. Mol. Struct.* **2000**, *553*, 187. (b) Kanappan, R.; Tanase, S.; Tooke, D. M.; Spek, A. L.; Mutikainen, I.; Turpeinen, U.; Reedijk, J. *Polyhedron* **2004**, *23*, 2285. (c) Elerman, Y.; Elmali, A.; Kabak, M.; Aydin, M.; Peder, M. *J. Chem. Crystallogr.* **1994**, *24*, 603.

Table 1. Crystal Data and Experimental Parameters for the Crystal Structure Analyses of 2, 4·CHCl₃, 6, and 8a^a

	2	4·CHCl ₃	6	8a
CCDC no.	659391	659386	659388	706853
empirical formula	C ₃₄ H ₂₈ N ₂ O ₄	C ₄₀ H ₃₁ Cl ₃ N ₂ O ₃ Si	C ₃₆ H ₃₀ N ₂ O ₃ Si	C ₄₀ H ₃₂ N ₂ O ₄ Si
<i>M_w</i>	528.58	722.11	566.71	632.77
collec _n <i>T</i> , K	93(2)	90(2)	90(2)	90(2)
cryst syst	monoclinic	monoclinic	orthorhombic	orthorhombic
space group	<i>P2₁/c</i>	<i>P2₁/n</i>	<i>Pbca</i>	<i>Pbca</i>
<i>a</i> , Å	12.5225(10)	10.8202(11)	16.553(1)	18.6908(4)
<i>b</i> , Å	8.4242(7)	25.228(2)	14.905(1)	17.3692(4)
<i>c</i> , Å	13.9239(10)	13.0459(12)	22.785(2)	19.7167(5)
<i>β</i> , deg	112.577(3)	104.665(6)	90	90
<i>V</i> , Å ³	1356.29(18)	3445.2(6)	5621.7(7)	6400.9(3)
<i>Z</i>	2	4	8	8
<i>ρ</i> _{calcd} , Mg/m ³	1.294	1.392	1.339	1.313
<i>F</i> (000)	556	1496	2384	2656
<i>θ</i> _{max} , deg	28.0	26.0	25.0	40.0
no. of collected rflns	16 715	46 978	11 865	177 492
no. of indep rflns	3275	6761	4949	19 826
no. of indep rflns (<i>I</i> > 2 <i>σ</i> (<i>I</i>))	2945	4361	3590	15 007
<i>R</i> _{int}	0.0186	0.1048	0.0566	0.0341
no. of params	185	443	381	426
GOF	1.072	1.015	0.923	1.098
<i>R</i> 1, <i>wR</i> 2 (<i>I</i> > 2 <i>σ</i> (<i>I</i>))	0.0357, 0.0952	0.0566, 0.1494	0.0427, 0.0942	0.0389, 0.1098
<i>R</i> 1, <i>wR</i> 2 (all data)	0.0400, 0.0979	0.1055, 0.1700	0.0813, 0.1025	0.0629, 0.1205
max, min resid electron dens (e Å ⁻³)	0.342, -0.185	0.577, -0.660	0.317, -0.520	0.696, -0.357

^a Radiation used: Mo K α , $\lambda = 0.710\ 73\ \text{\AA}$.

Table 2. Crystal Data and Experimental Parameters for the Crystal Structure Analyses of 3, 5a·CHCl₃, and 7·CHCl₃^a

	3	5a·CHCl ₃	7·CHCl ₃
CCDC no.	659385	659389	659387
empirical formula	C ₂₇ H ₂₂ N ₂ O ₃	C ₄₀ H ₃₁ Cl ₃ N ₂ O ₃ Si	C ₃₄ H ₂₇ Cl ₃ N ₂ O ₃ Si
<i>M_w</i>	422.47	722.11	646.02
cryst syst	triclinic	triclinic	triclinic
space group	<i>P1</i>	<i>P1</i>	<i>P1</i>
<i>a</i> , Å	8.7939(11)	10.9840(6)	10.7243(8)
<i>b</i> , Å	9.7102(12)	13.4905(3)	11.4283(9)
<i>c</i> , Å	13.0745(13)	13.6978(3)	13.9199(10)
<i>α</i> , deg	83.201(5)	119.198(1)	95.262(4)
<i>β</i> , deg	71.011(5)	98.988(2)	90.622(4)
<i>γ</i> , deg	84.206(5)	98.715(2)	116.653(4)
<i>V</i> , Å ³	1045.9(2)	1687.93(11)	1515.7(2)
<i>Z</i>	2	2	2
<i>ρ</i> _{calcd} , Mg/m ³	1.341	1.421	1.415
<i>F</i> (000)	444	748	668
<i>θ</i> _{max} , deg	28.0	30.0	30.0
no. of collected rflns	23 856	25 162	21 215
no. of indep rflns	4966	9728	8814
no. of indep rflns (<i>I</i> > 2 <i>σ</i> (<i>I</i>))	3848	7728	6599
<i>R</i> _{int}	0.0243	0.0234	0.0456
no. of params	298	447	434
GOF	1.081	1.334	1.058
<i>R</i> 1, <i>wR</i> 2 (<i>I</i> > 2 <i>σ</i> (<i>I</i>))	0.0436, 0.1217	0.0424, 0.1246	0.0483, 0.1390
<i>R</i> 1, <i>wR</i> 2 (all data)	0.0606, 0.1304	0.0579, 0.1308	0.0662, 0.1470
max, min resid electron dens (e Å ⁻³)	0.319, -0.223	0.527, -0.570	0.638, -0.820

^a Radiation used: Mo K α , $\lambda = 0.710\ 73\ \text{\AA}$. *T* = 90(2) K.

exhibits a distorted-octahedral coordination sphere about the silicon atom. Although the tetradentate ligand occupies the four equatorial positions and the relative orientation of the two axially Si-bound phenyl groups is very similar to their arrangement in the analogous complex of ligand **I**, the asymmetric ligand system causes some differences in the Si coordination sphere. Whereas the mirror symmetric molecule **I-SiPh**₂²¹ has bond lengths N–Si = 1.958(2), Si–O = 1.763(1), and Si–C = 1.967(3) and 1.955(3) Å, the Si–N bonds in **4** are somewhat longer (Si1–N1 = 1.966(2), Si1–N2 = 1.986(3) Å). The silicon–oxygen bond lengths (Si1–O1 = 1.758(2), Si1–O2 = 1.763(2) Å) are

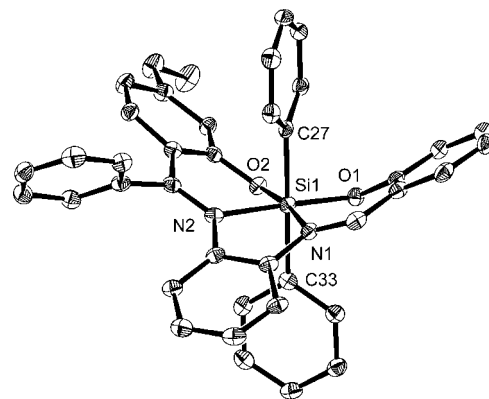


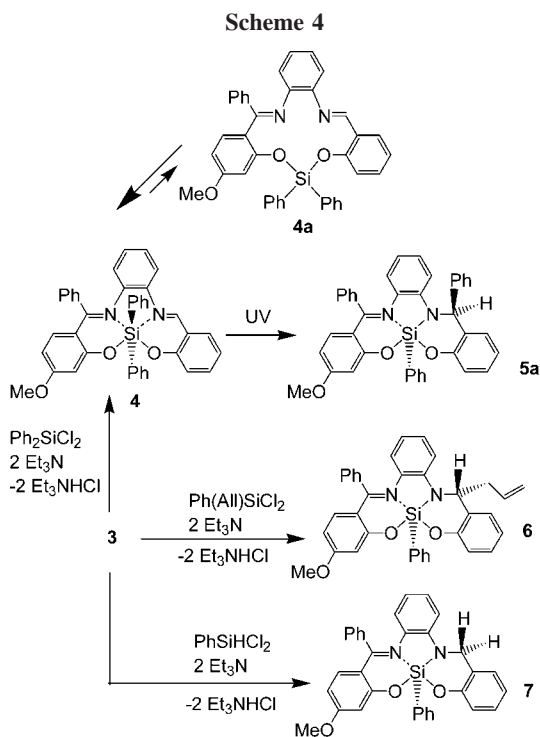
Figure 1. Molecular structure of **4** in the crystal of 4·CHCl₃ (ORTEP diagram with 50% probability ellipsoids, hydrogen atoms and chloroform molecule omitted, selected atoms labeled).

essentially similar to those in **I-SiPh**₂, and the Si–C bonds appear slightly shorter (Si1–C27 = 1.960(3), Si1–C33 = 1.946(3) Å), however, within the limits of their standard errors. In this tetradentate ligand system the salicylaldimine moiety, which forms the shorter silicon–nitrogen bond, would appear to be a better donor.

In the ²⁹Si NMR spectrum compound **4** has a signal at –168.7 ppm, which is shifted significantly downfield with respect to the ²⁹Si NMR signal of the structurally related compound **I-SiPh**₂ (–177.6 ppm). The *o*-phenylene bridge within the ligand system **3** is presumably the major origin of this downfield shift, as it has also been shown for other hypercoordinate silicon complexes that an *o*-phenylene instead of an ethylene bridge within a five-membered chelate causes a significant shift of the ²⁹Si NMR signal to lower field.²² In addition to the signal at –168.7 ppm, characteristic of a hexacoordinate Si complex, another (smaller) resonance appears at –37.7 ppm, characteristic

(21) Wagler, J.; Böhme, U.; Brendler, E.; Blaurock, S.; Roewer, G. Z. Anorg. Allg. Chem. **2005**, 631, 2907.

(22) One hexacoordinate silicon compound from ref 2c bearing a bidentate ethylene-bridged NN ligand exhibits a ²⁹Si NMR shift of –177.2 ppm, whereas an analogous complex with a phenylene-bridged NN ligand but similar bonding properties around the Si atom^{fm} has a ²⁹Si NMR signal at –165.3 ppm.



of Si compounds bearing a $\text{Ph}_2\text{Si}(\text{O-aryl})_2$ silicon environment. This signal arises from the isomer **4a** bearing a tetracoordinate silicon atom. Compounds **4** and **4a** coexist in an equilibrium, which can also be monitored by ^1H NMR behavior of the signals of the methoxy groups (**4**, 3.80 ppm, **4a**, 3.25 ppm). Upon heating, the intensity of the signals of **4a** increases, reverting to the initial ratio (**4**:**4a** = ca. 4:1) after cooling the solution to room temperature. However, equilibration is slow (not fully achieved within 30 min), and therefore, kinetic and thermodynamic investigations of this equilibrium by VT-NMR experiments were undertaken. (Whereas rapid equilibration in systems with bi- and even tridentate chelating ligand systems has been observed,^{16b,23} sometimes even rapid exchange on the NMR time scale, this equilibration **4** vs **4a** seems to be hindered by the rigid π -conjugated tetradentate ligand system.) From VT NMR experiments the thermodynamic parameters $\Delta H = -65.3$ kJ mol⁻¹ and $\Delta S = -209$ J mol⁻¹ K⁻¹ were estimated for the transition from the four- to the six-coordinate silicon complex. The above data, which correspond to the formation of two formally dative Si–N bonds, are in accord with the data reported from one of our previous studies ($\Delta H = -31.5$ kJ mol⁻¹ and $\Delta S = -116.7$ J mol⁻¹ K⁻¹ for the formation of one such bond).^{23a} Upon dissolution of **4** in CDCl_3 the equilibrium was established slowly, thus enabling us to also estimate the activation parameters $\Delta H^\ddagger = 159$ kJ mol⁻¹ and $\Delta S^\ddagger = 205$ J mol⁻¹ K⁻¹. (For details see the Supporting Information.)

As reported for hexacoordinate diorganosilanes with the symmetric ethylene-bridged tetradentate ONNO ligand **1**,¹⁴ compound **4** can also undergo UV-induced rearrangement of a phenyl group to an imine carbon atom. Irradiation of a suspension of **4** in THF with UV resulted in the diastereoselective formation of **5a** (Scheme 4). This isomer was identified as the only product by ^{29}Si NMR spectroscopy of the crude

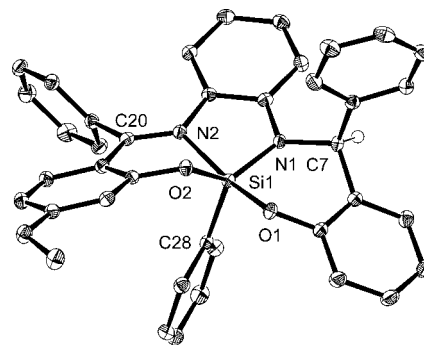


Figure 2. Molecular structure of **5a** in the crystal of **5a**· CHCl_3 (ORTEP diagram with 50% probability ellipsoids, most hydrogen atoms and chloroform molecule omitted, selected atoms labeled).

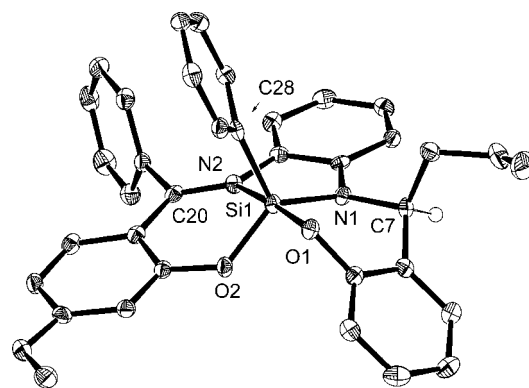


Figure 3. Molecular structure of **6** in the crystal (ORTEP diagram with 50% probability ellipsoids, most hydrogen atoms omitted, selected atoms labeled).

product solution, and its configuration has been proven by single-crystal X-ray diffraction analysis (Figure 2).

As found for such UV-initiated rearrangement reactions, the shifted substituent remains on the initial side of the idealized plane with respect to the tetradentate chelate (O1,N1,N2,O2). In the case of the above reaction the phenyl group is selectively shifted to the former salicylaldimine carbon atom C7.

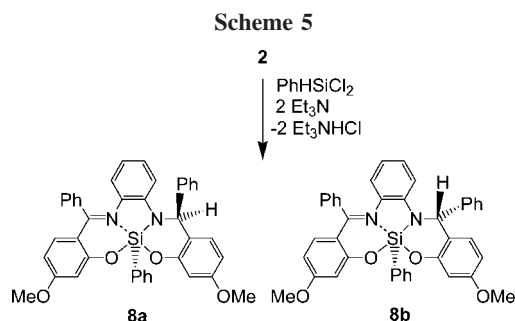
Reactions of **3** with both allylphenyldichlorosilane and phenyldichlorosilane²⁴ resulted in the instant formation of rearrangement products bearing pentacoordinate silicon atoms (**6** and **7**, respectively; Scheme 4). In both cases ^{29}Si NMR spectroscopy of the crude product solution proved the formation of only one silicon complex each. (Within the *s/n* limits of the spectra obtained, the presence of another isomer up to an amount of 5% with respect to the main product cannot be excluded.) Their crystal structures (Tables 1 and 2) reveal the selective allyl and hydrogen shift to the former salicylaldimine carbon atom C7.

In contrast with **5a**, which bears the migrated phenyl group on the opposite side of the idealized plane of the tetradentate ligand (anti), the allyl group in **6** is syn to the Si-bonded phenyl group (Figure 3). A possible mechanistic reason for that diastereoselectivity has been discussed previously.¹⁵

The hydrosilylation reaction between **3** and phenyldichlorosilane with formation of **7** (Scheme 4) does not allow for

(23) (a) Wagler, J.; Böhme, U.; Brendler, E.; Roewer, G. *Organometallics* **2005**, *24*, 1348. (b) Kalikhman, I.; Gostevskii, B.; Botoshansky, M.; Kafory, M.; Tessier, C. A.; Panzner, M. J.; Youngs, W. J.; Kost, D. *Organometallics* **2006**, *25*, 1252. (c) Gostevskii, B.; Silbert, G.; Ahear, K.; Sivaramakrishna, A.; Stalke, D.; Deuerlein, S.; Kocher, N.; Voronkov, M. G.; Kalikhman, I.; Kost, D. *Organometallics* **2005**, *24*, 2913.

(24) Hydrosilylation of imine^{24a} and diazo ligands^{24b} has recently been reported by other groups: (a) Kertsus-Banchik, E.; Kalikhman, I.; Gostevskii, B.; Deutsch, Z.; Botoshansky, M.; Kost, D. *Organometallics* **2008**, *27*, 5285. (b) Yamamura, M.; Kano, N.; Kawashima, T. *Tetrahedron Lett.* **2007**, *48*, 4033.



distinction between syn and anti diastereoselectivity of this hydrogen shift reaction. Therefore, ligand **2** was reacted with phenyldichlorosilane under the same conditions (Scheme 5). ^{29}Si NMR spectroscopy of the product mixture revealed the formation of two compounds (**8a** and **8b**) bearing pentacoordinate silicon atoms ($\delta(^{29}\text{Si})$ -104.4 and -105.1 ppm, ratio 10:1). Hence, hydrosilylation of **2** appears to be much more diastereoselective than hydrosilylation of the ethylene-bridged ligand **1**.²⁵ The major product of the **8a/8b** mixture was crystallized from acetonitrile. X-ray diffraction analysis (Table 3) revealed the predominant formation of **8a**, adding this hydrosilylation to the reactions producing the syn addition products. The molecular structure of **8a** is closely related to that of **5a**, the major differences being in the torsion of the Si-bound phenyl group due to packing effects and the presence of a second methoxy group at the ligand backbone.

Recently, Kost et al. reported the reactions between hypercoordinate chlorosilicon complexes and trimethylsilyl cyanide, which gave rise to the formation of hypercoordinate cyano silicon complexes and such bearing a cyano-functionalized former imine carbon atom (Scheme 6).²⁶ Therefore, we also investigated the cyano functionalization of our ONN'O' ligand system. Reaction of **3** with triethylamine and chlorotrimethylsilane (TMS-Cl) gave rise to the TMS derivative **9**, which was then treated with phenyltrichlorosilane to yield **10** (Scheme 7). Compound **10** has a hexacoordinate silicon atom in the solid state ($\delta_{\text{iso}}(^{29}\text{Si})$ -166.3 ppm) and exhibits poor solubility in chloroform. The Si-Cl bond of **10** can be activated by addition of SnCl_4 to **10** in chloroform to yield a solution of **11**. The cation of **11** in chloroform has a ^{29}Si NMR signal at -111.3 ppm, which is shifted somewhat upfield with respect to the signals of the other phenylsilicon compounds **5a**, **6**, **7**, and **8a**

(25) Hydrosilylation experiments have not been reported for ligand system **1** so far. In test reactions involving **1-H₂** and PhHSiCl_2 (or MeHSiCl_2) a striking lack of diastereoselectivity was found: in THF (20 mL) ligand **1** (1.0 g, 2.1 mmol) and triethylamine (0.80 g, 7.9 mmol) were stirred at 0 °C and phenyldichlorosilane (0.38 g, 2.2 mmol) was added dropwise. After 15 min the reaction mixture was filtered, the hydrochloride precipitate was washed with THF (5 mL), and the volatiles were removed from the filtrate under vacuum to yield a yellow foam. This crude product was dissolved in CDCl_3 and analyzed by ^{29}Si NMR (-113.3 and -114.9 ppm), ^1H NMR (4.88 and 5.06 ppm for $\text{HC}(\text{N},\text{Ar},\text{Ph})$), and ^{13}C NMR spectroscopy (67.2 and 69.1 ppm for $\text{C}(\text{N},\text{H},\text{Ph},\text{Ar})$) to reveal the hydrosilylation of one imine bond under formation of a mixture of two diastereomeric pentacoordinate silicon complexes in the ratio 3:2. Following the same procedure but using methylchlorosilane instead of phenyldichlorosilane, two diastereomers formed in the ratio 1:1 with their characteristic NMR shifts for the hydrosilylation products: ^{29}Si -101.6 , -102.6 ppm; ^{13}C 66.8, 69.0 ppm; ^1H 4.80, 4.94 ppm. In the case of the hydrosilylation reaction with methyltrichlorosilane, the product mixture also contained notable amounts (ca. 8%) of the siliconium chloride $(\text{ONNO})\text{SiMe}^+\text{Cl}^-$ (structure and spectroscopic data reported in ref 6b), which can be isolated by dissolving the crude product mixture in toluene (5 mL) to yield this byproduct as a white precipitate.

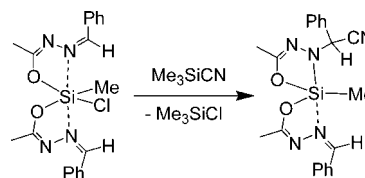
(26) Kalikhman, I.; Gostevskii, B.; Kertsnus, E.; Botoshansky, M.; Tessier, C. A.; Youngs, W. J.; Deuerlein, S.; Stalke, D.; Kost, D. *Organometallics* **2007**, *26*, 2652.

Table 3. Crystal Data and Experimental Parameters for the Crystal Structure Analyses of $11 \cdot 0.5\text{CHCl}_3$, **12b, and $14 \cdot 2\text{CHCl}_3$ ^a**

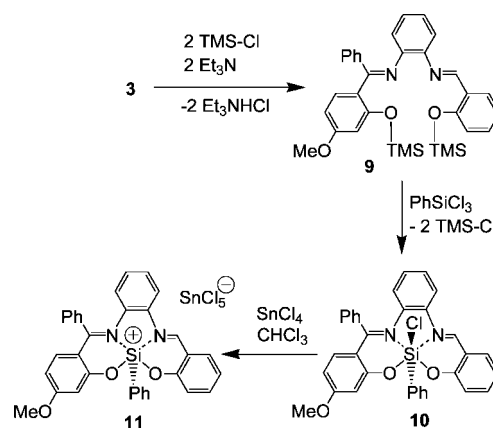
	$11 \cdot 0.5\text{CHCl}_3$	12b	$14 \cdot 2\text{CHCl}_3$
CCDC no.	659390	706854	706855
empirical formula	$\text{C}_{33.5}\text{H}_{25.5}\text{Cl}_{6.5}\text{N}_2\text{O}_3\text{SiSn}$	$\text{C}_{34}\text{H}_{25}\text{N}_3\text{O}_3\text{Si}$	$\text{C}_{40}\text{H}_{36}\text{Cl}_6\text{N}_2\text{O}_5\text{Si}$
M_w	881.26	551.66	865.50
cryst syst	triclinic	monoclinic	triclinic
space group	$P\bar{1}$	$P2_1/c$	$P\bar{1}$
a , Å	10.5139(5)	13.0425(7)	10.5362(2)
b , Å	11.3706(5)	10.0955(5)	12.6828(3)
c , Å	15.7917(7)	20.6130(11)	15.1854(3)
α , deg	91.089(3)	90	80.085(1)
β , deg	107.730(3)	95.221(2)	80.628(1)
γ , deg	90.590(3)	90	80.941(1)
V , Å ³	1797.64(14)	2702.9(2)	1954.65(7)
Z	2	4	2
ρ_{calcd} , Mg/m ³	1.628	1.356	1.471
$F(000)$	878	1152	892
θ_{max} , deg	35.0	27.0	25.0
no. of collected rflns	87 854	23 869	21 696
no. of indep rflns	15 833	5894	6648
no. of indep rflns ($I > 2\sigma(I)$)	11 719	4076	4860
R_{int}	0.0385	0.0573	0.0406
no. of params	477	371	564
GOF	1.121	1.022	1.098
R1, wR2 ($I > 2\sigma(I)$)	0.0324, 0.0751	0.0435, 0.0963	0.0482, 0.1183
R1, wR2 (all data)	0.0648, 0.0862	0.0752, 0.1057	0.0755, 0.1279
max, min resid electron dens (e Å ⁻³)	0.934, -1.151	0.348, -0.392	0.460, -0.514

^a Radiation used: Mo $K\alpha$, $\lambda = 0.71073$ Å. $T = 90(2)$ K.

Scheme 6

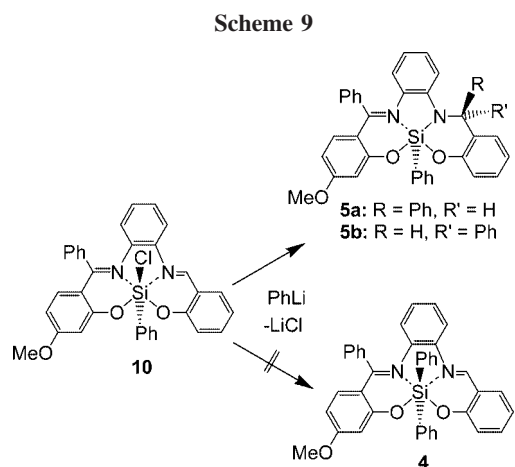
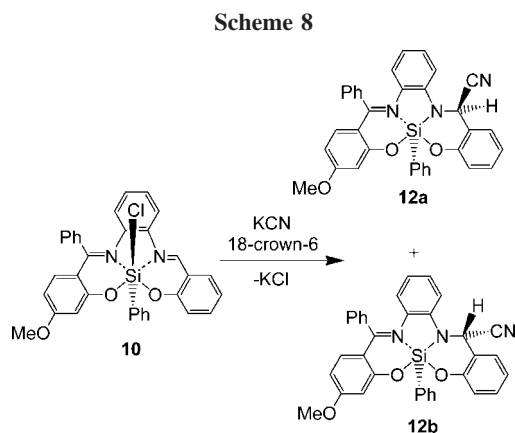


Scheme 7



($\delta(^{29}\text{Si})$ ca. -104 ppm) but clearly indicates pentacoordination of the Si atom.

Compound **10** was treated with KCN in CDCl_3 in the presence of 18-crown-6 to yield the mixture of diastereomers **12a/12b**, which gives rise to two ^{29}Si NMR signals ($\delta(^{29}\text{Si})$ -105.1 and -105.9) in the ratio 2:1 (Scheme 8). Hexacoordinate silicon complexes of the type $(\text{ONN}'\text{O})\text{Si}(\text{R})(\text{CN})$ were not observed. The regioselective attack of the cyanide at the salicylaldehyde carbon atom was concluded from the ^{13}C NMR shifts of the $(\text{R},\text{aryl},\text{N},\text{CN})$ substituted carbon atoms ($\delta(^{13}\text{C})$ 47.9 and 48.8 in the ratio 1:2), which are similar to one another and match the chemical shift range for $\text{R} = \text{H}$. One of these diastereomers (**12b**) crystallized from the chloroform solution (Figure 4). NMR spectroscopy (^{29}Si , ^{13}C , ^1H) of this predominant product revealed its purity.



To obtain more information about the syn vs anti product selectivity in these reactions with external nucleophiles, **10** was also treated with phenyllithium as a C-nucleophilic reagent (Scheme 9). The product mixture contained both diastereomers **5a** and **5b**, with the former being the major product ($\delta(^{29}\text{Si}) -104.3$ and -104.9 ppm, ratio 2:1).

In sharp contrast to the cyanide addition favored in syn fashion, these data suggest the favored formation of the anti-substituted products (referring to the relative positions of the Si-bonded carbon substituent and the carbanionic nucleophile). Furthermore, no indication was found for the formation of **4**, which would be inert once it had formed (unless irradiated with UV). This result suggests that the C-nucleophilic attack at complexes such as **10** occurs via direct approach of the C-nucleophile toward the imino carbon atom and not via initial

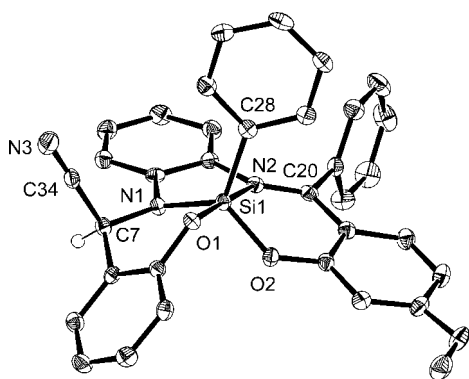
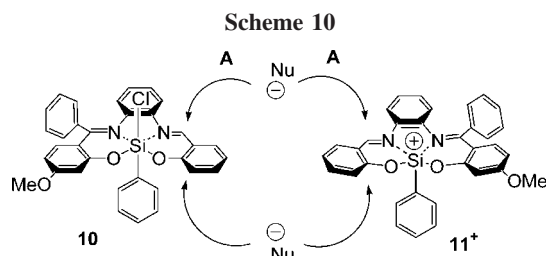


Figure 4. Molecular structure of **12b** in the crystal (ORTEP diagram with 50% probability ellipsoids, most hydrogen atoms omitted, selected atoms labeled).



C vs Cl substitution at the silicon atom. The discrepancy between the diastereoselectivities of the aforementioned nucleophilic attacks can be attributed to solvent effects. Whereas the reaction with cyanide was performed in chloroform, phenyllithium was added in THF. Hydrogen bridge donors (such as chloroform and dichloromethane) have already been shown to support ionic dissociation of hexacoordinate silicon compounds.⁶ Thus, one can expect contributions of pentacoordinate siliconium ions such as **11⁺** to the overall mechanism of the reaction with cyanide, whereas such ions should play a less pronounced role in thf solution (Scheme 10). In order to obtain structural information about the siliconium ion **11⁺**, its pentachlorostannate salt **11** was prepared by addition of SnCl_4 to **10** in chloroform and the structure was determined by X-ray diffraction analysis (Figure 5).

As in **5a** and related compounds, the Si atom of **11** is situated in a distorted-trigonal-bipyramidal coordination sphere. The pentachlorostannate counterion is not part of the Si coordination sphere; only one of its chlorine atoms points toward the silicon center but remains remote (separation $\text{Si1} \cdots \text{Cl1} = 3.901(1)$ Å). In contrast with the neutral complexes **5a**, **6**, **7**, **8a**, and **12b** the ONN'O' ligand is arranged in a different manner in **11**. The salicylaldehyde N atom occupies an axial position and the benzophenoneimine N atom an equatorial position. For comparison selected bond lengths and angles of the Si coordination spheres of all pentacoordinate Si complexes presented herein are given in Table 4.

Whereas **5a** and related compounds bear both a short covalent Si1–N1 bond and a much longer (formally dative) Si1–N2 bond, the silicon–nitrogen bond lengths of the cation of **11** are rather similar to one another. Differences between them might be explained by the axial vs equatorial positions of the respective N atom in the Si coordination sphere. For example, Akiba et al. reported N→P π -donation in the equatorial plane of pentacoordinate phosphoranes: the O–P σ^* MO of an equatorially situated oxygen atom enhances the equatorial N→P π -interaction.²⁷

The relative proportions of the axial vs equatorial Si–O (1.664(2) and 1.730(2) Å) and Si–N (1.846(2) and 1.937(2) Å) bond lengths in the complex **I-SiMe⁺**^{6b} are similar to those in the cation **11⁺**. Even the Si–C bond lengths (1.848(3) Å in **I-SiMe⁺**) are similar, although **11** bears a silicon-bonded phenyl group. In cation **11⁺**, however, the equatorial angle O1–Si1–N2 (129.7(1)°) is noticeably wider than the analogous angle in the cation **I-SiMe⁺** (115.8(1)°). This significant geometrical difference may be a result of the rigid *o*-phenylene bridge in the tetradentate ligand backbone of compound **11**. In contrast to the case for the hexacoordinate Si compound **4** with a rather planar arrangement of the ONN'O' ligand, the planes of the ON and O'N' chelates are folded toward one another in **11⁺**, thus

(27) Adachi, T.; Matsukawa, S.; Nakamoto, M.; Kajiyama, K.; Kojima, S.; Yamamoto, Y.; Akiba, K.; Re, S.; Nagase, S. *Inorg. Chem.* **2006**, *45*, 7269.

Table 4. Selected Bond Lengths (Å) and Angles (deg) of the Structures of **5a**, **6**, **7**, **8a**, **11**, **12b**, and **14**^c

	5a	6	7	8a	11	12b	14
Si1–C28	1.873(2) ^e	1.885(2) ^e	1.872(2) ^e	1.875(1) ^e	1.855(2) ^e	1.865(2) ^e	1.872(3) ^e
Si1–N1	1.760(1) ^e	1.755(1) ^e	1.741(1) ^e	1.759(1) ^e	1.951(1) ^a	1.755(1) ^e	1.746(2) ^e
Si1–N2	2.016(1) ^a	2.040(1) ^a	2.054(1) ^a	2.019(1) ^a	1.855(1) ^e	2.037(2) ^a	2.046(2) ^a
Si1–O1	1.717(1) ^a	1.724(1) ^a	1.708(1) ^a	1.714(1) ^a	1.673(1) ^e	1.722(1) ^a	1.719(2) ^a
Si1–O2	1.702(1) ^e	1.685(1) ^e	1.681(1) ^e	1.701(1) ^e	1.714(1) ^a	1.675(1) ^e	1.687(2) ^e
N1–C7	1.473(2)	1.479(2)	1.473(2)	1.471(1)	1.293(2)	1.454(2)	1.479(3)
N2–C20	1.318(2)	1.318(2)	1.306(2)	1.314(1)	1.338(2)	1.309(2)	1.312(3)
N1–Si1–O2	131.9(1) ^e	127.9(1) ^e	122.0(1) ^e	127.8(1) ^e	169.1(1) ^a	123.3(1) ^e	121.5(1) ^e
N2–Si1–O1	161.1(1) ^a	171.9(1) ^a	177.8(1) ^a	169.4(1) ^a	129.7(1) ^e	174.6(1) ^a	175.9(1) ^a
N1–Si1–C28	116.1(1) ^e	118.0(1) ^e	120.8(1) ^e	117.3(1) ^e	94.3(1)	117.8(1) ^e	119.5(1) ^e
N2–Si1–C28	92.5(1)	91.7(1)	86.9(1)	90.4(1)	115.0(1) ^e	89.8(1)	87.7(1)
O1–Si1–C28	99.0(1)	96.4(1)	95.0(1)	99.3(1)	114.9(1) ^e	95.1(1)	96.4(1)
O2–Si1–C28	110.9(1) ^e	113.2(1) ^e	115.3(1) ^e	113.6(1) ^e	95.1(1)	117.8(1) ^e	117.0(1) ^e

^a Axial and equatorial bonds and angles are indicated by superscript a and e, respectively. For **8a**, C20 and C28 are C27 and C35, respectively.

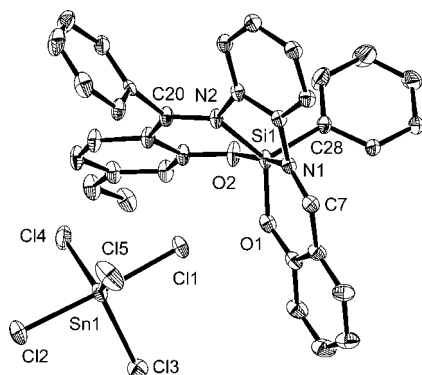
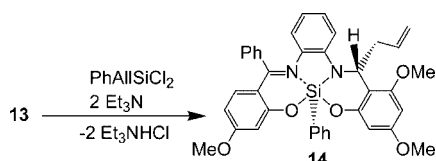


Figure 5. Molecular structure of **11** in the crystal of **11** · 0.5CHCl₃ (ORTEP diagram with 50% probability ellipsoids, hydrogen atoms and chloroform molecule omitted, selected atoms labeled).

Scheme 11



supporting nucleophilic attacks in a syn fashion with respect to the Si-bound phenyl group.

Finally, the electron-donating effect of the benzophenone-bound methoxy group on the pronounced regioselectivity of above reactions had to be ruled out. Therefore, ligand **13**, containing a dimethoxy-substituted salicylaldehyde moiety, was prepared in analogy to **3** (Scheme 3) and, in a representative reaction with allylphenyldichlorosilane, also yielded a product (**14**) which still underlines regioselectivity for reaction at the salicylaldehyde carbon atom (Scheme 11). The molecular structure of **14**, which has been determined crystallographically (Table 3), is similar to that of its analogue **6** (for bonding parameters see Table 4) and is therefore not further discussed in this context. Compound **14** was isolated in 59% yield. ²⁹Si NMR spectroscopy of the residual product solution provided no evidence for the formation of any pentacoordinate silicon complex other than **14**.

Conclusions

The tetradentate ligand system of compound **3** enabled us to elucidate both diastereo- and regioselectivity aspects of rearrangement reactions between various silanes and a tetradentate (ONN'O') diimine donor system. In addition to organylation reactions, we report hydrosilylation of an imine moiety of such

tetradentate ligand systems for the first time.^{24,25} Generally, the sterically more demanding benzophenoneimine site remains innocent and the salicylaldehyde moiety is altered by 1,3-shift reactions such as allyl transfer, hydrosilylation, and UV-induced 1,3-shift of a phenyl group.

Whereas these 1,3-shift reactions of the formal Si-bonded anionic nucleophiles “allyl[−]”, “H[−]”, and “Ph[−]” are very diastereoselective in most cases, reactions of the chlorosilicon complex (ONN'O')SiPhCl with external nucleophiles (PhLi, KCN) are much less diastereoselective; however, regioselective attack of the salicylaldehyde carbon atom was also observed for these reactions. Thus, the pronounced diastereoselectivity of the 1,3-shift reactions reported herein points to nonionic transfer mechanisms.

Ligand-dependent differences in the diastereoselectivity were found between the ethylene-bridged ligand system **1** and the *o*-phenylene-bridged tetradentate ligand systems **2** and **3**. Whereas hydrosilylation of **1** appeared rather nonselective,²⁵ reaction of **2** with phenyldichlorosilane exhibited pronounced diastereoselectivity for the syn product. Allyl shifts and UV-induced 1,3-shifts of an organic substituent, however, occur diastereoselectively in both ethylene- and *o*-phenylene-bridged ligand systems. Whereas in the latter cases the high diastereoselectivity can be attributed to the predetermined molecular geometry prior to the UV-initiated organyl shift and cyclic transition states involving a hexacoordinate Si atom for the allyl transfer,^{7,15} the lower diastereoselectivities for the hydride 1,3-shift reaction point to a rearrangement at an early stage of complex formation, the further development of which may then be determined by the flexibility of the tetradentate ligand system.

Experimental Section

Syntheses were carried out under an inert atmosphere of dry argon using standard Schlenk techniques and dry solvents. ¹H, ¹³C, and ²⁹Si NMR spectra (solution) were recorded on a Bruker DPX 400 spectrometer using TMS as internal standard. ²⁹Si CP/MAS spectra were recorded on a Bruker Avance 400WB spectrometer using a 7 mm rotor with KelF insert. Chemical shifts are also reported with TMS as the reference. Single-crystal X-ray diffraction analyses were carried out on a Bruker-Nonius X8 APEX2 CCD diffractometer using Mo K α radiation ($\lambda = 0.71073$ Å). The structures were solved with direct methods (all except **11** · 0.5CHCl₃) and Patterson methods (**11** · 0.5CHCl₃) using SHELXS-97. Structure refinement by full-matrix least-squares methods (refinement of F^2 against all reflections) was carried out with SHELXL-97. All non-hydrogen atoms were anisotropically refined. C-bonded hydrogen atoms were placed in idealized positions and refined isotropically. The O-bonded hydrogen atoms in the structures of **2** and **3** were located on residual electron density maps and isotropically refined without restraints.

Synthesis of Compound 4. To a solution of **3** (4.00 g, 9.50 mmol) and triethylamine (2.29 g, 22.6 mmol) in 40 mL of THF ($-10\text{ }^{\circ}\text{C}$) was added a solution of diphenyldichlorosilane (2.52 g, 9.90 mmol) in THF (10 mL) dropwise with stirring. The mixture was then stored at $8\text{ }^{\circ}\text{C}$ for 2 h, and the triethylamine hydrochloride precipitate was filtered off and washed with 10 mL of THF. From the yellow filtrate the solvent was removed under vacuum and the resulting orange-yellow solid was recrystallized from 15 mL of chloroform. After 1 day the crystalline product **4**·CHCl₃ was filtered, washed with chloroform (9 mL), and dried under vacuum. Yield: 4.46 g (6.20 mmol, 65%). ¹H NMR (CDCl₃): δ 3.79 (s, 3 H, OCH₃), 6.00 (d, 1 H, ar, ³J_{HH} = 9.6 Hz), 6.18 (d, 1 H, ar, ³J_{HH} = 8.4 Hz), 6.28 (d, 1 H, ar, ³J_{HH} = 8.8 Hz), 6.35–7.80 (m, 23 H, ar), 8.46 (s, 1 H, N=CH). ¹³C NMR (CDCl₃): δ 55.5 (OCH₃), 104.2, 107.4, 115.6, 116.2, 117.8, 119.3, 122.4, 124.2, 124.7, 125.5, 127.1, 127.5, 128.1, 129.0, 129.9, 133.7, 134.8, 135.3, 136.5, 137.3, 138.6, 138.8, 155.4, 158.2, 164.7, 166.8, 167.1, 168.4. ²⁹Si NMR (CDCl₃): δ -168.7. Anal. Found: C, 66.79; H, 4.32; N, 4.15. Calcd for C₄₀H₃₁N₂O₃SiCl₃: C, 66.53; H, 4.33; N, 3.88.

Synthesis of Compound 5a by UV Irradiation of 4. A stirred suspension of **4**·CHCl₃ (2.42 g, 3.40 mmol) in 130 mL of THF (at $15\text{ }^{\circ}\text{C}$) was exposed to UV (medium-pressure Hg lamp, λ_{max} 365–436 nm) for 5.5 h. From the resulting clear red solution the solvent was removed under vacuum, and the red solid product was recrystallized from 2 mL of chloroform. The red crystalline product **5a**·CHCl₃ was filtered, washed with chloroform (2 mL), and dried under vacuum. Yield: 1.32 g (1.80 mmol, 54.5%). ¹H NMR (CDCl₃): δ 3.93 (s, 3 H, OCH₃), 5.91 (d, 1 H, ar, ³J_{HH} = 8.0 Hz), 6.00 (s, 1 H, NCH), 6.27 (d, 1 H, ar, ³J_{HH} = 6.8 Hz), 6.38 (d, 1 H, ar, ³J_{HH} = 8.8 Hz), 6.55 (d, 1 H, ar, ³J_{HH} = 9.2 Hz), 6.65–7.70 (m, 22 H, ar). ¹³C NMR (CDCl₃): δ 55.9 (OCH₃), 61.9 (NCH), 103.8, 110.1, 112.0, 116.5, 116.9, 119.4, 119.6, 120.5, 126.2, 126.6, 126.7, 127.0, 128.2 (2 \times), 128.5, 129.0, 129.6, 129.8, 130.4, 130.8, 131.1, 133.1, 133.2, 136.4, 138.7, 143.5, 146.4, 154.6, 159.9, 165.5, 166.6. ²⁹Si NMR (CDCl₃): δ -104.2. Anal. Found: C, 66.27; H, 4.52; N, 4.15. Calcd for C₄₀H₃₁N₂O₃SiCl₃: C, 66.53; H, 4.33; N, 3.88.

Synthesis of Compounds 5a and 5b using Phenyllithium. To a suspension of **10**·0.5 (toluene) (0.38 g, 0.63 mmol) in 6 mL of THF (stirred at $-78\text{ }^{\circ}\text{C}$) was added a 1.8 M solution of PhLi in cyclohexane/diethyl ether (70/30) (0.35 mL, 0.63 mmol) dropwise. The mixture was warmed to room temperature and was stirred for a further 6 h. From the resulting red solution the solvent was removed under reduced pressure and the crude product was dissolved in CDCl₃ for ²⁹Si NMR spectroscopy: δ -104.3 and -104.9 (ratio 2:1).

Synthesis of Compound 6. To a $-10\text{ }^{\circ}\text{C}$ solution of **3** (0.50 g, 1.2 mmol) and triethylamine (0.29 g, 2.9 mmol) in THF (7 mL) was added a solution of allylphenyldichlorosilane (0.27 g, 1.2 mmol) in THF (3 mL) dropwise with stirring. The orange-red mixture was then stored at $8\text{ }^{\circ}\text{C}$ for 2 h, whereupon the amine hydrochloride precipitate was filtered off and washed with 5 mL of THF. From the orange-red filtrate the solvent was removed under vacuum and the resulting orange-yellow solid was recrystallized from 1.7 mL of chloroform. After 1 day the crystals were filtered, washed with 2 mL of chloroform, and dried under vacuum. Yield: 0.40 g (0.59 mmol, 51%). This product contains 0.9 mol of CHCl₃/mol of **6** in the crystals. From the filtrate the solvent was completely removed under vacuum and the solid residue was recrystallized from 0.4 mL of chloroform to yield further product (0.11 g, 0.17 mmol, 14%) with ca. 0.6 mol of CHCl₃/mol of **6** in the crystals. The variable chloroform content originates from the simultaneous crystallization of solvent-free crystals of **6** and crystals bearing one molecule of chloroform per molecule of **6**. Both compositions were identified by X-ray crystal structure analysis; however, only the crystals of the solvent-free compound were suitable for a satisfactory final structure refinement. ¹H NMR (CDCl₃): δ 2.77 (m, 2 H,

CH₂CH=CH₂), 3.89 (s, 3 H, OCH₃), 4.53 (m, 1 H, NCH), 5.03 (m, 2 H, CH₂CH=CH₂), 5.74 (m, 1 H, CH₂CH=CH₂), 5.86 (d, 1 H, ar, ³J_{HH} = 8.4 Hz), 6.29 (m, 1 H, ar), 6.37 (d, 1 H, ar, ³J_{HH} = 8.0 Hz), 6.55–7.55 (m, 18 H, ar). ¹³C NMR (CDCl₃): δ 38.3 (CH₂CH=CH₂), 55.7 (OCH₃), 59.5 (NCH), 104.1, 109.2, 111.1, 116.1, 116.4, 116.8, 119.2, 120.0, 126.5, 127.0, 127.3, 127.5, 127.8, 128.1, 128.4, 128.5, 129.1, 129.4, 129.7, 129.9, 130.5, 130.7, 131.7, 133.1, 135.6, 136.0, 138.8, 145.4, 155.7, 159.0, 164.5, 165.9. ²⁹Si NMR (CDCl₃): δ -104.3. Anal. Found: C, 66.04; H, 4.82; N, 4.53. Calcd for **6**·0.9CHCl₃ (C_{36.9}H_{30.9}N₂O₃SiCl_{2.7}): C, 65.74; H, 4.62; N, 4.16.

Synthesis of Compound 7. To a $-10\text{ }^{\circ}\text{C}$ solution of **3** (0.50 g, 1.2 mmol) and triethylamine (0.29 g, 2.9 mmol) in THF (7 mL) was added a solution of phenyldichlorosilane (0.22 g, 1.2 mmol) in THF (3 mL) dropwise with stirring. The red mixture was then stored at $8\text{ }^{\circ}\text{C}$ for 2 h, whereupon the amine hydrochloride precipitate was filtered off and washed with 4 mL of THF. From the red filtrate the solvent was removed under vacuum and the resulting orange-yellow solid was recrystallized from a mixture of 1.1 mL of chloroform and 0.1 mL of THF (the product remained dissolved in 1.1 mL of chloroform; crystallization commenced after addition of 0.1 mL of THF). The red crystals (average composition **7**·0.9CHCl₃·0.1THF; the THF content became obvious in ¹H NMR spectra) were filtered off and dried under vacuum. Yield: 0.54 g (0.84 mmol, 71%). ¹H NMR (CDCl₃): δ 3.89 (s, 3 H, OCH₃), 4.55 (d, 1 H, N-CH₂, ²J_{HH} = 14.0 Hz), 4.71 (d, 1 H, NCH₂, ²J_{HH} = 14.0 Hz), 5.86 (d, 1 H, ar, ³J_{HH} = 8.4 Hz), 6.27 (m, 1 H, ar), 6.37 (d, 1 H, ar, ³J_{HH} = 8.4 Hz), 6.60–7.60 (m, 18 H, ar). ¹³C NMR (CDCl₃): δ 47.8 (NCH₂), 55.8 (OCH₃), 59.5 (NCH), 104.3, 109.7, 110.7, 116.1, 116.5, 119.6 (2 \times), 119.9, 126.5, 127.0, 127.3, 128.3, 128.5, 129.1, 129.6, 130.1, 130.5, 132.6, 133.3, 136.0, 138.7, 146.4, 156.4, 159.4, 165.0, 166.1. ²⁹Si NMR (CDCl₃) δ -104.4. Anal. Found: C, 63.84; H, 4.41; N, 4.76. Calcd for **7**·0.9CHCl₃·0.1THF (C_{34.3}H_{27.7}N₂O_{3.1}SiCl_{2.7}): C, 64.24; H, 4.35; N, 4.37.

Synthesis of Compound 8a. To a $-10\text{ }^{\circ}\text{C}$ cold solution of **2** (3.00 g, 5.68 mmol) and triethylamine (1.80 g, 1.78 mmol) in THF (50 mL) was added phenyldichlorosilane (1.04 g, 5.88 mmol) dropwise with stirring. The orange-red mixture was then stirred at $0\text{ }^{\circ}\text{C}$ for 15 min, whereupon the hydrochloride precipitate was filtered off and washed with 10 mL of THF. From the filtrate most of the solvent was removed under vacuum to leave a red solution (ca. 10 mL), and a ²⁹Si NMR spectrum thereof was recorded (δ -105.1, -105.5; ratio 13:1). Within some hours compound **8a** precipitated from this crude product solution as a fine crystalline solid. The mixture was then stored at $8\text{ }^{\circ}\text{C}$ overnight, whereupon the solid product was filtered off, washed with a THF/hexane mixture (4 mL + 4 mL), and dried under vacuum (1.15 g). From the filtrate some more product precipitated at $8\text{ }^{\circ}\text{C}$ within 2 weeks (0.60 g). Yield: 1.75 g (2.77 mmol, 49%). ¹H NMR (CDCl₃): δ 3.61, 3.92 (2s, 6 H, OCH₃), 5.89 (s, 1 H, NCH), 5.93 (m, 1 H, ar), 6.25 (d, 1 H, ar, ⁴J_{HH} = 2.0 Hz), 6.28 (d, 1 H, ar, ⁴J_{HH} = 2.4 Hz), 6.30–7.70 (m, 22 H, ar). ¹³C NMR (CDCl₃): δ 55.1, 56.0 (OCH₃), 61.4 (NCH), 103.9, 105.7, 105.8, 110.1, 112.0, 116.6, 116.9, 119.4, 123.7, 126.1, 126.7, 127.0, 127.5, 128.1, 128.3, 128.5, 128.6, 128.9, 129.0, 129.3, 129.6, 129.8, 130.4, 133.1, 133.2, 136.4, 144.0, 146.5, 155.8, 159.9, 165.4, 166.6, 172.9. ²⁹Si NMR (CDCl₃): δ -104.4. Anal. Found: C, 75.91; H, 5.02; N, 4.40. Calcd for C₄₀H₃₂N₂O₄Si: C, 75.93; H, 5.10; N, 4.43.

Synthesis of Compound 9. To a stirred solution of **3** (0.50 g, 1.2 mmol) and triethylamine (0.36 g, 3.6 mmol) in THF (7 mL) at $-10\text{ }^{\circ}\text{C}$ was added a solution of chlorotrimethylsilane (0.39 g, 3.6 mmol) in THF (2 mL) dropwise. This mixture was stored at $8\text{ }^{\circ}\text{C}$ for 2 h, and then the amine hydrochloride precipitate was filtered and washed with THF (4 mL). From the filtrate the solvent was removed under vacuum to yield the crude product **10** as a yellowish oil of sufficient purity for further reaction. ¹H NMR (CDCl₃): δ -0.07, 0.27 (2s, 18 H, SiMe₃), 3.70 (s, 3 H, OCH₃), 6.18 (s, 1 H,

ar), 6.25 (d, 1 H, ar, $^3J_{\text{HH}} = 8.4$ Hz), 6.78 (m, 1 H, ar), 6.85–7.75 (mm, 13 H, ar), 8.58 (s, 1 H, N=CH). ^{13}C NMR (CDCl_3): δ 0.0, 0.3 (SiMe_3), 55.0 (OCH_3), 104.7, 105.1, 119.3, 119.5, 120.8, 121.4, 121.6, 123.8, 125.4, 127.6, 127.9, 128.1, 128.6, 129.8, 130.8, 131.8, 132.9, 140.5, 142.8, 145.3, 154.1, 155.6, 155.8, 160.6. ^{29}Si NMR (CDCl_3) δ 19.1, 20.9.

Synthesis of Compound 10. Compound **9** (prepared according to the above procedure) was dissolved in toluene (15 mL), and phenyltrichlorosilane (0.26 g, 1.2 mmol) was added dropwise. The mixture was then heated to reflux for 1 h and cooled to room temperature, and the resulting precipitate ($10 \cdot 0.5(\text{toluene})$) was filtered, washed with toluene (6 mL), and dried under vacuum. Yield: 0.59 g (1.0 mmol, 83%). ^1H NMR (d_6 -DMSO): δ 3.90 (s, 3 H, OCH_3), 6.35 (d, 1 H, ar, $^3J_{\text{HH}} = 8.4$ Hz), 6.51 (d, 1 H, ar, $^4J_{\text{HH}} = 1.2$ Hz), 6.53 (d, 1 H, ar, $^4J_{\text{HH}} = 1.6$ Hz), 6.75–8.10 (mm, 18 H, ar), 9.78 (s, 1 H, N=CH). ^{13}C NMR (d_6 -DMSO): δ 56.4 (OCH_3), 104.1, 109.6, 114.1, 118.2, 118.4, 120.2, 120.7, 123.4, 125.4, 126.2, 126.5, 128.2, 128.4, 128.5, 128.9, 129.0, 129.4, 129.5, 131.1, 133.5, 134.2, 135.3, 135.7, 138.8, 149.9, 160.6, 161.3, 164.1, 167.9, 171.1. ^{29}Si NMR (d_6 -DMSO): δ -167.9. ^{29}Si NMR (CP/MAS): $\delta_{\text{iso}} -167.7$. Anal. Found: C, 72.31; H, 5.04; N, 4.88. Calcd for $\text{C}_{36.5}\text{H}_{29}\text{N}_2\text{O}_3\text{SiCl}$: C, 72.20; H, 4.81; N, 4.61.

Synthesis of Compound 11. $10 \cdot 0.5(\text{toluene})$ (0.42 g, 0.70 mmol) was stirred in chloroform (10 mL), and tin tetrachloride (0.20 g, 0.77 mmol) was added, whereupon the initial suspension turned into a clear solution. From the crude solution a ^{29}Si NMR spectrum was recorded: δ -111.3. From this solution $11 \cdot 0.5\text{CHCl}_3$ crystallized. After storage at room temperature (1 week) and at 8 °C (another 1 week) the yellow crystals were separated from the solution by decantation, washed with chloroform (1 mL), and briefly dried under vacuum. Yield: 0.42 g (0.48 mmol, 68%). Anal. Found: C, 45.49; H, 2.90; N, 3.19. Calcd for $\text{C}_{36.5}\text{H}_{29}\text{N}_2\text{O}_3\text{SiCl}$: C, 45.66; H, 2.92; N, 3.18.

Synthesis of Compound 12b. To a suspension of $10 \cdot 0.5(\text{toluene})$ (2.1 g, 4.0 mmol) and potassium cyanide (0.30 g, 4.6 mmol) in chloroform (10 mL) was added 18-crown-6 (100 mg), and the mixture was stirred at room temperature for 24 h. The resulting (almost clear) orange-red solution was then filtered through diatomaceous earth and stored at 8 °C for 2 days. Within this time orange crystals of **12b** formed, which were then filtered off, washed with a chloroform/hexane mixture (1 mL + 1 mL; 1 mL + 2 mL), and dried under vacuum (0.75 g). Upon storage at -20 °C more crystalline product **12b** formed (0.38 g). Yield: 1.13 g (2.05 mmol,

51%). From the filtrate a ^{29}Si NMR spectrum was recorded, which revealed the presence of **12b** and **12a** in the approximate ratio 1:1 (δ -105.1 and -105.9, respectively). Data for **12b** are as follows. ^1H NMR (CDCl_3): δ 3.87 (s, 3H, OCH_3), 5.35 (s, 1H, NCH), 5.87 (d, 1H, 8.0 Hz), 6.37 (m, 1H), 6.42 (dd, 1H, 9.0 Hz, 2.6 Hz), 6.64 (d, 1H, 2.6 Hz), 6.8–7.6 (m, 17 H). ^{13}C NMR (CDCl_3): δ 48.9 ($\text{C}(\text{H},\text{CN},\text{aryl},\text{aryl})$), 55.8 (OCH_3), 104.7, 109.9, 110.7, 115.6, 118.4, 120.5, 120.8, 120.9, 123.4, 126.5, 126.8, 127.4, 127.7, 129.2, 129.5, 130.1, 130.2, 131.0, 132.3, 133.7, 135.2, 137.0, 142.9, 156.7, 159.2, 160.4, 166.0, 166.2. ^{29}Si NMR (CDCl_3): δ -105.1. Anal. Found: C, 74.19; H, 4.60; N, 7.64. Calcd for $\text{C}_{34}\text{H}_{25}\text{N}_3\text{O}_3\text{Si}$: C, 74.03; H, 4.57; N, 7.62.

Synthesis of Compound 14. At -10 °C ligand **13** (0.80 g, 1.65 mmol) was stirred in a solution of triethylamine (0.50 g, 4.95 mmol) in THF (10 mL), and allylphenyldichlorosilane (0.37 g, 1.70 mmol) was added dropwise. After 30 min the solvent was completely removed under reduced pressure and the solid was recrystallized from chloroform (10 mL). Yield: 0.84 g (0.97 mmol, 59%) of $14 \cdot 2\text{CHCl}_3$. (From the remaining solution a ^{29}Si NMR spectrum was recorded, which revealed only one signal in the range -80 to -120 ppm (-103.9) characteristic of compound **14**.) ^1H NMR (CDCl_3): δ 2.65–2.85 (m, 2 H, allyl), 3.78, 3.87, 3.89 (3s, 9 H, OCH_3), 4.85–5.15 (mm, 3 H, allyl, NCH), 5.7–5.9 (mm, 2 H, allyl, aryl), 6.1–7.6 (mm, 18 H, aryl). ^{13}C NMR (CDCl_3): δ 38.7 (CH_2), 50.6 ($\text{C}(\text{H},\text{allyl},\text{aryl},\text{aryl})$), 55.3, 55.6 (OCH_3), 90.7, 97.7, 104.3, 109.0, 111.6, 112.3, 115.7, 116.2, 116.2, 119.8, 127.0, 127.2, 128.4, 129.1, 129.4, 129.6, 129.9, 130.4, 131.7, 133.1, 135.9, 136.1, 138.9, 145.8, 156.3, 157.6, 158.9, 160.3, 164.2, 165.8. ^{29}Si NMR (CDCl_3): δ -103.9. Anal. Found: C, 56.50; H, 4.41; N, 3.35. Calcd for $\text{C}_{40}\text{H}_{36}\text{N}_2\text{O}_5\text{SiCl}_6$: C, 55.51; H, 4.19; N, 3.24.

Acknowledgment. This work was financially supported by the German Chemical Industry Fund.

Supporting Information Available: CIF files giving crystallographic data for **2**, **3**, $4 \cdot \text{CHCl}_3$, $5\text{a} \cdot \text{CHCl}_3$, **6**, $7 \cdot \text{CHCl}_3$, **8a**, $11 \cdot 0.5\text{CHCl}_3$, **12b**, and **14** and figures and text giving ORTEP diagrams of **2**, **3**, **7**, **8a** and **14**, experimental details of ligand syntheses (including NMR spectroscopic data), and details of the equilibrium between complexes **4** and **4a**. This material is available free of charge via the Internet at <http://pubs.acs.org>.

OM801049Q

New Bis(oxazoliny)phenyl–Ruthenium(II) Complexes and Their Catalytic Activity for Enantioselective Hydrogenation and Transfer Hydrogenation of Ketones

Jun-ichi Ito, Satoshi Ujiie, and Hisao Nishiyama*

Department of Applied Chemistry, Graduate School of Engineering, Nagoya University,
Chikusa-ku, Nagoya, 464-8603, Japan

Received October 3, 2008

Synthesis and characterization of ruthenium(II) complexes having a meridional bis(oxazoliny)benzene (*dm*-Phebox-*R*)H (**1a**: *R* = *ip*, **1b**: *R* = *ph*, **1c**: *R* = *dm*; *ip* = isopropyl, *dm* = dimethyl, *ph* = phenyl) ligand and their applications to enantioselective hydrogenation and transfer hydrogenation of simple ketones are described. Reaction of (*dm*-Phebox-*R*)H with RuCl₃·3(H₂O) in the presence of Zn and 1,5-cyclooctadiene (cod) afforded a ZnCl₄-bridged (Phebox)Ru dimer [(*dm*-Phebox-*R*)RuCl(CO)]₂(ZnCl₂) (**2a**, **2b**, and **2c**) in 73%, 58%, and 83% yield, respectively, through C–H bond activation. Treatment of **2a–c** with an excess amount of sodium acetylacetonate gave the corresponding acetylacetonato complexes (*dm*-Phebox-*R*)Ru(CO)(acac) (**3a–c**) in high yields. Such acetylacetonato complexes (**3**) were prepared by a one-pot reaction of **1** with RuCl₃·3(H₂O) in the presence of Zn and cod under reflux in ethanol, followed by treatment of acetylacetone at room temperature. The reaction of **2** generated in situ with CO (1 atm) also provided the corresponding dicarbonyl chloro Ru complexes (*dm*-Phebox-*R*)RuCl(CO)₂ (**4**) in moderate yields. New (Phebox)Ru complexes were found to exhibit catalytic activity toward hydrogenation of simple aromatic ketones in the presence of NaOMe under 30 atm of a hydrogen atmosphere to provide the corresponding secondary alcohols with high enantioselectivity (up to 98% ee). Transfer hydrogenation of bulky ketones was also catalyzed by **2** and **3** with high enantioselectivity (up to 97% ee).

Introduction

Since Noyori's ruthenium diphosphine/diamine system was discovered, ruthenium complexes with chiral bidentate ligands based on phosphorus and nitrogen atoms have been well established as highly effective precatalysts for enantioselective hydrogenation and transfer hydrogenation of ketones to generate optically active secondary alcohols.^{1,2} Thus far, a number of chiral diphosphine and diamine ligands have been developed because enantioselectivity is strongly dependent on the structure of these ligands. In connection with the design of chiral ligands for ruthenium catalysts, polydentate ligands including tridentate NNN,³ PNP,⁴ NPN,⁵ NNP,⁶ and PNO⁷ and tetradentate NNNN⁸

and PNNP⁹ ligands have successfully been applied to ruthenium-catalyzed enantioselective hydrogenation and transfer hydrogenation reactions (Chart 1).

Recently, pincer ruthenium complexes with tridentate PCP and NCN ligands have also been found to be suitable precursors for catalytic transfer hydrogenation.¹⁰ These pincer complexes have created stable and robust molecules, due to the metal–carbon σ -bond and five-membered metallacycles. In fact, van Koten and co-workers described ruthenium(II) complexes containing PCP and NCN ligands that showed high potential for the catalytic transfer hydrogenation of ketones in the presence of a base.^{10a} Recently, Baratta and co-workers developed new CNN tridentate ligands. Here the ruthenium complex exhibited high activity toward the catalytic transfer hydrogenation of ketones.¹¹ Application of those pincer Ru complexes for asymmetric transfer hydrogenation of ketones was also performed using a PCP ligand with chiral phosphorus centers, and provided modest

* Corresponding author. E-mail: hnishi@apchem.nagoya-u.ac.jp.

(1) Examples of reviews, see: (a) Noyori, R.; Ohkuma, T. *Angew. Chem. Int. Ed.* **2001**, *40*, 40–73. (b) Beller, M.; Bolm, C., Eds. *Transition Metals for Organic Synthesis*, 2nd ed.; Wiley-VCH: Weinheim, Germany, 2004. (c) Tang, W.; Zhang, X. *Chem. Rev.* **2003**, *103*, 3029–3070.

(2) (a) Ohkuma, T.; Ooka, H.; Hashiguchi, S.; Ikariya, T.; Noyori, R. *J. Am. Chem. Soc.* **1995**, *117*, 2675–2676. (b) Ohkuma, T.; Ooka, H.; Ikariya, T.; Noyori, R. *J. Am. Chem. Soc.* **1995**, *117*, 10417–10418.

(3) (a) Cuervo, D.; Gamas, M. P.; Gimeno, J. *Chem.–Eur. J.* **2004**, *10*, 425–432. (b) Jiang, Y.; Jiang, Q.; Zhang, X. *J. Am. Chem. Soc.* **1998**, *120*, 3817–3818. (c) Enthaler, S.; Hagemann, B.; Bhor, S.; Anilkumar, G.; Tse, M. K.; Bitterlich, B.; Junge, K.; Erre, G.; Beller, M. *Adv. Synth. Catal.* **2007**, *349*, 853–860.

(4) Jiang, Q.; Van Plew, D.; Murtuza, S.; Zhang, X. *Tetrahedron Lett.* **1996**, *37*, 797–800.

(5) Braunstein, P.; Naud, F.; Pfaltz, A.; Rettig, S. J. *Organometallics* **2000**, *19*, 2676–2683.

(6) Clarke, M. L.; Díaz-Valenzuela, B.; Slawin, A. M. Z. *Organometallics* **2007**, *26*, 16–19.

(7) (a) Yang, H.; Alvarez-Gressier, M.; Lugan, N.; Mathieu, R. *Organometallics* **1997**, *16*, 1401–1409. (b) Dai, H.; Hu, X.; Chen, H.; Bai, C.; Zheng, Z. *Tetrahedron: Asymmetry* **2003**, *14*, 1467–1472.

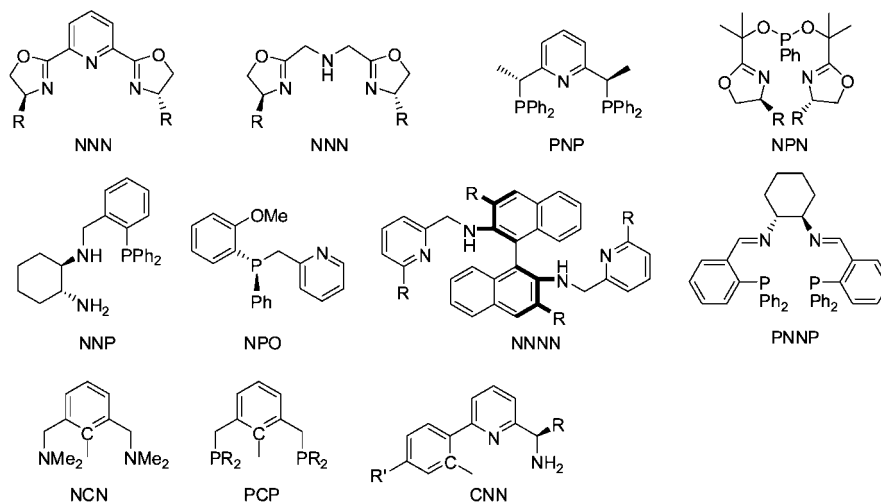
(8) (a) Karamé, I.; Jahjah, M.; Messaoudi, A.; Tommasino, M. L.; Lemaire, M. *Tetrahedron: Asymmetry* **2004**, *15*, 1569–1581. (b) Huang, H.; Okuno, T.; Tsuda, K.; Yoshimura, M.; Kitamura, M. *J. Am. Chem. Soc.* **2006**, *128*, 8716–8717.

(9) (a) Gao, J.-X.; Ikariya, T.; Noyori, R. *Organometallics* **1996**, *15*, 1087–1089. (b) Laue, S.; Greiner, L.; Wöltinger, J.; Liese, A. *Adv. Synth. Catal.* **2001**, *343*, 711–720.

(10) (a) Dani, P.; Karlen, T.; Gossage, R. A.; Gladiali, S.; van Koten, G. *Angew. Chem., Int. Ed.* **2000**, *39*, 743–745. (b) Amoroso, D.; Jabri, A.; Yap, G. P. A.; Gusev, D. G.; dos Santos, E. N.; Fogg, D. E. *Organometallics* **2004**, *23*, 4047–4054.

(11) Baratta, W.; Chelucii, G.; Gladiali, S.; Siega, K.; Toniutti, M.; Zanette, M.; Zangrando, E.; Rigo, P. *Angew. Chem., Int. Ed.* **2005**, *44*, 6214–6219.

Chart 1. Examples of Polydentate Ligands for Ru Catalysts



enantioselectivity.¹² Very recently, chiral CNN ligands were also used for the Ru- and Os-catalyzed enantioselective hydrogen transfer of ketones.¹³ In particular, the CNN-Os catalyst with a chiral diphosphine was found to be highly reactive to both hydrogenation and transfer hydrogenation of aromatic ketones with high turnover frequencies.^{13b}

A bis(oxazolinyl)phenyl moiety that provides a C_2 -symmetric and meridional environment around the metal center would create a suitable catalyst to distinguish the pro-chiral face of a substrate.¹⁴ Recently, we reported that transition metal catalysts with a bis(oxazolinyl)phenyl ligand (= Phebox), which is a meridional NCN ligand, have been successfully applied to the highly enantioselective conjugated reduction of α,β -unsaturated ester and ketones with hydrosilane.¹⁵ These results encouraged us to synthesize a (Phebox)Ru complex for enantioselective hydrogenation of carbonyl compounds. To the best of our knowledge, only one hypothetical (Phebox)Ru-catalyzed enantioselective cyclopropanation of alkene with diaza acetate has recently been reported.¹⁶ This paper reports the synthesis and full characterization of novel ruthenium(II) complexes with Phebox ligands via a feasible orthometalation method. The resulting (Phebox)Ru catalysts have been successfully applied to the enantioselective hydrogenation of simple aromatic ketones. Preliminary results were previously reported.¹⁷

Results and Discussion

Synthesis of (Phebox)Ru Complexes. Pincer (ECE)Ru complexes (E = N, P) have been prepared by the transmetalation of an organolithium compound,¹⁸ transcyclometalation with a

NCN pincer Ru complex,¹⁹ and C–H bond activation.^{20,21} Transmetalation of ruthenium chloride complexes, such as $[RuCl_2(nbd)]_n$ and $RuCl_2(PPh_3)_3$, with the organolithium compound $[Li\{C_6H_3(CH_2NMe_2)_2\}]_2$ is a reliable method for the synthesis of pincer (NCN)Ru complexes, as reported by van Koten and co-workers.¹⁸ (PCP)Ru complexes have also been obtained in high yield on the reaction of $C_6H_4-1,3-(CH_2PPh_2)_2$ with Ru chloride complexes via C–H bond activation.²⁰ Preparation of a related (NCN)Ru complex based on C–H bond activation of bis(pyridyl)phenyl and bis(pyrazolylmethyl)phenyl ligands was also reported.²¹

Preliminary experiments to synthesize a (Phebox)Ru complex by the reaction of $RuCl_2(PPh_3)_3$ with a (Phebox)Li compound²² resulted in the formation of a complex mixture. Consequently another method, namely, C–H bond activation of a ligand precursor, was tried. On the basis of the result, the 4,6-disubstituted Phebox ligand (*dm*-Phebox-*R*)H (**1**) proved to be a suitable precursor for the introduction of a transition metal;²³ we adopted the use of **1** as a starting material.

(12) Medici, S.; Gagliardo, M.; Williams, S. B.; Chase, P. A.; Gladiali, S.; Lutz, M.; Spek, A. L.; van Klink, G. P. M.; van Koten, G. *Helv. Chim. Acta* **2005**, *88*, 694–705.

(13) (a) Baratta, W.; Bosco, M.; Chelucci, G.; Zotto, A. D.; Siega, K.; Toniutti, M.; Zangrando, E.; Rigo, P. *Organometallics* **2006**, *25*, 4611–4620. (b) Baratta, W.; Ballico, M.; Chelucci, G.; Siega, K.; Rigo, P. *Angew. Chem., Int. Ed.* **2008**, *47*, 4362–4365.

(14) (a) Nishiyama, H. *Chem. Soc. Rev.* **2007**, *36*, 1133–1141. (b) Desimoni, G.; Faita, G.; Quadrelli, P. *Chem. Rev.* **2003**, *103*, 3119–3154.

(15) (a) Kanazawa, Y.; Tsuchiya, Y.; Kobayashi, K.; Shiomi, T.; Itoh, J.; Kikuchi, M.; Yamamoto, Y.; Nishiyama, H. *Chem.–Eur. J.* **2006**, *12*, 63–71. (b) Kanazawa, K.; Nishiyama, H. *Synlett* **2006**, 3343–3345.

(16) Takemoto, T.; Tsuzuki, Y.; Iwasa, S. *Abstr. Symp. Organomet. Chem. Jpn.* **2005**, *52*, 400.

(17) Ito, J.; Ujiie, S.; Nishiyama, H. *Chem. Commun.* **2008**, 1923–1925.

(18) Sutter, J.-P.; James, S. L.; Steenwinkel, P.; Karlen, T.; Grove, D. M.; Veldman, N.; Smeets, W. J. J.; Spek, A. L.; van Koten, G. *Organometallics* **1996**, *15*, 941–948.

(19) (a) Dani, P.; Karlen, T.; Gossage, R. A.; Smeets, W. J. J.; Spek, A. L.; van Koten, G. *J. Am. Chem. Soc.* **1997**, *119*, 11317–11318. (b) Dani, P.; Albrecht, V.; van Klink, G. P. M.; van Koten, G. *Organometallics* **2000**, *19*, 4468–4476. (c) Gagliardo, M.; Dijkstra, H. P.; Coppo, P.; De Cola, L.; Lutz, M.; Spek, A. L.; van Klink, G. P. M.; van Koten, G. *Organometallics* **2004**, *23*, 5833–5840. (d) Gagliardo, M.; Chase, P. A.; Lutz, M.; Spek, A. L.; Hartl, F.; Havenith, R. W. A.; van Klink, G. P. M.; van Koten, G. *Organometallics* **2005**, *24*, 4553–4557.

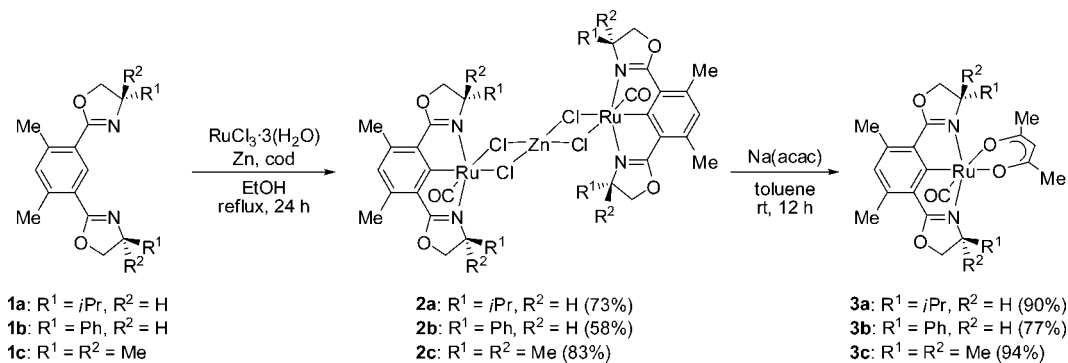
(20) (a) Jia, G.; Lee, H. M.; Xia, H. P.; Williams, I. D. *Organometallics* **1996**, *15*, 5453–5455. (b) Jia, G.; Lee, H. M.; Williams, I. D. *J. Organomet. Chem.* **1997**, *534*, 173–180. (c) van der Boom, M. E.; Kraatz, H.-B.; Hassner, L.; Ben-David, Y.; Milstein, D. *Organometallics* **1999**, *18*, 3873–3884. (d) Gusev, D. G.; Madott, M.; Dolgushin, F. M.; Lyssenko, K. A.; Antipin, M. Y. *Organometallics* **2000**, *19*, 1734–1739. (e) Ashkenazi, N.; Vigalok, A.; Parthiban, S.; Ben-David, Y.; Shimon, L. J. W.; Martin, J. M. L.; Milstein, D. *J. Am. Chem. Soc.* **2000**, *122*, 8797–8798. (f) Gusev, D. G.; Maxwell, T.; Dolgushin, F. M.; Lyssenko, M.; Lough, A. J. *Organometallics* **2002**, *21*, 1095–1100. (g) Amoroso, D.; Jabri, A.; Yap, G. P. A.; Gusev, D. G.; dos Santos, E. N.; Fogg, D. E. *Organometallics* **2004**, *23*, 4047–4054. (h) Precht, M. H. G.; Ben-David, Y.; Giunta, D.; Busch, S.; Taniguchi, Y.; Wisniewski, W.; Görls, H.; Mynott, R. J.; Theysen, N.; Milstein, D.; Leitner, W. *Chem.–Eur. J.* **2007**, *13*, 1539–1546.

(21) (a) Bekey, M.; Collin, J.-P.; Louis, R.; Metz, B.; Sauvage, J.-P. *J. Am. Chem. Soc.* **1991**, *113*, 8521–8522. (b) Beley, M.; Collin, J.-P.; Sauvage, J.-P. *Inorg. Chem.* **1993**, *32*, 4539–4543. (c) Koizumi, T.; Tomon, T.; Tanaka, K. *Bull. Chem. Soc. Jpn.* **2003**, *76*, 1969. (d) Harshorn, C. M.; Steel, P. J. *Organometallics* **1998**, *17*, 3487–3496.

(22) Motoyama, Y.; Okano, M.; Narusawa, H.; Makihara, N.; Aoki, K.; Nishiyama, H. *Organometallics* **2001**, *20*, 1580–1591.

(23) Ito, J.; Shiomi, T.; Nishiyama, H. *Adv. Synth. Catal.* **2006**, *348*, 1235–1240.

Scheme 1. Preparation of (Phebox)Ru Complexes



Simple heating of a mixture of $\text{RuCl}_3 \cdot 3(\text{H}_2\text{O})$ and **1a** ($\text{R} = i\text{Pr}$) in refluxing EtOH with Et_3N resulted in formation of complicated mixtures and gave no isolable ruthenium complexes. Reactions of **1a** with common ruthenium(II) complexes, such as $[\text{RuCl}_2(\text{cod})]_n$ ($\text{cod} = 1,5\text{-cyclooctadiene}$) and $[\text{RuCl}_2(\text{C}_6\text{H}_6)]_2$, also failed. After studying the reaction conditions, we found that treatment of **1a** with $\text{RuCl}_3 \cdot 3(\text{H}_2\text{O})$ in the presence of Zn and cod in ethanol under reflux for 24 h afforded a (Phebox)Ru complex, $[(dm\text{-Phebox-}ip)\text{RuCl}(\text{CO})_2(\text{ZnCl}_2)]$ (**2a**), through the C–H bond activation of **1a** (Scheme 1). The complex **2a** was isolated in 73% yield by purification with column chromatography on silica gel. On the other hand, when the reaction was carried out in the absence of cod, the yield of **2a** decreased to 32% and **1a** remained. Although we have not obtained details for the role of cod in the reaction, it was known that the reaction of $\text{RuCl}_3 \cdot 3(\text{H}_2\text{O})$ with cod and Zn in ethanol produces Ru(II) complexes prior to the formation of Ru(cod)-(cot).²⁴ Complexes **2b** and **2c** were prepared in 58% and 83% yields, respectively, in similar manners.

Complexes **2a–c** were characterized as (Phebox)Ru dimers containing a bridged ZnCl_4 moiety, on the basis of NMR and IR spectra and elemental analysis. The molecular structure was unambiguously confirmed by an X-ray diffraction study of **2c**. The ^1H spectrum of **2a** showed complex features due to the lack of a symmetry element in the molecule. The signals for the methyl groups on the isopropyl groups were independently observed to be eight doublet peaks at room temperature in C_6D_6 . The aryl protons on the phenyl groups separately appeared as two singlet signals. These spectral features indicate that the molecule consists of two Phebox units. In the ^1H NMR spectrum of **2a**, the shape of the methyl signals in the isopropyl groups depended on solvents. Whereas eight peaks were separately observed in C_6D_6 at room temperature, in CDCl_3 the methyl signals were observed to be broad peaks. With a decrease in the temperature, these signals split and separately appeared at -40°C . This feature implies that the complex is fluxional in solution.

The ^1H NMR spectrum of **2c** measured in C_6D_6 exhibited six singlet signals for methyl groups on two oxazolonyl groups and the phenyl group. AA'BB' signals for the CH_2 on oxazolonyl groups showed no symmetry in each (Phebox)Ru unit. On the other hand, the signal for the aryl protons on the phenyl groups was observed to be equivalent at δ 6.46, indicating that two (Phebox)Ru units are in the same environment.

Complexes **2a–c** have an unexpected CO ligand on the Ru center. The IR spectra of **2a–c** revealed characteristic peaks for a stretching vibration of the CO ligand at 1936, 1932, and

1937 cm^{-1} , respectively. The source of the CO ligand could be EtOH, which is oxidized to aldehyde followed by decarbonylation.²⁵ Gusev and co-workers have described that the Ru carbonyl complex $(\text{PCP})\text{Ru}(\text{CO})\text{Cl}$ was obtained by the reaction of $\text{RuCl}_3 \cdot 3(\text{H}_2\text{O})$ or $[\text{RuCl}_2(\text{cod})]_n$ with $\text{C}_6\text{H}_4\text{-1,3-(CH}_2\text{PPh}_2)_2$ in ethanol under reflux.^{20d}

Finally, the molecular structure of **2c** was confirmed by an X-ray diffraction study using crystals obtained by slow diffusion of pentane to a toluene solution at room temperature. The ORTEP diagram depicted in Figure 1 clearly shows that two (Phebox)Ru(CO) moieties are connected by ZnCl_4^{2-} . The Phebox ligand is meridionally coordinated to the Ru center through two nitrogen atoms and a carbon atom. The geometries on the Ru atoms are pseudo-octahedral with N–Ru–N angles of $156.4(3)^\circ$ and $155.6(3)^\circ$ and N–Ru–C_{ipso} angles of $77.7\text{--}78.8^\circ$. The Ru(1)–C(1) and Ru(2)–C(20) bond lengths of 1.969(8) and 1.995(7) Å are comparable to that of the (NCN)Ru complex (1.967(2) Å)¹⁸ and are shorter than those of (PCP)Ru complexes (2.03–2.13 Å).^{19,20} The coordination site of the CO ligand is perpendicular to the Phebox plane. The Ru(1)–Cl(1) and Ru(2)–Cl(3) bond lengths of 2.582(3) and 2.615(3) Å are slightly longer than the Ru(1)–Cl(2) and Ru(2)–Cl(4) lengths of 2.535(3) and 2.506(3) Å, probably due to the *trans* influence of the aryl group. These Ru–Cl bond lengths are significantly longer than those of other pincer-Ru chloride complexes (2.41–2.49 Å).^{18–20} The geometry on the Zn atom was described as pseudotetrahedral, with four large Cl–Zn–Cl angles ($113.71(8)\text{--}118.56^\circ$) and two small angles ($96.40(9)^\circ$ and $95.93(9)^\circ$).

The ZnCl_4 moiety of **2** was replaced by an acetylacetonato (=acac) ligand to give the corresponding mononuclear complex. Treatment of **2a** with sodium acetylacetonate in toluene at room temperature led to the mononuclear acac complex $(dm\text{-Phebox-}ip)\text{Ru}(\text{acac})(\text{CO})$ (**3a**) in 90% yield (Scheme 1). Similarly, **3b** and **3c** were obtained in 77% and 94% yields, respectively. Complex **3a** was synthesized by a successive procedure from the reaction of **2a** generated in situ, followed by treatment with acetylacetonate in 47% yield over two steps without isolation of **2a** (Scheme 2). This method easily allowed the preparation of a (Phebox)Ru complex with a different substituent on the oxazoline ring. For example, using the one-pot procedure, the phenyl analogue **3b** was obtained in 45% yield from **1b**. Complexes **3a–c** are air and moisture stable and can be purified by column chromatography and stored in air over months.

The ^1H NMR spectrum of **3a** shows four doublet signals for methyl protons of isopropyl groups at δ 0.62 (3H), 0.85 (3H), 0.90 (3H), and 0.92 (3H), due to the lack of symmetry elements

(24) Itoh, K.; Nagashima, H.; Ohshima, T.; Oshima, N.; Nishiyama, H. *J. Organomet. Chem.* **1984**, 272, 179–188.

(25) Poyatos, M.; Mata, J. A.; Falomir, E.; Crabtree, R. H.; Peris, E. *Organometallics* **2003**, 22, 1110–1114.

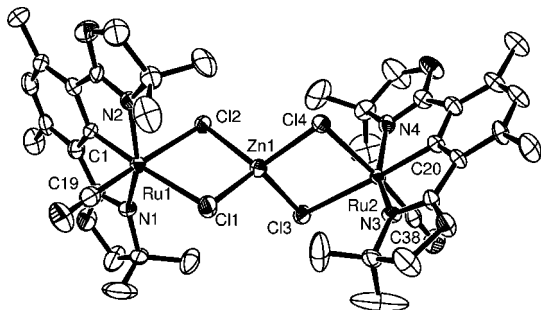
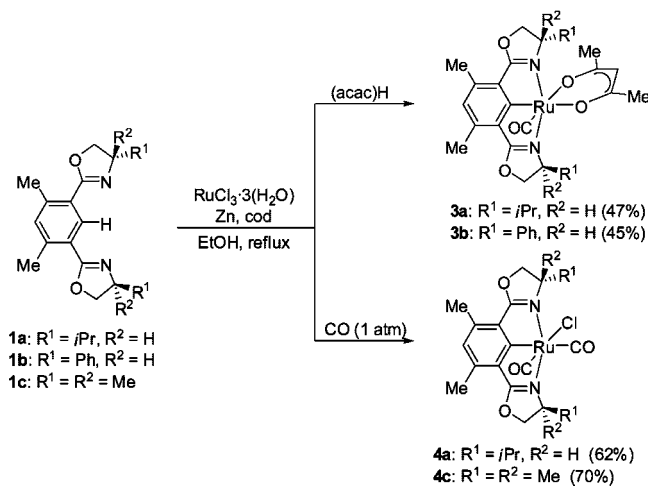


Figure 1. ORTEP diagram of **2c** at the 50% probability level. Hydrogen atoms have been omitted for clarity. Selected bond lengths (Å): Ru(1)–C(1) 1.969(8), Ru(1)–C(19) 1.863(10), Ru(1)–N(1) 2.113(7), Ru(1)–N(2) 2.111(7), Ru(1)–Cl(1) 2.582(3), Ru(1)–Cl(2) 2.535(3), Ru(2)–C(20) 1.995(7), Ru(2)–C(38) 1.825(9), Ru(2)–N(3) 2.129(6), Ru(2)–N(4) 2.112(7), Ru(2)–Cl(3) 2.615(3), Ru(2)–Cl(4) 2.506(3), Zn(1)–Cl(1) 2.289(3), Zn(1)–Cl(2) 2.287(3), Zn(1)–Cl(3) 2.265(3), Zn(1)–Cl(4) 2.314(3). Selected angles (deg): N(1)–Ru(1)–N(2) 156.4(3), N(3)–Ru(2)–N(4) 155.6(3), N(1)–Ru(1)–C(1) 77.8(3), N(2)–Ru(1)–C(1), 78.8(3), N(3)–Ru(2)–C(20) 78.2(3), N(4)–Ru(2)–C(20) 77.7(3), Cl(1)–Zn(1)–Cl(2) 96.40(9), Cl(1)–Zn(1)–Cl(3) 115.48(10), Cl(1)–Zn(1)–Cl(4) 118.56(10), Cl(2)–Zn(1)–Cl(3) 118.33(10), Cl(2)–Zn(1)–Cl(4) 113.71(8), Cl(3)–Zn(1)–Cl(4) 95.93(9).

Scheme 2. Preparation of (Phebox)Ru Complexes by the One-Pot Procedure



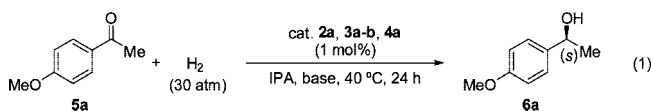
in the molecule. A set of signals assigned to the acac ligand were observed at δ 1.66 (3H), 2.04 (3H), and 5.13 (1H). In the IR spectrum of **3a**, an absorption assigned to the carbonyl ligand was observed at 1907 cm^{-1} , which is shifted to a lower frequency than that of **2a**. This result indicates that the back-donation to the carbonyl ligand from the Ru center in **3a** is larger than that in **2a**. The spectral data of **3b** and **3c** are consistent with a mononuclear structure having an acac ligand.

The molecular structures of **3b** and **3c** were confirmed by X-ray diffraction. The ORTEP diagrams of **3b** and **3c** are shown in Figure 2. As observed in **2c**, the Ru center is described to have a distorted-octahedral geometry with a meridionally coordinated Phebox ligand and a bidentate acac ligand. The coordination site of the CO ligand is perpendicular to the Phebox plane. The Ru–C(1) bond lengths of **3** are identical to those of **2c**. The Ru–O bond lengths *trans* to the *ipso*-carbon are slightly longer than those *trans* to a carbonyl ligand.

Related carbonyl complexes **4** were also obtained by the use of CO instead of acacH (Scheme 2). The crude complex **2a**, generated by treatment of **1a** with $\text{RuCl}_3 \cdot 3(\text{H}_2\text{O})$ in the presence

of Zn and cod in EtOH under reflux for 24 h, was exposed to CO (1 atm) to provide the dicarbonyl complex (*dm*-Phebox-*ip*) $\text{RuCl}(\text{CO})_2$ (**4a**) in 62% yield. The analogue (*dm*-Phebox-*dm*) $\text{RuCl}(\text{CO})_2$ (**4c**) was also obtained in 70% yield by a similar manner. In the ^1H NMR spectrum of **4a**, the signals of the four methyl groups of two isopropyl groups on the oxazoline rings were observed separately due to the lack of a symmetric element. The IR spectrum of **4a** exhibited two strong absorptions at 2037 and 1959 cm^{-1} assigned to the symmetric and asymmetric C=O stretching vibrations, respectively. The intensity of these peaks implied the *cis* arrangement of the CO ligands. These peaks are close to those of the related PCP-Ru dicarbonyl complexes [$2,6\text{-(Ph}_2\text{PCH}_2\text{)}_2\text{C}_6\text{H}_3\text{]}_2\text{RuCl}(\text{CO})_2$ (2028, 1966 cm^{-1})^{20b} and [$2,6\text{-(C}_2\text{H}_4\text{PCH}_2\text{)}_2\text{C}_6\text{H}_3\text{]}_2\text{RuCl}(\text{CO})_2$ (2018, 1945 cm^{-1})^{20g}. The spectral features of **4c** are similar to those of **4a**. The ^1H NMR spectrum of **4c** displayed the signals for the methyl groups on the oxazoline rings at δ 1.33 (s, 6H) and 1.46 (s, 6H). In the IR spectrum of **4c**, two C=O stretching vibrations were observed at 2032 and 1960 cm^{-1} .

Enantioselective Hydrogenation of Ketones. To test the catalytic ability of (Phebox)Ru complexes, hydrogenation of simple ketones using complexes **2–4** was examined. An initial reaction was carried out using 4-acetylmethoxybenzene (**5a**) in 2-propanol (IPA) with NaOMe under 30 atm of hydrogen pressure at 40 °C for 24 h (Table 1, eq 1). When the (Phebox)Ru dimer **2a** was employed as a catalyst for hydrogenation of **5a**, the corresponding alcohol (*S*)-1-(4-methoxyphenyl)-1-ethanol (**6a**) was successfully obtained in 99% yield with 65% ee (run 1). Complexes **3a** and **3b** were also found to be active to hydrogenation of **5a**, affording the *S*-alcohol **6a** with 64% and 56% ee, respectively (runs 2 and 3). On the other hand, **4a** provided only low enantioselectivity (17% ee; run 4). Other base sources such as NaOEt, NaOtBu, KOtBu, and LiOMe provided similar results (runs 5–8). However, the use of less basic K_2CO_3 and Cs_2CO_3 resulted in low yields and enantioselectivity (runs 9 and 10). Hydrogenation did not proceed in the absence of a base (run 11). Interestingly, the Ru catalysts **3** were recovered in ca. 50% yield by column chromatography after the catalytic reaction. In our catalysts, 2-propanol is the suitable solvent; low yields and ee's were observed using other solvents, such as methanol and ethanol (runs 12 and 13). Additionally, the use of toluene and THF resulted in notable decreasing of yields (<1%).



Next, examination of the scope and limitations of ketones was carried out using 1 mol % of **3a** and **3b** (Scheme 3, Table 2). Acetophenone derivatives with *p*-substituted methyl and phenyl groups resulted in high yields and moderate enantioselectivity of 65–79% ee (runs 1–4). In contrast, the hydrogenation reaction of the *p*-bromo-substituted ketone **5d** and the *m*-chloro-substituted ketone **5f** decreased in yields and enantioselectivity (runs 5, 6, 9, and 10). These reactions provided a small amount of acetophenone in 1–4% yields as a byproduct. Such a side reaction of dehalogenation might be a deactivation pathway of catalysts. Alkyl substituent ketones **5g** and **5h** maintained good enantioselectivities of 85% and 83% ee, respectively (runs 11–14). In the case of the 1-naphthylmethylketone derivatives **5j** and **5k**, substituents at the 4-position affected the yields and enantioselectivity. **5j** (R = H) was effectively reduced by **3a**, whereas **5k** (R = Me) was reduced

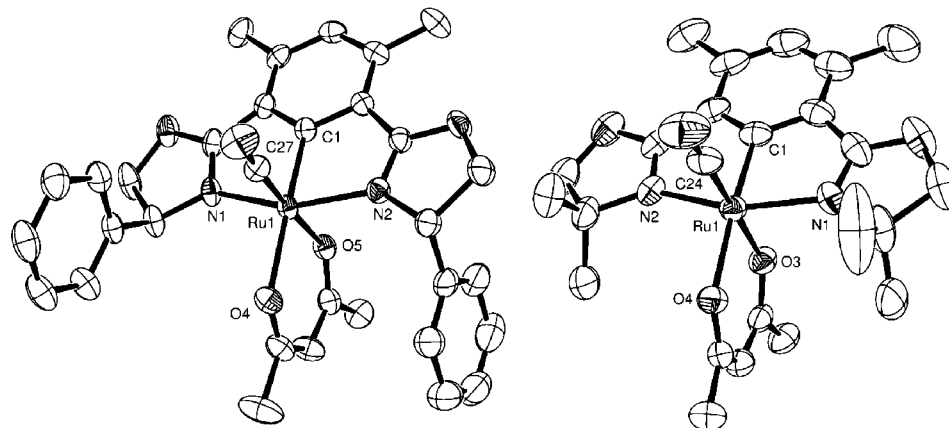


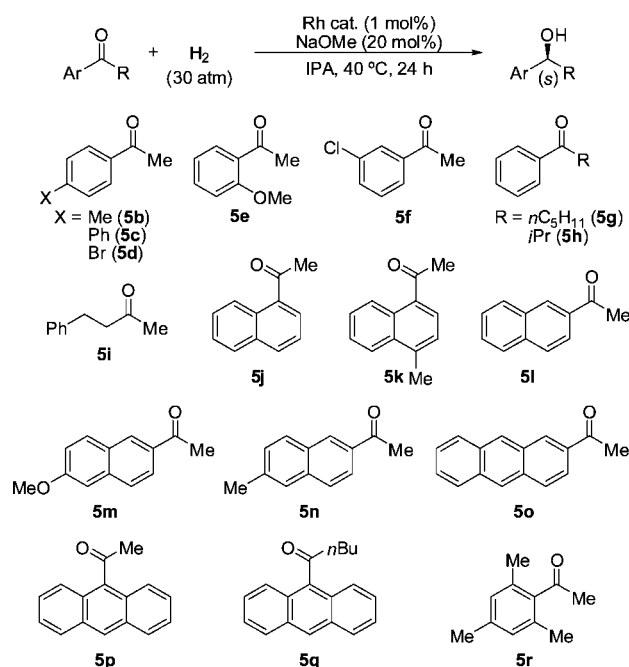
Figure 2. ORTEP diagram of **3b** (left) and **3c** (right) at the 50% probability level. Hydrogen atoms and solvents have been omitted for clarity. Selected bond lengths (Å) for **3b**: Ru(1)–C(1) 1.9635(18), Ru(1)–C(27) 1.8136(19), Ru(1)–N(1) 2.0908(16), Ru(1)–N(2) 2.0987(15), Ru(1)–O(4) 2.1609(14), Ru(1)–O(5) 2.1113(14). For **3c**: Ru(1)–C(1) 1.965(3), Ru(1)–C(24) 1.813(4), Ru(1)–N(1) 2.097(3), Ru(1)–N(2) 2.100(3), Ru(1)–O(3) 2.109(2), Ru(1)–O(4) 2.156(2).

Table 1. Enantioselective Hydrogenation of 4-MeOC₆H₄COMe (**5a**)^a

run	cat.	base	yield ^b	ee ^c
1	2a	NaOMe	99	65
2	3a	NaOMe	98	64
3	3b	NaOMe	87	56
4	4a	NaOMe	74	13
5	3a	NaOEt	99	56
6	3a	NaOtBu	99	67
7	3a	KOtBu	98	63
8	3a	LiOMe	98	51
9	3a	K ₂ CO ₃	3	22
10	3a	Cs ₂ CO ₃	11	37
11	3a		1	
12 ^d	3a	NaOMe	3	56
13 ^e	3a	NaOMe	13	27

^a Reactions were carried out under 30 atm of H₂ in the presence of cat. (1 mol %) and a base (20 mol %) in 2-propanol (10 mL) at 40 °C for 24 h. ^b Isolated yield. ^c Determined by HPLC. ^d Reaction was carried out in MeOH (10 mL). ^e Reaction was carried out in EtOH (10 mL).

Scheme 3. Hydrogenation of Ketones Catalyzed by (Phebox)Ru Complexes



by **3b** (runs 17–20). Enantioselectivities of 2-naphthylmethylketone (**5l**) with **3a** and **3b** were increased to 60% and 90%

Table 2. Enantioselective Hydrogenation of Ketones Catalyzed by **3**^a

run	ketone	cat.	yield ^b	ee ^c
1	5b	3a	98	79 (S)
2	5b	3b	95	65 (S)
3	5c	3a	99	77 (S)
4	5c	3b	99	69 (S)
5	5d	3a	22	4 (S)
6	5d	3b	8	14 (S)
7	5e	3a	98	81 (S)
8	5e	3b	98	72 (S)
9	5f	3a	97	6 (S)
10	5f	3b	72	0
11	5g	3a	96	85 (S)
12	5g	3b	97	51 (S)
13	5h	3a	97	71 (S)
14	5h	3b	95	83 (S)
15	5i	3a	95	5 (S)
16	5i	3b	96	15 (S)
17	5j	3a	98	74 (S)
18	5j	3b	59	22 (S)
19	5k	3a	33	2
20	5k	3b	97	77
21	5l	3a	99	60 (S)
22	5l	3b	99	90 (S)
23	5m	3b	99	93 (S)
24	5n	3b	98	75 (S)
25	5o	3b	87	96 (S)
26	5p	3b	29	94 (S)
27 ^d	5p	3b	94	97 (S)
28	5q	3b	nr	
29	5r	3b	60	90

^a Reactions were carried out under 30 atm of H₂ using **3** (1 mol %) and NaOMe (20 mol %) in 2-propanol (10 mL) at 40 °C for 24 h. ^b Isolated yield. ^c Determined by HPLC. ^d 48 h.

ee, respectively (runs 21 and 22). The substituents at the 6-position of the 2-naphthyl group affected the enantioselectivity (runs 23 and 24). Notably, the reduction of 2- and 9-anthracenyl-substituted ketones, **5o** and **5p**, led to 96% and 94% ee, respectively (runs 25 and 26). A long reaction time in the case of **5p** resulted in the increase in the ee (run 27). However, no reaction of the bulky ketones **5q** was observed (run 28). Sterically hindered ketone **5r** exhibited a good selectivity but a decrease in the yield (run 29).

To determine the relationship between the yield and the enantioselectivity, the hydrogenation of ketone **5l** catalyzed by 1 mol % of **3-ph** at 40 °C was monitored under 30 atm of hydrogen (Figure 3). After 12 h, the yield and enantioselectivity reached 99% and 88% ee, respectively. It is interesting to note that the enantioselectivity during the low conversion of **5l** was

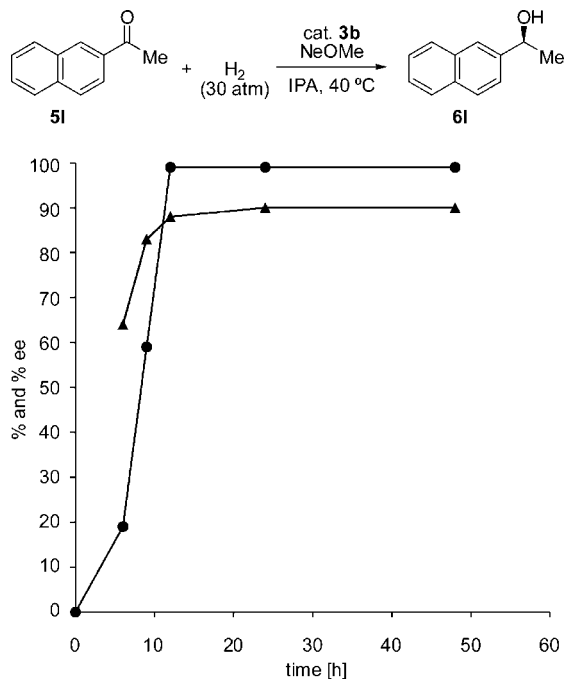


Figure 3. Plots of the yield (circles) and enantioselectivity (triangles) for hydrogenation of **5I** by **3b** (1 mol %) under 30 atm of H_2 in the presence of NaOMe (20 mol %) in 2-propanol at 40 °C.

Table 3. Enantioselective Hydrogenation of Ketones Catalyzed by **2b**^a

run	ketone	yield ^b	ee ^c
1	5I	99	89 (<i>S</i>)
2	5m	99	89 (<i>S</i>)
3	5o	97	95 (<i>S</i>)
4	5p	99	98 (<i>S</i>)
5	5q	99	97
6	5r	98	95

^a Reactions were carried out under 30 atm of H_2 using **2b** (0.5 mol %) and NaOMe (20 mol %) in 2-propanol (10 mL) at 40 °C for 24 h. ^b Isolated yield. ^c Determined by HPLC.

low with the slow initial reaction rate. This result suggests that an induction period is required for the generation of a catalytically active species.

As shown in Figure 3, hydrogenation of **5I** using **3b** for 6 h gave **6I** in 19% yields with 64% ee. On the other hand, the use of **2b** led to the increase in the yield to 99% after the same reaction time of 6 h; significant enhancement of the catalytic activity of **2b** was observed. This result encouraged us to perform a further study of hydrogenation of ketones using **2b**.

We adopted the same conditions as described in Table 3. In the presence of 1 mol % of **2b**, hydrogenation of **5I** under 30 atm of H_2 at 40 °C for 24 h proceeded smoothly to give the *S*-alcohol **6I** in 99% yield with 89% ee (run 1). This enantioselectivity was comparable to that observed in **3b**. Hydrogenation of **5m** using **2b** was also identical to that catalyzed by **3b** (run 2). On the other hand, improvement of yields and enantioselectivity was found in hydrogenation of sterically hindered ketones **5o–r**, which was not efficiently catalyzed by **3b**. For example, **5p** was reduced to the *S*-alcohol in 99% yield with 98% ee (run 4). In addition, hydrogenation of **5q** proceeded in 99% yield with 97% ee (run 5), whereas no reaction was observed in the case of **3b**. Similarly the yield and ee of hydrogenation of **5r** were improved by using **2b** (run 6). Enhancement of enantioselectivity in the case of **2b** is likely to relate to the increase in the yield of products. As described in

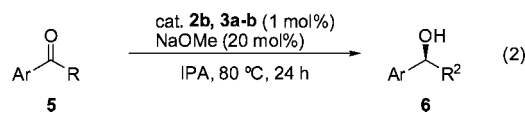
Table 4. Enantioselective Transfer Hydrogenation of Ketones^a

run	ketone	cat.	yield ^b	ee ^c
1	5I	2b	97	75
2	5I	3a	78	15
3	5I	3b	95	81
4	5m	2b	95	77
5	5m	3b	95	82
6	5o	2b	98	53
7	5o	3b	99	82
8	5p	2b	95	92
9	5p	3b	88	97
10	5r	2b	50	63
11	5r	3b	27	14

^a Reactions were carried out using **2b**, **3a**, and **3b** (1 mol %; Ru) and NaOMe (20 mol %) in 2-propanol (10 mL) at 80 °C for 24 h. ^b Isolated yield. ^c Determined by HPLC.

Figure 3, the induction period generated the catalytically active species that produced the alcohol with high enantioselectivity. Therefore an increase in the conversion of sterically hindered ketones **5o–r** using **2b** instead of **3b** would lead to an increase in the ee value of the alcohols.

Transfer Hydrogenation of Ketones. From the results of the enantioselective hydrogenation catalyzed by **2** and **3**, we attempted to carry out enantioselective transfer hydrogenation of ketones (Table 4, eq 2). Although reaction did not proceed at 40 °C, a reduced alcohol was obtained at 80 °C. The transfer hydrogenation reaction of **5I** catalyzed by **2b** provided the corresponding *S*-alcohol **6I** in 95% yield with 75% ee (run 1). Although the use of **3a** decreased the yield and enantioselectivity (15% ee; run 2), the use of **3b** increased the enantioselectivity (81% ee; run 3). As observed in hydrogenation, bulky ketones **5m–p** were found to be suitable substrates to **3b** (Table 3, runs 5, 7, 9). In most cases, the reaction with **3b** showed higher enantioselectivity than that with **2b**. However, hydrogenation of **5r** with both **2b** and **3b** resulted in low yields and enantioselectivity (runs 10 and 11). The formation of the *S*-alcohol in this reaction suggests that both the transfer hydrogenation and hydrogenation involve a similar transition state of a prochiral face for the determination of the ketone.

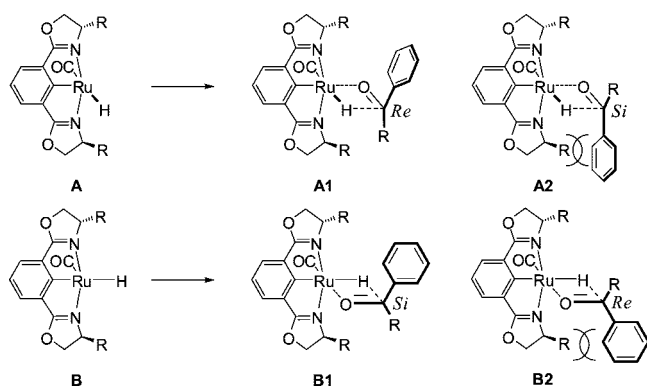


Proposed Transition State. Hydrogenation of ketones with (Phebox)Ru catalysts afforded alcohols with the *S*-absolute configuration. In the catalytic cycle, the monohydride intermediate (Phebox)Ru(H)(CO) may be formed by elimination of acac from **3** or $ZnCl_4$ from **2**, followed by the inter- or intramolecular activation of molecular hydrogen by a base (Scheme 4).²⁶ From judgment of the catalytic activity, replacement of $ZnCl_4$ in **2** is faster than that of acac in **3**. Alternatively β -H elimination of a Ru alkoxide intermediate, which is generated by exchange of the acac ligand or the $ZnCl_4$ salt with alkoxide, may provide the hydride intermediate in the case of transfer hydrogenation.^{26,27} Such a Ru alkoxide may also serve as a precursor to activation of hydrogen to generate the Ru hydride. To generate a vacant site on the Ru center, dissociation of the CO ligand could be ruled out. As the monohydride intermediate, two configurations, namely, *cis*-(Phebox)Ru(H)(CO) (**A**) and *trans*-(Phebox)Ru(H)(CO) (**B**), can be presumed. Each intermediate provides the

(26) Clapham, S. E.; Hadzovic, A.; Morris, R. H. *Coord. Chem. Rev.* **2004**, *248*, 2201–2237.

(27) Gagliardo, M.; Chase, P. A.; Brouwer, S.; van Klink, G. P. M.; van Koten, G. *Organometallics* **2007**, *26*, 2219–2227.

Scheme 4. Proposed Mechanism



corresponding 1:1 complexes with a ketone. In the catalytic systems of diphosphine/diamine Ru(II) complexes, a six-membered chelate mechanism using a metal-hydride and an amine proton at an outer sphere has been proposed.²⁸ Because of the absence of an amine fragment, the (Phebox)Ru system would involve an inner-sphere mechanism, namely, direct interaction of ketones with the Ru–H bond, as depicted in Scheme 4. To minimize nonbonded repulsion between the oxazoline substituent and the ketone, **A2** and **B2** could be ruled out. In the case of **A1**, hydride attack to the *re*-face side of the ketone is sterically favored to provide the corresponding *S*-alcohol. On the other hand, **B1** involves a hydride attack to the *si*-face side that provides the *R*-alcohol. Therefore, it was concluded that the catalytic hydrogenation might involve the **A1** intermediate rather than **B1** from the determination of the chiral face of the ketone. The hypothetical transition state of the (Phebox)Ru system is different from that of the bis(oxazolinyl)pyridine-Ru system reported by Gimeno and co-workers.^{3a}

Conclusion

The synthesis of novel Ru complexes with tridentate Phebox ligands was described via C–H activation using commercially available RuCl₃·3(H₂O) in the presence of Zn and cod. X-ray diffraction analysis of these complexes revealed the molecular structures, which consist of meridional Phebox ligands coordinated with the Ru–C bond. It was also found that these (Phebox)Ru complexes catalyze the enantioselective hydrogenation and transfer hydrogenation of ketones in 2-propanol with NaOMe as a base to afford the corresponding *S*-alcohols with high enantioselectivity, up to 98% ee.

Experimental Section

General Procedures. ¹H and ¹³C NMR spectra were obtained at 25 °C on a Varian Mercury 300 spectrometer and a Varian Inova 500 spectrometer. ¹H chemical shifts were reported in δ units, in ppm relative to the singlet at 7.26 ppm for CDCl₃ and 7.16 ppm for C₆D₆. ¹³C NMR spectra were reported in terms of chemical shift (δ, ppm) relative to the triplet at δ = 77.0 ppm for CDCl₃ and 128.0 ppm for C₆D₆. Infrared spectra were recorded on a JASCO FT/IR-230 spectrometer. Absolute toluene and THF were purchased from TCI. Column chromatography was performed with a silica gel column (Kanto Kagaku, silica gel 60). **1a** and **1c** were prepared by the reported method.²³

Synthesis of [(*S,S*)-*dm*-Phebox-*ph*]H (1b**).** According to the synthetic method of **1a**,²² **1b** was prepared using 4,6-dimethylisoph-

thalic acid²⁹ (1.94 g, 10.0 mmol), thionyl chloride (6.0 mL), (*S*)-(+)-2-phenylglycinol (2.74 g, 20.0 mmol), triethylamine (40 mL), and methanesulfonyl chloride (4.0 mL, 52 mmol). The crude product was purified by column chromatography on silica gel with ethyl acetate/hexane (1:5) to give **1b** (2.14 g, 5.42 mmol, 54%). Colorless solid; mp 103–104 °C. [α]_D²³ = –62.9 (*c* 1.00 in CHCl₃). ¹H NMR (300 MHz, CDCl₃, rt): δ 2.69 (s, 6H), 4.20 (dd, *J* = 8.1, 8.3 Hz, 2H), 4.74 (dd, *J* = 8.1, 10.2 Hz, 2H), 5.44 (dd, *J* = 8.3, 10.2 Hz, 2H), 7.19 (s, 1H), 7.27–7.39 (m, 10H), 8.45 (s, 1H). ¹³C NMR (75 MHz, CDCl₃, rt): δ 22.0, 70.3, 73.5, 76.5, 123.9, 126.1, 126.9, 128.1, 131.4, 134.0, 141.4, 142.0, 163.6. IR (KBr): ν 1635 cm⁻¹. Anal. Calcd for C₂₆H₂₄N₂O₄: C, 78.76; H, 6.10; N, 7.07. Found: C, 78.39; H, 6.11; N, 6.77.

Synthesis of [(*S,S*)-*dm*-Phebox-*ip*]Ru(CO)Cl₂(ZnCl₂) (2a**).** A 100 mL flask was charged with RuCl₃·3(H₂O) (523 mg, 2.0 mmol), **1a** (329 mg, 1.0 mmol), and Zn (327 mg, 5.0 mmol). Under an argon atmosphere, ethanol (20 mL) and 1,5-cyclooctadiene (0.61 mL, 5.0 mmol) were added, and the mixture was refluxed for 24 h. After removal of the solvent under reduced pressure, the residue was extracted with toluene and the extract was concentrated. The crude product was purified by column chromatography on silica gel with ethyl acetate/hexane (1:1) to give **2a** (373 mg, 0.25 mmol, 65%). Yellow solid; mp 209–210 °C (dec). ¹H NMR (500 MHz, C₆D₆, rt): δ 0.48 (d, *J* = 7.0 Hz, 3H), 0.61 (d, *J* = 7.0 Hz, 3H), 0.71 (d, *J* = 7.0 Hz, 3H), 0.76 (d, *J* = 6.5 Hz, 3H), 0.91 (d, *J* = 6.5 Hz, 3H), 0.92 (d, *J* = 6.0 Hz, 3H), 0.95 (d, *J* = 7.0 Hz, 3H), 1.16 (d, *J* = 6.5 Hz, 3H), 2.42 (s, 6H), 2.45 (s, 3H), 2.47 (s, 3H), 2.78 (m, 2H), 2.96 (m, 2H), 3.67–3.82 (m, 5H), 3.87–4.01 (m, 3H), 4.05–4.13 (m, 2H), 4.44 (m, 1H), 4.73 (m, 1H), 6.45 (s, 1H), 6.46 (s, 1H). ¹³C NMR (75 MHz, C₆D₆, rt): δ 14.7, 14.9, 15.4, 15.6, 19.4, 19.5, 19.6, 20.2, 29.3, 29.5, 29.6, 29.8, 67.2, 67.4, 70.0, 70.7, 130.0, 130.1, 140.0, 174.0, 174.5, 193.7, 195.3, 195.6. IR (KBr): ν 1936 cm⁻¹. Anal. Calcd for C₄₂H₅₄N₄O₆Cl₄Ru₂Zn: C, 45.03; H, 4.86; N, 5.00. Found: C, 45.04; H, 4.99; N, 4.83.

Synthesis of [(*S,S*)-*dm*-Phebox-*ph*]Ru(CO)Cl₂(ZnCl₂) (2b**).** Preparation procedure of **2b** was done in a similar manner with RuCl₃·3(H₂O) (523 mg, 2.0 mmol), **1b** (394 mg, 1.0 mmol), Zn (327 mg, 5.0 mmol), and 1,5-cyclooctadiene (0.61 mL, 5.0 mmol). The crude product was purified by column chromatography on silica gel with ethyl acetate/hexane (1:1) to give **2b** (366 mg, 0.59 mmol, 58%). Orange solid; mp 132–133 °C (dec). ¹H NMR (300 MHz, C₆D₆, rt): δ 2.52 (brs, 12H), 3.87 (t, *J* = 9.6 Hz, 2H), 3.95–4.11 (m, 6H), 4.53 (t, *J* = 9.2 Hz, 2H), 4.53 (dd, *J* = 6.6, 10.2 Hz, 2H), 6.60 (s, 2H), 7.13–7.54 (m, 12H). ¹³C NMR (75 MHz, C₆D₆, rt): δ 19.7, 66.5, 69.4, 77.7, 78.4, 127.2–130.3, 139.2, 140.2, 140.3, 140.7, 174.2, 175.5, 192.9, 198.4. IR (KBr): ν 2041, 1932 cm⁻¹. Anal. Calcd for C₅₄H₄₆N₄O₆Cl₄Ru₂Zn: C, 51.63; H, 3.69; N, 4.46. Found: C, 51.77; H, 3.88; N, 4.05.

Synthesis of [(*S,S*)-*dm*-Phebox-*dm*]Ru(CO)Cl₂(ZnCl₂) (2c**).** Preparation procedure of **2c** was done in a similar manner with RuCl₃·3(H₂O) (523 mg, 2.0 mmol), **1c** (300 mg, 1.0 mmol), Zn (327 mg, 5.0 mmol), and 1,5-cyclooctadiene (0.61 mL, 5.0 mmol). The crude product was purified by column chromatography on silica gel with ethyl acetate/hexane (1:1) to give **2c** (470 mg, 0.43 mmol, 86%). Yellow solid; mp 154–155 °C (dec). ¹H NMR (300 MHz, C₆D₆, rt): δ 1.26 (s, 6H), 1.31 (s, 6H), 1.54 (s, 6H), 1.81 (s, 6H), 2.41 (s, 6H), 2.49 (s, 6H), 3.61 (d, *J* = 8.6 Hz, 2H), 3.65 (d, *J* = 8.6 Hz, 2H), 3.69 (d, *J* = 8.3 Hz, 2H), 3.72 (d, *J* = 8.3 Hz, 2H), 6.46 (s, 2H). ¹³C NMR (75 MHz, C₆D₆, rt): δ 19.7, 27.8, 28.0, 28.9, 29.0, 65.9, 66.0, 81.9, 130.3, 139.7, 172.8, 193.8, 195.0. IR (KBr): ν 2030, 1937 cm⁻¹. Anal. Calcd for C₃₈H₄₆N₄O₆Cl₄Ru₂Zn: C, 42.89; H, 4.36; N, 5.26. Found: C, 42.63; H, 4.37; N, 4.81.

(28) Sandoval, C. A.; Ohkuma, T.; Muñiz, K.; Noyori, R. *J. Am. Chem. Soc.* **2003**, *125*, 13490–13503.

(29) (a) Schröder, A.; Karbach, D.; Güther, R.; Vögtle, F. *Chem. Ber.* **1992**, *125*, 1881–1887. (b) van der Made, A. W.; van der Made, R. H. *J. Org. Chem.* **1993**, *58*, 1262–1263. (c) Gerisch, M.; Krumper, J. R.; Bergman, R. G.; Tilley, T. D. *Organometallics* **2003**, *22*, 47–58.

Table 5. Crystallographic Data for 2c, 3b, and 3c

	2c	3b	3c
formula	C ₃₈ H ₄₆ Cl ₄ N ₄ O ₆ Ru ₂ Zn	C ₂₆ H ₃₆ N ₂ O ₆ Ru	C ₂₄ H ₃₂ N ₂ O ₆ Ru
fw	1064.10	573.64	545.59
cryst syst	triclinic	orthorhombic	tetragonal
space group	<i>P</i> $\bar{1}$	<i>P</i> 2 ₁ 2 ₁	<i>I</i> ₄ / <i>a</i>
<i>a</i> , Å	8.320(7)	11.9056(6)	31.843(5)
<i>b</i> , Å	10.286(9)	13.1663(6)	31.843(5)
<i>c</i> , Å	26.63(2)	18.7063(9)	10.133(3)
α , deg	97.657(17)	90	90
β , deg	91.08(2)	90	90
γ , deg	105.23(2)	90	90
<i>V</i> , Å ³	2176(3)	2932.3(2)	10274(4)
Z value	2	4	16
<i>D</i> _{calc} , g cm ⁻³	1.624	1.413	1.388
temp, °C	−120	−100	−100
μ (Mo K α), mm ⁻¹	1.525	0.577	0.647
radiation, λ , Å	0.71073	0.71073	0.71073
no. of rflns collected	15 663	21 035	35 149
no. of indep rflns	10 175 [<i>R</i> (int) = 0.0563]	6735 [<i>R</i> (int) = 0.0206]	5894 [<i>R</i> (int) = 0.0575]
<i>R</i> 1 (<i>I</i> > 2 σ (<i>I</i>))	0.0834	0.0240	0.0473
w <i>R</i> 2 (<i>I</i> > 2 σ (<i>I</i>))	0.2107	0.0607	0.1308
<i>R</i> 1 (all data)	0.1108	0.0248	0.0563
w <i>R</i> 2 (all data)	0.2296	0.0612	0.1383
parameters	508	365	301
GOF	1.078	1.080	1.154

Synthesis of [(*S,S*)-*dm*-Phebox-*ip*]*Ru*(acac)(CO) (3a). Method A: A 100 mL flask was charged with **2a** (408 mg, 0.36 mmol) and Na(acac) (264 mg, 2.16 mmol). Under an argon atmosphere, toluene (2 mL) was added and the mixture was stirred at room temperature for 12 h. After removal of the solvent under reduced pressure, the residue was purified by column chromatography on silica gel with ethyl acetate/hexane (1:5) to give **3a** (365 mg, 0.66 mmol, 90%). Method B: A 100 mL flask was charged with RuCl₃·3(H₂O) (523 mg, 2.0 mmol), **1a** (329 mg, 1.0 mmol), and Zn (327 mg, 5.0 mmol). Under an argon atmosphere, ethanol (20 mL) and 1,5-cyclooctadiene (0.61 mL, 5.0 mmol) were added and the mixture was refluxed for 24 h. After cooling to room temperature, acetylacetone (0.21 mL, 2.0 mmol) was added and the mixture was stirred for 20 h at room temperature. After removal of the solvent under reduced pressure, the resulting residue was extracted with toluene and the extract was filtrated. The concentrated filtrate was purified via column chromatography on silica gel with ethyl acetate/hexane (1:5) to give **3a** (258 mg, 0.47 mmol, 47%). Orange solid; mp 192–193 °C (dec). ¹H NMR (300 MHz, CDCl₃, rt): δ 0.61 (d, *J* = 6.9 Hz, 3H), 0.84 (d, *J* = 7.2 Hz, 3H), 0.90 (d, *J* = 6.9 Hz, 3H), 0.92 (d, *J* = 6.9 Hz, 3H), 1.66 (s, 3H), 1.86–1.95 (m, 1H), 2.03 (s, 3H), 2.06–2.12 (m, 1H), 2.51 (s, 6H), 3.73–3.79 (m, 1H), 4.00–4.05 (m, 1H), 4.43–4.65 (m, 4H), 5.13 (s, 1H), 6.56 (s, 1H). ¹³C NMR (75 MHz, CDCl₃, rt): δ 14.3, 15.6, 19.0, 19.28, 19.33, 19.37, 28.28, 28.34, 29.5, 30.2, 67.7, 69.0, 70.1, 70.8, 97.9, 126.4, 129.6, 129.7, 138.6, 173.7, 174.2, 185.7, 187.7, 194.7, 201.7. IR (KBr): ν 1907, 1594, 1512 cm⁻¹. Anal. Calcd for C₂₆H₃₄N₂O₅Ru: C, 56.20; H, 6.17; N, 5.04. Found: C, 56.13; H, 6.18; N, 5.22.

Synthesis of [(*S,S*)-*dm*-Phebox-*ph*]*Ru*(acac)(CO) (3b). The complex **3b** was prepared by using method A in 77% and method B in 45% yield. Orange solid; mp 201–202 °C (dec). ¹H NMR (300 MHz, CDCl₃, rt): δ 1.40 (s, 3H), 1.61 (s, 3H), 2.61 (s, 6H), 4.46–4.53 (m, 2H), 4.66 (s, 1H), 4.74 (t, *J* = 9.9 Hz, 1H), 4.98–5.11 (m, 3H), 6.64 (s, 1H), 7.09–7.35 (m, 10H). ¹³C NMR (75 MHz, CDCl₃, rt): δ 19.4, 19.5, 27.5, 28.3, 67.5, 68.1, 77.8, 98.0, 126.4, 127.1, 127.3, 127.4, 127.8, 127.9, 128.2, 129.6, 129.8, 139.25, 139.29, 139.4, 139.5, 174.8, 175.3, 184.3, 187.3, 194.0, 203.9. IR (KBr): ν 1913, 1594, 1518 cm⁻¹. Anal. Calcd for C₃₂H₃₀N₂O₅Ru: C, 61.63; H, 4.85; N, 4.49. Found: C, 61.67; H, 4.84; N, 4.77.

Synthesis of (*dm*-Phebox-*dm*)*Ru*(acac)(CO) (3c). The complex **3c** was prepared by using method A in 94% yield. Yellow solid; mp 195–196 °C (dec). ¹H NMR (300 MHz, CDCl₃, rt): δ 1.10 (s, 6H), 1.37 (s, 6H), 1.65 (s, 3H), 2.05 (s, 3H), 2.53 (s, 6H), 4.38 (d, *J* = 8.4 Hz, 2H), 4.42 (d, *J* = 8.4 Hz, 2H), 5.25 (s, 1H), 6.55 (s, 1H). ¹³C

NMR (75 MHz, CDCl₃, rt): δ 19.4, 27.2, 27.5, 28.4, 28.5, 63.9, 81.6, 98.8, 126.3, 130.1, 128.3, 172.6, 185.1, 187.4, 194.8, 201.3. IR (KBr): ν 1914, 1591, 1513 cm⁻¹. Anal. Calcd for C₂₄H₃₀N₂O₅Ru: C, 54.64; H, 5.73; N, 5.31. Found: C, 54.73; H, 5.80; N, 5.54.

Synthesis of [(*S,S*)-*dm*-Phebox-*ip*]*Ru*Cl(CO)₂ (4a). A 100 mL flask was charged with RuCl₃·3(H₂O) (523 mg, 2.0 mmol), **1a** (329 mg, 1.0 mmol), and Zn (327 mg, 5.0 mmol). Under an argon atmosphere, ethanol (20 mL) and 1,5-cyclooctadiene (0.61 mL, 5.0 mmol) were added and the mixture was refluxed for 24 h. After cooling to room temperature, the reaction atmosphere was replaced by 1 atm of carbon monoxide and the mixture was stirred for 20 h at room temperature. After filtration through Celite, the resulting filtrate was evaporated. The residue was purified via column chromatography on silica gel with ethyl acetate/hexane (1:5) to give **4a** (327 mg, 0.62 mmol, 62%). Dark red solid; mp 196–197 °C (dec). ¹H NMR (300 MHz, CDCl₃, rt): δ 0.83 (d, *J* = 6.9 Hz, 3H), 0.96 (d, *J* = 6.9 Hz, 3H), 0.98 (d, *J* = 6.9 Hz, 3H), 0.99 (d, *J* = 6.9 Hz, 3H), 2.13–2.21 (m, 1H), 2.30–2.35 (m, 1H), 2.53 (s, 3H), 2.54 (s, 3H), 3.83–3.89 (m, 1H), 4.02–4.06 (m, 1H), 4.53–4.61 (m, 2H), 4.63–4.72 (m, 2H), 6.75 (s, 1H). ¹³C NMR (75 MHz, CDCl₃): δ 14.5, 15.3, 19.25, 19.33, 19.7, 29.4, 29.8, 67.9, 70.4, 70.6, 70.7, 127.6, 127.8, 129.2, 140.2, 140.3, 174.3, 174.8, 191.8, 194.6, 199.2. IR (KBr): ν 2037, 1959, 1602, 1482, 1387 cm⁻¹. Anal. Calcd for C₂₂H₂₇N₂O₄ClRu: C, 50.82; H, 5.23; N, 5.39. Found: C, 50.45; H, 5.16; N, 5.38.

Synthesis of (*dm*-Phebox-*dm*)*Ru*Cl(CO)₂ (4c). The complex **4c** was prepared in a similar manner (343 mg, 0.70 mmol, 70%). Pale brown; mp 168–169 °C (dec). ¹H NMR (300 MHz, CDCl₃): δ 1.33 (s, 6H), 1.46 (s, 6H), 2.53 (s, 6H), 4.47 (d, *J* = 8.6 Hz, 2H), 4.52 (d, *J* = 8.6 Hz, 2H), 6.73 (s, 1H). ¹³C NMR (75 MHz, CDCl₃): δ 19.4, 27.6, 28.0, 64.9, 81.1, 128.4, 129.0, 140.1, 172.9, 191.6, 195.8, 199.4. IR (KBr): ν 2032, 1960, 1604, 1482, 1379 cm⁻¹. Anal. Calcd for C₂₀H₂₃N₂O₄ClRu: C, 48.83; H, 4.71; N, 5.69. Found: C, 48.64; H, 4.68; N, 5.60.

General Procedure for Hydrogenation. A stainless steel autoclave was charged with (Phebox)*Ru* catalyst (0.010 mmol), NaOMe (0.2 mmol), and ketone (1.0 mmol). After addition of 2-propanol (10 mL) under an Ar atmosphere, the autoclave was sealed. After purging with H₂, the H₂ pressure was adjusted to 30 atm. After being stirred at 40 °C for 24 h, the solvent was removed under reduced pressure. The residue was purified by column chromatography on silica gel with ethyl acetate/hexane (1:10), yielding a white solid of an alcohol. The enantioselectivity was determined by using HPLC with a proper chiral column.

(S)-(−)-1-(4'-Methoxyphenyl)ethanol (**6a**, Table 1, run 2):³⁰ [α]_D²⁵ −27.3 (c 5.11, CHCl₃), [lit.³⁰ gives [α]_D²⁵ −51.9 (c 0.718, CHCl₃, 64% ee (S))]. Chiral HPLC (Daicel Chiralpak AS-H, hexane/2-propanol, 95:5, 0.8 mL/min) showed 64% ee (*t*_R = 26.4 min, *t*_S = 36.1 min).

(S)-(−)-1-(4'-Methylphenyl)ethanol (**6b**, Table 2, run 1):³⁰ [α]_D²⁴ −40.3 (c 7.74, CHCl₃), [lit.³⁰ gives [α]_D²² −43.5 (c 0.994, MeOH, 99% ee (S))]. Chiral HPLC (Daicel Chiralcel OJ-H, hexane/2-propanol, 95:5, 0.8 mL/min) showed 79% ee (*t*_S = 15.3 min, *t*_R = 16.8 min).

(S)-(−)-1-(*p*-Biphenyl)ethanol (**6c**, Table 2, run 3):³¹ [α]_D²⁴ −29.5 (c 1.00, CHCl₃), [lit.³¹ gives [α]_D²⁸ −43.7 (c 0.75, CHCl₃, 99% ee (S))]. Chiral HPLC (Daicel Chiralcel OD, hexane/2-propanol, 95:5, 0.8 mL/min) showed 77% ee (*t*_S = 16.6 min, *t*_R = 19.1 min).

(S)-(−)-1-(4'-Bromophenyl)ethanol (**6d**, Table 2, run 6):³⁰ [α]_D²⁴ −2.4 (c 1.05, CHCl₃), [lit.³⁰ gives [α]_D²³ −37.9 (c 1.13, CHCl₃, 99% ee (S))]. Chiral HPLC (Daicel Chiralcel OD-H, hexane/2-propanol, 99:1, 0.8 mL/min) showed 14% ee (*t*_S = 36.6 min, *t*_R = 38.9 min).

(S)-(−)-1-(2'-Methoxyphenyl)ethanol (**6e**, Table 2, run 7):³⁰ [α]_D²⁵ −19.6 (c 2.33, CHCl₃), [lit.³⁰ gives [α]_D²³ −63.0 (c 1.10, CHCl₃, 99% ee (S))]. Chiral HPLC (Daicel Chiralcel OB-H, hexane/2-propanol, 95:5, 0.8 mL/min) showed 81% ee (*t*_S = 11.6 min, *t*_R = 20.1 min).

(S)-(−)-1-(3'-Chlorophenyl)ethanol (**6f**, Table 2, run 9):³⁰ [α]_D²⁴ −2.5 (c 5.95, CHCl₃), [lit.³⁰ gives [α]_D²³ −43.5 (c 1.08, CHCl₃, 99% ee (S))]. Chiral HPLC (Daicel Chiralcel OJ-H, hexane/2-propanol, 95:5, 0.8 mL/min) showed 6% ee (*t*_S = 12.7 min, *t*_R = 14.4 min).

(S)-(−)-1-Phenyl-1-hexanol (**6g**, Table 2, run 11):³¹ [α]_D²⁴ −15.5 (c 0.435, CHCl₃), [lit.³¹ gives [α]_D²⁴ −35.0 (c 0.88, CHCl₃, 92% ee (S))]. Chiral HPLC (Daicel Chiralcel OB-H, hexane/2-propanol, 95:5, 0.8 mL/min) showed 85% ee (*t*_{minor} = 23.1 min, *t*_{major} = 29.0 min).

(S)-(−)-2-Methyl-1-phenyl-1-propanol (**6h**, Table 2, run 14):³⁰ [α]_D²⁵ −27.5 (c 1.08, CHCl₃), [lit.³⁰ gives [α]_D²⁶ −49.1 (c 0.828, ether, 99% ee (S))]. Chiral HPLC (Daicel Chiralpak AD-H, hexane/2-propanol, 99:1, 0.8 mL/min) showed 83% ee (*t*_R = 20.4 min, *t*_S = 21.5 min).

(S)-(−)-4-Phenyl-2-butanol (**6i**, Table 2, run 16):³⁰ [α]_D²⁵ +3.8 (c 1.84, CHCl₃), [lit.³⁰ gives [α]_D²⁵ +21.0 (c 1.17, C₆H₆, 99% ee (S))]. Chiral HPLC (Daicel Chiralcel OD-H, hexane/2-propanol, 95:5, 0.8 mL/min) showed 15% ee (*t*_S = 12.5 min, *t*_R = 18.0 min).

(S)-(−)-1-(1'-Naphthyl)ethanol (**6j**, Table 2, run 17):³² [α]_D²⁵ −38.4 (c 1.68, CHCl₃), [lit.³² gives [α]_D²⁵ +78.9 (c 1.0, CHCl₃, 99% ee (R))]. Chiral HPLC (Daicel Chiralcel OD-H, hexane/2-propanol, 95:5, 0.8 mL/min) showed 74% ee (*t*_S = 20.6 min, *t*_R = 34.4 min).

(−)-1-(1'-(4'-Methylnaphthyl))ethanol (**6k**, Table 2, run 20): [α]_D²⁵ −39.1 (c 1.20, CHCl₃). Chiral HPLC (Daicel Chiralcel OD-H, hexane/2-propanol, 95:5, 0.8 mL/min) showed 77% ee (*t*_{minor} = 24.5 min, *t*_{major} = 28.1 min).

(S)-(−)-1-(2'-Naphthyl)ethanol (**6l**, Table 2, run 22):³³ [α]_D²⁵ −30.3 (c 0.996, CHCl₃), [lit.³³ gives [α]_D²⁵ +41.2 (c 0.50, EtOH, 95% ee (R))]. Chiral HPLC (Daicel Chiralcel OJ-H, hexane/2-propanol, 95:5, 0.8 mL/min) showed 90% ee (*t*_S = 33.4 min, *t*_R = 44.7 min).

(S)-(−)-1-((6'-Methoxy)-2-naphthyl)ethanol (**6m**, Table 2, run 23):³⁴ [α]_D²³ −40.4 (c 1.05, CHCl₃), [lit.³⁴ gives [α]_D²⁵ −39.6 (c 0.8, CHCl₃, 99% ee (S))]. Chiral HPLC (Daicel Chiralcel OD-H,

hexane/2-propanol, 95:5, 0.8 mL/min) showed 93% ee (*t*_S = 21.4 min, *t*_R = 30.9 min).

(S)-(−)-1-((6'-Methyl)-2-naphthyl)ethanol (**6n**, Table 2, run 24):³⁵ [α]_D²⁴ −33.7 (c 1.02, CHCl₃), [lit.³⁵ gives [α]_D²⁵ +33.4 (c 0.50, CHCl₃, 85% ee (R))]. Chiral HPLC (Daicel Chiralcel OD-H, hexane/2-propanol, 95:5, 0.8 mL/min) showed 75% ee (*t*_S = 18.1 min, *t*_R = 26.6 min).

(−)-1-(Anthracen-2-yl)ethanol (**6o**, Table 3, run 3): [α]_D²⁶ −23.5 (c 1.00, CHCl₃), Chiral HPLC (Daicel Chiralcel OD-H, hexane/2-propanol, 90:10, 0.8 mL/min) showed 95% ee (*t*_S = 17.2 min, *t*_R = 34.3 min).

(S)-(−)-1-(Anthracen-9-yl)ethanol (**6p**, Table 3, run 4):³⁶ [α]_D²⁶ −15.5 (c 1.00, CHCl₃), [lit.³⁶ gives [α]_D²² +11.47 (c 0.91, THF, 87.5% ee (R))]. Chiral HPLC (Daicel Chiralcel, AD-H, hexane/2-propanol, 90:10, 0.8 mL/min) showed 98% ee (*t*_R = 17.1 min, *t*_S = 26.5 min).

(+)-1-(Anthracen-9-yl)pentan-1-ol (**6q**, Table 3, run 5). [α]_D²⁷ +2.5 (c 2.23, CHCl₃), Chiral HPLC (Daicel Chiralcel AD-H, hexane/2-propanol, 95:5, 0.8 mL/min) showed 97% ee (*t*_R = 23.5 min, *t*_S = 26.7 min).

(S)-(−)-1-Mesitylethanol (**6r**, Table 3, run 6):³⁶ [α]_D²⁷ −60.6 (c 6.06, CHCl₃), [lit.³⁶ gives [α]_D²⁰ +37.3 (c 0.50, CHCl₃, 77% ee (R))]. Chiral HPLC (Daicel Chiralcel OD-H, hexane/2-propanol, 99:1, 0.8 mL/min) showed 95% ee (*t*_R = 25.8 min, *t*_S = 28.8 min).

General Procedure for Transfer Hydrogenation. A Schlenk tube was charged with (Phebox)Ru catalyst (0.010 mmol), NaOMe (0.2 mmol), ketone (1.0 mmol), and 2-propanol (10 mL). After being stirred at 80 °C for 24 h, the solvent was removed under reduced pressure. The residue was purified by column chromatography on silica gel with ethyl acetate/hexane (1:10), yielding a white solid of an alcohol. The enantioselectivity was determined by using HPLC with proper chiral columns.

X-ray Diffraction. Single crystals of **2c** were obtained by slow diffusion of pentane vapor in a toluene solution of **2c** at room temperature. Single crystals of **3b** and **3c** were obtained by solution of hexane/AcOEt. The diffraction data were collected on a Bruker SMART APEX CCD diffractometer with graphite-monochromated Mo K α radiation (λ = 0.71073 Å). An empirical absorption correction was applied by using SADABS. The structure was solved by direct methods and refined by full-matrix least-squares on *F*² using SHELXTL. All non-hydrogen atoms were refined with anisotropic displacement parameters. All hydrogen atoms were located on calculated positions and refined as rigid groups. The crystallographic and refined data are summarized in Table 5. CCDC 699555 (**2c**), 699556 (**3b**), and 699557 (**3c**) contain the supplementary crystallographic data for this paper. These data can be obtained free of charge from The Cambridge Crystallographic Data Center via www.ccdc.cam.ac.uk/data_request/cif.

Acknowledgment. This research was partly supported by a Grant-in-Aid for Scientific Research from the Ministry of Education, Culture, Sports, Science, and Technology, Japan (Concerto Catalysis; 460:18065011) and the Japan Society for the Promotion of Science (18350049, 20750073).

Supporting Information Available: Crystal data in CIF format. This material is available free of charge via the Internet at <http://pubs.acs.org>.

OM800953F

(30) Nakamura, K.; Matsuda, T. *J. Org. Chem.* **1998**, *63*, 8957–8964.

(31) Salvi, N. A.; Chattopadhyay, S. *Tetrahedron* **2001**, *57*, 2833–2839.

(32) Theisen, P. D.; Hesthcock, C. H. *J. Org. Chem.* **1988**, *53*, 2374–2378.

(33) Matharu, D. S.; Morris, D. J.; Kawamoto, A. M.; Clarkson, G. J.; Wills, M. *Org. Lett.* **2005**, *7*, 5489–5491.

(34) Koul, S.; Koul, J. L.; Singh, B.; Kapoor, M.; Parshad, R.; Manhas, K. S.; Taneja, S. C.; Qazi, G. N. *Tetrahedron: Asymmetry* **2005**, *16*, 2575–2591.

(35) Malkov, A. V.; Liddon, A. J. P. S.; Ramírez-López, P.; Bendová, L.; Haigh, D.; Kočovský, P. *Angew. Chem., Int. Ed.* **2006**, *45*, 1432–1435.

(36) Doucet, H.; Fernandez, E.; Layzell, T. P.; Brown, J. M. *Chem.—Eur. J.* **1999**, *5*, 1320–1330.

Kinetic Studies on the Oxidation of η^5 -Cyclopentadienyl Methyl Tricarbonyl Molybdenum(II) and the Use of Its Oxidation Products as Olefin Epoxidation Catalysts

Ahmad M. Al-Ajlouni,^{†,‡} Draganco Veljanovski,[†] Alejandro Capapé,[†] Jin Zhao,^{†,§} Eberhardt Herdtweck,[†] Maria José Calhorda,[⊥] and Fritz E. Kühn^{*,†}

Molecular Catalysis, Faculty of Chemistry, Technische Universität München, Lichtenbergstrasse 4, D-85747 Garching bei München, Germany, Department of Applied Chemical Sciences, Jordan University of Science and Technology, Irbid 22110, Jordan, Department of Chemistry, National University of Singapore, 3 Science Drive 3, Kent Ridge, 117543, Singapore, and Departamento de Química e Bioquímica, CQB, Faculdade de Ciências, Universidade de Lisboa, 1749-016 Lisboa, Portugal

Received September 22, 2008

The oxidation of η^5 -cyclopentadienyl(methyl)(tricarbonyl)molybdenum(II) (**1**) with excess *tert*-butylhydroperoxide (TBHP) initially yields η^5 -cyclopentadienyl(methyl)(dioxo)molybdenum(VI) (**2**), which further reacts with TBHP, forming η^5 -cyclopentadienyl(methyl)(oxo)(peroxo)molybdenum(VI) (**3**). The solid-state structure of **3** has been determined by single-crystal X-ray crystallography. Detailed kinetic studies have been carried out on the oxidation of **1** with TBHP as an oxidizing agent and on the catalytic activities of the resulting oxidation products, **2** and **3**, in olefin epoxidation. In the absence of oxidant, neither of the molybdenum species is able to transfer an O-atom to an olefin. However, both Mo(VI) species act as catalysts for the epoxidation of olefins with TBHP through the formation of active intermediates. It has been found that compound **3** reacts with excess TBHP to give an active intermediate, which exists in equilibrium with the catalyst precursor **3** with a K_{eq} close to 1. This intermediate is slowly formed in a reversible initial step. It reacts rapidly with an olefin, while it decomposes in the absence of olefin. Furthermore, the kinetic results indicate the formation of another active intermediate, originating from **2**, that is 3–5 times more active in epoxidation catalysis than the active intermediate formed from **3**. A mechanistic scheme is proposed, based on the kinetic results.

1. Introduction

Propylene oxide is an important intermediate in chemical industry, with an annual production of several million tons.¹ Propylene oxide is particularly important in the large-scale synthesis of propylene glycol, polyurethanes, and resins. A method that has been applied for a long time for the synthesis of propylene oxide is the chlorhydrine route. This method, however, consumes a considerable amount of Cl_2 and has a negative environmental impact. For the last decades significant research efforts both in industry and at universities have been dedicated to finding more efficient and environmentally benign synthetic pathways to propylene oxide and other valuable epoxides.² ARCO and Halcon described a catalytic process for the synthesis of epoxides in the late 1960s,³ and since then many research groups concentrated on mechanistic aspects of these catalytic reactions and on finding improved catalysts.^{4–6}

Among the variety of efficient catalysts known today for olefin epoxidation are some organometallic oxides containing

a metal in high oxidation state.⁷ Some of them can be conveniently synthesized from carbonyl precursors, such as $\text{Cp}'\text{Mo}(\text{CO})_3\text{R}$ (R = alkyl group).^{8–11} It has been found that

(4) (a) Fischer, E. O.; Vigoureux, S. *Chem. Ber.* **1958**, *91*, 1342. (b) Fischer, E. O.; Ulm, K.; Fritz, H. P. *Chem. Ber.* **1960**, *93*, 2167. (c) Cousins, M.; Green, M. L. H. *J. Chem. Soc.* **1963**, 889. (d) Nunes, C. D.; Valente, A. A.; Pillinger, M.; Rocha, J.; Gonçalves, I. S. *Chem.–Eur. J.* **2003**, *9*, 4380. (e) Abrantes, M.; Valente, A. A.; Pillinger, M.; Gonçalves, I. S.; Rocha, J.; Romão, C. C. *Inorg. Chem. Commun.* **2002**, *5*, 1069. (f) Abrantes, M.; Valente, A. A.; Pillinger, M.; Gonçalves, I. S.; Rocha, J.; Romão, C. C. *J. Catal.* **2002**, *209*, 237.

(5) (a) Herrmann, W. A.; Kühn, F. E. *Acc. Chem. Res.* **1997**, *30*, 169. (b) Deubel, D. V.; Frenking, G.; Gisdaks, P.; Herrmann, W. A.; Rösch, N.; Sundermeyer, J. *Acc. Chem. Res.* **2004**, *37*, 645. (c) Chong, A. O.; Sharpless, K. B. *J. Org. Chem.* **1977**, *42*, 1587. (d) Sheng, M. N.; Zajacek, J. G. *J. Org. Chem.* **1970**, *35*, 1839. (e) Sheldon, R. A.; van Doorn, J. A. *J. Catal.* **1973**, *31*, 427. (f) Sheldon, R. A.; van Doorn, J. A. A.; Schram, C. W. A.; de Jong, J. *J. Catal.* **1973**, *31*, 438.

(6) (a) Sheldon, R. A. *Recl. Trav. Chim.* **1973**, *92*, 253. (b) Thiel, W. R. *J. Mol. Catal. A: Chem.* **1997**, *117*, 449. (c) Wahl, G.; Kleinhenz, D.; Schorm, A.; Sundermeyer, J.; Stowasser, R.; Rummey, C.; Bringmann, G. *Chem.–Eur. J.* **1999**, *5*, 3237. (d) Poli, R. *Chem.–Eur. J.* **2004**, *10*, 332. (e) Chaumette, P.; Mimoun, H.; Saussine, L. *J. Organomet. Chem.* **1983**, *250*, 291. (f) Trost, M. K.; Bergman, R. G. *Organometallics* **1991**, *10*, 1172.

(7) (a) Kühn, F. E.; Santos, A. M.; Abrantes, M. *Chem. Rev.* **2006**, *106*, 2455. (b) Romão, C. C.; Kühn, F. E.; Herrmann, W. A. *Chem. Rev.* **1997**, *97*, 3197.

(8) (a) Fallor, J. W.; Ma, Y. *J. Organomet. Chem.* **1988**, *340*, 59. (b) Fallor, J. W.; Ma, Y. *J. Organomet. Chem.* **1989**, *368*, 45. (c) Bottomley, F.; Boyle, P.; Chen, J. *Organometallics* **1994**, *13*, 370.

(9) (a) Zhao, J.; Santos, A. M.; Herdtweck, E.; Kühn, F. E. *J. Mol. Catal. A: Chem.* **2004**, *222*, 265. (b) Radius, U.; Wahl, G.; Sundermeyer, J. Z. *Anorg. Allg. Chem.* **2004**, *630*, 848. (c) Robin, T.; Montilla, F.; Galindo, A.; Ruiz, C.; Hartmann, J. *Polyhedron* **1999**, *18*, 1485. (d) Pratt, M.; Harper, J. H. M.; Colbran, S. B. *Dalton Trans.* **2007**, 2746.

* Corresponding author. E-mail: fritz.kuehn@ch.tum.de.

[†] Technische Universität München.

[‡] Jordan University of Science and Technology.

[§] National University of Singapore.

[⊥] Universidade de Lisboa.

(1) (b) Weissmermel K., Arpe H. J. *Industrial Organic Chemistry*; Wiley: New York, 2003.

(2) (a) Bäckvall, J. E., Ed. *Modern Oxidation Methods*; Wiley-VCH: Weinheim, 2004. (b) Yudin, A. K., Ed. *Aziridines and Epoxides in Organic Synthesis*; Wiley-VCH: Weinheim, 2006.

(3) (a) Kollar J. (Halcon) US 3.350.422, US 3.351.635, 1967. (b) Sheng M. N., Zajacek G. J. (ARCO) GB 1.136.923, 1968. (c) Coltan, R.; Tomkins, I. B. *Aust. J. Chem.* **1965**, *18*, 447.

the latter catalyze the epoxidation of olefins with *tert*-butyl hydroperoxide (TBHP) and other alkyl hydroperoxides as oxidants.^{8,9}

The most thoroughly examined organometallic epoxidation catalyst known today is arguably methyltrioxorhenium, CH_3ReO_3 . In this particular case peroxy derivatives have been shown to be the active catalysts, and metal-attached η^2 -peroxy groups react with olefins when applied stoichiometrically.^{12–14} Compounds of formula $\text{Cp}'\text{Mo}(\text{CO})_3\text{R}$ and their oxidation products¹⁵ have not yet been examined in comparable detail, particularly with respect to mechanistic implications, and no active species beyond the Mo(VI)-dioxo species has been found or proposed to date. However, catalytic results show that their catalytic activity is considerable, and, in contrast to MTO they are both easier to derivatize and easier to immobilize.^{7–11,16} In this work, a detailed examination of the reaction mechanism of $\text{Cp}'\text{Mo}(\text{CO})_3\text{R}$ -based olefin epoxidation with TBHP as the oxidizing agent is presented, based on kinetic experiments. It involves a comprehensive investigation of the system starting with (1) the tricarbonyl, (2) the dioxo, and (3) the oxo peroxy compounds after adding excess TBHP in the presence and absence of olefin. Detailed kinetic studies have also been carried out on the activity of an oxo peroxy-derived active species with respect to olefin epoxidation with TBHP.

2. Results and Discussion

The title compound, $\text{CpMo}(\text{CO})_3\text{CH}_3$ (**1**), was synthesized and purified using a slightly modified literature method.¹⁷ When the carbonyl compound is treated with a TBHP excess of at least 5 equiv in dichloromethane, the Mo(VI)oxo-peroxy complex **3** is formed and can be isolated in good yields.

Compound **3** was characterized by UV–vis, IR, and NMR spectroscopy (see Experimental Section), and the structure was determined by single-crystal X-ray diffraction (see Supporting Information).

(10) Zhao, J.; Sakthivel, A.; Santos, A. M.; Kühn, F. E. *Inorg. Chim. Acta* **2005**, *358*, 4201.

(11) Honzicek, J.; Almeida Paz, F. A.; Romão, C. C. *Eur. J. Inorg. Chem.* **2007**, 2827.

(12) (a) Hroch, A.; Thiel, W. R.; Gemmecker, G. *Eur. J. Inorg. Chem.* **2000**, 1107, and references therein. (b) Kühn, F. E.; Groarke, M.; Benzce, É.; Herdtweck, E.; Prazeres, A.; Santos, A. M.; Calhorda, M. J.; Romão, C. C.; Gonçalves, I. S.; Lopes, A. D.; Pillinger, M. *Chem.–Eur. J.* **2002**, *8*, 2370–2383. (c) Veiros, L. F.; Prazeres, A.; Costa, P. J.; Romão, C. C.; Kühn, F. E.; Calhorda, M. J. *Dalton Trans.* **2006**, 1383. (d) Al-Ajlouni, A. M.; Valente, A. A.; Nunes, C. D.; Pillinger, M.; Santos, T. M.; Zhao, J.; Romão, C. C.; Gonçalves, I. S.; Kühn, F. E. *Eur. J. Inorg. Chem.* **2005**, 1716. (e) Al-Ajlouni, A.; Espenson, J. H. *J. Am. Chem. Soc.* **1995**, *117*, 9243. (f) Al-Ajlouni, A.; Espenson, J. H. *J. Org. Chem.* **1996**, *61*, 3969. (g) Espenson, J. H. *J. Chem. Soc., Chem. Commun.* **1999**, 479.

(13) (a) Herrmann, W. A.; Fischer, R. W.; Scherer, W.; Rauch, M. U. *Angew. Chem., Int. Ed.* **1993**, *32*, 1157. (b) Herrmann, W. A.; Fischer, R. W.; Rauch, M. U.; Scherer, W. *J. Mol. Catal.* **1994**, *86*, 243.

(14) (c) Kühn, F. E.; Santos, A. M.; Roesky, P. W.; Herdtweck, E.; Scherer, W.; Gisdakis, P.; Yudanov, I. V.; Di Valentin, C.; Rösch, N. *Chem.–Eur. J.* **1999**, *5*, 3603.

(15) (a) Legzdins, P.; Phillips, E. C.; Rettig, S. J.; Sánchez, L.; Trotter, J.; Yee, V. C. *Organometallics* **1988**, *7*, 1877. (b) Legzdins, P.; Phillips, E. C.; Sánchez, L. *Organometallics* **1989**, *8*, 940.

(16) (a) Zhao, J.; Herdtweck, E.; Kühn, F. E. *J. Organomet. Chem.* **2006**, *691*, 2199. (b) Zhao, J.; Jain, K. R.; Herdtweck, E.; Kühn, F. E. *Dalton Trans.* **2007**, 5567.

(17) (a) Burgmayer, S. J. N.; Templeton, J. L. *Inorg. Chem.* **1985**, *24*, 2224. (b) Abrantes, M.; Gago, S.; Valente, A. A.; Pillinger, M.; Gonçalves, I. S.; Santos, T. M.; Rocha, J.; Romão, C. C. *Eur. J. Inorg. Chem.* **2004**, 4914. (c) King, R. B.; Bisnette, M. B. *J. Organomet. Chem.* **1967**, *8*, 287. (d) Herrmann, W. A. In *Synthetic Methods of Organometallic and Inorganic Chemistry*; Herrmann, W. A., Ed. Georg Thieme Verlag: New York, 1997; Vol. 8, p 97. (e) Herrmann, W. A. In *Synthetic Methods of Organometallic and Inorganic Chemistry*; Herrmann, W. A.; Ed. Georg Thieme Verlag: New York, 1997; Vol. 8, p 98.

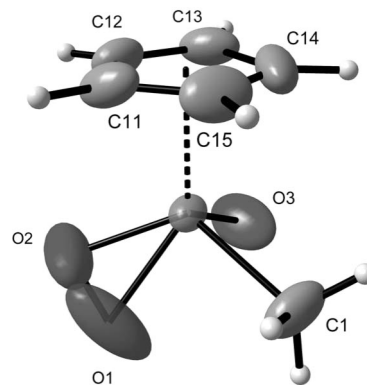
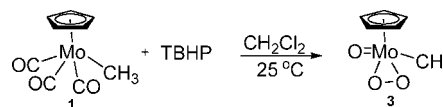


Figure 1. ORTEP-style plot of compound **3** in the solid state. Thermal ellipsoids are drawn at the 50% probability level. Details of the single-crystal X-ray diffraction studies are given in the Supporting Information.

Scheme 1. Synthesis of Mo(VI)oxo-peroxy Compound **3**



The single-crystal X-ray crystallographic analysis of compound **3** reveals that its solid-state molecular structure displays a slightly distorted “three-legged piano stool” conformation, in which the midpoint of the peroxy ligand is one of the legs of the piano stool. Two other structurally characterized Mo oxo-peroxy compounds and three W(VI)-oxoperoxy compounds of composition $\text{Cp}'\text{WO}(\text{O}_2)(\text{CH}_2\text{SiMe}_3)$ and $\text{Cp}'\text{WO}(\text{O}_2)\text{Cl}$ have a similar structural arrangement according to the literature.^{15a,18}

Kinetic Studies. Reaction of $\text{CpMo}(\text{CO})_3\text{CH}_3$ (1**) with TBHP.** The reaction of **1** with TBHP was carried out at room temperature and followed by NMR (in dry CDCl_3) and UV–vis (in dry CH_2Cl_2) spectroscopic techniques, respectively. The changes in the chemical shifts of the Cp and/or the methyl protons in the NMR spectra are particularly informative. When 0.06 mmol of **1** and 10 equiv of TBHP are mixed in 0.5 mL of CDCl_3 , the reaction starts immediately. The Cp signal of the carbonyl compound at 5.27 ppm decreases with time, and a new signal at 6.33 ppm appears. The area of this new signal reaches a maximum after 15 min, whereas the carbonyl compound peak is reduced to around 60% of its original size. The reduction of the signal at 6.33 ppm is associated with the buildup of a new signal at 6.29 ppm. After 2 h, the Cp signal of the carbonyl compound and the Cp signal at 6.33 ppm disappear completely, and only the signal at 6.29 ppm remains. The signal intensity–time curves are shown in Figure 2A. The ^{95}Mo NMR examination shows similar results. After 2 h the ^{95}Mo signal of **1** at -1424 ppm vanishes completely, and a new peak at -609 ppm, which has been assigned to the complex **3** is the only one observed.^{7a} An intermediate forming and disappearing in the same time frame as for the ^1H NMR experiments is observed at -346 ppm.

An experiment was designed to examine the compound (at 6.33 ppm), which is usually formed shortly after mixing TBHP with the carbonyl compound and later disappears. The above reaction was repeated and quenched after 15 min by adding MnO_2 . The filtrate is evaporated to dryness and extracted with diethyl ether to give a yellow solid. The product is analyzed by

(18) (a) Faller, J. W.; Ma, Y. *Organometallics* **1988**, *7*, 559. (b) Trost, M. K.; Green, M. L. H. *Organometallics* **1991**, *10*, 1172. (c) Chakraborty, D.; Bhattacharjee, H.; Krätzner, R.; Siefken, Roesky, H. W.; Usón, I.; Schmidt, H. G. *Organometallics* **1999**, *18*, 106.

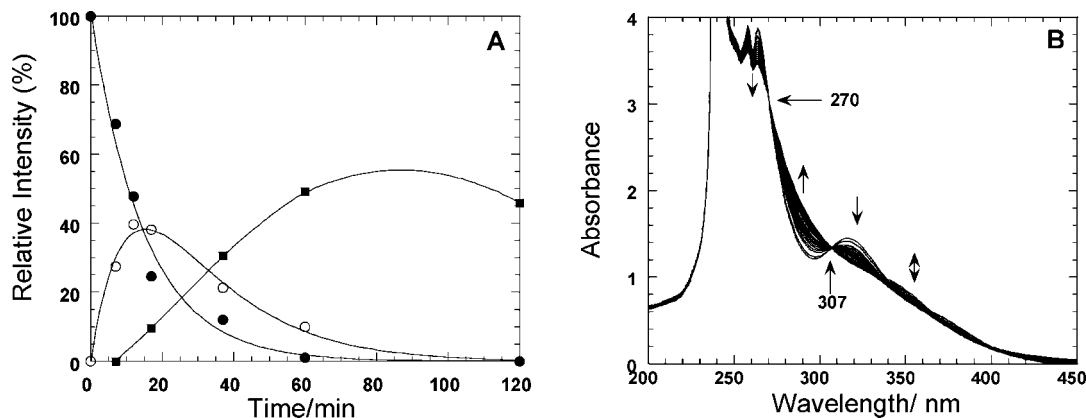
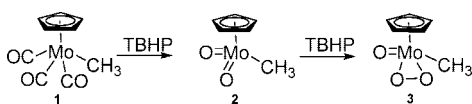


Figure 2. (A) Changes in the relative peak intensities with time of **1** (●) (at $\delta = 5.27$ ppm) and its products **2** (○) (at $\delta = 6.33$ ppm) and **3** (■) (at $\delta = 6.29$ ppm) during the reaction of **1** (0.06 mmol) with 10 equiv of TBHP in CDCl_3 at 20 °C. (B) UV-vis spectral changes (at 6 min intervals for the first 1 h and then every 10 min) for the reaction of **1** (0.33 mM) with TBHP (10 equiv) in CH_2Cl_2 at 20 °C.

Scheme 2. Proposed Reaction Pathway for the Oxidation of Compound **1**



¹H and ⁹⁵Mo NMR spectroscopy. The ¹H NMR spectrum shows a signal at 6.33 ppm and a signal at 1.45 ppm with 5:3 relative intensities, respectively. The ⁹⁵Mo NMR shows one signal at -346 ppm. A similar reaction profile can be obtained if the reaction is carried out in C₆D₆ under the same conditions, and the chemical shifts match with the NMR data for the dioxo-Mo(VI) compound, CpMoO₂CH₃ (**2**).^{15b} These results suggest that the formation of **3** from the reaction of the carbonyl compound **1** with TBHP proceeds via compound **2**, as shown in Scheme 2.

The yield of the final product, compound **3**, in the NMR experiments described above is less than 60% (with respect to **1**), due to a side reaction, which forms a highly insoluble precipitate. The latter was isolated as a blue solid, containing 42.3% of Mo, 18.7% of C, and 2.9% of H. Further characterization attempts were unsuccessful due to its insolubility in all common solvents. The blue solid can also not be redissolved by adding excess TBHP. It has been further tested as a catalyst in olefin epoxidation and was found to be completely inactive, even after prolonged reaction times.

The yield of compound **3** can be increased by increasing the TBHP/**1** ratio, suggesting that the major reaction pathway, which leads to the relatively stable product **3**, is favored. The side reaction pathway is totally suppressed with the addition of a substrate in the catalytic reaction.

The reaction progress was also followed by UV-vis spectroscopy with different concentrations and catalyst/TBHP ratios in CH₂Cl₂. One has strong absorptions at $\lambda_{\text{max}} = 256, 267,$ and 316 nm and a shoulder peak at $\lambda_{\text{max}} \sim 370$ nm. When the carbonyl complex (0.33 mM) is treated with a 10-fold excess of TBHP at room temperature, the absorbance at 316 nm decreases with time and the absorbance in the range 207–270 nm increases to give two clear isosbestic points at 307 and 270 nm (Figure 2B). These changes in absorbance are due to the formation of complex **2**. The reaction of **2** with TBHP proceeds, leading to an additional absorbance decrease in the range 307–335 nm and a slight increase in the absorbance in the range 335–400 nm, due to the formation of compound **3**. However, the isosbestic points due to this change are not all entirely clear; a possible explanation, based on further experimental evidence,

is given in the next section. It is worth mentioning, however, that under UV experimental conditions no precipitate was observed, possibly due to the higher TBHP excess that may decrease catalyst decomposition or side reactions.

The intensity-time curves and the changes in the UV absorbance with time can be used to determine the rate constants for the oxidation of the carbonyl compound **1** with TBHP to yield **2** and the formation of **3** from compound **2**. In the presence of excess TBHP, the reactions follow pseudo-first-order kinetics, and the decrease in the intensity of the signal at 5.27 ppm (Cp protons of the carbonyl compound) with time fits a first-order exponential decay equation ($I_t = I_\infty + (I_0 - I_\infty) \exp(-k_{\text{obs}}t)$). The value of the observed first-order rate constant was obtained from this fitting as $k_{\text{obs}} = (1.12 \pm 0.15) \times 10^{-3} \text{ s}^{-1}$. This indicates that the reaction is first-order with respect to the concentration of **1**. The buildup and the decay of the signal intensity at 6.33 ppm (Cp protons of **2**) was fitted to a biexponential (buildup and decay) equation to determine the pseudo-first-order constants for the formation of **2** ($k_f = (1.25 \pm 0.35) \times 10^{-3} \text{ s}^{-1}$) and for its reaction with TBHP ($k_r = (8.5 \pm 0.3) \times 10^{-4} \text{ s}^{-1}$). The rate constant k_f is also valid for the reaction of the carbonyl compound with TBHP and is in accord with the value obtained above from the time-dependent decrease of the carbonyl signal. These kinetic results confirm the observations made when **2** is prepared from **1** in the presence of excess TBHP. The oxoperoxy compound **3** starts appearing immediately after **2** is formed because the two rate constants for the formation of **2** and its reaction with TBHP to produce **3** are comparable.

Previous studies on CpMo(CO)₃Cl-type compounds indicate that the Mo-dioxo moiety is rapidly formed in the case of the Cl-containing compounds but reacts more slowly with additional TBHP to yield the final Mo-oxoperoxy product.^{18,15} From the results obtained here, it appears that the presence of a methyl group instead of a chloro ligand does not strongly affect the initial oxidation rate from Mo(II) to Mo(VI). However, the presence of a methyl group seems to enhance significantly the displacement rate of the oxo with the peroxy group on the Mo(VI) center. This difference in behavior of the Mo(VI) species between the Cl and the CH₃ derivative seems to become more pronounced in the further reaction between compound **3** and TBHP, where compound **3** can be transformed to an active species (**I**, see below), while the Cl derivative has been reported not to form an active catalyst in the presence of TBHP.¹⁸

Reaction of CpMoO(O)₂CH₃ (3**) with TBHP.** When **3** reacts with a large excess of TBHP (>100 equiv) in the absence of an olefin, a slight change of its UV-vis spectra occurs. After

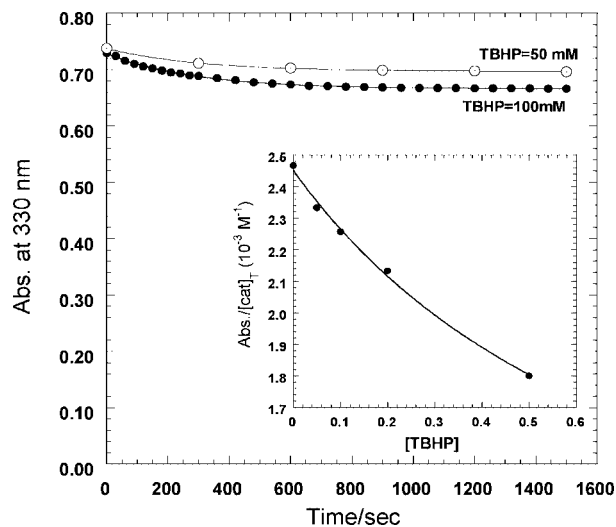


Figure 3. Changes in absorbance with time at 330 nm for the reaction of **3** with TBHP in CH_2Cl_2 at 20 °C. The inset shows a plot of $\text{Abs}_{\text{eq}}/[\text{Mo}]_{\text{T}}$ against $[\text{TBHP}]$; the solid line represents the calculated values based on eq 1 with $K_{\text{eq}} = 1.23$, $\epsilon_1 = 748 \text{ M}^{-1} \text{ cm}^{-1}$, and $\epsilon_p = 2460 \text{ M}^{-1} \text{ cm}^{-1}$.

mixing a 0.3 mM solution of **3** in CH_2Cl_2 (total volume 3 mL) with 0.15 mmol of TBHP at room temperature, the absorbance at 330 nm decreases exponentially with time and levels off after ~20 min. By adding more TBHP, the absorbance decreases further but never becomes zero even with very high TBHP excess (~1500 equiv), as shown in Figure 3. This must be due to the formation of an intermediate (**I**), which exists in equilibrium with **3**.



The equilibrium constant and the extinction coefficient of the intermediate were determined from the variation of the equilibrium absorbance with $[\text{TBHP}]$ using eq 1. This equation is derived from the equilibrium expression and the mass-balance equation ($[\text{Mo}]_{\text{T}} = [\mathbf{3}] + [\mathbf{I}]$). Complete derivation of eq 1 is shown in Appendix I (Supporting Information),

$$\frac{\text{Abs}_{\text{eq}}}{[\text{Mo}]_{\text{T}}} = \epsilon_1 + \frac{(\epsilon_p - \epsilon_1) K_{\text{eq}}}{1 + K_{\text{eq}}[\text{TBHP}]} \quad (1)$$

where Abs_{eq} is the absorbance at equilibrium, $[\text{Mo}]_{\text{T}}$ is the initial concentration of **3**, ϵ_1 and ϵ_p are the extinction coefficients of the intermediate and **3**, respectively.

A plot of $\text{Abs}_{\text{eq}}/[\text{Mo}]_{\text{T}}$ against $[\text{TBHP}]$ is shown as an inset in Figure 3. The data were fitted to eq 1, and the values of K_{eq} ($= 1.23 \pm 0.49$) and ϵ_1 ($= 748 \pm 430 \text{ M}^{-1} \text{ cm}^{-1}$ at 330 nm) were determined.

The absorbance–time curves in Figure 3 are exponential and fit to a first-order exponential equation, $A_t = A_{\infty} + (A_0 - A_{\infty}) \exp(-k_{\text{app}}t)$, to determine the values of k_{app} at each $[\text{TBHP}]$. The observed first-order rate constants (k_{app}) vary linearly with $[\text{TBHP}]$ in a relatively large intercept (Figure S3). Since the reaction between TBHP and **3** is reversible, the observed rate constant is the sum of the forward and the reverse rate constant. With TBHP being present in large excess over the catalyst, the observed rate constant can be expressed as

$$k_{\text{app}} = k_p[\text{TBHP}] + k_{-p} \quad (2)$$

Therefore, the intercept of the straight line represents the value of the reverse rate constant ($k_{-p} = 0.0032 \pm 0.0002 \text{ s}^{-1}$), and

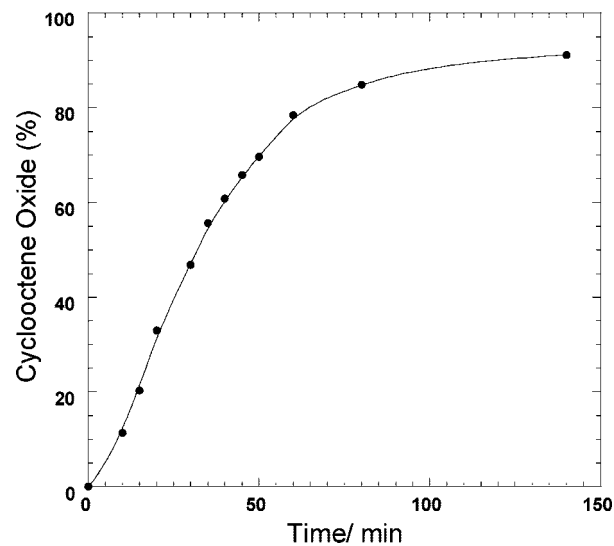


Figure 4. Yield of cyclooctene oxide against time. The reaction was carried out using 0.44 mmol of cyclooctene, 0.6 mmol of TBHP, and 0.05 mmol of **1** in CDCl_3 at 20 °C.

the slope expresses the forward rate constant ($k_p = 0.0047 \pm 0.0003 \text{ M}^{-1} \text{ s}^{-1}$). The value of the equilibrium constant ($K_{\text{eq}} = 1.47 \pm 0.36$) calculated from these kinetic data agrees with the value ($K_{\text{eq}} = 1.23$) obtained from eq 1 within the experimental error range of these measurements. After the equilibrium is established, a slow decrease in the absorbance continues with time, probably due to the decomposition of the catalytic system, in the absence of olefin and increases with the TBHP concentration and the solvent polarity.¹⁰

Catalytic Epoxidation. Epoxidations Starting from $\text{CpMo}(\text{CO})_3\text{CH}_3$ (1**).** Since the olefin does not react with TBHP without the catalyst being present, no corrections were needed for the uncatalyzed process. In the presence of an olefin, the epoxide is formed and the conversion to the epoxide proceeds to completion. Figure 4 shows the formation of cyclooctene oxide with time in an NMR experiment initially started with **1** (0.05 mmol), TBHP (0.6 mmol), and cyclooctene (0.44 mmol) and carried out in CDCl_3 at 20 °C. When TBHP was added last to a mixture of the catalyst and the olefin, the epoxide appears slowly in the first 10 min of the reaction. The rate then increases and becomes linear in the next 20 min, and the buildup continues exponentially.

This kinetic behavior is typical for a catalytic reaction where the catalyst precursor initially reacts with the oxidant to produce the active species in rates slower than or similar to the rate of the reaction of the active species with the substrate. In addition, the reaction rate in the later stages of the reaction becomes slower, indicating that the catalyst is partially deactivated. It has been previously reported that the accumulation of *t*-BuOH as a byproduct deactivates the catalyst, most likely by adduct formation.^{7,9,10,15}

In this catalytic system, **1** reacts with TBHP to form **2** and **3**. In one or both of them could be the active species, directly epoxidizing the olefin or acting as catalysts to activate TBHP toward epoxidation. To get further insight on the catalytic cycle, **3** was isolated and its activity tested with different substrates (cyclooctene, β -methylstyrene, and β -methoxystyrene).

In the absence of TBHP, both Mo(VI) species are inactive toward the epoxidation of cyclooctene and β -methoxystyrene at room temperature. However, when excess TBHP is added, the catalytic reaction proceeds. The epoxidation of cyclooctene and β -methylstyrene leads to the corresponding epoxides only,

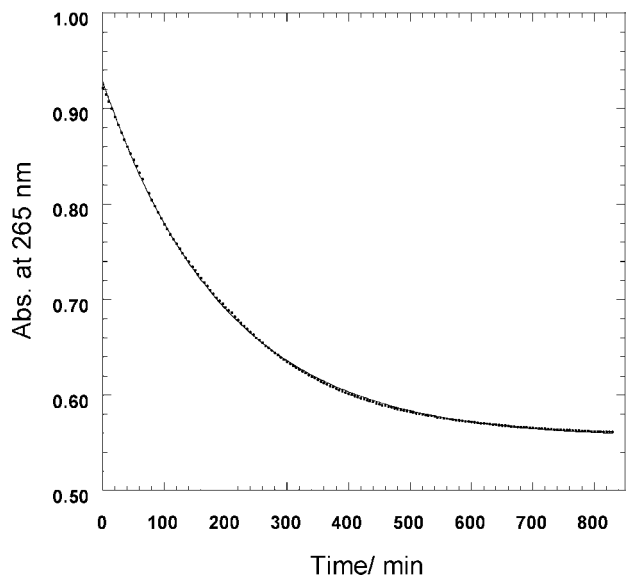
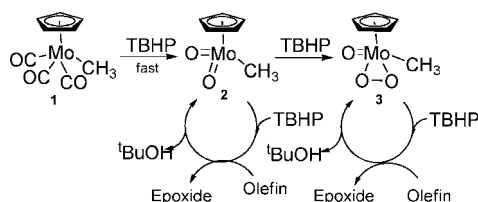


Figure 5. Absorbance–time curve at 265 nm for the oxidation of β -methoxystyrene (0.1 mM) with TBHP (10 mM) catalyzed by **3** (0.4 mM) in CH_2Cl_2 at 20 °C.

Scheme 3. General Reaction Scheme for the Oxidation of 1 by TBHP and the Epoxidation Activity of the Oxidation Products, 2 and 3



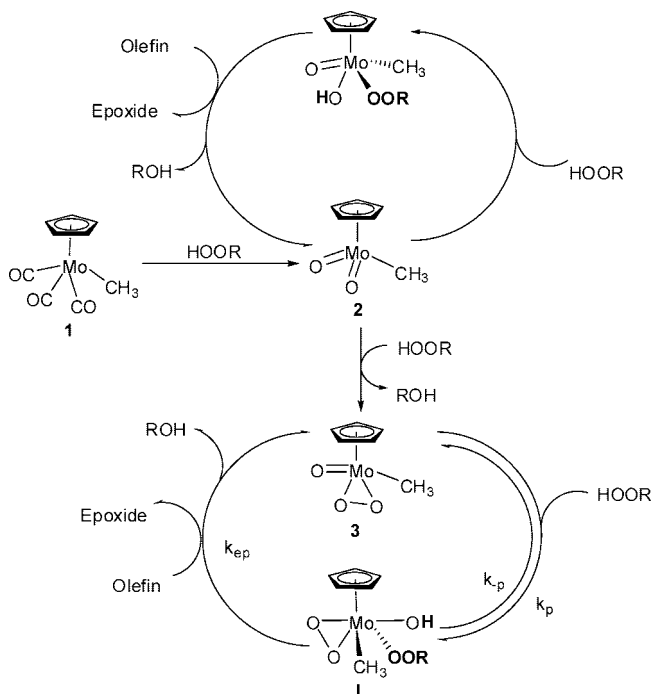
whereas the oxidation of β -methoxystyrene produces benzaldehyde. Similar behavior was observed for the oxidation of β -methoxystyrene with Re(VII)-peroxo species as a catalyst. The reaction initially produces the epoxide, which is not stable due to the electron-donating ability of the methoxy group, and undergoes C–C bond cleavage leading to benzaldehyde as the final product.^{12e}

A general pathway (Scheme 3) for this catalytic reaction can thus be proposed, involving three Mo species: the carbonyl (**1**), the dioxo (**2**), and the oxo-peroxo (**3**) complexes. Kinetically, it is possible to investigate the proposed pathways by studying each species separately.

Epoxidations Utilizing $\text{CpMoO}(\text{O})_2\text{CH}_3$ (3**).** Compound **3** was found to catalyze the epoxidation of cyclooctene and styrene with TBHP as oxidizing agent at room temperature. Figure 5 shows the change in the absorbance with time at 265 nm due to the epoxidation of β -methoxystyrene by the TBHP/**3** system. In the absence of TBHP, the olefin is not oxidized, nor does it react in any form with **3** (when **3** was mixed with cyclooctene or β -methoxystyrene, no changes were observed by NMR and UV spectroscopy). However, as discussed above, UV experiments show that **3** reacts with TBHP in the absence of olefin. This suggests that the epoxidation of the olefin is carried out by an active intermediate **I**, which is formed by the reaction of **3** with TBHP (Scheme 4).

Although both homolytic and heterolytic activation of peroxides by metal catalysts is possible, activation of TBHP by a homolytic cleavage of the O–O bond (which would generate reactive radicals, such as RO^\bullet or HO^\bullet) does not occur due to the reaction insensitivity to oxygen. Also, the olefin reactivity,

Scheme 4. General Mechanism for the Oxidation of $\text{CpMo}(\text{CO})_3\text{CH}_3$ (1**) and Catalytic Activity of the Resulting Complexes in the Presence of TBHP**



which was found to increase with the olefin nucleophilicity rather than with the radical stability, does not support a radical mechanism. Furthermore, radical mechanisms have not been proposed by the previous studies on epoxidations catalyzed by similar Mo compounds.⁶ Therefore, it appears reasonable to assume that the reactive intermediate (**I**), in equilibrium with the catalyst, transfers an O-atom to the olefin to form the epoxide and regenerate the catalyst (Scheme 4).

During the catalytic reaction, the concentration of **I** can be defined by either a steady-state approximation or a pre-equilibrium condition. The epoxidation rate according to Scheme 4 is expressed by eq 3:

$$\text{rate} = \frac{-d[\text{olefin}]}{dt} = k_{\text{ep}}[\text{olefin}][\text{I}] \quad (3)$$

If the rate equation is derived by means of a steady-state approximation for **I** with the mass balance expression, $[\text{Mo}]_{\text{T}} = [\text{3}] + [\text{I}]$, the rate of the reaction can be written as follows:

$$\text{rate} = \frac{k_{\text{ep}}k_{\text{p}}[\text{olefin}][\text{TBHP}][\text{Mo}]_{\text{T}}}{k_{-\text{p}} + k_{\text{p}}[\text{TBHP}] + k_{\text{ep}}[\text{olefin}]} \quad (4)$$

The kinetics of the epoxidation of β -methoxystyrene with TBHP catalyzed by **3** were investigated by following the absorbance change due to the consumption of β -methoxystyrene and the formation of the product(s) in the region 260–270 nm. Kinetic measurements were carried out with a constant concentration of β -methoxystyrene of 0.1 mM and a constant [TBHP] of 10 mM. The concentration of **3** was varied in the range 0.1–0.5 mM. Reaction mixtures were prepared in a spectrophotometric cell, the last added reagent being TBHP. The initial rates (i.r.) were calculated from the first 5% of the curves by using eq 5.

$$\text{initial rate} = -(1/b\Delta\epsilon_{\lambda})\Delta\text{Abs}_{\lambda}/\Delta t \quad (5)$$

where b is the optical path length, $\Delta\epsilon_{\lambda}$ is the total change in the molar absorptivity at λ , and $\Delta\text{Abs}_{\lambda}$ is the initial change in the absorbance.

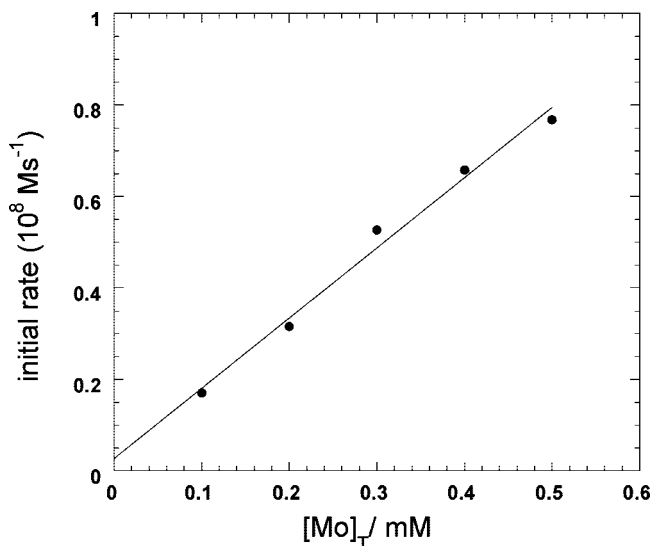


Figure 6. Linear variation of the oxidation initial rate of β -methoxystyrene against $[\text{Mo}]_{\text{T}}$ in CH_2Cl_2 at 20°C . $[\text{TBHP}] = 10\text{ mM}$, $[\beta\text{-methoxystyrene}] = 0.1\text{ mM}$.

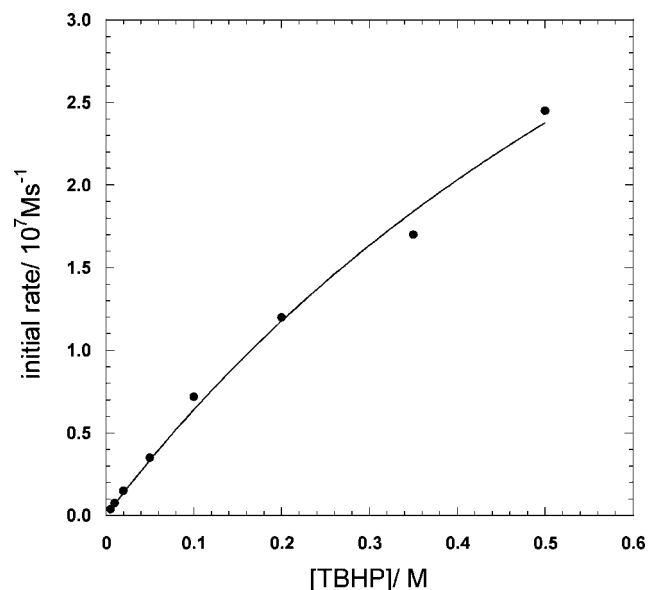


Figure 7. Variation of the oxidation initial rate of β -methoxystyrene (0.1 mM) with TBHP catalyzed by **3** (0.4 mM) in CH_2Cl_2 at 20°C . The data were fitted to eq 4 with the values of k_{p} ($= 0.0047\text{ M}^{-1}\text{ s}^{-1}$) and $k_{-\text{p}}$ ($= 0.0032\text{ s}^{-1}$) being held constant and k_{ep} ($= 18.3 \pm 3.8\text{ M}^{-1}\text{ s}^{-1}$) being varied.

The variation of the initial rate with the catalyst concentration is presented in Figure 6 and shows a linear dependence on $[\text{Mo}]_{\text{T}}$, as expected from eq 4. Using the determined values of k_{p} and $k_{-\text{p}}$ ($0.0047\text{ M}^{-1}\text{ s}^{-1}$ and 0.0032 s^{-1} , respectively) and the initial concentrations of β -methoxystyrene and TBHP, the value of k_{ep} ($\sim 16\text{ M}^{-1}\text{ s}^{-1}$) was determined from the slope.

Kinetic measurements were also carried out with a constant $[\text{Mo}]_{\text{T}}$ (**3**) of 0.4 mM and a constant concentration of β -methoxystyrene of 0.1 mM, varying the concentration of TBHP in the range 5–500 mM. A low concentration of β -methoxystyrene was used to allow direct measurement of the absorbance change, since β -methoxystyrene has a very strong absorptivity in the UV region ($\epsilon_{265} \approx 2 \times 10^4\text{ M}^{-1}\text{ cm}^{-1}$). A plot of the initial rate against $[\text{TBHP}]$ is shown in Figure 7. At low $[\text{TBHP}]$ ($\leq 20\text{ mM}$), the initial rate varies linearly and is first-order with respect to $[\text{TBHP}]$. The order decreases with increasing $[\text{TBHP}]$. This

kinetic behavior agrees with the rate law derived on the basis of a steady-state approximation (eq 4). Fitting the data in Figure 7 to eq 4 using the known values of k_{p} ($= 0.0047\text{ M}^{-1}\text{ s}^{-1}$) and $k_{-\text{p}}$ ($= 0.0032\text{ s}^{-1}$) leads to the epoxidation rate constant ($k_{\text{ep}} = 18.3 \pm 3.8\text{ M}^{-1}\text{ s}^{-1}$). This value of k_{ep} is close to the value estimated above from varying the concentration of the catalyst.

The reactions of *trans*- β -methylstyrene (UV method) and cyclooctene (NMR method) were studied similarly, and the values of k_{ep} for their epoxidation with TBHP catalyzed by **3** are 0.5 and $1.3\text{ M}^{-1}\text{ s}^{-1}$, respectively. These results show that the epoxidation rate constant (k_{ep}) increases with the olefin nucleophilicity:

β -methoxystyrene \gg cyclooctene $>$ *trans*- β -methylstyrene

β -methoxystyrene is the most nucleophilic olefin among the examined substrates (due to the presence of an OCH_3 group), and it is ca. 15 times more reactive than cyclooctene.¹²

Additionally, the epoxidation reaction is stereoselective. When *trans*- β -methylstyrene is oxidized only the *trans* epoxide is obtained. Epoxidations that occur by an external attack of the nucleophilic olefin onto the electrophilic oxygen of the M-alkylperoxo (or M-peroxo) group by a concerted O-transfer step are usually stereoselective, and coordination of the olefin to the metal center prior to the oxygen transfer step is less likely to happen.^{10,16}

Epoxidation Catalyzed by $\text{CpMoO}_2\text{CH}_3$ (2**).** The profile of the reaction between **1** (0.05 mmol), cyclooctene (0.44 mmol), and TBHP (0.6 mmol) in CDCl_3 at 20°C (Figure 4) indicates the presence of at least two catalytic systems formed from the initial Mo(II) precursor. Each catalyst activates TBHP (through an active intermediate) for the epoxidation of an olefin (as shown in Scheme 3). It was not possible to study the catalytic activity of **2** separately, because in addition to the epoxidation reaction, **2** also reacts with TBHP to form **3**, which also catalyzes the epoxidation of olefin as shown above. However, the values of the rate constants for the reactions of **1** with TBHP to yield **2** and **3** were determined in the absence of the olefin under the same conditions, and the rate constants for the epoxidation of cyclooctene by the TBHP/**3** catalytic system (k_{p} , $k_{-\text{p}}$, and k_{ep} in Scheme 4) were determined separately. Therefore, it is possible to estimate the relative rates of the epoxidation reactions by **2** from reactions initially started with the precursor **1** (see Appendix III in the Supporting Information). An initial rate method with the olefin existing in much higher concentration than the catalyst and TBHP was used. The initial rates were calculated from the initial 2–5% conversion of the olefin. Under these conditions, **3** is not involved, and the rate constant for the epoxidation of an olefin by **2**/TBHP was estimated. For cyclooctene, the epoxidation rate constant for reactions catalyzed by compound **2** are 3–5 times higher than those catalyzed by compound **3** under the same conditions, which might originate from the slightly different structure of the intermediates. This shows that **2** is more active than **3**. However, when TBHP is present in large excess over the olefin and the catalyst formation of **3** from **2** occurs at the beginning of the catalytic reaction, most of the epoxidation is carried out by the active species formed from **3** rather than that from **2**.

3. Conclusion

Based on detailed kinetic studies and experimental evidence, the mechanism shown in Scheme 4 has been proposed for the catalytic olefin epoxidation promoted by the precursor $\text{CpMo}(\text{CO})_3\text{CH}_3$ (**1**). In the presence of excess alkyl hydroperoxide (TBHP), $\text{CpMo}(\text{O})_2\text{CH}_3$ (**2**) and $\text{CpMo}(\text{O})(\text{O}_2)\text{CH}_3$ (**3**)

are formed. Whereas the isolated compound **3** is inactive for stoichiometric epoxidation of cyclooctene and styrenes, epoxidation with **3** does proceed in the presence of TBHP under formation of a reactive species **I**. The kinetic results of the variation of the reaction rate with the alkyl hydroperoxide are consistent with the formation of a σ -alkylperoxo intermediate species, as has been postulated for other Mo(VI)-based catalyst systems.¹² In the presence of excess olefin, the catalytic system is stable and the major pathway is the catalytic epoxidation reaction. As far as it can be concluded from the published literature, CpMo(CO)₃CH₃ differs in several aspects from the previously examined CpMo(CO)₃Cl with respect to its reaction behavior and applicability as catalyst. Work is currently undertaken in our laboratories to examine the apparently different catalytic behavior of the Cl derivative in more detail.

4. Experimental Section

4.1. Material and Methods. All preparations were carried out under an oxygen- and water-free argon atmosphere using standard Schlenk techniques. All solvents were derived from a MBraun solvent purification system. Cyclooctene and β -methoxystyrene (Aldrich) were used as received without further purifications. TBHP (Aldrich, 5.0–6.0 M solution in decane) was used after drying over molecular sieves to remove the residual water (<4% when received).

IR spectra were measured with a JASCO FT-IR-460 Plus spectrometer using KBr pellets. NMR spectra were measured applying a JEOL 400 and 400 MHz Bruker Avance DPX-400 spectrometer. The UV spectra were measured on a JASCO UV–vis V-550 spectrophotometer.

4.2. Synthesis of CpMo(O₂)OCH₃. CpMo(CO)₃CH₃ (1 mmol, 260 mg) was mixed with 10 equiv of TBHP (10 mmol) in 40 mL of dichloromethane at room temperature. The oxidation continued for 3 h, and then MnO₂ was added to quench the reaction. After another 1 h stirring, the solution was filtrated to removed MnO₂ and any solid residue. Then the solvent was evaporated under vacuum at 0 °C. The pale yellow solid was washed three times with hexane (3 × 5 mL) and dried under vacuum. Yield: ~140 mg (63%). Elemental analysis (C, 32.06; H, 3.76) is in agreement with the calculated values for C₆H₈O₃Mo (224.06): C, 32.17; H, 3.60. The spectral data of the pure compound are in agreement with those reported for the Mo-oxoperoxo compound, CpMo(O)(O₂)CH₃, prepared previously by the method of Legzdins.¹⁵ IR (KBr, ν cm⁻¹): 3102s (Cp), 3064w, 2987w, 2943w, 2895w, 1633bw, 1454w, 1420m, 1169m, 1067m, 1029m, 1002m, 951vs ($\nu_{\text{Mo=O}}$), 931s, 877vs ($\nu_{\text{O-O}}$), 849s, 831s, 774w, 748w, 575s, 565s ($\nu_{\text{Mo-O}}$). ¹H NMR (CDCl₃, 400 MHz, rt, δ ppm): 6.29 (5H, s, Cp), 2.12 (3H, s, CH₃). ¹³C NMR (C₆D₆, 100.28 MHz, rt, δ ppm):

109.3 (Cp), 24.7 (CH₃). ⁹⁵Mo NMR (C₆D₆, 26.07 MHz, rt, δ ppm): –609 ppm. ¹⁷O NMR (CDCl₃, 54.26 MHz, rt, δ ppm): 869 (oxo), 359, 336 (peroxo).

4.3. Kinetic Studies. Kinetic data were collected by using ¹H NMR and UV methods. The epoxidation of cyclooctene was monitored by NMR, and the epoxidation of β -methoxystyrene was followed by UV spectrophotometric technique. In every case the temperature was controlled at 20 °C. (a) The reactions studied by ¹H NMR were carried out in CDCl₃ in a total volume of 0.5–1.0 mL. The relative amounts of TBHP, the catalyst, and cyclooctene were chosen with concern for the requirements of the kinetic analysis, which was carried out by first-order or initial rate kinetics. The ¹H NMR spectra were recorded at 2–20 min increments over the 2–5 h reaction time. Under pseudo-first-order conditions, the changes in the intensity (*I*) of the cyclooctene signal(s) and/or the cyclooctene oxide with time were fit to a single-exponential decay: $I_t = I_\infty + (I_0 - I_\infty) \exp(-k_{\text{app}}t)$. (b) In the spectrophotometric (UV) method, the reaction mixtures were prepared in the reaction cuvette (optical path = 1.0 cm, *V_T* = 3.0 mL) with the last component added being TBHP or the olefin. Some experiments were carried out in cuvettes with short optical paths (0.1–0.2 cm) to allow direct measurement of the absorbance changes during the reaction when the catalyst or β -methoxystyrene were varied, because both have high molar absorptivities and contribute a large absorbance background at the wavelengths used. The data were obtained by following the loss of the β -methoxystyrene (or *trans*- β -methylstyrene) absorption in the range 260–270 nm. Initial rate and pseudo-first-order conditions were applied in different protocols. In the latter case, the pseudo-first-order rate constants were evaluated by nonlinear least-squares fitting of the absorbance–time curves to a single-exponential equation, $A_t = A_\infty + (A_0 - A_\infty) \exp(-k_{\text{app}}t)$.

Acknowledgment. A.M.A. thanks the Alexander von Humboldt Foundation for a Georg Forster Fellowship and Jordan University of Science and Technology for a sabbatical vacation. J.Z. thanks the Hochschul- und Wissenschaftsprogramm (HWP-II): Fachprogramm Chancengleichheit für Frauen in Forschung und Lehre for a postdoctoral grant. E.H. thanks Stephan D. Hoffmann for experimental assistance. M.J.C. thanks FCT and FEDER for financial support (POCI/QUI/58925/2004).

Supporting Information Available: X-ray data, complete derivations of eqs 1 and 4, and an estimation of the relative values for the rate constant of the catalysis with compound **2**. This material is available free of charge via the Internet at <http://pubs.acs.org>.

OM8009206

Opening of Bent Bi–C Bonds by Silanols To Give Stable $\text{Cp}_2\text{Mo}(\mu\text{-BiOR})_2\text{MoCp}_2$ Complexes

Christina Knispel,[†] Christian Limberg,^{*,†} and Michael Mehring[‡]

Humboldt-Universität zu Berlin, Institut für Chemie, Brook-Taylor-Strasse 2, D-12489 Berlin, Germany

Received September 5, 2008

First, the reactivity of molybdocene dihydride toward bismuth siloxides was studied. Depending on the stoichiometry, compounds of the type $[\text{Cp}_2\text{Mo}\{\text{Bi}(\text{OR})_2\}_2]$ ($\text{R} = \text{SiMe}_2\text{Bu}$, **1**, $\text{R} = \text{SiPh}_3$, **3**) or $[\text{Cp}_2\text{Mo}(\mu\text{-BiOR})_2\text{MoCp}_2]$ ($\text{R} = \text{SiMe}_2\text{Bu}$, **2^t**, $\text{R} = \text{SiPh}_3$, **4^t**) were obtained. Apart from **4** all of these compounds were characterized via single-crystal X-ray diffraction analyses, which revealed for the compound **2^t** a *trans* orientation of the two silanolate groups, similar to that found in case of the corresponding *tert*-butoxide derivatives. In contrast to those, however, the silanolates **2^t** and **4^t** proved to be stable in solution with respect to subsequent intramolecular silanol eliminations, which allowed for detailed NMR spectroscopic investigation. These studies revealed that on dissolution of **2^t** and **4^t**, they slowly enter into an equilibrium with isomers containing the two silanolate ligands in a *cis* configuration, **2^c** and **4^c**. However, the *cis* isomers cannot be isolated from the isomeric mixtures, as the *trans* isomer always precipitates first. Due to the thermodynamic stability of **2** and **4**, these complexes can also be obtained starting from $[(\eta^5\text{-Cp})\text{Mo}(\mu_2\text{-}\eta^5\text{-}\eta^1\text{-C}_5\text{H}_4)\text{Bi}]_2$, which contains bent Bi–C bonds and is formed from the *tert*-butoxide derivative of **2** and **4**, $[\text{Cp}_2\text{Mo}\{\text{Bi}(\text{O}^t\text{Bu})\}_2\text{MoCp}_2]$, **II^H**, by further alcohol elimination as the thermodynamically most favored product in that system: Reacting this compound with the silanols HOSiMe_2Bu and HOSiPh_3 provides **2^t** and **4^t**, respectively, which underlines that these complexes represent the thermodynamic holes within these corresponding systems.

Introduction

The unique property of $n\text{MoO}_3/\text{Bi}_2\text{O}_3$ phases to act as catalysts for the allylic oxidation of propene remains a subject of intense discussion.¹ This, as well as the fact that layered Mo/Bi oxide materials are known to belong to the “Aurivillius phases” showing interesting ferroelectric properties,² stimulates research with respect to the element combination Mo/Bi also on the molecular level.^{3–8}

Recently we have described the results of an investigation concerning the reaction between $[\text{Cp}_2\text{MoH}_2]$ and $[\text{Bi}(\text{O}^t\text{Bu})_3]$.⁷ First of all, the two hydride ligands are replaced by $\text{Bi}(\text{O}^t\text{Bu})_2$ moieties (**I^H**), and reaction with excess molybdocene dihydride leads to a tetranuclear complex **II^H** (see Scheme 1). C–H activation reactions initiated by complex-induced proximity effects in **II^H** subsequently favor further alcohol eliminations and formation of **III^H** and **IV^H** featuring until then unprecedented bonding situations, where planar $\mu_3\text{-}\eta^5\text{-}\eta^1\text{-Cp}$ and $\mu_2\text{-}\eta^5\text{-}\eta^1\text{-Cp}$ ligands bridge metal centers that are additionally linked via metal bonds. This unusual arrangement is made possible

through nonlinear orbital overlaps, i.e., “bent bonds”, between Bi and C atoms.⁷

It could further be noted that the derivatization of the $[\text{Cp}_2\text{MoH}_2]$ starting material to $[\text{MeCp}_2\text{MoH}_2]$ had massive consequences on (i) the solubilities and reactivities of the products **II**, **III**, and **IV**, (ii) the product ratio **III/IV**, and (iii) the reaction mechanism, which then proceeds via a monohydride intermediate **V** (Scheme 1).⁸ Moreover, different bismuth alkoxides react only to corresponding derivatives of **I**.^{3b}

This poses the question, which kind of reactivity is observed if bismuth *siloxides* are employed instead of alkoxides? A corresponding investigation seemed worthwhile, as we were still pursuing a stable derivative of **II** that can be employed in consecutive reactions for further functionalization or for the preparation of materials that contain the interesting metal-bonded Mo_2Bi_2 core. **II^H** and **II^{Me}**, the only compounds of that type known so far, cannot be employed in such studies: While **II^H**

* Corresponding author. Fax: (+49) 30-2093-6966. E-mail: christian.limberg@chemie.hu-berlin.de.

[†] Humboldt-Universität zu Berlin,

[‡] Technische Universität Chemnitz, Institut für Chemie, Strasse der Nationen 62, D-09111 Chemnitz, Germany.

(1) (a) Keulks, G. W.; Krenzke, L. D.; Notermann, T. M. *Adv. Catal.* **1978**, *27*, 183. (b) Grasselli, R. K.; Burrington, J. D. *Adv. Catal.* **1981**, *30*, 133. (c) Grasselli, R. K.; Burrington, J. D. *Ind. Eng. Chem. Prod. Res. Dev.* **1984**, *23*, 393. (d) Belagem, J.; Osborn, J. A.; Kress, J. J. *Mol. Catal.* **1994**, *86*, 267. (e) Grasselli, R. K. In Ertl, G.; Közinger, H.; Weitkamp, J., Eds.; *Handbook of Heterogeneous Catalysis*; VCH Verlagsgesellschaft mbH: Weinheim, 1997; p 2302. (f) Jang, Y. H.; Goddard, W. A., III. *Top. Catal.* **2001**, *15*, 273. (g) Hanna, T. A. *Coord. Chem. Rev.* **2004**, *248*, 429.

(2) Ould-Ely, T.; Thurston, T.; Whitmire, K. H. *C. R. Chim.* **2005**, *8*, 1906.

(3) (a) Hunger, M.; Limberg, C.; Kirchner, P. *Angew. Chem.* **1999**, *111*, 1171; *Angew. Chem., Int. Ed.* **1999**, *38*, 1105. (b) Hunger, M.; Limberg, C.; Kaifer, E.; Rutsch, P. *J. Organomet. Chem.* **2002**, *641*, 9.

(4) (a) Hunger, M.; Limberg, C.; Kirchner, P. *Organometallics* **2000**, *19*, 1044. (b) Limberg, C.; Hunger, M.; Habicht, W.; Kaifer, E. *Inorg. Chem.* **2002**, *41*, 3359. (c) Roggan, S.; Limberg, C. *Inorg. Chim. Acta* **2006**, *359*, 4698. (d) Klemperer, W. G.; Liu, R.-S. *Inorg. Chem.* **1980**, *19*, 3863. (e) Villanneau, R.; Proust, A.; Robert, F.; Gouzerh, P. *J. Chem. Soc., Dalton Trans.* **1999**, 421.

(5) (a) Clegg, W.; Compton, N. A.; Errington, R. J.; Norman, N. C.; Tucker, A. J.; Winter, M. J. *J. Chem. Soc., Dalton Trans.* **1988**, 2941. (b) Clegg, W.; Compton, N. A.; Errington, R. J.; Norman, N. C. *Polyhedron* **1988**, *7*, 2239.

(6) Bachmann, R. E.; Whitmire, K. H. *Inorg. Chem.* **1995**, *34*, 1542. (7) Roggan, S.; Schnakenburg, G.; Limberg, C.; Sandhöfer, S.; Pritzkow, H.; Ziemer, B. *Chem.–Eur. J.* **2005**, *11*, 25.

(8) Roggan, S.; Limberg, C.; Ziemer, B.; Brandt, M. *Angew. Chem.* **2004**, *116*, 2906; *Angew. Chem., Int. Ed.* **2004**, *43*, 2846.

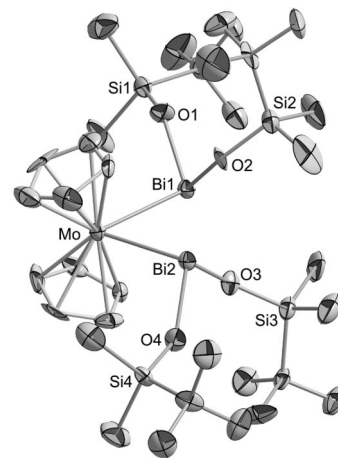
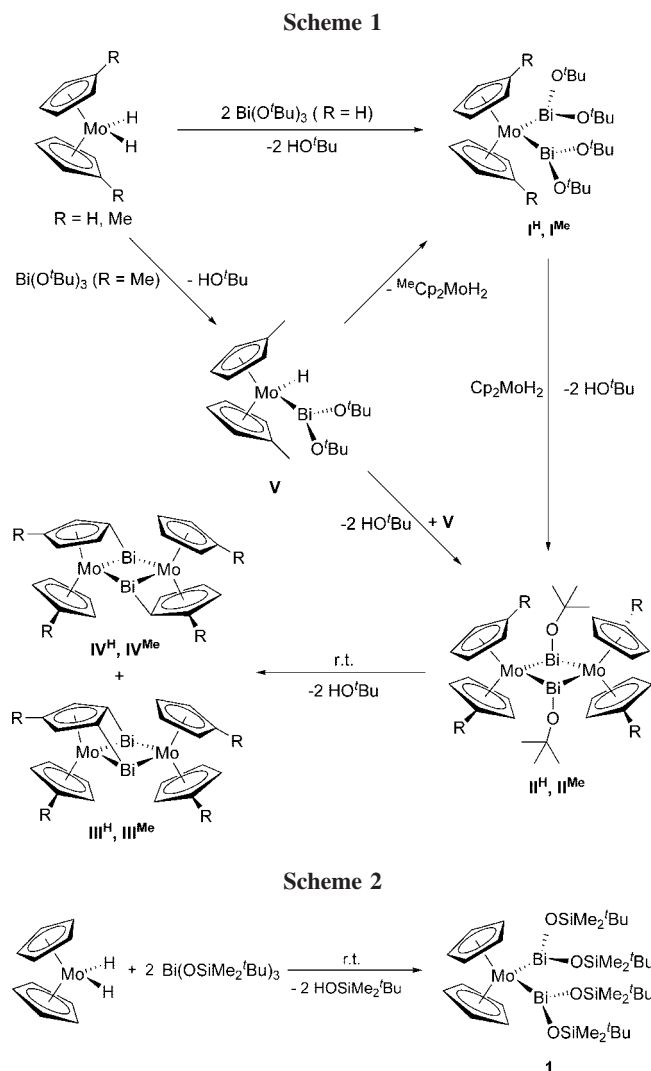


Figure 1. Molecular structure of complex **1**. Thermal ellipsoids are set at the 50% probability level. All hydrogen atoms were omitted for clarity. Selected bond lengths and distances (Å) and angles (deg): Mo–Bi1 2.8692(16), Mo–Bi2 2.8692(16), Bi1–Bi2 3.4384(10), Bi1–O1 2.098(14), Bi1–O2 2.130(13), Bi2–O3 2.128(14), Bi2–O4 2.128(13), Bi1–O3 2.975(12), Bi2–O2 2.902(13), Bi1–Mo–Bi2 73.6(3), O1–Bi1–O2 90.4(5), O3–Bi2–O4 90.3(5), Mo–Bi1–O1 104.9(4), Mo–Bi1–O2 92.6(4), Mo–Bi2–O3 94.1(3), Mo–Bi2–O4 104.2(4), O1–Bi1–O3 167.26(4), O2–Bi2–O4 168.99 (4).

forces between the two $\text{Bi}(\text{OR})_2$ moieties bound to the Mo center. In contrast to the alkoxide ligands at the bismuth atoms in I^{H} , which at least in the solid state are orientated in opposite directions,⁷ intramolecular secondary interactions¹¹ are observed between a siloxide ligand of one bismuth atom and the bismuth atom of the second $\text{Bi}(\text{OR})_2$ unit and vice versa. The corresponding Bi–O distances amount to 2.975(12) and 2.902(13) Å, and the O–Bi...O angles (O1–Bi1...O3 167.26(4)° and O4–Bi2...O2 168.99(4)°) are typical for such interactions, too. All other structural data are quite similar to those of I^{H} .

In the next step experiments were performed that aimed at synthesizing a stable derivative of I^{H} , $[\text{Cp}_2\text{Mo}(\mu\text{-BiOSiMe}_2\text{tBu})_2\text{MoCp}_2]$, **2**[†], by reaction of molybdocene dihydride with $[\text{Bi}(\text{OSiMe}_2\text{tBu})_3]$ in an equimolar ratio (Scheme 3). Reactions carried out in hexane were successful at ambient temperature or at 80 °C (where they proceed faster). Subsequently, cooling to 4 °C led to the precipitation of black crystals suitable for an X-ray crystal structure analysis (Figure 2).

The Mo–Bi bonds (2.9045(7) and 2.9572(8) Å) are in the same range as those in I^{H} (2.916(2) and 2.966(2) Å), and the same is true for the Bi–O bonds.⁷ The Bi–Mo–Bi' and Mo–Bi–Mo' angles of 74.65(2)° and 105.34(2)°, respectively, are indicative of an unstrained structure (compare the Bi–Mo–Bi angle of 73.6(3)° in **1**). The coordination sphere around each Bi center is a distorted pseudotetrahedron with angles between 103.29(15)° and 105.35(17)°. The siloxide ligands are in a *trans* configuration with respect to the planar Mo–Bi–Mo'–Bi' entity. While the distances between the siloxidic O atoms and the closest cyclopentadienyl protons, namely, those at C2 (and C2') and C6 (and C6') (C2–O' 2.1904(67) Å and C6–O' 2.3986(65) Å), are comparable to those observed in the *tert*-

is insoluble in common organic solvents, II^{Me} can be dissolved but rapidly reacts further to give III^{Me} .

Results and Discussion

A bismuth siloxide that seemed suitable for such a study is the monomer $[\text{Bi}(\text{OSiMe}_2\text{tBu})_3]$ described by Mehring and co-workers.⁹

Addition of a colorless solution of $[\text{Bi}(\text{OSiMe}_2\text{tBu})_3]$ in hexane to a solution of $[\text{Cp}_2\text{MoH}_2]$ (0.5 equiv) in the same solvent at ambient temperature led to an orange reaction mixture. Cooling to 4 °C yielded $[\text{Cp}_2\text{Mo}\{\text{Bi}(\text{OSiMe}_2\text{tBu})_2\}_2]$, **1**, in analytically pure form as deep orange crystals (Scheme 2). Hence, the replacement of the alkoxide ligands by the siloxide ligands does not alter the outcome of this reaction (compare Scheme 1). The molecular structure of **1** is depicted in Figure 1.

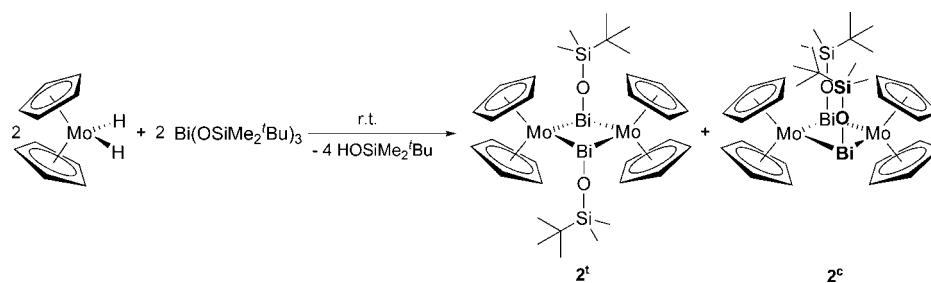
While the Bi1–Bi2 separation of 3.4384(10) Å is too long to be interpreted in terms of a Bi–Bi bond, the Bi1–Mo–Bi2 angle of 73.6(3)° is significantly smaller than the Bi–Mo–Bi angle in $[\text{Cp}_2\text{Mo}\{\text{Bi}(\text{O}^t\text{Bu})_2\}_2]$, I^{H} (75.66(4)°),⁷ and also smaller than the corresponding H–Mo–H angle in $[\text{Cp}_2\text{MoH}_2]$ (75.5°),¹⁰ which indicates that there are no apparent repulsive

(9) Mansfeld, D.; Mehring, M.; Schürmann, M. *Angew. Chem.* **2005**, *117*, 250; *Angew. Chem., Int. Ed.* **2005**, *44*, 245.

(10) Schultz, A. J.; Stearley, K. L.; Williams, J. M.; Mink, R.; Stucky, G. D. *Inorg. Chem.* **1977**, *16*, 3303.

(11) (a) Alcock, N. W. *Adv. Inorg. Chem. Radiochem.* **1972**, *15*, 1. (b) Landrum, G. A.; Hoffmann, R. *Angew. Chem.* **1998**, *110*, 1989; *Angew. Chem., Int. Ed.* **1998**, *37*, 1887. (c) Clegg, W.; Errington, R. J.; Fischer, G. A.; Hockless, D. C. R.; Norman, N. C.; Orpen, A. G.; Stratford, S. E. *J. Chem. Soc., Dalton Trans.* **1992**, 1967. (d) Barucki, H.; Coles, S. J.; Costello, J. F.; Gelbrich, T.; Hursthouse, M. B. *J. Chem. Soc., Dalton Trans.* **2000**, 2319.

Scheme 3

Table 1. Crystal Data and Experimental Parameters for the Crystal Structure Analyses of 1, 2^t, and 3

	1	2 ^t	3
formula	C ₃₄ H ₇₀ Bi ₂ MoO ₄ Si ₄	C ₃₂ H ₅₀ Bi ₂ Mo ₂ O ₂ Si ₂	C ₈₂ H ₇₀ Bi ₂ MoO ₄ Si ₄
weight, g mol ⁻¹	1169.16	1132.75	1745.64
temp, K	180(2)	150(2)	150(2)
cryst syst	orthorhombic	monoclinic	monoclinic
space group	P2 ₁ 2 ₁ 2 ₁	P2 ₁ /n	P2 ₁ /n
a, Å	10.8274(11)	11.2536(6)	23.6397(4)
b, Å	12.1563(12)	11.0845(7)	11.3979(2)
c, Å	34.104(4)	14.5150(10)	27.0463(4)
α, deg	90	90	90
β, deg	90	107.818(5)	107.421(2)
γ, deg	90	90	90
V, Å ³	4488.8(8)	1723.76(19)	6953.2(2)
Z	4	2	4
density, g cm ⁻³	1.730	2.182	1.668
μ(Mo Kα), mm ⁻¹	8.234	10.986	5.348
F(000)	2280	1072	3432
GoF	0.901	1.194	0.931
R ₁ [I > 2σ(I)]	0.0542	0.0494	0.0266
wR ₂ [all data]	0.0994	0.1000	0.0536
Δρ _{min} /Δρ _{max} , e Å ⁻³	2.534/−2.302	2.153/−2.066	1.133/−1.041

butylate substituted analogue, **III^H**,⁷ no evidence for further intramolecular silanol eliminations under formation of the complex **III^H** was observed on dissolution of **2^t**. Hence, in contrast to **II^H** and **II^{Me}** the siloxide-substituted derivative **2^t** is stable in solution over longer periods, and no C–H activation takes place, which allowed for more detailed NMR spectroscopic investigations. In the course of such studies it could be noticed that in solution **2^t** slowly enters into an equilibrium with a complex that was identified via ¹H, ¹³C(¹H)-HSQC, and ²⁹Si(¹H)-

HMBC NMR experiments as its isomer with the two siloxide ligands in a *cis* configuration. The ¹H NMR spectrum of **2^c** differs from that of **2^t** in the number of signals arising from the cyclopentadienyl moieties: The isomer **2^t** exhibits only one signal for these protons, while the *cis*-configured isomer **2^c**, due to the alignment of the siloxide ligands relative to the Mo₂Bi₂ plane, shows two signals (Figure 3). After one week the equilibration between **2^t** and **2^c** appeared to be adjusted, and the ratio found then was ca. 2:1 (the equilibrium constant *K* was determined as *K* = 0.46, which yields a Δ*G* = 1.92 kJ/mol).

All attempts to determine kinetic data failed because of the low rate of the equilibration process. Isomer **2^c** is likely to be formed by an inversion mechanism called “edge inversion” as proposed by Dixon and Arduengo.¹² This process represents a configurational inversion, where the ligands around a central group 15 element rearrange via a T-shaped planar transition state. This kind of inversion is characteristic for three-coordinated compounds of the heavier pnictogens, while in the case of nitrogen compounds they proceed via trigonal-planar transition states (“vertex inversion”).

The results of theoretical calculations and experimental investigations suggest the inversion barriers of pnictogen compounds to strongly increase with increasing mass of the central atom and with the number of electronegative substituents,¹² so that they are highest for the heaviest element bismuth. In fact, calculations performed for the inversion of a [Mo]-Bi(O*t*Bu)-[Mo] entity revealed a barrier of 133 kJ/mol, and

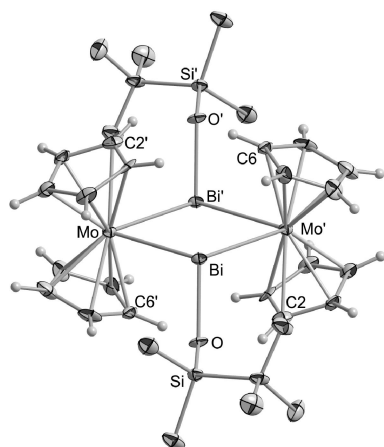


Figure 2. Molecular structure of complex **2^t**. Thermal ellipsoids are set at the 50% probability level. The *tert*-butyl and methyl hydrogen atoms were omitted for clarity. Selected bond lengths and distances (Å) and angles (deg): Mo–Bi 2.9045(7), Mo–Bi′ 2.9572(8), Mo–Mo′ 4.6613(9), Bi–Bi′ 3.5547(5), Bi–O 2.188(5), Mo–Bi–Mo′ 105.34(2), Bi–Mo–Bi′ 74.65(2), Bi–O–Si 120.9(3), Mo–Bi–O 103.29(15), Mo′–Bi–O 105.35(17), Bi–Mo′–Bi′–Mo 0.000(22).

(12) (a) Dixon, D. A.; Arduengo, A. J., III; Fukunaga, T. *J. Am. Chem. Soc.* **1986**, *108*, 2461. (b) Arduengo, A. J., III; Dixon, D. A.; Roe, D. C. *J. Am. Chem. Soc.* **1986**, *108*, 6821. (c) Dixon, D. A.; Arduengo, A. J., III. *J. Am. Chem. Soc.* **1987**, *109*, 338. (d) Dixon, D. A.; Arduengo, A. J., III. *Chem. Soc., Chem. Commun.* **1987**, 498.

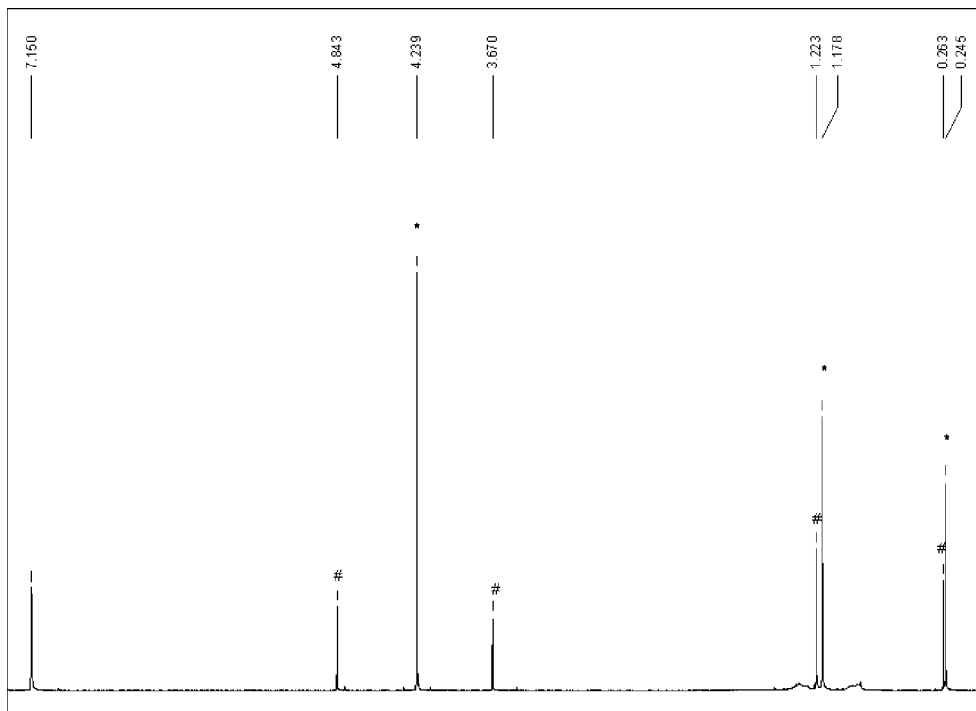
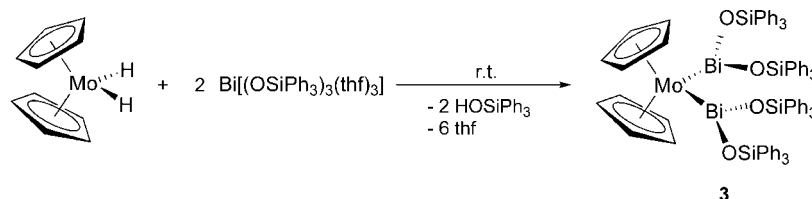
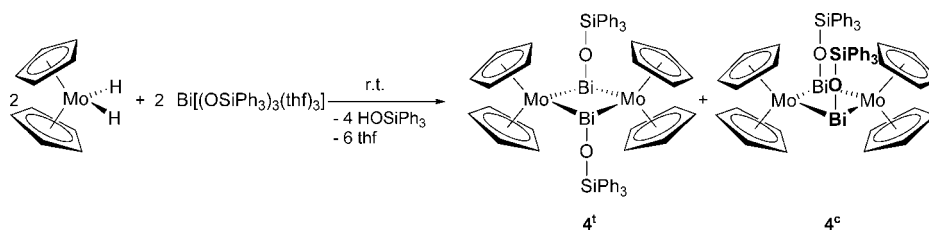


Figure 3. ^1H NMR spectrum of $2^t/2^c$ in C_6D_6 (equilibrium adjusted, * shifts belong to the isomer 2^t ; # shifts belong to the isomer 2^c).

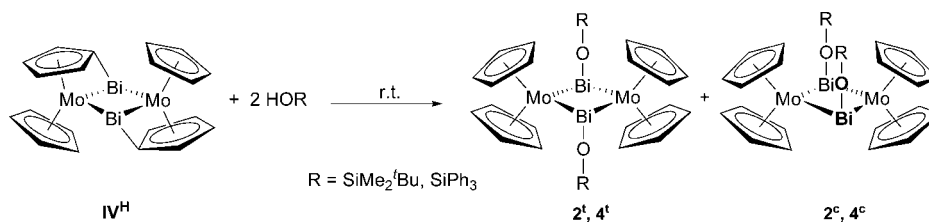
Scheme 4



Scheme 5



Scheme 6



indeed the transition state was found to be T-shaped (\rightarrow “edge inversion”).⁷ All that might explain the very slow rate observed for the isomerization of $2^t/2^c$.

To test the influence of the nature of the siloxide residue on the stability of compounds of the type $[\text{Cp}_2\text{Mo}(\mu\text{-BiOSiR}^1\text{-R}^2\text{R}^3)\text{MoCp}_2]$ and also on the *cis/trans* isomerization, we have analogously investigated the behavior of $[\text{Bi}(\text{OSiPh}_3)_3(\text{thf})_3]$.¹³

First, $[\text{Cp}_2\text{MoH}_2]$ was reacted with 2 equiv of $[\text{Bi}(\text{OSiPh}_3)_3(\text{thf})_3]$ as before in the case of $[\text{Bi}(\text{OSiMe}_2^t\text{Bu})_3]$ (Scheme 4).

After addition of hexane to the concentrated reaction mixture, $[\text{Cp}_2\text{Mo}\{\text{Bi}(\text{OSiPh}_3)_2\}_2]$, **3**, could be precipitated in good yields within one day in the form of orange crystals, which were analytically pure and suitable for X-ray diffraction analysis. The molecular structure of **3** is depicted in Figure 4.

As observed for **1**, one of the siloxidic O atoms of each $\text{Bi}(\text{OR})_2$ unit is obviously orientated toward the bismuth atom

(13) Massiani, M.-C.; Papiernick, R.; Hubert-Pfalzgraf, L. G.; Daran, J. C. *Polyhedron* **1991**, *10*, 437.

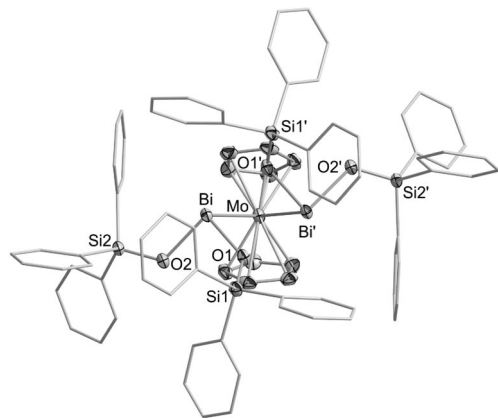


Figure 4. Molecular structure of complex **3**. Thermal ellipsoids are set at the 50% probability level. All hydrogen atoms were omitted for clarity. Selected bond lengths and distances (Å) and angles (deg): Mo–Bi 2.8528(4), Bi–Bi' 3.3497(3), Bi–O1 2.191(2), Bi–O2 2.176(2), Bi–O1' 2.786(2), Bi–Mo–Bi' 71.90(1), O1–Bi–O2 93.15(9), Mo–Bi–O1 92.99(6), Mo–Bi–O2 102.23(7), O2–Bi–O1' 168.75(9).

of the other Bi(OR)₂ moiety, and as the O–Bi···O angles amount to 168.7°, this again points to secondary bonding.¹¹ However, in spite of the sterically more demanding siloxide residues in comparison to SiMe₂tBu in **1**, the secondary interactions are stronger than those observed for **1**, as indicated by the much shorter distances (Bi···O1' 2.786(2) Å), which in turn lead to longer primary bonds (Bi–O2 and Bi'–O2' 2.176(2) Å as compared to 2.098(14) and 2.128(14) Å in **1**) and even to a somewhat shorter Bi–Bi' distance (3.3497(3) Å). All other bond lengths and angles compare well with those of **1** or the *tert*-butylate-substituted complex **1**^H.^{7,8}

Attempts to synthesize [Cp₂Mo{μ-Bi(OSiPh₃)₂MoCp₂}]**4**, by adjusting the stoichiometry of the two reagents [Cp₂MoH₂] and [Bi(OSiPh₃)₃(thf)₃] from 1:2 (as required for the formation of **3**) to 1:1 were successful at ambient temperature in toluene (Scheme 5). **4** precipitated from the reaction mixture in the form of a dark green solid, which is moderately soluble in thf and could be characterized by IR and NMR spectroscopy as well as by elemental analysis.

The NMR spectroscopic investigation of **4**^t again revealed an equilibrium in solution with a corresponding complex **4**^c, which even seems to be thermodynamically favored over **4**^t (ratio **4**^t/**4**^c found after one day was 4:5, equilibrium was not adjusted). However, all attempts to crystallize **4**^t by precipitation failed and led mainly to **4**^t.

Complex-induced proximity effects had allowed for the facile formation of **III**^H and **IV**^H, which represent the thermodynamically most favored compounds within the system [Cp₂MoH₂]/[Bi(O'Bu)₃] (Scheme 1) even though they contain strained bent bonds. As pointed out above, within **2**^t and **4**^t the Cp–H atoms are also located in close proximity to the siloxide O atoms, and hence the question arises why further intramolecular ROH eliminations yielding **IV**^H do not occur for them. A possible answer would be that within [Cp₂MoH₂]/[Bi(OSiR¹R²R³)₃] systems the complexes of the type [Cp₂Mo(μ-BiOSiR¹R²R³)MoCp₂] are lower in energy than **IV**^H. If this is true, **IV**^H should react with HOSiMe₂tBu and HOSiPh₃ to yield **2**^t and **4**^t, respectively, which was to be tested. Before that, we had performed many attempts to cleave the bent bonds within compounds **IV**, for instance with H₂, Me₃SiCl, HSiMe₂Ph, MeI, AlMe₃, HAl(*i*Bu)₂, ZnEt₂, Ph₃CH, PhCCH, PhMe₂SiH, and HS^tPr, without success. However, **IV**^H indeed reacted with

HOSiMe₂tBu and HOSiPh₃ to give the corresponding siloxide-substituted complexes **2**^t and **4**^t, which proves that their stability in fact has a thermodynamical basis (Scheme 6).

Conclusions

Employing bismuth siloxides allowed for the isolation of stable, soluble compounds of the type [Cp₂Mo(μ-BiOR)₂MoCp₂] (R = SiMe₂tBu, SiPh₃), which could also be obtained by the opening of bent Bi–C bonds within **IV**^H (achieved for the first time). These can now be investigated with respect to their reactivity, which will include studies concerning their redox behavior but also reactions that take advantage of the high affinity of silicon to fluorine, i.e., metathetical reactions under elimination of R₃SiF. This may also allow for the construction of scaffolds that contain several Mo₂Bi₂ units. The fact that [Cp₂Mo(μ-BiOR)₂MoCp₂] compounds are very deeply colored points to an increased density of low-lying orbitals due to the metal–metal bonding, and it would be interesting to extend such systems. Future research will address these issues.

Experimental Section

General Procedures. All manipulations were carried out in a glovebox or by means of Schlenk-type techniques involving the use of a dry and oxygen-free argon atmosphere. The ¹H, ¹³C{¹H}, and ²⁹Si NMR spectra were recorded on a Bruker AV 400 NMR spectrometer (¹H, 400.1 MHz; ¹³C{¹H}, 100.6 MHz; ²⁹Si, 79.5 MHz) in dry deoxygenated benzene-*d*₆, chloroform-*d*₁, or thf-*d*₈ as solvent. The spectra were calibrated against the internal residual proton and natural abundance ¹³C resonances of the deuterated solvent (benzene-*d*₆ δ_H 7.15 ppm, δ_C 128.0 ppm; chloroform-*d*₁ δ_H 7.26 ppm, δ_C 77.0 ppm; thf-*d*₈ δ_H 3.58, 1.73 ppm, δ_C 67.4, 25.5 ppm). The ²⁹Si NMR spectra were calibrated externally against TMS. For ²⁹Si resonances ²⁹Si(¹H)-HMBC NMR measurements were carried out. Microanalyses were performed on a HEKAtech Euro EA 3000 elemental analyzer. Infrared (IR) spectra were recorded in the region 4000–400 cm⁻¹ using samples prepared as KBr pellets with a Shimadzu FTIR-8400s spectrometer.

Materials. Solvents were purified, dried, and degassed prior to use. [Cp₂MoH₂],¹⁴ [(η⁵-Cp)Mo(μ₂-η⁵-η¹-C₅H₄)Bi]₂,⁷ [Bi(OSiMe₂tBu)₃],⁹ and [Bi(OSiPh₃)₃(thf)₃]¹³ were prepared according to the literature procedures.

Syntheses. [Cp₂Mo{Bi(OSiMe₂tBu)₂}]**1**. A colorless solution of [Bi(OSiMe₂tBu)₃] (20.5 mg, 0.09 mmol, 1 equiv) in 5 mL of hexane was added to a stirred yellow solution of [Cp₂MoH₂] (108.5 mg, 0.18 mmol, 2 equiv) in 5 mL of the same solvent at ambient temperature. During the addition the color changed from yellow to intense orange. After stirring the solution for 3 h at ambient temperature, the solution was cooled to 4 °C. Within 5 days **1** was obtained in the form of deep orange crystals (yield: 65 mg, 0.06 mmol, 62%). ¹H NMR (C₆D₆): δ 4.77 (s, 10H, Cp), 1.07 (s, 36H, tBu), 0.26 (s, 12H, Me), 0.18 (s, 12H, Me). ¹³C{¹H} NMR (C₆D₆): δ 83.8 (Cp), 27.1/19.9 (tBu), –0.6/–0.8 (Me). ²⁹Si NMR (HMBC expt, C₆D₆): δ 8.5 (SiMe₂tBu). IR (KBr): ν [cm⁻¹] 3100, 2950, 2923, 2881, 2852, 1470, 1461, 1443, 1427, 1405, 1385, 1359, 1251, 1242, 1107, 1005, 913, 883, 826, 768, 660, 571. Anal. Calcd for C₃₄H₇₀Bi₂MoO₄Si₄: C 34.93, H 6.04. Found: C 34.45, H 6.19.

[Cp₂Mo(μ-BiOSiMe₂tBu)₂MoCp₂]**2**. Route A: To a stirred, yellow solution of [Cp₂MoH₂] (241.2 mg, 0.4 mmol, 2 equiv) in 5 mL of hexane was added a colorless solution of [Bi(OSiMe₂tBu)₃] (91.2 mg, 0.4 mmol, 2 equiv) in the same solvent (5 mL) at ambient

(14) (a) Brauer, G. *Handbuch der Präparativen Anorganischen Chemie, in Drei Bänden*; Ferdinand Enke Verlag: Stuttgart, Band 3, 1981; p 1970. (b) Luo, L.; Lanza, G.; Fragala, I. L.; Stern, C. L.; Marks, T. J. *J. Am. Chem. Soc.* **1998**, *120*, 3111.

temperature. An orange solution was initially formed that spontaneously turned green-black after about 5 min. The reaction mixture was filtered into a Schlenk tube equipped with a Young valve and the filtrate heated to 80 °C for 3 h without stirring. After cooling to ambient temperature black needles of **2** precipitated, and after a further 24 h the overlaying solution was removed by filtration. The crystals were washed with hexane repeatedly to yield 165 mg (0.3 mmol, 73%) of pure **2^t**. Route B: HOSiMe₂tBu (16 μL, 13.3 mg, 0.1 mmol, 2 equiv) was added dropwise via injection to a stirred suspension of [(η⁵-Cp)Mo(μ₂-η⁵:η¹-C₅H₄)Bi]₂, **IV^H** (43.4 mg, 0.05 mmol, 1 equiv), in 5 mL of toluene at ambient temperature. Immediately the liquid phase turned green-black, and the suspension was stirred for 12 h at ambient temperature. The overlaying green-black solution was then filtered off, and all volatiles were removed from the filtrate. Drying under vacuum yielded **2^t** (35 mg, 0.03 mmol, 62%) in the form of a green-black microcrystalline solid.

¹H NMR (C₆D₆): **2^t** δ 4.24 (s, 20H, Cp), 1.18 (s, 18H, tBu), 0.25 (s, 12H, Me); **2^c** δ 4.84 (s, 10H, Cp), 3.67 (s, 10H, Cp), 1.22 (s, 18H, tBu), 0.26 (s, 12H, Me). ¹³C{¹H} NMR (C₆D₆): **2^t** δ 83.1 (Cp), 27.4/19.4 (tBu), -0.1 (Me); **2^c** δ 84.4/81.5 (Cp), 27.4/19.4 (tBu), -0.2 (Me). ²⁹Si NMR (HMBC expt, C₆D₆): **2^t** δ 6.7 (SiMe₂tBu); **2^c** δ 5.9 (SiMe₂tBu). IR (KBr): ν [cm⁻¹] 3098, 3053, 2947, 2916, 2878, 2845, 1466, 1458, 1439, 1420, 1404, 1383, 1356, 1244, 1207, 1180, 1101, 1078, 1053, 1003, 993, 903, 860, 826, 804, 779, 762, 658, 422, 401. Anal. Calcd for C₃₂H₅₀Bi₂Mo₂O₂Si₂: C 33.93, H 4.44. Found: C 33.57, H 4.42.

[Cp₂Mo{Bi(OSiPh₃)₂}₂] (**3**). A colorless solution of [Bi(OSiPh₃)₃(thf)₃] (9.1 mg, 0.04 mmol, 1 equiv) in 5 mL of toluene was added to a stirred yellow solution of [Cp₂MoH₂] (100.1 mg, 0.08 mmol, 2 equiv) in the same solvent (5 mL). The resulting orange solution was stirred at ambient temperature for 3 h. Afterward the reaction mixture was concentrated by evaporation of the solvent and layered with hexane. Solvent diffusion over a period of one day at ambient temperature resulted in orange crystals of complex **3** (yield: 54 mg, 0.03 mmol, 77%). ¹H NMR (CDCl₃): δ 7.45 (pseudo-d, 24H, Ph), 7.32 (pseudo-t, 12H, Ph), 7.16 (pseudo-t, 24H, Ph), 4.70 (s, 10H, Cp). ¹³C{¹H} NMR (CDCl₃): δ 138.7/135.4/129.0/127.6 (Ph), 83.9 (Cp). ²⁹Si NMR (HMBC expt, CDCl₃): δ -22.8 (SiPh₃). IR (KBr): ν [cm⁻¹] 3065, 3045, 3019, 3008, 2997, 1960, 1895, 1826, 1773, 1587, 1482, 1427, 1305, 1260, 1185, 1111, 1102, 1029, 997, 907, 835, 742, 700, 521, 511. Anal. Calcd for C₈₂H₇₀Bi₂MoO₄Si₄: C 56.41, H 4.04. Found: C 56.12, H 4.01.

[Cp₂Mo{μ-Bi(OSiPh₃)₂}₂MoCp₂] (**4**). Route A: To a stirred, yellow solution of [Cp₂MoH₂] (18.3 mg, 0.08 mmol, 2 equiv) in 5 mL of toluene was added a colorless solution of [Bi(OSiPh₃)₃(thf)₃] (100.1 mg, 0.08 mmol, 2 equiv) in the same solvent (2 mL) at ambient temperature. An orange solution was initially formed that spontaneously turned green-black after about 15 min, and a dark green solid precipitated. The resulting suspension was stirred for 3 h, the colorless solution was filtered off, and the residue was washed with toluene (2 × 2 mL). Drying under vacuum yielded **4^t**

(29 mg, 0.04 mmol, 50%) in the form of a dark green microcrystalline solid. Route B: A colorless solution of HOSiPh₃ (46.9 mg, 0.17 mmol, 2 equiv) in 5 mL of toluene was added to a stirred suspension of [(η⁵-Cp)Mo(μ₂-η⁵:η¹-C₅H₄)Bi]₂, **IV^H** (73.8 mg, 0.09 mmol, 1 equiv), in 5 mL of the same solvent at ambient temperature. During the addition the color of the liquid phase turned immediately from black to dark green under precipitation of a dark green solid. The resulting dark green suspension was stirred for 2 days, the overlaying solution was filtered off, and the residue was washed with toluene (2 × 4 mL). Drying under vacuum yielded **4^t** (71 mg, 0.05 mmol, 59%) in the form of a dark green microcrystalline solid.

¹H NMR (thf-*d*₈): **4^t** δ 7.60–7.54 (m, 12H, Ph), 7.27–7.24 (m, 18H, Ph), 4.52 (s, 20H, Cp); **4^c** δ 7.60–7.54 (m, 12H, Ph), 7.27–7.24 (m, 18H, Ph), 5.03 (s, 10H, Cp), 3.58 (s, 10H, Cp). ¹³C{¹H} NMR (thf-*d*₈): **4^t** δ 141.5/136.2/129.3/127.9 (Ph), 84.2 (Cp); **4^c** δ 141.5/136.2/129.3/127.9 (Ph), 85.7/82.4 (Cp). ²⁹Si NMR (HMBC expt, thf-*d*₈): **4^t** δ -24.6 (SiPh₃); **4^c** δ -24.6 (SiPh₃). IR (KBr): ν [cm⁻¹] 3060, 3048, 2994, 1957, 1887, 1822, 1586, 1482, 1425, 1404, 1366, 1259, 1184, 1155, 1110, 1101, 1065, 1029, 1005, 989, 914, 868, 832, 808, 788, 736, 703, 671, 519, 507, 458, 427, 420. Anal. Calcd for C₅₆H₅₀Bi₂Mo₂O₂Si₂: C 47.33, H 3.55. Found: C 47.06, H 3.54.

Crystal Structure Determinations. Suitable single crystals of **1** and **2^t** were obtained by cooling a concentrated hexane solution to 4 °C. Suitable single crystals of **3** were obtained by slow diffusion of hexane into a concentrated toluene solution of **3**. The crystal data were collected on a Stoe IPDS I or Stoe IPDS 2T diffractometer using Mo Kα radiation, λ = 0.71073 Å. In all cases, the structures were solved by direct methods (SHELXS-97)¹⁵ and refined versus *F*² (SHELXL-97)¹⁶ with anisotropic temperature factors for all non-hydrogen atoms. All hydrogen atoms were added geometrically and refined by using a riding model. Relevant crystallographic data are collected in Table 1.

Acknowledgment. We are grateful to the Deutsche Forschungsgemeinschaft, the Fonds der Chemischen Industrie, the BMBF, and the Humboldt-Universität zu Berlin for financial support. We also would like to thank P. Neubauer for crystal structure analyses, as well as Dr. B. Ziemer for helpful discussions concerning crystal structure analyses.

Supporting Information Available: X-ray crystallographic information files containing full details of the structural analysis of complexes **1**, **2^t**, and **3**. This material is available free of charge via the Internet at <http://pubs.acs.org>.

OM8008662

(15) Sheldrick, G. M. *SHELXS-97*, Program for Crystal Structure Solution; University of Göttingen, 1997.

(16) Sheldrick, G. M. *SHELXL-97*, Program for Crystal Structure Refinement; University of Göttingen, 1997.

Notes

Temperature-Dependent Nuclearity in Bis(benzimidazolyl) Nickel Complexes and Their Catalysis toward Conjugate Addition of Thiophenols to α,β -Enones

Way-Zen Lee,* Tzu-Li Wang, Huan-Sheng Tsang, Cheng-Yuan Liu, and Chien-Tien Chen*

Department of Chemistry, National Taiwan Normal University, Taipei 11650, Taiwan

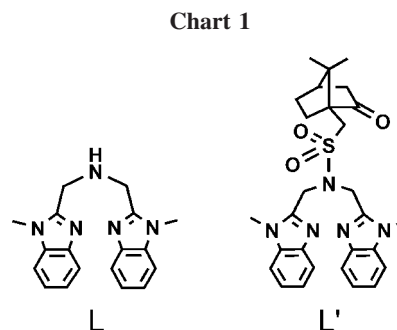
Ting-Shen Kuo

Instrumentation Center, Department of Chemistry, National Taiwan Normal University, Taipei 11650, Taiwan

Received September 30, 2008

Summary: The nuclearity of two previously prepared nickel complexes, $[\text{LNiCl}(\mu\text{-Cl})_2] \cdot 2\text{CH}_3\text{OH}$ (**1**) and $\text{L}'\text{NiCl}_2$ (**2**) ($\text{L} = \text{bis}(1\text{-methylbenzimidazolyl-2-methyl)amine}$ and $\text{L}' = \text{bis}(1\text{-methylbenzimidazolyl-2-methyl)-10-camphorsulfonamide}$), was found to be temperature-dependent. Mononuclear $[\text{LNi}(\text{CH}_3\text{OH})_2\text{Cl}]\text{Cl} \cdot 2\text{H}_2\text{O}$ (**3**) and dinuclear $[\text{L}'\text{NiCl}(\mu\text{-Cl})_2]$ (**4**) were obtained as crystals at -20°C . It is noteworthy that complex **2** can catalyze the conjugate addition of thiophenols to α,β -enones in high yields; in contrast, the same reaction catalyzed by $\text{NiCl}_2 \cdot \text{THF}$ or complex **3** was far less effective.

The nuclearity of a metal complex can be influenced by many factors, such as counterion,¹ solvent,² pH value,³ and ligand.⁴ For instance, a dinuclear nickel chloride complex bridged by a hexadentate poly(oxime) ligand may be converted to a mononuclear nickel complex, when the bonded chlorides are switched to innocent nitrate anions.^{1a} Recently, we observed that the nuclearity of nickel complexes could be controlled by employing a bis(benzimidazole) ligand.^{4a} Moreover, we discovered that the nuclearity of two previously prepared nickel complexes, $[\text{LNiCl}(\mu\text{-Cl})_2] \cdot 2\text{CH}_3\text{OH}$ (**1**) and $\text{L}'\text{NiCl}_2$ (**2**) ($\text{L} = \text{bis}(1\text{-methylbenzimidazolyl-2-methyl)amine}$ and $\text{L}' = \text{bis}(1\text{-methylbenzimidazolyl-2-methyl)-10-camphorsulfonamide}$; Chart 1), was also dependent on the temperature during their crystallization. The number of open sites on the nickel centers for the four bis(benzimidazolyl) nickel complexes was found to depend upon their nuclearity. It is well documented that nickel complexes with open site(s) can



be used as catalysts in organic synthesis.⁵ However, only a few nickel complexes have been reported to possess catalytic ability toward the conjugate addition of protic nucleophiles to α,β -unsaturated carbonyl compounds (i.e., Michael addition).⁶ Herein we wish to demonstrate that complex **2** can facilitate such a catalytic process in high yields.

As reported previously, complex **1** was prepared by the reaction of $\text{NiCl}_2 \cdot 6\text{H}_2\text{O}$ with the tripodal ligand **L** in methanol and was recrystallized at room temperature.^{4a} Interestingly, the mononuclear $[\text{LNi}(\text{CH}_3\text{OH})_2\text{Cl}]\text{Cl} \cdot 2\text{H}_2\text{O}$ (**3**) was obtained when the product isolated from the reaction was recrystallized at -20°C . The X-ray crystal structure of complex **3** revealed that the tripodal **L** was facially coordinated to the nickel center in **3**, and the complete coordination sphere of the nickel center was fulfilled by one chloride trans to the amine nitrogen of **L** and two methanol molecules trans to the imidazole nitrogens of **L** (Figure 1). The $\text{Ni}-\text{N}_{\text{amine}}$ bond is 0.127 Å longer than the average $\text{Ni}-\text{N}_{\text{imidazole}}$ bond, implying that the bonding by chloride is much stronger than that of the coordinated methanol molecules (Table 1). Although the nickel centers of **1** and **3**

* To whom correspondence should be addressed. E-mail: wzlee@ntnu.edu.tw (W.-Z.L.); chefv043@ntnu.edu.tw (C.-T.C.).

(1) (a) Bera, J. K.; Nethaji, M.; Samuelson, A. G. *Inorg. Chem.* **1999**, *38*, 218–228. (b) Deters, E. A.; Goldcamp, M. J.; Bauer, J. A. K.; Baldwin, M. J. *Inorg. Chem.* **2005**, *44*, 5222–5228.

(2) Kawata, S.; Breeze, S. R.; Wang, S.; Greedan, J. E.; Raju, N. P. *Chem. Commun.* **1997**, 717–718.

(3) (a) Kim, G.-S.; Zeng, H.; Neiwert, W. A.; Cowan, J. J.; VanDerveer, D.; Hill, C. L.; Weinstock, I. A. *Inorg. Chem.* **2003**, *42*, 5537–5544. (b) Liu, H.-J.; Hung, Y.-H.; Chou, C.-C.; Su, C.-C. *Chem. Commun.* **2007**, 495–497.

(4) (a) Lee, W.-Z.; Tseng, H.-S.; Kuo, T.-S. *Dalton Trans.* **2007**, 2563–2570. (b) Chen, C.-T.; Bettiger, S.; Weng, S.-S.; Pawar, V. D.; Lin, Y.-H.; Liu, C.-Y.; Lee, W.-Z. *J. Org. Chem.* **2007**, *72*, 8175–8185.

(5) (a) Younkin, T. R.; Connor, E. F.; Henderson, J. I.; Friendrich, S. K.; Grubbs, R. H.; Bansleben, D. A. *Science* **2000**, *287*, 460–462. (b) Gibson, V. C.; Spitzmesser, S. K. *Chem. Rev.* **2003**, *103*, 283–315. (c) Meinhard, D.; Wegner, M.; Kipiani, G.; Hearley, A.; Reuter, P.; Fischer, S.; Marti, O.; Rieger, B. *J. Am. Chem. Soc.* **2007**, *129*, 9182–9191.

(6) (a) Kanemasa, S.; Oderaotshi, Y.; Wada, E. *J. Am. Chem. Soc.* **1999**, *121*, 8675–8676. (b) Evans, D. A.; Thomson, R. J.; Franco, F. *J. Am. Chem. Soc.* **2005**, *127*, 10816–10817. (c) Soloshonok, V. A.; Cai, C.; Yamada, T.; Ueki, H.; Ohfuné, Y.; Hruby, V. J. *J. Am. Chem. Soc.* **2005**, *127*, 15296–15303.

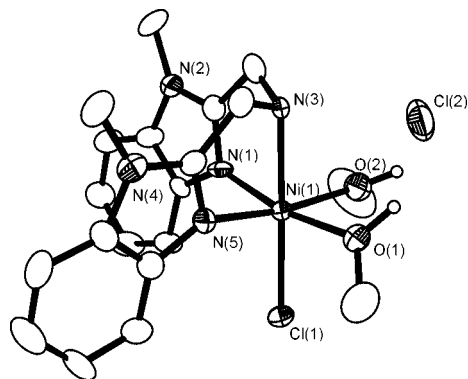


Figure 1. Thermal ellipsoid representation of $[\text{LNiCl}(\text{CH}_3\text{OH})_2]\text{Cl}\cdot 2\text{H}_2\text{O}$ (**3**) at the 50% probability level. Hydrogen atoms and solvent molecules of **3** are omitted for clarity.

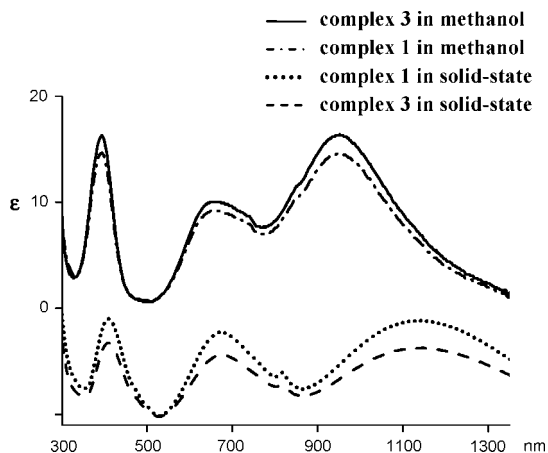


Figure 2. UV/vis spectra of $[\text{LNiCl}(\mu\text{-Cl})]_2\cdot 2\text{CH}_3\text{OH}$ (**1**) and $[\text{LNiCl}(\text{CH}_3\text{OH})_2]\text{Cl}\cdot 2\text{H}_2\text{O}$ (**3**) in methanol and the solid state.

Table 1. Selected Bond Lengths (Å) for Complexes **3** and **4**

	3	4
Ni1–N1	2.056	2.023
Ni1–N3	2.189	
Ni1–N5	2.068	2.060
Ni1–Cl1	2.367	2.378
Ni1–Cl1A		2.423
Ni1–Cl2		2.309
Ni1–O1	2.108	
Ni1–O2	2.095	

were independently coordinated with somewhat different ligands (two bridging chloride ions in **1** and two methanol molecules in **3**), the geometries of both complexes were octahedral in the solid state. The same geometries in **1** and **3** led to similar absorption profiles in their solid-state UV/vis spectra (Figure 2). It was quite obvious that mononuclear **3** was converted from dinuclear **1**, since **1** was composed of two identical $[\text{LNiCl}(\mu\text{-Cl})]$ fragments. Interestingly, one chloride remained coordinated to the Ni(II) ion of **3** and the other chloride was dissociated

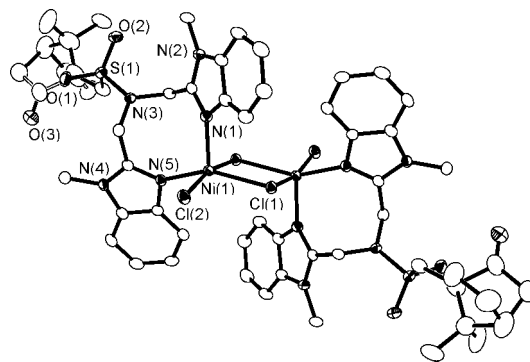
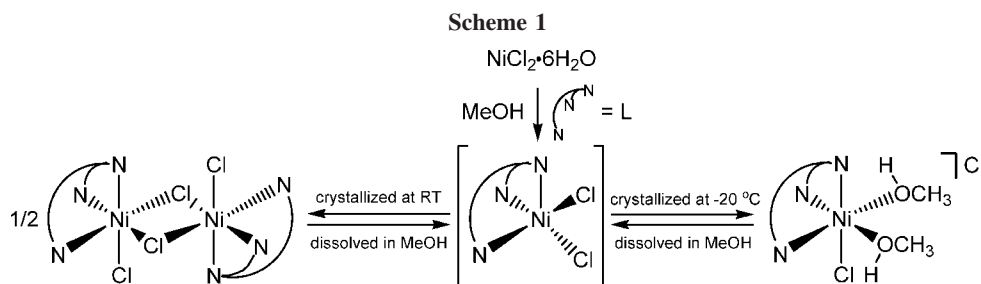


Figure 3. Thermal ellipsoid representation of $[\text{L}'\text{NiCl}(\mu\text{-Cl})]_2$ (**4**) at the 50% probability level. Hydrogen atoms of **4** are omitted for clarity.

from the nickel center. It was suspected that the dinuclear **1** was dissociated to form two $[\text{LNiCl}_2]$ fragments in methanol solution and crystallized out as **1** at room temperature or as **3** at $-20\text{ }^\circ\text{C}$ (Scheme 1). Notably, the coordination geometry of the species in solution was found to be different from those of complexes **1** and **3** in the solid state, as evidenced by their UV/vis spectra (Figure 2).

Similarly, complex **2** was prepared by the reaction of $\text{NiCl}_2\cdot 6\text{H}_2\text{O}$ with the tripodal ligand L' in methanol and was recrystallized at room temperature.^{4a} When the same solution was stored at $-20\text{ }^\circ\text{C}$, red crystals of dinuclear $[\text{L}'\text{NiCl}(\mu\text{-Cl})]_2$ (**4**) suitable for X-ray crystallographic analysis were obtained. The molecular structure of complex **4** revealed a dinickel core bridged by two chloride ligands, and each nickel was coordinated with a bidentate L' and a terminal chloride to construct a distorted-square-pyramidal geometry with a τ value of 0.26 (Figure 3).⁷ The two imidazole nitrogens of L' were coordinated at different positions on the nickel center: one at the axial position with a Ni–N bond length at 2.02 Å and the other at the equatorial plane with a longer bond length of 2.06 Å. Meanwhile, the length of the Ni–Cl_{terminal} bond is about 0.09 Å shorter than that of the average Ni–Cl_{bridged} bond (Table 1). The Ni_2Cl_2 core was flat with a Ni \cdots Ni distance of 3.62 Å. According to the UV/vis spectra of complexes **2** and **4** taken both in acetonitrile and in the solid state (Figure 4), **2** possessed the same tetrahedral geometry both in solution and in the solid state, whereas the dinuclear **4** was dissociated in solution to form 2 equiv of **2**, as depicted in Scheme 2. Recently, Shimazaki et al. reported a similar phenomenon.⁸ Their dinuclear nickel complex bearing a tripodal N_3O ligand and two bridging chlorides on each nickel ion was dissociated to form a five-coordinated mononuclear species in methanol.

Since complex **2** is only four-coordinated, we suspect that nucleophiles, such as carbonyl compounds, are capable of



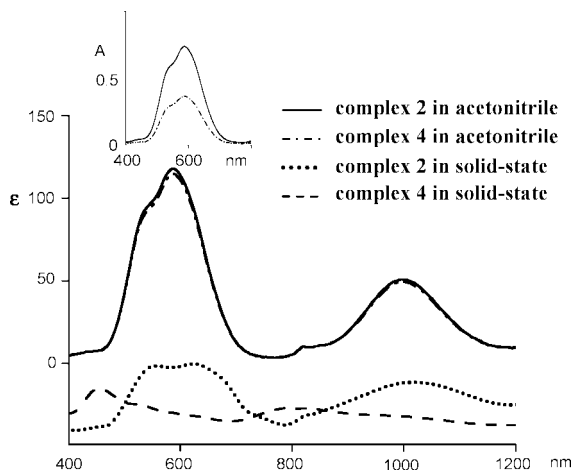
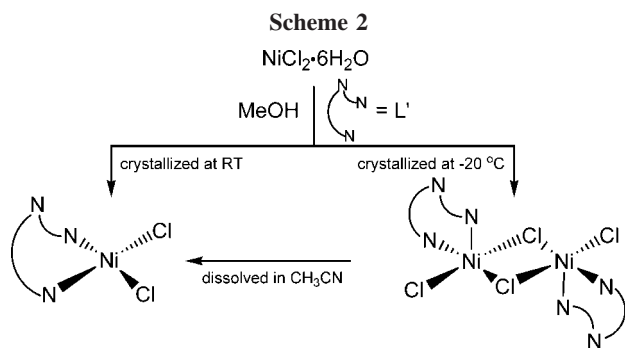


Figure 4. UV/vis spectra of $L'NiCl_2$ (**2**) and $[L'NiCl(\mu-Cl)]_2$ (**4**) in acetonitrile and the solid state. Inset: the intensity of the absorption band of **4** is double of that of **2** at the same concentration, illustrating that **4** was dissociated into 2 equiv of **2** in acetonitrile.



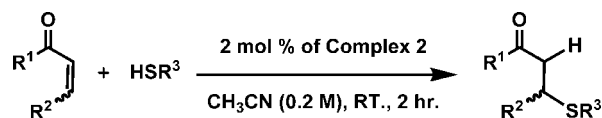
coordinating to the nickel center of **2** in solution. Bearing this idea in mind, we extended our investigation toward the conjugate addition of thiophenols to α,β -enones catalyzed by complex **2** with an incomplete coordination sphere.⁹ 2-Cyclohexenone (**5**; 2 equiv) was first selected as a test Michael acceptor, and 4-methoxythiophenol (**9**) was employed as a test Michael donor in the presence of catalyst **2**. An almost quantitative amount of 3-(4-methoxyphenylsulfanyl)cyclohexanone was produced in 2 h by using 2 mol % of **2** in acetonitrile (0.2 M of **9**) at room temperature (entry 1 in Table 2). Under the same reaction conditions, $NiCl_2 \cdot THF$ and complex **3** were employed as control catalysts for comparison to evaluate the catalytic ability of complex **2**. The product yields catalyzed by $NiCl_2 \cdot THF$ and by **3** are 65% and 75%, respectively. Apparently, complex **2** behaves as a more effective catalyst for the conjugate addition of thiophenols to α,β -enones. With this preliminary success, thia-Michael additions to other Michael acceptor classes such as but-2-enylbenzene (**6**), 5-methyl-3-hexenone (**7**), and *N*-but-2-enyl-1,3,2-oxazolidinone (**8**) by three 4-methoxythiophenol derivatives, 4-*tert*-butylthiophenol (**10**), 2-naphthylthiol (**11**), and 4-chlorothiophenol (**12**), were further explored. As the nucleophilicity of thiophenols is decreased by installing an electron-withdrawing substituent at the para position of thiophenols, the

(7) Selected bond angles (deg) of **4**: $N1-Ni1-N5 = 105.72$, $N1-Ni1-Cl2 = 97.06$, $N5-Ni1-Cl2 = 91.46$, $N1-Ni1-Cl1 = 102.40$, $N5-Ni1-Cl1 = 150.90$, $Cl2-Ni1-Cl1 = 92.42$, $N1-Ni1-Cl1A = 96.45$, $N5-Ni1-Cl1A = 87.25$, $Cl2-Ni1-Cl1A = 166.27$, $Cl1-Ni1-Cl1A = 82.26$.

(8) Shimazaki, Y.; Huth, S.; Karasawa, S.; Hirota, S.; Naruta, Y.; Yamauchi, O. *Inorg. Chem.* **2004**, *43*, 7816–7822.

(9) For conjugate additions of weak nucleophiles to α,β -enones or enoates catalyzed by vanadyl triflate, see: Lin, Y.-D.; Kao, J.-Q.; Chen, C.-T. *Org. Lett.* **2007**, *9*, 5195.

Table 2. Thia-Michael Additions of Thiophenols to α,β -Enones



Entry	Michael acceptor	Michael donor	Yield ^a
1			95% (1a)
2			95% (1b)
3			91% (1c)
4			37% (1d)
5			82% (2a)
6			82% (2b)
7			80% (2c)
8			37% (2d)
9			29% (3a)
10			29% (3b)
11			25% (3c)
12			15% (3d)
13			51% (4a) ^b
14			51% (4b) ^b
15			29% (4c) ^{b,c}
16			16% (4d) ^b

^a Isolated yield. ^b Reaction time: 12 h. ^c The yield of entry 15 was determined by ¹H NMR spectroscopy. ^d The yield for entry 1 catalyzed by $NiCl_2 \cdot THF$ is 65%, and that by complex **3** is 75%.

yields for the conjugate additions are decreased (entries 4, 8, 12, and 16 in Table 2). In addition, if the β -position of the alkene moiety in the enones is sterically more hindered, the yields of the conjugate additions are also decreased (entries 9–12 in Table 2). As represented in the thia-Michael additions to substrate **7**, the reaction rates drop by 2–3 times. To the best of our knowledge, this is the first successful example of conjugate additions to a sterically hindered α,β -unsaturated carbonyl compound by thiophenols catalyzed by nickel complexes. Another less reactive Michael acceptor class such as *N*-but-2-enyl-1,3,2-oxazolidinone (**8**) was also successfully converted to the corresponding products 3-(4-methoxyphenylsulfanyl)-2-oxazolidinone and 3-(4-*tert*-butylphenylsulfanyl)-2-oxazolidinone in about 50% yield with prolonged reaction time (12 h, entries 13 and 14 in Table 2).

In conclusion, we have revealed that the nuclearity of bis(benzimidazolyl) nickel complexes was governed not only

Table 3. Selected X-ray Crystallographic Data for Complexes 3 and 4

	3	4
empirical formula	C ₂₀ H ₂₇ Cl ₂ N ₅ NiO ₂	C ₆₀ H ₇₄ Cl ₁₂ N ₁₀ Ni ₂ O ₆ S ₂
fw	499.08	1638.23
<i>T</i> (K)	200(2)	100(2)
wavelength (Å)	0.71073	0.71073
cryst syst	monoclinic	triclinic
space group	<i>P2</i> / <i>m</i>	<i>P1</i>
<i>a</i> (Å)	13.5208(19)	12.0810(2)
<i>b</i> (Å)	8.1518(10)	12.3990(2)
<i>c</i> (Å)	26.366(4)	13.7750(3)
α (deg)	90	115.2590(10)
β (deg)	104.592(3)	92.7920(13)
γ (deg)	90	106.5790(13)
<i>V</i> (Å ³)	2812.3(6)	1753.60(6)
<i>Z</i>	4	1
<i>D</i> _{calcd} (g cm ⁻³)	1.179	1.551
μ (mm ⁻¹)	0.901	1.110
cryst size (mm)	0.36 × 0.17 × 0.04	0.40 × 0.26 × 0.12
goodness of fit	1.028	1.182
R1	0.0978	0.0608
wR2	0.2603	0.1641

Table 4. UV/vis Data of Complexes 1–4

complex	UV/vis λ _{max} /nm (ε/M ⁻¹ cm ⁻¹)
1	394 (15), 660 (9), 744 (8, sh), 952 (15) (in MeOH) 412, 674, 816, 1138 (solid)
2	551 (sh, 99), 587 (118), 997 (51) (in CH ₃ CN) 556, 624, 828, 1018 (solid)
3	394 (16), 660 (10), 740 (9, sh), 952 (16) (in MeOH) 409, 675, 817, 1147 (solid)
4	551 (sh, 98), 587 (115), 997 (50) (in CH ₃ CN) 455, 522, 800 (solid)

by the employed ligand but also by the crystallization temperature. Among NiCl₂·THF and the four bis(benzimidazolyl) nickel complexes, the coordinatively unsaturated complex **2**, L'NiCl₂, possessed effective catalytic ability toward the conjugate additions of thiophenols to α,β-enones, even for 5-methyl-3-hexenone (a hindered Michael acceptor) and *N*-but-2-enoyl-1,3,2-oxazolidinone (a sluggish Michael acceptor).

Experimental Section

Methods and Materials. All manipulations were performed under nitrogen using standard Schlenk and glovebox techniques. The synthesis of complexes **1** and **2** was described previously.^{4a} Methanol was dried in magnesium/iodine prior to use. Acetonitrile was distilled once from P₂O₅ and freshly distilled before use from CaH₂. Diethyl ether was dried in a sodium benzophenone still prior to use. 2-Cyclohexenone (**5**), 5-methyl-3-hexenone (**7**), 4-methoxythiophenol (**9**), 4-*tert*-butylthiophenol (**10**), 2-naphthalenethiol (**11**), and 4-chlorothiophenol (**12**) are commercially available and were used as received. But-2-enoylbenzene (**6**) was purchased and purified by column chromatography on silica gel (hexane/AcOEt, 9/1) before use. *N*-But-2-enoyl-1,3,2-oxazolidinone (**8**) was prepared according to the reported procedure from crotonyl chloride and 2-oxazolidinone.¹⁰ Electronic spectra were recorded on Hitachi

U-3501 and Hitachi U-4100 spectrophotometers equipped with an integrating sphere for reflectance measurements. IR spectra were recorded as Nujol mulls on a Perkin-Elmer Paragon 500 spectrometer. Elemental analyses of C, H, and N were performed on a Perkin-Elmer 2400 analyzer at the NSC Regional Instrumental Center at National Taiwan University, Taipei, Taiwan.

X-ray Structure Determination. Crystals of suitable size were selected under a microscope and mounted on the tip of a glass fiber, which was positioned on a copper pin. The X-ray data for complexes **3** and **4** were collected on a Bruker-Nonius Kappa CCD diffractometer employing graphite-monochromated Mo Kα radiation at 200 K and the θ–2θ scan mode. The space groups for all complexes were determined on the basis of systematic absences and intensity statistics, and the structures of **3** and **4** were solved by direct methods using SIR92 or SIR97 and refined with SHELXL-97. An empirical absorption correction by multiscans was applied to all structures. All non-hydrogen atoms were refined with anisotropic displacement factors. Hydrogen atoms were placed in ideal positions and fixed with relative isotropic displacement parameters. Selected crystallographic data for **3** and **4** are given in Table 3. Detailed crystallographic information for complexes **3** and **4** is provided in the Supporting Information (CIF).

[LNi(CH₃OH)₂Cl]Cl·2H₂O (3). Complex **3** was prepared by the same manner reported previously for complex **1**^{4a} but was recrystallized at –20 °C by the slow diffusion of diethyl ether into a methanol solution of **2** to form light green crystals (yield 0.342 g, 64%). Anal. Calcd for NiC₂₀H₃₁N₅Cl₂O₄: C, 44.89; H, 5.84; N, 13.09. Found: C, 44.48; H, 5.16; N, 13.38. IR (Nujol): 3406 cm⁻¹ (ν_{OH}), 3227 cm⁻¹ (ν_{NH}). UV/vis data are provided in Table 4.

[L'Ni(μ-Cl)Cl]₂ (4). Complex **4** was synthesized by the same reaction procedures reported previously for complex **2**,^{4a} and the isolated blue solution was kept at –20 °C for crystallization. Red crystals were obtained in a yield of 80.3% (0.522 g) from the acetonitrile solution of the purified product. Anal. Calcd for Ni₂C₅₆H₆₆N₁₀Cl₄S₂O₆: C, 51.80; H, 5.12; N, 10.79. Found: C, 52.35; H, 4.72; N, 11.00. IR (Nujol): 1743 cm⁻¹ (ν_{C=O}). UV/vis data are provided in Table 4.

General Procedure for the Conjugate Addition Catalyzed by Complex 2. To a blue acetonitrile solution (4 mL) of complex **2** (16.4 mg, 0.02 mmol) was added an α,β-enone (2.0 mmol) under a nitrogen atmosphere with stirring for 5 min. As a thiol (1.0 mmol) was added to the reaction mixture, the color of the solution became brick red. The resulting solution was stirred at room temperature for 2 h, and the solvent was evaporated under vacuum. The residue was then purified by column chromatography on silica gel (hexane/AcOEt 9/1) to give the conjugate adduct. Characterization of the conjugate addition products are listed in the Supporting Information.

Acknowledgment. We gratefully acknowledge financial support from the National Science Council of Taiwan (NSC Grant No. 97-2113-M-003-004 to W.-Z.L. and NSC Grant No. 97-2667-M-003-001 to C.-T.C.).

Supporting Information Available: CIF files giving X-ray crystallographic data for complexes **3** and **4** text and figures giving characterization data and ¹H and ¹³C NMR spectra of the conjugate addition products. This material is available free of charge via the Internet at <http://pubs.acs.org>.

OM8009427

(10) (a) Evans, D. A.; Chapman, K. T.; Bisaha, J. *J. Am. Chem. Soc.* **1988**, *110*, 1238–1256. (b) Evans, D. A.; Morrissey, M. M.; Dorow, R. L. *J. Am. Chem. Soc.* **1985**, *107*, 4346–4348.

Synthesis of Allylnickel Complexes with Phosphine Sulfonate Ligands and Their Application for Olefin Polymerization without Activators

Shusuke Noda, Takuya Kochi, and Kyoko Nozaki*

Department of Chemistry and Biotechnology, Graduate School of Engineering, The University of Tokyo, 7-3-1 Hongo, Bunkyo-Ku, Tokyo 113-8656, Japan

Received August 14, 2008

Summary: Phosphine sulfonate nickel complexes [(*o*-Ar₂-PC₆H₄SO₃)Ni(allyl)] (Ar = Ph, *o*-MeOC₆H₄) are prepared and used as catalysts for ethylene polymerization. The products were low molecular weight polyethylenes possessing only methyl branches. The activity for ethylene polymerization with the phenyl-substituted complex was comparable to that of *o*-methoxyphenyl-substituted complex in the absence of activator. Comparison with the corresponding allylpalladium complex revealed that the nickel catalysts produced polyethylenes with lower molecular weight and more branches than the palladium catalyst.

Introduction

Transition-metal-catalyzed insertion polymerization of olefins has been studied and used considerably due to its great ability to control polymer microstructures. Particularly, early transition metal catalysts, such as Ziegler–Natta catalysts, are most widely utilized for olefin polymerization. Recent intensive studies have also developed the use of late-transition metals as catalysts for olefin polymerization.¹ One of the most elegant examples is Brookhart palladium/ α -diimine catalysts used for copolymerization of ethylene with alkyl acrylates.² The palladium/ α -diimine catalysts produce unique amorphous-like highly branched polyethylenes with over 100 branches per 1000 carbon atoms via chain-walking. The catalysts were also successfully applied to copolymerization of ethylene/ α -olefins with alkyl acrylates for the first time. More recently, Drent and co-workers reported copolymerization of ethylene with alkyl acrylates^{3a} using in situ generated palladium catalysts bearing phosphine sulfonate ligands.³ Polymers produced by the catalysts have very few branches and acrylate units are incorporated into the polymer backbone. In recent years, the phosphine sulfonate palladium catalysts have been extensively studied^{4–7} because linear copolymers of ethylene and polar vinyl monomers may provide control over important properties such as toughness and adhesion. Studies by many researchers, including our group, have revealed that in situ generated and isolated phosphine sulfonate palladium catalysts also copolymerize ethylene with other polar vinyl monomers, such as vinyl ethers,^{5a} vinyl

fluoride,^{5b} acrylamides, vinyl pyrrolidone,⁶ and acrylonitrile.⁷ However, improvements in catalytic activity and molecular weight of produced polymers are still desired.

In contrast, several nickel catalysts have shown considerable catalytic activity and heteroatom tolerance. For example, Brookhart's nickel/ α -diimine catalysts display higher activity and produce polymers with higher molecular weight and fewer branches than the corresponding palladium catalysts. Grubbs and co-workers reported considerably active nickel catalysts bearing salicylaldiminato ligand for ethylene polymerization to generate high molecular weight polymers.⁸

Nickel catalysts bearing phosphine sulfonate ligands can be candidates for more desirable catalysts. Rieger and co-workers have reported the corresponding phenyl nickel catalysts with triphenylphosphine ligand and performed ethylene polymerization with or without activators, such as B(C₆F₅)₃ or Ni(cod)₂.^{4d,9} Although improvement in the activity is observed, molecular weights of the polymers are lower than those produced by the palladium catalysts. The possibility of triphenylphosphine or

(4) (a) Hearley, A. K.; Nowack, R. J.; Rieger, B. *Organometallics* **2005**, *24*, 2755–2763. (b) Schultz, T.; Pfaltz, A. *Synthesis* **2005**, 1005–1011. (c) Haras, A.; Michalak, A.; Rieger, B.; Ziegler, T. *J. Am. Chem. Soc.* **2005**, *127*, 8765–8774. (d) Nowack, R. J.; Hearley, A. K.; Rieger, B. *Z. Anorg. Allg. Chem.* **2005**, *631*, 2775–2781. (e) Kochi, T.; Yoshimura, K.; Nozaki, K. *Dalton Trans.* **2006**, 25–27. (f) Haras, A.; Michalak, A.; Rieger, B.; Ziegler, T. *Organometallics* **2006**, *25*, 946–953. (g) Haras, A.; Anderson, D. W. G.; Michalak, A.; Rieger, B.; Ziegler, T. *Organometallics* **2006**, *25*, 4491–4497. (h) Skupov, K. M.; Marella, P. M.; Hobbs, J. L.; McIntosh, L. H.; Goodall, B. L.; Claverie, J. P. *Macromolecules* **2006**, *39*, 4279–4281. (i) Kochi, T.; Nakamura, A.; Ida, H.; Nozaki, K. *J. Am. Chem. Soc.* **2007**, *129*, 7770–7771. (j) Liu, S.; Borkar, S.; Newsham, D.; Yennawar, H.; Sen, A. *Organometallics* **2007**, *26*, 210–216. (k) Newsham, D. K.; Borkar, S.; Sen, A.; Conner, D. M.; Goodall, B. L. *Organometallics* **2007**, *26*, 3636–3638. (l) Vela, J.; Lief, G. R.; Shen, Z.; Jordan, R. F. *Organometallics* **2007**, *26*, 6624–6635. (m) Bettucci, L.; Bianchini, C.; Claver, C.; Suarez, E. J. G.; Ruiz, A.; Meli, A.; Oberhauser, W. *Dalton Trans.* **2007**, 5590–5602. (n) Skupov, K. M.; Marella, P. R.; Simard, M.; Yap, G. P. A.; Allen, N.; Conner, D.; Goodall, B. L.; Claverie, J. P. *Macromol. Rapid Commun.* **2007**, *28*, 2033–2038. (o) Nakamura, A.; Munakata, K.; Kochi, T.; Nozaki, K. *J. Am. Chem. Soc.* **2008**, *130*, 8128–8129. (p) Borkar, S.; Newsham, D. K.; Sen, A. *Organometallics* **2008**, *27*, 3331–3334.

(5) (a) Luo, S.; Vela, J.; Lief, G. R.; Jordan, R. F. *J. Am. Chem. Soc.* **2007**, *129*, 8946–8947. (b) Weng, W.; Shen, Z.; Jordan, R. F. *J. Am. Chem. Soc.* **2007**, *129*, 15450–15451.

(6) Skupov, K. M.; Piche, L.; Claverie, J. P. *Macromolecules* **2008**, *41*, 2309–2310.

(7) Kochi, T.; Noda, S.; Yoshimura, K.; Nozaki, K. *J. Am. Chem. Soc.* **2007**, *129*, 8948–8949.

(8) (a) Wang, C.; Friedrich, S.; Younkin, T. R.; Li, R. T.; Bansleben, D. A.; Day, M. W.; Grubbs, R. H. *Organometallics* **1998**, *17*, 3149–3151. (b) Younkin, R. T.; Connor, F. E.; Henderson, I. J.; Friedrich, K. S.; Grubbs, H. R.; Bansleben, A. D. *Science* **2000**, *287*, 460–462.

(9) Very recently, two groups reported Ni phosphine sulfonate catalyzed ethylene polymerization independently. (a) Zhou, X.; Bontemps, S.; Jordan, R. F. *Organometallics* **2008**, *27*, 4821–4824. (b) Guironnet, D.; Rünzi, T.; Göttker-Schnetmann, I.; Mecking, S. *Chem. Commun.* **2008**, ASAP.

* E-mail: nozaki@chembio.t.u-tokyo.ac.jp

(1) (a) Boffa, L. S.; Novak, B. M. *Chem. Rev.* **2000**, *100*, 1479–1493. (b) Ittel, S. D.; Johnson, L. K.; Brookhart, M. *Chem. Rev.* **2000**, *100*, 1169–1203. (c) Gibson, V. C.; Spitzmesser, S. K. *Chem. Rev.* **2003**, *103*, 283–315.

(2) (a) Johnson, L. K.; Mecking, S.; Brookhart, M. *J. Am. Chem. Soc.* **1996**, *118*, 267–268. (b) Mecking, S.; Johnson, L. K.; Wang, L.; Brookhart, M. *J. Am. Chem. Soc.* **1998**, *120*, 888–899.

(3) (a) Drent, E.; van Dijk, R.; van Ginkel, R.; van Oort, B.; Pugh, R. I. *Chem. Commun.* **2002**, 744–745. (b) Drent, E.; van Dijk, R.; van Ginkel, R.; van Oort, B.; Pugh, R. I. *Chem. Commun.* **2002**, 964–965.

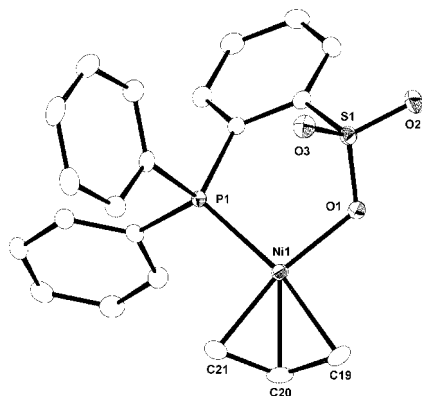
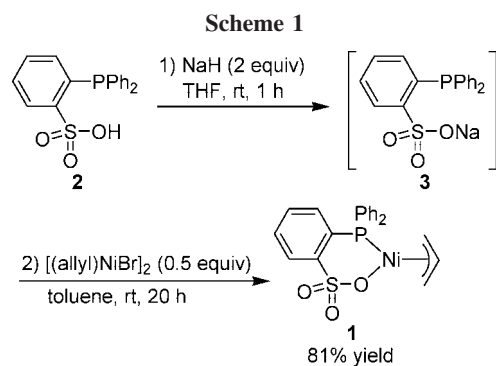


Figure 1. Molecular structure of **1**. Selected bond distances (Å) and angles (deg): Ni(1)–P(1), 2.1845 (16); Ni(1)–O(1), 1.9235 (18); Ni(1)–C(19), 2.066 (2); Ni(1)–C(20), 1.9979 (19); Ni(1)–C(21), 1.981 (2); C(19)–C(20), 1.399 (3); C(20)–C(21), 1.413 (3); and C(19)–C(20)–C(21), 117.98 (16).



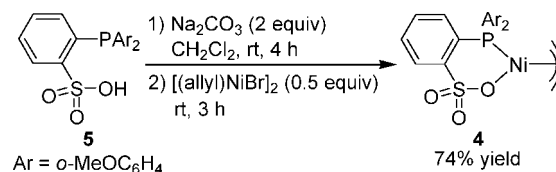
phosphine scavengers affecting polymerization lets us investigate activator- and additional phosphine-free phosphine sulfonate nickel catalysts. In this paper, we report the synthesis of allylnickel catalysts bearing phosphine sulfonate ligands and our examination on ethylene homopolymerization and copolymerization with polar vinyl monomers without any activators.

Results and Discussion

First, preparation of allylnickel complex bearing a phosphine sulfonate ligand (**1**) was examined (Scheme 1). When phenyl-substituted phosphine **2** was treated with NaH in THF, deprotonation proceeded smoothly to afford the corresponding sodium salt of the phosphine sulfonate ligand **3**, which is soluble in THF. A THF solution of **3** was obtained by filtration and directly used to form a nickel complex. Addition of this THF solution of **3** to a toluene solution of [(allyl)NiBr]₂ gave allylnickel complex **1**, which was isolated in 81% yield. The structure of complex **1** was confirmed by X-ray crystallography (Figure 1). As expected, the phosphine sulfonate ligand is bound to the nickel atom via one of the three oxygen atoms of the sulfonate group and the phosphorus atom to form a six-membered chelate. The allyl group binds to nickel in a η^3 fashion. The two terminal allyl carbons, the coordinating phosphorus and the oxygen, and the nickel are all placed in a single plane. The distance between the terminal carbon and the nickel is longer for the bond located trans to the phosphorus from that trans to the oxygen, reflecting the stronger trans influence of the phosphine than that of the sulfonate.

Synthesis of allylnickel complex with an *o*-methoxyphenyl-substituted ligand (**4**) was then investigated. However, treatment of sulfonic acid **5** with NaH in THF resulted in formation of

Scheme 2



the insoluble sodium salt of the ligand, which is difficult to separate from excess NaH. Therefore, sodium carbonate was used as an alternative weaker base. Sulfonic acid **5** was treated with sodium carbonate in CH₂Cl₂, followed by the addition of a toluene solution of [(allyl)NiBr]₂ to give the corresponding nickel complex **4**, which was isolated in 74% yield after recrystallization (Scheme 2). The structure of complex **5** was also confirmed by X-ray diffraction analysis.

Ethylene polymerization by the allylnickel complexes **1** and **4** was examined, and the results are summarized in Table 1. When the polymerization was performed at 80 °C, only a trace amount of polyethylene was generated (Table 1, entries 1 and 4). However, raising the reaction temperature to 100 °C led to formation of low molecular weight polymers (M_n 1400–1700) with activities of 7–9 g·mmol⁻¹·h⁻¹ (= 2–3 g·mmol⁻¹·h⁻¹·MPa⁻¹) and with relatively narrow polydispersities (M_w/M_n = 1.5–2.0) (entries 3 and 5). These results show ethylene polymerization with the allylnickel complexes can be performed in the absence of activators. The observed dramatic increase in the activity indicates that a higher reaction temperature is required for initiation than for propagation. Almost no product was given by in a shorter reaction time (entry 2). It indicates slow initiation with the allyl nickel complex. Rieger and co-workers reported that in the presence of B(C₆F₅)₃ as an activator, phenylnickel/PPh₃ complex of *o*-methoxyphenyl-substituted **5** catalyzed ethylene polymerization with high activities but that only a trace amount of polyethylene was obtained with the phenyl-substituted ligand **2**.^{4d} The importance of the *o*-methoxy group was emphasized. Therefore, it is noteworthy that, here in this study, phenyl-substituted complex **1** actually catalyzes ethylene polymerization with activity comparable to the methoxyphenyl-substituted catalyst **4**, both in the absence of activators. All obtained polymers had certain branches with 8–13 branches per 1000 carbon atoms. The number of branches is measured by ¹³C NMR using inverse-gated decoupling.¹⁰ The generated polyethylenes possess only methyl branches, and there are no longer side chains, such as ethyl, propyl, or butyl groups. It indicates that β -hydride elimination and reinsertion of the resulting olefin often occurs, but it occurs mostly at the chain end, and chain-walking further into the polymer chain does not proceed at a significant rate. Copolymerization with methyl acrylate is also examined, but as the result, only poly(methyl acrylate) is obtained.

Ethylene polymerization with the corresponding Pd complex bearing a phosphine sulfonate ligand was also examined. The use of allylpalladium complex [(*o*-Ar₂PC₆H₄SO₃)Pd(allyl)] (Ar = *o*-MeOC₆H₄) (**6**)^{4j} produced polyethylene with a higher molecular weight (M_n = 11500) and higher linearity (less than 1 branch per 1000 carbon atoms) but lower reactivity than nickel complexes under the same conditions (entry 6). The higher molecular weight and linearity indicate that allylpalladium complex **6** bearing phosphine sulfonate ligand has less tendency to undergo β -hydride elimination than the corresponding nickel

(10) (a) Guan, Z.; Cotts, P. M.; McCord, E. F.; McLain, S. J. *Science* **1999**, *283*, 2059–2062. (b) Cotts, P. M.; Guan, Z.; McCord, E.; McLain, S. *Macromolecules* **2000**, *33*, 6945–6952.

Table 1. Ethylene Polymerization with Phosphine-Sulfonate Allyl Complexes^a

entry	catalyst	temp (°C)	time (h)	yield (g)	productivity		M_n	M_w/M_n	branches (/1000C)
					(g · mmol ⁻¹ · h ⁻¹)	(g · mmol ⁻¹ · h ⁻¹ · MPa ⁻¹)			
1	1	80	15	trace	trace	trace	ND ^b	ND	ND
2	1	100	1	ND	ND	ND	ND	ND	ND
3	1	100	15	1.3	8.9	2.9	1400	1.5	8
4	4	80	15	trace	trace	trace	ND	ND	ND
5	4	100	15	1.0	6.8	2.2	1700	2.0	13
6	6	100	15	0.35	2.2	0.7	11600	2.3	<1

^a Conditions: 0.010 mmol of catalyst, ethylene pressure = 3.0 MPa, 2.5 mL of toluene. ^b Not determined.

complexes **1** and **4**. It is of interest to compare the difference between nickel complex **4** and palladium complex **6** in relation to the Brookhart's α -diimine complexes. The result that the nickel/phosphine sulfonate complexes produce polyethylenes with lower molecular weight and more branches than palladium/phosphine sulfonate is in sharp contrast to that the nickel/ α -diimine complexes are considered to produce more linear polyethylene with higher molecular weight than the corresponding palladium complexes. The origin of the difference is not clear at this moment.

The polymerization activity initiated by the allylpalladium **6** is lower than that by alkylpalladium complex: alkyl complex (*o*-Ar₂PC₆H₄SO₃)PdCH₃(2,6-lutidine) produced polyethylene with 15.0 g · mmol⁻¹ · h⁻¹ (= 5.0 g · mmol⁻¹ Pd · h⁻¹ · MPa⁻¹), M_n = 75 700, M_w/M_n 2.2, <1 branches over 1000 carbons at 80 °C.⁷ The lower activity with π -allyl complex **6** may originate from the higher activation energy requested for the olefin insertion into the Pd–C bond in the η^3 -complex when compared to methylpalladium complex.^{4j}

Conclusion

Phosphine sulfonate nickel complexes are prepared and used as catalysts for ethylene polymerization without addition of any activator. Structures of the obtained low molecular weight polyethylene were analyzed to detect only methyl branches. The activity for ethylene polymerization with **1** was comparable to that with **4**. Comparison with the corresponding allylpalladium complex **6** revealed that the nickel catalysts produced polyethylenes with lower molecular weight and more branches than the palladium catalyst.

Experimental Section

General Methods. All manipulations were carried out using the standard Schlenk technique under argon purified by passing through a hot column packed with BASF catalyst R3-11. ¹H (500 MHz), ¹³C (126 MHz), and ³¹P NMR (202 MHz) spectra were recorded on a JEOL JNM-ECP-500 spectrometer. Elemental analysis was performed by the Microanalytical Laboratory, Department of Chemistry, Faculty of Science, the University of Tokyo. Size exclusion chromatography analyses at 145 °C were carried out with a Tosoh instrument (HLC-8121) equipped with three columns (Tosoh TSKgel GMHr-H(20)HT) by eluting the columns with *o*-dichlorobenzene at 1 mL/min.

Dichloromethane, toluene, THF, and hexanes were purified by the method of Pangborn et al.¹¹ 2-(Diphenylphosphino)benzenesulfonic acid (**2**) and 2-{di(2-methoxyphenyl)phosphino}benzenesulfonic acid (**5**) were prepared according to literature

procedures.^{3b,4b} Phosphine sulfonate palladium complex **6** was prepared according to literature method.^{4j}

Preparation of [(*o*-Ph₂PC₆H₄SO₃)Ni(allyl)] (1**).** To a suspension of 50 mg of sodium hydride (2.05 mmol) in 20 mL of THF was added 205 mg of **2** (0.60 mmol), and the resulting mixture was stirred for 1 h at rt. The mixture was filtered and slowly added to a solution of 115 mg of [(allyl)NiBr]₂ (0.32 mmol) in 10 mL of toluene and stirred for 20 h at rt. The resulting mixture was filtered through Celite and evaporated to dryness. The residue was extracted with CH₂Cl₂. Slow diffusion of hexane into the concentrated CH₂Cl₂ solution afforded nickel complex **1** (128.3 mg, 0.29 mmol, 48% yield). ¹H NMR (CDCl₃): δ 8.21–8.18 (m, 1H), 7.56–7.38 (m, 12H), 7.08 (t, *J* = 8.4 Hz, 1H), 5.70–5.29 (m, 1H), 4.80–0.98 (br m, 4H). ¹³C{¹H} NMR (CDCl₃, –50 °C): δ 48.8 (CH₂, allyl), 116.2 (ArC), 119.7 (CH, allyl), 129.4, 129.8, 131.1, 131.9, 133.2, 135.3, 136.6, 148.7 (ArC, ArCH). ³¹P NMR (CDCl₃): δ 8.6. Anal. Calcd for C₂₁H₁₉NiO₃PS: C, 57.18; H, 4.34. Found: C, 56.96; H, 4.48.

Preparation of [(*o*-MeOC₆H₄)₂P(C₆H₄SO₃)NiCH₂CHCH₂] (4**).** To a solution of 436 mg of **5** (1.08 mmol) in 20 mL of CH₂Cl₂ was added 230 mg of sodium carbonate (2.17 mmol), and the reaction mixture was stirred for 4 h at rt. Then a solution of 210 mg of allylnickel bromide (0.584 mmol) in 20 mL of CH₂Cl₂ was added to the mixture and stirred for 3 h at rt. The resulting mixture was filtered through Celite. Slow diffusion of hexane into the concentrated CH₂Cl₂ solution afforded nickel complex **4** as a red-brown powder (405 mg, 0.808 mmol, 74% yield). ¹H NMR (CDCl₃): δ 8.20–8.17 (m, 1H), 7.52–7.46 (m, 3H), 7.30 (t, *J* = 7.4 Hz, 1H), 7.01–6.92 (m, 7H), 5.59–5.49 (m, 1H), 3.78 (s, 6H), 4.74–0.53 (br m, 4H). ³¹P NMR (CDCl₃): δ 41.7. Anal. Calcd for C₂₃H₂₃NiO₃PS: C, 55.12; H, 4.63. Found: C, 54.96; H, 4.64.

Ethylene Polymerization. To a 50 mL autoclave containing 0.010 mmol of metal complex and a stir bar was transferred 2.5 mL of toluene under argon atmosphere. The mixture was stirred at rt for 10 min and charged with 3.0 MPa of ethylene. The autoclave was heated, and the mixture was stirred for 15 h. After the reaction, MeOH was added to the cooled contents of the autoclave. Precipitated materials were collected by filtration and washed several times with MeOH. The remaining solid was dried under vacuum at 80 °C to afford polyethylene, which was analyzed without further purification.

Acknowledgment. This work was supported by a Grant-in-Aid for Scientific Research on Priority Areas “Advanced Molecular Transformations of Carbon Resources” from the Ministry of Education, Culture, Sports, Science and Technology, Japan.

Supporting Information Available: X-ray crystallographic data of **1** and **4** (CIF). This material is available free of charge via the Internet at <http://pubs.acs.org>.

(11) Pangborn, A. B.; Giardello, M. A.; Grubbs, R. H.; Rosen, R. K.; Timmers, F. J. *Organometallics* **1996**, *15*, 1518–1520.

Asymmetric β -Boration of α,β -Unsaturated Esters with Chiral (NHC)Cu Catalysts

Vanesa Lillo,[†] Auxiliadora Prieto,[‡] Amadeu Bonet,[†] M. Mar Díaz-Requejo,[§]
Jesús Ramírez,[†] Pedro J. Pérez,^{*,§} and Elena Fernández^{*,†}

Dpt. Química Física e Inorgánica, Universidad Rovira i Virgili, C/Marcel·lí Domingo s/n.
43005 Tarragona, Spain, and Departamento de Ingeniería Química, Química Física y Química Orgánica
and Laboratorio de Catálisis Homogénea, Departamento de Química y Ciencia de los Materiales, Unidad
Asociada al CSIC, Universidad de Huelva, Campus de El Carmen, 21007 Huelva, Spain

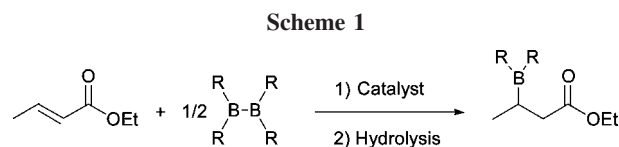
Received October 1, 2008

Summary: Copper complexes containing chiral *N*-heterocyclic carbene ligands catalyze the regioselective nucleophilic boryl attack at the β -carbon of α,β -unsaturated esters with enantioselectivities up to 74% ee, depending on the nature of the ester group.

In the past decade, the conjugate addition of boryl nucleophile to activated alkenes has opened up new perspectives in organoborane chemistry. The use of transition-metal-based catalysts to promote the heterolytic cleavage of diboron reagents, affording metal–boryl intermediates, is the key issue in these transformations. When employing α,β -unsaturated carbonyl compounds as starting materials, these boryl intermediates induce the regiocontrolled boryl migration to the β -position (Scheme 1).¹

Most of the catalysts described for this transformation are based on copper;² however, other catalytic systems based on Pt,³ Rh,⁴ or Ni⁵ are known and considered as attractive alternatives. This functionalization originates a stereogenic center at the β -carbon; therefore, the induction of enantioselectivity could be achieved with the appropriate catalyst.⁶ However, to the best of our knowledge, there is only one example in the literature which achieves the successful enantioselective β -boration/oxidation of α,β -unsaturated esters and nitriles. This was described by Yun and co-workers^{2c,7} using CuCl and the phosphines (*R*)-(*S*)-josiphos and (*R*)-(*S*)-NMe₂-PPh₂-mandyphos, with ee values up to 91%. Alternatively, Oestreich has recently reported the catalytic asymmetric addition of Me₂PhSi-Bpin across α,β -unsaturated acceptors to provide analogous chiral β -silyl carbonyl compounds.⁸

In a previous study, we found the catalytic capabilities of a series of copper complexes containing *N*-heterocyclic carbene (NHC)



ligands in the selective diboration of alkenes and alkynes.⁹ Recently, Hou and co-workers have also shown that related complexes effectively catalyze the carboxylation of organoboronic esters.¹⁰ With the aim of contributing to the development of asymmetric induction in the β -boration of α,β -unsaturated carbonyl compounds, we describe in this paper the results obtained with a chiral copper catalytic system, matching the advantages that chiral NHC ligands provide on the catalyst (donor properties, ease of synthesis, and robustness).¹¹

Results and Discussion

First we investigated the potential of several complexes containing the (NHC)*Cu⁺ core as the precursor of the catalyst for this reaction (Figure 1). The chiral NHC ligands display chirality either at the substituents at the nitrogen atom (L₁ and L₂) or at the backbone (L₃–L₅) of the NHC ring. The copper complexes employed as catalysts were those of general formulas (NHC)CuCl and [(NHC)Cu(NCMe)]BF₄ and were prepared in a manner similar to that for complexes 1–6.¹²

These catalyst precursors were employed for the β -boration of the model substrate ethyl *trans*-crotonate with B₂pin₂. A 2% catalyst loading with regard to substrate was used in all cases, in the presence of 3 mol % of NaOtBu and 2 equiv of MeOH, relative to alkene. In order to determine the degree of enantioselection, the initially formed organoboron compounds were derivatized into the acylated products, through consecutive oxidation and acylation steps (Table 1).

The use of chiral [(NHC)Cu(NCCH₃)]BF₄ complexes containing the ligands L₁ and L₂ led to quantitative conversion, although enantiocontrol on the stereogenic β -carbon was low (Table 1, entries 1 and 2). However, those complexes with ligands L₃–L₅

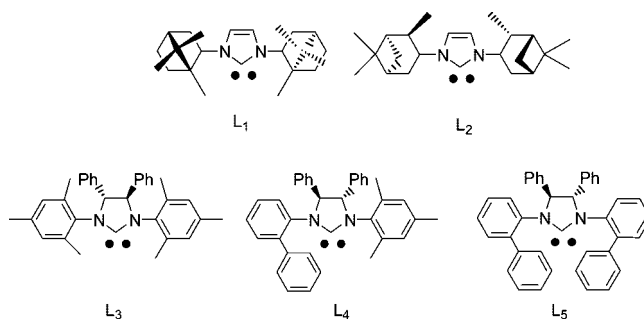


Figure 1. Chiral NHC ligands employed in this work.

* To whom correspondence should be addressed. E-mail: mariaelena.fernandez@urv.cat (E.F.); perez@dqcm.uhu.es (P.J.P.).

[†] Universidad Rovira i Virgili.

[‡] Departamento de Ingeniería Química, Química Física y Química Orgánica, Universidad de Huelva.

[§] Laboratorio de Catálisis Homogénea, Departamento de Química y Ciencia de los Materiales, Unidad Asociada al CSIC, Universidad de Huelva.

(1) (a) Marder, T. B. *J. Organomet. Chem.* **2008**, *34*, 46. (b) Dang, L.; Lin, Z.; Marder, T. B. *Organometallics* **2008**, *27*, 4443. (c) Kajiwara, T.; Terabayashi, T.; Yamashita, M.; Nozaki, K. *Angew. Chem., Int. Ed.* **2008**, *47*, 6606.

(2) (a) Ito, H.; Yamanaka, H.; Tateiwa, J.; Hosomi, A. *Tetrahedron Lett.* **2000**, *41*, 6821. (b) Takahashi, K.; Ishiyama, T.; Miyaara, N. *J. Organomet. Chem.* **2001**, *625*, 47. (c) Mun, S.; Lee, J.-E.; Yun, J. *Org. Lett.* **2006**, *8*, 4887. (d) Lee, J.-E.; Kwon, J.; Yun, J. *Chem. Commun.* **2008**, 733.

(3) (a) Lawson, Y. G.; Lesley, M. J. G.; Marder, T. B.; Norman, N. C.; Rice, C. R. *Chem. Commun.* **1997**, 2052. (b) Ali, H. A.; Goldberg, I.; Srebnik, M. *Organometallics* **2001**, *20*, 3962. (c) Bell, N. J.; Cox, A. J.; Cameron, N. R.; Evans, J. S. O.; Marder, T. B.; Duin, M. A.; Elsevier, C. J.; Bacherel, X.; Tulloch, A. A. D.; Toose, R. P. *Chem. Commun.* **2004**, 1854.

(4) Kabalka, G. W.; Das, B. C.; Das, S. *Tetrahedron Lett.* **2002**, *43*, 2323.

(5) Hirano, K.; Yorimitsu, H.; Oshima, K. *Org. Lett.* **2007**, *9*, 5031.

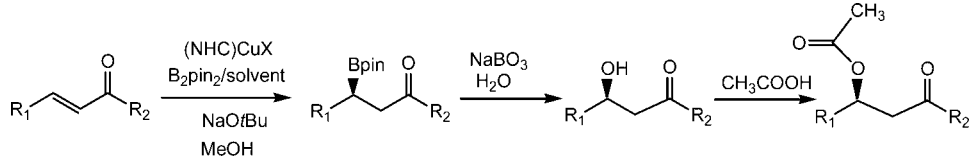
(6) (a) Burks, H. E.; Morken, J. P. *Chem. Commun.* **2007**, 4717. (b) Ramírez, J.; Lillo, V.; Segarra, A. M.; Fernández, E. C. R. *Chimie* **2007**, *10*, 138.

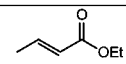
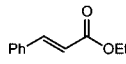
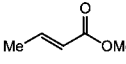
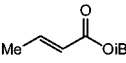
(7) Lee, J.-E.; Yun, J. *Angew. Chem., Int. Ed.* **2008**, *47*, 145.

provided moderate ee values (e.g. 58% ee with L_4). It seems that the nature of the anion does not affect either the conversion or the enantioselectivity (Table 1, entries 3–6). This could be the result of a common catalytic species of composition $(\text{NHC})\text{Cu}^+$ that could be reached from both starting materials. It seems obvious from these results that chirality at the backbone of the chiral NHC ligand plays an important role in inducing asymmetry in the β -boration reaction; therefore, the simultaneous contribution of IMes and biphenyl in L_4 provided the optimal benefits toward the asymmetric induction issue. Moreover, a comparison between the results obtained with L_4 - and L_5 -based catalysts indicate that C_1 symmetry provides better results than the corresponding C_2 -symmetric catalyst, which will be interesting information for any further catalyst development.

This improvement in the enantiocontrol of chiral $(\text{NHC})\text{Cu}^+$ complexes moved us to analyze the influence of the solvent and base on the β -boration of ethyl *trans*-crotonate. As inferred from data in Table 2, entries 8–10, the use of THF or toluene does not exert any effect on the reaction outcome. Similarly, when the base is changed from $\text{NaO}t\text{Bu}$ to NaOMe , NaOAc , or NaOH , small differences can be detected in the catalytic activity of $L_4\text{CuCl}$ (Table 1, entries 11–13). However, the absence of base in the β -boration of ethyl *trans*-crotonate with $L_4\text{CuCl}$ and $[\text{L}_4\text{Cu}(\text{NCCH}_3)]\text{BF}_4$ decreases the conversion rate significantly but slightly improves the enantioselectivity (Table 1, entries 14 and 15). Yun et al.^{2c} have postulated that the base is required to favor the formation of the LCu -boryl catalytic species from the catalyst precursor and the diboron reagent. We have also previously shown that η^2 -

Table 1. Chiral $(\text{NHC})\text{Cu}^+$ Complex Catalyzed β -Boration/Oxidation/Acylation of α,β -Unsaturated Esters^a



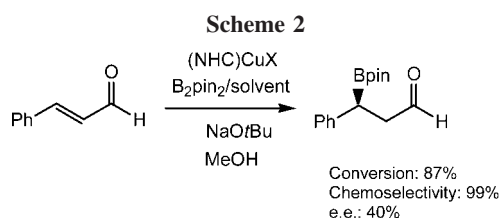
Entry	Substrate	Catalyst Precursor	Base	Solvent	Conv. (%) ^b	e.e. (%) ^c
1		$[\text{L}_1\text{Cu}(\text{NCCH}_3)]\text{BF}_4$	$\text{NaO}t\text{Bu}$	THF	93	10(R)
2	“	$[\text{L}_2\text{Cu}(\text{NCCH}_3)]\text{BF}_4$	$\text{NaO}t\text{Bu}$	THF	99	16(S)
3	“	$[\text{L}_3\text{Cu}(\text{NCCH}_3)]\text{BF}_4$	$\text{NaO}t\text{Bu}$	THF	99	25(S)
4	“	L_3CuCl	$\text{NaO}t\text{Bu}$	THF	96	31(S)
5	“	$[\text{L}_4\text{Cu}(\text{NCCH}_3)]\text{BF}_4$	$\text{NaO}t\text{Bu}$	THF	99	58(R)
6	“	L_4CuCl	$\text{NaO}t\text{Bu}$	THF	99	55(R)
7	“	L_5CuCl	$\text{NaO}t\text{Bu}$	THF	99	52(R)
8	“	L_4CuCl	$\text{NaO}t\text{Bu}$	Toluene	99	59(R)
9	“	L_4CuCl	$\text{NaO}t\text{Bu}$	CH_3CN	88	52(R)
10	“	L_4CuCl	$\text{NaO}t\text{Bu}$	CH_2Cl_2	99	57(R)
11	“	L_4CuCl	NaOMe	THF	99	51(R)
12	“	L_4CuCl	NaOAc	THF	73	50(R)
13	“	L_4CuCl	NaH	THF	99	53(R)
14	“	L_4CuCl	---	THF	<10	63(R)
15	“	$[\text{L}_4\text{Cu}(\text{NCCH}_3)]\text{BF}_4$	---	THF	25	62(R)
16		$[\text{L}_3\text{Cu}(\text{NCCH}_3)]\text{BF}_4$	$\text{NaO}t\text{Bu}$	THF	92	23(S) ^d
17	“	$[\text{L}_4\text{Cu}(\text{NCCH}_3)]\text{BF}_4$	$\text{NaO}t\text{Bu}$	THF	99	53(R) ^d
18	“	L_4CuCl	$\text{NaO}t\text{Bu}$	THF	99	61(R) ^d
19		$[\text{L}_3\text{Cu}(\text{NCCH}_3)]\text{BF}_4$	$\text{NaO}t\text{Bu}$	THF	96	31(R) ^d
20	“	$[\text{L}_4\text{Cu}(\text{NCCH}_3)]\text{BF}_4$	$\text{NaO}t\text{Bu}$	THF	96	48(R) ^d
21		$[\text{L}_3\text{Cu}(\text{NCCH}_3)]\text{BF}_4$	$\text{NaO}t\text{Bu}$	THF	99	15(R)
22	“	$[\text{L}_4\text{Cu}(\text{NCCH}_3)]\text{BF}_4$	$\text{NaO}t\text{Bu}$	THF	99	73(R)

^a Standard conditions: substrate/ Cu complex = 0.5/0.01, 3 mol % base, 1.1 equiv of bis(pinacolato)diboron (B_2pin_2), 2 equiv of MeOH, 2 mL of solvent, $T = 25^\circ\text{C}$, 6 h. ^b Determined by ^1H NMR spectroscopy. ^c Determined on the acylated product by GC-MS equipped with the chiral column β -cyclodex. ^d Determined on the β -alcohols by HPLC-MS equipped with the chiral column Chiralcel OD-H.

Table 2. Chiral (NHC)Cu⁺ Complex Catalyzed β -Boration of α -Methyl α,β -Unsaturated Esters^a

Entry	Substrate	Catalyst	Conv. (%) ^b	syn / anti ^b	syn e.e (%) ^c	anti e.e (%) ^c
1		L ₄ CuCl	99	60/40	54 ^d	5 ^d
2		L ₅ CuCl	97	52/48	68 ^d	25 ^d
3		L ₄ CuCl	94	64/36	57	11
4		L ₅ CuCl	99	60/40	35	8
5		L ₄ CuCl	65	55/45	70	20
6		L ₅ CuCl	82	53/47	56	37
7		L ₄ CuCl	93	70/30	74	5
8		L ₅ CuCl	99	65/35	39	42

^a Standard conditions: substrate/Cu complex = 0.5/0.01, 3 mol % of NaOtBu, 1.1 equiv of bis(pinacolato)diboron (B₂pin₂), 2 equiv of MeOH, 2 mL of solvent, *T* = 25 °C, 6 h. ^b Determined by ¹H NMR spectroscopy. ^c Determined on the acylated product by GC-MS equipped with the chiral column β -cyclodextrin. ^d Determined on the β -alcohols by HPLC-MS equipped with the chiral column Chiralcel OD-H.



diborane complexes can be involved in a pre-equilibrium step before the catalytic species (NHC)Cu-Bpin is formed.⁹

On the basis of the results obtained with the model ethyl *trans*-crotonate and with the aim of exploring the scope of this catalytic system, we did a series of experiments with a range of substrates under the optimized conditions. The reactions of ethyl *trans*-cinnamate with [L₃Cu(NCCH₃)]BF₄ and [L₄Cu(NCCH₃)]BF₄ provided quantitative conversion to the desired product (Table 1, entries 16 and 17), but again the enantioselectivity was better achieved when ligand L₄ was involved in the catalytic system, rising to 61% ee in the presence of the neutral catalyst precursor L₄CuCl (Table 1, entry 18). Similar catalytic performance was provided by [L₃Cu(NCCH₃)]BF₄ and [L₄Cu(NCCH₃)]BF₄ in the β -boration of methyl *trans*-crotonate ester (Table 1, entries 19 and 20). It is worth mentioning that the bulkiest species used, isobutyl *trans*-crotonate ester, behaved differently as far as the enantioselection induced by the metal center was concerned. Thus, the use of [L₃Cu(NCCH₃)]BF₄ afforded a 15% ee, whereas in the case of [L₄Cu(NCCH₃)]BF₄ this value rose to 73%. These results contrast

with the tendency observed by Yun et al.,^{2c,7} where enantioselectivity was independent of the nature of the ester moiety when CuCl/(*R*)-(*S*)-josiphos was used as catalytic system.

The metal-catalyzed β -boration of the most challenging α,β -unsaturated aldehydes has only been reported before in two examples through Rh^{13a} and Pt^{13b} catalysts, because this reaction suffers from a competitive 1,2-diboron addition reaction. Taking advantage of the benefits by copper-mediated B-addition reactions, we became motivated to carry out the (NHC)*Cu⁺-catalyzed β -boration of cinnamaldehyde, as a model substrate. In that case the use of L₃CuCl afforded quantitative conversion and total chemoselectivity on the desired product with 40% ee (Scheme 2), whereas in the case of L₄CuCl and L₅CuCl this value did not reach more than 10% ee. Despite these moderate values, this is the first attempt to obtain enantioselectivity in the β -boration of α,β -unsaturated aldehydes.

We have also studied another variable that could affect the degree of enantioselection: the existence of substituents in the starting alkene (Table 2). We have carried out the β -boration reaction with a series of α -methyl-substituted esters, such as methyl tiglate (R₁ = Me, R_{1'} = H, R₂ = OMe), ethyl tiglate (R₁ = Me, R_{1'} = H, R₂ = OEt), isopropyl tiglate (R₁ = Me, R_{1'} = H, R₂ = OiPr), and isobutyl angelate (R₁ = H, R_{1'} = Me, R₂ = OiBu). These experiments have been carried out with L₄CuCl and L₅CuCl as the catalyst precursors. As shown in Table 2, we observed very high quantitative conversions into the β -boryl products in most cases (Table 2, entries 1–8) indicating that α -substitution does not

diminish the borylation pathway. The syn/anti product ratio slightly favored the syn diastereoisomers, and ee values were markedly higher for the enantiomeric mixture of the syn products than for the anti products: the bulkiest isobutyl angelate substrate can be borated at the β position, with the highest ee value (74%) on the syn diastereoisomers (Table 2, entry 7).

Conclusions

We have found that complexes containing the (NHC)Cu core catalyze the selective β -boration of α,β -unsaturated esters and aldehydes under mild conditions. The use of chiral NHC ligands induced a certain degree of enantioselection in the final products, in a reaction for which only one precedent with asymmetric induction is known. The nature of the different NHC ligands and substrates employed in this work serves as the basis for developing more enantioselective catalysts for such transformations.

Experimental Section

General Considerations. All reactions and manipulations were carried out under an atmosphere of dry nitrogen, and the necessary organic solvents were dried, distilled, and degassed before use. Bis(pinacolato)diboron was used as purchased from Lancaster. The rest of the reagents were purchased from SigmaAldrich. Complexes 1–6¹² were prepared following literature procedures, as well as ligands L₁–L₄.¹⁴ NMR spectra were recorded on Varian Gemini 300 and Varian Mercury 400 instruments. Chemical shifts are reported relative to tetramethylsilane for ¹H, 85% H₃PO₄ for ³¹P, and BF₃–ether for ¹¹B.

Syntheses of the Ligand [L₅H][BF₄]. (a) Synthesis of (Bf)NHCH(Ph)CH(Ph)NH(Bf) (Bf = Biphenyl). Pd₂(dba)₃ (91.6 mg, 0.1 mmol), BINAP (147 mg, 0.2 mmol), (–)-(S,S)-1,2-diphenylethylenediamine (212.3 mg, 1 mmol), 2-iodo-1,1'-biphenyl (560 mg, 2 mmol), and NaO-*t*-Bu (288 mg, 3 mmol) were placed into an ampule inside a glovebox. Toluene (20 mL) was added, and the mixture was stirred for 120 h at 100 °C outside the glovebox. The solution was then cooled to ambient temperature and was quenched by the addition of water (5 mL). The aqueous layer was washed with CH₂Cl₂ (3 × 5 mL), the organic layers were combined, dried over MgSO₄, and filtered, and the solvent was removed under vacuum. Purification by silica gel chromatography (hexane–Et₂O 4:1) gave the diamine (Bf)NHCH(Ph)CH(Ph)NH(Bf) as a yellow solid (777 mg, 80%).

¹H NMR (CD₂Cl₂): δ 4.55 (d, *J* = 2.8 Hz, 2H, NCH), 4.64 (d, *J* = 2.8 Hz, 2H, NH), 6.13 (d, *J* = 7.6 Hz, 2H, arom), 6.66 (t, *J* = 7.5 Hz, 2H, arom), 6.92–6.95 (m, 2H, arom), 7.02–7.04 (m, 2H, arom), 7.07–7.09 (m, 4H, arom), 7.20–7.30 (m, 10H, arom), 7.48–7.57 (m, 6H, arom). ¹³C{¹H} NMR (CD₂Cl₂): δ 63.9 (NHC), 111.8 (arom), 117.6 (arom), 126.9 (arom), 127.7 (arom), 128.4 (arom), 128.7 (arom), 128.8 (arom), 129.1 (arom), 129.7 (arom), 129.8 (arom), 139.1 (arom), 139.9 (arom), 143.9 (arom).

(b) Synthesis of [L₅H][BF₄]. A mixture of the diamine obtained as above (516.7 mg, 1 mmol), ammonium tetrafluoroborate (125.8 mg, 1.2 mmol), and triethyl orthoformate (1.5 mL) was heated at 120 °C for 12 h. The solution was then cooled to ambient temperature. Purification by silica gel chromatography (20:1 CH₂Cl₂–CH₃OH) afforded an off-white solid of [L₅H][BF₄] (540 mg, 88%).

(8) Walter, Ch.; Oestreich, M. *Angew. Chem., Int. Ed.* **2008**, *47*, 3918.

(9) Lillo, V.; Fructos, M. R.; Ramirez, J.; Braga, A. A. C.; Maseras, F.; Díaz Requejo, M. M.; Pérez, P. J.; Fernández, E. *Chem. Eur. J.* **2007**, *13*, 2614.

(10) Ohishi, T.; Nishiura, M.; Hou, Z. *Angew. Chem., Int. Ed.* **2008**, *47*, 5792.

(11) (a) Herrmann, W. A. *Angew. Chem., Int. Ed.* **2002**, *41*, 1290. (b) Scott, N. M.; Nolan, S. P. *Eur. J. Inorg. Chem.* **2005**, 1815. (c) Hahn, F. E. *Angew. Chem., Int. Ed.* **2006**, *45*, 1358.

(12) Fructos, M. R.; de Frémont, P.; Nolan, S. P.; Díaz-Requejo, M. M.; Pérez, P. J. *Organometallics* **2006**, *25*, 2237.

(13) (a) Kabalka, G. W.; Das, B. C.; Das, S. *Tetrahedron Lett.* **2002**, *43*, 2323. (b) Ali, H. A.; Goldberg, I.; Srebnik, M. *Organometallics* **2001**, *20*, 3962.

¹H NMR (CD₂Cl₂): δ 4.74 (s, 2H, NCH), 6.69 (d, *J* = 8.0 Hz, 2H, arom), 7.22–7.41 (m, 20H, arom), 7.52–7.67 (m, 6H, arom), 8.98 (s, 1H, NCHN). ¹³C NMR (CD₂Cl₂): δ 75.7 (NHC), 127.2 (arom), 128.0 (arom), 128.2 (arom), 128.6 (arom), 128.7 (arom), 129.0 (arom), 129.1 (arom), 129.3 (arom), 129.4 (arom), 129.5 (arom), 129.6 (arom), 129.8 (arom), 129.9 (arom), 130.0 (arom), 130.6 (arom), 132.1 (arom), 134.1 (arom), 138.4 (arom), 138.7 (arom), 157.6 (NCHN).

Syntheses of the Neutral Complexes (NHC)CuCl and the Cationic Catalyst Precursors [(NHC)Cu(NCMe)]BF₄. The procedure was similar to that previously reported in the literature.¹² The imidazolium salt [LH][X] (X = Cl, BF₄) was dissolved (or suspended) in thf (5 mL), and 1.2 equiv of K⁺O[–]Bu was added to the stirred solution at room temperature. The mixture was stirred until a clear solution was obtained (1 h), and then 1 equiv of CuCl was added. Further stirring for 4 h led to a suspension that was filtered through Celite; the filtrate was then taken to dryness and the residue dissolved in a 1:1 mixture of CH₂Cl₂ and petroleum ether. Upon concentration until cloudiness, cooling to –20 °C overnight afforded an off-white, microcrystalline material of composition (NHC)CuCl (NHC = L₁–L₅). The cationic complexes [(NHC)Cu(NCMe)]BF₄ employed as catalyst precursors were prepared in the following manner. A solution of the neutral complex in acetonitrile was treated with 1 equiv of AgBF₄. After 15 min of stirring, the mixture was filtered through Celite and the filtrate was dried under vacuum to yield a solid of general composition [(NHC)Cu(NCMe)]BF₄. The spectroscopic data of these neutral and cationic compounds are given in the Supporting Information.

Typical Catalytic β -Boration of α,β -Unsaturated Esters and Aldehydes. Bis(catecholato)diboron (1.1 equiv) was added to a solution of the catalyst (2 mol %) and base (3 mol %) in tetrahydrofuran (2 mL) under nitrogen. The solution was stirred for 5 min, and the substrate (0.05 mmol) was then added with 2 mL of MeOH. The mixture was stirred for 6 h at room temperature. The products obtained were analyzed by ¹H NMR spectroscopy to determine the degree of conversion and the nature of the reaction products.

Oxidation Protocol. A solution of sodium perborate (2.5 mmol) in THF–water (1:1, 4 mL), was added to the mixture. The mixture was stirred vigorously for 4 h. After this time, it was quenched with a saturated solution of NaCl and then extracted into AcOEt (3 × 20 mL). The organic phase was dried over MgSO₄, followed by evaporation under reduced pressure to remove the solvent. The products obtained were analyzed by ¹H NMR spectroscopy to determine the degree of conversion and the nature of the reaction products. To determine the ee values of the β -alcohols, they were analyzed on an HPLC-MS instrument equipped with the chiral column Chiralcel OD-H.

Acylation Protocol. A solution of 3 mL of acetic anhydride and 5 mL of acetic acid in 25 mL of CHCl₃ was added to the β -alcohol product. The reaction mixture was stirred overnight at 50 °C. The next day the mixture was extracted with AcOEt (3 × 20 mL). The organic phase was dried over MgSO₄, followed by evaporation under reduced pressure to remove the solvent. The solution was analyzed in a GC-MS instrument equipped with the chiral column β -cyclodex to determine the ee values.

Acknowledgment. We thank the MEC for funding (CTQ2005-00324BQU, CTQ2007-60442BQU, and Consolider-Ingenio 2010 CSD-0003) and the Junta de Andalucía (P07-FQM-2870). V.L. thanks the MEC for an FPI grant.

Supporting Information Available: Text giving spectroscopic data for the new copper complexes employed as catalyst precursors. This material is available free of charge via the Internet at <http://pubs.acs.org>.

OM800946K

(14) (a) Lee, S.; Hartwig, J. F. *J. Org. Chem.* **2001**, *66*, 3402. (b) Seiders, T. J.; Ward, D. W.; Grubbs, R. H. *Org. Lett.* **2001**, *3*, 3225. (c) Lee, Y.; Hoveyda, A. H. *J. Am. Chem. Soc.* **2006**, *128*, 15604.